

Perugia, Italy July 2-13, 2007



IASPEI

**INTERNATIONAL ASSOCIATION OF SEISMOLOGY AND PHYSICS
OF THE EARTH'S INTERIOR**

INTER-ASSOCIATION SYMPOSIA AND WORKSHOPS

Excerpt of "Earth: Our Changing Planet. Proceedings of IUGG XXIV General Assembly Perugia, Italy 2007"
Compiled by Lucio Ubertini, Piergiorgio Manciola, Stefano Casadei, Salvatore Grimaldi

Published on website: www.iugg2007perugia.it

ISBN : 978-88-95852-24-9

Organized by

Perugia, Italy July 2-13, 2007



IRPI



High Patronage of the President of the Republic of Italy



Patronage of

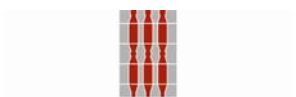
Presidenza del Consiglio dei Ministri

Ministero degli Affari Esteri

Ministero dell'Ambiente e della Tutela del Territorio e del Mare

Ministero della Difesa

Ministero dell'Università e della Ricerca



Regione Umbria

Presidenza della Giunta



Provincia di Perugia



Comune di Perugia

SCIENTIFIC PROGRAM COMMITTEE

Paola Rizzoli	<i>Chairperson President of the Scientific Program Committee</i>	<i>Usa</i>
Uri Shamir	<i>President of International Union of Geodesy and Geophysics, IUGG</i>	<i>Israel</i>
Jo Ann Joselyn	<i>Secretary General of International Union of Geodesy and Geophysics, IUGG</i>	<i>Usa</i>
Carl Christian Tscherning	<i>Secretary-General IAG International Association of Geodesy</i>	<i>Denmark</i>
Bengt Hultqvist	<i>Secretary-General IAGA International Association of Geomagnetism and Aeronomy</i>	<i>Sweden</i>
Pierre Hubert	<i>Secretary-General IAHS International Association of Hydrological Sciences</i>	<i>France</i>
Roland List	<i>Secretary-General IAMAS International Association of Meteorology and Atmospheric Sciences</i>	<i>Canada</i>
Fred E. Camfield	<i>Secretary-General IAPSO International Association for the Physical Sciences of the Oceans</i>	<i>Usa</i>
Peter Suhadolc	<i>Secretary-General IASPEI International Association of Seismology and Physics of the Earth's Interior</i>	<i>Italy</i>
Steve McNutt	<i>Secretary-General IAVCEI International Association of Volcanology and Chemistry of the Earth's Interior</i>	<i>Usa</i>



Abbreviations

IAG	International Association of Geodesy
IAGA	International Association of Geomagnetism and Aeronomy
IAHS	International Association of Hydrological Sciences
IAMAS	International Association of Meteorology and Atmospheric Sciences
IAPSO	International Association for the Physical Sciences of the Oceans
IASPEI	International Association of Seismology and Physics of the Earth's Interior
IAVCEI	International Association of Volcanology and Chemistry of the Earth's Interior
CLiC	Climate and Cryosphere
Ev-K2-CNR	Everest-K2 CNR Committee
GEWEX	Global Energy and Water Experiment
HKH-FRIEND	Hindu Kush-Himalayan Flow Regimes from International Experimental and Network Data
IABO	International Association for Biological Oceanography
IACS	International Association of Cryospheric Sciences
ICACGP	International Commission on Atmospheric Chemistry and Global Pollution
ICASVR	International Commission on Atmosphere-Soil-Vegetation Relations
ICCE	International Commission on Continental Erosion
ICCL	International Commission on Climate
ICCLAS	International Commission on the Coupled Land-Atmosphere System
ICCP	International Commission on Clouds and Precipitation
ICDM	International Commission on Dynamic Meteorology
ICGW	International Commission on Groundwater
ICIMOD	International Center for Integrated Mountain Development
ICMA	International Commission on the Middle Atmosphere
ICRS	International Celestial Reference System
ICSIH	International Commission on Snow and Ice Hydrology
ICSW	International Commission on Surface Water
ICT	International Commission on Trac
ICWQ	International Commission on Water Quality
ICWRS	International Commission on Water Resources Systems
IGAC	International Global Atmospheric Chemistry
IGS	International Glaciological Society
ILP	International Lithosphere Program
INQUA	International Union for Quaternary Research
ION	International Ocean Network

IRC	International Radiation Commission
PUB	Prediction in Ungauged Basins
SCAR	Scientific Committee on Antarctic Research
SEDI	Study of the Earth's Deep Interior
SPARC	Stratospheric Processes and their Role in Climate
UCCS	Union Commission for the Cryospheric Sciences
UNESCO	United Nation Educational, Scientific and Cultural Organization
UNITAR	United Nations Institute for Training and Research
WMO	World Meteorological Organization

Session code naming

The first letter of the session codes indicates whether the session is a Union, a Joint Interassociation or a single Association sponsored event, the second letter indicates the type of event: Symposium (S) or Workshop (W). For Joint events, the second letter indicates the Lead Association (with the abbreviations listed below) and the third indicates whether a session is a Symposium (S) or a Workshop (W). In some cases (namely IAGA, IAHS) Association session codes have an extra codification referring to a specific Theme or Division.

U	UNION
J	JOINT
G	IAG
A	IAGA
H	IAHS
M	IAMAS
P	IAPSO
S	IASPEI
V	IAVCEI

Some examples:

US002

is a **Union Symposium**; **JGW001** is a **Joint IAG Workshop** with IAG as the Lead Association;

MS003

is an Association (IAMAS) **Symposium**. **AS III 020** is an Association (IAGA) **Symposium** sponsored by its **III** Division.

JSS001 **Symposium** **(1716 - 1731)****Convener** : Prof. Ian Jackson

Physics and Chemistry of Earth Materials

JSS002 **Symposium** **(1732 - 1844)****Convener** : Dr. Kenji Satake, Dr. Gerassimos Papadopoulos**Co-Convener** : Prof. Efim Pelinovsky, Mrs. Paula Dunbar, Prof. Fumihiko Imamura

Tsunami: generation and hazard

JSS003 **Symposium** **(1845 - 1892)****Convener** : Prof. Jochen Zschau

Early-Warning Systems

JSS004 **Symposium** **(1893 - 1904)****Convener** : Dr. Gianluca ValensiseNon-instrumental seismometry - Quantification of past and future earthquakes:
balancing the geological, historical and contemporary strain records**JSS005** **Symposium** **(1905 - 1923)****Convener** : Dr. David Schwartz, Mrs. Suzanne Hecker, Dr. Gianluca Valensise, Dr. Kelvin Berryman**Co-Convener** : Dr. Paolo Marco De Martini, Dr. Eullia Masana, Dr. Daniela PantostiNon-instrumental seismometry - Global and regional parameters of paleoseismology;
implications for fault scaling and future earthquake hazard**JSS006** **Symposium** **(1924 - 1951)****Convener** : Dr. David Schwartz, Dr. Gianluca Valensise**Co-Convener** : Dr. Daniela Pantosti, Dr. Eullia Masana, Dr. Francisco Gutierrez

Non-instrumental seismometry - New Approaches to Paleoseismology and Earthquake Recurrence in the 21st Century

JSS007 **Symposium** **(1952 - 1976)**

Convener : Dr. Yoichi Sasai, Dr. Zlotnicki Jacques, Dr. Ciro Del Negro, Prof. Viacheslav Spichak

Co-Convener : Prof. Domenico Patella

Progress in electromagnetic studies on earthquakes and volcanoes - Volcanic structure and activities (same as JVS002)

JSS008 **Symposium** **(1977 - 2021)**

Convener : Dr. Malcolm Johnston

Progress in electromagnetic studies on earthquakes and volcanoes - Electromagnetic fields associated with earthquakes and active faulting

JSS009 **Symposium** **(2022 - 2066)**

Convener : Prof. Pier Francesco Biagi

Progress in electromagnetic studies on earthquakes and volcanoes - Crustal instabilities and earthquake precursors

JSS010 **Symposium** **(2067 - 2092)**

Convener : Dr. Valerio Tramutoli, Prof. Ramesh Singh

Co-Convener : Dr. Michel Parrot, Dr. Dimitar Ouzounov

Progress in electromagnetic studies on earthquakes and volcanoes - Seismo-electromagnetic studies using space technology

JSS011 **Symposium** **(2093 - 2186)**

Convener : Prof. Thorne Lay

Earth Structure and Geodynamics

Symposium **(2187 - 2215)**

JSS012**Convener** : Prof. Hitoshi Kawakatsu**Co-Convener** : Dr. Andrea Morelli, Dr. Shoichi Yoshioka, Prof. Tetsuo Irifune

Earth Structure and Geodynamics - Dynamics of Deep Mantle Slabs

JSS013**Symposium****(2216 - 2251)****Convener** : Prof. Sierd Cloetingh**Co-Convener** : Prof. Hans Thybo

The lithosphere

JSS014**Symposium****(2252 - 2327)****Convener** : Prof. Kevin P Furlong

Crustal structure and Tectonophysics - Crustal and lithospheric structure in active continental blocks and their boundaries

JSS015**Symposium****(2328 - 2338)****Convener** : Prof. Hans Thybo

Crustal structure and Tectonophysics - Large-scale multi-disciplinary programs for continental imaging

JSS016**Symposium****(2339 - 2358)****Convener** : Prof. Barbara Romanowicz

Underwater observatories

JSS017**Symposium****(2359 - 2394)****Convener** : Prof. David Chapman

Lithosphere thermal state and geodynamic processes: from measurements to models

JSW001

Workshop

(2395 - 2399)

Convener : Prof. Sri Widiyantoro

Subduction zone related volcanism and hazard mitigation



IUGG

XXIV2007

PERUGIA
I T A L Y



(S) - IASPEI - *International Association of Seismology and Physics of the Earth's Interior*

JSS001

1716 - 1731

**Symposium
Physics and Chemistry of Earth Materials**

Convener : Prof. Ian Jackson

Insight into the physical and chemical behaviour of Earth materials is essential for the interpretation of seismological, geochemical, geodynamic, and geomagnetic observations. Experimental techniques now provide direct access to the conditions of high pressure and temperature of subducting lithospheric slabs, the transition zone, lower mantle and core. Complementary theoretical studies predict behaviour of materials under extreme conditions difficult to realise in laboratory experiments. The structure and behaviour of mineral surfaces and crystal defects, as well as the bulk properties of crystalline and molten materials, are increasingly amenable to investigation. These developments in materials science promise a better understanding of the Earth's interior - from crust to core. Papers are invited on all aspects of contemporary research into the physics and chemistry of Earth materials

IUGG
XXIV2007
PERUGIA
ITALY



(S) - IASPEI - International Association of Seismology and Physics of the Earth's Interior

JSS001

Oral Presentation

1716

The relation between the rock variables and exponents and the lithology of nukhul formation at Ferian Oil Field, central part of the Gulf of Suez, Egypt.

Prof. Mahmoud Ghorab
GEOPHYSICS WELL LOGGING

In oil production, the prime importance is directed to define the types and amounts of fluids encountered in the concerned formations. These determinations require the calculation of the formation porosity, so the present work is devoted to show the effect of the lithology on the different reservoir characteristics specially porosity where the rock variables and exponent (m , n and a) are very important in the porosity calculation. The area of study lies in the central part of the eastern side of the Gulf of Suez, Egypt, where eight wells were selected (HH84-1, GG85-1, WFA-1, GS 206-1A, GS 196-1A, Tanka-1, Tanka-3 and Tanka-4) to calculate the rock variables and exponent (m , n and a) and their lithology. Different crossplots are used to define the rock variables and lithology for the Nukhul Formation. The " m " values are between 1.9 and 2.5 and " a " values are between 2.1 and 2.5 while the related lithologies are carbonate, shale, and sandstone. The petrophysical parameters like porosity and hydrocarbon saturation show that Nukhul Formation can be considered as a fair reservoir for oil production in the study area.

PERUGIA
ITALY



(S) - IASPEI - *International Association of Seismology and Physics of the Earth's Interior*

JSS001

Oral Presentation

1717

Investigation of extensional deformation of ductile rocks

Dr. Shayesteh Mehrabian

EARTH PHYSICS INSTITUTE OF GEOPHYSICS, UNIVERSITY OF TEHRAN IASPEI

Knowledge of the deformation and particularly ductile flow properties of both the crust and the mantle is important for better understanding a wide range of geological and geophysical processes. Models of earthquake distribution, extensional tectonics and convection all require appropriate flow laws for the rocks in the regions of interest. Structural and microstructural studies of in situ rocks or of samples from boreholes represent an important way for learning about natural rock deformation. Mechanical tests on rocks, over a wide range of temperature, pressure and strain rate followed up by microstructural studies of the deformed materials can provide additional information. Experimental deformation of rocks has provided much of the information on which the choice of constitutive laws is based. One of the aims of geological and geophysical studies is to gain a deeper insight into the physics of deformation mechanisms in rocks in order to be able to extrapolate constitutive equations obtained in experiments to inaccessible conditions of strain rate and time in nature. One problem of experimental techniques, however, is the inaccessibility of microstructural data during the deformation processes. In this study the main purpose is to simulate the behavior of a cylindrical marble rock sample of 10 mm diameter and 20 mm length in extension with necking under high temperature and pressure conditions and to compare the model results with the observed behavior of the rock sample in real high pressure/temperature laboratory experiments which performed by Rutter (1995). By using a numerical approach based on the finite element method the deformation of the sample is modeled. The discretised equations for a mesh of eight-node quadrilateral elements in the case of visco-plastic behavior, including power law flow, which is expected to correspond to the real situation, are solved. In order to be able to assess the capability of the model to simulate the ductile behavior, the geometry and boundary conditions are appropriate to experimental studies. The validation process of the numerical frame-work has been made by using the analytical calculations for a single element with uniform deformation conditions. From the obtained results of the numerical calculations it appears that responses of the program in terms of displacement-force curves are very similar to the experimental results and the deformed shape corresponds to diffusive necking deformation along the sample length. It can be concluded that the strain-dependent flow law together with a consideration of the temperature gradient can be applied to establish a framework for the numerical modeling of the necking phenomenon or potentially the evolution of localized shear zones. Hence this approach with a constitutive model offers a capability to simulate some aspects of rock deformation in extension at least up to 20% bulk strain, and can be used to set up more realistic and complex applications to a wide range of conditions for comparison with the experimental results.

Keywords: deformation, visco plastic, constitutive flow law

(S) - IASPEI - *International Association of Seismology and Physics of the Earth's Interior*

JSS001

Oral Presentation

1718

Plane strain and axisymmetric models to simulate the mechanical behavior of a rock sample

Mr. Shervin Mizani

Electrical and Computer Engineering School of Electrical and Computer Engineering IASPEI

In this study a finite element program is developed for the analysis of static instability and consequent flow of an elasto-plastic solid in the cases of plane strain and axisymmetric by using correspondence principle in the theory of rheological mechanics. The steps are as follows: firstly, declarations of the quantities for the finite element mesh, the finite element calculations and the constitutive models are specified. Then the necessary files which are used in the calculation procedures are opened. After that the geometrical data as generated by the mesh generator is read from a file to specify the geometry of the problem. Then the material parameters and the applied boundary conditions are read in. Next the nodal freedom matrix is composed by considering restraint nodes or restraint freedoms of nodes along restraint sections of the boundary. The numerical implementation concerns three main processes, namely: (i)-The check of the initial stress state, which involves the calculation of the initial load vector. (ii)-The specification of the global stiffness matrix, by considering the corresponding solution procedures. (iii)-Application of displacement increment steps, which involves a Newton-Raphson iteration method for the equilibrium equation solution in each iteration. With respect to the point that in the finite element calculation the estimated stress distribution must be in equilibrium with the external load, this is achieved by calculating the stress distribution for any set of nodal displacements. The program deals with plane strain and axisymmetric deformation using eight-node rectangular elements for the elastic, elasto-plastic and viscous behavior of a rock sample. The finite element mesh has been kept regular to simplify the presentation and to minimize the volume of data required. The simple geometries enable the nodal co-ordinates and freedom numbers to be generated automatically. The program is quite capable of analyzing geometrically more complex problems, by simply replacing the mesh file generated by another program, a so-called mesh generator. The starting geometry, the initial boundary conditions and material properties which are used as inputs to the numerical models are obtained from experimental deformation. In general there are three output files for this program which are used for storage of basic and necessary results, commonly include the calculation results of the program for the latest step in terms of nodal displacements and invariants of stress and strain. Some calculated results are demonstrated in relevant figures as displacement-force, nodal displacement vectors, deformed mesh, contours of deviatoric stresses and strains at integration points for various cases.

Keywords: plane strain, axisymmetric, rock behavior

(S) - IASPEI - *International Association of Seismology and Physics of the Earth's Interior*

JSS001

Oral Presentation

1719

**Constraining the Composition and Thermal State of the Earth's Mantle
from Inversion of Geophysical Data**

Dr. Amir Khan

Niels Bohr Institute University of Copenhagen IASPEI

James Connolly, Nils Olsen

We jointly invert seismic data (global ISC P and S wave travel times), electromagnetic sounding data (long-period inductive responses in the form of C-responses) and gravity data (mean mass and moment of inertia) using a recently developed method to rigorously invert different geophysical data jointly for compositional and thermal parameters. The inversion combines thermodynamic phase equilibrium calculation and physical properties, with a fully non-linear stochastic inverse algorithm, based on a Markov chain Monte Carlo (MCMC) method, to explore the range of model parameters consistent with the observations, i.e. Earth's mantle geotherm and composition within the system CaO-FeO-MgO-Al₂O₃-SiO₂. Through our choice of parameters, the method provides a means of naturally linking various a priori unrelated geophysical data in the inversion. Our results are indicative of a chondritic mantle composition and a lower mantle geothermal gradient that is slightly superadiabatic.

Keywords: mantle, composition, temperature

PERUGIA
ITALY



(S) - IASPEI - *International Association of Seismology and Physics of the Earth's Interior*

JSS001

Oral Presentation

1720

Ultrahard nano-polycrystalline diamond: novel material for high-pressure mineral physics studies

Prof. Tetsuo Irifune

Geodynamics Research Center Ehime University IASPEI

Hitoshi Sumiya

Since we first reported the synthesis of binderless nano-polycrystalline diamond (NPD) with extremely high hardness by direct conversion of graphite at high pressure and high temperature (Irifune et al., 2003; 2004; Sumiya and Irifune, 2004), we have been extensively working to synthesise the NPD with larger dimensions and higher quality. NPD rods of up to ~5 mm in diameter and ~a few mm thick without any visible cracks can now be synthesized on a routine basis using large multi-anvil apparatus. We found thus synthesised NPD rod can be polished to various forms, although it needs substantially longer time compared with that needed for polishing a single crystal diamond. Moreover, the NPD was found to maintain its hardness at temperatures substantially higher than single crystal diamond. Applications of NPD to high-pressure generation have been made by using multi-anvil apparatus combined with in situ X-ray observations. We used a pair of NPD rods as the third-stage anvils for the 6-8-2 compression system, originally devised by Endo et al. (1985), and found that the pressures as high as ~90 GPa were produced at room temperature, which were maintained at temperatures up to ~1200K. It is suggested that NPD can also be used for further higher pressure generation and other mineral physics studies using various high pressure apparatus, such as laser heated diamond anvil cell, Drickamer anvil apparatus, etc.

Keywords: diamond, high pressure, multi-anvil



(S) - IASPEI - *International Association of Seismology and Physics of the Earth's Interior*

JSS001

Oral Presentation

1721

High-temperature elasticity of high-pressure minerals: new insights from gas-medium ultrasonic interferometry

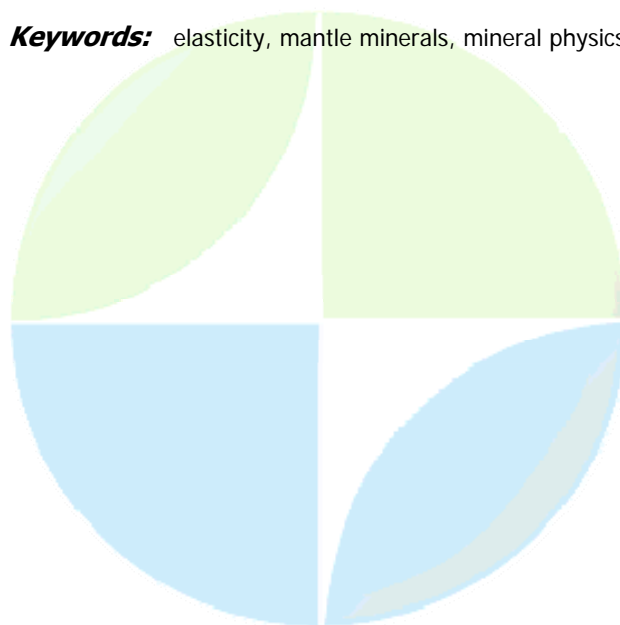
Prof. Ian Jackson

Research School of Earth Sciences Australian National University IASPEI

Gabriel D. Gwanmesia, Sytle M. Antao, Jennifer Kung, Sally M. Rigden, Robert C. Liebermann

The internally heated gas-medium high-pressure apparatus provides an attractive environment for the study of high-temperature elasticity of geological materials under essentially hydrostatic conditions. Use of a compound steel-alumina acoustic buffer rod, and a soft-iron cup as a refractory pressure-transmitting medium surrounding the cylindrical sample, allows precise measurements of elastic wave speeds by ultrasonic interferometry to 1300C at 300 MPa confining pressure. However, for the necessarily small (<3 mm) specimens of high-pressure minerals to be tested over temperature ranges limited to < 700C by their metastability, an NaCl cup provides a closer approach to hydrostatic conditions. This latter method has recently been applied to fine-grained polycrystalline specimens of pyrope garnet, magnesioferrite spinel, ScAlO₃ perovskite and the wadsleyite and ringwoodite polymorphs of Mg₂SiO₄. Compressional and shear wave speeds are usually measured under identical conditions of pressure and temperature with dual-mode transducers with ~0.1% precision yielding well-resolved, essentially linear temperature dependencies of wave speeds and elastic moduli. The resulting constraints on the temperature dependence of the elastic bulk and shear moduli are most useful when integrated, along with other relevant thermoelastic data, into the thermodynamically self-consistent theory of Stixrude and Lithgow-Bertelloni. This comprehensive, parametrically economical theory is based on fundamental thermodynamic relations, generalized to anisotropic strain and represented by Taylor series in Eulerian strain, thus describing elasticity as well as the usual bulk thermodynamic properties. Comparison of the temperature dependence of elastic wave speeds from gas-medium studies with similar data obtained at the much higher pressures of solid-medium apparatus provides new constraints on the elusive mixed pressure-temperature derivatives important in extrapolation to deep-mantle conditions.

Keywords: elasticity, mantle minerals, mineral physics



(S) - IASPEI - *International Association of Seismology and Physics of the Earth's Interior*

JSS001

Oral Presentation

1722

The transition from elastic to viscoelastic behaviour: grain-size sensitive relaxation in polycrystalline MgO

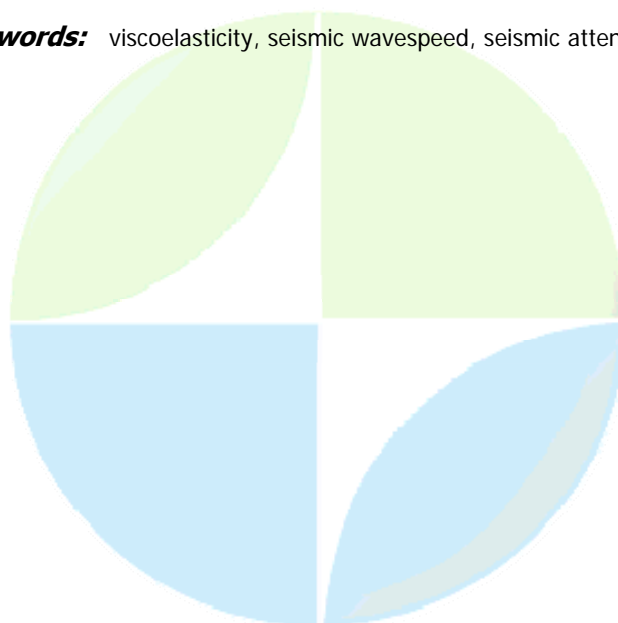
Dr. Auke Barnhoorn

Research School of Earth Sciences Australian National University IASPEI

John D. Fitz Gerald, Akira Kishimoto

Strictly elastic behaviour gives way at sufficiently high temperatures and long periods to viscoelastic behaviour manifest in reduced seismic wave speeds and associated attenuation. In order to further explore the nature of this transitional mechanical behaviour, we have performed seismic-frequency forced-oscillation experiments at high temperatures on a suite of newly prepared MgO polycrystals (of high purity and low porosity). The samples were fabricated from powders of 50 nm grain size with temperature-time trajectories varied to allow different amounts of grain growth resulting in samples with stable average grain sizes of <1, 3, 8 and ~100 micron, respectively. Torsional forced-oscillation experiments were conducted on precision-ground cylindrical specimens at 200 MPa confining pressure over the temperature range of 20-1300C. Sinusoidally varying torques were applied at 10 different oscillation periods between 1 and 1000 s with amplitudes equivalent to maximum shear stresses of 0.3 MPa, resulting in maximum shear strains of 3E-5 at the highest temperature. For temperatures below 900C, the behaviour is essentially elastic for all grain sizes. However, at higher temperatures (~900-1300C) the forced-oscillation and complementary torsional microcreep tests show that there is significant anelastic and viscous behaviour. The measured shear modulus and dissipation are both strongly frequency and grain size dependent with the highest levels of dissipation and the lowest levels of shear modulus in the most fine-grained sample. Fitting of the combined shear modulus and dissipation data to an extended Burgers model captures the complete transition from elastic behaviour through a broad anelastic absorption band to the onset of viscous deformation. Collapse of the data using a master variable approach indicates that grain-boundary sliding processes play an important role in the viscoelasticity of fine-grained polycrystalline MgO. The results of this study contribute to an emerging more general understanding of viscoelastic relaxation in fine-grained geological and ceramic materials.

Keywords: viscoelasticity, seismic wavespeed, seismic attenuation



(S) - IASPEI - *International Association of Seismology and Physics of the Earth's Interior*

JSS001

Oral Presentation

1723

The role of mechanochemical production for the CO₂ released from the seismic area of Apennine Chain

Dr. Francesco Italiano
Sezione di Palermo INGV IAVCEI

Giovanni Martinelli, Sonia Pizzullo, Paolo Plescia

The evidence that a large amount of carbon dioxide is released through wide areas in the absence of clear contribution from the mantle or from mantle-derived fluids leads to the hypothesis that an additional energy source has to be considered to justify the origin of the released CO₂. The CO₂-dominated gases released along the Thyrrenian sector of the Apennine chain come from both geothermal and seismic areas: they are mainly marked by ³He/⁴He ratios of radiogenic signature, but some cases (i.e Larderello geothermal area) where a mantle signature is evident. Experimental results clearly confirm the possibility of producing CO₂ by grinding carbonate rocks as an effect of the total dissociation of calcite. Laboratory experiments carried out by a ring mill demonstrate that stress application on calcite and calcite/clay mixture produces CO₂ and CH₄ and, even though the experimental approach cannot be compared to a natural system, it shows a way to model the processes occurring on fault planes where mineralogical phases are involved and modified with the total reorganization of the crystalline lattice and the contemporary production of a gas phase. The evidence that the mechanochemical production of CO₂ and CH₄ plays an important role over the entire Apennine chain leads to the consideration that similar greenhouse gas production has to be evaluated on a global scale.

Keywords: co2 production, mechanochemical, seismic areas



(S) - IASPEI - *International Association of Seismology and Physics of the Earth's Interior*

JSS001

Oral Presentation

1724

Viscosity of Magmatic Liquids: A model for volcanology

Prof. Kelly Russell
earth & ocean sciences

Daniele Giordano, Don Dingwell

Viscosity of silicate melts is the single most important physical property governing the transport and eruption of magma. The viscosity of naturally-occurring silicate magmas can span more than 10 orders of magnitude (10⁻¹-10¹⁴ Pa s) due to variations in temperature (T), melt composition, and due to varying proportions of suspended solids and/or exsolved fluid phases. Dissolved volatile contents of H₂O and F are of particular importance because small variations in their concentrations generate large (> 10⁵) and strongly nonlinear changes in melt viscosity. The task of creating a comprehensive model for viscosity of natural melts has long been a goal of earth scientists, but the challenge has been to include these volatile effects, together with multicomponent melt compositional effects, in the framework of a non-Arrhenian model. Here, we present an empirical model for predicting the viscosity of natural volatile-bearing silicate melts. The model has an oxide mole % basis of SiO₂, Al₂O₃, TiO₂, FeO, CaO, MgO, MnO, Na₂O, K₂O, P₂O₅, H₂O, and F₂O-1) and covers over fifteen log units of viscosity (10⁻¹-10¹⁴ Pa s). Temperature dependence of viscosity (η) is modelled by the VFT equation [$\log \eta = A + B/(T(K) - C)$]. The calibration is based on ~1540 published viscosity measurements at T(K) on melts of known composition. The chemical model uses a total of 17 empirical coefficients. The parameter A is assumed constant and to represent the high-temperature limit to silicate melt viscosity ($A = \eta \sim 10^{-4.6}$ Pa s). Compositional effects are ascribed to the parameters B and C. Additional attributes of the viscosity model include: i) its experimental basis spans virtually the entire compositional range found in naturally-occurring volcanic rocks, ii) the model captures the effects of 10 major and minor oxide components and the volatile components H₂O and F, iii) it is computationally continuous across the entire compositional and temperature spectrum of the database, iv) it is capable of accommodating both strong (near-Arrhenian T-dependence) and fragile (very non-Arrhenian T-dependence) behaviour of silicate melts, and v) it reproduces observed relationships between melt composition and transport properties such as glass transition temperature (T_g) and fragility (m). The model reproduces the T(K)-log η relationships for melts not used for calibration purposes indicating that it can be extrapolated past the original database. This attribute makes our model important for predicting transport properties of melts that do not allow direct experimental measurement (e.g., peridotite, kimberlite, or high-T, volatile-rich melts). In addition, because the model uses a single computational strategy independent of whether melts are hydrous or anhydrous and strong or fragile, the model allows for accurate, continuous prediction of melt properties as a function of evolving temperature and melt composition (e.g., volatile loss or gain). This property ensures that dramatic shifts in predicted viscosity are real (e.g., due to $\Delta(T-X)$ conditions) as opposed to numerical artefacts. This model will undoubtedly lead to more realistic computational models of volcanic processes. In summary, this computational model transforms a quarter-century of experimental study of melt viscosities, into a parameterisation which can support numerical modelling of magmatic and volcanic phenomena.

Keywords: viscosity, silicate melt, model

(S) - IASPEI - International Association of Seismology and Physics of the Earth's Interior

JSS001

Poster presentation

1725

Feature of the analyses of heterogeneous ores

Dr. Artush Tamrazyan
IUGG, IASPEI JSS IASPEI

At X-ray radiometric approximation (XRA) of ores in conditions in situ or at their processing and enrichment, object of research are not homogeneous, heterogeneous environments. To present time a plenty of the works, the influences of heterogeneous effect devoted to studying on results XRA is known. However, all questions of the theory of heterogeneous effect, especially ways of his(its) account yet are not solved. We receive analytical formulas for calculation of streams of secondary radiations from heterogeneous environments with the various sizes and distributions of heterogeneous. Taking into account, that distribution of ore grains in the heterogeneous environment has probability character for reception of a full picture cases their discrete binomial and continuous (normal) distributions are considered. With the purpose of finding - out of character of influence of large sizes particles and the law of their distribution to size of a stream of secondary radiations, the settlement data are compared to results of experimental researches. For experiment with fractionated chalcopyrite and syenite some groups of test in which contents of ore grains varied both the sizes, and were made. From comparison settlement and experimental data it is visible, that at the big sizes of particles calculations on binomial distribution are better coordinated with experiment, and with the small sizes the good consent with experiment is observed for normal distribution. The received data allow to conclude, that in the initial stage of processing and enrichment of ores distribution of ore inclusions in the environment submits binomial law, and in the following stages of processing when the sizes of particles and therefore, the quantity of grains in individual volume their distribution is close to the normal law is increased decrease. Knowing character of change of the law of distribution of ore grains in ore in different stages of its development, the appropriate ways of realization X-ray radiometric method, taking into account influence of effect of heterogeneity easily get out.

Keywords: x ray radiometric



(S) - IASPEI - *International Association of Seismology and Physics of the Earth's Interior*

JSS001

Poster presentation

1726

Natural magnetite nanoparticles from an iron-ore deposit: grain size effects in magnetic properties

Dr. Luis M. Alva-Valdivia

Paleomagnetism Universidad Nacional Autonoma de Mexico IAGA

We report natural magnetite nanoparticles, 0.514 nm, from the mineralized zones of Pea Colorada iron-ore deposit. Crystallographic identification of magnetite nanostructures was done using high resolution transmission electron microscopy. Micrometric scale magnetite was magnetically reduced and divided into distinct range fractions: 8556 m, 5630 m, 3022 m, 2215 m, 1510 m, 107 m, and 7-2 m. Reduced magnetite was characterized by X-ray diffraction, high resolution transmission electron microscopy and high angle annular dark field. Magnetic properties show drastic changes when grain size exceeds the frontier from micro to nanometric sizes. The magnetic susceptibility obtained from frequency percent (fd%), report high values (13%) for the 214 nm fractions, attributed to dominant fractions of superparamagnetic particles, confirming the Mossbauer spectroscopy results. fd% < 5% variations in fractions from 567 m occur due to the presence of stable single domain grains. Nanometric and 0.2 to 7 m grain size magnetite particles require a magnetic field up to 152 mT to reach saturation during the isothermal remanent magnetization experiment. Coercivity of magnetite increase when the grain size decreases probably due to coupling effects. The magnetic susceptibility vs. temperature curves show that reversibility is due to magnetite nanoparticles.

Keywords: magnetite nanoparticles, grain size, magnetic properties



(S) - IASPEI - International Association of Seismology and Physics of the Earth's Interior

JSS001

Poster presentation

1727

Halite fluid inclusion geochemistry of evaporite deposits in central iran

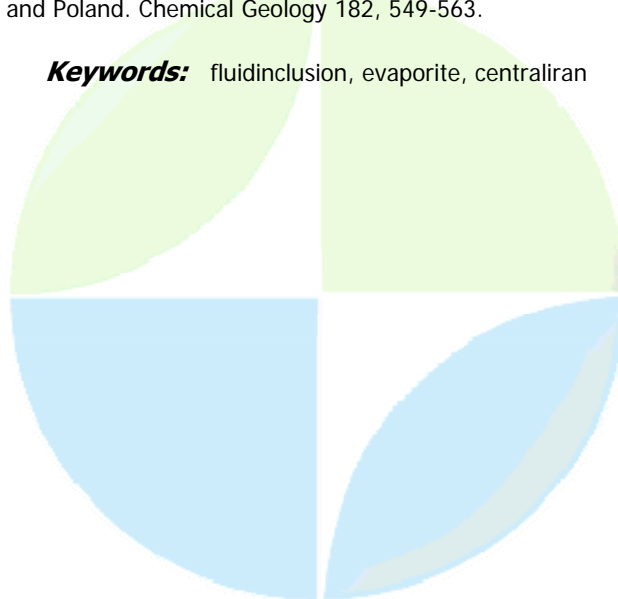
Mrs. Zeinab Shariatinia

GEOLOGY-SEDIMENTOLOGY SCHOOL of Geology-University of Tehran Tehran14155 IASPEI

Cendon Dioni I, Pueyo Juan Jose, Rahimpour- Bonab Hussain, Hezarhani Ardeshir

The chemical analyses of major ions in primary halite fluid inclusions is widely used for the determination and characterization of brine chemistry and its evolution in ancient evaporite basins through the Phanerozoic (eg. AYORA et al., 2001; BRENNAN and LOWENSTEIN, 2002; HORITA et al., 2002; KOVALEVICH et al., 2002). The purpose of this study is to show the major ion compositional evolution and halite crystallization pathway in the Miocene, M1 member of the Upper Red Fm. (N, Great Kavir Basin, Iran). We show how the Rift setting of the Great Kavir Basin, exerted the main control on the modification of seawater major ion chemistry. Influx of Ca-Cl₂ brines modified the earlier evaporated seawater into Ca- Mg- Na- Cl brines. In this case, the Ca²⁺ concentration of the evolving brine exceeded overall concentrations of SO₄²⁻, HCO₃⁻, and CO₃²⁻ ions, which is expressed as $mCa^{2+} > \sum(mSO_4^{2-} + mHCO_3^- + mCO_3^{2-})$. From this modified brine MgSO₄-poor potash salts (mainly halite, sylvite and carnallite) precipitated. The study of major ion variation for evaporite deposits in the mentioned area reveals that the evaporation path in the Great Kavir Basin was not the same as present-day seawater. The geochemical diagrams (e.g. Mg vs. SO₄ and K) show that major ions followed different evolution trends. Seemingly, an externally Ca-Cl₂ influx would have overridden the chemical signature of evaporated seawater within Great Kavir Basin. As a result, sylvite instead of K-Mg-sulfates precipitated, similar to that observed in other rift settings such as the Danakil Depression (Ethiopia) in Quaternary evaporates where secular seawater compositional changes can not justified the observed lithologies. Ayora C., Cendon D. I., Taberner C., and Pueyo J. J. (2001) Brine-mineral reactions in evaporite basins: Implications for the composition of ancient oceans. *Geology* 29(3), 251-254. Brennan S. T. and Lowenstein T. K. (2002) The major-ion composition of Silurian seawater. *Geochimica et Cosmochimica Acta* 66(15), 2683-2700. Horita J., Zimmermann H., and Holland H. D. (2002) Chemical evolution of seawater during the Phanerozoic: Implications from the record of marine evaporites. *Geochimica et Cosmochimica Acta* 66(21), 3733-3756. Kovalevich V. M., Peryt T. M., Beer W., Geluk M., and Halas S. (2002) Geochemistry of Early Triassic seawater as indicated by study of Rt halite in the Netherlands, Germany and Poland. *Chemical Geology* 182, 549-563.

Keywords: fluidinclusion, evaporite, centraliran



(S) - IASPEI - *International Association of Seismology and Physics of the Earth's Interior*

JSS001

Poster presentation

1728

Effect of mineral content of granitoids of the ukrainian shield on the change of their elastic parameters in different thermobaric conditions of the lithosphere (by experimental data)

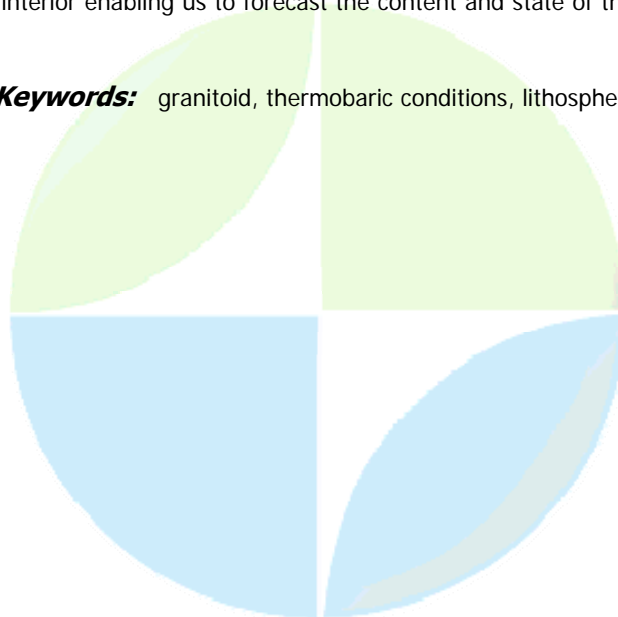
Mrs. Elena Karnaukhova

Physical Properties of the Earth's substance S.I.Subbotin Inst. of Geophysics of NASU IASPEI

Korchin Valery

On an example of optimal sampling of the Ukrainian Shield (USh) granitoids whose main rock-forming minerals are quartz, plagioclase, potassium feldspar, biotite, some dependences of their elastic parameters on the mineral content at pressures and temperatures are shown. The increasing amount of quartz in the rock decreases the change of the elastic velocities by pressure, while the growth of the plagioclase content of biotite increases them. The growth of the potassium feldspar content first increases and then decreases the velocity change. For the Ukrainian Shield rocks the elastic velocity of longitudinal polarization (V_p) values increase abruptly in the programmed PT regimes of the experiments at depths of 0-7 km. After reaching a definite limit, they begin to decrease nearly to the depth of 7-15 km and then increase again. Thus, on the curves of the depth distribution of velocity, inversion zones are distinguished which change their width with depth (ΔH) and diminish the velocity maximally (ΔV_p). The existence of these zones is due to the essentially opposite effect of pressures and temperatures (corresponding with definite depths) on the rocks. To solve the problem set the method of the multidimensional correlation-regression analysis was used together with the explosion seismology data. It was shown that different-gradient change of the velocity with depth sometimes corresponds with a definite change of the mineral content of the rocks the main effect being exerted by the regional deep pressures and temperatures. Only with notable change of V_p with depth appreciable mineral content change may be expected. E.g., if the velocity inversion zones show $\Delta V_p > 0,3 \text{ km} \cdot \text{s}^{-1}$ the mineral content change should also be suggested. In this case the rocks should first of all be enriched with quartz, while the intensive velocity growth seen after the inversion zone immediately (above 16 km) may be due to the increased plagioclase and pyroxene content of the rocks, the quartz content being decreased. The obtained experimental data of a broad spectrum of rocks are used for petrographic modeling of the Earth interior enabling us to forecast the content and state of the mineral matter of the lithosphere.

Keywords: granitoid, thermobaric conditions, lithosphere



(S) - IASPEI - *International Association of Seismology and Physics of the Earth's Interior*

JSS001

Poster presentation

1729

Reconstruction of the complicated stress state of a massif using data of elastic anisotropy as well as structural and textural measures of rocks

Dr. Valery Korchin

Physical Properties of the Earth's substance S.I.Subbotin Inst. of Geophysics of NASU IASPEI

Burtny Peter, Karnaukhova Elena

The crystalline rocks usually form textures by irreversible changes of mineral matter under the effect of stress fields, temperature and different geochemical processes. The rocks may "flow" at definite PT-parameters in the deformation process and form here with structures with linear, planar and linear-planar orientation of crystals, grains, detests. The structural and textural characteristics of rocks are closely related with elastic anisotropy. According to the character of the anisotropy of the physical parameters of the textured media, the latter may be differentiated by the classes of symmetry associated with the history of their formation and by the symmetry of the external effects. After having defined the elastic symmetry of rock it is not difficult to recover the directions of the fields of the external effects. But the difficulty of these studies consists in distinguishing the causes of the initial anisotropy of rocks and the inhomogeneity of the change of their elastic parameters in different directions caused by non-structural features. These problems can be solved by combined studies of elastic-anisotropic properties of mineral matter in different thermodynamic conditions. Vp was measured in 9 oriented polyhedrons of rocks and that Vs in 18 directions under hydrostatic pressure and the programmed PT-conditions corresponding with rock sampling sites. The elastic anisotropy and the structural and textural features of samples of a core of rocks of the Krivoy Rog ultradeep borehole from zones of destruction and non-destroyed areas will studied. The effect of paleotectonic and technological stress in rocks on their destruction in boring is founded. The studies show that in their geologic evolution the rocks (plagiogranites) formed textured structures with clear-cut elastic-anisotropic characteristics typical of transversely isotropic media. Then, under the effect of recent tectonic processes characteristic of synclinea, structural transformations of the rock occur that are detected by petrographic studies as secondary changes of the initial structure or texture and are marked by elastic anisotropy distortions. The character of the elastic anisotropy of the borehole rocks at different pressures and temperatures indicates the orientation of the action of tectonic forces not compensated by lithostatic pressure. Most probable is the orientation of the relaxation of these forces at an angle of 45 to the borehole shaft. They produce the maximal destructive effect in plagiogranites when their layering is oriented along the core generant (vertical dip of layering), while the stress is mainly relaxed in the stratification plane caused by the microcrack orientation and micropore localization under the effect of recent tectonic stress and movement. In the crushing zone, the rocks most probably experience the effect of tensile stress (unlike the overlying layers) due to under thrust, which also favour the borehole shaft destruction during discovering of these horizons by boring.

Keywords: high pressure and temperature, anisotropy

(S) - IASPEI - *International Association of Seismology and Physics of the Earth's Interior*

JSS001

Poster presentation

1730

Analysis of P-V-T relationship and melting of the pyrope mineral

Dr. Kripa Shanker Singh

physics R.B.S.COLLEGE,AGRA,INDIA(AFFL.-DR.B.R.A. UNIV.) IASPEI

ABSTRACT The melting behaviour of any solid under extreme conditions has attracted the attention of theoretical and experimental workers [Wang et al, Journal of alloys and Compounds 31 (2001) 51]. Knowledge of the volume properties of minerals at simultaneously high temperatures and pressures is needed for quantitative understanding of the Earth's deep interior [Fiquet et.al, Phys. Chem. Minerals 27 (1999) 103]. Pyrope ($Mg_3Al_2Si_3O_{12}$) is an important geophysical mineral present in Earth's interior. Thermoelastic and physical properties of this mineral are of considerable interest and importance to both material scientists and geophysicists alike. Thermoelastic and thermodynamic properties including bulk modulus and its variation with temperature and pressure, and melting of this mineral are of central importance for understanding the behaviour at temperature and pressure conditions relevant to Earth's interior [O.L. Anderson, Equations of State of Solids for Geophysics and Ceramic Sciences, Shanker et.al, Physica B 245 (2001) 190]. Studies on melting assume significance in view of the fact that it covers the widest range of pressures and temperatures [Wang et al, Physica B 293 (2001) 408]. The pressure-volume-temperature relationship have been studied for the pyrope mineral. Values of volumes at simultaneously elevated temperatures and pressures have been evaluated using the Rydberg - Vinet [Phys. Rev. B 35 (1987)] 1945, J.Phys.Condens. Matter 1 (1989) 1941] equation of state for isothermal compression and the Singh - Suzuki [Singh, High Temp. - High Pressure 34 (2002) 379] equation for isobaric thermal expansion. Values of volumes at melting temperatures corresponding to elevated pressures have been obtained and found to compare well with the experimental values.

Keywords: pyrope mineral, melting, equation of state



(S) - IASPEI - *International Association of Seismology and Physics of the Earth's Interior*

JSS001

Poster presentation

1731

Comparison between different microscopic properties of a 2D lattice on its macroscopic behaviours

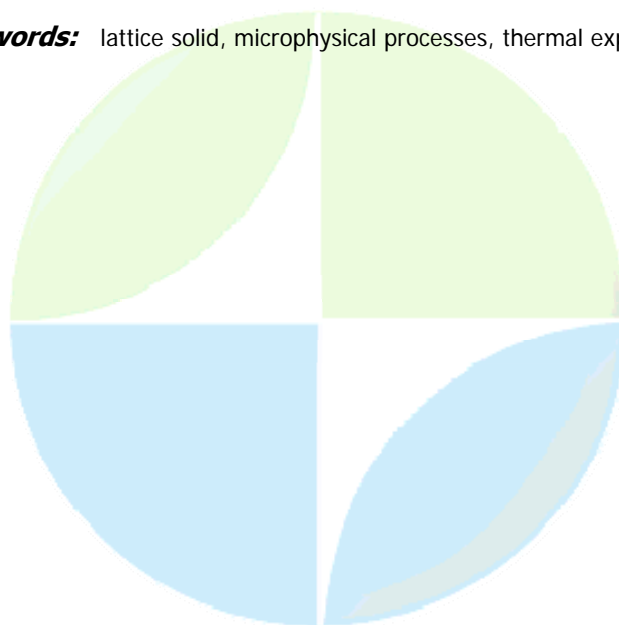
Dr. Shayesteh Mehrabian

EARTH PHYSICS INSTITUTE OF GEOPHYSICS, UNIVERSITY OF TEHRAN IASPEI

Ahmad Amini

A set of 2D numerical biaxial compression experiments has been performed to illustrate simulation of fracturing behavior using the random lattice. Unlike laboratory experiments and field studies, numerical experiments allow all quantities to be measured at any scale resolved by the model. With advances in numerical simulation methodology and High Performance Computing, they provide a means to study the processes underlying earthquake phenomena, emergent behavior such as space-time patterns for long seismicity sequences or localization phenomena, and the impact of different potentially important microphysics on fault behavior. Numerical experiments of biaxial compression using a random lattice illustrate that the new approach is capable of simulating typical rock fracture behavior using only simple radial interactions between particles. This 2D lattice solid model (LSM) is a particle-based numerical model that was developed to simulate the nonlinear dynamics of earthquakes. Occurrence of many microphysical processes can strongly affect the macroscopic behavior of the faulting processes but in previous works only few of them (such as friction) have been considered in the numerical experiments. Using simple particle interaction, the model can be calibrated with laboratory experiments of rock fracture. However, not all macroscopic parameters can be matched with laboratory results so more complex particle interactions may be required. In this study, thermal expansion and pore fluid pressure which affect the macroscopic behavior of rocks are incorporated in the model. With the capability of easily adding new features in the model such as rotational dynamics, microscopic breakage through bending, fluid and thermal effects, the model can be more easily calibrated against laboratory observations and provides a means to simulate complex phenomena such as localization processes, and to study the dynamics of complex systems such as fault zones. With the ability to add new microphysics, the model is presently capable of simulating physical processes such as friction, fracture, granular dynamics and thermal effects including thermo-mechanical and thermo-porous feedback.

Keywords: lattice solid, microphysical processes, thermal expansion



(S) - IASPEI - *International Association of Seismology and Physics of the Earth's Interior*

JSS002

1732 - 1844

Symposium

Tsunami: generation and hazard

Convener : Dr. Kenji Satake, Dr. Gerassimos Papadopoulos

Co-Convener : Prof. Efim Pelinovsky, Mrs. Paula Dunbar, Prof. Fumihiko Imamura

The 2004 Indian Ocean tsunami, the worst tsunami disaster in history, had a significant impact on tsunami research, warning and hazard mitigation systems. To fully document the 2004 tsunami, IUGG Tsunami Commission formed working groups to collect and compile field survey data, instrumental sea level data and satellite data. Regional tsunami watch systems are being set up in basins and oceans in the world with a guidance of UNESCO IOC. Tsunami hazard maps are implemented in many coastal communities world-wide using the state-of-the-art numerical modeling techniques. Probabilistic tsunami hazard assessments have been introduced in many coastal areas in the world. This joint session offers forums for information exchange and discussion on such developments of tsunami research, particularly after the 2004 Indian Ocean tsunami, as well as case studies of recent tsunamis. A part of this session will be carried out as Workshop on Wave and water level data assessment and product development for Tsunamis. Following the 2004 Indian Ocean Tsunami, the need for assessing the availability, quality, access tools, archive, and analysis techniques of current and historic wave and water-level data for tsunami event analysis became apparent. The objective of this workshop is to establish standard procedures for data assessment and data archive for tsunami event analysis. The lessons learned from this workshop and subsequent re-analysis of the data could apply to other extreme water level events.

XXIV2007

PERUGIA
I T A L Y



(S) - IASPEI - *International Association of Seismology and Physics of the Earth's Interior*

JSS002

Oral Presentation

1732

Planning For Tsunami And Natural Disaster Mitigation - Issues On Ecological And Social Risk: Lessons from South Asian Tsunami

Dr. Lalit Chaudhari
Research ISDR IAHS

Dr.A.G.Bhole, Dr.R.C.Bhattachajee, Prof.N.K.Gupta, Mr.Vijay Singhal

South Asia is more vulnerable to Geo disasters and impacts of climate changes in recent years. On 26 December 2004 massive waves triggered by an earthquake surged into coastal communities in Asia and East Africa with devastating force. Hitting Indonesia, Sri Lanka, Thailand and India hardest, the deadly waves swept more than 200 000 people to their deaths. Also in an another extreme climate change phenomenon during last week of July 2005 , causing heavy rains and flooding situation in the Mumbai ,and state of Maharashtra .More than 20 million population in the Mumbai metro region alone and 50 million all over the state are witnessing the social- economical and ecological risks and impacts due to climate changes . The economic losses to coastal ecosystem, agriculture, irrigation, aquaculture, drinking water resources, coastal industries and infrastructure are very high due to extreme geo-disasters that are linked with environmental and climate changes .The ecosystem, economic system, agriculture and aquaculture system in this region are severely affected and need systematic rehabilitation. Also mitigating the geo-disasters, marine hazards and rehabilitation during post tsunami period , scientific knowledge is needed, requiring experienced research communities who can train the local population during tsunami rehabilitation. ISDR,AVCCE, India and CGSI jointly started the initiatives on the problem identifications in management of risks in geo-disasters, tsunami rehabilitation etc., to investigate problems related to social-economic and ecological risks and management issues resulting from the December tsunami and Geo- disaster, to aid mitigation planning in affected areas and to educate scientists and local populations to form a basis for sustainable solutions. This presentation reviews the status and issues of Geo-risks, marine risks along Indian coast focusing on technical issues, problems and damage arising from the extreme floods, tsunami in agriculture, aquaculture, irrigation, drinking water, coastal infrastructure, coastal ecosystems and coastal economic systems. This study signifies that climate changes and risk management ,Geo disasters and Tsunami education is needed for mitigating potential Geo-marine risks in this region for capacity building for climate changes and rehabilitation issues based on local resources. The paper will also explore the issues concerned with achieving environmental, social and economic sustainability through corporate strategies and innovative geosciences information delivery and Tsunami education for the affected communities. The paper also discusses role of information technology and its application for marine hazards; risk management and sustainability aspects that deal with coastal resources development, management and Tsunami disaster management planning.

Keywords: tsunami, marinerisk, geo disaster andtsunami

(S) - IASPEI - *International Association of Seismology and Physics of the Earth's Interior*

JSS002

Oral Presentation

1733

A Tsunami Detection and Warning-focused Tide Station Metadata Web Service

Dr. John Marra

NOAA NESDIS NCDC IDEA Center

Uday S. Kari, Stuart A. Weinstein

The Indian Ocean Tsunami of 26 December 2004 made it clear that information about tide stations that could be used to support detection and warning (such as location, collection and transmission capabilities, operator identification, etc.) are insufficiently known or not readily accessible. Parties interested in addressing this problem united under the U.S. National Oceanic and Atmospheric Administration (NOAA) NESDIS/NCDC/IDEA Centers PRIDE program and in 2005 began an effort to develop a distributed metadata system describing tide stations starting with pilot activities in a regional framework and focusing on tsunami detection and warning systems being developed by various agencies.* A summary of discussions and concepts related to this effort is described in the UNESCO document IOC/INF-1226 of April 2006. This paper describes progress to date in this PRIDE-sponsored effort. Specifically, it describes the components of a pilot tide station metadata web service, including an XML-based schema that exposes, at a minimum, information in the NOAA National Weather Service (NWS) Pacific Tsunami Warning Center (PTWC) station database needed to use the PTWCs Tide Tool application. The schema includes as optional elements, information recommended in the IOTWS/WG2 Message Formats Content document generated at the ICG/PTWS-XXI meeting held in Melbourne Australia on May 3-5 2006. This paper also describes a web-enabled client application that harvests information from the web service and displays it via a graphical user interface that supports GIS-based queries. Where available from the source, real time tide-station data can be accessed and viewed via this application. Going beyond exposing and harvesting tide station metadata, a tsunami bulletin schema based on PTWC Operations (Watchstander) manual and legacy business processes (specifically, PACBUL) has also been developed as part of this effort. In this regard, an XML bulletin generator has been prototyped and deployed on a test platform. Development of the type of distributed tide station web service focused on tsunami detection and warning systems described here will also contribute to other marine hazard warning systems (such as storm surges), as well as sea level change monitoring and research. * National Environmental Satellite Data and Information Service (NESDIS), National Climatic Data Center (NCDC), Integrated Data and Environmental Applications (IDEA) Center, Pacific Region Integrated Data Enterprise (PRIDE).

Keywords: tsunami, tidestations, service orientedarchitecture

(S) - IASPEI - *International Association of Seismology and Physics of the Earth's Interior*

JSS002

Oral Presentation

1734

Geological recognition of tsunami and storm deposits in two coastal areas of Portugal

Mr. Pedro J M Costa

Earthquake Engineering and Seismology Division, IC IST Technical University of Lisbon

Suzanne A. G. Leroy

Abrupt marine invasions such as tsunamis and storms are particularly devastating for coastal areas. They may also leave a permanent record in sedimentary deposits. In historical times the most destructive tsunami that affected Europe was the Lisbon AD 1755. The effects and consequences of the AD 1755 tsunami are presented. Sedimentological criteria to identify abrupt marine invasions in the stratigraphic column are discussed. This work aims to contribute to a better understanding of the signature left by abrupt marine invasions in coastal stratigraphy by investigating the nature of the sedimentary record associated with tsunamis in a region of their known impact. A wide range of proxies was used to detect tsunami and storm deposits in two coastal areas of Portugal. The techniques used include stratigraphic description, grain size analysis, digital and x-ray photography, magnetic susceptibility, macrofossils analysis, geochemical analysis and ^{210}Pb and Optically Stimulated Luminescence dating. The investigated areas (e.g. Lagoa de bidos (Central Portugal) and Martinhal (South Portugal)) were affected by the AD 1755 tsunami. The locations have similar geomorphological features and are both susceptible to major abrupt marine invasions. Results show that an abrupt event deposited unique sedimentary units in both locations. A similar age for the event was established. A considerable number of tsunami sedimentary characteristics were detected in both units. Moreover, other abrupt marine invasions were detected in the lithostratigraphy of the study areas. However, a key outcome of this research is the demonstration of the difficulty of distinguishing between sedimentary deposits laid down by tsunamis, and those deposits resulting from storm action; consequently the geological record of tsunamis almost certainly underestimates their frequency.

Keywords: tsunami, storms, portugal



(S) - IASPEI - *International Association of Seismology and Physics of the Earth's Interior*

JSS002

Oral Presentation

1735

Kuril Islands Tsunami of november 15, 2006. (Examination of Tsunami enhancement at crescent city, California)

Dr. Juan Horrillo

JSS42 Historical and contemporary observations IAPSO

Zygmunt Kowalik, Williams Knight

Application of global tsunami propagation models to the Indian Ocean Tsunami of December 2004 and to the Kuril Islands Tsunami of November 2006 shows the importance of tsunami modifications through secondary source generation at ridges, seamounts and passages between islands or continents. Tsunami modification depends on the strength of these secondary sources, which in turn depend on tsunami interactions with these prominent bathymetric features. Interactions between wave fronts derived from primary and secondary sources lead to difficulties in arrival time prediction for the largest amplitude portion of the tsunami. These interactions make it apparent that improvements in both the modeling techniques and the physics described in numerical models must be supported by high resolution bathymetry. A numerical model for global tsunami propagation with spatial resolution of one minute was applied to the Kuril Islands Tsunami of November 15, 2006. As the computational domain is resolved with over 100 million grid points, the application was parallelized and run on a supercomputer. Numerical results were compared to sea level data collected by Pacific DART buoys and tide gauges along the U.S. West Coast. Numerical results were found to be highly sensitive to the spatial resolution applied to these prominent bathymetric features. The high resolution model is applied to explain the origin of the large-amplitude portion of the tsunami at Crescent City, California, which arrived roughly two hours after the initial wave.

Keywords: tsunami, kuril, 2006



(S) - IASPEI - *International Association of Seismology and Physics of the Earth's Interior*

JSS002

Oral Presentation

1736

A Comparison Study of Two Numerical Tsunami Forecasting Systems

Dr. Diana Greenslade

Bureau of Meteorology Research Centre Australian Bureau of Meteorology IASPEI

Vasily Titov

Recent tsunami events, e.g. Sumatra 2004 and Java 2006 have demonstrated the need for providing accurate and timely tsunami warnings. Improvements in the availability of sea-level observations and advances in numerical modelling techniques are increasing the potential for tsunami warnings to be based on numerical model forecasts. Numerical tsunami propagation and inundation models are well developed, but they present a challenge to run in real-time; partly due to computational limitations and also due to lack of detailed knowledge on the earthquake rupture details. For these reasons, current tsunami forecast systems are based on pre-computed tsunami scenarios. A tsunami scenario is a single tsunami model run that is calculated ahead of time with the initial conditions carefully selected so that they are likely to represent an actual tsunamigenic earthquake. This paper will present a comparison of two tsunami scenario databases: the NOAA/PMEL system, currently being implemented at NOAA Tsunami Warning Centers and the Bureau of Meteorology system, which is being developed for the Australian Tsunami Warning System. Both scenario databases are based on the MOST numerical model, but there are some differences in the way the scenarios are constructed. The databases will be described, and a comparison of results for the Tonga event (May 3, 2006) will be presented. The tsunami forecasts will be compared to each other and to available observations, including those from two DART buoys located near Hawaii.

Keywords: tsunami, forecast, modelling



(S) - IASPEI - International Association of Seismology and Physics of the Earth's Interior

JSS002

Oral Presentation

1737

Geology and archaeology evidence of megatsunami impact in Easter Island from tsunamigenic tectonic event in Southern Chile: May 22, 1960 (M 9.5) and December 16, 1575 (M 8.5) Earthquakes

Prof. Oscar Gonzalez-Ferran

GEOLOGY AND GEOPHYSIC UNIVERSITY OF CHILE IAVCEI

Cortez Carolina, E .Lorca, E .Zarate, R Mazzuoli, S .Rapu

Easter Island (2709S / 10926W) one of the most isolated land in the Earth at the southeastern Pacific Ocean, famous for the giant megalithic monument of the Rapa Nui culture, building during the century XIII XVII, declared by UNESCO as a World Heritage Site since 1995, had been the most important and the best elements for register and preservation some geophysical hazard in the past, as earthquakes, tsunamis and landslide. Into the archaeological ruins, we have been recognise two main groups of Ahus: the oldest semipiramidal which represent to hoard up ruins; and the youngest ahu-moai, the biggest and mainly collapsed by earthquakes. The Island is entirely compound by young volcanic rocks, characterized by a rough triangular shape with 160 Km², represent the small emerged portion of the large submarine volcanic complex, that rise from about 3000 m. over the oceanic Nazca plate. Geological and geophysics hazard research along the coast perimeter of the island, which is characterized by the high cliff at the three volcanic corner, and about 70% flat and broadly beaches of basaltic lava flows without sand, where are developed a sequence of small rocky pocket beaches, inlets and boulder-blocky-pebbles in the marine abrasion zone, which are quite narrow. On this coast line, where set up about 90% the biggest megalithic monuments. We discover the enormous impacts caused by the big mega tsunamis occurred in May 1960 and December 1575, not only for the geological evidences as a great amount of marine detritus deposit run up along the southeastern coast and strong erosion of the Poike volcano cliff, also for the huge catastrophic impact to archaeological ruins of AHU MOAI by the 1960, and double impact to the AHU SEMIPIRAMIDAL by the 1575 and 1960 tsunamis. The measure the inundation areas, the variation of the high wave, where maximum was estimated about 30 m. high near the Poike cliff-Tongariki valley and 10 to 15m. toward southwest and the run up characteristics deposits variables between few meters and near one kilometre in land and also remove big moai which weight more than 40 ton.. and many basaltic block more than 6 ton, for hundred meters in land. These research had give an important information about the magnitude of these two mega tsunamigenic impact in the Easter Island, located about 4500 kms. north west from the earthquakes epicentre at the subduction zone in southern Chile. We present here six sections: Tongariki; Hanga Maihiku; Hanga Tetenga; Akahanga-Ura uranga Te Mahina; Koe-Koe and Hanga Poukura-Hanga Tee. Five of them were lucky not have been remove by archaeologist and conserved unaltered the tsunamis and earthquakes evidences through time, complemented with photographic documentation before and after the events. On the base these information we present the Tsunami Hazard Chart for Easter Island, which also is correlated with the tsunami numerical modelling techniques from distance.

Keywords: easter island, megatsunami archaeotsunami, field survey data hazard map

(S) - IASPEI - *International Association of Seismology and Physics of the Earth's Interior*

JSS002

Oral Presentation

1738

Progress in Tsunami Forecasting

Dr. Eddie Bernard

*National Oceanic and Atmospheric Administration Pacific Marine Environmental Laboratory
IAPSO*

Vasily Titov

The strengthening of the U.S. tsunami hazard mitigation program has led to many improvements in tsunami detection, forecasting, and mitigation activities. Progress on tsunami forecasting will be the focus of this presentation. Examples of experimental forecast products (tsunami amplitude over time forecasts) from the March 2006 Tonga, the November 15, 2006 Kurile, and the January 12, 2007 Kurile tsunamis will be presented to illustrate the capability of the forecasting methodology. The forecast products will be compared with tide data to quantify the accuracy of the forecast technology.

Keywords: tsunami, forecast

XXIV2007

PERUGIA
ITALY



(S) - IASPEI - *International Association of Seismology and Physics of the Earth's Interior*

JSS002

Oral Presentation

1739

Tsunami associated with the Mw 7.1 earthquake over Luzon Strait on 26 December 2006

Dr. Wing Tak Wong

Geophysics, Time and Port Meteorological Services Hong Kong Observatory IASPEI

Kin-Wai Li, Mr Wang-Chun Woo

At 20:26 Hong Kong Time on 26 December 2006, an earthquake of moment magnitude Mw 7.1 (Ms 7.2) occurred over the Luzon Strait near Taiwan Island. The earthquake wreaked havoc in Hengchun, Taiwan and damaged many submarine telecommunication fibre cables in the Luzon Strait which connected Hong Kong to overseas. At a distance of more than 600 kilometres from the epicentre, many residents in Hong Kong felt the earth tremor. Based on reports from local residents, the intensity at Hong Kong was III to IV on the Modified Mercalli Intensity Scale. The peak ground acceleration measured by strong motion accelerographs at Hong Kong was 0.003 to 0.004 g. After the occurrence of the earthquake, the Hong Kong Observatory issued a Tsunami Information Bulletin, the first of its kind, to advise the people of Hong Kong that the earthquake might have generated a tsunami but the tsunami height at Hong Kong would not be significant. At Tai Miu Wan tide gauge station in the eastern part of Hong Kong, a train of tsunami waves was recorded shortly after midnight. The crest of the first wave arrived around 00:10 on 27 December, with an amplitude of about 11 cm crest-to-trough. The wave recurred with lesser amplitudes at intervals of about 10 to 20 minutes for 2 to 3 hours. A post-analysis using a numerical tsunami model based on high resolution bathymetry and topography predicted an arrival time and amplitude commensurate with the tidal records. The event provided useful data for verification of the numerical model which could be used to support future tsunami forecasting in Hong Kong.

Keywords: tsunami, luzon strait, numerical model



(S) - IASPEI - *International Association of Seismology and Physics of the Earth's Interior*

JSS002

Oral Presentation

1740

Numerical Simulations of the 2004 Indian Ocean Tsunamis: Coastal Effects

Prof. Philip Liu

School of Civil and Environmental Engineering Cornell University IASPEI

Xiaoming Wang

The 2004 Sumatra earthquake and the associated tsunamis are one of the most devastating natural disasters in the last century. The tsunamis flooded a huge coastal area in the surrounding countries, especially in Indonesia, Thailand and Sri Lanka, and caused enormous loss of human lives and properties. In this paper, tsunami inundations in Trincomalee, Sri Lanka and North Banda Aceh, Indonesia were simulated by using a finite difference model based on the shallow-water equations. The calculated tsunami heights and inundations in these two regions are compared with the field measurements and observations. Fairly good agreement is observed. Numerical results confirm again that the local bathymetric and topographic characteristics play important roles in determining the inundation area. Numerical simulations further indicate that although nonlinearity becomes important in many dynamic aspects when tsunamis approach the shore, its influence on determining the inundation area is relatively small in the regions examined for this tsunami event. Finally, the potential capability of sediment transport and a force index on a virtual structure in flooded areas are introduced and discussed.

Keywords: tsunami, inundation, sediment

PERUGIA
ITALY



(S) - IASPEI - *International Association of Seismology and Physics of the Earth's Interior*

JSS002

Oral Presentation

1741

Short-term Inundation Forecasting for Tsunamis in the Caribbean Sea Region

Prof. Aurelio Mercado-Irizarry

Department of Marine Sciences University of Puerto Rico IAPSO

Wilford Schmidt

After the 2004 Indian Ocean tsunami, the USA Congress gave a mandate to the National Oceanographic and Atmospheric Administration (NOAA) to assess the tsunami threat for all USA interests, and adapt to them the Short-term Inundation Forecasting for Tsunamis (SIFT) methodology first developed for the USA Pacific seaboard states. This methodology would be used with the DART buoys deployed in the Atlantic Ocean and Caribbean Sea. The first step involved the evaluation and characterization of the major tsunamigenic regions in both regions, work done by the US Geological Survey (USGS). This was followed by the modeling of the generation and propagation of tsunamis due to unit slip tsunamigenic earthquakes located at different locations along the tsunamigenic zones identified by the USGS. These pre-computed results are stored and are used as sources (in an inverse modeling approach using the DART buoys) for so-called Standby Inundation Models (SIMs) being developed for selected coastal cities in Puerto Rico, the US Virgin Islands, and others along the Atlantic seaboard of the USA. It is the purpose of this presentation to describe the work being carried out in the Caribbean Sea region, where two SIM's for Puerto Rico have already being prepared, allowing for near real-time assessment (less than 10 minutes after detection by the DART buoys) of the expected tsunami impact for two major coastal cities.

Keywords: tsunamis, caribbean, modeling



(S) - IASPEI - *International Association of Seismology and Physics of the Earth's Interior*

JSS002

Oral Presentation

1742

Experiments and an improvement of model on the inundated flow with floating bodies

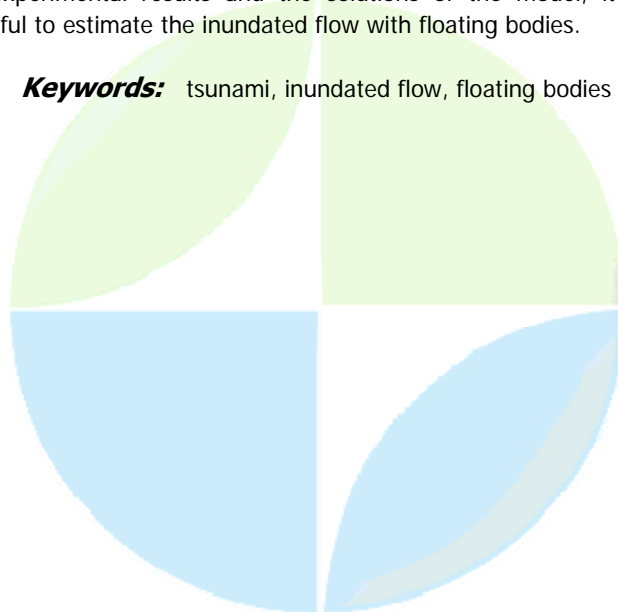
Prof. Hideo Matsutomi

Department of Civil and Environmental Engineering Akita University IASPEI

Takeshi Yamaguchi, Midori Fujii

Inundated flow with floating bodies such as debris, driftwood, cars, bikes and so on was witnessed and videotaped in Banda Aceh at the time of the 2004 Indian Ocean Tsunami, and attracted a great deal of public attention, as did the collision force of such floating bodies. In light of the circumstances, a model to estimate such a flow was presented by the authors in 2005. However, it was confirmed that the model could only be applied to the flow with fluid like oil or the flow with a small amount of solid floating bodies in which their effect as a resistance body to the flow was small (Matsutomi et al. 2006). This study aims to improve the model for estimating the moving velocity of floating bodies, i.e., current velocity of inundated flow with floating bodies in a steady state. The improved model adopts the notion of the conventional bore theory regarding the floating bodies as a hypothetical fluid with the same density as those in the downstream region of the bore, and takes account of the effect of resistance due to the floating bodies piling up at the surge front of inundated flow. Physical experiments are carried out to grasp the behavior of floating bodies at the surge front of inundated flow and to model the inundated flow more exactly. The experimental flume is 0.3m wide, 0.5m high and 11.0m long with a horizontal bed. Inundated flows are generated by rapidly pulling up a gate, installed 5.0m from the upstream end of the flume. Two ultrasonic wave gauges are installed at the distance of 3.5m and 5.5m from the gate respectively to measure the time series of surface elevation of the inundated flow. The state of the inundated flow is videotaped from the upper and the left sides of the flume to grasp the behavior of floating bodies, and to estimate the moving velocity u_2 and the void ratio e of floating bodies. The experimental conditions are that the initial water depth h_1 in the upstream region of the gate is three cases of 0.20, 0.25 and 0.30m, the initial void ratio is three cases of 0.4, 0.6 and 0.8, the dimensions of each floating body is three cases of 1.8x1.8x1.8cm (cube), 1.8x1.8x5.4cm and 1.8x1.8x10.8cm, and hemlock fir is adopted as the floating bodies. Through examinations and comparisons of the experimental results and the solutions of the model, it is concluded that the improved model is useful to estimate the inundated flow with floating bodies.

Keywords: tsunami, inundated flow, floating bodies



(S) - IASPEI - International Association of Seismology and Physics of the Earth's Interior

JSS002

Oral Presentation

1743

Tsunamigenic risk for North Atlantic shorelines

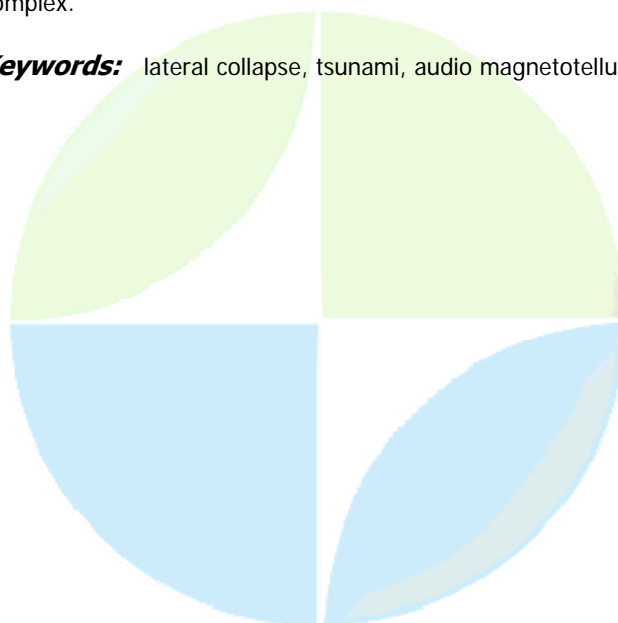
Mr. Nicolas Coppo

Institute of Geology and Hydrogeology University of Neuchtel - Switzerland IASPEI

Pierre-Andr Schnegg, Pierik Falco, Roberto Costa

Among the high-intensity on-Earth tsunami generating events, seismicity, submarine landslides, and volcano lateral collapses are the most important (Holcomb and Searle, 1991; Ward, 2001). Recent off shore bathymetry studies demonstrated the huge accumulation of debris flow deposits spreading over more than 100 km off the northern Tenerife (Canary Islands) coast line, inherited from past lateral collapses (Watts and Masson, 1995). Although mechanics and dynamics triggering such catastrophic events follow from combined complex processes (vertical caldera collapse, flank destabilization, hydrothermal pressurization, seismic events), potential movable volume is the unavoidable parameter to quantify and constrain the tsunamigenic area. In the same archipelago, mathematical modelling of the La Palma potential landslide concluded that high amplitude waves may cross all the Atlantic Ocean with harmful effects (Ward and Day, 2001) in few hours. However, because of often steep and inaccessible volcano flanks, the geological and geophysical ignorance of lateral flank structures may lead to wrong estimation of a potential movable volume. New geophysical results (audio-magnetotellurics recorded in the 0.001-1 s period range) provide for the first time a good estimation of the volume of the Icod Valley (Tenerife, Canary Islands) potential giant landslide threatening northern Atlantic Ocean shorelines. Two profiles image its electrically conductive roots with a characteristic U-shaped morphology thought to be the consequence of previous landslides. This conductive layer (20-70 m) corresponds to a plastic breccia within a clayish matrix reached in some galleries that perforate the volcanic edifice for water supply. It is overlaid by the recent resistive (200-2000 m) lavas from the Pico Teide Pico Viejo complex with up to 1000 m thickness in the middle of the Icod Valley. Around 15 km separate two high conductive bodies that delimit the lateral extension of the valley. Its length is estimated at 13 km. Considering that the top conductive layer might be the sliding surface of the potential Icod Valley lateral landslide, we show that northern Atlantic Ocean shorelines might be exposed to a destructive tsunami generated by a subaerial lateral collapse of at least 120 km³ during a future strong volcanic activity of the Teide-Pico Viejo complex.

Keywords: lateral collapse, tsunami, audio magnetotellurics



(S) - IASPEI - International Association of Seismology and Physics of the Earth's Interior

JSS002

Oral Presentation

1744

Analysis of tsunamis generated by two great Kurile earthquakes of 15 November 2006 and 13 January 2007

Prof. Yuichiro Tanioka

Institute of Seismology and Volcanology Associate Professor IASPEI

Yohei Hasegawa, Tatsuo Kuwayama

Two great earthquake, Mw 8.3 and 8.1, occurred off Simushir Island along the Kurile trench on November 15, 2006, and January 13, 2007, respectively. The 2006 earthquake was a typical underthrust event occurred along the plate interface between the Pacific plate and the Okhotsk plate. The 2007 earthquake was an intraplate event occurred in the outer-rise region with a normal fault type mechanism. Both earthquakes generated tsunamis which observed at the many tide gauges along the Pacific coast in Japan, Russia, and USA. Some damages were reported at Sanriku in Japan and at Crescent City in USA by the tsunami generated by the 2006 earthquake. No damages were reported for the 2007 earthquake. The tsunamis were first arrived at the tide gauges in Japan about 2-4 hours after the origin times of the earthquakes. The significant phenomenon of those tsunamis in Japan was large later phases observed about 7-10 hours after the origin times of the earthquakes. In this study, we first numerically computed two tsunamis, and compared the observed and computed tsunami waveforms to estimate the seismic moments of two earthquakes. We also try to discuss the generation mechanisms of the large later phases observed at tide gauges in the Japan. For the 2006 earthquake, eight tsunami waveforms observed at three tide gauges in Japan, Hanasaki, Miyako, and Chichijima, two tide gauges in Hawaii, Hilo and Kahului, and three tide gauges in the west coast of USA, Port Orford, Arena Cove, Port San Louis, were used to estimate the slip amount of the earthquake. The thrust type fault plane (strike 220 degree, dip 25 degree, rake 96 degree) which estimated by Yamanaka (http://www.eri.u-tokyo.ac.jp/sanchu/Seismo_Note/2006/EIC183.html) was used for the tsunami computation. The length and width of the fault model were 200km and 80km, respectively. For the 2007 earthquake, four tsunami waveforms observed at three tide gauges in Japan, Hanasaki, Miyako, and Chichijima, and one ocean bottom pressure sensor (DART system) installed by the NOAA-PMEL. The normal fault plane (strike 220 degree, dip 37 degree, rake -108 degree) which also estimated by Yamanaka (http://www.eri.u-tokyo.ac.jp/sanchu/Seismo_Note/2007/EIC184.html) was used for the tsunami computation. The length and width of the fault model were 130km and 30km, respectively. By comparing the observed and computed tsunami waveforms, we estimated the slip amounts of 5.1 m for the 2006 earthquake and 6.4 m for the 2007 earthquake. By assuming the rigidity of 4×10^{21} Nm/s², the seismic moment is calculated to be 3.3×10^{21} Nm (Mw8.3) for the 2006 earthquake and 1.0×10^{21} Nm (Mw8.0) for the 2007 earthquake. This estimated seismic moment is consistent with that shown in the Harvard CMT catalog, 3.37×10^{21} Nm (Mw8.3) for the 2006 earthquake and 1.65×10^{21} Nm (Mw8.1) for the 2007 earthquake. This implies that the excitations of seismic waves and tsunamis are consistent with each other. The preliminary analysis of the computed tsunami indicated that the large later phase observed in Japan can be caused by the scatter of the tsunami at the shallow region near Emperor Seamounts.

Keywords: tsunamis, kurile, earthquakes

(S) - IASPEI - International Association of Seismology and Physics of the Earth's Interior

JSS002

Oral Presentation

1745

Mega-tsunami of the world ocean: did they occur in the recent past?

Dr. Viacheslav Gusiakov

Department of Geophysics Inst. of Compl Mathematics and Math. Geophysics IASPEI

Abbott Dallas, Bryant Edward, Masse William

The comprehensive historical tsunami database collected at the Novosibirsk Tsunami Laboratory, contains data on more than 2250 historical events occurred in the World Ocean from 1628 BC to present. Even if the historical data set is obviously incomplete for many areas, especially for older times, the world catalog contains enough data to estimate an average run-up heights for the largest seismically-induced tsunamis resulted in wide-spread damage and large number of fatalities (1755 Lisbon, 1868 and 1877 Chile, 1952 Kamchatka, 1957 Aleutians, 1960 Chile, 1964 Alaska, 2005 Sumatra). This average run-up does not exceed 30-35 meters on the nearest coast with 10-12 meters at the distance more than 5000 km. Somewhat larger waves (up to 40-45 m) can be generated by volcanic explosions followed by volcanic cone collapse (Santorini 1628 BC, Kuwae 1453, Unzen 1792, Tambora 1815, Krakatau 1883). Landslide-generated tsunamis have the largest recorded heights (up to 525 m) but normally these events are very local with the width of inundated area from hundred meters to several kilometers (1958, 1936, 1853 Lituya Bay, 1936 Norway, 2000 Greenland). Meanwhile, many parts of the World Ocean coastline contain the prominent features of catastrophic impact of water currents and waves that came from the ocean. They are large boulders, weighing well above one hundred tons, lying on the top of vertical cliffs at the height up to 60 m and large vortexes cut-down in rather resistive coastal rocks. On a smaller scale, these features include sculptured bedrocks, grooves, canyons, cavettos and flutes, found in areas where hurricanes and severe tropical storms are not common. Sedimentational features of water impacts include mega-ripples found in the north-western Australia and so-called chevrons (parabolic and blade-like sand dunes) that are common along many parts of the Indian Ocean coast. In southern Madagascar, chevrons reach altitude of 205 m with 30-35 km in-land penetration. The high energy water flux of that scale could be generated by Storegga-class submarine landslides or Santorini-class volcanic explosions, but for this area does not have nearby active volcanoes or large sedimentation basins having potential for large-volume submarine sliding. Not widely acknowledged presently, but still real possibility is creating of these coastal features by catastrophic oceanic waves generated by deep-water impacts of large comets or asteroids. In the Indian Ocean, several crater candidates (Burckle, Mahuika, Kukla, Flinders) have been found recently by geomorphological analysis of detailed bathymetric maps They are geologically young and analysis of nearby deep-sea cores shows the presence of some elements and minerals typical for oceanic impact structures. The paper discusses the consistency of these data with spatial and azimuthal distribution of the large-scale erosional and sedimentational features found at the Australian and Madagascar coast.

Keywords: tsunami, run up, impacts

(S) - IASPEI - *International Association of Seismology and Physics of the Earth's Interior*

JSS002

Oral Presentation

1746

Destructive tsunami-like waves (meteotsunamis) at the Balearic Islands: observations and numerical modelling

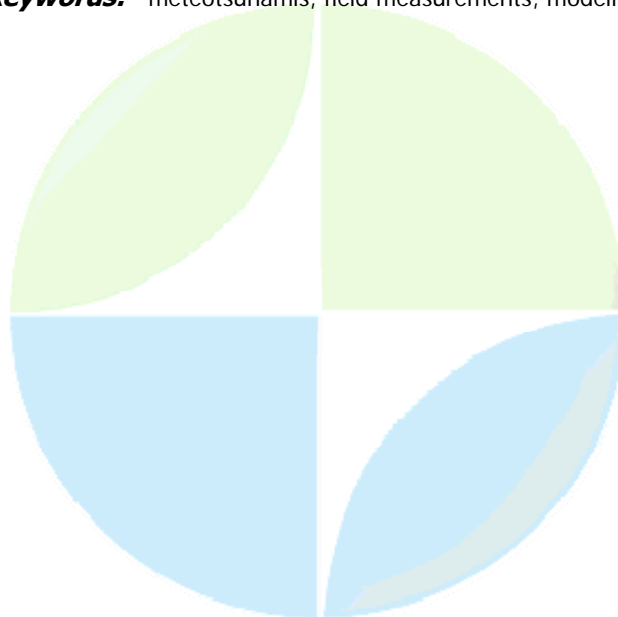
Dr. Ivica Vilibic

Physical Oceanography Laboratory Institute of Oceanography and Fisheries IAPSO

Sebastian Monserrat, Alexander B. Rabinovich, Hrvoje Mihanovic

In light of enhanced activity in the study of tsunamis and their source mechanisms, we consider tsunami-like destructive waves generated by atmospheric disturbances such as atmospheric waves, pressure jumps, frontal systems, and squalls. Such hazardous sea level oscillations (meteotsunamis) occur regularly in the region of the Balearic Islands (Western Mediterranean) where they are known as rissaga. Destructive rissagas with heights 2 m take place every 4-5 years. A recent devastating rissaga event occurred on 15 June 2006 in Ciutadella Harbour (Menorca Island) with reported wave heights greater than 4 m. More than 40 boats were damaged and the event caused an economic loss of several tens millions of euros. Unfortunately, there were no working tide gauges in the inlet or on the shelf during the event. However, we have been able to use previous observational data to formulate an efficient 2D numerical model of extreme long waves generated in this region. Specifically, we use data for the period 1989-1999 with focus on the comprehensive hydrophysical experiment LAST-97 undertaken in 1997 which included a triangle of precise microbarographs and eight bottom pressure gauges installed on the shelf and in bays/inlets of the Mallorca and Menorca islands. We re-examine these data to estimate magnitude, speed and direction of travelling atmospheric disturbances and associated generated long ocean waves. To understand the generation mechanism of meteotsunami waves, we also consider those cases for which strong atmospheric disturbances did not produce a noticeable sea level response. Parameters of the atmospheric disturbances are used as inputs to the numerical model. Simulated ocean waves are in good agreement with observation. The verified model is then used to simulate the 2006 event. Finally, the sea level measurements and numerical computations are used to assess general tsunami issues for the Balearic region which is also prone to tsunamis of seismic origin; a very recent and well-known example is the 2003 Algerian tsunami.

Keywords: meteotsunamis, field measurements, modelling



(S) - IASPEI - *International Association of Seismology and Physics of the Earth's Interior*

JSS002

Oral Presentation

1747

Possibility of tsunami source detection by using ocean radar

Dr. Tomoyuki Takahashi

Department of Civil and Environmental Engineering Akita University IASPEI

Shinpei Takahashi, Shoichiro Kojima

In the 2004 Indian Ocean tsunami, many people who don't know tsunamis were killed by the tsunami. It shows that disaster information is important to mitigate damage caused by tsunamis. To provide appropriate disaster information for the administrations and residents, a tsunami warning system is necessary. A reliability of the tsunami warning system depends largely on its capacity for detecting tsunamis. The present tsunami warning systems don't detect tsunami generation directly, but they try to do indirectly by using observed seismic waves. Unfortunately, the detection method may underestimate some kinds of tsunamis. Then, it is expected to carry out a new observation of the ocean surface directly, widely and two-dimensionally. To realize such a tsunami source monitoring, remote sensing is promising. The aim of our research is to develop the tsunami detection system by using remote sensing and to add the new system to the present tsunami warning system. In this study, we focus on an ocean radar as one of the remote sensing. The ocean radar has some advantages, such as a moderate price and easy maintenance, by comparison with other remote sensing systems, e.g. satellites. The present ocean radar, however, requires a certain time for analysis and needs large velocity on the ocean surface, because it uses doppler spectrum to analyze the ocean surface condition. It is difficult to detect tsunami source and its initial propagation in the deep region by the present analyzing method. Then, a new detection index is proposed in this study. It is sea surface disturbance in the tsunami source. We assume that an abrupt ocean bottom crustal deformation increases small waves in the sea surface and they cause heavy back scattering of electromagnetic wave transmitted by the radar. Hence the back scattering strength is used directly as the detection parameter to investigate the tsunami source. The ocean radars are established in Ishigaki Island and Yonaguni Island in Okinawa Prefecture, Japan. The analyzed radar data were recorded from April 1, 2004 to March 31, 2006. In this period, 46 earthquakes were occurred in the observed region and the significant three earthquakes (M6.5, M4.4 and M4.3) are selected for analysis. The back scattering strength is examined between 1 minute before and 2 minutes after their main shocks. Therefore, no particular transition of the back scattering strength is found for M4.4 and M4.3 earthquakes. On the other hand, for M6.5 earthquake, the back scattering strength became larger rapidly around its epicenter when the main shock occurred. The result, however, is not enough to confirm that the back scattering strength can reveal the sea surface disturbance, because the M6.5 earthquake is not large for tsunamigenic earthquakes. Then, larger sea surface disturbance due to Typhoon Matsa in 2005 are also analyzed. The typhoon had the minimum central atmospheric pressure of 950 hectopascals and the maximum wind velocity of over 40 m/s. Accordingly, it is confirmed that the back scattering strength became larger when it passed over the ocean radar observation region.

Keywords: sea surface disturbance, back scattering strength, tsunami warning system

(S) - IASPEI - *International Association of Seismology and Physics of the Earth's Interior*

JSS002

Oral Presentation

1748

**The 26 December 2004 Sumatra Tsunami in the Atlantic Ocean:
Observations and Analysis**

Dr. Alexander Rabinovich

*Russian Academy of Sciences, Moscow, Russia Tsunami Laboratory, Institute of Oceanology
IASPEI*

Philip Woodworth, Richard Thomson

The $M_w = 9.3$ megathrust earthquake of December 26, 2004 off the west coast of Sumatra in the Indian Ocean generated a widespread catastrophic tsunami. This was the first global tsunami to occur during the "instrumental era", and it was accurately recorded by a large number of tide gauges throughout the World Ocean, including many tide gauges in the Atlantic Ocean, at sites located ten to twenty five thousand kilometers from the source area. The Mid-Atlantic Ridge is shown to have served as a wave-guide for the 2004 event, efficiently transmitting tsunami energy from the source area to far-field regions of the Atlantic coasts of South and North America. Statistical characteristics (wave height, period, and arrival time) and spectral properties of the tsunami waves observed in the Atlantic are examined and summarized. This is the second part of a three-part study of the Working Group on Tide Gauge Measurements of the 2004 Sumatra Tsunami, IUGG Tsunami Commission. This first part focused on the Indian Ocean (PAGEOPH, 2007) while the third part will focus on the Pacific Ocean.

Keywords: 2004, sumatra, atlantic

PERUGIA
ITALY



(S) - IASPEI - *International Association of Seismology and Physics of the Earth's Interior*

JSS002

Oral Presentation

1749

Probabilistic SMF Tsunami Hazard Assessment for the upper East Coast of the United States

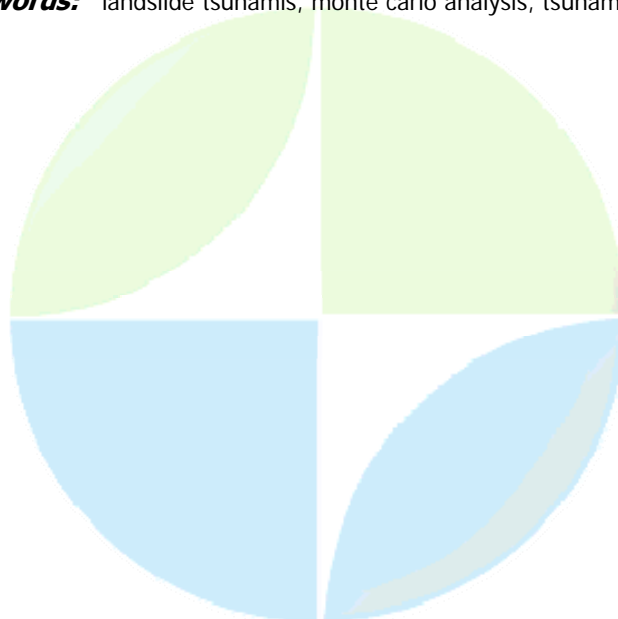
Prof. Stephan Grilli

Department of Ocean Engineering University of Rhode Island

Stefan Maretzki, Christopher Baxter

While much work has been done for the United States west coast, the level of tsunami hazard on the east coast of is not well understood. This information is critical for the population, emergency services, and industry of the region. Assessing this hazard is particularly difficult because of the lack of tsunami observations in the historical record and the uncertainty regarding the return periods of large-scale events that have been proposed, such as a large transoceanic tsunamis possibly caused by a collapse of the Cumbre Vieja volcano in the Canary Islands, or a large co-seismic tsunami initiated in the Puerto Rican subduction zone. It is believed, however, that one of the most significant tsunami hazards in this region could result from local submarine mass failures (SMF), which could cause concentrated damage in coastal communities located near the failures. This paper presents results of a probabilistic analysis performed to estimate the hazard, expressed in terms of runup (at a given probability of occurrence), of SMF tsunamis triggered by earthquakes along the upper northeast coast of the United States. A Monte Carlo approach is employed, in which distributions of relevant parameters (seismicity, sediment properties, type and location of slide, volume of slide, water depth, etc.) are used to perform large numbers of stochastic stability analyses of underwater slopes, based on standard geotechnical methods (Maretzki, 2006). When slope failure occurs, initial tsunami characteristic height and runup are estimated, based on earlier numerical work (Grilli and Watts, 2005; Watts et al., 2005), for specified return periods of seismic events. The 100 year hazard associated with SMF tsunamis along the US east coast is found to be quite low at most locations, as compared to the typical 100 year hurricane storm surge in the region (5 m). Two sites, however, located near Long Island, New York and Atlantic City, New Jersey, showed an elevated risk of higher tsunami runup (5.0-7.5 m). These two sites are the focus of more detailed ongoing modeling studies.

Keywords: landslide tsunamis, monte carlo analysis, tsunami runup



(S) - IASPEI - *International Association of Seismology and Physics of the Earth's Interior*

JSS002

Oral Presentation

1750

Lessons from Tsunami evacuation in the recent tsunamis including the 2004 Indian ocean

Prof. Fumihiko Imamura

disaster control research center Tohoku University IASPEI

We investigated the tsunami information/warning and response of the people including evacuation in recent tsunamis including the 2004, in order to discuss the essential role of the early tsunami warning. There three stages for carrying out safety evacuation after the earthquake; the first is to collect the information of tsunami warning and natural phenomenon such as strong shakes and abnormal on the coast, the second is to make decision of evacuation based on the risk perception, the third is to select proper route and place for safety evacuation from tsunami attack. Unless the three stages should be completed adequately, people could not be survived. We found the balance between tsunami warning and risk bias in individual on response. If the risk on the warning overcome the risk bias, they could make the decision of evacuation, which suggest us an idea of proper and essential role of the warning system. Moreover, in diary life, the functions with risk communication and education so on are important to decrease the risk bias.

Keywords: tsunami warning, awareness, risk perception

PERUGIA
I T A L Y



(S) - IASPEI - *International Association of Seismology and Physics of the Earth's Interior*

JSS002

Oral Presentation

1751

Long wave runup on the plane beach

Prof. Efim Pelinovsky

Nonlinear Geophysical Processes Chief Scientist IAPSO

Didenkulova Irina, Soomere Tarmo, Zahibo Narcisse

The problem of the long wave runup on a beach is discussed in the framework of the rigorous solutions of the nonlinear shallow-water theory. An interesting moment here is the analysis of the runup of a certain class of asymmetric waves, the face slope steepness of which exceeds the back slope steepness. Shown is that the runup height increases when the relative face slope steepness increases whereas the rundown weakly depends on the steepness. Another new result concerns an influence of initial wave form on extremal (maximal) characteristics of the wave on a beach (runup and rundown heights, runup and rundown velocities and breaking parameter). It is suggested to define a wave length for solitary waves on a 2/3 level of the maximum height (it is connected with length of significant wave in oceanology). In this case formulas for extremal runup characteristics are universal and the influence of initial wave form on extremal runup characteristics is weak.

Keywords: tsunami, runup



(S) - IASPEI - International Association of Seismology and Physics of the Earth's Interior

JSS002

Oral Presentation

1752

Overview of the restoration program from the giant earthquakes and tsunamis project

Prof. Teruyuki Kato

Earthquake Research Institute The University of Tokyo IAG

Kenji Satake, Koshun Yamaoka, Fumihiko Imamura, Hirokazu Iemura

A giant earthquake occurred off Sumatra Island, Indonesia and generated large tsunami in Indian Ocean on December 26, 2004. This event caused devastating disasters in the countries surrounding the Indian Ocean. Motivated by this event, we have initiated a multi-disciplinary and international research project called the Restoration Program from the Giant Earthquakes and Tsunamis which is supported by the Japanese government. The ultimate goal of the project is to propose an effective measure to mitigate disasters from giant earthquakes and tsunamis such as the 2004 event. We tackle this problem by interdisciplinary and international approaches. Synergetic works among different academic disciplines are important for ultimate restoration from the disasters due to earthquakes and tsunamis. The knowledge on the mechanism of earthquakes and tsunamis is to be utilized to elaborate the software and hardware system of early warning system and to construct a strong and resilient city against earthquake and tsunami. Education and outreach of such basic knowledge of earthquakes and tsunamis, function of early warning system and earthquake resistant construction are indispensable for effective mitigation of human casualties in a society. The project consists of four sub-theme of natural science, civil engineering and social science as follows: 1) Clarification of mechanism of the giant earthquake and tsunami and its prediction: This sub-theme tries to clarify the mechanism of giant earthquake and tsunami using various geophysical schemes such as seismology, paleoseismology and geodesy. 2) Research on developing human resource for enforcing the human power against the natural disaster: This sub-theme is mostly devoted to build capacities of human power for resilient community against earthquake and tsunami through education and outreach. 3) Research on effective use of tsunami warning system and mitigation of tsunami hazard: This sub-theme tries to propose an effective measure of monitoring, transmitting and disseminating tsunami information in real time manner for tsunami disaster mitigation. 4) Restoration program and city planning from the disasters due to giant earthquakes and tsunamis: This sub-theme searches for coastal disasters due to earthquake and tsunami and tries to propose an effective plan for restoration from the earthquake and tsunami. Each sub-theme is composed of 3-5 research subjects and the program strongly encourages synergetic efforts among international community of related scientists through international workshops and symposia as well as related field researches. The term of the project is three years from April 2005 to March 2008, so that the project will terminate in the next year. However, we try to build up long lasting international researchers community for earthquake and tsunami, particularly in the Asian countries, toward our ultimate goal of mitigating disasters related to giant earthquakes and tsunamis that may occur in other areas along the subducting plate boundaries over the globe.

Keywords: earthquake, tsunami, restoration

(S) - IASPEI - International Association of Seismology and Physics of the Earth's Interior

JSS002

Oral Presentation

1753

A tsunami hazard model for New Zealand

Dr. William Power
Natural Hazards GNS Science

Gaye Downes, Mark Stirling, Kelvin Berryman, Warwick Smith

How does the risk of tsunami compare to that from other natural hazards, and which locations are most vulnerable? These questions were frequently asked in the aftermath of the 2004 Boxing Day tsunami, and in this presentation we describe our attempts to answer them. We developed a probabilistic model for estimating the tsunami hazard along the coast of New Zealand due to plate-interface earthquakes around the Pacific Rim and local earthquakes around New Zealand. To do this we constructed statistical and physical models for several stages in the process of tsunami generation and propagation, and developed a method for combining these models to produce hazard estimates using a Monte Carlo technique. These models and the results we obtained from them will be described.

Keywords: tsunami, probabilistic, hazard



(S) - IASPEI - *International Association of Seismology and Physics of the Earth's Interior*

JSS002

Oral Presentation

1754

Tsunami terminology - do we all talk the same language?

Mrs. Gaye Downes
IASPEI

William L Power

What is run-up? Consult any of a number of scientific papers, dictionaries, glossaries, scientific institution websites, and you will get one or more of several definitions that differ in key aspects. For example, what run-up is a measure of, where it is measured, and to what reference level it is measured. Run-up is only one of a number of frequently-used tsunami terms that have more than one definition or are often misinterpreted, resulting in considerable misunderstanding and confusion among the scientific community and among those, such as emergency managers and planners, who use the scientific information. This presentation will look at some of the problems we have encountered and invite consideration of the need to critically review existing tsunami terminology.

Keywords: tsunami terminology



(S) - IASPEI - International Association of Seismology and Physics of the Earth's Interior

JSS002

Oral Presentation

1755

Reconsideration of the tsunami source model of the 1755 Lisbon Tsunami

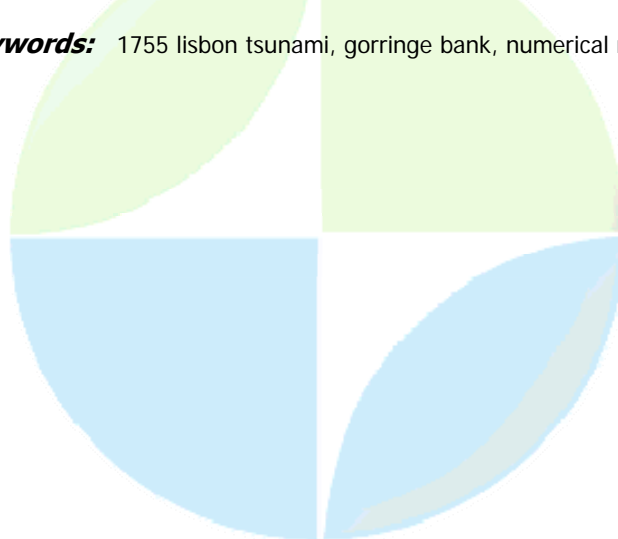
Dr. Angela Santos

Civil Engineering and Environmental Engineering Tohoku University IASPEI

Shunichi Koshimura, Fumihiko Imamura

The November 1st, 1755 Lisbon Earthquake, one of the most catastrophic events to have ever occurred in Portugal, Spain and Morocco, caused severe damage and casualties. The tsunami generated by this earthquake is well documented in the historical accounts, being reported throughout the Atlantic Ocean, reaching not only Portugal, Spain and Morocco, but also the Madeira and Azores Archipelagos, England, Ireland and the Caribbean. In spite of all the available information, the overall picture of this event remains unknown. On the other hand, there are uncertainties regarding the tsunami travel time, since some historical descriptions have ambiguous or unclear interpretation. One example is Cape St. Vincent, where we considered a travel time between 6 and 18 minutes. In other places we did not have access to the original documents, so we considered the travel time mentioned in previous studies. Since there are discrepancies in those articles, we also considered a possible range for determination of tsunami travel time. This occurred in: Huelva, 35-60 minutes; Porto Santo, 30-60 minutes; Figueira da Foz, 35-55 minutes. Other historical accounts are very accurate and we considered the exact value mentioned: Cadiz, 78 minutes; Funchal, 90 minutes; Safi, 30 minutes. The Gorringe Bank is the largest tectonic structure around this area, and with 200 km by 80 km, is enough to generate an $M_w=8.7$ earthquake. Johnston (1996) proposed possible source mechanisms with lengths ranging from 100 km to 500 km. In this study we followed Johnston (1996) proposal and reconsidered the possible tsunami source model for this event, taking account of the uncertainties of tsunami travel time suggested above. First, considering the range of tsunami travel time obtained from the historical accounts, we determined the spatial extent of tsunami source area by using wave ray analysis. Secondly, referring the fault parameters proposed by Johnston (1996), we calculated the initial sea surface displacement by using the theory of Okada (1985). Thirdly, we conducted the tsunami propagation model based on the non-linear shallow water theory. The model results were validated from the point of view of consistency with the reported tsunami travel time. The good agreement between the model and historical accounts for the travel time was obtained in some locations, leading us to conclude that the subsurface rupture length should be between 150 km and 300 km. Therefore, Gorringe Bank area could be a potential source for the 1755 tsunami and further study on that area should be carried out.

Keywords: 1755 lisbon tsunami, gorringe bank, numerical model



(S) - IASPEI - *International Association of Seismology and Physics of the Earth's Interior*

JSS002

Oral Presentation

1756

**Deposits of the tsunami of December 26, 2004, In Northern Indonesia:
Simelue Island and the medan coast of Sumatra Island**

Dr. Razzhigaeva Nadya
paleotsunami paleotsunami

Larissa Ganzey, Tatiana Grebennikova, Elena Ivanova

Sediments deposited during the tsunami of December 26, 2004, in coastal areas that differ in their structure and orientations relative to the tsunami front are studied with defining of the factors controlling particular features of the sedimentation under different wave intensities. The data obtained by the international expedition that studied the aftereffects of the tsunami in question from January-February, 2005. The sediments were studied along profiles orthogonal to the shoreline with available estimates of the tsunami run-up heights and distances. The lithology of tsunami-related deposits and data on various fossils (diatoms, foraminifers, and mollusks) are analyzed. The data obtained demonstrate that the sedimentation patterns during the tsunami were substantially variable in different coastal areas, which is explained by some other reasons in addition to the different wave transformation on the coasts with different configuration. A significant role in this process belongs to the geomorphologic structure and composition of the flooded zone and underwater coastal slope. Variably oriented coseismic motions is one of the factors influencing the sedimentation patterns. The most intense erosion occurred in the Northern part of Simelue Island, where the tsunami run ups exceeded 10 m. The thickness of the eroded layer amounts at least to 1.5 m. Coral reefs suffered the most intense erosion, particularly in the areas of coseismic uplifting and on the low shores subjected to a direct tsunami impact. The lithology of tsunami deposits depends on both the particular features of the tsunami and, largely, on the material sources. Under tsunami run ups up to 3-5 m high, when the erosion zone is limited by the upper part of the coastal slope, the beach, and adjacent old ramparts, the tsunami deposited well-sorted sands texturally similar to their counterparts from the beach and draining area. The textural characteristics of the sands are well sustained both vertically and horizontally. When the material from destroyed reefs is the main source for the tsunami deposits, they become more heterogeneous. Their most intense destruction occurred in the areas of coseismic uplifting. Here near the shoreline, the tsunami deposited moderately and poorly sorted sands, in the extended flooded zone, high tsunami run ups result in the sorting of this material, its grain size decrease, the disappearance of the coarse-grained fractions, and a unimodal grain-size distribution. The taxonomic composition of the microflora and fauna in the tsunami sediments shows that they mainly originate from the sediments of the erosion zone, coral reefs, and the upper part of the coastal slope. The paleotsunami deposits discovered are compared with their recent counterparts. Grants RFBR 05-05-64063, FEB RAS I № 06-I-OH3-106.

Keywords: tsunami, sediments

(S) - IASPEI - *International Association of Seismology and Physics of the Earth's Interior*

JSS002

Oral Presentation

1757

Tsunami intensity as a quantification tool: the example of Mediterranean and Connected Seas

Mrs. Anna Fokaefs
IASPEI

Eleni Daskalaki, Gerassimos A. Papadopoulos

Quantification of tsunami waves is not an easy task given that adequate magnitude scales have not introduced so far. Alternatively, tsunami intensity is a tool that makes possible to describe semi-quantitatively the effects of a tsunami wave in particular coastal sites. Traditional 6-grade tsunami intensity scales were introduced since 20s. A few years ago the so-called Papadopoulos-Imamura 12-grade scale was developed and applied in several tsunamigenic regions of the world. Mapping of a real intensity distribution as well as correlations between intensity and physical parameters of the wave (e.g. wave height, distance of penetration inland) can be performed. Therefore, the tsunami intensity is a potential tool for the post-event effect study, for the development of scenarios of expected effects from future tsunamis as well as for comparative studies. Such possibilities are shown with the example of the Mediterranean and connected Seas. Intensities for hundreds of tsunami events have been estimated in both the classic 6-grade and 12-grade scales and correlations between the two scales are investigated. Intensities have been estimated for a long number of observation points of the large tsunami of 9 July 1956 in the South Aegean Sea and the intensity field has been mapped as a prototype example.

Keywords: tsunami, intensity, scale

PERUGIA
ITALY



(S) - IASPEI - *International Association of Seismology and Physics of the Earth's Interior*

JSS002

Oral Presentation

1758

Development of a Decision Matrix for Early Tsunami Warning in the Mediterranean and Connected Seas

Dr. Gerassimos Papadopoulos

IUGG Tsunami Commission National Observatory of Athens IASPEI

Eleni Daskalaki, Katerina Orfanogiannaki

After the generation of the large Indian Ocean 2004 tsunami a systematic effort started for the establishment of regional, national and local early tsunami warning systems in Europe under the coordination of IOC-UNESCO. One of the most important requirements for the development of operational tsunami warning systems is the existence of a reliable procedure for decision making about the tsunamigenic or non tsunamigenic nature of a particular earthquake in real-time conditions. In this contribution we introduce a first approach of a tsunami warning decision matrix for the most tsunamigenic region of Europe that is for the Mediterranean Sea. Connected Seas, such as the Marmara Sea, the Black Sea and the Atlantic Ocean offshore are also included. The decision matrix developed is empirical and is based on two main data compilations. The first is the catalogue of earthquakes of the instrumental era of seismology, that is from 1900 to 2006. Earthquakes occurring either offshore or on land at distance no more than 30 km from the closest shoreline are considered. We perform completeness analysis and determine earthquake magnitude cut-off for several time intervals from magnitude-frequency and magnitude-time diagrams. The second data compilation is the tsunami catalogue for the time period from 1900 to 2006. We perform completeness analysis and determine tsunami intensity cut-off for several time intervals from intensity-frequency and intensity-time diagrams. The 12-grade Papadopoulos-Imamura tsunami intensity scale is used. We correlate complete data sets of earthquakes and tsunamis and produce empirical probabilities for the tsunamigenic nature of a particular earthquake according to the earthquake magnitude class, focal depth, epicentral location and focal mechanism. Such probabilities make a good basis for the construction of a tsunami warning decision matrix in the Mediterranean Sea region.

Keywords: early, tsunami, warning



(S) - IASPEI - *International Association of Seismology and Physics of the Earth's Interior*

JSS002

Oral Presentation

1759

Stromboli Island (Italy): tsunamis generated by submarine landslides

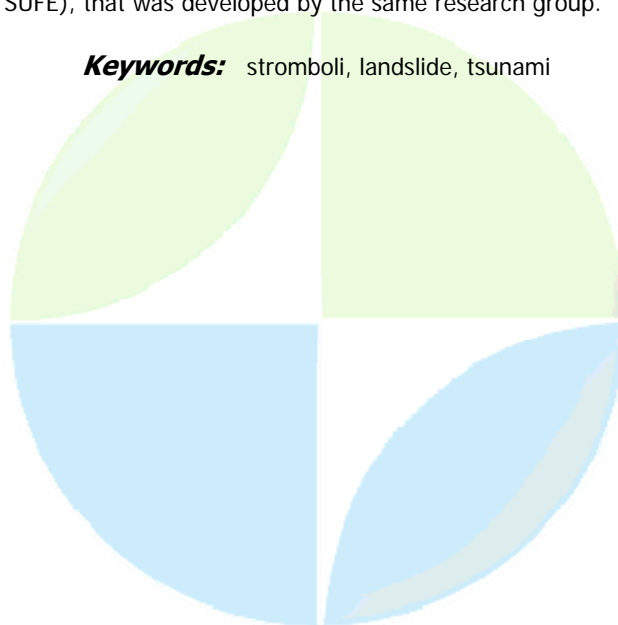
Dr. Alberto Armigliato

Dipartimento di Fisica, Settore Geofisica Università di Bologna IASPEI

Stefano Tinti, Filippo Zaniboni, Gianluca Pagnoni

The strong volcanic activity of Stromboli island, located in South-East Tyrrhenian Sea (Italy), is well known: the morphology of the volcanic complex has been deeply changed by the frequent catastrophic events that characterized its history. The last one (or ones), in the Holocene, formed the Sciara del Fuoco scar (in the North-Western flank of the island), an evident big depression that extends also under the sea. The sliding mass had an estimated total volume of around 1 km³, and the simulations of such (possibly multiple) event carried out by our group evidenced the impact of really catastrophic waves on the coasts of South Italy. In addition to large disastrous events, minor failures take place recurrently in the Sciara del Fuoco, due to accumulation of ejecta along the slope, to the steep angle typical of volcanic flanks, to the tremors induced by volcanic activity: all these elements contribute to submarine and sub-aerial mass instabilities. These have potential for tsunami generation as was shown by the December 30th 2002 failures that occurred here. Big tsunami waves were set up that travelled all around the island, reaching the height of over 10 meters and causing severe damage in the waterfront area, but fortunately no casualties. These events justify the constant monitoring of the Sciara del Fuoco, together with the large effort to study its characteristics and evolution, but this is not the only place of Stromboli where mass failures are to be expected. Several submarine incisions were evidenced by bathymetric surveys all around the island, that can be interpreted as results of past events and also can be seen as possible source areas of future events. In this work we consider three alternative scenarios for landslides generating tsunamis around Stromboli flanks, with volume comparable to the December 2002 events. The first is placed in the Strombolicchio plain, north of the island; the second is found near the southern extreme of the island, at Punta Lena, and the third is located in the Eastern coast, in the area named Forgia Vecchia. The landslide simulations is carried out through a Lagrangian block model (UBO-BLOCK1) developed at the University of Bologna, while the computation of the tsunami generation and propagation around the island and in the Aeolian Archipelago is performed through a finite-element tsunami model (UBO-TSUFE), that was developed by the same research group.

Keywords: stromboli, landslide, tsunami



(S) - IASPEI - *International Association of Seismology and Physics of the Earth's Interior*

JSS002

Oral Presentation

1760

National ocean service operation of tide stations in support of tsunami detection

Mr. Stephen Gill

Allison Allen, Natalia Donoho, Stephen Gill, Tom Mero, Rolin Meyer, Manoj Samant, Robert Aspinall

The United States National Oceanic and Atmospheric Administration (NOAA) funds several water level observation networks in support of operational tsunami warning capability. These observing systems include NOAA-funded stations operated by the University of Hawaii Sea Level Center, stations operated by the NOAA Tsunami Warning Centers (TWCs), the NOAA-operated DART network, and the stations of the NOAA National Water level Observation Network (NWLON). This paper describes the NOAA National Ocean Service (NOS), Center for Operational Oceanographic Products and Services (CO-OPS) contribution to tsunami warning. CO-OPS is responsible for operating the NWLON which has supported tsunami warning since 1948. NOS continues to expand the NWLON to collect multi-purpose data for a variety of applications, including real-time water levels for navigation, sea level trends, habitat restoration, computation of tidal datums, and coastal hazard mitigation. After the December 2004 Indian Ocean tsunami, CO-OPS was tasked to coordinate with the TWCs to expand and upgrade the tsunami warning capabilities of the NWLON. A plan was developed to upgrade existing NWLON stations with new Data Collection Platforms (DCPs), implement data formats, and fill observation gaps. Work began in 2005 to upgrade 33 existing water level stations and install 16 new stations in priority areas in the Pacific Ocean and the Caribbean . By September 2006, all 33 targeted upgrades had been completed, as well as 15 of the 16 planned installations. And by September 2007, CO-OPS plans to have completed the upgrade of all coastal NWLON stations with new DCPs to satisfy tsunami requirements. As of January 2007, a total of 100 NWLON stations are operating in support of the National Weather Service (NWS)s tsunami warning capabilities. Even though this information will still be transmitted via the Geostationary Operational Environmental Satellite (GOES) for both the primary and backup DCPs, for the first time the upgraded DCPs will be transmitting 1-minute averaged water levels every six minutes. 6 and 1-minute data are available to the TWCs directly through GOES, through remote phone dial-in, and through the CO-OPS web page. These stations also store 15-second data on a flash drive for post event analyses and modeling. The 15-second data can be manually downloaded from the station itself or remotely using the DCPs modem. The strategy developed by CO-OPS and the TWCs has involved more than just the expansion of the NWLON and new hardware, but an expansion of a total capability, as evidenced by the CO-OPS support to computing harmonic constants for each DART buoy site, so that effective de-tiding can take place for resolution of the tsunami signals.

Keywords: noaa, tide, station

(S) - IASPEI - *International Association of Seismology and Physics of the Earth's Interior*

JSS002

Oral Presentation

1761

Numerical studies of multiple submarine slope failures and tsunamis near Seward, Alaska, during the M9.2 1964 earthquake.

Mrs. Elena Suleimani

Geophysical Institute University of Alaska Fairbanks IASPEI

Peter Haeussler, Keith Labay, Roger Hansen

We are creating tsunami inundation maps for Seward, Alaska, in the scope of the National Tsunami Hazard Mitigation Program. Tsunami potential from tectonic and submarine landslide sources must be evaluated in this case for comprehensive mapping of areas at risk for inundation. Seward is a community located at the head of Resurrection Bay, in southern Alaska, which was hit hard by both tectonic and landslide-generated tsunami waves during the 1964 earthquake. Resurrection Bay is a glacial fjord fed by several rivers and creeks draining nearby glaciers and depositing sediments into the bay at a high rate. Sediment accumulation on the steep underwater slopes contributes to the landslide tsunami hazard in the Resurrection Bay. We constructed a 5-m grid of combined topography and bathymetry for the northern part of Resurrection Bay. The data is of exceptional quality and includes (1) a 2006 LIDAR survey of the entire area of interest, (2) a 2001 multi-beam survey of the bathymetry of all of Resurrection Bay, and a (3) 2006 survey of the Seward harbor and surrounding areas. Gaps between the LIDAR and multi-beam surveys were minimal, with the exception of a shallow tidal area at the head of the bay. Where gaps exist, interpolation was used to create a smooth transition between the surveys. All pre-1964 (1905 to 1961) bathymetric surveys from NOAA smooth sheets were digitized, with corrections applied for coseismic subsidence, post-seismic uplift, sea level rise, and rounding errors. We then compared these to a 2001 NOAA multi-beam survey to assess the location and size of submarine slides. More than 100 million m³ of sediment moved during the 1964 earthquake, with much of it flowing about 10 km to the south into a bathtub-shaped depression in the fjord bottom. There were four major slides in the bay with volumes in excess of 14 million m³. A slide along the Seward waterfront, which is likely responsible for most of the initial damage, has a volume of about 19 million m³, and left behind a blocky lag deposit. To reconstruct the sequence of waves observed at Seward on March 27, 1964, we model tsunami waves caused by superposition of the local landslide-generated tsunamis and the major tectonic tsunami, which arrived about 30 minutes after the start of the earthquake. We use a three-dimensional numerical model of an incompressible viscous slide with full interaction between the slide and surface waves to simulate Seward slope failures and associated tsunami waves. The long-wave approximation is used for both water waves and slides. The equations of motion and continuity for the slide and for surface waves are solved simultaneously using an explicit finite-difference scheme.

Keywords: tsunami, landslide, modeling

(S) - IASPEI - *International Association of Seismology and Physics of the Earth's Interior*

JSS002

Oral Presentation

1762

Central Kuril Earthquake and Tsunami of 15 November 2006: Pre-event geophysical field survey and post-event seismicity

Dr. Evgueni Kulikov

Russian Academy of Sciences Tsunami lab, Shirshov Institute of Oceanology IASPEI

L.I. Lobkovsky, V.B. Baranov, A.I. Ivaschenko, E.A. Kulikov

Following the catastrophic 2004 Sumatra earthquake and global tsunami, seismic zones around the Pacific Ocean were thoroughly examined based on the seismic-gap theory. The Central Kuril seismic gap of about 500 km was defined as the zone of a highest risk of a possible catastrophic event. The last major earthquake in this zone was in 1780, while the southwest and northeast regions of this zone are bordered by the 1918 and 1915 earthquake source areas, respectively. The point of main concern was the northeastern shelf of Sakhalin Island in the Sea of Okhotsk, the area of active oil and gas exploration. To examine the Central Kuril seismic gap zone, two detailed marine geophysical expeditions were conducted on the R/V Michail Lavrentiev by the Russian Academy of Sciences in 2005 and 2006. The main purposes of these expeditions were examination of the tectonic structure of the seismic gap, identification of cross-shelf fault areas, and estimation of the possible source area of the expected earthquake. Based on results of these expeditions, numerical modeling of several scenarios involving possible major tsunamis was undertaken. The earthquake of 15.11.2006 occurred very close to the expected source region. Parameters of the actual tsunami were also similar to that predicted, except that fortunately the NW coast of Sakhalin Island was sheltered from the waves by the Simushir coast. Simulated tsunami wave forms were found to agree very closely with the open-sea island and deep-ocean DART records.

Keywords: tsunami, seismic gap



(S) - IASPEI - *International Association of Seismology and Physics of the Earth's Interior*

JSS002

Oral Presentation

1763

Solving the Semantics Problem

Dr. Luis Bermudez

Research and Development Monterey Bay Aquarium Research Institute

Adopting metadata specifications is not sufficient to achieve interoperability due to the heterogeneity of the values in metadata annotations. For example, stage, gage height and water elevation are different representations of the same concept. These values may be used as values for a metadata element. If the semantic heterogeneities are not solved among these elements then they will appear to be referring to different phenomena. Therefore, searching for stage data will not retrieve all the possible results. The Marine Metadata Interoperability (MMI) project is working to address this issue, as well as other semantic conflicts. The work is guided by community collaborations and supported via the MMI site (<http://marinemetadata.org>). The main activities that MMI focuses to achieve semantic interoperability are: 1) encouraging the use of already existing vocabularies; 2) providing best practices about publishing controlled vocabularies so that they are interoperable in the Semantic Web; 3) hosting workshops to create and map controlled vocabularies; 4) providing tools and guidance to solve semantic heterogeneities.

Keywords: semantic web, ontologies, interoperability

XXIV 2007
PERUGIA
I T A L Y



(S) - IASPEI - *International Association of Seismology and Physics of the Earth's Interior*

JSS002

Oral Presentation

1764

U.S. states and territories national tsunami hazard assessment, historic record and sources for waves

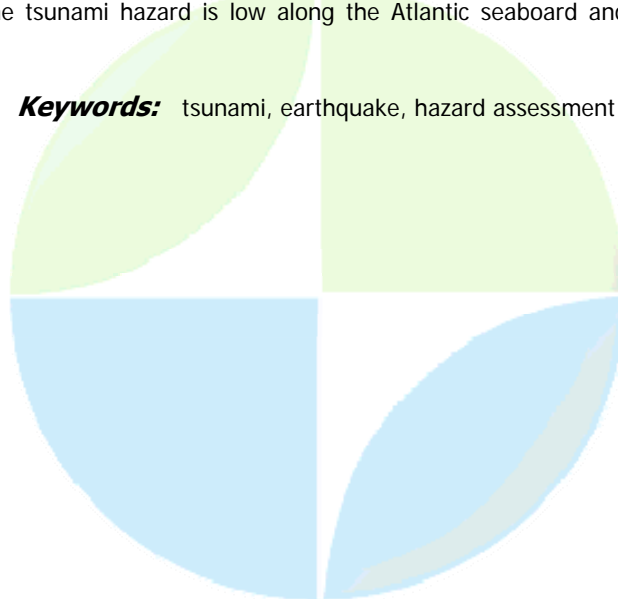
Mrs. Paula Dunbar

National Geophysical Data Center National Oceanic and Atmospheric Administration

Craig Weaver

In 2005, the U.S. National Science and Technology Council (NSTC) released a joint report by the subcommittee on Disaster Reduction and the U.S. Group on Earth Observations titled Tsunami Risk Reduction for the United States: A Framework for Action (Framework). The first specific action called for in the Framework is to Develop standardized and coordinated tsunami hazard and risk assessments for all coastal regions of the United States and its territories. Since the National Oceanic and Atmospheric Administration (NOAA) is the lead agency for providing tsunami forecasts and warnings and NOAA's National Geophysical Data Center (NGDC) catalogs information on global historic tsunamis, NOAA/NGDC was asked to take the lead in conducting the first national tsunami hazard assessment. Earthquakes or earthquake-generated landslides caused more than 85% of the tsunamis in the NGDC tsunami database. Since the United States Geological Survey (USGS) conducts research on earthquake hazards facing all of the United States and its territories, NGDC and USGS partnered together to conduct the first tsunami hazard assessment for the United States. A complete tsunami hazard and risk assessment consists of a hazard assessment, exposure and vulnerability assessment of buildings and people, and loss assessment. This report is an interim step towards a tsunami risk assessment. The goal of this report is to provide a qualitative assessment of the tsunami hazard at the national level. The core of the assessment involved dividing the NGDC historical tsunami database based on the measured runup heights and the number of runups at each height. Although tsunami deaths are a measure of risk rather than hazard, the known tsunami deaths found in the NGDC database search compare favorably with the qualitative assessment based on frequency and height. The second assessment method used the USGS estimates of recurrence of possible tsunami-generating earthquakes near American coastlines to extend the NOAA/NGDC tsunami database back in time. Combining the two techniques shows that the American tsunami hazard is highest for all Pacific basin states, possessions, and those in the Caribbean. The number of high runups in Alaska and Hawaii indicate that the tsunami hazard is very high in those states. In contrast, the tsunami hazard is low along the Atlantic seaboard and very low for the Gulf coast states.

Keywords: tsunami, earthquake, hazard assessment



(S) - IASPEI - *International Association of Seismology and Physics of the Earth's Interior*

JSS002

Oral Presentation

1765

Supplementary Post-Tsunami Survey of 2004 Indian Ocean Tsunami in Sumatra Island and the database

Prof. Koji Fujima

Dept. of Civil and Environmental Eng. National Defense Academy

Indian Ocean Tsunami, occurred on 26 December 2004, caused heavy damages in many countries in Indian Ocean. After the tsunami, many field investigations were performed to measure the tsunami-trace height, to examine the damage situation, and to make a suggestion for recovery planning. However, in Indonesia, the surveys with measurement were concentrated in Banda Aceh city and northwest part of Sumatra, north of latitude 5.4 degrees N (Lho-nga and Leopung), although the epicenter was estimated as 3.4 degree N. Therefore, 13 experts organized the survey team and carried out the supplementary post-tsunami survey from Leopung to Meulaboh, latitude 4.1 degrees N, through 29 July to 6 August, 2006. The length of survey area is 180 km and the number of survey point is about 30. The measured runup height between Leopung and Calang, 100 km south of Banda Aceh, was 13 to 20 m, and the inundation height was 8 to 10 m. As a reference, runup height from Lho-nga and Leopung (13km length) was 20 to 30 m and the inundation height was 12 to 20 m. Because the low-lying land lies between Calang and Meulaboh, it was impossible to measure the runup height. However, the measured inundation height was 3 to 5.5 m, thus the runup height might become round 10 m if there was a hill in this region. The present survey shows the tsunami height distribution along the northwest coast of Sumatra. In the present survey area, many big bridges were destroyed by the tsunami. On the contrary, there were the small bridges which were left without destruction. In addition, beach erosion is severe between Calang to Meulaboh, the coastline moved over 100 m landward at the maximum. The mechanism of bridge destruction and beach erosion should be investigated for tsunami disaster reduction. The database of measurement data of Indian Ocean tsunami was established including the present data.

Keywords: tsunami, survey, sumatra



(S) - IASPEI - *International Association of Seismology and Physics of the Earth's Interior*

JSS002

Oral Presentation

1766

Tsunami wave characteristics in Alberni Inlet, British Columbia, Canada

Dr. Josef Cherniawsky

Isaac Fine, Alexander Rabinovich, Fred Stephenson

Spectral analysis of sea level records of recent tsunami events and calculations with numerical models are used to study tsunami wave propagation and resonance characteristics on the southwest shelf and coast of Vancouver Island, British Columbia, and in particular, inside Alberni Inlet. This 45-km long fjord has experienced significant tsunami waves in the past. The town of Port Alberni, located at the head of the fjord, was severely affected by the March 27 (Good Friday) 1964 tsunami that originated from a magnitude 9.2 earthquake in Prince William Sound, Alaska. Property damage in Port Alberni was estimated at more than 8 million dollars. Tsunami-alert sirens warned the residents to move to higher ground and helped to avoid fatalities. Tide gauges in Port Alberni and at two locations on the Pacific Coast, Bamfield and Tofino, recorded clearly the incoming tsunami waves. However, the Port Alberni maximum wave heights of up to 5 m were by a factor of 4 larger than in Bamfield, or Tofino, exhibiting relatively strong amplification inside the inlet. We use spectral analyses of observed tide gauge records and compare these to spectra of time series generated by two numerical models, a nested-grid finite-difference model initialized with scenarios from nearby and remote earthquakes and a local finite-difference model that is forced at its open boundary with red-noise signal.

Keywords: tsunami wave, propagation, resonance

PERUGIA
ITALY



(S) - IASPEI - *International Association of Seismology and Physics of the Earth's Interior*

JSS002

Oral Presentation

1767

Tsunami vulnerability assessment for the city of Banda Aceh using the tsunami numerical model and the post-tsunami survey data

Dr. Shunichi Koshimura

Graduate school of engineering Tohoku University

Takayuki Oie, Hideaki Yanagisawa, Fumihiko Imamura

The 2004 Indian Ocean tsunami disaster attacked the city of Banda Aceh, Indonesia. According to the post-tsunami survey conducted by Japan International Cooperation Agency (JICA), this tsunami resulted more than 70,000 of casualties corresponding to 27 % of population before disaster and more than 12,000 of house damage. The extent of tsunami inundation zone reached approximately 2 km inland from the shoreline. The present study aims to understand Banda Aceh's vulnerability against the tsunami disaster, by using the numerical model of tsunami propagation and run-up, and GIS analysis with post-tsunami survey data in terms of casualties and structural damage. The post-tsunami survey data were obtained by an effort of JICA mission of the study on the urgent rehabilitation and reconstruction support program for Aceh province and affected areas in north Sumatra. Using the high-resolution land elevation data, we performed a coastal inundation modeling for the 2004 Indian Ocean tsunami that attacked the city of Banda Aceh. The model is based on a set of non-linear shallow water equations with bottom friction in the form of Mannings formula according to the land use condition. The equations are discretized by the Staggered Leap-frog finite difference scheme. To create the computational grids for tsunami model, we use the GEBCO digital bathymetry data, SRTM data, local bathymetric charts of northern Sumatra (1:500,000 and 1:125,000) and land elevation data obtained by digital photogrammetric mapping. The grid size varies from 1860 m to 23 m from the source region to the coast of Banda Aceh, constructing a nested grid. The Final grid size within the city of Banda Aceh is 23 m, and the data is based on the land elevation data provided by JICA. The model results in terms of local inundation depth and the extent of inundation zone are consistent with the actually measured and interpreted data from satellite imagery. Also, using GIS analysis combined with the detailed survey data in terms of the damage on structures and casualties, we developed the tsunami inundation depth-damage diagram to understand Acehs vulnerability against tsunami disaster. Throughout the present analysis, we found that number of destroyed structures and the percentage of casualties significantly increase for 2 or 3 m as local tsunami inundation depth. In order to reduce the tsunami hazard and mitigate the damage of possible tsunami disaster, Acehs reconstruction planning should consider the possible countermeasures such as sea walls or vegetations in order to reduce the local tsunami inundation depth to at least 2m.

Keywords: tsunami, vulnerability, numerical model

(S) - IASPEI - *International Association of Seismology and Physics of the Earth's Interior*

JSS002

Oral Presentation

1768

Forces on the structures in urban area due to tsunamis

Dr. Yoshinori Shigihara

Civil and Environmental Engineering National Defense Academy

Koji Fujima, Charles Simamora

The Indian Ocean Tsunami of December 26, 2004 caused significant damage to coastal areas. The tsunami created breaking waves run up the shoreline as surges, or bores. They inundated in urban area, and broke down most kinds of structures such as residential houses, industrial plant and cargo transporter. Since the best way to preserve the human life from the tsunami is that people run away to a higher place as much as possible, a refuge building in coastal region may exert great effect for saving life. In order to evacuate people safely in the buildings, structure of the building must hold against the gigantic tsunami load. Therefore, estimation method of force against tsunami on the structures is required. The objective of this study is to investigate tsunami forces on the structures in urban area. We carry out laboratory experiments, analytical and numerical model are developed to simulate the behavior of tsunami. Two dimensional wide wave tank (11m in length and 7m in width) used for the experiment is 60cm depth with 1/3 slope connected to 5cm shelf region, the solitary wave is generated from the wave generator. The structure models are installed on-shore, we measured total force against tsunamis, pressure, time history of the water level in off-shore, time history of inundation depth and vector of velocity in time on-shore. The maximum measured force related to distance from the shoreline and that related to occupied rate of buildings are discussed. Also, to determine the tsunami force quantitatively, we introduce relationships among tsunami forces, water level on-shore and current velocity around the structures. Results of the laboratory experiments are simulated with Finite Difference Method (FDM) and Finite Volume Method (FVM), and both model results are compared to clarify which numerical models well simulate the tsunami force. In order to discuss the accuracy of simulation model, suitable grid size, grid number and grid shape in numerical domain are investigated.

Keywords: tsunami, structure, tsunami force



(S) - IASPEI - *International Association of Seismology and Physics of the Earth's Interior*

JSS002

Oral Presentation

1769

A Probabilistic Tsunami Hazard Assessment for Western Australia

Dr. Phil Cummins

Geospatial and Earth Monitoring Division Geoscience Australia IASPEI

David Burbidge, Hong Kie Thio

The occurrence of the Indian Ocean Tsunami on 26 December, 2004 has raised concern about the lack of information on the tsunami threat, which makes it difficult to determine appropriate mitigation measures. In addition to a warning system, such measures may include inundation maps and decision-making tools that would enable planning and emergency management officials to manage the tsunami threat. A first step in the development of such measures is a tsunami hazard assessment, which gives an indication of which areas of coastline are most likely to experience tsunami, and how likely such events are. Here we present the results of a probabilistic tsunami hazard assessment for Western Australia (WA). Compared to other parts of Australia, the WA coastline experiences a relatively higher frequency of tsunami occurrence. This hazard is due to earthquakes along the Sunda Arc, south of Indonesia. Our work shows that large earthquakes offshore of Java and Sumba are likely to be a greater threat to WA than those offshore of Sumatra or elsewhere in Indonesia. A magnitude 9 earthquake offshore of the Indonesian islands of Java or Sumba has the potential to significantly impact a large part of the West Australian coastline. The level of hazard varies along the coast, but is highest along the coast from Carnarvon to Dampier. Tsunami generated by other sources (e.g. large intra-plate events, volcanoes, landslides and asteroids) were not considered in this study, which limits our hazard assessment to recurrence times of 2000 years or less.

Keywords: tsunامي, hazard, modelling



(S) - IASPEI - *International Association of Seismology and Physics of the Earth's Interior*

JSS002

Oral Presentation

1770

Earthquake-generated tsunamis in the Mediterranean Sea: scenarios of potential threats to the coast of Italy

Dr. Stefano Lorito

Department of Seismology and Tectonophysics INGV

Mara Monica Tiberti, Roberto Basili, Alessio Piatanesi, Gianluca Valensise

We calculated the impact on the Italian coasts of a large set of tsunamis resulting from earthquakes generated by selected fault zones of the Mediterranean Sea. Our approach merges updated knowledge on the regional tectonic setting and scenario-like calculations of expected tsunami impact. We focussed on potential source zones located at short, intermediate and large distance from our target coastlines. For each zone we determined a Maximum Credible Earthquake and described the geometry, kinematics and size of its associated Typical Fault. We then let the Typical Fault float along strike of its parent source zone and simulated all tsunamis it could trigger. Simulations are based on the solution of the nonlinear shallow water equations through a finite-difference technique. We investigate the tsunami threat to Italy coasts by both analyzing the travel-times and maximum water elevation field, and aggregate the results to quantify the threat from each source zone as a whole. We found a highly variable impact for tsunamis generated by the different zones. For example, a large Hellenic Arc earthquake will produce a much higher tsunami wave (up to 5 m) than those of the other two source zones (up to 1.5 m). This implies that tsunami scenarios in the Mediterranean Sea must necessarily be computed at the scale of the entire basin. The procedure can be easily replicated for other coastal areas of the Mediterranean. Our work represents a pilot study for constructing a basin-wide tsunami scenario database to be used for tsunami hazard assessment and early warning.

Keywords: tsunamis, mediterranean, seismotectonics



(S) - IASPEI - International Association of Seismology and Physics of the Earth's Interior

JSS002

Oral Presentation

1771

Standards and benchmarks for tsunami modeling

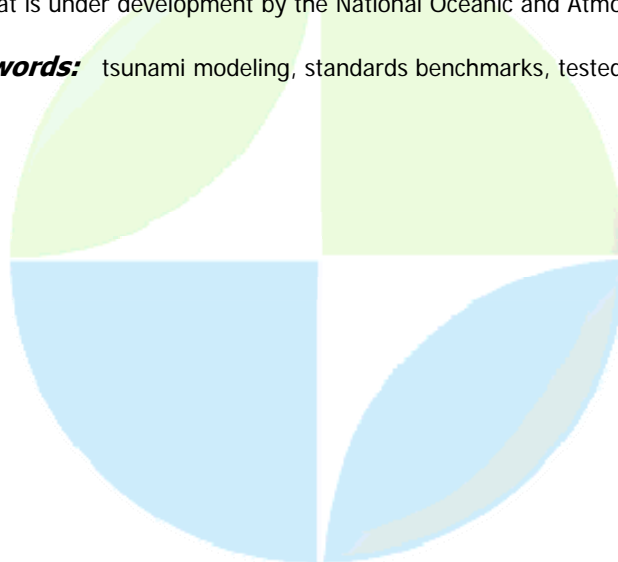
Prof. Utku Kanoglu

Department of Engineering Sciences Middle East Technical University IASPEI

Costas Synolakis, Eddie Bernard, Vasily Titov, Frank Gonzlez

A substantial number of new tsunami codes, more than 20 by some accounts, have been employed in the aftermath of the December 26, 2004 Boxing Day tsunami. Predictions from these new untested models are being presented at international meetings even though results differ from established paleotsunami measurements by factors as large as four. These substantial differences have attracted press attention, requiring hazard mitigation professionals to provide public explanations of the discrepancies. Since an increased number of nations in tsunami-prone regions around the world must develop tsunami mitigation plans, both validation and verification are essential for all numerical models used in planning. Validation refers to the process of ensuring that the model solves the parent equations of motion accurately, and is accomplished through comparison with analytical solutions. Verification refers to the process of ensuring that the model represents geophysical reality, and is accomplished through comparison with both laboratory measurements and field measurements. The gold standard for inundation numerical codes must include validation, verification, and the essential step of formal documentation in the peer-reviewed scientific literature. This process must be considered continuous; it is essential that even proven models be routinely reviewed and subjected to additional testing and documentation as new knowledge and data are acquired. So far, only a few existing numerical models have met these standards, and such models must be the only choice for inundation forecast modeling; the consequences of failure are too serious to risk a lower standard. A forecast system also requires accurate tsunami measurements and well-tested numerical procedures for inverting the measurements to produce predictions with a proven model. Clearly, however, there is no absolute certainty that even a properly validated and verified numerical code will produce accurate, real-time inundation forecasts; this is why multiple models should be implemented to improve forecast system robustness. We discuss analytical, laboratory, and field benchmark tests by which tsunami models can be validated, verified and formally documented in peer-reviewed journals indexed by ISI. This painstaking process may appear onerous, but is the only defensible methodology when human lives are at stake. Model standards and procedures that reflect this approach are being adopted for implementation in the U.S. Tsunami Forecasting System that is under development by the National Oceanic and Atmospheric Administration.

Keywords: tsunami modeling, standards benchmarks, tested model



(S) - IASPEI - *International Association of Seismology and Physics of the Earth's Interior*

JSS002

Oral Presentation

1772

Archive and Access of Global Water-Level Data: from the Coast to the Deep-ocean

Mrs. Kelly Stroker
NOAA NGDC IASPEI

Paula Dunbar

NOAA's National Geophysical Data Center (NGDC) operates the World Data Center (WDC) for Solid Earth Geophysics (including tsunamis). NGDC is one of three environmental data centers within NOAA's Environmental Satellite Service. The WDC/NGDC provides the long-term archive, data management, and access to national and global tsunami data for research and mitigation of tsunami hazards. Archive responsibilities include the global historic tsunami event and run-up database, the bottom pressure recorder data, and access to event-specific tide-gauge data, as well as other related hazards and bathymetric data and information. Recently, NGDC has assumed the responsibility to archive the high-resolution water level data. Currently, NGDC is archiving the pressure and temperature data recorded by NOAA's deep-ocean tsunameters. The next step would be to incorporate the water level data from coastal tide-gauge stations around the globe. There is a significant gap in data management for the coastal water level data in that no formal archive currently exists and it is quite a challenge to obtain water level information from various sources due to the lack of a central portal. It is envisioned that the retrospective water level data will be available through web services, using an XML-based schema. NGDC and the WDC are committed to distributing data in standard formats and the water level data would be no exception. Images of the station locations would be available through the Open Geospatial Consortium Web Map Services (WMS) and station metadata would be available through Web Feature Services (WFS). As part of the World Data Center, NGDC is committed to working with its international and national partners to develop a method for long-term sustainability of this important data.

Keywords: tsunami, water level, tidegauge



(S) - IASPEI - International Association of Seismology and Physics of the Earth's Interior

JSS002

Oral Presentation

1773

Tsunami damage in Crescent City, California from the November 15, 2006 Kuril event

Prof. Lori Dengler

Geology Department Humboldt State University

Annabel Kelly, Burak Uslu, Aggeliki Barberopoulou, Solomon Yim

On November 15, the harbor at Crescent City in Del Norte County, California was hit by a series of tsunami surges generated by the $M_w = 8.3$ Kuril Islands earthquake. The surges caused an estimated \$5.9 million in losses to the small boat basin, damaging the floating docks and several boats. The event highlighted the vulnerability of harbors from a relatively modest tsunami, problems in with the tsunami warning system for a marginal event, and the particular vulnerability of the Crescent City harbor area. It also illustrated a persistent problem for tsunami hazard mitigation a lack of awareness of both government officials and the public of the duration of tsunami hazard. Crescent City is particularly susceptible to tsunami events. Twenty-four tsunamis have been recorded since 1938, nine with amplitudes of 0.5 meters or larger including two previous events originating from the Kuril Islands. On November 15, tsunami alert bulletins were issued by the North American Tsunami Warning Center in Palmer, Alaska. When the alerts were cancelled at 6:40 AM PST, Crescent City had never been placed in a warning or watch situation. Projections for tsunami amplitudes on the order of a meter prompted the warning center to initiate an informal dialog with State Warning Centers and resulted in a local decision to clear beaches and harbor areas in Humboldt and Del Norte Counties, California before the arrival of the first expected wave at 11:48 AM PST. However there was no direct contact with the regional weather forecast offices and no advice directly conveyed to local jurisdictions. Water level data from the two previous Kuril events was not readily available to county emergency managers. There was confusion at the local level about what amplitude meant, the duration of the event and the appearance of a moderate tsunami in a harbor environment. Two people were on the docks believing the event was over when the strongest surges (1.8 m peak to trough) arrived around 2:15 PM. They were fortunately able to get to safety as the docks began breaking up. Wave activity continued with amplitudes on the order of 0.5 m for more than 8 hours, through the next high tide cycle. As a result of the November 15 event, interim procedures were adopted by the Tsunami Warning Center to provide advice if forecasts indicate that tsunami water heights may approach warning- level thresholds. On January 13, 2007 a similar Kuril event occurred and hourly conferences between the warning center and regional weather forecasts were held with a considerable improvement in the flow of information to local coastal jurisdictions.

Keywords: tsunami, crescent city, mitigation

(S) - IASPEI - *International Association of Seismology and Physics of the Earth's Interior*

JSS002

Oral Presentation

1774

Potential landslide tsunami waves offshore Ischia island, (Italy)

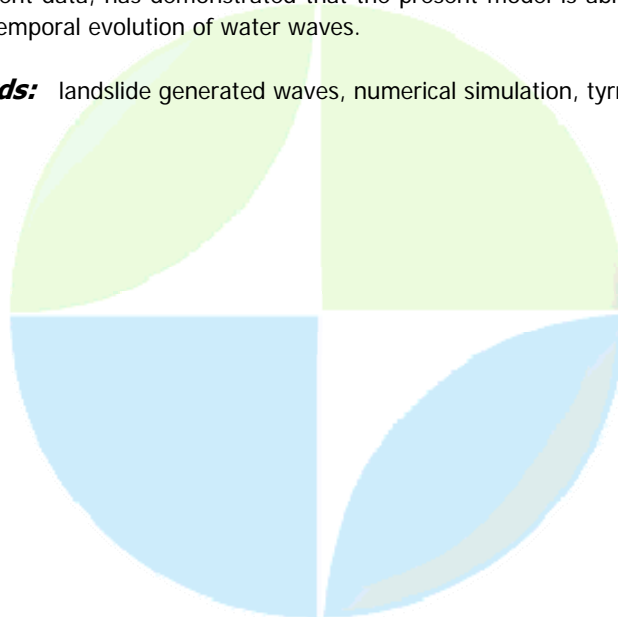
Dr. Violante Crescenzo

IAMC-CNR Institute for Coastal Marine Environments National Research Council IAHS

Chiara Biscarini, Silvia Di Francesco

Recent submarine explorations at Ischia island, a volcanic complex located north-west of the Gulf of Naples, Italy, showed evidences of debris avalanches and catastrophic collapses including an amphitheatre scar to the south, and hummocky deposits in the southern, western and northern offshore. The island is characterised by a series eruptions that continuously modified its morphology, and by an high rate of tectonic uplift of the central sector, the Mt Epomeo, that has raised up to 780 m in the past 30 ky with an average rate of 20 mm/y. The studied mass movements in the form of mud-debris flows, debris slides, rock-falls and debris avalanche radiate from Mt Epomeo as a consequence of its volcano-tectonic uplift and have an age spanning from prehistory to the present. Debris volumes range from 0.1 km³ from smaller events to more than 2-3 km³ for the largest avalanche, whose run-out is probably larger than 45 km as deduced from large blocks occurring in the southern continental slope until 1100 m depth. In the northern offshore an engraved fan-shaped valley, likely related to the emplacement of a very recent landslide event, is laterally constrained to the west by a relevant depositional levee. For all these events, large masses of volcanic material have entered the sea both in shallow waters and in deep waters likely producing tsunami waves spreading all over the Tyrrhenian sea and possibly into the bay of Naples. To test we work out a 3D simulation of the potential tsunami event associated to one of the major landslide events. The numerical model is based on geological data, so that the fluid dynamic simulation allows to investigate, evaluate and represent the three-dimensional water waves generation and propagation resulting from landslide phenomena. The problem is schematised as a multiphase multicomponent fluid flow (compressible air, water and landslide material) and the numerical tool is a finite volume transient fluid dynamics model based on coupling mass and momentum conservation (Navier Stokes) equations to a Volume Of Fluid (VOF) model, which actually keeps and updates the field of volume fraction of one fluid in each cell and is widely used to track the interface of two immiscible fluids, such as water and air. A previously performed validation with both laboratory and real event data, has demonstrated that the present model is able to predict with a high level of accuracy the temporal evolution of water waves.

Keywords: landslide generated waves, numerical simulation, tyrrhenian sea



(S) - IASPEI - *International Association of Seismology and Physics of the Earth's Interior*

JSS002

Oral Presentation

1775

Tsunami moment magnitudes (Mwt) of the 1 April 1946 Unimak and the 28 March 1964 Alaska tsunamis

Dr. Liujuan Tang

NOAA Center for Tsunami Research Research Scientist

Vasily V. Titov, Christopher Chamberlin, Yong Wei, Michael Spillane

Previous studies of seismic, geodetic and water-level data have provided the possible sources for some destructive tsunamis in Pacific (Kanamori and Ciper, 1974, Johnson et al, 1994, 1996, Johnson and Satake, 1999). Derived based on low-resolution tsunami propagation models, most of these source estimates are subject to debate and adjustment. NOAA Center for Tsunami Research (NCTR) is developing the next generation tsunami forecast system and implementing it at NOAAs Tsunami Warning Centers (TWCs). It includes DART detection, inversion to a pre-computed propagation database, and site-specific inundation forecasts by Stand-by Inundation Models (SIMs). The propagation database contains of 836 synthetic unit tsunami scenarios at the major subduction zones in Pacific Ocean, using the Method of Splitting Tsunami (MOST) numerical model. With resolution of 60-90 meter in nearshore area, SIM is optimized for speed and accuracy to provide 4-hour event inundation forecast less than 10 minutes. In addition, a Reference Inundation Model (RIM) with higher resolution of 10-30 meter was also developed to provide numerical references for each SIM, as well as a useful tool for tsunami hazard mapping projects. The components of the forecast system provide a unique chance to re-investigate the historical destructive tsunamis by inversion of the coastal water level data with the high-resolution quality inundation and propagation models. Application of this approach gives tsunami moment magnitudes of $M_{wt} = 8.5$, for 1 April 1946 Unimak tsunami and $M_{wt} = 9.0$ for the 28 March 1964 Alaska tsunami. Excellent model-observation comparisons, including first arrivals, wave periods and amplitudes for first waves of over 2 hours, are achieved at coastal tide stations in Hawaii, Alaska and U.S. West Coast respectively. Modeled inundation limit at Hilo for the 1946 tsunami agrees well with the observations.

Keywords: tsunami moment magnitude



(S) - IASPEI - *International Association of Seismology and Physics of the Earth's Interior*

JSS002

Oral Presentation

1776

Tsunamis Recorded on the Pacific Coast of Canada: 1994-2007

Mr. Fred Stephenson

Fisheries and Oceans Canadian Hydrographic Service IASPEI

Alexander B. Rabinovich

In the last 15 years there have been 14 tsunami events recorded at tide stations on the Pacific Coast of Canada. Ten of these events were from distance sources covering almost all regions of the Pacific, as well as the December 26, 2004 Sumatra tsunami. Three of the tsunami events were from local or near-field earthquakes and one was a meteorological tsunami. The earliest four events, which occurred in the period 1994 - 1996, were recorded on analogue recorders, and these tsunami records were recently re-examined, digitized and analysed. The other 10 tsunami events were recorded using digital instrumentation with one minute sampling intervals. Each of these tsunamis was recorded at two or more of the tide gauge stations, and all 14 of the events were recorded at Tofino and Bamfield on the outer B.C. coast. The tide station at Tofino has been in operation for 100 years and these recent observations add to the dataset of tsunami events compiled previously by S. Wigen for the period 1906-1980. For each of the tsunami records statistical and spectral analysis was carried out to determine the arrival times, amplitudes, frequencies and wave train structure. As a result of these observations, and the resulting analyses, it was confirmed that significant background noise at one key station creates serious problems in detecting tsunami waves. As a result, the station has now been moved to a new location with better tsunami response. The number of tsunami events observed in the past 15 years also justified re-establishing a tide gauge at Port Alberni, where large tsunami wave amplitudes were measured in March 1964. The data obtained at Port Alberni during future tsunami events will increase our understanding of tsunami response at this location, as well as other similar locations at the heads coastal inlets.

Keywords: observations, canada, pacific



(S) - IASPEI - *International Association of Seismology and Physics of the Earth's Interior*

JSS002

Oral Presentation

1777

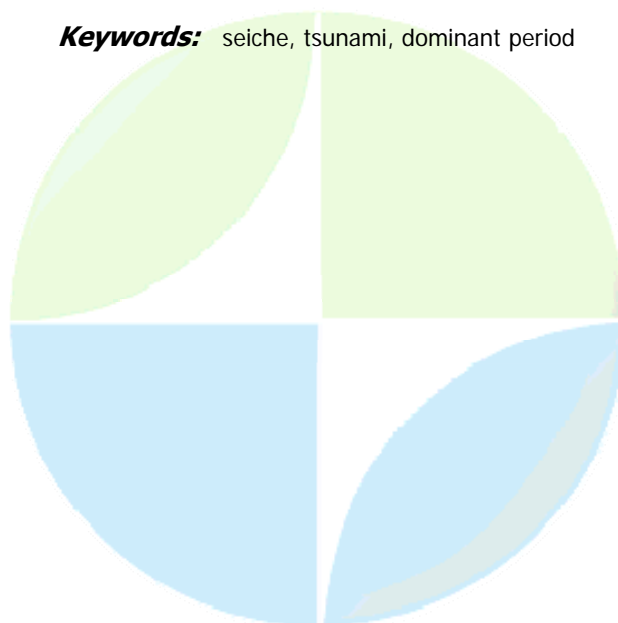
Observations of Seiche at Japanese coast in the Japan Sea and the significance to tsunami amplification

Prof. Kuniaki Abe

dental hygien Niigata Junior College, Nippon Dental University IASPEI

In situ observations of seiche were conducted at 55 points of bay heads and ports facing to the Japan Sea in . Sea level was detected with a pressure gauge for 6 hours per point in time interval of 1 minute and the total data was prepared in the period from November 11, 2002 to December 25, 2006. The time histories were decomposed into amplitude spectra and the most dominated period component was identified for each observation point. The result shows that the values vary from 7 to 167 min and level of 10 minutes occupies 25 % in all the observation points. These periods are approximated to ones of the fundamental mode under the consideration of the length and the sea depth. Moreover, the frequently observed periods of 10 to 30 minutes correspond to typical periods of tsunamis which are excited by large earthquakes, especially in . Therefore, we studied a relation of the dominant period with one of tsunami in bays and ports. We used tide gauge records of tsunamis observed in the 1993 Hokkaido nanse-oki, the 1983 Nihonkai chubu and the 1964 Niigata Earthquakes. Responses of tide stations were reduced based on the recovery time obtained by Satake et al.(1988). The amplitude spectra were calculated for the record of 6 hours from the earthquake origin time with the same method as for the seiche. Selecting 30 seiches observed at the neighborhoods of the tide stations we compared the dominant periods with ones of the tsunamis observed at the same bays. Appearance of the same dominant period between seiche and tsunami at the same bay was counted for all the observation points in each tsunami. The same period of seiche was defined for the period within the error of 50 %. The ratios reach to 38, 44 and 8% for 1993, 1983 and 1964 tsunamis, respectively. This value is an indicator of resonance of tsunami to bay and port. The difference is caused by one of typical period mainly related to source size and sea depth in the source. In this case sea depth is an important factor. The typical sea depths are 3000, 2000 and 70 m for 1993, 1983 and 1964 tsunamis, respectively (Abe, 2007). It is concluded that the difference directly is reflected to one of period and brought the difference of resonance.

Keywords: seiche, tsunami, dominant period



(S) - IASPEI - *International Association of Seismology and Physics of the Earth's Interior*

JSS002

Oral Presentation

1778

The Kuril Island Tsunamis of 15 November 2006 and 13 January 2007: A comparative analysis

Dr. Richard Thomson

Department of Fisheries and Oceans Institute of Ocean Sciences

I.V. Fine, A.B. Rabinovich, E.A. Kulikov

Two major tsunamigenic earthquakes have recently occurred near the Central Kuril Islands . The trans-Pacific tsunami generated by the $M_w = 8.3$ earthquake of 15 November 2006 was the largest since that generated by the 1964 Alaska earthquake. Wave heights exceeding 1 m were recorded as far as the Hawaiian Islands, Oregon, California and . Significant damage took place in the port of Crescent City (California) located roughly 6600 km from the source. Maximum waves recorded at this site were up to 177 cm. Marked tsunami signals were identified in records from the Kuril Islands, Japan, Alaska, Canada, Peru, New Zealand and various Pacific islands. Two months later, on 13 January 2007, a $M_w = 8.2$ earthquake occurred in the same region with a source located slightly seaward from the source of the November 2006 earthquake. Although weaker than the 2006 tsunami, the 2007 tsunami was also clearly recorded at many sites in the Pacific Ocean, including the Kuril, Aleutian, and Hawaiian islands, California and . Both tsunamis have been examined in detail using coastal tide gauges, bottom-pressure open-ocean stations and satellite altimetry. Numerical models have formulated for both events. Simulated tsunami wave forms were found to agree closely with the offshore island and deep-ocean DART records. The energy flux of the waves was mainly directed southeastward toward the Hawaiian Islands and . A pronounced feature of both tsunamis was their high-frequency content, with typical wave periods from 5 to 20 minutes. Dispersion was found to play an important role in the propagation and transformation of these waves. Despite their similarities, the two tsunamis were markedly different and even had opposite polarity in that the first trans-Pacific wave for the first event was positive while that from the second event was negative.

Keywords: kuril islands



(S) - IASPEI - International Association of Seismology and Physics of the Earth's Interior

JSS002

Oral Presentation

1779

A comparison of tsunamis in Caribbean and Mediterranean; history, possibility, reality

Prof. Ahmet Cevdet Yalciner

Civil Engineering Ocean Engineering IAPSO

Efim Pelinovsky, Tania Talipova, Narcisse Zahibo, Andrey Zaitsev, IRina Didenkulova, Ceren Ozer, Isil Insel, Hulya Karakus, Andrey Kurkin, Irina Nikolkina

The Caribbean sea is one of the biggest marginal seas in the planet and located in between latitudes 7oN and 23oN, and longitudes -88oE and -60oE. It is bordered on the North and East by the West Indies archipelago, on the South by South America mainland, and on the West by the Central American isthmus. The Caribbean sea is well known center of attraction with its tropical climate, storms, rain, clear waters, sun and reefs. The Mediterranean sea is one of the biggest marginal seas in the planet and located in between latitudes 30oN and 47oN, and longitudes -5oE and 43oW. It is bordered on the North and West by Europe, on the south by Africa, on the East by Asia. Sicily divides the sea to eastern and western basins. The Mediterranean sea is well known and is the center of attraction with its breeze, clear waters, sun and remnants of ancient civilizations. There are three main geographical features of the Caribbean Sea, which are i) Outer ring of mainly coral islands with white sand beaches from the Bahamas, to the Turks and Caicos, the Cayman Islands, ii) Inner ring of more volcanic islands, with black sands, includes the islands of the Greater Antilles - Cuba, Haiti, Dominican Republic and Puerto Rico. iii) The alluvial coast of Guyana, Suriname and French Guiana (Cayenne) on the South American mainland between the vast estuaries of the Orinoco and the Amazon. The fault zones around eastern Mediterranean basin are Hellenic Arc, North Anatolian Fault Zone (NAF), East Anatolian Fault Zone (EAF), Cyprus Arc, and Dead Sea Fault. There are series of volcanoes Vesuvius, Etna, Stromboli, Milos, Antimilos, Antiparos, Santorini, Christiana, Colombus, Kos, Yali, Nisiro and others in the Mediterranean. Hellenic arc is one of the important tsunami prone areas for the far old propagation of tsunamis. Numerous earthquakes and associated tsunamis in history in the Caribbean and Mediterranean seas seem as the precursor of the future similar events. In this study oceanographical, geographical, geological and geophysical characteristics of the Caribbean and Mediterranean Seas are presented and discussed briefly. For comparison the general characteristics of historical tsunamis occurred in both seas documented in literature are tabulated. The estimated zones of tsunami sources in relation to the earthquake activities are presented. The numerical modeling is applied to several different tsunami cases. For illustration of the generation, propagation and coastal amplification of tsunamis, the simulations of different tsunami scenarios for Caribbean and Mediterranean are developed, compared and discussed.

Keywords: tsunami, caribbean, mediterranean

(S) - IASPEI - International Association of Seismology and Physics of the Earth's Interior

JSS002

Oral Presentation

1780

The July 17, 2006 Central Java Tsunamis

Mr. Widjo Kongko

coastal dynamic research center agency for the assessment & application of techno.

Gegar Prasetya, Rahman Hidayat, Dinar C. Istiyanto, Sungsang U. Sujoko

The offshore area of the Java fore-arc from historical record had lack of moderate and large earthquake or low seismic potential, only the area between 109E to 112E is more active in the past, however, its relatively lack of shallow event. The 17th July 2006 earthquake with magnitude Mw 7.6 happened within that area and generated tsunamis. The tsunamis hit the south coast along the central Java Island and neighborhood shoreline and killed 650 people. From the field survey that had been done, the tsunamis consist of 3- 5 waves with interval from 5 to 10 minutes. The sea receding first, and the second waves was the highest. It takes 30 50 minutes for tsunamis to reach the coast and the waves run up and flow depth varies between 1 m to 4. 6 with exceptional wave run up were found at Nusa Kambangan Island about 10 20 m. This exceptional run up possibly due to second generating mechanism such as submarine slumping or landslide at the offshore of the Nusa Kambangan Island. The cause of many death tolls were possible due to the earthquake was not felt by most of the people who lived on the coast according to the eyewitnesses, however, it could be minimized if the warning system is operational within this region. Unfortunately, there is no warning had been issued, and the warning systems still not in place even though the Great Sumatran Earthquake and Tsunamis had already brought a lot of effort into the warning system in Indian Ocean region since it happened 2 years back. This event, again, a raise how important the integration of early warning system based on technology available and people who really had genuine commitments on this matter, and continuous education and preparedness of the people who lived along the coast that facing to the subduction zone. This implies the future re-development and hazards management of Indonesian Coast.

Keywords: central java tsunamis, warning system, hazards management



(S) - IASPEI - International Association of Seismology and Physics of the Earth's Interior

JSS002

Oral Presentation

1781

Archiving of tsunami event data

Dr. Laura Kong

International Tsunami Information Center IOC of UNESCO IASPEI

Charles S. McCreery

Since the 1990s, more than 15 tsunamis have been significant enough to cause damage locally or regionally. International post-tsunami survey teams have been deployed to collect measurements of runup, flow depth, inundation, scour, sediment deposits, and eyewitness observations of the arriving tsunami wave. At the same time, sea level time series recordings of tsunami events are sought out by scientists, who often first inquire to the tsunami warning centers, such as the Pacific Tsunami Warning Center (PTWC) in operation since 1949, since they are often the first to know that a tsunami has occurred. As a United Nations tsunami-dedicated information resource since 1965, the International Tsunami Information Center (ITIC) receives information starting immediately after the PTWC issues a watch or warning notification. Much of these data are shared with tsunami researchers and professionals through ITIC's Tsunami Bulletin Board list serve. The ITIC also regularly publishes a newsletter and hosts an event web site which starts to compile tsunami event information and data soon after an event occurs. For long-term archiving, the National Geophysical Data Center (NGDC), which hosts the World Data Center for Solid Earth Geophysics Tsunamis (WDC-Tsunamis), has the mission to preserve and archive relevant, quality-controlled data for all significant tsunami events. Recognizing the long-standing commitment of these three international organizations to tsunamis and the important value to researchers and hazard mitigation specialists of high-quality, verified, and authenticated information on tsunamis, the NGDC, ITIC, and PTWC propose to work collaboratively together to collect, synthesize, quality-control, catalogue, and archive all available data and observations from significant tsunami events. Within this context, a common standardized catalogue schema will be established by reviewing existing databases and soliciting input from data providers and users to determine a system that best meets everyone's needs. The group will seek input from the IUGG Tsunami Commission, its members, and especially its working groups that have been tasked to collect data from the December 26, 2004 tsunami. The effort plans to build upon and enhance existing capabilities and services of the NGDC and ITIC with the goal of developing more efficient and thorough mechanisms for seeking out data, for encouraging the contribution of observations by both scientists and the public, and for making quality collected information available to many in a user-friendly environment. In this talk, we will review the status of our quality control efforts and present tools for collaboration, user input, and data access.

Keywords: tsunami event, sea level data, archive

(S) - IASPEI - *International Association of Seismology and Physics of the Earth's Interior*

JSS002

Oral Presentation

1782

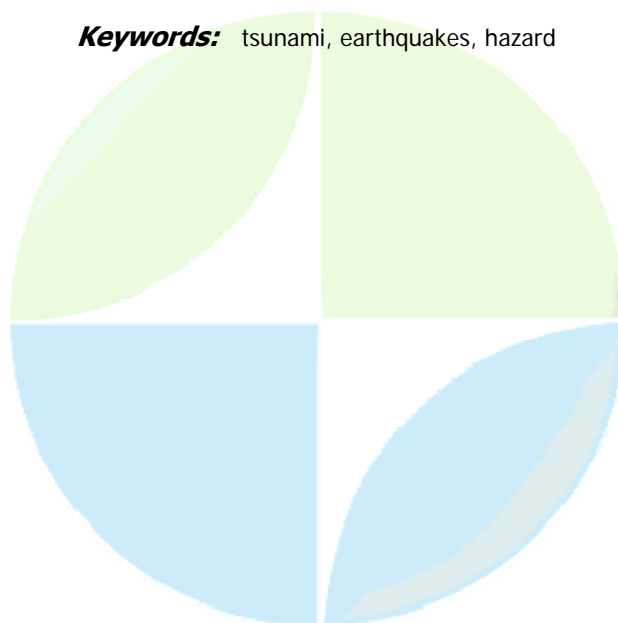
Probabilistic tsunami hazard analysis - results for the Pacific and Indian Oceans

Dr. Hong Kie Thio

Jascha Polet, Paul Somerville

We have developed a series of probabilistic tsunami hazard maps for the coasts of western North America Australia and along the Indian Ocean based on fault source characterizations of the circum-Pacific subduction zones as well as local offshore faults. The maps show the probabilistic offshore exceedance waveheights at 72, 475, 975 and 2475 year return periods, which are the return periods typically used in Probabilistic Seismic Hazard Analysis (PSHA). Our method follows along similar lines as (PSHA) which has become a standard practice in the evaluation and mitigation of seismic hazard in particular with respect to structures, infrastructure and lifelines. Its ability to condense complexities, variability and uncertainties of seismic activity into a manageable set of ground motion parameters greatly facilitates the planning and design of effective seismic resistant buildings and infrastructure. Because of the strong dependence of tsunami wave heights on bathymetry, we use a full waveform tsunami waveform computation in lieu of attenuation relations that are common in PSHA. By pre-computing and storing the tsunami waveforms at points along the coast generated for sets of subfaults that comprise larger earthquake faults, we can rapidly synthesize tsunami waveforms for any slip distribution on those faults by summing the individual weighted subfault tsunami waveforms. This Green's function summation provides accurate estimates of tsunami height for probabilistic calculations, where one typically integrates over thousands of earthquake scenarios. We have carried out tsunami hazard calculations for western North America and Hawaii, and based on a comprehensive source model around the Pacific and Indian Oceans. We will present the tsunami hazard maps and discuss how these results are used for probabilistic inundation mapping, including a follow-up inundation study of the San Francisco Bay area that is based on disaggregation results of the probabilistic analysis. We will also show that even for tsunami sources with large uncertainties (e.g. submarine landslides) a probabilistic framework can yield meaningful and consistent results.

Keywords: tsunami, earthquakes, hazard



(S) - IASPEI - *International Association of Seismology and Physics of the Earth's Interior*

JSS002

Poster presentation

1783

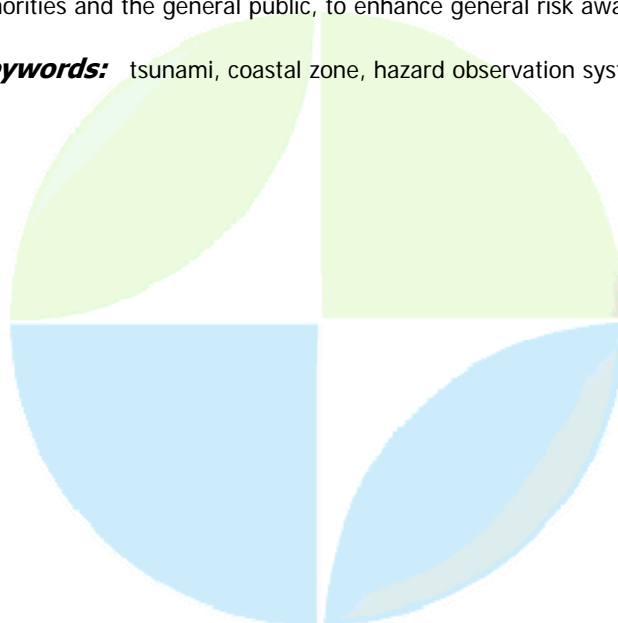
The Southeast Asia Tsunami Disaster Aftermath: Development of New Approaches to Coastal Zone Hazard Observation and Warning Systems

Prof. Evgeny Kontar

Experimental Methods Lab P.P.Shirshov Institute of Oceanology IAPSO

On January 2005 IOC/UNESCO and IUGG Tsunami and GeoRisks Commissions issued the statements on the greatest submarine earthquake and tsunami of the early 21st century and recommended that the countries around the Indian Ocean set up a Disaster Management Center and a warning system in order to monitor the Indian Ocean in relation to all kinds of natural hazards, especially those related to coastal regions. Assessment of potential of geo-hazards and their risks to populated coastal areas is becoming an important domain of scientific research and mitigation management. Coastal zone, shelf and continental slope are quickly becoming new major areas of industrial technological development owing to growing population in coastal regions and vast natural resources such as fish, oil, and gas available in these areas. Understanding risks of natural and human-made coastal zone hazards contributes to strengthening the scientific and technological basis of a number of industries including oil/gas production and transport. Traditional ways to evaluate risks of submarine earthquakes and tsunamis (e.g., through analyzing historic data) are often not comprehensive enough and may result in lower estimates of the actual risks of these hazards, while a combined approach developed recently at P.P.Shirshov Institute of Oceanology of the Russian Academy of Sciences provides more accurate evaluations, which may affect significantly human research and industrial activities in the coastal areas. We report here some new ideas, approaches and preliminary results in the development of tsunami warning systems based on a complex monitoring system using the deep-ocean cable installations and bottom observatories located in the vicinity of the oil and gas drilling platforms which are cable connected to data processing centers. Operation of such systems is to be combined with satellite survey as well as with scientific cruise investigations. Also we report here some results of the EU project which was designed to disseminate information to scientific and industrial communities on combined risks of submarine contaminated groundwater discharge, saltwater intrusion, coastal zone earthquakes, landslides, and tsunamis. This information can be introduced targetting potential risk groups, including local coastal zone authorities and the general public, to enhance general risk awareness.

Keywords: tsunami, coastal zone, hazard observation systems



(S) - IASPEI - *International Association of Seismology and Physics of the Earth's Interior*

JSS002

Poster presentation

1784

The simple model of Tsunami propagation simulator by using SITPROS Model

Dr. Wattana Kanbua

Thai Meteorological Department Director of Marine Meteorological Center IAPSO

Somporn Chuai-Aree

A new model for the tsunami propagation simulator is constructed. The boundary condition at the shore line is controlled by the total depth and can be set to the zero normal velocity. This model, with spatial resolution of two minute, is applied to the tsunami On December 26, 2004, 00:58 (UTC), 07:58 (Local Time, Thailand), a great earthquake occurred off the west coast of northern Sumatra, Indonesia. The magnitude of this earthquake was 9.0 and this was the fourth largest earthquake in the world since 1900. We deduce the shallow water wave equation and the continuity equation that must be satisfied when a wave encounters a discontinuity in the sea depth. Our procedure also includes a new mathematical model for tsunami generation, propagation, real-time simulation and visualization. The model is so called SiTProS (Siam Tsunami Propagation Simulator). Thailand is one of the countries affected by the Tsunami natural disaster on 26 December 2004. In order to provide up to the minute, precise prediction tsunami propagation simulator model with fast and accurate prediction.

Keywords: tsunami generation, tsunami propagation simulator, real time simulation

PERUGIA
ITALY



(S) - IASPEI - *International Association of Seismology and Physics of the Earth's Interior*

JSS002

Poster presentation

1785

Application of RS and GIS in Tsunami hazards assessment and Rehabilitation in Car Nicobar Islands

Dr. Arun Kumar

Department of Earth Sciences, Manipur University Associate Professor

Th. Dolendro

The present studies deal with the 26 December 2004 tsunami hazards assessment at Car Nicobar Island, located at a distance of 200 miles approximately from the epicenter of the Great Indonesian Earthquake (M9.3). A considerable part of the island has been damaged as a result of the Great Earthquake triggering and followed by Great Tsunami events. The application of Remote Sensing and GIS techniques is used to characterize the tsunami damages. The IRS 1D LISS- 3 (Pre) and IRS P-6 (Post) digital data are used to assess the changes in the various coastal features of the island. The tsunami height, run up elevation, water flow direction, erosion, sand deposition, and coastal subsidence are main indicators for the main aspects of the damages assessment. The digital image processing of the pre and post satellite data is carried out, which is supplemented with the detailed field studies at the island. The digital elevation model (DEM) is generated to demarcate the water inundation, flow direction and extent of the sea water submergence. 10-15 meters of water inundation on the island is marked and the flow direction of tsunami water is observed along the NW and SE direction by using 1 meter DEM. The existing beaches are now extended by 60 meters as sediment deposition on the SW part while 152.54 meter width of the beach is inundated on its SE part of the island. The new sand deposition at Kakana and Aukchung beaches are of 2.5 meters high and 10-12 meters wide, which is observed by comparing the pre and post satellite data. Similarly, the submergence at Malacca beach is 1.25 meters which has caused 170 meters wide stretch of the beach into permanent submergence. This submergence has also caused the loss of coral at Malacca beach. There are evidences for the earlier tsunami events based on the study of sand pits at island. The modeling of the tsunami run up and topography of the island has been attempted. There is good correlation between the tsunami run up, inundation distance and tsunami height. The application of GIS has been made in demarcating the safer sites for rehabilitation work in the island. The erstwhile villages on the island were located within the 1 km distance from the sea, therefore, the minimum distance of 1 km has been proposed for rehabilitation of the villages. The 1 km zone has been used for the plantation by various district level authorities. The application of remote sensing and GIS is proved to be very useful in assessment of tsunami hazards as well as rehabilitation measures in the island.

Keywords: tsunami, assessment, rehabilitation

(S) - IASPEI - *International Association of Seismology and Physics of the Earth's Interior*

JSS002

Poster presentation

1786

Restoration of Tsunami Incident by Remote Measurements of the Surface Water Oscillations

Dr. Tatiana Voronina

JSS002 Inst. of Comput. Math. & Mathem. Geophysics SD RAS IASPEI

During the past few years, the tsunami events that occurred in the Pacific and the Indian Oceans had caused to turn to on the inverse tsunami problem. The inversion problem to infer the initial sea perturbation is considered as a usual ill-posed problem of the hydrodynamic inversion of tsunami tide-gage records. Mathematically, this problem is formulated as inverse problem of mathematical physics for restoration of the initial water displacement in the source area by the water level oscillations observed at a number of points distributed in the ocean. We assume that the time dependency of the source function to be described by the Heavyside function. The forward problem, i.e. the calculation of synthetic tide-gage records from the initial water elevation field, is based on a linear shallow-water system of differential equations in the rectangular coordinates. This system is approximated by the explicit-implicit finite difference scheme on a uniform rectangular grid, so the system of the linear algebraic equations is obtained. The ill-posed inverse restoration problem is regularized by means of the least square inversion using the truncated SVD approach. In this method, the inverse operator is regularized with the help of its restriction on the subspace spanned on a finite sample of the first right singular vectors. The so-called r-solution is a result of the numerical process. The quality of the solution obtained is evaluated as relative errors (in L_2 -norm) in restoration of the source function. The results are fairly satisfactory, if the receivers have a good azimuthally coverage with respect to source area. It is necessary to recognize that the results obtained strongly depend on the signal-to-noise ratio due to the ill-posedness of the problem. As a model of initial water displacement we used displacement representing the bottom deformation due to the typical tsunamigenic earthquakes with reverse dip-slip or low-angle thrust mechanisms. This paper represents the algorithm of the solution of the inverse problem dealing with an arbitrary bottom topography having some basic morphological features typical of the island arc regions with inner and outer boundaries. We have shown that to attain a reasonable quality of the source restoration in this case we need, at least seven records distributed over the space domain and their azimuthally coverage plays the key role in obtaining the satisfactory results of inversion. The algorithm proposed enables us to evaluate the potential of a certain observation system in restoring the initial tsunami waveform.

Keywords: ill posed inverse problem, numerical modeling, regularization

(S) - IASPEI - *International Association of Seismology and Physics of the Earth's Interior*

JSS002

Poster presentation

1787

Processes affecting tsunamis propagating towards wide continental shelves, and their role in coastal impacts

Dr. Chris Wilson

K. J. Horsburgh, B. J. Baptie, A. Cooper, D. Cresswell, R. M. W. Musson, L. Ottemoller, S. Richardson, S. L. Sargeant

We investigate the propagation of tsunamis, towards the European shelf break, from a source at the Azores-Gibraltar Fault Zone in order to explore aspects of oceanographic interest for tsunami propagation over a broad continental shelf. We use six different initial conditions, based on the November 1755 Lisbon earthquake, to force a nested model of the northeast Atlantic. The sensitivity of tsunami propagation to tides, Earth's rotation, and topographic forcing is examined. Our results show that topographic features at the shelf edge interact with the almost planar wave front, forming complex intensified beams. The practical consequences of this interaction are highly variable wave heights around affected coasts over very local scales. Despite this, wide continental shelves afford a degree of protection from tsunamis. Due to refraction and wave spreading only a fraction of the tsunami energy reaches the northwest European shelf, which itself provides a further buffer through reflection and frictional dissipation. We find that even with an earthquake of magnitude 8.7 Mw, and a fault orientation favourable to northward energy transfer, the hazards for European shelf seas are comparable to those during winter storm conditions. The uncertainties arising from the combination of source orientation and bathymetric interaction suggest that any assessment of tsunami risk, for places where they are likely, should consider a large ensemble of initial conditions.

Keywords: tsunami, shelf, model



(S) - IASPEI - *International Association of Seismology and Physics of the Earth's Interior*

JSS002

Poster presentation

1788

The potential use of coastal tide gauge data in the Australian Tsunami Warning System

Mr. Stewart Allen

Bureau of Meteorology Research Centre Australian Bureau of Meteorology IASPEI

Diana Greenslade

The Australian Bureau of Meteorology (the Bureau), in conjunction with Geoscience Australia is currently developing an operational tsunami warning system. One planned component of this warning system is to run a numerical tsunami model in real-time, initialised with seismic information and assimilating sea-level data. DART buoys are typically located offshore in deep water and provide an ideal data stream that can be assimilated into a tsunami propagation model. The Bureau is currently also expanding and enhancing its coastal tide gauge network. These tide gauges provide another data stream that can be used for model verification and could potentially also be used for data assimilation. Tide gauges are almost always in enclosed harbours, bays or ports and the variability seen in tide gauge records of tsunamis will contain variability due to the tsunami interacting with the local small-scale topography, e.g. shoaling, seiching, reflections, diffraction, refraction, wave-breaking etc. These effects are not represented in the relatively coarse resolution of a tsunami propagation model. The relationship between the signal of a tsunami at a tide gauge and the offshore wave is strongly dependent on location and determining the relationship between the two is a challenge. There is therefore a need to analyse the tide gauge signal and location to determine what, if any, characteristics of a tsunami can be extracted from the observed signal and used for model verification and/or assimilation. In this presentation, initial results from an analysis of some existing Australian tide gauge data will be presented.

Keywords: tsunami, tidegauge, modelling



(S) - IASPEI - *International Association of Seismology and Physics of the Earth's Interior*

JSS002

Poster presentation

1789

Tsunami sources of November 2006 and January 2007 Kuril earthquakes

Dr. Yushiro Fujii

IISEE Building Research Institute IASPEI

Kenji Satake

We have performed tsunami simulations for the Kuril earthquakes which occurred on November 15, 2006 (46.577N, 153.247E, Mw=8.3 at 11:14:16 UTC according to USGS) and January 13, 2007 (46.288N, 154.448E, Mw=8.2 at 04:23:20 UTC according to USGS), and found that the seismic moment of the Nov. 2006 event was larger than that of the Jan. 2007 event. The tsunamis generated by these two earthquakes were recorded at many tide gauge stations located in and around the Pacific Ocean. The DART buoy systems installed and operated in deep oceans by National Oceanic & Atmospheric Administration (NOAA) also captured these tsunamis. We have collected and downloaded the tide records at 90 or more stations from Japan Meteorological Agency (JMA), Japan Coast Guard (JCG), Geographical Survey Institute (GSI), Sakhalin Tsunami Warning Center (STWC), West Coast & Alaska Tsunami Warning Center (WCATWC), NOAA and their web sites. The observed tsunami records indicate that the Nov. 2006 tsunami was twice or three times larger than that of the Jan. 2007 tsunami. For the tsunami simulation, we adopted the following fault models. For the Nov. 2006 event, the fault model is based on Global CMT solution (strike: 214, dip: 15, rake: 90, length: 200 km, width: 100 km, average slip: 4 m, rise time (source duration): 100 s). For the Jan. 2007 event, the fault model is based on Yagis model (strike: 215, dip: 45, rake: -110, length: 160 km, width: 40 km, average slip: 5 m, rise time: 50 s). The seismic moment ratio for these fault parameters is 2.5:1, assuming the same rigidity. The computed tsunami waveforms from the above fault models explain well the observed ones at most of tide and DART stations, indicating that the seismic moment of the Nov. 2006 event was twice or third times larger than the Jan. 2007 event.

Keywords: kuril earthquake, tsunami source, tide gauge data



(S) - IASPEI - *International Association of Seismology and Physics of the Earth's Interior*

JSS002

Poster presentation

1790

Simulation of tsunami propagation in Arabian Sea due to earthquakes in Makran: a possible scenario

Dr. Vijay Prasad Dimri

National Geophysical Research Institute, India Director, N.G.R.I., India

Kirti Srivastava, D.Srinagesh

The Makran subduction zone is seismically active and the notable earthquake from this region is the great earthquake of Mw 8.1 which occurred on 27th November 1945. The unique nature of the Makran subduction zone is that it has been divided into two segments based on morpho-tectonic features and the contrasting features in seismicity patterns and the varying rupture histories between the eastern and western segments. The eastern Makran has experienced large thrust earthquakes and continue to experience small to moderate sized thrust earthquakes whilst the western Makran has no established historical records of any large earthquake in the historic times or the modern instrumentation. The absence of notable interplate seismicity in western Makran could be due to varying alternatives like the plate boundary is locked or the subduction is a seismic in nature. In view of the alternating hypothesis for the occurrence of great earthquakes along the 900 km long Makran subduction zone we have carried out a simulation study to assess the potential of a Tsunami hazard along the west coast of India by considering different sources for the above region. The 1945 earthquake was used in simulating the tsunami and estimating the height of the Tsunami at various gauge locations and its arrival time at these gauges. The significant results from this study show that the Tsunami wave heights at different gauge locations in the west coast of India vary from 0.2-0.8 m. However, if the wave travels onto the land the heights of the Tsunami wave would be 8-10 times larger than the estimated gauge height. We have also analyzed the potential of Tsunami hazard due to an earthquake in the locked western Makran and estimated the wave heights at different gauge locations on the West coast of India.

Keywords: makran, tsunami, wave height



(S) - IASPEI - *International Association of Seismology and Physics of the Earth's Interior*

JSS002

Poster presentation

1791

Tsunami deposits in the western Mediterranean: the remains of the 1522 Almera earthquake

Prof. Klaus Reicherter

Neotectonics and Natural Hazards RWTH Aachen University

Peter Becker-Heidmann

The 1522 Almera earthquake ($M > 6.5$) affected large areas in the western Mediterranean and caused more than 2000 casualties. Different epicentral areas have been suspected, mainly along the 50 km long sinistral Carboneras Fault Zone (CFZ), however no on-shore surface ruptures and paleoseismological evidences for this event have been found. High-resolution sea floor imaging (narrow beam sediment profiler) yields evidence for an offshore rupture along a strand of the CFZ that is supported by evaluation of historic documents. Based on these data, a new epicentral area precisely at the observed sea floor rupture area is proposed at N 36 42, W 2 23 in the Gulf of Almera. Drilling in lagunas and salinas of the Cabo de Gata area proved sedimentary evidence for paleo-tsunamis along the Spanish Mediterranean coast. Several coarse grained intervals with fining-up and thinning-up sequences, rip-off clasts, broken shells of lamellibranchs and foraminifera show erosive bases. The coarse-grained intervals show up to three sequences divided from the next one by a small clayey layer. These intervals are interpreted as a tsunami trail and correspond to three individual waves. We have also found multiple intercalations of those tsunamites downhole, which is interpreted as either an expression of repeated earthquake activity or tsunami-like waves induced by submarine slides triggered seismic shaking in the Gulf of Almera. The coast of southern Spain, the Costa de Sol, is one of the touristic hot spots in the Mediterranean Europe and very densely populated. Hence, the impact on the vulnerability is of great concern for society and economy, considering destructive earthquakes in costal residential and industrial areas, especially a holiday and recreation area in the western Mediterranean region. Our evidence suggests a certain tsunami potential and hazard for offshore active and seismogenic faults in the western Mediterranean region.

Keywords: tsunamites, tsunami deposits, western mediterranean



(S) - IASPEI - International Association of Seismology and Physics of the Earth's Interior

JSS002

Poster presentation

1792

New theory for tsunami propagation and estimation of tsunami parameters

Dr. Ilia Mindlin

Applied Mathematics State Technical University of Nizhny Novgorod, Rus IAPSO

A numerable set of specific basic waves on the sea surface are found analytically. It is shown that any tsunami is a combination (not superposition: the waves are nonlinear) of the basic waves, and, consequently, the tsunami source (i.e., the initially disturbed body of water) can be described by the numerable set of the parameters involved in the combination. In this way, the problem of theoretical reconstruction of a tsunami source is reduced to the problem of estimation of the parameters. The tsunami source can be modelled approximately with the use of a finite number of the parameters. Two-parametric model is discussed thoroughly. A method is developed for estimation of the model's parameters using the arrival times of the tsunami at certain locations, the maximum wave-heights obtained from tide gauge records at the locations, and the distances between the earthquake's epicentre and each of the locations. In order to evaluate the practical use of the theory, four tsunamis occurred in Japan are considered. For each of the tsunamis, the tsunami energy, the duration of the tsunami source formation, the maximum water elevation in the wave originating area, dimensions of the area, and the average magnitude of the sea surface displacement at the margin of the wave originating area are estimated on the basis of data recorded by tide gauges. The results are compared (and, in the author's opinion, are in line) with the data known from the literature. It should be mentioned that, compared to the methods employed in the literature, there is no need to use bathymetry (and, consequently, refraction diagrams) for the estimations. The present paper follows earlier works [1, 2] very closely and extends their theoretical results. Example. The following notations are used below: E for tsunami energy (in Joules), H for the maximum water elevation in the wave originating area (in metres), R for the mean radius of the wave origin, h for the averaged magnitude of the sea surface displacement at the margin of the wave origin (in centimetres), T for the duration of the tsunami source formation (in seconds). Variant a): estimates obtained using a model of tsunami generated by initial free surface displacement; variant b): estimates obtained using a model of tsunami triggered by a sudden change in the velocity field of initially still water. The asterisk shows that the value of the parameter is known in the available literature. The Hiuganada earthquake of 1968, April, 1, 9h 42m (J. S. T.) A tsunami of moderate size arrived at the coast of the south-western part of Shikoku and the eastern part of Kyushu. a) $E=1.91 \cdot 10^{12}$, $H=3.43$, $R=22$, $h=17.2$; b) $E=8.78 \cdot 10^{12}$, $H=1.38$, $R=20.4$, $h=9.2$, $T=16.4$; $E^*=1.3 \cdot 10^{13}$ ([3], attributed to Hatori), $E^*=(1.4 \ 2.2) \cdot 10^{12}$ ([3], attributed to Aida), $R^*=21.2$, $h^*=20$ [4] (variant a) since was obtained by means of inverse refraction diagram.) 1. Mindlin I.M. Integrodifferential equations in dynamics of a heavy layered liquid. Moscow: Nauka*Fizmatlit, 1996 (Russian). 2. Mindlin I.M. Nonlinear waves in two-dimensions generated by variable pressure acting on the free surface of a heavy liquid. J. Appl. Math. Phys. (ZAMP), 2004, vol.55, pp. 781 - 799. 3. Soloviev S.L., Go Ch.N. Catalogue of tsunami in the West of Pacific Ocean. Moscow, 1974 (Russian). 4. Hatory T., A study of the wave sources of the Hiuganada tsunamis. - Bull. Earthq. Res. Inst., Tokyo Univ., 1969, vol. 47, pp. 55-63.

(S) - IASPEI - International Association of Seismology and Physics of the Earth's Interior

JSS002

Poster presentation

1793

Modeling of the UHF Radar signature of a tsunami approaching coastal areas: application to tsunami warning

Prof. Stephan Grilli

Department of Ocean Engineering University of Rhode Island

Marc Saillard, Sara Dubosq

During the catastrophic 12/26/04 tsunami, perhaps for the first time, satellite remote sensing (radar altimetry) was able to provide transects of tsunami elevation across the Indian Ocean while the event unfolded (e.g., Jason 1). Here we similarly use well established Ultra High Frequency (UHF) radar technology, to develop a method that could provide warning of an incoming tsunami to coastal populations. When a tsunami reaches the continental shelf, the mostly depth-uniform current it induces, indeed greatly increases in speed (maybe up to 10-20 cm/s) and starts causing significant Doppler shifts in ocean surface waves, particularly those of smaller wavelength (high frequency). Such shifts may be recognized as a typical signature, by a shore-based UHF radar, and thus trigger a warning, provided proper numerical simulations and sensitivity analyses have been performed ahead of time. Since tsunamis very much slow down due to decreasing water depth, from the shelf break to shore, warning times 5-15 minutes could be conceivable, depending on the shelf width. Here, we use a Higher Order Spectral (HOS) Method to model fully nonlinear sea states caused by wind, down to typical UHF wavelength of order 10 cm, as well as Doppler shifts and wave shoaling and refraction caused by a slowly varying depth uniform current. The latter current is obtained from tsunami propagation modeling, using a standard long wave model, for some selected case studies. UHF radar backscattering is modeled by a Boundary Element Method solving Maxwells equations, developed and validated in earlier work. We present initial results of this modeling study, in terms of spatio-temporal UHF radar signatures corresponding to some tsunami case studies. In particular, we apply this methodology to southern Thailand, based on earlier modeling work we performed for tsunami runup caused in Thailand for the 12/26/04 tsunami.

Keywords: tsunam modeling, remote sensing, warning systems



(S) - IASPEI - *International Association of Seismology and Physics of the Earth's Interior*

JSS002

Poster presentation

1794

Numerical modeling of tsunami waves in the French West Indies

Dr. Narcisse Zahibo

Physics Universitu Antilles Guyane IASPEI

Narcisse Zahibo, Efim Pelinovsky, Ahmet Yalciner, Andrey Zaitsev, Irina Nikolkina

Problem of tsunami risk for the French West Indies in Lesser Antilles (Caribbean Sea) is discussed. The catalogue of historic events is created, it includes the eighteen events are selected as true and almost true. Ten events have been generated by underwater earthquakes in Caribbean Sea; seven events - by the volcano eruptions in Lesser Antilles, and one is a teletsunami from the 1755 Lisbon earthquake. Numerical simulation of the several historic events (1755 Lisbon, 1867 Virgin Islands, 2003 Montserrat) in the framework of nonlinear shallow water equations is performed. Results of calculations are in good agreement with observed historic data.

Keywords: tsunami

XXIV2007

PERUGIA
I T A L Y



(S) - IASPEI - International Association of Seismology and Physics of the Earth's Interior

JSS002

Poster presentation

1795

Mechanism of damage to road embankment caused by tsunamis

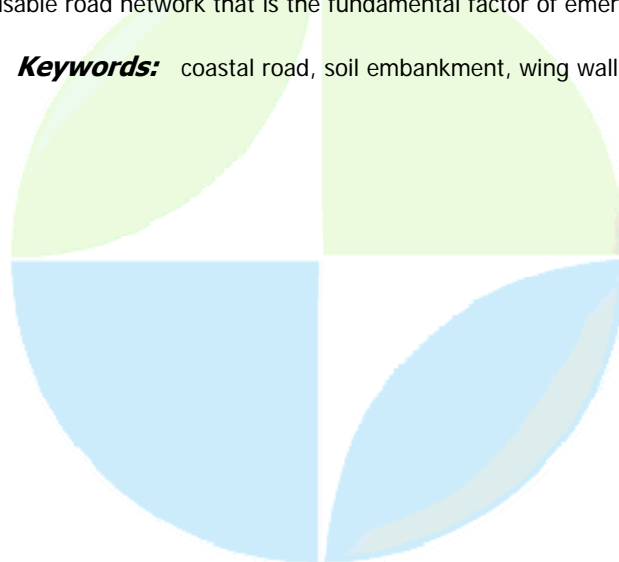
Mr. Hiroyuki Fujii

Dep. Coastal eng. INA corporation, Japan

Nobuo Shuto

The Golden 24 is a universal law to save many human lives when a catastrophic disaster occurs. Damage caused by such a huge tsunami as the 2004 Indian Ocean tsunami is a good example. It is quite important to send rescue teams, medical assistance and vital goods as many and as soon as possible to the damaged areas. In order to support such human activities in an emergency, a hardware, i.e., coastal roads, is a vitally necessary infrastructure. Among several causes of coastal traffic hindrance, the present paper aims to understand the physical mechanism of damage to road embankments made of soil in order to find how to reinforce or improve them. There are two major causes of damage to soil embankment. The one is scouring due to overflowing tsunami. The other is erosion near bridge abutment due to tsunamis that concentrate to openings. A rough estimate whether a road embankment made of soil would be damaged or not was given by one of the present authors as a function of the height of embankment and the overflow depth. In order to explain more in details, a numerical scheme to simulate the process of scouring is developed, on comparing with large-scale hydraulic experiments for river dikes for which the overflowing time is much longer compared to tsunamis. The hydraulic experiments carried out in the Public Works Research Institute, Ministry of Construction, revealed; (1) the critical depth appeared near the shoulder, then (2) the flow separated and reattached. (3) After the reattachment, the flow over the rear slope was supercritical. (4) When the flow hit the toe of embankment, high impact pressure was measured, and (5) a hydraulic jump appeared to return a sub-critical flow. This process is simulated in the numerical model by the present authors, except for the flow separation and reattachment near the shoulder. Calculated shear stress, if compared with the strength of the embankment soils, shows the area that should be covered by solid materials. When a tsunami is stopped by a road embankment of long extension, the flow concentrates toward openings such as rivers, canals and channels. The velocity of the concentrating flow is simulated to compute the shear stress on the embankment slope. The slope near the bridge abutments should be covered by such structure as wing walls to resist the tsunami-induced shear stress. This simulated result may give a measure of the length of the wing walls. The model proposed herein paper also provides a basis to examine the usable road network that is the fundamental factor of emergency response

Keywords: coastal road, soil embankment, wing wall



(S) - IASPEI - International Association of Seismology and Physics of the Earth's Interior

JSS002

Poster presentation

1796

Walking Tours by Use of Tsunami Digital Library (TDL)

Dr. Sayaka Imai

Department of Computer Science Gunma University

Yoshinari Kanamori, Nobuo Shuto

We are developing a Tsunami Digital Library (TDL) which can store and manage documents about tsunami, news paper articles, tsunami run-up simulations, field work data, videos, etc., in Japan. Every person interested in data about the tsunami can get the information through the internet. We also offer a multilingual interface. Currently some documents and explanations of tsunami videos have been translated into English and French. TDL is here (<http://tsunami.dbms.cs.gunma-u.ac.jp/>). We have proposed a public education on the tsunami disaster which utilizes TDL for citizens in coast areas struck by the tsunami. We can visualize the change of tsunami disasters by clicking coast areas on the map in TDL. This shows a kind of virtual walking tours in TDL, and also is an effective public education. We can plan some walking tours in TDL based on spatio-temporal domain, the region or the era in Japan. For example, if you have any interest in the 1896 Meiji Sanriku Great Tsunami, you can travel Sanriku prefectures on the map, and see a lot of records on the tsunami by clicking villages, towns or cities along coasts in those prefectures. On the other hand, if you want to know the tsunami disasters of all eras on a town, you have to input the town name as key word, and can obtain the records on all eras related with the town. Furthermore, TDL will also contribute to a public education for tourists who go very occasionally sightseeing in the areas struck by the tsunami. This means TDL supports an actual walking tour. We have developed the necessary TDL environments to support such walking tours as follows: (1) Keyword retrievals TDL uses XML technology. The documents containing figures, pictures and tables are represented in XML structure, and managed under an XML database system (Oracle 10g). The schemas of these documents depend on the type of the documents, reports or newspapers. Therefore, each document has a different schema. In order to make a traversal retrieval crossing whole documents, it is necessary to use a unified schema which integrates all schemas for XML documents. We have designed an integration schema by XML, and implemented the system to retrieve some requested data from TDL through keyword input on Web. (2) Retrievals by mobile phones When tourists visit the coast area struck by the tsunami, a lot of facts of the tsunami disasters are automatically retrieved from TDL and displayed on mobile phones to attract their attention. Therefore, it is necessary to retrieve the region name of the place where tourists are in. We have obtained the place information from the area code when we use the i-mode of NTT Docomo mobile phones. There are restrictions of the number of display characters and the computing powers in mobile phones. Then, we have to submit some remarkable contents, concerning the number of bodies, destroyed houses and ships, and a summary of the document to mobile phones. TDL for mobile phones is here (<http://tsunami.dbms.cs.gunma-u.ac.jp/iTDL/>)

Keywords: tsunami digital library, mobile phone, xml database

(S) - IASPEI - *International Association of Seismology and Physics of the Earth's Interior*

JSS002

Poster presentation

1797

Manifestations of the Indian Ocean tsunami of 2004 in satellite nadir-viewing radar backscatter variations

Dr. Yuliya Troitskaya

Institute of Applied Physics Institute of Applied Physics IAPSO

Stanislav Ermakov

The catastrophic tsunami of 26 December 2004 emphasized the need in a functioning global system of tsunami early warning. A space-borne system of tsunami monitoring would have been an ideal solution because of global coverage and instant access to the information. At present, the only known way of tsunami satellite remote sensing is via space-borne altimetry, which, unfortunately, is of limited practical value: to register a tsunami a satellite should be exactly above the wave in question. In this context, it would have been preferable to employ side-looking instruments providing large-scale panorama of the sea surface, for example, synthetic aperture radars. The latter are routinely used for registering signatures of atmospheric and oceanic phenomena caused by variations of the surface scattering properties mostly determined by the short wind waves (sea roughness). The key open question was, whether a tsunami can produce such a signature, that is, cause modulation of the short waves sufficient for instrumental registration. Here we report on the first experimental evidence for space-observed manifestation of the open ocean tsunami in the microwave radar backscatter (in C- and Ku-bands; wave-lengths 6cm and 2 cm respectively). Significant (a few dB) variations of the radar cross section synchronous with the sea level anomaly were found in the geophysical data record of the altimetry satellite Jason-1 for the track which crossed the head wave of the catastrophic tsunami of 26 December 2004. The simultaneous analysis of the available complementary data provided by the satellite three-channel radiometer enabled us to exclude meteorological factors as possible causes of the observed signal modulation. A possible physical mechanism of modulation of short wind waves due to transformation of the thin boundary layer in the air by a tsunami wave is discussed. The results open new possibilities of monitoring tsunamis from space.

Keywords: radar backscatter, tsunami, wind waves



(S) - IASPEI - *International Association of Seismology and Physics of the Earth's Interior*

JSS002

Poster presentation

1798

An Integrated Numerical Simulation for Tsunami and Seismic Wave Propagation Generated by Subduction-Zone Large Earthquakes

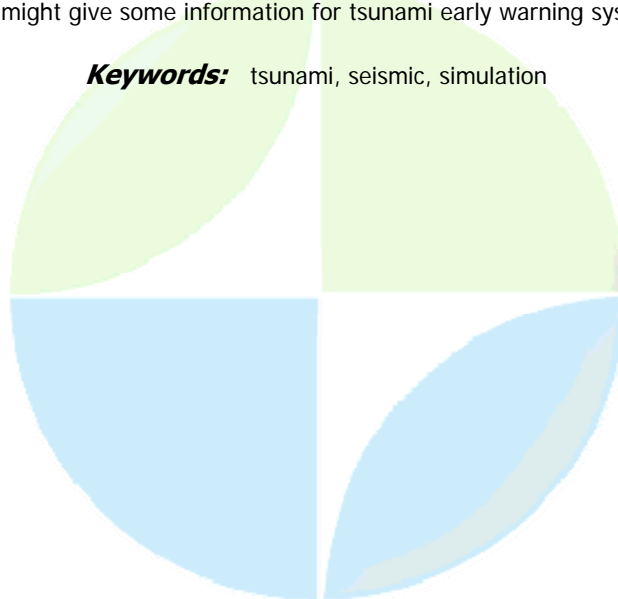
Dr. Tatsuhiko Saito

Earthquake Research Institute the University of Tokyo IASPEI

Takashi Furumura

We develop an integrated simulation model for tsunami and seismic wave propagation to make accurate prediction of tsunami disasters caused by subduction-zone earthquakes. We employ a 3D FDM simulation technique for evaluating the spatial and temporal deformation of sea floor caused by the earthquake, and the resultant vertical movement of the sea-floor deformation is used as tsunami source model. Unlike the conventional tsunami simulation models that usually assume a simple half-space subsurface structure and calculates static deformation of sea-floor, our new model includes the effects of 3D heterogeneous structure near the source region and dynamic deformation process of sea floor. In order to demonstrate the effectiveness of our new model, we conducted a seismic and tsunami simulation for the 1944 Tonankai earthquake (Mw8.1) that occurred in the Nankai Trough, Japan. At first, we calculated the seismic wavefield using a detail source rupture model for the earthquake and a 3D heterogeneous structure of the Nankai-Trough subduction zone. This model includes detail structure of the subducting plate and low-velocity oceanic sediment at the top of the plate. The FDM simulation for seismic wave takes about 100 minutes on the Earth simulator supercomputer using 24 nodes (192CPUs) of processors and 290GB of computer memory for evaluating seismic wave propagation of 200 s. Then, using the simulation results as tsunami source, we evaluate the tsunami propagation by FDM based on the linear long-wave theory. The tsunami simulation was conducted on a cluster of 16 AMD Opteron processors, which takes about 10 minutes for calculating 60 minutes of tsunami propagation. The seismic simulation using 3D structural model shows large deformation of the seafloor in localized region compared with that derived assuming homogeneous half-space structure. This is because, in inhomogeneous subsurface structure, the seismic strain is accumulated in small elasticity portion. As a result, tsunami wave of our simulation has larger maximum amplitude than that calculated with homogeneous half-space medium. Also, the deformation of sea floor associated with the Rayleigh waves also excites weak tsunami in the direction of fault rupture propagation as a forerunner of major tsunami signals which might give some information for tsunami early warning system.

Keywords: tsunami, seismic, simulation



(S) - IASPEI - International Association of Seismology and Physics of the Earth's Interior

JSS002

Poster presentation

1799

Tsunami waveform analysis for historical large tsunamis generated by the large earthquakes along the Kurile trench

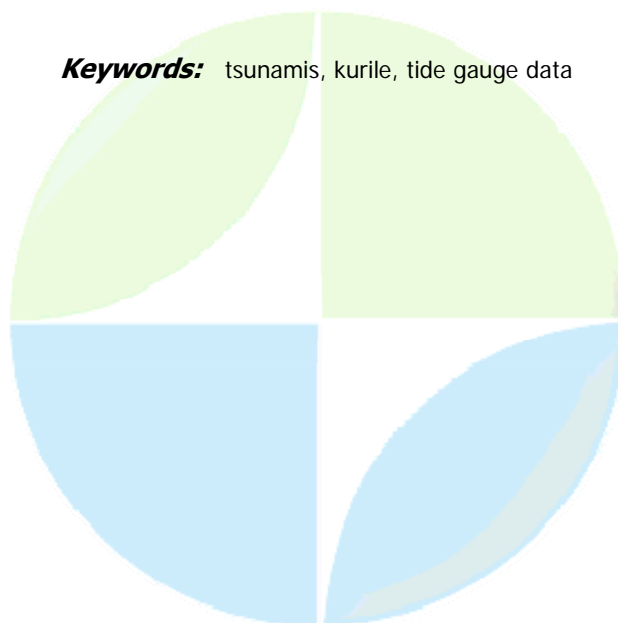
Prof. Yuichiro Tanioka

Institute of Seismology and Volcanology Associate Professor IASPEI

Kenji Satake, Paula Dunbar

Many large earthquakes have occurred along the Kurile trench due to subduction of the Pacific plate beneath the Kurile Islands, and large tsunamis have been generated by those earthquakes. The large earthquakes occurred in this region in the late 19 century or in the early 20 century are not well studied because of lack of seismological data. However, tsunami waveform data observed at tide gauges around the Pacific Ocean are available for some of those historical earthquakes. In this paper, we analyze the observed tsunami waveforms to study the source processes of those historical large earthquakes, especially the 1894 Nemuro-oki and 1918 Kurile earthquakes. The fault model of the 1894 Nemuro-oki earthquake is estimated using the observed tsunami waveform at Ayukawa in Sanriku, Japan. The most recent large earthquake in this area is the 1973 Nemuro-oki earthquake. The source model of the 1894 earthquake has to be compared with that of the 1973 Nemuro-oki earthquake. The tsunami numerical computation is carried out using the finite different approximation of the linear long-wave equations. By comparing the observed and computed tsunami waveforms, we conclude that the fault length of the 1894 Nemuro-oki earthquake is approximately 200 km, much larger than that of the 1973 Nemuro-oki earthquake, 40-80 km. The slip amount is estimated to be 2.4 m by comparison of observed and computed amplitudes between the largest peak and the first trough. The total seismic moment of the 1894 Nemuro-oki earthquake is 2.9×10^{21} Nm ($M_w 8.3$) by assuming the rigidity of 6×10^{10} N/m². This estimate is much larger than the estimated seismic moment of the 1973 Nemuro-oki earthquake. The 1918 large Kurile earthquake occurred off the central Kurile Islands. The epicenter of this earthquake is located at southwest of the source areas of the recent 2006 and 2007 large Kurile earthquakes. The tsunami waveforms for the 1918 earthquake are observed at three tide gauges in Japan, Kushiro, Choshi, and Chichijima. The tsunami waveforms are also observed at tide gauges in Honolulu, Hawaii, and in San Francisco. Those tsunami data are collected to analyze the source process of the earthquake.

Keywords: tsunamis, kurile, tide gauge data



(S) - IASPEI - *International Association of Seismology and Physics of the Earth's Interior*

JSS002

Poster presentation

1800

Evaluation of real-time simulation at 2006 and 2007 Kuril Islands Tsunami

Mr. Ikuo Abe

Disaster Control Research Center Tohoku University IASPEI

Fumihiko Imamura

When a tsunami was generated by the Kuril Islands earthquake $M=7.9$ on November 15, 2006, a tsunami warning was issued 15 minutes after earthquake shock in Japan, based on the JMA tsunami warning system. Although a tsunami warning was canceled about 5 hours later, maximum wave heights of a tsunami at several points were observed after this cancellation, and the damage of fishing boat such as overturn and sink were reported due to the maximum wave and current in the next morning. If a season, time and weather condition were different, the damage should be larger. Furthermore, an earthquake with tsunami occurred at neighboring location of 2006 on January 13, 2007. A warning continues for six hours and no damage was reported. However, maximum wave heights in the west coast of Japan were recorded. The sequence of two tsunamis suggests us several problems; accuracy of quantitative forecasting system, timing of canceling warning, damage on boats by current/vortex, and less than 10 % of evacuation at communities along the coast. We compiled there problems and issues in the tsunami warning and evacuation. In order to overcome such a problems, the tsunami warning system should be improved by taking consideration of evidences and issues in the 2006 and 2007 Kuril Islands tsunamis. Recently, a performance of computer becomes higher, and we can simulate more detailed information in a short time. As instance, we evaluated possibility of the real time tsunami simulation about Kuril Islands tsunami. In its evaluation, we used the information to be provided just after an earthquake shock, estimating magnitude, location and depth at several time stages, and try to estimate the errors at each step. As a result, we found that there was uncertainty of around 40% in initial conditions.

Keywords: realtime simulation, uncertainty, initial conditions



(S) - IASPEI - International Association of Seismology and Physics of the Earth's Interior

JSS002

Poster presentation

1801

Vulnerability of the Argentina coasts to tsunami effects

Dr. Roberto Antonio Violante

Argentina Hydrographic Survey IGCP 464 Argentina Delegate IAPSO

Walter Dragani

The Southwestern Atlantic coastal regions have been traditionally considered of low hazard probabilities of being affected by tsunamis. The main reason is the geotectonic emplacement in a stable, tectonically inactive, passive continental margin. However, some geological, topographical and oceanographic aspects of the region should be reviewed as they could favor the occurrence of destructive events or increase damage. The Scotia arc, located in the southernmost extreme of South America, is a highly dynamic convergent margin with frequent occurrence of earthquakes and volcanic eruptions. The most recent example was a 7.3 magnitude (Richter scale) earthquake occurred in 2003 with epicenter near Orcadas Islands (60.55S- 43.49W), which induced an ocean wave that was rapidly cushioned by the neighboring oceanic ice-field. The Argentina coasts were affected by the consequences of the 2004 Sumatratsunami. It produced small sea-level fluctuations measured at tide gauge stations in different coastal emplacements between 37 - 39S, where short waves in the tidal curves with maximum heights of 27 cm and wave periods between 20-120 minutes were recorded (Dragani et al., 2004). Also the neighboring Brazilian coasts recorded the phenomena (Frana and de Mesquita, 2006). Considering the configuration and relative geographical position of the Argentina coasts, the vulnerability to long ocean waves originated by submarine events like earthquakes, volcanic eruptions and slides in the Scotia Arc and surroundings cannot be rejected. The smooth and gently sloping continental shelf is a feature that can behave as a ramp for ocean waves approaching to the coast driven by either climatic or geological processes. The variable shelf width (decreasing from 600 to 170 km from South to North) and the morphology of the adjacent continental slope should be considered as probable factors affecting ocean waves movement. Regarding coastal morphology, there is an alternation of areas with different susceptibility to damaging effects coming from processes and events originated in the ocean. They are: a) low-lying regions located few meters above sea level (river mouths, deltas, estuaries, coastal plains, etc.), considered as probable hazard areas with high potential of populations damage; and b) high cliffed coasts elevated several tens of meters above sea level which should not offer any substantial risk except for their possibilities of suffering strong erosion and structural instability derived from it. The interplay between coastal and submarine morphology, oceanographic and climatic aspects as well as geological processes should be considered under an integrated perspective for evaluating the real potential of the region to the impact of tsunamis.

Keywords: tsunami, argentina continental margin, scotia arc

(S) - IASPEI - *International Association of Seismology and Physics of the Earth's Interior*

JSS002

Poster presentation

1802

South Java tsunami reconnaissance

Dr. William Power
Natural Hazards GNS Science

Stefan Reese, Jim Cousins, Neville Palmer, Iwan Tejakusuma, Saleh Nugrahadi

A team of scientists from GNS, NIWA and the Indonesian Agency for the Assessment and Application of Disaster Mitigation Technology (BPPT) undertook a reconnaissance mission to the South Java area affected by the tsunami of 17th July 2006. The team used GPS-based surveying equipment to measure ground profiles and inundation depths along 17 transects across affected areas near the port city of Cilacap and the resort town of Pangandaran. The purpose of the work was to acquire data for calibration of models used to estimate inundations, casualty rates and damage levels. Water depths were typically 2 to 4 m where housing was seriously damaged. Damage levels ranged from total for older brick houses, to about 50% for newer buildings with reinforced concrete beams and columns, and to 5-20% for multi-storey hotels with heavier RC columns. Punchout of weak brick walls was widespread. Death and injury rates were both about 10% of the population exposed.

Keywords: tsunami, java, reconnaissance

XXIV2007
PERUGIA
I T A L Y



(S) - IASPEI - International Association of Seismology and Physics of the Earth's Interior

JSS002

Poster presentation

1803

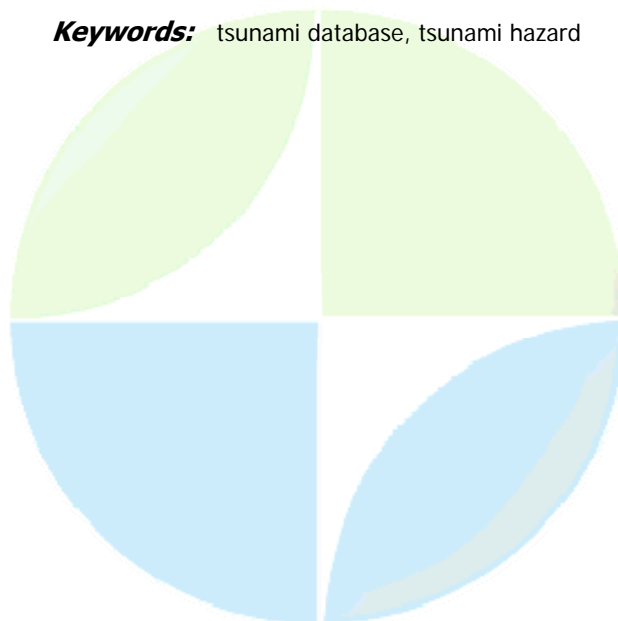
Revision and update of the tsunami database for New Zealand

Mrs. Gaye Downes
IASPEI

Willem P. De Lange

In the last decade there have been many advances in the science of tsunamis, and tsunami hazard and risk assessment. Despite these advances, the historical record of tsunami impact, once almost the only tool for tsunami-hazard assessment, continues to have an important role. This presentation reports on recent revisions and updates of the tsunami database. In New Zealand's short written historical record of just over 165 years, more than 50 local, regional and distant source tsunamis have occurred, some very isolated landslide-generated events in confined waters (e.g. fiords), some observable on tide-gauge records only, some local events large enough to be detectable elsewhere in the Pacific, and others large enough to have caused disastrous impact, had they occurred at a time and place of more significant coastal settlement. New Zealand has had a fairly comprehensive tsunami database since 1986 (de Lange & Healy, 1986). Recent events, such as the small 4 May 2006 tsunami (max. peak-to-trough in NZ, 0.35 m) and the December 2004 Sumatra tsunami (max peak-to-trough, 1.05 m), have been added. In addition, in-depth searching of historical records in the last five years has uncovered new historical tsunamis and extensive further data on known tsunamis. At present, the tsunami database is being developed as an Excel spreadsheet. Many fields are incorporated, including source parameter fields (with references) and impact fields, with separate entries for tide-gauge data (for example, maximum crest-to-trough heights, amplitude, first motion and predominant period), and observed data (for example, run-up, maximum inundation, brief referenced extracts from historical documents), as well as event summaries and key references to publications on specific events. The Excel database will be converted to a Web-based searchable interface, with tools to download and display data. In addition to the Excel database, transcribing of historical accounts is also in progress. These materials provide resources for researchers, emergency managers and planners, and for public education and community awareness. De Lange, W P and Healy, T R (1986). New Zealand tsunamis 1840-1982. *Journal of geology and geophysics* 2, 115-134.

Keywords: tsunami database, tsunami hazard



(S) - IASPEI - International Association of Seismology and Physics of the Earth's Interior

JSS002

Poster presentation

1804

Applicability of high-precision topographic model for tsunami simulation

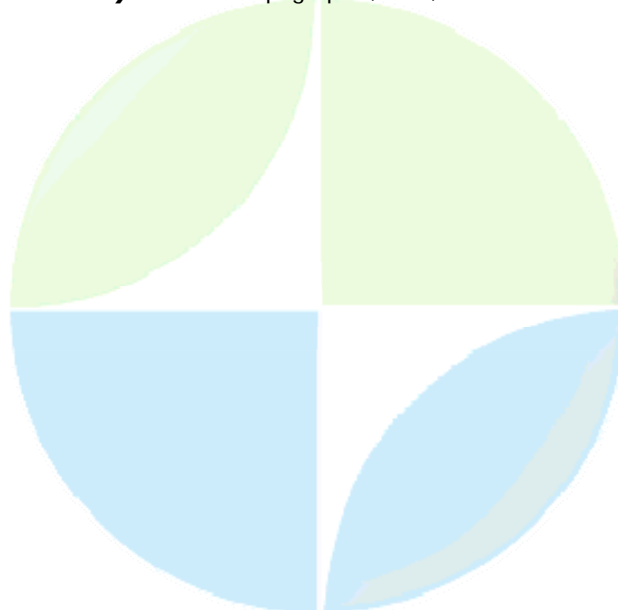
Mr. Yoichi Murashima

Disaster Control Research Center Tohoku University IASPEI

Fumihiko Imamura, Shunichi Koshimura

As seen in 2004 Indian Ocean Tsunami, one of the main causes of damage expansion was lack of information tsunami disaster in inundation area. The importance of hazard maps is steadily increasing. At this time it is essential to provide detailed information, such as inundation area, tsunami damage, evacuation centers and evacuation routes. Since developing model to predict tsunamis inundation area is still in progress and is discussed among researchers, the reliability and accuracy of topographic data is also essential, which change the results of run-up heights and inundation area from the simulation. Therefore, a study on accuracy and grid size of topographic model in the simulation is the target in our research. Recently, not only inundation area but also inundation depth and flow distribution information is supplied by tsunami simulation. And it is a major issue that using topographic model has impact on the results of tsunami simulation. In Japan, the 50m mesh elevation data from the Geographical Survey Institute Japan is available in Japan at a low price and it is widely used in tsunami simulation well. However, in recent years, it has become possible to measure elevation with adequate precision for detailed topographic models on an extensive scale, several meters, by airborne laser profilers LiDAR, Light Detection and Ranging, which has high measurement density and can measure minute topographical changes. Nowadays, detailed topographic models which use data by LiDAR are being used for tsunami prediction (Imamura et al, 2004; Tsubaki et al 2006; Iwate Prefecture, 2004). In this study, the method of topographic models with LiDAR is introduced for tsunamis case. We discuss whether or not the proposed topographic models made from DEM used LiDAR data and re-extracting data of dikes and embankments is appropriate for prediction of inundation area. In addition, we study the accuracy with grid size of topographic model which are suited for run-up tsunami simulations for such as hazard maps, through the comparisons among the cases with the different resolutions including 50 m data by GSIJ.

Keywords: topographic, lidar, simulation



(S) - IASPEI - *International Association of Seismology and Physics of the Earth's Interior*

JSS002

Poster presentation

1805

Application of Ocean Bottom Tsunami Gauge Data for Real-Time Tsunami Forecasting

Mr. Hiroaki Tsushima

Graduate School of Science Tohoku University IASPEI

Ryota Hino, Hiromi Fujimoto, Yuichiro Tanioka

Tsunami forecasting is one of the most effective methods to mitigate tsunami hazards. Now, in , tsunami warning can be issued within three minutes after the occurrence of earthquakes. This warning is based only on the seismic data and therefore has some problems; no one can assess the validity of the forecasting until tsunami reaches coasts and, in principle, tsunami amplitudes may be underestimated when tsunami earthquakes, which generate tsunamis much larger than those expected from their magnitudes estimated by seismic data, occur. To avoid these problems, tsunami data observed at offshore should be effectively used for the forecasting because the offshore stations can detect tsunami earlier than it reaches to the coastal area. In this study, we develop an algorithm for real-time tsunami forecasting system using offshore Ocean Bottom Tsunami Gauge (OBTG) data. To forecast coastal tsunami in real-time, we plan to use pressure data measured by cabled OBTGs. The offshore tsunami waveforms are inverted for a coseismic sea-floor vertical displacement distribution, which is used to calculate coastal tsunami waveforms before actual tsunami arrives. Owing to calculate Greens functions in advance, we can accomplish the successive calculation about one minute. Due to use more OBTG data in inversion as time lapses after a tsunami occurs, the reliability of forecasting is expected to improve. In order to check whether our method is practical before tsunamis reach the coasts, we performed numerical test assuming the case of the 1896 Sanriku tsunami earthquake ($M_s=7.2$, $M_t=8.6$). We use only four OBTGs, presently operating in the Tohoku-Hokkaido region. Tsunami waveforms were calculated using the source parameters by Tanioka and Satake (1996), and regarded as the observed waveforms. Then, we compared the observed tsunami waveforms with those calculated by our forecasting scheme for coastal tide stations. This test shows that our method can provide more reliable forecasting results, as time lapses. Five minutes before the earliest arrival time to the coast, our method can provide very good estimation of arrival time and amplitude of first and maximum wave at most tide stations along the Pacific coast of the Tohoku-Hokkaido region. We also applied our method to the actual tsunami observations in the 2003 Off-Fukushima earthquake ($M6.8$); the tsunami was recorded by both two OBTGs and coastal tide stations. In the result, the calculated tsunami waveforms match to the observations within five minutes in arrival times and within 70 % of the first waves in amplitudes at three coastal tide stations. On the other hand, we found that the accuracy of the tsunami wave height forecasting is subject to effects of azimuthal dependence of tsunami radiation, which is significant for large interplate underthrusting earthquakes. The result of our numerical experiment shows that the accuracy of the wave height forecasting will considerably improve if we build additional four OBTG stations between the two existing cabled system.

Keywords: tsunami forecasting

(S) - IASPEI - *International Association of Seismology and Physics of the Earth's Interior*

JSS002

Poster presentation

1806

Study on behavior of drifting bodies due to tsunami and its numerical simulation using EDEM

Mr. Naoki Fujii

Port and Coastal Engineering Department Tokyo Electric Power Services Co.,Ltd IASPEI

Ken Yanagisawa, Fumihiko Imamura

When large earthquakes such as Tokai and Tonankai in happen, the coastal area in particular industrial zone would suffer damage due to tsunami. The damage of the structure is basically classified into two types. The first is caused by hydrodynamic force of tsunami itself, and drifting bodies due to tsunami causes the other one. Ships, cars and destroyed objects could be drifting bodies. As seen in 2004 Indian Ocean Tsunami, drifting/floating bodies together with tsunamis attacked to coastal area and destroyed the offshore and land structures. The importance of such kind of tsunami effect is realized recently. Therefore it is an important to develop the tool for predicting behavior of the drifting bodies interacted by the tsunami at coastal area. In this study, a behavior of drifting bodies due to tsunami is investigated and modeled. Firstly, experimental tests are carried out. Secondly, we introduce Extended Distinct Element Method -EDEM- into numerical simulation to reproduce experimental results. This EDEM has a characteristic to be able to express various shape of drifting bodies by connecting among several elements. In order to understand the behavior of drifting bodies, especially in complex stream regime, we carried out drifting experiment with a harbor in large two-dimensional wave tank. The behavior of drifting bodies is measured its displacement and drifting path by the video system. Several notable behaviors of drifting bodies were observed, such as rotation with vortex occurred in the harbor, running on the land and running over the breakwater. Secondly, we aim to develop the model of drifting bodies with EDEM, which consists of several elements connected by spring, dash pot and slider, and can take into count hydrodynamic force for drifting bodies on the sea. Tsunami simulation with nonlinear long wave theory gives temporal velocity on each element. Horizontal force acting on drifting bodies is calculated by Morrisons equation. Vertical force is calculated by buoyancy based on the tsunami wave height, gravity and drag force. The drifting behavior is calculated by solving the momentum equation based on the horizontal/vertical forces. The feasibility of EDEM is discussed through comparisons with the result of experiments. We made the numerical simulation model for the behavior of drifting bodies due to tsunamis based on a physical experiment. As a result, it is confirmed that EDEM can reproduce well the behavior of drifting bodies due to tsunami, including complex behavior such as rotation in the harbor, running on the land and running over the breakwater.

Keywords: tsunami drifting body, extended dem

(S) - IASPEI - *International Association of Seismology and Physics of the Earth's Interior*

JSS002

Poster presentation

1807

Precise algorithm for tsunami wave rays and travel-time computations

Dr. Andrey Marchuk

International Tsunami Commission Member of the International Tsunami Commission IASPEI

Calculation of tsunami travel-times is still important for the tsunami prognosis and investigation of historical tsunamis. The methods based on the Huygen's principle are the most widely used in the areas with complicated topology and bottom relief. The main disadvantage of this method is limitation of possible directions of the wave-ray segments that connect neighboring grid-points. The proposed algorithm defines travel-times more accurately by taking into account all directions of the ray segments. Corrected travel-time values can be used for restoring the ray-traces which connect the source with all other grid-points of the computational area. The method was tested on some primitive models of bottom relief. The shapes of tsunami isochrones and wave rays are approaching theoretical solutions.

Keywords: tsunami, travel time, wave rays

XXIV2007

PERUGIA
I T A L Y



(S) - IASPEI - *International Association of Seismology and Physics of the Earth's Interior*

JSS002

Poster presentation

1808

Comprehensive analysis of the bathymetric data for the North Pacific

Dr. Andrey Marchuk

International Tsunami Commission Member of the International Tsunami Commission IASPEI

Anatoly Bezhaev

Gridded digital bathymetry is widely used for numerical modeling of tsunami generation, propagation and run-up. The quality of these data is of great importance for reliability of the results of numerical simulation of tsunami. At present time tsunami investigators mainly use segments of the global Smith-Sandwell and GEBCO digital gridded bathymetry. The comparison of these data, bathymetric and navigation charts for the Aleutian-Alaska region discover some significant data mismatches. The user interface for gridded, vector and raster bathymetric data comparison was created. Using this interface make it possible to find areas with insufficient density of existing digital data and to choose data for digitizing and for further creating the new gridded bathymetry.

Keywords: digital, bathymerty



(S) - IASPEI - International Association of Seismology and Physics of the Earth's Interior

JSS002

Poster presentation

1809

Historical and holocene paleotsunami deposits on Minor Kurile Arc

Dr. Razzhigaeva Nadya
paleotsunami paleotsunami

Larissa Ganzey, Tatiana Grebennikova, Andrey Kharlamov, Alexander Ya. Ilev

The data obtained describes the results of grain size and mineralogical study of tsunami 1994 deposits on Shikotan, Tanfiliev and Kunashir Islands. Investigations carried out within the coast with different configuration, geomorphologic structures, lithodynamic environments and tsunami character. Tsunami deposits composition were mainly controlled by erosion-accumulative processes during tsunami events and are in many respects inherited from sources material. Tsunami deposits include marine diatoms, rich assemblages were found within areas, where material from offshore redeposited. Data of deposits of earlier historical tsunami from the same sections are discussed too. The study of these deposits indicates similar development of erosion-accumulative processes during tsunami events with the same intensity and gripping the material for the same sources. Paleotsunami traces were studied in Shikotan and Zeleniy Islands coastal peat bogs and lacustrine sequences that were deposited during last 6 ka. The results will be used for detail catalog of tsunami events for South Kurile Region. The age of these events was based on radiocarbon dating and tephrochronology, some tsunami parameters (wave height, inundation area) for different coasts, and frequency were estimated. The marine origin of the sands was confirmed by some analysis including diatom data. Paleotsunami frequency was irregular, high reiteration of the events took place during Late Holocene. The data are presented for concrete coasts. Largest amount of paleotsunami sands were found on Pacific side of Shikotan Island. Some sites with numerous tsunami sands may be used as key sections. Grain size composition of tsunami sands was analyzed and compared with other coastal facies. Sources of paleotsunami material were established. Tsunami sediments are consisting of terrigenous and pumice sands which had different sedimentation features. Some tsunami and volcanic eruptions were synchronously. Grants RFBR 05-05-64063, FEB RAS I № 06-I-OH3-106.

Keywords: tsunami, sediments



(S) - IASPEI - *International Association of Seismology and Physics of the Earth's Interior*

JSS002

Poster presentation

1810

Pointwise and distributed reflection of long waves from a beach

Dr. Ira Didenkulova

Department of Nonlinear Geophysical Processes Institute of Applied Physics RAS IAPSO

Soomere Tarmo, Zahibo Narcisse

Wave reflection from underwater obstacles and beaches is a classical problem of the water wave theory in the ocean of variable depth. Pointwise reflections are realized on the non-analytical points of the depth profile $h(x)$, when the function $h(x)$, or its first derivative has jumps (steps, breaks and so on). Distributed reflection is realized for the most typical bottom profiles including non-reflected beaches. The pointwise and distributed reflection contribution in the real process of the onshore tsunami wave propagation is analyzed.

Keywords: tsunami, reflection



(S) - IASPEI - *International Association of Seismology and Physics of the Earth's Interior*

JSS002

Poster presentation

1811

Tsunamigenic potential of recently mapped submarine mass movements offshore eastern Sicily (Italy): numerical simulations and implications for the 1693 tsunami

Dr. Alberto Armigliato

Dipartimento di Fisica, Settore Geofisica Università di Bologna IASPEI

Stefano Tinti, Andrea Argnani, Filippo Zaniboni, Gianluca Pagnoni

Eastern Sicily has long been recognised to be among the most exposed regions in Italy and in the entire Mediterranean to tsunami hazard and risk. The historical tsunamis recorded along the Ionian coasts of Sicily were generally associated to moderate-to-large magnitude earthquakes: the most famous is the 11th January 1693 tsunami, whose parent earthquake is believed to be the largest magnitude event of the Italian history ($M=7.4$). Indeed, the possibility of tsunami generation by coastal and submarine mass movements cannot be ruled out: the destabilisation of mass bodies induced by the volcanic activity of Mount Etna, by the relevant seismic activity of the region or by a combination of these two factors, together with the steep bathymetric gradients found in correspondence with the Hyblaean-Malta escarpment just few kilometres offshore eastern Sicily, represents a highly hazardous combination of factors as regards tsunami generation. Recent offshore surveys, including the multichannel seismic survey MESC2001, carried out from 27 July to 16 August 2001, on board the R/V Urania of the Italian National Council of Researches (CNR), mapped a number of possible landslide bodies along the Hyblaean-Malta escarpment. Understanding the tsunamigenic potential of these mass instabilities is not only important from the point of view of the tsunami hazard assessment along the coasts of eastern Sicily, but it can also be useful in evaluating their possible role in the generation of historical events, such as the January 11, 1693 tsunami. A lively debate exists on the source of the 1693 event, and one of the key questions is whether the $M=7.4$ earthquake was the only source of the tsunami, or other causes (such as submarine landslides, possibly triggered by the earthquake) contributed to the tsunami generation. So far, numerical investigations of the event have been based only on the first hypothesis, and they pointed out that the characteristics of the tsunami deducible from the available historical accounts (size and spatial extension of effects) can be reproduced only by assuming an offshore tectonic source. The main goal of this study is to make a first attempt to investigate the second of the aforementioned hypotheses. Taking into account the largest of the mass movements mapped by MESC2001, we model numerically the dynamics of the landslide and the generation and propagation of the ensuing tsunami. In particular, the sliding motion is simulated with Lagrangian block models, UBO-BLOCK1 and UBO-BLOCK2, developed at the University of Bologna, while the tsunami generation and propagation is carried out through the finite-element code UBO-TSUFE, implemented by the same research team. The main computed tsunami features are discussed, such as the time evolution of the tsunami field, the spatial distribution of the minimum and maximum tsunami heights along the eastern Sicily coastline, as well as the amplitude, period and first polarity of the tsunami waves in selected coastal stations. We compare the numerical results with the historical evidences and try to draw some preliminary conclusions on the possible role of the mapped landslides in generating the 1693 tsunami.

Keywords: eastern sicily, 1693 tsunami, landslide

(S) - IASPEI - *International Association of Seismology and Physics of the Earth's Interior*

JSS002

Poster presentation

1812

Assessing vulnerability to tsunami: a pilot study in Seaside, Oregon

Mrs. Paula Dunbar

National Geophysical Data Center National Oceanic and Atmospheric Administration

Dale Dominey-Howes, Jesse Varner, Maria Papathoma-Khle

The results of a pilot study to assess the risk from tsunamis for the Seaside-Gearhart, Oregon region will be presented. To determine the risk from tsunamis, it is first necessary to establish the hazard or probability that a tsunami of a particular magnitude will occur within a certain period of time. Tsunami inundation maps that provide 100-year and 500-year probabilistic tsunami wave height contours for the Seaside-Gearhart, Oregon, region were developed as part of an interagency Tsunami Pilot Study (1). These maps provided the probability of the tsunami hazard. The next step in determining risk is to determine the vulnerability or degree of loss resulting from the occurrence of tsunamis due to exposure and fragility. The tsunami vulnerability assessment methodology used in this study was developed by M. Papathoma and others (2). This model incorporates multiple factors (e.g. parameters related to the natural and built environments and socio-demographics) that contribute to tsunami vulnerability. Data provided with FEMA's HAZUS loss estimation software and Clatsop County, Oregon, tax assessment data were used as input to the model. The results, presented within a geographic information system, reveal the percentage of buildings in need of reinforcement and the population density in different inundation depth zones. These results can be used for tsunami mitigation, local planning, and for determining post-tsunami disaster response by emergency services. (1) Tsunami Pilot Study Working Group, Seaside, Oregon Tsunami Pilot Study Modernization of FEMA Flood Hazard Maps, Joint NOAA/USGS/FEMA Special Report 103, 7 appendices, U.S. National Oceanic and Atmospheric Administration, U.S. Geological Survey, U.S. Federal Emergency Management Agency, 2006. (2) Papathoma, M., D. Dominey-Howes, D., Y. Zong, D. Smith. 2003. Assessing Tsunami Vulnerability, an example from Herakleio, Crete. *Natural Hazards and Earth System Sciences*, 3, 377389.

Keywords: tsunami, vulnerability, risk



(S) - IASPEI - *International Association of Seismology and Physics of the Earth's Interior*

JSS002

Poster presentation

1813

Tsunami modelling along Morocco atlantic coast preliminary results

Prof. Maria Ana Baptista
DEC ISEL, CGUL, IDL IASPEI

R. Omira 1,2, J. M. Miranda,1, P.M.M. Soares1,3, J.Luis, 4, E. A.Toto,2

Morocco, by its geographical situation with two marine limits, lengthens along the Atlantic coast in the west, and along the Mediterranean coast in north, is the country of Western Africa more exposed to the risk of the tsunamis coming from the Atlantic and the Mediterranean. In high populated coastal areas between Rabat and Casablanca the tsunami risk is almost unknown. Data on the 1755.11.01, transoceanic tsunami, report strong devastation from Tangier to Agadir. In the last century the 1969.02.28 Horseshoe fault (HSF) earthquake Mw 8.0 generated a small tsunami, with maximum amplitude recorded at Casablanca. Recently, another event stroke Morocco and southern Iberia but its moderate magnitude (Mw=6.1) prevented the triggering of a significant tsunami. In this study we present the preliminary results tsunami propagation and inundation results for Rabat and Casablanca areas. Modelling was performed with COMCOT code, from Cornell University. The simulation domain covers the eastern part of the Atlantic Ocean offshore Morocco and the Gulf of Cadiz, from the most prone tsunami generation area. Three nested grid layers of different resolution (0.008, 0.002 and 0.0005) are incorporated to obtain a good description of bathymetric and topographic effects near shore. Results of the numerical simulations are discussed in terms of wave heights, flow depth and maximum velocity. This study was funded by projects FCT/TESS and NEAREST STREP 37110 UE.

Keywords: tsunami, morocco, hazard



(S) - IASPEI - *International Association of Seismology and Physics of the Earth's Interior*

JSS002

Poster presentation

1814

Numerical modelling of the 2006 Java tsunami

Mrs. N. Rahma Hanifa

Geodesy Institute Technology Bandung INDONESIA IAG

Fumiaki Kimata, Takeshi Sagiya, Hasanuddin Z. Abidin, Parluhutan Manurung

The M7.8 earthquake occurred on July 17, 2006, at 08:24 UTC or 15:24 in local time, in the coast of Pangandaran, Java Island, , excited a deadly tsunami of 3 to 8 meters that inundated the southern coast of Java. This event was a tsunami earthquake based on the fact that the earthquake generated a much larger tsunami than expected from its seismic waves, the rupture lasted for unusually long time, and that the source mechanism was a low angle thrust type (Ammon et. al., 2006). The tsunami propagation has been modeled solving the non linear equations for shallow water . The initial condition for water surface is computed from Okada's (1985) formulas, using several different seismic parameters. The tsunami propagation is simulated by a finite-difference numerical model using a system of multiple grids with one and two minutes grid sizes. The best estimated parameter are; average slip 12 meter and rupture area of 70x200 km with rigidity of 10 GPa. The computed waves are in fair agreement with the recorded tide at Benoa tide station. The numerical results obtained along the southern coast of Java, confirm the run up observations.

Keywords: tsunami, modeling, java 2006

PERUGIA
ITALY



(S) - IASPEI - *International Association of Seismology and Physics of the Earth's Interior*

JSS002

Poster presentation

1815

Micropaleontological analysis of 2004 Indian Ocean Tsunami sediments

Prof. Koji Minoura

Geology and Paleontology Non IAPSO

Daisuke Sugawara, Naoki Nemoto, Shinji Tsukawaki, Tetsuya Shinozaki, Fumihiko Imamura, Kazuhisa Goto

The 2004 Indian Ocean Tsunami, which is one of the largest tsunamis on record, attacked the coastal areas around the Indian Ocean on 26 December 2004. The tsunami invaded the coast of Thailand with waves reaching up to 9 meters high (Matsutomi et al., 2005). At Pakarang Cape the tsunami left thousands of carbonate boulders on the shore. Satellite images exhibit no signs of the boulders before the tsunami, whereas show distribution of them after the tsunami. The coastal areas are not in the affect of strong tropical cyclones, and thus the storms were not responsible for the emplacement of the boulders at the cape. These scientific results, together with the reports of local residents regarding the absence of such boulders before the tsunami, indicate that the boulders were highly likely to have been transported as a result of the 2004 Indian Ocean Tsunami. Our numerical calculations indicate that the reef flat was mostly exposed above the sea surface just before the tsunami attack due to seawater receding. The first wave reached to the reef edge approximately 130 minutes after the tsunami generation, and the maximum current velocity of the first tsunami was calculated to be from 8 to 15 m/s between the reef edge and 500 m offshore, and less than 6 m/s on the reef flat. We do not know the origin of such destructive tsunami currents in the sea, and we cannot make clear the reworking mechanism of carbonate boulders on the forereef slope. In this context the understanding of current formation is an urgent necessity of study for evaluating the effect of tsunamis on the environment. It can be hypothesized that fluid motion by tsunami currents cause bedload transport of grains on the sea bottom. Rapid grain shearing over the static bed disturbs the ecological adaptation of in- and epi-faunal organism. Such kind of destructive tsunamis occurred repeatedly in the ocean on a geological time scale, and probably impacted on the ecology and evolution of benthic living things. In this study we adopted micropaleontological methods for elucidating the erosion-reworking mechanism of tsunami currents. We have stocks of surface sediment samples dredged in the offing of Pakarang Cape before the tsunami (April 2002). By comparing the faunal compositions of benthic foraminifers in the samples with those in sediments collected after the tsunami (April 2005, February 2006), we could make clear the origin of tsunami currents in the offshore bottom. The preliminary results on the benthic foraminiferal analysis indicate that the currents by the 2004 Indian Ocean Tsunami were formed on the forereef of around 30 m in depth. The difference in faunal assemblages between the samples of 2005 and 2006 shows the ecological recovery of faunal communities to have been made within a year. We know well on-land tsunami hazards, however undersea effects by tsunami waves are mysterious. Living things in the coastal areas receive continually exogenous impacts, and they have ecological adaptability for environmental catastrophes. By applying this characteristic of shallow sea benthic foraminifers, we might be able to elucidate the origin of tsunami currents that bring on destructive damages on the coast

Keywords: numerical calculation, benthic foraminiferal analysis, coral reef

(S) - IASPEI - *International Association of Seismology and Physics of the Earth's Interior*

JSS002

Poster presentation

1816

Tsunami detection by wavelet analysis of DART records

Dr. Victor Morozov

Tsunami laboratory 117997 Moscow, Russia, Nakhimovskiy ave 36 IASPEI

Wavelet analysis has been applied to bottom pressure DART records for detection tsunami signals related to seismic events from 1986 to 2007 in Pacific Ocean. Wavelet analysis of the bottom pressure oscillations reveals that the high frequency components of tsunami signals were markedly dispersive. The observed dispersion was found to be in a good agreement with theoretical estimates of the dispersion derived from the group velocity of the waves.

Keywords: dart, tsunami, dispersion



(S) - IASPEI - *International Association of Seismology and Physics of the Earth's Interior*

JSS002

Poster presentation

1817

Numerical experiment of the oil spread caused by the 1964 Niigata Earthquake Tsunami

Dr. Yoko Iwabuchi
Civil Eng. Tohoku Univ.

Shun-Ichi Koshimura, Fumihiko Imamura

A complex tsunami damage involving floating objects driven by a tsunami is a new aspect of tsunami disaster in industrialize coastal region. The most commonly observed feature of this complex tsunami disaster is that the destruction of storage of flammable materials by collision with tsunami-driven objects or by the hydrodynamic force of tsunami may result spread of large fires, flammable materials such as spilled oil and ignited material advected and diffused by the tsunami current in a harbor or on inundated land. In the 1964 Niigata Earthquake , oil were leaked from tanks in coastal industrial region. The tsunami inundation flow which was happen subsequently cause expansion of oil spreading and fire damage (Iwabuchi et al. 2006) . Despite of the risk of all industrialize coastal region and the significance of the damage by tsunami, little has been done on estimating the complex damage to waterfronts. Current situation of estimatiing tsunami damage is based only on counting assets possibly exposed in a tsunami inundation zone, so the features of complex tsunami disaster is not well understood. We have developed the water-oil 2-layer model to draw up disaster-affected scenario for disaster prevention planning or as a tool for designing of oil dike. Here, we conduct a numerical experiment of the oil spread caused by the past tsunami event. Firstly, the simulation of propagation and run-up for the 1964 Niigata Earthquake tsunami was carried out. Most fault parameters were based on the source mechanism proposed by Aki (1966). Two large rivers, the Shinano and Agano, in the devastated area are vital for determining tsunami devastation, especially the area above the Agano River mouth, where bathymetry data must be extremely precise to calculate the tidal level at the Matsugasaki Station during the event. The model tsunami shows good agreement with tidal records. However, calculated inundation area was underestimated. The ignorance of the remarkable subsidence caused by liquefaction and fountain flow is likely to be one of the main causes of that underestimation. The findings suggest that the subsidence caused by liquefaction should be considered to predict tsunami inundation area. Using both numerical analysis of 1-layer tsunami model and historical records enables us to confirm that tsunami inundation flow make the oil spreading area more extensive in the coastal industrial region. Secondly, we take the 1964 Niigata Earthquake Tsunami as an example, numerical experiments were carried out to apply our 2-layer model. We proposed the processes that oil layer was transported by tsunami inundation flow. The practical issues were clarified by numerical simulation for examples.

Keywords: tsunami, 2 layer, oil

(S) - IASPEI - International Association of Seismology and Physics of the Earth's Interior

JSS002

Poster presentation

1818

The implications of non-linearity and dispersion in a tsunami scenario database

Mr. Arthur Simanjuntak

Australian Bureau of Meteorology Research Centre Australian Bureau of Meteorology

Diana J.M. Greenslade

The Australian Bureau of Meteorology has developed a 1st generation operational model-based tsunami prediction system (T1) as a component of the Australian Tsunami Warning System. The T1 system is based on a database of pre-computed tsunami scenarios. For each earthquake source location, the T1 system provides solutions from four different earthquake magnitudes and chooses the closest scenario. A natural extension of this system would be to provide an interpolation of these scenarios to obtain the solution for a specific intermediate earthquake magnitude. Implicit in this is the assumption of wave linearity, which has been shown to hold in the open ocean but unlikely to be accurate in shallow water. Furthermore, since the ruptures for each earthquake magnitude differ from each other not only in the amount of slip but also width and length, the initial conditions would have different horizontal wavelengths from each other. This will have implications as the waves disperse and encounter bathymetric features. The importance of dispersion is proportional to the distance travelled by the waves and inversely proportional to depth. In this presentation, the potential for scenario interpolation will be investigated by means of numerical experiments and simple scaling arguments. The assumption of linearity and the effect of dispersion will be investigated separately. Specifically, we will explore some non-dimensional parameter space beyond which the non-linearity and dispersive effects start to dominate and therefore render simple magnitude interpolation inappropriate.

Keywords: linearity, dispersion, simulation



(S) - IASPEI - *International Association of Seismology and Physics of the Earth's Interior*

JSS002

Poster presentation

1819

Development of numerical tsunami simulation technique in near field

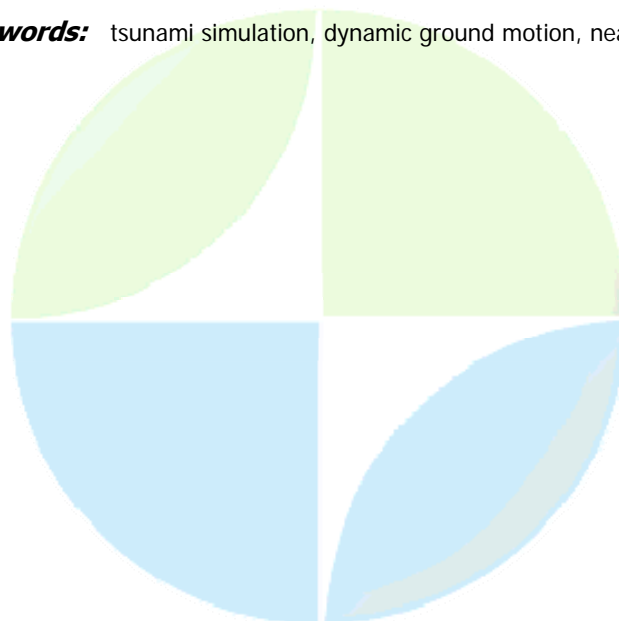
Mr. Shusaku Inoue

Interdisciplinary Graduate School of Science and Technology Tokyo Institute of Technology IASPEI

Gota Kubo, Tatsuo Ohmachi

People living in costal areas of Japan are always exposed to tsunami risks because Japan has a long costal line and active seismicity. And seismic faulting in and around Japan often takes place very close to the coastline, and tsunamis would attack coastal cities within a few minutes. And also not a few cities may be included in tsunami source areas. Accordingly, we think it necessary to consider dynamic effects of tsunami generation followed by propagation and runup. Up to now, many researchers have investigated tsunami behaviors by means of experiments and computer simulations. Among them, lots of computer simulations have been carried out for not only academic but also practical purposes, and lots of simulation techniques have been developed. From an engineering viewpoint, there seems to be few techniques that can successfully simulate the near field tsunami. For this reason, we have developed a new technique called dynamic tsunami simulation. Our developed simulation technique was intended to apply near field tsunamis. The technique consists of two steps of simulation. The first is to simulate seabed displacements. The boundary element method (BEM) is employed here because it can give us time histories of dynamic displacement of irregular seabed resulting from a seismic faulting with a satisfactory level of accuracy. The second is to simulate seawater disturbance using the finite difference method (FDM). In the second simulation for fluid domain, the Navier-Stokes equation is used as a governing equation. Thus, this simulation can take account of dynamic ground motion effects in the tsunami generation. We have recently added new functions to our previous technique to make it more useful. The new functions are, for example, a technique to simulate tsunami runups, and also a nesting technique to deal with a large area effectively with a sufficient accuracy. In our technique, the SOLA procedure and the height function are used. We have validated our technique by comparing simulation results with runup height of solitary wave derived from theoretical and experimental results. After all, we have found that our newly developed technique works well, especially for near-field tsunamis.

Keywords: tsunami simulation, dynamic ground motion, near field



(S) - IASPEI - *International Association of Seismology and Physics of the Earth's Interior*

JSS002

Poster presentation

1820

Finite Fault Modelling for Tsunamigenic Earthquakes in Australasia using Seismic and Sea Level Data

Dr. Phil Cummins

Geospatial and Earth Monitoring Division Geoscience Australia IASPEI

Toshitaka Baba, Hong Kie Thio, Ming-Hai Jia

Since the 2004 Sumatra-Andaman earthquake and Indian Ocean Tsunami, there has been a vast increase in the monitoring of large earthquakes and tsunami-related sea level changes, especially in the Australasian region. The increase in data has resulted in much better coverage of tsunami sources in this region, much of it in real-time. In this presentation we consider how well this increased monitoring allows us to characterise these sources, by performing finite fault inversions using combinations of seismic, sea level and GPS data. While tide gauge data is often limited by its sensitivity to poorly known local bathymetry, there are an increasing number of ocean bottom pressure measurements which record tsunami waveforms unaffected by shallow bathymetry, and we investigate the potential of these for constraining earthquake source properties. Two fundamental questions investigated are: (1) Can earthquake source models be inferred with sufficient accuracy to be used to validate teletsunami modeling? (2) Can accurate source models be developed in near-real-time? We discuss our results for modelling recent tsunamigenic earthquakes with a view towards answering these questions.

Keywords: earthquake, tsunami, modeling

PERUGIA
ITALY



(S) - IASPEI - *International Association of Seismology and Physics of the Earth's Interior*

JSS002

Poster presentation

1821

Tsunami Risk in the Northern Bay of Bengal

Dr. Phil Cummins

Geospatial and Earth Monitoring Division Geoscience Australia IASPEI

This presentation is a synthesis of the results of geologic and geodetic studies of the northern Bay of Bengal, combined with an analysis of historical accounts of the 1762 Arakan earthquake and a simulation of the tsunami that may have accompanied it. I show that these are all consistent with active subduction in the Myanmar subduction zone, and hypothesize that the seismogenic zone associated with it extends into the Bay of Bengal beneath the Bengal Fan. These results suggest that a very large and vulnerable population is exposed to a high earthquake and tsunami risk. Other reports that have characterised this hazard as low may have not considered the possibility that the seismogenic zone extends offshore, as is suggested by GPS surveys, the active Bengal Fold System, and the historical accounts of subsidence on the coast of Chittagong during the 1762 Arakan earthquake. Although the 2004 Indian Ocean Tsunami was difficult to foresee, some of the warning factors were there and should have been recognized by the earth science community. This presentation attempts to draw attention to similar warning factors in the Bay of Bengal, where the cost in human lives of a large earthquake and tsunami may be much larger.



(S) - IASPEI - *International Association of Seismology and Physics of the Earth's Interior*

JSS002

Poster presentation

1822

Constraints on the source of the 20th February 1743 tsunamigenic earthquake in Apulia, Italy, from numerical tsunami modelling and geological evidences

Dr. Alberto Armigliato

Dipartimento di Fisica, Settore Geofisica Università di Bologna IASPEI

Stefano Tinti, Giuseppe Mastronuzzi, Paolo Sans, Gianluca Pagnoni

According to the most recent version of the Italian Tsunami Catalogue, the 20th February 1743 tsunami was generated by a strong earthquake ($M=6.9$) which severely hit the Salento peninsula (Apulia) and the Greek Ionian Islands, and that was felt in a very large area, including Calabria, the Messina Straits and Naples. The maximum damage due to the earthquake was suffered by the towns of Nard and Francavilla Fontana in southern Apulia, where most buildings were ruined. The cities of Taranto and Brindisi were also heavily damaged. The earthquake was responsible for more than 160 victims. Historical accounts on the tsunami are scarce: the only available report describes some tsunami effects in the harbour of Brindisi, where the sea withdrew. On the other hand, the impact of the tsunami waves along the Ionian and Adriatic coasts of Apulia appears to be well documented from the geological point of view. A recent detailed study on large boulder accumulations along the southern Apulia coasts and on their depositional characteristics allowed not only to put them in relation to the 1743 event with a reasonable degree of confidence, but also to formulate some hypotheses on the possible source area (SSE of Apulia), on the direction of impact of the tsunami waves and on the highest tsunami runup (11 m). Based on these results and on some basic information coming from local tectonics, we take into account a small number of seismic sources and for each of them we simulate numerically the ensuing tsunami. More specifically, for each studied fault we compute the coseismic deformation of the sea bottom and take it to be identical to the tsunami initial condition. The subsequent tsunami wave propagation is computed by means of a finite-element numerical code, UBO-TSUFE, developed at the Department of Physics of the University of Bologna, which implements and solves the Navier-Stokes equations in the shallow-water approximation. For each run, we compare the numerical results with the available geological and historical evidences: attention is posed especially on the tsunami wave propagation direction, on the polarity of the first wave arrivals in some selected coastal stations in southern Apulia and on the spatial distribution of the extreme water elevations along the coastlines. The results are discussed in order to draw some preliminary conclusions on the most probable source area and geometry for the 1743 tsunamigenic earthquake.

Keywords: apulia, numerical modelling, tsunami deposits

(S) - IASPEI - *International Association of Seismology and Physics of the Earth's Interior*

JSS002

Poster presentation

1823

Physical Simulation of Drain Mechanism of Tsunami Generation

Mr. Pavel Korolev

Boris Levin

As a result of 1999 Izmit earthquake a split sea and sinking of the water level were observed in Izmit Gulf. A cause of this effect may be cracks, breaks in the fault zone. Really great cracks with length tens kilometers and width some meters are occurred on the Earth surface in the time of strong earthquakes. Such kind of cracks were observed as a result of recent Neftegorsk (1995), Altai (2003) earthquakes in Russia. Not excluded that similar processes can occur on the sea bottom. As a result of water withdrawal tsunami could be generated. This process was simulated physically on the experimental water tank measuring 3.0 x 0.6 x 0.4 meters. In the central part of tank at the bottom there is a device with slots simulating cracks opening. Conditions of water waves generation depending on initial water depth, slots width, time of slots opening are ascertained. This work is supported by Russian Foundation for Basic Research, grant 07-05-00363, and Program of Leading Scientific Schools NSH 8043.2006.5.

Keywords: tsunami generation, drain mechanism, simulation



(S) - IASPEI - *International Association of Seismology and Physics of the Earth's Interior*

JSS002

Poster presentation

1824

How very-high resolution 3D DEM contribute to quantitative tsunami damage forecast: the study case of Sri Lanka

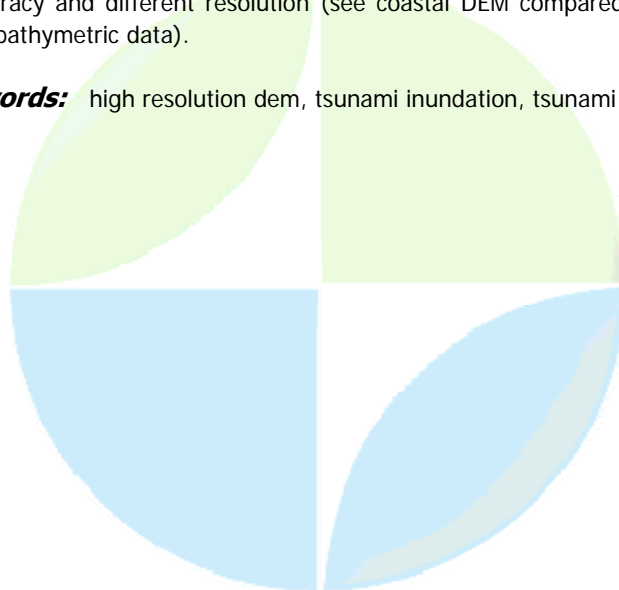
Dr. Alberto Armigliato

Dipartimento di Fisica, Settore Geofisica Università di Bologna IASPEI

Stefano Tinti, Fabrizio Ferrucci, Roberto Tonini, Sara Gallazzi, Gianluca Calabretta

Tsunami damage assessment and forecast requires both sophisticated numerical modelling and support of data sets reflecting our knowledge of the physical coastal environment and of the socio-economic values exposed to the risk. The problem is complex and no standard methodology has been so far introduced to make quantitative assessment and to provide local communities and responsible authorities with basic agreed-upon tools to make quantitative estimates of tsunami impact. Here we explore the contribution that very-high resolution 3D mapping from airborne and spaceborne techniques may give to quantitative estimates resulting from tsunami modelling. The area of application is Sri-Lanka, that was severely hit by the 26th December 2004 disastrous tsunami of the Indian Ocean, that killed more than 290,000 people, and in Sri Lanka took a fatality toll of more than 30,000. This paper is based on the data provided by the project HyperDEM, that was born from an inter-Governmental agreement established between Italy and Sri Lanka and was funded by the Italian Ministry for Foreign Affairs. The project work was mainly based on the integration of airborne LiDAR and spaceborne RaDAR campaigns that were undertaken between autumn 2005 and summer 2006. The post-processing data products are a Digital Ground Model (DGM) and a Digital Surface Model (DSM). DGM represents the Earth elevation cleaned of vegetation and manufacts and it is suitable for mapping the water penetration in vegetated areas with little presence, or absence, of manufacts, while DSM includes them and it is indicated for a detailed inundation mapping in urban areas. The terrain resolution in some urban areas was of 1 metre, providing a very detailed topography which, if properly combined with an accurate bathymetric data set, is well suited to the computation of detailed inundation map by means of numerical models. In this study we concentrate on the city of Galle, placed along the south-western coast of Sri-Lanka, where more than 4,000 persons were killed by the 2004 tsunami and the quay was completely destroyed. We consider tsunami simulations models where use is made of high-accuracy 3D DEM and discuss uncertainties in tsunami inundation maps resulting from combination of data with different level of accuracy and different resolution (see coastal DEM compared to offshore and near-shore lower-accuracy bathymetric data).

Keywords: high resolution dem, tsunami inundation, tsunami damage



(S) - IASPEI - *International Association of Seismology and Physics of the Earth's Interior*

JSS002

Poster presentation

1825

Numerical simulation of tsunamis around Shanghai on the East China Sea Coast Due To Great Nankai, Japan, earthquakes

Dr. Tomoya Harada

Research Center for Urban Safety and Security Kobe University IASPEI

Katsuhiko Ishibashi

There has been a controversy among Japanese scientists whether Chinas Shanghai and its vicinity on the East China Sea coast were struck by large tsunamis or not due to the great interplate Nankai earthquakes along the Pacific coast of southwest Japan. Chinese historical documents report remarkable water disturbances in rivers, canals, ponds and wells around Shanghai in 1498, 1707 and 1854. The dates in 1707 and 1854 coincide with those of the Nankai earthquakes and the date in 1498, with that of a large earthquake in southwest Japan. Tsuji and Ueda (1997) claimed that these water disturbances meant large tsunamis and that the 1498 earthquake had also been the Nankai earthquake. Utsu (1988) and Ishibashi (1998), on the contrary, considered the water disturbances not to be tsunamis but seiches caused by long-period seismic waves. In this study, in order to terminate this controversy, we carried out the numerical simulation of tsunami propagation in the East China Sea for the 1707 Hoei, the 1854 Ansei and the 1946 Showa Nankai earthquakes, though the computation was the first-order approximation. We assumed six static fault models of the 1707, 1854 and 1946 earthquakes proposed by Ando (1975, 1982) and Aida (1979, 1981a, b). Tsunami propagations were computed by the finite-difference method for the linear long-wave equations in the area of 120-140E and 2036N using 1-minute bathymetry data provided by GEBCO. The time step of the computation is 3.0 sec to satisfy a stability condition of the grid system. The friction with Mannings roughness coefficient of 0.03 is provided at the ocean bottom where the water depth is shallower than 100m. Initial conditions of tsunami propagation are ocean bottom deformation due to earthquake faulting, which were computed by Okadas (1985) program. Concerning boundary conditions, the total reflection on the coast and open boundary to outside the computational area were used. As the results, tsunamis caused by great Nankai earthquakes propagate into the East China Sea mainly through the Tokara strait, and they reach the coast around Shanghai about nine hours after the earthquake occurrence. The tsunami height on the China coast is not large, less than 1 meter, even for presumably overestimated fault slip of the 1707 Hoei Nankai earthquake model. Thus, water disturbances recorded in China are considered not to be tsunamis but effects of seismic waves. However, it should be noted that tsunami and seismic effect due to the next Nankai earthquake, which is anticipated to recur around the middle of this century, may affect to considerable extent to the modernized society of China. We thank Yuichiro Tanioka for providing us his tsunami computation program.

Keywords: tsunami simulation, east china sea, great nankai earthquake

(S) - IASPEI - International Association of Seismology and Physics of the Earth's Interior

JSS002

Poster presentation

1826

Modelling Tsunami Inundation in the Gulf of Cadiz - Preliminary Results

Mrs. Vnia Lima
DEC ISEL IASPEI

J M Miranda, M.A. Baptista, M. Olabrieta, L.Otero, P M M Soares, M Gonzalez, E Carreno

North East Atlantic European coasts were hit in the past by large, destructive tsunamis. The European Tsunami Catalogue (ETC) includes several large events in the Gulf of Cadiz, generated by moderate and strong magnitude earthquakes. The city of Cadiz suffered severe damage during the 1st November 1755 Lisbon tsunami. The coeval historical information enables extensive evaluation of run in and run up data for the city and harbour of Cadiz. In this study we present the preliminary results of numerical modelling for one of the critical sites in the North Atlantic area. Modelling was performed with COMCOT code, from Cornell University. The simulation domain covers the eastern part of the Atlantic Ocean offshore Morocco and the Gulf of Cadiz, from the most prone tsunami generation area. Three nested grid layers of different resolution (0.008, 0.002 and 0.0005) are incorporated to obtain a good description of bathymetric and topographic effects near shore. Results of the numerical simulations for an event similar to the 1755 earthquake and tsunami are discussed in terms of wave heights, flow depth and maximum velocity. This study was funded by project TRANSFER STREP 37058 UE

Keywords: tsunami, waveheight, flowdepth

PERUGIA
ITALY



(S) - IASPEI - *International Association of Seismology and Physics of the Earth's Interior*

JSS002

Poster presentation

1827

Tsunami hazard estimation for the southern Kuril Island coast

Dr. Victor Kaystrenko

Russian Academy of sciences Institute of Marine Geology and Geophysics

The Russian Far Eastern coast is a one of the most tectonically active margin of the Pacific area with frequent tsunami occurrence. After catastrophic tsunami in November 1952 that destroyed the most part of the Severo-Kurilsk town, up till now more than 40 tsunami were recorded on the Far East coast of our country, the height being more than 5 meters in 7 cases, and in 1952, 1963, 1969, 1994 the wave heights being up to 15 meters in some points. Tsunami hazard distribution along the Russian coast is not homogeneous and tsunamis are most frequent events on the Southern Kuril Island coast. It is known that a sequence of earthquakes exceeding an elected magnitude is really the Poissonian one and its main parameter is the recurrence function $F(h_0)$ which is a mean frequency of tsunamis with height more then elected "threshold" h_0 . Analysis of the natural data showed that this function depends from two parameters: $F(h_0) = f \exp(-h_0/H^*)$. Parameter H^* is calibrate (characteristic) tsunami height depended from the coastal point of tsunami observation, and f is the regional tsunami frequency, that varying very slowly along the Pacific coast and can be considered as a regional constant. Using the least square method these parameters have been calculated from the historical tsunami data set. Finally, characteristic tsunami heights H^* were evaluated for 18 points on the Southern Kuril Island coast. Tsunami frequency for this region is $f = 0.17$ 1/year and its standard deviation is $\sigma(\ln(f)) = 0.13$. These parameter allowed to estimate tsunami risk for this region. The work was supported by the grants of the Russian Foundation of Basic Research 05-05-64733 and FEB RAS I # 06-I-ON3-106.

Keywords: tsunami, hazard, risk

PERUGIA
ITALY



(S) - IASPEI - *International Association of Seismology and Physics of the Earth's Interior*

JSS002

Poster presentation

1828

Numerical analysis of tsunami caused by seabed deformation

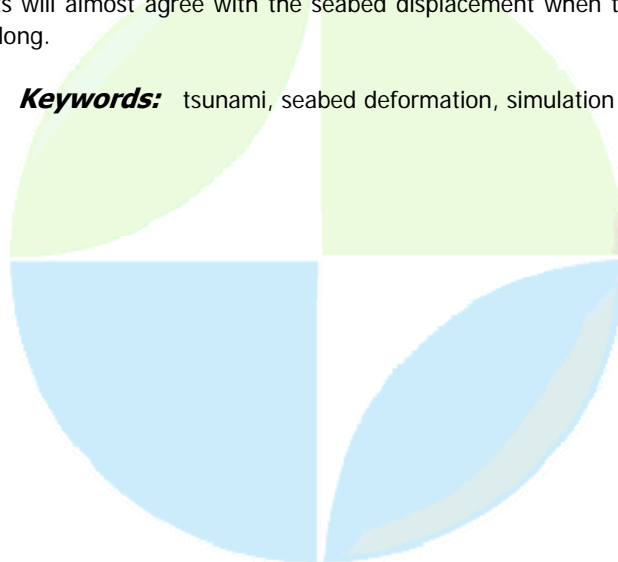
Dr. Toshinori Ogasawara

Department of Civile and ENvironment

Shigeki Sakai, Akifumi Wakamatsu

The seismic intensity scale of the Meiji Great Sanriku Tsunami of 1896 was small scale but the tsunami height was very large. The maximum wave height was 32 m. Such an earthquake is called a tsunami earthquake or a slow earthquake. Note that tsunami heights are not necessarily proportional to earthquake magnitude. This is one of reasons that the tsunami heights in coast lines cannot be forecast easily. In the present forecast of tsunami, wave heights are estimated by water surface disturbances due to the seismic fault model. The model is based on the fault parameters calculated by the observed seismic wave, which are the length, the depth, and the dip angle etc. The information of the initial wave profile generated by a seabed deformation is more important for the accuracy of tsunami forecast. This study makes clear how the physical quantities related to the seabed deformation exert an influence on the tsunami generation. In particular, the relationships between the physical quantities and the maximum wave height are described. Here, the physical quantities represent the vertical velocity, the width, and the shape of the seabed deformation. Numerical analysis on the tsunami generation was done for various seabed deformations. This numerical method defined a two-dimensional water tank of fluid domain. The water depth was set to four types from 1,000 m to 4,000 m. Tsunami sources used the vertical displacement field of sea bottom directly computed by using a time-domain solution involving the boundary element method. The width of seabed deformation was changed from 20 km to 100 km. The speed of seabed deformation was changed at a constant velocity and the maximum displacement was set to 3.0 m. The waves generated by the seabed deformation permeate the open boundary on the both side of tank. As a result, when the seabed deformation was low-speed at 0.01 m/s, the maximum wave heights were proportional to the width of seabed deformation. However, when the seabed deformation became 100 m, the wave heights were found to almost reach as high as the seabed deformation. On the other hand, when the seabed deformation was high-speed at 0.3 m/s, if the seabed deformation width exceeded more than 20 km the wave heights agreed with the seabed deformation. It is concluded from the result that the width of seabed deformation is strongly required at the determination of the maximum wave height at tsunami generation. Further, the results show that the initial wave heights will almost agree with the seabed displacement when the width of the seabed deformation becomes long.

Keywords: tsunami, seabed deformation, simulation



(S) - IASPEI - *International Association of Seismology and Physics of the Earth's Interior*

JSS002

Poster presentation

1829

Rupture Process of the California Earthquake of 18 April 1906 from (near-field) Tsunami Waveform Inversion

Dr. Stefano Lorito

Department of Seismology and Tectonophysics INGV

Alessio Piatanesi, Anthony Lomax

Keywords: tsunامي, inversion, source

IUGG

XXIV2007

PERUGIA

I T A L Y



(S) - IASPEI - *International Association of Seismology and Physics of the Earth's Interior*

JSS002

Poster presentation

1830

Seismic and Tsunami Monitoring in the Puerto Rico and Caribbean Region

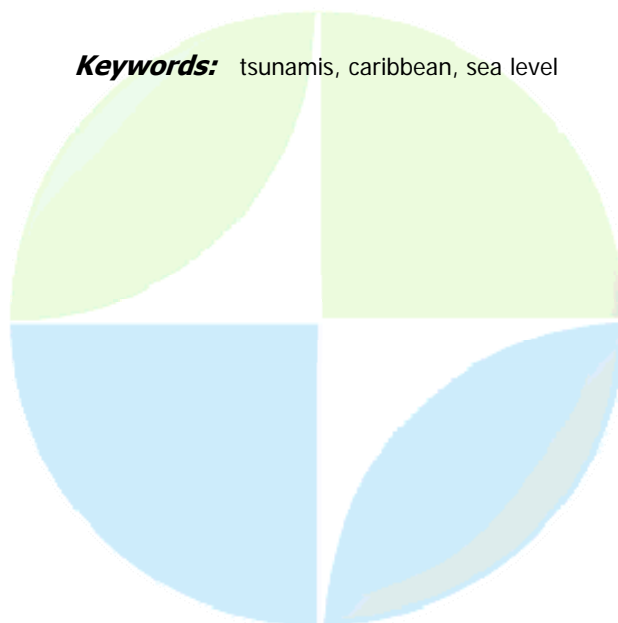
Prof. Aurelio Mercado-Irizarry

Department of Marine Sciences University of Puerto Rico IAPSO

Christa Von Hillebrandt-Andrade, Victor Huerfano

The US Commonwealth of Puerto Rico has a population of 3.8 million (2000 Census), which amounts to a higher population density than any state. The island, approximately 160km from east to west by 50km from north to south, is bounded by off-shore active faults on all sides. Numerous local and regional events in the recorded history with $M > 7.0$, three of which have generated destructive tsunamis, have caused extensive damage to local infrastructure. The most recent significant ground motions and (local) tsunami in Puerto Rico occurred as a consequence of $M 7.3$ earthquake on October 11, 1918. Efficient emergency response in the event of a large earthquake or tsunami will be crucial to minimizing the resultant loss of human life and disruption of lifeline systems. State of the art seismic and sea level monitoring are necessary to be able to provide an appropriate response to such a disaster. The seismicity of the island, as well as the northeastern Caribbean region in general (including the US and British Virgin Islands), is monitored jointly by the Puerto Rico Seismic Network (PRSN) and the Puerto Rico Strong Motion Program (PRSMP), both operating within the University of Puerto Rico at Mayagez. As of 2000 the PRSN has been developing a Tsunami Warning System for the region. For the detection and reporting of potentially tsunamigenic earthquakes it monitors over 150 channels of seismic data from the Caribbean and adjoining regions. The goal is to be able to timely and precisely detect all earthquakes of at least magnitude 5 in the Caribbean region. As part of the warning system the PRSN is also in the process of installing six tsunami ready tide gauge stations in Puerto Rico and a GOES satellite receiver at its facilities for the data from these and other tide gauges of the regions, including the 10 tide gauges NOAA operates in Puerto Rico and the Virgin Islands. The tide gauges also meet the standards for long term sea level studies. The data from the five DART buoys which were deployed by NOAA in the spring of 2006 in the Caribbean and adjacent waters are also being incorporated into the monitoring system, and Short-term Inundation Forecasting computational grids have been developed for two major coastal cities, with three additional ones being worked on during 2007, including the USVI.

Keywords: tsunamis, caribbean, sea level



(S) - IASPEI - International Association of Seismology and Physics of the Earth's Interior

JSS002

Poster presentation

1831

Global Tsunami Deposits Dtabase

Mrs. Vinita Ruth Brocko

IASPEI

Paula K. Dunbar

Historical tsunami and tsunami deposit data are important for assessing the tsunami hazard of a region. The past record provides clues to what might happen in the future, such as frequency of occurrence and maximum wave heights. Instrumental and even written records often do not span enough time to assess the full range of a regions tsunami hazards. Tsunamis have been reported since ancient times, but without mechanical, digital or human observation, all that remain of tsunamis occurring before records were kept are the deposits they have left behind. Historical events for which deposits have been studied provide criteria for identifying tsunami in the geologic record (ground truth for the modelers and photogrammetrically-inclined). A comprehensive database of historical tsunami events and their effects has been in progress for decades, continued by present work at NGDC. Beginning with a massive literature search undertaken by colleagues at the University of Hawaii, we extend the record of tsunami backward in time by developing a new database, one of tsunami deposit locations, their estimated age and descriptions of the deposits themselves. Events known only by proxy information are included, but flagged to highlight the absence of a physical deposit. Sort by any populated field, including event, location, region, age of deposit, author, publication type (extract information from peer reviewed publications only, if you wish), grain size, composition, presence/absence of plant material, etc. Use the GTDD to find tsunami deposit references for a given location, event or author; previous work published in your field area; deposits similar to your field area; of potential collaborators. You may also download public domain documents pertinent to tsunami deposits.

Keywords: paleotsunami, tsunami deposits, global database



(S) - IASPEI - International Association of Seismology and Physics of the Earth's Interior

JSS002

Poster presentation

1832

Analytical solution for long wave directivity

Prof. Utku Kanoglu

Department of Engineering Sciences Middle East Technical University IASPEI

Vasily Titov, Baran Ayd N, Costas Synolakis

The spatial and temporal evolution of a finger-like pattern from a finite-dimension source is referred to as its directivity. Ben-Menahem (1961, Bull. Seismol. Soc. Am. 51, 401-435) recognized it and defined a directivity function generated by the source length and the rupture velocity. Later, Ben-Menahem and Rosenman (1972, J. Geophys. Res. 77, 3097-3128) used linear theory to calculate the two-directional radiation pattern from a moving source. Ben-Menahem and Rosenman (1972) showed that tsunami energy radiates primarily at a right angle to a rupturing fault and showed the dependence of directivity on the seafloor rupture and wave celerity, using the path of 1964 Great Chilean tsunami as an example. One example of their work is presented in Synolakis and Bernard (2006, Phil. Trans. R. Soc. A 364, 2231-2265) for the 2004 Boxing Day Tsunami. Okal (2005, Pers. Comm.) quickly eliminated the shorter source proposed in the immediate aftermath of this tsunami, in favour of the larger source, based on qualitative assessment of the radiation field on the basis of the directivity of the source. Okal (2003, Pure Appl. Geophys. 160, 2189-2221) discussed the details of the analysis of Ben-Menahem (1961) and the distinct difference between the directivity patterns of landslide and dislocation generated tsunamis. Okal (2003) considered directivity pattern differences with the field observation of 1964 Alaska event concluding that a large slow earthquake and landslide must occur concurrently. Carrier and Yeh (2005, CMES-Computer Modeling in Engineering and Science, 10(2), 113-121) presented an analytical study for the tsunami propagation with finite crest length over a flat bathymetry and discussed directivity. However, the solution of Carrier and Yeh (2005) appears to have two drawbacks. One, they were not able to compute the integrals numerically for the farfield. Therefore, Carrier and Yeh (2005) proposed a solution using complete elliptic integral of the first kind, with a singularity and, in continuation of conservation of difficulty, they proposed a self similar approximate solution for large times. Two, Carrier and Yeh (2005) analytically modelled only the propagation of Gaussian shaped finite-crest wave profiles, involving approximations in their solution. However, most realistic initial waveform are N-wave like, Tadepalli and Synolakis (1994, Proc. R. Soc. Lond. A 445, 99112). We introduce a new exact analytical solution for the linear shallow water-wave equation over a flat bottom for a finite-crest length source. Our solution can be applied any given initial wave profile with finite-crest length. We discuss several features of directivity along with field observations of the December 26, 2004 Boxing Day Tsunami.

Keywords: tsunami directivity, finite tsunami source

(S) - IASPEI - *International Association of Seismology and Physics of the Earth's Interior*

JSS002

Poster presentation

1833

**Study on the effect of coastal forest against tsunami, Case study on 2006
JAVA Tsunami around Pngandaran, Indonesia**

Dr. Kenji Harada

Disaster Reduction and Human Renovation Inst. Reserch Scientist IASPEI

Aditya Riadi Gusman, Hamzah Latief, Yuichi Nishimura, Yoshiaki Kawata

At the 2004 Indian tsunami, many stories on tree and forest were reported. Some people were survived due to catch on tree. Some area was small damage by the forest effect of tsunami mitigation and blocking driftage. These effects of coastal forest against tsunami were known before 2004 tsunami. However several primary studies were discussed, the tsunami mitigation effect cannot be established quantitatively. Regardless of this, coastal forest are used as the countermeasures to mitigate tsunami impact in the rehabilitation and reconstruction plan. In such conditions, the concern and importance for the role of coastal forest and mangrove on protection are growing big from many specialized fields. The workshop on the coastal forest and tsunami are organized in 2006 by FAO (Food and Agriculture Organization of United Nation) in Khao Lak, Thailand. In this workshop, various authorities related in coastal forest and tsunami are joined and discussed on the role of coastal forest. The key results for evaluation of this workshop are (1) The level of knowledge and understanding of the functions of forests and trees in coastal protection is still insufficient and there is a lack of multidisciplinary research and cooperation in this field, (2) The degree of protection offered by coastal bioshields depends on a number of variables, including: i) the characteristics of the hazard itself, ii) the geomorphologic features of the site and iii) the characteristics of the bioshield, (3) Care must be taken to avoid making generalizations about the protective role of forests and trees based on evidence from one or a few areas, (4) The options for protection include: soft solutions hard engineering solutions and a hybrid of the two. If none of these are appropriate and viable, it may be necessary to zone coastal land use to prevent (further) settlement and construction of valuable assets in the vulnerable zone. And scientific knowledge should be translated into policy-relevant information for decision makers and into technical guidelines. In this study, the coastal forest effect and its limit are discussed based on some tsunami field investigation. The field investigation in the 2006 Java tsunami was carried out on coastal forest conditions and tsunami inundation level around Pangandaran and Cilacap, Indonesia. In this field survey case, species of tree are Coconuts tree, Casuarina, Pandanus and Mangrove. On the type of tree, the shape of tree, tree height, location from sea and so on are different and we measured these conditions. Shuto(1987) is analyzing on the effect of coastal forest from five tsunami events. The limit conditions of coastal forest effect are shown in the case of pine tree in Japan. Our measurement data and some other field survey data in 2004 Indian Ocean Tsunami of are collecting and combined for compare the effect of coastal forest against tsunami and limitation. From these analyses, the limit conditions are shown depend on the kind of tree and local conditions.

Keywords: coastal forest, java tsunami 2006, bioshield

(S) - IASPEI - International Association of Seismology and Physics of the Earth's Interior

JSS002

Poster presentation

1834

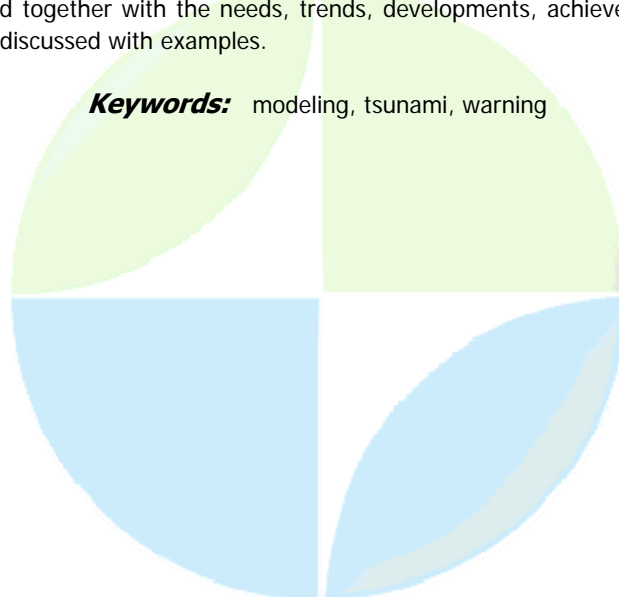
Tsunami modeling; trends, needs, achievements and benefits

Prof. Ahmet Cevdet Yalciner

Civil Engineering Ocean Engineering IAPSO

There are several components of assessment and mitigation of disasters. One of them (for tsunamis) is numerical modeling. There have been several questions came out for the assessment of tsunami risk in the oceans and enclosed seas after the most disastrous event of December 26, 2004, Indian Ocean tsunami. This event caused increasing interests on tsunamis by scientists from different disciplines, and also interests from general public and decision makers and disaster managers at coastal communities in local, national and international level. Tsunami modeling is one of the most important tools needed for assessment of tsunamis, using for warning issues and developing educational and training materials. Tsunami modeling covers i) mathematical description of the problem with initial and boundary conditions with proper approximations and assumptions, ii) solutions of the governing equations with different techniques, iii) simulation, iv) visualization. Beyond these v) analysis of the results, vi) interpretation of the tsunami parameters, vii) understanding of their effects in the inundation zone, and viii) developing mitigation measures accordingly and viii) using them for educational and public relation purposes. There are several issues for achieving the modeling results to be more accurate and useful. One of the main needs for developments in tsunami modeling is estimating the characteristic parameters of triggering mechanisms and simulating them in more realistic level. Length of the rupture segment(s) and width of the ruptured plane(s), strike angle(s) of each segment(s), dip and slip angles, displacement(s) of the ruptured segment(s) are the main inputs for computation of the co-seismic tsunami source characteristics (initial water level distribution for the static source). Most of these parameters can only be estimated by compilation of seismic, geophysical and tidal data some time after the event. Since numerical modeling is one of the essential supplementary tools for TEWSs, more advanced (using parallel processing algorithms and cluster technology), accurate and faster numerical models must be achieved for the best supplement to well developed TEWSs. Satisfying both i) accurate (with additional nonlinear terms such as dispersion and much finer grid sizes) and ii) sufficiently faster numerical modeling for TEWS will need some more time. In the presentation, the stages of tsunami modeling, new demands such as more accurate for academic purposes or faster for operational purposes are discussed together with the needs, trends, developments, achievements, and benefits of tsunami modeling are discussed with examples.

Keywords: modeling, tsunami, warning



(S) - IASPEI - *International Association of Seismology and Physics of the Earth's Interior*

JSS002

Poster presentation

1835

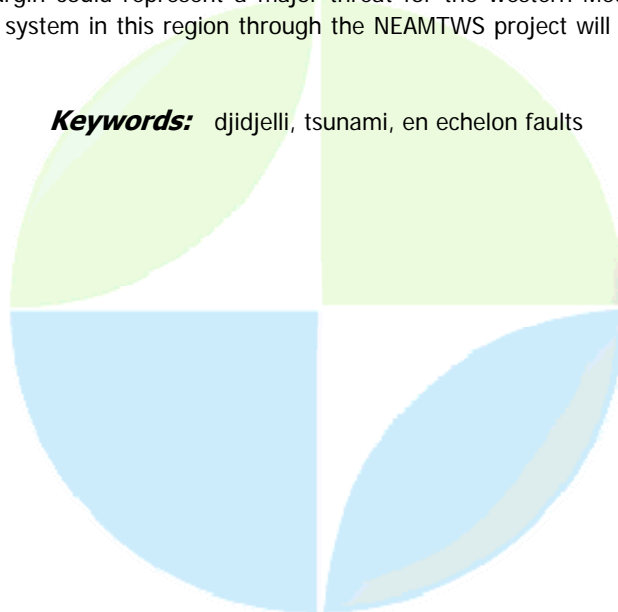
The tsunami of Djidjelli (Eastern Algeria) of August 22 th, 1856: the seismotectonic context and its modelling

Prof. Yelles-Chaouche Abdelkarim
Seismology C.R.A.A.G. IASPEI

J. Dverchre, A. Domzig, B. Mercier De Lpinay, N. Babonneau, H. Hbert, J.Roger, A. Kherroubi, D. Graindorge, R. Bracne, A. Cattaneo, V.Gaullier, B. Savoye, P. Leroy, R. Ait Ouali

The Djidjelli tsunami of August 22 th, 1856, at 10 p.m. is the first event well known in . It occurred after the earthquake which hit the region and destroyed the city of Djidjelli, a small city located 300 km east of Algiers (the capital of). One day before, a first seismic shock happened in the same area causing damages. The tsunami was well described by authors as Roth (1950) or Ambraseys (1982) who reported many details of the effects on the Algerian coast. These authors indicated that a seawave of 2 m or 3m was generated by the earthquake. It flooded the lower part of the town and propagated until the Balearic island. Effects of the tsunami were felt all around the western Mediterranean region. Although the tsunami was attributed to an offshore seismic event with a location of about 15 miles from the coast, its seismotectonic context remained unknown until the recent Maradja2 survey carried out in November 2005. This survey conducted by the French R/V The Suroit allowed to map the bathymetry of the eastern margin of from Dellys to Annaba . From the data collected, a morphotectonic map of the eastern region of has been obtained. Off Djidjelli, four tectonic active structures are outlined along the foot of the slope. They correspond to a set of en echelon faults with an E-W orientation. From the seismic profiles, these structures correspond to thrust ramps dipping towards the south. This pattern explains the occurrence of the double shock and the occurrence of the tsunami on the August 22th. This later could have also triggered marine landslides. Some instabilities are still observed along the margin. Using numerical modelling of the tsunami waves due to the earthquake only, we discuss the effect of tsunami due to the source inferred, compared to the available observations, especially in the Balearic islands. The Djidjelli and the last Boumerdes May 21st, 2003 tsunamis are considered as the most important ones which occurred on the Algerian margin. Their occurrence demonstrates that seismicity along the Algerian margin could represent a major threat for the western Mediterranean region. The installation of an alert system in this region through the NEAMTWS project will be an important tool to mitigate the risk.

Keywords: djidjelli, tsunami, en echelon faults



(S) - IASPEI - *International Association of Seismology and Physics of the Earth's Interior*

JSS002

Poster presentation

1836

Distribution of run-up heights of the tsunami of the South off Central Java earthquake of July 17th, 2006

Dr. Yoshinobu Tsuji

Disaster Mitigation Sciences Associate professor, Earthquake Research Institute IASPEI

Seh-Sub Han, Fachrizal, Indra Gunawan, Teruyuki Kato

A huge tsunami was generated by the south off central Java earthquake of July 17th, 2006, and more than 500 people were killed at the villages on the Indian Ocean coast of Java Island including the international resort point of Pangandaran. We conducted field surveys twice. The first one made by Kato during July 25th to 29th July on the coast from Pangandaran to Pameugpeuk about 150kilometers west of Pangandaran. The second one was made during August 4 to 8 from Genup east to Parangtritis, near Yogyakarta about 200 kilometers east of Pangandaran. The maximum run-up height is 7.7 meters at Pangandaran where 137 peoples were killed due to the tsunami. The length of our surveyed coast is totally 400kilometers. The run up heights at these villages on the section of the surveyed coasts keeps the values of generally 5 to 7 meters and did not attenuated up to the east end of our surveyed coast. The tsunami magnitude in Imamura-Iida's scale is estimated at 3. We made interviews to the habitants and found out that the shaking of the earthquake was weak even at the coasts nearest to the epicenter. Most of the people living on the coasts west of Cilacap did not feel shaking, so it is suggested that this event was induced by a kind of tsunami earthquake.

Keywords: tsunami run up height, tsunami of indonesia, tsunami earthquake

PERUGIA
I T A L Y



(S) - IASPEI - International Association of Seismology and Physics of the Earth's Interior

JSS002

Poster presentation

1837

Mechanism of the Totomi-Oki earthquake of the November 7, 1855

Dr. Yoshinobu Tsuji

Disaster Mitigation Sciences Associate professor, Earthquake Research Institute IASPEI

Yuichi Namegaya, Yoshikane Murakami

On October 15, 2006 a large earthquake M7.9 of a plate boundary dip slip typed one occurred in the south sea region of the central part of Kuril Islands , and accompanied with it a small tsunami was observed at tide gauges on the pacific coasts of the Japanese Island . About two month after it, On January 13th , 2007 another large earthquake M8.2 occurred in the same sea region at the point slightly outside of the trench axis, and its mechanism was estimate as a normal typed one in the sinking plate . The Totomi-Oki Earthquake of November 7, 1855 occurred in the sea region off Tokai district about one year after the Ansei Tokai Earthquake M8.4 of December 23, 1854. A small tsunami of the height of 1 to 2 meters was recorded at several points on the pacific coast, and strong shaking of seismic intensities 6-7 (in JMA scale) were recorded on the plains of Shizuoka prefecture. The crust at Sagara port, near the Cape of Omaezaki, uplifted by about one meter at the Ansei tokai earthquake, but it was subsided by about 60 centimeters accompanied with the Tootomi-Oki earthquake. The crust of Irie village on the east coast of the lagoon Hamana had been subsided and the residential area and the rice fields became lagoon bed after the main shock of the Ansei Tokai earthquake. But after the Totomi-Oki earthquake the crust was uplifted and the residential and rice field areas recovered as before. It is suggested that that the mechanism of the Totomi-Oki earthquake is a normal typed one, which was generated in the Philippine Sea plate. It is suggested that the relationship between the Ansei Tokai Earthquake and the Totomi-Oki earthquake is the same as the two events which occurred in the sea area of Kuril Islands in the recent days. The same typed events also recorded in the few years after the Ansei Nankai Earthquake of December 24, 1854 in an old document written by a person lived in Kochi castle town.

Keywords: normal typed earthquake, earth quakes pair of dip slip, and normal typed ones



(S) - IASPEI - *International Association of Seismology and Physics of the Earth's Interior*

JSS002

Poster presentation

1838

Miocene conglomerates formed by Huge tsunami

Dr. Toru Tachibana

Reserch org. Environmental Geology of Setouchi

Yoshinobu Tsuji, Yuichi Namegaya

Some tsunami sediments need huge tsunami to interpret the sedimentary processes. The Miocene conglomerates, Tsubutegaura Conglomerates, is one of them. These conglomerates including meter-order gravels were deposited in deep water (about several hundred meters depth), and show sedimentary structures formed under not only gravity flows but also strong traction currents. Most possible agents of such traction currents are tsunamis. Nevertheless, there is a doubt whether tsunami-induced currents are able to move large gravels in deep water environments. We attempted two researches; (1) the tsunami simulation to estimate the velocity of tsunami-induced currents, based on the paleogeography and the reconstructed tectonic setting, (2) the estimation of the threshold velocities of large gravels. Results of research (1) using similar parameters of the 2004 Sumatora Earthquake showed that maximum velocity of the estimated bottom current reached 6m/s in 500m depth. Considering results research (1) and (2), tsunamis are possible to transport large gravels in deep water. Tsubutegaura Conglomerates are interpreted to be formed by the huge tsunami caused by large earthquake like the Sumatora Earthquake. Tsunami have been thought to be no major agents in deep water environments except extraordinary events like meteorites-induced tsunami. But tsunami may have occasionally deposited the sediments in deep water environments.

Keywords: deep water environments, conglomerates, miocene



(S) - IASPEI - *International Association of Seismology and Physics of the Earth's Interior*

JSS002

Poster presentation

1839

Large Scale Landslide Tsunami Experiments

Dr. Hermann Fritz

Civil and Environmental Engineering Georgia Institute of Technology

Fahad Mohammed, Jeseon Yoo

Tsunamis are commonly associated with submarine earthquakes. However more than 10% of all tsunamis are generated by landslides or landslide like volcano collapses with subaerial, partially submerged or submarine origins. Landslides may pose perceptible tsunami hazards to areas commonly regarded as immune. A large number of historic and prehistoric slope failures have been reported covering a broad range of landslide volumes and resulting tsunamis. In recorded history landslide generated tsunamis have attained local wave heights and runup heights of more than 100m and 500m, respectively, thereby locally exceeding maximum wave and runup heights of tectonic tsunamis by more than an order of magnitude. The coupling between the landslide motion and the generated tsunami waves is of critical importance given the characteristic trans-critical landslide versus tsunami velocity Froude numbers. Landslide generated tsunamis were investigated in the three-dimensional tsunami basin at OSU based on the generalized Froude similarity. The landslide emplacement characteristics were controlled by means of a novel pneumatic landslide tsunami generator. Deformable landslides of subaerial and submarine origin were modeled with granular materials. State-of-the-art measurement techniques such as particle image velocimetry (PIV), a digital video system comprising multiple above and underwater video cameras, multiple acoustic transducer arrays, hydrophones, as well as resistance wave and runup gauges were applied. The wave generation was characterized by an extremely unsteady three phase flow consisting of the slide granulate, water and air entrained into the flow. PIV provided instantaneous surface velocity vector fields, which gave insight into the kinematics of the wave generation process. At high impact velocities flow separation occurred on the slide shoulder resulting in a hydrodynamic impact crater. The recorded wave profiles were extremely directional, unsteady, non-linear and located in the intermediate water depth wave regime.

Keywords: landslide tsunami, osu, piv



(S) - IASPEI - International Association of Seismology and Physics of the Earth's Interior

JSS002

Poster presentation

1840

Field survey reveals extreme runup of the 17 July 2006 Java tsunami

Dr. Hermann Fritz

Civil and Environmental Engineering Georgia Institute of Technology

W. Kongko, A. Moore, B. Mcadoo, J. Goff, C. Harbitz, B. Uslu, N. Kalligeris, V. Titov, C. Synolakis

On Monday July 17, 2006 at 08:19:28 UTC (15:19:28 local time), a magnitude Ms 7.7 earthquake occurred 200 km off the south coast of western Java in Indonesia. According to Reymond and Okal (2006), this earthquake involved very slow rupture through $\Theta = 6.1$ compared to the usual $\Theta = 4.9$. Similarly, its T waves recorded at Diego-Garcia feature a parameter γ deficient by two orders of magnitude compared to those of typical events from the Sumatra series. This slow earthquake generated a tsunami that severely damaged coastal communities along the southwest and south-central Java provinces. The estimated tsunami death toll exceeds 600 along a 200 km stretch of coastline, with over 400 fatalities in and around the tourist resort of Pangandaran. Flow depths of up to 5 m caused the destruction of 3000 houses in Pangandaran. A lifeguard reported that, mercifully, the tsunami hit on Monday afternoon, when there were few tourists on the beaches compared to the preceding Sunday. This tsunami was difficult to mitigate because the affected area was too close to the epicenter for an early warning system to have been effective, and there was little or no felt ground shaking. Lifeguards sitting on elevated concrete towers had difficulties in recognizing the initial ocean withdrawal, because large wind waves breaking at the coast masked most of the shoreline recession that preceded the main wave. An International Tsunami Survey Team was deployed within one week and the investigation covered more than 600 km of coastline. Measured tsunami heights and run-up distributions were uniform over large areas; however there was a pronounced peak on the south coast of Nusa Kambangan, where the tsunami impact carved a sharp trimline in a forest at elevations up to 21 m and 1 km inland. Local flow depth exceeded 8 m along the elevated coastal plain between the beach and the hill slope. We infer that the focused tsunami and runup heights on the island suggest a possible local submarine slump or mass movement.



(S) - IASPEI - *International Association of Seismology and Physics of the Earth's Interior*

JSS002

Poster presentation

1841

Development of high-resolution coastal digital elevation models for the U.S.: seamlessly integrating bathymetric and topographic data to support tsunami forecasting and modeling efforts

Mrs. Lisa Taylor

NOAA National Geophysical Data Center geophysicist

Barry W. Eakins

The National Geophysical Data Center (NGDC), an office of the National Oceanic and Atmospheric Administration (NOAA), is building high-resolution digital elevation models (DEMs) for select coastal regions. These combined bathymetric/topographic DEMs are used to support tsunami forecasting and modeling efforts at the NOAA Center for Tsunami Research, Pacific Marine Environmental Laboratory (PMEL). The DEMs are part of the tsunami forecast system SIFT (Short-term Inundation Forecasting for Tsunamis) currently being developed by PMEL for the NOAA Tsunami Warning Centers, and are used in the MOST (Method of Splitting Tsunami) model developed by PMEL to simulate tsunami generation, propagation, and inundation. We present our methodology for creating the high-resolution coastal DEMs, typically at 1/3 arc-second (~10 meters) cell size, from bathymetric, topographic, and shoreline data obtained from various sources, including federal, state, and local government agencies, academic institutions, and private companies. These diverse digital datasets are collected using numerous methodologies, in different terrestrial environments, and at various scales and resolutions. We discuss problems encountered in building the DEMs and lessons learned, including: the importance of establishing common vertical datums, accounting for morphologic change in the coastal zone, and evaluating source data sets for reliability, consistency and accuracy.

Keywords: digital elevation models, tsunami forecasting, bathymetry



(S) - IASPEI - *International Association of Seismology and Physics of the Earth's Interior*

JSS002

Poster presentation

1842

Ocean data and information network for Africa (ODINAFRICA) sea level data facility

Dr. Mika Odido

The Ocean Data and Information Network for Africa (ODINAFRICA) has launched a sea level facility the IODE Project Office in Ostend . This facility which can be accessed at <http://www.sealevelstation.net> has the following roles: (i) Data capture via GTS and archive in relational database as an OdinAfrica backup to national and GLOSS data centres, (ii) Web-display of sea level stations status map, allowing quick visual inspection of the network, (iii) semi-automatic data quality control, (iv) real time provision of data (including plots and raw data), (v) database services, through which historical data can be retrieved, (vi) generation of data reports and access to station metadata, and (vii) provision of tide-gauge operator alert (by email or SMS) in case of equipment mal-function. The facility is built in a transplantable format with a view to having it mirrored at a location in Africa . The data will also be mirrored on the websites of the respective National Oceanographic Data and Information Centres (NODCs) participating in ODINAFRICA. The facility has been developed in collaboration with the Flemish Marine Institute (VLIZ).

Keywords: sea level, tide gauge, tsunami

PERUGIA
ITALY



(S) - IASPEI - International Association of Seismology and Physics of the Earth's Interior

JSS002

Poster presentation

1843

Tsunami disaster prevention Management in Iwate Prefecture, Japan

Mr. Kenichi Yoshida

Department of Prefectural Land Developm Iwate Prefecture, Japan IASPEI

Shigeki Sakai, Toshinori Ogasawara, Koshiya Shin, Tomoko Yamazaki, Nobuo Shuto, Takashi Furukawa, Tsutomu Mikami

Since Iwate Prefecture has suffered extensive damage from tsunamis in the past, much effort has been directed towards the maintenance of sea walls, water gates and other tsunami disaster prevention facilities. However, as a result of i) the serious worsening of the economic situation, ii) the development of tsunami simulation technology and the predicted occurrence of a tsunami that could outstrip previous estimates of size, disaster prevention measures in Iwate are currently shifting from the maintenance of disaster prevention facilities to evacuation strategies. In order that prefectural residents are able to evacuate in the instance of a tsunami, knowledge and understanding of tsunamis and improvement in their awareness of disaster prevention is necessary. However, there are many prefectural residents who have limited understanding of tsunamis, while in the majority of schools in the prefecture, there are no lessons given in disaster prevention. Futherstill, much time has elapsed since the occurrence of past tsunami-related disasters and the consequent deterioration of prefectural citizens' knowledge of disaster prevention, is of great concern. In this report, Miyako City (Iwate Prefecture) is cited as a model case of how the inclusion of tsunami disaster prevention education in children's school curriculum and the provision of disaster prevention workshops for adults, have been used to effect improvement in regional citizens' awareness of disaster prevention. When an initial attempt was made to introduce tsunami disaster prevention studies in schools, one issue that became clear was the ① the lack of tsunami disaster prevention educational materials ② limited understanding of the subject on the part of the teachers. Given this situation, tsunami disaster prevention educational materials have been developed in cooperation with teachers from elementary and junior high schools. The materials consist of a DVD compilation of video images that allow viewers to experience at first hand the terror of a real tsunami, a diagram that explains the mechanism of a tsunami in simple terms, experiments and photographs of past sea defenses and damage from past tsunamis. To allow teachers to select and use the educational materials they require for inclusion in a particular lesson plan, the materials have been put together and categorized using a motif system. As from now, slightly over 90% of schools in Miyako City will be integrating the tsunami disaster prevention educational materials into their school curriculums. Workshops attended by regional citizens, members of regional administration and university members have been set up to address problems and issues relating to tsunami evacuation. Prefectural citizens living in areas that are potentially susceptible to inundation by tsunamis have been encouraged to walk the actual path that will lead them to the evacuation area, check on problems and issues that often arise during an evacuation, discuss policy aimed at reducing damage and create an action program as part of their tsunami evacuation strategy. In the beginning, prefectural citizens took a passive stance on the tsunami disaster prevention strategy but after the workshop, there was much visible improvement in their disaster prevention awareness, culminating in maintenance of evacuation routes, the production of maps detailing evacuation routes in the event of an emergency (disaster prevention maps) and other such activities.

Keywords: tsunami disaster, evacuation, disaster education

(S) - IASPEI - International Association of Seismology and Physics of the Earth's Interior

JSS002

Poster presentation

1844

Distribution of asperities of the 1854 Ansei Nankai earthquake

Dr. Yuichi Namegaya

Geological Survey of Japan National Institute of Advanced Industrial Science IASPEI

Yoshinobu Tsuji

Are the locations of the asperities of each gigantic earthquake belonging to the series of the Nankai earthquakes located commonly at the same places? In order to clarify this, the locations of asperities of two Nankai earthquakes, the 1854 Ansei Nankai earthquake and the 1946 Showa Nankai earthquake should be estimated and compared to each other. Distribution of asperities of the 1946 Showa Nankai earthquake is estimated by Tanioka and Satake (2001) by using inversion method on the tide gauge records of the tsunami wave. They pointed out that there are three asperities; the south off Susaki city, Kochi prefecture; the east off the cape Muroto; and sea area south off Kii peninsula. However, the distribution of asperities of the 1854 Ansei Nankai earthquake has not been estimated, because there are no data of the tide gauge records of the tsunami. Only the distributions of the tsunami maximum heights, the crustal deformations, and the seismic intensities estimated from the old documents are available for the 1854 Ansei Nankai earthquake. In this study, we developed the nonlinear inversion method to solve the distribution of asperities by using the data of the tsunami maximum heights and the crustal deformations. We estimated the distribution of asperities to make the sums of square of differences of the maximum tsunami heights between the recorded and calculated minimum. As the result, the distribution of asperities of the 1854 Ansei Nankai earthquake is similar to that of the 1946 Showa Nankai earthquake, but the amount of dislocations of the former is larger than that of the latter.

Keywords: 1854 ansei nankai earthquake, asperity, joint inversion



(S) - IASPEI - *International Association of Seismology and Physics of the Earth's Interior*

JSS003

1845 - 1892

**Symposium
Early-Warning Systems**

Convener : Prof. Jochen Zschau

Early warning systems can reduce the negative impacts across the globe of extreme events such as earthquakes, tsunamis, volcano eruptions, landslides, tropical storms, floods, extreme space weather and others. They provide timely information that allows individuals exposed to a hazard, to take action to avoid or reduce their risk and prepare for effective response. Dependent on the type of hazard the warning time available may range between only a few seconds in case of earthquakes to months and years in case of creeping disasters such as droughts. Although rapid information- and early warning technologies are now available to a great extent, their potential in the field of disaster mitigation is not used to any appreciable extent, showing that the user needs are not yet addressed sufficiently. Integrated earth observation, the development of real-time analysis, modelling and simulation methods, their integration with appropriate facilities for data processing, visualization and rapid information systems and their application to early warning in conjunction with disaster management, therefore, remains one of the major challenges of applied earth system sciences. The session will discuss the latest scientific/technological developments, projects, programs and best practices in the field of early warning. This will be done for various disaster types, from global to local scale and with special regard to the user needs. Contributions are particularly welcome if they address the aspect of multi-hazard early warning.

XXIV2007

PERUGIA
I T A L Y



(S) - IASPEI - *International Association of Seismology and Physics of the Earth's Interior*

JSS003

Oral Presentation

1845

Post-Tsunami Survey and the Development of a Tsunami Warning System for Kenyan Coastal Region

Dr. Balla Maggero

Oceanography & Marine Services Kenya Meteorological Services IAMAS

Ali Mafimbo, Antony Kibue

Kenya is among the countries in the Western Indian Ocean region that was affected by the tsunami. Though the impact was much less compared to the devastation in countries closer to the epicenter. Malindi bay and Lamu were most affected because they are wide, shallow and open. There are no coral reefs to shield the bay from the waves propagating from the deep sea. The fishing industry in Malindi and Lamu was most affected due to destruction of fishing gear, boats and man-hours lost. Occurrence of the tsunami at the coastal area of Kenya has revealed that the country is ill prepared to deal with such a catastrophe since there are no early warning mechanisms in place. Though the effects of the tsunami were less in Kenya as compared to countries close to the epicenter, a number of impacts were experienced in the country. This is a clear pointer to more serious impacts should another tsunami of higher magnitude strike our countrys coastline. Therefore, it calls for concerted efforts to put mechanisms in place for purposes of mitigating the negative impacts of such events whenever they occur in future. In this report, we presents findings from a post-Tsunami survey conducted by marine experts from Oceanography & Marine Department of the Kenya Meteorological Service and Kenya Marine & Fisheries Institute, catastrophic modeling results, some recommended precautionary measures and recent progress at the Oceanography & Marine Department in developing a Tsunami Warning System for this region.

Keywords: tsunami, waves, impact



(S) - IASPEI - *International Association of Seismology and Physics of the Earth's Interior*

JSS003

Oral Presentation

1846

Flood warning system for Bangladesh

Mr. Mohammad Khaled Akhtar
Early-Warning System IASPEI

Bangladesh is highly vulnerable to the floods and associated disasters. The world's highest mountain, the Himalayan, in the north and the Bay of Bengal in the south make unique geographical setting for the country. Bangladesh is a low-lying country in the Meghna delta located at the confluence of three major rivers; the Ganges, the Brahmaputra and the Meghna. During recent years several large floods have caused disasters in Southeast Asia. The inundation and flooding in Bangladesh is a serious setback. Flood forecasting in a deltaic region like Bangladesh is a difficult problem. Flood occurs almost every year in Bangladesh with varying intensity and magnitude. In a normal year, 20% of the country is inundated by river spills and drainage congestions. Approximately 37% of the country is inundated by floods of 10 years return period. Devastating floods of 1988 and 1998 inundated more than 60% of the country. Recent floods of 2004 also caused lots of damage to the country economy. Structural measures for flood management began in Bangladesh in the late 60s to completely eliminate flood in the project area but later on non-structural measures has also been adopted for flood management. However, with the modern technological advancement flood forecasting and warning services (a non structural measure) acquired the highest position to minimizing flood damage and losses because of Tens of millions people live in flood plains. Moving them out is not an option but providing adequate safety against large floods combined with a risk reduction system supported by an early warning is desirable. With the presence of improved data exchange programme through the neighboring country and access to the result of numerical meteorological models like ECMWF are only option for the country to significantly increase forecasting lead times and improve forecast accuracy near border areas. Considering the present situation, this paper aims to develop a system which can improve the early warning system by increasing the accuracy of the forecasted boundary discharge with the help of remotely sensed data as well as meteorological models.

Keywords: flood, warning, forecasting



(S) - IASPEI - International Association of Seismology and Physics of the Earth's Interior

JSS003

Oral Presentation

1847

Win: a new SOA for risk management

Mrs. Araceli Pi Figueroa
Business Development Starlab

Christian Alegre, Marina Martinez-Garcia

The Wide Information Network (WIN) Integrated Project (EU FP6 Call 2 DG IST) integrates existing reference results and initiatives to contribute to the design, the development, and the validation of the European risk management info-structure. This info-structure will be a major element of the future European Spatial Data Infrastructure (ESDI) and of Single European Information Space for what concerns the environment and risk management. WIN results, including the data information models, the service oriented architecture with its set of generic services and workflow management facility, constitute an efficient and open framework, useful on various environmental and risk management contexts. The last year of WIN project will be focused on validation, experimentation, evaluation and preparation of the deployment of the solution, in several thematic. Two domains of experimentation are defined: Marine and Coastal domain with experimentations related to oil-spill monitoring and response process, and Land risk management domain, with experimentations on fire and floods disaster management in relation with French and other countries Civil protections. Planned experimentations will allow to evaluate benefits of WIN and in particular the capability of WIN to support end-to-end oil spill monitoring and response process, managing all required information, and the capability of WIN to improve risk management for what concerns fire and floods, through its unified wide catalogue and its GIS capabilities. WIN deployment roadmap targets at a wide range of opportunities at European and regional level, on several thematic like shoreline monitoring, water resources management, and various land-based risks management domains.

Keywords: riskmanagement, architecture, infostructure



(S) - IASPEI - *International Association of Seismology and Physics of the Earth's Interior*

JSS003

Oral Presentation

1848

MarCoast Network: a provision of EO-Based services for marine and coastal applications

Mrs. Araceli Pi Figueroa
Business Development Starlab

Jrme Bruniquel, Marina Martinez-Garcia

The MARine & COASTal environmental information services project (MarCoast) is part of the GMES Service Element (GSE) programme, managed and funded by the European Space Agency (ESA). The project started with a consortium composed of 32 partners from 10 European countries, and gathers all key actors in the field of marine and coastal applications. Additional activity is expected to expand the initial scope of the delivered services, both in term of geographical coverage and/or added services. MarCoast targets to deliver a single portfolio of marine and coastal services at the European scale. The portfolio is composed of 6 service lines which are: Oil spill surveillance and customised information, Oil spill drift forecast, Water quality monitoring and alert, HAB monitoring, evolution and forecasting, Water quality assessment service, Met-Ocean data. One of the specificity of MarCoast, as for each GSE project, is the strong commitment of users; this commitment is formalized through Service Level Agreement (SLA), signed between the service provider and the user. Signed SLA is mandatory to start any service activity. MarCoast makes use of all sensors dedicated to marine applications, such as SAR systems (ASAR and RSAT-1) for oil spills, ocean colour sensors (MERIS and MODIS) for water quality applications. Altimeter, radiometers, and scatterometer sensors support the production of metocean data. In the future, GMES sentinels 1 and 3 will be the 2 main missions on which MarCoast services will rely on. MarCoast is a unique opportunity to gather in the same project end-users, service providers and system developers. As such, it demonstrates that GMES services are about to reach the needed level of maturity that will ensure sustainability.

Keywords: operational, marine, services



(S) - IASPEI - *International Association of Seismology and Physics of the Earth's Interior*

JSS003

Oral Presentation

1849

Remote sensing/GIS application for early warning systems of natural hazard: case study of Victoria Island, Lagos Nigeria.

Mr. Olumuyiwa Sonuga
PHYSICS UNIVERSITY IASPEI

The rate of environmental changes at the Victoria Island coast of Lagos State, Nigeria is a major problem and the environment is under the threat of loss of lives, properties and land became vulnerable to landslide, soil erosion and land use such as residential, industrial buildings and utilities has repeatedly devastated by coastal storms and flooding thereby resulting in environmental hazards. Already, an occurrence of 0.2meters of sea level rise resulted to a loss of 3,100 square kilometer of landmass to flooding. Studies have shown that population growth, migration, urbanization, human and natural activities at the costal areas are the major factors influencing the occurrence of the hazards. As a result of population growth in the country, the rate at which people migrate to Lagos State is high resulting into high rate of urbanization which has led to construction of buildings whereby obstructing the flow of water through the drainage channels to drain excess water has cost massive loss of land, bulk age of sewage. Remote Sensing and GIS technologies have been employed in this study to asses the extent of coastal land loss and damages in Victoria Island of Lagos. Satellite images for different years between 1990 and 2003 of the study area were compared and results shows that natural processes have destroyed vegetation and land cover areas.

Keywords: coastal storms, flooding, hazards



(S) - IASPEI - International Association of Seismology and Physics of the Earth's Interior

JSS003

Oral Presentation

1850

Web Based Global System for loss assessment due to strong earthquakes

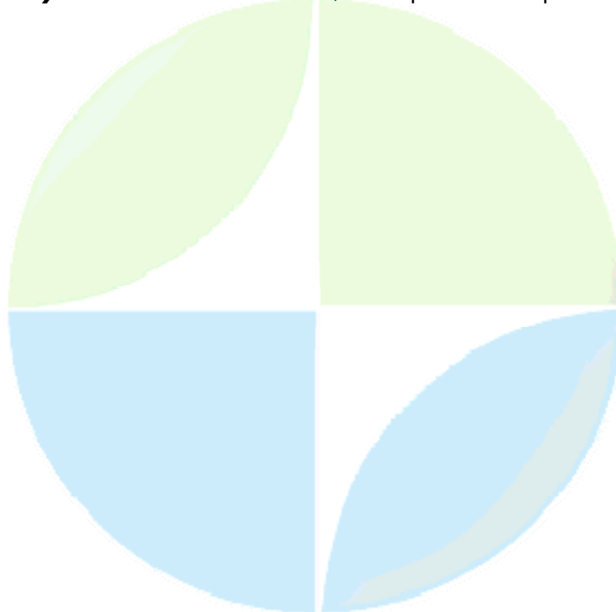
Dr. Nina Frolova

Seismological Center of IGE, Rus. Acad. of Sci. Senior Scientific Researcher, Ph.D. IASPEI

Valery Larionov, Jean Bonnin

According to the recommendations of IDNDR Working Groups on scientific and technological aspects of Early Warning Systems (EWS) in order to fulfill a risk reduction functions such Systems should not be interpreted as technical instruments for detecting, forecasting impending event and issuing alert and, therefore, they should consists of four sub-systems: a warning sub-system, a risk reduction sub-system, a preparedness sub-system and a communication sub-system. A risk reduction sub-system may allow potential damage extent and social loss due to scenario earthquakes to be generated and/or estimate expected consequences due to just occurred event in emergency mode. Risk reduction sub-system may be designed and developed for individual decision makers usage. Another variant is to develop the web-based sub-system, which may be accessible to all interested decision makers and experts at international, regional, national, local or urban level. The paper describes the framework of the global web-based risk reduction sub-system, its mathematical models for shaking intensity distribution, damage to buildings and structures, number of fatalities and injuries, as well as its data bases on build environment and population distribution. The sub-system is now under development within the NATO-Russia Project Analysis and Synthesis of Loss Estimation and Risk Assessment Methodologies for Prediction and Prevention of Catastrophes. Extremum family systems developed during the last ten years are prototypes of the new web-based open tool, which will be accessible to any registered end-user. The tool will provide possibility of distributed data bases usage and to update the data bases on regional attenuation laws, vulnerability functions of different elements at risk by joint efforts. In the case of strong earthquake the Internet conferences may be organized in order to give additional possibility to experts to take a proper decision about expected damage and loss. One of the principle advantages of the new web-based sub-system for loss assessment due to strong earthquakes is usage of common data bases and simulation models, which are updated by joint efforts.

Keywords: web based tool, earthquake consequences



(S) - IASPEI - *International Association of Seismology and Physics of the Earth's Interior*

JSS003

Oral Presentation

1851

FLASH: A new EU project for the early warning of Mediterranean flash floods

Prof. Colin Price

Geophysics and Planetary Sciences Tel Aviv University IAMAS

Yoav Yair, Alberto Mugnai, Kostas Lagouvardos, Maria-Carmen Llasat, Silas Michaelides

A new European Union FP6 project titled FLASH will run from 2006-2009 in an attempt to improve our knowledge of historic flash floods in the Mediterranean region, while trying to improve short term (hours) and mid term (days) forecasts of heavy precipitation events. Flash floods are a serious problem in the Mediterranean region in particular, and in Europe in general, resulting from large weather systems with embedded severe thunderstorms that deposit large amounts of rainfall in short periods of time. Since lightning activity can be detected and monitored continuously from thousands of kilometers away, this new EU project will use lightning data, together with other available observations, to better detect and track the location, intensity and timing of heavy convective precipitation events. We plan to develop algorithms to provide on-line nowcasts and forecasts of areas at high-risk of heavy precipitation and flooding across the Mediterranean. Our experimental products will be provided in real time to end-users and stakeholders for use in their planning activities. The societal benefits of such advanced warnings will be investigated, especially in relation to risk management.

Keywords: flashfloods, lightning, mediterranean

PERUGIA
ITALY



(S) - IASPEI - International Association of Seismology and Physics of the Earth's Interior

JSS003

Oral Presentation

1852

Earthquake Detection and Rapid Magnitude Determination by the Fast Wavelet Transform

Prof. Frederik Simons

Ben D. E. Dando, Richard M. Allen

Earthquake early warning systems must save lives. It is of great importance that networked systems of seismometers be equipped with reliable tools to make rapid determinations of earthquake magnitude in the few to tens of seconds before the damaging ground motion occurs. A new fully automated algorithm based on the discrete wavelet transform detects as well as analyzes the incoming first arrival with unmatched accuracy and precision, estimating the final magnitude to within a single unit from the first few seconds of the P wave. The curious observation that such brief segments of the seismogram may contain information about the final magnitude even of very large earthquakes, which occur on faults that may rupture over tens of seconds, is central to a debate in the seismological community which we hope to stimulate by this presentation. Wavelet coefficients of the seismogram can be determined extremely rapidly and efficiently by the fast lifting wavelet transform. Extracting amplitudes at individual scales is a very simple procedure, involving a mere handful of lines of computer code. Scale-dependent thresholded amplitudes derived from the wavelet transform of the first 3--4 seconds of an incoming seismic P arrival are predictive of earthquake magnitude, with errors of one magnitude unit for seismograms recorded up to 150 km away from the earthquake source, over a surprisingly wide magnitude range. Our procedure is a simple yet extremely efficient tool for implementation on low-power recording stations. It provides an accurate and precise method of autonomously detecting the incoming P wave and predicting the magnitude of the source from the scale-dependent character of its amplitude well before the arrival of damaging ground motion. Provided a dense array of networked seismometers exists, our procedure should become the tool of choice for earthquake early warning systems worldwide.

Keywords: earthquakes, hazards, wavelets



(S) - IASPEI - *International Association of Seismology and Physics of the Earth's Interior*

JSS003

Oral Presentation

1853

Detection of precursory changes in source parameters: A probable short-term forecasting model for the small- to moderate- size intraplate earthquakes in the Kachchh seismic zone, Gujarat, India

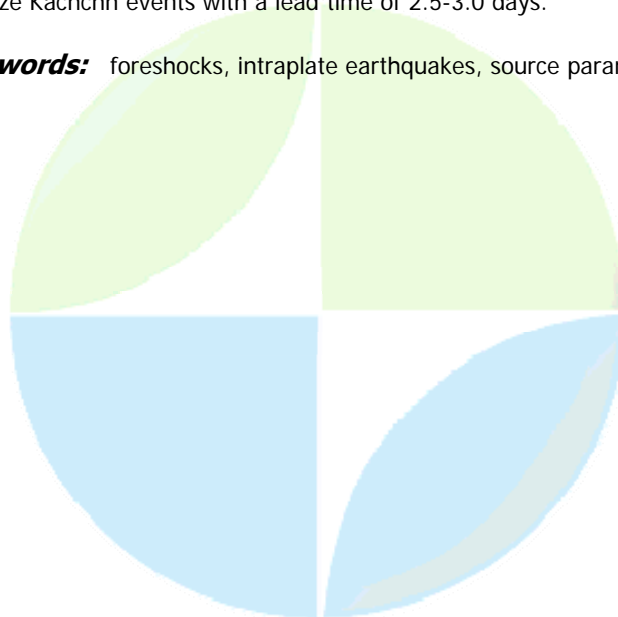
Dr. Prantik Mandal

Seismology NGRI, HYDERABAD, INDIA IASPEI

R.K.Chadha, Mr. C. Styamurty, Mr. I.P. Raju, Mr. N. Kumar

Precursory changes in corner frequency as well as stress drops have been noticed about 2.5-3.0 days prior to nine main earthquakes (M_w 3.8-5.6) of the 2001 M_w 7.7 Bhuj earthquake sequence, which occurred in the Kachchh seismic zone during 2002-2006. The studied sequences suggest 2-8 numbers of foreshocks, which have occurred within a circular area of 10-15 km from the epicenter of the mainshocks during 80-160 hours period prior to the mainshocks. Since August 2002, the seismic activity in Kachchh has been monitored by a close digital network consisting of 5-8 three-component digital seismographs and 10-20 three-component digital accelerographs, which enabled us to relocate the considered nine earthquake sequences using the joint hypocentral determination (JHD) technique resulting in a reliable and accurate hypocentral parameters estimates (error in the epicentral location < 500 meter, error in the focal depth estimation < 1000 meter). The focal depths are varying from 2 to 35 km. The estimated corner frequency (f_c), source radius (r), stress drop (D_s) and moment magnitude (M_w) for foreshocks of nine studied sequences are ranging from 3.21 to 9.81 Hz, 128.4 to 487.5 m, 3.21 to 12.39 MPa, and 2.3 to 4.2, respectively. For all the nine earthquake sequences, we observed a precursory decrease of 66-82 % in the corner frequency and a precursory increase of 65-98 % in the stress drops during the 60-70 hours period prior to the mainshocks. We also noticed an increase of 30-60 % in the fault length during the above-mentioned precursory period. The foreshocks for the studied nine Kachchh earthquake sequences are found to be of Mogi's type-II classification, which follow multiple rupture model of foreshock generation. Following dilatancy model, it can be inferred that the observed an increase of 30-60% in fault length associated with a decrease in corner frequency and increase in stress drop over most of the precursory period can be attributed to the presence of fluids at the focal depths (15-30 km depth range), which may be considered as the probable precursors for predicting moderate size Kachchh events with a lead time of 2.5-3.0 days.

Keywords: foreshocks, intraplate earthquakes, source parameters



(S) - IASPEI - International Association of Seismology and Physics of the Earth's Interior

JSS003

Oral Presentation

1854

Natural Hazard Monitoring: a early warning method to delineate potentially affected areas by Hurricane using a GIS model

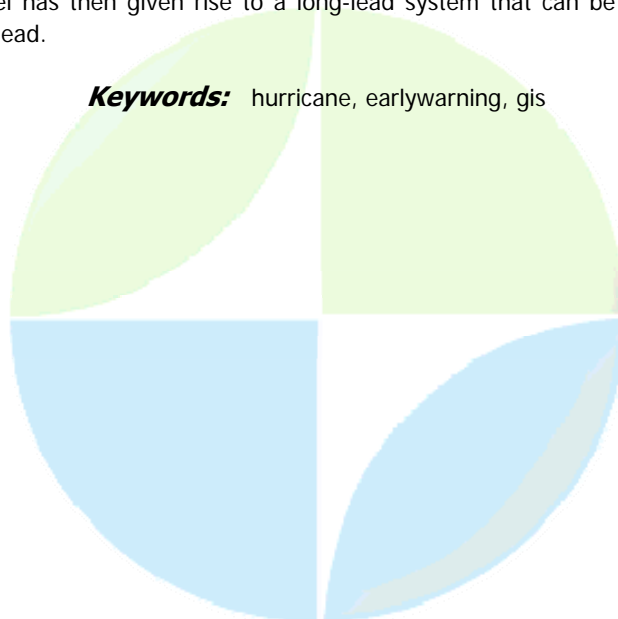
Dr. Andrea Taramelli

Dipartimento di Scienze della Terra Università degli Studi di Perugia

Laura Melelli, Massimiliano Pasqui, Alessandro Sorichetta, Bernardo Gozzini

This research integrates the concept that the subject of natural hazards and the use of existing remote sensing system in the different phases of a disaster management for a specific hurricane hazard, is based on the applicability of GIS model for increasing preparedness and providing early warning. The modelling of an hurricane event in potentially affected areas by GIS has recently become a major topic of research. In this context the disastrous effects of hurricanes on coastal communities and surroundings areas are well known, but there is a need to better understand the causes and the hazards contributions of the different events related to an hurricane, like storm surge, flooding and high winds. This blend formed the basis of a semi-quantitative and promising approach in order to model the spatial distribution of the final hazard along the affected areas. The applied model determines a sudden onset zoning from a set of available parameters that include topography, bathymetry, storm track into coast proximity and river network. For all these parameters, key attributes based on SRTM and bathymetry data, are the river network delineation (based on the Strahler methodology) the slope data and coastline bathymetry identification. Complementary data for the final model includes remote sensed density rain dataset, elevation datasets for selected coastal drainage basins, and existing hurricane tracks inventories together with hurricane structure model (different buffers related to wind speed hurricane parameters in a GIS environment). To assess the overall susceptibility, the hazard results were overlaid with population dataset and landcover. The approach, which made use of a number of available global data sets, was then validated on a regional basis using past experience on hurricane frequency study over an area that covers both developed and developing countries in the Caribbean region. As a final result we can state that remote sensing data analysed together with meteorological and environmental data in an integrated GIS system give a spatially resolved picture of the surface conditions and, in our context, information on the occurrence, extent and severity of hurricane hazard. The applied GIS model has then given rise to a long-lead system that can be set-up to allow such a early warning to go ahead.

Keywords: hurricane, earlywarning, gis



(S) - IASPEI - *International Association of Seismology and Physics of the Earth's Interior*

JSS003

Oral Presentation

1855

Weather and constant plane crashes: a case study of Nigeria

Dr. Deborah Olorode
Physics University IASPEI

Dr Catherine Ikhile

ABSTRACT: This paper examines the incidence of constant plane crashes in Nigeria and the weather connection. The Nigerian weather condition for the past twelve years (12 yrs) was examined using weather elements of rainfall, temperature, relative humidity, sunshine and wind speed for three major towns , Lagos Benin City and Port Harcourt. Results reveal that changing weather conditions over these years are in line with global climate change. Nigeria has a spotty air safety record with more than eleven crashes since 1995, killing over 600 people. It is concluded that Nigerian Government embark on drastic measures and source for facilities to manage the bad weather condition which has contributed to the constant plane crashes in Nigeria.

Keywords: aircraft, plane crashes, weather



(S) - IASPEI - *International Association of Seismology and Physics of the Earth's Interior*

JSS003

Oral Presentation

1856

An evolutionary approach for real-time magnitude estimation for earthquake early warning

Dr. Maria Lancieri

RISSC-LAB INGV, Osservatorio Vesuviano

Aldo Zollo

Regional earthquake early warning systems relies on the possibility of achieving fast and reliable estimates of location and magnitude/moment of an occurred, potentially destructive event, in order to predict peak ground motion quantities at a distant target infrastructure. Recent studies showed the possibility of predicting the final event magnitude using measurements of the predominant frequency and/or the low-frequency peak displacement amplitude in the very early portion of P-wave signals. In particular, the recent analysis of near-source strong motion records from the European Data Base revealed a clear correlation between distance corrected peak displacement amplitudes and magnitude for events in the magnitude range 4-7.4 (Zollo, Lancieri and Nielsen, 2006). In the present work we analyze a Japanese strong motion data-set (extracted from K-Net and KiK-net) with the aim to investigate the relationship between the early P- and S- wave peak displacement and magnitude and its use for an evolutionary estimate of magnitude for earthquake early warning application. About 2700 records from 256 Japanese earthquakes have been analyzed with magnitude ranging from 4 to 7 with maximum depth of 50Km and hypocentral distance smaller than 60Km. The records come from the Kyoshin strong motion network, which collects data from 1000 strong-motion station deployed over the whole Japanese archipelago, with an average inter-station distance of 25 Km. The accelerometric records have been integrated twice, and band pass filtered between 0.075 and 3Hz. In order to correct the early peak amplitudes for the distance attenuation effect, we evaluated an attenuation relationship between the logarithm of the distance, the magnitude and the peak displacement read on short time windows after the P-wave and the S-wave arrivals. While using a duration of 2-sec after the first P-arrival the peak displacement appears to saturate with magnitude around $M=6$, this effect is removed using windows larger than 3-sec for which a linear relationship is found between the logarithm of displacement peak amplitude and magnitude. On the other hand the saturation effect is not visible on S-wave peak even for very short time windows (1 sec). Assuming the existence of a strong motion network, densely deployed in the epicentral area of an impending earthquake, we illustrate a Bayesian approach to estimate the magnitude and its uncertainty from the P- and S-peak information available at each triggered station as a function of time from the event occurrence. We show the application of the proposed procedure to the Japan earthquake data-set by simulating the real-time estimation of several moderate to large magnitude events along with time evolution of its confidence level.

Keywords: magnitude estimation, evolutionary, bayesian approach

(S) - IASPEI - *International Association of Seismology and Physics of the Earth's Interior*

JSS003

Oral Presentation

1857

Recent Progress in Infrasonic Early Warning Systems

Dr. Milton Garces

Infrasound Laboratory University of Hawaii, Manoa IAVCEI

David Fee, Michael Hedlin, Robin Matoza, Hugo Yepes, David McCormack, Rene Servranckx, Henry Bass

The emerging global infrasound network has stimulated a growing number of infrasound projects devoted to natural hazard applications. These applications include monitoring volcanic eruptions, extreme weather, large ocean swells, bolides and tsunamis. The Acoustic Surveillance for Hazardous Eruptions (ASHE) project aims to develop and evaluate the capability to use low frequency sound to provide robust, low-latency notifications of volcanic eruptions over regional distances. We describe current field deployments of several small, autonomous infrasound arrays in Washington state (US) and Ecuador. The arrays in Washington have detected diverse eruption signals from Mount St. Helens, and the arrays in Ecuador have captured eruptions from Tungurahua and Sangay Volcanoes, as well as Galeras in Ecuador. These stations send continuous real time data to a central facility where automatic analysis techniques for eruption detection are being prototyped. Plans are in place to send automated notification products on a test basis to a participating ICAO-designated Volcanic Ash Advisory Center for comparison and possible integration with their existing warning systems.

Keywords: infrasound, volcanoes, ashe



(S) - IASPEI - International Association of Seismology and Physics of the Earth's Interior

JSS003

Oral Presentation

1858

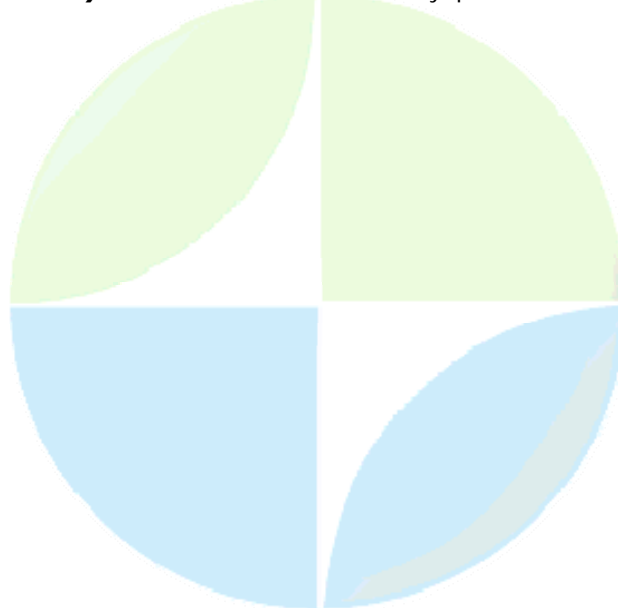
Real-time, probabilistic and evolutionary earthquake location for seismic early warning

Dr. Claudio Satriano
RISSC-Lab AMRA Scarl

Anthony Lomax, Aldo Zollo

An effective early warning system must provide probabilistic estimates of the location and size of a potentially destructive earthquake within a few seconds after the event is first detected. In this work we present an evolutionary, real-time location technique, based on a robust, equal differential time (EDT) misfit function, a very fast, global-search algorithm, and a probabilistic approach for describing the hypocenter estimation. The location technique, at each time step, relies on the combined information from triggered arrivals and not-yet-triggered stations. With just one recorded arrival, the hypocentral location is constrained to be within the Voronoi volume around the first triggering station. The Voronoi volume is defined by the current time and the travel times to the not-yet-triggered stations; this volume shrinks as time passes, even if no new arrivals become available. With two or more triggered arrivals, the location is constrained by the intersection of the Voronoi volume defined by the remaining, not-yet-triggered stations with the EDT surfaces for all pairs of triggered arrivals. (At each point on an EDT surface the difference in the predicted travel times to two stations equates the difference in the observed arrival times at the two stations.) As time passes and more triggers become available, the evolutionary location converges to a standard EDT location. We show several tests of the real-time location technique using arrivals generated by different automatic picking procedures for strong-motion data from moderate to large earthquakes worldwide. The results indicate that useful, probabilistic location estimates, suitable for early-warning applications, can be achieved with very few recording stations (1-2), while, in comparison, a standard location algorithm usually needs 3 or more stations to begin constraining the hypocenter. We also present an event binding procedure for the real-time location technique to detect multiple sources and associate phase arrivals when different events occur close in time.

Keywords: location, evolutionary, probabilistic



(S) - IASPEI - *International Association of Seismology and Physics of the Earth's Interior*

JSS003

Oral Presentation

1859

Use of high-frequency geoacoustic effect for a location of earthquakes preparation areas

Dr. Boris Shevtsov

Far Eastern Branch Russian Academy of Science IAGA

Anatolii Kuptsov, Igor Larionov, Yurii Marapulets, Andrei Perezhogin, Raya Sagitova, Gleb Vodinchar

High-frequency (0-10 kHz) geoacoustic precursors of earthquakes are considered. It is shown, that during preparation of seismic events as result of increase in deformations, intensity and anisotropy of geoacoustic emission grow, and sound signals have as a first approximation a direction on an epicenter. The measurements of deformations carried out with the help of laser interferometer have shown, that high-frequency acoustic noise is the result of slip in the surface sedimentary breeds which are taking place in an condition of elastic pressure. Having in view the solution for tensor of elastic pressure and features of sound sources in the breeds the physical model of geoacoustic signal generation is created. It has explained three experimental results. In the first why the high-frequency geoacoustic effect arises on distances of hundred kilometers from epicenters. Second, why the earthquakes giving geoacoustic effect have strongly anisotropic spatial distribution around the point of measurements. Thirdly, why acoustic signals have a direction on an epicenter, and what explains the deviation of signal bearing. In the report, the opportunity of use of high-frequency geoacoustic effect for geodeformations monitoring and location of earthquake preparation areas is discussed.

Keywords: geoacoustic, location, earthquake



(S) - IASPEI - *International Association of Seismology and Physics of the Earth's Interior*

JSS003

Oral Presentation

1860

Ground Effects of Space Weather: climatology and forecast of extreme events

Dr. Larisa Trichtchenko

Natural Resources Canada Research Scientist

Impacts of space weather events on ground infrastructures arise from the combined effects of large variations in geomagnetic field, ground conductivity structure, and topology of the affected network. These impacts range from slow, cumulative multi-year excessive corrosion of the pipeline systems to fast (in minutes) collapse of power grids during geomagnetic storms (Hydro-Quebec in March 1989, part of Sweden power grid in October 2003). Space Weather Regional Warning Centre in Ottawa, has long-time experience in working closely with industry to better address the needs for studies of climatology and for the forecast of the extreme events. For this session we present a short summary of our recent projects with industrial partners on both aspects. The first topic is the development of the methodology for assessing the effects of geomagnetically induced currents on pipeline infrastructure in . This includes statistical studies of the occurrences of different levels of geomagnetic activity, global and regional models of the ground conductivity and effects of the infrastructure topology. As a result, sequence of statistical maps for different areas of is produced. The second aspect, forecast of the extreme events for statistically different zones of geomagnetic activity in will be demonstrated using examples of the latest space weather events (2000-2007). Here we address the issue of importance of the proper provision of real-time ground and space data for forecast of ground effects of space weather events for local users.

Keywords: space weather



(S) - IASPEI - *International Association of Seismology and Physics of the Earth's Interior*

JSS003

Oral Presentation

1861

Real-time monitoring of earthquake activity in Australasia

Dr. Phil Cummins

Geospatial and Earth Monitoring Division Geoscience Australia IASPEI

Spiro Spiliopoulos, Jonathan Bathgate, Marco Maldoni

Since the 2004 Sumatra-Andaman earthquake and Indian Ocean Tsunami, considerable effort has been directed towards improving regional monitoring of large earthquakes in Australasia. As part of its response to the 2004 disaster, the Australian Government is developing the Australian Tsunami Warning System, which includes a facility for real-time monitoring of earthquake activity in the Australasian region. As part of its attempt to rapidly characterize earthquake sources, this facility has implemented a system (based on the commercially available software platform Antelope) for real-time data acquisition and automatic detection, location, and magnitude estimation. In addition, it is implementing systems for automated CMT estimation and manual Mwp estimation. To our knowledge this is the first warning centre in the region that is implementing this array of techniques in a warning context. In this presentation we present an analysis of the performance of this real-time earthquake monitoring system, discuss the challenges to earthquake monitoring in the region, and canvas plans for the future.

Keywords: early warning, earthquake, tsunami

PERUGIA
ITALY



(S) - IASPEI - *International Association of Seismology and Physics of the Earth's Interior*

JSS003

Oral Presentation

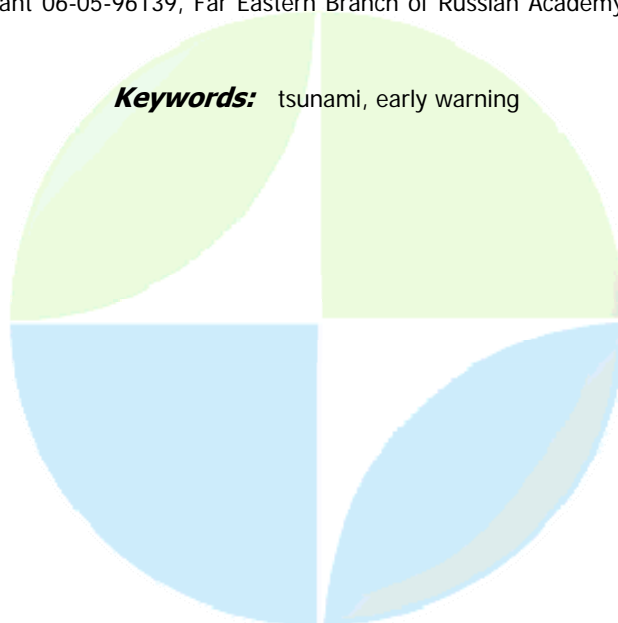
1862

A Possible Method of Tsunami Early Warning

Dr. Yury Korolev

At present Tsunami Warning Services (TWS) in US, Japan and Russia works well enough not missing significant tsunamis. At the same time TWS commit a great many false tsunami alarms (up to 75-78% of total alarms since it came into existence). It is obvious, that false tsunami alarms are accompanied by various losses. As a result of some recent false tsunami alarms on Hawaii the average cost of lost business and productivity was estimated to be \$ tens millions in every event. It is possible to reduce a number of false alarms using additional information on a formed tsunami obtained in the open ocean. Use of this information can provide more accurate prediction. The method of the short-term tsunami forecast using information of remote level gauge is presented in this paper. This method is based on well-known reciprocity principle. This method permits to calculate the form of tsunami wave near every specific coast point. The sea level information in remote point and the only seismological information about time of beginning and co-ordinates of the earthquake are needed for tsunami wave form prediction. The suggested method for tsunami estimation from the data of a sea level gauge was tested by means of the numerical model with actual bathymetry. To calculate tsunamis (expected ones) tsunami sources were applied which were chosen as macroseismic ones corresponding to recent tsunamis. Use of proposed method shows that the main wave parameters of predicted tsunami agree sufficiently well with parameters of expected tsunami. The presenting method may be applied for short-term tsunami forecast regardless of tsunami generation genesis. Tsunami may be seismic one, subsea landslide one or others. The presenting method can be used on-line not only by regional tsunami warning service but also by local tsunami warning services. So, tsunami warning may be declared for sites where tsunami to be of real threat. Putting this method or analogue ones into use will permit to reduce a number of false tsunami alarms. It seems that requirements (recommendations) to TWS in future may be as follows. TWS must announce tsunami alarm to those point only where tsunami to be of real threat. This alarm must be accompanied by information about predicted tsunami: number of waves, their heights, expected time of alarm canceling. This work is supported by Russian Foundation for Basic Research, grant 06-05-96139, Far Eastern Branch of Russian Academy of Sciences, grant 06-III-A-07-248.

Keywords: tsunami, early warning



(S) - IASPEI - International Association of Seismology and Physics of the Earth's Interior

JSS003

Oral Presentation

1863

Early warning decision support system based geo-information technology and spatial planning for earthquakes reduction and assessment in Syria

Mr. Hussain Saleh

Department of Civil Engineering Ghent University IAPSO

Georges Allaert

With the rapid development of economic construction and urbanization in , highly dense population, infrastructure and traffic, caused a lot of troubles to the main cities. Great change becomes to integrated management and more to eco-environmental safety construction, especially to the prevention for disasters destroyed structure as earthquake. It is not possible to completely avoid earthquakes, but the sufferings can be minimized by creating proper awareness of these disasters and its impact through developing a suitable early warning system, disaster preparedness and management of disasters for accelerating the delivery of knowledge and advanced geo-information technology to the end users. In addition, several factors can help in reducing these impacts such as working directly with complex urban areas in building capacity, institutional development and information sharing, and influencing policy. Therefore, a cost effective and feasible disaster information system must depend on an effective spatial planning in which disaster occurrence is considered explicitly as a prime parameter. The main innovative aspect of this developed system is the integration of the geographical and environmental data collection and data management tools with simulation and decision tools for earthquake reduction and assessment. This system is linked with a large, open, and executable database which has been created with robust data access and data mining capabilities. This centralized database, which is available via the internet, is a valuable source of information for policy making such as earthquake hazards and impacts, transportation, public facilities, emergency services, elevation, land use/zoning and high resolution imagery. Based on historical earthquake hazard records and socioeconomic database of Syrian cities, the hazard risk index, the vulnerability index, and the response ability index can be established, and then the earthquake effect index will be obtained. These assessment indexes with corresponding digital maps, can be used to measure earthquake risk management performance and to analyze the spatial features of seismic risk reduction in urban areas. This system, which is connected to an internet browser for transferring local capability to each client, is interactive tool that allows decision makers and specialized members to view useful information and maps for various earthquake scenarios. This will assist city planners and public safety officials to understand the spatial context in which multiple hazards impact urban environments. Also, this will support disaster-planning processes, comprehensive disaster risk assessment, reduction, and management activities. This paper constitutes a crucial step in integrated strategies of earthquake at complex urban areas by elucidating how artificial intelligence and long-term sustainable spatial planning could be efficiently introduced in the design process of these strategies to create early warning that can potentially provide vital information that is quicker, better, and at lower cost for reducing earthquake damage in . Another innovative direction of this research will show how a novel approach parallelisation and hybridisation of dynamic optimisation methods coupled with local search procedures can effectively; simplify handling data, minimize the execution time, and facilitate the design modelling approach based on simulation and optimisation process. Furthermore, a sensitivity analysis using anticipatory process will be performed in order to handle robustness and simulate an appropriate behaviour of the design parameters in real-time

Keywords: complexurbanarea, hazardriskindex, spatialplanning

(S) - IASPEI - *International Association of Seismology and Physics of the Earth's Interior*

JSS003

Oral Presentation

1864

Spatial forecasting of tropical cyclone wind hazard and impact for emergency services: example utilising tropical cyclone Larry.

Mr. Bob Cechet

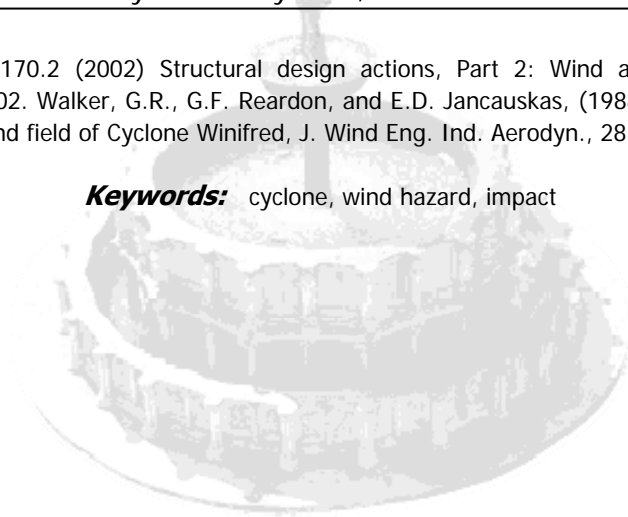
Risk Research Group Geoscience Australia

Craig Arthur, Mark Edwards, Krishna Nadimpalli, Babu Divi

Tropical Cyclone Larry crossed the Australian coastline near the far north Queensland town of Innisfail in March, 2006. At landfall, the eye of Tropical Cyclone Larry extended about 20 to 25 kilometres and a vessel sheltering in the South Johnstone River to the east of Innisfail recorded winds gusting to 225 km/h while gusts as high as 294 km/h were recorded on the nearby peaks of the Bellenden Ker mountain range (1450 metres) and 187 km/h was recorded at the Ravenshoe wind farm (about 75 kilometres from the coast) as the weakening cyclone moved inland. The Australian Bureau of Meteorology was able to forecast the cyclone track 24 hours prior to landfall with a good indication of its size, intensity and speed of movement. No spatial hazard or impact tool for determining local wind gust hazard and impact is currently available in the Australian region. It is conceivable that post-impact assessment analysis tools could be utilised, forced by a forecast of the cyclone characteristics, to supply spatial information for emergency planning (i.e. determine worst affected [severe wind] regions based on direction, topographic and prognostic cyclone characteristics). Tropical Cyclone Larry was classified as a midget cyclone because of the limited range of its destructive winds. Furthermore, coastal communities were not exposed to cyclonic winds and airborne debris for long periods as the cyclone moved relatively quickly at landfall. Low tides at the time also ensured there was no significant storm surge. Tropical Cyclone Larry impacted the coast at both high lateral speed and at low tide, causing only wind-related damage. This presentation outlines the methodology employed for spatial wind hazard assessment in the Tropical Cyclone Larry impact zone. In this process the regional maximum gust wind speed was estimated using the Aon Re cyclone model and the local wind adjustment factors were adapted from the Australian/New Zealand wind loadings standard (AS/NZS 1170.2, 2002) utilising modifications that enabled the process to be undertaken in a computational framework on a GIS platform. The impact of severe wind varies considerably between equivalent structures located at different sites due to the local roughness of the upwind terrain, the shielding provided by upwind structures and topographic factors. Wind multipliers quantify how local effects adjust the regional wind speeds (defined as open terrain at 10 m height) at each location. The local wind effects were evaluated and mapped, and this information has been compared with the damage assessed for engineering structures (residential, commercial & industrial). This analysis formed part of a post-impact assessment however the utility of this information for both emergency planning and building standards will also be demonstrated. A body of literature exists on the topic of boundary layer flow over small-scale topography. It is interesting, and extremely relevant to this investigation, that one of the very few studies that has explicitly considered the effects of topography on surface wind speeds in land-falling tropical cyclones, examines a Category 3 cyclone that passed through Innisfail in the 1980s. Walker et al. (1988) deals with the landfall of Cyclone Winifred on the far North Queensland coast of in February 1986, with a track similar to Cyclone Larry but approximately 20 kilometres to the north. During Cyclone Winifred the region of maximum winds was closer to the township of Innisfail than for Cyclone Larry. In this assessment, we apply to the whole Tropical Cyclone Larry impact region similar wind engineering principles to Walker et al. (1988) and derive a geospatial assessment of the maximum gust wind speeds. In addition, and with the aid to heuristically-derived damage (vulnerability) functions, we determine the damage in a spatial sense and compare it with the post-event field survey of 3000

structures. AS/NZS 1170.2 (2002) Structural design actions, Part 2: Wind actions, Australian/New Zealand Standard, 2002. Walker, G.R., G.F. Reardon, and E.D. Jancauskas, (1988): Observed effects of topography on the wind field of Cyclone Winifred, J. Wind Eng. Ind. Aerodyn., 28, 79-88

Keywords: cyclone, wind hazard, impact



IUGG
XXIV2007
PERUGIA
ITALY



(S) - IASPEI - *International Association of Seismology and Physics of the Earth's Interior*

JSS003

Oral Presentation

1865

The operational forecasting of the tide and surge over Irish waters

Dr. Shiyu Wang

Ray Mcgrath, J. A. Hanafin, Tido Semmler

During the last century, and especially in recent decades, serious flooding events have occurred over coastal ocean areas. Generally, coastal flooding and coastal erosion are issues with serious economic and social impacts. It is essential to establish a warning or prediction system to minimize the risk to lives and property. Over Ireland, flooding is associated mainly with heavy rainfall which can lead to enhanced river-flow and over-topping of river banks. However, coastal flooding events are often more serious, particularly those associated with storm surge. In this study, the Regional Ocean Model System (ROMS) of Rutgers University was run to simulate a strong tide and surge event over Irish waters. The meteorological forcing data are taken from ERA40 data. The model is evaluated against tidal gauge data and satellite altimeter data for short and long term simulation. The results show the high resolution ROMS model can simulate the basic tide and the surge very well, especially in the south Irish Sea. On the basis of evaluation study, a preliminary storm surge forecasting system was set up for Irish waters. The model is driven by hourly meteorological forcing fields from the HIRLAM forecasting system used by Met ireann. The preliminary results show that this system has very good forecasting capability for predicting surge in the first 24-36 hours.

Keywords: storm surge, roms, hirlam



(S) - IASPEI - *International Association of Seismology and Physics of the Earth's Interior*

JSS003

Oral Presentation

1866

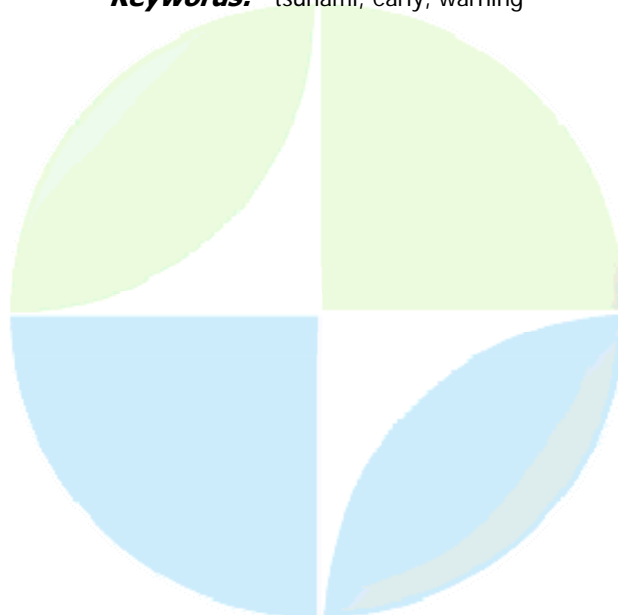
Status of the GITEWS project The German-Indonesian contribution to the Indian Ocean tsunami early warning system

Dr. Alexander Rudloff
Geophysics IASPEI

Joern Lauterjung, Gitews Project Team

On the road to an effective Tsunami Early Warning System for the Indian Ocean first milestones have been achieved. About ten seismological broadband sensors have been installed throughout Indonesia, on the Islands of Nias, Sumatra, Java, and Kalimantan. Some GPS stations and tide gauges have also been installed. A new version of the seismological software package SeisComP will be released soon. The marine equipment, consisting of GPS buoys and ocean bottom sensors, has been testing since November 2005. New deployments with modified components are planned for mid 2007. New bathymetric data has been collected through several research vessel cruises. Together with integrated images from earlier collections all data covers an area of more about 100.000 square kilometres, mainly off coast Sumatra. The bathymetry builds the base for the unstructured grid of the tsunami modelling group. A couple of sensitivity analysis and wave propagation tests have been calculated and a simplified run-up was integrated. The architecture of the Early Warning and Mitigation centre (EWMS), a Decision Support System (DSS) and a communication concept have been planned. The capacity building branch has started with 8 PhD candidates from the Indian Ocean region for a special programme, working at their home institutes and at German partner institutes. Since the project and its activities address nearly all Indian Ocean rim countries, cooperation with countries like Sri Lanka, Yemen, Tanzania, and South Africa are planned or already realized. The project is carried out through a large group of scientists and engineers from GeoForschungsZentrum Potsdam (GFZ) and its partners from German Aerospace Centre (DLR), Alfred-Wegener-Institute for Polar and Marine Research (AWI), GKSS Research Centre, Leibniz-Institute for Marine Sciences (IFM-GEOMAR), United Nations University (UNU), Federal Institute for Geosciences and Natural Resources (BGR), German Agency for Technical Cooperation (GTZ), as well as from Indonesian and other international partners. Website: <http://www.gitews.org>

Keywords: tsunami, early, warning



(S) - IASPEI - *International Association of Seismology and Physics of the Earth's Interior*

JSS003

Oral Presentation

1867

Can an Early Warning System in Northern Italy be Useful ?

Mrs. Paola Traversa

LGIT CNRS - UJF Grenoble - France IAVCEI

Lai Carlo, Strobbia Claudio

The aim of an Earthquake Early Warning System (EEWS) is to provide the community with a pre-alarm of a few seconds before a potentially damaging ground motion strikes sensible objectives. In order to make a EEWS effective and useful it is therefore essential to properly assess a) the expected pre-alarming times for a given site and seismotectonic context and b) the intensity of ground motion generated at the site by a possible earthquake scenario. An adequate consideration of these issues is essential in the implementation of a feasibility study of an EEWS and this is particular relevant in areas like Northern Italy characterized by low to medium seismicity. At the purpose of assessing the potential usefulness and reliability of an EEWS in the hospitals of Lombardy Region, we have carried out a series of numerical simulations of ground motion caused by two realistic earthquake scenarios corresponding to fault ruptures along potentially active seismogenic structures. In order to validate the results of the numerical simulations with real records, the earthquake scenarios have been chosen to correspond to two seismic events recently occurred in Northern Italy. The synthetic seismograms have been calculated using two computer programs based on an extended kinematic model of the source which fully solve the inhomogeneous elastodynamic problem. The results of numerical simulations were compared in the time domain with real recordings showing very good agreement in terms of amplitudes of ground motion and its spatial decay. The synthetic seismograms also allowed to estimate the temporal separation or phase delay between the first arrivals of P and S phases at given locations as a function of distance from the seismic source. This is the basis for estimating the pre-alarm times that can be used to automatically shut-down the functioning of sensitive equipments and prevent catastrophic chain failures. Using a simple geometrical model, a sensitivity study was carried out to assess the influence of relevant seismological parameters used in the numerical simulations. This study revealed a rather strong correlation between the time separation of P and S first arrivals and the thickness of the layers of the crustal model adopted in the analyses. More specifically the travel times-distances curves turned out to be mainly affected by the characteristics of the two thickest layers of the crustal model. Finally a preliminary investigation has been made with regard to the influence of possible site amplification effects which may alter the intensity of simulated ground motion calculated for the standard stiff ground (outcropping rock) conditions.

Keywords: early warning, italy, simulation

(S) - IASPEI - *International Association of Seismology and Physics of the Earth's Interior*

JSS003

Oral Presentation

1868

Monitoring geophysical precursors to natural hazards

Mrs. Steinunn S. Jakobsdttir

Physics Department Icelandic Meteorological Office IASPEI

The Geophysical Monitoring Section of the Icelandic Meteorological Office has the obligation to monitor and - if possible - to forecast natural hazards such as earthquakes, volcanic eruptions and glacial floods (jkuhlaup). Three types of networks are operated in real-time for this purpose: the SIL seismic network, the ISGPS continuous GPS network and a volumetric strain network. The SIL seismic system was designed in the Nordic SIL-project (1988-1995) as a tool for earthquake prediction research and monitoring. Automatic earthquake locations and continuous GPS and strain time-series are available at: <http://hraun.vedur.is/ja/>. An automatic alert system monitors changes in seismicity and sends reports via SMS, e-mail and by audio messages to computers at the Office. In the EU projects PRENLAB 1&2 (1996-2000), SMSITES (2000-2003), RETINA (2002-2003), PREPARED (2003-2005) and FORESIGHT (2004-2006) SIL seismic data, including two magnitude ~6.5 earthquakes in June 2000, was used for earthquake prediction research. Different methods have been developed within these projects in order to extract information from the data, focussing on highlighting possible precursors. These methods are now being implemented in the monitoring system. A Spectral Amplitude Grouping (SAG) method from the PREPARED project is running automatically, displaying the results through a web page. In the SAFER project (2006-2008), a data-base of active faults will be made available for the daily operation, making it possible to relate earthquakes to known faults in near real-time. Within FORESIGHT, real-time corrections to volumetric strain data were made for earth tides and air pressure, and an automated detector will soon be in use within the alert system. The presentation will summarize methods that are already implemented or will be implemented in the near future and it will discuss some of the insights gained from these approaches.

Keywords: monitoring, precursors



(S) - IASPEI - *International Association of Seismology and Physics of the Earth's Interior*

JSS003

Oral Presentation

1869

On the potential of multi-temporal satellite records analysis for extreme flooding events monitoring

Dr. Teodosio Lacava
IMAA CNR

Filomena Sannazzaro, Nicola Pergola, Valerio Tramutoli

In the past satellite remote sensing techniques have been widely used within the flood risk management cycle. In particular, there have been many demonstrations of the operational use of satellite data for detailed monitoring and mapping of floods and for post-flood damages assessment. When a real-time monitoring is requested (e.g. in the emergency phase or for early warning purposes) to assist civil protection activities, high temporal resolution satellites (mainly meteorological, with revisiting times from hours to minutes) can play a strategic role. In this paper a new AVHRR technique for near real time monitoring of flooded areas, based on the general Robust Satellite Techniques (RST) approach, is presented. Its performances are evaluated, in comparison with other well known approaches, in the case of the flood event which occurred in during April 2000 involving the Tisza and Timis Rivers. In fact, compared with previously proposed techniques, the proposed approach: a) is completely automatic (i.e. unsupervised with no need for operators intervention); b) improves flooded area detection capabilities strongly reducing false alarms; c) automatically discriminates (without the need for ancillary information) flooded areas from permanent water bodies. Moreover it is globally applicable and, because of the complete independence on the specific satellite platform, easily exportable on different satellite packages.

Keywords: flood, multi temporal analysis, optical data



(S) - IASPEI - *International Association of Seismology and Physics of the Earth's Interior*

JSS003

Oral Presentation

1870

Monitoring soil wetness variations by a multi-temporal microwave satellite records analysis

Dr. Teodosio Lacava
IMAA CNR

Elena Vita Di Leo, Nicola Pergola, Valerio Tramutoli

In the last few years, remote sensing observations have become a useful tool for providing hydrological information, including the quantification of the main physical characteristics of the catchments, such as topography and land use, and of their variables, like soil moisture or snow cover. Moreover, satellite data have also been largely used in the framework of hydro-meteorological risk assessment and mitigation. Recently, an innovative Soil Wetness Variation Index (SWVI) has been proposed, using data acquired by the microwave radiometer AMSU (Advanced Microwave Sounding Unit), flying aboard NOAA (National Oceanic and Atmospheric Administration) polar satellites. The proposed index, developed by a multi-temporal analysis of AMSU records (RST - Robust Satellite Techniques), seems able to reduce the problems related to vegetation and/or roughness effects. Such an approach has been tested on the analysis of some flooding events which occurred in Europe in past years. Results obtained up to now seem to confirm the reliability of the proposed approach verifying its sensitivity in the identification of pre-precipitations soil conditions, particularly useful for warning system purposes, as well as for monitoring space-time dynamic of the considered event. In this paper, preliminary results obtained by the analysis of data related to the flooding event occurred in Europe during summer 2003 are presented. The assessment of the reliability of such results have been made comparing them with data acquired by AMSRE (Advanced Microwave Scanning Radiometer - Earth Observing System), a more recent radiometer with spectral features better than AMSU in retriving soil moisture.

Keywords: soil moisture, multi temporal analysis, microwave



(S) - IASPEI - *International Association of Seismology and Physics of the Earth's Interior*

JSS003

Oral Presentation

1871

Early warnings of forest fires with MSG-SEVIRI data

Dr. Giuseppe Mazzeo

Dipartimento di Ingegneria e Fisica dell'Ambiente Universit degli Studi della Basilicata

Carolina Filizzola, Francesco Marchese, Rossana Paciello, Nicola Pergola, Valerio Tramutoli

A Robust Satellite Technique (RST) permits us to automatically identify anomalous space-time signal transients related to actual hazardous events distinguishing them from signal occurrences of similar intensity but originated by the natural space-time variability of land coverage and/or atmospheric conditions. In this paper, the RST (Robust Satellite Technique) method has been successfully applied for the monitoring of major natural and environmental risks, exploiting MSG-SEVIRI potential for forest fire detection. The RST scheme is based on a multi-temporal analysis of co-located satellite records and on an automatic change detection scheme. The index of local (in space and time) change, which is at the basis of the classical RST approach, is here integrated with a differential index, computed by using RST preion as well, which permits us to identify the very start of a forest fire event, exploiting the high temporal repetition of the sensor. A possible real-time implementation of such a scheme will be discussed, analysing its actual potential and its possible contribution to the development of a reliable and efficient early warning system. Moreover, the exportability of this approach (already applied both to polar e.g. NOAA/AVHRR- and geostationary data e.g. Meteosat 5, 7, GOES) guarantees its complete applicability to other present or future sensor data.

Keywords: fire detection, multitemporal analysis, seviri



(S) - IASPEI - *International Association of Seismology and Physics of the Earth's Interior*

JSS003

Oral Presentation

1872

Robust Satellite Techniques (RST) for early warnings in security applications

Dr. Carolina Filizzola
IMAA CNR

Rosita Corrado, Antonio De La Cruz, Rossana Paciello, Nicola Pergola, Valerio Tramutoli

RST technique is based on a preliminary multi-temporal analysis performed on several years (variable in dependence of the availability of homogeneous historical data-set) of satellite records, which is devoted to characterize the signal (in terms of its expected value and variation range) for each pixel of the satellite image to be processed. On this basis, anomalous signal patterns are identified by using a local change detection index, named ALICE (Absolutely Local Index of Change of Environment). RST was initially applied to the prevision and NRT (Near Real Time) monitoring of major natural and environmental hazards: seismically active areas, volcanic activity, hydrological risk as well as forest fires and oil spills are the main fields of RST application. In all cases, the technique demonstrated how meteorological satellites, which presently offer the highest time repetition (from few hours to few minutes), despite their low spatial resolution, can be used to timely detect events interesting small portions (< 100m²) of Earth surface. In this paper, RST algorithm has been applied for security applications like accidents or sabotages along pipeline networks, exploiting the high temporal resolution of SEVIRI (Spinning Enhanced Visible and Infrared Imager) sensor aboard Meteosat Second Generation (MSG) platform. In particular, SEVIRI MIR (Medium Infra Red) signal has been used in order to timely identify hot spots due to pipeline accidents or sabotages, as a possible real-time implementation for an early warning system.

Keywords: multitemporal analysis, seviri, security



(S) - IASPEI - *International Association of Seismology and Physics of the Earth's Interior*

JSS003

Oral Presentation

1873

Tsunami Early Warning: the approach of NEAREST EU Project.

Dr. Nevio Zitellini

ISMAR Sede Bologna Consiglio Nazionale Ricerche IASPEI

Maria Ana Baptista, Juanjo Danobeitia, Wilfried Jokat, Paolo Favali, Hans Gerber, Jose Morales, Fernando Carrilho, Azelarab El Mouraouah, Herculano Caetano

In the last decade a pool of European institutions has mapped the location of the potential tsunamigenic sources in the Gulf of Cadiz (SW Portugal). These sources are mostly tectonic in origin, are located near the SW Iberian continental margin and are confined and geometrically well constrained. The locations knowledge of these tectonic structures allowed us to optimally position a Tsunami Early Warning System (TEWS) Prototype based on the operation of an abyssal a multi-parameter seafloor observatory. This station will be deployed during summer 2007 offshore Southwest Portugal on behalf the EU project NEAREST (Integrated observations from Near Shore Sources of Tsunamis: towards an early warning system). The TEWS methodological approach will be based on the cross-checking of time series acquired on land by seismic networks and tide gauge stations and by a multi-parameter deep-sea platform, this latter equipped with near real-time communications to an onshore warning centre. Land and sea data will be integrated to be used in the prototype of TEWS. The proposed method can be extended to other near-shore potential tsunamigenic sources, as for instance the Central Mediterranean), Aegean Arc and Marmara Sea.

Keywords: tsunami early warning system, multi parameter observatory, tsunami source identification



(S) - IASPEI - *International Association of Seismology and Physics of the Earth's Interior*

JSS003

Oral Presentation

1874

The potential for Earthquake Early Warning using ElarmS in Italy

Mr. Marco Olivieri
CNT, INGV INGV

Richard M. Allen, Gilead Wurman

The new INSN (Italian National Seismic Network) is a dense network of broadband stations deployed for monitoring Italian seismicity. The network consists of 250 stations with a typical station spacing of ~40 km. Earthquake early warning is the rapid detection of an event in progress, assessment of the hazard it poses, and transmission of a warning ahead of any significant ground motion. We explore the potential for using the INSN real-time network for the purpose of earthquake early warning. We run the ElarmS early warning methodology off-line using a data set of more than 200 events with magnitude between 2.5 and 6.0. A scaling relation for magnitude determination from the dominant period of the first seconds of signal following the P-onset is developed from the dataset. The standard deviation in the magnitude estimates using this approach is 0.4 magnitude units and all event magnitude estimates are within 0.75 magnitude units of the true magnitude. Given the existing distribution of seismic stations it takes an average of 10 sec after event initiation before the P-wave has been detected at 4 stations. If we require a detection at 4 stations before issuing the first alert then the blind zone, within which no warning would be available, has a radius of ~37 km. The ElarmS methodology can provide a warning earlier than this but with a greater uncertainty. An assessment of past damaging earthquakes across Italy shows that applying ElarmS with the existing seismic network could provide warning to population centers in repeats of past events. For example, in a repeat of the 1980 Irpinia earthquake Naples could receive ~15 sec warning. The variations in the size of the blind zone and warning times for different regions can be used as a guide to selecting strategic locations for future station deployments.

Keywords: italy, earthquake, monitoring



(S) - IASPEI - International Association of Seismology and Physics of the Earth's Interior

JSS003

Oral Presentation

1875

Rapid ground-shaking map computation for early-warning applications

Dr. Vincenzo Convertito

Osservatorio Vesuviano Istituto Nazionale di Geofisica e Vulcanologia IASPEI

De Matteis Raffaella, Zollo Aldo, Cantore Luciana, Iannaccone Giovanni

Rapid assessment of strong ground-shaking maps after a moderate-to-large earthquake is crucial to identify most probable damaged areas. For rapid response, this is fundamental for directing first-aid emergency rescues, for loss estimation and the planning of emergency actions. Ground-shaking maps are computed by integrating and interpolating both recorded and predicted data. As a consequence, key elements in computing ground-shaking maps are the tool used to predict selected ground motion parameter (e.g., Pga, Pgv, Sa(T)) and the adopted gridding and interpolation techniques. These elements are crucial particularly in the areas not covered by the seismic network. We propose a procedure for rapid computation of ground-shaking maps for moderate-to-large earthquakes. The procedure uses a new interpolation technique based on the triangulation of the region of interest by selecting regional attenuation relationships for ground motion predictions. The proposed method allows to account for earthquake specific effects, such as rupture extension, radiation pattern and directivity integrating the recorded and estimated ground motion values. The method is tested off-line on a set of earthquakes and the results are compared with those obtained by using the software ShakeMap. From one side, the comparison is devoted to outline the main differences between the different interpolation and gridding techniques. On the other hand, the same comparison allows to emphasize the use of regional attenuation relationships particularly for low magnitude earthquakes.

Keywords: ground shaking map, attenuation relationships, near real time



(S) - IASPEI - International Association of Seismology and Physics of the Earth's Interior

JSS003

Oral Presentation

1876

Tsunami early warning system in Thailand

Mrs. Sumalee Prachuab

Meteorological Department, Thailand Director Seismological Bureau IASPEI

The Indian Ocean Tsunami that occurred on 26 December 2004 was one of the greatest natural disaster in the world. The destructive occurred in many countries in Asia around the Indian Ocean and as far as the east coast of Africa . Total report of dead, among these countries more than 200,000. In , total casualties in six provinces along the Andaman coast namely, Ranong, Phang-Nga, Phuket, Krabi, Trang and Satun are approximately 5,395 dead with 8,457 injured and 2,932 still missing. The earthquake occurred around 8 oclock (Local time) on Sunday and the first tsunami wave reach spent 2 hours striking the Phuket Province . Wave period is found to vary from 5 to 15 minutes and wave heights vary from 3 to 10 metres where Khao Luk in Phang-Nga Province was the highest tsunami wave and most destructive in Thailand. Tsunami Early Warning (TEW) could reduce the lost of lives on December 2004 if TEW has established and functioned for the Indian Ocean . The basic required for TEW are very rapid or real-time earthquake and sea-level evaluation, especially the first estimate of the magnitude, location and depth of epicenter is needed immediatly. However, evacuation plans are necessary in order to save human lives at location attacked by tsunami. Tsunami wave will hit different parts of coast line with different strength and wave height. The effective plans with reliable inundation maps are required. In order to produce such maps, a suitable wave model has to be adopted by using adequate Bathymetric and topographic maps. In the TEW has been established under the National Disaster Warning Center (NDWC) in May 2005. The NDWC acts as the center coordinating with other governmental agencies concerned. In case of the big destructive disasters will occur and have to evacuate the people, NDWC will make decision to announce the warning to people in effected areas. The Thai Meteorological Department (TMD) is the organization responsible for monitoring, analyse and warning for all natural hazards including earthquake information and Tsunami Warning to the public.

Keywords: tsunami, warning, bathymetric



(S) - IASPEI - *International Association of Seismology and Physics of the Earth's Interior*

JSS003

Poster presentation

1877

New Approaches to Coastal Zone Hazard Early Warning Systems

Prof. Evgeny Kontar

Experimental Methods Lab P.P.Shirshov Institute of Oceanology IAPSO

Coastal zone, shelf and continental slope are quickly becoming new major areas of industrial technological development owing to growing population in coastal regions and vast natural resources such as fish, oil, and gas available in these areas. Understanding risks of natural and human-made coastal zone hazards contributes to strengthening the scientific and technological basis of a number of industries including oil/gas production and transport. Traditional ways to evaluate risks of earthquakes and tsunamis (e.g., through analyzing historic data) are often not comprehensive enough and may result in lower estimates of the actual risks of these hazards, while a combined approach developed recently at P.P.Shirshov Institute of Oceanology of the Russian Academy of Sciences provides more accurate evaluations, which may affect significantly human research and industrial activities in the coastal areas. We report here some new ideas, approaches and preliminary results in the development of tsunami warning systems based on a complex monitoring system using the deep-ocean cable installations and bottom observatories located in the vicinity of the oil and gas drilling platforms which are cable connected to data processing centers. Operation of such systems is to be combined with satellite survey as well as with scientific cruise investigations. Also we report here some results of the EU project which was designed to disseminate information to scientific and industrial communities on combined risks of submarine contaminated groundwater discharge, saltwater intrusion, coastal zone earthquakes, landslides, and tsunamis. This information can be introduced targeting potential risk groups, including local coastal zone authorities and the general public, to enhance general risk awareness.

Keywords: early warning systems, hazards, coastal zone



(S) - IASPEI - *International Association of Seismology and Physics of the Earth's Interior*

JSS003

Poster presentation

1878

Early-Warning Mapping for cavities in abandoned subsurface mines

Dr. Vyacheslav Palchik

Geological and Environmental Sciences Ben-Gurion University of the Negev IASPEI

A surface landslide caused by collapse of abandoned subsurface mines is a problem in many parts of the world. The landslides can cause damage to buildings on the overlying surface, hinder the economic use of such territories, and sometimes result in loss human life. Cavities in the abandoned openings at a depth up to 80 m in Donetsk city (Ukraine) are potentially dangerous from the point of view of landslides and, therefore, earlywarning map of these cavities is needed. Unfortunately, there are no reliable plans of the mining excavations and it is impossible to enter such openings. Empirical model which relates to the physical characteristics of the overlying strata was proposed to predict the existence of such cavities in abandoned underground workings at shallow depth. The model shows combined influence of different rock layers and uniaxial compressive strength of the immediate roof over underground openings on existence of the cavities in the openings. Large thicknesses of sandstones in the rock mass or relatively high uniaxial compressive strength rock in the immediate roof contribute to the existence of cavities in abandoned workings. On the other hand, sandstones of small thickness, weak alluvium, argillites and sandy shales only give additional weight on immediate roof of the opening and allow collapse of the rock mass. On this basis, early warning mapping for cavities in abandoned subsurface mines defines locations of these cavities depending on rock strength, thicknesses, alteration and types of rock layers, thickness of alluvium in overburden.

Keywords: mapping, cavities, landslide



(S) - IASPEI - *International Association of Seismology and Physics of the Earth's Interior*

JSS003

Poster presentation

1879

Millimetric ground movements from space radars: European Space Agency's GMES TERRAFIRMA PROJECT

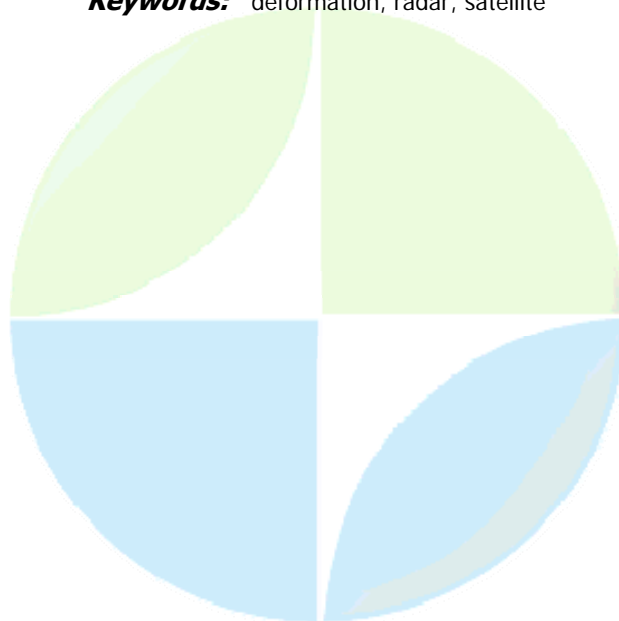
Dr. Chris Browitt

Geoscience Edinburgh University IASPEI

Alice Walker

In the early 2000s, following almost a decade of using differential interferograms to observe centimetric ground movements, particularly for earthquakes, the Polytecnico Milano, and its spin-out company TRE, pioneered a new processing approach which has yielded results at a millimetric scale. With around 30 radar scenes utilized, rather than two, a longer term, high precision view is obtainable, with widespread applications. These range from deformation in earthquake and volcanic zones, ground vulnerability mapping and landslide risk assessment, to geotechnical issues in relation to groundwater abstraction and recharge, compressible soils, mines and engineered excavations. Differential subsidence observed in alluvial flood plains can lead to improved flood risk assessments as is evident from the application of this Persistent Scatterer INSAR technique in New Orleans. In order to build more awareness of this potential, the European Space Agency has sponsored a project, entitled GMES TerraFirma, to capitalize on its ERS1, ERS2 and ENVISAT data archives. Many city and landslide sites in Europe have already been processed to reveal their ground movement histories for up to 14 years, and by the end of 2007 it is intended that every European Union country will have at least one city, with satellite radar coverage processed to reveal small ground movements of around 1 millimetre per year. That information will be in the hands of national geoscience centres and engineers for expert interpretation utilising their own data and expertise. They, in turn, will engage with the relevant authorities in their countries to ensure take up, and action on the hazards revealed which will be seen in great detail; in many cases, for the first time. It is intended that these national cities will lead to national initiatives for further studies across each country, and that the examples will be shared across borders to ensure that the community of Europe benefits from the experience of its collective experts and from our European Space Agency's investments in leading edge technology for practical purposes.

Keywords: deformation, radar, satellite



(S) - IASPEI - *International Association of Seismology and Physics of the Earth's Interior*

JSS003

Poster presentation

1880

An experimental model of data receiver for gravitational disturbance research and earthquake prediction with 3 to 16 days forestalling

Prof. Nikolay Egorov

Faculty of Applied Mathematics and Control Process St.Petersburg State University

Valeriy Smirnov, Boris Bogdanovich

Gravitational field of the Earth is researched for more than 300 years. Nowadays reliable mathematical models and data analysis methods are developed, which makes possible to solve various gravimetric problems. Using advanced gravimetric methods we can analyze time-dependent changes of gravitational force: changes caused by tidal effects and Earth's rotation; and caused by mass redistribution inside the Earth. All gravitational disturbances may be divided into 2 groups: caused by effect of external (space) objects, like the Sun, the Moon, etc.; caused by movement of tectonic masses in the Earth's crust and mantle. The latter movements causes intense earthquakes. Modern experimental techniques of gravitational disturbances recording are strictly limited both for disturbances of tectonic origin, and for ones of space origin. Possible recording of local gravitational disturbances in different regions of the Earth would make it possible to predict probable earthquake sources with some days forestalling, which could save their lives for hundreds thousands of people. The developed data receiver for gravitational disturbance recording is a dynamical electro-mechanical device, which provides the ability to determine direction on the sourced of gravitational impact. The main element of the data receiver is a brass gyroscope, operating in negative acceleration mode. In this rotation mode the gyroscope reacts on change of the Sun (Moon) position relating the data receiver by change of period of revolution. As a result the output signal is changed and may be recorded using a plotter. The sensitivity level depends also on: angular velocity of rotation; length of deceleration pulse; direction angle to possible source of gravitational impact. The data receiver shows high sensitivity level in recording small gravitational impacts from space objects. It is possible to record also high disturbances caused by internal effects. In principle, all tectonic movements may change gravitational potential of the Earth. Using map of the Earth's crust breacs, we have carried out an experiment of data receiver orientation on some of tectonically active areas. We have registered several high gravitational impacts, with 400 to 500 μ s change of preiod of revolution. (In contrast, for space gravitational impacts, the change was about 75 to 200 μ s.) The times of recording were correlated with information about earthquakes. In all cases the signals were recorded with 3 to 10 (and more) days forestalling. E.g., for earthquake in Iran, 2 April 2006, the signal was recorded on 29 March 2006. Now an experimant is in progress, on scanning and monitoring some seismologically active Earth's regions using the data receiver.

Keywords: gravitational, disturbance, earthquake

(S) - IASPEI - *International Association of Seismology and Physics of the Earth's Interior*

JSS003

Poster presentation

1881

Anisotropy of high-frequency geoacoustic emission at different stages of seismic event preparation

Dr. Yury Marapulets
FEB RAS IKIR FEB RAS IASPEI

Anatoly Kuptsov, Igor Larionov, Mihail Mischenko, Albert Sherbina, Valery Gordienko

Research of anisotropy was carried out by vector-phase combined acoustic receiver installed in a natural reservoir (Mikizha lake) in Kamchatka. It was determined that in the angle range of 10 - 60 degrees there is a local area which generates the major quantity of geoacoustic signals. The intensity of signals from this area increases iteratively in diurnal time interval before a seismic event under the influence of growing deformation processes.

Keywords: geoacoustic emission, vector phase acoustic receive



(S) - IASPEI - *International Association of Seismology and Physics of the Earth's Interior*

JSS003

Poster presentation

1882

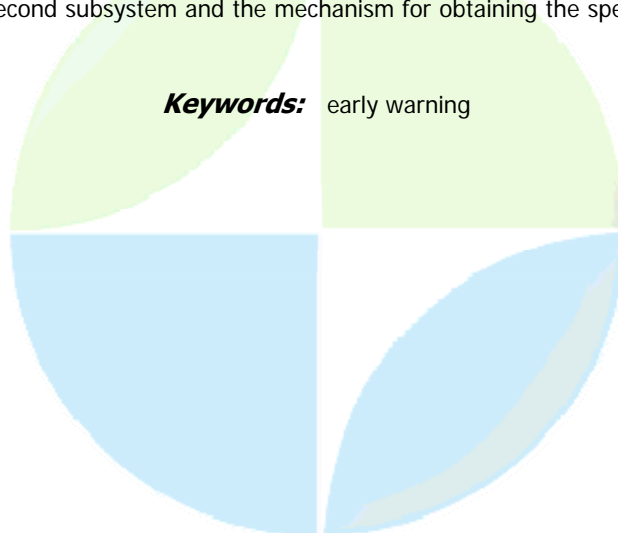
Development of structural features for earthquake early warning systems

Dr. Alvaro Antonyan

Armenian National Survey for Seismic Protection President of Armenian NSSP IASPEI

The territory of Armenia is wholly located at the one of the seismically most active regions of the world. Destructive earthquakes dated back as far as the 6th Century BC. According to the data of the Armenian historiography the following destructive earthquakes were known: Dvin (851-893, M6.5), Talin Arouch (972, M6.5), Ararat (1319,1840,M7.5), Garni (1679,M7.0), Tsakhkadzor (1827, M6.5), Spitak (1988M 7.0). These earthquakes caused thousands of deaths and great economic losses in Armenia. Only during the Spitak 1988 devastating earthquake more than 25,000 people lost their lives, 20,000 people were injured, and 515,000 people were homeless. Most of the buildings and structures in all the cities and villages of the Northern part of Armenia were almost completely destroyed. In present, the buildings and structures in Armenia are designed for ground acceleration values of 0,1-0,2g, that correspond to 7-8 value by MSK-64 intensity scale according to seismic zonation map operating in the territory of Armenia up to 1994. It is obvious that the expected value of seismic impact (0.4g) considerably exceeds the designed values of accelerations of existing buildings and structures and the hazard of great destruction of buildings and structures is evident in case of the possible strong earthquake in Armenia. Development of Earthquake Early Warning Systems (EEWS), providing information about upcoming destructive earthquake is getting essential. In this paper we have developed the new concept of EEWS for Yerevan city. The new system will consist of the two components: 1.Current seismic hazard assessment and early non-urgent warning (preparation phase): the current seismic regime is evaluated, and in case of relevant hazard the warning will be submitted to the Government and related governance bodies, and, if necessary, to public and communities; 2. Urgent warning (earthquake hit urban area and rapid information is necessary): the principles of action of the urgent EEWS was developed on the base of velocities difference between electromagnetic waves propagation and seismic waves. It was focused on the solution of the following tasks: possibility and efficiency of EEWS creation, configuration of EEWS and determination of necessary number of seismic stations, gain in time the warning in case of upcoming strong earthquake and others. The first subsystem is dealing with the results of the current seismic hazard which based on the monitoring data of the more than 40 seismological, geophysical and geochemical, and hydrodynamic, and geodynamic parameters as well as on the sizes of anomaly and their correlation with the seismic events, and testing. The appropriate software has been developed. The structure of the second subsystem and the mechanism for obtaining the special seismic signal have been developed.

Keywords: early warning



(S) - IASPEI - International Association of Seismology and Physics of the Earth's Interior

JSS003

Poster presentation

1883

Can the offshore pressure sensors contribute to early tsunami warning system?

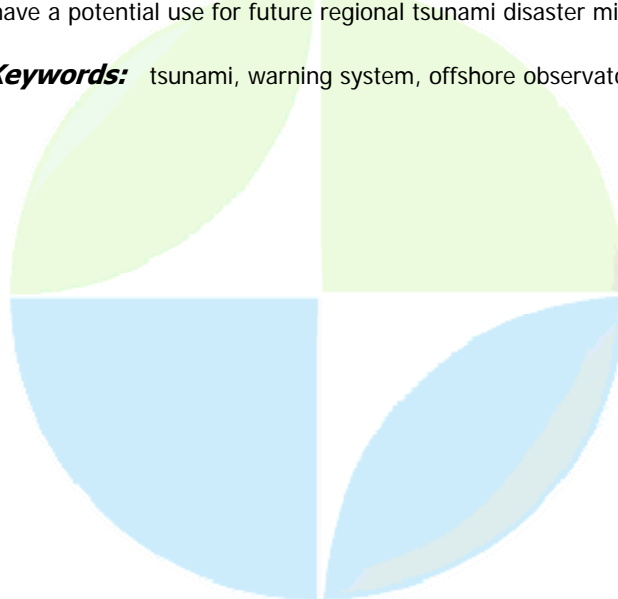
Dr. Hiroyuki Matsumoto

Deep Sea Research Department JAMSTEC IASPEI

Hitoshi Mikada, Kenichi Asakawa, Katsuyoshi Kawaguchi

Early tsunami warning system is necessary, in particular for those regions that have historically never experienced devastating tsunami disasters, such as the 2004 Indian Ocean tsunami disaster. In Japan, seven permanent offshore cabled observatories, in which bottom pressure sensors are included have been operated by various research institutions and universities since 1970s. Two case studies of early tsunami detection by the bottom pressure sensors are introduced together with demonstrating by the tsunami computation; one is by the off Kii-peninsula, Japan earthquake (M7.4) in 2004 and the other is by the Kuril Islands earthquake (M8.3) in 2006. Water pressure fluctuations during the 2004 off Kii-peninsula earthquake was successfully obtained by the offshore cabled observatory off Muroto, SW Japan, approximately 200 km west of the earthquake epicenter, i.e, the tsunami source, and the tsunami signals were processed from the acquired dataset after applying moving average filtering. As a result, two pressure sensors could detect the tsunami signals 20 minutes before the first tsunami arrival at Muroto, the nearest coast to the observatory. Tsunami amplitude observed by the pressure sensors was less than 0.1 m, while that observed at the coast was 0.5 to 1 m. On the other hand, the tsunami from the mega-thrust earthquake taken place off Kuril Islands on 15 November 2006 was also observed by the other offshore cabled observatory off Kushiro, NE Japan, 800 km away from the epicenter. Although most of the tsunami energy propagated toward off the Pacific Ocean, about one hour later, the series of the tsunami signals was observed by three bottom pressure sensors. The tsunami amplitude was approximately 5 cm, whereas that observed at the coast were a few tens of centimeters. In case of the Kuril Islands earthquake, the tsunami could be detected 20 min earlier than that arrived at the eastern tip of Japan. This means that the offshore observatory off Kushiro possibly become the most rapid warning strategy against tsunamis generated along the Kuril trench. Our recent experiences of tsunami observation suggest that the bottom pressure sensors make us possible to detect tsunami itself in advance. From a viewpoint of early tsunami warning or forecasting, the bottom pressure sensors would surely have a potential use for future regional tsunami disaster mitigation.

Keywords: tsunami, warning system, offshore observatory



(S) - IASPEI - *International Association of Seismology and Physics of the Earth's Interior*

JSS003

Poster presentation

1884

Storm surges/Wave Operational Ocean Model in KMA

Dr. Sung Hyup You

Marine Meteorology & Earthquake Research Lab. METRIKMA

Sangwook Park, Jang-Won Seo

The Korea Meteorological Administration (KMA) has operated numerical ocean wave prediction system since 1992. Prior June 1999, the 1st generation wave model (DSA-5) was operated twice in daily over the Northeast Asia region. With introduction of NEC SX5 supercomputer in 1999, the 3rd generation wave model (WAM) was implemented with two wave prediction systems the ReWAM (Regional Wave Model) and the GoWAM (Global Wave Model). At present, KMA (Korea Meteorological Administration) has operated the wave model and storm surge model based on CRAY X1E system. The study shows development and verification of operational ocean model and future plan of KMA. The operational storm surge model (STOM : Storm surge/Tide Operational Model) area covers 115-150E, 20-52N based on POM (Princeton Ocean Model) (Blumberg and Mellor, 1987) with 1/12 horizontal resolutions including the Yellow Sea, East China Sea and the East Sea, marginal seas around Korea. From July, 2006 the STOM have been applied to formal forecasting model in KMA. Sea surface wind and pressure from the Regional Data Assimilation and Prediction System (RDAPS) is used for forcing input of storm surge model. In this model, the level of storm surge calculated by the difference between tide level and sea level change caused by meteorological effects. The newly developed operational wave model is WAVEWATCH III which is a third generation wave model developed by Tolman (1989). The Regional WAVEWATCH III (RWW3) covers the northwestern Pacific Ocean from 115 E to 150 E and from 20 N to 50 N similar to STOM. The horizontal grid intervals are 1/12 in both latitudinal and longitudinal directions. The RWW3 is integrated from a state of rest and forced by the RDAPS wind stress produced by KMA. From 2007, the RWW3 will be applied to formal forecasting model in KMA. The Coastal WAVEWATCH III (CWW3) covers 6 coastal areas around Korea peninsular. The horizontal grid intervals are 1/120 for each area. Under the renewal process of power computing packs at KMA on the year 2005, the CRAY X1E system (14.5 Teraflops) replaced NEC SX5 (224 Gigaflops). Establishing of newly devised ocean prediction system is underway in conjunction with high computing environment. The main focus of new wave system lies in accommodating coastal wave/surge processes. The west and the south coastal area of Korean peninsular is one of the challenging places in ocean modeling for reasonable prediction of nearshore wave conditions and tides.

Keywords: stormsurges, wave, operationaloceanmodel



(S) - IASPEI - *International Association of Seismology and Physics of the Earth's Interior*

JSS003

Poster presentation

1885

Earlywarning system for risk mitigation due to the landslides triggered by seismic activity

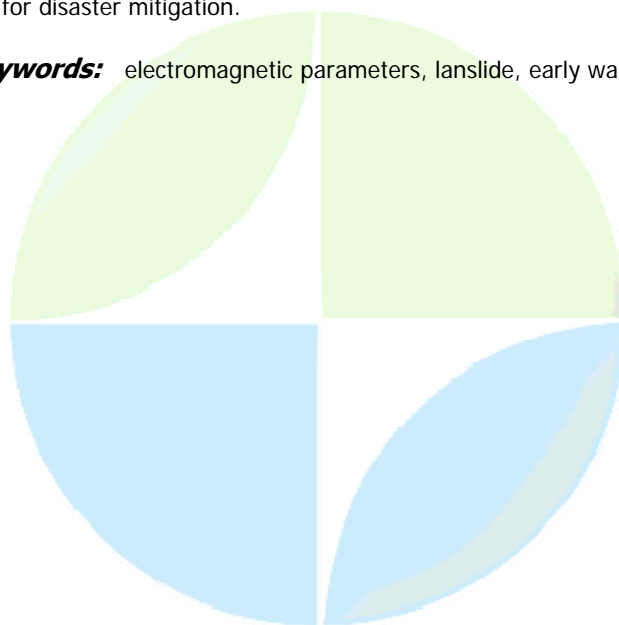
Dr. Dumitru Stanica

Electromagnetism and Lithosphere Dynamics Institute of Geodynamics of the Romanian Academy IAGA

Maria Stanica, Constantin Diacopolos

The goal of the paper is to present a specific electromagnetic monitoring system, to better understand its efficiency for broad application in the landslide study and risk mitigation. The main objective was to implement this complex system that may provide early-warning against the risk arising from landslides (test sites) triggered by the earthquakes (EQs) occurred in the seismic active Vrancea zone (Romania). The activities that have been accomplished consist of: (i) innovation in integrated geo-sensors structure for network conditions; (ii) implement and continuous improvement of the real-time monitoring system depending on the landslide test sites conditions; (iii) real time signals processing for pattern recognition in pre disaster and at disaster circumstances; (iv) assessment and quantification of the geodynamic precursory parameters related to the landslide phenomenon for risk mitigation; (v) provision of early-warning against the risk arising from landslide process. Thus, the specific methodology and software packages have been applied for obtaining, in real time, all the important electromagnetic parameters and to point out their anomalous behaviour versus the specific pattern pre-established in non geodynamic conditions. Additionally, by combining different data types and analysis techniques, and also by merging electromagnetic parameters with geoelectric tomographic images and with low frequency electric signals occurred prior the stress to reach a critical value, a compelling dynamical paradigm, in which is emphasized a correlation between electromagnetic parameters and the earthquakes magnitudes, was carried out. In consequence, by analyzing the data from the Provita de Sus (test site), it was possible to assign the increase of the landslide activity related to the local fault which has been reactivated by the EQs occurred in the Vrancea zone. In the end, this paper illustrate the stage of the system implementation and to what extent the results carried out in the test (Provita de Sus) site may contribute on understanding such kind of phenomenon in order to provide the information necessary for disaster mitigation.

Keywords: electromagnetic parameters, lanslide, early warning



(S) - IASPEI - *International Association of Seismology and Physics of the Earth's Interior*

JSS003

Poster presentation

1886

New seismic system for acquisition and analysis in Israel

Dr. Vladimir Pinsky

Seismology Geophysical Institute of Israel POB 182, Lod, Isra

Andrei Polozov, David Kadush, Veronic Avirav, Abraham Hofstetter,

For updated seismic monitoring and preparedness to future large earthquakes as well as for improved waveform data exchange with other seismic systems in the world and for the progressive earthquake related research Geophysical Institute of Israel (GII) now carries out modernization of Israel Seismic Network (ISN) and the ISN acquisition system (ISNAS) in the frame of the contract between the GII and Nanometrics Co. The ISNAS is based on satellite and radio real-time communication and close-to-real time automatic waveform analysis. The project consists of four stages: 1) Transformation of the trigger-based acquisition to the continuous waveform recording; 2) Replacement of the part of the existing stations to the new ones; 3) Changing of the seismic network configuration; 4) Modernization of the existing software for processing the continuous data. The ISNAS structure comprises four networks: 1) Site network (between data loggers and satellite transmitter); 2) Network between the stations and the data center hub; 3) Data center acquisition network, including communication between the hub and the servers and connection between the main and the backup center. 4) Analysis network internal GII network. The ISNAS includes several types of acquisition: radio-link, new satellite, broad-band frame relay communications based on the SeedLink and Naqs servers. The system includes new algorithms of real-time detection, picking and location as a part of the JSTAR analysis system, developed in GII.

Keywords: real time, satellite communication, seismic acquisition



(S) - IASPEI - *International Association of Seismology and Physics of the Earth's Interior*

JSS003

Poster presentation

1887

Real time sea level data transmission from tide gauges for tsunami monitoring

Dr. Simon Holgate

Permanent Service for Mean Sea Level Proudman Oceanographic Laboratory IAPSO

Peter Foden, Jeff Pugh, Philip Woodworth

The Asian tsunami of December 2004 was the most devastating in modern history. Following this event, the Intergovernmental Oceanographic Commission held a meeting under the auspices of the Global Sea Level Observing System (GLOSS) where new recommendations were made for tide gauge installations. GLOSS guidelines were amended so that new tide gauge installations which are part of the GLOSS network include tsunami monitoring capability and transmit sea level data of suitably high frequency and intervals (e.g. 1 minute sea level samples sent every 15 minutes). Here we present the development and implementation of "tsunami enabled" tide gauges at Proudman Oceanographic Laboratory, which allow real time data to be returned from almost anywhere on Earth. The system is based around off the shelf components where possible. At its centre is a low power, embedded Linux platform, which performs the data logging and communications. The sensors used so far have been the OTT Hydrometry Kalesto radar and PS1 pressure sensors which are queried over a serial interface. Telemetry is through the Inmarsat Broadband Global Area Network (BGAN) system which allows a bi-directional broadband connection over ethernet, permitting remote reconfiguration when required. Data transmission is via SMS messages which contain 1 minute values from 3 sensors and are returned over Inmarsat's private network every 5 minutes.

Keywords: tsunami, tide gauge, real time



(S) - IASPEI - *International Association of Seismology and Physics of the Earth's Interior*

JSS003

Poster presentation

1888

CUSCO base meridian for the study of geophysical data

Prof. Teodosio Chavez_campos
iaga no

Israel Chavez Sumarriva, Nadia Chavez Sumarriva, Liliana Sumarriva Bustinza

In order to have a better comprehension of the different phenomena occurring on the earth and the management of a data base in real time, that is currently studied by the seven associations (IASPEI, IAVCEI, IAPSO, IAHS, IAG, IAMAS and IAGA) of the International Union of Geodesy and Geophysics (IUGG) and others. We propose that the Meridian of Cusco (72 W), would become a Base Meridian, the same as the Greenwich Meridian. This is based in the entrance of the Vernal point to the Aquarius Constellation, defining the vernal point as "a sensitive axis of maximum conductivity" as it is demonstrated by the stability of the geomagnetic equator (inclination of the field is zero grades) in the year 1939, calculated with the IGRF from the year 1900 up to the 2007 and it is confirmed with tabulated data of the Magnetic Observatory of Huancayo (Peru). From that date until this year (2007) the geomagnetic equator it is fluctuating between 12-14 South, on the other hand in the area of Brazil it has advanced very quickly towards the north, and approximately 108 km. above the earth surface it is located the equatorial electrojet, that is more intense during equinoxes in South America (Peru and Bolivia).

Keywords: vernalpoint, equatorialelectrojet, geophysicaldata



(S) - IASPEI - *International Association of Seismology and Physics of the Earth's Interior*

JSS003

Poster presentation

1889

Toward an integrated early-warning system in Serbia

Dr. Peter Labak

Department of Seismology Geophysical Institute IASPEI

Slavica Radovanovic, Erik Bystricky, Andrej Cipciar

Serbia is located in the Balkan area - one of the most earthquake prone areas in Europe. However, up to year 2004 real time data exchange and analysis had been missing in the country. The modernization of Serbian seismic network achieved within the Slovak-Serbian project DIRECTE (2004-2005) allows to collect and process earthquake data in real time. 12 seismic stations on the territory of Serbia collect data in real-time. The data center in Beograd uses real-time data from neighboring seismic networks and performs real time localization of earthquakes in Serbia. The packages SeisComp and Autoloc (GFZ Potsdam), Seisgram (A. Lomax), Seismic Handler (K. Stammer) and archiving tool (GPI SAS Bratislava) are used for processing of earthquake data. Similarly as earthquakes, floodings are of interest in significant part of Serbia. Therefore, a pilot project on real time monitoring of rain-falls is underway. The goals of ongoing projects ShareDIRECTE and IMPART in the field of dissemination of real-time data and their use for Civil protection purposes is presented.

Keywords: early warning, earthquakes, floodings

PERUGIA
ITALY



(S) - IASPEI - International Association of Seismology and Physics of the Earth's Interior

JSS003

Poster presentation

1890

Reliability of automatic location procedures in north - western Italy

Dr. Chiara Turino

Dip. Te. Ris. University of Genova IASPEI

Scafidi Davide, Morasca Paola, Ferretti Gabriele, Spallarossa Daniele

Reliable automatic procedure for locating earthquake in real or quasi-real time is strongly needed for seismic warning system, earthquake preparedness and producing Shakemaps. The accuracy of automatic location algorithm is influenced by several factors such as errors in picking seismic phases, network geometry and velocity model uncertainties. The main purpose of this work is to investigate on the performances of two automatic procedure for the real-time location of earthquakes in North - Western Italy. The automatic-picking algorithm consists on a waveform pre-processing based on adaptive band-pass filter, self-calibrated by a signal to noise analysis, and on a two-steps picking procedure. Firstly, an initial pick of P and S phases is obtained with an algorithm based upon abrupt changes in the ratio of a short term and long term running average of the signal (Allen, 1978). The second step uses the re-picking program MannekenPix, to improve initial P-phase picking. The location problem is then solved by both a standard location procedure (Hypoellipse) and a probabilistic, non linear one based on the software NonLinLoc. The reference locations are determined by the Hypoellipse code considering manually-revised data. The comparison is made on a dataset composed by more than 500 seismic events for the period 2000 - 2007, geographically selected from 43 N30' to 46N and from 6 E30' to 11E, with local magnitude greater than 2.0. The results point out the accuracy of the automatic-phase picking of P phases while, regarding the S phases, the automatic procedure is able to recognize a smaller number of arrival times than the manual one. Furthermore, the NonLinLoc software is proved to be more efficient than the standard Hypoellipse code, leading to more accurate and reliable automatic locations mainly when outliers (wrong picks) are present.

Keywords: automatic location, picking



(S) - IASPEI - *International Association of Seismology and Physics of the Earth's Interior*

JSS003

Poster presentation

1891

4D geoelectrical tomography as a tool for real-time landslide monitoring: a test-bed in southern Italy

Dr. Colangelo Gerardo

Dipartimento Infrastrutture e Mobilit Direzione Generale

Aniello Vietro, Giuseppe Basile, Vincenzo Lapenna, Antonio Loperte, Angela Perrone, Antonio Satriani, Luciano Telesca, Giovanni Calice, Nicola Pergola, Valerio Tramutoli

A novel approach based on GRID technologies has been proposed to remotely control active and passive geoelectrical sensors for obtaining in real-time high-resolution 4D tomographic electrical images of landslide bodies. In the next future this technology could be applied and integrated in the hydrogeological early warning systems. The prototype system has been implemented assembling hardware components (multimeter, multichannel cables, electrical impolarizable probes, TDR sensors and probes for soil and meteo-climatic parameter measurements) and developing new software routines for geoelectrical data control and processing. The system allows to measure the self-potential voltage differences between electrodes putted into the ground at different depth (0,2m 1,0m and 2,0m) distributed along a profile with 45,0m length with 5.0m of spacing. Combining the SP data for the different depth we produces a high resolution tomography image along a vertical section crossing the profile representing the probability to find electrical point sources. Furthermore, the system can be used for active geoelectrical measurements: electrical currents can be automatically injected into the ground obtaining subsurface resistivity images of landslide body. Then, the integration of passive and active geoelectrical measurements allows us to detect the time-dependent-changes of water content in vadose zone and to evaluate the geometrical features of landslide body. The remote control of geoelectrical and meteo-climatic sensors with GRID technologies was the key for obtaining in near-real-time electrical tomographic images before, during and after strong rainfall precipitation periods and, consequently, to analyse the complex dynamics of subsurface water infiltration processes. An advanced, javabased, system of tools for remote management and control of the sensors is, in fact, able to automatically change acquisition parameters (e.g. sampling frequency) of the in situ instrumentation on the base of some triggering threshold of crucial measured meteorological parameter (e.g. rain rate). Finally, the first results obtained during an experimental field test carried in Lucanian Apennine Chain (Southern Italy) in collaboration with Regional Civil Protection is presented and discussed. The study area is located close the Tito and Picerno villages and it was interested by diffuse and large surface deformation phenomena after a strong rainfall and snow events occurred on March 2006.

Keywords: grid technologies, geoelectrical tomography, self potential signals

(S) - IASPEI - International Association of Seismology and Physics of the Earth's Interior

JSS003

Poster presentation

1892

Robust Satellites Techniques for oil spill detection and monitoring

Mr. Daniele Casciello

DIFA PHD

Pergola Nicola, Tramutoli Valerio, Lacava Teodosio

In last years, the environmental pollution of the sea due to technological hazards, as the oil spills, outcoming from different sources (oil rigs releases, illegal vessels discharges, tanker accidents, etc.) still continue. As stated in different conferences, there is an urgent need for improved management of the sea and coastal zones in terms of monitoring and mitigation of technological hazards. Satellite remote sensing could contribute in multiple ways, in particular for what concerns early warning and real-time (or near real-time) monitoring. Several satellite techniques exist, mainly based on the use of SAR (Synthetic Aperture Radar) technology, which are able to recognise, with sufficient accuracy, oil spills discharged into the sea. Unfortunately, such methods cannot be profitably used for real-time detection in whatever geographic area, because of the low observational frequency assured by present satellite platforms carrying SAR sensors (which can offer observation frequency from few hours up to few minutes at medium and low latitudes). On the other hand, the potential of optical sensors aboard meteorological satellites, has not been yet fully exploited and no reliable techniques have been developed until now for this purpose. A new satellite technique for oil spill detection and monitoring is discussed in this paper. It is based on the general approach called RST (Robust Satellite Technique, Tramutoli, 2005) which was already applied for monitoring other natural hazards related to volcanic activity, earthquakes (Tramutoli, 2001), floods, forest fires (Tramutoli, 1998). Briefly, RST approach is an automatic change-detection scheme that considers a satellite image as a space-time process, described at each place (x, y) and time t , by the value of the satellite derived measurements $V(x, y, t)$. Generally speaking an Absolute Local Index of Change of the Environment (ALICE) is computed and this index permits to identify signal anomalies, in the space-time domain, as deviations from a normal state preliminarily defined, for each image pixel, (e.g. in terms of time average and standard deviation) on the base only of satellite observations collected during several year in the past, in similar observational conditions (same time of the day, same month of the year). By this way local (i.e. specific for the place and the time of observation) instead than fixed thresholds are automatically set by RST which permit to discriminate signal anomalies from those variations due to natural or observational condition variability. Using AVHRR observations in the Thermal (TIR), the approach was applied to Kuwait and Saudi Arabia oil spill event occurred in January 1991 during the Gulf War (Cross, 1992, Casciello et al., 2004), to the Seky Baynunah event occurred in March 1994 (Tseng, 1995) and now applied for the San George Argentina Uruguay event occurred in February 1997 (Liu et al., 2000). To reduce problems of TIR fluctuations due to the meteorological and climatological conditions a Robust Estimator of TIR anomalies (RETIRA) was implemented and used too. This estimator, was quite effective to reduce this kind of problems, and also to enhance the anomalous signals on the sea due to the oil polluted areas with a good detection capability and a good reliability too (up to 0% of false alarms) in different observational conditions. Thanks to the high repetition rate offered by NOAA polar satellites, the proposed method offers a first opportunity to plan high-frequency monitoring systems for oil spill at global scale. Although these results need to be confirmed by further analyses on number of events and in different observational conditions, this work surely encourages to continue the research in this field. Moreover, the complete independence of the RST approach on the specific sensor and/or satellite system, will ensure its full exportability on the new generation of Earth Observation satellite sensors which, thanks to their improved capabilities, could actually guarantee timely, reliable and accurate information.

Keywords: oilspills, avhrr, thermalinfrared



IUGG

XXIV2007

PERUGIA
I T A L Y



(S) - IASPEI - International Association of Seismology and Physics of the Earth's Interior

JSS004

1893 - 1904

Symposium

Non-instrumental seismometry - Quantification of past and future earthquakes: balancing the geological, historical and contemporary strain records

Convener : Dr. Gianluca Valensise

General scopes related to Symposia on Non-instrumental seismometry. During the past 20 years, the seismic hazard assessment practice has increasingly relied on the quantification of past and future seismicity based on non-instrumental disciplines such as active tectonics, paleoseismology, historical seismology. Over the years, these disciplines have been turned from merely descriptive to progressively more quantitative. Quantification involves not only significant parameters of the earthquake source for recent and more distant earthquakes (e.g. fault location, fault length, coseismic slip, rupture complexity), but also the rate of earthquake production and recurrence properties of a fault, the development of segmentation models, the description of the geometric conditions leading to dynamic triggering. The symposium intends to acknowledge the enormous progress achieved in this area of seismology in recent years and particularly since the mid-1990s, emphasize their mutual relationships and show how they integrate with conventional instrumental methods. Due to its long-standing tradition in the analysis of the historical earthquake record and to its contribution to the development of methodologies in earthquake geology, Italy qualifies as an especially appropriate country to take a leading role in this symposium. This is the first of four related symposia: JSS004, JSS005, JSS006, JSS007. Below the scopes of JSS004. One of the outstanding issues in modern seismic hazard assessment practice is the comparison of the earthquake record with the geologic and geodetic evidence for ongoing tectonic strain. The correct estimation of past earthquakes on the one hand and of geologic and tectonic parameters on the other hand forms the basis for assessing the maximum credible earthquake, the size of impending earthquakes, and the expected rate of earthquake production in any given region. Significant over- or under-estimations of the earthquake potential may derive from such diverse conditions as source complexity during historical earthquakes, poor assessment of fault size, dynamic fault interaction, failed identification of active fault trends, and aseismic creep. This session intends to draw on scientists from different lines of expertise who are willing to cross conventional disciplinary boundaries and compare their approaches, results and residual uncertainties. We especially welcome contributions from these areas, or contributions that combine them into unconventional schemes: - quantification of the historical earthquake record; - quantification of the geologic record, including field studies of cumulative tectonic strain and the development of fault segmentation schemes; - partitioning of geodetically-derived strain onto individually identified or areal active tectonic structures. Papers are expected to emphasize the impact of the proposed results or approaches in the improvement of i) the understanding of the seismic cycle of major faults, and of ii) mid- to long-term seismic hazard estimates.

(S) - IASPEI - *International Association of Seismology and Physics of the Earth's Interior*

JSS004

Oral Presentation

1893

Re-evaluation of historical catalogues in the Indian Region.

Dr. Hari Narain Srivastava

SEISMOLOGY GLOBAL HYDROGEOLOGICALSOLUTIONS IASPEI

Historical earthquake catalogues in the Indian Region were generally based on the felt reports published in the News Papers, writings of Courts and Historians, archaeological, and Paleo seismological investigations. Many new damaging earthquakes ranging in seismic intensity from VIII to XII on MM scale were added in the catalogue based on the above. However, closer examination of some of these earthquakes has brought out discrepancies in the time, of occurrence and in some cases even their location. During the early instrumental era, recent re-interpretation of the great Kangra earthquake of 1905 in western Himalaya based on limited seismological data has raised many questions, due to the inference about two earthquakes one in Kangra and the other near Dehradun. Further look at the data has reaffirmed the occurrence of only one earthquake of 1905 in Kangra. The other inferred earthquake near Dehradun was only a consequence of site response called secondary meizoseismal area similar to that observed during great earthquakes of Bihar Nepal (1934), Bhuj (2001) and Mexico (1985). The historical earthquakes based on limited data often requires a more closer look which can be undertaken only if old the seismograms are preserved for new researches. Microfilming of historical earthquakes was initiated in India Meteorological Department. This was in accordance with the first phase of IASPEI. Program on Historical seismograms and earthquakes. However, the slow methodology and problems in their preservation has now led to the modern method of digital scanning of the record. New results have been discussed based on historical data on Indian earthquakes.

Keywords: historical, earthquakes, india



(S) - IASPEI - *International Association of Seismology and Physics of the Earth's Interior*

JSS004

Oral Presentation

1894

Modeling the tsunami-associated, magnitude \geq 8.5, AD365 earthquake sequence in the Eastern Mediterranean

Prof. Stathis Stiros

Civil Engineering Patras University, Greece IAG

Antonis Drakos

Different pieces of evidence (historical, archaeological, geomorphological, marine biological, radiocarbon datings) provide evidence for a destructive tsunami, coastal uplift and subsidence and earthquake devastation in various parts of the Eastern Mediterranean, especially the Nile Delta, Cyprus, Crete, Libya and Sicily in the 4th c. AD. A systematic comparative analysis and evaluation of these data revealed that all these effects can be assigned to a single seismic sequence in AD365, in agreement with ancient reports for a universal earthquake of unprecedented scale. A least-constrained elastic dislocation analysis revealed that the up to 9m uplift of western Crete can be associated with a reverse-fault earthquake of minimum magnitude 8.5 cutting through to the sea-bottom SW of Crete, in broad agreement with modern seismological evidence. Still, widespread damage in ancient buildings testifies to short period, conspicuously nearly local seismic waves. Furthermore, while there is new evidence for tsunami deposits in Crete, preliminary modeling makes difficult the faulting offshore SW Crete to account for the reported extreme tsunami damage in the Nile Delta, commemorated for centuries as the Day of Horror. We can therefore propose that the AD365 seismic sequence consisted of a number of major shocks, offshore Crete, offshore and possibly between and Sicily.

Keywords: ad365 earthquake sequence, elastic dislocation, tsunami



(S) - IASPEI - International Association of Seismology and Physics of the Earth's Interior

JSS004

Oral Presentation

1895

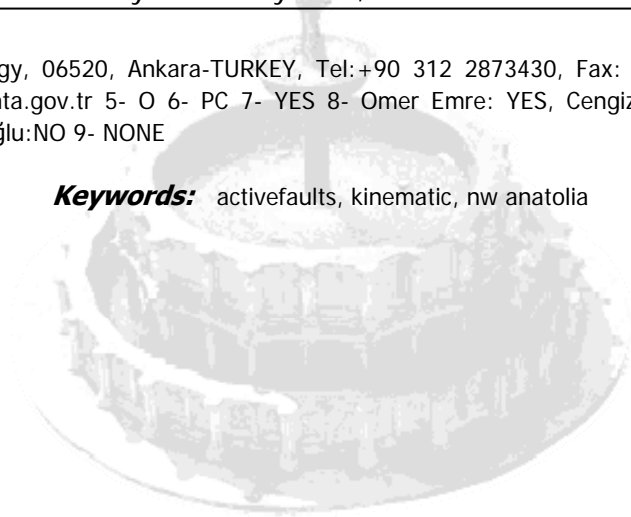
Active fault geometry and kinematics of NW Anatolia, new insights from revision of active fault map of Turkey

Mr. Cengiz Yildirim
Geology MTA IASPEI

The revision of the Active Fault Map of Turkey has been carried out by the MTA and this study presents the preliminary results of the project in NW Anatolia. NW Anatolia is a transition zone between the Aegean extensional tectonic regime and the North Anatolian transform fault system (NAFS). The NAFS turns into a broad deformation zone and bifurcates into two strands as the northern and the southern in the Marmara region. Lateral motion of the Anatolian block is essentially accommodated by the northern strand in the Sea of Marmara. However, the southern strand is included in the NW Anatolian transition zone as a major splay bifurcating from the master strand of the NAFS. The transition zone (NATZ) is structurally delimited by the Sındırgı-Sincanlı fault and the Bergama-Zeytinadağ fault zones from the Aegean graben system in the south. However, the eastern boundary of the zone is connected to the Eskişehir and the Tuzgözü fault zones delimiting the eastern boundary of the Aegean extensional regime. In this study, about forty active faults were mapped in detail and the active faults were classified into four sub-classes as earthquake rupture, active fault, potentially active fault and neotectonic fault or lineament. The new data reveal that the active faults were localized along four major bend systems concave to the south in the region, namely the Bandırma-Biga, Manyas-Gönen, Bursa and Balıkesir bends. The Bandırma-Biga bend is connected to the westernmost tip of the southern strand or splay of the NAFS. However, in the east the Bursa bend is connected to the Eskişehir fault zone via the Dodurga fault. Both the eastern and the western flanks of the bends are controlled by right lateral strike slip faults. However, the faults trending NE-SW are transpressional and those trending E-W and NW-SE are transtensional just at the apex of the bends. This structural pattern accommodates a counter-clockwise rotation of the sub-blocks delimited by the active faults. The Manyas-Gönen bend and the Bursa bend are the best examples of the bend kinematics of the region. The Bursa fault of E-W and NW-SE trends at the apex of the bend display normal dip-slip characteristics, however, the Ulubat fault which is located immediately to the west of the bend is a reverse oblique right lateral strike slip fault. The findings from this study are consistent with the seismologic and the GPS data. The overall geometry of the bends are parallel to the Gediz graben and to the large bend of the NAFS in the Sea of Marmara. Our data imply that bend geometry due to block rotations dominates the kinematics of active faults in NW Anatolia. The active faults in the southern Marmara and the Biga peninsula are the Yenice-Gönen, Manyas, Orhanlı, Ulubat and Bursa faults forming the Manyas-Gönen and the Bursa bends that can not be directly connected with the NAFS. These two bends connect to inner west Anatolia instead of to the NAFS. The geometry of the bends is controlled by the paleotectonic structures and the granitic plutons as in the Bursa and Manyas-Gönen bends. The 1855 historical earthquakes originated on the reverse strike slip Ulubat fault and then the normal dip-slip Bursa fault on the Bursa bend. In the 20th century, a similar earthquake sequence occurred on the Manyas-Gönen bend during the 1953 Yenice-Gönen (M:7.2) and the 1964 Manyas earthquakes. The Yenice-Gönen earthquake nucleated on the restraining flank of the Manyas-Gönen bend, whereas the 1964 Manyas earthquake (M: 6.9) nucleated on the releasing flank of the bend and occurred on a dip-slip oblique normal fault. Hence we suggest that the earthquake sequences in the region primarily initiate on the restraining flanks and then propagate toward the releasing flanks of the bends. Submission Information 1-JSS004 2- Non-instrumental seismometry - Quantification of past and future earthquakes: balancing the geological, historical and contemporary strain records 3-Active tectonic, Kinematic, NW-Anatolia 4-Cengiz YILDIRIM, MTA

Department of Geology, 06520, Ankara-TURKEY, Tel: +90 312 2873430, Fax: +90 312 2854271, e-mail: cengizyildirim@mta.gov.tr 5- O 6- PC 7- YES 8- Omer Emre: YES, Cengiz Yildirim: YES, Ahmet Doğan: NO, Fuat Şaroğlu: NO 9- NONE

Keywords: activefaults, kinematic, nw anatolia



IUGG

XXIV2007

PERUGIA
I T A L Y



(S) - IASPEI - *International Association of Seismology and Physics of the Earth's Interior*

JSS004

Oral Presentation

1896

Deglacial earthquakes in Fennoscandia can be reconciled with stable-craton-core earthquake rates

Dr. John Adams

Geological Survey of Canada Geological Survey of Canada IASPEI

It is believed that the weight of the Greenland and Antarctic ice sheets inhibits current earthquake activity (Johnston's 1987 hypothesis), and that when the Scandinavian ice sheet melted the stored strain energy was released in a burst of large earthquakes in immediate deglacial times. I test the hypothesis that, allowing for this effect, the long-term seismicity rate in Sweden is substantially the same as that of other Stable Craton Cores (SCCs). I tried to reconcile the per-unit-area rate of magnitude > 6 earthquakes from a) the low contemporary seismicity rate in Sweden, b) the high seismicity rate that occurred immediately following deglaciation, and c) the much lower rate from the past 8000 years (both b and c were taken from available paleoseismic catalogs) with the global SCC rate. The reconciliation needs an assessment of the completeness of the information and some additional assumptions. I conclude that the Swedish deglacial earthquakes appears to represent the release of ~50,000 years strain accumulation at a typical stable craton seismic activity release rate. In the long term, about 8 to 15 earthquakes of moment magnitude 6.0 or greater might be expected within a 100-km radius of a site during a future 100,000 year period (the full uncertainty is much larger than this best-estimate range). Past history indicates that much of this activity might be concentrated into a relatively short time window in the more distant future, or alternatively the analysis places a limit on the probability of a $M > 6$ event in the near future.

Keywords: deglacial, earthquakes, sweden



(S) - IASPEI - *International Association of Seismology and Physics of the Earth's Interior*

JSS004

Oral Presentation

1897

The Earthquake Cycle in the San Francisco Bay Area: 1600-2007

Dr. David Schwartz

IASPEI

William Lettis, James J. Lienkaemper, Suzanne Hecker, Keith Kelson, Thomas Fumal, John Baldwin, Gordon Seitz, Tina Niemi

The San Francisco Bay Area lies within the Pacific-North American plate boundary. The historical record of earthquakes in the Bay Area is considered complete at magnitude 5.5 back to 1850. The striking contrast between the large number (29) of moderate magnitude earthquakes (M 5.6-6.4) from 1850 to 1906 and their general absence between the M7.9 1906 San Francisco earthquake and the present day is a fundamental observation leading to the concepts of the earthquake cycle, the acceleration of regional seismicity prior to a great earthquake, and stress shadows. There is no accurate quantification of either the number or magnitude of moderate events prior to 1850 for comparison. Paleoseismic studies cannot easily identify moderate-size earthquakes, but they do extend the record of larger surface-faulting events. Recent investigations of the region's major plate strike-slip faults now provide a longer view of the Bay Area earthquake cycle. Preliminary paleoearthquake chronologies for the region's major faults have been developed; these have durations of 1000 to 3000 years. Although the completeness of individual fault chronologies is variable, the paleoearthquake history across the entire Bay Area fault system since 1600 is essentially complete. Evidence of surface faulting that is post-1600 and pre-1776 (founding of Mission Dolores) is found on the northern San Andreas (SAN), Santa Cruz Mountains San Andreas (SAS), northern Hayward (NH), southern Hayward (SH), Rodgers Creek (RC), northern Calaveras (NC), San Gregorio (SG), and Green Valley (GVY) faults. The timing of these, listed in order of their mean radiocarbon age (with age-range uncertainties in parentheses), is: SH 1620 (1605-1645); SAS 1640 (1600-1670); GVV 1700 (1685-1776); NH 1705 (1670-1776); SG 1720 (1695-1776); SH 1730 (1685-1776); RC 1740 (1690-1776); SAN 1750 (1720-1776); and NC 1760 (1670-1830). (Given dating uncertainties, the actual ordering of earthquakes may have been different). Offset data, which reflect magnitude, are limited. However, measured point-specific slip (RC, 1.8-2.3m; SG, 3.5-5.0m; SAN 3.0m) and modeled average slip (SH, 1.9m) indicate large magnitude earthquakes on these regional faults. Major observations of the Bay Area earthquake cycle are: 1) between 1600 and 1838 the San Andreas fault failed in a series of large earthquakes rather than as a single, multi-segment 1906-type rupture; 2) a regional cluster of large earthquakes occurred between 1670-1776 (and the actual interval was likely shorter); 3) the estimated moment release of the cluster (irrespective of the sequence of events) is comparable to the moment release of 1906; and 4) the cluster was followed by a regional quiescence of large earthquakes (paleo stress shadow?), with only two (1838, 1868) until 1906. The Bay Area paleoseismic record has the potential to extend these types of observations through multiple earthquake cycles.

Keywords: earthquake cycle, clustering, paleoseismology

(S) - IASPEI - *International Association of Seismology and Physics of the Earth's Interior*

JSS004

Oral Presentation

1898

**GPS Constraints on Seismic Hazards in Continental Intraplate Regions:
Eastern Canada Example**

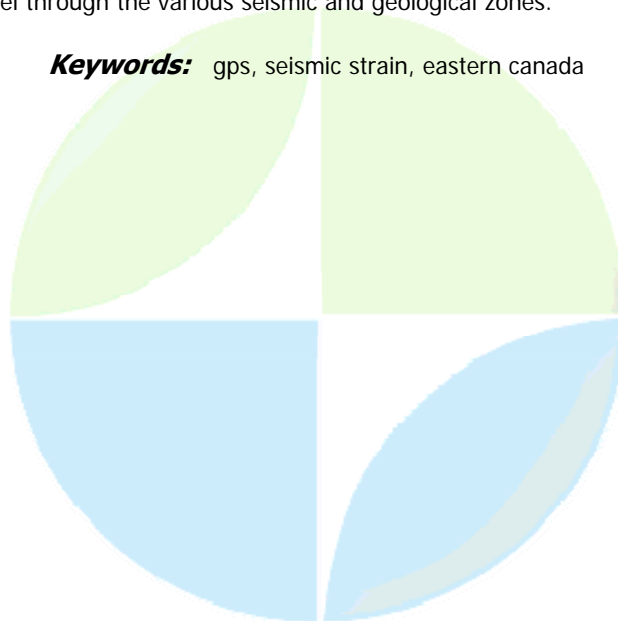
Dr. Stephane Mazzotti

Geological Survey of Canada Pacific Geoscience Centre IAG

Joseph Henton, John Adams

Compared to the long return periods, the historical and instrumental records of intraplate earthquakes only provide a relatively short seismicity snapshot. In addition, the lack of a physical understanding of what controls the earthquake distributions make seismic hazard assessments in continental intraplate regions particularly challenging. Thus, hazard models are often a reflection of the earthquake records, based on the assumption that the hazard is higher in the zones of (known) recent high activity. An alternative model is to consider that the hazard is controlled by large-scale geological structures where the seismicity migrates on a time scale of hundreds to thousands of years. Eastern Canada provides a good test ground for this alternative hypothesis. Most of the seismicity is concentrated in patches along the St. Lawrence and Ottawa valleys, which follow the late Precambrian Iapetus rift and aulacogen system. All known large earthquakes have occurred along this major paleo-tectonic structure. We use a combination of continuous and campaign GPS data to try to map crustal strain rates in eastern and discriminate between the two hazard models (historical vs. geological seismic zones). The GPS data cover periods of 4-12 years with a spatial density of 100-200 km. To a first order, the horizontal velocity field shows a systematic south-east motion of ~ 1 mm/yr, with respect to stable North America, which decreases eastward and possibly reverts to a slight north-west motion in the far-field. The vertical GPS velocities show a clear south-east tilt from ~ 8 mm/yr uplift near Hudson Bay to ~ 2 mm/yr in New England. These velocity fields can be attributed to post-glacial rebound from the fading of late Holocene Laurentide ice sheet. The GPS strain rate field is not as well defined and at the limit of resolution of the existing dataset. However, preliminary results suggest that crustal strain may concentrate in the areas of highest historical seismicity along the rift structure of the St. Lawrence valley. A direct strain seismic moment relationship allows us to convert the GPS strain rate to earthquake recurrence statistics, which in turn can be used to constrain the seismic hazard models. We discuss the impact of including the GPS data on the hazard level through the various seismic and geological zones.

Keywords: gps, seismic strain, eastern canada



(S) - IASPEI - *International Association of Seismology and Physics of the Earth's Interior*

JSS004

Oral Presentation

1899

The use of morphotectonic data to infer seismotectonic parameters of normal faults in Crete, Greece

Prof. Riccardo Caputo

Dept. Earth Sciences University of Ferrara IASPEI

Monaco C., Tortorici L.

Morphotectonic features reveal recent seismic activity on normal faults on Crete allowing slip-rates, palaeoearthquake magnitudes and earthquake recurrence intervals to be inferred. The investigated faults show major escarpments (100s m high, 10s km long), separating uplifted Mesozoic rocks from Quaternary deposits. During Holocene, slip-rates out-paced erosion/sedimentation rates and 5-15 m-high fresh scarps formed at the base of the major escarpments. Based on our field observations and following empirical relationships between magnitude, surface rupture length and maximum co-seismic vertical displacement, it is possible to infer some of the principal seismotectonic parameters of the investigated faults. Long-term slip-rates range between 0.5 and 1.3 mm/a, maximum expected magnitudes between 6.3 and 6.6 (or 6.5-6.8, considering the worst case scenario), while mean recurrence intervals range between 260 and 870 years. These geologically-inferred estimates are comparable with those obtained by geodetic data, the historical and instrumental seismicity allowing to improve seismic hazard estimates in Crete.

Keywords: holocene, fault scarps, seismic hazard



(S) - IASPEI - *International Association of Seismology and Physics of the Earth's Interior*

JSS004

Oral Presentation

1900

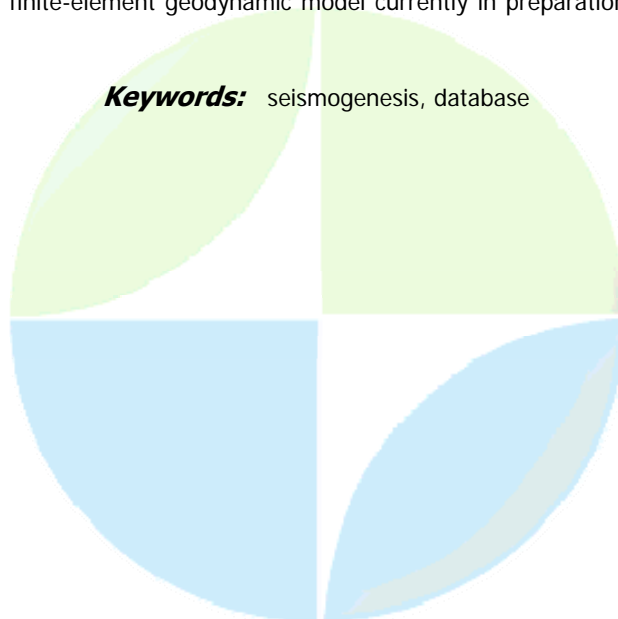
Assessing the completeness of an active fault database: the Italian case history

Dr. Roberto Basili

Sara Scriveri, Gianluca Valensise, Diss Working Group

For most applications a fault database is effective only to the extent that it ensures a certain level of completeness, i.e. if all existing fault zones are captured and correctly described. For this reason, and in addition to mapping the potential sources of individual large earthquakes, the new version of the Italian Database of Individual Seismogenic Sources (DISS, v. 3.0.2: <http://www.ingv.it/DISS/>) describes the countrys earthquake potential in terms of a new category of potential sources, the Seismogenic Areas. These are narrow, elongated portions of the territory that are intended to represent the surface projection of active and potentially seismogenic fault systems capable of earthquakes of M 5.5 and larger. Seismogenic Areas were designed to combine the historical record with a number of lines of geologic and tectonic evidence that are normally insufficient to determine the existence of potential sources of individual earthquakes. For this reason Seismogenic Areas are described using the same geometric and kinematic parameters as the standard sources, but are more loosely defined and are not internally segmented. More importantly, they aim at a complete description of the earthquake potential that may allow them to be used in new generation SHA schemes. How can the completeness of Seismogenic Areas be tested? We subdivided Italy into eight zones that are believed to be relatively homogeneous from the geodynamic point of view. For each zone we calculated two earthquake moment rates, respectively from all 81 Seismogenic Areas and from over 300 historical earthquakes having $M \geq 5.5$ (<http://emidius.mi.ingv.it/CPT1/>) that fall within it. The results show that for six zones the moment rate from Seismogenic Areas justifies the rate derived from seismicity: in one case it exceeds it, and in the last case it underestimates it. This suggests that the Seismogenic Areas are already reasonably complete, although at this stage we cannot exclude that large real uncertainties within a given zone might compensate among them and simulate a good match. This and other limitations of the test should be overcome when Seismogenic Areas will be tested against the strain rates derived for the whole country using a finite-element geodynamic model currently in preparation (see Barba et al., this session).

Keywords: seismogenesis, database



(S) - IASPEI - *International Association of Seismology and Physics of the Earth's Interior*

JSS004

Oral Presentation

1901

Numerical modelling of strain rates in Italy

Dr. Salvatore Barba

Seismology and Tectonophysics Istituto Nazionale di Geofisica e Vulcanologia IASPEI

Carafa Michele Mc

Italy is earthquake country, but investigating active faults is difficult as many if not most of them are hidden or positively blind. Geological strain rates in can be confidently assessed only in very few seismogenic areas, and seismic hazard studies generally rely only on earthquake rates from catalogues. GPS networks are still rather sparse and their resolving power is limited by the peculiar configuration of the country. Our work attempts to bridge this knowledge gap by constructing a geodynamic model that may be used to assess strain-rates in most of known fault zones and possibly to identify as yet unknown seismogenic areas. We computed the strain-rate in integrating several datasets: seismic events, active faults, GPS measurements, stress and strain indicators, and tectonic regime. Different ways to assess strain rates have obvious advantages and disadvantages, due to the different spatial coverage of data, different temporal scale, and probably different physical significance with respect to the future strain rates. Using different classes of observations, we increase the spatial coverage of the separate datasets and show the inconsistencies where the datasets overlap. Although we do not face how the different observations relate to the future strain rate, being the physical relationships not yet clear, the integration guarantees a more robust result than the datasets taken separately. By means of a trial-and-error procedure, we build a series of 3D dynamical models of and surrounding regions, compute the velocities, stress, and strain in the thin-shell approximation by using the finite element code SHELLS (Bird, 1999, *Computers & Geosciences*, 25(4), 383-394), and compare the model predictions with the available observations. We test many free parameters in acceptable ranges, including boundary conditions, fault friction, rheology, etc., and study the models or family of models whose predictions deviate less from the data. We build the structure of the models based on the most recent information on the crustal structure, faults, and rheology. The range of boundary conditions and the ideas of basal shear tractions are adopted from the literature. To compare the predictions with the observations, we use regional published datasets and compute the deviation of each model with each dataset. Last, we combine the single deviations assigning a weight to each dataset based on a possible estimate of the signal that cannot be modelled by our approach. We find that our model predictions satisfactorily agree with data (we do not reproduce 17-33% of tectonic regime observations, the predicted azimuth deviates of 26-30 degrees, and the RMS of velocities is 1.2-1.4 mm/y). In the most active areas, we find a strain-rate of 10-16-10-14 s⁻¹, compatible with the estimates of other authors but with somewhat a different pattern that accounts for the different datasets. Most importantly, we show that using only one class of observations leads to very different results depending on the choice of the data, whereas our results appear to be more robust.

Keywords: strain rates, italy, numerical models

(S) - IASPEI - International Association of Seismology and Physics of the Earth's Interior

JSS004

Poster presentation

1902

Where are all the young faults scarps in eastern Canada?

Dr. John Adams

Geological Survey of Canada Geological Survey of Canada IASPEI

Seismicity rates in eastern Canada (east of the Rockies) suggest a rate of 7 $M \geq 4$ (approximate completeness threshold) per year and $\beta = 2.09$. Thus we predict about 0.1 $M \geq 6$ events/year, each of a size that had it occurred in the top of the crust should have produced a surface rupture. This rate needs to be reduced by about a factor of ~ 10 , viz ~ 5 to allow for distribution of events in depth through the seismogenic crust and also ~ 2 to allow for underwater surface ruptures. For the past 100 years (when knowledge of $M6$ events is fairly complete) we should have had $0.1 \cdot 100 / 10 = \sim 1$ ruptures; we know of just one: the 1989 Ungava surface rupture, though a few other earthquakes might have undiscovered surface ruptures. Furthermore a rate of 0.01 p.a. suggests that in the circa 10,000 years since eastern Canada was deglaciated, $\sim 100+$ surface ruptures should have been formed. Arguably we know none, though some candidates are beginning to emerge, and evidence of earthquake shaking events is accumulating. If the Canadian ice sheets had the same effect of suppressing the seismicity for $\sim 50,000$ years as in Fennoscandia, we should have had $\sim 500+$ deglacial $M \geq 6$ events occurring near the ice margin of the day, i.e. 5 times more than the postglacial number. None have been confirmed as yet. Excuses might be made for the Canadian craton, as behaving differently from the Scandinavian craton due to the scale of its glaciation, or due to all the deglacial scarps forming under the ice and thus rapidly destroyed (perhaps as in southern Sweden?). But the gap between the predicted and the known remains profound.

Keywords: paleoseismic, fault scarp, canada



(S) - IASPEI - *International Association of Seismology and Physics of the Earth's Interior*

JSS004

Poster presentation

1903

Variation of slip velocity of repeating earthquakes and its dependence on focal depths

Dr. Keisuke Ariyoshi

DONET (JAMSTEC) Seismological Society of Japan, AGU IASPEI

Toru Matsuzawa, Ryota Hino, Akira Hasegawa, Yoshiyuki Kaneda

We investigated depth dependence of the slip velocity of small repeating earthquakes using 3-D numerical simulations of a subduction zone involving large and small asperities based on a rate- and state-dependent friction law. Our results reveal that the postseismic slip of a large earthquake trigger slow slip (with slip velocity lower than that of the spontaneous rupture of the small asperity) rupture of the small asperity located at a depth of 45 km [Ariyoshi et al., 2007, GRL], whereas rapid slip (with higher slip velocity) one at a depth of 5 km. Uchida et al. [2003, GRL] showed that the repeating earthquakes in the NE Japan subduction zones occur constantly, conforming to the rate of the plate convergence for the depth range of $> \sim 40$ km. On the other hand, the shallow ($< \sim 10$ km) focus repeating earthquakes tend to be activated only for the postseismic period of large interplate earthquakes and cumulative slip estimated by them is less than that expected from the plate convergence rate. Considering that frictional instability of asperities in shallower part is less than those deeper due to low effective normal stress, most of the observed shallow repeating earthquakes may be rapid slip events triggered by the postseismic slip of the neighboring large asperities, and the corresponding small asperities give rise to (aseismic) slow slip events otherwise.

Keywords: effective normal stress, repeating earthquake, rate and state dependent law



(S) - IASPEI - *International Association of Seismology and Physics of the Earth's Interior*

JSS004

Poster presentation

1904

GPS-geodetic monitoring of the South West Seismic Zone (SWSZ) of western Australia: progress after two observation epochs in 2002 and 2006

Dr. Mark Leonard

Geoscience Australia Geohazards IASPEI

The Australian south-west seismic zone (SWSZ) is a northwest-southeast-trending belt of intra-plate earthquake activity that occurs in the southwest of Western Australia, bounded by 30.5S to 32.5S and 115.5E to 118E. This is one of the most seismically active areas in , with nine earthquakes over magnitude 5.0 that have occurred in the SWSZ between 1968 and 2002, the largest of these was the M6.8 Meckering earthquake in 1968. Since the SWSZ lies as close as ~150 km from the ~1.4 million population of the Perth region, it poses a distinct seismic hazard. However, little is currently known about the magnitude and orientation of this deformation, and whether there is any associated ongoing surface expression. It is also not known how this intra-plate activity compares with that observed elsewhere in or elsewhere on Earth. Earthquake activity recorded by Geoscience over the past four decades suggests that the SWSZ could be deforming with strain rates between 10^{-9} /yr and 10^{-8} /yr, or with displacements between 0.1 mm/yr and 1 mm/yr across the 200km width of the currently active SWSZ. This estimate is derived by applying the Kostrov formula for a moment release of 3.3×10^{19} Nm in the 34 years from 1968 to 2002. Early geodetic studies of the SWSZ that used both terrestrial and Global Positioning System (GPS) techniques were inconclusive, due mainly to the imprecision of the technologies used in relation to the likely small amount of any surface deformation. Therefore, in 2002 a new 48-point campaign-reoccupation GPS network was established across the SWSZ to attempt to detect surface deformation, using ground-level forced-centred monuments. The first two observational epochs were in May 2002 and May 2006. In both surveys, the dual-frequency carrier-phase GPS data were collected continuously at each monitoring point over a 5-7 day observation period. For the both campaigns, after excluding outlying sites (due to equipment malfunctioning), the estimated internal horizontal precision was 1.0 mm; the vertical precision was generally better than 4 mm. Comparison of these two repeat surveys shows that strain rates in the order of 10^{-9} /yr can, in principle, ultimately be resolved if the deformation across the SWSZ occurs uniformly, but that the four-year time interval between the existing two surveys is at present not adequate to detect deformation with confidence given the noise in the estimated coordinates at each epoch. Further repeat surveys after, say, eight and 12 years should begin to reveal any observable deformation significantly in excess of this observational error. These preliminary results suggest that the higher range of estimated of strain rates (10^{-8} /yr) is unlikely.

Keywords: gps, strain rate, earthquake

(S) - IASPEI - *International Association of Seismology and Physics of the Earth's Interior*

JSS005

1905 - 1923

Symposium

Non-instrumental seismometry - Global and regional parameters of paleoseismology; implications for fault scaling and future earthquake hazard

Convener : Dr. David Schwartz, Mrs. Suzanne Hecker, Dr. Gianluca Valensise, Dr. Kelvin Berryman

Co-Convener : Dr. Paolo Marco De Martini, Dr. Eullia Masana, Dr. Daniela Pantosti

For the General scopes see introduction to symposium JSS004. This session deals mainly with the integration of earthquake and fault rupture parameters across the seismological/geological/geophysical boundaries exploring the difference in scaling between large and small earthquakes. Another interesting aspect we would like to discuss concerns the evidence for linear or nonlinear relationship between average displacement and fault length for large dip-slip and strike-slip earthquakes. These have been the topic of considerable debate in the last years and we hope that the contributions to the session will advance our knowledge at both global and regional scales. The session includes, but is not restricted to, the following topics: - relationships between paleoseismological parameters (surface rupture length and average surface displacement) and earthquake magnitude estimates; - comparison of paleoseismological parameters obtained from the pre-instrumental epoch as against modern earthquakes studies; - comparison of source parameters obtained by different methodologies (geodesy, geology, seismology and geophysics). We particularly welcome contributions based on results from fieldwork, high-resolution geophysical measurements, remote sensing studies and analogue models. We also encourage presentations dealing with problems of under- or over-estimation of earthquake magnitude resulting from spatial variability of slip and scarp degradation processes at the surface.

PERUGIA
ITALY



(S) - IASPEI - *International Association of Seismology and Physics of the Earth's Interior*

JSS005

Oral Presentation

1905

Empirical relations among magnitude and rupture characteristics, through mechanical modeling of interacting faults and fault patches

Mr. Olaf Zielke
SESE ASU

Ramon J Arrowsmith

Determining the magnitude of paleo-earthquakes is as difficult as it is important. These data are crucial components to assess seismic hazard: knowing the slip and date of the last major earthquake that occurred on a specific fault, the derived long-term slip-rate can be used to estimate the timing of the next large event assuming that they are time predictable. Furthermore, long-term slip-rates define the slip-distribution within a fault system constraining the regional stress field a crucial component to run increasingly realistic fault models. Such models may characterize the seismic hazard at fault system level by incorporating processes such as fault interaction. In order to determine paleo-magnitudes, earthquake-related geomorphic features such as rupture length, average surface displacement, or maximum surface displacement are utilized, assuming that an earthquake of a specific size will cause surface features of correlated size. The well known Wells & Coppersmith (1994) paper defined empirical relationships between these and other parameters, based on events with known magnitudes and rupture characteristics. However, because their study depended on a limited number of observed events, the uncertainties on their correlations are rather large, coefficients ranging from 0.71 to 0.95. In addition, they were only able to differentiate between the three general fault types (strike, normal, reverse). Therefore, the effect of oblique slip on rupture characteristics was not addressed affecting the derived relationships. We have developed a boundary element model, based on derivations by Okada (1992) that simulates faulting and fault interaction of any number of arbitrarily oriented, located, and loaded faults. For the study presented here, we simulate faulting along a single fault divided into a large number of (~5000) elements and utilize a simple Coulomb static/dynamic friction law to create synthetic seismic catalogs: Each time step the faults are tectonically loaded. When the stress on an element exceeds its static frictional strength, it starts to slip, corresponding to the stress drop to its dynamical frictional strength. Due to a fault interaction algorithm, this may cause other elements to fail as well, cascading into events of all sizes, populating the synthetic seismic catalog. This catalog will be used to develop a new set of more complete magnitude vs. rupture characteristics plots in the sense of Wells & Coppersmith (1994). Several enhancements justify this approach: A) We can use seismic catalog of any length. B) Our catalog will be not limited to large, rare, surface rupturing earthquakes but contain the full spectrum of possible magnitudes. C) The uncertainty in the correlations will be small, providing a more realistic assessment of variability. D) How different parameters such as oblique slip, fault sinuosity, or fault roughness affect the magnitude vs. rupture characteristics relationships can be explored. In addition to a full exploration of relevant parameters from Wells & Coppersmith, we will also study system level properties such as fault sinuosity, fragmentation, slip obliquity, etc. Since these are parameters that can be constrained in the field, our experiment will help paleo-seismologist to interpret their findings in a more complete way that treats faults not as individual, isolated entities but as part of a system of interacting structures.

Keywords: mechanical modeling, interaction, synthetic seismicity

(S) - IASPEI - *International Association of Seismology and Physics of the Earth's Interior*

JSS005

Oral Presentation

1906

A 48-KYR-long slip rate history along the Jordan Valley segment of the Dead Sea fault

Prof. Mustapha Meghraoui
IASPEI IASPEI IASPEI

The 110-km-long fault rupture of the Jordan Valley section of the Dead Sea fault exhibits significant late Quaternary active deformation. We document systematically offset drainage over three regions along the active fault trace. The mostly dendritic drainage is formed by gully incisions and river streams carving into the soft Lisan lacustrine sediments and may be arranged into six distinct generations, as a function of their depth. Considering incisions underwent similar erosion/deposition processes, depth reflects age and incisions may consequently be sorted chronologically. Besides, from the history of past lake level fluctuations and intense rainfall episodes, we identify six climatic events likely to have triggered the onset of gully incisions. In addition, we measured lateral offsets affecting the drainage from the analysis of aerial photographs and filed control points. Combined observations yield an accurate dating from the onset of incisions and thus, for the maximum age of cumulative displacements they recorded. The deduced slip rate displays a long-term average value of 5 mm/yr, in good agreement with geodetic measurements. A detailed analysis reveals strong variations over short time spans with a threefold increase from 3.5 mm/yr to 11 mm/yr during a 2000-yr-long period. This original behavior is interpreted as a result from alternating periods of quiescence and increased seismic activity (clustering). Considering the last large earthquake in the Jordan Valley occurred in AD 1033, the fault may have accumulated 3.5 m to 5 m of slip deficit. This pleads for a Mw 7.4+ earthquake yet to be released along the Jordan Valley fault segment.

Keywords: faulting, earthquake, offset



(S) - IASPEI - *International Association of Seismology and Physics of the Earth's Interior*

JSS005

Oral Presentation

1907

Paleoearthquake surface rupture in a transition zone from strike-slip to oblique-normal faulting

Dr. Vasiliki Mouslopoulou

School of Geological Sciences University College Dublin

A. Nicol, T. A. Little, J. G. Begg

Landforms displaced by the North Island Fault System (in New Zealand) over the last c. 30 kyr indicate a gradual northward change from right-lateral strike-slip to oblique-normal faulting (c. 60° in the slip vector pitch) near its intersection with the Taupo Rift. We analyse fault data from 20 trenches and displacements along active traces to explore whether changes in late Quaternary fault slip vectors principally arise due to earthquake rupture arrest in the transition zone and/or to variations in slip vector pitch during individual earthquakes that span the transition zone. Results show that earthquake rupture arrest occurs along the strike of the North Island Fault System with, at least 80% of all events during the last 10-13 kyr terminating across the zone of late Quaternary (c. 30 kyr) kinematic transition from strike-slip to oblique-normal slip. The strike of the faults across the kinematic transition is unchanged, and we suggest that rupture was arrested there due to a 20-30° northward shallowing of the fault-dip across this zone. Rupture arrest decreases earthquake lengths and magnitudes which, when combined with recurrence intervals from trenching, locally decreases the seismic hazard in the region of the faults. Rupture arrest alone cannot account for the observed change in slip vectors and some northward steepening of slip vectors during individual earthquakes is required. Changes in coseismic slip vectors may arise due to the northward decrease in fault-dip and associated steepening of the principal compressive stress axis (σ_1) which, in turn, is due to fault interactions between the North Island Fault System and the adjacent active Taupo Rift.

Keywords: earthquakeslip vectors, fault segmentation, fault trench



(S) - IASPEI - *International Association of Seismology and Physics of the Earth's Interior*

JSS005

Oral Presentation

1908

Scaling of paleoseismological parameters of 550 behavioral segments in Japan

Dr. Toshikazu Yoshioka

Active Fault Research Center Geological Survey of Japan, AIST IASPEI

Yasuo Awata, Yuichiro Fusejima, Fujika Miyamoto

Active faults in Japan are segmented into about 550 behavioral segments based on geometry of fault strand separated by discontinuities of larger than about 2 km and bends, timing of paleo-faulting and slip-rate. 550 behavioral segments consist of about 290 reverse faults, 40 normal faults and 220 strike-slip faults. The maximum value in length among all behavioral segments is 66 kilometers and the average value in length is about 20 kilometers. We gather paleoseismological data to construct the active fault database in Japan, and evaluate paleoseismological fault parameters of each behavioral segment, such as the fault length, the dip and strike, the long-term slip rate, the displacement-per-earthquake, the recurrence interval, and the elapsed time after the last faulting. To evaluate these parameters, we use observed field data (mid-range value if they have some uncertainty) after the data source references. In case there is no field data on the behavioral segment, we adopted the values calculated from other parameters. We examined the relationships between these paleoseismological parameters of the behavioral segments of active faults in Japan. In 65 behavioral segments, the displacement-per-earthquake (D; net slip, most frequency-occurring value) was estimated from field data. There is a good correlation between the lengths of behavioral segments (L) and D. The values of D of the reverse faults are slightly higher than the values of the strike-slip faults. The average ratio between D (m) and L (km) is about 0.15 in the reverse faults except for the Ichinose and Iriyamase segments, and 0.12 in the strike-slip faults. The relationship between D and the long-term slip rate (S) is also obvious. Behavioral segments with higher S tend to have higher values of D in over 1.0 mm/yr in S. However, the values of D are almost flat in less than 1.0 mm/yr in S.

Keywords: fault, segment, parameter



(S) - IASPEI - *International Association of Seismology and Physics of the Earth's Interior*

JSS005

Oral Presentation

1909

The role of complex step-over geometry on the 1939 earthquake rupture propagation in the Niksar Region, North Anatolian fault system

Dr. Omer Emre

Geology Dept General Directorate of Mineral Research and Explor IASPEI

The 1939 Erzincan earthquake (M: 7.9) is the largest event in a sequence of earthquake in 20th century along the North Anatolian Fault System (NAFS) produced a 360 km-long surface rupture. The event nucleated in the eastern end of the rupture and unilaterally propagated toward to west. The rupture extended along the master strand of the NAFS between Erzincan and Niksar basins. However, a part of 65 km-long western portion of the rupture directed towards on the Ezinepazar splay. Three years later, the 1942 earthquake (M: 6.9) occurred on Erbaa-Niksar fault on the master strand. It produced a 47 km-long surface rupture. We performed detail mapping on fault and step-over geometry to discuss fault interaction in the both events. In the region, the master strand of NAFS consists of Reşadiye segment and Erbaa-Niksar fault. However, Karayaka reverse fault and strike-slip Esencay and Ezinepazar faults are major splays. Niksar pull-apart basin located on the main strand which has an 11 km width and separates the eastern and the central NAFS. The basin characterized by serial normal fault on the both margins. The Erbaa-Niksar fault divides into two main geometric sections by a 12 km-long restraining step-over which is characterized with reverse fault zone and push-up structure. The length of the Esencay fault is 70 km. It is also divided into two sections by a restraining step-over which is 7.5 km-long and 1.5 km width. Eastern section of the fault includes a serial subsection in left stepping. Ezinepazar fault that included in the 1939 rupture as the western tip segment runs into Anatolian micro-plate. A local releasing step-over separates Reşadiye and Ezinepazar segment. Although displacements were 3.5-4.0 m along Reşadiye segment east of Niksar basin, the amount of the maximum displacement was about 2 m on the Ezinepazar segment of the 1939 rupture. Hence, the amount of lateral slip abruptly decreased on the Ezinepazar segment. However, the data indicated that a 26 km eastern section of the Erbaa-Niksar fault and normal faults on the both margin of Niksar releasing step-over ruptured during the both 1939 and 1942 events. Surface faulting of the 1939 event terminated at the restraining step-over on the Erbaa-Niksar fault. However, the surface faulting of 1942 event covered entire fault including the 26 km-long eastern section. On the other hand, there is no data for surface faulting on an 18 km-long the eastern section of the Esencay fault. We concluded that structural complexity in the region played a significant role on the deviating of the 1939 rupture from the master strand to the Ezinepazar splay. This study reveals that not only Niksar releasing step-over but also two large restraining step-over on the Niksar-Erbaa and Esencay faults were other barriers to the rupture propagation of the 1939 event on the master strand and surface faulting jumped to Ezinepazar splay. We also suggest that Karayaka and Esencay faults did not ruptured during the earthquake sequence of 20th century along the NAFS should be taken into consideration as the most important source faults for the seismic hazard assessment of the region.

Keywords: stepover, 1939 rupture, nafs

(S) - IASPEI - *International Association of Seismology and Physics of the Earth's Interior*

JSS005

Oral Presentation

1910

Magnitude distribution of linear morphogenic earthquakes in the Mediterranean Region: insights from palaeoseismological and historical data

Prof. Riccardo Caputo

Dept. Earth Sciences University of Ferrara IASPEI

Mucciarelli M., Pavlides S.

We analyse the earthquake magnitude distribution of 'linear morphogenic earthquakes' that reactivated dip-slip normal faults within the Mediterranean Region. Information on past events is obtained following two distinct methodological approaches: the geological one (morphotectonic investigations coupled with palaeoseismological excavations) and the historical one (contemporaneous surveys of coseismic ruptures). In order to homogenise the different datasets, and therefore enabling a comparison, we calculated moment magnitudes (M_w) starting from seismic moments (M_0) estimates. The cumulative distributions thus obtained for the two datasets show similarities and differences. To interpret these differences, we generate random datasets reproducing the distribution of the real data, based on the log-normal distributions of the coseismic vertical displacement and the rupture length. The analysis of larger synthetic catalogues suggests that coseismic displacements are systematically underestimated for moderate-to-strong palaeoseismologically-observed events (5.0-6.5), while the opposite occurs for very strong (>6.7) historically-observed past earthquakes. The possible causes and consequences for seismic hazard analyses are also discussed.

Keywords: seismotectonic, holocene, seismic hazard



(S) - IASPEI - *International Association of Seismology and Physics of the Earth's Interior*

JSS005

Oral Presentation

1911

Maximum Fault Displacements in Extensional Regimes: a Geologic Perspective

Mrs. Suzanne Hecker

Earthquake Hazards U.S. Geological Survey

Timothy E. Dawson, David P. Schwartz

The characterization of ground motions at very low probabilities of exceedance is important for long-lived critical facilities. As part of an interdisciplinary effort to evaluate the possibility of extreme ground motions at the proposed high-level nuclear waste repository at Yucca Mountain, Nevada (Basin and Range Province, USA), we are addressing the issue of earthquake-source capability. Our approach is to inventory maximum (or largest observed) historical and paleoseismic displacements on normal faults both regionally and globally. To date, we have identified in the literature earthquake displacements for 144 faults or fault sections in regions of Cordilleran extension in the interior western United States, including data from seven historical surface ruptures. Most prehistoric ruptures have been studied at only one or two locations and, consequently, the relation of observed to maximum displacement is uncertain. However, site-selection practices and preferential preservation of large scarps favor sampling of above-average displacements. We have found that, with a few potential exceptions, normal faults in the western United States have produced net coseismic vertical displacements no larger than about 6 m at a point. We note that the largest historical displacement (5.8 m in the 1915 Pleasant Valley, Nevada, earthquake) is essentially as large as any identified in the prehistoric record. Interestingly, faults with large maximum displacements (> 4 m) are twice as common (normalized to total number of faults) in the Rocky Mountains region, beyond the margin of classic Basin and Range physiography, than in the rest of the extensional province. Normal faulting in much of the Rocky Mountains is localized along, and has perhaps reactivated, parts of preexisting thrust faults. We speculate that the youthful, immature nature of most faults in this relatively unextended region promotes higher static-stress drops.

Keywords: paleoseismology



(S) - IASPEI - *International Association of Seismology and Physics of the Earth's Interior*

JSS005

Oral Presentation

1912

Scaling Relations of Segmented Strike-slip Surface Ruptures

Mr. Yasuo Awata

Active Fault Research Center Geological Survey of Japan, AIST IASPEI

Most of long surface ruptures composed of more than one segment and many of large earthquakes are multiple-rupture events. To understand and model the static earthquake source parameter, 16 strike-slip surface ruptures with lengths of 13-180km and maximum displacement up to 11.5m were segmented based mainly on geometry of fault strand and slip distribution, and supplementary on paleoseismicity and seismic rupture process. Then, the scaling relation of sizes of segmented surface rupture is analyzed. A surface rupture is composed of one to five segments with length of several to 48 km, and the number of segments (N_s) is linearly proportional with the total rupture length (L_t). A segment consists of a straight main section where displacement is large and continuous, and tail sections at both ends where displacement suddenly decreases and dies out. The size of tail section is proportional to the length of the segment. A segment is further divided into smaller segments by indistinct jogs and changes in slip distribution. These geometric similarity and nested array of smaller segments suggest the hierarchical self-similarity of fault structure. The maximum displacement of a segment (D_{sm}) is linearly proportional to the length of the segment (L_s), and the scaling relations is $D_{sm} (m) = 0.17 L_s (km)$. This relation suggests that the stress drop on individual segment is almost constant. In addition, the equation estimates that the world largest displacements of strike-slip surface rupture; ca.12-13 m occurred on a segment shorter than about 100 km? These scaling relations of segment can depicts the relations among M_o , L_t and W (fault width), which have been discussed since 1980s. The linear proportions between D_{sm} and L_s , and number of segments and L_t are consistent with the well-known scaling relations; M_o is proportional to L^{**2} for $W < L < 10W$, and L for $L > 10W$. The saturation of fault displacement in case of very-long surface rupture can be explained by the upper limit of segment size, which is probably governed by the thickness of seismogenic layer of the crust.

Keywords: fault segmentation, surface rupture, scaling relation



(S) - IASPEI - International Association of Seismology and Physics of the Earth's Interior

JSS005

Oral Presentation

1913

Empirical and Theoretical Fault Scaling Relations

Dr. Mark Leonard

Geoscience Australia Geohazards IASPEI

It has been widely observed that the rupture area of small earthquakes ($M_0 < 10^{21} \text{Nm}$ or $M < 8$) have aspect ratios > 4 . To account for this I suggest that all earthquakes where the aspect ratio is between 1 and 5 follow the power law relation $W \sim L^P$ (where W =width, L =length). This relation, with $P=0.67$ (0.6-0.7), applies to both dip slip and strike slip interplate earthquakes and intraplate earthquakes. Combining this relation with $M_0 = \mu D W L$ (where D = average displacement) gives a series of theoretical moment-area ($\log M_0 \sim C_1 \log A$) and moment-length ($\log M_0 \sim C_2 \log L$) relations which depend only on the relationship between D and L . Relations were developed for four displacement models: (1) $D \sim W = L^P$, (2) $D \sim \sqrt{A} = L^{(1+P)/2}$, (3) $D \sim L$, and (4) $D \sim L^{(2-P)}$. Model 1 has constant stress drop, model 2 preserves the $C_1 = 3/2$ relation and model 4 preserves the $C_2 = 3$ relation. By combining published data sets (e.g. Wells and Coppersmith (1994), Henry and Das (2001) and Romanowicz and Ruff (2002)) the relative merit of each of these relations is estimated by testing how well C_1 and C_2 fit the data. For interplate dip-slip earthquakes the preferred P is 0.67 for fault lengths ranging from 4 km to 1000 km and for intraplate dip-slip earthquake faults with length ranging from 2 to 40 km. Similarly $P = 0.67$ for interplate strike-slip earthquakes for fault lengths ranging from 4 to 40 km (above which they become width limited) The $\log M_0 \sim \log L$ and $M_0 \sim \log A$ data are consistent with models 1 & 2 but not with 3 & 4. The closest fitting model is 1, with $C_1 = 1.4$ & $C_2 = 2.33$, followed closely by 2, with $C_1 = 1.5$ & $C_2 = 2.5$. WC94 found $C_1 = 1.47(0.045)$ & $C_2 = 2.23(0.06)$. These theoretically and empirically consistent models have application to hazard and paleoseismic studies, rupture and ground motion modelling, and may have application for estimating maximum credible earthquakes in dip-slip tectonics.

Keywords: scaling, relations, faults



(S) - IASPEI - *International Association of Seismology and Physics of the Earth's Interior*

JSS005

Oral Presentation

1914

Seismic characterization of the Vilaria Fault in NE Portugal: Comparison between a segmentation model and paleoseismology

Dr. Thomas Rockwell

Geological Sciences San Diego State University

Chris Madden, Tim Dawson, Lewis Owen, Susan Villanova, Paula Figueiredo, Joo Fonseca

As part of a seismic hazard assessment for a new dam in NE Portugal, we studied the geomorphology and conducted paleoseismic trenching along the Vilaria fault in northeastern Portugal to explore the fault's late Quaternary rupture history. The Vilaria fault is a major, 250 km-long sinistral strike-slip structure orientated NNE to SSW. This fault has no historical seismicity for large earthquakes, although it may have generated a moderate (M5.8) earthquake in 1858 (Villanova, 2004). Evidence of continued left horizontal displacement is shown by the presence of Cenozoic pull-apart basins as well as late Quaternary stream deflections. We identified three major segments based on structural complexities, with the dam adjacent to the 75 km-long central segment. Based on an inferred rupture of this length, we would expect earthquakes of about M7.2 with about 1.6 m of average displacement using the Wells and Coppersmith (1994) regressions. Combined with the very sparse published inferences on the Quaternary slip rate, about 0.5 mm/yr (Cabral, 1989; 1995), we estimate a return period for such events of about 3000 years. To test this segmentation model and more directly determine the seismic hazard posed by the Vilaria fault, we excavated a number of trenches at three sites along the central segment. At one site at Vale Meo winery, we determined the occurrence of 2-3 events in the past 14-18 ka, suggesting a return period of 5-9 ka. In the same area, a small offset rill suggests 2.2 m of slip in the MRE. At another site along the Vilaria River alluvial plain, northeast of the Vale Meo site, we excavated several trenches in late Pleistocene and Holocene alluvium, and exposed the fault displacing channel deposits dated to between 18 and 32 ka. In a succession of closely-spaced parallel cuts and trenches, we traced the channel riser into and across the fault to resolve 9 m of cumulative slip, which yields a slip rate of 0.3-0.5 mm/yr, consistent with but a bit lower than earlier estimates. This displacement is also about four times that inferred from the deflected channel at Vale Meo, consistent with its older age. Combining the information of timing at Vale Meo winery and displacement at Vilaria argues for earthquakes in the M7.2-M7.4 range, similar to that inferred from the segmentation model, but suggests that the displacements are slightly larger and the return periods longer. It also demonstrates that there are potential seismic sources in Portugal that are not associated with the 1755 earthquake or the Tagus Valley and, although rare, large events on the Vilaria fault could be quite destructive for the region.

Keywords: vilarica, paleoseismology, portugal

(S) - IASPEI - *International Association of Seismology and Physics of the Earth's Interior*

JSS005

Oral Presentation

1915

A 15,000-Year-long synthetic earthquake catalogue for the Central Taupo Rift, New Zealand, derived from earthquake geology and historic data

Dr. Pilar Villamor

Hazards Group GNS Science, New Zealand IASPEI

Pilar Villamor, Kelvin Berryman, Terry Webb, Mark Stirling, Nicola Litchfield

For a section of the central Taupo Rift of North Island, we have characterized all fault sources and assigned earthquake magnitudes based on a new fault rupture scaling relation developed for this region (see Webb et al in this symposium). The new scaling model, with formal estimates of uncertainty, relates fault rupture length (based on earthquake duration) to seismic moment. This fault rupture scaling is appropriate for this region because it is derived from historic data within the Taupo Rift itself and satisfactorily replicates the observed historic surface fault parameters (e.g., the 1987 Edgcumbe Earthquake). Estimates of earthquake magnitudes are thus primarily based on fault length. However in the central Taupo Rift, because the fault pattern is very complex, with closely spaced faults that merge and bifurcate along strike, it is difficult to uniquely identify the fault traces that combine to form a single surface rupture. Also, data from paleoseismic trenches and historic events (the 1987 Edgcumbe Earthquake) indicate that single event displacement (SED) can be highly variable (<0.1 to 2.5 m) from event to event on an individual fault. SED variability suggests that a fault can rupture in different modes: primary versus secondary faulting (primary faulting contributes to earthquake hazard while secondary faulting does not); or primary segmented (representing small to moderate earthquake magnitude) versus primary unsegmented rupture (representing moderate to large earthquake magnitude). The fault scaling relation provides a basis for assigning typical SED values to fault length, and from this we can differentiate between primary and secondary faulting, and segmented versus unsegmented fault rupture. A synthetic earthquake catalogue has been developed from fault sources by assigning earthquake magnitude to faults, or parts of faults, consistent with SED values observed in fault trenches. Earthquake recurrence has either been observed directly in the fault trenches, or estimated from slip rate values obtained from geomorphic features divided by the derived SED values appropriate to the fault length. There are a few large independent faults with maximum lengths of ~ 30 km which are indicative of earthquakes of ~Mw 6.9. There are some apparently shorter faults that generate more frequent, smaller earthquakes. We have merged the paleoseismic with the historic record into a single catalogue. The field data are reasonably complete for the last 15,000 years, generating a long term frequency-magnitude relation for earthquakes with associated surface rupture. We find that within the considerable uncertainties involved in generating the catalogue the two datasets form a single Gutenberg-Richter distribution from Mw 4.0 to 6.9.

Keywords: fault scaling relation, taupo rift, synthetic catalogue

(S) - IASPEI - *International Association of Seismology and Physics of the Earth's Interior*

JSS005

Oral Presentation

1916

Derivation of New Zealand fault rupture scaling relations that reconcile seismological and geological data

Dr. Kelvin Berryman

Hazards Group GNS Science IASPEI

Terry Webb, Kelvin Berryman, Pilar Villamor, Mark Stirling, David Rhoades

Two factors have encouraged us to investigate a physically-based understanding of fault rupture scaling of large events. By large events we mean those that rupture the ground surface and are preserved in earthquake geology records. Firstly, recent literature indicates that large strike-slip earthquakes show a change in fault rupture scaling when the full seismogenic width is ruptured, and secondly, field observations of active faulting in do not fit with the often-used Wells & Coppersmith (1994) empirical regressions. In this study we have reviewed international literature regarding scaling relations for large earthquakes where the full seismogenic width is ruptured, and find that slope 2 is the most appropriate regression slope relating seismic moment ($\log M_0$) and fault rupture length ($\log L$) for two regions of New Zealand the normal faults of the Taupo Rift, and the low slip rate (< 5 mm/yr) or low total displacement, strike-slip, reverse and oblique faults, within the plate boundary deformation zone. We developed fault rupture scaling relations by using rupture duration in historic events (with well-determined moment magnitude) as a proxy for fault rupture length, and fault area by incorporating fault dip and information on seismogenic thickness. Average subsurface slip may then be derived from seismic moment, and we demonstrate how this relation, when modified to account for differences between subsurface and surface displacement, is in good agreement with earthquake geology observations. Recognising changes in fault rupture scaling when width-limited rupture is achieved is an important factor in fault rupture scaling in two quite different tectonic regions of , and we suggest this may also be true for all tectonic regions, worldwide.

Keywords: fault rupture scaling, width limited rupture, new zealand



(S) - IASPEI - *International Association of Seismology and Physics of the Earth's Interior*

JSS005

Oral Presentation

1917

Displacement-length scaling relations of normal faults and paleoearthquakes in the active Taupo Rift, NEW ZEALAND

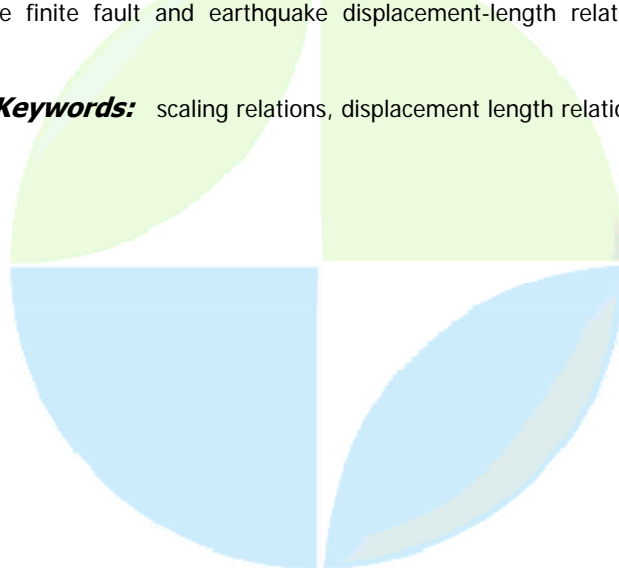
Prof. John Walsh

Fault Analysis Group, School of Geological Sciences University College Dublin IASPEI

A. Nicol

The relation between maximum displacement and length provides important information about the scaling properties of faults and earthquakes. Displacement-length plots typically reveal slopes of 1-1.5 for ancient fault systems and 1 for historical earthquakes. Active normal faults in the Taupo rift, however, have slopes of 0.5-0.7 for paleoearthquakes and faulted volcanic surfaces ranging up to ca. 60 ka in age. These low slopes are attributed to two principal factors: sampling bias and fault interaction/intersection. The bulk of our data are from a digital elevation model of displaced geomorphic surfaces with a vertical resolution of ~2 m. Displacements less than ~2 m are not routinely imaged in the model resulting in an under-sampling of small faults and a reduction in lengths of at least 100-200 m. Both of these sampling artefacts introduce a systematic under-sampling of low displacement-length faults particularly for those faults with lengths of <1 km, and therefore lead to a decrease in the slope of the displacement-length relation. Fault interaction and displacement transfer in the rift locally enhances the growth of short faults (e.g., <2 km) that are often immediately adjacent to, and at the terminations of, the larger faults. Although many of these short high-displacement faults may not be physically linked (i.e. hard-linked) with other structures, their displacements are transferred to adjacent faults by deformation of the intervening rock volume, a kinematic scenario referred to as soft-linkage. Whatever the nature of linkage between faults (i.e. hard- or soft-), complementary displacement transfer permits all faults to be components of a single kinematically coherent system, with faults therefore displaying interdependent, and complex, earthquake histories. The accentuated displacement transfer associated with fault interactions and intersections, nevertheless means that related faults are marked by higher than average displacement changes and by high displacement-length ratios, irrespective of time scale. Since the rift comprises many (>100) short interacting/intersecting faults they are together responsible for a decrease in the slope of the displacement-length relation. As extension continues to accrue across the rift, we suggest that such short faults are either temporally or permanently abandoned, or are incorporated into larger faults, scenarios which result in an increase in the slope of both the finite fault and earthquake displacement-length relations with fault system maturity.

Keywords: scaling relations, displacement length relation



(S) - IASPEI - *International Association of Seismology and Physics of the Earth's Interior*

JSS005

Oral Presentation

1918

Variable paleoearthquake recurrence intervals arising from fault interactions, Taupo Rift, New Zealand

Dr. Andy Nicol

Geohazards solution Section GNS Science

Paleoearthquakes at the Earth's surface often produce variable recurrence intervals on individual faults. The origin of these variations and the extent to which they result from systematic processes is unresolved. To address this question we analyse displacements of geomorphic surfaces and of tephra horizons in 29 trenches excavated across normal faults in the Taupo Rift. Each trench typically yields information on 3-6 paleoearthquakes that ruptured the surface over the last 16-23 kyr. Recurrence intervals on 25 faults, which are distributed across the 15 km wide rift and record ca. 30-40% of the total extension, were constrained by geochemical fingerprinting and radiocarbon dating of up to 12 stratigraphic layers. Recurrence intervals range from ca. <1 ka to 15 ka, with the variability for individual faults often reaching an order of magnitude. We find that much of the variability in recurrence intervals on individual faults reflects a temporal and spatial clustering of paleoearthquakes on timescales of 5-10 kyr. The timing of periods of earthquake clustering are typically different for individual faults which, together with the uniform rate of total extension across the rift during the last 60 kyr, suggests that fluctuations in recurrence intervals were not driven by changes in the rift boundary conditions. Instead, we propose that the variable recurrence intervals arise principally due to fault interaction, which is achieved by faults intersection and deformation of the rock volumes between faults that do not intersect. All faults in the rift are components of a single kinematically coherent system for which the earthquake histories of each fault are interdependent. The largest faults in the system exert the greatest influence on the location and timing of paleoearthquakes and appear to be capable of stimulating or retarding paleoseismicity on smaller faults.

Keywords: earthquake recurrence, fault interaction, taupo rift



(S) - IASPEI - *International Association of Seismology and Physics of the Earth's Interior*

JSS005

Poster presentation

1919

Paleoseismic features as indicators of earthquake hazards in Iran

Mrs. Mahsa Abd Etedal

Institute of Geophysics, Tehran, Iran Institute of Geophysics IASPEI

Giuseppe Delfino

This paper is intended to provide a perspective on the use of paleoseismological studies in the seismic hazard in Iran. Paleoseismology involves the geologic study of the past behavior of active faults. The evolution of paleoseismological studies in the past clearly demonstrates that in order to properly understand the seismic potential of a region, and to assess the associated hazards, it is necessary to take full advantage from the geological evidence of past earthquakes. The large amount of paleoseismological data collected in recent years shows that each earthquake source creates a signature on the geology and the geomorphology of an area that is unequivocally related with the order of magnitude of its earthquake potential. This signature is defined as the seismic landscape of the area. The scientific contribution of this approach refer to: confirmation of Holocene fault activity, slip-per-event and average slip rate of a given fault (or segment), seismic potential of known faults, fault segmentation, fault interaction as consequence of stress loading by stick-slip on contiguous faults, time-space distribution of seismic activity along a given tectonic feature, seismotectonic association of historical earthquakes and landscape evolution on the short term and its implications on the long-term evolution.

Keywords: paleoseismology, iran, slip



(S) - IASPEI - *International Association of Seismology and Physics of the Earth's Interior*

JSS005

Poster presentation

1920

Seismicity investigation of Shiraz Region with remote sensing and GIS

Mrs. Azam Nemati

tehran shomal university student IASPEI

Central Zagros is one of the well-defined seismoactive areas in IRAN. My study area is located in Folded Zagros and bonded by latitudes 27 N and 30 N and longitudes 51 E and 53E. At first seismic activity of this territory is studied by using Geological, Geomorphological and Seismological methods. On the available geology maps there are not any near trend between epicenters and active faults. This problem comes from Salted Hormoz layer, evaporated sediment that underlain and their plastic property. For solving this problem we use Remote Sensing Data such as ETM+ images, RADAR images that detect in scansar mode with 50m resolution and SRTM DEM. We merge panchromatic band with multispectral bands in ETM+ data and provide an image with 15m spatial resolution. For seismic data we use IIEES, USGS and Tehran geophysics institute catalogs. Using of remote sensing data is a relatively new technique that can be used to study deformation and identify lineaments. Multisensor remotely sensed, has a wide view angle and high spatial resolution are very useful for lineament analysis and neotectonic mapping in this area also a shaded relief Digital Elevation model (DEM) could be useful for the quantitative approach of activity of faults- segments (morphotectonic analysis, estimation of the displacement, erosion rate versus uplift rate, etc). We identify linear features by visual analysis from surface and morphotectonic evidence and some software filter (sharp edge, sun angle and etc). Finally the use of satellite images, earthquakes and GIS analysis show that these are very powerful tools for identification of blind faults and their characteristics.

Keywords: seismicity, shiraz, remotesensing



(S) - IASPEI - *International Association of Seismology and Physics of the Earth's Interior*

JSS005

Poster presentation

1921

Magnitude versus faults surface parameters: quantitative relationships from the Aegean Region.

Prof. Riccardo Caputo

Dept. Earth Sciences University of Ferrara IASPEI

Pavlidis S.

Historical and seismotectonic data from the broader Aegean Region have been collected and all possible information relative to ground deformation associated to earthquakes that hit the area have been re-evaluated. All events associated to co-seismic surface faulting have been selected and further investigated, while geomorphologic and geological criteria have been used to recognise and characterise the seismogenic faults associated to these morphogenic earthquakes (sensu Caputo, 1993). In particular, in order to perform seismic hazard analyses, we compiled a list of all earthquakes where the surface rupture length (SRL), the maximum vertical displacement (MVD) or the average displacement (AD) is available. We thus obtained reliable values of these source parameters for 36 earthquakes, of which 26 occurred during the 20th century, 6 in the 19th century and the three remaining earlier. Magnitude versus SRL and MVD have been compiled for estimating empirical relationships. The calculated regression equations are: $M_s = 0.90\log(\text{SRL}) + 5.48$ and $M_s = 0.59\log(\text{MVD}) + 6.75$, showing good correlation coefficients equal to 0.84 and 0.82, respectively. Co-seismic fault rupture lengths and especially maximum displacements in the Aegean Region have systematically lower values than the same parameters world-wide, but are similar to those of the Eastern Mediterranean-Middle East region. The envelopes of our diagrams are also calculated and discussed for estimating the worst-case scenario. Furthermore, for all investigated seismogenic structures, based on several geological criteria, we measured the 'geological' fault length (GFL), representing the total length of the neotectonic faults showing cumulative recent activity, and compared SRL with GFL. Eventually, from the distribution of GFL versus magnitude we also infer an important geological threshold for the occurrence of morphogenic earthquakes at about 5.5 degrees.

Keywords: seismic hazard, morphogenic earthquakes, seismotectonics



(S) - IASPEI - *International Association of Seismology and Physics of the Earth's Interior*

JSS005

Poster presentation

1922

Reconciling neotectonic and seismic recurrence rates in SW Australia

Dr. Mark Leonard

Geoscience Australia Geohazards IASPEI

Dan Clark

The southwest corner of Western Australia is an area of stable continental crust (SCC) with the geology being Proterozoic and the area undergoing no tectonic activity in the last 40Ma. However in the last 50 years it has had the highest level of seismicity of any area of worldwide SCC. It has not been glaciated in the last 20Ma and has had a cool dry climate for at least the 200ka, thus providing an ideal environment to preserve fault scarps. The availability of high resolution digital elevation model data (DEM) in this area has led to the identification of over 50 new features that are thought to be scarps of surface rupturing earthquakes (Clark 2006 & Clark and Leonard 2007). Half of these scarps have been the subject of field work and all are thought to be fault scarps. One feature has been trenched and the presence of a fault scarp verified (Estrada et al. 2006). Using recently developed fault scaling relations (Leonard 2007) the fault length and displacement are used to estimate magnitude and in some cases identifying multiple events, these scarps have been used to generate a neotectonic earthquake catalogue. Between M6.5 & 7.2 the Log N vs Mag plot of the data has a slope of 1, indicating that the neotectonic derived catalogue is complete above M6.4. Below M6.4 the number of earthquakes rapidly decreases, with 20% of the expected number of M6.2 earthquakes and 3% of M6.0 earthquakes being identified via neotectonic methods. This is likely a combination of the lower likelihood of the earthquakes causing a surface rupture and the smaller rupture more rapidly reducing in size to below the detection threshold. Scarps formed by earthquakes of $\geq M7.3$ appear over represented with M7.4-7.5 earthquakes being overrepresented by a factor of perhaps 3-6. This could be explained by the longer preservation age of these large scarps. The three key results of this study are: 1. Under the right geological and climatological conditions fault scarps from $\geq M6.5$ earthquakes can be preserved for 100ka or more and scarps from $>M7.3$ earthquakes for perhaps $>150ka$. With approximately 50% of M6.3 and 100% $>M6.4$ earthquakes in SCC are expected to form scarps. 2. M_{max} in stable continental crust is more likely to be M7.3-7.5 than the M7.0-7.2 generally used in hazard studies. 3. The recurrence rate for this neotectonic catalogue and historical earthquakes in the whole SCC of Australia are similar. However the contemporary level of seismicity in this area is an order of magnitude higher than that needed to generate the scarps. This supports the hypothesis that seismicity in SCC is episodic and migrates on time frames of 1-10ka.

Keywords: paleoseismicity, recurrence, earthquake

(S) - IASPEI - *International Association of Seismology and Physics of the Earth's Interior*

JSS005

Poster presentation

1923

Scaling source dimension of the Mw 6.7 JUNE 5, 1688 Sannio southern-Apennines earthquake, using geophysical, geological and morphometrical data

Dr. Rosa Nappi
INGV OV IASPEI

Alessio Giuliana, Bellucci Sessa Eliana, Vilardo Giuseppe, Pierfrancesco Burrato

The identification of the seismogenetic source of the Mw = 6.7, 1688 Sannio normal faulting earthquake is still a subject of scientific debate. This is due to several reasons comprising a) the possible incompleteness of the damage pattern, b) the difficult or not straightforward recognition of the induced surface deformation, c) the probable occurrence of blind or hidden faulting, and d) the low tectonic deformation rates and youthfulness of the source. According to the magnitude scaled with Wells and Coppersmiths relationships the earthquake ruptured a 30 km-long, 16 km-wide normal fault. However, published works propose seismogenetic sources for this earthquake slightly smaller than the expected from the empirical relationships alone. Similar results were obtained for other large historical events in central-southern Apennines. This may reflect either a routinely overestimation of the magnitude of earthquakes listed in the historical catalogue, or an underestimation of the geologically determined seismogenetic sources. The goal of this paper is to collect original information for identifying the seismogenetic source of the 1688 earthquake, making use of seismological, geological and morphometrical data. In particular, the seismological data used in this study are relative both to the historical and recent seismic activity in the Sannio area, which in instrumental times was characterized by low energy seismic sequences (1990-92 and 1997, Md = 4.1). As regards the morphometrical analysis, we studied the Tammaro basin area (Sannio, Southern Apennines) for identifying the long term surface deformation induced by the seismogenetic fault of the 1688 earthquake. The reason of our choice is due to a) the hypothesis of the 1688 source location inside this basin, suggested by the seismogenetic source database DISS v. 3.1, b) the presence along the Tammaro river of young geomorphological features useful for revealing tectonic surface deformation, and c) clustering of recent seismic events inside this area along hypothetical boundaries of the master fault. Our analysis has been carried out by integrating the morphometrical data derived by processing of a very high resolution DTM (5x5 m pixel), with the geological and geomorphological data derived from photo-interpretation and field surveys in a GIS environment. The preliminary results have provided the following conclusions: a) the topographical parameters extracted from DTM show significant NW-SE lineaments on the right hand side of the valley of the Tammaro river; this evidence is further constrained by morphological analyses carried out both from orthophoto and from field surveys, that confirm the presence of a structural mountainside corresponding to the above lineaments; b) the low energy sequences, which were progressively activated, do not coincide with the main structural lineaments exposed at surface, but highlight the activity of buried structures likely acting as segment-boundaries and constraining the dimension of the 1688 seismogenetic source.

Keywords: 1688 earthquake

(S) - IASPEI - *International Association of Seismology and Physics of the Earth's Interior*

JSS006

1924 - 1951

Symposium

Non-instrumental seismometry - New Approaches to Paleoseismology and Earthquake Recurrence in the 21st Century

Convener : Dr. David Schwartz, Dr. Gianluca Valensise

Co-Convener : Dr. Daniela Pantosti, Dr. Eullia Masana, Dr. Francisco Gutierrez

For the General scopes see introduction to symposium JSS004. Paleoseismology is now a well-established discipline whose major goal is the identification and dating of past earthquakes in the geological record. It provides the fundamental data for developing an understanding of the behavior of seismogenic faults in time and space and the primary recurrence information for seismic hazard assessment. Paleoseismology has evolved during the past 30 years and is now practiced worldwide. As the field moves into the 21st century there is recognition of the need to: develop longer earthquake chronologies, reduce uncertainties in recurrence times, and develop better knowledge of earthquake recurrence on sources that do not easily lend themselves to traditional paleoseismic analysis (trenching). We invite contributions on topics that include NEW: -statistical analyses of paleoseismic recurrence data, particularly for correlating the occurrence of past events along faults ; -approaches to identify paleoearthquakes on blind or remote (ie, subduction zone) earthquake sources and in logistically difficult settings such as urban environments; -technologies that increase the length of the paleoseismic record and paleoearthquake chronologies at investigation sites on major faults; -dating techniques of paleoearthquakes; -approaches to quantify slip in paleoearthquakes for better estimates of paleo-earthquake magnitudes

XXIV 2007

PERUGIA

I T A L Y



(S) - IASPEI - *International Association of Seismology and Physics of the Earth's Interior*

JSS006

Oral Presentation

1924

Paleoliquefaction features as a tool for paleoseismic studies of blind and offshore located faults: preliminary field search in Algeria

Dr. Bouhadad Youcef

seismic hazard department Earthquake engineering center (Algeria) IASPEI

The tellian Atlas chain of Algeria belongs to the African-Eurasian tectonic plates boundary compressive belt where earthquakes are not randomly distributed but may be easily correlated with geological structures. The tectonic style is represented, mainly, by thrust faults which may be blind located offshore and/or onshore. Recent strong earthquakes of El-Asnam, 1980 ($M_s=7.3$) and Boumerdes, 2003 ($M_w=6.8$) induced extensive liquefaction features in the epicentral areas. Preliminary field search indicates that paleoliquefaction features may be found in these areas. Therefore, it may constitute a precious geological tool for paleoseismic studies knowing that either in the case of blind faults or offshore located faults trace of faulting is inaccessible.

Keywords: paleoliquefaction blind fault



(S) - IASPEI - *International Association of Seismology and Physics of the Earth's Interior*

JSS006

Oral Presentation

1925

Beyond marine terraces: investigating Holocene coastal uplift using transgressive marine sediments and fluvio-tectonic terraces at the Pakarae River mouth, North Island, New Zealand.

Dr. Kate Wilson

Geohazards Solutions GNS Science IASPEI

Kelvin Berryman, Nicola Litchfield, Ursula Cochran, Tim Little

This study describes two new techniques used to extend the paleoseismic record and constrain the geometry of an active offshore fault at the Pakarae River mouth locality, East Coast, North Island, New Zealand. Seven marine terraces dating back to 7 ka have previously been used to estimate the magnitude and frequency of coastal uplift events at Pakarae, the site of highest uplift (3.2 mm yr⁻¹) along the Hikurangi margin. To attain a longer record and to verify the sudden, coseismic nature of uplift events, a method of using the fluvio-estuarine sedimentary sequence underlying the highest marine terrace was developed. We compared the paleoenvironmental facies architecture of the uplifted fluvio-estuarine sequence with typical incised valley sequences deposited on stable coastlines. Two sharp estuarine-to-fluvial transitions dated at 9 ka and 8.5 ka indicate rapid sea level regressions. Their occurrence during a period of eustatic sea level rise suggests coseismic uplift events caused temporary estuary abandonment. A further uplift event between 8.5 and 7.35 ka is inferred from the significant difference between the amount of sediment preserved from this period and the predicted sediment thickness according to the eustatic sea level curve. This technique enables us to extend the record of coastal uplift events back to 10 ka and overcome the limitation of marine terraces, which only record uplift since eustatic SL stabilisation. The second technique uses fluvial terraces that appear to grade to the marine terraces and thus are also interpreted to be coseismic. A longitudinal profile shows these terraces fan out downstream and thus their distribution defines the upstream limit of uplift. These data, coupled with along-coast correlations with marine terraces at Puatai Beach and Waihou Bay (9 and 15 km northward), provide constraints on the geometry of uplift. Forward-elastic dislocation modelling indicates the fault is likely to be a steeply northwest-dipping reverse fault lying close to the shoreline; there is possibly involvement of plate interface slip. Techniques such as these are vital for understanding seismic hazard of subduction zones such as the Hikurangi margin. With no historical large subduction interface earthquakes, investigations along the coastline need to be able to distinguish upper plate faulting effects, if we are to isolate plate interface events. Furthermore, the methods described here contribute to defining an offshore fault that is too close to the coast for marine geophysical investigation.

Keywords: terraces, subduction, geomorphology

(S) - IASPEI - International Association of Seismology and Physics of the Earth's Interior

JSS006

Oral Presentation

1926

Earthquake clustering along major continental faults: the influence of strain pattern and geometrical complexities on rupture propagation

Prof. Mustapha Meghraoui
IASPEI IASPEI IASPEI

The temporal clustering of large earthquakes is a salient characteristic of major continental faults in active zones. Decisive examples are large earthquake clusters along the East Anatolian fault (1820 1905), the North Anatolian fault (1912 1999), the Dead Sea fault (1137 1293), the southern San Andreas fault (1502 1680), the Kunlun Fault (1937 2001), the Tien Shan fault system (1885 1992) and Bulnay-Bogd fault system (1905 1957). Recent projects and faulting studies with paleoseismic investigations along the Dead Sea Fault (DSF), the East Anatolian Fault (EAF) and the North Anatolian Fault (NAF) provided a wealth of field data and results on the physical characteristics of earthquake ruptures. Using individual and cumulative slip, and the rich historical seismicity catalogue and archeoseismic investigations along fault strike, I examine the length of earthquake ruptures and timing of past earthquakes. The detailed mapping of rupture zones showing structural restraining bends, releasing step-overs, patch and segment boundaries, and slip distribution along strike illustrate their geometrical complexities. I observe that the long-term behaviour of fault segments and/or patches determines the occurrence of seismic sequences and the location of seismic gaps. In most cases, the clustering of large earthquakes migrate along fault segments and show off sequence seismic events. The mechanical coupling between off sequence distant earthquakes and laterally propagating ruptures depend mostly on the stress change at fault discontinuities and related block tectonics. The temporal clustering and multi-segment earthquakes ruptures in the past with coupling between step-overs and stress change suggests the size and probable length of future large earthquakes along major continental faults.

Keywords: earthquake, faulting, clustering



(S) - IASPEI - *International Association of Seismology and Physics of the Earth's Interior*

JSS006

Oral Presentation

1927

Archeoseismic and paleoseismic records of Baelo Claudia (Gibraltar Arc area, southern Spain)

Prof. Klaus Reicherter

Neotectonics and Natural Hazards RWTH Aachen University

Pablo G. Silva, Teresa Bardaj, Javiten Lario, Christoph Grtzner, Marcel Peltzer, Peter Becker-Heidmann

The western Betic Cordilleras have experienced several moderate and partly strong earthquakes and earthquake-related hazards (landslides and tsunamis) during the last 2000 years. The ruins of the Roman village of Baelo Claudia (Tarifa) yield evidence for the first historic earthquake damage on the Iberian Peninsula. Roman settlement started in the II Cent. BC, last relicts are from the V-IV Cent. AD. We have found indications for two earthquakes, which destroyed Baelo. During the I. Cent. AD, probably an earthquake occurred, the village was restored and rebuilt (40-60 AD; Silva et al., 2005). Ground Penetrating Radar and geo-electrical studies were carried out in the ruins, across fault zones to map and mirror fossilized and active faults. Although kinematic indicators in the ruins of Baelo Claudia are often badly preserved, we encountered in several buildings typical evidence for coseismic deformation, i.e. high-energy events, e.g. shock-induced break-outs in the pavement, pull-ups, and joints in the flagstones of the Decumanus Maximus. Orientation of these indicators is systematic, pointing to a shock from the SW, and folding in NW-SE direction. The Isis temple area is partly excavated. Drums of fallen columns, wall and pillar collapses are directed in S to SW direction, and testify to coseismic building deformation. A crude stratigraphy based on Roman pottery allows us to date the collapse event in the IV. Century AD. The amphitheatre of the I. Cent. AD suffered not only earthquake and/or landsliding deformation, but also a lot of restoration. Open cracks in the walls and inclined walls are interpreted as generated by slow deformation. On the other hand, big fallen blocks of the tiers are attributed to coseismic damage. The eastern aqueduct outside the city walls crosses a little creek. The western part of the aqueduct collapsed downhill, and some of the arcs show rotational displacement around a horizontal axis, this might be interpreted as a slow deformational feature originating probably from small creek-parallel landslides. The city wall surrounds the village, and was built for representative and not defensive purposes. The walls are inclined up to 10 with varying directions. Keystones of arcs are subsided due to extension. The walls are partly displaced up to 17 cm, and/or rotated against each other. During the excavation older rests of a former city wall has been encountered, this wall is topped by a "demolition horizon" with big blocks of wall boulders. This horizon may correspond to the 40-60 AD earthquake outlined by Silva et al. (2005). Silva, P.G. et al., 2005. *Archeoseismic Record at the ancient Roman city of Baelo Claudia (Cdiz, South Spain)*. *Tectonophysics* 408: 129-146. Acknowledgements This work has been supported by the Spanish-German Acciones Integradas Program HA2004-0098. The authors are grateful to the Director of the Archeological Site of Baelo Claudia, Angel Muoz Vicente for facilitating the work.

Keywords: archeoseismology, paleoseismology, roman remains

(S) - IASPEI - *International Association of Seismology and Physics of the Earth's Interior*

JSS006

Oral Presentation

1928

**Active faulting and holocene paleoseismic record offshore Portugal,
Southwest Iberian Margin**

Dr. Eulalia Gracia

Unitat de Tecnologia Marina CSIC - Barcelona IASPEI

Alexis Vizcaino, Rafael Bartolom, Alessandra Asioli, Carlota Escutia, Jordi Garcia Orellana, Pedro Terrinha, Antonio Villaseor, Susana Diez, Sara Martinez, Juanjo Daobeitia

Crustal deformation in the southwestern margin of the Iberian Peninsula is controlled by the NW-SE convergence of the African and Eurasian Plates (4.5-5.6 mm/yr) at the eastern end of the Azores-Gibraltar zone. This convergence is accommodated through a wide deformation zone characterized by moderate magnitude seismicity although great earthquakes ($M_w > 8$), such as the 1755 Lisbon Earthquake and Tsunami and the 1969 Horseshoe Earthquake, have also occurred in the region. A multidisciplinary geological and geophysical dataset acquired during the last 10 years in the course of successive marine surveys revealed a number of active NE-SW trending west-verging thrusts (e.g. Marques de Pombal, Sao Vicente, and Horseshoe faults) and WNW-ESE strike-slip faults located offshore southern . The recognition of deformed Quaternary units together with swarms of shallow seismicity associated with surface ruptures suggest that faults located beneath these ruptures are active. For instance, a detailed swath-bathymetry data together with new high-resolution multichannel seismic profiles crossing the external part of the Gulf of Cadiz evidence a 150 km long WNW-ESE dextral strike-slip fault reaching up to the seafloor. This newly mapped structure may be a plausible candidate for the 1969 Earthquake ($M_w 8.0$) which epicentre is located few km away in the Horseshoe Abyssal Plain agreeing with the calculated fault plane solution. Associated to the active faults, mass transport deposits and submarine landslides are commonplace. Textural, mineralogical and geochemical analyses of marine sediments collected in the area in eight different sites stretching from the Tagus to the Horseshoe Abyssal Plains revealed the presence of numerous turbidite intervals. Although a number of mechanisms may be suggested to account for turbidite triggering, in the case of the SW Iberian Margin, earthquakes are the most likely explanation for synchronous, widely-spaced distribution of turbidites during the Holocene, when sea level was relatively stable. A total of 9 widespread turbidite events have been recognized for the Holocene. Precise dating of the two recentmost events (E1 and E2) based on ^{210}Pb and ^{137}Cs geochronology provides ages of 1971 \pm 3 AD and 1908 \pm 8 AD, respectively. These ages correspond to high-magnitude historical and instrumental earthquakes that occurred in the region: the 1969 Horseshoe Earthquake ($M_w 8.0$) and the 1909 Benavente Earthquake ($M_w 6.0$). The following 14C calibrated ages of turbidite events (E3 to E5) correlate with important historical earthquakes and paleotsunami deposits from the Gulf of Cadiz area, such as AD 1755, BC 218, and 5200 BP. Considering also the deepest events (E6 to E9) ranging from 7000 BP to 10400 BP we obtain a recurrence interval of about 1500 yr for the Holocene. Such a good correlation between turbidites and instrumental and historical seismic events suggests that the turbidite record can be used as a paleoseismic indicator in a low-convergence rate margin, constituting a valuable tool for assessment of earthquake and tsunami hazard along the coasts of the Iberian Peninsula and North Africa.

Keywords: marine paleoseismology, seismogenic faults, turbidite

(S) - IASPEI - *International Association of Seismology and Physics of the Earth's Interior*

JSS006

Oral Presentation

1929

Estimation of an upper limit on prehistoric peak ground acceleration using the parameters of intact speleothems in Hungarian caves

Dr. Katalin Gribovszki

Geodetic and Geophysical Research Institute Hungarian Academy of Sciences

Gy. Szeidovitz, G. Suranyi, Z. Bus, Sz. Leel-Ossy

The examination of speleothems in the Hajno'czy and Baradla caves (northeastern Hungary) allows estimating an upper limit for horizontal peak ground acceleration generated by paleoearthquakes. The density, the Young's modulus and the tensile failure stress of the samples originating from a broken speleothem have been measured in laboratory, while the natural frequency of speleothems was determined by in situ observations. The value of horizontal ground acceleration resulting in failure, the natural frequency and the inner friction coefficient of speleothems was assessed by theoretical calculations. The ages of the samples taken from a stalagmite of 5.1 m high (Baradla cave) at different heights has been determined by ICP-MS analysis and alpha spectrometry. According to our result the speleothem were not excited by a horizontal acceleration higher than 0.05 g during the last 60-70 000 years. This acceleration level is lower than the PGA value determined in previous seismic hazard assessment studies for a much shorter period of time.

Keywords: speleothem, prehistoric earthquake, pga

PERUGIA
ITALY



(S) - IASPEI - *International Association of Seismology and Physics of the Earth's Interior*

JSS006

Oral Presentation

1930

Magnetic fabric of earthquake-triggered structures

Dr. Shmuel Marco

Geophysics and Planetary Sciences Tel Aviv University IASPEI

The microscopic fabric of clastic sediments reflect their transport, deposition, and deformation history. We characterize the fabric of clastic dikes and seismite layers by measuring the anisotropy of magnetic susceptibility (AMS). We assume that different sources of dike fill have different microfabrics, which manifest in different magnetic fabrics. We studied over 250 Holocene clastic dikes, exposed by deep fluvial incision into the lacustrine 70-15 ka Lisan Formation in the Dead Sea basin. Typically, they are vertical, up to 30-40 m high, and up to 0.4 m thick. In map view they appear in a radial arrangement spanning a sector of 60 degrees with projected strikes that converge at a structural dome above a rising salt diapir. Field relations and AMS analyses show that 'passive' dikes filled from above have vertical K_{min} directions, compatible with sedimentary features. Conversely, horizontal to sub-horizontal K_{min} directions occur in dikes that show segmentation typical of horizontal propagation of the fractures and lateral material transport. Vertical zoning of the clay and silt symmetric about the center of the dikes is regarded as evidence of multiple injection events. We conclude that the upward indentation of a salt diapir induced a local stress perturbation, which triggered the formation of a radial set of fractures. Subsequently the fractures were filled by horizontal injection of fine clastics pressurized by earthquake vibrations. Sedimentation from above occurred where the tops of the dikes reached the surface and remained open.

Keywords: earthquakes, magnetic susceptibility, clastic dikes



(S) - IASPEI - International Association of Seismology and Physics of the Earth's Interior

JSS006

Oral Presentation

1931

Latent bias in temporal constraints of paleoseismic events in coastal plains: an example from the Shonai-Heiya-Toen Fault in Northeast Japan

Dr. Shinji Toda

Active Fault Research Center Geological Survey of Japan, AIST

Temporal parameters of paleoseismicity to calculate earthquake probabilities on active faults are commonly influenced by the preservation of datable sediments. The recent rapid accumulation of paleoseismic data in Japan reminds us that paleo-earthquakes recorded in sediments are mostly incomplete despite numerous excavations. We are aware of the limitations of geological method on the faults particularly in coastal plains where sea level change directly controls the local sedimentation and erosion during the datable time range of the radiocarbon analysis (in the past 50ka). Here we first present a typical example of temporal bias of datable sedimentary units from the Shonai-heiya-toen fault in northern Honshu, Japan, which mostly lacks sedimentary units in the period between 15 25 ka. We then argue how temporal bias of the analyzed radiocarbon ages yielded from trench walls affects estimates of average recurrence time. To evaluate such latent bias of preservation of paleoseismicity, we not only examined the actual detail geological data themselves but also performed Monte Carlo simulations using both synthetic earthquakes and observed radiocarbon ages. We computed the following procedures: 1) Repeating earthquakes on a fault are synthetically produced by log-normal probability density function with predetermined recurrence time (T_{rs}) and coefficient of variation 0.5. 2) Several radiocarbon samples (changeable parameter) are picked up from the actual C14 data recovered from the Shonai-Heiya-toen fault. 3) Using the picked-up radiocarbon samples, some of the synthetic earthquakes is constrained by sandwiching two ages. 4) If the number of the paleoseismic events determined is more than one event, we calculate the average recurrence time (T_{ro}) during the recent 10,000-yr and 50,000-yr periods. 5) We iterate 1-4 procedures 1000 times and make a histogram of the estimated average recurrence times. We then compare the mean recurrence time (T_{rom}) from numerous T_{ro} with the synthesized recurrence time (T_{rs}). As the results of the simulations, ten random C14 sampling from a trench leads to estimate the recurrence time twice as long as the real one for the 50ka case. Even we increase the number of samples up to 30, we still overestimate the recurrence time, in other words $T_{rom} > T_{rs}$. It clearly attributes to several missing events originated from the deficiency of sediments or possible erosion in the last glacial climax (MIS 2) due to sea level regression. For the 10ka case, we tend to overestimate T_{rom} for $T_{rs} < 3000$ yr together with C14 samples fewer than ~20. In contrast, we underestimate T_{rom} for $T_{rs} > 5000$ yr even increasing the number of samples. We speculate that 10,000-yr time window tricks us that it befalls the shorter intervals produced by the combination of $T_{rs} > 5000$ yr and coefficient of variation 0.5.

Keywords: paleoseismicity, recurrence time, earthquake probability

(S) - IASPEI - *International Association of Seismology and Physics of the Earth's Interior*

JSS006

Oral Presentation

1932

Record of Surface Ruptures on the San Jacinto Fault at Hog Lake, Southern California, Implications for Patterns of Recurrence From a 16 Event 3800 Year Record

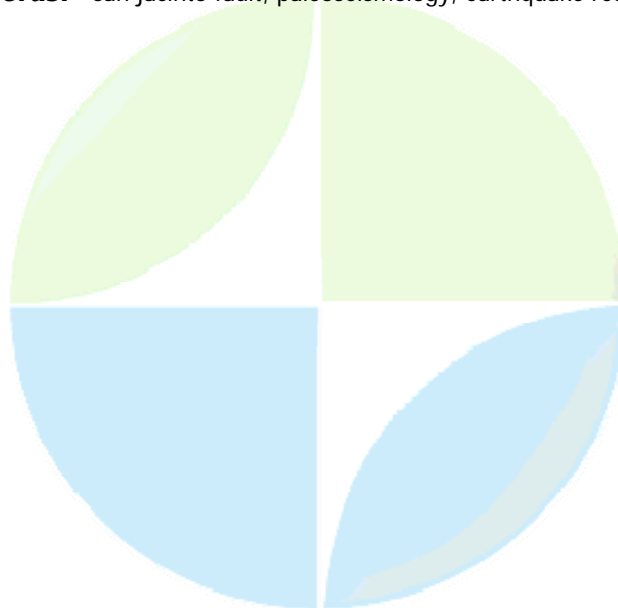
Dr. Thomas Rockwell

Geological Sciences San Diego State University

Gordon Seitz, Tim Dawson, Jeri Van Horn, Tim Middleton

Paleoseismic excavations at the Hog Lake site along the central San Jacinto fault near Anza have yielded one of the longest continuous records of earthquakes on the planet, with at least 16 events in the past 3.8 ka, yielding a long-term recurrence interval of about 240 years. The most recent event is likely the November, 1800 earthquake based on radiocarbon dating and historical damage records, so the fault may be nearing failure. The penultimate event is ca 1570, consistent with the long-term inferred RI. However, interestingly, there was a flurry of five surface ruptures between about AD 1000 and 1410 during which the southern San Andreas fault was relatively quiet (at Wrightwood), leading to an interval RI of less than 100 years. In contrast, we see evidence for only two events at Anza between about AD 250 and 1000 (RI = ~400 years), during which the SAF at Wrightwood experienced a flurry of at least seven events (between AD 500 and 1000). These observations suggest that the fault mode switches between quasi-periodic and clustered behavior, possibly influenced by ruptures on the San Andreas fault. Mapping of the surface slip associated with the past two events based on offset channels suggests about 3-4 m of slip per event in the Anza area. The slip distribution defined by 350 measurements of over 200 separate channels suggests rupture of the entire Clark fault from Hemet to Clark Valley, a distance of about 115 km. Using 3.5 m for the average slip event combined with the average long-term recurrence interval of 240 years, we calculate a slip rate of about 15 mm/yr, consistent with geodetic observations. Our observations suggest that the San Jacinto and San Andreas faults may trade off in slip accommodation in southern California for periods of up to a half millennium or more. Further, it is clear from these records that average return times based on only a few events may lead to substantial errors in estimation of hazard.

Keywords: san jacinto fault, paleoseismology, earthquake recurrence



(S) - IASPEI - International Association of Seismology and Physics of the Earth's Interior

JSS006

Oral Presentation

1933

A New Approach to Paleoseismic Event Correlation -

Dr. Glenn Biasi

Seismological Laboratory University of Nevada Reno

Ray J. Weldon

When there is more than one paleoseismic site on a fault, the issue arises of correlating events between them. As the number of paleoseismic sites increases, the number of possible correlations and combinations among them becomes unmanageable. Correlation based on dating evidence alone remains uncertain even with high quality radiocarbon evidence. These realities seriously complicate the use of paleoseismic data for estimation of recurrence intervals and seismic hazard. We present a new approach that permits estimates of seismic hazard and multiple-site earthquake recurrence without having to solve the correlation problem per se. The most important input data for our approach are reasonably complete paleoseismic records and approximate dates for the events. To begin we develop a complete list of all possible single and multiple-site ruptures allowed within the event dating uncertainties. Each individual paleoseismic event is counted as a rupture. We compare each event with the neighboring site chronology, and make another rupture of any which overlap with the first. If two overlap in time, both become new ruptures. Each rupture is extended in turn to a third site chronology to make new rupture(s). Lack of dating overlap keeps this process from expanding as the outer product of the number of events. Ruptures are also extended through sites with no evidence of the rupture, but penalized for contradicting the paleoseismic record there. The pool of all possible ruptures thus includes all the available event data for the fault. Paleoseismic displacement estimates or displacements drawn from an average displacement model are used to extrapolate ruptures beyond the outside sites in each rupture. Rupture length is used with regression relations to assign each rupture an average displacement and simple displacement profile. To constrain the rupture history of the fault we construct rupture scenarios by drawing from the pool of all possible ruptures. Sampling is constrained so that every event is included each scenario exactly once. The scenario becomes a possible rupture history for the fault at some level of probability. A large suite of scenarios is developed in this manner. To extract likely scenarios from the suite, scenarios are graded for consistency with dating evidence (do dates overlap strongly or weakly?) and by comparing the displacement totaled over the ruptures at any given point on the fault with the total predicted independently from the geodetic or geologic slip rate and elapsed time since the oldest event. Other grading criteria may also be applied, such as by using per-event displacement measurements. Ensembles of scenarios become more or less likely actual histories of the fault. They may then be used directly in seismic hazard assessment using ground motion prediction methods, or indirectly to estimate the likely fractions of shorter or longer ruptures, frequency of multiple segment ruptures, etc. We illustrate the method with paleoseismic data from the southern San Andreas fault in California. Results have been provided as inputs to the most recent assessments of the Working Group on California Earthquake Probabilities.

Keywords: paleoseismology, seismic hazard, san andreas fault

(S) - IASPEI - *International Association of Seismology and Physics of the Earth's Interior*

JSS006

Oral Presentation

1934

The seismic potential of a silent and slow moving fault: the Carboneras fault (Eastern Betic Shear Zone, southern Spain)

Dr. Eullia Masana

Ximena Moreno, Eullia Grcia, Pere Santanach, Hector Perea, Joao Cabral, Patricia Ruano, Oriol Piqu, Raimon Palls

Africa and Iberia converge at a very slow rate (4.5 to 5.6 mm/yr) through a diffuse collisional plate boundary. The seismicity is low to moderate and widespread over a very wide area suggesting a number of slow moving faults. Because of this, many of the seismogenic faults in Iberia have not yet generated a large historical earthquake and remain may hidden. We aim to detect these and characterise their seismic potential. The seismogenic behaviour of the Alhama de Murcia fault has yet been evidenced by previous paleoseismic studies. This fault belongs to the Eastern Betic Shear Zone (EBSZ), composed by several left-lateral and reverse faults that crop out from Alicante to the north down to Almeria to the south (at both tips the system is entering the Mediterranean). The morphological signature of the faults composing the EBSZ is similar to that of the Alhama de Murcia suggesting than the rest of the faults may also be active and possibly seismogenic. The Carboneras fault, the aim of this study, is the southernmost fault of the system. It shows very few instrumental earthquakes but its morphological expression indicates recent left-lateral slip. After a geomorphological study, based on aerial photograph analysis and field work, the northwestern side of La Serrata range was selected, as the most suitable area for a detailed paleoseismological study. We present the first paleoseismological results at the El Hacho site, to the south of La Serrata range. Microtopography, GPR, Electric tomography, and a detailed geomorphological analysis were used to select the best sites to trench and to understand the recent behaviour of the fault. Four trenches across the fault and a 3D trench where analysed. Evidence of a minimum of four reverse component paleoearthquakes where interpreted based on sealed fault branches and colluvial wedges. TL, U/Th and radiocarbon dating indicated that the four events have taken place since 55 ka BP and previous to 1180 yr BP. This suggests a mean recurrence time of 14 ka and a very short elapsed time. Marine studies (swath-bathymetry, TOPAS, high-resolution MCS, magnetic, gravity and core sampling) are also in course and will be integrated to the onshore data to obtain a complete image of the behaviour of the fault. The offshore change in strike of fault was interpreted as a possible segment boundary. Down to this boundary, the maximum magnitude that the Carboneras fault could generate is Mw 7.2 although no evidence is found about the effectiveness of the mentioned segment boundary. The paleoseismic results will contribute to obtain more realistic values of the seismic hazard of this highly populated area. The methodological results are also of interest in the Iberian Peninsula where we suppose that many seismogenic faults are historically silent and at the same time they enter the sea and need to be studied integrating onshore-offshore data.

Keywords: eastern betic shear zone, carboneras fault, slow moving faults

(S) - IASPEI - *International Association of Seismology and Physics of the Earth's Interior*

JSS006

Oral Presentation

1935

Statistical approaches to earthquake recurrence in novel off-fault paleoseismic archives

Prof. Amotz Agnon
AGU IASPEI

Off-fault archives extend records of large earthquakes to 300 ka. Statistics are required in the interpretation of such records. Three statistical approaches have been used in the validation and interpretation of such records: (1) temporal correlation between arguably equivalent archives with precise dates; (2) temporal correlation between dense and sparse records with large dating uncertainties; (3) resolving power of records in which each event obliterates a finite interval that precedes the event horizon. (1) The laminated lacustrine sequences of the Holocene Dead Sea offer dating precision approaching annual. The historical record contemporaneous with the lacustrine one is sometimes better resolved, where the former provides a yardstick for the latter. Yet the absolute dating of the laminated sequence is traditionally limited by the inaccurate radiocarbon method. The floating laminar chronology can be correlated to the historical chronology by anchoring on the precisely measured intervals. The correlation is validated by estimating the probability for a similar matching between two random series, about 2 to the power of the number of intervals. In the case of the historical Dead Sea record, this number is smaller than 10¹⁰. (2) A dated record of damaged cave deposits, 40 km west of the trace of the Dead Sea transform, can be correlated with the clustered record of late Quaternary laminated lake deposits. Within the U-Th dating uncertainty, each event in the cave deposits can fit a cluster in the lake deposits. This can be interpreted as a filtered series in the remote site, where only events that exceed a threshold leave a mark. A simple criterion for assessing correlation stems from estimating the chance that a each member in a random series of events in the remote site will have a counterpart in the time spanned by the clusters of the in-rift site. (3) The resolving power of archives based on breccia layers (mix-layers) and homogenites suffer from an inherent limitation: each event is detected by the obliteration of layering which could potentially include additional events. Using the observed distributions of recurrence and obliterated intervals we estimate the expectancy for merging of events. The logarithmic distributions observed in the Pleistocene Dead Sea seismites yield an analytical expression for expectancy. In the limit of small ratio of obliterated to recurrence interval the expectancy equals that very ratio. The historical record of the last two millennia validates the analysis, where 30 events are resolved and five are merged into their successors. A possible implication is that we live in the most active period on record.

Keywords: logarithmic distribution, recurrence interval, paleoseismology

(S) - IASPEI - *International Association of Seismology and Physics of the Earth's Interior*

JSS006

Poster presentation

1936

Complex holocene deformation in the Lower Tagus Valley, Portugal, with probable tectonic origin

Dr. Joao Fonseca
IASPEI

Susana Pires Vilanova, Pedro Costa, Sandra Heleno, Vittorio Bosi

Palaeoseismological investigations on the Lower Tagus Valley, Portugal, led to the identification of holocene deformation, dated with C14 and archaeological artefacts. The deformation consisted on a set of NW-SE dipping planes with variable dip angles, with reverse N-S slip. The deformation was interpreted as indicative of compressive active tectonics. Alternatively, other authors attributed to the same structures a gravitic origin. This research was recently resumed, with resource to boreholes and improved outcrop exposure due to new roadcuts. This new phase led to the following additional results: 1) a gravity-driven landslide, with a sub-horizontal sliding plane, can in fact be identified in the new exposure, close to the trenches. 2) However, a sub-vertical contact surface striking about N50E and showing normal slip can also be identified in the new outcrop, directly underneath the old trenches. The surface remains steep down to a depth of 9 meters at least, making it difficult to reconcile with a gravitic origin. NW-SE extension, as implied by the new structure now discovered, is at odds with the usually adopted stress field for Western Portugal. This suggests that the structure is a secondary fault, with small dimension. Our preferred interpretation is that it belongs to a more complex pattern of tectonic deformation yet to be constrained by further study, of which the landslide is also a secondary effect. Such further study is key to the assessment of the contribution of intraplate seismicity to the seismic hazard in Portugal, and in particular in the Greater Lisbon region.

Keywords: paleoseismology, active fault, seismic hazard



(S) - IASPEI - *International Association of Seismology and Physics of the Earth's Interior*

JSS006

Poster presentation

1937

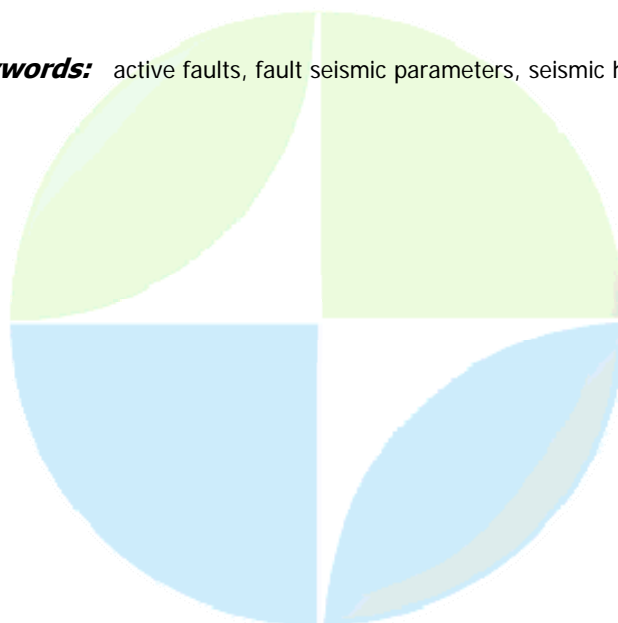
Identifying active faults and obtaining their seismic parameters in low strain zones: The northwestern margin of the Valencia trough

Dr. Hector Perea

Eullia Masana, Pere Santanach

The detection of the active faults and the determination of the parameters that describe their seismic cycle (maximum magnitude earthquake, recurrence period and time elapsed since the last event) is one of the key points that could help to the improvement of the seismic hazard studies in zones of low seismicity. The faults localized in these regions are characterized by low slip rates (< 0.01 mm/yr) and long seismic cycles (10 to 3 to 10 to 5 years). We propose different approaches with the objective of identifying the active faults in a zone of low strain rates, the north-western margin of the Valencia trough: a) spatial association between earthquakes, instrumental and historical, and faults to detect those responsible of the present and historical earthquakes; b) paleoseismological studies; c) geomorphological analysis of mountain fronts to identify the main patterns of those associated to active faults, those associated to non active faults and those not associated to faults; and d) analysis of seismic reflection profiles in offshore zones to localize the faults that are offsetting the seismic reflectors corresponding to the plio-quadernary sedimentary layers. Using this information the faults are classified in five different groups according with the observed characteristics: a) seismogenic faults (2 in the study area); b) faults that record present and accumulated activity (8); c) faults that record accumulated activity (18); d) faults that record present activity (32); and e) faults that do not record activity (186). The next step is the obtainment of the seismic parameters of the detected active faults. Maximum magnitude earthquake and recurrence interval are obtained from the length and slip rate of the faults. However, these parameters can only be obtained for faults classified in groups a, b and c. The time elapsed since the last event can only be get trough paleoseismological studies and these are not always feasible in low slip rate faults. The knowledge of these parameters allows the inclusion of some of the active faults in a probabilistic seismic hazard assessment. This study highlights the importance of identifying active faults and studying their seismic parameters to be included in any probabilistic seismic hazard assessment.

Keywords: active faults, fault seismic parameters, seismic hazard



(S) - IASPEI - *International Association of Seismology and Physics of the Earth's Interior*

JSS006

Poster presentation

1938

Liquefaction induced deformation in sediment column and their significance in paleoseismic studies: Examples from India

Dr. Prabha Pandey

National Geophysical Research Institute, Hyderabad Scientist

Anand Kumar Pandey

Liquefaction induced features are commonly observed in region of recurrent seismicity and their paleoseismic significance lies in their frequent occurrence and straightforward recognition in trenches. A number of regional and local agencies play part in triggering the liquefaction; earthquake wave is one such triggering agent producing seismically induced liquefaction (SIL) on regional scale. They occur mainly in the saturated soft sediments of beach, barrier and fluvial deposits. The manifestations of SIL are dependent on the type and variability in the sediment column that are affected by the driving mechanism and boundary conditions. The normal and reverse density gradients in the saturated sediment column plays important role in defining the surface and subsurface manifestations of liquefaction features. These features have been recognized in sediments as old as Proterozoic but the practical interest is limited only to the Quaternary sediments. We discuss the process of liquefaction and associated deformation features in sedimentary column primarily formed during an earthquake with examples from different documented earthquakes in past century and other mezoseismal regions in India. Further, the significance of SIL in the magnitude determination of source earthquake will be discussed.

Keywords: liquefaction, paleoseismicity



(S) - IASPEI - *International Association of Seismology and Physics of the Earth's Interior*

JSS006

Poster presentation

1939

Ground penetrating radar for archeoseismological investigations - a case study from Baelo Claudia, Southern Spain

Mr. Christoph Gruetzner

Neotectonics and Natural Hazards Group RWTH Aachen University, Germany

Klaus Reicherter, Pablo G. Silva

The Roman ruins of Baelo Claudia are situated at the Straits of Gibraltar in the province of Cdiz (Spain), close to the village of Tarifa. With about 2.000 inhabitants, the city was one of the larger roman settlements on the Iberian Peninsula and delivered tons of Garum, an ancient fish-dip made of tuna, to the capital. In the 1st century, an earthquake destroyed wide parts of the infrastructure. Because of the economic importance the city was rebuild during the Imperial Phase. Later in the 4th century, when the Roman star already had begun to sink, another destructive earthquake hit Baelo Claudia. It can be observed in the ruins - the columns and house walls fell on clean pavement and are partly preserved in this situation - that the event marked more or less the end of Roman settlings in this place. The seismic source or faults of the earthquakes are not yet clear. Paleoseismological studies showed, however, that both, the Carrizales and Cabo de Gracia Faults, in the immediate environs of Bolonia might produce a seismic event big enough to destroy the city. For our study 7 km of ground penetrating radar (GPR) profiles have been collected in the ruins, using the 300 MHz GSSI antennas and the SIR2 system. The frequency of 300 MHz provides a good compromise between penetration depth and resolution. In addition, some 240 cm low-frequency profiles have been taken in order to image the deeper structures of the area. We aim to find coseismic features like landslides and liquefaction or even buried faults inside the ancient city. As well we collected subsurface information of the buildings (tilted or destroyed walls and buildings that are still covered by the post-Roman colluvium). Besides the geological information, the investigation helps the local archeologists with their future excavations, as many unknown tombs and constructional features have been discovered during the survey. Our data do not imply an unknown active fault in the area but document earthquake-related damages like fallen boulders, tilted walls and the deformation of a buried aqueduct as well as the structure of a small scarp, crossing the city. The post-Roman colluvium can be easily mapped and distinguished from building rests and from older deeper-lying sediments. This layer marks the event horizon of the last earthquake after which the settling stopped. The thickness of the colluvium (or the depth of the event layer) provides information about erosion and sedimentation processes in the area, including mass wasting. Furthermore, GPR provides a reliable tool in finding promising locations for probing and/or trenching.

Keywords: paleoseismology, archeoseismology, groundpenetratingradar

(S) - IASPEI - *International Association of Seismology and Physics of the Earth's Interior*

JSS006

Poster presentation

1940

Paleoseismology in Iran; aims, previous record and future panorama

Mr. Alireza Babaie Mahani

institute of geophysics MS.c student of seismology IASPEI

Shayesteh Mehrabian, Majid Bagheri

Being placed in Alp-Himalaya orogenic belt, Iran is one of the most geologically active regions in the world. Northward movement of the Arabian plate and stability of the Turan plate in the north has caused Iran plateau to become squeezed in between. All of these conditions have transformed Iran to one of the most exclusive places for occurring earthquakes in the world. The energy of earthquakes in Iran is released along the faults in different seismotectonic regions. Earthquake catalogues in Iran consist of instrumental and historical data. The Instrumental data are limited, in the most optimistic situations, to some decades ago. Historical data can go back to some centuries or a millennium. In the regions where earthquakes occur frequently with short recurrence intervals, for example in Zagros, by instrumental data bank we can have an assessment of hazard in this region. In north of Iran, Alborz-Azarbayejan province, Historical data can increase our knowledge in order to have an assessment of the hazard. In contrast, in the regions of E-NE of Iran neither Instrumental nor historical data can reveal the history of occurring earthquakes in the past. In these parts of Iran the earthquakes occur with long recurrence intervals, much longer than our data range, so the role of paleoseismic investigations can be determined here to detect earthquakes that occurred some millennia ago. These investigations usually have been done by digging trenches across the faults to obtain some information such as: determining the exact sense of movement of faults; identifying and dating paleoearthquakes on the faults; measuring the slip rate of the faults and the recurrence interval of the paleoearthquakes. This information is then used for seismic hazard analysis of the regions specially where there are not enough data (instrumental and historical) for the assessment of the earthquake hazard. In this study we tend to deal with this kind of work; the aim of paleoseismic studies in different parts of Iran, the history of these studies and also the future panorama of this interdisciplinary subject.

Keywords: paleoseismology, iran, seismichazardanalysis



(S) - IASPEI - *International Association of Seismology and Physics of the Earth's Interior*

JSS006

Poster presentation

1941

**Applying Different Techniques in Studying an Active Strike-slip Fault;
Example of a Seismotectonic Study in the Southern Alps, NW Slovenia**

Mrs. Vanja Kastelic

University of Ljubljana, Department of Geology M.Sc IASPEI

Jure Bajc, Mladen Ivčić

We combine several techniques to obtain better insight into earthquake processes on the active fault zone in NW Slovenia. This particular fault system is of major concern with respect to seismic hazard in Slovenia one of the strongest events in the last century occurred there, the $M_w = 5.6$ in 1998 and $M_w = 5.2$ in 2004. In areas with absence of recent sedimentation or with active erosion processes, no young sediments or sedimentary rocks are present. Therefore, studying the seismic history of a fault in such an area cannot be done by standard paleoseismological investigation technique like trenching. Quantitative assessment of deformation that occurred on a particular fault must be approached by alternative methods due to lack of typical geological markers, such as displacements between stratigraphy or lithological boundaries. The Julian Alps (Eastern part of Southern Alps) in NW Slovenia are a region where both, absence of recent deposits and lack of geological markers is typical. The 1998 and 2004 earthquakes occurred along a NW-SE striking fault that runs through this region. We applied detailed structural mapping of the area along the fault trace, computed the stress orientation from measured kinematic data, and enriched both results with joined hypocenter (re)locations and focal mechanism calculation. The combination of the results of these different techniques provides better understanding of the seismicity of the area. We show that the fault exhibits a segmented geometry of individual fault segments and step-over zones of local transpressional basins that bound these segments. The geometrical relation between the length of individual segments and their overlap and separation distances in the step-over zones play an important role in spatial distribution of earthquake sequence. The step-over zone with overlap to separation ratio around 1:1 was easily breached by $M_w = 5.6$ event, while the one exhibiting the ratio around 5:1 was not breached by the same event and the aftershock cluster stopped at this step-over zone. Comparison of the fault area marked by the aftershocks and the fault area, obtained from the scaling relation between the magnitude and the area that ruptured, shows that the aftershocks span a significantly larger area than the segment that was activated during the main event. On the other hand, the aftershocks that occur within the first few hours after the main shock do mark the activated fault area of the main event reasonably well. Comparison between both methods shows, that in case of good local coverage of seismic stations in the epicentral area distributed evenly in all direction from the epicenter, polarity of first arrivals technique gives very good and reliable focal mechanisms. These in turn allow detailed seismotectonic interpretation of the earthquake processes in the area. The solution of focal mechanisms computation for both main earthquakes, that yield dextral strike-slip deformation, are also in a very good agreement with results obtained from field measurements of kinematic indicators and the solution of inversion of the data used for calculating stress orientation. Results give a N-S oriented direction for the maximum compressive stress and a strike-slip solution for the kinematic behaviour of the fault within this tectonic phase.

Keywords: active tectonics, fault segmentation, fault plane solution

(S) - IASPEI - International Association of Seismology and Physics of the Earth's Interior

JSS006

Poster presentation

1942

Sedimentological imprint of past earthquakes in the Algerian margin from slump and turbidite record (Maradja Project)

Dr. Nathalie Babonneau

IUEM - Universit de Brest UMR 6538 Domaines Ocaniques

Nathalie Babonneau, Antonio Cattaneo, Jacques Dverchre, Bruno Savoye, Karim Yelles, Gabriela Dan, Anne Domzig, Pierre Giresse, Rachid Matougui, Bernard Merci De Lpinay, Henri Pauc, Virginie Gaullier, Faouzi Djadid

As shown by the 2003 M 6.9 Boumerdes earthquake, northern is affected by moderate to large seismic activity damaging the Algerian coastal cities. Seismic activity results from the convergence motion between African and European plates. It occurs through large earthquakes, activating fault segments partly located offshore and causing important effects on the stability of the sediments on the Algerian continental slope. Sedimentological and geophysical data acquired offshore during the Maradja cruises (2003 and 2005) allow to identify possible Quaternary sediment instabilities generated by seismic events. The submarine slope morphology is characterised by deep canyons, indicating high efficient sediment transport by gravity processes, from the shelf break to the deep basin. Morphological and sedimentological studies of the margin suggest that several types of gravity deposits with a possible seismic origin exist. Slumps and debris flow deposits appear on multibeam-based seafloor morphology. They are mainly located at the foot of the continental slope and on steep canyon flanks, and are sometimes linked to subsurface fault motion. These sedimentary structures have a typical size of a few kms. Using detailed sonar imagery (SAR), high resolution seismics and core data, we made a first estimation of the age and distribution of slumps and debris flows. The link with seismic events is difficult to build, since deposits have limited spatial extent and rare vertical superposition. For the moment, a consistent chronostratigraphic framework cannot be established for these structures and prevents us to obtain event recurrence intervals. Large turbidity currents flowing offshore may well represent the result of sediment destabilisation induced by seismic activity, as testified by direct recording of catastrophic mass flows immediately following some of the most destructive historical earthquakes. During the 1954 Orlansville, the 1980 El-Asnam and the 2003 Bourmerdes earthquakes, numerous deep-sea communication cables were broken by turbidity currents directly triggered by seismic events. Currents, probably initiated in canyon heads, propagated as far as 100 km and more from the Algerian coast into the basin. These events are recorded as turbidite deposits in the abyssal plain and in levees of turbidite channels. A detailed sedimentological and morphological study of the margin (especially in the Algiers area) is performed in order to estimate the location of the initial instabilities in the canyons, the paths of active sediment transport and the main flow characteristics of the turbidity currents. Using this knowledge of transport and sedimentation processes, we establish a coring strategy for a cruise programmed in August 2007 in order to attribute an age to the largest deep turbidite sequences and estimate the recurrence time of these events in the different structural segments of the margin. This approach will help to gain important informations on the recurrence of great earthquakes along the Algerian margin in the last 10,000 years and on their actual imprint on the seafloor.

Keywords: paleoseismicity, algerian margin, slope instability

(S) - IASPEI - *International Association of Seismology and Physics of the Earth's Interior*

JSS006

Poster presentation

1943

A fresh fault scarp identified in an urban district by LiDAR survey: A case study on the Itoigawa-Shizuoka Tectonic Line, central Japan

Dr. Hisao Kondo

Active Fault Research Center Geological Survey of Japan/AIST

Shinji Toda, Koji Okumura, Keita Takada, Tatsuro Chiba

A light detection and ranging (LiDAR) survey that provides us high-resolution DEM has been successfully applied to the field of active tectonics recently to reveal invisible and obscure active faults, especially in forested areas. Here, we apply the LiDAR to an urban district in which detailed fault mapping is normally difficult due to densely built-up area in central Japan. Matsumoto City, which is located on a ca. 3 km square basin along the middle section of the Itoigawa-Shizuoka Tectonic Line active fault system (ISTL), one of the major active fault systems in Japan, shows us a large gap of the fault continuity. As the result of the survey, we found obvious fault scarps in the densely populated area. For the LiDAR, the data were acquired from a Cessna, which basically flew at the position of 750m above ground surface with laser scanning angle of 15 degrees. Along the expected fault traces, in order to avoid loss of laser returns to ground surface insulated with buildings, data was acquired from the position of 1000m above ground surface with a scanning angle of 12 degrees. GPS position control and Inertial Measurement Unit (IMU) data were combined with the time of flight for the laser data to produce DSM data. After filtering process to remove noise data, and laser returns to buildings and vegetations, DEM data at 0.5-m-grid interval was processed. Based on the high-resolution DEM, a continuous one-meter-high scarp was clearly recognized on alluvial fan surfaces in the urban district, west of the Matsumoto castle built in the ca. 16th century. Since the trend of west-facing scarp is almost perpendicular to the general flow-direction of streams, the scarp can be geomorphologically interpreted as tectonic origin. Taking distribution of adjacent active faults into considerations, the newly found fault traces probably contribute to form a pull-apart basin related to a fault step-over between the Gofukuji fault and the East Matsumoto Basin faults of which predominant slip component are left-lateral strike-slip. Since the Gofukuji fault has 14% earthquake probability for the next 30 years based on previous paleoseismic studies, the existence of such a fault scarp in urban district and its tectonic interpretation in Matsumoto City is crucial not only for evaluation of the future surface rupturing and direct strong shaking from the source but also for fault segmentation of the ISTL. Thus, the application of the current LiDAR survey technology to other urban areas would provide advantages in various aspects of seismic hazard mitigation.

Keywords: paleoseismology, lidar

(S) - IASPEI - *International Association of Seismology and Physics of the Earth's Interior*

JSS006

Poster presentation

1944

NEotectonic derived models for crustal deformation in a stable continental region setting: insight from the Southwest Of western Australia.

Dr. Mark Leonard

Geoscience Australia Geohazards IASPEI

Dan Clark

In recent times, high resolution digital elevation models (DEMs) have emerged as an important tool for finding and characterising earthquake related geomorphology, and particularly fault scarps. The results of a reconnaissance investigation of two DEM datasets covering a large portion of southwest and central Western Australia are presented. A total of thirty-three new fault scarps of probable Quaternary age have been identified, bringing the total number of neotectonic features in the area to sixty. The scarps are spatially isolated and range in length from ~15 km to over 45 km, and from ~1.5 m to 20 m in height. Most scarps where a displacement sense could be determined from the DEM data suggest reverse displacement on the underlying fault. In the few instances where high-resolution aeromagnetic data is coincident with a scarp location the ruptures are seen to exploit pre-existing crustal weaknesses. Twenty-one of the features have been verified as fault scarps by ground-truthing, and range in apparent age from perhaps less than a thousand years to many tens of thousands of years. Only four have been quantitatively examined to determine source parameters (e.g. timing of events, recurrence, magnitude). However, three important characteristics are revealed in the extant data: 1) recurrence of surface breaking earthquakes on an individual fault is typical (ie. areas hosting active fault scarps are earthquake-prone), 2) temporal clustering of events is apparent on many faults (ie. large earthquake recurrence in active phases might be much less than during inactive phases), and 3) significantly larger events than have been seen in historic times ($MW > 7.2$) might be expected in the future, Australia-wide. This rich neotectonic record also provides an opportunity to understand the characteristics of intraplate deformation at the scale of the entire Precambrian shield region (the Yilgarn Craton). An uniform distribution of the northerly trending scarps suggests that strain is uniformly accommodated over the Yilgarn Craton at geologic timescales, and that the easterly-trending compressive contemporary stress field has pertained for hundreds of thousands of years or more. This evidence supports a model whereby the lower, ductile part of the lithosphere is uniformly strong and deforms uniformly, and the upper (seismogenic) layer accommodates this large-scale flow by localised, transient and recurrent brittle deformation in zones of pre-existing crustal weakness. The proposed model implies uniform seismic hazard across the southwest of Western Australia, but at a timescale much greater than useful for most seismic hazard assessment applications. Palaeoseismological data on individual faults is playing an important role in bridging the gap between this seismicity model and the historic record of seismicity in , upon which all current seismic hazard assessments are based.

Keywords: neotectonic, paleoseismicity, earthquake

(S) - IASPEI - *International Association of Seismology and Physics of the Earth's Interior*

JSS006

Poster presentation

1945

Rupture characteristics and deformation partitioning in the Himalayan front of NW Himalaya: evidence from a post 1335 AD earthquake

Dr. Anand Pandey

National Geophysical Research Institute Scientist

Prabha Pandey, G.D. Singh, G.V. Ravi Prasad, K. Dutta, D. K. Ray, Madhukar Milki

The Himalayan Frontal Thrust (HFT) is the southernmost terrain defining intracrustal fault marked by the underthrusting of the Indo-Gangetic alluvium under the Siwaliks of the Sub-Himalaya. The HFT is physiographically recognized as an abrupt topographic break separating the Siwalik range from the Piedmont/alluvial plain. The Sub-Himalayan belt in the hangingwall of the HFT has attained a height of ~900 m above MSL (or ~600 m relative relief with reference to the HFT outcrops) during Late-Quaternary period. Invariably, the Siwalik rocks are observed in anticlinal disposition close to HFT zone and the folding has been attributed to fault-bend folding. This led to the growth and upliftment of different levels of strath terraces in response to the fold growth related to activity on HFT. Some recent active tectonic studies and paleoseismic investigations have argued for the growth related to episodic seismic slip on the HFT. The surface ruptures of some past earthquakes have also been documented in the HFT zone, which is recognized as the locus of primary earthquake rupture front of the active Himalayan mountain belt. We explored the mountain front and HFT zone on the same line in parts of NW Himalaya. Three levels of strath terraces and shear zone patterns in the growing Dhanaura anticline have been mapped along transverse stream sections in Himachal Sub-Himalaya. A surface rupture scarp (5-7 m high) with considerable lateral extension has been identified in HFT zone. A trenching experiment across the scarp in lower T1 terrace near village Kathgarh has been carried out. The trenches lie between two previously explored trenches (Kumar et al., 2006) at 1 and 5 km on either side in the region. In the trench section, two imbricate splays of surface rupture fault are observed, thrusting the Middle Siwalik mudstone/sandstone over the Holocene deposits. The Holocene terrace deposits have been folded by fault-propagation mechanism with thinning and truncation of the overturned limb by the fault. The charcoal samples within 50cm of the pre-earthquake surface in the footwall, marked by soil development, have yielded calibrated ^{14}C ages older than AD 1335 (2 σ) suggesting that the event postdates the deposit containing charcoal. However, a distinctly contrasting structural expression in the trench has been observed with reference to the previous trenches by Kumar et al., 2006. Analyzing the deformation characteristics of rupture in the trenches and in the outcrops within the HFT zone, it is obvious to infer that the rupture is partitioned into various splay faults near the surface giving rise to variability in their structural expressions. This also suggests that the rupture front behaves more like an echelon fault system in the Himalayan front rather than a single discrete fault.

Keywords: paleoseismology, rupture, himalaya

(S) - IASPEI - *International Association of Seismology and Physics of the Earth's Interior*

JSS006

Poster presentation

1946

Evidence of recent activity along the offshore Carboneras fault (SE Iberian margin) based on high-resolution acoustic and seismic imaging

Mrs. Ximena Moreno

Unitat de Tecnologia Marina CSIC IASPEI

Eullia Grcia, Eullia Masana, Rafael Bartolom, Graziella Bozzano, Eduardo Rubio, David Casas, Claudio Lo Iacono, Alessandra Asioli, Klaus Reicherter, Juan Jos Daobeitia, Pere Santanach

Neogene and Quaternary shortening at the Eastern Betic Cordillera (southern Iberian margin) is due to the European-African convergent boundary, and is mainly accommodated by a left-lateral strike-slip fault system referred to as Eastern Betics Shear Zone (EBSZ). The Carboneras Fault, with a length of almost 50 km onshore and more than 100 km offshore is one of the largest structures of the EBSZ. Along the Carboneras Fault the instrumental seismicity is low, suggesting either non seismic behaviour or long recurrence intervals (104 years) as found in adjacent structures. However, paleoseismological data onshore reveals that this fault had seismogenic behaviour during late Quaternary, with at least four earthquake events in the last 55 ky. Recently published marine geophysical data from the HITS 2001 cruise reveals the seafloor morphology along the offshore Carboneras Fault segment as an upwarped 5-10 km wide deformation zone bounded by subvertical faults. Geomorphic features, similar to the ones found onland, evidence a left-lateral strike-slip deformation with some vertical slip component. Last summer, we carried out the IMPULS 2006 cruise onboard the RV Hesprides. The main objectives were to characterize the structure and geometry of the offshore Carboneras Fault, to determine the recent activity and paleoseismic parameters of the fault, and to investigate the southern termination and the relationship with the Trans Alborn Shear Zone. A total of 46 high-resolution multichannel, single channel and magnetic profiles and up to 60 TOPAS sub-bottom profiler, gravimetric, swath bathymetry/backscatter data were acquired. In addition, nine gravity cores were also obtained along the Carboneras Fault and associated structures during the IMPULS and CARBMED (RV Meteor M69/1, 2006) cruises. High-resolution multichannel seismic profiles illustrate the shallow geometry and structure variability along the Carboneras Fault Zone. Preliminary observations of the succession of seismic profiles from shelf to the basin denotes morphostructural changes along the main trace of the fault: possible flower-structure morphologies in the shelf zone, underlapping restraining step-over in the central segment, and buried pressure ridges towards the south segment. The very shallow geometry of the fault is depicted by TOPAS profiles showing fault scarps, displaced reflectors (faulted horizons and mass-transport deposits) and horizons sealing faulted layers. The main objective of the coring survey was to sample and date specific horizons identified on the TOPAS profiles. Sediment grain size and physical properties measurements (magnetic susceptibility, density and p-wave) show that sediment cores are mainly composed of gravity-driven deposits intercalated by hemipelagic muds. AMS radiocarbon dating of the Holocene to Late Pleistocene units will provide a sediment rate and a fine chronology for these specific horizons, allowing to estimate a Late Quaternary vertical slip rate for the marine segments of the Carboneras Fault and a recurrence interval of past earthquakes. These parameters are of paramount importance to assess seismic hazard models in the Iberian Peninsula, especially when considering high magnitude earthquakes and long recurrence rates.

Keywords: carbonerasfault, alboransea, marinepaleoseismology

(S) - IASPEI - *International Association of Seismology and Physics of the Earth's Interior*

JSS006

Poster presentation

1947

In search of tsunami deposits along the eastern coast of Sicily (Italy)

Dr. Alessandra Smedile

Scienze Geologiche Universit di Catania IASPEI

Maria Serafina Barbano, Paolo Marco De Martini, Daniela Pantosti, Paola Del Carlo, Flavia Gerardi, Pierpaolo Guarnieri, Claudia Pirrotta, Mario Cosentino

Eastern Sicily has been affected in historical times by large earthquakes followed by devastating tsunamis, such as the 1169, 1693 and 1908 events. In order to provide a long term assessment for tsunami recurrence and related hazard, we developed a multi-disciplinary study aimed to recognize and date historical and paleo-tsunami deposits. We have compiled a georeferenced database storing information on the effects of known tsunamis (hit localities, inundation areas, run-up heights, etc.). On the basis of these data coupled with a geomorphological approach (satellite images and aerial photographs analysis and field surveys), we selected several sites, such as coastal lakes (Ganzirri, Gornalunga), marshes and lagoons (Fiumefreddo, Priolo and Vendicari oases), potentially suitable for preserving tsunami deposits. 50 test gouge cores have been dug by hand and engine coring. Sedimentological and paleontological analyses were carried out in order to reconstruct the paleoenvironment with specific attention to potential paleo-tsunami sandy layers. Magnetic and X-ray analyses evidenced susceptibility variations and peculiar small-scale sedimentary structures not detectable through the standard stratigraphic analysis. Moreover, morphometric and mineralogic analyses were performed on selected samples through a EDS equipped SEM. Tephra identification and radiocarbon dating were accomplished to constrain sedimentation rates and to correlate potential paleo-tsunami sandy layers with historical earthquakes. Although several of the investigated sites resulted unfavourable for the preservation of paleo-tsunami deposits, because revealed prevalently fluvial or marine deposits or highly modified settings, a few sites contain probable paleo-tsunami information. For example, three sandy/detrital layers, possibly related to paleo-tsunami events, were found at different depths within a silty-clay to clay prevailing sequence at the Anguillara site (Mascali, north of Catania). The paleontological analysis pointed out that the two uppermost sandy layers (about at 70 cm and 200 cm) were barren, whereas the assemblage found in the third, deeper sample (at about 350 cm) consisting of metamorphic rounded clasts, echinoderms fragments, sponges spicules and high concentration of roots and seeds, was totally different from the rest. The magnetic susceptibility highlighted lithological differences and few peaks related to volcanic material. The radiocarbon dating, carried out on a charcoal piece sampled just below the deepest suspicious layer, yielded an age of 1425-1510 AD, suggesting as candidate tsunami responsible for this layer the 1693 earthquake. Also at the Priolo lagoon, south of the town of Augusta, extensive coring has highlighted a couple of sandy/detrital layers (at -90 and -160 cm, respectively), showing a distinct micro- and macro-fossil assemblage. The tsunami-related origin of these layers remains matter of debate and further specific analyses are in progress to confirm or discard this hypothesis.

Keywords: paleo tsunami, eastern sicily

(S) - IASPEI - *International Association of Seismology and Physics of the Earth's Interior*

JSS006

Poster presentation

1948

Tbilisi fault, its forming and seismic activity of Tbilisi environs

Mrs. Tamari Tsamalashvili

Seismic Hazard Assessment Seismic Monitoring Centre of Georgia

On the basis of field observation, analysis of boring and geophysical data is shown that formation of Tbilisi olistostrmes of Middle Eocene age was connected with submeridional, long developed, consedimetation hidden deep fault (normal fault) tracing mainly along the right bank of Kura River. Complex of geomorphic, hydrogeologic, seismic data and distribution of rocks temperature field show the existence in Tbilisi environs, close to revealed old hidden deep fault, of young submeridional fault, which in the kinematic sense represents reverse-right-slip fault. Tbilisi fault is characterized by seismic activity and with it is bound up both Tbilisi earthquake of April 25, 2002 and a number of historical earthquakes.

Keywords: normal, hidden, fault

XXIV2007

PERUGIA

I T A L Y



(S) - IASPEI - *International Association of Seismology and Physics of the Earth's Interior*

JSS006

Poster presentation

1949

First paleoseismological evidence at the Plio-Quaternary Munbrega Half-graben (Iberian Chain, NE Spain)

Dr. Francisco Gutierrez

Earth Sciences Department University of Zaragoza

Eullia Masana, Lvaro Gonzalez, Jess Guerrero, Pedro Lucha

The Iberian Chain, in the NE of Spain, is an intraplate Alpine orogene created by the tectonic inversion of Mesozoic basins (orogenic stage, late Cretaceous-early Neogene). In the central sector of the orogene, westward propagation of a rifting process has given rise to Mio-Pliocene grabens and later Plio-Quaternary half-grabens locally superimposed on the western margins of the pre-existing basins (postorogenic stage). The Munbrega Plio-Quaternary Half-graben is a 19 km long and up to 3 km wide NW-SE trending neotectonic depression superimposed on the western margin of the Calatayud Neogene Graben. The poorly exposed fill of this recently captured basin consists of more than 30 m of fine-grained and gravel sheetflood alluvial fan facies capped by a petrocalcic horizon that displays the stage V of Machettes sequence. The NE active margin of the fault-angle depression corresponds to a prominent horst structure flanked by the Munbrega E and Munbrega W Faults. The Munbrega W Fault, which controls the development of the Munbrega depression, has generated a well-defined mountain front with triangular facets. In the north-western sector of the half-graben, the master Munbrega W Fault offsets an Upper Pleistocene mantled pediment creating a straight uphill-facing scarp. This pediment deposit grades distally into a 20 m thick terrace of the Jaln River whose aggradation surface is located at 45 m above the current channel. A 40 m long trench was dug perpendicularly to the 7.5 m high antislope fault scarp in order to conduct a paleoseismological investigation. This is the first trench ever dug across an active fault in the Iberian Chain. The sediments exposed in the trench walls show numerous deformational structures within a 25 m wide band, including fissure fills, cross-cut synthetic and antithetic normal faults, grabens, a roll-over, a monoclinical flexure, and a reverse fault that may correspond to an oversteepened normal fault. The higher thickness of the alluvial sequence in the downthrown sector of the fault zone suggests that deposition has been controlled by the fault activity (syntectonic sedimentation). A cumulative vertical displacement of 7.45 m has been estimated on the deformed mantled pediment deposit. Retro deformation of the trench units suggests three paleoearthquakes post-dating 70 ka sediments (OSL dating). This investigation demonstrates the seismogenic potential of the Munbrega W Fault. The mappable length of the structure (ca. 20 km) indicates that earthquakes Mw as large as 6.5 might be expected on this fault.

Keywords: iberian chain, normal faults, trenching paleoseismology

(S) - IASPEI - *International Association of Seismology and Physics of the Earth's Interior*

JSS006

Poster presentation

1950

**Earthquake recurrence of the DZCE fault (North Anatolian Fault Zone):
integrating geomorphological and paleoseismological analyses**

Dr. Stefano Pucci

Sismologia e Tettonofisica Istituto Nazionale di Geofisica e Vulcanologia

**Daniela Pantosti, Paolo Marco De Martini, Giuliana D'Addezio, Nikolaos Palyvos,
Phil E.F. Collins, Cengiz Zabcı**

To learn about recurrence of large earthquakes on the DZCE segment of the North Anatolian Fault Zone, that ruptured on November, 12, 1999 (Mw 7.1) with a predominant right-lateral kinematics, systematic geomorphological and paleoseismological analyses were integrated. Geo-morphological mapping along the fault trace permitted to analyze fault-related cumulative landforms and drainage pattern settings in order to provide new estimates on Quaternary slip rate of the fault. Remnant of an old alluvial fan modeled by fluvial terraces and 41 right-hand stream deflections were reconstructed, described and used as offset geomorphic markers. Two correlated Late Pleistocene, terrace risers, offset of about 300 and 900 m, respectively, were dated by means of OSL method about 21 kyr BP and 60 kyr BP. Moreover, the onset of the offset of the streams deflected for a total of ~100 m was radiocarbon dated about 7000 yr BP. These data translate to a constant rate of deformation of 14.0 ± 1.8 mm/yr for the last 60 kyr. On the basis of characteristic-earthquake model and under constant slip rate assumptions, it is possible to estimate that stream deflections across the DZCE Fault may be explained by repetition of 20-30 1999-like earthquakes during the last 7000 years, thus the recurrence time for surface rupturing events of the DZCE Fault is 28060 years. With the aim to reconstruct the record of last large earthquakes, 10 trenches at five sites were excavated. By merging information obtained from all trenches, evidences for four surface faulting earthquakes prior to 1999 one were found. These paleoearthquakes are dated on the basis of radiocarbon, ²¹⁰Pb and archaeological information and can be summarized as follows: 1) AD1685-1900, possibly end of 19th century; 2) AD1685-1900, possibly close to AD1700; 3) AD1185-1640; 4) possibly AD800-1000. Some of them can be correlated to historical earthquakes occurred on AD967, 1719, 1878 or 1894. These paleoseismological results, merged with those from previous papers, are suggestive of bimodal recurrence distribution (~400 and 200 yrs) yielding overall average recurrence time of ~300 yrs for the past two millennia, compatible with that calculated from the geomorphic markers analysis. Under the assumption of characteristic earthquake, bimodal paleoearthquakes distribution indicate slip rate fluctuations during the past two millennia, with clustered high strain release for the past 300-400 yrs. These results suggest Wallace-type strain release model for the DZCE fault, and average strain accumulation of 13.3 mm/yr, comparable with slip rate results for the past 60 kyr obtained by geomorphic marker analysis.

Keywords: paleoseismology, geomorphology, DZCE

(S) - IASPEI - *International Association of Seismology and Physics of the Earth's Interior*

JSS006

Poster presentation

1951

Ground Based Imaging Spectroscopy and Supervised Classification algorithms. New tools for the 21st century earthquake geologist.

Dr. Daniel Ragona

Geological Sciences San Diego State University

Tom Rockwell, Bernard Minster

We present a new methodology to assist the description, interpretation and archival of stratigraphic and structural information from field exposures. Portable hyperspectral scanners were used in the field or lab to collect high-quality spectroscopic information at high spatial resolution (pixel size ~ 0.5 mm at 50 cm) over frequencies ranging from visible to short wave infrared (VNIR-SWIR). A variety of robust algorithms generated fast and accurate mapping of the images supplying the geologist with new information to facilitate the interpretation process. This methodology, named hereinafter Ground-Based Imaging Spectroscopy (GBIS), provide a new set of tools that complement the traditional techniques of geological analysis. The principal benefits can be categorized in three groups. 1) Acquisition of a new type of data. High-resolution VNIR-SWIR hyperspectral datasets provide textural and mineralogical information at each pixel of the image, in some cases invisible to the human eye. 2) Quantitative analysis of the spectra using robust algorithms allows fast classification of the images generating alternative ways of mapping and correlation. 3) Data sharing and archival. Hyperspectral datasets constitute an objective description of the geological materials that can be digitally transmitted to a world-wide base of colleges for further analysis and interpretation. It is also an ideal format to construct GIS-type data bases of geological exposures, samples and cores. These advantages can benefit earthquake geology studies that require objective high-resolution geological description to resolve the earthquake history at a site. To evaluate the methodology we acquired high-spatial resolution spectral data of a large sample (60 x 60 cm) and four cores of faulted sediments from a paleoseismic excavation site using portable push broom Specim hyperspectral scanners. These data, which contains hundreds of narrow contiguous spectral bands between 400 and 2403 nm, were processed to obtain the reflectance spectra at each pixel. The dataset was analyzed using traditional spectroscopic methods and processed in a variety of ways to enhanced stratigraphic and structural relationships not obvious to the human eye. Additionally we used a neural network algorithm (MLP) to generate classification models of eight different types of materials (classes) observed on the samples. The best models were applied to the hyperspectral dataset to obtain detailed and accurate classification maps of the samples. The results of classification show that hyperspectral images classified with supervised algorithms can be used to properly map sediments, even those of very similar compositions and grain sizes. In conclusion, Ground-Based Imaging Spectroscopy is a very useful complement to traditional geological description techniques. It not only provides new ways to visualize the geological data but also can be used as a quantitative tool for fast and objective classification of geological materials in field or lab settings.

Keywords: paleoseismology, hyperspectral, neuralnetworks

(S) - IASPEI - International Association of Seismology and Physics of the Earth's Interior

JSS007

1952 - 1976

Symposium

**Progress in electromagnetic studies on earthquakes and volcanoes -
Volcanic structure and activities (same as JVS002)**

Convener : Dr. Yoichi Sasai, Dr. Zlotnicki Jacques, Dr. Ciro Del Negro, Prof. Viacheslav Spichak

Co-Convener : Prof. Domenico Patella

Magnetic, electric and electromagnetic methods are intensively applied to imaging volcanic structures and monitoring volcanic activity. The knowledge of volcanoes' interior is crucially important for understanding the dynamics of the feeder as well as for proper interpretation of EM signals. Both aspects lead to a more complete description of the time varying EM phenomena related to on-going volcanic processes. The contributions along the following lines are encouraged: 1) EM methods to study the volcanic structures, the associated geothermal fields and hydrothermal systems; 2) Joint interpretation of EM, seismic, gravimetric and other geophysical/geological data; 3) Land-based and satellite EM monitoring of active volcanoes, geothermal fields and hydrothermal systems; 4) Space and time changes of EM signals related to volcanic activity; 5) Modeling of EM manifestations of volcanic processes.

XXIV2007

PERUGIA
I T A L Y



(S) - IASPEI - *International Association of Seismology and Physics of the Earth's Interior*

JSS007

Oral Presentation

1952

Three - Dimensional resistivity model of the Volcano Elbrus (Northern Caucasus) revealed from MT and satellite data

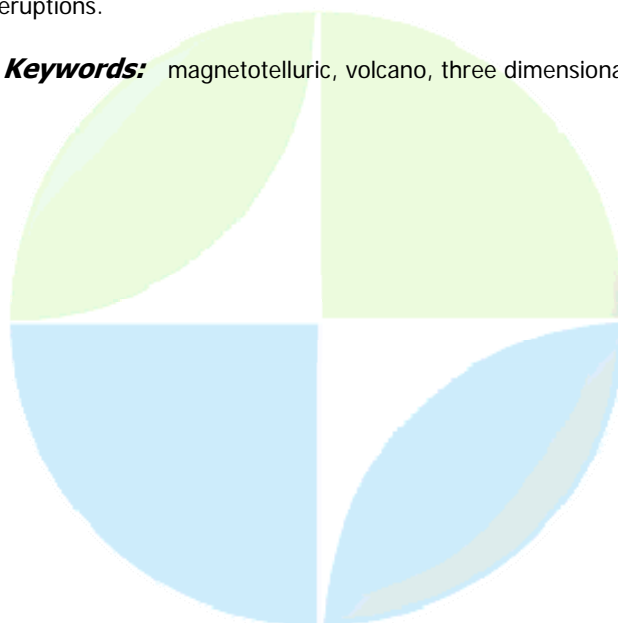
Prof. Viacheslav Spichak

EM data interpretation methodology Geoelectromagnetic Research Center IPE RAS IAVCEI

Borisova Valeriya, Fainberg Edward, Khalezov Alex, Goidina Aleksandra

Construction of the 3D resistivity model of the volcano requires array EM survey provided over the whole surface, which is often difficult due to its relief surface and inaccessibility of some zones surrounding the summit. This problem could be overcome by using a new approach, which combines analysis of both ground and satellite data. It is based on the method of the correlation similitude, which enables to fill the gaps in the EM data using other geological and/or geophysical data, correlating with the resistivity values. In particular, the latter ones could consist from the tectonic fragmentation of the rocks obtained by analysis of the satellite photographs of the surface using the method developed in (Nechaev, 1999). In turn, it is based on the estimation of the coefficient of the tectonic fragmentation (CTF) from the specific lineaments' lengths determined by the photographs of the studied area. The approach mentioned above was used in order to construct a 3D resistivity model of the Elbrus volcano (northern Caucasus) by MT data measured along one longitudinal profile crossing its summit. Two-dimensional inversion of the MT data resulted in a resistivity values in the same nodes of the grid, where the CTF was determined. A special neural network based technique was used in order to extract the subset of these nodes, which supports the biggest correlation ratio between these two parameters. At the next step an artificial neural network was taught to correspondence of these parameters determined only in the selected nodes followed by reconstruction of the resistivity distribution in the whole area from the CTF values. The analysis of the constructed resistivity model resulted in detection of the relatively conductive body at the depth 40 km (conductivity - 0.04 S/m, dimensions in vertical axis, latitude and longitude being equal to 20 km, 35km and 15km, accordingly), which can be treated as a magma chamber. The model of the Elbrus volcano can be used for solution of two important tasks related to the monitoring of its activity: optimization of the EM survey network and determination of the background level for detection of the time and spatial variations of the manifestations of the tectonic activity leading to the eruptions.

Keywords: magnetotelluric, volcano, three dimensional



(S) - IASPEI - *International Association of Seismology and Physics of the Earth's Interior*

JSS007

Oral Presentation

1953

Artificial neural network analysis of MT and geothermal data to delineate the 3-D structure of Tattapani geothermal Region, Central India

Dr. Saurabh Verma

Geophysical Exploration and Modeling National Geophysical research Institute, India IAGA

Artificial neural network modeling employing magneto-telluric and heat flow data is done to derive the 3-D structure of the Tattapani geothermal region, Sarguja district, M.P., India. The region represents one of the most prominent geothermal fields in central India that comprises several hot springs with temperatures ranging between 50 to 98 0C. The geothermal activity is governed by the major ENE-WSW trending Tattapani fault and cross faults oriented in NE-SW direction. A number of 300-350 m deep boreholes drilled within an area of 4 x 0.5 sq km yield temperatures in the range 1000C to 2100C that is also corroborated by the geochemically computed base temperature. Analysis of MT data reveals the 3-D depth-wise distribution of resistivity from which the temperatures are derived employing the borehole data. The ANN algorithm to generate the 3-D structure of the geothermal field utilizes these data sets along with the measured heat flow data. Correlation with the local structural and the regional tectonic framework highlights the factors that control the dynamics of geothermal fluids in the region.

Keywords: tattapani geothermal field, 3d geothermal structure, ann analysis mt and heat flow

PERUGIA
I T A L Y



(S) - IASPEI - *International Association of Seismology and Physics of the Earth's Interior*

JSS007

Oral Presentation

1954

Multi-scale tomography of volcano-electric sources. Its use in the localization and characterization of hydrothermal fluid movement of Piton de la Fournaise volcano from 1992-2005.

Dr. Ginette Saracco

Geophysique & Planetologie CNRS-CEREGE IAVCEI

Guillaume Mauri, Philippe Labazuy, Frederique Moreau

Previous wavelet analysis studies have shown the usefulness of applying complex wavelet tomography to study the hydrothermal systems of active volcanoes and define quantitative parameters (depth, orientation, effective degree of sources) linked to volcanic eruptions (Saracco et al 2004). Twelve SP profiles collected between 1992 and 2005 on the top of the summit cone are analyzed here by continuous wavelet transform. We show clearly the existence of 5 major fluid circulation cells, which move with the time, inside the Piton de la Fournaise hydrothermal system. These hydrothermal fluid cells are spatially located between 1600m to 200m-depth. The depth are directly related to shallow magma intrusions. Moreover, the fluid displacements are directly influenced by the eruptive activity. Initially, between 1992-1998, the quiescent period is characterized by deeper hydrothermal fluid cells (1600m). With the resumption of eruptive activity, the fluids moved upward to shallow depths due to pressurization of the hydrothermal system around 200m-depth. After a constant pressurization of the hydrothermal system (2001-2003), a weak and slow depressurization of the hydrothermal system appears and hydrothermal fluids moved slowly downwards (200m ->400m). This implies the beginning of a weak depressurization of the hydrothermal system. This change in direction of source migration suggests a quasi-constant activity of the Piton de la Fournaise, but with future eruptions likely being of small magnitude. Wavelet tomography allows for a 3D determination of hydrothermal fluid displacement directly influenced by shallow magmatic intrusion through the time. It is a promising new method for improved forecasting of changes in the hydrothermal system of active volcanoes and for detecting electrical precursors of changes in eruptive activity.

Keywords: multi scale tomography, hydrothermal sources movment, complex wavelet transform



(S) - IASPEI - *International Association of Seismology and Physics of the Earth's Interior*

JSS007

Oral Presentation

1955

High Density Helicopter-Borne Aeromagnetic Survey in Aso Volcano

Dr. Mitsuru Utsugi

Aso Volcanology Laboratory Kyoto Univ. IAGA

Yoshikazu Tanaka

Recently, geomagnetic field observation is successfully applied to many active volcanos to detect the volcano-magnetic changes, i.e., geomagnetic field changes associated with the volcanic activities. These observations are usually based on the continuous or repeated observation stations setting on the ground near the active area. From these observations, we can obtain high accurate information about the temporal geomagnetic field changes. But we can obtain only limited information about the special distribution of geomagnetic changes because of it is quite difficult to maintain many observation stations under the extremely bad environment around the active area of volcano. To interpret the geomagnetic field changes to underground heat transfer, we have to know the special distribution of the geomagnetic changes. To obtain the detailed information about the spatial distribution, we tried to use the aeromagnetic survey. Based on the aeromagnetic survey, we can get many data of spatial distribution of the field easily. Our goal is to detect the volcano-magnetic changes from the repeated aeromagnetic survey. The main problem of aeromagnetic repeated observation is the difficulty of the observation point control. In the two flights, it will be impossible to flight exactly same position. So that, it is very difficult to separate observed field changes to temporal variation due to the volcanic activities and the spatial variation due to the difference of the observation points. If the detailed distribution of geomagnetic field is obtained on quiet period of the volcano, and the field intensity on the arbitrary point around the active area is estimated interpolating the observed data, we can correct the spatial variation of the repeated aeromagnetic survey data caused by the difference of flight position, and it may be possible to detect the field changes associated with the volcanic activities. For this purpose, we made very high density and low altitude helicopter-borne aeromagnetic survey on Aso Volcano, central Kyushu Island of Japan, in July 2002. The survey area was NS1200 x EW1200 x 300m region above the Nakadake crater which is the most active area on Aso volcano. In this survey, we used a high-resolution portable cesium magnetometer. The sampling time of measurements was 0.1 second. The flight was made in 8 heights (1370, 1400, 1450, 1500, 1540, 1570, 1600 and 1640 m from the sea level). The total numbers of measurements were about 8200. Using these data, we tried to estimate the special distributions of the geomagnetic field around the Nakadake crater. Observed data likely contain some noise or miss-observed data. To extract these inadequate data, we applied the technique of equivalent anomaly method. This method is usually used to calculate the upward continued aeromagnetic data. Based on this method, inharmonic component of observed data is carried away and the harmonic field distribution can be estimated in the upper region of the flight surface. In this study, we used this method to extract harmonic component from the observed data. The accuracy of the obtained distribution over the Nakadake crater is about 10nT, and if comparatively larger scale eruption is occurred, we can detect the volcano-magnetic changes using our estimated distribution of the geomagnetic field.

Keywords: aeromagneticsurvey, volcanomagneticiceffect

(S) - IASPEI - *International Association of Seismology and Physics of the Earth's Interior*

JSS007

Oral Presentation

1956

Time dependent piezomagnetic changes in viscoelastic medium

Dr. Gilda Currenti

Ciro Del Negro, Malcolm Johnston, Yoichi Sasai

Temporal changes in piezomagnetic field can arise from changes in magma pressure, evolution of the source geometry, or rheologic properties of the host rock. Especially in volcanic areas, the presence of inhomogeneous materials and high temperatures produce a lower effective viscosity of the Earth's crust that calls for considering anelastic properties of the medium. We have investigated time dependent piezomagnetic changes due to viscoelastic properties of the medium surrounding volcanic sources. Piezomagnetic properties are carried by grains of titanomagnetite, which occupies only a small fraction of ordinary rock volume and are supposed to be elastic, while the non-magnetic surrounding matrix is assumed to behave viscoelastically. Under this assumption, only the medium parameters show a viscoelastic behavior. From all the possible rheological models, we investigate two cases in which the bulk modulus is purely elastic and the shear modulus relaxes as: (i) a standard linear solid (SLS) and (ii) a Maxwell solid. We applied the correspondence principle to the analytical elastic solutions for pressurized spherical sources and dislocation sources in order to find out the time dependent piezomagnetic fields in a viscoelastic medium. In particular, the shear stress and hence the piezomagnetic field completely disappears after the relaxation process for Maxwell rheology. For a SLS rheology, the piezomagnetic field is found to decrease over time and reach some finite net offset value. These different behaviors can provide helpful hints in understanding the temporal evolution of piezomagnetic anomalies in volcanic regions.

Keywords: piezomagnetism, viscoelasticity, modeling



(S) - IASPEI - *International Association of Seismology and Physics of the Earth's Interior*

JSS007

Oral Presentation

1957

Interpretation of SP anomalies on Kaimondake volcano, Japan

Dr. Hideaki Hase

Institute of Seismology and Volcanology Hokkaido University IAVCEI

Tsuneo Ishido, Wataru Kanda, Shinyou Mori

Self-potential (SP) anomalies were observed on active volcanoes and geothermal areas. The SP anomalies are mainly formed by streaming potential associated with groundwater flow in porous media. Electric charge of the streaming potential is generally positive (when the zeta potential is minus), so that a positive SP anomaly at the upper part of volcano can be interpreted as a sign of hydrothermal upwelling. Therefore, the interpretation of SP anomalies is important for detecting hydrothermal circulation and is also used for evaluation of volcanic activities. Recently, SP numerical simulations have been conducted (e.g., Ishido and Pritchett, 1999; Hase et al., 2005), which allow to discuss a quantitative interpretation of flow directions and fluxes of groundwater. Hase et al. (2003) has conducted several zeta potential experiments of volcanic rocks and clarified that the zeta potentials of rocks have variety values in area-by-area. This result implies that groundwater flow by only gravity force can cause a characteristic SP anomaly because of the zeta potential variety influenced by heterogeneous structure. A characteristic positive SP anomaly was observed at the summit area of Kaimondake volcano, despite there is no indication of geothermal activities (Kanda et al., 2004). Zeta potential experiments of rock samples from the volcano were conducted by Hase et al. (2004). The result of zeta potential shows negative in all samples, however, the zeta potentials were significantly different by each rock stratum in the volcano. In this presentation, we will show the result of SP numerical simulations to take into account the zeta potential variations of rocks for the volcano and will discuss the cause of the SP anomaly.

Keywords: self potential, zeta potential, kaimondake



(S) - IASPEI - *International Association of Seismology and Physics of the Earth's Interior*

JSS007

Oral Presentation

1958

Electromagnetic monitoring of La Fournaise volcano (Indian Ocean): Fuzzy pattern recognition algorithms

Prof. Alexey Gvishiani

Geophysical Center RAS Russian Academy of Sciences IASPEI

J. Zlotnicki, A. Gvishiani, J.L. Le Moul, M.Rodkin, S. Agayan, Sh. Bogoutdinov

Numerous studies investigate electromagnetic (EM) precursors of volcanic eruptions (and earthquakes). Active volcanoes are excellent natural laboratories for such electric and magnetic studies. Indeed: (1) usually, volcanoes are not highly populated, so the level of anthropogenic noise is low; (2) the area to be monitored is typically small, till 10 km from the volcano, (as compared to several hundreds km long seismic faults), so a limited number of data sensors (≤ 15) is required to install sufficiently dense network; (3) volcanic activity generally produces a large number events (seismicity, ground deformation, EM, geochemistry, etc) which can be recorded during a short time period. This study is devoted to the basaltic, 2640 m high, La Fournaise volcano, located in the South-eastern part of Reunion Island (France, Indian Ocean). The more or less regular volcanic activity allows detailing electric, magnetic, and EM signals associated to the eruptive phases. Precursory total magnetic force (TMF) and electric (ES) signals to eruptions have been already reported. These signals can appear a few weeks before the outburst, and the amplitude can reach a few nT for TMF and some hundreds of mV/km for ES. Signals are enhanced when the magma migrates towards the ground surface in the last hundreds meters. These signals are low frequency events, from a few minutes to several weeks or months. Nowadays, we investigate the EM signals in higher frequency domains. A sharp increase in the sampling rate of data, up to several kHz, takes place. Manual time series processing by a visual expertise becomes more and more difficult, not enough objective, and time consuming. Thus, the problem of automation of visual data processing becomes an important one. We introduce an alternative approach to visual analysis of data with the building of algorithms based on fuzzy-logics and statistics. These algorithms carry out the morphological examination of time series, and identify pre-supposed signals in successive segments of the EM records. Both, a sample of a real record or some ideal pattern formulated by the expert is used to formulate the recognition procedure. The application of algorithms allows to find out anomalies in electric and magnetic data, and to discriminate between anomalies of different type corresponding to diverse physical processes (heavy rains, changes in the hydrothermal activity, etc.). The algorithms can be used in monitoring systems for automation and for revealing characteristic morphological sequences in huge data sets.

Keywords: fuzzy logic algorithms, data processing, volcanic activity

(S) - IASPEI - International Association of Seismology and Physics of the Earth's Interior

JSS007

Oral Presentation

1959

Electromagnetic and Geochemical monitoring of the slow unrest of Taal volcano (Philippines)

Dr. Zlotnicki Jacques

Magma and Volcanoes Laboratory CNRS IAGA

Zlotnicki Jacques, Sasai Y., Toutain J.P., Villacorte E.U., Cordon Jr, Bernard A., Sabit J., Harada M., Hase H., Sincioco J., Punongbayan Jane, Nagao T.

Taal volcano (121E, 14N), in Philippines, is a 311m high stratovolcano in which a 75m deep, 1.2km in diameter, lake (Main Crater Lake, MCL) fills the centred crater (Main crater, MC). This acid lake (pH ~2-3) is partially connected to Taal Lake (TL) which surrounds the volcano inside a pre-historical large caldera. Since 1572, 33phreatic to phreatomagmatic eruptions have occurred, some of them causing several hundreds casualties. In regard to the duration between two consecutive eruptions, Taal volcano should have already erupted with 88% of probability. Moreover, several phases of strong seismic activity accompanied by ground deformation, opening of fissures and surface activity were recorded between 1992 and 1994. Upraise of sporadic seismicity started again in October 2004, with occurrence of felt earthquakes in 2005 and 2006. In November 2006, a geysering activity took place in MCL and disappeared a week later. Taal activity appears to be controlled by dikes injection and magma supply, and buffered by a hydrothermal system that releases fluids and heat through boiling and subsequent steaming. In early 2005, a multi-disciplinary project for studying the hydrothermal activity started. Combined self-potential, total magnetic field, ground temperature, and carbon dioxide soil degassing surveys, as well as satellite thermal imaging of MCL water, are now performed. The different methods are combined to analyse the hydrothermal/volcanic activity in the northern part of central crater and on its outer northern slope. High temperatures and high concentrations of carbon dioxide, as well as self-potential and magnetic anomalies, outline large-scale hydrothermal degassing, this process being enhanced along the tectonic features of the volcano and in a lesser extent along the East-West northern flank active fissures opened during the 1992-1994 seismic activity. Heat and fluids released from the hydrothermal system delineate a general NW-SE trend in the northern part of MC and may be related to a suspected NW-SE fault along which seismicity takes place and dikes are believed to intrude triggering volcanic crises. Since 2005, reiteration of reference profiles evidence self-potential, total magnetic field, CO2 degassing and ground temperature changes with time. T The observations suggest that most of heat and fluid transfer operate close to the acid lake. However, the northern flank of the volcano is reactivated during seismic crises and this sector could be subjected to a flank failure. PHILVOLCS EM team: P. K. B. Alanis, L. Saquilon, I. Narag, R. Seda, A. Ramos, W. Reyes, Paolo D. Reniva

Keywords: imaging monitoring, electromagnetism, geochemistry

(S) - IASPEI - *International Association of Seismology and Physics of the Earth's Interior*

JSS007

Oral Presentation

1960

Large magnetic changes at Etna Volcano (Italy) observed before and during the 2006 eruption

Dr. Rosalba Napoli

Istituto Nazionale di Geofisica e Vulcanologia Istituto Nazionale di Geofisica e Vulcanologia

Gilda Currenti, Ciro Del Negro, Davide Giudice

The latest eruption of Mt Etna, occurred from July to December 2006, was characterized by episodic eruptive activity involving a number of explosive and effusive vents in the summit craters. From the beginning of 2006 significant geomagnetic changes were recorded by the permanent magnetic network of Mt Etna. The present network consists of 6 scalar magnetometers and 3 magnetic gradiometers. Stations are located at elevations ranging between 1700 and 3000 m a.s.l. along a North-South profile crossing the summit craters. All magnetic stations are equipped with Overhauser effect magnetometer (0.01 nT sensitivity) and synchronously sample the Earth's magnetic field every 5 seconds. Between January and July 2006, after differential magnetic fields were filtered from the seasonal thermal noise by Independent Component Analysis, a slow and continuous decrease in the magnetic field total intensity greater than 5 nT was observed at almost all the sites of the southern flank of Mt Etna. Magnetic data indicate that changes in the magnetization within the volcano are caused by thermomagnetic effects. The location of the demagnetized region, which is supposed to be the region heated by high-temperature liquids and gases originating from magma, was estimated by the spatial distribution of the variation rate. At the beginning of November 2006 a large and sharp decrease of the geomagnetic field was detected at the station of MFS. The anomaly reached the maximum amplitude of more than 150 nT in about two months with a variation rate of about 10 nT/day. At the end of January 2007 the phenomenon was still in progress, even if the variation rate drastically decreased to 0.5 nT/week. The large anomaly could be of thermomagnetic origin engendered by lava flows emitted by an effusive vent on 6 November, which threatened station and stopped at about 30 m from the magnetic sensor.

Keywords: geomagnetic changes, mt etna



(S) - IASPEI - *International Association of Seismology and Physics of the Earth's Interior*

JSS007

Oral Presentation

1961

Imaging of Electrical and Thermal Structure of a Shallow Magmatic Intrusion Associated with the 2000 Eruption of Usu Volcano

Dr. Takeshi Hashimoto

Institute of Seismology and Volcanology Faculty of Science, Hokkaido University IAGA

Yasuo Ogawa, Shinichi Takakura, Hiroyuki Inoue, Yusuke Yamaya, Mitsuru Utsugi, Tetsuji Koike, Hiroshi Hasegawa, Hiroshi Ichihara, Hideyuki Satoh, Toru Mogi

1. Introduction * Usu Volcano, southwestern Hokkaido in northern , experienced the 4th (and the final) eruption in the 20th century in March, 2000. The eruption resulted in the ground upheaval of about 80 m due to a shallow intrusion of magma beneath the western part of Nishiyama, the NW piedmont of the volcano. Many geophysical investigations have been implemented in this area during and after the eruption. None of them, however, have yet achieved a clear imaging of the intruded magma. As for the electrical structure, Akita and Shibata (2003) conducted the shallow resistivity survey by audio frequency magnetotellurics. They reported that the shallow part of this area is very conductive, and therefore, it seemed that the investigation of the deeper structure down to the intrusion depth requires lower frequency band. We thus planned a magnetotelluric survey up to 0.001 Hz in 2006. Six wide-band MT sites aligned in the NE-SW direction (orthogonal to the regional strike), crossing the upheaval center, were interfilled with several audio-frequency sites to achieve a high horizontal resolution as well as the vertical reach. * 2. Electrical resistivity structure * Acquired MT responses were inverted to a 2D resistivity structure by using the inversion process developed by Ogawa and Uchida (1996). As seen in the previous survey, the general resistivity of this area is quite low (0.1 to 10 Ohm-m). This feature well explains the poor variation of surface self-potential reported by Hase et al. (2007). Surface resistivity shows about 10 Ohm-m, corresponding to the volcanic deposits. A very low resistivity (VLR: 0.1 to 1 Ohm-m) underlies with a thickness of some hundred meters. This layer is imaged at 200 to 400 m deep beneath the upheaval center, while it does from 500 to 1000 m deep in the northern and southern side of the cross-section, just like an umbrella-shaped structure. It is probable that a highly conductive clay mineral (montmorillonite) immersed in high salinity fluid is responsible for the VLR. The bottom of this VLR then possibly corresponds to the thermal transition (about 200 C) from montmorillonite to other minerals such as illite of higher resistivity. The bump of the VLR below the upheaval center may be related to the isotherm due to a magmatic intrusion. The intruded magma should be situated below this VLR, though it is not imaged as an isolated body in the resistivity cross-section. * 3. Implication from geomagnetic changes * Some of the authors (Hokkaido University) have started magnetic repeat measurements over the upheaval area since 2003, about three years after the surface manifestation ended, anticipating the subsequent geomagnetic changes related to subsurface thermal activity. Surprisingly, it has been revealed that markedly rapid magnetic changes up to 50 nT/yr was still going on. The change looks quite linear with respect to the time, showing no plateauing even seven years after the eruption calmed down. The magnetic total field has increased to the south, while it has decreased to the north of the upheaval center, suggesting the increasing magnetization at 400 m deep. Such change is normally interpreted as cooling at the source region; namely, the rock is getting more magnetized as the magnetic minerals in the rock freeze themselves to the present geomagnetic field. This mechanism requires that the source region must have been heated in advance to a high temperature enough to produce the effective, enormous, and persisting thermal magnetization in the subsequent cooling phase. Such an extensive pre-heating at 400 m deep is unlikely, taking account of the discussion in the resistivity section. * One of the alternative mechanisms is the thermo-viscous magnetization (TVM) in a lower temperature range. Magnetic minerals exposed to an external field may

be gradually magnetized with time along the present geomagnetic field. Heating of a rock body, even in a range far below the Curie temperature, may cause dramatic decrease of the relaxation time, resulting in considerable amount of TVM acquisition (e.g. Dunlop, 1983). The TVM therefore seems more consistent with the temperature information deduced from the magnetotellurics than simple cooling magnetization process. * It is worth considering such TVM effect on a rock with initial remanent magnetization of opposite sense to the present geomagnetic field (i.e. reversely magnetized body). In such a situation, magnetic field change due to TVM will be similar to the one due to thermal demagnetization (TD). TVM effect can, however, be even more efficient, especially in a low temperature range, since it rotates the reversed component in place of simple erasing as in the case of TD. It is still an open question whether the magnetization of the upheaved mound of Usu is normal or reversed. However, the latter is probable since the relevant area is situated at the geological boundary between the reversed Tertiary volcanic basement and recent Usu somma basalt. Aeromagnetic survey of this area (Okuma et al., 2002) and a marked geomagnetic change in the initial stage of the 2000 eruption (Satoh et al., 2002; Hashimoto et al., 2007) also support the reversal. The ongoing rapid and persistent changes in the total field may be accounted for such effective TVM at low temperature. * 4. Summary and conclusions * We conducted MT resistivity survey over the magmatic intrusion of the 2000 eruption of Usu Volcano. An umbrella-shaped very low resistivity (VLR: 0.1 to 1 Ohm-m) layer was found beneath the upheaval center at some hundred meters deep. This umbrella structure is probably related to the intrusion. Montmorillonite is a plausible candidate for the VLR, while the bottom of the VLR may correspond to the isotherm (c.a. 200 C) of transition to more resistive clay mineral. Meanwhile, results from the geomagnetic monitoring in the post-eruption stage suggest that a rock body at about 400 m deep is acquiring the magnetization to the present geomagnetic field. It is more consistent with the resistivity results to interpret this ongoing change is due to the TVM at a low temperature range rather than considering the simple thermal demagnetization.

Keywords: usu volcano, magnetotellurics, geomagnetic field



(S) - IASPEI - *International Association of Seismology and Physics of the Earth's Interior*

JSS007

Oral Presentation

1962

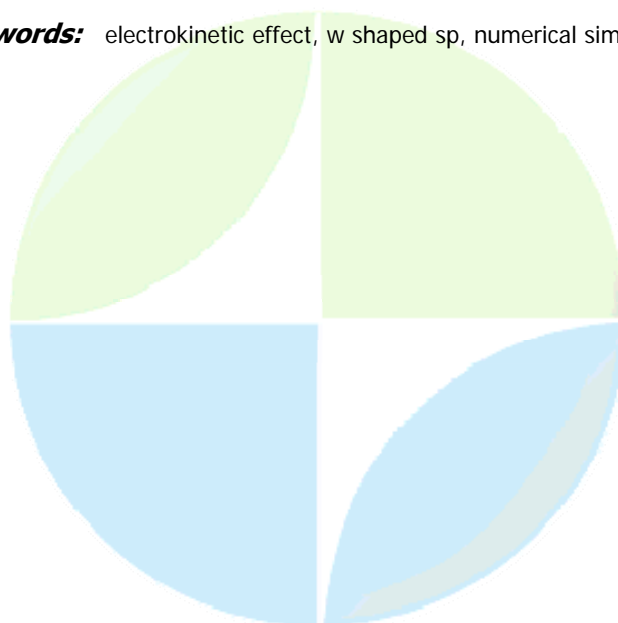
Self-potential evolution associated with volcanic activity

Dr. Tsuneo Ishido

Institute for Geo-Resources and Environment Geological Survey of Japan, AIST IASPEI

The self-potential (SP) distributions have similar features on a number of volcanoes: SP first decreases several hundred millivolts to more than one volts as one climbs the slopes of the volcano, then rapidly recovers to the level measured on the flank of volcano as the summit crater is approached. Consequently, the entire SP profile along a survey line starting from the foot, passing near the summit and reaching the foot on the opposite side often has the shape of the letter "W". Numerical simulations by Ishido (2004) showed that the primary cause of the "W"-shaped SP distribution is a combination of the electrokinetic drag current associated with the downward liquid flow in the unsaturated and underlying saturated layers and the presence of a shallow conductor near the volcano summit. If the shallow conductor contacts a deep conductive layer, this conductive structure provides a current path between the low-potential shallow and high-potential deep regions, resulting in increase in SP around the summit. Assuming a plausible value of zeta potential and liquid-saturation dependency of drag current, the terrain-related SP on the peripheral area is calculated as about -1 mV/m, which is typical of the magnitudes observed at a number of volcanoes. The calculated "W"-shaped profile is stable even with periodic groundwater recharge, which is also consistent with field observations. The "W"-shaped SP distribution is sometimes not symmetrical and short wavelength anomalies are obvious near the volcano summit. In addition to heterogeneous resistivity and coupling-coefficient distributions, local increase or decrease in liquid-phase saturation associated with smaller or larger permeabilities or fumarole activities is thought to be responsible for the local SP anomalies. The calculated amplitude of high SP around the summit crater is sensitive to the conductivity structure, which is thought to change over time due to volcanic activities such as magma ascent, development of hydrothermal convection, etc. Evolution of high SP near the summit crater with (electrically conductive) magma ascent is expected to be largely affected by the continuity of the pre-existing conductive structure between the near surface and deep regions. These topics will be discussed on the basis of axi-symmetrical 3D numerical simulations of electrokinetic potential produced by subsurface fluid flow.

Keywords: electrokinetic effect, w shaped sp, numerical simulation



(S) - IASPEI - *International Association of Seismology and Physics of the Earth's Interior*

JSS007

Oral Presentation

1963

Three-dimensional inversion of resistivity structure for CSEM method and its application to the ACTIVE system in Izu-Oshima Island, Japan

Dr. Takao Koyama

Earthquake Research Institute University of Tokyo IAGA

Yuji Takahashi, Hisashi Utada, Yuichi Morita, Hidefumi Watanabe, Tsuneomi Kagiya

We developed a numerical solver of three-dimensional inverse problems for resistivity structure by the CSEM method. The forward calculation is based on the modified IDM (Singer, 1995; Avdeev et al, 1997), and is originally modified to drastically reduce both the computation time and memories by giving the 1-D Greens functions in horizontal wavenumber-domains analytically. The inversion algorithm is based on the hybrid method by the steepest descent and the quasi-Newton methods (Koyama, 2001). We apply it on the ACTIVE (Array of Controlled Transient-electromagnetics for Imaging a Volcanic Edifice) system installed at Mt. Mihara in Izu-Oshima Island, central Japan, which is a kind of the CSEM (Takahashi, 2006). Now the ACTIVE system is operated every other day; 1 Hz square currents (J) are injected at the electric line embedded at about 1 km distance in the south east of Mt Mihara and five stations observe the vertical magnetic field (Z). We try to detect the temporal change of the resistivity structure and elucidate the volcanic activity of the Mt. Mihara, analyzing the responses Z/J. In our presentation, by using the change of the responses Z/J and the 3-D inversion code, we estimate the change of the resistivity beneath the Mt. Mihara. We discuss also further plans to install other receivers and transmitters to effectively detect the magma ascent in the future.

Keywords: csem, inversion, resistivity



(S) - IASPEI - *International Association of Seismology and Physics of the Earth's Interior*

JSS007

Poster presentation

1964

Inspection of the dike position by total intensity data in the 2000 eruption of Miyake-jima volcano

Dr. Yoichi Sasai

Disaster Prevention Division, Tokyo Metrop. Govt. Disaster Prevention Specialist (Chief) IAVCEI

Mitsuru Utsugi, Eisuke Fujita, Makoto Uyeshima, Jacques Zlotnicki

Several remarkable magnetic changes were observed before and during the 2000 eruption of Miyake-jima volcano, such as the precursory changes since 1996, those prior to and associated with the formation of a sinkhole in the summit, those associated with the tilt-step events, the enormous ones during the caldera formation and so on (Sasai et al., 2002, Zlotnicki et al., 2003). However, any significant change in the total intensity was not observed at stations well distributed on the island at the time of the magma intrusion started on June 26. Only an exception was that a 3-components flux-gate magnetometer operated by NIED at a station on the western slope of the volcano (MKA) recorded a large amount of changes up to 200 nT. Ueda et al. (2006) showed that the said magnetic changes could be explained by the piezomagnetic effect due to an intrusive dike in the NW-SE direction emerged beneath around MKA. This is the 3rd example of the piezomagnetic change due to dike intrusion, i.e. in the cases of 1986 Izu-Oshima (Sasai et al., 1990) and 2002 Mt. Etna eruption (Del Negro et al., 2003). These three observations indicate that magnetic data strongly constrain the position of an intrusive dike. Ueda et al.'s piezomagnetic calculation is based on the mechanical model inferred from tiltmeter and GPS data (Ueda et al., 2005). This model consists of three intrusive dikes and a contractive one, which reproduced the deformation data in three time periods from 18:30, June 26 to 6:00, June 27. The magnetic changes at MKA were ascribed to the dike in the second time period (19:00-01:00). On the other hand, Fujita et al. (2002) searched for a single opening dike plus a shrinking Mogi source to best fit the tilt change at each one hour interval from 18h, June 26 to 01h, June 27. From 21h to 24h, mostly E-W oriented dikes intruded in the southern part of the volcano toward eastern side of the island, which were not well represented by Ueda et al.'s (2005) model. Our problem is that the total intensity at TAR station, located at the southern coast, gradually decreased from June 26 to July 10 by about 10 nT in contrast to other stations which showed no significant variations. However, even a dike closest to TAR proposed by Fujita et al. can not properly explain the observation there in terms of the thermal-magnetic nor piezomagnetic effect. The only plausible explanation was the piezomagnetic effect due to the shrinkage of the magma reservoir which continuously feeded magma to the dike intruded into the western sea. Del Negro et al., EPSL, 2004. Fujita et al., Bull. Earthq. Res. Inst., Univ. Tokyo, 77, 67-75, 2002. Sasai et al., J. Geomag. Geoelectr., 1990. Sasai et al., EPSL, 203, 769-777, 2002. Ueda et al., GJI, 161, 891-906, 2005. Ueda et al., EPSL, 245, 416-426, 2006. Zlotnicki et al., 205, 139-154, 2003.

Keywords: dyke intrusion, piezomagnetism, thermal demagnetization

(S) - IASPEI - *International Association of Seismology and Physics of the Earth's Interior*

JSS007

Poster presentation

1965

Magnetic and electric field variations associated with the tilt-step event during the caldera formation of Miyake-jima volcano in 2000.

Dr. Yoichi Sasai

Disaster Prevention Division, Tokyo Metrop. Govt. Disaster Prevention Specialist (Chief) IAVCEI

Makoto Uyeshima, Motoo Ukawa, Jacques Zlotnicki, Eisuke Fujita, Hideki Ueda

In the 2000 eruption of Miyake-jima volcano, central Japan, a new caldera was formed on the summit of the volcano. It started from a sudden depression of the summit area in the existing Hatcho-Taira caldera on July 8. The new sinkhole of 900 m in diameter and 200 m in depth enlarged up to 1.6 km in diameter and 500 m deep until the August 18 largest eruption. A rapid ground deformation called the tilt-step event took place once or twice a day during the caldera formation period (July 8 to August 18), which was a sudden step-like inflation of the volcano edifice followed by a gradual shrinkage for several hours (Ukawa et al., 2000). The velocity waveform of the ground motion was a single sinusoidal wave of 50 seconds duration. The magnetic field showed a step-like change within one minute, which was observed by proton magnetometers at several sites on the island with its measurement interval of 1 minute (Sasai et al., 2002). The electric field also varied with this event as detected by the long baseline (a few km distance) SP measurement system using telephone cables with a sampling interval of 10 seconds. Unlike magnetic case, the electric field showed a single bay-like variation very similar to the velocity waveform (Sasai et al., 2002). Recently, two more clear evidences have been found for the electric and magnetic variations, namely the short-span (150 m) multi-channel SP measurement with 2 seconds sampling on the southwestern side (Zlotnicki et al., 2003), and 3 components magnetic data by two flux-gate magnetometers with 1 second sampling on the north- and south-western side of the volcano. All these EM data are compiled to clarify the generating mechanism of this unique volcano-tectonic phenomenon, which should be essentially related to the caldera formation process (Fujita et al., 2002). Since the time-dependent behavior is different between magnetic and electric signals, the generation source must be different. The magnetic variation is most probably ascribed to the piezomagnetism of rocks due to stress changes, while the electric one to the electrokinetic effect due to the groundwater movement induced by rapid stress changes and/or fluid injection from the pressure source. Fujita et al., 2002, Cyclic jerky opening of magma sheet and caldera formation during the 2000 Miyakejima volcano eruption, *Geophys. Res. Lett.*, 29, 10.1029/2001GL013848. Sasai et al., 2002, Magnetic and electric field observations during the 2000 activity of Miyake-jima volcano, central Japan, *Earth Planet. Sci. Lett.*, 203, 769-777. Ukawa et al., 2000, The 2000 Miyakejima eruption: Crustal deformation and earthquakes observed by the NIED Miyakejima observation network, *Earth Planets Space*, 52, xix-xxvi. Zlotnicki et al., 2003, Resistivity and self-potential changes associated with volcanic activity: The July 8, 2000 Miyake-jima eruption (Japan), *Earth Planet. Sci. Lett.*, 205, 139-154.

Keywords: tilt step, piezomagnetic effect, electrokinetic effect

(S) - IASPEI - *International Association of Seismology and Physics of the Earth's Interior*

JSS007

Poster presentation

1966

A dense aeromagnetic survey on Kuju volcano, central Kyushu Japan

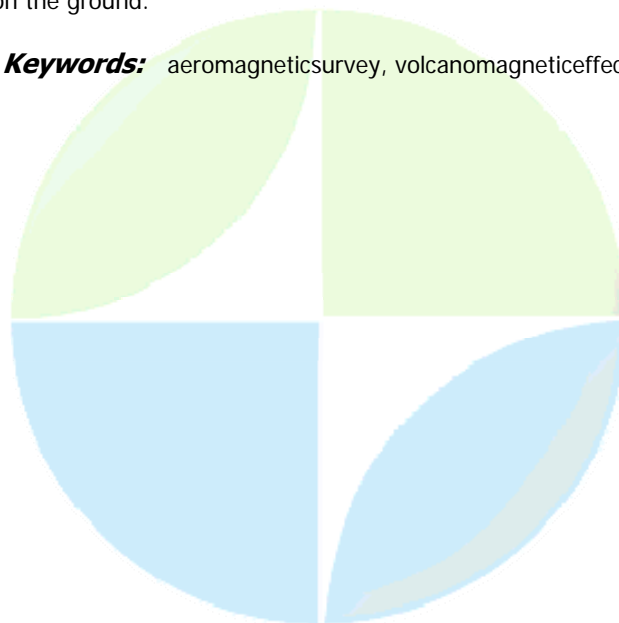
Dr. Mitsuru Utsugi

Aso Volcanology Laboratory Kyoto Univ. IAGA

Yoshikazu Tanaka

Kuju volcano is a one of active volcano on central Kyushu Island, Japan. This volcano is located in the NE of Aso Caldera, and it consists of many stratovolcanoes and lava domes. Kuju volcano is active through Holocene and has several historical eruption records. The historical eruption records do not suggest magmatic eruptions but phreatic or hydrothermal eruptions. Most youngest magmatic eruption, estimated from geological record is about 1.7ka erupted Kurodake lava dome and pyroclasticflow in the eastern part of Kuju. On this volcano, small scale eruption was began at October 11, 1995 in the northern flank of Hossyo dome, the central part of Kuju volcano without remarkable seismicity. About 400m long fissure running west to east effused ash and small lahar. Ash fall was observed in Kumamoto city, 60km NW of the volcano. But activity was decreased soon and in October 12, there was only white vapor fumarole about 400m high. The fissure formed several sub-fissures and craters. They are named a1, a2, a3 craters, and b, c, d, e sub-fissures. Just after this eruption, Kyoto University installed 5 magnetometers around new craters and started continuous geomagnetic field observation. From this observation, very large geomagnetic temporal change was observed. The amplitude of the total change during 1995 to 2006 becomes over 500nT in the maximum. On this volcano, low-altitude aeromagnetic survey was carried out by JMA (Japan Meteorological agency) on Jun. 1996 to observe the subsurface heat anomalies. For from this period to present, magnetic field has changed over 300nT on the ground. To detect this field change, we made very dense aeromagnetic survey on this volcano in Dec. 2004. From obtained data, we calculated upward continuation of observed data, and estimated field intensity on each observation points of last aeromagnetic survey in 1996. Comparing the field intensity of 1996 surveys and estimated value of 2004, the change in a feature pattern was detected. A magnetic field decrease was detected by centering on the northeast of crater chain, which was created by 1995 eruption, on the north side and the pattern of an increase was detected in the south. Its amplitude is about 100 nT in maximum. This pattern and the amplitude are corresponding to the result of obtaining from the observation on the ground.

Keywords: aeromagneticsurvey, volcanomagnetic effect



(S) - IASPEI - *International Association of Seismology and Physics of the Earth's Interior*

JSS007

Poster presentation

1967

Piezomagnetic modeling associated with hydrothermal pressurization.

Dr. Ayako Okubo

Geophysics Research Group Geological Survey of Japan, AIST IAGA

Wataru Kanda

Continuous observations of geomagnetic total intensity have been carried out on many active volcanoes (e.g., Tanaka, 1993; Del Negro et al., 2004). Geomagnetic field variations observed at many volcanoes suggest stress changes, temperature changes and/or inside those volcanoes. Such volcanomagnetic effects are largely controlled by a behavior of volcanic fluids or hydrothermal systems that transport heat and mass from the deep source. Therefore we have developed a postprocessor to calculate the geomagnetic field changes due to the piezomagnetic effect caused by hydrothermal pressurization. Here, we used a 3-D, steady state, poroelastic model, because of the lack of symmetry in stress-induced magnetization. Our method of piezomagnetic modeling are summarized as follows; (1) we computed the elastic effective stress field with the spatial distribution of body forces (due to both gravity and seepage force) and appropriate boundary conditions using the finite element method. (2) On the basis of this calculated elastic effective stress field, distributions of the stress-induced magnetization were estimated from a linear relationship between the magnetization changes and the stress components (Sasai, 1980). (3) Piezomagnetic changes were calculated by using the method proposed by Sasai and Ishikawa (1978). In this study, we carried out numerical experiments on the effect of host-rock permeability and the influence of caprock, as a factor to change the physical state within the volcanic edifice.

Keywords: piezomagnetic modeling, hydrothermal pressurization, postprocessor



(S) - IASPEI - *International Association of Seismology and Physics of the Earth's Interior*

JSS007

Poster presentation

1968

Shallow Resistivity Structure of Asama Volcano and Its Implication for Magma Ascent Process of 2004 Eruptions

Dr. Koki Aizawa

Tokyo Institute of Technology Tokyo Institute of Technology IAGA

Yasuo Ogawa, Takeshi Hashimoto, Takao Koyama, Wataru Kanda, Electromagnetic Research Group For Asama Volcano

Asama volcano, which sits 150km northwest of Tokyo, is one of the most active volcanoes in Japan. Historical records show many eruptions that are mainly characterized by Vulcanian eruptions. Its recent eruptions took place in 2004 at the summit crater without remarkable precursors. Geodetic data and the hypocenter distributions [e.g., Takeo et al., 2006] suggest that magma ascent route is not simple, and the conduit does not directly link the summit crater to deep magma chamber. Because shallow structure may give the constraints on volcanic activities [Tanaka et al., 2002] and can control type of eruptions [Kagiya et al., 1999], imaging the upper part of volcanoes is important. In this paper, we will argue the resistivity structure shallower than 5km obtained by dense magnetotelluric (MT) survey. The MT data were taken along the four survey lines across the volcano. The total number of measurement sites was 74. The resistivity profiles obtained by two-dimensional inversions are mainly characterized by resistive surface layer and underlying conductive layer. Important feature of the profiles is that in a depth range of a few hundred meters to a few kilometers, three resistive bodies exist, being surrounded by highly conductive regions. Two of three resistive bodies correspond to the old eruption centers; one corresponds to the 24ka collapse caldera, and the other does to the 21ka lava dome. Taking into account that the geothermal activities exist near the old eruption centers, the highly conductive zone is considered to be hydrothermal system. In this study, we interpret the resistive bodies as old and solidified intrusive magma that are still driving hydrothermal system in the surrounding area. The solidified magma bodies are considered to be resistive due to its low porosity. Self-potential survey was also conducted along the MT profiles. The obtained SP data show the distinct "W"-shaped SP profiles [Ishido, 2004], and suggests the existence of hydrothermal and hydrogeological zone within the volcano. The SP profiles seem to have correlation with the top surface of the highly conductive regions, which is interpreted as hydrothermal system. The SP data may support our interpretation of the resistivity structure. The resistive body beneath the 24ka collapse caldera is located above the swarm of tectonic earthquakes at the depth of 3km. Geodetic data suggests that magma intruded beneath this resistive body. We suggest that magma ascent was hampered by old and solidified remnant magma at the depth of 3km beneath the collapse caldera, and that a part of the magma migrated horizontally to the east and finally ascended to the summit, resulting in the 2004 eruptions. This study raises the possibility that solidified remnant magma in volcanoes is controlling present magma movement.

Keywords: magnetotellurics, resistivity, self potential

(S) - IASPEI - *International Association of Seismology and Physics of the Earth's Interior*

JSS007

Poster presentation

1969

Magnetic imaging of the feeding system of oceanic volcanic islands: El Hierro (Canary Islands)

Dr. Isabel Blanco-Montenegro

Departamento de Física Universidad de Burgos IAGA

Iacopo Nicolosi, Alessandro Pignatelli, Massimo Chiappini

El Hierro is the youngest of the Canary Islands, a volcanic archipelago in the central Atlantic, near the African coast. The subaerial part of the island shows a characteristic shape with three convergent ridges that have been interpreted as a triple-arm rift system. These ridges are separated by wide, horseshoe embayments, related with the occurrence of at least four giant landslides. Recent works based on high-resolution bathymetry, however, have shown that in the submarine portion of the island the rift structure is much more complex. We have analyzed an aeromagnetic anomaly dataset acquired in 1993 by the Spanish Instituto Geográfico Nacional in order to obtain a structural model of the island from a magnetic point of view. A digital elevation model of the volcanic edifice was divided into a mesh of prismatic cells, each of them with its top corresponding to the topographic height (or bathymetric depth, in the marine area) and its bottom at the constant depth of 4000 m below the sea level. A three-dimensional (3D) inversion algorithm was applied to the magnetic anomaly data that has provided us with a magnetization distribution containing valuable information about the inner structure of the island. We have completed the study with a forward modelling along some representative profiles. The magnetic model has allowed us to obtain new evidences about the rift structure of El Hierro. In particular, high magnetization values have been interpreted as intrusion complexes on which rifts zones are rooted. Their location confirms the hypothesis of a complex rift structure in the marine area, suggesting that sometimes rift axes might be shifted with respect to previous interpretations. In addition, the areas affected by giant collapses are characterized by very low magnetization values, showing that magnetic anomalies can provide fresh information about this kind of catastrophic event.

Keywords: oceanic volcanic islands, magnetic anomalies, intrusion complexes



(S) - IASPEI - *International Association of Seismology and Physics of the Earth's Interior*

JSS007

Poster presentation

1970

Looking at Tenerife (Canary Islands) from a magnetic perspective

Dr. Alicia Garcia

Volcanology Spanish Research Council IAVCEI

Nieves Snchez, Massimo Chiappini, Roberto Carluccio, Riccardo De Ritis, Iacopo Nicolosi, Alessandro Pignatelli, Isabel Blanco-Montenegro

Tenerife is one of the largest and complex oceanic volcanic islands on our planet. A large variety of investigations has been conducted during the last decade aimed at improving the knowledge of the volcanic evolution of the region. After the relevant increase of seismic activity which started in 2004, Spanish and Italian authorities have worked together to establish a research consortium to develop an appropriate plan for assessing the hazard in this region. Remotely sensed data such as high resolution aeromagnetism can shed new light on the volcanic and tectonic setting. This technique is, in fact, particularly suitable to study these areas due to the high magnetic contrasts linked to volcanic structures. Furthermore, surveying poorly accessible sites with airborne geophysics can be expeditious and effective. Joint Spanish and Italian efforts have been therefore ongoing to study the area from a magnetic perspective, acquiring new data during April 2006. A towed-bird, optically pumped magnetometer was used in a high resolution helicopter-borne magnetic survey which was conducted all over Tenerife and its marine surrounding sector. The obtained magnetic anomaly images, compiled at the geomagnetic epoch 2006.4, reveal a complex pattern which is suggestive of the composite evolution of the entire system.

Keywords: magnetic anomalies, teide, aeromagnetism



(S) - IASPEI - *International Association of Seismology and Physics of the Earth's Interior*

JSS007

Poster presentation

1971

Lightning and electrical activity during the 2006 eruption of Mt. Augustine

Prof. Ronald Thomas

none none IASPEI

S.R. McNutt, G. Tytgat, P.R. Krehbiel, W. Rison, H. Edens

We observed a sequence of lightning and electrical activity during one of Mount St. Augustine's eruptions by using a combination of radiofrequency time-of-arrival and interferometer measurements. The system was developed and has been used to study lightning during thunderstorms. In thunderstorms we obtain a detailed 3-D picture of each lightning flash. For a storm these give us information to identify the charge structure in the cloud. For thunderstorm studies we use at least 8 ground receiving stations, but for Mount St. Augustine we were only able to setup two stations. With two stations we were able to determine the azimuthal direction to the sources, their power, the time history and relationship to other pulses. On one lightning flash we used an interferometric effect to infer altitude. The observations of Augustine volcano indicate that the electrical activity had two modes or phases. First, there was an explosive phase in which the ejecta from the explosion appeared to be highly charged upon exiting the volcano, resulting in numerous apparently disorganized discharges and some simple lightning. The net charge exiting the volcano appears to have been positive. The second phase, which occurred in the plume that followed the most energetic explosion, produced conventional-type discharges. Although the plume cloud was undoubtedly charged as a result of the explosion itself, the fact that the lightning onset was delayed and continued after and well downwind of the eruption indicates that in situ charge separation charging of some kind was occurring, presumably similar in some respects to that which occurs in normal thunderstorms.

Keywords: lightning, volcano, electromagnetic



(S) - IASPEI - *International Association of Seismology and Physics of the Earth's Interior*

JSS007

Poster presentation

1972

A magnetotelluric study along Satluj valley thermal springs in NW Himalaya

Dr. Abdul Azeez K. K.

MT Division National Geophysical Research Institute, India IAGA

K. Ravi Shankar, Dhanunjaya Naidu, Sharana Basava

Northwestern part of the Indian Himalaya depicts the most complex tectonic structures resulted from the Cenozoic India-Asian collision and the subsequent underthrusting of Indian plate that resulted in the Himalayan mountain range. There are not many attempts to understand the geophysical signatures related to the deep structure of the Indian Himalaya that can provide more insights to the tectonic settings in the region. We present the magnetotelluric (MT) study carried out along the Sutluj valley thermal springs in NW Himalaya. The Sutluj valley crosses major tectono-stratigraphic units of the Himalaya and evidence active geodynamics in the form of seismicity and hot springs. The present ENE-WSW trending MT profile, parallel to the Sutluj valley, spans over the Lesser Himalayas, Higher Himalayan Crystallines and Tethys Himalayas. The profile cut across the Main Central Thrust (MCT) a major tectonic feature in the Himalaya that separate Higher Himalayan crystallines with the Lesser Himalayas. Broad Band MT measurements are made at 17 locations along the profile with an average site spacing of 10 km. The data are processed with robust algorithms to obtain the MT impedance estimates. The MT impedances are analyzed to determine the electrical strike in the area and inverted using a non-linear conjugate gradient algorithm to deduce the two-dimensional conductivity distribution along the profile. The obtained conductivity structure is described and its tectonic implications on the thermal manifestations in the area are discussed.

Keywords: magnetotelluric, thermal springs, himalaya



(S) - IASPEI - International Association of Seismology and Physics of the Earth's Interior

JSS007

Poster presentation

1973

A shallow resistivity structure of Kuju Volcano, Central Kyushu, Japan

Dr. Wataru Kanda

Sakurajima Volcano Research Center DPRI, Kyoto University IAGA

Yoshikazu Tanaka, Mitsuru Utsugi, Yasuaki Okada, Hiroyuki Inoue

Kuju volcano is a composite volcano, consisting of more than 20 lava domes or cones, located on central Kyushu, Japan. In Oct. 1995, a phreatic explosion occurred after a few hundred years of dormancy with opening of several new vents at the eastern flank of Mt. Hossho, one of the domes of the Kuju complex. The new vents were located about 300m south of a pre-existing fumarolic field called Iwo-yama. The activity continued to middle of 1996 with occasional ash ejections. Although seismicity around Mt. Hossho showed a decreasing tendency after 1995 to 1996 eruptive activities, fumarolic activity around Iwo-yama has been still in high level. Heat discharge rate has been estimated as 500-1000 MW that is several times higher than that before eruption (~100MW). Proton-precession magnetometers were installed shortly after the 1995 eruption to obtain the continuous records of the total intensity (Tanaka et al., 1996). Total intensities showed rapid increase at sites located south of the pre-existing fumarolic area, while it decreased at a site located north, indicating that magnetization of the volcanic rocks occurred beneath around Iwo-yama area by cooling. We conducted Audio-frequency MagnetoTelluric (AMT) surveys in Aug. 2005 and 2006 around Iwo-yama area. The data were successfully collected at 22 locations and interpreted by 2-D inversion (Ogawa and Uchida, 1996). Although the data quality was not good at the marginal sites of the section, following features of resistivity structure were obtained. (1) High resistivity of several hundreds to a thousand ohm*m is found near the surfaces of the profile, which correspond to the andesitic lavas of Mt. Hossho and Naka-dake. This surface layer is thicker at the northern flank of Mt. Hossho where two lava-flow units are seen. (2) Conductive layer of less than 3 ohm*m is seen at the depths between 200m and 600m beneath the northern flank of Mt. Hossho and beneath Naka-dake. This conductive layer is mainly composed of hydrothermally altered rocks and also contains ground water. It appears to be shallower near the fumarolic area, indicating that high temperature zone is inflated due to higher heat flux related to intense fumarolic activity of Iwo-yama. (3) Relatively resistive zone of 10 - 30 ohm*m lies beneath Iwo-yama area. This less conductive body seems to decouple the conductive layer. Magnetization source is located at this part. Since the highest fumarolic temperature still exceeds 200 degrees, this less conductive body may be vapor rich zone. Gravity data suggested that a great amount of water has flowed into the shallow part beneath the pre-existing fumarolic area. The estimated resistivity section is consistent with this idea. Since water contained in the conductive layer has flowed into and cooled the less conductive zone, geomagnetic variations have shown a cooling process. However, high temperature magmatic gases have been still supplied from the deep thermal source to Iwo-yama area, so that the central part of the less conductive zone is still in high temperature state.

Keywords: resistivity, fumarolic activity, phreatic eruption

(S) - IASPEI - *International Association of Seismology and Physics of the Earth's Interior*

JSS007

Poster presentation

1974

**Multi-electrode resistivity surveys around a cyclic hydrothermal system:
the hot lakes of the Waimangu geothermal area, New Zealand**

Mrs. Aurlie Legaz
IASPEI

Andre Revil, Jean Vandemeulebrouck, Tony Hurst

We conducted a series of multi-electrode surveys around the Waimangu hydrothermal area (New-Zealand), using 1.26 km of cable with 20 m electrode spacing. The resistivity survey had two aims, firstly to obtain a better picture of the structure and thermal state underlying the current thermal activity, and secondly to see whether we could detect changes in resistivity under Inferno Crater Lake, a main feature of the valley, which displays a cyclic behaviour in temperature and level (about 30 days). Direct current electrical resistivity measurements were performed along two profiles; a Wenner configuration gave the most consistent results, producing a detailed image of the electrical resistivity in the top 200 metres. Along the first outline, there were very low resistivity zones under recently active thermal areas. Surface low resistivity areas were globally well correlated with high temperatures and high CO₂ fluxes. Two surveys were conducted on the second outline, past Inferno Crater, at different stages of the Inferno cycle: we observe resistivity changes near the crater, indicating hydrothermal fluid movement associated with the cycling of Inferno Crater, which was overflowing during the first survey, but was a couple of metres lower by the time of the second survey. This work was primarily to further investigate the cyclic behaviour of Inferno Crater Lake, but also gives an indication of the sensitivity and repeatability of resistivity techniques in shallow geothermal environments; Inferno Crater can be considered as a textbook case, which gives us an insight into the displaced volume of fluid, through the cycles. Therefore, the interest of the study is to measure the electrical response of observed subsurface fluid movements, with a view to generalising the method to volcanic and geothermal environments.

Keywords: resistivity, hydrothermal environments, fluid movements



(S) - IASPEI - *International Association of Seismology and Physics of the Earth's Interior*

JSS007

Poster presentation

1975

Temporal changes of resistivity and self potential at the Onikobe geyser, NE Japan

Prof. Yasuo Ogawa

Volcanic Fluid Research Center Tokyo Institute of Technology IAGA

Seiji Mishima, Keisuke Saho

A geyser, as a proxy for a volcano, is useful in studying the fluid dynamics for an phreatic eruption using geophysical measurements. We have studied the temporal changes of resistivity and self-potential at Onikobe geyser, Northeast Japan, in order to understand the fluid dynamics of the geyser. We deployed 23 potential electrodes around the Onikobe geyser and 5 current electrodes to inject DC current (200-300mA). We could monitor the resistivity and self potentials at 23 potential electrodes at every 2 seconds using 24bit seismic data loggers. We have observed the decrease (up to 5%) of apparent resistivity starting from approx 15 seconds prior to the effusion. The spatial pattern of the decrease does not have a simple radial symmetry, but in general closer sites to the pit have larger amount of decrease. On the other hand, if we inject current in another location 5m away from the vent, then we observed increase of apparent resistivity at the time of the effusion. The larger increase was centered at the opposite side of the current injection location. This puzzle was qualitatively solved using the three-dimensional resistivity modeling utilizing FEM. The final model showed that at the effusion the vacant space beneath the pit is filled with mixture of vapor and hot water. Self potential source was investigated for typical phases of the effusion cycle. The most significant SP increase was observed just after the effusion and modeled point current source as sought at 4m below surface at 4m away from the pipe, which means that the fluid is supplied to the reservoir though porous media causing electrokinetic effect. The SP decreases as the reservoir is filled. Just before effusion, as the fluid goes into a shallow minor plumbing system, another small current source appears. During effusion, the vapor-fluid interface is responsible for the divergence of the drag current and it is located at the casing pipe.

Keywords: geyser, resistivity, self potential



(S) - IASPEI - *International Association of Seismology and Physics of the Earth's Interior*

JSS007

Poster presentation

1976

Self-potential anomalies around Ontake volcano, Central Japan - the earthquake swarm and summit areas -

Dr. Ryokei Yoshimura

Disaster Prevention Research Institute Kyoto University IAGA

Ken'Ichi Yamazaki, Yasuaki Okada, Naoto Oshiman, Makoto Uyeshima

Ontake stratovolcano is located in the southern end of the Norikura Volcanic Chain, central Japan, close to the junction of the Izu-Bonin and Mariana and Southwestern Japan volcanic arcs. It is almost conical and made of andesite. Earthquake swarm activity has been continuously observed around the eastern flank of Ontake since 1976. A phreatic explosion occurred in 1979 at a fissure on the southwestern slope of the Kengamine, the main peak of Ontake. And a large earthquake with the depth about 2 km and a magnitude of 6.8 occurred in 1984 in the southeastern flank of the volcano. Recently, Kimata et al. (2004) revealed uplift ground deformation above the earthquake swarm area by using repeated leveling. Furthermore, Magnetotelluric soundings estimated a low resistivity region with the depth about 2km beneath the uplift area [Kasaya et al., 2002]. In order to investigate a relationship between tectonic movements and subsurface low resistivity zone, we carried out self-potential (SP) measurements from 2003 and 2006 around the earthquake swarm and the summit areas of Ontake volcano. As the result of SP measurements around the seismic swarm area, a torus-shape positive SP anomaly has been detected at the eastern part of survey profile. This anomaly is located between recent active clusters of earthquakes and near the ground uplift detected by Kimata et al. [2004]. They suggest that the uplift is associated with a region of low resistivity [Kasaya et al. 2002] and anomalous increases in chemical compositions of springs [Tanaka et al. 2003], imaging potential shallow hydrothermal activity. Generally, an upflow caused by a hydrothermal convection produces positive current sources in the direction of flow. The comprehensive positive sense anomaly supports potential shallow hydrothermal activity. Recently, we established a continuous SP observation network with the aim of monitoring the hydrothermal activity by reference to the obtained SP distribution. This network uses metallic telephone lines for measuring SP with 1 sec sampling. We also found the positive sense anomalies up to about 2V p-p around the northern part of summit area. This large anomaly may be not irrelevant to recent eruption vents. Younger vents are located near the positive anomalies. In this presentation, we will report a detail of SP results and introduce outline of continuous SP observation network which has been started since late February, 2007.

Keywords: self potential, ontake volcano, earthquake swarm

(S) - IASPEI - *International Association of Seismology and Physics of the Earth's Interior*

JSS008

1977 - 2021

Symposium

**Progress in electromagnetic studies on earthquakes and volcanoes -
Electromagnetic fields associated with earthquakes and active faulting**

Convener : Dr. Malcolm Johnston

Electromagnetic fields are both expected and observed during seismic and aseismic fault rupture. Furthermore, as a consequence of this rupture, secondary fields are generated by coupling of ground motion into the atmosphere and ionosphere. These phenomena relate directly and indirectly to source processes driving these tectonic events and may reflect the roles of fluids in active faulting. Unfortunately, not all aspects of these measurements, or theories proposed to explain them, are well understood. This session will focus on the following areas of investigation: 1) Measurements of electric and magnetic fields near and during active faulting; 2) Heterogeneity in electromagnetic structure around seismic and aseismic rupture region including lower crust; 3) Controlled laboratory observations and observations from natural laboratories such as dam loading/filling, and crustal loading/failure; 4) Theoretical considerations regarding source generation mechanisms; 5) Measurement resolution, data quality, identification, separation and removal of spurious signal sources; 6) Multi-parameter measurements (strain, tilt, pore pressure, displacement, etc) together with EM measurements that can place better constraints on the physics of source processes before, during and after earthquakes.

XXIV2007

PERUGIA
I T A L Y



(S) - IASPEI - *International Association of Seismology and Physics of the Earth's Interior*

JSS008

Oral Presentation

1977

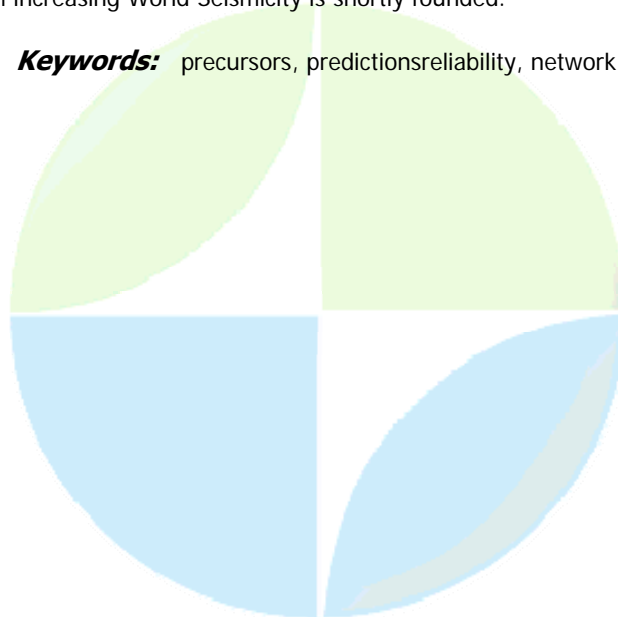
On the complex earthquake precursors research and reliability test of predictions regional/global NETWORK- collaboration PrEqTiPlaMagInt

Prof. Strachimir Cht. Mavrodiev

Theoretical and Environmental physics INRNE, BAS, Sofia IASPEI

Some results of collaboration PrEqTiPlaMagInt, which is trying to create the earthquake research and prediction NETWORK in Balkan-Black Sea region are presented: The correlation between geomagnetic quakes and the incoming extremum (minimum or maximum) of tidal gravitational potential (there is unique correspondence between the geomagnetic quake signal and the maximum of the monitoring point of the energy density of the predicted earthquake). The statistic evidence for reliability of geomagnetic quake as reliable time earthquake precursor is based on distributions of the time difference between time of occurred and predicted earthquakes for the period 2002- 2006 for Sofia region and 2004- 2006 for Skopje. The predictions are valid for the earthquakes with magnitude greater than 3 at distance up to some 700- 800 km. The distance dependence of the prediction accuracy on the magnitude is presented. A reliability of predictions made for the 2006 spectral earthquake numbers, The possibility for systematic of earthquake parameters Richter Magnitude, Seismic Moment, Intensity and Depth, The World statistic of tide-earthquake correlation for different depth and magnitude, The model of the increasing World seismicity as consequence of Anthropogenic Global Warming. A regional NETWORK for prediction the earthquakes time, place (epicenter, depth), magnitude by using reliable precursors is proposed and shortly analyzed. The researching of precursors is based on complex geophysical monitoring under, on and above Earth surface and usual seismological monitoring of the region. The proposed investigation for establishing of regional NETWORK is based on contemporary data acquisition system for preliminary archiving, testing, visualizing, and analyzing the relevant geophysical data. The theoretical part of the Project include wide interdisciplinary research based on the unification of standard Earth sciences and using of nonlinear inverse problem methods for discovering the empirical and hidden dependences between variables. By means of special software the complex environmental and real time analyzed Satellite data can be used to prepare regional daily risk estimations. A proposal for including in the Stern estimation for economical costs because of Global Warming the cost from increasing World Seismicity is shortly founded.

Keywords: precursors, predictionsreliability, network



(S) - IASPEI - *International Association of Seismology and Physics of the Earth's Interior*

JSS008

Oral Presentation

1978

ULF seismomagnetic signals analysis

Prof. Valery Korepanov

Laboratory for EM Investigations Lviv Center of Institute of Space Research IAGA

Baldev Arora, Fedir Dudkin, Gautam Rawat, Ashok Sharma

The existence of electromagnetic (EM) precursors of earthquakes (EQ) is widely discussed. The EQ EM precursors in ULF band are the most promising between the known ones. They generally are based on movement of conductive fluid or charges in the Earth's magnetic field (inductive effect), piezoelectric or piezomagnetic effects. However the problem of their reliable detection has not yet been solved first of all because of low level of precursor signal and of the comparatively high level of ambient EM interference. Many examples of their observations before the EQ are given in the scientific papers as well as in many cases the EQ occur without preliminary EM activity. So, it appears that these precursors are very different in their peculiarities and they vary not only at diverse places but also for different time even in the same place. Apparently this fact depends on the specifics of geological formation and the types of EM signal source in seismoactive zones and yields a rather modest progress in EQ prediction practice. This report is an attempt to explain some experimental facts with observed seismogenic ULF emissions. First the model of the source of EM variations connected with EQ preparation process is proposed and discussed. It is shown that the range of distances for which the components of anomalous EM field are detectable mainly depends on the signal-to-noise ratio at the observation place. The approach to the determination of the EQ epicenter location is proposed based on multi-points observations of ULF electromagnetic signals collected in the monitored area. The main principle of the data processing using this method is based on the assumption that at relatively small distance between EQ epicenter and observation points (no more than 100-200 km), we are always in near zone of electromagnetic wave propagation what allows us to use as informative carrier only signal amplitude. This peculiarity can be used for enhancing the signal-to-noise ratio by processing simultaneously the time-synchronous signals collected in different points. To realize this efficiently, the critical requirements to the observation system are discussed. The design features of the automatic ULF observation system LEMI-30 with large dynamic range and free from time mismatch necessary for continuous monitoring of EQ EM precursors are discussed and the example of its practical realization is presented. Some known examples of ULF magnetic pre-EQ activity successful registration are analyzed and a new multi-points observations results obtained with LEMI-30 systems in India during medium magnitude EQs at Koyna active fault are reported. This study was partially supported by STCU grant 3165.

Keywords: electromagnetic, precursor, earthquake

(S) - IASPEI - *International Association of Seismology and Physics of the Earth's Interior*

JSS008

Oral Presentation

1979

Re-examining the reported magnetic precursor to the 1989 Loma Prieta earthquake using magnetic field data collected in the US and Japan during September and October 1989

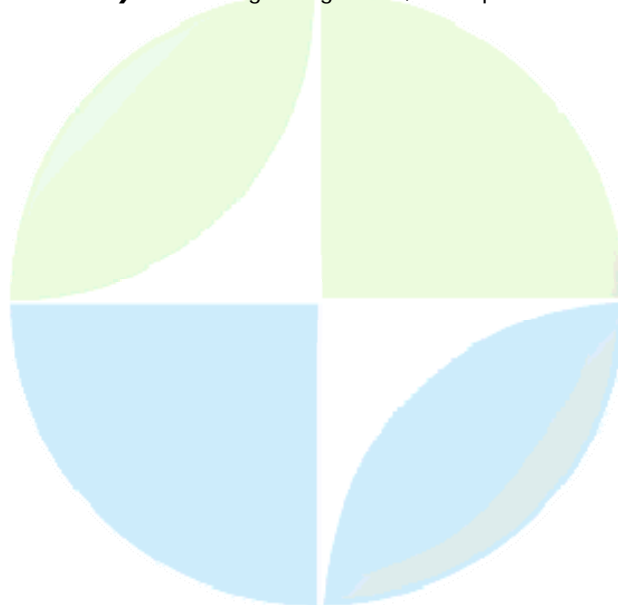
Dr. Jeremy Thomas

National Geomagnetism Program USGS Denver, CO IAGA

Jeffrey J. Love, Malcolm J. S. Johnston

One of the most well-known and perhaps the most compelling reports of an electromagnetic precursor is the ultra low frequency (ULF, 0.01-10 Hz) magnetic variations measured prior to the Ms 7.1 Loma Prieta earthquake of October 17, 1989 in Northern California by Fraser-Smith et al., 1990, GRL, 17, 1465-1468 (referenced as FS90). According to FS90, an ULF search coil magnetic field sensor (magnetic latitude of 42.70), located 7 km from the epicenter, measured unusual activity for more than a month prior to the earthquake. A later study by Campbell, 2005, Eos Trans. AGU, 86(18), Abstract GP23A-01, using USGS magnetic observatory data, reported that the claimed precursory activity was probably not related to the earthquake, but was, instead, driven by solar-terrestrial phenomena. In this paper, we present geomagnetic-field data measured by the Kakioka Magnetic Observatory in Japan and by the USGS in Fresno and Tucson prior to, and during, the Loma Prieta earthquake. The 1-second magnetic field data from Kakioka (magnetic latitude of 28.90 and 8,284 km from the epicenter) are filtered into several frequency band-pass channels for direct comparison with the precursory activity reported by FS90. The 1-minute magnetic field data from Fresno and Tucson (magnetic latitudes of 43.2 and 39.90 and distances of 201 and 1,162 km from the epicenter, respectively) are filtered just below the frequencies reported by FS90, since the data rate at these observatories was too slow for a direct comparison. We investigate these data and explore whether the claimed precursor was a local, regional, or global phenomenon. We briefly present more recent measurements of ULF magnetic fields at similar band-passes to FS90 to quantify the typical noise background at these frequencies. Based on our analyses, we discuss the likelihood of possible sources for the claimed magnetic precursor, such as magnetospheric activity, man-made noise, and processes related to the earthquake.

Keywords: geomagnetism, earthquakes



(S) - IASPEI - *International Association of Seismology and Physics of the Earth's Interior*

JSS008

Oral Presentation

1980

Comments on seismomagnetic effects from the long-awaited 28 September 2004 M6.0 Parkfield earthquake by M.J.S. Johnston, Y. Sasai, G.D. Egbert, R.J. Miller

Prof. Panayiotis Varotsos

Physics Department University of Athens IASPEI

Seiya Uyeda

Johnston et al. [1] list four criticisms on Seismic Electric Signals (SES) [2]. (1) There are no similar co-seismic signals observed when the primary earthquake energy is released. Actually, signals at the time of EQ observed routinely in Greece, Japan, Indonesia and even at Parkfield were all co-seismic wave. However, this does not negate SES. SES generation takes place during the slow stress increase and has little to do with sudden stress release. Why stress release does not generate observable signals is a separate question. (2) No clear physical explanation exists describing how the SES signals can relate to EQs occurring sometimes hundred of kilometers away. This statement is untrue. Structural inhomogeneity may be the key: The EQ fault may be orders of magnitude more conductive than the surrounding, providing a conductive path for SES[2]. This explains why SES reveals the so called selectivity. In other words, unless the observation point is at a sensitive site, SES can not be observed. (3) no independent data (strain, seismic, pore pressure etc) exists that supports the proposed earthquake/SES relationship. Again, these authors do not seem to understand the SES generation mechanism well. SES is a critical phenomenon in the sense that it is generated when the stress reaches a certain level, requiring no sudden changes. Some geophysical parameters may coincidentally show anomalies. In fact, recent studies by natural time analysis have shown that pre-mainshock seismicity exhibits important changes just after SES, but that is not a prerequisite for SES generation. (4) The SES signals have the form expected from rectification/saturation effects of local radio transmissions (Pham et al., 1998). However, Pham et al.[3] argument proves nothing[4]. They observed SES-looking noises in Greece and stated that what we observe were all such noises. We also observed them but have discarded by applying our noise discriminating criteria. Johnston et al. did not see SES at Parkfield EQ. Their results from a single station alone do not prove that SES did not exist. As stated above, SES are recorded only at a sensitive site, whereas they have not made any selective site search. Thus, it seems much too premature to conclude either Parkfield EQ was not preceded by SES or useful prediction of damaging earthquakes seems unlikely using electromagnetic data. [1] M.J.S. Johnston et al., BSSA. 96, no.4B, S206-S220 (2006). [2] P. Varotsos, The Physics of Seismic Electric Signals, TerraPub, Tokyo, 338pp (2005). [3] V.N. Pham et al., GRL. 25, 2229-2232 (1998). [4] N. Sarlis et al., GRL. 26, 3245-3248 (1999).

Keywords: seismic electric signals, parkfield

(S) - IASPEI - *International Association of Seismology and Physics of the Earth's Interior*

JSS008

Oral Presentation

1981

New approaches of the monitoring of porosity, permeability, shear and bulk modulus and dynamic viscosity of the pore fluid in vicinity of seismoactive fault zone

Prof. Mikhail Gokhberg

Igor Garagash, Nikolai Kolosnitsin

New method of seismoactive region parameters like porosity, permeability and shear modulus is proposed by means of extraction of the electric component related with tidal oscillations. Theoretical models are developed which show that the electric fields are connected with inhomogeneous petrophysical properties of the crust (both in vertical and horizontal direction). Generation of the electrotelluric field (ETF) by geodynamic processes in the earth crust is considered. It is supposed that the ETF arises due to electrokinetic effect caused by deformation of the earth crust. Based on this model, the new technique of the ETF measurement is proposed. The possibility to use the electrical fields caused by the tidal waves for calibration of the measurements is also considered. It is shown that the tidal variations of the pore pressure and electrical fields essentially depend on medium permeability, porosity, and viscosity of a fluid. It is also shown that by using observations of the field it is possible to determine mechanical and petrophysical properties of deformable medium. Examples of extraction of electric field components from the long-term observations are given

Keywords: electric, petrophysical, mechanical

PERUGIA
ITALY



(S) - IASPEI - International Association of Seismology and Physics of the Earth's Interior

JSS008

Oral Presentation

1982

Dynamic Seismo-Electromagnetic Effects.

Dr. Malcolm Johnston

Earthquake and Volcanic Hazards U.S. Geological Survey IASPEI

Karl Kappler

Electromagnetic (EM) signals during earthquakes are expected to result from dynamic stress field radiation and sensor movement driven by ground motion. In the epicentral region, small signals at the time of rupture initiation might also be expected from direct EM radiation from the source. EM signals preceding rupture may also occur from initiation of the fault failure process but these are likely to be smaller than those associated with the main seismic energy release. High-resolution EM data within a kilometer of the San Andreas fault and directly above the end of the rupture from the recent M6 Parkfield, California earthquake on September 28, 2004, allows some quantification of these various processes. During the earthquake, the EM instruments operated continuously at 40 sps as the rupture propagated below the buried sensors. A second EM system installed 115 km to the northwest allows correction for large-scale common-mode noise from the ionosphere and magnetosphere. The resolution of magnetic fields at 1 Hz was about 3 picotesla while that in electric field was about 6 microvolt/km. A search for direct source rupture effects expected at this site up to 3 seconds before the P wave arrival shows no apparent signal above the noise during this time. Magnetic and electric field "seismograms" occurred during the seismic wave arrivals with peak-to-peak (P-P) magnetic signals of about 0.4 nT in the north and east directions and 8 nT in the vertical and P-P electric signals of about 60 microvolts/km in the north and east directions. These appear to track the ground velocity seismograms closely with the peak amplitudes occurring during the larger S wave arrivals. Regarding different contributions to the EM seismograms, preliminary models show that stress changes from the dynamic radiation field could generate local oscillating fields of 0.1 nT. In comparison, expected sensor translation of up to 30 cm/sec in a resistive medium of about 3.0 ohm-m through the Earth's geomagnetic field could generate magnetic and electric fields of 0.1 nT and less than 100 microvolts/km, respectively, in the EM seismogram. While we are attempting to predict and remove translation and rotation effects, at this point both crustal stress cycling and sensor translation/rotation are apparently important contributors to these signals. Regarding precursory behavior, these EM data show no indications of unusual noise above the 95% confidence limits of 20 picotesla and 20 microvolts/km, respectively, in the ultra-low-frequency (ULF) bands (0.01 Hz to 20 Hz) during the week before the earthquake. This conflicts with suggestions that magnetic noise some 50 times larger may have preceded the 1989 ML7.1 Loma Prieta earthquake and electric fields some 1000 times larger may have preceded earthquakes of this magnitude in Greece. On the other hand, static offsets at this site caused by the earthquake corresponded to about 0.2 nT as expected from geodetic and seismological models of the earthquake assuming a total remanent and induced magnetization of 2 A/m in the medium and a stress sensitivity of 0.002/MPa.

Keywords: dynamic seismogram, electromagnetic, earthquake

(S) - IASPEI - International Association of Seismology and Physics of the Earth's Interior

JSS008

Oral Presentation

1983

MT 3D modeling of seismogenic zone Duzce in NW Turkey. Rokityansky I.I., Savchenko T.S., Tank S.B.

Mr. Tymur Savchenko

In 1999 two catastrophic earthquakes: Izmit and Duzce occurred in the western part of the North Anatolian Fault Zone. In 2005 joint Turkish-Ukrainian team made MT observations in 17 sites in the Duzce seismogenic zone. Results of the processing, MT tensor analysis and 2D inversion were presented at 18th EM Workshop at el Vendrel, Spain, September 2006 (Kaya et al., 2006). Results of 2D inversion of E- and B-polarization MT data yield very good conducting crustal layer with integral conductance several thousands Simenses under northern part of NS profile. Such conductor must create strong magnetovariational anomaly at periods several hundreds – few thousands seconds. But induction vectors do not support the existence of such anomaly. This contradiction of MTS and MVP data in the framework of 2D approach leads us to supposition that MT field behavior is essentially 3D at long periods. This idea also supported by parameter Skew at long periods. At short periods $T < 0.1-1$ s, parameter Skew is small, additional impedances are much smaller than principal ones and data can be considered as 1D. In this approach interpretation was made for every site and conductivity distribution of uppermost sedimentary layer along profile was received (Rokityansky et al., 2007). Having rather complex data along a profile we do not hope to get reliable results of 3D inversion. So, we preferred the direct problem 3D modeling, selecting 3D model to fit the results of short period data 1D inversion and manipulating parameters of upper layer outside of profile by qualitative consideration of the shunting effect. Shunting effect is a reduction of electric field (and MTS RHO curve) in surface conductor because of electric charges accumulation at the conductor edges. The effect is well studied for B-polarization in 2D and this result can be qualitatively applied for 3D situation. 6 northern sites of the profile are located in sedimentary basin with specific resistivity 2 Ohmm and integral conductance around 300 S. The northern MTS curve pxy rises much steeper than eastern curve pyx and their difference attain 1.8 orders at long period 500-1000 s. It can be interpreted as small shunting effect for pxy and much stronger one for pyx. The sedimentary basin in the area is almost isometric (30 km from N to S, 40 km from E to W). We supposed that eastern and western borders of the basin are high resistive (we accepted it in the starting model be 2000 Ohmm, but in the final model it was reduced to 600 Ohmm) while northern and southern borders do not prevent free current flow in N-S direction. We have no information to the North from our profile and supposed that surface layer has resistivity 5 Ohmm that sufficient for minimization of shunting effect. In the southern direction we have observations and know that near surface resistivity rise up to 1000 Ohmm at the distance 5 km from sediments under sites 1-6. It means that currents can flow in the southern direction only at some depth. We introduced vertically submerging to the depth 10 km conductor under site 6, which exactly coincide with North Anatolian Fault Zone active during Duzce earthquake 12.11.1999, and continued to the South as horizontal layer at the depth 10 km with conductance 100 S. Using code (W. Siripunvaraporn, G. Egbert, M. Uyeshima, 2006) we calculated 7 3D models with slightly varying parameters to improve the fitting with really observed impedance tensor. The fitting was satisfactory and we make the conclusion that North Anatolian Fault zone under site 6 together with southward deep conductor provides outflow of NS currents from sediments under sites 1-5 in the southern direction. The system of vertical and horizontal conductors can be replaced by fault steeply submerging in south direction.

Keywords: 3dmodeling, seismogeniczones, mts

(S) - IASPEI - *International Association of Seismology and Physics of the Earth's Interior*

JSS008

Oral Presentation

1984

Three dimensional resistivity structures in intra-plate earthquake zones in Hokkaido, northern Japan

Mr. Hiroshi Ichihara

Institute of Seismology and Volcanology Hokkaido University IASPEI

Toru Mogi, Ryo Honda, Yusuke Yamaya

Clarifying heterogeneous subsurface structures in intraplate earthquake areas is an important element in understanding mechanisms of the intraplate earthquakes, i.e. how/where the stress concentrates and how/where the fault ruptures. In this paper, we focus on two intraplate earthquake areas in Hokkaido district, Northern Japan. Hokkaido locates in a complex tectonic setting, where the Okhotsk, Pacific and Amurian plate are colliding with each other. One of the intraplate earthquake areas is Teshikaga region where there had been occurring 12 large earthquakes ($> M5$) during 1938 and 1967 (Hirota, 1969). Teshikaga region is located in a volcanic belt formed along the northern margin of the fore-arc sliver of the Kurile arc. The other one is focal area of the 2004 Rumoi-nanbu earthquake (MJMA 6.1), located near the boundary between the Okhotsk and Amurian plates. In order to image heterogeneity of the crustal structure, we performed wide-band MT surveys around these intraplate earthquake areas. As a preliminary study, several 2-D resistivity models were analyzed. In both areas, these resistivity profiles were compared with gravity data and geological structure to discuss relationships between the intraplate earthquakes and crustal structures. In Teshikaga region, a high resistivity (> 300 ohm-m) body is imaged at 0-5 km in depth with a horizontal width of 10-20 km, in the focal area of most of the 1938-1969 earthquakes. Comparisons with borehole (NEDO, 1985) and density structure indicate that the high resistivity zone seems to represent Miocene volcanic rocks. On the contrary, conductive zones, which are regarded as Quaternary-Pliocene sediments, are distributed around the resistive body. This suggests that the earthquakes occurred around boundary between rigid rocks and non-rigid rocks by stress concentration to the heterogeneity. The 2-D models also clarified that the fault of the 1938 earthquake corresponds to the wall of the Kutcharo caldera. Three profiles of 2-D resistivity images were obtained around the focal area of the 2004 Rumoi-Nanbu earthquake. All images are roughly comprised of two layers: upper conductive layer, existing surface to 3-5 km in depth, and lower resistive layer. Comparisons of the resistivity image with the surface geology and drilling data indicate that the upper conductive layer and the lower resistive layer correspond to Cretaceous-Tertiary sediment rocks and older igneous rocks, situating as its basement, respectively. On the basis of this correspondence, we found a clear upheaval structure in one profile across center of the focal area. This structure implies steep variation in rigidity around the focal area. The rigidity variation suggests local accumulation of strain, which probably triggered the earthquake. The gravity anomaly (Honda et al., 2007) and the anticline structure observed in surface geology indicate that this structure extends along strike direction of the fault. In order to clarify above subsurface structures including along strike variation, we constructed three dimensional resistivity structure using 44 sites and 29 sites of magnetotelluric data at Teshikaga and Rumoi area, respectively. The resistivity modeling was operated using the 3-D forward modeling code developed by Fomenko and Mogi (2002). Around these seismogenic zones, both models show heterogeneous structures, where resistive body surrounded by conductive zones. The 3-D analyses also resolve incoherencies in 2-D modeling and result in accurate modeling. This enabled us to discuss lower crustal heterogeneity under the focal area, resistivity of which is difficult to detect because of existence of shallower conductive layers.

Keywords: magnetotelluric, intra plateearthquake

(S) - IASPEI - *International Association of Seismology and Physics of the Earth's Interior*

JSS008

Oral Presentation

1985

Seismomagnetic investigations in Serbia and its future

Mrs. Milena Cukavac

Seismomagnetism Geomagnetic Institute IASPEI

Seismomagnetic method of investigations is one of various methods of investigations seismic activity in epicentral regions. In the complex of geophysical and other methods for investigation various appearance connected with preparation and manifestation of earthquake, seismomagnetic investigations have very important role. Tectonic deformations or movements in the Earth's crust can be related to certain changes in magnetization which are registered in local changes of geomagnetic field near a tectonically active region. Supposed relation should be supported by detected anomalies in some other geophysical or physical fields or parameters as well. There is presently no recognizable pattern of occurrence of precursory phenomena. We need long-term measures of precaution against earthquakes. Repeated geophysical surveys (for instance seismomagnetic survey) are required for revealing temporal variations of physical rock properties associated with the accumulation of stress. Changes in earth's magnetic field observed prior to earthquakes are to be expected. Whether these changes can be regarded as a significant earthquake precursor is still controversial. Geomagnetic Institute has been performing seismomagnetic investigations in the regions of the Montenegro, Rudnik, Svilajnac and Kopaonik, since 1979. Within the areas of seismically active regions on the established grid of fixed measuring sites, seismomagnetic survey is periodically renewed in order to observe local changes in the geomagnetic field with a view to ascertaining the presence and manifestations of the seismomagnetic effect. Investigations in the wider area of Kopaonik were initiated immediately after the May 18, 1980 earthquake ($M=6,0$). Since than total field intensity surveys have been carried out, using the network of the stations in the wider area affected by the earthquake. Obtained results enabled us to follow spatial and temporal variations of local field changes. The distribution of these changes exhibits characteristic pattern which can be related to the seismicity in certain time period. Surveys have been carried out with proton precession magnetometers applying the following measuring procedure. At each site successive readings were done by proton magnetometer comprising the interval of about 15 minutes, while continuous records of referent station were used to correct values for daily variation. Before discussing the spatial and temporal changes of total intensity, account on the important geological, tectonic and seismological feature of the investigated area will be given. By the comparison of spatial form of successive measurements we can obtain different seismicity of the region. It might reflect pre and co earthquake processes in the wider area of epicentral region. These seismomagnetic investigations in Serbia have relevance because of the long period of measurements but there is necessity for different methodology that imply continuous measurements in seismically active regions.

Keywords: seismomagnetism, precursor, survey

(S) - IASPEI - International Association of Seismology and Physics of the Earth's Interior

JSS008

Oral Presentation

1986

Luminescence Associated With Uni-Axial Rock Fracture Experiments

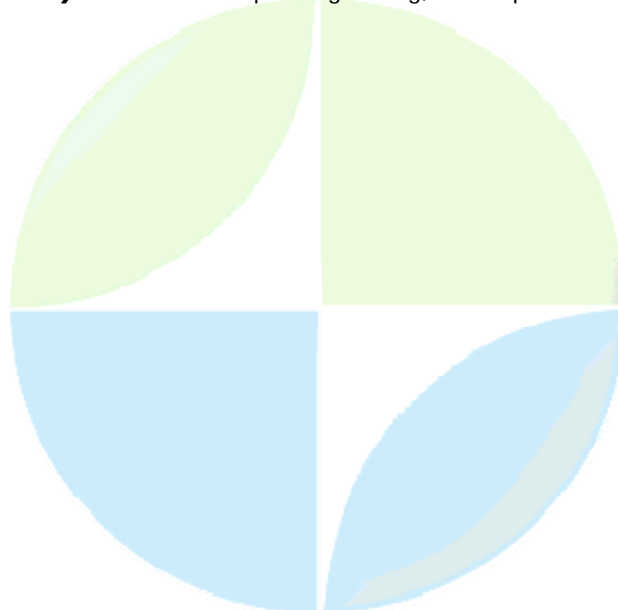
Dr. Mamoru Kato

Graduate School of Human and Environmental Studies Kyoto University IASPEI

Yuta Mitsui, Takashi Yanagidani

The sky being illuminated before and during an earthquake is one of the phenomena that are often referred as macroscopic anomaly. Such phenomena are termed as earthquake lightening, and reports of observations can be found in ancient documents in , and . The first unambiguous photographs of the illuminated sky were taken during swarm activities in Matsushiro, , in mid-1960s, and reports of similar observations, some of which are less credible than others, follow large earthquakes in , such as 1995 Kobe Earthquake, as high interest in this phenomenon, in accord with high interest in short-term earthquake prediction, is shared in . Brady and Rowell [1986] was first to experimentally investigate luminescence during rock fracture, and postulated from spectrographic observations that luminescence is caused by exoelectrons emitted from fresh rock surfaces which are created during fracture. In other experimental studies on electromagnetic behavior of rocks subjected to compression [e.g., Yoshida, 2001], piezoelectric effect of quartz is asserted to play an important role, and it appears that luminescence and emission of other electromagnetic waves do not share the same origin. We have experimentally studied luminescence of rock in uniaxial compression. Rock samples such as granite, sandstone, and basalt are prepared in both dry and wet conditions, and are compressed with high strain rates in ambient atmosphere. Luminescence of rocks is weak but visible to naked eye when conditions are met. Photographic records of faint luminescence with digital cameras are also possible. Emission of light is instantaneous, and appears to be dominant at the final explosive failure. Its intensity significantly decreases when samples are in wet condition. Mineralogy controls luminescence, as, for example, quartz-rich samples usually emit stronger light than quartz-poor samples. Grain size is another controlling parameter, as we observe stronger light from granite with coarser grains. These observations are not successfully explained by the exoelectron hypothesis of Brady and Rowell, but rather suggest that discharge of piezoelectric field is primarily responsible for luminescence.

Keywords: earthquake lightening, rock experiment



(S) - IASPEI - *International Association of Seismology and Physics of the Earth's Interior*

JSS008

Oral Presentation

1987

Effect of seismic activities in the F2 region ionospheric electron and ion temperature

Mr. Ramesh Chand

Earth Sciences Indian Institute of Technology Roorkee, India IASPEI

M. Israil, D.K. Sharma, J. Rai

Ionospheric perturbations by seismic activity have been studied by analyzing ionospheric electron & ion temperature data during earthquake. The data recorded by Retarded Potential analyzer (RPA) payload aboard the Indian SROSS-C2 satellite during period from January 1995 to December 2000 are used for the present analysis. Details of earthquake events are obtained from USGS website. Pre & post earthquake ionospheric electron & ion temperature data were compared to the corresponding data recorded during the earthquake hours. The analysis of ionospheric temperature data shows anomalies in ionospheric temperature. 27 earthquake events from Indian region were analysed which shows the anomalous behavior in electron & ion temperature. Out of the events studied 12 indicates increase in electron temperature by an amount of 1.2 to 1.5 times the normal temperature whereas 13 earthquake events shows the increase in ion temperature by amount 1.2 times the normal temperature. We have also found decrease in ion and electron temperature in 3 events. Our analysis indicates the increase in temperature in majority of the events studied in the present investigation. In Seismically active region the emission of gases generates acoustic gravity wave, reaches to ionospheric height which is responsible for the ionospheric perturbation. The seismogenic vertical electric field and associated electromagnetic radiation reaches up to ionospheric height, induces joule heating are responsible for the ionospheric temperature perturbation.

Keywords: ionospheric temperature, seismic activity



(S) - IASPEI - International Association of Seismology and Physics of the Earth's Interior

JSS008

Oral Presentation

1988

Seismo-electromagnetic emissions and VHF pulsed radio signals (P-H pulses) observations over one solar orbit - More questions than answers.

Mr. Phillip Hollis-Watts

CRC Mining Western Australian School of Mines

Christopher R Windsor

Electromagnetic radiation has been observed and measured during the deformation/fracture of 'rock' over various scales by many authors for many years (Warwick et al, 1982 to Freund et al, 2007). One form of emission, termed P-H pulses (pulsed VHF signals) was originally observed by the first author prior to a $M=5.9$, earthquake (EQ) that occurred 10:28, 28 Dec. 1989 (Local Time) at Newcastle, NSW, Australia. P-H pulses, the early monitoring equipment and some interpretations and discussions have been given by Pulinets and Hollis-Watts, 2003 and in Pulinets and Boyarchuk, 2004. In 2006, an improved measurement station was established at Esperance, WA. This station is manually operated which restricts observation frequency and duration but does allow each observation to be checked and confirmed. A systematic assessment began involving measurements at 0.5 hour intervals averaging over 10 hours per day from 20 October 2005 to 20 October 2006 with a hiatus during February and March, 2006. This assessment was conducted over one Earth orbit of the Sun, in an attempt to firstly, determine any daily, monthly, annual variations, secondly to determine any astronomical and atmospheric effects and thirdly to officially record and report any anomalous 'spikes' for comparison to EQs recorded within the Geoscience Australia, 2007 earthquake database. The EQ events of magnitude 0 to 9.99 were taken from Geoscience Australia Earthquake Database over the period considered for a coordinate range of Lon. 60 to 180 and Lat.+40 to -50. A total of 225 of these events are recorded across continental Australia (proportioned by state with WA: 59%, SA:15%, NSW: 11%, NT: 8%, VIC: 4%, TAS: 2% QLD: 1%). 75 events are also recorded across an Asian arc North of Australia from Pakistan to Fiji. The data show a characteristically low magnitude (1 to 4) pattern for continental Australia relative to the significant magnitude events (>5) recorded for the chosen Asian arc. They also show 103 events (or 46% of the total continental occurrence) are recorded in the relatively seismic Yilgarn Craton of WA. It is interesting to note that relatively high principal normal stress magnitudes and ratios of horizontal to vertical stress have been measured in the upper crust within the Yilgarn Craton (Brown and Windsor, 1990). The P-H pulses per minute were monitored from the single station at Esperance, WA with two amplitude levels (on VHF 148 MHz). An annual reduction in pulses per minute is observed with retreat from the Sun with a daily cycle that peaks at ca. midnight (local time). Transformation of time to $x = \sin(kt)$, where $k = (2\pi/\text{LOD})$ and least squares regression with $y = (\text{P-H pulses /minute})$ visibly indicates a linear relation limited by an r^2 coefficient of ca. 0.56. They are compared with the time series of heliocentric radial range to Esperance, WA at Lon. 121 53', Lat. 33 51', computed on 23/02/2007 using the Ephemeris Solar System Dynamics Program, NASA/CIT/JPL, 2007 (<http://ssd.jpl.nasa.gov/>). This visible suggested relation will be tested properly after anomalous spikes have been censored. Different types of short-time anomalies were identified possibly related with the earthquakes and close volcano eruptions having different envelope and spectrum characteristics. Work is now concentrating on statistical analysis of the various data time series in an attempt to test any correlated effects. At this stage our observations have produced more questions than answers and these will be discussed in the paper proper. At this stage we note:

- Cycles in P-H pulses that appear associated with astronomical geometry.
- Not as of yet, identified effects from severe electrical storms, pressure and precipitation and reported coronal ejections.
- Consistent measurement (i.e. over 100,000 frames) of more positive spikes than negative indicating a flux which is not a recognised form of EM

interference. • A short duration anomaly that may precede an EQ and a relatively long duration anomaly that appears to be co-volcanic (with distinctly different FFTs). The issue of a P-H pulse anomaly representing an EQ precursor requires considerable assessment that has not been attempted here. The rock physics of Freund, 2002 coupled with the ionospheric physics given by Pulnits and Boyarchuk, 2004 indicate lithosphere-ionosphere coupling may be possible through electromagnetic emissions. However, here, we have only reported intermittent observations from a single, manually operated station. Several automated terrestrial stations with continual measurement and synchronised vectoring of the signal would provide a much better test, (as would a satellite based system). References Brown, E.T. and Windsor, C.R., 1990. Near surface in situ stresses in Australia and their influence on underground construction. Keynote lecture, Proc. 7th Aust. Tunneling Conf, Sydney. Nat. Conf. Pub. No. 90/8 pp 18-48. IE Aust. Canberra. Freund, F.T. 2002. Charge generation and propagation in rock. J. Geodynamics, 33, 545-572. Freund, F. T., Takeuchi, A., Lau, B.W. S., Al-Manaseer, A., Fu, C.C., Bryant, N.A. and Ouzounov, D. 2007. Stimulated infrared emission from rocks: assessing a stress indicator. eEarth, 2, 1-10. (www.electronic-earth.net/2/1/2007/) Geoscience Australia, 2007. Australian earthquake database at www.ga.gov.au Pulnits, S. and Hollis-Watts, P. 2003. P-H Pulses – the new type of seismoelectromagnetic emission. Paper EAE03 – A 07035. AGU –EUG Joint Assembly, Nice France. Pulnits, S. and Boyarchuk, K. 1995. Ionospheric Precursors of Earthquakes. Springer: Berlin : Germany P.315. NASA/CIT/JPL, 2007. Solar System Dynamics Ephemeris Program at <http://ssd.jpl.nasa.gov/> Rowe, A.J. and Grayson, M. 1996. Shake, rattle and roll. The Medical Journal of Australia. V.165. No. 10/11. Warwick, J.W., Stoker, C. and Meyer, T.R. 1982. Radio emission associated with rock fracture: Possible application to the great Chilean earthquake of May 22, 1960. J. Geophys. Res. 87:2851-2859.

Keywords: vhf pulsed emission, p h pulses, stress

XXIV2007

PERUGIA
I T A L Y



(S) - IASPEI - International Association of Seismology and Physics of the Earth's Interior

JSS008

Oral Presentation

1989

On the physical mechanism of vertical electric field generation over active tectonic faults

Prof. Sergey Pulinets

Space Physics Department Institute of Geophysics

The anomalously high vertical electric field gradients before strong earthquakes were reported by many authors. At the same time there are a lot of cases when no electric field anomalies were registered before earthquakes. This contradiction does not permit to consider the electric field as a precursor up to now. The problem can be resolved if the nature of the observed (or not observed) anomaly will be clear. It is well established that the main source of the atmospheric boundary layer (BL) ionization providing its conductivity over the continents is natural ground radioactivity. So the natural radioactivity is one of the important parts of the Global Electric Circuit (GEC). The major contribution to this radioactivity is provided by the radon emanation and its progeny. Lithosphere-Atmosphere-Ionosphere Coupling (LAIC) model developed recently explains the thermal anomalies observed before earthquakes as a latent heat released by water vapor condensed on ions produced by radon ionization (Pulinets et al., 2006). It means that the thermal anomalies could serve as indicators of the increased radon release. The thermal anomalies monitored by the remote sensing satellites clearly show the anomalies along the active tectonic faults what is consistent with the radon behavior established earlier. The size of the thermal anomalies for the strong earthquakes of order of hundreds thousand square kilometers implies the important changes of atmospheric electricity over these areas. The sharp increases of the atmospheric electric field before earthquakes can be explained by the formation of large ion clusters (result of water condensation on ions) with very low mobility. Low mobility leads to the drop of BL conductivity and sharp increase of potential drop (and consequently vertical electric field gradient) near the ground surface. Large particle formation before earthquakes is confirmed by Aeronet network measurements at California and Mexico with time scales similar to those of thermal and ionospheric anomalies. We can say that some kind of haze is formed over earthquake preparation area few days before earthquakes changing the electric properties of BL. Another possibility (with no strong electric field on the ground surface) can be realized in the case of the sharp increase of the latent heat release. In this case the ions will be raised by the convective thermal flux in the upper layers of atmosphere. In this case the electric field can be amplified (Sorokin et al., 2005) or even generated (Morozov, 2006) providing high values of electric field in upper atmosphere and ionosphere and consequent ionosphere modification (ionospheric precursors). This type of electric field anomalies can be checked only by balloon or rocket measurements of the vertical profiles of electric field. The only experimental support for this model up to now is formation of so called earthquake clouds what confirms the raise of ions as centers of condensation up to levels of several kilometers of altitude. Ionospheric anomalies observed before the earthquakes (especially in equatorial regions) can be explained only by anomalous electric field effects from the point of view of their morphology. References Morozov V. N., The influence of convective current generator on the global current, *Nonlin. Processes Geophys.*, 13, 243-246, 2006 Pulinets S. A., Ouzounov D., Karelin A.V., Boyarchuk K. A., Pokhmelnikh L. A., The physical nature of the thermal anomalies observed before strong earthquakes, *Physics and Chemistry of the Earth*, 31, 143-153, 2006 Sorokin V. M., A. K. Yaschenko, V. M. Chmyrev, and M. Hayakawa, DC electric field amplification over seismically active faults, *Natural Hazards and Earth System Sciences*, 5, 661-666, 2005

Keywords: atmospheric electric field, radon, ionization

(S) - IASPEI - *International Association of Seismology and Physics of the Earth's Interior*

JSS008

Oral Presentation

1990

Statistical relation of Pc1 pulsations at low latitude to Earthquake occurrence

Dr. Jacob Bortnik

Dept. of Atmospheric and Oceanic Sciences University of California, Los Angeles

James W. Cutler, Clark Dunson, Thomas E. Bleier

There have been numerous suggestions in the literature that seismic activity may be preceded by a variety of phenomena, including ultra-low-frequency (ULF) magnetic pulsations, and changes in the local ionospheric electron number density. In the present study, we test this hypothesis using 8 years of search-coil magnetometer data recorded in Parkfield, California. We use a newly developed identification algorithm to automatically detect and classify all wave events in the Pc1 (0.2-5 Hz) frequency range in our data set, and compare these events to a catalog of local Earthquakes. Pc1 events are believed to be generated in the equatorial magnetosphere, propagate along magnetic field lines to the high latitude ionosphere, and further propagate to low latitudes within the F2-layer ionospheric density duct leaking down to the ground due to the finite conductivity of the E-layer. Thus, we look for changes in detected Pc1 characteristics coincident with Earthquakes, which would act as a proxy for local ionospheric changes. Results of our statistical analysis are presented and discussed in the context of pre-seismic ionospheric modifications.

Keywords: earthquake, precursors, ulf

PERUGIA
ITALY



(S) - IASPEI - International Association of Seismology and Physics of the Earth's Interior

JSS008

Oral Presentation

1991

Understanding Electromagnetic Properties of Dry and Wet, Stressed and Unstressed Igneous Rocks: Progress Report

Prof. Friedemann Freund

Earth Science Division, Code SGE NASA Ames Research Center IAGA

Vern Vanderbilt, Akihiro Takeuchi, Bobby W.S. Lau, Milton Bose

The discovery of a new type of electric currents that can be stress-activated in igneous rocks (1) opens a window of opportunity for controlled laboratory experiments and for considering source generation mechanisms. Laboratory experiments demonstrate that the propagation of the electronic charge carriers is not impeded by water films in water-soaked rock, though cm-thick layers of liquid water reverse the direction of the current flow. The charge carriers that propagate through rocks are defect electrons in the oxygen anion sublattice (positive holes or pholes for short). They are introduced into the matrix of nominally anhydrous minerals during cooling from magmatic or high-grade metamorphic temperatures when hydroxyl pairs (traces of dissolved H₂O) split off H₂ molecules and convert to peroxy links. The oxygens in the peroxy links thereby change from the 2- to the 1- valence state. Stress causes dislocations to move, breaking peroxy links and activating pholes alongside with loosely bound electrons. The electron-phole pairs are long-lived (hrs to days). Our hypothesis is that the boundary between stressed and unstressed rock acts analogous to a semiconductor pn junction, impeding electron flow across the boundary in one direction while promoting flow of pholes. Whereas pholes can stream out of the stressed rock into the unstressed rock, electrons need an n-type contact to flow. We report on the magnitude of the transient currents that can be expected, when pholes and electrons both flow out of the stressed rock volume and reconnect, thereby closing the electric circuit. (1) Freund et al. 2006, Phys. Chem. Earth 31, 389-396; Freund & Sornette, 2007, Tectonophys. 431, 33-47.

Keywords: pre earthquake signals, telluric currents, electromagnetic emissions



(S) - IASPEI - *International Association of Seismology and Physics of the Earth's Interior*

JSS008

Oral Presentation

1992

ULF magnetic transfer function approach for monitoring of crustal activity

Dr. Katsumi Hattori

Department of Earth Sciences, Faculty of Science Chiba University IASPEI

H. Ishikawa, M. Harada, I. Takahashi, C. Yoshino, N. Isezaki, T. Nagao

The southern part of Kanto District, Central Japan is situated in front of the triple junction of three plates (Pacific, Philippine Sea, and Eurasia), and the tectonic activity associated is remarkable. In order to investigate the electromagnetic phenomena associated crustal activity, the precise ULF electromagnetic measurement network has been established. At each station, three magnetic components and two horizontal electric components are observed. There are two arrays with interstation distance of 5 km in Izu and Boso Peninsulas. In this paper, the features of interstation transfer functions (ISTF) have been investigated. ISTF means the correlation between the site and the reference site. Usually FFT is used for estimating transfer function but wavelet transform is applied in this paper. We analyzed data observed at Mochikoshi and Seikoshi stations in Izu Peninsula in the periods of 2000-2003 (4 years). The distance between two stations is about 5 km. As a reference station, Kakioka operated by Japan Meteorological Agency is used for estimating transfer functions in this paper. The distance from our stations is about 150 km. In comparison to the mechanical data, we analyzed the strain data observed Toi station, which locates about 5km from Seikoshi station. Main results are as follows; (1) There are three anomalous changes in the magnetic transfer function. (2) The above three anomalous changes are seemed to be associated with the crustal activities, which are not only earthquake activities associated with 2000 Izu island swarm and M5.1 earthquake near Izu stations but also crustal activities without earthquakes. (3) The magnetic anomalous changes are started a few days prior to the mechanical changes.

Keywords: ulfmagnetic transfer function, wavelet transform, crustal activity monitoring



(S) - IASPEI - *International Association of Seismology and Physics of the Earth's Interior*

JSS008

Oral Presentation

1993

Electromagnetic wave Anomaly of Earthquake and Signal Processing to Detect Precursor

Prof. Masayasu Hata

Computer Science Div. Chubu University IASPEI

Takashi Fujii, Ichi Takumi, Hiroshi Yasukawa

We have been studying an earthquake precursor of environmental electromagnetic waves (EM) at ELF band of 30-300Hz for the last twenty years. The observed signals contain local anomalous radiation of earthquakes as well as global background noise due to tropical thunderstorm. The global noise distorts the earthquake prediction. A method of global noise elimination is discussed by Independent Component Analysis (ICA). The second signal processing is to extract a precursor relevant to earthquake. For the processing, the linear predicting coefficient (LPC) method is applied. The LPC error was well acknowledged as a precursor of earthquakes exceeding magnitude five. In the paper, a new approach to extract precursor out of noisy ELF environmental signal by making use of Linear Predicting Coefficient, LPC signal model is introduced. For the case of Off-West-Fukuoka earthquake with M7.0, an anomalous magnetic flux radiation of about $10\text{pT}/\sqrt{\text{Hz}}$ with $1\text{pT}/\sqrt{\text{Hz}}$ background noise was detected about four days before the event at Tijiwa town Nagasaki Prefecture, 120km south of the epicenter, and five aftershocks exceeding M5.0 also followed respectively the anomalous radiations within one days delay. The radiation area was determined near the epicenter for both the main and aftershocks, by direction finding of the detected anomaly signal from two sites of Tijiwa and Tomochi through the signal amplitude ratio of EW to NS of sensing loop coils. These two facts may confirm the existence of EM precursor.

Keywords: electromagnetic wave anomaly, elf band, lpc



(S) - IASPEI - *International Association of Seismology and Physics of the Earth's Interior*

JSS008

Oral Presentation

1994

Magnetotelluric survey around source region of the 2003 Tokachi-Oki earthquake

Prof. Toru Mogi

Institute of Seismology and Volcanology Hokkaido University IAGA

Kengo Tanimoto, Yusuke Yamaya, Hiroyuki Kamiyama, Takeshi Hashimoto, Venera Doblica, Takanori Kajiwara, Makoto Uyeshima, Yasuo Ogawa

The 2003 Tokachi-oki earthquake ($M_w=8.0$) occurred at 26th September. The hypocenter was determined at 80 km off of the Erimo area, the southern part of Hokkaido, Northern Japan. The source region, including the asperity and aftershock region, spread to about 100km wide in NW and NE direction over the upper plane of the Pacific plate. The lower edge of the source region reached beneath the Erimo area at a depth of 50km. The Pacific plate is subducting at rate of about 8 cm/year to the NW direction beneath Hokkaido along the Japan-Kuril trench, a depth of about 6000m, situated at 100km off from the land. We carried out wide band magnetotelluric survey, covered frequency range over 320 to 0.8×10^{-4} Hz, at 25 sites in the Erimo area to clarify the resistivity structure of the source region. The sites were arrayed in a grid in about 50x50 km area, and the site array enables us to construct three-dimensional resistivity model. The survey area faced to Pacific Ocean and the data obtained at the coast area were seriously affected by a sea effect. We are constructing three dimensional resistivity model including sea to become reality. The resistivity structure reveals resistive subducting plate at deeper part of the area and its complex shape in this area.

Keywords: magnetotelluric, resistivity



(S) - IASPEI - *International Association of Seismology and Physics of the Earth's Interior*

JSS008

Oral Presentation

1995

Multipoint measurements of ULF magnetic field activity in south-eastern Europe during August 2004-February 2005: DFA approach and results

Dr. Petko Nenovski

physics of the ionosphere geophysical institute, sofia IASPEI

Massimo Vellante, Irina Pilarska, Konrad Schwingenschuh, Umberto Villante, Mohammed Boudjada, Viktor Wesztergom, Elena Cristea, I. Cholakov, Emil Botev

This report deals with detrended fluctuation analysis (DFA) of ground-based ULF magnetic field data from the South-Eastern Geomagnetic Measurement Array (SEGMA). DFA approach is applied to ULF signals and their fractal properties are studied depending on geomagnetic and local conditions. The ULF activity is analyzed in two time windows: 10-90 sec and 90-450 sec. We investigate all the magnetic field components (H, D, and Z) both in day and night conditions. Both regional (at all SEGMA stations) and local effects (at one station only) are found in the DFA index dynamics: i) regional effects correlate with the magnetospheric activity controlled by Kp index, and ii) local ones are characterized by gradual (long term) DFA index decrease in the Z component observed only in the shorter time window 10-90 sec. The latter persists days over diurnal trends. Several moderate earthquakes ($4.3 < m < 5.5$) have occurred in the Adriatic region in August 2004-February 2005. Changes in diurnal trends of the DFA index 5 days prior to earthquakes are under study. Attempts to explain all specifics in the DFA dynamics are undertaken.

Keywords: ulf magnetic field, dfa index dynamics, diurnal trend

PERUGIA
ITALY



(S) - IASPEI - *International Association of Seismology and Physics of the Earth's Interior*

JSS008

Oral Presentation

1996

ULF common mode signal estimation with a network of sensors in California

Mr. Clark Dunson
IASPEI

Tom Bleier, Dr. James Cutler, Dr. Jacob Bortnik

Three of the problems facing those who attempt to investigate the ULF geomagnetic signals for relationships to seismicity are: 1) The magnitudes of the natural field fluctuations are often large compared with the signals of interest because of the normal geomagnetic activity; 2) Each site in a monitoring network has a different assortment of cultural noise sources contaminating the signals; and 3) Local impedance variations cause different signal reflections at each site. Prior work computing residual or local signals has been complicated by a number of difficulties, among them a dearth of signals to compare, often 1-3 instruments. Development of the high-sensitivity QF1005 sensor network and associated Data Center has allowed deployment of some of these techniques across a larger network (10+ instruments, including 30+ channels). Therefore, this presentation illustrates enhancements to calculations of the Intra-Station Transfer Function and the Common Mode Signal Estimator made possible by the larger array of sensors. The effects seen in different signal regimes (Pc3&4 vs. Pc1&2) will also be highlighted and discussed.

Keywords: estimation, noise, distributed

PERUGIA
ITALY



(S) - IASPEI - *International Association of Seismology and Physics of the Earth's Interior*

JSS008

Oral Presentation

1997

Formation of Carbon Films on New Fracture Surfaces: Implications for Continental-Collision-Zone Conductivity Anomalies

Dr. Al Duba

working group on EM induction Geomagnetism IAGA

E. Mathez, S. Karner, A. Kronenberg, J. Roberts

Electrical resistivity of dense crystalline quartzite is reduced by carbon films deposited on fractures during failure experiments performed at $T=400$ C in the presence of carbon-bearing fluids. Hollow cylinders of Sioux quartzite, jacketed by silver, were hydrostatically loaded to failure by applying pressurized argon gas at the outer diameter (reaching ~ 290 MPa at a rate of 0.1 MPa/s) while maintaining a constant pore pressure at the inner diameter. Pore fluids consisted of CO, CO₂, CH₄, a 1:1 mixture of CO₂ and CH₄ (each with pore pressures of 2.0 to 4.1 MPa) and air (at atmospheric pressure). Biaxial-stress states are calculated using elastic-stress solutions that account for the applied pressures and hollow-cylinder dimensions. For the inner wall of the cylinders, effective radial stress (s_r) is zero and calculated effective differential stresses ($s_q - s_r$) reach 1225 MPa. Failure of hollow Sioux quartzite cylinders occurred by the formation of mode II shear fractures that transect the cylinder wall. The distribution of carbon in the run products was mapped by electron probe. Samples deformed in CO₂ and air contained little or no carbon above the small amount that exists in the undeformed rock. Samples deformed in CO contain ubiquitous carbon films on the fracture surfaces that formed during deformation. Because carbon is absent on other free quartz surfaces that existed during the experiments, we conclude that the carbon films formed preferentially on the fractures as they formed. The radial resistivity of dry, undeformed Sioux quartzite cylinders is extremely large in the ambient laboratory atmosphere (>23 MW-m). The radial resistivity of Sioux quartzite cylinders that failed in pore fluids that promote carbon deposition are lower (2.8 to 4.6 MW-m for CO tests; 15.2 to 18.4 MW-m for CO₂:CH₄ tests). The results of this study help to isolate the role of carbon deposition on fresh fracture surfaces in altering the electrical properties of rocks with little initial porosity from that of carbon deposition on fractures and preexisting equant voids of porous rocks. Taken together, our results and those of Roberts et al. (1999) indicate that electrical conductivity in rocks may be enhanced due to carbon deposition on grain and/or fracture surfaces. Our results are important for studies linking variations of crustal electrical properties to seismogenesis, as well as to illuminate physico-chemical mechanisms that may be exploited to monitor injection sites for carbon sequestration. Furthermore, this work offers an explanation of the genesis of shallow, linear conductivity anomalies observed in continental-collision zones in Europe, in the Andes, in the Himalayas, and in South Africa.

Keywords: conductivity anomaly, continental collision zones, carbon sequestration

(S) - IASPEI - International Association of Seismology and Physics of the Earth's Interior

JSS008

Oral Presentation

1998

A method for parameterization of magnetic ULF signals

Dr. James Cutler
IASPEI

Jacob Bortnik, Clark Dunson, Tom Bleier

We analyze long-term (1995-2007) ultra low frequency (ULF, less than 10Hz) tri-axial magnetometer data measured in California. We process data from fourteen ULF sensor systems installed along active California zones that are operated by Quakefinder, Stanford University, and UC Berkeley with data collections starting in 2005, 2004, and 1995 respectively. L-shell values of the sensors range from 1.6 to 1.9. Twelve years of data as measured by two UC Berkeley systems provides the basis for determining typical signals levels in California through a full solar cycle. More recent data collected by Quakefinder and Stanford allows us to measure the extent of wide-area signals and characteristics of additional local signal environments. In this analysis, we develop statistical summaries of measured signal strength parameterized according to sensor site, coil orientation, frequency range, time of day, season, and global geomagnetic activity (Kp index). For each parameter, we calculate the mean, median, variance, and quartiles of the magnetic signal recorded at multiple ULF stations, and use these quantities as baseline values from which signals are assumed to deviate. With these statistical quantities, we construct expected signals as a function of the six parameters and subtract them from absolute measurements to obtain signal residues. Results show that this technique can be effective in reducing large background variations and thereby increasing the signal to noise ratio (SNR), allowing much lower amplitude signals of local origin to be detected. Network-wide trends in parameterized statistics are discussed. We also describe the use of parameterization output to create data quality metrics, determine sensor health, remove of wide area signals, and indentify local noise signals. We then examine time periods surrounding earthquake near the sensors, and to improve SNR, we superpose multiple earthquake events and discuss the results in light of possible seismogenic ULF signal sources.

Keywords: ulf, magnetic, parameterization



(S) - IASPEI - *International Association of Seismology and Physics of the Earth's Interior*

JSS008

Oral Presentation

1999

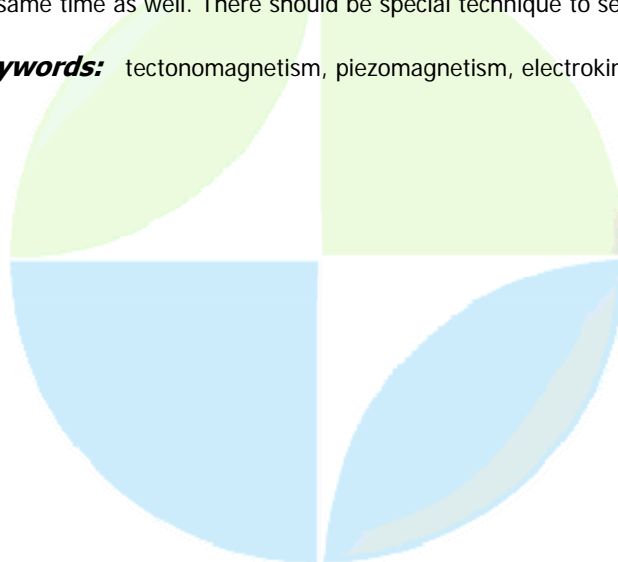
Short and long range impact of seismoelectromagnetic effects

Dr. Farshed Karimov

Seismology Institute of Earthquake Engineering and Seismology IASPEI

Space-time development of seismotectonic process initiates space-time patterns of seismoelectromagnetic effect (SME). There are different physical processes can take place in an earthquake preparation zone. For instance deformation of earth crust solid phase, underground fluid flow from locally stressed crust or opposite direction flow at dilatancy stage. As far as SME can be generated both by solid phase deformation or underground fluid flow the character of SME pattern can be diverse. If SME signal is radiating directly from the source solid deformed volume for instance by virtue of piezoelectric or piezomagnetic effects one can detect the signal quite immediately at any distance, limited by the discrimination level only. Its a case of long range SME effect. Such effect is likely to be expected for rocks in the source with high enough piezoelectric or piezomagnetic properties. For the underground flow SME radiation mechanism one can expect less or more shift in time appearance of the signal, depending on site location within the source preparation zone or away from it. Really it takes time for spreading of fluid flow within or out of the preparation zone. Electrokinetic stream intensity is varying in space and time and therefore the SME signal turns up dependent on how fluid flow is distributing and spreading. Its an example of short range SME effect. Such effect is likely to be expected for the intensive enough underground fluid streams, high enough rocks zeta-potential, high enough rocks porosity, low enough liquid viscosity and high underground fluid ion concentration. Such delay can take place also for the ionosphere spreading of SME, carrying by electric currents. Mean term tectonomagnetic effects of earthquake preparation observed in the seismic areas present a type of SME effects. There are rocks with very low magnetization and piezomagnetic effects majoring in the Tajikistan and one can scarcely expect sizable piezomagnetic origin of tectonomagnetic variations. In contrast, there are wide spread porous rocks with underground liquids which can be regarded as an electrolyte. Straight tectonomagnetic signal space-time shift has been observed as well during Nurek reservoir water level seasonal variations up to 50 meters. The speed of underground water flow as much as several kilometers per day, measured by means of bore holes, correlates with space-time shift of the local tectonomagnetic effect in the vicinity of the water reservoir, featuring short range character of that SME effect. Its principally possible that both impacts from long and short range effects will turn up comparable at the same time as well. There should be special technique to separate each other.

Keywords: tectonomagnetism, piezomagnetism, electrokinetics



(S) - IASPEI - *International Association of Seismology and Physics of the Earth's Interior*

JSS008

Poster presentation

2000

A review of selected problems in seismoelectrodynamics

Prof. Anatol Guglielmi

Solar-Terrestrial Physics Institute of Physics of the Earth, Moscow, Russia IAGA

Tsegmed Battulai, Dovbnya Boris, Zotov Oleg

The report presents an analytical review of the following selected topics: (1) Generation mechanisms of the co-seismic electromagnetic variations; (2) Detection of the seismoelectromagnetic waves by the spectral-polarization method; (3) Seismomagnetic sounding of the earth crust; (4) The impact of the earthquakes on the ionospheric ULF electromagnetic wave activity; (5) The possible impact of the industrial electromagnetic fields on the seismicity. A set of illustrative examples is analyzed in detail including the Sumatra event of 26 December 2004. The emphasis is on the relation between the theory and experiments. The actual unsolved problems are outlined. It is proposed the idea of a seismoelectromagnetic research area intended for conducting special methodological experiments in seismoelectrodynamics. The work was partly supported by grant RFBR 06-05-64143.

Keywords: earthquakes, electrodynamics



(S) - IASPEI - International Association of Seismology and Physics of the Earth's Interior

JSS008

Poster presentation

2001

The relationship between seismo-electric/magnetic field and earthquake magnitude

Dr. Xiaoping Fan

Earthquake Administration of Jiangsu Province China Earthquake Administration IASPEI

Li Qinghe, Yang Congjie

Observational, theoretical and laboratory studies have revealed seismo-electric/magnetic is a natural phenomenon. The currents/potential changes and abnormal electromagnetism appear in some earthquake preparation zone especially. Varotsos(1996) given the empirical relationship between seismic electric signal (SES) amplitude E and earthquake magnitude M based on observation data. The recent discussion on the relation between SES amplitude and earthquake magnitude has divided the point of view into two parts: one accept it and the other reject, the key reason which reject it is that the relationship has not the strongly theoretical support. Based on dipolar emitter source model, the paper study the radiant characters of seismo-electric/magnetic fields in earthquake prepare zone firstly, then analysis the relation between radiant intensity of seismo-electric/magnetic fields and earthquake magnitude, and last discuss the influence factor of the mechanisms of seismo-electric/magnetic type. The results show that dipolar emitter source model is one of the most possible mechanisms of inspiring seismo-electric/magnetic field, conversion mechanisms of seismo-electric/magnetic are the main mechanisms which inspire the radiant of seismo-electric/magnetic fields in earthquake prepare zone but not only. The relation between the logarithm of seismo-electric/magnetic field and earthquake magnitude is linear which slop depends on the fractal character of earthquake prepare zone.

Keywords: seismo electric/magnetic, earthquake magnitude



(S) - IASPEI - *International Association of Seismology and Physics of the Earth's Interior*

JSS008

Poster presentation

2002

The micro-satellite Compass-2 for investigation of the ionosphere disturbances related to seismic, meteo and human activity.

Prof. Yuri Ruzhin

IZMIRAN, Russian Academy Vice director

Kuznetsov V.D., Danilkin V.A., Dokukin V.S.

The micro-satellite COMPASS-2 launched on May 26, 2006. The satellite project has an exploratory character and aims first of all to detect the ionosphere plasma anomalies linked to seismic, meteo and human activity, precisely determining their characteristics, such as the EM frequency spectrum and plasma density structures of disturbances in the ionosphere and the upper atmosphere, and the corresponding precipitations of particles, systematically. It will provide the necessary data to work out theories and models likely to explain their origin. The observations made by the COMPASS-2 has the very great advantage of very rapidly covering almost the whole of the active seismic regions in the world and monitoring the effects of a large number of earthquakes. COMPASS-2 has the capacity to carry out precise and systematic measurements around the Earth and thus to collect a maximum number of events (<http://www.compass.izmiran.ru> for more details about the mission). Without modifying the payload, COMPASS-2 is capable for example of studying the influence of storms in relation between Sun and Earth, and of assessing the impact of human activities on the ionosphere. The detailed COMPASS-2 mission and payload description and also some first results of measurements will be presented.

Keywords: micro satellite, ionosphere, earthquakes



(S) - IASPEI - *International Association of Seismology and Physics of the Earth's Interior*

JSS008

Poster presentation

2003

The Magnetic Storm influence on the Pre-seismic Ionosphere Anomaly (a case study)

Mr. Vitali Shpakovski

IZMIRAN, Russian Academy Scientist IASPEI

I. E. Zakharenkova, Yu.Ya. Ruzhin, I.I.Shagimuratov, N.Yu. Tepenitsina

The ionosphere total electron content (TEC) variations obtained by using the GPS measurements before Hokkaido earthquake of September 25, 2003 (M8.3) is investigated. The pre-seismic plasma anomaly appeared as the local TEC enhancement (plasma cloud) located in the vicinity of the forthcoming earthquake epicenter. These structures are generated at the similar local time in ionosphere during 5 days prior to the main shock. It is shown that according to its main parameters (locality, affinity with the epicenter, dome-shaped zone of manifestation and time of existence) the detected ionospheric anomaly may be associated to the future seismic activity. It is necessary to mention that geomagnetic storm took place one day prior to the main shock and usually it is appeared at ionosphere as global disturbance (or ionosphere storm). It is shown that the spatial-temporal TEC variations can be presented as superposition of ionospheric storm effects and the ionosphere anomaly of seismogenic origin. As result, the intensification of the pre-seismic plasma anomaly due to magnetic storm action (up to 85-90% of non-disturbed level) became visible at ionosphere 18 hours (one day) before Hokkaido earthquake

Keywords: pre seismic, ionosphere, earthquake



(S) - IASPEI - *International Association of Seismology and Physics of the Earth's Interior*

JSS008

Poster presentation

2004

Analytical study on piezomagnetic effect due to 3-D magnetic structure and its applications to the earthquakes in Japan

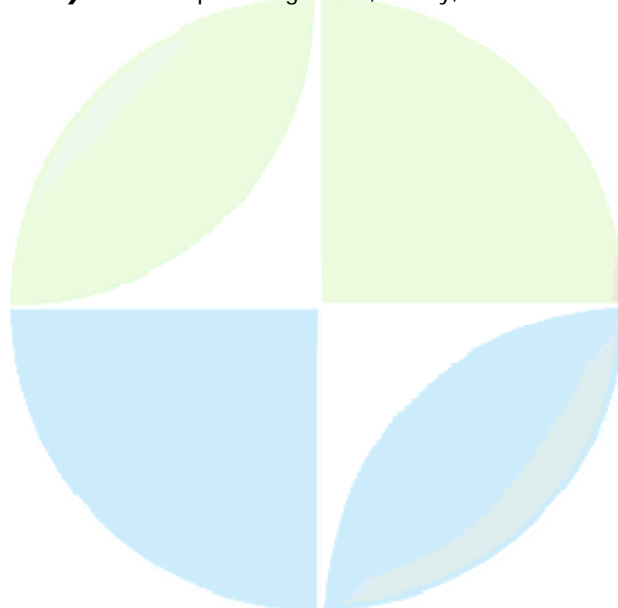
Prof. Yasunori Nishida

Institute of Seismology and Volcanology Faculty of Science IAGA

Mitsuru Utsugi, Toru Mogi

We developed an analytical form of the piezomagnetic field due to a non-uniformly magnetized medium. In order to represent the non-uniform distribution of the crustal magnetization, we divide the crust into a number of blocks assuming that each block has its own magnetic properties. The piezomagnetic potential derived from a single block is expressed by a definite surface integral of an integrand, which includes the magnetization change and displacement of the medium, over the boundary surface of the block (the representation theorem by Sasai, 1991). We show the surface integral is reduced analytically to the line integral which has the integrand including elliptic integrals. The line integral is calculated numerically to represent the piezomagnetic potential. This method of analysis is advantageous to fast computation of the piezomagnetic fields. No co-seismic geomagnetic changes related with the 2003 Tokachi-oki earthquake (M8.0) and the 2004 Kushiro-oki earthquake (M7.1) in Hokkaido, Japan were observed at a magnetic station whose epicentral distances were about 120 km and 50 km, respectively. Applying the above-mentioned analytical method, model calculations showed that co-seismic piezomagnetic fields did not amount to 1 nT at the station in both cases when we assumed the relevant fault parameters, in-situ Curie temperature depth, subsurface 3-D magnetic structure and stress sensitivity of rocks. Therefore, it may be reasonable that we could not detect the piezomagnetic signals at the station. We also made model calculations to forecast the piezomagnetic amplitudes caused by M7.9 and M8.5 earthquakes predicted to occur along the southern Kurile trench and by M7.8 earthquake in the central Japan (Tokai earthquake) in the future. The model calculations reveal the piezomagnetic fields up to about 4 nT and 7 nT are expected in the eastern part of the Hokkaido island for the M7.9 and M8.5 earthquakes and +25 nT on the Sagami trough for the M7.8 earthquake, encouraging magnetic observations hereafter.

Keywords: piezomagnetism, theory, observations



(S) - IASPEI - *International Association of Seismology and Physics of the Earth's Interior*

JSS008

Poster presentation

2005

Possible association between some geomagnetic anomalies and Vrancea (Romania) significant earthquakes occurred in the years 2004-2007

Dr. Moldovan Iren-Adelina

Bioseismic and magnetotelluric studies National Institute for Earth Physics IASPEI

Dumitru Enescu, Adrian-Septimiu Moldovan

The association between geoelectromagnetic anomalies and Vrancea earthquakes of moment magnitudes $3.7 \leq MW \leq 5$ was first proved by studying the magnetic and seismic data in the period 1997 - 2004. This finding was extended in 2004 to a broader magnitude range $3.7 \leq MW \leq 6.3$. While Vrancea earthquakes had never exceeded $Mw=5$ for nearly seven years, they did so in October 2004, culminating with a seism of $Mw = 6.3$ on October 27, 2004. The hypocentral coordinates of the Vrancea earthquake of October 27, 2004, are: 45.8 N, 26.7 E and $h=100$ km. Its macroseismic intensity was $I_0=VII$ as a maximum (on the Mercalli scale) and $I = VI$ in Bucharest. Further data with respect to Vrancea seismic activity in the period 2004-2007 were taken from the seismic bulletins of the National Institute for Earth Physics. The working data are represented by geomagnetic data as recorded at Muntele Rosu. The study proves that observable precursory anomalies in the geomagnetic impedance have preceded all Vrancea earthquakes of moment magnitudes $Mw \geq 4.0$ occurred in 2004-2007 years. This study confirms the main result obtained in the first period, namely that the great majority of Vrancea earthquakes of magnitudes higher than 4 are associated with precursory anomalies in the geomagnetic impedance. It also seems that neither the precursor time nor the amplitude of the precursory magnetic anomaly can be linked reliably with the magnitude of the anticipated earthquake.

Keywords: geomagnetic anomaly, earthquake, moment magnitude



(S) - IASPEI - *International Association of Seismology and Physics of the Earth's Interior*

JSS008

Poster presentation

2006

MEMFIS - Multiple Electromagnetic Field and Infrasond Monitoring Array at Plostina - Vrancea. An attempt to guess what's cooking.

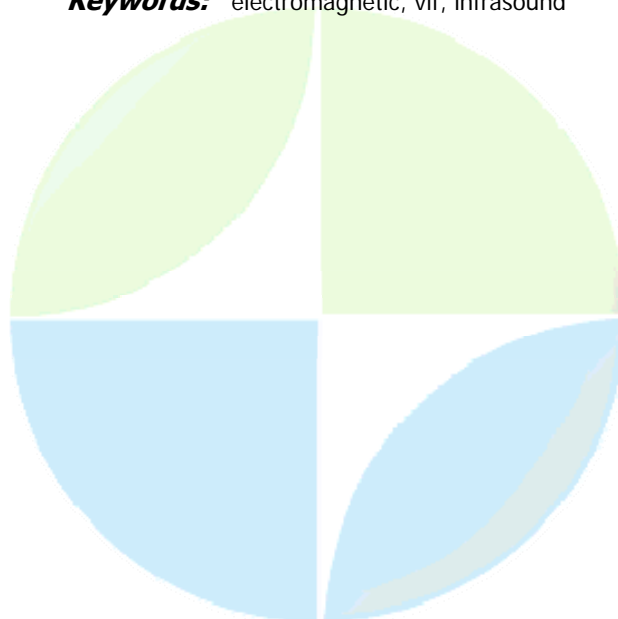
Mr. Adrian-Septimiu Moldovan

Electronic devices department CS AZEL - DESIGNING GROUP Ltd. IASPEI

Iren-Adelina Moldovan, Constantin Ionescu, Simion Ersen, Aurelia Ersen

The paper presents a complex monitoring system that is partially deployed at Plostina site, Romania - PLOR. Plostina is located at 45.8512 N latitude and 26.6499 E longitude, it's close to the epicentral zone in Vrancea and is one of the seismic stations under the administration of the National Institute for Earth Physics (NIEP), Romania. Starting with July 2006, NIEP, AZEL - Designing Group S.R.L., University of Bucharest-Faculty of Physics and Institute for Spatial Sciences made a research consortium who's project "Complex Multidisciplinary Research System On Precursory Phenomena Associated With Strong Intermediate Vrancea Earthquakes, In Conformity With The Latest International Approaches - MEMFIS" is financed by the Romanian Ministry of Research and Education, through the Programme "Excellency Research". Using specific instrumentation that will provide information on acoustic (both earth's seismic and atmosphere's infrasonic activities), electric, magnetic and electromagnetic fields, the consortium will verify if there are correlations which could be established between the behavior of these fields and the preparatory stage of strong intermediate earthquakes in Vrancea zone. In this purpose, NIEP and AZEL will develop an array in the shape of a triangle, that will consist in three independent data collecting points, equipped with seismic sensors, infrasond stations, triaxial fluxgate magnetometers and electrometers. In the same time, the observations will be improved by differential measuring methods involving simultaneous, time-synchronized, data acquisition from sensors located far from the epicentral zone (Surlari, Magurele and international observatories of geomagnetic field) and will take place in ULF and sub-ULF bands, between 0.001Hz and 25Hz. The paper also presents the actual structure of the array, the auxiliary equipments and data communication protocol and format, as well as the next steps the partners will take toward a reliable and high quality acoustic and electromagnetic surveillance array in Romania.

Keywords: electromagnetic, vlf, infrasond



(S) - IASPEI - *International Association of Seismology and Physics of the Earth's Interior*

JSS008

Poster presentation

2007

HRT wave precursor to the Sumatra earthquake

Dr. Wei Qian

Dept. of Physics University of Toronto IASPEI

Four PS100, which is a newly developed anti-interference high-precision geoelectric measurement system, stations in Sichuan and Yunnan, China have recorded the harmonic resonance waves of geoelectricity driven by tidal forces (HRT wave) precursor to the Mw 9.0 Sumatra earthquake. At resonance $T=T_0$, where the wattles component of the impedance is equal to zero, the RT wave peak will be very large, sharp and an earthquake is impendent within 1-3 days. As preliminarily estimated, the phase velocity of the RT longitudinal waves was $V_l \approx 307 \text{ km/h}$, and the vireual wave velocity $V_v = (V_l v_t) / (V_l - v_t)$ was 207 km/h. Hence, as long as the arrival time difference of the 2 RT waves at one station is known, it is possibl to calculate the epicentral distance of a coming earthquake quantitatively. For the earthquake, the free period of oscillation was $T_0 = 4 \sim 5 \text{ h}$, from which the magnitude of the coming earthquake can be determined. Both the arrival time difference and the virtual wave velocity during and before the earthquake are almost equal to each other, the RT waves during the earthquake were emitted by the fault failure, and the RT waves appearing 2 days before the earthquake were emitted by the early failure of the fault in the hypocenter region of the earthquake. If we have a reasonably designed the PS100 network, it will be possible to quantitatively predict the three factors of a coming earthquake. Since the 1966 M 7.2 Xingtai earthquake, permanent observatories have been set up in some of the major earthquake zones in China to investigate earthquake precursor of geoelectric resistivity and current field. Precursors to the 1976 M 7.8 Tangshan earthquake has been found, e.g. decrease of geoelectric resistivity, geo-resistivity impulse related to tidal force M2 wave, and geo-current filed changes related to tidal force MSf. A model of short-term earthquake precursor of tidal force has been established in accordance. The PS100 anti-interference high-precision geoelectric measurement system has been developed to overcome the instability of electrode polarization, the interference of the natural electromagnetic field, and especially the interference of random current due to industrialization, which will prevail on the globe. This system utilizes the Code Division Multiple Access (CDMA) technique and the concept of black box to geoelectric measurement instrument. It applies convolution and deconvolution to the encoded input time series and the observed output time series, and identifies the true value of geo-resistivity with eliminated electromagnetic interference. Specification tests have been conducted by China National Institute of Metrology regarding the anti-interference ability of the PS100 system. A PS100 system had measured the resistivity of a 0.01% measuring resistance, on which interference voltage from a signal generator (as source of the interference) was applied. The results indicate that when the signal-to- noise ratio was between 20dB and 0dB, both the difference between the detected and true values and the standard deviation of multiple measurements were better than 0.1% (between 0.01% at 20dB and 0.1% at 0dB).

Keywords: earthquake precursors, geo electricity, pore fluids movement

(S) - IASPEI - *International Association of Seismology and Physics of the Earth's Interior*

JSS008

Poster presentation

2008

Effects of water content on the converse piezoelectric effect in granite with an Atomic Force Microscope

Mrs. Yuko Esaki

OSAKA UNIVERSITY GRADUATE SCHOOL OF SCIENCE IASPEI

Piezoelectric effect of quartz and behavior of piezo-compensating electric charges are possible mechanism of various seismo-electromagnetic phenomena 1). In order to argue such electromagnetic phenomena quantitatively on this hypothesis, it is important to know the piezoelectric effects of granites in real state: real rocks show various water contents in the actual earth's crust. We have adopted a converse piezoelectric measurement using an Atomic Force Microscope (AFM) 2). By this method, we can obtain a small displacement of granite sample of a few nm ranges. Then we changed the water content of a granite sample and measured the piezoelectric coefficient using the AFM. The water content was referred as a mass difference of the sample after a few days of inundation and that after drying at 60 degrees Celsius for 2 hours. The piezoelectric coefficient of the granite sample decreased from 610-13 C/N after the inundation to 210-13 C/N after drying. The mass change was around -0.07%. The water contributed to the decrease of sample mass was supposed as adsorption water on this experiment condition. Preliminarily, the piezoelectric effect seems to be affected by water content in the rock. In our presentation, experimental results with precise control of water content will be reported. 1) M.Ikeya: *Why do Animals Behave Abnormally before Earthquakes? - Birth of Electromagnetic Seismology* NHK Publisher, Tokyo(1998)(in Japanese) 2) T. Matsuda, C.Yamanaka and M.Ikeya : *Jpn.J.Appl.Phys.*44,pp.968971(2005)

Keywords: granite, water content, converse piezoelectric effect



(S) - IASPEI - *International Association of Seismology and Physics of the Earth's Interior*

JSS008

Poster presentation

2009

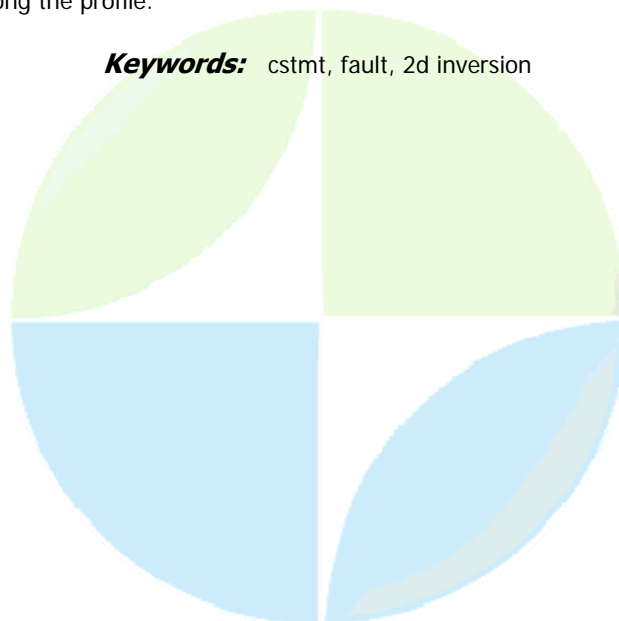
1-D AND 2-D interpretation of bam fault CSTMT data

Mr. Davood Moghadas
Institute of Geophysics student IAGA

Saeid Hashemi Tabatabaei

In recent years, EM methods are widely used for detection and producing detailed subsurface resistivity structure of faults. One such study of faults is reported here. We experienced Controlled Source Tensor Magnetotelluric (CSTMT) method to recognize a fault zone in Bam area (South-eastern of Iran). The CSTMT is an electromagnetic method used for shallow studies. It aims at mapping of shallow subsurface resistivity structures. Depending on the porosity, fluids and clay minerals there in, geological structures have different responses to the electromagnetic waves. Fault zones have resistivity contrast particularly when water and other fluids flow through them; therefore they can be recognized easily by electromagnetic methods. The tensor RMT technique (CSTMT) has additional high resolution capabilities because at every point along the profile, a detailed tensor sounding is performed. Bam lies within the western of two north-south, strike-slip fault systems located on each side of the aseismic Lut desert, which together accommodate the relative motion between central Iran and Afghanistan, part of the Eurasian plate. An earthquake devastated the town of Bam on December 26, 2003. Surface displacements reveal that over 2 m of slip occurred at depth on a fault that had not previously been identified. This fault located in south of bam is a strike slip fault which extends from the centre of Bam southwards for about 12 km. The region is an almost flat, featureless and sloping gently east. The CSTMT survey was carried out in summer 2006 using EnviroMT system from Uppsala University, Sweden. Data were collected along a profile with 19 stations and with an approximately W-E direction which was perpendicular to the fault. The frequency range used in this method is from 1-25 KHz. 1-D inversion approach presented by Pedersen (2004) was applied on the determinant, TE and TM mode data. We also obtained 2-D models using inversion algorithm proposed by Siripunvaraporn and Egbert (2000). We assumed 0.05 error floor on the impedance elements. In this essay, we discuss inversion and interpretation of CSTMT data collected from bam south fault. Two dimensional inversion results agree well with data sections and regional geology. The CSTMT field measurements resolved well the resistivity contrasts along the profile.

Keywords: cstmt, fault, 2d inversion



(S) - IASPEI - *International Association of Seismology and Physics of the Earth's Interior*

JSS008

Poster presentation

2010

The piezomagnetic field in association with a subduction and a slow slip on a plate boundary

Dr. Ken'Ichi Yamazaki

Earthquake Research Institute The University of Tokyo IAGA

Makoto Uyeshima, Tsutomu Ogawa, Shigeru Koyama

Earthquake Research Institute of the Univ. of Tokyo has deployed continuous geomagnetic observation sites in Tokai area, central . In this area, large interplate earthquakes have occurred repeatedly due to subduction on the Philippine Sea Plate, and one of the objectives of our geomagnetic observations is to detect tectonomagnetic signals in association with the subduction process. Recently, data at one site shows a characteristic variation. Until 2000, geomagnetic total forces had decreased at a rate of 1 nT/year. This decrease had stopped during a period from 2000 to 2004. And it started decreasing again since 2005. The period during which the decrease had stopped corresponds to the Tokai Slow Slip Event which was detected by geodetic observations, and the variation found in the total forces may have some relation to the Slow Slip Event. To investigate the possible relation between the changes in the geomagnetic total force and the Tokai Slow Slip Event, we performed piezomagnetic modelings. In general, piezomagnetic fields are generated by the heterogeneities of the initial magnetization of the crust and/or those of the stress field. To clarify which heterogeneity is dominant in generation of the observed changes in Tokai area, we conducted two types of numerical modelings, one for the uniformly magnetized crust with the realistic stress field, and one for the uniform regional stress field with the highly magnetized rock bodies near the station. In the former case, the stress field variation calculated from the slip distribution estimated by the geodetic data (Ohta et al., 2004) was substituted to the calculation. In the latter case, simple magnetization structures suggested from aeromagnetic surveys and geological studies are used. Estimated changes obtained from the latter model is by one order of larger than that from the former case. Therefore, the latter effect is more plausible. Whether this effect can be the generating mechanism of magnetic changes or not is depend on the stress sensitivity of the crust. Our simulation results have indicated that the sensitivity as large as $1 \times 10^{-7} (\text{Pa}^{-1})$ is required to generate 1nT/yr changes on ground. However, this values is far larger than those obtained by past studies. Stress sensitivities determined from determined from laboratory experiments for intact rocks are the order of 1×10^{-9} . Those obtained by experimental studies for some porous rocks (Hamano, 1983) and observational studies (e.g., Davis and Stacey, 1972) are the order of 1×10^{-8} . This difference indicates that the stress sensitivities of crusts may vary widely according to the phenomenon which the crust experiences.

Keywords: piezomagnetic field, subduction, slow slip

(S) - IASPEI - *International Association of Seismology and Physics of the Earth's Interior*

JSS008

Poster presentation

2011

A magnetotelluric study to recognize a fault zone in Markazi province, Iran

Mr. Masoud Ansari

Institute of Geophysics Student IASPEI

Behrooz Oskooi

Magnetotelluric (MT) is a passive exploration technique that utilizes a broad spectrum of naturally occurring geomagnetic variations and natural electric field as a power source measurable at the earth's surface, to investigate the distribution of electrical resistivity in the subsurface. For MT studies, Electromagnetic fields that are naturally induced in the earth, have wave periods ranging from about 10 to 10 s. The depth of investigation of MT method is much higher than that of other electromagnetic methods. The Zagros orogenic belt of Iran, as part of the Alpine-Himalayan mountain chain, extends for about 2000 km in a NW-SE direction from the East Anatolian Fault of eastern Turkey to the Oman Line in southern Iran. The Zagros orogenic belt is the result of the opening and closure of the Neo-Tethys oceanic realm. Therefore detection of Zagros basement has an important role in hydrocarbon exploration. In Jul-Aug 2006 carried out a magnetotelluric (MT) survey across Zagros area to recognize the geological formations and features. Arak is located in the central of Iran with the coordinate of 04' 50.4" N , 40' 38.4" E. MT measurements were planned at 32 sites over a length of 160 km along an E-W profile from Arak to Broujerd. MT data were processed using a processing code from Smirnov (2003), aiming at a robust single site estimates of electromagnetic transfer functions. We obtained one-dimensional (1-D) and two-dimensional (2-D) inversion models using codes from Pedersen (2004) and Siripunvaraporn and Egbert (2000). As results, we could respectively depict the geological structure in the area by recognition the fault zone of Talkhab fault.

Keywords: magnetotelluric, inversion, talkhab



(S) - IASPEI - *International Association of Seismology and Physics of the Earth's Interior*

JSS008

Poster presentation

2012

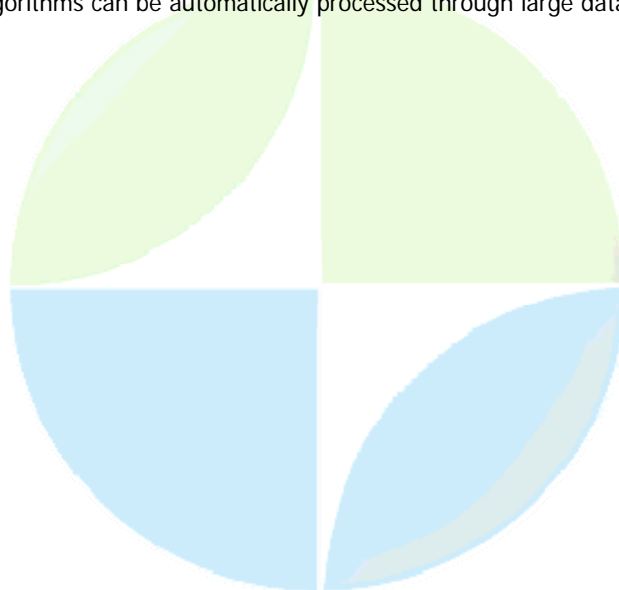
Complex Electromagnetic monitoring of Corinth Gulf seismic area (Greece): Fuzzy logic algorithms time series pattern recognition

Dr. Zlotnicki Jacques

Magma and Volcanoes Laboratory CNRS IAGA

Gvishiani A., Le Moul J.L., Rodkin M., Agayan S., Bogoutdinov Sh., Vargemezis G.

During several decades many studies have focused on the search of electric, magnetic and/or electromagnetic (EM) precursors of earthquakes (and volcanic eruptions). In particular, electric signals in the ULF band (less than 10Hz) have largely been investigated, and some results of possible precursor signals were revealed and discussed. But, these signals are not systematically observed in every seismic area. Our study is devoted to Corinth Gulf seismic area. During the last years, an EM monitoring system of three stations was developed with the objective to do systematic observations, from DC up to several kHz. These ground based studies are done in the frame of Demeter mission, whose goal is to identify and correlate forerunners EM signals to earthquakes, at the ground surface and on board of the micro-satellite Demeter. The three EM stations bound a seismic gap, along which a magnitude 6 earthquake is expected. At the three stations, horizontal electric and three components magnetic fields are recorded at 100Hz. At two stations, horizontal electric and magnetic fields are also recorded at 1kHz, while these fields are measured, every hour, at 10 kHz during 5 minutes in the centre of the seismic gap. Up to now, small earthquakes ($M < 4$) have been recorded in the vicinity of the stations ($< 100\text{km}$). Most of the earthquakes which hypocenters are along the seismic gap have produced co-seismic electric signals. The EM monitoring system gives a huge flow of electric, magnetic, EM, and seismic data that hardly can be fully examined manually. Besides, the features of data are very complicated, and the non-formal criteria are sometimes used in experts data processing. Thus, we introduce a new data processing methodology, based on artificial intelligence approach, fuzzy-logics and statistics, which avoids non-formal EM signal identification. Such approach also gives the possibility to systematically study huge volumes of data. These algorithms carry out the morphological examination of time series with the purpose to recognise signals in successive segments of the records. Both, a sample of a real record or some ideal pattern formulated by expert, are used to set the recognition procedure. The algorithms are able to allocate signals in electric and magnetic data, and to discriminate between signals of different morphology. These algorithms can be automatically processed through large datasets.



(S) - IASPEI - *International Association of Seismology and Physics of the Earth's Interior*

JSS008

Poster presentation

2013

The INGV tectonomagnetic network: future developments in the MEM Project

Dr. Fabrizio Masci

Osservatorio Geofisico di L'Aquila Istituto Nazionale di Geofisica e Vulcanologia

Paolo Palangio, Cinzia Di Lorenzo, Manuele Di Persio, Antonio Meloni

The MEM Project (Interreg IIIA Adriatic Cross Border Programme) has been activated in the INGV (Italian Istituto Nazionale di Geofisica e Vulcanologia) Observatory of LAquila since 2004. The leader partner of the project is the Abruzzo Region. One of the purposes of the MEM project is the electromagnetic monitoring of the geodynamic processes related to the seismic activity. To that end inside this project the upgrade of the INGV tectonomagnetic network was scheduled. The INGV tectonomagnetic network was installed in Central Italy since the middle of 1989 to investigate possible seismomagnetic effects related to earthquakes occurrences. The network is part of the INGV L'Aquila Geomagnetic Observatory. Here, we are reporting the actual state and the future developments of the network. At the present time, total geomagnetic field intensity data are collected in four stations using proton precession magnetometers. During 2007 the network will be updated with new other stations with the aim to thicken the network and to extend the research area. Each network station will be supplied with a new overhauser magnetometer and a 3-axes magnetometer. Some tests, carried out to select the location of the new stations, are shown. Here we also report the 2006 dataset of the network stations showing a different approach in the data analysis that takes into account the inductive effects on the total geomagnetic field intensity by means of the inter-station transfer functions.

Keywords: tectonomagnetism



(S) - IASPEI - *International Association of Seismology and Physics of the Earth's Interior*

JSS008

Poster presentation

2014

Network-MT surveys in Central Japan

Dr. Makoto Uyeshima

Earthquake Research Institute the University of Tokyo IAGA

Tsutomu Ogawa, Satoru Yamaguchi, Hiroaki Toh, Hideki Murakami, Ryohei Yoshimura, Naoto Oshiman, Shigeru Koyama, Toshiya Tanbo, Weerachai Siripunvaraporn

In Central Japan, there runs the Niigata-Kobe tectonic zone in its backarc side, seismic and volcanic active zone beneath the Northern Japan Alps, and low-frequency seismic zone of non-volcanic origin in its forearc side. All these crustal activities are considered to be directly or indirectly related to the existence or movement of the crustal fluids such as water or melt. Electrical conductivity is an underground physical property which is sensitive to the existence of such crustal fluids and their connectivity. Thus, aiming at elucidating mechanism of the various kinds of crustal activities occurring beneath Central Japan, we have started the Network-MT survey to determine regional and deep electrical conductivity structure down to the upper mantle since the end of 2005. In this study, we introduce its first and second surveys on a 260 km NNW-SSE trended survey line from Noto Peninsula, Ishikawa Pref. to Toyama, Nagano Pref. together with a 45 km sub-survey line along the Atotsugawa Fault from Higashimozumi to Hatogaya, Gifu Pref. The ENE-WSW trended Atotsugawa Fault is located along the Niigata-Kobe tectonic zone. We will show characteristics of the Network-MT responses from 8s to several 10^4 s, and 2-D and 3-D inversion interpretations by using those responses. We will discuss on relationship between electric and seismic structures, and that between structures with distribution of hypocenters in the survey area.

Keywords: resistivity structure, network mt observation, niigata kobe tectonic zone



(S) - IASPEI - *International Association of Seismology and Physics of the Earth's Interior*

JSS008

Poster presentation

2015

Electric and magnetic field variations due to the seismic dynamo effect associated with blasting

Prof. Yoshimori Honkura

Department of Earth and Planetary Sciences Tokyo Institute of Technology IAGA

Shintaro Nagaoka, Yasuo Ogawa

Electric and magnetic (EM) field variations are observed during seismic-wave passage at the observations site, if the ground motion is sufficiently strong. We have proposed the mechanism of generation of these EM fields as the seismic dynamo effect. So far we have demonstrated some examples obtained in association with earthquakes, such as the 1999 Izmit earthquake and its aftershocks, but well-controlled blasting provides us with a more suitable case for the generation of EM fields due to the seismic dynamo effect. In October, 2006, a seismic reflection and refraction experiment was carried out in the central part of Japan by the volcano research group, and we set up two MT observation systems about a few hundred meters away from one of the blasting points; one in the west and the other in the south. We could successfully observe EM field variations, as expected. One signal was simultaneous with the blasting time, suggesting that it reflects the electric current used for triggering the blasting. Variations following this signal are due to the seismic dynamo effect. The results of this observation indicate that EM field variations seem to have started before the arrival of seismic wave.

Keywords: electric, seismic, blasting



(S) - IASPEI - *International Association of Seismology and Physics of the Earth's Interior*

JSS008

Poster presentation

2016

Numerical modeling of self-potential variation associated with very long-period seismic pulse observed in the 2000 Miyake-jima volcanic activity

Mr. Osamu Kuwano

Shingo Yoshida, Masao Nakatani, Makoto Uyeshima

Transient self-potential (SP) variations were observed simultaneously with tilt-step events of the 2000 Miyake-jima volcano activities (Sasai et al. 2002). Very long-period seismic pulses (VLP pulses) with a duration of about 50s (Ukawa et al., 2000; Fujita et al., 2002, 2004) were excited in these event. In this study, we attempt to model the observed SP variation, assuming it was due to electrokinetic effect accompanying fluid flow caused by VLP strain field. Though there have been many studies related to SP variations due to electrokinetic phenomena accompanying crustal activities, most of them have aimed to detect or evaluate static SP around faults or volcanoes. Few studies considered transient phenomena (e.g., Pride et al., 2004). First, using Okadas (1992) program, strain field caused by VLP pulse was calculated. Moment tensor of VLP pluses obtained by Kumagai et al. (2001) was used here. Fluid flow was then obtained as poroelastic response. Then electric field at the surface was obtained by integrating all streaming current sources induced by fluid flow. The simulation result agreed well with observed SP variation, in terms of both amplitude and magnitude.

Keywords: electrokinetic

PERUGIA
ITALY



(S) - IASPEI - International Association of Seismology and Physics of the Earth's Interior

JSS008

Poster presentation

2017

Resistivity structure at damage area of the 2006 Mid Java earthquake

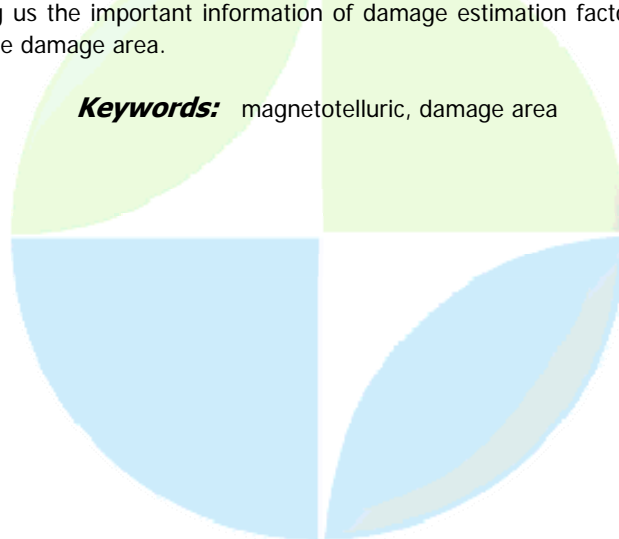
Prof. Toru Mogi

Institute of Seismology and Volcanology Hokkaido University IAGA

Yasuo Ogawa, Nurhasan, Djedi S. Widarto

We carried out the AMT and wide band MT survey at the damage area of the Mid Java Earthquake (M6.3) that occurred at 27th May, 2006. The damage area was distributing in the plain extending to the south of Yogyakarta district where thick soft sediment were deposited. Generally, an extent of damage due to shaking of a ground depends on the velocity contrast of S wave between basement rocks and sediments distributing in the surface, and thickness of the sediments as well. Our purpose of the survey was to clarify what subsurface structure was cause of the severe damage. We set 20 AMT sites along the line of WNW-ESE direction (A line) and 14 sites on the line of NNE-SSW direction (B line). These lines were through the damage zone in the center part and crossed each other. The wide band MT sites set at every other site and 11 sites were on the A bline and 7 sites were on the B line. The AMT, using the Phoenix MTU5A system, covers frequency range at 10kHz to 10 Hz and measured natural electromagnetic field over 1.5 to 2 hours at each site. The wide band MT covers at 320Hz to 0.01Hz and measured at overnight of 12 to 15 hours in this survey. We performed data process using the MTU standard data process to obtain apparent resistivity and phase, and using the Groomy-Berly decomposition to find strike direction. The apparent resistivity and phase at 1 to 0.1 of dead band showed almost large error, but another frequency ranges were relatively better quality. The strike directions in higher frequencies were not clear in all sites. This means that the resitivity structure is almost layer form at a shallower depth. We derived resitivity section image across the damage area using the 2D inversion code developed by Ogawa and Uchida (1996). The resistivity image showed conductive layer, less than 10 ohm-m, is distributing in the plain and its thickness increase at the center where the conductive layer was 1.5km thick and severe damage was happened. The conductive layer was not found beyond the east side of the plain and entering mountainous area where the resistive layer was distributing to a shallower depth. We interpret that the shallower conductive layer found under the plain is correspond to the soft sediment layer and the thick sediment caused to the sever damage. The resistivity contrast between the basement layer and the sediment was about 10 times. Probably contrast of S wave velocity between these layer was estimated to about 30% based on the relation between resitivity and S wave velocity change. As a conclusion of this survey, the MT study has possibility of providing us the important information of damage estimation factor through the resitivity image covered over the damage area.

Keywords: magnetotelluric, damage area



(S) - IASPEI - *International Association of Seismology and Physics of the Earth's Interior*

JSS008

Poster presentation

2018

Electrical resistivity structure around the hypocentral region of DLF events in the Kii peninsula, southwest Japan

Dr. Naoto Oshiman

Disaster Prevention Research Institute Kyoto University IAGA

Tkehiro Nagano, Rokei Yoshimura, Satoru Yamaguchi, Makoto Uyeshima

Recently, very high dense seismic observation network, called Hi-net in Japan, revealed the existence of deep low-frequency (DLF) events (or deep non-volcanic tremors) at depths of about 35km along the subducting Philippine Sea plate, southwest Japan (Obara, 2002). Their generation mechanism has not been well understood, yet. Crustal fluids are, however, strongly thought to generate such DLF events, taking their characteristics into consideration. In order to investigate electrical resistivity structure around the hypocentral region of the DLF events, southwest, we conducted the magnetotelluric (MT) soundings in the Kii peninsula. We made wide-band MT measurements at 16 sites along the survey line of about 70 km across the epicentral area of the DLF events in the Kii peninsula, in September, 2005. Apparent resistivity and phase of the TM mode of the wide-band MT, together with those of longer-period MT and Network-MT measurements, were used for determining a two-dimensional resistivity structure model. In the obtained best-fit model, a low resistive region is seen at depths around the hypocenters of the DLF events located in the middle of the profile, suggesting that crustal fluids from the subducting Philippine Sea plate exist around the region.

Keywords: resistivity, mt

PERUGIA
ITALY



(S) - IASPEI - *International Association of Seismology and Physics of the Earth's Interior*

JSS008

Poster presentation

2019

Crustal heterogeneity on electrical resistivity around the Niigata-Kobe Tectonic Zone, Chubu Region, Japan

Dr. Ryokei Yoshimura

Disaster Prevention Research Institute Kyoto University IAGA

Hiroaki Toh, Makoto Uyeshima, Naoto Oshiman, Research Group For Crustal Resistivity Structure

Wideband magnetotelluric (MT) soundings were carried out around the concentrated deformation zone, Chubu region, Japan (NKTZ: Niigata-Kobe Tectonic Zone pointed out by Sagiya et al.[2000]). The NKTZ becomes one of important target areas in "the 2nd new Program of and Observation for Earthquake Prediction" (Hirata, 2004). A multidisciplinary research around the NKTZ, especially the Atotsugawa fault, using dense GPS, seismological observations and investigation of crustal resistivity structure has been started since 2004. In October 2004, we obtained the electric and magnetic fields data at 30 sites across the central part of the NKTZ in which the Ushikubi, Mozumi-Sukenobu, Atotsugawa, Takayama-Oppara faults are located. Observed data at all sites were processed by the remote reference technique. Using Phase Tensor analysis (Caldwell et al., 2004), we verified the data showed strong two-dimensionality in the long period (1-1000sec). Apparent resistivity and phase in TM mode, phase in TE mode and tipper were used for two-dimensional inversions. Obtained model shows inhomogeneity in the middle and lower crust. Additionally in 2005, to reveal heterogeneity along the fault plane, we carried out MT survey along the Atotsugawa fault. A seismic gap and a creep-like crustal movement were observed along the Atotsugawa fault. Obtained preliminary inversion result shows lateral inhomogeneity correlated with heterogeneity in seismicity along the fault, which suggested that the seismic gap on the Atotsugawa fault plane seems to be modeled as a high resistive block. We will report outline of the both MT surveys and also discuss results compared with seismic and GPS data.

Keywords: magnetotellurics, atotsugawa fault, tectonic zone



(S) - IASPEI - *International Association of Seismology and Physics of the Earth's Interior*

JSS008

Poster presentation

2020

Deep electrical imaging of Parbati Beas Valley geothermal region of NW Himalayan region

Dr. Veeraswamy Koppireddi
Magnetotellurics N.G.R.I. IASPEI

K.Ravi Shyankar, G.Dhanunjaya Naidu, Sarana Basava, K.K.Abdul Azeez

Parbati Beas valley of NW Himalaya forms one of the important geothermal regions. The well known structural features such as MCT and MBT forms part of the region. The important hot spring locations such as Manikaran, Vashisht etc can also be seen. After successful delineation of a large anomalous conductive zone near Puga region related to major geothermal reservoir, much attention is being paid to this region to explore the area for possible exploitation of resources. Two long profiles oriented one nearly in NS direction and the other in NE-SW direction with 30 broadband stations have been completed to map the deep geoelectrical structure with a station interval of about 5 km. Single site robust processing of the data gave consistent MT response functions after removal of local distortion effects using decomposition technique. The data are modeled with both TE and TM mode response functions using non-linear conjugate gradient algorithm. Anomalous shallow conductive features derived from the data are indicative of the possible presence of geothermal reservoir and deeper anomalous features are interpreted due to the presence of major tectonic features in the region.

Keywords: beas parbati valley, himalayas, geothermal region

PERUGIA
ITALY



(S) - IASPEI - *International Association of Seismology and Physics of the Earth's Interior*

JSS008

Poster presentation

2021

Seismomagnetic studies in central Italy: 16 years of monitoring by the INGV network

Dr. Domenico Di Mauro

Geomagnetism Dept. INGV - Roma2, ROME - ITALY IAGA

Manuele Di Persio, Stefania Lepidi, Fabrizio Masci, Giuliana Mele, Antonio Meloni, Paolo Palangio

According to several studies, earthquakes and volcanic eruptions, produce variations in the absolute value of the local geomagnetic field intensity. To detect possible effects related to seismic activity in central Italy, INGV installed a network of four magnetometers in a region extending from 41 to 43 N and 12 to 15 E, since 1989. Total geomagnetic field intensity was synchronously sampled at the magnetometer sites and averaged on a daily basis. Observed averaged values were then differentiated with respect to the data recorded at the permanent nearby Geomagnetic Observatory of LAquila (42 23 N, 13 19 E). The study area is characterized by active faulting and seismicity, and by historical destructive earthquakes. In the search of potential significant magnetic field variations of tectonic origin, data were recorded for about 16 years only with some interruptions due to temporary instrumental failures. This data set represents a long series of geomagnetic total field intensity measurements that is valuable to study the secular variation in a tectonically active area. Some anomalous variation of the differential geomagnetic field intensity are discussed in relation to the seismic activity for the whole dataset until 2006.

Keywords: seismomagnetism, tectonomagnetism



(S) - IASPEI - *International Association of Seismology and Physics of the Earth's Interior*

JSS009

2022 - 2066

Symposium

**Progress in electromagnetic studies on earthquakes and volcanoes -
Crustal instabilities and earthquake precursors**

Convener : Prof. Pier Francesco Biagi

Tectonic activity produces permanent and/or temporal alterations of geophysical, geodetic, geochemical and hydrological state of the earth crust. These alterations, earthquakes being the most typical, reflect the crustal instabilities at critical state. It has been reported that often even the atmosphere/ionosphere is affected by such instabilities - the phenomenon now called the lithosphere-atmosphere-ionosphere (LAI) coupling. Different methods of geosciences are in operation to monitor the crustal instabilities. The earthquake precursors, in particular the electromagnetic precursory phenomena, constitute one of the important targets of crustal instability research. The crucial point here is that all these phenomena are inter-related and to understand them, we have to treat the earth's crust as a system. The scope of this session includes: 1) All kinds of evidence of crustal instabilities, involving seismicity, magmatism, strain anomalies, active faulting, fault creep and underground fluid perturbations, in addition to EM anomalies, and their inter-relationships; 2) All empirical and statistical variations of crustal phenomena, preceding or coming with earthquakes and their inter-connections. Instrumentation, measurement techniques and methods of data analysis for pre-co-post crustal instabilities; 3) Theoretical models to explain the physical mechanisms behind instabilities and their precursors.

XXIV 2007

PERUGIA
I T A L Y



(S) - IASPEI - International Association of Seismology and Physics of the Earth's Interior

JSS009

Oral Presentation

2022

Recent results on seismic electric signals (SES)

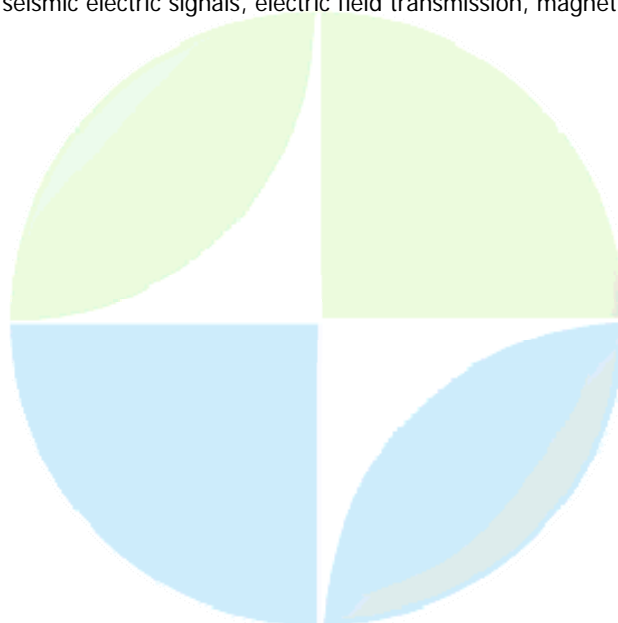
Prof. Panayiotis Varotsos

Physics Department University of Athens IASPEI

Efthimios S Skordas, Nicholas V Sarlis

Seismic Electric Signals (SES) are low frequency (1 Hz) electric signals that precede earthquakes. [P. Varotsos and K. Alexopoulos, Tectonophysics 110, 73 (1984); *ibid* Tectonophysics 110, 99 (1984)] Since the 80s, it has been suggested that they are emitted from the focal area when the stress reaches a critical value. During the last several years, our knowledge on the SES has been advanced through detailed experimental and theoretical studies, which among others include the following: First, for SES activities preceding major earthquakes and for epicentral distances ~100 km, the electric field arrives 1 to 2 s before the time derivative of the horizontal magnetic field [P. Varotsos, N. Sarlis and E. Skordas, Phys. Rev. Lett. 91, 148501 (2003)]. An explanation, should consider, beyond criticality, the fact that the transmission through a weakly conductive medium like the Earth, of low frequency electromagnetic fields, obeys diffusion type equations. Second, in the aforementioned case it is also observed that the electric field components of SES exhibit markedly different time evolution. This difference, if properly measured, is of profound importance since it can reveal the distance of the measuring site from the epicenter of the impending earthquake [P. Varotsos, N. Sarlis and E. Skordas, Appl. Phys. Lett. 86, 194101 (2005)]. Third, the introduction of the new concept of natural time [P. Varotsos, N. Sarlis and E. Skordas, Practica Athens Acad. 76, 294 (2001)] revealed new properties of the SES activities that were hitherto unknown. For example, the study of the normalised power spectrum in the natural time domain shows that all SES activities fall on a universal curve which coincides to that expected from the theory of critical phenomena [P. Varotsos, N. Sarlis and E. Skordas, Phys. Rev. E 66, 011902 (2002)]. Furthermore, the SES activities exhibit infinitely ranged temporal correlations and hence memory which is markedly stronger than that found from the analysis of electric signals emitted from man-made sources [P. Varotsos, N. Sarlis and E. Skordas, Phys. Rev. E 67, 021109 (2003); *ibid* 68, 031106 (2003)].

Keywords: seismic electric signals, electric field transmission, magnetic field variations



(S) - IASPEI - International Association of Seismology and Physics of the Earth's Interior

JSS009

Oral Presentation

2023

Analysing complex time series in natural time

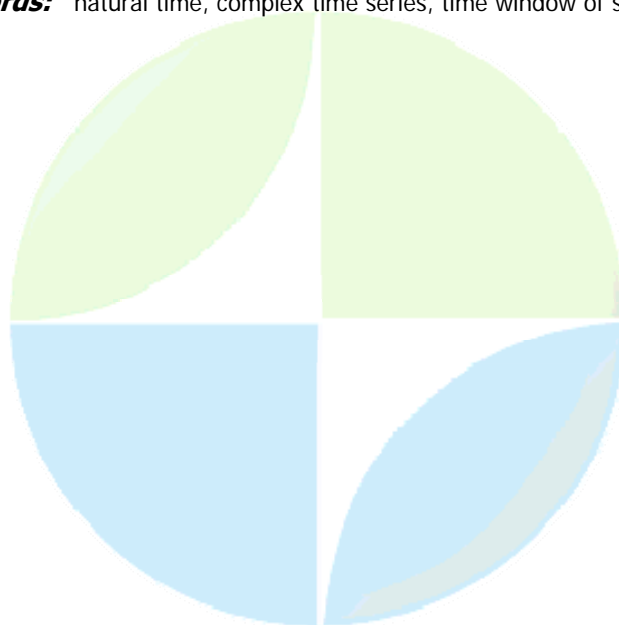
Prof. Panayiotis Varotsos

Physics Department University of Athens IASPEI

Nicholas V Sarlis, Efthimios S Skordas

Novel dynamical features hidden behind time series in complex systems can emerge upon analysing them in a time domain, termed natural time, that has been introduced recently [P. Varotsos, N. Sarlis and E. Skordas, *Practica of Athens Academy* 76, 294 (2001); *ibid Phys. Rev. E* 66, 011902 (2002)]. This analysis enables the study of the dynamical evolution of a complex system and identifies when the system enters the critical stage. Relevant examples have been published in a large variety of fields including biology, physics and earth sciences. As a first example, we mention the analysis of the electrocardiograms which may herald a cardiac arrest [P. Varotsos, N. Sarlis, E. Skordas and M. Lazaridou *Phys. Rev. E* 70, 011106 (2004); *ibid* 71, 011110 (2005)]. Second, natural time analysis enables the distinction between the precursory electric signals, termed Seismic Electric Signals (SES) and similar looking electric noise emitted from artificial (man-made) sources. Third, the data of avalanches of the penetration of magnetic flux into thin films of type II (high-Tc) superconductors as well as those of a three dimensional pile of rice (which are typical systems that have been suggested as following the so-called Self Organised Criticality) getting progressively closer to the critical state conform to the features suggested, on the basis of natural time, to describe critical dynamics [N. Sarlis, P. Varotsos and E. Skordas, *Phys. Rev. B* 73, 054504 (2006)]. Fourth, the analysis of seismicity subsequent to the SES detection allows the determination of the occurrence time of the impending strong earthquake(s) within a narrow range around a few days at the most [P. Varotsos, N. Sarlis and E. Skordas *Practica Athens Acad.* 76, 294 (2001); *ibid Acta Geophys. Pol.* 50, 337 (2002)]. Details on the latter procedure, which has been applied to recent strong earthquakes in Greece [P. Varotsos, *Proc. Jpn. Acad. Ser. B* 82, 86, 2006; P. Varotsos, N. Sarlis, E. Skordas, H. Tanaka and M. Lazaridou, *Phys. Rev. E* 73, 031114 (2006); *ibid Phys. Rev. E* 74, 021123 (2006)], the SES activities of which have been identified and submitted for publication well in advance, are presented

Keywords: natural time, complex time series, time window of strong eqs



(S) - IASPEI - *International Association of Seismology and Physics of the Earth's Interior*

JSS009

Oral Presentation

2024

VLF transmitter signals received on satellite for global diagnostics of ionospheric perturbations associated with seismicity

Dr. Alexander Rozhnoi
electromagnetic iperas IASPEI

Molchanov Oleg, Solovieva Maria, Akentieva Olga, Berthelier Jean Jackiy, Parrot Michel, Lefeuvre Francuas, Hayakawa Masashi, Yamauchi Takeshi, Biagi Pier Francesco, Castellana Laura

We present two methods of the global ionosphere diagnostics using VLF signals received on board a satellite in association with two cases of strong seismic activation. The method of reception zone changes reveals an evident effect before and during the great Sumatra earthquake with long-time duration of the order of one month. The result leads to the conclusion on the size of perturbation area of the order of several thousands kilometers. Disadvantage of this method is in its difficulty to separate preseismic and postseismic effects. In contrast, the difference method allows us to overcome this difficulty and it shows the appearance of preseismic effect for several days for seismic activation near Japan. However, we need such an analysis for reliability in regular satellite data to be checked by ground reception of subionospheric VLF signals. It is not so obvious that both of these satellite and ground effects are excited by the same generation mechanism on the ground. So, these look as complementary. The work was supported by ISTC under Grant 2990.

Keywords: radiowaves, seismicity, satellite



(S) - IASPEI - *International Association of Seismology and Physics of the Earth's Interior*

JSS009

Oral Presentation

2025

Observation evidences of Atmospheric Gravity Waves induced by seismic activity from analysis of subionospheric LF signal spectra

Dr. Alexander Rozhnoi
electromagnetic iper IASPEI

Solovieva Maria, Molchanov Oleg, Biagi Pier Francesco, Hayakawa Masashi

We analyze variations of LF subionospheric signal amplitude and phase from JJY transmitter in Japan (F= 40 kHz) received in the station Petropavlovsk-Kamchatsky during seismically quiet and active periods together with the periods of magnetic storms. After 20 s averaging the frequency range of the analysis is 0.28 -15 mHz that corresponds to the period range T from 1 to 60 minutes. Changes in spectra of LF signal perturbations are found several days before and after three large earthquakes , which happened in November 2004 (M=7.1), August 2005 (M=7.2) and November 2006 (M=8.2) inside Fresnel zone of Japan-Kamchatka wavepath. Comparing the perturbed and background spectra we have found the evident spectrum increase in a range of T= 10-25 minutes that is in compliance with theoretical estimations on lithosphere-ionosphere coupling by AGV waves (T> 6 minutes). Similar changes are not found for the periods of magnetic storms The work was supported by ISTC under Grant 2990.

Keywords: radiowaves, seismicity, ionosphere

PERUGIA
ITALY



(S) - IASPEI - International Association of Seismology and Physics of the Earth's Interior

JSS009

Oral Presentation

2026

Natural time analysis of seismicity in Japan and California

Prof. Seiya Uyeda

Approach to critical state of seismicity a few days before mainshocks was indicated in areas other than Greece. Time series of seismicity before 2000 Izu-island (M6 class), 1995 Kobe (M7.3), 2004 Niigata Chuetsu (M6.8), 2003 Tokachi-oki (M8.0) in Japan, and 2004 Parkfield earthquakes (M5.9) in California. The 2000 swarm activity in Izu-island region, lasting for about two months with some 7,000 shocks with magnitude $M \geq 3$ and five $M \geq 6$ shocks, was preceded by a pronounced seismic electric signal (SES) activity with innumerable signals that started a few months prior to the swarm onset. It has been shown first that the seismicity subsequent to the electrical activity approached to the critical stage a few days before the occurrence of the first $M \geq 6$ shock, and second that the electrical signals also have the properties characteristic to a critical stage. These features were similar to those found earlier in Greece. Seismicities before 1995 M7.3 Kobe, 2003 M8.0 Tokachi-Oki, and 2004 M6.8 Niigata Chuetsu earthquakes (EQs), in Japan, have been analyzed in the natural time-domain. For the Kobe and Tokachi-oki EQs, the occurrence time of the impending mainshocks were assessed with accuracy of the order of a few days, when the computation had started 1-2.5 months before the mainshocks. In the present cases where there was no SES data, the starting dates of computation were sought by trial and error approach. For the Chuetsu event, the results were uncertain. The same type of analysis has been made on seismicity after 2003 San Simeon EQ and before 2004/09/28 Parkfield EQ in California. In circular and elliptic areas with different sizes around San Andreas Fault, magnitude 2.2-2.6 EQs (Catalog: NCEDC) were shown to reach critical point 5 days before the mainshock of the Parkfield EQ, when the calculation was started on 2004/05/01.

Keywords: natural time, critical state, seismicity



(S) - IASPEI - *International Association of Seismology and Physics of the Earth's Interior*

JSS009

Oral Presentation

2027

Anomalies in VLF radio intensities related to seismicity during November-December 2004: a comparison of ground and Demeter satellite results

Prof. Pier Francesco Biagi

Department of Physics University of Bari IASPEI

Castellana Laura, Maggipinto Tommaso, Piccolo Roberto, Minafra Antonio, Ermini Anita, Capozzi Vito, Solovieva Masha, Molchanov Oleg, Hayakawa Masashi, Rozhnoi Alexander

A previous study of the VLF signals radiated by two ground transmitters located in Germany ($f = 16.6$ kHz) and in France ($f = 18.3$ kHz) and received on board of the French DEMETER satellite, revealed a drop of the signals (scattering spot) in the time interval November 23 December 12, 2004, probably connected with the occurrence of large earthquakes ($M = 5.4-5.5$) in Europe. From the beginning of 2002 a receiver is into operation at Bari University (Southern Italy) and the intensity and the phase of the VLF/LF radio signals radiated by GB ($f = 16$ kHz, United Kingdom), FR ($f = 20.9$ kHz, France), GE ($f = 23.4$ kHz, Germany), IC ($f = 37.5$ kHz, Island) and IT ($f = 54$ kHz, Sicily, Italy) are monitoring with a 5s sampling rate. In this study, the intensity data collected by the Bari receiver from October 2004 to January 2005 have been analysed in order to compare the results with those obtained by the DEMETER. Drops of the GB, FR, GE and IC signals were revealed before the middle of November and a drop of IT signal appeared before December 10. The possible effect of the geomagnetic activity and of the meteorology was investigated and a correspondence with the drop of the signals in November clearly appeared; on the contrary no correspondence stood up with the drop in December that is a peculiarity of the IT signal. So, a seismic effect can be considered and an agreement with the results obtained by the DEMETER seems to appear. A doubtful point is the appearance of such an effect only on the IT radio signal and not on the other ones (GB, FR, GE, IC).

Keywords: disturbances, radio signals, seismicity



(S) - IASPEI - *International Association of Seismology and Physics of the Earth's Interior*

JSS009

Oral Presentation

2028

Earthquake precursors detected through the analysis of mutual interactions of hydrogeochemical signals

Mrs. Laura Castellana

Department of Biomedical Sciences University of Foggia IASPEI

Pier Francesco Biagi

Many studies showed that changes in hydrogeochemical time series can be related to earthquakes. In particular, the detection of seismic precursors is traditionally carried out associating the spectral content of the time series analyzed to the occurrence of seismic events. The limit of this approach is twofold: first it is based on a posteriori signal analysis, second each groundwater parameter is analysed singularly and their mutual correlations are not investigated. Here correlations are meant both as interactions among hydrogeochemical parameters and as interactions between these parameters and the occurrence of seismic precursors. To overcome these drawbacks, we use a classifier that, appropriately trained on a finite and limited number of examples (training set), learns to predict the occurrence of seismic events in new observations of hydrogeochemical data. The training set is composed of l couple of examples $\{(x_i, y_i)\}$, $i=1, \dots, l$, where the vector x_i is the temporal window, large m , of the signal and y_i is a label identifying the signal pattern, i.e. $y_i = 0$ or $y_i = 1$ or $y_i = 2$ if x_i is a no-seismic signal or precursor signal or co-post seismic signal, respectively. Under this perspective, the problem of detecting hydrogeochemical precursors becomes the problem to predict the correct output y_j relative to never seen before input pattern x_j . The prediction accuracy and the number of false positives provide a quantitative measure of the capability of the multivariate predictor in discriminating no-seismic/ precursor/ co-post seismic signal. Furthermore, these quantities provide also an estimate of correlations between hydrogeochemical data and earthquakes, because the higher prediction accuracy, the better correlations among these quantities. The dataset used in this study is composed of thirteen geochemical time series collected in Kamchatka (Russia) peninsula, since 1977. The predictor we worked with is K Nearest Neighbour classifier. In order to compute the prediction accuracy, we use the Leave-K-Out-Cross-Validation (LKOCV) procedure, a statistically well founded method for estimating the accuracy of predictors by using a finite number of observations. We applied K Nearest Neighbour classifier to study the correlations among ions (Na^+ , Cl^- , Ca^{++} , HCO_3^- and H_3BO_3), among parameters (pH, Q and T) and finally among gases (N_2 , CO_2 , CH_4 , O_2 and Ar) in order to establish if their interactions improve the prediction accuracy of seismic precursors. The results show the model order is proportional to the prediction accuracy. This is a proof that information collected some months before the event under analysis are necessary to improve the classification accuracy. In particular, we obtained a prediction accuracy of 78% in a temporal window of size $m=80$.

Keywords: precursors, knn classifier, prediction

(S) - IASPEI - International Association of Seismology and Physics of the Earth's Interior

JSS009

Oral Presentation

2029

Changes of the electromagnetic parameters used as possible seismic premonitory signals

Dr. Dumitru Stanica

Electromagnetism and Lithosphere Dynamics Institute of Geodynamics of the Romanian Academy IAGA

Maria Stanica, Nicoleta Vladimirescu

Identification of electromagnetic (EM) precursory parameters related to the seismic activity is still under scientific debate and requires new reliable information about their possible interrelation with changes of electrical conductivity occurred prior to the geodynamic process. The paper emphasizes the anomalous behaviour of the EM parameters as possible premonitory signals under the circumstances of the specific geotectonic characteristics of the Vrancea zones intermediate depth seismicity. In this respect, measurements of geomagnetic field have been performed since 2001 year and recording network has consisted of two high sensitive geomagnetic systems placed at the Surlari National Geophysical Observatory and Provita de Sus Geodynamic Observatory. Every recording system consists of data logger with 6 channels and A/D converter of 24 bits resolution, three-axis magnetic field sensor (frequency range: DC- 1kHz) and a laptop for real time data storage and processing. One of the horizontal components of the three-axis magnetic sensor has always been orientated perpendicular to the geological strike in order to record its time variation. It is well known that a large-scale regional conductivity anomaly causes a regional amplification of the vertical magnetic component B_z as well as spatial changes of the horizontal magnetic component perpendicular to strike ($B_{per.}$). Subsequently, a specific approach regarding the electromagnetic precursory parameters ($B_{zn}=B_z/B_{per.}$ and $p_n=\rho_{||}/\rho_z$, where $\rho_{||}$ is resistivity parallel to strike and ρ_z is vertical resistivity), selected according to the temporal invariability criterion for a 2D geoelectric structure in non-seismic condition, taking into consideration their daily mean distribution versus intermediate depth seismic events recorded simultaneously, was elaborated. These changes of electrical conductivity inside of the Vrancea seismogenic slab and its surroundings, before the earthquakes to occur, as a sequence of the lithospheric conductivity changes produced maybe by the dehydration of the rocks associated with rupturing processes and fluid migration through faulting systems are reflected by the anomalous behaviour of the B_{zn} and p_n parameters and, finally, several conclusions concerning mutual interrelation within a span of 6 years interval are inferred. We claim that this specific methodology together with more complete approach of EM phenomena can improve the seismic hazard assessment.

Keywords: electromagnetic, precursory parameters, seismicity

(S) - IASPEI - International Association of Seismology and Physics of the Earth's Interior

JSS009

Oral Presentation

2030

Some basic problems related to ground based seismo-electromagnetics

Prof. Seiya Uyeda

1. Anomalies immediately before earthquakes (EQs) When the lead time of alleged EM precursors are long, they may be less convincing. However, when anomalies are observed minutes before EQs, it would be much more convincing. We introduce such anomalies (pulses of msec duration) observed by the VAN group for a long time. 2. Co-seismic anomalies One of the most common objections to seismo-EM is no co-seismic signals. In fact, although signals at the time of EQ have been routinely observed, they were always observed only when seismic waves arrived. They are co-seismic wave signals. So far, therefore, it is true that no reliable true co-seismic signals have been observed. If true co-seismic signal does not exist, can that be a reason for denial of pre-seismic signals? Not necessarily. It can rather provide key information for understanding the mechanism of EQ and seismo-EM. Certainly lab experiments show high frequency EM emission at rock fracture, which suggests the same may happen at EQ. However, high freq. signals at focal depth would not reach earth surface. Even if they do, usual DC-ULF field apparatus cannot record them. This is one explanation for non observation of true co-seismic signals. However, there may be a flaw in this: since fracture along faults of large EQ will take some time, measurable low freq. convolution component will inevitably be generated. This might lead to the conclusion that EQ does not generate even high freq. signals, possibly because EQ is not fracture but sliding of existing faults. Although this view is not warranted at the moment as information on EM effects of fault sliding with high speed at EQ is scanty, it might open new perspectives. In any case, EQ is a stress releasing event whereas precursory phenomena occur during the slow stress increasing process. They are different physical processes. 3. No pre-seismic EM signals at 2004 M6 Parkfield EQ. USGS scientists state that since nothing was observed at Parkfield, EM in general is unlikely useful for short-term prediction. Although we have some doubt about their methodology and data analysis, here we tentatively accept their results and seek some reason for non existence of EM at Parkfield and existence elsewhere. One possibility is as follows: San Andreas Fault is known for its weakness. Therefore, it may be suspected that EQ takes place before any EM signal is generated. For generation of DC-ULF precursory EM signals, two main models are suggested. One is the solid state physics model by the VAN group and the other is the more popular electrokinetic model. Both models need certain level of stress to operate, which may be higher than San Andreas Fault can sustain.

Keywords: pre seismic pulses, co seismic anomalies, parkfield

(S) - IASPEI - *International Association of Seismology and Physics of the Earth's Interior*

JSS009

Oral Presentation

2031

Standardised procedure for satellite remote sensing thermal anomalies and earthquakes

Dr. Hari Narain Srivastava

SEISMOLOGY GLOBAL HYDROGEOLOGICALSOLUTIONS IASPEI

Satellite based radiometers like NOAA AVHRR, and SSM/I which sense the thermal emission originating from the earth surface are now being increasingly used to study thermal anomalies originating near the earth surface. Such observations are generally found to be precursory in nature although a few such anomalies are also co-seismic or post seismic. Under a programme sponsored by the Dept. of Science and Technology a few such observations have been reported in some parts of world including India. In order to obtain a coherent approach from operational point of view it is necessary to standardize such observations with respect to epicenter distance, focal depth, magnitude of earthquakes and meteorological conditions particularly the dynamic weather systems. Keeping in view that earthquake occurrence is chaotic in nature the data can be utilized to evolve probabilistic approach based on either the synthesized probability or Principal Component Analysis. Results have been examined using this approach.

Keywords: thermal, anomalies, earthquakes

PERUGIA
ITALY



(S) - IASPEI - *International Association of Seismology and Physics of the Earth's Interior*

JSS009

Oral Presentation

2032

Observation report of quasi-electrostatic for Wenan earthquake

Prof. Yougang Gao

college of Telecommunications Beijing University of Posts and Telecommunications IASPEI

Li Yantang

In the paper, the abnormality variation of quasi-electrostatic field observed by Handan Earthquake Observatory Station corresponding to Wenan earthquake, Hebei province(5.1, with Eastern Longitude and Northern Latitude),happened on July 4,2006, 301km away from the observatory station, is presented. Observation of quasi-electrostatic field responding to Wenan earthquake show that our record system can detect abnormality variation caused by sources about 300~400Km, The most abnormality appear about one month before the main earthquake. It is found that the abnormality variation is a course with weak strong weak quietude - occurrence. And the dominant frequency is 0.1~0.7Hz.

Keywords: abnormalityvariation, quasi electrostatic field, dominant frequency



(S) - IASPEI - International Association of Seismology and Physics of the Earth's Interior

JSS009

Oral Presentation

2033

Patterns preceding major earthquakes in Central Himalaya

Prof. Harsh Gupta

National Geophysical Research Institute Raja Ramanna Fellow

Dodla Shashidhar, Metilda Pereira

Himalaya is seismically or one of the most active intra-continental region in the world where devastating earthquakes have occurred. In the Global Seismic Hazard Assessment Program estimates of peak ground acceleration in Himalayan region have been made. However it is useful if regions likely to be affected by major earthquakes are identified on long-term basis. A successful study was made in 1986 where based on the concept of "precursory swarm and quiescence" an area of 50x40 was identified to be the site of a future 8 magnitude earthquake to occur before the end of 1990. This medium term forecast came true with the occurrence of an M 7 earthquake on 8 August 1988. We are now making an effort to identify other parts of Himalayan belt where precursory swarm and quiescence precede major earthquakes. One such region is central Himalaya where we discovered that three major earthquakes namely 19 January 1975 Kinnaur earthquake of M 6.8, 19 October 1991 Uttarkashi earthquake of M 7.0 and 28 March 1999 Chamoli earthquake of M 6.6 were preceded by precursory swarm and quiescence. For the Kinnaur earthquake a well-defined swarm activity with 5 shocks of $M \geq 5$ was observed during 1963-1968 followed by a seismic quiescence during the period 1968 - 1975 before the main shock of 1975. A similar pattern was also observed for the Uttarkashi and Chamoli earthquakes. With a swarm activity well before 20 years during 1966-1969 for Uttarkashi earthquake, followed by seismic quiescence from 1970-1990 with only one event of $M > 5$ in 1979. For the Chamoli earthquake the swarm and quiescence activity is not very clear probably due to the occurrence of Uttarkashi earthquake in 1991 in the immediate vicinity. In any case, a seismic quiescence was observed during 1992-1999. The purpose of this study is to extend this concept to other Himalayan regions, which might have gone through the precursory swarm and are currently in the quiescence period preparing for a future earthquake.

Keywords: himalaya, precursory swarm quiescence, forecast



(S) - IASPEI - *International Association of Seismology and Physics of the Earth's Interior*

JSS009

Oral Presentation

2034

Statistical study of the relationship between seismic electric signals and earthquakes at Koze-Shima Island, Japan

Dr. Masashi Kamogawa

Department of Physics Tokyo Gakuzei University

Yoshiaki Orihara, Toshiyasu Nagao, Seiya Uyeda

Geoelectric potential difference monitoring has been conducted in Koze-shima Island about 170 km south of Tokyo. During the monitoring period (May 14, 1997 - June 25, 2000), there were 20 anomalous geoelectric changes that practically satisfy the criteria for Seismic Electric Signals (SES) in the VAN method. In the same period, 25 earthquakes of which magnitude was greater than 3 within 20 km focal distance occurred. Some selectivity relation, including SES polarities, was noticed. In this paper, statistical correlation between the anomalous geoelectric changes and the earthquakes is examined. When 30-day leadtime was chosen, anomaly appearance rate (AAR) and earthquake occurrence rate (EOR) were 44 % and 55 %, even no selectivity was considered. Note that AAR was defined by the ratio of the number of SES appearances and the number of EQs and EOR was defined by the ratio of the number of EQ occurrences and the number of SES appearances. The AAR exceeded 2 sigma of AARs and EORs in simple random testing. In order to ascertain the correlation, the leadtime, area, and magnitude dependences are also examined. If the selectivity map is taken into account, both AAR and EOR are much higher.

Keywords: earthquakes, ses, kozu island

PERUGIA
ITALY



(S) - IASPEI - *International Association of Seismology and Physics of the Earth's Interior*

JSS009

Oral Presentation

2035

Towards extraction of precursory changes from noisy electromagnetic data

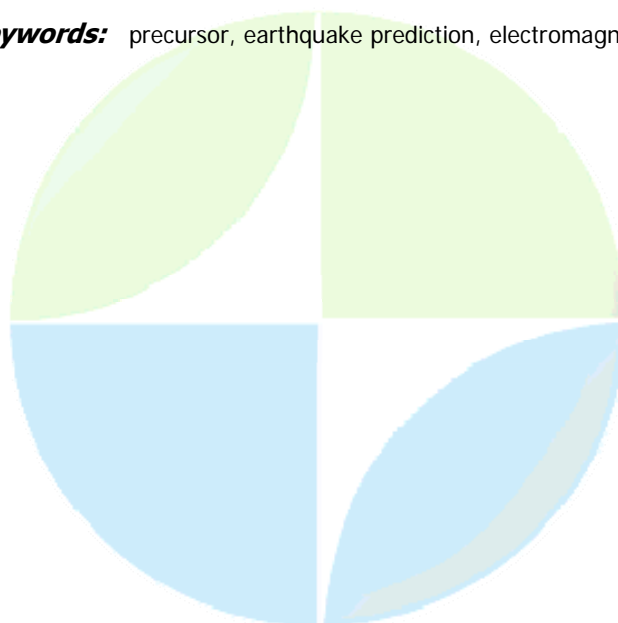
Prof. Toshiyasu Nagao

Earthquake Prediction Research Center Tokai University IASPEI

Takayuki Kawakami, Keizo Sayanagi, Jun Izutsu, Makoto Harada, Makoto Uyeshima, Tada-Nori Goto

There are a number of reports that electromagnetic data contain precursory changes related to earthquakes and volcanic eruptions. However, artificial noises, such as leakage current from DC-driven trains and electromagnetic noises from factories, are extremely large in Japan over wide frequency ranges. Therefore, it is very difficult to extract precursory conductivity changes and telluric current changes due to electrokinetic effects by using the conventional techniques (magneto-telluric method, apparent resistivity monitoring, and spontaneous potential monitoring, etc.). During the last decade, some researchers have been claiming that well-considered information processing techniques (principal components analysis; PCA, independent components analysis; ICA, fractal/multi-fractal analyses, and so on) are tools quite useful to extract precursory changes. Their approaches sometimes seemed working well. However, most of the cases, they only demonstrated that some abnormal changes were observed before impending earthquakes and volcanic eruptions. The abnormal changes, however, could have been due to other causes. In order to improve the situation, it is considered that we should pay more attention to remove the theoretically explainable changes (magnetic pulsations and their induction components, tidal components due to earth and ocean, etc.) at first by using the well-designed remote reference techniques (e.g., inter-station transfer function technique using wavelet transformation). Then, we apply the information processing techniques to extract precursory changes and consider their theoretical backgrounds. Analyzed data in this study is telluric current data since 1996 at Ito Station, east coast of Izu Peninsula and ocean bottom electro-magnetic data off Izu Peninsula since 2005. In the region, during the study period, we had three severe seismic swarms in 1996, 1998 and 2006. Izu Peninsula, being close to Metropolitan Tokyo, is a region of very high artificial noise. If we succeed in extracting meaningful precursory changes in this region, we believe that it is an enormous progress in seismo-electromagnetics.

Keywords: precursor, earthquake prediction, electromagnetics



(S) - IASPEI - *International Association of Seismology and Physics of the Earth's Interior*

JSS009

Oral Presentation

2036

The transfer functions between geomagnetic changes and neutral current of 500kV power line

Dr. Jun Izutsu

Earth Watch - Safety Net Research Center Chubu University IASPEI

Junji Kanaya, Tomiichi Uetake, Makoto Harada, Toshiyasu Nagao

The electromagnetic anomalies related to earthquakes have been reported since 1980s, including the pre-seismic anomalous telluric current (e.g. VAN method). We have been examining the neutral current of transformers of the commercial power line system to see if it shows transient anomalies associated with earthquakes. This study was motivated by Higuchi (2000), reporting a large change of neutral current (over 30A) at a substation in west Japan before and after a nearby M3.0 earthquake. Since 2002, we have monitored the neutral current by using a clamp sensor at three substations in seismically active areas in east Japan, i.e., Shin-Hadano, Shin-Fuji and Higashi-Yamanashi substations. The neutral current is sensitive to factors such as the geomagnetic changes and artificial noises (especially, DC driven electric trains) like conventional telluric current (Izutsu et al., 2006). In this study, we examine the observed neutral current data and compare them with geomagnetic field observed at Kakioka magnetic observatory and try to show the relationship between geomagnetic field and neutral current quantitatively. We calculate transfer function between geomagnetic field data (for input) and neutral current data (for output). Instead of the conventional Fourier transform, we have used continuous wavelet transform (Harada et al., 2004). Although the transfer functions for short-period geomagnetic changes were not clearly determined because of artificial noises of neutral current data, the transfer functions for long-period geomagnetic changes (longer than 300 sec) were determined with small errors. By this result, we can discriminate the influence of geomagnetic changes from observed neutral current data and it would make it easy to discriminate the anomalous signals possibly associated with earthquakes from noises.

Keywords: neutral current, geomagnetic induced current, transfer function



(S) - IASPEI - International Association of Seismology and Physics of the Earth's Interior

JSS009

Oral Presentation

2037

Analysis on The Dynamical Nature of Seismo-Electromagnetic Signal

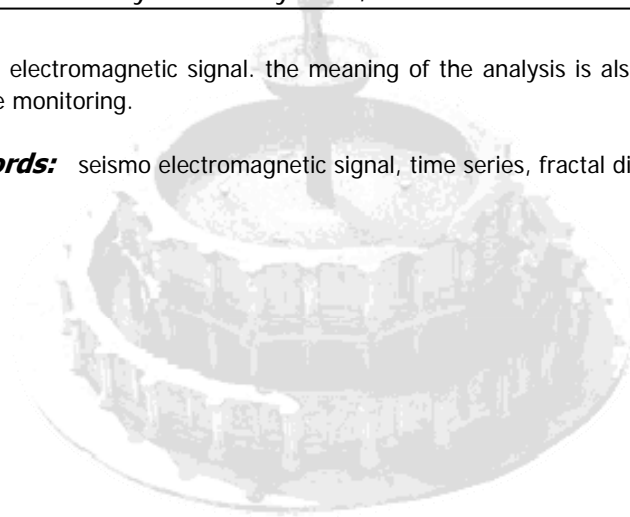
Dr. Dong Jiping

Research & Development Center China Academy of Space Technology IASPEI

Electromagnetic phenomena have been recognized as a promising candidate for the short-term earthquake prediction (Hayakawa, 2005). There are a lot of reports concerning about electromagnetic signal observed in a wide frequency range from ULF to HF before earthquakes occur. Electromagnetic radiation during experiments of rock fracture also convinces us that seismo electromagnetic signal comes directly from seismic source, considering that earthquakes occur when rock body fractures suddenly due to high stress in crust. It seems that seismic electromagnetic signal is closely related to fracturing process of rocks in crust. So as to this, Several radiation mechanisms of seismic electric magnetic signal, such as stress variation effect in seismogenic zone, piezoelectricity or piezomagnetic effect, and electromagnetic emission associated with microscopic cracking in rocks, have been brought forward. Comparing to field observation, none of these mechanisms can explain all abnormal behavior of seismic electric magnetic signal, but electron emission effect with microscopic cracking in rocks is relatively some reasonable and with catholicity. For example, no observable stress variation corresponds to characteristic time of minutes or hours for abnormal Electromagnetic observation, and piezoelectricity or piezomagnetic effect need large number of orderly arrange dcrystalloids in crust. There are three main viewpoints about the mechanism of electron emission effect with rock cracking. The first viewpoint is surface charging mechanism, suggesting that the surface charge on crack walls in rock is caused by appearances of excited hole and electron trapping centers (point defects) on a newly created surface of rocks when fault asperities are sheared. The second is based on that seismic electromagnetic signal is caused by emission of electrons in crack tip end and the model of compressed atoms. Even a electric quadrupole model is proposed by Guo Ziqiang etc to simulate the extending process of microscopic cracking in rocks and frequency spectral bandwidth gotten as 0.5 1.0MHz. The emission of electrons in crack tip end and the model of compressed atoms are supported by the third opinion, and otherwise, a capacitor model is proposed as a supplement suggesting that charging and discharging in crack tip happens in the extending process of microscopic cracking and the lower or higher frequencies are explained well. After all, the radiation mechanism of seismo electromagnetic signal is still not known well. It seems much difficult for us to check which model is more reasonable by observation in field around ground. There is still much uncertainty in actual observational, such as amplitude, time series and direction and so on. The uncertainty seems relative to the dynamic radiation process. Another convincing evidence of seismic electromagnetic radiation caused by fracturing process of rocks is that there found abundant cracks in rocks. Once the stress in crust reaches a certain value, the seismological system would get into a nonlinear phase and the numberless cracks in focal dimension scope would fracture thus macroscopical seismic electromagnetic signal would be generated and observed. Considering that seismological Gutenberg - Richter Equation accords with power law, a typical fractal phenomena, much similar to the behavior of fragmentation in mining and eruption, as well as tectonic distributing. Some authors regard power law as a characteristic of self- similar seismological system and others suggest that it is a reflection of self-organized critical phenomenon. Although Gutenberg - Richter Equation is statistically got for global events and for a period of time, it is still often used for a certain region and for a longer time. In the paper, the power law is used to tiny cracks in crust rocks with different fractal dimensions for different scales. By the introduction of furcated fractal dimension, the radiation mechanism caused by fracturing process of rocks is analyzed related to the

time series of seismic electromagnetic signal. the meaning of the analysis is also discussed for ground observation and space monitoring.

Keywords: seismo electromagnetic signal, time series, fractal dimension



IUGG
XXIV2007
PERUGIA
ITALY



(S) - IASPEI - *International Association of Seismology and Physics of the Earth's Interior*

JSS009

Oral Presentation

2038

Instabilities, electric currents and earthquake precursors associated with volcanic activity

Prof. Friedemann Freund

Earth Science Division, Code SGE NASA Ames Research Center IAGA

Michelle Mcmillan, John Keefner, Joshua J. Mellon, Rachel Post

Deviatoric stresses can activate electronic charge carriers that normally lie dormant in rocks¹. The existence of these charge carriers was previously unknown. We studied electric currents flowing down strain gradients and temperature gradients². The charge carriers in question are defect electrons in the oxygen anion sublattice known as positive holes or pholes for short. They are introduced into the matrix of minerals during cooling when hydroxyl pairs (due to traces of dissolved water) split off hydrogen molecules and convert to peroxy links. The two oxygens in the peroxy links convert from the 2- to the 1- valence state. When deviatoric stresses act on cool rocks or when temperatures rise above ~500C, peroxy links dissociate activating pholes and loosely bound electrons. The pholes are capable of streaming out of the stressed or hot rocks (source) into the surrounding less stressed or cool rocks, generating potentially powerful currents. Whether or not these currents develop, when and how they flow depends on whether or not the electrons can also flow out of the source and recombine with the pholes, thereby closing the electric circuit. The interplay between pholes and electrons is expected to control the magnitude of dipoles, the intensity of the transient currents and of their associated EM fields. Understanding these processes may help us interpret EM signals generated by dynamically evolving feeder systems beneath volcanoes. 1 Freund et al. 2006, Phys. Chem. Earth 31, 389-396; Freund and Sornette, 2007, Tectonophys. 431, 33-47. 2 McMillan and Freund, AGU 2006 Fall Mtg, MR21A-0001

Keywords: electric currents, electromagnetic emissions, instabilities



(S) - IASPEI - *International Association of Seismology and Physics of the Earth's Interior*

JSS009

Oral Presentation

2039

Precursors of geomagnetic anomaly and earthquake locations

Prof. Jann-Yenq Liu

National Central University ISS, National Central University IAGA

Chieh-Hung Chen, Horng-Yuan Yen

Geomagnetic anomalies associated with major earthquakes have been reported by many scientists. When an earthquake occurs, its location, magnitude, and onset time are reported. The location of an earthquake with a latitude, longitude, and depth is named the hypocenter while its vertical projection on the Earth's surface is called the epicenter. Scientists found that the chance of observing the anomalies is proportional to the magnitude of fore coming earthquakes but inversely to the distance from the magnetometer station to the epicenter (the epicenter system). However, sometimes geomagnetic anomalies might not be observed even when some major earthquakes occurred nearby geomagnetic stations. On the other hand, other scientists found that the conductivity and/or current along a fault (or slip plane), which could be significantly changed during the earthquake preparation period, disturb nearby geomagnetic field strengths. Therefore, they employed the earthquake fault instead of the epicenter to be a reference for studying the geomagnetic anomalies (the fault system). Similarly, magnetometers near faults sometimes might also fail to register any geomagnetic anomalies before large earthquakes. Both success and failure cases suggest that the epicenter and fault reference systems need be reconsidered. In this paper, we construct new a reference system, by taking the epicenter and fault into account, examining the relationship between geomagnetic anomalies and $M \geq 5.0$ earthquakes occurred in during 1988-2001.

Keywords: seismo geomagnetic, earthquake, magnetometer



(S) - IASPEI - International Association of Seismology and Physics of the Earth's Interior

JSS009

Oral Presentation

2040

Multi-parametric monitoring of crustal stress propagation in a very active tectonic area such as the Cephallonia island (Greece)

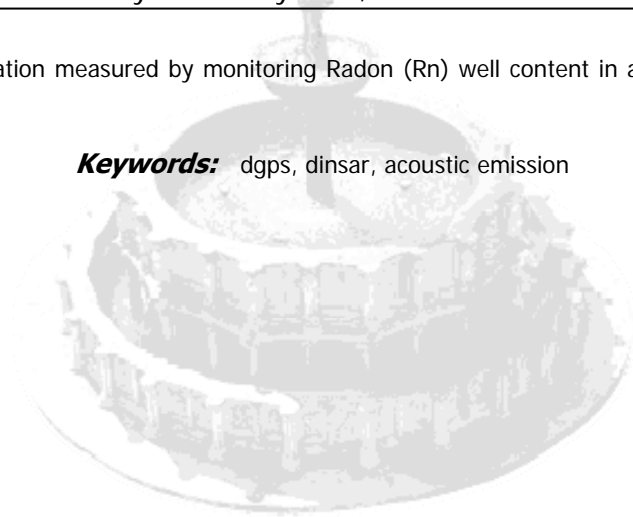
Dr. Maurizio Poscolieri

Giovanni P. Gregori, Evangelos Lagios, Matteo Lupieri, Gabriele Paparo, Issaak Parcharidis, Vassilis Sakkas

Since 2003 both ground-based and spaceborne techniques were applied for monitoring crustal deformations in the Cephallonia Island located in a seismically active area of Western Greece. In particular, ground deformation studies based on Differential GPS (DGPS) and Differential Interferometric SAR (DInSAR) analyses were extended to all Central Ionian Islands. Local GPS networks were installed in Cephallonia (2001), Ithaca (2004) and Zakynthos (2005). The Cephallonian network was re-measured five times and Zakynthos' once as of July 2006. The studies yielded detailed information regarding both local and regional deformations that are occurring in the area. For Cephallonia Island, DInSAR analysis (1995 to 1998) indicated ground deformation up to 28 mm located in small sections of the island. DGPS measurements for a subsequent period (2001 to 2006) revealed a clockwise rotation of the island with respect to a centrally located station in Aenos Mount. The horizontal component of deformation generally ranged from 6-34 mm, with the largest values at the western and northern parts of the island. Considering the vertical deformation, two periods are distinguished. The first one (2001 to 2003) is consistent with anticipated motions associated with the main geological and tectonic features of the island. The second one (2003 to 2006) has been tentatively attributed to dilatancy in which relatively small uplift (20-40 mm) has occurred along the southern and south-eastern parts of the island, while larger values (>50 mm) happened at the western part (Paliki Peninsula). These large magnitudes of uplift over an extended area (>50 km), in conjunction with an accelerated Benioff strain determined from the analysis of the seismicity in the broader region, are consistent with dilatancy. This effect started some time after 2003 and is probably centred in the area between Zakynthos and Cephallonia. If this interpretation is correct, it may foreshadow the occurrence of a very strong earthquake(s) in the above designated region during 2007-2008. In order to support this inference, Acoustic Emission data at high (200 kHz, HF AE) and low (25 kHz, LF AE) frequencies were collected in a ground station working since February 2003 in the centre of Cephallonia Island. Such point-like AE records, with high temporal resolution, provided: (i) relative time variation of the applied stress intensity, envisaging the amount of stress that affects some crustal portion, on a scale size which depends on the specific tectonic setting. (ii) the state of fatigue of stressed crustal slab, which is characterised by the typical time series of the released AE signals. Such aspect was examined by applying the fractal analysis to the AE records temporal sequence. This can provide information about the temporal evolution of the system in terms of increasing fatigue, eventually addressed towards a paroxysmal crisis (e.g. the seismic shock). The preliminary results concerning the HF AE showed a clear annual variation, whose regularity envisages some likely astronomical modulation. Such annual variation resulted during 2004 clearly in phase with other HF AE time series collected in the Italian peninsula. It proves, therefore, a planetary phenomenon, which shows up as a periodic stress wave regularly crossing the Mediterranean area. As far as the LF AE data are concerned, a conspicuous crisis of crustal stress seems to cross the broader area of Cephallonia, appearing just like one well defined soliton lasting from about April 2004 through the beginning of 2005. Some other perturbation could have been more recently started. The entire area appeared involved in some remarkable seismic activity during such soliton crossing. In addition, this multi-parametric study utilizes ancillary information obtained by analyzing digital topographic data

(DEM) and soil exhalation measured by monitoring Radon (Rn) well content in a gauge nearby the AE station. <s />

Keywords: dgps, dinsar, acoustic emission



IUGG
XXIV2007
PERUGIA
I T A L Y



(S) - IASPEI - *International Association of Seismology and Physics of the Earth's Interior*

JSS009

Oral Presentation

2041

Preliminary report on the observation of the electromagnetic field and other geophysical parameters by real-time deep sea floor observatory in Sagami Bay, Japan

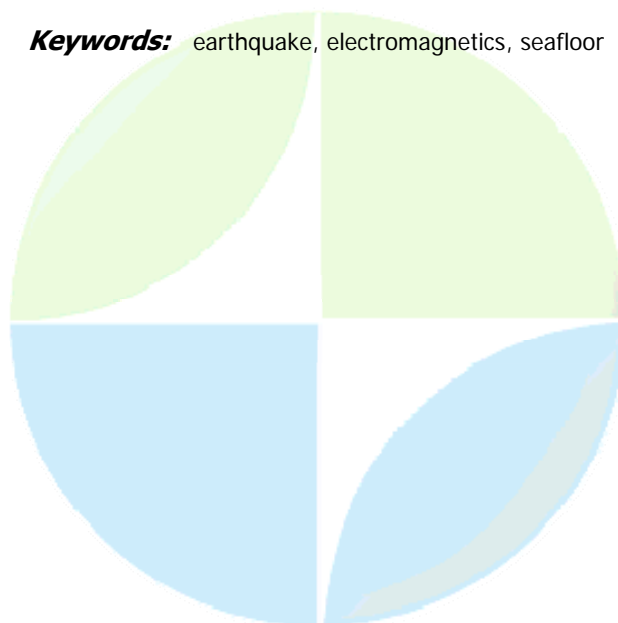
Dr. Keizo Sayanagi

Institute of Oceanic Research & Development Tokai University IAGA

Tada-Nori Goto, Toshiyasu Nagao, Kenichi Asakawa, Kyohiko Mitsuzawa, Eiichiro Araki, Takafumi Kasaya, Shigehiko Morita, Tomoki Watanabe, Masataka Kinoshita

Recently, water in the crust has become of major interest for generation of earthquakes and magma. Electromagnetic (EM) fields are generally sensitive to the distribution, movement and state of the water. Therefore, measurements of the EM fields would provide key information to understand seismic and volcanic activities. There is, however, little or no EM data sufficient to discuss the water under seafloor. From this standpoint, we have developed a long-term and real-time observation system of the EM fields on the seafloor since 2000. Sagami Bay south of Tokyo is one of the most convenient regions to try such an experiment because it is close to Japan and tectonically active. In that region, the Philippine Sea plate is subducting beneath Japan along the Sagami Trough, and the Izu Peninsula is colliding with the Honshu Arc. In January, 2005, we installed an ocean bottom electromagnetometer (OBEM) on the seafloor off Hatsushima Island in Sagami Bay. The installation was carried out by a remotely operated vehicle, the Hyper Dolphin, and its support vessel, the Natsushima. The OBEM was connected with the Real-Time Deep Sea Floor Observatory. The observatory was established at a depth of 1174 m by JAMSTEC in 1993, and has been linked to the land station on Hatsushima Island by optical fiber cable. The OBEM has measured two horizontal components of electric field and three components of magnetic field with a sampling rate of 8 Hz for more than two years. The magnetic field data clearly show daily variations of the geomagnetic field and geomagnetic storms. Some variations of the electric field suggest changes of bottom current. Spectra of the EM fields also indicate tidal components such as S2 and M2. Additionally, changes of the EM fields due to seismic waves have been observed when some earthquakes occurred in the eastern part of Japan. In this paper, we will mainly report on changes of the EM fields related to the 2006 seismic activities east off Izu Peninsula in Sagami Bay, Japan.

Keywords: earthquake, electromagnetics, seafloor



(S) - IASPEI - *International Association of Seismology and Physics of the Earth's Interior*

JSS009

Oral Presentation

2042

**Study of self potential anomalous fluctuations in a seismic active zone of
Lucano Apennine (southern Italy): recent results**

Dr. Colangelo Gerardo

Dipartimento Infrastrutture e Mobilit Direzione Generale

Vincenzo Lapenna, Luciano Telesca

In the last years geoelectrical fluctuations measured in seismic areas have been attributed to stress and strain changes, associated with earthquakes. The complex nature of this problem has suggested the development of monitoring networks based on multiparametric remote stations, in order to perform geophysical monitoring for a long time period and with a high spatial resolution. Since 2000 a geophysical monitoring network able to detect geoelectric, seismometric and geochemical parameters was installed in a seismically active area of southern Apennine chain. The main seismic activity of this area is originated by three faults systems: the complex setting of Irpinia normal faults, the Potenza strike-slip fault and the system of Val d'Agri normal faults. On May 2004 at Tito station a 20 m depth hole was drilled to measure in-depth the vertical component of the self-potential (SP) signals. We analysed and discussed the correlation between anomalous temporal fluctuations in SP signals and local seismic events.

Keywords: geoelectrical signals, earthquakes, time series

PERUGIA
ITALY



(S) - IASPEI - International Association of Seismology and Physics of the Earth's Interior

JSS009

Oral Presentation

2043

The electromagnetic device optimization modeling of seismo-electromagnetic processes

Prof. Taner Sengor

Electronics and Communication Engineering Yildiz Technical University

This paper concerns itself with modeling the seismicity-related geo-data as the self-optimization process of an electromagnetically equivalent device and developing a less accurate but fast model. A mapping is established between the parameter space of the geo-data and the characteristics of the electromagnetically equivalent device model. The temporal variations of the geo-data are correlated to the self-optimizing the specific characteristics of the electromagnetically equivalent device in the model presented in this paper. The relationship said here gives a possibility of predicting the geo-data. Using the inverses of the mapping said above generates the evaluations giving the predictability conditions involving restrictions. The inversion of the mapping exploits a fine model at predicting the natural iterations of the geo-data at future on both the region under the observation and some locations non-related to the observation region either geologically or seismically or phenomenologically relating to the earth. The electromagnetically equivalent device model is called EEDM in short. The crustal structures are considered as a complex network of distributed circuits involving slot antenna arrays, open waveguides, cavities, transmission strip lines, attenuators, frequency converters, dividers, couplings in the EEDM [1]-[5]. The variations at the geo-data alter the electromagnetic characteristics of the distributed complex network explained above. The mapping said in previous paragraph is based on the transformations among either the temporal and the spatial variations of both geo-data and the electromagnetic characteristics of the distributed complex network; i.e., phase velocity, attenuation factor, phase constant, input impedance, output impedance, relaxation factor, etc. The finite difference time domain method is used at the evaluations. The temporal variations at the mapping of EEDM at specific locations extract the mechanisms explaining the relationship among the characteristics of the distributed complex network and seismic phenomena at future. [1] T. Sengor, "Full wave analysis of earthquake sequences with waveguide and cavity effects: application in Aegean Sea - Izmir earthquakes of 2005 related to the coupling of great earthquakes of 2004," European Geosciences Union Geophysical Research Abstracts, Vol. 8, 00752, SRef-ID:1607-7962/gra/EGU06-A-00752, ISSN: 1029-7006, European Geosciences Union General Assembly 2006, Vienna, Austria, 02-07 Nisan 2006. [2] T. Sengor, "The electromagnetic radiation mechanism in faults: aperture antenna array in fractal structure," European Geosciences Union Geophysical Research Abstracts, Vol. 8, 00945, SRef-ID:1607-7962/gra/EGU06-A-00945, ISSN: 1029-7006, European Geosciences Union General Assembly 2006, Vienna, Austria, 02-07 Nisan 2006. [3] T. Sengor, "The genes and seismicity genetics of the NAF: conflicts of historical earthquake theses," European Geosciences Union Geophysical Research Abstracts, Vol. 8, 00951, SRef-ID:1607-7962/gra/EGU06-A-00951, ISSN: 1029-7006, European Geosciences Union General Assembly 2006, Vienna, Austria, 02-07 Nisan 2006. [4] T. Sengor, "The Observational Findings Before The Great Earthquakes Of December 2004 And The Mechanism Extraction From Associated Electromagnetic Phenomena," Book of XXVIIIth URSI GA 2005, pp. 191, EGH.9 (01443) and Proceedings 2005 CD, New Delhi, India, Oct. 23-29, 2005. [5] T. Sengor, "The interaction mechanism among electromagnetic phenomena and geophysical-seismic-ionospheric phenomena with extraction for exact earthquake prediction genetics," 10th SA of the IAGA 2005, Abst. CD., GAI, C109, No.: IAGA2005-A-0134, Toulouse, France, July18-29, 2005.

Keywords: seismo electromagnetic, earthquake prediction, space mapping

(S) - IASPEI - International Association of Seismology and Physics of the Earth's Interior

JSS009

Oral Presentation

2044

The Tor Caldara CO2 Diffuse Degassing Structure (DDS): $^{222}\text{Rn}/^{220}\text{Rn}$ output before and after the August, 22, 2005 Anzio Earthquake ($M_w=4.6$).

Dr. Fedora Quattrocchi

Voltattorni N., Cantucci B., Cinti D., Gasparini C., Pizzino L., Procesi M.

Soon after a ^{222}Rn and ^{220}Rn survey in soil gases, performed (June 2005) in the frame of the Diffuse Degassing in Italy risk assessment project, a moderate earthquake ($M_w=4.6$) occurred in the Anzio offshore, on August, 22, 2005, only 5 miles from the Tor Caldara Diffuse Degassing Structure (DDS onward). Having available the pre-earthquake ^{222}Rn and ^{220}Rn grid-map on around 50 soil-gas points and being ^{222}Rn both a stress-pathfinder and a discriminative component of activated-faults, a mirror-like survey was repeated on the same 50 sites, soon after the close earthquake. Later, during a quiescent-aseismic period (December, 2005), a CO_2 flux survey was performed for the same 50 sites, adding detailed measurements (more than 100 sites) for the highest flux sectors. The aim of this survey was both to have an overall picture of the background CO_2 flux and to calculate the total budget of CO_2 flux throughout the DDS, to better interpret the ^{222}Rn and ^{220}Rn areal surveys before and after the seismic event. Herewith, we distinguish the contribution of organic, diffusive and advective CO_2 flux. Hints of convection and strong degassing linked to the fracture field, inside the DDS, have been envisaged on selected points, where continuous monitoring stations could be strategic, for seismic, volcanic and NGH surveillance. Despite we found higher ^{222}Rn values in soils after the earthquake, suggesting an enhanced local degassing probably linked to a stress signal throughout the DDS as a whole, the results highlight an unmodified shape and location of the ^{222}Rn anomalies before and after the earthquake. This evidence excludes both that the activated seismogenic segment has affected in some ways both the DDS degassing patterns and that fracture field changed. A similar result could be expected if the activated fault was oriented along the DDS itself and reached the surface. This evidence is well correlated with the reconstructed focal mechanism of the earthquake, pertaining to the transfer structure of the Ardea Graben, located along a peripheral sector of the degassing Alban Hills volcano and intersecting the DDS Tor Caldara itself. The shape and location of ^{222}Rn anomalies inside the DDS for both the surveys are strictly inversely correlated with the areal CO_2 flux data. The geometry of the degassing pathways is probably linked to the barrier action (sealing power) of the clays cropping out in the study area. These clays are generated by the strong leaching of the outcropping sedimentary Pleistocene rocks due to the huge flux of volcanic gas-rich fluids.

Keywords: tor caldara, diffuse degassing structure, quiescent aseismic period

(S) - IASPEI - *International Association of Seismology and Physics of the Earth's Interior*

JSS009

Poster presentation

2045

New aspects on the statistical properties of seismicity

Prof. Panayiotis Varotsos

Physics Department University of Athens IASPEI

Efthimios S Skordas, Haruo Tanaka, Nicholas V Sarlis

We report a similarity of fluctuations in equilibrium critical phenomena and nonequilibrium systems [P. Varotsos, N. Sarlis, H. Tanaka and E. Skordas, Phys. Rev. E 72, 041103 (2005)], which is based on the concept of natural time [P. Varotsos, N. Sarlis and E. Skordas, Practica of Athens Academy 76, 294 (2001); *ibid* Phys. Rev. E 66, 011902 (2002)]. The worldwide seismicity as well as that of the San Andreas fault system and Japan are analyzed. An order parameter is chosen and its fluctuations relative to the standard deviation of the distribution are studied. We find that the scaled distributions fall on the same curve, which interestingly exhibits, over four orders of magnitude, features similar to those in several equilibrium critical phenomena, e.g., two-dimensional Ising model, as well as in nonequilibrium systems, e.g., three-dimensional turbulent flow. Furthermore, it is explained, from first Principles, why in the Gutenberg-Richter law the so called b-value is usually found to be around unity varying only slightly from region to region. The explanation is achieved just by applying the analysis in the natural time domain, without using any adjustable parameter [P. Varotsos, N. Sarlis, E. Skordas and H. Tanaka, Proc. Jpn. Acad. Ser. B 80, 429 (2004); P. Varotsos, N. Sarlis, E. Skordas, H. Tanaka and M. Lazaridou, Phys. Rev. E 74, 021123 (2006)].

Keywords: seismicity, Gutenberg Richter law, non equilibrium systems

PERUGIA
I T A L Y



(S) - IASPEI - *International Association of Seismology and Physics of the Earth's Interior*

JSS009

Poster presentation

2046

Detection of time and direction of earthquakes with the parameters of natural ULF/ELF magnetic field

Dr. Alexandr Schekotov

Institute of the Physics of the Earth senior researcher IASPEI

Evgeny Fedorov, Viktor Chebrov, Valery Sinitsin, Evgeny Gordeev, Gennady Belyaev, Nadejda Yagova, Masashi Hayakawa

Natural ULF/ELF preseismic emission, registered at Karimshino complex observatory (Lat=52.83 N, Long=158.13 E, Kamchatka, Russia), is used to obtain not only the most probable time of the EQ and its azimuth. It was shown in (Schekotov et al., 2006) that several days before an earthquake the signal polarization changes so that the signal orientation indicates the appearance an additional source in the seismic zone. The spectrum of the preseismic emission varies with time: it is enriched with high (above 20 Hz) frequencies at the early stage of the earthquake preparation while low frequencies (several Hz) dominate at its last stage. The maximum of averaged over frequency occurs 1-5 days before an earthquake. For this interval of maximal, the pulse component of the field is revealed and its average azimuth is calculated. This azimuth approximately agrees with the azimuth of the forthcoming earthquake. This research is supported in a frame of ISTC project 2990.

Keywords: seismoelectromagnetics, elf

PERUGIA
ITALY



(S) - IASPEI - *International Association of Seismology and Physics of the Earth's Interior*

JSS009

Poster presentation

2047

**Mechanisms of seismic effects in the atmosphere revealed from sounding
by VLF, LF and HF radio signals**

Dr. Oleg Molchanov

Institute of the Physics of the Earth principal researcher IASPEI

Masashi Hayakawa, Pier Francesco Biagi

Besides the direct impact by seismic pulses a slower preseismic and postseismic influence upon the atmosphere and ionosphere was recently theoretically discussed in relation to the observed effects in the atmosphere and ionosphere. The clear agent of such an influence is gas/water release at the ground surface resulting in the changes in the air temperature and density and in the density and distribution of the charged particles (due to emanation of radioactive gases like Rn222 and aerosol particles). The changes usually supposed in a thin near-ground layer (source layer) with thickness of several hundreds meters, because of slow vertical diffusion of the heavy gases and temperature variations. Extension of influence above the source layer is possible either by induced electric field (other variant is modification of background electric field) or by excitation of atmospheric gravity waves (AGW) with upward power flux. We discuss both types of models in explanation to short-time precursory effects revealed from sounding by VLF, LF and HF radio-signals.

Keywords: seismoelectromagnetics, atmosphere

PERUGIA
ITALY



(S) - IASPEI - *International Association of Seismology and Physics of the Earth's Interior*

JSS009

Poster presentation

2048

About correlation of social tension and damaging earthquakes

Dr. Oleg Molchanov

Institute of the Physics of the Earth principal researcher IASPEI

It was found some correlation between unleash of social perturbations like wars and appearance of the great damaging earthquakes. The main features of the correlation are the following: a) Number of damaging earthquakes increased after beginning of the war. Time delay is several months in a case of local wars at Caucasus area and it is 1-5 years for the global wars; b) Decrease of damaging earthquake number occurred several years before great wars on global statistics; c) Such a correlation does not exist for total number of large earthquakes. The explanation is possible in terms of biotic regulation concept.

Keywords: seismicity, sociology



(S) - IASPEI - *International Association of Seismology and Physics of the Earth's Interior*

JSS009

Poster presentation

2049

Groundwater geochemical disturbances related to seismicity revealed in Kamchatka (Russia) during the last 30 years: further results

Prof. Pier Francesco Biagi

Department of Physics University of Bari IASPEI

Maggipinto Giuseppe, Maggipinto Tommaso, Piccolo Roberto, Minafra Antonio, Ermini Anita, Capozzi Vito, Khatkevich Yuri, Gordeev Evgeni

For many years, ion and gas content data have been collected from the groundwater of six deep wells and two natural springs in the southern area of the Kamchatka peninsula, Russia. In previous studies developed in 1998-2000, the possibility that the hydrogeochemical time series contained precursors was investigated. The technique used was to filter the raw data from short and long variations, to assume that each signal with an amplitude larger than three times the standard deviation is an irregularity and then to define anomalies as irregularities occurring simultaneously in the data for more than one not correlated parameter at each measurement site. Using this method, as main result, preseismic anomalies with a duration of some month were revealed on the occasion of the March 2, 1992 ($M = 7.0$) and January 1, 1996 ($M = 6.9$) earthquakes, i.e. the largest events occurred quite near to the hydro-geochemical network in last thirty years. Another result was a preseismic anomaly with a duration of some days pointed out on the occasion of the July 21, 1996 earthquake ($M = 7.1$), that was a very shallow event. The previous anomalies appeared only in some measurement site of the network. Now the more extended (up to December 2005) data sets were investigated using directly the raw data, without any filtering technique. The present analysis has confirmed the previous results adding some information as the appearance of possible preseismic anomalies in other measurement sites of the network and the existence of long term (some year) precursors and of post seismic effects.

Keywords: precursors, geochemistry, kamchatka



(S) - IASPEI - *International Association of Seismology and Physics of the Earth's Interior*

JSS009

Poster presentation

2050

Study of ground data VLF radio anomaly related to seismicity revealed by DEMETER satellite on 2004: phase analysis

Dr. Tommaso Maggipinto
Department of Physics University of Bari

P.F. Biagi, L. Castellana, R. Piccolo, A. Minafra, A. Ermini, V. Capozzi, M. Solovieva, O. Molchanov, M. Hayakawa

The studies on VLF signals collected by ground receivers continue to reveal the existence of disturbances related to the seismicity. Recent papers report anomalies in VLF data collected from satellite too. In particular, the analysis of the VLF signals received on board of the French DEMETER satellite, revealed a drop of the signals (scattering spot) in the time interval November 23 December 12, 2004, probably connected with the occurrence of large earthquakes ($M = 5.4-5.5$) in Europe. The lithosphere-atmosphere coupling model provides the theoretical explanation of the very complex relations linking earthquakes and precursors. In this framework, we have analysed the phase of the VLF/LF radio signals radiated by GB ($f = 16$ kHz, United Kingdom), FR ($f = 20.9$ kHz, France), GE ($f = 23.4$ kHz, Germany), IC ($f = 37.5$ kHz, Island) and IT ($f = 54$ kHz, Sicily, Italy) and received at Bari (Italy), during October-December 2004. At first the wavelet analysis was applied on the phase data and clear anomalies were revealed on the FR and IC signals at the end of November. So, an agreement with the results obtained by the DEMETER seems to appear. Then the standard deviation of the phase data sets was investigated and a clear short drop was revealed on the GE signal on 26-27 November. This anomaly could be a precursor of one of the previous earthquakes and this result goes beyond the ones obtained by satellite analysis.

Keywords: earthquakes, vlf radiosignals, statistical analysis



(S) - IASPEI - *International Association of Seismology and Physics of the Earth's Interior*

JSS009

Poster presentation

2051

Introductory remarks to integrated EMSEV sessions

Prof. Seiya Uyeda

(IAGA/IASPEI/IAVCEI) Working Group of Electromagnetic Studies on Earthquakes and Volcanoes (EMSEV) was established in 2001, with the purpose of promoting international and interdisciplinary cooperation in the new field of research now called Seismo-electromagnetics. Members share a common interest to understand earthquakes and volcanoes, but their scientific background is extremely diverse often using different languages, namely from ground based geophysics to ionospheric physics, space science and solid state physics, to name a few. Therefore, mutual understanding for the common cause is of crucial importance. During the past several years, EMSEV has enjoyed high activities. For this meeting in Perugia, the second IUGG General Assembly for EMSEV, we have planned an integrated symposium entitled Progress in electromagnetic studies on earthquakes and volcanoes, consisting of the following sessions. JSS007: Volcanic structure and activities. Convenors: V. V. Spichak; J. Zlotnicki, Y. Sasai, D. Patella and C. Del Negro JSS008: Electromagnetic fields associated with earthquakes and active faulting. Convenors: M. Johnston; N. Oshiman, and A. Meloni JSS009: Crustal instabilities and earthquake precursors. Convenors: P. F. Biagi; M. Hayakawa, J-Y Liu, T. Nagao JSS010: Seismo-electromagnetic studies using space technology. Convenors: R. Singh; S. Pulnits, M. Parrot, D. Ouzounov, and V. Tramutoli Although separated in different sessions, it is hoped that active fruitful discussions among participants with different backgrounds be made since the subject matters are all inter-connected.

Keywords: emsev, earthquakes, volcanoes



(S) - IASPEI - *International Association of Seismology and Physics of the Earth's Interior*

JSS009

Poster presentation

2052

Association of the Negative Anomalies of the Quasistatic Electric Field in Atmosphere with Kamchatka seismicity

Dr. Sergey Smirnov

Far Eastern Branch Russian Academy of Sciences IAGA

One hundred three cases of a bay-like depression in the strength of the E_z component of the quasistatic electric field in the near-Earth atmosphere, observed from 1997 to 2002 on Kamchatka, have been analyzed statistically. It has been shown that the most probable length of a bay is 40--60 min. The most probable drops in E_z are minus 106--300 V/m. The dependence of these values on an earthquake class and a distance to the epicenter was not found. The probability of earthquake prediction over 24 h before an earthquake based on the E_z anomaly is 36%.

IUGG

XXIV2007

PERUGIA
I T A L Y



(S) - IASPEI - *International Association of Seismology and Physics of the Earth's Interior*

JSS009

Poster presentation

2053

**Modification of the signals from VLF transmitters in seismic regions-
studies of the DEMETER measurements**

Dr. Jan Blecki

Space Research Centre Polish Academy of Sciences IAGA

Ewa Słomińska, M. Parrot, J. Słomiński, J. J. Berthelier

Many past researches describe anomalous behaviour in electromagnetic measurements, associated with seismic and volcanic activity. Some of these signals have been used in the studies of the possibility of the earthquake prediction, as pre and post seismic events that occur few hours or even few days before main shock. However, due to the subtle and poorly understood nature of earthquake precursors activity, it is necessary to examine as many data sets as possible, in order to gain more complete understanding of the physical mechanism involved in the precursors signal generations. The main goal of our work is statistical studies on electromagnetic signals in VLF range. The choice of spectrum frequency for analyzes is strictly connected with the net of VLF transmitters situated in different world regions, but in the seismic regions. We are focused on analyzing of spectrograms for electric and magnetic field registered by DEMETER microsatellite, trying to describe normal behaviour of the signal without any seismic influence, and its evolution associated with earthquake events.

Keywords: vlf signals, earthquakes and vlf signals, demeter measurements

PERUGIA
ITALY



(S) - IASPEI - *International Association of Seismology and Physics of the Earth's Interior*

JSS009

Poster presentation

2054

Magnetotelluric study of mount ST. Helens Washington, USA: phase tensor analysis preliminary results

Prof. Ray Cas

School of Geosciences Monash University IAVCEI

G. J. Hill, J. P. Cull, T. G. Caldwell, H. M. Bibby, W. Heise, M.K. Burgess, L.G. Mastin

Our attempts to understand the processes that drive volcanism can be greatly enhanced by imaging the location and geometry of magma storage systems and by imaging the internal structure of volcanic complexes. The majority of efforts have been seismically based, using technologies adapted from petroleum and mineral exploration. Recently, however, there have been efforts to incorporate additional survey and data types, GPS and gravity successfully at Okmok, thermal and acoustic studies of Stromboli, self potential at Misti, and recently magneto-tellurics at Ruapehu. These multidisciplinary studies unequivocally add to the understanding of these volcanic systems, either by providing supporting evidence or suggesting alternative viable interpretations. We have undertaken a magneto-telluric study of Mount St. Helens a quaternary stratovolcano located in south-western Washington, USA, lying along the western front of the Cascade Range between Mt. Hood to the south and Mt. Rainier to the north, Mt. St. Helens is located in a region of transition both geologically and geophysically. Phase tensor and induction arrow analysis from 37 broadband magnetotelluric (~0.01 2000 s) sounding sites show the regional conductivity structure in a ~1000 km² area around the volcano is 3-D at all period scales. Phase tensor analysis indicates that Mount St. Helens lies on the boundary of a large regional conductor to the north east of the volcano which begins at a depth of ~25 km and extends into the lower crust. The phase tensor analysis indicates a shallow response (

Keywords: magnetotellurics, mtsthelens



(S) - IASPEI - *International Association of Seismology and Physics of the Earth's Interior*

JSS009

Poster presentation

2055

Electric current emissions from brittle materials suffering near fracture mechanical stress

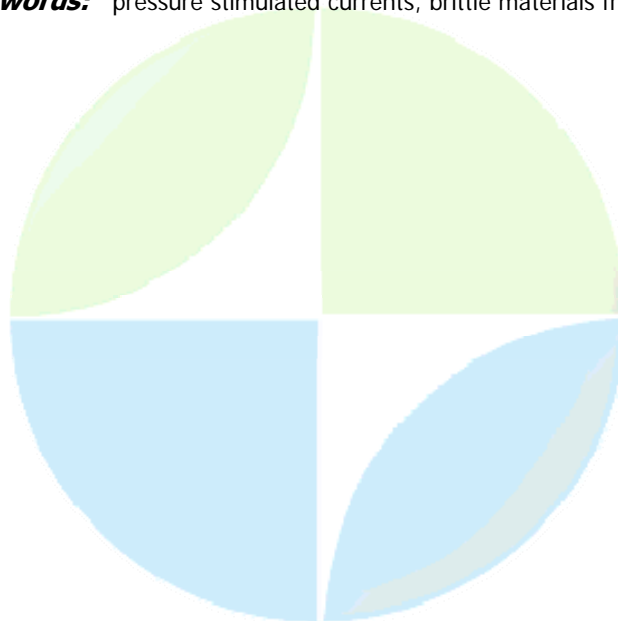
Dr. Ilias Stavrakas

Department of Electronics Technological Educational Institution of Athens

Panayiotis Kyriazis, Antonis Kyriazopoulos, Cimon Anastasiadis, Dimos Triantis, Filippos Vallianatos

Pressure stimulated current (PSC) effects have been studied on various materials. In a number of previous presentations the applied mechanical stress has been correlated with the emitted current. In the present work current emissions are studied on a set of natural brittle materials like marble and amphibolite as well as on composite man-made materials like cement paste. Specifically, the stress was applied on the referred samples close to mechanical failure along with emitted PSC measurements. The recordings manifest that, dynamic phenomena, like macro-crack propagation and failure plane creation, result in current emissions. In these experiments despite the fact that the stress level was maintained practically constant in the vicinity of failure, significant PSC emissions of long duration were observed. The emitted PSC can be attributed to charge rearrangements due to dynamic change of the sample structure while new cracks are formed and the existing ones extend. In general, both the existence and interpretation of the PSC are consistent with the Moving Charged Dislocations (MCD) theory which relates the emitted current to crack formation and propagation and to the consequent strain variation. Strain recordings in the range near fracture support these findings since strain variations have been recorded without any change of stress. A deep and fast PSC reduction has always been recorded before fracture predicting the inevitable failure. This effect can be attributed to two coexisting causes: The former is related to the lack of any obvious triggering, i.e. stress or strain in the bulk of the material, that could lead to charge rearrangement since in this stage all the applied stress is localized at the edges of the main macro-crack that guides the failure plane. The latter is related with the observation that the failure plane limits significantly the available paths for the charges to move across the sample bulk which makes the detection of any emitted PSC even more difficult.

Keywords: pressure stimulated currents, brittle materials fracture



(S) - IASPEI - International Association of Seismology and Physics of the Earth's Interior

JSS009

Poster presentation

2056

Day-time variations of foF2 connected to strong earthquakes

Dr. Mikhail Rodkin

Geophysical Center Russian Academy of Sciences IASPEI

Elena Liperovskaya, Vadim Bogdanov, Claudia-Veronica Meister, Victor Liperovsky

In the present work, the authors continue their search for earthquake precursors and study of the behavior of some characteristic parameters of the ionosphere occurring during the earthquake preparation processes and after the earthquakes. The F-layer is the most dynamic regular layer of the ionosphere being considerably modified by different reasons. The foF2 frequency characterizing the maximum of the electron concentration in this layer is one of the parameters of the ionosphere that is regularly measured during vertical sounding experiments. Here the variability of the foF2 frequency connected with the strong earthquakes is investigated statistically, more than 100 events with magnitude $M > 6.0$ are taken into examination. These earthquakes have a depth less than 80 km, and they happened at a distance less than 1000 km from the vertical sounding station. The used foF2 frequency hourly data were registered at the stations: Wakkanai, Akita, Kokubunji, and Yamagawa () since 1957 until 1990. The authors find an increase in the variability of the foF2 frequency at time scale 1-2 hours during 5-10 days before the event and the decrease in the variability of the foF2 frequency since the day before until a few days after an earthquake. Analyzing the diurnal behavior of the effect, they find that it occurs at day-time in period between 11 h and 15 h LT. Diurnal variability depends on the season, on 11-years Solar variations cycle, and on geomagnetic variations. In the work we use the data recorded in time intervals with weak heliomagnetic disturbances (Wolf number below 100 and $\Sigma Kp < 30$). The amplitude of the modification may be larger than 10%, and the statistical reliability of the effect amounts to more than 0.95. No effect is obtained for the strong earthquakes with depths more than 80 km. Also, no effect is found for weaker earthquakes with $M < 6.0$. The revealed change in the foF2 variability with the modifications of the electrical conductivity could be connected with an injection of radon into the lower atmosphere.

Keywords: ionosphere, earthquakes, f layer



(S) - IASPEI - *International Association of Seismology and Physics of the Earth's Interior*

JSS009

Poster presentation

2057

Ionospheric anomalous changes observed by GPS-TEC and NmF2 possibly associated with large earthquakes

Mr. Masahide Nishihashi

Graduate Course of Science Chiba University IASPEI

Hau-Kun Jhuang, Katsumi Hattori, Jann-Yenq Liu, Sarmoko Saroso, Djedi S. Widarto

A lot of anomalous electromagnetic phenomena possibly associated with large earthquakes have been reported. Recently, scientists found an apparent reduction in GPS-TEC values occurred within 1.5 days prior to $M \geq 6.0$ earthquakes in Taiwan. However, those recent studies were not cross-checked by simultaneous data sets observed at other places to confirm the ionospheric anomalies being earthquake related. In this study, we retrieved GPS-TEC records, routinely published in the global ionosphere maps (GIM). Simultaneous data in various other locations outside of Taiwan are examined to see whether the anomalies observed in Taiwan before the 1999 Chi-Chi earthquake (Mw7.6) and Chia-Yi earthquake (M6.4) are local or global effects. The result shows that the anomalies in Taiwan three days before the Chi-Chi earthquake (18 September), and one and three days before the Chia-Yi earthquake (19 and 21 October) are local phenomena. It means that the ionospheric-disturbed areas were localized around Taiwan, and did not spread all the way to Tokyo in Japan. We conclude that the disturbed areas are at least less than about 2200km in radius and may be much smaller. We also obtained similar tendency in the case of the 2004 Sumatra-Andaman earthquake (M9.0).

Keywords: gps tec, nmf2, ionospheric disturbances



(S) - IASPEI - *International Association of Seismology and Physics of the Earth's Interior*

JSS009

Poster presentation

2058

Electromagnetic monitoring of regional geodynamical processes in the frame of MEM Project

Dr. Paolo Palangio

Osservatorio Geofisico di L'Aquila Istituto Nazionale di Geofisica e Vulcanologia

Cinzia Di Lorenzo

The MEM Project (Interreg IIIA Adriatic Cross Border Programme) has been activated in LAquila since 2004. The leader partner of the project is the Abruzzo Region. The main scientific objective of the project is the characterization of the electromagnetic background noise in the frequency band from 0.001 Hz to 100 kHz in Earth-Ionosphere cavity. Further scientific objectives of the MEM Project are the model realization of the electric and magnetic fields generated in a 3-dimensional earth by induction sources in the lithosphere and the study of electromagnetic signals produced in the Earth interior. The study of electric and magnetic phenomena linked to tectonic processes allow us to locate the electromagnetic sources by means of interferometric methods. The first station of the MEM interferometric array has been installed in LAquila near the INGV Geomagnetic Observatory (42 23 N, 13 19E, 682m a.s.l.) and it is working from the middle of 2005. Here we report the preliminary results obtained in the LAquila MEM station concerning the non inductive field analysis by means of the Earth impulse response functions.

Keywords: tectonomagnetism



(S) - IASPEI - *International Association of Seismology and Physics of the Earth's Interior*

JSS009

Poster presentation

2059

Effect of Noise from DC-Driven Trains to Goelectrical Potential Difference and its Reduction at Hakuba Area, Japan

Dr. Katsumi Hattori

Department of Earth Sciences, Faculty of Science Chiba University IASPEI

Hisashi Ishikawa, Ichiro Takahashi, Yoichi Noda, Toshiyasu Nagao, Nobuhiro Isezaki

The variations of goelectrical potential differences in Hakuba area, Nagano Prefecture, Japan have been investigated. The noises originated from the DC-driven trains were found to contaminate into the natural goelectrical potential data. The most intense influence of trains occurred when the train was running nearby measuring dipoles. The gradient of the potential was deflected towards the railways and/or the position of the train, exhibiting a certain correlation between the power supply data at substation data and the goelectrical potential data at measuring site. Extracting the high correlation part ($r > 0.7$), idealized train noise can be computed by the least square method. The reduction of train noise by more than 60 % was achieved by subtracting the idealized noise from observed data.

Keywords: goelectrical potential diff, noise reduction, dc driven train

PERUGIA
ITALY



(S) - IASPEI - *International Association of Seismology and Physics of the Earth's Interior*

JSS009

Poster presentation

2060

Singular Spectral Analysis and Principal Component Analysis for Signal Discrimination of ULF Geomagnetic Data Associated with 2000 Izu Island Earthquake Swarm

Dr. Katsumi Hattori

Department of Earth Sciences, Faculty of Science Chiba University IASPEI

Aya Serita, Daishi Kaida, Chie Yoshino, Masashi Hayakawa, Nobuhiro Isezaki

In order to extract any ULF signature associated with earthquakes, the singular spectral analysis (SSA) and the principal component analysis (PCA) have been performed to investigate the possibility of discrimination of signals from different sources (geomagnetic variation, artificial noise, and the other sources (earthquake-related ULF emissions)). We adopt SSA to the time series data observed at closely spaced stations, Seikoshi (SKS), Mochikoshi (MCK), and Kamo (KAM) stations. Then, PCA is adopted to the time series data sets filtered at 0.01 Hz of NS component at three stations. In order to remove the most intense signal like the first principal component, we make the differential data sets of SKS-MCK and MCK-KAM for the above data. The major findings are summarized as follows. (1) It is important to apply simultaneously SSA and PCA. SSA gives the structure of signals and the number of sensors for PCA is estimated. This makes the results more convincing. (2) There is a significant advantage using PCA with differential data sets of filtered (0.01Hz band) signal between SKS-KAM and MCK-KAM in NS component for removing the most intense signal like global variation (solar-terrestrial interaction). This yields that the anomalous changes in the second principal component were detected more clearly, and the contribution of the second principal component is found to be 20-40%. It is enough to prove mathematical accuracy of the signal. Further application is required to accumulate events. These facts demonstrate a possibility of monitoring the crustal activity with using the SSA and PCA.

Keywords: singular spectral analysis, principal component analysis, ulf geomagnetic data



(S) - IASPEI - *International Association of Seismology and Physics of the Earth's Interior*

JSS009

Poster presentation

2061

Hydrostructural and hydrothermal models for the studies of the hydrogeochemical precursors of the seismic activity: examples from Serchio and Magra grabens (Northern Apennines, Italy)

Prof. Francesco Baldacci

Dipartimento di Scienze della Terra Universit di Pisa IASPEI

Botti Flavia, Cioni Roberto, Molli Giancarlo, Pierotti Lisa, Sozzari Andrea

In order to identify eventual earthquake precursors four hydrothermal emergencies have been selected and monitored with a Continuous Automatic Monitoring Network (CAMN). During the Tortonian-Quaternary, deformation connected to the late and post collisional phases, the tectonic units outcropping in the examined areas have been affected by low-angle and high-angle normal faults respectively; these extensional structures confer a "semigraben"-like geometry on Magra and Serchio intermountain basins. Four hydrostructural sections have been elaborated and integrated with seismic data: they are representative both for the Apuan side of the "Serchio Graben" (Galliciano) and for the Apenninic one (Pieve Fosciana and Bagni di Lucca), as well as for the NW Apuan Alps (Equi Terme). Seismic sources responsible for the strongest earthquakes ($M = 6.5$ earthquake of September 1920) are present in Garfagnana ("Serchio graben") and in Lunigiana ("Magra graben"); the extensional regime in these areas is confirmed by the focal mechanisms of recent earthquakes. The geochemical monitoring (continuous and discontinuous) of selected water points in Garfagnana-Lunigiana area begun on November 2002: the main physical and physico-chemical parameters have been monitored continuously, while the chemical parameters have been measured on a monthly basis. The Equi Terme spring (NaCl water type, $T=17.826.2$ and TDS from 1.2 to 5.5 g/l) originates from a mixing, at a different degree, of karst shallow Ca-HCO₃ water and deep Na-Cl water. Galliciano spring (Na-Ca-Cl water type, $T=23.724.9$, TDS from 3.1 to 3.9 g/l and CO₂ concentration in dissolved gases around 2.5%) originates from a mixing process between a deep component (a mixture of two different deep water-types) and a shallow groundwater. The deep component (Na-Cl type) rises-up along the NW-SE normal faults system at the NE side of the Apuan Alps, while the shallow component (diluted Ca-bicarbonate water) circulates in the upper carbonatic reservoir. The Pieve Fosciana well (Na-Cl type, $T=36.5C$, TDS=5.9g/l and CO₂ concentration in dissolved gases of ~7.5%) and the Bernab (Bagni di Lucca) spring (Ca-SO₄ type, $T=40.5C$, TDS=2.5g/l) are artesian emergencies. Their chemical and physico-chemical characteristics, acquired by the water in the deep aquifer, are maintained unchanged during their ascent to the surface. At the end, hydrogeochemical and isotopic data, with their hydrostructural context, allowed to define the conceptual models of groundwater flow, related to the examined aquifers. The results of three years of continuous monitoring, integrated into their hydrostructural context, have been: i) monitoring stations detect even small variations of the measured parameters; ii) definition of the conceptual models of the groundwater flow related to the examined water points; iii) in most locations, the observed trend of the acquired parameters is consistent with the periodic manual sampling results, and confirms the mixture of different water types, that the hydrogeochemical model expects. The absence of seismic events with a sufficient energy precluded the possibility to detect anomalies, except for the Equi site, where an increase in the dissolved CO₂ content was observed twelve days before a $M 3.7$ earthquake occurred at a distance of 3 Km North of the monitoring station.

Keywords: geochemical precursors, seismic activity, structural hydrothermal model

(S) - IASPEI - *International Association of Seismology and Physics of the Earth's Interior*

JSS009

Poster presentation

2062

Some characteristics of pre-seismic VHF wave scattering

Prof. Toru Mogi

Institute of Seismology and Volcanology Hokkaido University IAGA

Takeo Moriya, Isao Yamamoto, Masamitsu Takada

In order to confirm that VHF FM (frequency modulation) radio waves propagate beyond the line-of-sight before earthquake occurrences, we installed five observatories in Hokkaido, Japan, and started our observation in December 2002. Shortly before each of many earthquakes, which occurred in and around the northern Honshu and Hokkaido until August 2006, the anomalous reception of FM waves, which were considered as caused by scattering during transmission, was confirmed. We found that the logarithm of the total summation of the duration times of anomalous transmission, $\text{Log}(T_e)$, is related to the maximum seismic intensity and magnitude (M) of the earthquake, which is going to occur around the FM broadcasting station, though T_e seems to be a function of many other parameters including the hypocentral depth and distance and the surface condition of the epicenter (sea or land). For the earthquake group that occurred beneath the southern Hidaka Mountains, Hokkaido, plots of $\text{Log}(T_e)$ versus the maximum seismic intensity of the earthquakes show that there is a linear relation between these two parameters. The seismically active depths of the hypocenters were concentrated in a narrow range from 48 to 54 km, and for those earthquakes, the plots of $\text{Log}(T_e)$ versus M also show a clear linear relation. Moreover, we succeed to measure the azimuth of the scattering waves, which appeared before two earthquakes, by using interferometer. It became clear that azimuth of the scattering waves direct the epicenter roughly. It appears that these pre-seismic scattered VHF waves may indeed be useful earthquake precursors.

Keywords: precursor, vhfwave



(S) - IASPEI - International Association of Seismology and Physics of the Earth's Interior

JSS009

Poster presentation

2063

Wavelets in the analysis of seismoelectromagnetic signals

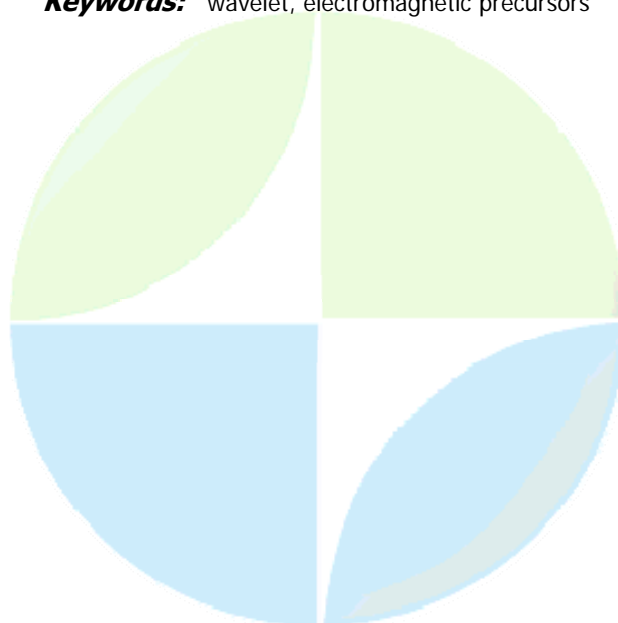
Mr. George Hloupis

Laboratory of Geophysics & Seismology Technological Educational Institute of Crete

George Hloupis, Filippos Vallianatos, John Makris, Dimos Triantis

The study of electromagnetic field recordings before the occurrence of a significant seismic event has been proposed by many researchers as a possible indication of an earthquake precursor. In a considerable set of cases, along with these proposals, a theoretical model has been developed in order to explain suavisly the observed recordings. There is no arguing that what all the prementioned efforts tried to reveal is a set of signals than can be proved that were generated from an earthquake generation mechanism. On this direction, the initial and crucial step is the revealing of the candidate earthquake precursor (CEP) from the whole recording which is a two-step process. Primary, there must be an identification of a CEP signal using well-known automated methods and possible knowledge databases. Eventually the isolation method of the CEP signal must be able to separate it from acquaint periodic events (daily and seasonal variations) as well as independent non-seismic events (i.e. industrial noise). Without knowing the exact earthquake generation mechanism we cannot allege that we can identify CEP signals based on their characteristics. An alternative approach is to identify CEP signals based on pattern recognition methods. The purpose of this study is to propose a pattern recognition scheme for CEP signals based on wavelet analysis. Wavelets has been widely used in various studies in order to derive non-stationarities and hidden irregularities from underlying signals. At the same time their intrinsic ability to split the signal in different scales provides an analysis frame where we can rapidly identify and isolate the signals under interest. The proposed method uses electric and magnetic recordings from an 1Hz acquisition system. The recorded signals after appropriate preprocessing they analyzed using wavelets and classified according to their scale-to-scale behavior. The recording period separated into three sub-periods: One consisting the Kythira (36.21 North, 23.41 East) earthquake and two without any significant seismic activity. From the results we can exclude some interesting indicators of CEP signals primarily in electrical field recordings.

Keywords: wavelet, electromagnetic precursors



(S) - IASPEI - *International Association of Seismology and Physics of the Earth's Interior*

JSS009

Poster presentation

2064

Multiscale Entropy analysis of self-potential time series associated to the Mw=7.4 earthquake of 14 September 1995 in Mexico.

Dr. Cervantes De La Torre

Departamento de Sistemas Universidad Autonoma Metropolitana IASPEI

A. Ramirez-Rojas, C. G. Pava-Miller, F. Angulo-Brown

We have obtained self-potential time series at several sites during diverse periods, along the Pacific Coast of Guerrero State in Southern Mexico a very active seismic zone linked to the Middle American Trench, during this period at the vicinity of our stations have occurred 10 EQs with $M_w \geq 5.9$, the strongest of these EQs ($M_w = 7.4$) occurred in September 14, 1995 with epicenter at 110 Km., the Acapulco station. The theory of nonlinear dynamical systems provides new tools and quantities for characterization of irregular time series data. In this work we present a multiscale entropy analysis of our self potential time series.

Keywords: seismo, fractal dimension, nonlinear time series



(S) - IASPEI - *International Association of Seismology and Physics of the Earth's Interior*

JSS009

Poster presentation

2065

A multifractal study of self-potential time series

Dr. Cervantes De La Torre

Departamento de Sistemas Universidad Autonoma Metropolitana IASPEI

A. Ramirez-Rojas, C. G. Pava-Miller, F. Angulo-Brown

In many seismically active zones in the world there exist research programs for the study of precursory phenomena of seism. One technique used since more than twenty five years ago consists in monitoring the so-called self-potential (electric field of the ground). We have obtained self-potential registers from the State of Guerrero's Coast during more than five years; these data sets constitute the so-called self-potential time series. In this work we report the fractal and multifractal study of the Acapulco, Coyuca, Ometepec and Tecpan stations; we study of quantifiers of chaotic behavior such as Lyapunov exponent and generalized dimensions associated to the self-potential time series

Keywords: seismo, multifractals, nonlinear time series

XXIV2007

PERUGIA
ITALY



(S) - IASPEI - *International Association of Seismology and Physics of the Earth's Interior*

JSS009

Poster presentation

2066

Thermal neutrons' response to the earthquakes depending on the direction of their epicenter (based on Kamchatka observations)

Dr. Ekaterina Sigaeva

Space Physics Research Department Skobeltsyn Institute of Nuclear Physics

Yuri Kuzmin, Oleg Nechaev

Long-term ground-based observations have shown that thermal neutrons' flux is very sensitive regarding different processes both in the near-Earth space and in the Earth's crust due to the dual nature of the neutron flux near the Earth's surface. The first source of neutrons is bound up with the high-energy particles of cosmic rays, which produce neutrons in the interactions with the elements of the atmosphere. The second source originates from the natural radioactive gases of the Earth's crust. The calculations have shown that the impact of the second source strongly depends on geographical location of the observation point, i.e. on the local conditions of the gases' emission. One of the most promising applications of the thermal neutrons' observation is development of a new method for earthquake prediction. The observations in the seismic area of Kamchatka have shown that this region is very 'rich' in the neutrons' flux variations of different nature, including local effects (climate, weather, etc.) Therefore it's very important to separate the geodynamical variations from the rest. The analysis has shown that it's necessary to take into consideration not only the magnitude of the following earthquake and the remoteness of its epicenter from the experimental unit, but also the direction from the epicenter to the unit, and consequently the propagation path of the seismic waves. The paper presents the results of the neutrons' data analysis compared with the directions of the earthquakes' epicenters to the experimental unit. It is shown that for Kamchatka region there is a preferable direction along the boundary of the Pacific and Euro-Asian tectonic plates, and the majority of the strong earthquake with the epicenters in a sufficiently broad area along this boundary 'produce' the increased neutrons' flux at Kamchatka unit.

Keywords: thermal neutron, epicenter direction



(S) - IASPEI - *International Association of Seismology and Physics of the Earth's Interior*

JSS010

2067 - 2092

Symposium

**Progress in electromagnetic studies on earthquakes and volcanoes -
Seismo-electromagnetic studies using space technology**

Convener : Dr. Valerio Tramutoli, Prof. Ramesh Singh

Co-Convener : Dr. Michel Parrot, Dr. Dimitar Ouzounov

During the last decade, the possibilities have been shown that large events in the solid earth and oceans, such as earthquakes, volcanic activity and tsunamis, may affect the atmosphere and ionosphere through yet unresolved process the lithosphere-atmosphere-lithosphere (LAI) coupling. LAI coupling was postulated from ground-based observations associated with earthquakes. The recent investigations using multi satellite sensors have been actively pursued. Significant changes in total electron concentration (TEC) in the ionosphere, ground surface temperature anomaly by thermal infrared (TIR) emission and/or cloud cover associated with several large earthquakes have been observed over the epicentral region. Latest observations from the DEMETER satellite seem to provide evidence of Very Low Frequency (VLF) electrical and magnetic signals prior to some earthquakes. However, convincing results are still insufficient and the physical understanding of the link between the solid earth processes and surface/atmospheric/ionospheric precursory events is largely unclear. Topics to be discussed in this session include: 1) Case studies of satellite observation related to seismo-electromagnetic observations comparison with ground-based observations; 2) Theory on the physical mechanism of the connection between the process in the earth crust and atmospheric-ionospheric phenomena prior to main earthquakes; 3) Thermal infrared (TIR) emission phenomena, cloud cover and TEC anomalies, possibly related to major earthquakes, and volcanic/geothermal activities and their comparisons with ground-based relevant data, such as meteorological, radon emission and ionosonde data; 4) Possible usefulness of space technology in tsunami early warning.

PERUGIA
I T A L Y



(S) - IASPEI - *International Association of Seismology and Physics of the Earth's Interior*

JSS010

Oral Presentation

2067

Detection of electromagnetic precursors by demeter satellite before earthquakes

Mr. Shourabh Bhattacharya

Space Science Laboratory, Department of Physics Barkatullah University, Bhopal, India

Shivalika Sarkar, A.K.Gwal, M.Parrot

One of the major advancements related to study of earthquake phenomenology is the investigation and analysis of electromagnetic signatures that are observed before seismic activities. They are also termed as earthquake precursors due to their existence before seismic activities. These electromagnetic precursors found prior to seismic activities can be a vital diagnostic tool, the long term investigation of which may establish them as one of the promising short term precursors of earthquakes. Moreover, significant anomalies are found to exist predominantly in the Ultra Low Frequency (ULF) /Extremely Low Frequency (ELF) range due to their greater penetration depth, as compared to other higher frequency ranges. In this paper, the authors discuss some important results in terms of electromagnetic emissions occurring as short term electromagnetic precursors in the ULF/ELF range which have been observed in the ionosphere, with the help of DEMETER satellite. The DEMETER satellite was launched in June 2004, and is aimed to study the ionospheric perturbations linked with seismic activities.

Keywords: demeter, earthquakes, electromagnetic precursors

PERUGIA
ITALY



(S) - IASPEI - *International Association of Seismology and Physics of the Earth's Interior*

JSS010

Oral Presentation

2068

Seismogenic ionospheric disturbances and planned satellite experiment

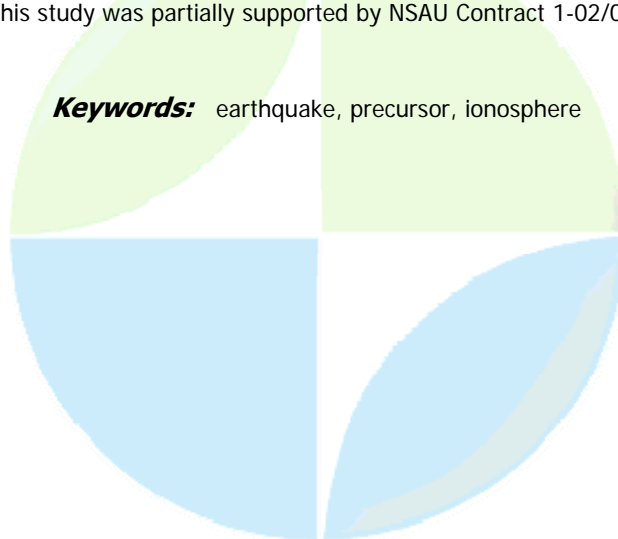
Prof. Valery Korepanov

Laboratory for EM Investigations Lviv Center of Institute of Space Research IAGA

Georgy Lizunov, Yury Yampolsky, Fedir Dudkin

A great number of experimental observations of ionospheric disturbances stimulated by seismic events are described in numerous papers and books. But till now two key (principal) questions of these investigations are still open: what is a transport mechanism of co-seismic and especially pre-seismic perturbations to the ionospheric altitudes; how big has to be the energy of pre-seismic (precursory) signals in order the ionospheric precursors of seismic events could be observed at the background of natural variations from other sources. Taking into account a great importance of any information about such catastrophic natural hazards as earthquakes, volcano eruptions, tsunamis for the mankind, every progress at this way is welcome. In this paper both these questions are discussed. First the experimental results obtained with satellite and ground measurements of some physical parameter variations are analyzed, and the conclusion is made that the best candidate for such an energy transport from ground to ionosphere are atmospheric gravity waves (AGW). The executed experiments and theoretical analysis allowed restoring the AGW parameters which may create an observable ionospheric response to the lithosphere/atmosphere powerful processes. The probability to find the answer to the second question how big should be energy of lithospheric source in order it may be projected at the ionospheric heights is discussed. The calculations were made to estimate this energy from above which gave non-realistic value. But from another hand enough simple calculations show that quite realistic thermal variation about 0.3 K is already enough for AGW generation which evolution with height will create rather strong density perturbation in E-region about 10%. So, this needs further study, both theoretic and experimental. New satellite mission IONOSATS is planned now for detailed experimental study of the described processes. The IONOSATS project is proposed by National Space Agency of Ukraine for the First European Space Program, as well as for Space Weather (SW) Program as a part of GMES. One of the project purposes is long-term spatial-temporal monitoring of main field and plasma parameters of ionosphere with the aim to extract the signatures of natural and technogenic catastrophic events in the lower atmosphere and at the Earth's surface with the help of a cluster of 3 LEO microsattelites. Tentative launch data is 2010 year. All spacecrafts will have the same payload including AC and DC magnetometers, electric field probes, Langmuir probes, neutral particle density and temperature probes. This study was partially supported by NSAU Contract 1-02/03 and the STCU Project -3165.

Keywords: earthquake, precursor, ionosphere



(S) - IASPEI - *International Association of Seismology and Physics of the Earth's Interior*

JSS010

Oral Presentation

2069

Progress in Understanding of Lithosphere-Atmosphere-Ionosphere Coupling

Prof. Sergey Pulinets

Space Physics Department Institute of Geophysics

Dimitar Ouzounov, Alexander Karelin, Kirill Boyarchuk

The Lithosphere-Atmosphere-Ionosphere Coupling (LAIC) model created recently is able to explain simultaneously the thermal anomalies observed in the boundary layer (BL) of atmosphere and ionospheric anomalies observed in all layers of the ionosphere before strong earthquakes by common physical mechanism, having as a principle source the air ionization by increased radon release over active tectonic faults. We name these anomalies as thermal and ionospheric branches of the model. But these branches are not independent; they interact and provide the energy one to another for self-development. Electric properties of the large ion clusters change the chemical potential (work function of evaporation) what makes the clusters more stable and permit to attach more water molecules and consequently to release more latent heat. The thermal energy released during the process of water molecules attachment to ions creates the upward convective flux which is the source of the additional electric field generation and amplification. The intermediate products of this interaction between branches are increased concentration of the aerosols in the boundary layer and formation of so called earthquake clouds. All the parts of the presented model are supported by satellite and ground based measurements of atmospheric and ionospheric parameters of major recent earthquakes.

Keywords: lai coupling model, ionization, thermal ionospheric anomalies



(S) - IASPEI - *International Association of Seismology and Physics of the Earth's Interior*

JSS010

Oral Presentation

2070

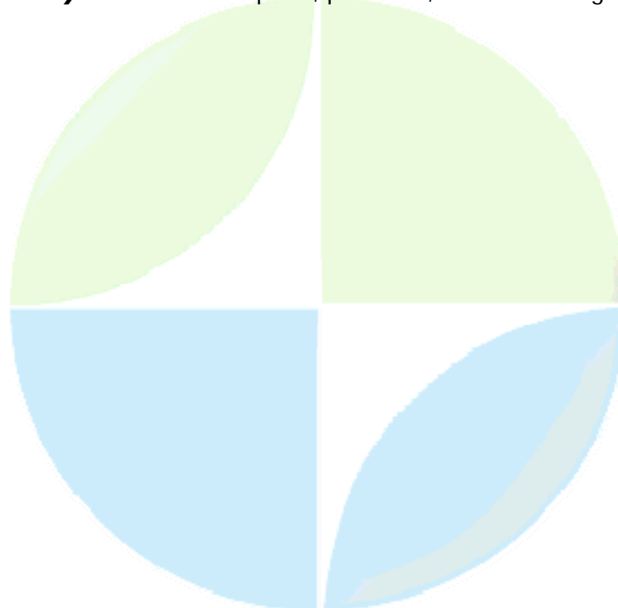
Multisensor Approach of Analyzing Atmospheric/Ionospheric EM Signals Connected with Major Earthquake Activities

Dr. Dimitar Ouzounov
WG EMSEV EMSEV IAGA

Sergey Pulinets, Guido Cervone, Menas Kafatos, Michel Parrot, Patrick Taylor

We present a possible relationship between tectonic stresses, electro-chemical and thermodynamic processes in the Earth's crust and atmosphere with ionospheric plasma and ground-atmosphere electromagnetic (EM) field variations as a potential signature of electromagnetic (EM) phenomena that are related to earthquake activity, either pre-, co- or post-seismic. Using data from: (1) polar orbiting MODIS, onboard NASA's Terra and Aqua; (2) AIRS (on Aqua); (3) NOAA/AVHRR; (4) geosynchronous weather satellites (GOES and METEOSAT); (5) DEMETER and; (6) GSP/TEC; we have analyzed: surface emissivity; sea and land surface temperature (LST); emitted earth radiation (OLR); air temperature; surface latent heat flux (SLHF); Total Electron Content, TEC (GPS /TEC); quasi-continuous electrical fields; and thermal plasma parameters. A reference level was created from multi-year data (LST, SLHF, OLR, and VLF) by systematically comparing them with recent satellite observations to determine meaningful statistics that can be applied to anomalous signals prior to an earthquake. Our rationale for using this complement of observations is that there is insufficient spatial and temporal coverage of any one of these pre-cursor signals on the global scale. The advantage of our approach is to enable multiple and previously validated physical measurements to be integrated into one framework with the latest theoretical models of seismo-electromagnetic generation and propagation and to provide feedback on data gaps that may then be acquired in the future from new missions. The significance of our satellite based multi-sensor approach was defined through analyzing recent (2000-2006) worldwide strong earthquakes and applying the techniques used to capture the EM anomalies. This joint approach provides an opportunity for a comprehensive study of Earth's electromagnetic environment, and can be used to understand the relationship between seismic-tectonic processes in the solid Earth and surface-atmosphere-ionosphere variability.

Keywords: earthquake, precursor, remote sensing



(S) - IASPEI - *International Association of Seismology and Physics of the Earth's Interior*

JSS010

Oral Presentation

2071

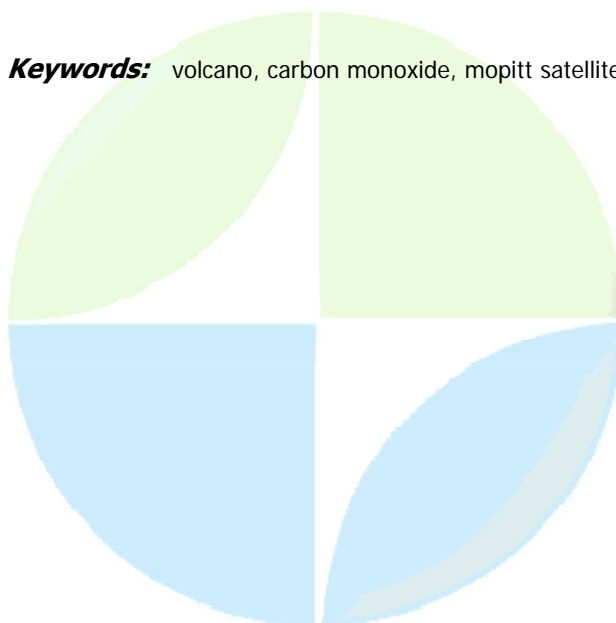
Monitoring slow unrest of Taal Volcano (Philippines) using carbon monoxide from MOPITT satellite

Mr. Senthilkumar Jambulingam
CIVIL ENGINEERING STUDENT IAVCEI

Ramesh P. Singh, J. Zlotnicki, Y. Sasai, J. Sincioco

Taal volcano (121E, 14N) is located 60 km south of Manila, Philippines. Since 1572, 33 eruptions have occurred. The volcano is considered as one of the most devastating volcanoes in Philippines, due to the sudden and explosive eruptions. Taal volcano shows new phases of low but noticeable activities since the last 1976-1977 eruption. Between 1992 and 1994, seismicity was strongly found to increase and was accompanied by ground deformations (several tens of cm) and surface fissures. After October 2004, seismicity sporadically occurs and several earthquakes are felt. Geysering phenomena was finally observed in November 2006. The 311 m high Taal stratovolcano is located in a large pre-historical caldera filled by a lake, and the crater of the volcano itself is filled by an acidic lake of about 1.2 km in diameter. These hydrologic characteristics, associated with dikes injection below the volcano generate a very powerful hydrothermal activity which partly controls the onset of eruptions. Efforts have been made to use remote sensing technique since it will be difficult to access the area close to the volcano, in case of eruption. Analysis of multi sensor parameters available from optical and microwave sensors every day have been carried out. Unfortunately, up to now, these sensors have low resolution. As a result it is difficult to monitor small changes in land surface and meteorological parameters. However, the gases emitted from the volcano bring changes in the chemistry of the atmosphere over the volcano and the surrounding region. The multi sensor parameters which provide information about the land, meteorological and atmospheric parameters have been analyzed during the period 2001 to 2007. Due to low resolution of sensors not much changes in various parameters are noticed. The MOPITT (Measurement of Pollution in the Troposphere) sensor onboard Terra satellite daytime and nighttime vertical carbon monoxide (CO) mixing ratio data over the volcano shows significant variations in mixing ratio from ground up to 500 hPa pressure level. The correlation of ground parameters observed near the Taal volcano and vertical carbon monoxide mixing ratio confirms the slow increase of activity of Taal volcano.

Keywords: volcano, carbon monoxide, mopitt satellite



(S) - IASPEI - *International Association of Seismology and Physics of the Earth's Interior*

JSS010

Oral Presentation

2072

Possible influence of seismic activity on the propagation of anomalous whistlers recorded in space

Dr. Livio Conti

Dep. of Physics, Roma Tre University Researcher

Aurora Buzzi, Michel Parrot, Jean-Louis Pincon, Vittorio Sgrigna, David Zilpimiani

An analysis reported in literature on whistlers-waves detected by ground-based observatories, has suggested the possible influence of seismo-electromagnetic emissions on the propagation of anomalous whistlers. In the present work a geographic and temporal correlation between earthquakes of moderate and large magnitude and anomalous whistlers has been investigated but using data collected in space by the DEMETER satellite. Both method of analysis and preliminary results on one year data will be presented and discussed.

Keywords: whistler, earthquake, demeter

XXIV2007

PERUGIA
I T A L Y



(S) - IASPEI - *International Association of Seismology and Physics of the Earth's Interior*

JSS010

Oral Presentation

2073

Precursors in ionospheric GPS TEC of the 26 December 2004 M9.3 Sumatra earthquake

Prof. Jann-Yenq Liu

National Central University ISS, National Central University IAGA

Yuh-Ing Chen

An M9.3 earthquake, the largest one in the recent 5 decades, occurred in Sumatra Indonesia at 00:58:53 UT (universal time) on 26 December 2004. A time sequence of global ionosphere maps (GIMs) derived from worldwide ground-based receivers of the global positioning system (GPS) is used to monitor changes of the ionospheric total electron content (TEC). It is found that near the epicenter the ionospheric electron density anomalously decreases in the afternoon period on 21 December 2004 which is day 5 prior to the earthquake. The spatial distributions of the decreased anomalies further indicate that the ionospheric fountain is significantly disturbed and electrodynamic is important.

Keywords: seismo ionospheric, gps, tec



(S) - IASPEI - *International Association of Seismology and Physics of the Earth's Interior*

JSS010

Oral Presentation

2074

Review of pre-seismic lithosphere - atmosphere - ionosphere coupling study

Dr. Masashi Kamogawa

Department of Physics Tokyo Gakuzei University

Pre-seismic anomalous states in the atmosphere and ionosphere as well as those in the telluric currents and ultra-low frequency electromagnetic waves have been reported since the 1970s. These pre-seismic phenomena have not yet been universally accepted, partly because the low occurrence frequency of large earthquakes has hindered establishing their statistical significance. Recent achievements in this respect, however, seem to be highly encouraging for promoting further studies on the pre-seismic lithosphere-atmosphere-ionosphere (LAI) coupling. Liu et al. (JGR, 2006) constructed a set of quantitative definitions for ionospheric anomalies (depression of foF2) and examined the statistical correlation between thus defined ionospheric anomalies and all the Taiwan $M \geq 5$ earthquakes (184 in number) during the period 1994-1999. The results indicated that anomalies appeared within 5 days before the earthquakes. Examining the validity of the pre-seismic anomalous transmission of VHF electromagnetic waves beyond the line-of-sight, Fujiwara and Kamogawa et al. (GRL, 2004) statistically demonstrated the existence of atmospheric anomalies lasting for a few minutes to several hours before earthquakes. They found that the anomalies were significantly enhanced within 5 days before $M \geq 4.8$ earthquakes. If the pre-seismic atmospheric - ionospheric anomalies are real, some phenomena causing them should be detectable on the ground. If such causal phenomena are identified, the concept of lithosphere - atmosphere - ionosphere coupling (LAI coupling) will be greatly strengthened. Possible mechanisms for energy-transport channels from the lithosphere to the atmosphere-ionosphere are summarized as follows: First, the atmospheric electric field generated on/near the ground surface during the pre-seismic period may cause the ionospheric anomalies. Such an atmospheric electric field may be caused by ions generated from radon emissions. Actually, a number of reports have been published for pre-seismic radon emissions. However, such pre-seismic electric fields on the ground followed by pre-seismic ionospheric anomalies have not yet been observed. Alternatively, it has been proposed that atmospheric gravity waves propagate up to and disturbs the ionosphere before earthquakes. The proposed sources of the gravity waves are long-period ground oscillations or thermal anomalies. This proposed linkage is inferred from the observations of co-seismic ground vibrations and tsunami exciting atmospheric gravity waves which propagate into ionosphere. However, there is no report of pre-seismic long-period ground oscillations being detected, even by sensitive superconducting gravimeters. Although some reports claim the existence of pre-seismic rises of temperature, infrared radiation, and surface latent heat flux, it is difficult to explain how such anomalies disturb the ionosphere through the atmosphere. As discussed in this abstract, the cause and effect relationships may still be unestablished but pre-seismic atmospheric-ionospheric anomalies do exist and searching for the lithospheric connection remains an important research endeavor.

Keywords: earthquake, ionosphere, atmosphere

(S) - IASPEI - *International Association of Seismology and Physics of the Earth's Interior*

JSS010

Oral Presentation

2075

A robust multitemporal satellite approach for thermal volcanic activity monitoring

Dr. Francesco Marchese
DIFA University of Basilicata

Nicola Pergola, Carolina Filizzola, Maurizio Ciampa, Valerio Tramutoli, Irina Coviello

In the world there are more than 1500 active volcanoes, many of these are located in very densely populated regions representing a serious risk both for local residents and infrastructures. From decades satellite remote sensing is used to study thermal volcanic activity thanks to low cost data, high observational frequencies and global coverage. Recently, a new multi-temporal satellite approach, named RST (Robust Satellite Techniques) has been applied to several recent eruption of Mount Etna, Stromboli and Merapi volcanoes showing to be suitable to successfully detecting and monitoring hot volcanic features, strongly reducing false alarms occurrences. An automatic satellite monitoring system, based on this approach, has also been developed at IMAA (Institute of Methodologies for Environmental Analysis) to monitor Italian volcanoes in near real time, processing AVHRR data. This system is capable of providing, a few minutes after the direct acquisition of raw data, thermal anomaly maps and alert log files, reporting the exact geographic location of hot spots and their relative intensity. RST approach has been successfully implemented also on new geostationary satellite MSG-SEVIRI, with improved performances in terms of sensitivity and reliability. Moreover, the geostationary attitude of SEVIRI assures a higher observational frequency allowing us to promptly identifying new eruptive events at very early stage within an actual early warning context. A summary of recent RST results for thermal volcanic activity monitoring, both using polar and geostationary satellites, will be shown and discussed also in terms of operational purposes.

Keywords: hotspots, volcanoes, satellite



(S) - IASPEI - International Association of Seismology and Physics of the Earth's Interior

JSS010

Oral Presentation

2076

Robust Satellite Techniques (RST) for seismically active areas monitoring:

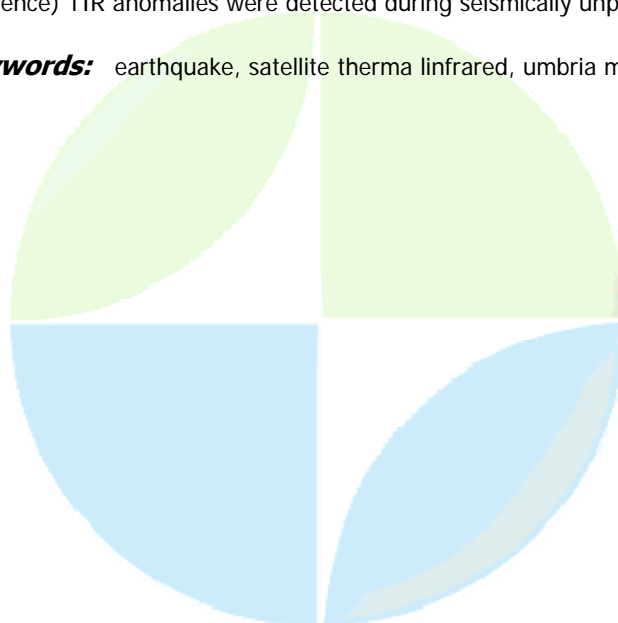
Dr. Carolina Aliano

DIFA UNIBAS

Rosita Corrado, Carolina Filizzola, Pergola Nicola, Valerio Tramutoli

In the last 20 years an increasing number of studies based on TIR satellite data have reported space-time fluctuations of earths emitted TIR radiation during a time (from weeks to days) before earthquake occurrence. Several authors interpreted such thermal signals as seismic precursors, suggesting different explanatory models. More recently, a Robust Satellite data analysis Technique (RST) was proposed which has turned out as a suitable tool for satellite TIR surveys in seismically active regions. Compared with other methods, RST offers an unambiguous (statistically founded) definition of TIR anomaly and improved capability to identify anomalous space-time TIR signal variations even in very variable observational (satellite view angle, land topography and coverage, etc.) and natural (e.g. meteorological) conditions. In this work RST is applied for the first time to a seismic sequence for better understanding the relationship between TIR anomaly intensity and earthquake magnitude and/or depth, being the same the geologic conditions. The 1997-1998 Umbria-Marche seismic sequence was considered because the region of Central Appennines is one of the more degassing area in . The enhanced green-house gas emission is in fact one of the proposed cause for the appearance of TIR anomalies in relation with seismic activity. Nine years of Meteosat TIR observations have been analyzed in order to characterize the TIR signal behaviour in absence of significant seismic activity at each specific observation time and location. Space-time TIR signal transients have been then analyzed, both in presence (validation) and in absence of (confutation) seismic events, looking for possible space-time relationships. The main ($M_b > 4$) seismic events of the sequence have been considered as test cases for validation, and relatively unperturbed periods (no earthquakes with $M_b > 4$) were taken for confutation purposes. The observations show that the area of interest is affected by positive time-space persistent TIR anomalies during periods of seismic activity. Such anomalies generally overlap the principal tectonic lineaments of the region, sometimes focusing in the vicinity of the earthquake epicentre. As far as the confutation analysis is concerned, the results well highlight that no similar (in terms of relative intensity and space-time persistence) TIR anomalies were detected during seismically unperturbed periods.

Keywords: earthquake, satellite therma linfrared, umbria marche



(S) - IASPEI - *International Association of Seismology and Physics of the Earth's Interior*

JSS010

Oral Presentation

2077

Multi Sensor Response and Its Relation with the Observed Earthquake Activities in the Koyna region (India)

Prof. Ramesh Singh

Civil Engineering IIT Kanpur IASPEI

Senthil Kumar, Guido Cervone, Anup K Prasad

Koyna region lies near the western coast of where frequent seismicity are observed since 1967. Efforts have been made to study the response of multi sensor satellite over the Koyna region available during day and night. From these satellite data, information on the surface as well as at different pressure levels are deduced. The long term analysis of multi sensor parameters during the period 2000 2006 show anomalous behavior which are not found to be associated with observed seismicity. However, the combined behavior of multi sensor parameters show one to one relation with the observed earthquake activities in the Koyna region. The complimentary behavior of multi sensor parameters will be discussed in the early warning of an impending earthquake in the Koyna region.

Keywords: koyna, earthquake, remotesensing



(S) - IASPEI - *International Association of Seismology and Physics of the Earth's Interior*

JSS010

Oral Presentation

2078

Statistical studies of ionospheric parameters observed by the satellite DEMETER during seismic activity

Dr. Michel Parrot
LPCE CNRS IAGA

F. Li

DEMETER is an ionospheric micro-satellite launched on a polar orbit at an altitude of 710 km. Its main scientific objective is to study the ionospheric perturbations in relation with seismic activity, and then, its scientific payload allows to measure electromagnetic waves and plasma parameters all around the Earth except in the auroral zones. Two specific parameters are taken into account in this paper: the electron density and the electrostatic turbulence. First the paper will show specific events where the electron density and the electrostatic turbulence are perturbed prior to large earthquakes above the future epicentre. Although, these examples have been carefully selected (close in time and space to the earthquakes, abnormal variations relative to the background level for the same location, the same local time and the same magnetic activity) it is always possible that the perturbations are due to other natural mechanisms because the ionosphere is highly variable and mainly under the control of the sun. Only a statistical analysis of the data is able to remove this ambiguity. As there are now more than two years of data, a statistical study has been set about the variation of these parameters during the seismic activity. The statistic is done as functions of the geographic position, the local time, and the magnetic activity. Geographical maps with average data are obtained to be used as background levels, and the superposed epoch method is applied to merge the data recorded during seismic activity. Comparison is done when we remove the aftershocks from the statistics.

Keywords: demeter, ionosphere, micro satellite



(S) - IASPEI - *International Association of Seismology and Physics of the Earth's Interior*

JSS010

Poster presentation

2079

TEC variations over the Mediterranean during the seismic activity period of Kythera earthquake of 12th January, 2006

Prof. Michael Condadakīs

Department of Geodesy and Surveying Aristotle University of Thessaloniki IASPEI

D. N. Arabelos, G. Asteriadis, S.D. Spatalas, Ch. Pikridas

TEC variations over a particular site sustain variations of different causality, global (earth revolution, earth rotation, earth-tides, variations of the geomagnetic field etc.) or local (atmospheric or underground explosions, earthquakes, volcanoes etc.). A lot of work has been done by a great number of researchers on the characteristics of ionospheric variations according to their causality (wave - length, attenuation and velocity and way of propagation). In order that TEC variations over a particular site be used as earthquake precursory diagnostic a concrete sense of the interrelation of TEC variations over different sites as well as their respond of the geomagnetic field variations would be of great interest. In this paper the TEC data of eight GPS stations of the EUREF network (AUT1, Thessaloniki and TUC2, Crete in Greece, MAT, Matera and LAMP, Lampedusa in Italy, GAIA in Portugal, RABT in Rabat, EVPA, Evpatoria in Ukrain and TRAB, Trabson in Turkey) were analyzed using wavelet analysis in order to detect any frequency dependence of the correlation of TEC over different stations. In the same time frequency dependence of Dst and TEC variations are searched in order to detect any correlation. The main conclusion of this analysis is that the constituents of TEC variation with periods <3h are more suitable in searching for earthquake precursors. On the base of this conclusion the analyzed TEC series are searched for possible precursory phenomena. Variation in TEC constituents with periods <3h over the stations AUT1 and TUC2 occurred 10days of the seismic activity may be attributed to this tectonic activity.

Keywords: tec, seismic activity, gps network



(S) - IASPEI - *International Association of Seismology and Physics of the Earth's Interior*

JSS010

Poster presentation

2080

Comparison of foF2 variations observed prior to two major earthquakes in Italy and during a magnetic storm

Dr. Valeri Khagai

Solar-Terrestrial Physics IZMIRAN, Troitsk, Moscow Region 142190, Russia IASPEI

Legenka Anna Dmitrievna, Kim Vitaly Pavlovich

We have examined time variations of the critical frequency foF2 for low geomagnetic activity before two major earthquakes ($M = 6.0$ and $M = 5.3$) which occurred in Italy on January 7, 1962 and April 5, 1998, respectively, and during the geomagnetic storm of January 10, 1962 using measurements from several ground-based ionosondes. It is found that there took place noticeable (more than 1.5 the standard deviation) transient perturbations of foF2 with respect to the foF2 monthly median from about 24 to several hours before the earthquakes over the restricted region (with horizontal dimensions of the order of 800 - 1000 km) around the earthquake epicenter. During the magnetic storm, severe disturbances of the F region peak electron density were observed on a global scale. Peak magnitudes of the foF2 disturbances associated with the storm by more than a factor of 3 exceed those ones measured before the earthquakes at the same locations. We suggest that the foF2 perturbations preceding the earthquakes are likely initiated by some pre-earthquake seismic activity.

Keywords: earthquakes, magnetic storm, fof2 disturbances

PERUGIA
ITALY



(S) - IASPEI - International Association of Seismology and Physics of the Earth's Interior

JSS010

Poster presentation

2081

Earthquake Clouds

Prof. Ugur Kaynak

Dept. of Geophysics-Kou-Turkey Retired

Roland Karel

We decided to work about the earthquake clouds after the ionosphere investigations begin to announce that there are some relationship between the ionosphere and lithosphere. These relationships are based on the huge amount of electric discharges from surrounded strained rocks of a stressed fault zone. On the other hand, the ionosphere affected from huge amount of the bearing particle coming from Sun by the solar winds. This phenomenon also will affect the lithosphere but only by the induction effect to the natural displacement currents. When the fault planes begin to emanate electrons to the lower troposphere by the piezoelectric effect, the newer electrostatic forces of these electron clouds will disturb the entire electric and magnetic systems located on the closed environments of it, until the ejected electron clouds will be reabsorbed by the main capacitor of the earth. Just on this exaggerated electron bearing condition of the lower troposphere, there may be two kind of coulombic bearing earthquake clouds produced from lithosphere and induced ionosphere. The lower earthquake clouds induced from the emanated electron clouds directly, called here as electrostatic earthquake clouds and stratospheric ice clouds that known as jet-streams called ionic earthquakes clouds when they deviated from their flying route because of their positive charges. Another earthquake clouds are the thermal earthquakes clouds emanating of the water vapor and other gases. (Such as radon, argon, methane) Their main gas and vapor ejections column namely tornado type earthquake clouds called first by the Japanese investigators. Also there are normal thermal clouds produced by the volcanic craters, warm tectonical lakes, hot water springs, and warm rivers streaming in the frozen territories. Because of these abundant types of the thermal clouds, it is very difficult to distinguish the thermal earthquake clouds from the normal one.

Keywords: electrostatic clouds, ionic earthquakes clouds, thermic earthquakes clouds



(S) - IASPEI - *International Association of Seismology and Physics of the Earth's Interior*

JSS010

Poster presentation

2082

Simultaneous disturbances of high-frequency geoacoustic emission and of electric field in the near-ground air

Dr. Yury Marapulets

FEB RAS IKIR FEB RAS IASPEI

Oleg Rulenko, Mihail Mischenko, Albert Scherbina

By the means of a complex of synchronous measurements of rock acoustic emission at the frequencies 0,1-10000 Hz and of vertical potential gradient of electric field in the near-ground air their simultaneous disturbances, appearing during deformation of near-surface rocks, were determined for the first during. The disturbances may be observed in seismically calm periods and at the final stage of earthquake preparation. They indicate one more form of influence of the lithosphere on the near-ground atmosphere.

Keywords: acoustic emission, electric field

XXIV2007

PERUGIA

I T A L Y



(S) - IASPEI - *International Association of Seismology and Physics of the Earth's Interior*

JSS010

Poster presentation

2083

Occurrence of precursory effects of Kythira 2006 earthquake in GPS TEC variations

Mrs. Irina Zakharenkova

Irk Shagimuratov, Andrzej Krankowski, Galina Yakimova

Total electron content of the ionosphere (TEC) is one of the most effective parameter to investigate the ionospheric effects associated with natural and technogenic hazards. GPS technique gives opportunities to detect spatial and temporal changes of the ionosphere during geomagnetic and seismic events. In this report we present the specific features of TEC behavior as possible precursors of Southern Greece earthquake of January 8, 2006 (M6.8). The epicenter position was 36N, 23E. For this purpose we used both the TEC data of nearest to the epicenter Euref-IGS stations and TEC maps over Europe. The favorable circumstance for this analysis was the quiet geomagnetic situation during the period previous to the earthquake. One day prior to earthquake the characteristic anomaly was found out as the day-time significant increase of TEC level at the nearest stations up to the value of 50% relative to the background condition. To estimate the spatial dimensions of seismo-ionospheric anomaly the differential mapping method was used. The ionosphere modification as the cloud like increase of electron concentration situated in the immediate vicinity from the forthcoming earthquake epicenter was revealed. The amplitude of modification reached the value of 50% relative to the non-disturbed condition and was in existence from 10 UT till 22 UT. The area of significant TEC enhancement had the sizes of about 4000 km in longitude and 1500 km in latitude. The revealed anomaly we have associated with precursors of the seismic event amenably to its peculiarities (its locality, affinity with the epicenter, cloud like zone of manifestation, characteristic time of existence).

Keywords: precursors, ionosphere



(S) - IASPEI - *International Association of Seismology and Physics of the Earth's Interior*

JSS010

Poster presentation

2084

Modification of the ionosphere before strong earthquakes of Japan region on the base of GPS measurements

Mrs. Irina Zakharenkova

Irk Shagimuratov, Yuriy Ruzhin, Nadezhda Tepenitsina

The searches of the seismo-ionospheric effects with using space technologies have been extensively discussed in the last years. The huge opportunities in this field are provided by satellite navigation system GPS. The global and dense network of ground-based GPS stations enables to realize the permanent monitoring of the ionosphere in the global scale with high spatial-temporal resolution. In this report the analysis of the ionospheric total electron content (TEC) variations obtained by using the GPS measurements before strong earthquakes is presented. We have investigated the modification of the ionosphere before strong earthquakes occurred during 2000-2006 in Japanese region. In this analysis the diurnal TEC variations from GPS net were used. For detailed picture of TEC behavior, TEC observations along the individual satellite flights were considered. The spatial modification of the ionosphere was investigated with use of TEC maps (global maps at the IONEX format and regional maps with high spatial-temporal resolution). Some general peculiarities of the ionospheric effects associated with seismic activity are found out. The pre-seismic behavior of TEC was detected within several days before the main event. Anomaly appeared as the local TEC enhancement (plasma cloud) located in the vicinity of the forthcoming earthquake epicenter. These structures are generated in the ionosphere for several days prior to the main shock. During the process of the earthquake approach the amplitude of plasma modification increases, and it has reached the value of 35-60% relative to the non-disturbed level. The ionosphere region of strong positive disturbance has extended larger than 1500 km in latitudes and 3500-4000 km in longitudes. The TEC enhancement reached the value of 70-90% relative to the quite level for very strong events ($M > 7.0$). For the earthquake that took place on the background of the high geomagnetic activity the positive effect will be discussed.

Keywords: ionosphere, gps, precursors



(S) - IASPEI - *International Association of Seismology and Physics of the Earth's Interior*

JSS010

Poster presentation

2085

Spatial distribution of ionospheric GPS-TEC and NmF2 disturbances prior to the 1999 Chi-Chi and Chia-Yi Earthquakes

Mr. Masahide Nishihashi

Graduate Course of Science Chiba University IASPEI

Hau-Kun Jhuang, Katsumi Hattori, Jann-Yenq Liu

Many anomalous electromagnetic phenomena possibly associated with large earthquakes have been reported. Recently, scientists found an apparent reduction in GPS-TEC within 1 - 5 days prior to beyond M6.0 earthquakes in Taiwan. However, those studies did not match simultaneous data sets of other sites to confirm the observed ionospheric anomalies are related to local earthquakes. In this study, we retrieved GPS-TEC data sets, routinely published in the global ionosphere maps (GIM). Simultaneous data of ionosonde records and GPS-TEC data sets of various locations such as Taiwan and Japan were examined to check whether the anomalies observed in Taiwan during the 1999 Chi-Chi earthquake (Mw7.6) and Chia-Yi earthquake (M6.4) episodes are local or global effects. The result shows that the anomalies in Taiwan three days before the Chi-Chi earthquake (18 September), and one and three days before the Chia-Yi earthquake (19 and 21 October) are local phenomena. It means that the ionospheric-disturbed areas were localized around Taiwan, and did not spread all the way to Tokyo in Japan. We conclude that the disturbed areas are at least less than about 2200km in radius and may be much smaller.

Keywords: gps tec, nmf2, taiwan earthquakes

PERUGIA
ITALY



(S) - IASPEI - *International Association of Seismology and Physics of the Earth's Interior*

JSS010

Poster presentation

2086

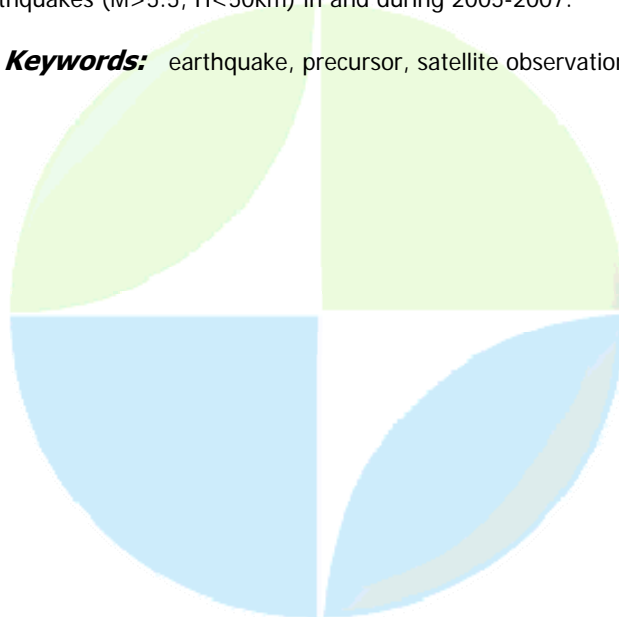
Joint Satellite and Ground Based EM observation and Search for Earthquake Precursors

Dr. Dimitar Ouzounov
WG EMSEV EMSEV IAGA

Katsumi Hattori, Sergey Pulinets, Masashi Kamogawa, Masahide Nishihashi, Michel Parrot, J.Y. Liu

Previous studies have shown that there were precursory electromagnetic signals associated with several recent earthquakes observed on the ground and space. Goal of this work is to merge our new approach of recording and analyzing multi-sensor satellite and ground data to our studies of pre-, co- and post-seismic signals. Recent advances in solid earth sciences, GPS/TEC and remote sensing capabilities give us assurance that the scientific understanding and data availability are appropriate at this time to initiate this joint search for the possible earthquake precursors. Our approach is based on data fusion of satellite data obtained from thermal infrared observations from Terra, Aqua, GOES, POES and space plasma parameters variations from DEMETER, simultaneously with ground based multi parameter continuous measurements of GPS/TEC, ion concentration, R_n , atmospheric electrical field, magnetic array and corona probe from Japan (Iyogatake station, Chiba University) and Taiwan (NCU). We use existing satellite sensors and ground observations and the physical link between both measurements are given by Lithosphere-Atmosphere-Ionosphere coupling (LAIC) model. This mechanism is a coupling between the boundary layer of atmosphere and the ionosphere due to increased tectonic activity before strong earthquakes. The simultaneous co-existence of several mechanisms manifesting this coupling enhances the possibility of revealing and tracking future EM seismogenic signals much easier and more reliably. Our first results show that is very unlikely that a single existing method (magnetic field, electric field, thermal infrared (TIR), Surface Latent Heat Flux SLHF, and GPS/TEC) can provide a successful solution for monitoring pre-earthquake phenomena on the global scale. However, simultaneous satellite and ground measurements as an integrated web should provide the necessary information by combining the information provided by multiple sensing sources, both on the ground and from space. The significance of joined satellite and ground based EM precursor search was defined through analyzing most recent major earthquakes ($M > 5.5$, $H < 50\text{km}$) in and during 2005-2007.

Keywords: earthquake, precursor, satellite observation



(S) - IASPEI - *International Association of Seismology and Physics of the Earth's Interior*

JSS010

Poster presentation

2087

On the physical causes of enhanced infrared emission known as Thermal Anomalies

Prof. Friedemann Freund

Earth Science Division, Code SGE NASA Ames Research Center IAGA

Akihiro Takeuchi, Bobby W.S. Lau, Nevin A. Bryant

Ever since large, rapidly changing areas of enhanced infrared emission have been noted in night-time satellite images in association with impending seismic activity, the search has been on to find an explanation for this intricate phenomenon. We pursue a different line of inquiry - different from what has been proposed before - which comes from the recognition (1) that deviatoric stresses activate dormant electronic charge carriers that exist in rocks in form of peroxy links, $O_3Si-OO-SiO_3$. They release defect electrons, highly mobile charge carriers in the oxygen anion sublattice (positive holes or pholes for short), chemically O^- . The pholes propagate at speeds on the order of 20050 m/sec, propagate through dry and wet rocks, through sand and soil. They become trapped at the surface. It costs mechanical energy to dissociate peroxy at depth. Some of this energy is recovered when pholes recombine at the surface, leading to vibrationally highly excited O-O bonds, which can get rid of their excess energy (i) by emitting photons at specific wavelengths in the mid-IR region, (ii) by kicking and exciting their neighbors, thereby thermalizing and causing a very thin surface layer to heat up. The theoretically predicted narrow mid-IR emission bands due to the deactivation of highly excited O-O bonds have been experimentally confirmed with a large block of anorthosite, a feldspar rock, measuring the IR emission ~50 cm from the stressed rock volume (2). (1) Freund et al. 2006, Phys. Chem. Earth 31, 389-396; (2) Freund et al. 2007, eEarth, 2, 1-10.

Keywords: earthquake precursors, thermal infrared anomalies, stimulated infrared emission



(S) - IASPEI - *International Association of Seismology and Physics of the Earth's Interior*

JSS010

Poster presentation

2088

Analysis of thermal neutron ground observations in accordance with space observations of seismo-electromagnetic phenomena

Dr. Ekaterina Sigaeva

Space Physics Research Department Skobeltsyn Institute of Nuclear Physics

Irina Myagkova, Ekaterina Muravieva, Yuri Kuzmin

Long-term ground-based observations have shown that thermal neutrons' flux is very sensitive regarding different processes both in the near-Earth space and in the Earth's crust due to the dual nature of the neutron flux near the Earth's surface. The first source of neutrons is bound up with the high-energy particles of cosmic rays, which produce neutrons in the interactions with the elements of the atmosphere. The second source originates from the natural radioactive gases of the Earth's crust. The calculations have shown that the impact of the second source strongly depends on geographical location of the observation point, i.e. on the local conditions of the gases' emission. Besides any change of these conditions will result in variations of the thermal neutrons' flux. For instance, tidal wave's influence on the Earth's crust leads to presence of harmonics in the thermal neutrons' observations, which are well known from gravity surveys. The recent observations of the thermal neutrons' flux in the seismic-active area of Kamchatka resulted in a conclusion that the most part of the strong earthquakes occurred in the sufficiently broad area along the boundary of the Pacific and Euro-Asian tectonic plates "produce" increased neutrons' flux at Kamchatka experimental unit. At the same time there are a lot of local effects (including climate, weather, etc.) which also lead to changes of neutrons' flux. Therefore it's very important to separate the variations of geodynamical nature from the rest in order to use them as earthquake precursors and to develop a new method of earthquake prediction. One of the possible ways for such separation can be implemented by means of analysis of the neutrons' flux data and the seismo-electromagnetic data obtained by space missions. In this paper the results of cross-section analysis of the neutrons' data and the charged particles' precipitation under the Earth's radiation belts in order to find the characteristics of geodynamic variations of the neutrons' flux are presented.

Keywords: neutron, precursor, seismo electromagnetic



(S) - IASPEI - *International Association of Seismology and Physics of the Earth's Interior*

JSS010

Poster presentation

2089

Analysis of ionospheric electrostatic turbulence over seismic regions using DEMETER plasma and wave measurements

Dr. Tatsuo Onishi

Jean-Jacques Berthelier

Several recent results have pointed out the existence of ionospheric disturbances associated with seismic activity. Of great interest, in particular, is the possible occurrence of disturbances prior to the main shock that can be thought as ionospheric precursors of earthquakes. One of the goals of the DEMETER mission is to perform an in-situ study of the ionospheric plasma and waves in order to search for events associated to seismic activity and to characterize pre- and post-seismic effects. Using measurements of the electric components of plasma waves in the ULF/ELF/VLF ranges provided by the ICE instrument and thermal plasma measurements from the IAP instrument, we have studied the natural emissions that are observed over seismically active regions with an initial focus on the low frequency electrostatic turbulence and plasma irregularities. The electromagnetic interferences onboard DEMETER have been maintained to a low level. However, it is expected that events associated with seismic activity have a weak intensity, and we have paid a careful attention to detect the occurrence of electromagnetic interferences, understand their origin and estimate their effect on power spectra. Similarly we have tried to recognize as far as possible natural emissions that arise from space weather effects and are not linked with seismic activity in order to minimize their impact on the statistical distribution of low level signals. In order to distinguish the true pre-seismic events from post-seismic disturbances, a number of earthquakes were carefully selected from the earthquake database so as not to include other seismic events of significant importance during the 5 preceding days within the same seismic region. In this talk we shall present the most important aspects of the methodology that have been followed to analyze the data and discuss current results from this on-going study.

Keywords: demeter, vlf, electrostatic



(S) - IASPEI - *International Association of Seismology and Physics of the Earth's Interior*

JSS010

Poster presentation

2090

Statistical study of anomalous fluctuations of whistler data recorded by DEMETER

Dr. Aurora Buzzi

Physics Roma Tre University IASPEI

Livio Conti, Michel Parrot, Jean-Louis Pincon, Vittorio Sgrigna, David Zilpimiani

It has been carried out a statistical analysis on the spatial and temporal distributions of whistlers detected by the RNF experiment on board the micro-satellite DEMETER. Several cuts and constrains (on the geomagnetic conditions, whistler propagation modes, etc.) have been applied to data in order to discriminate possible whistler anomalous fluctuations with respect to the mean monthly and geographical background values. Assuming a ducted propagation of whistler-waves along the magnetic field line, a few mathematical estimators of the signal-to-noise ratio have been introduced to estimate the statistical significance of anomalous signals. Aim of the study is to search whistler fluctuations possibly associated with earthquakes.

Keywords: whistler, earthquake, demeter



(S) - IASPEI - *International Association of Seismology and Physics of the Earth's Interior*

JSS010

Poster presentation

2091

Possible physical mechanisms of the TEC enhancements observed before earthquakes

Mrs. Irina Zakharenkova

Alexander Namgaladze, Irk Shagimuratov, Oleg Zolotov, Oleg Martynenko

The GPS derived TEC enhancements before earthquakes were discovered using global and regional TEC maps, TEC measurements over individual stations as well as measurements along individual GPS satellite passes. This pre-seismic behavior of TEC was detected within several days before the main event. Anomaly appeared as the local TEC enhancement located in the vicinity of the forthcoming earthquake epicenter. Such structures were generated in the ionosphere for several days prior to the main shock. The amplitude of plasma modification reached the value of 30-90% relative to the non-disturbed level. The ionosphere region of strong positive disturbance extended larger than 1500 km in latitudes and 3500-4000 km in longitudes. The possible physical mechanisms which can cause this positive effect associated with seismic activity are discussed. Among them the thermosphere-ionosphere interaction and electrodynamic mechanisms of the ionospheric earthquake precursors' formation are contemplated. The vertical plasma drift caused by the eastward electric field is considered as the most probable cause of the observed TEC enhancements. The electric potential distribution at the near-epicenter region boundary required for such electric field maintenance is proposed. The results of the corresponding numerical model calculations of the electric field and its effects in the ionospheric F2-layer and plasmasphere are presented.

Keywords: gps tec, precursors, earthquake



(S) - IASPEI - *International Association of Seismology and Physics of the Earth's Interior*

JSS010

Poster presentation

2092

**Seismo-anomalies of ground- and space-based observations during
M \geq 5.0 earthquakes in Taiwan**

Mrs. Yi-Ying Ho

National Central University Institute of Space Science IAGA

Taiwan is located on the western side of circum-pacific seismic zone, where the interaction between the Philippine Sea plate and the Eurasian plate is intense and complicated and therefore it offers an excellent opportunity for studying pre-earthquake anomaly phenomena. To search pre-earthquake electromagnetic anomalies, a program on integrated Search for Taiwan Earthquake Precursors (ISTEP) has been carried out since 1 April 2002. A comprehensive ground-based observation of eight networks of electrodes, magnetometers, Corona probes, FM tuners, Doppler sounders, all sky imagers, ionosondes, and GPS receivers has been constructed and applied. Recently pre-earthquake anomalies have been observed by using satellites, such as DEMETER launched on 29 June 2004, FORMOSAT-3/COSMIC launched on 14 April 2006, etc. In this paper, measurements of the ISTEP networks and the satellites of M \geq 5.0 earthquakes in the area are examined and discussed.

Keywords: istep, demeter, formosat 3



(S) - IASPEI - *International Association of Seismology and Physics of the Earth's Interior*

JSS011

2093 - 2186

**Symposium
Earth Structure and Geodynamics**

Convener : Prof. Thorne Lay

Integrated theoretical, observational and experimental studies involving seismology, geodynamics and geomagnetism are essential for advances in understanding of the dynamics of our planet. Fundamental problems such as the driving mechanisms for plate tectonics, the fate of subducted slabs, the role of water in the transition zone, the existence and nature of any mantle plumes, the isolation of geochemical reservoirs in the mantle, the structure and processes in the lowermost mantle boundary layer, and the chemical and physical interactions between the core and mantle all require multidisciplinary approaches. These topics will all be addressed in this symposium. Seismology provides constraints on the structure and amplitudes of heterogeneity in elastic properties and density and on elastic anisotropy using many imaging and modeling approaches. Geodynamics provides insights on the thermo-chemical nature of mantle convection, boundary layer behavior, interaction of flow with phase transitions, time evolution, and deformation processes using numerical modeling and laboratory experiments. These two fields interact closely, combined with constraints from mineral physics, geochemistry and geomagnetism to develop quantitative understanding of how the planet works. Both disciplinary and multidisciplinary papers drawing from these fields are invited for this symposium. This symposium will be subdivided into 5 multidisciplinary sessions: 1) lithosphere and asthenosphere structure and processes (L) 2) subduction zones and deep slabs (S) 3) mantle upwellings and plumes (P) 4) transition zone structure (T) 5) D" and mantle-core interactions (MC)

XXIV 2007

PERUGIA
I T A L Y



(S) - IASPEI - *International Association of Seismology and Physics of the Earth's Interior*

JSS011

Oral Presentation

2093

Continental growth and preservation of geochemical mantle heterogeneity in spite of whole-mantle convection

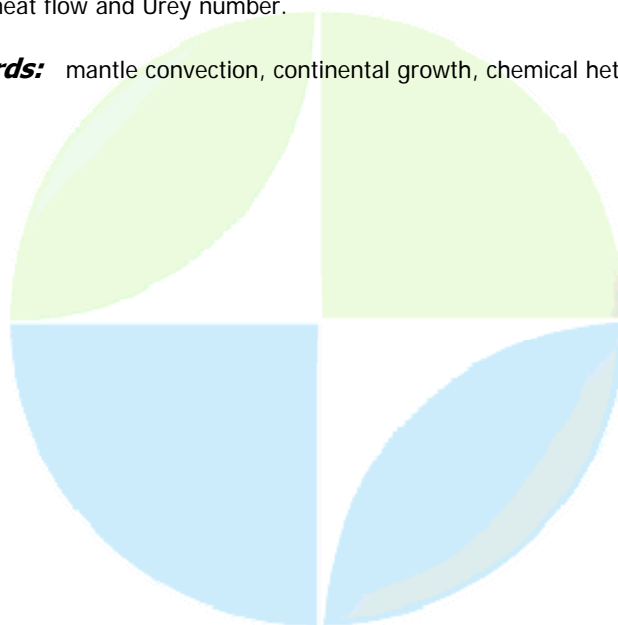
Prof. Uwe Walzer

Institut f. Geowissenschaften Friedrich-Schiller-Universitaet Jena IASPEI

Roland Hendel, John. Baumgardner

The focus of this paper is the numerical simulation of the chemical differentiation of the Earth's mantle. This differentiation induces the generation and growth of the continents and, as a complement, the formation and augmentation of the depleted MORB mantle. Here, we present a solution of this problem by an integrated theory in common with the problem of thermal convection in a 3-D compressible spherical-shell mantle. The conservation of mass, momentum, energy, angular momentum, and of four sums of the number of atoms of the pairs ^{238}U - ^{206}Pb , ^{235}U - ^{207}Pb , ^{232}Th - ^{208}Pb , ^{40}K - ^{40}Ar is guaranteed by the used equations. The whole coupled thermal and chemical evolution of mantle plus crust was calculated starting with the formation of the solid-state primordial silicate mantle. No restricting assumptions have been made regarding number, size, form, and distribution of the continents. It was, however, implemented that moving oceanic plateaus touching a continent are to be accreted to this continent at the corresponding place. The model contains a mantle-viscosity profile with a usual asthenosphere beneath a lithosphere, a highly viscous transition zone and a second low-viscosity layer below the 660-km mineral phase boundary. The central part of the lower mantle is highly viscous. This explains the fact that there are, regarding the incompatible elements, chemically different mantle reservoirs in spite of perpetual stirring during more than 4.49 billion years. The highly viscous central part of the lower mantle also explains the relatively slow lateral movements of CMB-based plumes, slow in comparison with the lateral movements of the lithospheric plates. The temperature- and pressure-dependent viscosity of the model is complemented by a viscoplastic yield stress, S_y . The paper includes a comprehensive variation of parameters, especially the variation of the viscosity-level parameter, η , the yield stress, S_y , and the temporal average of the Rayleigh number. In the η - S_y plot, a central area shows runs with realistic distributions and sizes of continents. This area is partly overlapping with the η - S_y areas of piecewise plate-like movements of the lithosphere and of realistic values of the surface heat flow and Urey number.

Keywords: mantle convection, continental growth, chemical heterogeneity



(S) - IASPEI - *International Association of Seismology and Physics of the Earth's Interior*

JSS011

Oral Presentation

2094

Tomographic Imaging of the Kachchh seismic zone, western India : A mechanism for stress concentration in the lower crust

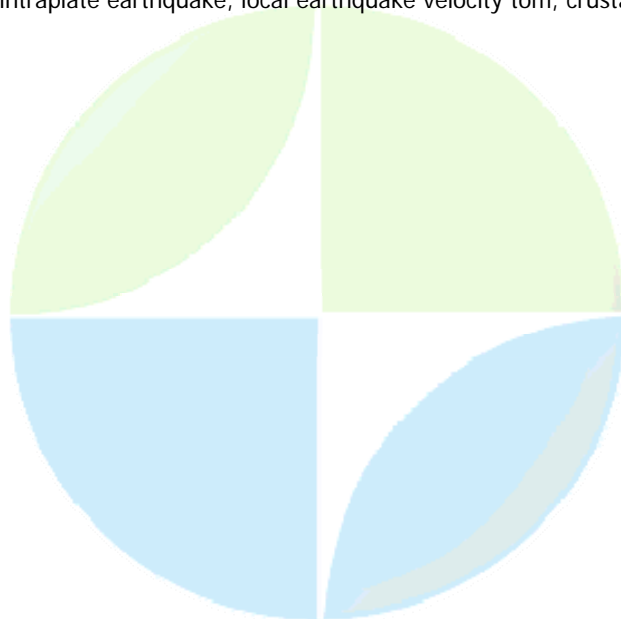
Dr. Prantik Mandal

Seismology NGRI, HYDERABAD, INDIA IASPEI

Dr. R.K. Chadha

Aiming at obtaining a model for the causative mechanism of the continued occurrence of earthquakes in Kachchh, Gujarat for about last six years, we estimated high-resolution three-dimensional V_p , V_s and V_p/V_s structures in the aftershock zones of the 2001 Mw7.7 Bhuj and 2006 Mw5.6 Gedi earthquakes. We used 13,862 P and 13,736 S wave high-quality arrival times from 2303 events recorded by the 5-18 three-component seismograph stations during 2001-06. Seismic images revealed a marked spatial variation in the velocities (up to 10% in V_p , up to 15% in V_s , and up to 4% increase in V_p/V_s) in the 10-42 km depth range beneath the Bhuj aftershock zone. Relatively more increase in V_p than V_s , and an increase in V_p/V_s in the crust beneath the seismically active causative fault (North Wagad Fault, NWF) zone in Kachchh, Gujarat suggests a rigid, mafic crust beneath the region. They also delineate an increase of 8% in V_p and 14% in V_s , and a decrease of 4% in V_p/V_s in the almost vertical rupture zone of the 2006 Gedi earthquake extending up to 12 km depth. This high velocity body associated with the Gedi mainshock is inferred to be a gabbroic intrusive. The Banni region and the Wagad uplift are found to be associated with high velocity intrusive bodies (inferred to be mafic) extending from 5 to 35 km depth, which might have intruded during the rifting in early Jurassic (~160 Ma). Aftershock activity mainly confines to the zones characterized by high V_p , high V_s and low V_p/V_s ratio, which might be representing the strong, competent and brittle parts of the fault zone / intrusive bodies that could accumulate large strain energy for generating aftershocks for more than five years. A few patches of slow (V_p and V_s) and high V_p/V_s between 10 to 30 km depth have also been detected on the causative 40° south dipping north Wagad fault (NWF) for the 2001 mainshock, which may be attributed to the fluid filled fractured rock matrix. Interestingly, the 2001 Bhuj mainshock hypocenter is found to be associated with such a low velocity patch.

Keywords: intraplate earthquake, local earthquake velocity tom, crustal mafic intrusive



(S) - IASPEI - *International Association of Seismology and Physics of the Earth's Interior*

JSS011

Oral Presentation

2095

Upper mantle seismic anisotropy structure beneath central and southwestern Japan subduction zone

Dr. Mohamed Salah

Tetsuzo Seno, Takashi Iidaka

In central and northeast Japan, the Pacific plate is subducting from the east beneath the Okhotsk plate along the Japan Trench in the WNW direction, while in southwest Japan, the Philippine Sea plate is subducting along the Nankai Trough and the Ryuku Trench in the NW direction. Analysis of seismic anisotropy in the crust and mantle wedge above subduction zones opens up a new source of information about rising magma in the region, the induced mantle flow and the stress state in the forearc and back-arc regions, because the physical property estimated from shear wave anisotropy is related to the dynamic processes inside the Earth. For this reason, we detect shear wave polarization anisotropy in the crust and upper mantle above the subducting Pacific plate from local shallow, intermediate, and deep earthquakes beneath central-southwestern Japan. We analyze local S phases from 198 earthquakes that occurred in the subducting Pacific plate and are recorded at 42 Japanese F-net broadband seismic stations. This data set yields a total of 980 splitting parameter pairs for the central-southwestern Japan subduction zone. The measured splitting pattern is generally complicated especially beneath Kanto-Tokai. Dominant fast polarization directions of shear waves obtained at most stations in the Kanto-Izu-Tokai area are oriented nearly WNW-ESE, which are sub-parallel to the Sagami Trough or parallel to the subduction direction of the Pacific plate. At some stations, however, fast polarization directions are also oriented in NE-SW directions especially in the north of Izu Peninsula and Tokai district. Fast directions obtained at stations located in Kii Peninsula are generally oriented ENE-WSW, almost perpendicular to the Pacific plate subduction, although some directions have NW-SE trends. Delay times vary considerably and range from 0.1 to 1.25 s. These lateral variations suggest that the nature of anisotropy is quite different between the regions beneath the studied areas. Beneath Kanto-Tokai, the slab morphology is relatively complicated as the Philippine Sea slab is overriding the Pacific slab. This is also a region where the Izu-Bonin forearc is subducting in the east and the collision of the Bonin ridge occurs in the west. This complex tectonic setting may induce lateral heterogeneity in the flow and stress state in the forearc mantle wedge, on very short length scales. Fast directions beneath Kii Peninsula and its eastern extension, on the other hand are trench-parallel, which is sometimes seen in the back-arc regions.

Keywords: shear wave splitting, central southwestern japan, subduction zone

(S) - IASPEI - *International Association of Seismology and Physics of the Earth's Interior*

JSS011

Oral Presentation

2096

An 1-2-1 Model for the Evolution of the Earth's Mantle Structure and Their Implications for Supercontinent Cycles and True Polar Wander.

Prof. Shijie Zhng

Department of Physics University of Colorado IASPEI

Nan Zhang, Zheng-Xiang Li, James H. Roberts

The present-day Earth's mantle is predominated by long-wavelength structures including circum-Pacific subducted slabs and Africa and Pacific super-plumes. These long-wavelength structures are largely controlled by the history of plate tectonic motion. Although it dictates the evolution of mantle structure, global plate tectonic history prior to 120 Ma is poorly constrained except for continental motions that can be reliably traced back to >1 Ga. An important observation of continental motions in the last 1 Ga is the two episodes of formation and breakup of super-continents Pangea and Rodinia. We formulated 3D global models of mantle convection with temperature- and depth-dependent viscosity to study the formation of mantle structure. We found that for the upper mantle with 30 times smaller viscosity than the lower mantle and moderately strong lithosphere, in the absence of continents, mantle convection is characterized by a hemispherically asymmetric structure in which one hemisphere is largely upwellings, while the other hemisphere contains downwellings (i.e., degree-1 convection). We also found that the lithosphere plays an essential role in producing degree-1 convection. This is the first study in which degree-1 mantle convection is observed in mobile-lid/plate-tectonic convection regime at high Rayleigh number. This result suggests that degree-1 convection may be a dynamically preferred state for the Earth's mantle. We suggest that the evolution of mantle structure is controlled by a cyclic process of formation and breakdown of degree-1 convection modulated strongly by continents. The formation and breakup of supercontinents are surface manifestation of this cyclic process. During the degree-1 convection state, the upwellings in one hemisphere push all continents into the other hemisphere with the downwellings to form a supercontinent. The non-subducting nature of continents dictates that subduction in the downwelling hemisphere occurs along the edge of the supercontinent upon its formation. The insulating effect of a supercontinent and return flow from the circum-supercontinent subduction should heat up sub-continental mantle and lead to formation of another upwelling system below the supercontinent (i.e., largely degree-2 platform) and eventually to breakup of the supercontinent. After the breakup of a supercontinent, the mantle with two large upwellings, similar to that for the present-day Earth, is then evolved back to degree-1 convection state. This cyclic process also has implications for the Earth's true polar wander. We found that after the sub-continental upwelling is formed, the two upwellings should be centered at the equator due to their positive geoid and true polar wander effects. This may explain the equatorial locations of the supercontinent Pangea and Rodinia before their breakup.

Keywords: supercontinents, convection, true polar wander

(S) - IASPEI - *International Association of Seismology and Physics of the Earth's Interior*

JSS011

Oral Presentation

2097

Crust and mantle structure from the Northern Indian Shield to Western Himalaya and Ladakh using receiver functions

Dr. Shyam Rai

Seismic Tomography National Geophysical Research Institute IASPEI

K. Suryaprakasam, Keith Priestley, Vinod Gaur

We analysed over 2000 P-S converted receiver functions from 24 broadband seismograph locations from the northern edge of the Indian shield to the western Himalaya and Ladakh- Karakoram to model the structure of the crust and the underlying mantle transition zone. Crustal structure is imaged through joint inversion of the receiver functions with the surface wave group velocity measurements while the mantle transition zone discontinuities are mapped through the common depth point stacking of the mantle converted receiver functions. The Moho depth beneath northern India is ~38 km that progressively deepens to ~55 km beneath Higher Himalaya and ~75 km beneath the Ladakh and Karakoram. Upper crust beneath northern India is more felsic ($V_s < 3.4$ km/s) compared to the crust in southern part like Dharwar craton where the shear velocity is > 3.6 km/s. Unlike the central Tibet and Nepal, the crust beneath western Himalaya, Indus suture and Ladakh does not contain signature of low velocity. In the mantle transition zone (MTZ), beneath the Gangetic plain we mapped the 410 km discontinuity at ~392 km depth while the discontinuity at the base of the transition zone splits into 660 and 715 km with the MTZ thickness ~ 260 km. These observations support the presence of high velocity slab beneath the Gangetic plain and Himalaya whose interaction with the upper mantle was responsible for the observed complexity of 660 km discontinuity possibly due to phase transformation from garnet to perovskite. We interpret this as the signature of fossil slab broken off the subducting Indian margin or the Tethys. In contrast, beneath Ladakh 410 is at its normal depth and the average MTZ thickness is 242 km suggesting distinct thermal state of mantle between Himalaya and Ladakh.

Keywords: western himalaya, receiver function, crust mantle



(S) - IASPEI - *International Association of Seismology and Physics of the Earth's Interior*

JSS011

Oral Presentation

2098

Mantle convection beneath Mongolian-Baikal Rift zone and its geodynamic implications

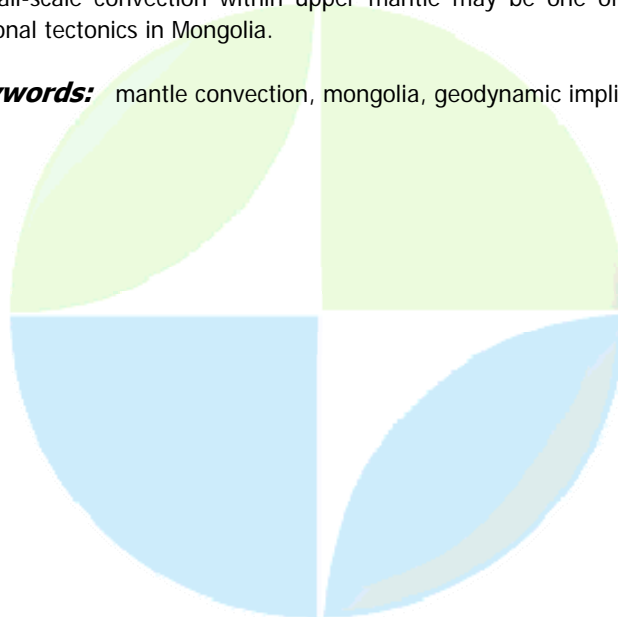
Dr. Xiong Xiong

Key Laboratory of Dynamic Geodesy Institute of Geodesy and Geophysics, CAS IASPEI

Jiye Wang, Rongshan Fu

Mongolia occupies a peculiar place in Asia, which is characterized by very complicated tectonics under the impact of the India-Asia collision to the south and the subduction of Pacific Plate to the east. It recently became clear that Mongolia, which is one of the least studied and poorly understood of the tectonically active regions of the world, plays a key role in deciphering the intracontinental deformation processes. Although it is generally agreed upon that Mongolia is a direct consequence of the India-Asia collision and the subsequent compression between Asia and the northward advancing Indian continent, the collision and compression model alone cannot account for all regional tectonic features of Mongolia. Therefore, other mechanisms may superimpose upon the India-Asia collision and compression, and the small-scale convection within upper mantle is believed to be one of the candidates, which is responsible for intraplate and regional tectonic processes. Relating regional gravity anomalies and mantle convection, we calculated the small-scale mantle convection pattern and resulted stress at the lithospheric base beneath Mongolia by using isostatic gravity anomalies. The numerical results indicate that the Mongolia and its adjacent areas are characterized by a very complicated pattern of mantle flow and convection-generated stress field in deep. The low activity of the mantle flow and small magnitude of the convection-generated stress suggest that the Siberia Platform is a stable tectonic unit, which is short of active dynamic process in deep. The eastern Mongolia is another area where mantle convection and its impact are weak. This is consistent with the present-day low tectonic activity in these areas. Beneath the Baikal Rift Zone exists an upwelling mantle plume, which is identical to the low-velocity anomalies originated from the 670km discontinuity imaged by seismic tomography. The Hangay-Hóvsgól Plateau is underlain by mantle upwellings, resulting in extension stress regime. A complicated pattern of mantle flow and convection-generated stress is exhibited in the western Mongolia. The consistency between the surface tectonic features and the mantle flow pattern, as well as the resulted stress field, suggests that the small-scale convection within upper mantle may be one of the main mechanisms which control the regional tectonics in Mongolia.

Keywords: mantle convection, mongolia, geodynamic implication



(S) - IASPEI - *International Association of Seismology and Physics of the Earth's Interior*

JSS011

Oral Presentation

2099

Upper mantle anisotropy beneath the Ltzow-Holm Bay Region, East Antarctica in relation to past tectonic events

Dr. Yusuke Usui

Transdisciplinary Research Integration Center Research Organization of Information and Systems IASPEI

Masaki Kanao, Atsuki Kubo, Yoshihiro Hiramatsu, Hiroaki Negishi

The analysis of seismic anisotropy has developed into a powerful tool to know deformations in the Earth's interior. Upper mantle anisotropy is mainly produced by lattice preferred orientation of highly anisotropic mantle peridotites in the lithosphere and/or asthenosphere. The origin of such anisotropy is generally attributed to the deformations of present plate motion reflected the mantle flow and paleo tectonic events of collision and/or break-up of craton. We investigate the upper mantle anisotropy using broad-band seismic data recorded at a few seismic stations in Ltzow-Holm Bay (LHB), East Antarctica, and discuss the origin of the anisotropy, the history of the Antarctic plate motion and the effects of continental collision and/or break-up. We calculate the splitting parameter (f , dt) for teleseismic SKS waves using Silver and Chan [1991]. f is fast direction of split shear wave and dt is the delay time of two split waves. The splitting parameters are determined by minimizing the energy of the transverse component by net grid search technique with intervals of 1(deg.) and 0.1s, respectively. The error estimate of each combination of splitting parameters can be given by 95% confidence level of F test. The delay times at all stations are the same degree in comparison to the average value (1.2s) of the results in global continental studies, and the fast polarization directions are systematically parallel to near coast line in the LHB. For most of all stations we used, azimuthal variations of the splitting parameters do exist. In this case, we modeled two-layer model of azimuthal anisotropy. From a geodynamic point of view, since two layers may correspond to anisotropy in the lithosphere and asthenosphere, such a model is reasonable. Investigations of seismic anisotropy may contribute to ideas about influence of recent or fossil mantle flows and/or the tectonic evolution of the study regions. Fast polarizations directions of the lower layer are generally parallel to the directions of Absolute Plate Motion (APM). The directions are about N120E and the velocity is about 1cm/yr in this study region. The APM velocities are slow for East Antarctica and the delay time is small relative to upper layer. We consider that it is reasonable that the structures of lower layers anisotropy might have been produced asthenospheric mantle flow. The upper layers don't coincide with the APM direction. We should consider the anisotropic structure which is past tectonic events of East Antarctica. The direction of Gondwana continent break up was NW-SE. This is perpendicular to the observed direction. In general, the fast polarization directions are consistent with NE-SW paleo-compressional stress. We consider that the anisotropy of upper layers is caused by lithospheric deformation during Pan-African orogen event (~500Ma).

Keywords: seismic anisotropy, upper mantle, antarctica

(S) - IASPEI - *International Association of Seismology and Physics of the Earth's Interior*

JSS011

Oral Presentation

2100

P-wave velocity structure of the mantle beneath the South Pacific superswell revealed by joint ocean floor and islands broadband seismic experiments

Dr. Satoru Tanaka
IFREE JAMSTEC IASPEI

**Masayuki Obayashi, Daisuke Suetsugu, Hajime Shiobara, Hiroko Sugioka,
Toshihiko Kanazawa, Yoshio Fukao, Guilhem Barruol**

Three-dimensional P-wave velocity structure of the mantle beneath the South Pacific superswell is determined to depths of 1600 km through passive broadband seismic experiments at the ocean floor and islands in the period 2003 to 2005. We collected approximately 1500 relative times of long-period P-waves by using a waveform cross-correlation and PREM as initial reference model. Then, ellipticity corrections are applied and a linear trend as a function of an epicentral distance is removed from the relative times to obtain travel time residuals for each event. The residuals are used for delay time tomography. The resultant structure shows lateral heterogeneities of magnitudes of approximately 1%. A low velocity region is found beneath the north of the Society hotspot and the center of the superswell at a depth of 1600 km. At 1200 km depth, we observe a change in the pattern, which linearly occurs beneath the Society to Pitcairn hotspots. Another low velocity region is obliquely elongated from 800 km to 400 km depth toward the Marquesas hotspot. An isolated low velocity region is identified beneath the Society hotspot at 400 km depth. These features are generally consistent with those obtained by global tomography that contains the P-wave travel times newly observed here, which is particularly discussed in another paper by Obayashi et al. in this session.

Keywords: south pacific superswell, tomography



(S) - IASPEI - *International Association of Seismology and Physics of the Earth's Interior*

JSS011

Oral Presentation

2101

Frequency distribution of seismic wavespeed as evidence for bodies of distinct material in the lowermost mantle, and analogies with the lithosphere.

Dr. Bernhard Steinberger

Center for Geodynamics Geological Survey of Norway IASPEI

Kevin Burke, Trond H. Torsvik, Mark A. Smethurst

Frequency or occurrence of shear-wave tomography models close to the CMB shows a distinct bimodal distribution, with a larger peak at higher velocities and a smaller peak at lower velocities. The relative size of the peak at higher velocities gets larger higher up in the mantle. Correspondingly, regions of strong lateral gradient in shear wave speed frequently occur along approximately at the - 1 % shear wave anomaly contour surrounding the Large Low Shear Velocity Provinces (LLSVs) above the CMB. This provides further evidence for bodies of distinct material in the lowermost mantle. They occupy a surface area of ~ 20 % close to the CMB, which reduces to ~ 10 % 300 km above the CMB, and thus contain about 2 % of mantle material. Large Igneous Provinces (LIPs), when reconstructed to their eruption sites, cluster above the margins of these bodies at their base, which we term Plume Generation Zones [PGZ]. Thus we find a correspondence between processes at the base of the mantle and its top: While subduction frequently occurs at the edges of continents, which are chemically distinct and positively buoyant, the return of material from the "slab graveyards" in the form of mantle plumes occurs at the edges of LLSVs, which appear to be also chemically distinct and negatively buoyant. Different from continents, though, LLSVs appear not to have substantially moved or deformed -- possibly because their upper parts are at a depth with rather high viscosities of about 10^{23} Pas. The scenario proposed here has implications, which can be tested through seismic and geochemical observations and geodynamic modelling.

Keywords: cmb, plumes, llsvs



(S) - IASPEI - *International Association of Seismology and Physics of the Earth's Interior*

JSS011

Oral Presentation

2102

Three-dimensional shear wave speed structure beneath the South Pacific superswell

Dr. Takehi Isse
JAMSTEC IFREE IASPEI

***Daisuke Suetsugu, Hajime Shiobara, Hiroko Sugioka, Kazunori Yoshizawa,
Toshihiko Kanazawa, Yoshio Fukao, Guilhem Barruol***

We determined three-dimensional shear wave speed model beneath the South Pacific superswell down to a depth of 200 km by analyzing broadband data from ocean bottom seismograph and island stations temporary deployed in the French Polynesia region. The temporal data covers period from 2003 to 2005 for the BBOBS stations deployed on the seafloor and from 2001 to 2005 for the island stations deployed during the PLUME project. This enables us to study the upper mantle structure beneath the Superswell with an unprecedented high resolution. We measured the dispersions of fundamental mode of Rayleigh waves at periods between 40 and 140 seconds by using a two-station method. Resolution analyses indicate that these temporary stations may locally improve the lateral resolution to about 400 km. We observe superficial slow anomalies associated to the spreading ridges such as the Lau Basin and two kinds of hotspot signatures: We found pronounced and continuous slow anomalies down to at least 200 km depth near the Society, McDonald, Marquesas, and Pitcairn hotspots whereas the slow anomalies beneath the Samoa, Rarotonga and Arago hotspots are only present at depths shallower than 80 km.

Keywords: surface wave tomography, bbobs, superswell

PERUGIA
ITALY



(S) - IASPEI - *International Association of Seismology and Physics of the Earth's Interior*

JSS011

Oral Presentation

2103

Subduction roll-back, slab break-off and induced strain in the uppermost mantle beneath Italy

Dr. Lucia Margheriti
CNT INGV IASPEI

Francesco Pio Lucente

Differences in the splitting amount of SKS waves that traverse the upper mantle beneath the Italian region identify four areas of internally coherent delay times, providing evidences for mantle strain partitioning. If compared with the uppermost mantle structure of subduction imaged by tomography, the sequence of these areas displays a straightforward parallelism. Under certain assumptions, the highlighted correspondence between areas of coherent splitting amount and areas of coherent velocity perturbations offers new insights on the last evolution phases of subduction in Italy and on the way they affect the mantle strain.

Keywords: anisotropy, mantle strain



(S) - IASPEI - *International Association of Seismology and Physics of the Earth's Interior*

JSS011

Oral Presentation

2104

Lowermost mantle structure of the western part of the Pacific low velocity province constrained by the Vietnamese broadband seismograph array

Dr. Nozomu Takeuchi

Earthquake Research Institute Univ of Tokyo IASPEI

Takeuchi (2007, GJI) recently conducted broadband waveform inversion for the whole mantle SH velocity structure. The inversion fully utilize later phase date (including major and multi-orbit body waveforms) to improve the resolution. The resultant model reveals the different natures of the two major upwelling systems: the strong low velocity anomalies beneath Africa extend for more than 1000 km from the core-mantle boundary (CMB), whereas those beneath the Pacific are restricted to 300-400 km from the CMB. The final goal of this study is to obtain independent evidence for the different natures of the upwelling regions through analyses of seismograph array data. The western part of the Pacific low velocity province is focused on in this study, because the array data which well resolve the velocity profiles of this region were not previously available. The Vietnamese broadband seismograph array, which was deployed by the Ocean Hemisphere Project, has ideal geometry for this purpose: the array and epicenters of Fiji-Tonga and Vanuatu events are nearly on the same great circle, which provides S and sS data with wide variety of bottoming depths (distributing between about 150-1300 km from the CMB). The analysis of S and sS apparent velocity data indicates the existence of the low velocity zone at the lowermost mantle. Its thickness is smaller than 400 km, and it seems to be smaller than 150 km in some region. The horizontal scale length of thickness variations is small (about 500 km). The analysis of ScS-S and sScS-sS travel times indicates the existence of sharp side boundary of the Pacific low velocity province. The location of the boundary is precisely consistent to that indicated by Sdif travel time analysis (Toh, Romanowicz & Capdeville 2003, PPV workshop). These results suggest the existence of chemical heterogeneities which are confined in 400 km from the CMB.

Keywords: cmb, seismology



(S) - IASPEI - *International Association of Seismology and Physics of the Earth's Interior*

JSS011

Oral Presentation

2105

Cratonic keels and a two-layer mantle tested: mantle expulsion during Arabia-Russia closure linked to westward enlargement of the Black Sea, formation of the Western Alps and subduction of the Tyrrhenian (not the Ionian) Sea.

Mr. Miles Osmaston
IASPEI

Two of the most controversial questions concerning mantle behaviour are the great depth of cratonic tectospheric keels (e.g. [1, 2]) and whether the base of the upper mantle is a substantial barrier to flow [3]. Individually the arguments for each are indecisive but if both are true there should be major dynamical consequences for plate motions, susceptible to direct observation [4]. If keels extend nearly to 660km the principal considerations are: Where does the mantle come from to put beneath a widening ocean? and Where does it go when two cratons approach one another? The former, in an Atlantic-Arctic context, was explored in [4]; here we explore the latter in an Alpine belt setting. My recent studies show that the Western Alps were primarily the result of ~250km westward motion of northern Adria/Italy in the early Oligocene, using a formerly-straight Insubric-Pusteria-Gailltal fault-Line, before the Giudicaria NE-ward offset differentially compressed the Eastern Alps. This dextral motion is recorded in a shear zone extending all the way to the Black Sea coast in the Dobruja area, north of the probably Neo-Archaean Moesian block, well known for its (W-ward) 'indenter' behaviour, and it may explain the present deep seismicity below the SE Carpathians. Westward flow of mantle from between the converging Arabian and Russian tectospheres has evidently driven this motion by impinging upon the cratonic keel of Moesia, opening the western Black Sea. This westward motion of the entire Balkan Peninsula appears to have built the Apennines. Their previous history is probably this. The crust of the former westward-extending 'Greater Italy' was extensively undercut by basal subduction tectonic erosion in the early-mid Cretaceous, creating a flat-slab interface with its downbend near the present coastline. Subduction then ceased and the undercut region subsided (recorded in Apennine stratigraphy) as the underlying ocean floor cooled until Oligocene. Initial closure of the proto-Tyrrhenian Sea by Corsica-Sardinia established a west-dipping vergence which was imposed upon the undercut 'Italian' margin as closure continued. This pushed the now-cool underlying oceanic plate past the former downbend, establishing slab pull which has pulled open parts of the Tyrrhenian floor. Thus the easterly vergence of the Apennine front is not due to subduction of Apulia-Ionian Sea. Rather, the Tyrrhenian floor plate must downbend sharply beneath the narrow fault-bounded Gioia (marginal) Basin, doubling back westward beneath itself to bring the subducted crust into suitable position for sourcing the Aeolian arc. This doubling-back is attributable to the westward mantle flow developed further East. [1] Gu, Dziewonski & Agee (1998) EPSL 157 ; [2] Agee (1998) Rev. Mineral. 37 ; [3] Osmaston, IUGG2003; [4] Osmaston (2006) in ICAM IV, OCS Study MMS 2006-003 Also:- <http://www.mms.gov/alaska/icam>

Keywords: tectospheresandmantleflows, blackseaopening, tyrrheniansubduction

(S) - IASPEI - *International Association of Seismology and Physics of the Earth's Interior*

JSS011

Oral Presentation

2106

Density, shear and compressional velocity models of the Vrancea seismogenic zone

Dr. Rosaria Tondi

Seismology INGV Bologna IASPEI

Ulrich Achauer, Lucian Besutiu

Keywords: tomography, gravity, subduction

IUGG

XXIV2007

PERUGIA

I T A L Y



(S) - IASPEI - *International Association of Seismology and Physics of the Earth's Interior*

JSS011

Oral Presentation

2107

Thermal evolution and geometry of the descending lithosphere beneath the SE-Carpathians

Dr. Alik Ismail-Zadeh

Geophysical Institute Karlsruhe University IASPEI

Gerald Schubert, Igor Tsepelev

We develop a thermal model of the crust and mantle beneath the SE-Carpathians based on the inversion of P-wave velocity anomalies of recent seismic tomography images into temperature and on heat flow measurements. The model of the present crustal and mantle temperature is assimilated into the geological past, and the prominent Miocene thermal state of the lithospheric slab, descending in the region, is restored quantitatively from its diffuse present state. In Miocene time the slab geometry clearly shows two portions of the sinking body: one of them has NW-SE orientation and can be associated with the interface between the East European and Scythian platforms, and another portion has a NE-SW orientation and is related to the present descending slab. Above a depth of 60 km the slab had a concave thermal shape, confirming the curvature of the Carpathian arc, and a convex surface below that depth. The slab maintained its convex shape until it split into two parts at a depth of about 220 km. We suppose that this change in the slab geometry, which is likely to be preserved until the present, can cause stress localization due to the slab bending and subsequent stress release resulting in large mantle earthquakes in Vrancea. Our results also support the hypothesis of dehydration and partial melting of the descending lithosphere as the cause of the reduction in seismic velocities beneath the Transylvanian Basin.

Keywords: vrancea earthquakes, slab dynamics, data assimilation



(S) - IASPEI - *International Association of Seismology and Physics of the Earth's Interior*

JSS011

Oral Presentation

2108

Crustal and sub crustal structure of the Italian peninsula as inferred from local seismic tomography

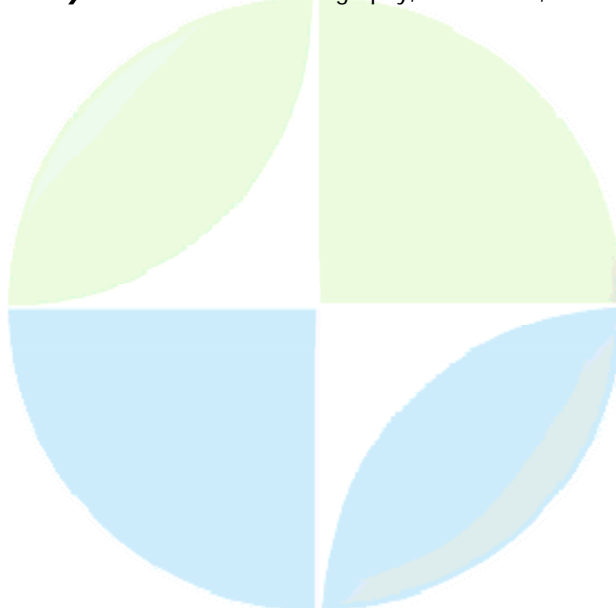
Dr. Davide Scafidi

Dip. Te. Ris. Universit degli Studi di Genova IASPEI

Stefano Solarino, Claudio Eva

We investigate the P wave velocity structure and the V_p/V_s ratio beneath the Italian peninsula down to 100 km depth by seismic local earthquake travel time tomography. Our aim is not only to define and confirm the gross structural frameworks of the crust and of the upper mantle, which are somewhat already known, but, in particular, to provide more details either on the shape of the complex subduction that acts on the peninsula either on the transition zones between continental and oceanic crusts. Since both goals require an appropriate rather than a standard approach, many actions have been taken to achieve the result. The experiment is based on data published by the International Seismological Centre (ISC). More than 60.000 P phase readings and about 25.000 S phase readings for the period 1997-2005, as recorded by various seismic networks around the Italian peninsula, have been inverted employing SIMULPS, the well constrained and worldwide adopted tomographic code. The joining of an adequate dataset and the introduction of some alternative strategies in the travel time tomographic routine (grid designing, ray tracing of the forward problem, appropriate data selection) results in a fair cross-firing all over the large inverting area and partly ensures ray sampling also for deeper layers. Although results are partly biased by the uneven resolution of the tomographic images and by the variable maximum resolved depth, we discuss the structural framework of the most debated areas of the peninsula as they appear from our V_p and V_p/V_s 3-D inversion. In particular, a very shallow Moho is evident in the Ligurian Sea with anomalously low V_p/V_s values; a gentle subduction is visible under the western Alps; a change in the vergence of the subduction is seen in the eastern part of the Alpine chain, where the Adriatic Moho seems to subduct under the European one. Finally, the slab of the Calabrian arc is confirmed as very steep in the Tyrrhenian Sea, while in the Apenninic area an overlap of different types of crust (oceanic-transitional over continental) is shown, without a clear slab geometry.

Keywords: seismic tomography, subduction, slab



(S) - IASPEI - *International Association of Seismology and Physics of the Earth's Interior*

JSS011

Oral Presentation

2109

Preliminary Body-wave Tomography of the Cameroon Volcanic Line: Linear Anomaly in a Convecting Mantle

Prof. Angela Marie Larson

Department of Geosciences The Pennsylvania State University IASPEI

Andy Nyblade, Doug Wiens, Rigobert Tibi, Patrick Shore, Garrett Euler, Bekoa Ateba, Joseph Nnange, Charles Tabod, Yongcheol Park

The Cameroon Volcanic Line (CVL) is a 1600km feature traversing both continental Cameroon in west Africa and the offshore islands of Bioko (part of Equatorial Guinea), Sao Tome and Principe, and Annobon (also part of Equatorial Guinea). The CVL is a fairly linear feature, suggestive of the movement of the African plate over a stationary hotspot, but the volcanic rock ages of the CVL range from 42Ma to the present (with present volcanism occurring in the center of the line at Mt. Cameroon), contrary to what would be expected from a stationary hot spot. Several hypotheses have been proposed for the formation of the CVL. One possible explanation has been that there may be a plume rising to the surface along of previously weakened linear zone. In this scenario, the magma may rise sporadically to the surface at different points along the line thereby explaining the apparent lack of age progression. The Cameroon Seismic Experiment was deployed in Cameroon from January 2005 to January 2007, with 8 stations active the first year and an additional 24 stations installed in January 2006. The data from the 32 broadband seismometers is currently being used for a body-wave tomography study to study the upper mantle structure beneath Cameroon. Preliminary results from a P wave travel time tomography suggest a linear negative velocity anomaly paralleling the CVL. This linear feature may be the result of a localized mantle convection cell resulting from edge flow from the nearby Congo Craton to the southeast instead of a plume rising from the lower-to-mid mantle. These tentative results will be presented and used to evaluate all possible models for the origin of the Cameroon Volcanic Line.

Keywords: body waves, tomography, africa



(S) - IASPEI - *International Association of Seismology and Physics of the Earth's Interior*

JSS011

Oral Presentation

2110

Short wavelength topography on the inner core boundary

Prof. Barbara Romanowicz

Berkeley Seismological Laboratory University of California at Berkeley IASPEI

Aimin Cao, Yder Masson

Constraining the topography of the ICB is important for studies of core-mantle coupling and the generation of the geodynamo. We present evidence for significant temporal variability in the amplitude of the inner core reflected phase PKiKP for an exceptionally high quality earthquake doublet, which occurred in the South Sandwich Islands within a ten year interval (1993/2003) and was observed at the short period Yellowknife seismic array (YK). While individual waveforms of the PP phase and its coda are highly similar for the doublet in a relatively wide frequency range of 0.5 to 2 Hz, the PKiKP amplitude for the 2003 event is 7.2 times larger than that for the 1993 event, and the corresponding amplitude ratio of PKiKP/PKiKP for the 2003 event is 3.1 times larger than that for the 1993 event in the frequency range of 1 to 2 Hz. We show that the PKiKP for the 2003 event is normal and the PKiKP for the 1993 is anomalous, most likely due to defocusing at the ICB. From the size of the amplitude anomaly, which is not accompanied by a significant travel time anomaly, we infer that this observation, complemented by data from several other doublets, indicates the presence of topography at the inner-core boundary, with a horizontal wavelength on the order of 10 km. Such topography could be sustained by small scale convection at the top of the inner core, and is compatible with a rate of super-rotation of the inner core of $\sim 0.1\text{-}0.15$ deg/year. Alternatively, if the inner core is not rotating, decadal scale temporal changes in the ICB topography would provide an upper bound on the viscosity at the top of the inner core of about 10^{16} Pas.

Keywords: inner core, topography, structure



(S) - IASPEI - *International Association of Seismology and Physics of the Earth's Interior*

JSS011

Oral Presentation

2111

Locating scatterers in the mantle using array analysis of PKP precursors from an earthquake doublet

Prof. Barbara Romanowicz

Berkeley Seismological Laboratory University of California at Berkeley IASPEI

Aimin Cao

Well separated individual PKP precursors observed at the Yellowknife seismic array (YK) for a high quality doublet of earthquakes provide a good opportunity to study the corresponding scatterer locations and examine the stability of our adopted method of array analysis. Based on the comparison of the waveforms of non-linearly stacked individual precursors and those of PKIKP phases, for the first time, we are able to determine that most of these precursors originate from scattering of the PKPbc (rather than the PKPab) branch above the B caustic on the receiver side. This allows a reliable location of the scatterers in the lower mantle. The depths of the scatterers range from 2890km (the CMB) to 2270km, and their surface projections range from southern Ontario to northern Saskatchewan in . These locations are associated with transitions from slow to fast velocities in mantle tomographic models and follow the expected general dip direction of fossil slabs under north America. This suggests that the subducted slab remnants under north America have retained their compositional signature. Average uncertainties in precursor slowness and back-azimuth are as small as 0.08s/deg and 1.4deg, respectively, indicating that it may be possible to locate such scatterers in the future using single earthquakes.

Keywords: scatterers, lower mantle, structure



(S) - IASPEI - International Association of Seismology and Physics of the Earth's Interior

JSS011

Oral Presentation

2112

Deep earthquakes and orogenic processes: toward a new interpretation

Dr. Giancarlo Scalera

Geodynamics Istituto Nazionale di Geofisica e Vulcanologia IASPEI

Earthquakes are not uniformly distributed either along mountain belts and arcs or in depth. An especially uneven distribution is present all along the Mediterranean margin between Africa and Eurasia. The zones in which the deeper earthquakes originate are shown, and their regional and global context is examined. Abandoning the traditional 2-D sections perpendicular to the trench-arc-backarc zones, with the help of 3-D plotting on larger scale, which can visualize the entire extent of a Wadati-Benioff zone, a characteristic inhomogeneous pattern of hypocentres along the alleged subduction zones is revealed in the Italian region as well under Mediterranean and circum-Pacific active margins. Using the recent global catalogues of relocated earthquakes, filaments of hypocenters are recognizable instead of planar or spoon-like patterns. These filaments taper downwards, resembling the shapes of trees, columns, smoke from chimneys, and leading to the idea of an origin in a narrow region of disturbance. Because very hardly a subductive process can produce similar deep hypocentral distributions, a new interpretation of the Wadati-Benioff zones and of their overimposed orogenic zones is proposed. The resulting global tectonics framework involves non-collisional orogenic processes deriving from global expansion, rifting, isostasy, surfaceward flow of deep material, gravitational spreading, and mantle phase changes. The associated model of evolution of an orogen can be linked to the volume increase of an isostatically uprising mantle column which segments slowly overcome a solidus-solidus limit of the temperature-pressure phase diagram. The outpouring of the exceeding material drives the gravitational nappes to overthrust the sediments of the pre-existing trough, forcing them on a burial path which emulate the subduction process, but without reaching depths greater than 50-70 km. At the boundary between uplifting material and down-pushed crust and lithosphere, phenomenon like metamorphism, mixing, migmatization, upward transport of fragments of the buried lithosphere etc. are possible. The mere existence of the earthquakes in the brittle portion of the lithosphere (first few tens of kilometres of depth) is at odd with the existence of the two ways subduction channel a low viscosity channel. Earthquakes are the more important circumstantial evidence of local storing and releasing of deviatoric stress, which can be cause of local overpressure. Then the possibility that lenses-like HP-UHP exhumed fragment could be mechanical product of great earthquakes occurrence at depth not exceeding few tens of kilometres should be considered. This model of evolution of a fold belt is in agreement with the tomographically revealed P-wave and S-wave high-velocity anomalies underlying with different slopes most orogens and arcs, and the obtainable topographic heights are consistent with the values of volume increase that are associated to the main mineralogical phase transitions. In this view, a discontinuous upward movement of mantle materials can be linked to the observed discontinuous evolution of the orogens and to the widespread observation of uplifted coastal terraces. Finally, the rate of rifting between two lithospheric fragments is a decisive factor in causing the evolution of the orogen toward a true fold belt (low rifting rate) or in a continuously enlarging depression (high rifting rate), leading to a true marine and oceanic sea-floor generation. Indeed, some zones like Tonga-Kermadec-New Zealand-Macquarie seems to suggest all these aligned different zones trench and expanding ridge, mature fold belt, oceanic ridge respectively as different moments of a unique orogenic process.

Keywords: deep earthquakes, geodynamics, mountain building

(S) - IASPEI - *International Association of Seismology and Physics of the Earth's Interior*

JSS011

Oral Presentation

2113

Temperature and composition of the upper mantle as inferred from long period seismic waveforms

Dr. Fabio Cammarano

Earth and Planetary Science UC Berkeley IASPEI

Using long period seismic waveforms and a novel inversion approach which includes constraints from mineral physics, we find that lateral variations of temperature can explain a large part of the data in the upper mantle. The additional compositional signature of cratons emerges in the global model as well. Above 300 km, we obtain seismic geotherms that span the range of expected temperatures in various tectonic regions. Below 300 km, average velocities and gradients with depth are well constrained by the long period data used, except near the mantle discontinuities. We find that seismic data globally require a slower transition zone and an overall faster shallow upper mantle than reference pyrolitic models. Despite the large uncertainties in mineral physics data, the observations are not compatible with a thermal interpretation assuming dry pyrolite. A gradual enrichment in a garnet-rich component throughout the upper mantle may help reconcile the observed discrepancies. A hydrated transition would help to lower the transition zone shear velocities, as required, but the high velocities and gradients we found above the wadsleyite stability field are not consistent with this hypothesis. Exploiting the different ways in which thermal and compositional variations affect the phase and amplitude of seismic waveforms, we are now proceeding to include in our inversion the amplitude effects and invert simultaneously for temperature and composition.

Keywords: mantle, seismology, mineral physics



(S) - IASPEI - *International Association of Seismology and Physics of the Earth's Interior*

JSS011

Oral Presentation

2114

Hydrogen enhanced melting beneath the East Pacific Rise near 9 degrees 30 N

Dr. Kerry Key

Scripps Institution of Oceanography University of California, San Diego IAGA

Steven Constable

A 200 km wide electrical conductivity profile obtained across the fast spreading East Pacific Rise at 9 degrees 30 N using 38 broadband seafloor magnetotelluric sites reveals a broad, deep, and asymmetric mantle conductor. High conductivity below 60 km depth requires hydrogen (water) enhanced partial melting beginning at 200 km depth and reaching a maximum at 80 km with 1-5% melt fraction estimated. Hydrogen enhanced conductivity may also contribute to the deep conductor, but this requires a mechanism to increase hydrogen concentration as mantle rises beneath the ridge in order to match the observed conductivity increase. The mantle is devoid of melt above 30 km as well as to 60 km depth west of the ridge, but a highly conductive region 30 km east of the axis and 40 km deep suggests melt ponding beneath a freezing horizon and episodic migration to the crust, supporting earlier evidence of off-axis melt supply and eruptions.

Keywords: mid ocean ridge, mantle melting, conductivity

PERUGIA
ITALY



(S) - IASPEI - *International Association of Seismology and Physics of the Earth's Interior*

JSS011

Oral Presentation

2115

Ridge jumps associated with plume-ridge interaction: Weakening of the lithosphere by upwelling asthenosphere

Mr. Eric Mittelstaedt

Geology and Geophysics University of Hawaii, Manoa IASPEI

Garrett Ito

Interaction of mantle plumes and young lithosphere near mid-ocean ridges can lead to changes in spreading geometry by shifts of the ridge-axis toward the plume such as seen at Iceland and the Galapagos. Previous work has shown that, with a sufficient magma flux, magmatism alone may weaken the plate sufficiently to initiate a ridge jump, but the contribution of upwelling asthenosphere to plate weakening and ridge-jumps is poorly understood. Using the FLAC (Fast Lagrangian Analysis of Continua) algorithm, we solve the equations of continuity, momentum and energy to examine deformation in near-ridge lithosphere associated with relatively hot upwelling asthenosphere and seafloor spreading. The cold portion of the lithosphere is treated as an elastic-plastic material and experiences brittle failure while the lower lithosphere and asthenosphere obey a non-Newtonian viscous rheology. Combined with a freely deformable surface this allows for simulation of gravitational effects on topography and dynamic faulting. Using a new 2-D dual-grid method, we achieve better than 0.5 km resolution within the lithosphere over a domain 100 km wide and 50 km deep and 5 km resolution in the mantle over a domain 1200 km wide and 400 km deep. The upper region of the box is initially set to a square-root of age thermal profile while a hot patch is placed at the bottom to initiate a single asthenospheric upwelling. The effect of upwelling asthenosphere on ridge jumps is evaluated by varying three parameters; the plume excess temperature, the spreading rate and the lateral location of the hot patch relative to the ridge axis. Preliminary results show plume related thinning (i.e. weakening) of the lithosphere over a wide area (100s of kms) with the rate of thinning dependent upon the thermal excess temperature of the plume. Initially thinning occurs as the plume approaches the lithosphere and asthenospheric material is forced out of the way. As the plume material comes into contact with the lithosphere, thinning of the boundary layer occurs through thermal weakening and mechanical removal of material. Thinning of the lithosphere is one of two primary factors in achieving a ridge jump. The other is high stresses capable of initiating rifting at this weakened location. Model stresses induced by the buoyant asthenosphere are significant fractions of the lithospheric yield strength near the plume and reach a maximum at the center of plume upwelling. The stresses decrease with distance from the plume center and increase with increasing spreading rate. Ridge jumps induced by upwelling asthenosphere alone are not observed which suggests that additional effects, such as off-axis magmatism, are important to ridge jump formation.

Keywords: hotspot, rifting, plume ridge

(S) - IASPEI - International Association of Seismology and Physics of the Earth's Interior

JSS011

Oral Presentation

2116

Water flow into the mantle transition zone

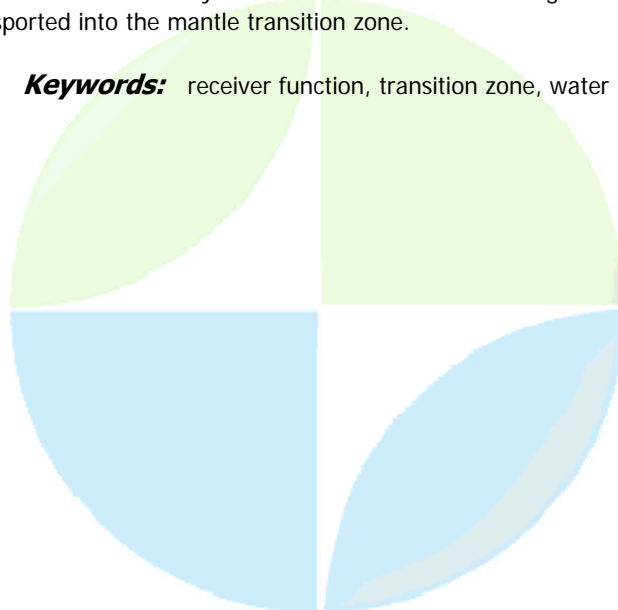
Dr. Takashi Tonegawa

Earthquake Research Institute University of Tokyo IASPEI

Kazuro Hirahara, Takuo Shibutani, Katsuhiko Shiomi, Hiroo Kanamori

It has recently been proposed that the mantle transition zone is a water reservoir in the Earth's interior. Transition zone minerals, such as wasleyite and ringwoodite, have unusual properties in comparison with the upper and lower mantle minerals. The solubility of water in the upper and lower mantle minerals is less than 0.2 wt%, whereas several experimental researches have shown that the wasleyite and ringwoodite can contain significant amounts (~several wt%) of water in the crystal structure, and some seismic researches have also estimated the amount of water in the transition zone. One of the problems for water in the transition zone is why water exists in the transition zone that is shut out by anhydrous minerals in the upper and lower mantle. We applied receiver function (RF) analysis with Hi-net tiltmeter recordings, provided by NIED, that are observed at 700 stations in Japan and contain relatively lower frequency component (~1000 sec). For deconvolution to calculate RF, since tiltmeter recordings have just horizontal component, we obtained source-time function by stacking all of vertical components observed at F-net broadband stations. We applied a bandpass filter of 0.02-0.16 Hz. Usually, radial receiver function is stacked to image seismic discontinuities, but in this study we used transverse receiver function that is usable to detect P-to-S phase converted at a dipping layer, such as subducting slab. In RF transects, the top surface of the Pacific slab descending underneath the Japanese Islands could be traced down to a depth of 400 km or greater. In addition, another seismic discontinuity just above the slab surface would be traced by positive RF amplitude, which is likely to be related to water transportation from the Earth's surface to the mantle transition zone. Although, in subducting process, most of hydrous minerals in the oceanic crust lose water by dehydration reaction at depths of 100 km, lawsonite can preserve it up to 9~10 GPa (~300 km) under low temperature condition. The water expelled from lawsonite would rise and react with the mantle wedge peridotite, and hence phase A will be formed in the mantle wedge (Komabayashi et al., 2005). The seismic discontinuity just above the Pacific slab detected in this study seems to correspond to the upper limitation of the existence of phase A in the mantle wedge. This discontinuity detected down to 410 km or greater implies that the water within phase A is transported into the mantle transition zone.

Keywords: receiver function, transition zone, water



(S) - IASPEI - *International Association of Seismology and Physics of the Earth's Interior*

JSS011

Oral Presentation

2117

Ab initio modeling of seismic velocity structure of deep mantle

Prof. Taku Tsuchiya

Geodynamics Research Center Ehime University

Jun Tsuchiya

We calculated the acoustic velocities of perovskite and postperovskite in MgSiO_3 , Fe_2+SiO_3 and Al_2O_3 compounds, using the density functional method for a pressure range of the Earth's lower mantle. Both Fe and Al have considerable effects to decrease shear moduli of Mg-phases at deep mantle pressures, though the effects on the bulk moduli are small. We have also found that both Fe and Al influence elasticity of ppv more than that of pv. Therefore velocity contrasts between pv and ppv are expected to decrease with increasing Fe and Al contents. Using these data, we have modelled velocity structures of the deep mantle region. Positive velocity variations are suggested to hardly be produced in pv with the MORB composition. Research supported by Ehime Univ Project Fund.

Keywords: postperovskite, elastic wave velocity, ab initio method



(S) - IASPEI - *International Association of Seismology and Physics of the Earth's Interior*

JSS011

Oral Presentation

2118

Iranian Model Determination for Crust and Upper Mantle using Pn and Sn Tomography

Dr. Shadi Tabatabai

Institute of Geophysics University of Tehran IASPEI

Eric Bergman, M.R. Gheitanchi

This paper has a primary motive to map Pn and Sn velocities beneath most part of Iranian Plate in order to test 3D mantle models and to develop and test a method to produce Pn and Sn travel time correction surfaces that are the 3D analogue of travel time curves for a 1D model. To the EHB data we apply the tomographic method of Barmin et al. (2001), augmented to include station and event corrections and an epicentral distance correction. The Pn and Sn maps are estimated on a $20^\circ \times 20^\circ$ grid throughout Iranian Plate. We define the phases Pn and Sn as arriving between epicentral distances of 30° and 150° . After selection, the resulting data set consists of about 42,000 Pn and 10,800 Sn travel times distributed inhomogeneously across Iranian Plate. The Pn and Sn maps compare favorably with recent 3D models of P and S in the uppermost mantle. The rms misfit to the entire Iranian data set from the Pn and Sn model increases linearly with distance and averages about 1.5 s for Pn and 3.1 s for Sn. Further research remains to determine if these results improve regional location capabilities.

Keywords: iran, upper mantle, tomography

PERUGIA
ITALY



(S) - IASPEI - *International Association of Seismology and Physics of the Earth's Interior*

JSS011

Oral Presentation

2119

Crust and upper mantle structure in the Caribbean Region by group velocity tomography and regionalization

Dr. Mariangela Guidarelli

Department of Earth Sciences University of Trieste

O'Leary Gonzales, Leonardo Alvarez, Giuliano Francesco Panza

An overview of the crust and upper mantle structure of the Central America and Caribbean region is presented as a result of the processing of more than 200 seismograms recorded by digital broadband stations from SSSN and GSN seismic networks. Group velocity dispersion curves are obtained in the period range from 10 s to 40 s by FTAN analysis of the fundamental mode of the Rayleigh waves; the error of these measurements varies from 0.06 and 0.09 km/s. From the dispersion curves, seven tomographic maps at different periods and with average spatial resolution of 500 km are obtained. Using the logical combinatorial classification techniques, eight main groups of dispersion curves are determined from the tomographic maps and eleven main regions, each one characterized by one kind of dispersion curves, are identified. The average dispersion curves obtained for each region are extended to 150 s by adding data from a larger scale tomographic study (Vdovin et al., 1999) and inverted using a non-linear procedure. A set of models of the S-wave velocity vs. depth in the crust and upper mantle is found as result of the inversion process. In six regions we identify a typically oceanic crust and upper mantle structure, while in other two the models are consistent with the presence of a continental structure. Two regions, located over the major geological zones of the accretionary crust of the Caribbean region, are characterized by a peculiar crust and upper mantle structure, indicating the presence of lithospheric roots reaching, at least, about 200 km of depth.

Keywords: tomography, caribbean, regionalization



(S) - IASPEI - *International Association of Seismology and Physics of the Earth's Interior*

JSS011

Oral Presentation

2120

Geodynamic development of the European lithosphere imprinted in its structure and topography of the lithosphere-asthenosphere boundary

Dr. Jaroslava Plomerova

Seismology Geophysical Institute, Czech Acad. Sci. IASPEI

Vladislav Babuska

Topography of the lithosphere-asthenosphere boundary and structure of the continental lithosphere record the geodynamic development of outer parts of the Earth. Though driving mechanisms of plate tectonics throughout the planet history are enigmatic, architecture of the continental plates can help to answer questions how and when the plates were assembled and to what extent they were later deformed. We model the lithosphere thickness and anisotropic structure of European continent, in tectonic provinces of different ages and of various settings. We observe noticeable differences in the lithosphere thickness varying from ~60km beneath some basins (e.g., the Pannonian Basin, the Po Plain), parts of Variscan Massifs (e.g., the southern French Massif Central, the Rhenish Massif) or the Phanerozoic North-German Platform, to about 200-220 km in the orogenic roots (e.g., the Western and Eastern Alps) and beneath large parts of the Precambrian Baltic Shield, with one of the oldest continental cratons on the planet. Our models, based on array travel-time deviations, consider seismic anisotropy, and are in good agreement with estimates of lithosphere thickness based on surface waves, magnetotelluric soundings, or xenolith studies. At scale lengths of a few hundred kilometres, domains with a consistent large-scale orientation of seismic anisotropy can be recognized in the continental lithosphere. We invert and interpret jointly anisotropic parameters of body waves (P residual spheres and shear-wave splitting) for 3D self-consistent anisotropic models of the mantle lithosphere. Velocity anisotropy of lithosphere domains is approximated by hexagonal or orthorhombic symmetry of fossil olivine fabrics with generally plunging symmetry axes, while mostly sub-horizontal anisotropy due to the present-day flow is generally modelled in the asthenosphere below the continental plates. Due to different orientations of seismic anisotropy within the lithosphere and asthenosphere, the velocity contrast at the lithosphere-asthenosphere boundary can be larger than it could be produced by compositional variations and by a thermal state. We interpret the anisotropic domains as fragments of mantle lithosphere retaining an old fossil olivine fabric, which was created before these micro-continents assembled. Dynamic forces acting in young orogenic regions with active tectonics could deform the mantle part of the lithosphere. However, unlevelled relief of the LAB and variable fabrics even in the Precambrian lithosphere support an idea that lithospheric roots have been formed during an early form of plate tectonics, i.e., by systems of successive paleosubductions (Babuska and Plomerov, 1989), or other subduction-related processes, like a thrust stacking of oceanic (proto-cratonic) lithospheres and accretion of magmatic arcs, acting since Archean (Flowers et al., 2004; Condie et al., 2006).

Keywords: lithosphere thickness, mantle fabric, geodynamic development

(S) - IASPEI - *International Association of Seismology and Physics of the Earth's Interior*

JSS011

Oral Presentation

2121

Seismic observations of mantle discontinuities, and their mineral physical interpretation

Dr. Arwen Deuss

Earth Sciences University of Cambridge IASPEI

Jennifer Andrews

Seismological studies on mantle discontinuities have been successful in observing the transition zone discontinuities at 410 and 660 km depth, as well as discontinuities in the lower mantle at a whole range of depths. The characteristics of discontinuities place important constraints on the style of mantle convection in the Earth. Here, we study mantle discontinuities using large collections of stacked PP precursors, SS precursors and receiver functions. Such stacks show clear reflections from the transition zone discontinuities and provide a means of investigating hypotheses about the mineral physical nature of discontinuities in the Earth's mantle. The 410 km discontinuity is observed in all data types and is characterised by a simple single peak. The 660 km discontinuity, however, shows a much more complex structure. It had been apparently absent in previous studies of PP precursors, posing major problems for models of mantle composition. We reported, for the first time (see Deuss *et al.* 2006), that the 660 km discontinuity can be seen in PP precursors, SS precursors as well as receiver functions. Our observations reveal a very complicated global structure with single and double reflections ranging in depth from 640 to 720 km. A weaker and possibly non-global discontinuity at approximately 520 km depth is also present in SS and PP precursors, but does not show up consistently in receiver functions. We find that this 520 km discontinuity is split in certain regions, while in other regions one discontinuity is observed. These observations are explained by the presence of multiple phase transitions on a global scale in the transition zone. Pyrolite and piclogite mantle models contain a mixture of olivine and garnet. The phase transitions of olivine and garnet explain the seismic observations of double peaks (or splitting) at the 520 and 660 km discontinuities. Computations of reflection amplitudes for different mantle models show that our observations are consistent with a pyrolite composition. We conclude that transition zone discontinuities cannot be interpreted in terms of olivine phase transitions only and we imply that phase transformations in the garnet components are of major importance for understanding the structure of the Earth's mantle and its convective state. Our three data types also support evidence for reflections from lower mantle discontinuities, the most consistent ones being at approximately 800 and 1150 km depth. Discontinuities at 1100-1220 km have been proposed before by some regional studies and would be consistent with tomographic models, particularly in subduction zone areas.

Keywords: mantle discontinuities, phase transitions, transition zone

(S) - IASPEI - *International Association of Seismology and Physics of the Earth's Interior*

JSS011

Oral Presentation

2122

Strain rate field calculated from GPS measurements in Chinese Continent

Dr. Shoubiao Zhu

Geophysics Institute of Crustal Dynamics, CEA IASPEI

Yongen Cai, Yaolin Shi

In previous studies, the strain rate in China has been computed from GPS measurements using different methods, resulting in quite different estimates of the strain rate. In this study, we use the kriging method to interpolate the scattered GPS velocity data to grid values, and then calculate the strain rate for each volume element, using a method similar to the derivation of shape functions in the finite element algorithm. We found that this approach can provide an accurate and stable strain rate field for the Chinese continent. The result shows that the orientations of principal strain rates are consistent with those of the P axis and T axis of focal mechanisms. The distribution of maximum shear strain rate clearly delineates some major active fault zones surrounding the Tibetan Plateau. The maximum shear strain rate is comparable with that obtained from the analysis of seismic moment release. In part of the Tibetan plateau, containing normal faults and pull-apart grabens, we obtain an extensional state of strain. The absolute value of the strain rate in the west of China is approximately 5 times larger than that of the east China, and the pattern of the strain rate field in most of the Chinese continent is controlled by the India/Eurasia collision.

Keywords: strain rate field, gps measurements, chinese continent

PERUGIA
ITALY



(S) - IASPEI - International Association of Seismology and Physics of the Earth's Interior

JSS011

Oral Presentation

2123

Mantle derived CO₂ degassing in Italy

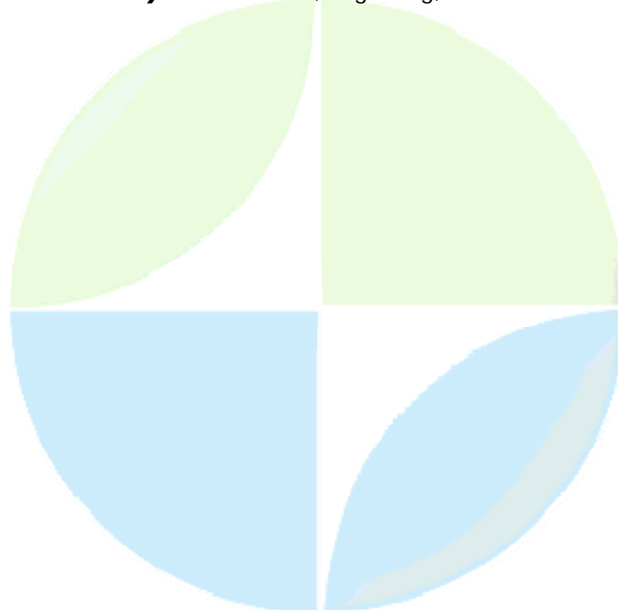
Dr. Carlo Cardellini

Dipartimento di Scienze della Terra Universit di Perugia IAVCEI

Chiodini Giovanni, Frondini Francesco, Caliro Stefano, Avino Rosario, Baldini Angela, Granieri Domenico, Morgantini Nicola

Central and southern are affected by an active and intense process of CO₂ Earth degassing. Recent studies, pointed out the presence of two large CO₂ degassing structures (62000 km²): a northern one, the tuscan roman degassing structure (TRDS) and a southern one, the campanian degassing structure (CDS). These two structures are characterized by the presence of numerous CO₂ rich gas emissions. The deeply derived CO₂ released by these two structures was estimated in about 9.2 Mt/y and resulted globally relevant, being about 10% of the estimated global CO₂ discharge from subaerial volcanoes. Based on the extension and magnitude of the CO₂ degassing and on the geochemical-isotopic features of the gas released, it is our opinion that the two degassing structures are the surface expression of two large plumes of fluids derived by a crusally metasomatised mantle. These CO₂ rich fluids heat the crust and saturate with gas the crustal permeable structures. The existence of a mantle wedge metasomatised by crustal materials is also strongly suggested by the geochemical features of the magmas of the Tuscany, Roman magmatic provinces. At regional scale, was also observed a strong relation between CO₂ degassing and the earthquakes location. The anomalous CO₂ flux suddenly disappears in the Apennine in correspondence of a narrow band where most of seismicity concentrates. Here, at the eastern borders of TRDS and CDS plumes, the CO₂ from the mantle intrudes and accumulate in crustal traps generating overpressurised reservoirs two of which have been reached by 4-5 km deep wells in the northern Apennine. These CO₂ overpressurised level can play a major role in triggering the Apennine earthquakes by reducing fault strength and potentially controlling the nucleation of earthquakes. Understanding the mechanism of mantle degassing, its flux through the crust, and its contribution to crustal deformation can provide useful information for the reconstruction of the geodynamic scenario of our region, as well as in many other tectonically active regions of the world.

Keywords: co₂, degassing, mantle



(S) - IASPEI - *International Association of Seismology and Physics of the Earth's Interior*

JSS011

Oral Presentation

2124

Interaction between mantle upwellings and lithosphere as derived from seismic anisotropy in Africa and Pacific

Prof. Jean-Paul Montagner
Geophysics Seismology IASPEI

Jean-Paul Montagner, Michel Cara, Eleonore Stutzmann, Eric Debayle, Genevive Roult, Jean-Jacques Lévêque

The interaction of continental and oceanic lithospheres with mantle upwellings, has been investigated for East Africa and Pacific by using 3D anisotropic tomographic model derived from broadband seismic data. The simultaneous use of Rayleigh and Love surface waves enables to retrieve both azimuthal and radial anisotropies with a lateral resolution of 500km. The joint interpretation of seismic velocity and anisotropy in the upper 400 km of the mantle enables to map mantle flow in the upper mantle and provides information on the complex interaction between mantle upwellings and lithosphere. In agreement with numerical modeling, it is shown that the flow pattern in the asthenosphere is significantly affected by mantle upwellings. Two kinds of mantle upwellings can be distinguished. The first one, such as the Afar plume in Africa originates from deeper than 400 km. From a geochemical point of view, it is characterized by enrichment in primordial ^3He and $^3\text{He}/^4\text{He}$ ratios higher than those along mid-ocean ridges (MOR). The second one, associated with Cenozoic volcanic provinces (Darfur, Tibesti, Hoggar, Cameroon) or close to the Mid-Atlantic ridge (Ascension, St Helena, Tristan, Canary, ...), with $^3\text{He}/^4\text{He}$ ratios similar to, or lower than MOR, is a consequence of shallower upwelling, presumably asthenospheric instabilities (secondary convection). An unexpected strong positive radial anisotropy is observed below Afar and Hawaii similar to the one found below Iceland (Gaherty, 2001), which is more difficult to explain from a geodynamic and mineralogical point of view. Both azimuthal and radial anisotropies show a stratification of anisotropy at depth, corresponding to different physical processes (shape preferred orientation, lattice preferred orientation) and also related to differential motion between different layers at depth.

Keywords: anisotropy, lithosphere plume interaction, upwelling



(S) - IASPEI - *International Association of Seismology and Physics of the Earth's Interior*

JSS011

Oral Presentation

2125

The effect of plate boundary evolution in 3D Cartesian geometry mantle convection models

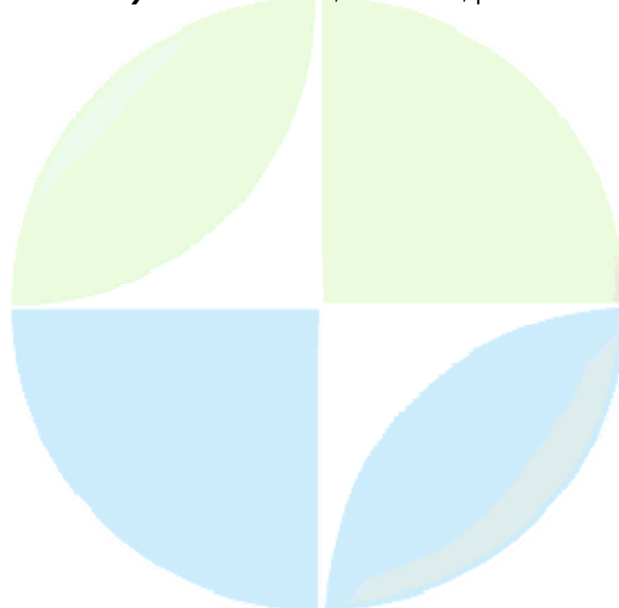
Prof. Julian Lowman

Physical and Environmental Science University of Toronto IASPEI

Andrew D. Gait, Carl W. Gable

Plate boundary locations, and therefore plate dimensions, can change significantly over time periods that are relatively short compared to the mantle overturn time-scale. However, the influence of plate geometry evolution on mantle convection has not been widely studied in 3D convection models. Here, we examine the effect of mobile plate boundaries on the time-dependence of the mean surface velocity, the surface velocity field and mantle and core heat flow. We investigate the effect of evolving plate geometries in high Rayleigh number, three-dimensional Cartesian mantle convection calculations featuring multiple plates with dynamically determined motion. Plate motion is determined by specifying that each plate move rigidly with a velocity that results in a net shear stress of zero at the base of the thick, viscously defined, lithosphere. This condition ensures that the specified plate motion neither drives nor resists the buoyancy driven flow. The time-dependent plate velocities determine the evolution of the plate geometry. Plate boundaries evolve as triple junctions are moved with a velocity that is equal to the average of the velocity of the three surrounding plates. In a $3 \times 3 \times 1$ solution domain geometry, we compare the time-dependence of the convection obtained in cases where plate geometry is able to evolve, with cases where the geometry remains fixed. We investigate time-dependence in three distinct viscosity stratification models. We compare the time-dependence of the plate velocities and the mantle and core heat flux in these calculations and examine the consistency of the results in three large geometry calculations (obtained with $6 \times 6 \times 1$ Cartesian geometry solution domains featuring a minimum of 9 plates). We find that an evolving plate geometry results in more rapid and more dramatic variations in all global measures of the vigour of the convection. However, the presence of a high viscosity lower mantle dampens the time-dependence of the convection, even over periods in which the plate geometry evolves considerably.

Keywords: mantle, convection, plates



(S) - IASPEI - *International Association of Seismology and Physics of the Earth's Interior*

JSS011

Oral Presentation

2126

Global modelling of the dynamic geoid: a role of the transition zone.

Dr. Mikhail Kaban

Dept. 1 GeoForschungsZentrum IASPEI

Valery Trubitsyn, Irina Rogozhina

Joint inversion of the observed geoid with other geophysical data (primarily seismic tomography and surface plate velocities) is a powerful tool to determine structure and properties of the mantle. However, despite of the massive efforts, the obtained results are remarkably various and the generalized dynamic model of the Earth does not exist at the moment. One of the reasons might be underestimation of the impact of the transition zone. The tomography models, which were used in the previous works, have been obtained without considering this effect. This can lead to strong artificial seismic velocity anomalies and, consequently, to false inferences on the density structure of the mantle. We use the tomography model of Gu et al. (2003), in which mantle velocities have been estimated in a joint inversion with the transition zone discontinuities. The velocity-to-density scaling factor and density jump at the discontinuities are determined independently to fit the observed geoid and surface plate velocities. For the 400-km discontinuity we obtain the scaling factor and density jump, which are very close to the mineral physics prediction, therefore, we can conclude that these effects are really decoupled in the tomography model. By contrast, the velocity-to-density scaling factor for the 670-km discontinuity doesn't differ remarkably from that one for the standard tomography model, while the calculated density jump is much less than the PREM value. One possible explanation for such a disagreement is that the seismically determined 670-km discontinuity might represent to a large extent compositional boundaries related to lithospheric slabs and mantle plumes near the 670-km discontinuity.

Keywords: dynamic geoid, mantle convection



(S) - IASPEI - *International Association of Seismology and Physics of the Earth's Interior*

JSS011

Oral Presentation

2127

New constraints on structure and dynamics of the lithosphere and asthenosphere from global upper-mantle tomography

Dr. Sergei Lebedev

Earth Sciences Utrecht University IASPEI

Rob D Van Der Hilst

We derive structural constraints from our new shear-speed model of the upper mantle. The model is a result of the application of the Automated Multimode Inversion (AMI) (Lebedev et al. 2005) to a large global dataset of over 60000 vertical-component seismograms. AMI extracts structural information from both surface waves and regional S and multiple-S waves and provides resolution of a few hundred km (varying with data sampling) everywhere the upper mantle (0--660 km). An elaborate filtering, windowing, and weighting procedure enables highly complete and balanced use of the information contained in the seismogram regarding Earth structure. Unlike other methods for tomographic mantle imaging, AMI has also been benchmarked with numerical wave-propagation modelling, both the method and its underlying assumptions thus validated. We observe that low-Sv-velocity anomalies beneath mid-ocean ridges and back-arc basins extend down to 100 km depth only; this agrees with estimates of primary melt production depth ranges there. Seismic lithosphere beneath cratons bottoms at depths up to 200 km. Pronounced low-velocity zones beneath cratonic lithosphere are rare; where present (South America; Tanzania) they are neighbored by volcanic areas near cratonic boundaries. The images of these low-velocity zones may be showing hot material - possibly of mantle-plume origin - trapped or spreading beneath the thick cratonic lithosphere. We suggest that sub-horizontal flow of asthenosphere from beneath cratons is the immediate cause of the intraplate, hotspot-like volcanism observed near cratonic boundaries. High-velocity lithosphere is observed beneath the southern part of the Tibetan Plateau, but beneath its northern part the lithosphere is seismically slow. This is consistent with a large part of Tibetan lithosphere being weak, suggesting that previously proposed scenarios involving the dominance (or even formation) of rigid, possibly cratonic lithosphere beneath Tibet are unlikely.

Keywords: craton, hotspot, tibet



(S) - IASPEI - *International Association of Seismology and Physics of the Earth's Interior*

JSS011

Oral Presentation

2128

When hot thermochemical instabilities trigger subduction and continental growth

Dr. Anne Davaille

Dynamique des Fluides Geologiques IPGP

Nicholas Arndt

Cratons generation often starts with massive mafic-ultramafic volcanism, to climax about 30 m.y. later with intrusion of voluminous granitoids. In terms of mantle dynamics, the first episode could be created by a mantle plume, while the second corresponds to subduction. To understand this sequence of events, we have studied the circulations induced by the onset of thermochemical hot instabilities at the bottom of the mantle, using laboratory experiments. A strongly temperature-dependent viscosity fluid, glucose syrup, was used. Initially a thin layer of syrup, made denser by the addition of salt, was at the bottom of the tank. Then the tank was heated from below and cooled from above. The temperature and velocity fields were measured in situ using thermochromic liquid crystals and PIV. The experiments were run for low buoyancy numbers, in the regime where episodic hot thermochemical doming occurs. The presence of denser material at the bottom of the tank delays the onset of hot instabilities, and convection usually starts by cold downwellings. Then hot domes develop from the hot chemically denser layer, with a morphology of cavity plumes since they are less viscous. When they hit and spread under the top surface, they peel off the cold thermal boundary layer there. This triggers a ring of enhanced cold instabilities around each thermochemical dome. The velocity of the cold downwellings is significantly increased compared to its value in absence of domes. Scalings laws derived from the experimental data suggest that this sequence of events is similar to what was observed on Earth in the archaean. Moreover, such a mechanism could explain geophysical observations around the Ontong-Java and Caribbean plateaus.

Keywords: convection, plumes, subduction



(S) - IASPEI - *International Association of Seismology and Physics of the Earth's Interior*

JSS011

Oral Presentation

2129

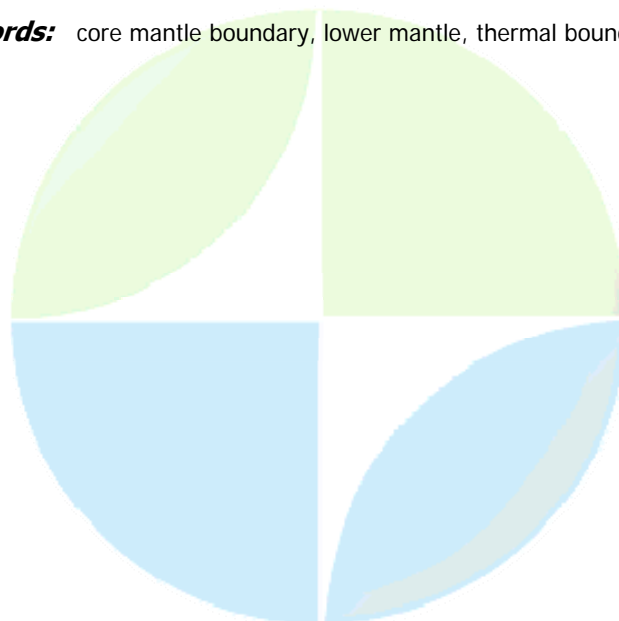
Post-Perovskite in the Deep Mantle - What Can it do for You?

Prof. Thorne Lay

Earth and Planetary Sciences University of California IASPEI

For several decades seismologists have observed reflections from the lowermost mantle that can be accounted for by abrupt increases in shear velocity and/or compressional velocity. Interpretation of these velocity changes has been difficult, as their origin may be petrological or mineralogical, and they may or may not involve dynamically generated fabrics. The discovery of post-perovskite, a high pressure polymorph of magnesium-silicate perovskite that should exist for P-T conditions near those of the core-mantle boundary, provides a specific hypothesis for the origin of lowermost mantle reflectivity. Consideration of the diversity of seismic models and observations in the context of this specific mineralogical context indicates that the phase change may plausibly account for a subset of seismic observations, but there are many features that are not easily reconciled with an isochemical phase change. For example, relatively weak P wave reflectivity is predicted for the phase change, but in some locations the compressional velocity increases are observed to be strong. In other regions, more than one seismic reflection appears to occur, some involving velocity increases and some involving velocity decreases. When the effects of temperature and chemistry on the post-perovskite phase transition are considered, it is possible to develop scenarios in which two or more discontinuities might be anticipated, either as a result of double-crossing of the phase boundary in a steep thermal gradient or the presence of multiple phase boundaries in a mixture of distinct petrologies. It is intriguing that seemingly realistic scenarios involving the phase change can be reconciled with significant seismic complexity, but testable demonstration of the scenarios is rather elusive. The reason this topic is attracting so much attention is that the occurrence of the phase change has important implications for dynamics of the thermal boundary layer in D", for detection of chemical heterogeneity, for development of seismic anisotropy in the boundary layer, and for determination of temperature gradients in the deep mantle. Examples will be discussed of how the post-perovskite context leads to implications for deep mantle chemistry, the fate of subducted lithosphere, the origin of deep mantle plumes, and the heat flux through the core-mantle boundary.

Keywords: core mantle boundary, lower mantle, thermal boundary layer



(S) - IASPEI - *International Association of Seismology and Physics of the Earth's Interior*

JSS011

Oral Presentation

2130

Regional Scale Variation of the top Layer of the Inner Core Beneath Pacific

Prof. Shingo Watada

Earthquake Research Institute University of Tokyo IASPEI

Differential traveltimes of seismic core phases have been used to probe the surface layer of the inner core, although, the differential traveltimes data show large scatter relative to a reference earth model. The origin of the scatter has been speculated, for example, sharp seismic velocity boundaries in the top of the mantle and strong heterogeneity above the CMB, or in the inner core. The large aperture dense seismic array, Hi-net, is suitable for the study of the regional scale variation of core phases because its short station spacing enables us to measure the traveltimes of short-period body waves from waveforms without spatial aliasing. The pattern PKPcd-df and PKPbc-df differential traveltimes from deep focus earthquakes in South America shows a clear systematic gradient within the Japanese islands. For example 0.5 s difference occurs over a 300 km distance for PKPbc-df, suggesting a short scale variation of P-wave velocity of the top 300 km of the inner core. The core phases propagate in the inner core in the east-west direction beneath the Pacific where strong anisotropy is not expected. Rich short-scale heterogeneity in addition to the well documented hemispheric structure in the inner core may hide in the scatter of the differential traveltimes of core phases over the globe. The scale and size of the regional structural variation of the inner core revealed by a large-aperture dense seismic array will provide observational constraints for the style of convection of the inner core.

Keywords: traveltimes, seismic core phases, inner core

PERUGIA
ITALY



(S) - IASPEI - *International Association of Seismology and Physics of the Earth's Interior*

JSS011

Poster presentation

2131

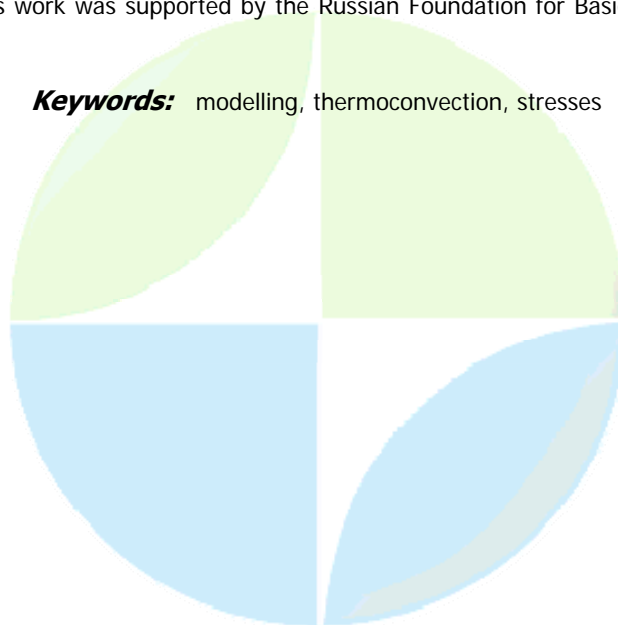
**The evolution of mantle viscous stresses caused by supercontinental cycle:
numerical modelling**

Dr. Alexander Bobrov

Theoretical Geodynamics Group Institute of Physics of the Earth, Russian Acad.Sc IASPEI

Numerical modelling are carried out of the fields of the main normal stresses values in the mantle, the maximal shear stresses, and also their spatial orientation in each point. Calculations are fulfilled for sequence of stages of a supercontinental cycle (Wilson cycle) on numerical two-dimensional model of assembling and dispersing continents, driven by mantle flows; in turn, the flows themselves are forming under thermal and mechanical influence of continents. Without such self-consistent interaction, Wilson cycle would be impossible, and all structure of currents and stress fields would be another, qualitatively differing from taking place in the real Earth. Our computer modeling demonstrates a number of realistic features of the process; closing and then opening ocean; appearance of the marginal seas and inclined subduction zones, etc. Mantle sources of radiogenic heat are also included in the model (in the considered case they contribute one third of full thermal flow at the surface). Results of model calculations have shown, that areas of the maximal shear stresses are located in the upper parts of descending mantle flows, in particular, in the upper parts of inclined subduction zones. The model gives that the sizes of such area where shear stresses are equal or exceed 35 MPa (350 bar), are approximately 200 x 200 km. These magnitudes are about 10 times more the stress values in the bulk of the mantle model (3 - 5 MPa). At the same time the upgoing mantle flows are, with respect to downgoing ones, more slow and wide, having significantly less stress magnitudes. Further, the area before a leading edge of moving continent is outlined: the pair consisting of a descending and an ascending mantle streams, close located to each other (similar to Andian subduction zone of South America and closely located East-Pacific raising) which exists during rather long time, forming the mantle area of essentially (approximately in 2.5 times in comparison with average value) increased stresses. Later, in process of advance of continent, the ascending mantle flow deviates aside continent, and the rest of a descending flow becomes more flat, comes under continent and gradually disappears; stresses in it also gradually decrease. The picture is qualitatively similar to a situation at Pacific margin of North America. This work was supported by the Russian Foundation for Basic Research (project 05-05-65190).

Keywords: modelling, thermoconvection, stresses



(S) - IASPEI - *International Association of Seismology and Physics of the Earth's Interior*

JSS011

Poster presentation

2132

Geodynamics of the Active continental Margins of the Far East, Russia

Prof. Alexander Rodnikov

Geophysical Center Russian Academy of Sciences IAVCEI

The Geodynamics of the active continental margins of Far East (Russia) was investigated under InterMARGINS Project along the deep sections of the tectonosphere, including the lithosphere and the asthenosphere. A distinctive feature of the transition zone from the Eurasian continent to the Pacific Ocean is the presence of an asthenospheric layer in the upper mantle and the upwelling of the diapirs of a hot anomalous mantle, which controlled the formation of the geological units of the active continental and oceanic margins. There is an obvious correlation of the geological features, tectonomagmatic activity, and the structure of the upper mantle. The active regions, such as the island arcs and the rifts of the marginal seas, correlate with a thick, magma-generating asthenosphere. It is expressed in the growth of heat flow in the younger tectonic zones caused by the upwelling of asthenospheric diapirs into the lithosphere, which involves tectonomagmatic reworking. Rifts in the marginal seas and island arcs may be accompanied by intense mineralization. The combination of high heat flow, volcanicity and hydrothermal activity in these structures, in the past and at present, can lead to the formation of sulphides and other mineral deposits.

Keywords: geodynamics, lithosphere, asthenosphere

PERUGIA
ITALY



(S) - IASPEI - *International Association of Seismology and Physics of the Earth's Interior*

JSS011

Poster presentation

2133

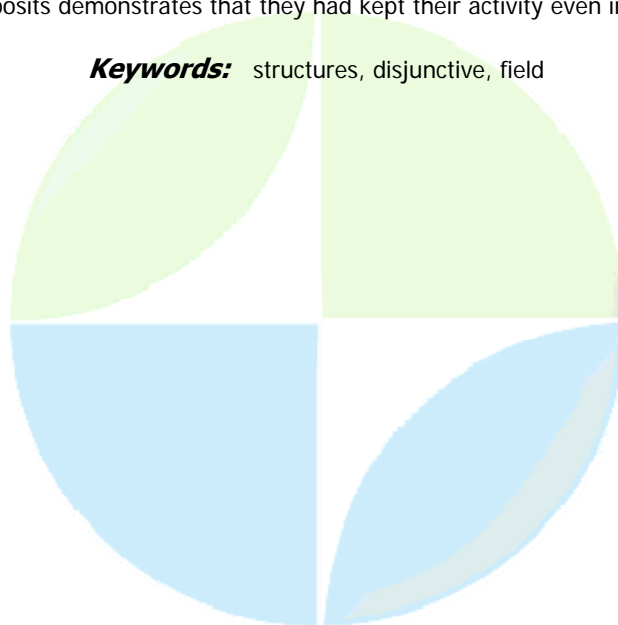
Disjunctive-plicative lateral structures of Tien-Shan; their delineation and role in pre-mesozoic geology of the region

Prof. Oleg Mordvintsev

Regional thematic Uzbekgeophysic IASPEI

In Central Asia, systems of breaking dislocation of various directions are widely developed, among them are north-west, sub-latitude, to less degree sub-meridional and north-east, as well as some other directions. The structures of north-east strike have not been specially studied till present time. Analysis of the material on subsurface geology of Uzbekistan, with some degree of confidence, let us assert that they are not only one of the earliest disjunctive plicative structures in the region (age of start of formation is Pre-Paleozoic), but even most of long-living active even till present. Nine such zones were delineated within Western Uzbekistan, which divide the territory into the blocks essentially distinguished by the character of magnetic field and gravity field, in some cases, differences in blocks minerageny were established. In the north, they strike right up to Bolshoy Karatau ridge (Kazakhstan), in the west, they come to Kopetdag (Turkmenistan). Materials on depth CDP showed their clear fixing on seismic sections, besides, which is very important, from the beginning of entry (0.2 s) and till its end (4.5 s). In order to define time of start of formation of these structures, their reflection in relief of crystalline basement surface was followed, where they mostly show as flexure-fracturing zone (FFZ). The divided zones have their own specific character of structural surface morphology. Upper to the section, amplitude of movement on FFZ is leveling, and on Pre-Jurassic surface their tracing was conducted on the zones of morphostructures contacts, as well as on distribution of magmatic magnetoactive objects and differences in substance content of basement and intermediate structural stage. One of the most important factors of depth of penetration of breaking dislocations into the Earth crust can serve the character of distribution of average density of the Earth crust. Correlation of FFZ position with the scheme of distribution of average density of the Earth crust showed presence of certain dependencies (timing of local anomaly, passing through the areas of anomalies sign change). This emphasizes the early age of start of formation of FFZ, that influences basement development in the period of its becoming. Their show in Hercynian basement of Southern Tien-Shan and Bukhara Khiva region sedimentary cover deposits demonstrates that they had kept their activity even in later periods.

Keywords: structures, disjunctive, field



(S) - IASPEI - *International Association of Seismology and Physics of the Earth's Interior*

JSS011

Poster presentation

2134

The investigation of aftershock process of strong earthquakes of the Eastern-Anatolian fractured zone

Dr. Mariam Mkrtchyan
IAGA ISS011 IASPEI

The Eastern Anatolian fractured zone is one of the seismoactive zones of the Armenian plateau. It covers folding structures of Eastern Tavros, Bitlis and joints in the area of Lake Van with Zagros belt. Submeridian seismicity of the Levant fracture from the south adjoins to the Eastern Anatolian zone. The zone, which is to the south of Tavros is considered to be less active in comparison with Northern Anatolian fractured zone. In the past in the given area earthquakes are recorded with the maximal intensity of no more than $M \sim 4.5$. But for a short period of time from the seismicity standpoint two strong earthquakes occurred in this area: 22.05.71.; 0:16h44m; $\varphi=38.87N$; $\lambda=40.48E$; $h=22\text{km}$; $M_s=6.8$ Bingol area and 06.09.75.; 0:09h20m; $\varphi=38.50N$; $\lambda=41.00E$; $h=26\text{km}$; $M_s=6.7$ in Lice to the northeast of Diyarbakir. The recorded earthquakes as significant seismic events are less studied and an attempt is made in this work to pay more attention to the investigation of these earthquakes in particular the aftershock process of earthquakes which had occurred in the region are genetically connected with seismotectonic zone of Erzincan seismoactive node and Bitlis zone of fractures. The aftershocks analysis earthquake 22.05.71. 0:16h44m in the time showed, that the majority of aftershocks including strong aftershocks occurred during the first 24 hours after the main earthquake. Aftershocks are distributed to the northeast, southwest, at the end of the fault emanated on the surface. The main earthquake occurred nearer to the northwest edge of a fault. The main part of aftershocks is concentrated here. The strongest aftershock with $M=4.8$ occurred about 2 days later after the main earthquake, the aftershocks which were nearer to the main shock in time were weaker. The depth of focuses was 20-25 km. The focal mechanism of earthquakes is left-lateral strike-slip. After the 06.09.75. 0:09h20m earthquake over a period of 31.12.75.- 26 strong aftershocks occurred with $M \geq 4.0$. The main shock and aftershocks are distributed in the limit $\varphi=38.5-39.0N$; $\lambda=40.50-41.0E$. The mean depth is 25-30km. The focal mechanism of the 06.09.75 earthquake and its aftershocks is thrust fault. The detailed analysis aftershock process of these earthquakes showed that: - the space development of aftershock sequence after a strong earthquake is important for the current estimation of seismic hazard. - the epicenter of the most strongest aftershock is quite near to the epicenter of the main earthquake. - the focal mechanism of the strongest aftershocks follows the focal mechanism of the main shock.

Keywords: strongaftershocksmechanism

(S) - IASPEI - *International Association of Seismology and Physics of the Earth's Interior*

JSS011

Poster presentation

2135

Normal Modes for Kinematics of A Triaxial Earth

Prof. Wen-Jun Wang

Dept of Geodynamics, School of Surveying and Land Chinese Academy of Sciences

Wenbin Shen, Han-Wei Zhang

The Earth orientation is determined according to Euler dynamical equations as well as Euler kinematical equations. Solving Euler kinematical equations on behalf of multiple solutions of free wobbles and secular wander, three groups of solutions from Euler kinematical equations index that Earth possesses no regular precession but free precessions. The first group of free precessions has 46.46 days periodic precession for Eulers precession angle, 36.44 days periodic nutation for Eulers nutation angle and 30.01 days periodic free spinning oscillation for the rigid Earth case. By this discovery, the 40-50 day oscillations or so-called MJO (Madden-Julian Oscillations) can be clearly claimed possessing free precession background of Earth rotation. Other two groups of free precession solutions also provide detectable variations for the Earth orientation.

Keywords: earth orientation, euler kinematical equations, eulers angles free precession



(S) - IASPEI - *International Association of Seismology and Physics of the Earth's Interior*

JSS011

Poster presentation

2136

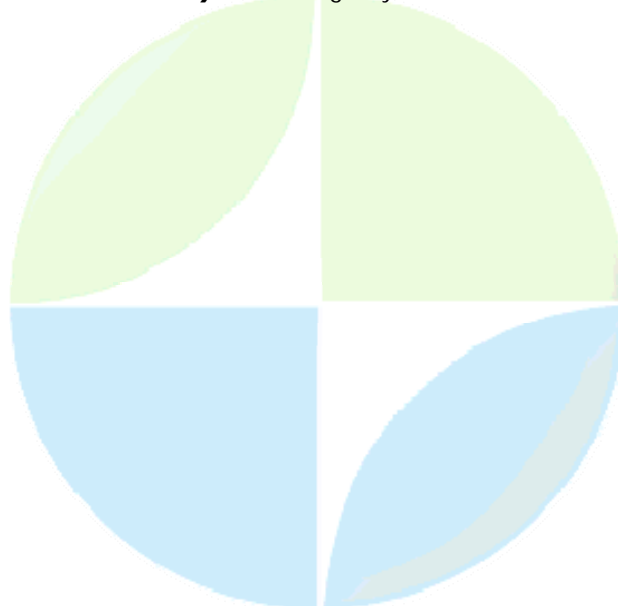
Complex geophysical research of earth CTUST deep structures and geodynamics of territory of Armenia

Dr. Hmayak Hovhannisian
IASPEI

Karine Vardanyan

More complete data at present about the construction of Earth crust deep structures and geodynamics of territory of Armenia are obtained on a basis of gravimetric, geothermal, seismological, geodetic and other geophysical data. The experience of the long-term research in Armenia showed that a complex interpretation of gravimetric, geothermal, seismological data is the important means of decrease in multivalence and increase in the truth of constructions of structural - dynamic models of the Earth crust. As a result of quantitative interpretation of gravitational and thermal fields in a complex with deep seismic sounding (DSS) data, seismometry, the data of the stations " Earth " and "Turtle" and geodesy the three-dimensional structural-dynamic model of the Earth crust is plotted in scale 1:200000. It is stated that the Earth crust of territory of Armenia has a heterogeneous, three-layer structure. The borders of layers coincide with the surfaces of crystal base, Konrad and Mochorovichich. The localization places of vertical nonhomogeneties are established coinciding with the zones of deep breaks. According to the data of velocities of Earth surface modern vertical and horizontal (GPS) motion changes in time of gravitational and geomagnetic fields, seismic regime, and also a thermal stream, made an estimation of relative geodynamic activity of blocks as well as its delimited zones of deep breaks. The calculation of deep temperatures, their changes for the last million years within a frame of the generalized regional thermal model shows, that near the borders of a volcanic belt of territory of 15-23 km depths, where the changes in temperatures reaching the order of 10-12-10-13 , are enough for the accumulation of thermoelastic pressure, exceeding durability of breeds. As a result of complex interpretation of high-speed, gravitational and thermal models on a structural - dynamic model of seismoactive layer is allocated, the sole of which is placed at depths of 13-30km according to the data of earthquakes hypocenters.

Keywords: geodynamics



(S) - IASPEI - *International Association of Seismology and Physics of the Earth's Interior*

JSS011

Poster presentation

2137

Earth's structure with the gravimetric tomography method

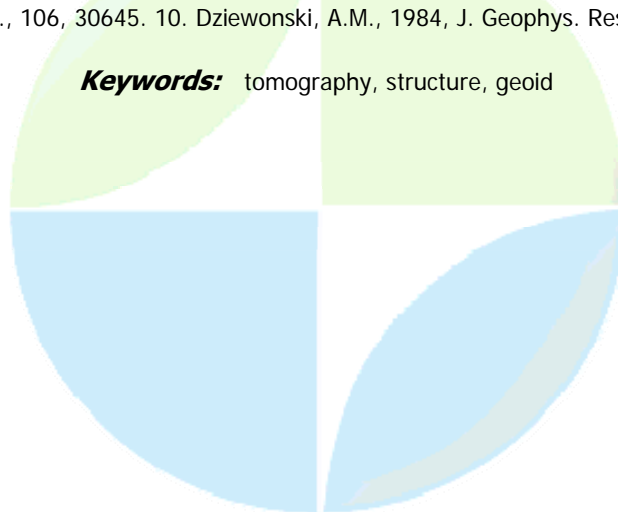
Dr. Rudolf Greku

IASPEI IASPEI

Alexander A. Kulikov, Tatyana R. Greku

Experienced geophysicists supposed a relationship between depth of disturbing layers and the geoid harmonics [1, 2]. In later researches on modeling of the Earth the geoid was used as observable referenced data to integrate their or compare with seismic or geodynamic data [3, 4]. The inverse decision of the geopotential-density problem was proposed in a book [5]. Our gravimetric tomography technique is based on realization of this algorithm for determination of harmonic dense anomalies (relatively the PREM density model) through the spherical harmonics of the EGM96 gravity potential model. Spherical harmonics are used also for determination of the layers depths disturbing geopotential. Maps of the lateral distribution of density inhomogeneities at different layers and vertical cross sections along characteristic directions over the world, dynamic features within the Antarctic and Arctic Polar regions in all range of depths up to 5300 are presented in the paper. Comparison of the gravimetric tomography data with the seismic tomography data from [6, 7, 8, 9] is given. In particular, the gravimetric tomography data are coordinated with seismic images of the Antarctic regions from the work [9]. It is shown that the main structural bodies are similar by signs and the spatial distribution at the lateral slices in depths of 150 km and 400 km. Areas with low-velocity anomalies are corresponding to the less dense structures by the gravimetric tomography and vice versa. But the areal enclosing of different structures is not coincided everywhere. It concerns especially to the shallower crustal layers where the seismic tomography models have a less resolution. The plume zones can be also visible with the gravimetric tomography at deeper layers. Known low-velocity layer on the core-mantle boundary underneath the Pacific and Africa [10] is indistinguishable by the gravimetric tomography density models. At the same time these models are coordinated here with the models of density within the mantle from [8]. 1. Allan R.R., *Nature*, 1975, 236: 22. 2. Gainanov A.G., 1981, *Geology and Geophysics of the Eastern Indian Ocean Floor*, Moscow, Nauka, 256 (in Russian). 3. Ricard Y., Richards M., Lithgow-Bertelloni C., Le Stunff Y., 1993, *J. Geophys. Res.*, 98, 21895. 4. Forte A.M., Woodward R.L., Dziewonski A.M., 1994, *J. Geophys. Res.*, 99, 21857. 5. Moritz H., 1990, *The Figure of the Earth*, Wichmann, Karlsruhe. 6. Dziewonski A.M., Hager B.H., OConnell R.J., 1977, *J. Geophys. Res.*, 82, 239. 7. Romanowicz B., 2003, *Annu. Rev. Earth Planet. Sci.*, 31:303. 8. Ishii M., Tromp J., 2004, *Physics of the Earth and Planetary Interiors*, 146: 113. 9. Ritzwoller M.H., Shapiro N.M., Levshin A.L., Leahy G.M., 2001, *J. Geophys. Res.*, 106, 30645. 10. Dziewonski, A.M., 1984, *J. Geophys. Res.*, 89, 5929.

Keywords: tomography, structure, geoid



(S) - IASPEI - *International Association of Seismology and Physics of the Earth's Interior*

JSS011

Poster presentation

2138

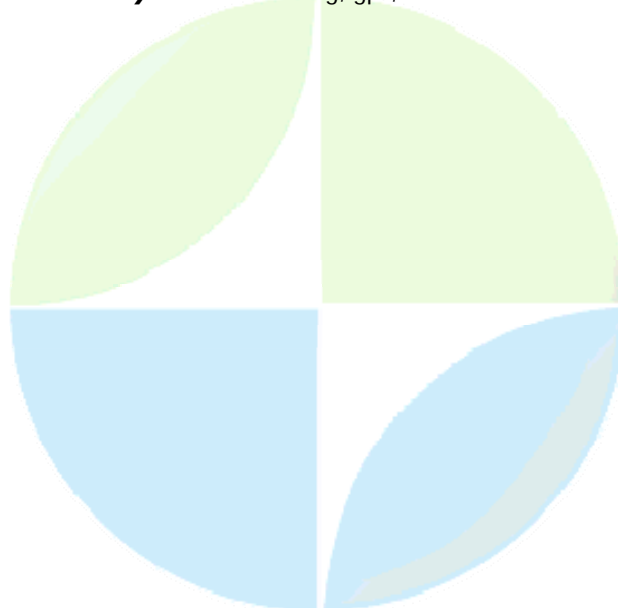
Behavior of the high-dam building and surrounding areas derived from leveling and GPS measurements, Aswan-Egypt

Dr. Abdel-Monem Mohamed

Geodynamics National Research Institute of Astronomy & Geophys IAG

Several leveling lines were established at different levels along the High-Dam building during its construction. One of those leveling lines is at the up-stream berm (186m), two of them are at the up and down stream parapets (196m) and the others are at the downstream berm (179, 162, 145, 130, 114m). Precise leveling measurements were carried out, along these leveling lines, each month since 1970 and continue till now. Analysis of the leveling data from the different leveling lines for the period from 1970 to 2006 were carried out in order to study the behavior of the High-Dam building during this period, especially the rock filled part of the High-Dam building. The results from the analysis reveals different tendencies of settling for the different parts, different sections and similar positions at different levels of the High-Dam building. The rates of settling of the High Dam body are stable since 1975. No significant correlations were found between the rates of settling and water level changes at the down-stream side of the High Dam, while at the up-stream side some part of correlation were remarked between the rates of settling and the seasonal variations of the water level in the lake (cycles of charge and discharge) especially during the first ten years (1970- 1980). Also, no significant correlations were found between the rates of settling and the earthquake occurrence in the area of the northern part of lake Nasser. For monitoring the horizontal movements in the High Dam area, a local GPS network consisting of 10 geodetic stations was established in 2000. The measurements were carried out during the period from 2002 to 2006. nine campaigns of GPS were carried out in the study area. The measurements are correlated to the water level changes in the lake, as well as to the seismic activity in the area. The displacements for each epoch of observations were calculated and the deformation analysis was performed. The horizontal displacements vary between 1 to 2 mm/yr. The horizontal rates and strain accumulations are small, which reflect the stable situation, and demonstrates a new information about the present state of the High Dam body and surrounding areas.

Keywords: leveling, gps, deformation



(S) - IASPEI - *International Association of Seismology and Physics of the Earth's Interior*

JSS011

Poster presentation

2139

The Joint Inversion Study on the Driving Forces Acting on the Block Boundaries and Tectonic Stress Field of China Mainland and Its Adjacent Areas

Dr. Zhixing Du

Key Laboratory of Foundational Geo-information Shandong University of Science & Technology IASPEI

Fanlin Yang, Xiushan Lu

China situates on the southeast of Eurasian plate. It is joined with the Pacific-oceanic plate in the east and with the Indian plate in the south. The development and interaction of three plates shape the present tectonic framework. As one of the most drastic districts of new global tectonic change and present tectonic motion, it is an uncommon and superior district to study the inner continent and its marginal lithosphere and geodynamics. It plays an important role in geoscience study and is broadly concerned by geoscience scientists. In recent decades, geoscience scientists did a lot of work in the fields of tectonic structure, geophysical field, infrastructure, seismic activity and tectonic motion. It established a good base for the study of driving source of tectonic motion of inner block. This paper after expatiating the status and evolution of the inversion study on the driving forces acting on the boundaries of China mainland and its adjacent areas and the tectonic stress field, the inversion computation of them is made by means of the finite element of genetic method according to the displacement observations obtained from the Crustal Movement Observation Network of China and tectonic stress fields, and the specific implementation procedure including the selection of the parameters, the computation conditions of model, the method of inversion, the analysis of inversion results and their interpretation for inversion computation is given out in detail. The following conclusions can be drawn from analyses: (1) the main driving forces that formed the displacement field in Chinese mainland and tectonic stress field are still from the collision of Indian plate with Eurasian plate. (2) Although the driving forces of Pacific plate and Philippine plate are smaller than that of Indian plate, yet they are the significant factors that affect eastern China. (3) The back basin of Japan sea arc is continuously extending possibly because of the drag to continent formed after the oceanic crust dropped back. (4) The forces from north prevent the northern motion of China which are relatively big resistive forces. (5) Neijiang river fracture and Xilamulun river fracture has the sign of motion, but the exact motion mode is still uncertain.

Keywords: tectonic stress fields, crustal movement observation, joint inversion

(S) - IASPEI - *International Association of Seismology and Physics of the Earth's Interior*

JSS011

Poster presentation

2140

The stress field of the Hyuga-Nada Region, Southwest Japan, deduced from ocean-bottom seismic observations

Dr. Kenji Uehira
IASPEI

Hiroshi Yakiwara, Tomoaki Yamada, Masanao Shinohara, Toshihiko Kanazawa, Kodo Umakoshi, Kazuhiko Goto, Hiroki Miyamachi, Ryota Hino, Kimihiro Mochizuki, Kazuo Nakahigashi, Masaji Goda, Hiroshi Shimizu

The Philippine Sea (PHS) plate is subducting beneath the southwest Japan arc along the Nankai trough at a rate of about 5 cm per year. The seismic activity in the boundary between the PHS and the Eurasian (EU) plates varies spatially along the Nankai trough. Especially the region from off coast of Shikoku to the Bungo channel and Hyuga-nada has large variation of seismicity. In addition, recent studies reveal that a coupling rate between two plates has variety. A plate coupling rate should affect a stress field in the vicinity of plate boundary. In other words, there is a possibility that a plate coupling rate can be estimated by a stress field near a plate boundary. To estimate a stress field, precise hypocenter distribution is needed. It is difficult to obtain precise hypocenter distribution without Ocean Bottom Seismometer (OBS), since the interesting area is under water. Because a stress field is usually estimated by many focal solutions, it is important that a whole area is covered with a seismic network. We used the data of OBSs and temporary stations from 2002 to 2004 and permanent stations for this analysis. The stress field was estimated using a stress tensor inversion method by polarity of first arrivals from earthquakes. The obtained stress field has spatial heterogeneity, especially near the boundary between the PHS and the EU plates. The direction of minimum principal axis of the PHS slab is parallel to the direction of subduction. This means that stress field of the PHS slab is down-dip tension. The direction of maximum principal axis is almost perpendicular to the plate boundary, but there is a little variation. The northern region of the study area has small angle between maximum principal axis and the normal vector to the plate boundary, on the other hand, the direction of maximum principal axis in the southern region has large deviation from the normal direction to the plate boundary. The shear stress of plate boundary is estimated to be smaller in the north, and larger in the south. The slip distribution estimated by using waveform data of large earthquake and geodetic data is thought to indicate the state of the plate coupling. There is a good correlation between the slip distribution at large earthquakes and the angle between maximum principal axis and the plate boundary. Although slip distribution has not been obtained in the southern area, it is estimated that subducting plate in the southern region couples with the landward plate stronger than the northern region. On the boundary region, Kyushu-Palau ridge, which has northwest-southeast strike and exists on the PHS plate, subducts beneath the Kyushu arc. According to the velocity structure obtained from a seismic tomography, there is high V_p/V_s ratio region at mantle wedge in the northern part of Hyuga-nada. The geographical features, and/or the serpentinization material may cause the spatial variation of the state of stress in Hyuga-nada.

Keywords: stress field, seismic coupling, hyuga nada

(S) - IASPEI - *International Association of Seismology and Physics of the Earth's Interior*

JSS011

Poster presentation

2141

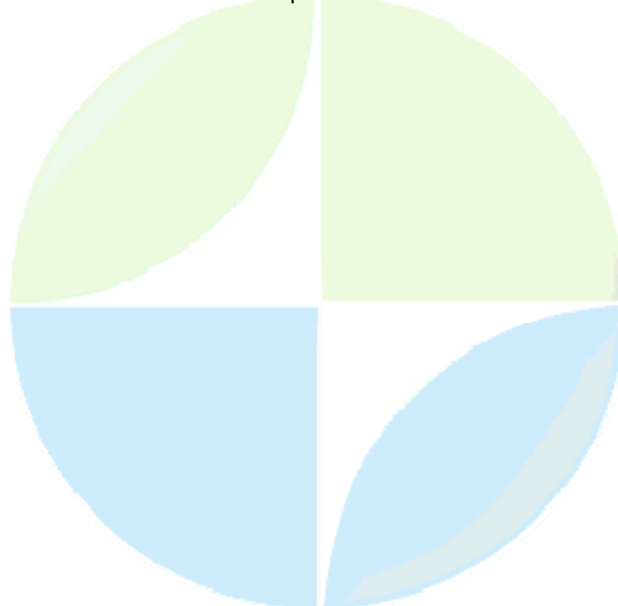
Influence of the atmospheric and oceanic circulation on the movement of the lithosphere plates and on the earthquakes

Prof. Nikolay Sidorenkov

Hydrometcentr of Russia Hydrometcentr of Russia IAG

The non-tidal irregularities of the Earth rotation are mainly due to the exchange between the angular momentum of the solid lithosphere and its fluid environment - the atmosphere and the hydrosphere. This exchange occurs at the expense of the moments of the frictional forces and pressure forces pushing on mountain ranges. The lithosphere is cracked on a set of the lithosphere plates. The atmosphere and ocean are acting on the lithosphere plates, and only then this action is being transmitted to the Earth's interior. Under the lithosphere, there is a layer of the lower viscosity - an asthenosphere in which the lithosphere plates are capable to float. On the decade time scale, the lithosphere plates can move in the horizontal direction under the action of the friction stresses and pressure, which the atmosphere and ocean produce on the exterior surface of the plates. The atmospheric and oceanic forcing causes the drift of the lithosphere along the asthenosphere. Evidence in favour of this hypothesis is presented. The moment of forces effecting on an individual plate, determines the vector of the movement of the plate. The estimations of the orders of magnitudes of the atmospheric and oceanic forces effecting on a separate plate and of the stresses of the interaction between plates are given. Under the effect of the atmospheric and oceanic forces the plates interact with the circumjacent plates through the frontal contacts. The stresses may reach such high values (10^6 - 10^7 N/m²), at which the discontinuity and displacement of plates from each other occur, and triggers the earthquakes. The mechanical action of the atmosphere and ocean on the lithosphere plates defines relative movement between the plates and can be cause of the earthquakes. The empirical facts, which evidence for the benefit of this conclusion, are given. It is necessary to carry out the monitoring of the atmospheric and oceanic forces separately for every lithosphere plate. The time series of these forces make it possible forecasting of a seismic activity.

Keywords: atmospheric & oceanic forces; variations in earth rotation; movement of lithosphere plate



(S) - IASPEI - *International Association of Seismology and Physics of the Earth's Interior*

JSS011

Poster presentation

2142

Three-dimensional seismic velocity structure in the Off-Miyagi and Off-Fukushima forearc Region

Mr. Yojiro Yamamoto

RCPEV, Graduate School of Science Tohoku University IASPEI

Ryota Hino, Kensuke Suzuki, Tomoaki Yamada, Masanao Shinohara, Toshihiko Kanazawa, Masayuki Tanaka, Yoshiyuki Kaneda, Kenji Uehira

The Japan Trench is a plate convergent zone where the Pacific Plate is subducting below the NE Japan arc. Interplate coupling along the plate interface is estimated to be strong by a backslip modeling of the land GPS observation in the middle to southern part of the arc (Suwa et al., 2006). However, the middle part (the off-Miyagi region) and the southern part (the off-Fukushima region) show different characteristics of the interplate seismic activity. In the off Miyagi region, the large earthquakes ($M > 7$) with thrust mechanisms have occurred at an interval of about 40 years, and an interplate earthquake of $M 7.2$ occurred in this region on 16 August 2005. In the off-Fukushima region, few large interplate earthquakes have occurred while the background microseismicity is very high. In 2005, we deployed 51 OBSs in the off-Miyagi and off-Fukushima regions to observe the interplate seismicity, including the 2005 off-Miyagi earthquake ($M7.2$) and its aftershocks. Using the OBSs data with those of the onshore seismic stations, we performed a 3D seismic tomography in order to clarify whether there are some differences in the seismic velocity structures between the off-Miyagi and the off-Fukushima regions, corresponding to the differences in the seismic activity. In our results, the subducting oceanic crust and the mantle wedge of the overriding plate were imaged as the landward dipping low velocity (V_p : ~ 7.0 km/s, V_s : ~ 4.0 km/s) layer and the high velocity (V_p : ~ 8.0 km/s, V_s : ~ 4.5 km/s) layer above it, respectively. Most of the earthquakes were relocated along the plate boundary, including the mainshock and the aftershocks of 2005 earthquake. Comparing spatial extents of the rupture areas of the 1978 and 2005 earthquakes and the velocity variation in the mantle wedge, we found that the location of high V_p anomaly corresponds to the rupture areas of the large interplate earthquakes. This suggests that the heterogeneity of the upper plate delimits the extent of the rupture area of large interplate earthquakes. The V_p in the mantle wedge of the off-Fukushima region is slower than that in the off-Miyagi region. Previous airgun-OBS experiment studies indicated that there is a low V_p (~ 7.5 km/s) area at the toe of the mantle wedge in the off-Fukushima (Miura et al., 2003), while the V_p of the mantle wedge in the off-Miyagi is high (~ 8.0 km/s) (Ito et al., 2005, Miura et al., 2005). The V_p variation in the mantle wedge imaged by the present seismic tomography is consistent with their results.

Keywords: subduction zone, velocity structure, mantle wedge

(S) - IASPEI - *International Association of Seismology and Physics of the Earth's Interior*

JSS011

Poster presentation

2143

Crustal and upper mantle structure beneath central South America deduced from ScS reverberation waveforms and receiver functions

Dr. Keiko Kuge

Department of Geophysics Kyoto University IASPEI

Yusuke Okaue

We investigated the crust and upper mantle structure beneath the central South America, approximately at 20 degree south, where the Nazca plate is subducting beneath the western coast and the Brazilian craton resides in the east. Our approach is to model ScS reverberation waveforms and receiver functions at GSN stations. ScS reverberation waveforms are sensitive to the path-averaged S-wave velocities, attenuation, and depths and reflection coefficients of discontinuities in the crust and mantle. Our procedure to determine these parameters follows that of Kato et al. (2001) utilizing ray-based theoretical waveform modeling and grid search optimization. Finiteness of source time duration is additionally taken into consideration in synthesizing waveforms of a great earthquake in this study. Depths of mantle discontinuities were separately estimated from arrival times of PS conversion phases on receiver functions. We also modeled receiver functions from early P coda to determine crustal structure. We found significant differences in the crust and uppermost mantle between the western coast and eastern continent. The Moho beneath the station NNA on the western coast is deeper than beneath the station BDFB in the eastern continent. While the Conrad and Moho beneath BDFB were estimated at depths of 22 and 40 km, respectively, discontinuities at depths of 25, 35, 60, and 70 km were detected beneath NNA. Some phases on the receiver functions imply an inclination of the discontinuities at 60-70 km depths, and the discontinuities can be the manifestations of the top of the subducting Nazca plate. A high value of Q (>400) was obtained for the upper mantle beneath NNA, but not beneath BDFB. This value is much higher than predicted from the expected mantle transition zone temperature, and an origin of this high Q might exist in the uppermost mantle. These observed differences between the east (NNA) and west (BDFB) could be attributed to the subducting Nazca plate. In the transition zone, the 410-km discontinuity is shallow beneath the western coast, which is consistently found in both studies. The mantle transition zone is thinner in the western coast (260 km) than in the eastern continent (270km), but it is thicker in either area than that beneath Japan. On the receiver functions in the western coast, we were able to identify a phase possibly from the 520-km discontinuity. Using SS reflection coefficients from the ScS reverberations and PS conversion coefficients from the receiver functions, we attempted to obtain constraints on density and V_s contrasts at mantle discontinuities. For the 410-km and 660-km discontinuities, the upper bounds of density contrast are 7-9 % and 15-20 %, respectively, while the upper bounds of V_s contrast are 6-14 % and 7-20 % or more, respectively.

Keywords: south america, crust, upper mantle

(S) - IASPEI - *International Association of Seismology and Physics of the Earth's Interior*

JSS011

Poster presentation

2144

Shear wave splitting and subduction structure in Southern Italy

Dr. Lucia Margheriti
CNT INGV IASPEI

Paola Baccheschi, Michael S. Steckler

In the current work we present a large collection of shear wave splitting measurements in the Calabrian Arc-Tyrrhenian basin subduction system. The dataset consists of SKS teleseismic phases (earthquakes with delta 87 - 112 and magnitude greater than 6.0) and of local S phases (events deeper than 150 km). We used the method of Silver and Chan to obtain the splitting parameters: fast direction (ϕ) and delay time (δt). Shear wave splitting results reveal the presence of a strong seismic anisotropy with a complex pattern of fast directions in the subduction system below the region. We interpret the trench-parallel ϕ observed along the orogen in Calabrian Arc and in Southern Apennines as a mantle flow below the slab, likely due to the pressure induced by the retrograde motion of the slab itself. The pattern of trench-perpendicular ϕ in the Apulian Platform foreland seems to be not a direct result of the roll-back motion of the slab and may be explained as frozen-in lithospheric anisotropy or as asthenospheric flow deflected by the complicated structure of the Adriatic microplate. Results obtained with S phases show an extremely complex pattern of fast directions and delay times. We related this strong fast directions variability to the complex structure and composition of the slab itself and of the wedge above it .

Keywords: splitting, mantle flow



(S) - IASPEI - International Association of Seismology and Physics of the Earth's Interior

JSS011

Poster presentation

2145

Electrical conductivity of wadsleyite

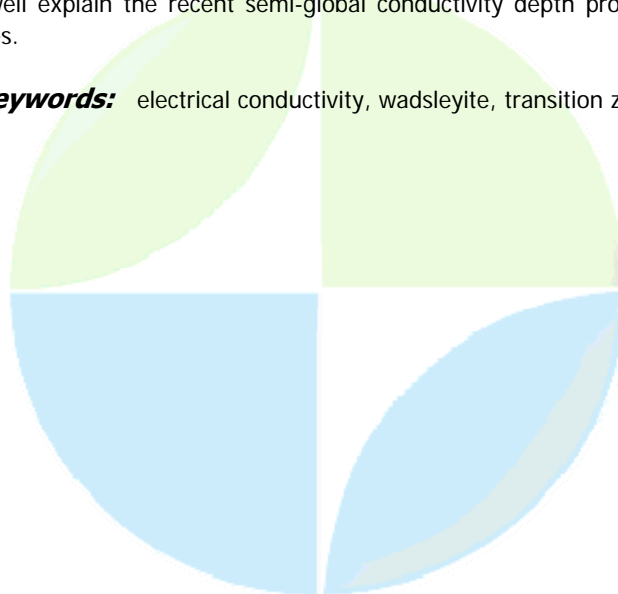
Mr. M.A. Geeth Mahinda Manthilake

Institute for Study of the Earth's Interior Okayama University, Japan

T. Matsuzaki, T. Yoshino, S. Yamashita, E. Ito, T. Katsura

Electrical conductivity of wadsleyite was measured in its stability field in order to examine the conductivity variation associated with the olivine-wadsleyite phase transition. All high pressure experiments were carried out at 16 GPa using KAWAI-type multi-anvil apparatus under controlled oxygen fugacity. Water-doped and undoped samples were used to examine the effect of water on conductivity. Two water-doped wadsleyite samples with initial water contents of 0.3 0.01 and 1.2 0.02 wt % were used for the conductivity measurements. The temperature ranges were 500-2000 K for water-undoped samples and 350-1000 K for water-doped samples. All recovered samples from the water-undoped experiments show a few hundred ppm of water (maximum 910 ppm) incorporated into the sample. Above 1500 K, the electrical conductivity values of water-undoped wadsleyite show good agreement among different runs. The average activation enthalpy is about 1.7 eV. We consider that the small polaron conduction dominates above this temperature. Below 1000 K, the conductivity systematically increases with increasing water content. Activation enthalpy of each conductivity path show systematic decrease from 1.0 to 0.55 with the increasing water contents from 0.008 to 1.2 wt %. This observation suggests the proton conduction as a dominant mechanism at the low temperatures. Electrical conductivity of anhydrous wadsleyite in the mantle transition zone is about 310-2 S/m. Hydration enhances the conductivity of wadsleyite, by containing 0.1 % of water, the conductivity of wadsleyite increases by 0.3 log units. At 1.0 wt % of water, the conductivity becomes 110-2. The conductivity jump associated with the dry olivine-wadsleyite transition is only 0.7 log units. The hydration of olivine and wadsleyite decreases conductivity jump if water is distributed homogeneously at the bottom of the upper mantle and top of the transition zone, and it should become ~0.5 log units by 0.1 % hydration. If water is partitioned between olivine and wadsleyite, the water content of wadsleyite should be 5 times higher than the olivine, resulting in the conductivity jump of ~0.9 log units. This study shows the contribution of water to the conductivity is smaller at the mantle transition zone temperatures and it is difficult to detect water less than 0.1 wt % from electrical conductivity data. Our dry wadsleyite data well explain the recent semi-global conductivity depth profiles obtained from the electromagnetic studies.

Keywords: electrical conductivity, wadsleyite, transition zone



(S) - IASPEI - *International Association of Seismology and Physics of the Earth's Interior*

JSS011

Poster presentation

2146

Comparative study concerning intermediate seismicity dynamics within some seismic nests of the world

Mrs. Luminita Zlagnean

Solid Earth Dynamics Institute of Geodynamics of the Romanian Academy

Lucian Besutiu

Intermediate-depth earthquakes usually occur within subduction zones. Their intra-continental presence is rather rare and always constrains on the mechanism of subduction. In fact, there are only three such regions on the Earth: Hindu-Kush (Afghanistan) centered at 36.5N and 71E, Bucaramanga (Colombia) at 6.9N and 73 W, and Vrancea (Romania) at 45.8N and 26.5E. The common feature of the seismicity in these areas is the strange spreading of the hypocenters within a confined almost vertically extended volume of lithosphere (nest) completely different as compared to the situation in the subduction zones. The paper aims at analysing some peculiarities of the above-mentioned seismic nests, starting with their geographical and tectonic setting and going on with a statistical analysis of the seismic events. Vrancea nest appears at the junction of three major lithospheric compartments: Intra-Carpathian microplate, Moesian microplate and East-European plate. Hindu-Kush is located at the western end of a broad deformation belt, within the collision zone between Indian and Eurasian plates, while Bucaramanga nest locates in the convergence zone of the four tectonic units: Panama Block and South American, Carribean and Nazca plates. Comparative analysis regarding geometry and space - time dynamics of the intermediate-depth seismicity within the three seismic nests was made based on statistics approach. Two seismic catalogues were used as raw data. The IRIS catalogue (1964 - 2004) was used for location and magnitude of the earthquakes in the Hindu-Kush and Bucaramanga nests, and the ROMPLUS catalogue (1940 - 2004) provided information on the Vrancea events. In order to perform the above-mentioned analysis a similar approach as previously used for studying dynamics of the Vrancea intermediate-depth seismicity was employed. On the overall, time-series of earthquakes were clustered in several time spans, generally ranging between two major seismic events. Besides, an analysis of earthquake frequency versus depth clearly showed a spatial clustering of the intermediate-depth seismicity in all studied areas. Among the peculiarities revealed by the above-mentioned analysis it is worth mentioning: (i) high velocity bodies associated to seismic zones were revealed by seismic tomography in all three cases: however, while intermediate earthquakes occur inside the high velocity body in Vrancea and Hindu-Kush nests, in Bucaramanga they locate at its boundary; (ii) a vertical clustering of the lithosphere, somehow different from one seismic nest to another, was revealed by the presence of increased earthquake frequency zones at various depth; (iii) time-space dynamics of the intermediate-depth seismicity within thus revealed lithospheric clusters may slightly differ with the depth and nest location; (iv) a strange seasonal variation of seismicity within the nests, that seems to relate to the longitude, was revealed with no explanation. By comparing each to another, Vrancea and Hindu-Kush nests exhibit closer peculiarities, while Bucaramanga seems to behave closer to the subduction zones. The present research has been partly funded by the Romanian National Authority for Scientific Research through the grant CEEEX-732/2006.

Keywords: seismic nest, earthquakes statistics, geodynamics

(S) - IASPEI - *International Association of Seismology and Physics of the Earth's Interior*

JSS011

Poster presentation

2147

3-D geomagnetic impulses: Synopsis of field components at the CMB

Dr. Ludwig Ballani

Geodesy and Remote Sensing GeoForschungsZentrum Potsdam (GFZ) IAG

Hans Greiner-Mai, Dietrich Stromeyer, Ingo Wardinski, Jan Hagedoorn, Aude Chambodut

Geomagnetic impulses ('jerks') were discovered at first in one field quantity: the dY/dt secular variation component. Because of the integral 3-D character of the field, every episodic process affects all the three field components, however often in a different way. Thus, for a comprehensive description of such processes, which give important hints for the investigation of the core-mantle boundary region, all field components should be checked commonly. We analyse several global data sets within the time span 1980-2000 with respect to the occurrence of geomagnetic impulses (around the year 1991) in the single components. We study their mutual correlations, and try to clarify its common (vectorial) structure at the earth surface. Utilising these findings and assuming a mantle conductivity model (radially dependent, weak conducting and bordered by a high-conductive base layer) in a second step, we apply the non-harmonic downward continuation method to track and to analyse the distribution of geomagnetic impulses for all single field components at the CMB where they appear at an earlier stage as seen at the earth surface. Subsequently, we merge the different components for a synoptical vectorial view of the impulses found. The results of these determinations, which include the effect of a conducting mantle for the first time, mark only an initial step. Further decompositions of the space-time behavior of the vectorial impulse will be necessary to understand in more detail the physical mechanism behind.

Keywords: jerk, magnetic field components, core mantle boundary



(S) - IASPEI - *International Association of Seismology and Physics of the Earth's Interior*

JSS011

Poster presentation

2148

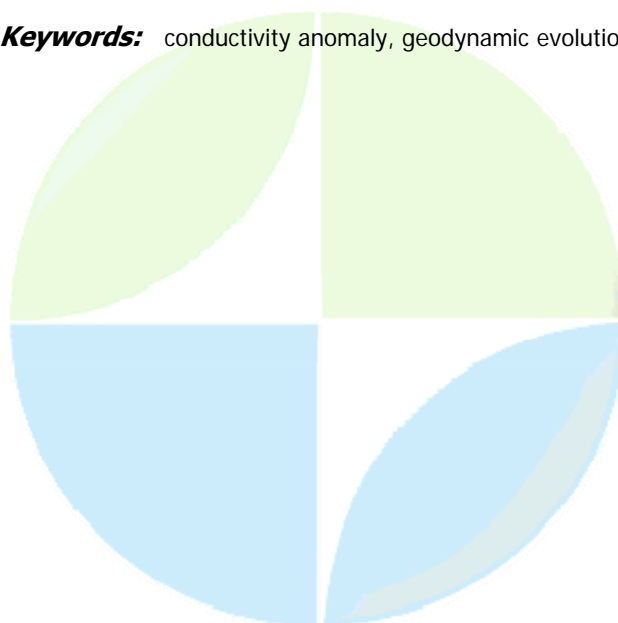
Origin and evolution of Northwest Indian conductor derived from geomagnetic deep sounding and thermo-geodynamical processes

Dr. S N Prasad

Geophysics National Geophysical Research Institute (NGRI) IASPEI

Aravalli cratonic province situated in the northwestern part of Indian shield, forms one of the most unusual late Archean Proterozoic terrain consisting of complex geotectonic elements and geophysical features. This region has been associated with long sustained rejuvenation since late Archeans which continued till the end of Mesozoic period. Geomagnetic deep sounding studies, which were conducted to study the deeper structures of this region, led to discovery of a major conductivity structure having a conductivity of 1 ohm. m (termed here as northwest Indian conductor), which strikes across the western part of Ganga basin and extends into foot hills of Himalaya. Modeling result indicates the depth to the top of this conductor at 32 km, which extends at least to the depth of 82 km, while lateral extent is about 110 km. This conductor is stated to be the northward continuation of Aravalli belt which was formed much before the collision of India with Eurasia. However, even after several investigations, the cause of the conductivity anomaly still remains a subject of considerable debate. Present study suggests the cause of high conductivity to be the presence of serpentinized olivine basalt peridotite at subcrustal depths and its consequent dehydration, which conforms with the prevailing thermal regime of the underlying lithosphere. Our calculations indicate melting conditions between the depths of 70 and 100 km beneath Aravalli belt, which would correspond to insitu temperatures of about 600 to 800°C, required for serpentinisation between the depths where conductive structure is located. However, if the conductivity anomaly is influenced solely by the melting, then in all likelihood it would be related in some way or other to the rise of isotherms caused by upwarped and molten asthenosphere sitting at a very shallow depth of 40-50 km beneath a prominent thermal anomaly zone situated around western margin of India. In this zone, temperature gradients and heat flow are high reaching to about 78°C/km and 97 mW/m² respectively and Moho is thinned to about 17-22 km. It is felt that the currents induced in the adjoining areas are channeled through the delineated zone of high heat flow which provides a passage to the anomalous flow of induced currents.

Keywords: conductivity anomaly, geodynamic evolution



(S) - IASPEI - *International Association of Seismology and Physics of the Earth's Interior*

JSS011

Poster presentation

2149

Celestial geodynamics and solution of the fundamental problems of geodesy, gravimetry and geophysics

Prof. Yury Barkin

Laboratory of Gravimetry Sternberg Astronomical Institute IAG

The motion of the planet consisting of an external shell (mantle) and a core (rigid bodies), connected by a viscous-elastic layer and mutually gravitationally interacting with each other and with external celestial body (considered as material point) is studied (Barkin, 2001; 2002; Barkin, Vilke, 2004). Relative motions of a core and a mantle are studied in the assumption that the centres of mass of a planet and an external perturbing body move on unperturbed Keplerian orbits around of the general centre of mass of the system. The core and mantle of a planet have an axial symmetry and have the different principal moments of inertia. Differential action of the external body on the core and mantle cause the periodic relative displacements of their centres of mass and their relative turns. Approximate solution of the problem was obtained on the basis of methods of linearization, averaging and small parameter method. The obtained analytical results are applied to the study of the possible relative displacements of the core and mantle of the Earth under gravitational action of the Moon. For suggested two-body Earth model and in the simple case of circular (model) orbit of the Moon a phenomenon of periodic oscillations of the core with the fortnightly period and with an amplitude 11.5 mm was observed. More remarkable phenomenon is a cyclic turn with same period (13.7 days) of the core relatively to the mantle with "big" amplitude 152 m (at core surface). In another model problem the deformations of elastic mantle due to relative displacements of the core are studied. The mantle we consider as elastic (homogeneous and isotropic) layer, and core as a rigid spherical body. In the undeformed state centers of mass of the mantle and core coincide and shells have concentric positions. We admit that mantle and core are subjected by differential action from the side of external celestial bodies. Due to this action shells undergo by the forced mutual mechanical interaction. The core pushes on the mantle and deforms its inner surface and all mantle layers. We give an analytical description of mentioned deformations of the mantle by the small displacements of the core. Here we consider restricted treatment of problem and believe that displacements of the core relatively of center of mass of the planet (by undeformed mantle) are given. Formally it means that here we do not take into consideration deformations of the mantle under attraction of the external celestial body. In accordance with linear theory of elasticity it can be studied separately. An analytical description of the possible geocenter displacements is given. Obtained results confirm a general Barkin's model (1999, 2002) that induced relative shell oscillations can control and dictate cyclic and secular processes of energization of planets and satellites in definite rhythms and in different time scales. The phenomena of inversion changes of the Earth figure, its tension states and deformation fields in opposite hemispheres, inversion of gravity in opposite hemispheres, the directed redistribution of the oceanic and atmospheric masses from one hemisphere to opposite hemisphere, density inverse changes in opposite hemispheres, inversion of variations of activity of the planetary processes (seismicity, volcanism, geyser activity) and others have been predicted and studied on the base of developed geodynamical model Barkin (1995-2007). The following fundamental problems of geodesy, astrometry, gravimetry and geophysics have been explained and solved: 1. secular drift and periodic motions of the geocenter and the core of the Earth; 2. directed mass redistribution of the Earth; 3. the Earth pole secular drift; 4. the Earth non-tidal diurnal acceleration; 5. lengthening (shortening) of parallels of the South (North) hemisphere; 6. contrast and asymmetric expansion and contraction of hemispheres; 7. non-tidal gravity variations due to the Earth core displacements; 8. height variations at the Earth surface; 9. inversion phenomena in activity of

volcanism and seismicity of the Earth; 10. the sea level rise and sea surface changes in the last century; 11. the solution of the "attribution problem" about mechanisms of the secular sea level rise (SLR); 12. hour variations of natural processes and others. Referenses Barkin Yu.V. (2002) Explanation of endogenous activity of planets and satellites and its cyclicity, News of Russian Academy of Natural Sciences, Section of the Earth sciences. Issue 9, December 2002. pp. 45-97. In Russian.

Keywords: geodynamics, geodesy, geophysics



IUGG

XXIV2007

PERUGIA
I T A L Y



(S) - IASPEI - *International Association of Seismology and Physics of the Earth's Interior*

JSS011

Poster presentation

2150

Mantle wedge dynamics versus crustal seismicity in the Apennines (Italy)

Dr. Francesca R. Cinti

Sismologia e Tettonofisica Istituto Nazionale di Geofisica e Vulcanologia IASPEI

Guido Ventura, Francesca Di Luccio, N. Alessandro Pino

In the Apennines subduction (Italy), earthquakes mainly occur within the overriding plate, along the chain axis. The events concentrate in the upper 15 km of the crust above the mantle wedge, and focal solutions indicate normal faulting. In the foreland, the seismogenic volume affects the upper 35 km of the crust. Focal solutions indicate prevailing reverse faulting in the northern foreland and strike-slip faulting in the southern one. The deepening of the seismogenic volume from the chain axis to the foreland follows the deepening of the Moho and isotherms. The seismicity above the mantle wedge is associated with uplift of the chain axial zone, volcanism, high CO₂ flux, and extension. The upward pushing of the asthenospheric mantle and the mantle-derived, CO₂-rich fluids trapped within the crust below the chain axis causes this seismicity. All these features indicate that the axial zone of Apennines is affected by early rifting processes. In northern Italy, the widespread and deeper seismicity in the foreland reflects active accretion processes. In the southern foreland, the observed dextral strike-slip faulting and the lack of reverse focal solutions suggest that accretion processes are not active at present. In our interpretation of the Apennines subduction, the shallower seismicity of the overriding plate is due to the dynamics (uprising and eastward migration) of the asthenospheric wedge.

Keywords: apennines crustal seismicity, rifting, subduction

PERUGIA
ITALY



(S) - IASPEI - International Association of Seismology and Physics of the Earth's Interior

JSS011

Poster presentation

2151

Some regularities of the plate motion and space redistribution of big earthquakes

Prof. Yury Barkin

Laboratory of Gravimetry Sternberg Astronomical Institute IAG

Jose Manuel Ferrandiz, Miguel Garcia Ferrandez

The general regularities in the motion of lithosphere plates and in spatial distribution of epicenters of the largest seismic events on the Earth surface in 20 century are investigated. Plates and earthquakes by the closest image are connected with each other. The seismicity is most brightly shown on boundaries of plates, and seismic belts (zones) determine these boundaries and configurations of the plates. On the other hand it is enough sure the parameters of global lithosphere rotation are determined (Greep, Gordon, 1990; Argus, Gordon, 1991; Barkin, 2000). The certain geometrical, kinematic and dynamic regularities of plate motion have been established (Barkin, 2000). The maximal tension at sliding of lithosphere and, accordingly, the strengthened accumulation of elastic energy and the most active displays of seismic activity should take place along the inclined equator of rotating lithosphere. Therefore we had the right to expect, that the pole P_w of the axis of global rotation of lithosphere, the pole P_m of the angular momentum of relative motion of plates and the pole P_s of a planetary (most active) seismic belt should have a close positions to each other. Results of the fulfilled research have confirmed the made assumption. Thus, the global rotation of lithosphere organizes (in planetary scale) and directs seismic events, and its equator of rotation is set actually the position of a planetary seismic belts (zones) of the most active seismic events, as it is observed actually. The dynamic model of lithosphere plates and lithosphere with various powers of oceanic and continental areas (Barkin, 2000) has been used for analysis. Only surface displacements are considered in this model in accordance with known kinematical theories NNR-1 and HS-2 (Greep, Gordon, 1990; Argus, Gordon, 1991). The special computer method of axography (Ferrandez Garcia et al., 2002) has been used for determination of the most active poles (P_s) of latitudinal and longitudinal alignment in positions of epicenters of large earthquakes in 20th century (coordinates in degrees): 1) 65.5 S, 60.5 E. (the analysis of 112 largest earthquakes in 20th century); 2) 53.5 S, 45.5 E (392 earthquakes with $M > 7$); 3) 54.5 S, 41.5 E (112 earthquakes); 4) 52.5 S, 56.5 E (392 earthquakes) etc. Various indexes of longitudinal (1, 2)), latitudinal (3)) and equatorial ordering (4)) (Ferrandez Garcia et al., 2000) have been used. The obtained coordinates of a pole of a seismic belt are coordinated with each other and with corresponding coordinates of the following poles (Barkin, 2000b): pole 49.0 S, 65.0 E of angular velocity of global rotation of lithosphere; pole 45.4 S, 57.6 E of the angular momentum of relative motion of lithospheres plates under theory HS2-NUVEL1; pole 48.1 S, 63.5 E of the angular momentum of global rotation of lithosphere. It is shown, that the vector of the principal moment of forces of inertia L_D of lithosphere (together with the Earth) is located in an equatorial plane and directed to descending node of seismic belt W_s (longitude 145.4 E). The centre of mass of lithosphere C_l with coordinates 41.0 N, 36.0 E is located near to the big seismic belt. The pole P_s is located on the other big seismic belt covering big northern arch of Pacific ocean, with ascending unit on equator (a longitude 105.0 E and an inclination about 55.0 degrees), up to seismic zones of South America. With poles of a vector of the moment of inertia forces of lithosphere, caused by the Earth rotation, the extended zones of active seismicity are connected. They form of the spirals located in the field of longitudes 90-180 E (spirals are twirled clockwise) and 270-360 E (are twirled counter-clockwise) with the general orientation in a direction the north - south. Their origin can be connected with the dynamic role of forces of inertia for non-spherical lithosphere. The moments of these forces and the corresponding motions of plates result in additional

accumulation of elastic energy and influence on the spherical turns of plates. Three ring zones with the centers located on the basic seismic belt (with coordinates 30 N, 85 E; 15 N, 120 E; 5 S, 290 E) are marked. Ring zones are closely connected to arc zones on plate boundaries and it serves as the indication, that activation of seismicity and structure and position of ring zones are determined by the general mechanism.

Keywords: lithosphere, rotation, seismicity



IUGG

XXIV2007

PERUGIA
I T A L Y



(S) - IASPEI - International Association of Seismology and Physics of the Earth's Interior

JSS011

Poster presentation

2152

Earthquakes and the State of Stress in the Outer Rise

Dr. Jascha Polet

Institute for Crustal Studies University of California at Santa Barbara IASPEI

Hong Kie Thio

The outer rise represents a long wavelength upwarping of the oceanic plate just before it dives into the mantle. A temporal and spatial correlation may exist between interplate and intraplate (both in the outer rise as well as at greater depths within the subducting plate) earthquakes, with intraplate events possibly serving as stress gauges of the subduction earthquake cycle. To examine spatial and temporal patterns in intraplate seismicity, we have compiled a catalog of worldwide shallow intraplate earthquakes, using an automated search algorithm based on local subduction geometry and the focal mechanisms from the Global CMT catalog. With this catalog, we have confirmed the preferential occurrence of normal faulting outer rise events after large interplate thrust events, in particular after tsunami earthquakes. Compressional outer rise events also appear more frequently after interface events, an observation that is difficult to explain using only a simple elastic bending model in combination with an in-slab compressional or extensional force. We also examined the orientation of the fault planes of the outer rise earthquakes with respect to the local subduction zone reference frame. To explain our results, we propose that a significant number of tensional outer rise earthquakes occur on pre-existing seafloor fabric and that compressional outer rise events are more likely to occur in response to local perturbations of the stress field caused by, for example, the subduction of bathymetric features. We will also show the results of a comparison of the mechanisms of the outer rise earthquakes with seafloor bathymetry and refraction data for specific regions. In addition to the analysis of the intraplate earthquake catalog, we also intend to present the results of an investigation of the January 13 Kuril Islands Mw=8.1 normal faulting outer rise earthquake, which occurred in close proximity to an Mw=8.3 interplate event two months earlier. We are primarily interested in determining the depth extent of its rupture process through the modeling of seismic waveforms and tsunami data.

Keywords: subduction, earthquake, outer rise



(S) - IASPEI - *International Association of Seismology and Physics of the Earth's Interior*

JSS011

Poster presentation

2153

Roles of lateral viscosity variations caused by stiff subducting slabs and weak plate margins on long-wavelength geoid anomaly

Dr. Masaki Yoshida

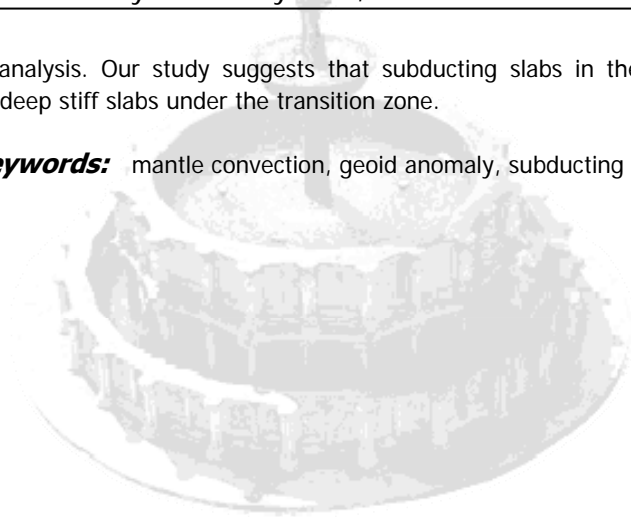
Institute for Research on Earth Evolution (IFREE) JAMSTEC IASPEI

Tomoeki Nakakuki, Motoyuki Kido

The observed geoid anomaly shows very broad highs over the subduction zones, especially over the circum-Pacific trench, when the longest-wavelength components (the spherical harmonic degree are 2 and 3) are subtracted (Hager, 1984). Our previous work (Yoshida, 2004) has shown that the long-wavelength geoid anomaly is significantly affected by the lateral viscosity variations (LVVs) in the mantle, i.e., stiff (high viscous) subducting slabs and weak (low viscous) plate margins related to the plate-tectonic mechanism, by the use of the 2-D mantle convection model. In this study, we have examined possible effects of such LVVs on the long-wavelength geoid by using 3-D spherical shell models. In contrast with a traditional propagator matrix method by Hager, our new numerical approach can treat the mantle flow including LVVs. The finite volume method is used for the discretization of basic equations governing the instantaneous mantle flow with spatially variable viscosity. To construct more actual global density models compared with our previous models (Yoshida et al., 2001; Yoshida, 2004), we have used a model coupled with (1) the global subducting slab model based on the seismicity in the upper mantle, and (2) the S-wave global tomography model (Becker and Boschi, 2002) in the lower mantle. The radial viscosity variation is layered; the lithosphere, the upper mantle, the transition zones, the lower mantle, and the bottom boundary layer. The low viscous asthenosphere is also considered. The reference viscosity is fixed at 1021 Pa s in the upper mantle. The viscosity contrast between the lithosphere and the mantle is taken to be 104.5, which is the actual effective viscosity of the lithosphere. The viscosity of the plate margins is determined by using the global strain-rate model (Kreemer et al., 2003). First we have calculated the geoid anomaly by using a no-LVV model, in which the stiff subducting slabs and the weak plate margins are not considered. The result shows that geoid highs over the subduction zones arise only when the vertical viscosity contrast between the upper mantle and the lower mantle (RLM) is around 103. This value seems to be one order larger than the viscosity contrast suggested by the post-glacial rebound analysis (e.g., Peltier, 1998). We have next imposed the stiff subducting slabs only in the upper mantle, the viscosity of which is the same as that of the lithosphere, on the no-LVV model. The geoid anomaly shows regionally strong negative pattern over the subduction zones, especially, the Jawa and the South America trenches, even when RLM is significantly high, 104. This is because the surface deformations in such regions strongly depress due to the mechanically strong coupling between the lithosphere and stiff subducting slabs. When we have imposed weak plate margins on this model, the geoid pattern remains largely unchanged. Here we have systematically examined the effects of the viscosity contrast of subducting slabs in the range between 100 (i.e., no viscosity contrast) and 104.5 on patterns of the geoid anomaly. We have confirmed that when the viscosity contrast of the subducting slabs is around 101 to 102, the geoid anomaly over the subduction zones becomes positive pattern over such regions, if RLM is around 103. Imposing weak plate margins on this model reproduces the broadly positive anomaly which explains the observation. If RLM is lower than 102, the geoid anomaly over the subduction zones still remains broadly negative. These results indicate that the viscosity of subducting slabs is significantly weaker than that of lithosphere. When the low viscous layer under the transition zone, i.e., the second asthenosphere (Cserepes and Yuen, 2000) is included, the broadly positive anomalies over the subduction zones emerge when RLM is 101.5 to 102, which is within the range of the viscosity contrast derived from the

post-glacial rebound analysis. Our study suggests that subducting slabs in the upper mantle is not strongly coupled with deep stiff slabs under the transition zone.

Keywords: mantle convection, geoid anomaly, subducting slab



IUGG

XXIV2007

PERUGIA I T A L Y



(S) - IASPEI - *International Association of Seismology and Physics of the Earth's Interior*

JSS011

Poster presentation

2154

Folds evolution and basin development in the hinterland of an orogen: the Almanzora neogene-quaternary corridor (SE Betic Cordillera, Spain)

Mr. Antonio Pedrera

Departamento de Geodinamica Universidad de Granada

Jess Galindo-Zaldvar, Ana Ruz-Constn, Carlos Duque-Calvache, Ngel Carlos Lpez-Garrido, Carlos Marn-Lechado, Carlos Sanz De Galdeano, Inmaculada Serrano

The Almanzora Corridor is an E-W elongated depression located on the internal zones of the Betic Cordillera. Its growth is associated with a complex structural interaction dominated by folding and related faulting, developed in a changing stress scenario. (a) During the Early Tortonian, a N-S directed compression is associated to the northwards propagation of deformation, with progressive folds growth, first starting in Sierra de Los Filabres antiform and then, in Sierra de Las Estancias antiform. (b) Later, since Tortonian, an anticlock-wise rotation in stress field occurred, the shortening direction changed to NW-SE with an orthogonal associated extension. Therefore, the maximum stress axis became oblique to the previous E-W oriented Sierra de Los Filabres fold producing dextral shear deformation along a wide band located along the corridor and Sierra de las Estancias. Geophysical data (2D gravity models, 2D MT images, hypocenter distribution and earthquake focal mechanism solutions) show the presence of large low-angle crustal detachments that allow the folds growth in their hanging walls since the Tortonian. The main outcropping active faults are NW-SE and E-W normal faults. The crustal thickening process is still active in the Central Betic. Both the low and high-angle faults, active in a variable stress field, are the responsible of the present-day seismicity of the region pointing the need of the crustal studies to characterize the seismic hazard.

Keywords: paleostress evolution, fault overprinting, fault related fold



(S) - IASPEI - *International Association of Seismology and Physics of the Earth's Interior*

JSS011

Poster presentation

2155

3D Seismic Velocity Structure and geometry of plate boundary around the rupture area of the 1968 Tokachi-Oki Earthquake

Dr. Asako Kuwano

Earthquake Reserach Institute University of Tokyo IASPEI

Ryota Hino, Masanao Shinohara, Tomoaki Yamada, Kimihiro Mochizuki, Kazuo Nakahigashi, Shinichi Sakai, Toshihiko Kanazawa, Yojiro Yamamoto, Akira Hasegawa, Shinichiro Amamiya, Yoshio Murai, Tetsuotakanami

We obtained precise hypocenter distribution and the three dimensional seismic velocity structure in the rupture area of the 1968 Tokachi-Oki earthquake ($M_w=8.3$), the largest interplate earthquake in the last four decades in Japan Trench subduction zone, by a seismic tomographic inversion technique using data obtained by Long-term OBS observation in 2005 and the aftershock observation in 1995. The long-term observation was conducted for eight months using 18 LOBSs. The hypocenter distribution simultaneously determined with P and S wave velocity structure shows landward dipping planar shape. The planar distribution is thought to indicate that an interplate seismicity is dominant in the study region. The subducting oceanic crust and the slab mantle were well imaged as dipping layers with V_{ps} of 7 and 8 km/s. The seismic velocity in the mantle wedge varies along the trench axis direction. Its velocity just above the rupture area of the 1968 earthquake seems to be larger than that of the surrounding area and takes its maximum value near the location of the large coseismic slip estimated by the local strong motion records of the 1968 earthquake. From the obtained focal depth distribution of the interplate earthquakes, we found that the strike and the dip of the plate boundary change at the northern limit of the rupture area of the 1968 earthquake. It perhaps suggests that the geometry of the plate boundary is one of important factors controlling the spatial extent of the coseismic rupture propagation.

Keywords: subduction, crustal structure, japan trench



(S) - IASPEI - International Association of Seismology and Physics of the Earth's Interior

JSS011

Poster presentation

2156

Seismic tomography model on Google Earth

Dr. Yasuko Yamagishi

IFREE JAMSTEC

Hiroshi Yanaka, Seiji Tsuboi

Visual presentation of various geophysical and geochemical data together gives us intuitive sight of the Earth's interior. Especially, an overlay plot of geochemical data of rock and seismic tomography data are useful for correlating internal temperature anomalies to geochemical anomalies. Each data, however, has its own format and own presentation tool. In this study, we aim to display both geochemical data of rock and seismic tomography data together. We adopt Google Earth as a geoscience data browser. Google Earth makes use of a XML called KML to display graphical features. We have developed softwares to convert geochemical data of rock and seismic tomography data to KML files. The seismic tomography data are provided by ASCII text files. Our software converts the original seismic tomography data to a KML file for each depth. It can deal with both global and local tomography data. The software can extract a part of the original data so that you can select a displayed area of the tomography model. In addition, you can produce a KML file of a vertical cross section along any profile you like. The vertical cross section of the seismic tomography model stands on the Earth's surface. You can choose where to display the data at each depth, either on the Earth's surface or above the surface. The altitude at which the tomography data is displayed on Google Earth is equal to the distance from CMB to the depth of the model. This tomography data is positioned in the vertical cross section. We have developed softwares to convert geochemical data and seismic tomography data to KML files, which give us overlay views of these data on Google Earth. We are now planning to provide our conversion software as an online software (<http://www.jamstec.go.jp/pacific21/TMGonGE/home.html>).

Keywords: seismic tomography, google earth



(S) - IASPEI - International Association of Seismology and Physics of the Earth's Interior

JSS011

Poster presentation

2157

To the problem of mechanism definition of earthquakes focuses of Armenia

Dr. Mariam Mkrtchyan
IAGA ISS011 IASPEI

In contradiction to the generally accepted definition method of earthquake focus our approach provides for the accuracy estimation solution for each of nodal plane each taken separately. It becomes possible by definition of the limitedly admissible turning of the nodal plane around an axis N and direction SLIP. It allows in a quantitative way to formalize the geometric limitation of the confident sectors of pressure and tension. The introduction of such accuracy solution characteristics is accounted for the necessity of quantitative information on pressure and tension spheres with the aim of study of tectonic fields of tensions and deformations according to the data on the earthquake focus mechanism. The data on the earthquake focus mechanism allow describing by definitely spatial and temporal groups of focuses the field of tectonic tensions existing in seismoactive spheres of lithosphere. The obtained characteristics by describing this field of orientations of main axes tensions in every earthquake focus allow in their, turn to solve the apportionment problem of breach of plane realized in a focus proceeding from analysis relation between orientations of these axes with a direction of strike-slip motion on each of these 2 nodal planes each taken separately. For the definition of the fault plane realized in a focus the data on tectonic tension orientations were used for the of Armenia obtained on the basis of the earthquake focus mechanism analysis with $M \geq 4.5$ over a period of 1960-2000 years. Thus the utilization of this method gave an opportunity to come to the description of multivariant solutions of focus mechanism to more complex and more informative record. The algorithm program is based on the method of maximal probability. As a result of this the totality of solutions of the given confident level (85%) is revealed compatible with the true sphere characterizing the uncertainty degree of the unknown solution. As a result of a count the values of angular coordinates X and Y are established corresponding to the maximal value of probability function and also the values of coordinates $l_x, l_y, \theta_x, \theta_y$ in 85% of confidence interval sphere. The choice of confidence interval sphere is simple in view of discreet disposition of the stations on the surface of the Earth. At a quite uniformity and density of disposition of the stations many solutions are obtained having the same probability. In the end the values of angular coordinates of pressure and tension axes are established corresponding to maximal value probability function and 85% of confidence interval sphere disposed at an angle of 45° to X and Y axes. As a result of dimensional analysis of confidence interval spheres of X,Y,P,T axes all the solutions are conditionally divided into 3 groups. Thus in case of compact I and II groups of confidence of the possible solution spheres the obtained results may be considered as confident. In case of confidence of the III group with the majority of solution types the joint analysis of aftershock sphere definition results is required and directions of rupture formation in earthquake focus. The analysis and accuracy estimation of the earthquake focus definition mechanism with the utilization of the modern program provides with the increase of the confidence of the obtained solutions.

Keywords: mechanismdirectiondefinition

(S) - IASPEI - *International Association of Seismology and Physics of the Earth's Interior*

JSS011

Poster presentation

2158

Surface Wave Tomography beneath the Gulf of California Rift Zone

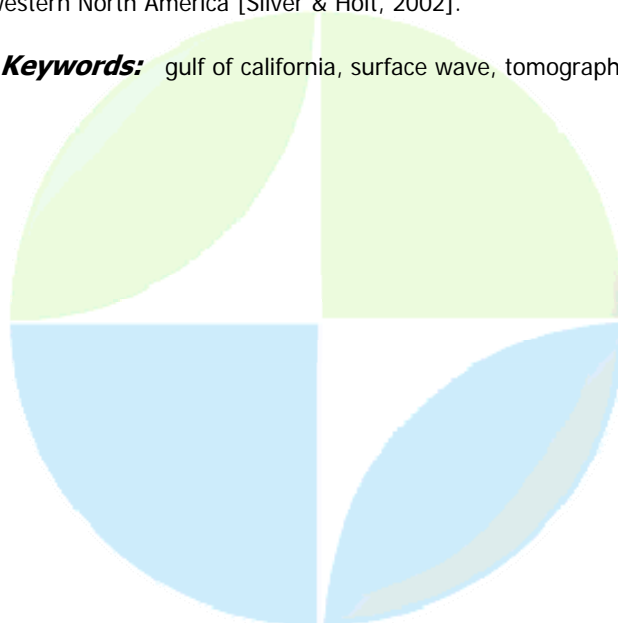
Mrs. Xiaomei Zhang

Department of Earth Sciences Utrecht University

Hanneke Paulssen, Sergei Lebedev, Thomas Meier

We present an average 1-D shear velocity model and a set of fundamental mode Rayleigh wave phase velocity maps including azimuthal anisotropy of the Gulf of California (GofC). The study was based on applying the two-station-method to earthquake data recorded by the NARS-Baja network. The 1-D shear velocity model space search result confirms the presence of a low velocity zone in the upper mantle of the GofC, which was suggested by regional and global models as well. The sensitivity of our phase velocity period band (10–250 s) reaches into the transition zone (660 km). The Monte Carlo search suggests low shear velocities to this depth, which indicates that the source of the low velocities has a deep mantle origin. Therefore the common feature of the entire region is slower shear velocities than PREM down to the transition zone. From the phase velocity tomography with anisotropy (period 10–100 s, depth range 0–250 km), we observe a change in pattern of the lowest velocity regions as a function of period (depth). At 30 s the lowest phase velocities are found beneath the plate boundary in the Gulf (related to upwelling underneath the ridge). At periods larger than 50 s, the lowest velocities are found beneath the northern GofC (possibly related to a slab gap in the subducted Farallon plate). In the low period band (≤ 20 s) we distinguish two different directions of azimuthal anisotropy. In the northern part of the GofC the fast axes move from NNW (10–14 s) to NW (20 s) as the period increases. In the southern part the fast axes moves from ENE to EW. The fast NW axes are coherent with Pacific plate motion or the strike slip plate boundary motion. The fast EW axes in the southern part seem to be associated with gulf extension. In the period band in-between 20 to 40 s, the amplitudes of the anisotropy become very low; this could be due to upwelling underneath the Gulf. In the period band above 40 s, we lose resolution of the azimuthal anisotropy in the southern part due to lack of data. The fast axes in the northern part move from NW (at 50 s) to EW (at 100 s). The NW direction can be associated with the direction of Pacific Plate motion, and the EW fast axes agree with the fast direction of SKS-splitting measurements for southern California and northern Baja [Obrebski et al., 2006] and mantle flow beneath western North America [Silver & Holt, 2002].

Keywords: gulf of california, surface wave, tomography



(S) - IASPEI - *International Association of Seismology and Physics of the Earth's Interior*

JSS011

Poster presentation

2159

Upper Mantle Anisotropy from Shear Wave Splitting on the Southeastern Passive Margin of Arabia, Dhofar Region, Oman

Dr. Ali Al-Lazki

Seismology Sultan Qaboos University IASPEI

Cindy Ebinger, Michael Kendall, George Helffrich, Sylvie Leroy, Christel Tiberi, Graham Stuart, Khalfan Al-Toobi

As part of the Dhofar-Socotra Broadband Seismic Experiment, eighteen broadband stations were temporarily deployed on the southeast margin of Arabia in Dhofar region, Sultanate of Oman. The Dhofar-Socotra seismic experiment stations were deployed for the period September-2005 to August-2006 and covered an area of about 250km along and 100km across the margin. The spacing between stations is about 20 kilometers. The objective of this deployment is to map the structure and rheology of the crust and upper mantle of the young Gulf of Aden passive margins. This deployment is aimed at studying the transition zone across the passive margin. In this study we use shear wave splitting methodology to map upper mantle lateral anisotropy variation beneath the study area. We have categorically selected events that were at epicenter distances larger than 85 degrees. The SKS and few PKS splitting results show roughly N-S orientations for stations located on the eastern parts of the study area. This agrees with observation on stations located on the exposed Arabian shield region, in the Kingdom of Saudi Arabia. Since most of the events were coming from east, this made the analyses more difficult (i.e., only one shear-wave is excited). However, a more NW-SE orientation is consistently observed on the three most westerly stations. Generally the splitting magnitudes are small (~0.6sec). Anisotropy variations were observed to occur along the margin (not across). Such variations require careful analysis of the pre-Tertiary rocks and basement that are masked by the Tertiary deposits.

Keywords: shear wave splitting, gulf of aden, passive margin



(S) - IASPEI - International Association of Seismology and Physics of the Earth's Interior

JSS011

Poster presentation

2160

Local-scale surface-wave tomography of the Japanese islands I: A two-station approach

Dr. Kazunori Yoshizawa

Natural History Sciences Hokkaido University IASPEI

Kazuaki Miyake, Kiyoshi Yomogida

Seismic surface waves provide us with useful information on three-dimensional heterogeneous and anisotropic structures in the crust and uppermost mantle. To investigate the local-scale heterogeneity using surface waves, a two-station method or a multiple station method has been widely used to estimate local phase speed dispersion as a function of frequency. With the recent deployment of high-density broad-band seismic networks, it is now possible to reconstruct a high-resolution local seismic model working with such conventional methods of surface wave analysis. In this study, we apply a classical two-station method to the F-net broad-band seismic network (NIED) in Japan, and reconstruct phase speed distribution in the period range between 20 and 150 seconds. In this study, we used F-net broad-band seismic stations as well as several stations in Japan that are affiliated with the global seismic network. We chose seismic events with moment magnitude greater than 6.0 and depth shallower than 100 km. Prior to waveform processing, the response characteristics of all the seismograms are corrected. Surface-wave arrivals are automatically picked depending on the epicentral distance based on appropriate group speed ranges (Rayleigh: 2.6-3.1 km/s; Love: 3.0-5.5 km/s). Phase spectra for seismograms are then calculated, and are applied to two-station phase speed measurements. Two-station pairs are chosen with the following criteria: the difference in azimuth from a source is less than 0.5 degrees, and the distance between two-stations are longer than 50 km. An average station interval of F-net is less than 100 km, which is suited to estimate the local phase speed dispersion between two stations down to a relatively short period of 20 seconds. Preliminary results of Rayleigh-wave phase speed distributions at periods shorter than 50 s show a prominent slow anomaly in central Japan (the Chubu region), which is likely to be related to a thick continental crust beneath this region. In the south-western part of Japan, we can see high phase speed anomalies corresponding to the subducting Philippine-Sea plate and a slow anomaly related to mantle wedge in the period range between 20 and 70 seconds. In the eastern Japan, large-scale high speed anomalies corresponding to the subducting Pacific plate can also be identified. The results of this study suggest that local phase speed dispersion curves are well retrieved by the simple two-station method with the dense F-net broad-band seismic network. Although we have employed the classical two-station method based on a great-circle path approximation, this simple approach may need to be improved by a quantitative evaluation of the effects of off-great-circle propagation. In particular, such effects should be of importance in the period range shorter than 30 seconds at which surface waves are affected strongly by the heterogeneous crustal structure.

Keywords: surface waves, phase speed, two station method

(S) - IASPEI - *International Association of Seismology and Physics of the Earth's Interior*

JSS011

Poster presentation

2161

Local-scale surface wave tomography of the Japanese islands II: A multi-station approach

Dr. Kazunori Yoshizawa

Natural History Sciences Hokkaido University IASPEI

Haruka Takezoe, Kiyoshi Yomogida

Phase speed distributions of fundamental-mode Rayleigh waves beneath the Japanese islands are reconstructed by using a newly developed multi-station method with a regional broad-band seismic network, F-net, which has been deployed by the NIED (National Research Institute for Earth Sciences and Disaster Prevention, Japan). We estimate local phase speeds and arrival angles of the fundamental-mode Rayleigh waves from a group of stations using the multi-station method in a period range between 40 and 130 seconds. To avoid some unwanted effects caused by higher modes as well as ambient noise, we restrict seismic events at depth shallower than 50 km and with surface-wave magnitude greater than 6.0. In our multi-station analysis, we consider at first regular grids with a 1-degree interval in both longitude and latitude. Each grid point is supposed to be the center of a circle with radius of 150 km. F-net stations located in each circle are used as a group to measure local phase speed dispersion, and one of the stations in each group is set to be the reference station. We then measure phase differences for the rest of stations in the group with respect to the reference station. Perturbations of phase speeds and arrival angles are expanded in a set of B-spline functions, whose coefficients are determined by a least-squares inversion. Unlike the conventional two-station method, the array-based multi-station method does not require any concept of a ray path, and, therefore, we may allow a large deviation of an actual ray path from the great-circle direction. The local phase speeds estimated by the multi-station analysis are then used to invert for phase speed maps working with a bilinear interpolation using regular grids with a 1-degree interval. The results show that the phase speeds in a period range between 40 and 50 seconds in the Chubu region (central Japan) are 6-15 % slower than those estimated from a model based on PREM with crustal correction using an average crust model in Japan, suggesting a thicker crust beneath this region. In addition, the phase speeds in the same period range are 3-10 % higher than the reference values in the Chugoku and the eastern Kyusyu regions, indicating the effect of the subducting Philippine Sea plate. In a period range longer than 60 seconds, the phase speeds in the eastern Japan (from Hokkaido to the northern Kanto) tend to be 2-6 % faster than the reference, suggesting the effect of the subducting Pacific plate with higher shear wave speeds beneath these regions.

Keywords: surface waves, phase speed, array analysis

(S) - IASPEI - *International Association of Seismology and Physics of the Earth's Interior*

JSS011

Poster presentation

2162

Seismic structure and seismicity of the rupture areas of the Tonankai, Nankai earthquakes derived from long-term sea floor earthquake observation

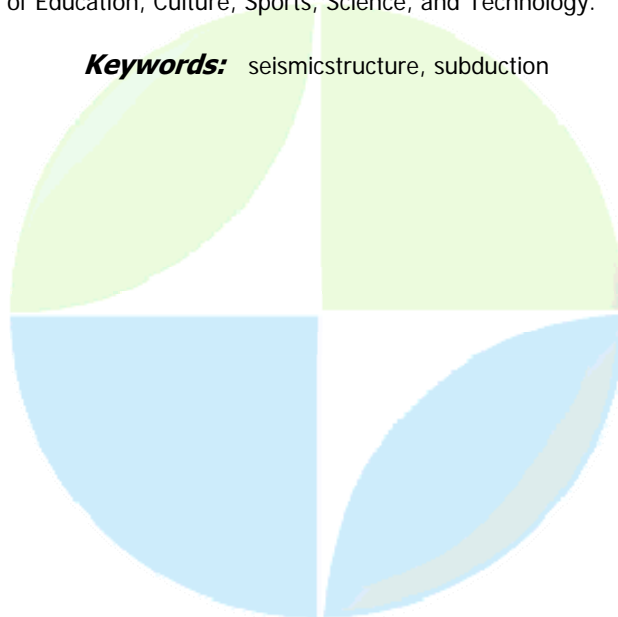
Dr. Kazuo Nakahigashi

Earthquake Research Institute Univ. of Tokyo IASPEI

Asako Kuwano, Tomoaki Yamada, Kimihiro Mochizuki, Masanao Shinohara, Shinichi Sakai, Toshihiko Kanazawa, Kenji Uehira, Hiroshi Shimizu

The large earthquakes with estimated magnitudes around 8 repeatedly occurred throughout history along the Nankai Trough. The recurrence periods are approximately 100 years after 1361, and the latest events are the 1944 Tonankai and the 1946 Nankai earthquakes. The Nankai Trough seismogenic zone is one of the most well-studied subduction seismogenic zone in the world. However, hypocenters were not able to be determined accurately by the land seismic network. Therefore, we began earthquake observations on the estimated rupture areas of the Tonankai and the Nankai earthquakes, to understand the seismic activities around the rupture area, using long-term type ocean bottom seismographs (LTOBSs). In this study, we present the seismic structure obtained by seismic tomography method and using LTOBSs and land station data. We started the observation in 2003, using 9 LTOBSs. We retrieved them and deployed 23 LTOBSs in 2004. In 2005, we recovered these 23 LTOBSs, and, with additional 2 new LTOBSs, we deployed a total of 25 LTOBSs in a region from southwest offshore of Shikoku to Cape Shionomisaki covering toward the trench axis. Those 25 LTOBSs are currently in operation. The spatial intervals among LTOBSs were about 20km. This seismic network covered the Tonankai and the Nankai rupture area. In addition, the seismic surveys with controlled sources were conducted to obtain a shallow part structure beneath LTOBSs in 2003, 2004, and 2006. Data from the recovered LTOBSs were corrected for the time drifts, and seismic events were extracted along with the data from land seismic stations according to the JMA catalogue. P and S arrivals were then manually picked. We relocated the hypocenters of those extracted events using the manually picked arrival times, and applied tomographic analyses about the crustal structure. The results of these analyses will be reported. This work is a part of the Research on the Tonankai and Nankai earthquakes funded by the Ministry of Education, Culture, Sports, Science, and Technology.

Keywords: seismicstructure, subduction



(S) - IASPEI - *International Association of Seismology and Physics of the Earth's Interior*

JSS011

Poster presentation

2163

Determining the Location of the Fault Plane for the Nankai Subduction Zone, Southwest Japan

Dr. Bogdan Enescu

Earthquake Hazards Division Disaster Prev. Res. Inst. IASPEI

Jim Mori

We estimate the location of the thrust plane for large earthquakes in the Nankai subduction zone, southwest Japan, by using high quality locations of small earthquakes. We assume that the small events in the depth range of 10 to 80 km are occurring close to the plate interface or within the subducted oceanic crust a few kilometers below. We are studying the region near the Kii Peninsula, where seismic experiments have already produced a good starting velocity model (Ito et al., 2006). We have collected waveform data at 70 seismic stations, from 450 earthquakes ($M > 1.7$) with hypocenter locations determined by both Japan Meteorological Agency (JMA) and National Institute for Earth Science and Disaster Prevention (NIED), Japan. In order to recalculate the hypocenters, we are using P- and S-waves arrival times determined by JMA, as well as high-precision differential travel times from waveform correlations of P-waves. For all possible earthquake pairs with catalog-derived distances of less than 15 km apart, waveforms on vertical component, recorded at common seismic stations, were cross-correlated to obtain differential travel times. The waveforms were filtered to 2-10 Hz and sliced in 2.00 sec. (200 time sample) windows around the P-arrival time determined by NIED. Two waveforms were considered similar if their correlation coefficient equalled or exceeded a threshold of 0.6. We are using the absolute and relative travel time data together with a double-difference tomography approach (Zhang and Thurber, 2003) to obtain an improved 3D velocity structure and better locations for the earthquakes.

Keywords: earthquake relocation, nankai subduction zone, velocity structure



(S) - IASPEI - International Association of Seismology and Physics of the Earth's Interior

JSS011

Poster presentation

2164

Seismotectonics of the southern Tyrrhenian compressive region, Italy

Dr. Debora Presti

Earth Science Dept. University of Messina IASPEI

Andrea Billi, Claudio Faccenna, Giancarlo Neri, Barbara Orecchio

The application of a new technique of earthquake location (Bayloc) and the evidences inferred by structural data in the south-Tyrrhenian area have contributed to the definition of the tectonic architecture and active kinematics of the seismogenic apparatus of the plate compressive margin in this region. Compressional displacements have resumed at the rear of the Maghrebic orogenic wedge since about 700-500 ka and are presently accommodated along a seismic belt in the south-Tyrrhenian area, where a passive margin has developed during late Neogene-Quaternary times. Main seismological results show that the studied compressive belt is characterized by spatially-discontinuous epicentral clusters with major NW-SE and SW-NE trends and by hypocentral clusters dipping toward the north at angles greater than 60. These seismic clusters are here interpreted as high-angle, S-verging, reverse fault zones constituting an early tectonic architecture of the recently-inverted (i.e. younger than about 700-500 ka) passive margin, which developed during late-Neogene-Quaternary time at the border of the Tyrrhenian backarc basin. Brittle deformations in the Quaternary volcanic island of Ustica are consistent with the geometry and kinematics of the seismic belt as deduced from the seismological data. The south-Tyrrhenian active belt may constitute an early stage of subduction of the Tyrrhenian oceanic crust beneath Sicily. A similar scenario has been hypothesized also for the westward prolongation of the south-Tyrrhenian belt off Sicily. On the basis of instrumental and historical seismic data, combined with tectonic and morphological information, a maximum seismic potential corresponding to magnitudes between 6.0 and 7.0 is proposed for the south-Tyrrhenian seismic belt as the most likely scenario. The segmented geometry of this belt should prevent from the occurrence of stronger earthquakes. These data may result important for mitigating the seismic and tsunamic hazards in such a densely populated region.

Keywords: seismicity, tectonics, dynamics



(S) - IASPEI - *International Association of Seismology and Physics of the Earth's Interior*

JSS011

Poster presentation

2165

SKS splitting measurements beneath Northern Apennines region: a case of oblique trench retreat

Mrs. Silvia Pondrelli

Sezione di Bologna INGV IASPEI

Salimbeni Simone, Margheriti Lucia, Park Jeffrey, Levin Vadim

We present here the new observations of seismic anisotropy obtained from SKS corerefracted shear waves analysis. We studied 34 teleseismic earthquakes recorded by the temporary seismic network of RETREAT project in the Northern Apennines region. For each single-event couple we calculate the anisotropic parameters (delay time and fast polarization direction) by minimizing the energy in the transverse component. Our measurements confirm the existence of two domains. The Tuscany domain, on the west with respect to the Apennines, shows mostly NW-SE fast axes directions, with a rotation toward E-W direction moving toward the Tyrrhenian Sea. The Adria domain, east of the Apennines orogen, shows more scattered measurements, with prevailing N-S to NNESSW directions; also a back-azimuthal dependence is evidenced. The transition between the two domains is abrupt in the northern part of the study region while southward it is more gradual. The detected anisotropy is located principally in the asthenosphere. Only beneath the Adria domain, where the presence of a double layer structure seems possible, a lithospheric contribution is not excluded. An interpretation of the anisotropy pattern as produced by mantle deformation is used to describe a differential evolution of the trench retreat process along the Northern Apennines orogen. The orogen-parallel anisotropy in the study region is beneath the inner part of the chain instead of beneath the crest, as occurs all along the rest of the Apennines, and no orogen-normal measurements are found. Compared to the anisotropy pattern of the typical slab retreat taking place perpendicular to the slab strike (as seen in the Northern Central Apennines), in the northernmost part of the orogen the anisotropy pattern suggests that a more oblique retreat occurred in the most recent part of the orogen's history.

Keywords: seismic anisotropy, apennines, subduction



(S) - IASPEI - *International Association of Seismology and Physics of the Earth's Interior*

JSS011

Poster presentation

2166

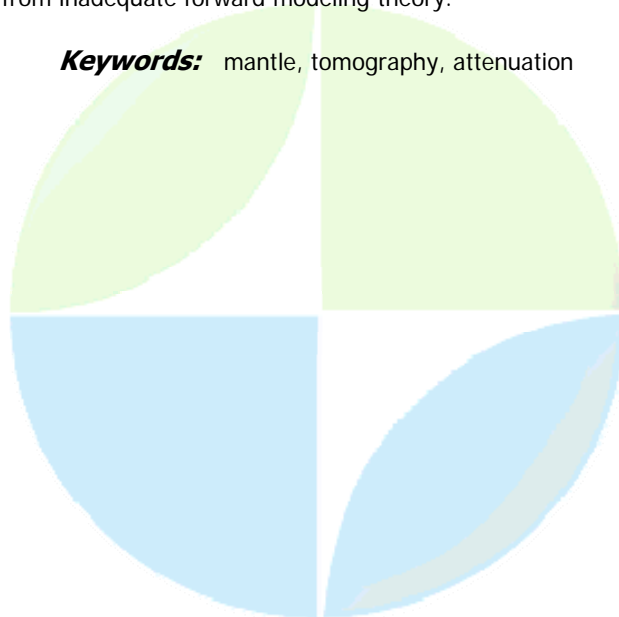
3D models of the upper mantle developed using the coupled spectral element method

Mr. Vedran Lekic

Department of Earth and Planetary Science University of California

Seismic waveforms contain information on the elastic and anelastic structure of the earth. High quality data from global seismic networks combined with approximate waveform modeling techniques that rely on first-order perturbation theory have made possible the development of high resolution global models of shear wave velocity and, recently, radial anisotropy (e.g. Panning and Romanowicz, 2006), with reliable details of wavelength 1000 km or less. However, mapping the 3D distribution of seismic attenuation has lagged behind due to difficulties in accounting for purely elastic effects of scattering and (de)focusing that result from often poorly constrained gradients of elastic structure. Furthermore, even when elastic structure is known, inaccuracies in forward modeling can obscure the anelastic signal. Therefore, anelastic 3D models only exist presently for the upper mantle and only resolve wavelengths larger than 2000 km (degree 12 in spherical harmonics). The models agree qualitatively, and, in particular, show correlation with velocity structure in the uppermost ~250 km of the mantle. However, the quantitative agreement is not as good, and the amplitudes of lateral variations, which are critical for interpretation in terms of physical processes, are not well constrained. Therefore, development of high resolution global models of attenuation is predicated upon both better retrieval of gradients of elastic structure and implementation of a forward modeling theory that accurately predicts the effects of elastic structure on seismic waveforms. In the first step of the development of a new generation 3D Q model of the upper mantle, we have applied the coupled Spectral Element Method (cSEM, Capdeville et al., 2003) which allows a complete description of the seismic wavefield to the forward modeling of long period (60s) waveforms. We present preliminary models of elastic structure developed from a waveform dataset of 3 component surface waves and overtones recorded at more than 100 stations of the IRIS/GSN, GEOSCOPE, GEOFON and various regional networks. In particular, cSEM allows accurate modeling of crustal effects, especially beneath continental shields, where conventional methods that rely on first order perturbation theory are inadequate. We explore the contamination of elastic models of the mantle that can result from inadequate forward modeling theory.

Keywords: mantle, tomography, attenuation



(S) - IASPEI - *International Association of Seismology and Physics of the Earth's Interior*

JSS011

Poster presentation

2167

P-wave mantle tomography with a focus on the South Pacific superswell obtained from traveltimes and relative traveltimes data

Dr. Masayuki Obayashi
IFREE JAMSTEC IASPEI

Satoru Tanaka, Junko Yoshimitsu, Daisuke Suetsugu, Hajime Shiobara, Hiroko Sugioka, Toshihiko Kanazawa, Yoshio Fukao, Guilhem Barruol

We collected approximately 1500 relative times of long-period P-waves by using a waveform cross-correlation from the broadband seismic waveforms data at the ocean floor and islands in the South Pacific superswell region during 2003 to 2005 (Tanaka et al. in this session). We also collected 600 first arrival times by manual picking from the same waveform data. A three-dimensional P-wave velocity structure of the whole mantle is obtained with a combination of these data and the ISC first arrival times. The tomographic image in the eastern area of the superswell is improved and different from that obtained with only the ISC data. The resultant structure shows plume like slow anomalies throughout the mantle of which details change depth by depth. At the depths greater than 1800 km, the slow anomalies observed in the western part of the superswell, i.e. the slow anomalies exist beneath the Society hotspot while there is no slow anomaly beneath the Marquesas, McDonald and Pitcairn hotspots. The slow anomalies beneath the Society hotspot extends to the Pitcairn hotspot at 1500km depth. In the upper mantle, there is a broad slow anomaly below the superswell in which strong anomalies are localized beneath the Society, McDonald and Pitcairn hotspots. The distribution of the newly revealed slow regions approximately coincides with that found in the regional tomogram (Tanaka et al. in this session).

Keywords: south pacific superswell, mantle plume, tomography



(S) - IASPEI - *International Association of Seismology and Physics of the Earth's Interior*

JSS011

Poster presentation

2168

Deformation experiments on Marble under true triaxial stress states

Mr. Shotaro Nakayama

Earthquake Prediction Research Center Earthquake Research Institute

Hiromine Mochizuki, Masao Nakatani, Shingo Yoshida

Although effect of the intermediate principal stress virtually has been done, to our knowledge, it has been only known for a brittle regime (e.g. Mogi, 1971). However, because of the stress states in the deep crust with directional tectonic force, it is obviously important to clarify the deformational behavior of rocks during plastic flow under true triaxial stress states, in which the intermediate principal stress is not equal to the minimum or maximum principal stress. We performed deformation experiments by applying three principal stresses independently: σ_1 by vertical pistons, σ_2 by horizontal pistons and σ_3 by confining pressure. All tests, true and conventional triaxial compression tests, at constant piston displacement rates were conducted using marble at dry and wet conditions. Temperature was 300 C and effective confining pressure was 220 MPa for the all experiments. True triaxial compression tests at high temperature and pressure were successfully performed, and two stress-strain curves, σ_1 - σ_3 vs. ϵ_1 and σ_2 - σ_3 vs. ϵ_2 , were obtained. From experiments carried out at different strain rates, it was found that flow stress, σ_1 - σ_3 , significantly increased with σ_2 . Description of a flow property under true triaxial stress state using the Von Mises equivalent flow stress and strain rate, which was suggested by Paterson (1987), has been tried. A sample deformed under a true triaxial stress state was cut in three planes, each of which was perpendicular to each principal stress. All of them showed clear evidence of microstructures which was not seen in an undeformed sample. In addition, there were slight differences in microstructures of the 3 planes which were presumably caused by a true triaxial stress state.

Keywords: true triaxial, flow, marble



(S) - IASPEI - *International Association of Seismology and Physics of the Earth's Interior*

JSS011

Poster presentation

2169

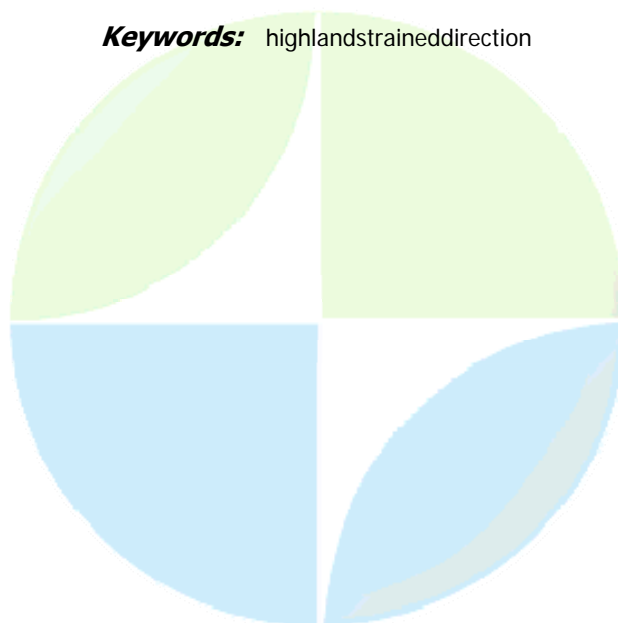
The analysis of the strained state of main seismotectonic zones of Menian upland

Dr. Eduard Gyodakyan
JSS011 Poster Presentation IASPEI

Naira Geodakyan

The spatial distribution sources of earthquakes of Armenian highland specifies on the naturally located linear structures of sources of earthquakes well correlating with tectonic zones of disturbances. The strong earthquakes are confined to areas of intersection of the longitudinal and cross folding and to Anatolian and Zagross fault zones. For definition of the strained state of main seismotectonic zones the data of mechanisms of the sources more than 185 earthquakes with $M > 4$ are involved. The analysis of the parameters of sours mechanisms specifies, that the majority of planes of rupture have dip at an angle $\alpha=450$, that is the earthquakes with abrupt planes of rupture dip prevail, characteristic at movements in sources of earthquakes, corresponding to throw and upthrow depending on orientation of axes of compression and tension strains. Precise conformity of a direction of one of planes of the break with directions of seismic hazardous zones is revealed. The data on directions of compression axes show, that almost on all seismotectonic zones the axes of compression having a nearhorizontal directions prevail, except for the zone of extend from Erzinjan to Northeast. Earthquakes with compression axis which make an angle more than 300 with a horizon here are observed. On all main seismotectonic zones prevailed directions of tension axes placed by some corners, except for seismic active zones of Javakhet highland and southern part of Transcoucasus zone, where tension axes orientations are nearer to a perpendicular direction. The dominant types of motions characteristic for separate sites of researched area are revealed. The northeast part Armenian highland is characterized by the up throw-thrust motions and the area between Taur and Anatolia - mainly by faults with the elements of left lateral slip. Earthquakes near the Lake Van characterized with down slips and in northern part of the motions of up throw type prevail. The analysis of the strained state of the region as a whole specifies on dominant strains of compression in a horizontal plane in a direction 150-200 northeast and on tension strain in a vertical plane 300-600.

Keywords: highlandstraineddirection



(S) - IASPEI - *International Association of Seismology and Physics of the Earth's Interior*

JSS011

Poster presentation

2170

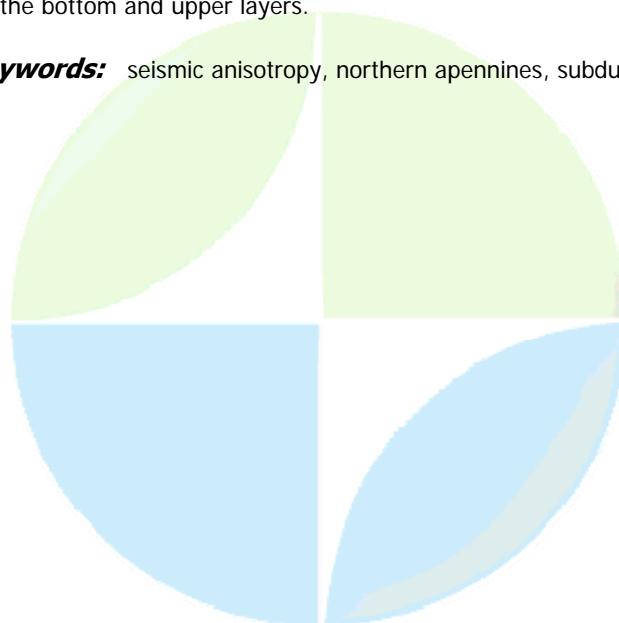
Complex anisotropy structure beneath the Po-Plain and Northern Apennines (Italy): measurements and modelling

Dr. Simone Salimbeni
INGV Bologna IASPEI

Margheriti Lucia, Levin Vadim, Park Jeffrey

The multidisciplinary RETREAT project (REtreating-Trench, Extension and Accretion Tectonics) is focused on the development of a 3D self-consistent dynamic model of the syn-convergent extension in the Northern Apennines (Italy). A temporary seismic network equipped with 35 seismic stations recorded between October 2003 to September 2006. We used the data recorded by these stations, added to those from permanent stations (MedNet and INGV network), to analyse seismic anisotropy. Previous SKS splitting analysis done for this region allowed to define some anisotropic domains. The Tuscany domain (Tyrrhenian side) shows a homogeneous NW-SE fast axes directions; the Po-Plain domain (Eastern side of the Apennines) shows a N-S to NE-SW directions. These two domains are separated by an abrupt transition zone (30-40 Km) located in correspondence of the Apenninic crest. In the Po-Plain domain, the splitting parameters are strongly dependent on backazimuth of earthquakes analysed; consequently, the presence of a complex structure (probably multilayers or dipping anisotropy) has been supposed beneath this region. To evaluate if at depth a double layer structure can justify our dataset distribution, we use the approach of Menke and Levin (2003), applying the cross convolution method they propose to discriminate whether a two-layer anisotropic model fits better than a simple one-layer model. Two time-series containing the event data and theoretical earth model are constructed. Varying the earth model it is possible to identify the one that minimizes the misfit with observed data and that is then considered the best. The method can work either on the single event recordings or also on group of events data recorded at the same station. The analysis confirm the more simple structure beneath the Tuscany side of study region, where a single anisotropic layer with a NW-SE fast polarization direction is in agreement with SKS splitting analysis. The anisotropic structure beneath the Po Plain is the main goal of the study. Here our results confirm the presence of a multi-layered structure, where a mainly NW-SE directions and delay time greater than 2.0 sec and NE-SW fast polarizations and smaller delay times are found respectively for the bottom and upper layers.

Keywords: seismic anisotropy, northern apennines, subduction



(S) - IASPEI - *International Association of Seismology and Physics of the Earth's Interior*

JSS011

Poster presentation

2171

Crustal and upper mantle structure beneath the Deccan Volcanic Province of India

Dr. Mohan Gollapally

Earth Sciences Indian Institute of Technology Bombay

Pankaj Kr. Tiwari

An experiment was launched during 1999-2006 to map the crustal and upper mantle discontinuities beneath the Deccan Volcanic Province (DVP) through deployment of broadband seismographs in phases at thirteen sites along a 600 km long profile in western India. The Receiver function analysis using about 1200 teleseismic events enabled imaging the Moho and the mantle discontinuities beneath DVP and the adjoining regions. The crustal thicknesses are estimated to range between 33 and 38 km averaging 36.2 km at all stations in DVP suggesting a normal crust. The P-to-s conversion times from the 410 and 660 km discontinuities beneath DVP are normal, as per IASP91 model. In comparison, the P410s and P660s from the mantle discontinuities beneath the Cambay rift and the Gulf of Cambay are delayed by 0.5 to 1s respectively with respect to the IASP91 model. The delays suggest presence of zones of low velocities (LVZs) in the upper mantle, coinciding with the low velocity track presumably representing the Deccan plume track starting from north Cambay. However, the LVZs are dominant only in the Gulf of Cambay and appear to extend north into the Cambay rift with diminished magnitude contrary to that expected for a plume track. Contrasting upper mantle images beneath DVP and the adjoining offshore region suggests the absence of anomalous thermal or compositional anomalies in the upper mantle beneath DVP, south of the Narmada rift, while possible rift related signatures in terms of LVZs are preserved beneath the Gulf of Cambay.

Keywords: deccan volcanic province, mantle discontinuities, receiver function



(S) - IASPEI - *International Association of Seismology and Physics of the Earth's Interior*

JSS011

Poster presentation

2172

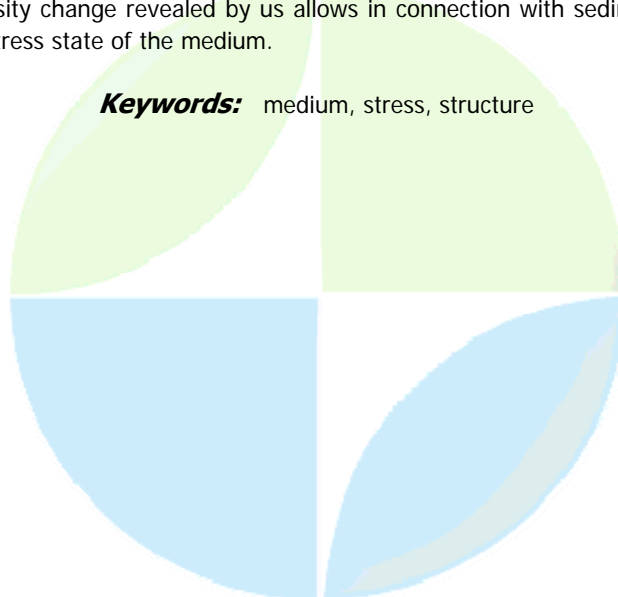
What parameters make up, what we call site effects

Prof. Ikram Kerimov

Scientific Centre of Seismology, Azerbaijan Director, Prof. Dr. IASPEI

The seismology undergoes a qualitative leap in understanding numerous physical processes in the medium and their influence the propagation and spreading of seismic radiation and seismic effects over a very long distance. Finding induced seismicity phenomena has allowed us to better understand the nature of the often discovered errors in evaluation of parameters of seismic proof construction. One of a bigger achievement between others is a discovery of the site effects. The study had been conducted since 1976 in tens of active and non-active regions and have lead us to a conclusion that one of the most important parameters of the medium, which influences the site effects, is the state of the medium, but not just its structure. That allows introducing necessary corrections to the mentioned expected reaction of the medium and, furthermore, to other issues related to creation of seismic and geophysical networks, monitoring of natural events, finding out possible earthquakes precursors and so. Moreover these two most important parameters react in differently to strong and weak influences, which must be taken into account in order to solve various seismic related problems using the earthquakes, explosions or microseisms registrations. For instance, investigations of influences of sedimentary layer thickness on seismic noise intensity distribution showed that for aseismic zones when thickness changes from 1 to 15 km the noises level changes from several hundred to several thousand of conventional units of measurements. But for seismic zones the noises level much lower and changes from 15-20 to 85-90 units. The opposite situation is observed during registration of strong signals: earthquakes and explosions. The analysis of the number of registered seismic events showed first that an increase in sediment thickness leads to a decrease in the number of registered events and secondly that the quantity of registered events in a seismic zone exceeded greatly the quantity of events registered in an aseismic zone. The next results we have got analyzing influences of stress state of the medium to registered information. As the level of stress state of the medium increases intensity of microseisms permanently decreases. Surprisingly in quiet areas it is considerably higher than in active zones, approximately in 4-12 times. From that point of view becomes understandable a physical meaning of so called seismic gap appearing during the period of earthquakes sources activation. Thus, the specificity of seismic noise intensity change revealed by us allows in connection with sedimentary layer thickness to judge the level of stress state of the medium.

Keywords: medium, stress, structure



(S) - IASPEI - *International Association of Seismology and Physics of the Earth's Interior*

JSS011

Poster presentation

2173

Error analysis of strain rates from GPS measurements based on Monte-Carlo method

Dr. Shoubiao Zhu

Geophysics Institute of Crustal Dynamics, CEA IASPEI

Yaolin Shi

The strain rates in Chinese continent have been computed from GPS data by many researchers, resulting in quite different estimates of the strain rates. Moreover, until now, researchers have not presented the errors of the strain rates yet, which are very important in geodynamics. In order to solve this problem, we propose the method to calculate the errors of strain rates, computed from GPS vectors with measurement errors, on the base of Monte Carlo technique. Taken the Qinghai-Tibet plateau as an example, independent computation of strain rate is repeated for large numbers of times (4000 times in this research) and the components of strain rates, as well as the errors, are obtained by statistical theory. The result shows that the errors of strain rates in NS, WE directions and shear components, respectively, are larger in Himalayas and both in the middle and in the east of the plateau than those in other places. The distribution of the statistical average strain rates is similar to the one calculated from the GPS vectors without considering the errors of the GPS observation. In general, the strain rate in whole Qinghai-Tibet plateau is accurate and stable. Also the result suggests that the errors of the strain rates computed from GPS measurements are mainly originated from the errors of GPS data. The accuracy of GPS survey does not meet the requirements for precisely computing the strain rates in the region where there is a small value of deformation, for example in east China with the relative errors of strain rates greater than 100%.

Keywords: strain rate field, error analysis, monte carlo method



(S) - IASPEI - *International Association of Seismology and Physics of the Earth's Interior*

JSS011

Poster presentation

2174

Investigation of Moho depth and its variations in Kope Dagh

Mrs. Elham Mohammadi

geophysics graduate student IASPEI

Mohammad Reza Gheitanchi

In this study, to find Moho depth with small error, we selected about 40 teleseismic events ($m > 5.5$ & $30 < \Delta < 95$) for investigation of Moho depth in Kope Dagh that were recorded in 4 short period seismic stations of Ghuchan seismic network. We used converted P to S phases from Moho using receiver function method. The majority of receiver functions indicate that the depth of Moho is about 40 km in this region.

Keywords: crust



(S) - IASPEI - *International Association of Seismology and Physics of the Earth's Interior*

JSS011

Poster presentation

2175

D" structure investigated using source array migration

Mr. Jeremy Chaloner

Department of Earth and Ocean Sciences University of Liverpool IASPEI

Christine Thomas, Andreas Rietbrock

The D" region of the lowermost mantle has been much studied in recent years. Better understanding of its structure will shed light on mantle convection systems and core-mantle interactions. Most studies of the lowermost mantle utilise reflected waves off the top of the D" discontinuity. This discontinuity is found in many locations, but especially where tomographic models indicate higher than average seismic velocities. Extending studies into areas of slower seismic velocities will be significant, since coverage of such areas is sparse at present. We investigate D" structure under the western Pacific, north-west of the Marshall Islands, by using earthquakes in the Philippines to construct a source array. Using recordings of up to 300 earthquakes in the Philippine Sea recorded at KIP in Hawaii, we stack records of earthquakes with suitably similar source mechanisms to perform a migration. This is used to attempt to detect reflectors in D" for both P and S-waves. This region is shown in tomographic studies to be seismically slow near the core-mantle boundary. This means that the presence and nature of a D" velocity discontinuity will have strong implications for the role of post-perovskite in creating this discontinuity. In addition the double crossing model (perovskite to post-perovskite and back to perovskite) can be tested.

Keywords: d double prime, mantle, core mantle boundary



(S) - IASPEI - *International Association of Seismology and Physics of the Earth's Interior*

JSS011

Poster presentation

2176

Lower mantle structure from scattered and diffracted PKP waves

Dr. Christine Thomas

Earth and Ocean Sciences University of Liverpool IASPEI

J.-Michael Kendall

The lowermost mantle region (D") is important to understand the dynamics of the mantle and the core-mantle interactions. In several regions reflections from the D" discontinuity are observed, however, the imaging in regions that show slow velocities in tomographic models is still hampered by the source-receiver combinations currently available. Some of the regions with slow seismic velocities have been found to exhibit strong scattering. The scatterers are thought to be close to the core-mantle boundary, but scattering throughout the mantle has also been reported. In this study we are testing new regions of the lower mantle using PKP waves recorded at the temporary EAGLE array in and the GRSN () with epicentral distances between 130 and 143 degrees. The earthquake locations are in the South Pacific for both arrays. The PKP waves to show strong scattering of PKPab waves which arrive as precursors to PKPdf and in addition large PKP-b diffracted amplitudes. In contrast, the events recorded at the GRSN show scattering of PKPab as precursors to PKPdf but much smaller PKP-b diffracted amplitudes. Explanations for the observed waveforms and amplitudes are strong low-velocity regions just above the core-mantle boundary, only a few 10s of km thick for the South Pacific to path. These strong low velocity regions act as waveguides for the PKP-b diffracted waves. They cannot be smooth layers but must show a certain roughness to produce the high-frequency scattering observed in the data. The path to needs small scatterers but there is no specific requirement for strong low velocity zones.

Keywords: lower mantle, diffracted waves



(S) - IASPEI - International Association of Seismology and Physics of the Earth's Interior

JSS011

Poster presentation

2177

**Shear-wave splitting analysis using aftershocks of the 28th May 2004
Baladeh-Iran earthquake**

Mrs. Masoumeh Dilmaghani

Azad University, Science And Research Department ministry of education of Iran IASPEI

Seyed Mojtaba Mirmajidi, Dr.Ahmad Sadikhuy, Prof.Mohammad Reza Gheitanchi

One of the best ways to study deformation in Earth's interior is detection and interpretation of seismic anisotropy, or the dependence of seismic velocities on wave propagation and polarization direction. In an anisotropic medium, shear wave split into two approximately orthogonal polarizations that travel at different velocities and write characteristic easily -identifiable signatures into three components seismic wave's trains. In this paper, we present the result of shear-wave splitting in the crust of central Alborz using aftershocks of the 28th May 2004, Baladeh-Iran earthquakes. Clear shear-wave splitting was observed on the records of the selected aftershocks. The polarization of the faster shear wave is aligned in the direction of microcracks, and coincides with the direction of the maximum horizontal compressive tectonic stress in the region. These effects are interpreted in terms of effective anisotropy of the upper crust in the region. It seems that, this shear-wave splitting in the crust is almost caused by propagation through stress-aligned fluid-saturated microcracks. It was concluded that when shear wave is polarized parallel to the crack surface, the velocity is uniform, but the velocity curve varies clearly if shear wave is polarized perpendicular to the crack surface.

Keywords: crustal anisotropy, shear wave splitting, fast wave direction

PERUGIA
ITALY



(S) - IASPEI - *International Association of Seismology and Physics of the Earth's Interior*

JSS011

Poster presentation

2178

Determination of minimum 1-D velocity model for north west Iran region, using simultaneous inversion of local earthquake travel times.

Mr. Esmail Bayramnejad
Institute of Geophysics University of Tehran

Earthquakes travel times inversion for determination of velocity structure of crust is one of the most important objectives in seismology. In simultaneous inversion method, the parameters of earthquakes and velocity model are determined initially and are improved in inversion steps. In this study, we used more than 22000 calculated travel times for first arrivals of 6000 earthquakes occurred in north west Iran region (bounded 36N-40N & 44E-50E) to estimate P wave velocities and thickness of crust in this region. We used this information to determine several initial models. At first we selected 181 earthquakes with magnitudes 4 or above that were well located. Then, we used the simultaneous inversion method to obtain the best initial and final improved model. The obtained model tested again with travel times of 2940 earthquakes with magnitudes greater than 2.5 in six independent sets. The results were in good agreement, specially for depths deeper than 8 km. The results show two low velocity shallow layers with thickness of 3 km and 2 km and with corresponding average velocity of 4.8 and 5.4 km/s for P wave. Also, a sharp change of velocity was detected in depth 23 km, where the P wave velocity increase from 6.1 km/s to 6.6 km/s. The depth of Moho was obtained to be 45 km while the P wave velocity in upper mantle was evaluated to be 8.0 km/s.

Keywords: velocity model, simultaneous inversion, travel times

PERUGIA
ITALY



(S) - IASPEI - *International Association of Seismology and Physics of the Earth's Interior*

JSS011

Poster presentation

2179

Estimation of the crustal structure beneath Isfahan(Iran) obtained from receiver functions of short period data.

Mrs. Zahra Alikhani

azad univrsity,department of science and research azad university IASPEI

Dr.Forough Sodudi, Dr.Ahmad Sadid Khuy

In this study data from 68 events recorded at 4 short period stations of Isfahan network are used to investigate the crustal structure beneath this region. Regarding the low seismicity occurred in this area, receiver function method is useful tool to obtain crustal structure of Isfahan region which considered to be as a part of stable intraplate. Receiver function are computed from teleseismic events with magnitude greater than 5.5 and epicentral distance between 30-95 deg. Resulted receiver function provide informations on MOHO, depth, velocity model, and number of crustal layers, which belong to important seismological parameters.

Keywords: receiverfunction, crustalstructure, shortperiod



(S) - IASPEI - *International Association of Seismology and Physics of the Earth's Interior*

JSS011

Poster presentation

2180

Kirchhoff migration imaging of reflectors and scatterers in the lowermost mantle beneath Central America

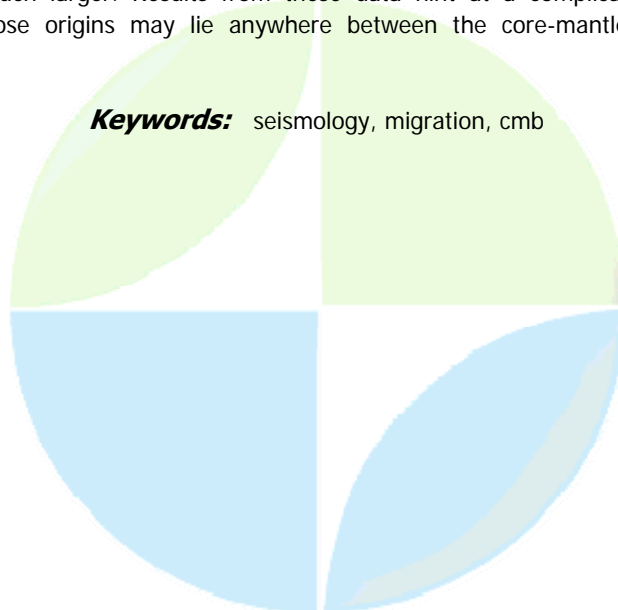
Mr. Alexander Hutko

Earth Sciences University of California, Santa Cruz IASPEI

Thorne Lay

We use tens of thousands of seismograms from South and Central American earthquakes recorded by western North American seismic networks to image the lowermost mantle beneath Central America using a 3D Kirchhoff migration method. P wave studies of the deep mantle often rely on some form of stacking of many records in order to enhance the signal-to-noise ratio of weak phases generated by deep structure, such as reflections off of the D" discontinuity. These methods, however, often assume one-dimensional structure, which is at odds with the evidence for significant heterogeneity. Kirchhoff migration is a three-dimensional stacking method that allows interactions with structure outside of the source-receiver plane, thus illuminating a much larger volume. The D" discontinuity beneath Central America has been readily observed in S wave studies and may be the result of the shear wave velocity increase associated with the recently discovered perovskite to post-perovskite phase transition. This phase transition is expected to have weaker effects on P wave velocities than on S wave velocities and the sharpness of this transition is unknown. Using data at post-critical distances, we observe structures consistent with a P velocity discontinuity about 200 km above the core-mantle boundary (CMB). Observing this using short period data suggests that the boundary must be less than a few 10s of km thick, while observation with lower frequency broadband data exclude the possibility of it being a thin layer. Whether this discontinuity is co-located for both P and S waves is difficult to resolve. Both the broadband and the short period P wave data sets also reveal a sharp out-of-plane scatterer, which may be located close to the CMB. The short period data also indicate reflectivity about 400 km above the CMB, well above the D" discontinuity, and similar reflectivity is observed under the Central Pacific. This feature appears to be more consistent with a discontinuity than a scatterer, is hinted at in the broadband data set and is not observed with S waves. We also present results using P wave data from pre-critical distances. While reflection and scattering coefficients are much lower at these distances, the imaging volume is much larger. Results from these data hint at a complicated lower mantle with multiple features whose origins may lie anywhere between the core-mantle boundary and many hundred km above it.

Keywords: seismology, migration, cmb



(S) - IASPEI - *International Association of Seismology and Physics of the Earth's Interior*

JSS011

Poster presentation

2181

Current state of deformation processes in an earth's crust of the Caucasian region

Mrs. Gedakian Naira

SS011 Poster Presentation IASPEI

Deformation processes in the Caucasian region on the basis of definitions of mechanisms of the centers of strong Earthquakes are considered. For the analysis of a field of deformations tool data of strong earthquakes for the period with 1970 on 1990 with magnitude $M > = 5.4$ and ≤ 7.0 are used. The size of speed of deformation essentially depends on a choice of seismogenic volume in this connection components of tensor average speed of deformation are certain both for region as a whole, and for the separate areas chosen for consideration. On the basis of settlement sizes the component of tensor average speed of deformation for separate elements with the equal areas on a terrestrial surface, is lead the detailed analysis of the most intensive areas of deformations in the Caucasian region. Quantitative characteristics of dominating deformation processes in horizontal and vertical planes are given. Orientations a component of tensor deformations testify that in the central part of region there are intensive vertical movements. In a southeast and a southwest deformation processes are focused mainly in a horizontal plane, but their direction variously. Thus the southeast direction of a vector of horizontal making speed of deformation in Taur-Anatolia parts of region is replaced on near meridional its orientation in the central part of region in area of Armenia, and then, passes on southwest in the structures adjoining to coast of Caspian sea.

Keywords: earth



(S) - IASPEI - *International Association of Seismology and Physics of the Earth's Interior*

JSS011

Poster presentation

2182

Mantle Convection Models with Temperature and Depth-dependent Thermal Expansivity

Mrs. Sanaz R. Ghias

Earth & Space Science Graduate Student IASPEI

Gary T. Jarvis

This study investigates the effects of temperature- and depth-dependent thermal expansivity in 2D mantle convection models in both plane-layer and cylindrical-shell geometries. For simplicity, most previous mantle convection models have used a constant coefficient of thermal expansion, a , although there are some limited earlier studies of the effects of temperature and depth-dependent coefficient of thermal expansion in plane layer models. We consider a to have the form $a(z,T) = a_z(z)a_T(T)$ and employ the results of separate mineral physics experiments to determine the functional forms of $a_z(z) = 1/(1+2.0255e-4z)^3$, and $a_T(T) = a_0 + a_1T + a_2/T^2$. Note that $a_z(z)$ decreases with depth while $a_T(T)$ increases with T . We find that the depth-dependence and temperature-dependence of a each have a significant effect on the mean surface heat flux (or Nusselt number) and the mean surface velocity of the convecting system. For $a = a_z(z)$, the decrease of a with depth causes a decrease of surface heat flux by about 25% and a decrease in mean surface velocity by about 40%, relative to the constant- a case, in either geometry. Consequently, studies of the effects of depth-dependence of a alone would seriously underestimate these surface parameters. However, when $a = a_z(z)a_T(T)$ (i.e., the temperature-dependence of a is also included) our predicted values of surface heat flow and velocity increase; $a_T(T)$ compensates for the effects of $a_z(z)$. Compared to models with $a = a_z(z)$, for Earth-like conditions our predicted values increase by 34% and 75%, respectively, in Cartesian coordinates, and by 23% and 60%, respectively, in cylindrical geometry.

Keywords: convection, thermal expansivity



(S) - IASPEI - *International Association of Seismology and Physics of the Earth's Interior*

JSS011

Poster presentation

2183

Comparison of Long Period Normal Modes from the Sumatra Earthquake Using Superconducting Gravimeters and GSN Seismometers

Prof. David Crossley

Earth and Atmospheric Sciences Saint Louis University IAG

Yan Xu

We have analyzed the available superconducting gravimeter (SG) data from the Sumatra earthquake of 2004, and compared it to similar data from seismometers of the GSN network. Our goal was to determine whether SG data can add information about the Earth through the refinement of parameters such as seismic Q and M_0 , the seismic moment of the earthquake, the latter through its effect on normal mode amplitudes. SGs are known to have very good amplitude calibration (0.01-0.1%), and SG data is now becoming available through IRIS for the use of the seismic community. Our results to date show that the determine of the Q factor of modes such as $0S_0$ is very good, but there are difference in the amplitudes determined from SGs and seismometers that may, or may not, be due to calibration effects. We will show a comparison between theoretical and observed amplitudes for low frequency modes in the range 0.3-2.0 mHz..

Keywords: normal modes, superconducting gravimeters, sumatra



(S) - IASPEI - *International Association of Seismology and Physics of the Earth's Interior*

JSS011

Poster presentation

2184

The Earth's seismicity statistics

Dr. Natalia Bulatova

Earth Structure and Geodynamics JSS011 IASPEI

The quantitative results (in 2D- and 3D- form) of time latitude dependence in the statistical analysis for the dates taken from the catalogues IASPEI and NEIC from 1900 to 1999 years and from 1982 to 2006 years, correspondently, are presented in this work. The dates (more 180 000 events) are observed separately for the groups $M=3, 4, 5, 6$ and 7 ; and the new information by modeling the earthquake epicenters activity temporary migration and connection of the Earth's seismicity with the temporary cyclical variations parameters of the Sun and the Moon was displayed.

Keywords: seismicity, geodynamics

XXIV2007

PERUGIA
I T A L Y



(S) - IASPEI - *International Association of Seismology and Physics of the Earth's Interior*

JSS011

Poster presentation

2185

Geodynamic significance of the 105 meridian of eastern longitude.

Dr. Lidia Ioganson

laboratory of Seismotectonics Institute of Physics of the Earth RAS

The 105 meridian of Eastern longitude is considered to be the critical meridian by many researches. Along this pure geographical line the essential changes of geological pattern and deep structure are observed to the West and East from it. In the area of Eastern-Siberia craton and this line is a specific axis of symmetry in distribution of the rupture trend complicating the tectonic units of the Southern mountain margins of the Eastern-Siberia craton and Mongolia. In the Chinese area this zone divides the domain of the thick continental crust of the Western China and domain of thin crust in the Eastern China . The vast area of anomalous mantle is connected to this zone within Central Asia . As to seismicity this zone is a divider between high seismic Western Mongolia and low seismic Eastern Mongolia . In this zone is marked by the chain of strong earthquakes. The zone of 105 meridian of Eastern longitude most likely represents the specific type of joint of the large continental blocks and acts from ancient geological epoch being tectonically active modern zone in its southern part.

Keywords: 105, geodynamic significance



(S) - IASPEI - International Association of Seismology and Physics of the Earth's Interior

JSS011

Poster presentation

2186

Flat to normal subduction Nazca Plate transition between latitudes 31.5-33.5S as seen from small earthquakes ($M < 4.5$)

Prof. Renzo Furlani

Subcom. de Sismología y Fís. del Int. de la Tierra Member

About 1500 small earthquakes ($M < 4.5$) recorded in a temporary network of 15 broadband seismographs on west-central show a highly not uniform seismicity distribution of the subducted Nazca Plate just within its transition from flat at the north to normal at the south, and within a 95-250 km depth range. To the north, the seismicity clusters are closely located on the Juan Fernandez ridge trace, obtained from magnetic data extrapolation, which trends predominantly to east and slightly to northeast. Smoothing spline surface approximations show topographic highs and lows presumably related to the original shape of the ridge, although in average corresponds to the southernmost flat portion of the plate. To the south and southeast the seismicity shows well defined narrow alignments. They start at the above mentioned clusters and trend at least three of them to the southwest, one to the southeast, and one to the east. In spite of their lined shape, they define a surface which still sub-horizontal close to the south of the clusters, but further on recover the normal dip subduction of $\sim 30^\circ$ showing faces to the south, south-east and east. We speculate about the relative possibility that the alignments are reactivated faults formed at the outer trench ridge, or new ones due to the contortion of the plate, or a result for the combination of the two processes. The vertical wide of the faults gives some chance that they might be ongoing tears in the plate. An outstanding feature is the pronounced bend between the contorted plate and the normal shaped subduction to the south of $\sim 33^\circ S$. First motion focal mechanisms are mostly normal with the T axis along the maximum slope direction of the different oriented front subduction faces. In the bend, near the plate re-subduction surface a mechanism shows horizontal compressive stresses. In an overall view the plate morphology shows the influence of the subducted Juan Fernandez ridge predominant progression to the east, but also the influence of its displacement to the south relative to the upper continental lithosphere.

Keywords: nazca, subduction, morphology



(S) - IASPEI - *International Association of Seismology and Physics of the Earth's Interior*

JSS012

2187 - 2215

Symposium

Earth Structure and Geodynamics - Dynamics of Deep Mantle Slabs

Convener : Prof. Hitoshi Kawakatsu

Co-Convener : Dr. Andrea Morelli, Dr. Shoichi Yoshioka, Prof. Tetsuo Irifune

Seismic tomography has revealed the presence of fast seismic velocity anomalies, which are likely to be associated with the subducted oceanic lithospheres, in and around the mantle transition zone of the current and past subduction zones. Although the existence of such "stagnant slabs" is now well established, their cause, fate and impact on the tectonics, dynamics and evolution of the earth system are not well understood. We solicit contributions from a wide variety disciplines of earth science to eventually answer questions like "Why do slabs stagnate, and why/where do they disappear?", "What occurs when they fall into the deep mantle?". Contributions may include: detailed geophysical mapping of subducted slab (including oceanic crust) signatures in the deep mantle, dynamic modeling and high-pressure experiments to delineate the fate of subducted slabs, possible connection between stagnant slabs and surface tectonics and volcanisms, etc...



(S) - IASPEI - *International Association of Seismology and Physics of the Earth's Interior*

JSS012

Oral Presentation

2187

Seismic Evidence for Deep Water Transportation in the Mantle

Prof. Hitoshi Kawakatsu

*Ocean Hemisphere Research Center Earthquake Research Institute, University of Tokyo
IASPEI*

Shingo Watada

Water in the mantle is expected to play essential roles in various significant problems of geodynamics, and delineating its location and abundance in the mantle may be considered as one of the most important issues in the current earth science. How water is transported into the mantle, however, has never been clear, except that it is generally believed the subducting hydrated oceanic crust is the major carrier, preventing earth scientists from accurately estimating the overall water circulation budget of the earth system. We present seismic evidence indicating the transportation of water into the deeper portion of the mantle wedge of the subduction zone beneath northeastern Japan. The reflectivity profiles of seismic waves obtained from migrated receiver functions of teleseismic earthquakes recorded by the dense Japanese seismic network, Hi-net, show strong signature of the dehydration of the subducting oceanic crust in the depth interval of 50-90km. Below this depth range, a low-velocity layer on the top of the subducting plate, which we infer as a channel of serpentinite that brings water into the deep mantle, is observed. The overall feature of our image is remarkably similar to the result of the numerical simulation of the water transportation beneath the Japan arc, and thus provides a strong line of evidence for deep water transportation within the mantle wedge of the subduction zone. Our result indicates that a significant amount of water (several weight percent H₂O) must be transported at least to a depth ~ 130-150km through this channel, and may significantly affect the overall water circulation budget in the earth system.

Keywords: dehydration, receiver function, serpentinite



(S) - IASPEI - *International Association of Seismology and Physics of the Earth's Interior*

JSS012

Oral Presentation

2188

Variation of Seismic Discontinuity Depths at ~660 km: Role of Garnet Associated with Stagnant Slab

Prof. Fumiko Tajima

Earth and Planetary Systems Science Hiroshima University IASPEI

Ikuo Katayama, Tsuyoshi Nakagawa

The role of mid-oceanic ridge basalt (MORB) with its primary component of garnet is important in slab dynamics. Early 1990s, seismic tomography models visualized the bulk of stagnant slab in long wavelength images. However, structural variation is apparent within the zones of high velocity anomaly (HVA), i.e., stagnant slab, in the transition zone. Waveform modeling of triplicated regional broadband waves that have ample information to resolve the finer structure in the transition zone derived P wave velocity models M3.11, M2.0 or others associated with stagnant slab (Tajima and Grand, 1995, 1998). Model M3.11 is characterized by HVA of up to +3% in the deeper part of the transition zone and depression of the discontinuity depth to 690 km. This model is consistent with the structure predicted for a cold slab in the stable field of ringwoodite (Ringwood and Irifune, 1988). Model M2.0 is characterized by HVA which is similar to that in M3.11 indicating the existence of a flattened cold slab in the transition zone, but not accompanied by broad depression of the 660 km discontinuity. Taken the profile for the assemblage of ringwoodite, the lack of depression of the 660 km discontinuity may be interpreted with the temperature which is normal beneath the flattened slab. However, the observed change of structure from M3.11 to M2.0 in the northwestern Pacific is more rapid than what can be expected from the temperature gradient associated with cold slab. Instead, we postulate the change of geochemical properties with stagnant slab at the bottom of the upper mantle, in which the contrast of MORB and peridotite involves. Results of two recent experiments under high pressure and temperature conditions are supportive for this hypothesis. Sano et al. (2006) has shown that the Clapeyron slope of hydrous garnet at the phase transformation is positive, and there may be no depression of the phase transformation depth if $T < 1200$ deg C. Given this condition, if the region primarily consists of hydrous MORB (garnet) at the bottom of the upper mantle, the structure may be delineated by model M2.0. The other result of experiments in rheology suggests lower viscosity of garnet than olivine under water rich conditions (Katayama and Karato, 2006). This will cause the garnet-rich MORB layer can flow relative to the surrounding mantle. The MORB layer is denser than peridotite in the transition zone, and consequently descend over the peridotite layer to form a zone of M2.0, and the two zones of HVA with or without depression of the discontinuity depth exist next to each other.

Keywords: stagnant slab, discontinuity depth variation, hydrous morb

(S) - IASPEI - *International Association of Seismology and Physics of the Earth's Interior*

JSS012

Oral Presentation

2189

Seismic reflectors in the lower mantle beneath the Mariana subduction zone

Dr. Daisuke Suetsugu

Institute for Research on Earth Evolution JAMSTEC IASPEI

Masayuki Obayashi, Hiroko Sugioka

We detected later phases of various types on Hinet records of a deep earthquake in the Mariana subduction zone (Jan. 7, 2002; 19.02N, 145.05E, $h=619\text{km}$, $M_w5.9$). Distinct impulsive later phases were observed in western Japan at 12, 30, and 42 sec from the first P-waves. We performed an array analysis (a beam forming) to the Hinet data to determine the arrival times, approaching azimuths and slownesses (corresponding to incident angle) of the later phases. The obtained slownesses and particle motions of the later phases suggest that the phases are S to P converted waves originated from the lower mantle reflectors beneath the Mariana subduction zone. We determined locations and inclination angles of the reflectors by following Takenaka (2000) using the obtained slownesses, azimuths, and travel times. The reflectors are located at 690, 800, 850, and 940 km. Comparing with a tomographic image by Obayashi et al. (2006), the 690 km and 940 km reflectors are located in the Mariana slab penetrating into the lower mantle. The former may be interpreted as the post-spinel transition and the latter may be originated by heterogeneities in the lower mantle Mariana slab. The 800 km and 850 km reflectors, on the other hand, are located outside the Mariana slab, of which origins are not identified yet. We will perform amplitude and waveform analyses to investigate the nature of the reflectors (e.g., simple velocity increase or decrease, low velocity zone, and so forth) to identify the origins of the reflectors.

Keywords: lower mantle, mariana, seismic reflector



(S) - IASPEI - *International Association of Seismology and Physics of the Earth's Interior*

JSS012

Oral Presentation

2190

Correlation between seismic and electric parameters in stagnant slabs

Prof. Pascal Tarits

EArth Sciences Geomagnétisme IAGA

The fate of water transported by subducting slabs down into the mantle is studied from the joint analysis of electric and seismic tomographic models. Water seems to have a strong influence on mantle electrical conductivity even in very small quantity (a few 100 ppm). As a result, the knowledge of electrical conductivity versus depth obtained from deep magneto-telluric (MT) techniques may provide insight on the amount of water released by the slab. The effect of water on seismic velocities at the upper mantle depths is complicated and difficult to identify from the many tomographic models available. Here, we analyse two deep MT sounding realized over stagnant slabs: one in the French Alps, from which mantle conductivity values down to ~1000 km were obtained and one in China (Ichiki et al. 2001). We study their correlation with seismic profiles obtained from a variety of tomography models.

Keywords: deep magnetotellurics, seismic tomography, stagnant slab



(S) - IASPEI - *International Association of Seismology and Physics of the Earth's Interior*

JSS012

Oral Presentation

2191

Three-dimensional shear-wave speed structure beneath the Philippine Sea by land and ocean bottom broadband data

Dr. Takehi Isse
JAMSTEC IFREE IASPEI

Hajime Shiobara, Hiroko Sugioka, Kazunori Yoshizawa, Daisuka Suetsugu, Aki Ito, Hitoshi Kawakatsu, Azusa Shito, Adam Claudia, Toshihiko Kanazawa, Yoshio Fukao

We obtained three-dimensional shear-wave speed structures beneath the Philippine Sea and surrounding region from seismograms recorded by land-based and long-term broadband ocean bottom seismographic stations. As a part of the Stagnant Slab Project, twelve broadband ocean bottom seismometers (BBOBSs) were deployed in the period from 2005 to 2006 in and around the northern Philippine Sea region. The BBOBS stations improved the spatial distribution of seismic stations in the Philippine Sea. We measured phase speeds of the fundamental and first three higher modes of Rayleigh waves for the source-station pairs within a latitudinal range from -10S to 55N and a longitudinal range from 110E to 165E, using a fully non-linear waveform inversion method by Yoshizawa and Kennett (2002). We obtained 4814, 468, 838 and 835 phase speed dispersion curves of the fundamental and first three higher modes of Rayleigh waves in a period range between 40 and 167 second, respectively. The measured multi-mode phase speeds are inverted to a 2-D shear wave phase speed structure using the inversion technique by Yoshizawa and Kennett (2004), which allows us to incorporate the effects of finite frequency as well as ray path deviation from the great-circle. The use of the multi-mode phase dispersion data should resolve better the depth variation of shear wave speed than the conventional analysis method of fundamental mode dispersion. Corrections for the off-great circle propagation and finite frequency effects should improve resolution and accuracy of a 2-D phase speed model as in the present case where the lateral variation in seismic wave speed is large and sharp. We inverted the multimode dispersion curves of phase speed maps to the shear wave speed model. The reference 1-D model is based on PREM except for the crust for which we adopted the CRUST2.0 model. We obtained a shear speed structure under the Philippine Sea region with resolution better than that by Isse et al. (2006), because the number of phase dispersion curves and BBOBS stations are increased, particularly in the southern part of the Philippine Sea region. The inverted model has a good resolution in the upper 240 km of the mantle. In the upper 120 km, the shear wave speed structure is well correlated with the age of provinces. At depth greater than 160 km, the patterns is dominated by fast anomalies of the subducted slabs of the Pacific plate and three slow anomalies beneath the center of the Philippine sea plate, the west Caroline basin and the Caroline islands.

Keywords: surface wave tomography, bbobs

(S) - IASPEI - *International Association of Seismology and Physics of the Earth's Interior*

JSS012

Oral Presentation

2192

The fate of morb crust at the core-mantle boundary

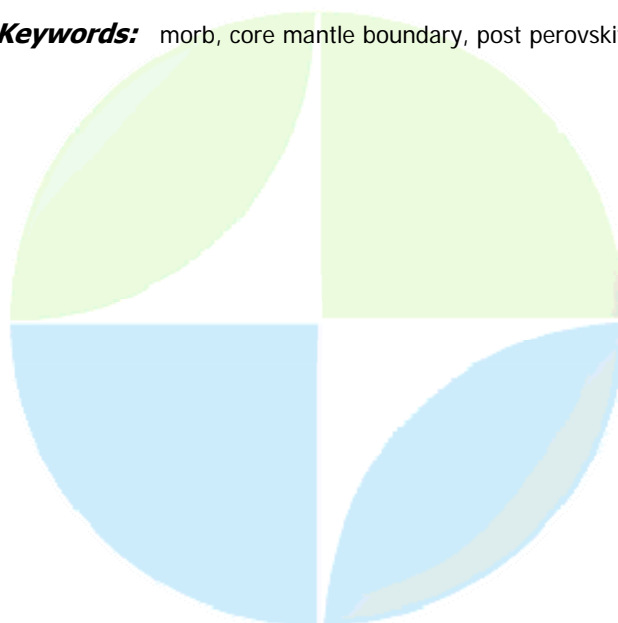
Prof. Kei Hirose

Department of Earth and Planetary Sciences Tokyo Institute of Technology

Kenji Ohta, Thorne Lay, Nagayoshi Sata, Yasuo Ohishi

Subduction of mid-oceanic ridge basalt (MORB) gives rise to strong chemical heterogeneities in Earth's mantle, possibly down to the core-mantle boundary. The subducted MORB is denser than the surrounding mantle by about 3% at the base of the mantle (Hirose et al., 2005), so if slabs penetrate to the D region, MORB material could be stable there. Geodynamical simulations have demonstrated that this magnitude of density contrast can induce separation of MORB crust from the balance of the slab and the dense MORB-enriched materials may have accumulated in dense, chemically distinct piles at the bottom of the mantle (Christensen and Hofmann, 1994; Tackley, 1998; McNamara and Zhong, 2004). These piles may be formed underneath upwelling regions. However, direct seismological evidence for the presence of MORB piles in the lowermost mantle has not been presented, in part because the velocities properties of MORB are not well characterized for lowermost mantle conditions. We precisely determined the phase relations in both pyrolite and MORB compositions at high pressures and temperatures corresponding to lowermost mantle conditions, based on in-situ X-ray diffraction measurements at BL10XU of SPring-8. Pressures were estimated from the new P-V-T equation of state of Au (Sata et al., 2007), which is consistent with the MgO pressure scale proposed by Speziale et al. (2001). Experimental results demonstrate that the post-perovskite phase transition occurs in pyrolite between 116 and 121 GPa at 2500 K, while post-perovskite and SiO₂ phase transitions occur in MORB at ~4 GPa lower pressure at the same temperature. Theory predicts that these phase changes in pyrolite and MORB cause shear wave velocity increase and decrease, respectively. Near the northern margin of the large low shear velocity province in the lowermost mantle beneath the Pacific, reflections from a negative shear velocity jump near 2520-km depth are followed by reflections from a positive velocity jump 135 to 155-km deeper. These negative and positive velocity changes are consistent with the expected phase transitions in a dense pile containing a mixture of MORB and pyrolitic material. This may be a direct demonstration of the presence of subducted MORB crust in the deep mantle.

Keywords: morb, core mantle boundary, post perovskite



(S) - IASPEI - *International Association of Seismology and Physics of the Earth's Interior*

JSS012

Oral Presentation

2193

Elastic wave velocities of pyrolite and MORB at P, T conditions of the mantle transition region

Prof. Tetsuo Irifune

Geodynamics Research Center Ehime University IASPEI

Yuji Higo, Yoshio Kono, Toru Inoue, Ken-Ichi Funakoshi

We have developed techniques for precise measurements of elastic wave velocities for polycrystalline sintered bodies of high-pressure phases at pressures to ~20 GPa and temperatures to 1700K, equivalent to those of the middle part of the mantle transition region (MTR), by a combination of Kawai-type multianvil apparatus, ultrasonic interferometry, and synchrotron radiation. We have been measuring elastic wave velocities of ringwoodite and majorite in a pyrolite composition, and the garnetite with a MORB compositions using the same techniques. We found the velocities of the majorite garnet with both pyrolite and basaltic compositions are substantially lower than the earlier estimates based on the measurements for garnets with simpler compositions under lower P-T conditions. The present results suggest that pyrolite yields seismic velocities consistent with those of typical seismological models at least in the middle part of the MTR, while MORB provides slightly lower velocities at these depths. Further extension of the P, T conditions for such measurements, toward those of the upper part of the lower mantle, is currently being pursued.

Keywords: ultrasonic, elasticity, high pressure

PERUGIA
ITALY



(S) - IASPEI - *International Association of Seismology and Physics of the Earth's Interior*

JSS012

Oral Presentation

2194

The influence of water on seismic wave speeds and attenuation in the mantle wedge: an exploratory experimental study

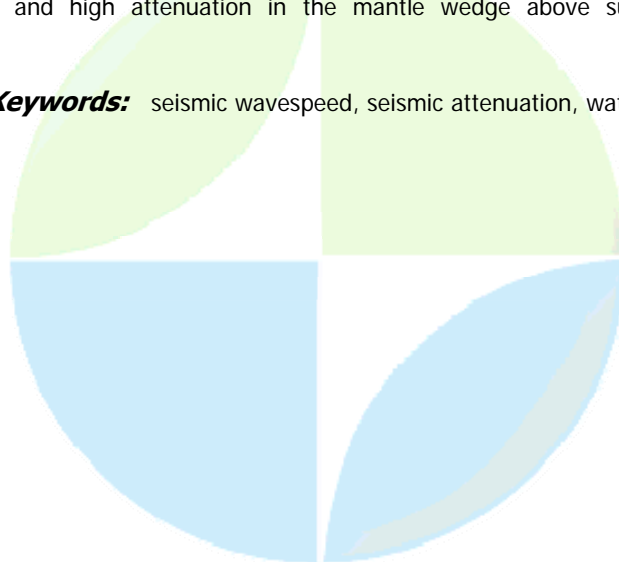
Dr. Yoshitaka Aizawa

Seismology, Volcanology and Disaster Mitigation Nagoya University IASPEI

Auke Barnhoorn, Ulrich H. Faul, John D. Fitz Gerald

Water, either as a free fluid phase or dissolved in nominally anhydrous minerals, may strongly influence seismic wave speeds and attenuation especially in subduction zones where water is released into the mantle wedge by dehydration of subducting oceanic lithosphere. As the first step in a new experimental campaign, we have performed torsional forced-oscillation experiments on a natural rock, Anita Bay (NZ) dunite, consisting mainly of the dominant upper-mantle mineral olivine along with accessory hydrous phases. These experiments were conducted at teleseismic frequencies (mHz-Hz) under conditions of high temperature to 1300C and high confining pressure (200 MPa) within internally heated gas-medium high-pressure apparatus. Both oven-dried and pre-fired specimens wrapped in Ni/Fe foil within the (poorly) vented assembly were recovered essentially dry after 50-100 h of annealing at 1300C followed by slow staged cooling. The results for three such specimens indicate broadly similar absorption-band viscoelastic behaviour, but with systematic differences in the frequency dependence of strain-energy dissipation, attributed to differences in the small volume fraction of silicate melt and its spatial distribution. It has been demonstrated that a new assembly involving a welded Pt capsule retains aqueous fluid during prolonged exposure to high temperatures - allowing the first seismic-frequency, high-temperature measurements under high water pore pressure. A marked reduction in shear modulus, without concomitant increase in dissipation, observed at temperatures >1000C is attributed to the widespread wetting of grain boundaries resulting from hydrofracturing and the maintenance of conditions of low differential pressure (confining pressure minus pore pressure). During staged cooling, accompanied by decreasing pore pressure and progressive restoration of significant differential pressure, a different microstructural regime is encountered in which the fluid is increasingly accommodated in arrays of isolated grain-boundary pores. The more pronounced viscoelastic behaviour observed within this regime for the Pt-encapsulated specimen than for the essentially dry specimens is tentatively attributed to enhanced grain-boundary sliding facilitated by the presence of interconnected pore fluid and lower grain-boundary viscosity. Such processes may help explain localized regions of low seismic wave speeds and high attenuation in the mantle wedge above subducting, dehydrating lithosphere.

Keywords: seismic wavespeed, seismic attenuation, water



(S) - IASPEI - *International Association of Seismology and Physics of the Earth's Interior*

JSS012

Oral Presentation

2195

Challenge to image deep mantle slab by seafloor electromagnetic survey

Dr. Kiyoshi Baba

Earthquake Research Institute University of Tokyo

Tada-Nori Goto, Takafumi Kasaya, Takeo Ichikita, Takao Koyama, Hisayoshi Shimizu, Makoto Uyeshima, Hisashi Utada

Electromagnetic survey is one of the geophysical method to image Earth's interior and has a complementary nature with seismic surveys. Electrical conductivity of mantle minerals primarily depends on temperature. It also changes largely when partial melt exists and the melt is interconnected. Moreover, water dissolved in minerals strongly enhances the electrical conductivity. Constraining these parameters, electromagnetic method can contribute to mantle dynamics studies. We have run a seafloor electromagnetic survey project in Philippine Sea in order to image Pacific slab stagnated beneath the area and surrounding mantle. Observations at seafloor is necessary to resolve the geometry of the slab because existing data sets are based on the observation by land geomagnetic stations and submarine cables, which are distributed coarsely and unevenly. Although it is difficult to establish steady observation stations at seafloor, iterative maneuver observations using ocean bottom electromagnetometers (OBEMs) can acquire the data required to image the stagnant slab. The project iterates one-year-long survey three times. Earthquake Research Institute, University of Tokyo and Institute for Research on Earth Evolution (IFREE), Japan Agency for Marine-Earth Science and Technology (JAMSTEC) have resourced the project with their OBEMs. All of the OBEMs are the products of Tierra Tecnica Ltd. The OBEMs measure time variations of three components of the magnetic field, two components of the electric field and the instrumental tilts with one-minute intervals for one year. In the first phase, we deployed 11 OBEMs in October, 2005 and recovered all of them successfully in November, 2006. R/V Kairei of JAMSTEC was utilized for both cruises. In the second cruise, we deployed another 12 OBEMs so that the second phase was started. We found that all the recovered OBEMs recorded mostly good data. We have been analyzing the data sets of the first phase. The time series are cleaned, corrected for the record timing, the instrumental tilts, and the components of daily variations and tides. Then, magnetotelluric (MT) and geomagnetic depth sounding (GDS) responses are estimated. The effect for the land-ocean distribution and seafloor topography on the responses are examined and stripped by using three-dimensional numerical modeling. We will report the detail of the observation, the data quality and some results of the preliminary analysis. The current data set can constrain the upper mantle structure although we need to wait the data accumulation by the second and third observation phases to reach the desired objectives.

Keywords: seafloor em survey, electrical conductivity, philippine sea

(S) - IASPEI - *International Association of Seismology and Physics of the Earth's Interior*

JSS012

Oral Presentation

2196

Deep azimuthal seismic anisotropy in the western Anatolia and Aegean subduction zone

Mrs. Gulten Polat
seismology IASPEI

Shear wave splitting due to source-side mantle anisotropy is estimated from broadband teleseismic and local S waves using a suite of Aegean subduction zone events. The data have been recorded by Kandilli Observatory and Earthquake Research Institute (KOERI) stations, at the depth of more than 60 km, from 2000 to 2007. We assume that there are at most two anisotropic regions along the ray path: one on the source-side and the other one on the receiver-side. It has been known that receiver-side splitting is known from analysis of SKS waves. Aim of this study is to investigate the kinematics of subduction; its influence on mantle convection and related deformation by using seismic anisotropy. From the combined analyses of SKS, local S, and teleseismic S waves, we have concluded that there must be azimuthal seismic anisotropy in the deep part of the mantle around the consuming slab. The splittings of the waves recorded at the stations in the western have allowed us to constrain the orientation and depth distribution of the anisotropy both below and above the slab. In the lithospheric mantle beneath the western part of the Anatolia, S- wave fast propagation directions are parallel to the direction of the extension of the Aegean region. Obtaining SKS and local S wave splitting, our results at BALB, ANTB and DALT stations show that fast split shear wave direction is about NE and delay time greater than 1 sec. These findings give information about the nature of the deformation and the coupling between the subducted lithosphere and surrounding asthenosphere. These results are consistent with the presence of azimuthal seismic anisotropy in the asthenosphere below the slab. Local S phases recorded at Southern Aegean Region (SAR) stations, yield fast directions that are not similar to the pattern of the SKS results at the depth of 133 km. We have found high delay times among the S phases in this region (SAR). This situation can be explained with the important coupling between cold slab and the intense mantle convection.

Keywords: aegeanslab, anisotropy, mantleconvection



(S) - IASPEI - *International Association of Seismology and Physics of the Earth's Interior*

JSS012

Oral Presentation

2197

Stagnant slab configuration in the vicinity of the 660-km discontinuity

Dr. Masayuki Obayashi
IFREE JAMSTEC IASPEI

Junko Yoshimitsu, Yoshio Fukao

Arrivals times of the direct P-waves hand-picked on seismograms from the broadband seismometer networks OHP (Ocean Hemisphere Project), JISNET (Japan-Indonesia Seismic Network), SPANET (South Pacific Seismic Network), SKIPPY, Hi-net and IRIS were added to the ISC data in our P-wave tomography with a focus on the western Pacific region. We measured PP-P differential travel times on the IRIS records, which were also used in the tomography. The result shows clearer images of the subducting slabs than the previous ones (Fukao et al., 2001). The Japan and Izu-Bonin slabs horizontally flatten most extensively in a depth range of about 450 - 600 km. The horizontal spreads become small gradually towards the 660-km discontinuity. The northern Kurile, Mariana and Java slabs are apparently stagnant below 700 km depth. The depth range between 600 and 700 km with the 660-km discontinuity in it is marked by a trench-parallel slab-like feature of which vertical extent varies from region to region. These characteristics are observed regardless of how the model mantle is divided into layers or whether the model mantle discontinuities are of the zeroth or higher orders. Recently the 660-km discontinuity undulation under the Japanese islands has been obtained from ScS reverberations (Tono et al., 2005) and P-S conversions (Niu et al., 2005; Ramesh et al., 2005) using the Hi-net data. According to their results, the 660-km depression is greatest in the area where our P-wave tomography shows a slab-like feature in the relevant depth range. The 660-km discontinuity is still depressed but with less amount in the area where the slab horizontally spreads most extensively in our tomographic model. There is little indication that slabs lie horizontally directly above the 660 km-discontinuity.

Keywords: subducting slab, 660 km discontinuity, tomography



(S) - IASPEI - *International Association of Seismology and Physics of the Earth's Interior*

JSS012

Oral Presentation

2198

Phase relations in stagnant slabs: Seismic velocity structure and bending moments

Prof. Craig Bina

Earth and Planetary Sciences Northwestern University IASPEI

Deep subhorizontal extensions of subduction or stagnant slabs constitute unusual thermobaric environments, in that subducted material may gradually undergo nearly isobaric thermal assimilation. The petrological consequences, in terms of equilibrium or metastable phase relations, should affect both apparent seismic velocity structure and slab morphology [e.g., Bina, 2006]. Evidence for slab stagnation may appear in several forms. Seismic extensions of stagnant slabs may appear as shallowing in apparent dip angles of deep seismicity distributions [e.g., Chen et al. 2004]. Aseismic extensions may appear as subhorizontal deflections of fast velocity anomalies in P-wave and S-wave seismic tomography [e.g., Fukao et al., 2001, Suetsugu et al., 2006]. Lateral depth variations along the 660-km seismic discontinuity in migrated receiver functions [e.g., Kawakatsu and Watada, 2005] may be mapped into thermal anomalies by assuming correspondence to equilibrium deflection of the perovskite-forming transition in ringwoodite. We have constructed kinematic thermal models [cf. Negredo et al., 2004] of stagnant slabs and undertaken thermodynamic modeling [e.g., Fei et al., 1991, Akaogi et al., 2002] of the consequent thermal perturbation of high-pressure phase transitions in mantle minerals. For such models we have estimated seismic velocity anomalies, as might be imaged by seismic tomography, and corresponding seismic velocity gradients, as might be imaged by boundary-interaction phases. We have also calculated associated thermo-petrological buoyancy forces and bending moments which (along with other factors such as viscosity variations and rollback dynamics [Christensen, 2001]) may contribute to slab deformation and morphology. We have considered effects of variations in depth of stagnation, post-stagnation dip angle, phase transition sharpness, and transition triplication due to multiple intersection of stagnant-slab geotherms with equilibrium phase boundaries. Japan is our primary study area.

Keywords: stagnation, thermodynamics, buoyancy



(S) - IASPEI - *International Association of Seismology and Physics of the Earth's Interior*

JSS012

Oral Presentation

2199

Stagnant slab: A review

Dr. Yoshio Fukao
IFREE JAMSTEC IASPEI

Masayuki Obayashi, Deep Slab Project Group

Subducted slabs tend to be, in general, once horizontally flattened at various depths in a range roughly between 400 and 1000 km. We call a slab in this tendency stagnant slab. We review the recent progress in the related subjects. The stagnant slab image behind the Japanese arc is especially suitable to detail its fine structure by addition of a large amount of arrival time data from Chinese networks, by comparison of the broadband waveforms of P and S waves grazing the stagnant slab, and by spatially correlating the stagnant slab image to the 660-km depression revealed by analyses of near-station P to S conversions. Many of these studies support the simple idea of cold stagnant slab, which is also supported by the recent electromagnetic tomography delineating remarkably well the seismic images of the stagnant slab under south Europe as a low conductive body. Several attempts have been made to simulate numerically the characteristic configuration of the stagnant slab and the associated 660-km topography in the northwestern Pacific. The factors affecting the deep slab configuration are the trench retreat, Clapeyron slope of the 660, viscosity jump across the 660 and grain size-dependent softening of ringwoodite in the cold slab. Combination of these factors in reasonable ranges generates a variety of slab configuration, including horizontally deflected slab either above or below the 660. The recent high pressure experiments imply that the Clapeyron slope of the 660 depends on water content. This dependence, together with the tomographic map at 660 km depth and the undulation map of the 660, suggest that the stagnant slab behind the Izu-Bonin trench is not anomalously hydrous.

Keywords: stagnant slab, transition zone, 660km discontinuity



(S) - IASPEI - *International Association of Seismology and Physics of the Earth's Interior*

JSS012

Oral Presentation

2200

Numerical Models of the Fate of Detached Slabs

Prof. Gary Jarvis

*Earth and Space Science, York University, Toronto IASPEI, Canadian Geophysical Union
IASPEI*

Julian P. Lowman, Hosein Shahnas

We examine the rate of sinking of subducted slabs in a series of idealized three-dimensional and two-dimensional simulations using a 3D Cartesian plane-layer model, and a 2D cylindrical-shell model, of mantle convection. Our goal is to account for the inference from seismic tomographic studies that some slab remnants have persisted at mid-mantle depths for 150 My or more while others have descended to the base of the mantle, in much less time, where they have spread laterally for great distances along the core-mantle boundary. We consider the influence of initial slab dimensions, viscosity stratification, slab dip angle, mineral phase transitions and three dimensionality on the time required to clear the upper half of the mantle of all thermal traces of an initial upper mantle subduction zone. We find that upper mantle slabs will persist in the upper 1500 km of the mantle for times in excess of 150 My if there is a viscosity jump by a factor of 30 or more at a depth of 670 km. In contrast, if the initial slab structure reaches deep into the lower mantle, it will draw all of the upper portions of the slab into the lower half of the mantle in less than 150 My, unless the viscosity increases in the lower mantle by a factor of 300 or more. We find that sinking rates of slab remnants are relatively insensitive to the presence of phase transitions when the viscosity increase at 660 km is sufficiently large. The age of slab remnants depends most strongly on the viscosity stratification and the total depth extent of the original slab.

Keywords: truncated, slab, models



(S) - IASPEI - *International Association of Seismology and Physics of the Earth's Interior*

JSS012

Poster presentation

2201

The mantle discontinuity depths in the stagnant Pacific slab beneath the Philippine Sea

Dr. Daisuke Suetsugu

Institute for Research on Earth Evolution JAMSTEC IASPEI

Hajime Shiobara, Hiroko Sugioka, Aki Ito, Hitoshi Kawakatsu, Azusa Shito, Claudia Adam, Toshihiko Kanazawa, Yoshio Fukao

We determined depths of the mantle discontinuities (the 410-km and 660-km discontinuities) in the Pacific slab stagnant in the mantle transition zone beneath the Philippine Sea using data from a broadband ocean bottom seismograph (BBOBS) network. As a part of the Stagnant Slab Project (2004-2008), twelve BBOBSs were deployed on the seafloor in the northern Philippine Sea. We analyzed nine-twelve months long data recovered by the cruise (KR06-14) with the JAMSTEC research vessel KAIREI to determine the mantle discontinuity depths beneath the northern Philippine Sea and westernmost Pacific. Among them, eight stations have continuous records longer than nine months, which were used in the further analysis. We employed the Velocity Spectrum Stacking of receiver functions (Gurrola et al., 1994). We stacked receiver functions at three stations located above the stagnant Pacific slab imaged by a seismic tomography to determine the discontinuity depths in and around the stagnant slab. The 410-km and 660-km discontinuity depths and the thickness of the mantle transition zone are 384 km, 692 km, and 308 km, respectively, assuming the iasp91 model for a velocity correction. As a comparison, we estimated the discontinuity depths beneath a normal Pacific region from three BBOBS stations in the westernmost Pacific Ocean, giving 392 km and 651 km for the 410-km and 660-km discontinuity depths, respectively. The 660-km discontinuity is significantly deep in the stagnant Pacific slab. Assuming that the deep 660-km discontinuity is solely caused by a cold temperature environment of the stagnant slab, the thick mantle transition zone around the stagnant slab is estimated to be 300 K colder than beneath the normal Pacific Ocean.

Keywords: transition zone, bbobs, philippine sea



(S) - IASPEI - *International Association of Seismology and Physics of the Earth's Interior*

JSS012

Poster presentation

2202

Effect of superhydrous phase B and phase D on the density of hydrated slabs in the deep mantle

Dr. Konstantin Litasov

Dept. Mineralogy, Petrology and Economic Geology Faculty of Science, Tohoku University

Eiji Ohtani

Recent geophysical data indicate that at least locally upper mantle and transition zone may be substantially hydrated. High-pressure experiments reveal existence of several dense hydrous magnesium silicates (DHMS) stable along the subduction slab geotherms in a peridotite composition. After breakdown of serpentine and chlorite at 6 GPa the most important of them, with increasing pressure, are phase A, phase E, superhydrous phase B (SuB), and phase D. SuB and phase D are most important hydrous phases of post-spinel assembly at the top of the lower mantle. After transformation of hydrous ringwoodite to Mg-perovskite and ferropericlavite at the 660-km depth, the density of hydrated slabs may be reduced by subsequent formation of SuB and/or phase D. Pressure-volume-temperature relations have been measured for SuB and Fe-bearing phase D using synchrotron X-ray diffraction with a multianvil apparatus of SPring-8 facility. A fit of P-V-T data for superhydrous phase B to high-temperature Birch-Murnaghan equation of state yields $K_0 = 135.8 \pm 2.6$ GPa; $K = 5.3 \pm 0.2$; $dK/dT = -0.026 \pm 0.003$ GPa/K and zero-pressure thermal expansion $\alpha = \alpha_0 + \alpha_1 T$ with $\alpha_0 = 3.2 \pm 1.0 \times 10^{-5}$ K⁻¹ and $\alpha_1 = 1.2 \pm 0.4 \times 10^{-8}$ K⁻². A fit of P-V-T data for phase D to high-temperature Birch-Murnaghan EOS yields $K_0 = 139.6 \pm 3.0$ GPa; $K = 6.6 \pm 0.4$; $dK/dT = -0.023 \pm 0.008$ GPa K⁻¹ and zero-pressure thermal expansion $\alpha = \alpha_0 + \alpha_1 T$ with $\alpha_0 = 3.4 \pm 0.2 \times 10^{-5}$ K⁻¹ and $\alpha_1 = 0.4 \pm 0.6 \times 10^{-8}$ K⁻². Present EOSs enables accurate estimation of the density of SuB and phase D in pyrolitic composition in the deep mantle conditions. The density reduction of hydrated subducting slab at the top of the lower mantle due to presence of about 10 vol.% of SuB/phase D (with extrapolation to Fe-bearing composition) would be 1.5-2.0%. This indicates that hydrated slab (>1 wt.% H₂O) may be buoyant in the surrounding mantle rocks and does not penetrate into the deep lower mantle.

Keywords: subduction, mantle, hydration



(S) - IASPEI - *International Association of Seismology and Physics of the Earth's Interior*

JSS012

Poster presentation

2203

**Upper boundary of the pacific plate subducting under Hokkaido, Japan,
estimated from ScSp phase**

Dr. Kiyoshi Yomogida

Earth and Planetary Dynamics Hokkaido University IASPEI

Kinue Osada, Kazunori Yoshizawa

Geometry of the upper boundary of the subducting Pacific plate or slab was estimated in the Hokkaido region, Japan, using the ScSp phase: the converted phase to P wave at the boundary from the S wave reflected at the core-mantle boundary and propagating nearly vertically (i.e., ScS phase). Taking the advantage of a dense seismic network named "Hi-net" recently deployed across the Japanese islands, we applied several seismic array analyses with the recorded waveform data for a large nearby deep earthquake, in order to enhance weak ScSp signals in record. At first, we set up five blocks for the region in the subducting direction of the plate. After aligning the travel time of the ScS phase and stacking seismograms among stations in a same sub-block perpendicular to the plate subduction, we searched for the optimal plate model (i.e., two-dimensional geometry of the upper boundary of the plate) for each block. The model was parameterized with six depths, and the seismograms were stacked based on the travel time of ScSp as time lag at each sub-block, so that the optimal model would yield the maximum amplitude of ScSp after stacking. The searches were done, using ray tracings of the ScSp phase with a reference velocity model and the non-linear inversion scheme called Neighbourhood Algorithm. The optimal model of each block was combined each other by cubic spline interpolation, in order to construct three-dimensional geometry of the upper boundary of the plate. We then performed the frequency-wavenumber (f-k) spectral analysis to refine the above result. Assuming each station as a reference point, we made each beam output with adjacent 7 stations as a function of wavenumber vector (k_x , k_y) and frequency. The peak of its power spectrum was considered as the ScSp signal, estimating the wavenumber vector, that is, the azimuth of arrival and slowness, so that we can estimate the position and depth of the corresponding S-to-P conversion. In the frequency range of 0.5 to 1.5 Hz, we could estimate the conversion points for 21 stations, and refined the geometry of the upper boundary already obtained by the above non-linear stacking approach. The final plate model was compared with the distribution of intraplate earthquakes in the Pacific plate. This comparison clearly reveals that the upper seismic zone merges with the lower from 150 to 200 km in depth, by systematically deviating away from the upper boundary of the plate.

Keywords: scsp phase, subducting slab, array analysis

(S) - IASPEI - *International Association of Seismology and Physics of the Earth's Interior*

JSS012

Poster presentation

2204

Preliminary study on formulation of a slab stagnation model unifying thermal convection and kinetics

Dr. Shoichi Yoshioka

Earth and Planetary Sciences Kyushu University IASPEI

I present preliminary formulation to unify thermal convection and thermo-kinetic coupled numerical models to reveal physical mechanism of slab stagnation around a depth of 660 km, which has been identified by seismic tomography. I developed the former in Yoshioka and Sanshadokoro (2002). Regarding the latter, I also developed its basic part in Yoshioka et al. (1997). I will modify the latter model, incorporating the latest results in high pressure and high temperature experiments such as the effect of water, and grain nucleation inside and along grain boundaries associated with phase transformations in a slab. In this unified model, although I carry out calculation of thermal convection in a conventional method, I calculate temperature distribution, taking account of latent heat release associated with phase transformations in a slab in the energy equation. From the temperature and pressure distributions, I calculate nucleation and growth rates of grains of high pressure phase of olivine based on its kinetics, and obtain grain sizes and degree of phase transformation. From the grain sizes, I estimate final grain size distributions after union of each grain associated with decrease in surface energy, using a grain growth law. In the portion dominated by diffusion creep, I calculate viscosity distribution in the slab from these grain sizes, and let it reflect in the momentum equation. I solve the coupled problems using the three basic equations as a time marching problem, by employing numerical methods such as finite difference method, ADI method, Runge-Kutta method, and DASPK method. Then, I will develop a numerical model to calculate dynamic behavior of a slab in the mantle transition zone, temperature distribution in the slab, and viscosity distribution in the slab calculated from the grain sizes simultaneously.

Keywords: slab, convection, kinetics



(S) - IASPEI - *International Association of Seismology and Physics of the Earth's Interior*

JSS012

Poster presentation

2205

Anelasticity in the mantle surrounding Izu-Bonin subduction zone inferred from BBOBS waveform data

Dr. Azusa Shito

Ocean Hemisphere Research Center University of Tokyo

Hajime Shiobara, Hiroko Sugioka, Aki Ito, Claudia Adam, Hitoshi Kawakatsu, Toshihiko Kanazawa

Anelasticity in the upper mantle surrounding Izu-Bonin subduction zone is estimated by using the amplitude spectra of P wave recorded by Broad Band Ocean Bottom Seismometer (=BBOBS). As a part of Stagnant Slab Project we deployed 12 BBOBS from October 2005 to October 2006 in and around the Philippine Sea. The sites were equipped with three components Guralp CMG-3T sensors recorded at 200 Hz. This is the first challenge of regional scale and long term BBOBS array. The BBOBS waveform data will provide us much information on physical property of subduction zone. We analyze regional (< 15 degree) earthquake that sample the Pacific slab, mantle above the Pacific slab (=mantle wedge), and the mantle beneath the Pacific slab. The waveform data from events in Izu-Bonin slab were recorded by the BBOBS array with adequate signal to noise ratio. We estimated t^* of P wave using high frequency spectral decay and calculated the path averaged quality factor; Q_p by using the observed travel time. Time domain signals are windowed with the window length of 6s; before 1s and after 5s onset of manually picked P wave. This window includes main pulse of the waveform and excludes later phases. Then amplitude spectra and the slope are calculated over the frequency range 0.75 to 4.0 Hz. The results clearly show low-Q mantle and high-Q slab. For shallow event (< 150km), the estimated Q_p are 100-200 above the Pacific slab, and are 500-1000 in the mantle beneath the Pacific slab. For deep event (> 400km), the estimated Q_p are 200-300 both above and beneath the Pacific plate. However, the waveforms especially from shallow events are complex may be due to effects of multi-path. Therefore, we should trace the raypath more carefully for further discussion. In the presentation, we will show the results of estimation of t^* and discuss anelastic structure and the tectonic implications.

Keywords: anelasticity, mantle, bbobs



(S) - IASPEI - *International Association of Seismology and Physics of the Earth's Interior*

JSS012

Poster presentation

2206

Detailed Structure of Upper Mantle Discontinuities in the Tonga and Mariana Subduction Zones

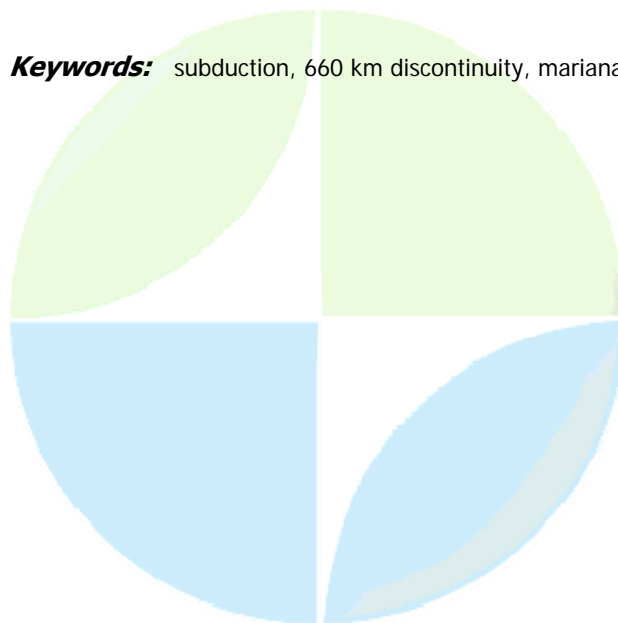
Dr. Rigobert Tibi

Earth and Planetary Sciences Washington University

Douglas A. Wiens

Recordings of deep Tonga earthquakes from two arrays of 12 broadband seismographs each in the Fiji and Tonga islands are stacked and searched for reflections and conversions from upper mantle discontinuities in the Tonga subduction zone. To enhance the low-amplitude discontinuity phases s_{410p} , P_{660p} and S_{660p} , deconvolved seismograms from each event/array pair are aligned on the maximum amplitude of the direct P wave and subsequently slant-stacked. For the 410-km discontinuity, the results show no systematic variations in depth with distance to the cold slab. The 660-km discontinuity varies between 656 and 714 km in depth. For the southern and central parts of the subduction zone, the largest depths occur in the core of the Tonga slab. For the northern part, two separate depressions of the 660 are observed. These anomalies are interpreted as being induced by the active, steeply subducting Tonga deep zone and a subhorizontally lying remnant of subducted lithosphere from the fossil Vityaz trench, respectively. Interpreting the deflections of the 660 in terms of local temperatures implies a thermal anomaly of -800K to -1200K at 660 km depth. Except for the southern region where it may thicken, the width of the depressed 660 region implies that the Tonga slab seems to penetrate the 660 with little deformation. We use P-to-S converted phases from teleseismic data recorded at island and ocean bottom stations in Mariana to investigate the upper mantle structure in the region. Results of the analysis show evidence for double seismic discontinuities at the base of the transition zone near the Mariana slab. A shallower discontinuity is imaged at depths of ~650-715 km, and a deeper interface lies at ~740-770 km depth. The large lateral extent at near constant depths for both features is consistent with horizontal interfaces rather than small-scale scatterers. The amplitude ratios of the seismic signals suggest that the shear velocity contrasts across the two interfaces are comparable. These characteristics support the notion that the discontinuities are the results of the phase transformations in olivine (ringwoodite to post-spinel) and non-olivine component (ilmenite to perovskite), respectively, for the pyrolite model of mantle composition.

Keywords: subduction, 660 km discontinuity, mariana



(S) - IASPEI - *International Association of Seismology and Physics of the Earth's Interior*

JSS012

Poster presentation

2207

The crystallographic preferred orientation of MgSiO₃ Ilmenite and its implications for the anisotropy of the subducted slab

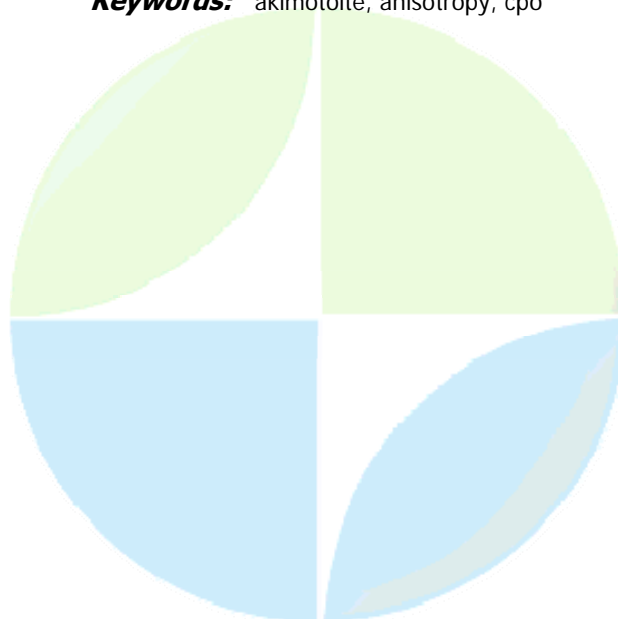
Mrs. Rei Shiraishi

Science Tohoku University IASPEI

Eiji Ohtani, Kyuichi Kanagawa, Akira Shimojuku, Masaaki Miyahara

Akimotoite, the ilmenite structured MgSiO₃, which is the major constituent of the harzburgite layer of subducting slabs, is likely to be the most anisotropic mineral in the mantle transition zone. From the characteristic of anisotropy, Anderson [1989] predicted that if ilmenite aggregate is lined up by plastic deformation, a cold slab could be extremely anisotropic. Therefore, the deformation-induced crystallographic preferred orientation of akimotoite provides important information on seismic anisotropy in the mantle transition zone. Plastic deformation experiments of MgSiO₃ polycrystalline ilmenite (akimotoite) at high pressures and temperatures were carried out at confining pressure of 20GPa to 22GPa, temperature of 1273-1573K using a Kawai-type multi-anvil apparatus installed at Tohoku University. The sample was sandwiched between alumina pistons, which induced high differential stresses inserted in the furnace assembly. Two type-modified assemblies, uni-axial compression geometry and simple shear geometry were used for deformation experiment. Crystallographic orientations of deformed ilmenite grains were measured by the electron backscatter diffraction (EBSD) technique at Chiba University. A c-axis maximum parallel to the compression direction develops at higher temperatures (T=1473-1573K), while c-axes are oriented parallel to the shear direction at the lowest temperature (T=1273K). This change in crystallographic preferred orientation of akimotoite may be due to a change in dominant slip system with temperature. In order to confirm this, TEM observations are now in progress. Seismic anisotropy of deformed MgSiO₃ polycrystalline ilmenite calculated from the crystallographic orientation data is strong; azimuthal anisotropy is 4.7% for P wave and 3% for S wave, and S wave polarization anisotropy is up to 4.2%. Anisotropy of polycrystalline akimotoite is at least 4-5 times as large as that of 60% wadsleyite and 40% garnet (Tommasi et al., 2004) and akimotoite probably has a much greater impact on the anisotropy for the subducted slab.

Keywords: akimotoite, anisotropy, cpo



(S) - IASPEI - International Association of Seismology and Physics of the Earth's Interior

JSS012

Poster presentation

2208

Sensitivity of geomagnetic transfer functions to stagnant-SLAB-type electrical conductivity heterogeneity

Dr. Hisayoshi Shimizu

Earthquake Research Institute University of Tokyo IAGA

Yuta Baba, Takao Koyama, Kiyoshi Baba, Hisashi Utada

Electrical conductivity structure in the Earth obtained by using observed geomagnetic and geoelectric field provides important and independent information to discuss the dynamics and material in the Earth. First 3D semi-global mantle conductivity model in the northern Pacific obtained by Koyama (2001) was examined together with the seismic velocity by Fukao et al. (2003) in the same region, and Fukao et al. (2004) pointed out that temperature anomaly cannot be the cause of anomalously high conductive region beneath Philippine Sea in 350-550 km depth. Koyama et al. (2006) estimated using the Nernst-Einstein relationship (Karato, 1990) with standard geotherm model (Ito and Katsura, 1989) and the diffusivity of hydrogen in wadsleyite at high pressure (Hae et al., 2006) that the high electrical conductivity in the area can be explained if 0.3 wt. per cent of water exist in the region. The estimate is an important constraint to discuss the dynamics in the mantle. Although observationally determined electrical conductivity structures have already been employed for further interpretations, the estimates have much room to improve the credibility and accuracy. Koyama (2001) employed GDS (Geomagnetic Deep Sounding) and magnetotelluric responses in the period range of 5-15 days in the 3D inversion. The fit of model output with observed data seems fine, but more geoelectromagnetic information may be utilized to improve the credibility of the conductivity model. In this study, we are going to seek the plausibility to employ the ratio of horizontal geomagnetic components between geomagnetic stations (horizontal transfer function; HTF hereafter), which has sensitivity to 3D heterogeneities, as new information to constrain the conductivity structure. We estimated HTFs at stations in the north-western Pacific in reference to the horizontal component at Kakioka, and compared them with the HTFs calculated by using three dimensional conductivity model by Koyama (2001) as a trial. Observed and modeled HTFs have large differences, more than the estimation error of the observed HTFs, at some stations. HTF can be a promising candidate to be included in further inversion on conductivity structures. We are going to present the results of the sensitivity test of HTF and GDS responses against synthetic three dimensional conductivity structures. Preliminary calculations supposing 1000km scale checkerboard type lateral conductivity heterogeneities, having an order of magnitude contrast, at 350-850km depth embedded in one-dimensional reference model (Utada et al. 2003) imply that the signature due to lateral heterogeneities are larger than the estimation error of HTF and GDS responses at stations in geomagnetic mid latitudes in the period range of 5-60 days. Discussions on the sensitivity in with respect to the size and depth of the heterogeneity, conductivity contrast, and period of the response functions are presented in the paper.

Keywords: electrical conductivity, response functions

(S) - IASPEI - *International Association of Seismology and Physics of the Earth's Interior*

JSS012

Poster presentation

2209

Gaussian-beam receiver function synthetics in a 3-D heterogeneous medium with velocity discontinuities at the Japan subduction zone

Prof. Kazuro Hirahara

Geophysics, Graduate School of Science Kyoto University IASPEI

Takashi Tonegawa, Takuro Shibutani

We have constructed receiver functions (RFs) observed at high-density broadband and short-period stations over the Japan Islands to map the Moho beneath the Japan Islands, the slab top and the oceanic crust of the Pacific and the Philippine Sea slabs, and the lower boundary of the Pacific slab, 410 and 660 km velocity discontinuities. The mapping, however, depends on the reference velocity model. Only radial RFs (RRFs) have been employed, though the transverse RFs (TRFs) have considerable amplitudes in relation to subducting slabs. We propose RF tomography which combines the travel time tomography and the RF analyses to obtain the 3-D velocity structure including velocity discontinuities. RF tomography requires iterative forward modeling of RFs in a 3-D heterogeneous medium. The recent advancement of computer power enables us to synthesize short-period waveforms with SEM and FDM. However, iterative synthesizing of RFs in RF tomography is still formidable. We extend a computer code GBM3D (Sekiguchi, 1992), which can treat only the waves from the source in the model space and the plane waves incident vertically at the bottom. Therefore, we implement calculation of teleseismic waveforms with arbitrarily incident angles in the followings. As in the original code, we assume the 3-D heterogeneous velocity, Q and density structure in each layer which are interpolated by 3-D cubic spline functions and the layer boundaries are represented by 2-D ones. We set the dense grids at the bottom and calculate the slowness vectors and travel times at the grids from a teleseismic source, assuming a 1-D earth model outside of the modeling space. From each grid, we execute kinematic and dynamic ray-tracings for a variety of phases, and sum up beams with Gaussian weights to synthesize waveforms at stations. It has been pointed out that GBM has the several tuning parameters and seems to be less reliable in some cases. For almost vertical incident teleseismic waves, calculations are stable if ray beams with enough density are summed. Then RRFs and TRFs are calculated from the synthetic waveforms. We present the modeling of RFs which include the P_s phases converted at the Moho and the upper mantle discontinuities with comparisons of observed RFs observed at several regions. The first is the Kii Peninsula region where the Philippine Sea slab subducts steeply with a 3-D complex configuration, and RF analyses (e.g., Yamauchi et al., 2003) have provided the structure of the slab top and the subducting oceanic crust. The second is the Tohoku region, where RF analyses have clarified the subducting oceanic crust overlying the Pacific slab and the lower boundary of the slab, and other phases. The third is the 410 km and 660 km discontinuities across and around the stagnant Pacific slab.

Keywords: receiver function, gaussian beam method, subducting slab

(S) - IASPEI - *International Association of Seismology and Physics of the Earth's Interior*

JSS012

Poster presentation

2210

Upper mantle structure beneath Japan and Okhotsk Sea from Rayleigh wave analysis

Dr. Ekaterina Litvina

Department of Natural History Sciences Hokkaido University

Kiyoshi Yomogida

The lithospheric structure beneath the Seas of Japan and Okhotsk is investigated by the multimode dispersion analysis of Rayleigh wave in the period range of 35-150 s, incorporating finite frequency effects. Broadband waveform data from 353 events with magnitude greater than 5.5 from 1990 to 2005 recorded at 25 stations of the Global Seismographic Network are used in this study. Locations and origin times of the earthquakes are taken from the IRIS catalogue. The centroid moment-tensor solutions are provided by the Harvard CMT catalogue. The recorded waveforms are processed by the three-stage inversion technique of Yoshizawa & Kennett (2004). The phase velocity dispersion curves of Rayleigh waves are measured for the fundamental mode and the first higher mode by waveform fitting. Next, the dispersion information from all the paths is combined to produce multimode phase velocity maps as a function of frequency. Initial phase velocity maps are derived from a linear inversion based on the assumption that each surface wave path follows its great-circle. Subsequently, the 2-D phase velocity maps are updated by including the ray tracing and finite frequency effects. Finally, 1-D S-wave velocity profiles are inverted from each local dispersion information. Three dimensional S-velocity models can be reconstructed from the set of updated multimode phase velocity maps. This method offers the advantage of incorporating various styles of information such as multimode dispersion, off-great circle propagation, and finite frequency effects for surface waves in a common framework. The obtained shear velocity model is resolved down 300 km in depth. Lateral resolution is estimated from a checkerboard tests, which shows the average resolution of 4 degrees in the study region. The subducting Pacific plate is clearly imaged as a high velocity anomaly up to 6 percents. A low velocity anomaly beneath the Seas of Japan and Okhotsk is associated with the mantle wedge. The absolute S wave velocities in the mantle wedge at depth of 125 km are approximately 4 km/s, probably indicating the presence of partial melt in this area. A small-scale high velocity anomaly is located in the northern part of the Sea of Okhotsk. The position of this anomaly correlates well with the high velocity anomaly found in the P-wave tomography of Gorbatov et al. (2000), which may be interpreted as a relict of the subducted Okhotsk plate. We also performed a preliminary mapping of azimuthal anisotropy in this region. In the eastern margin of the Sea of Japan, we found abrupt change in the fast direction of Rayleigh-wave phase speed in the period range from 40 to 120 seconds near the plate boundary between the North-American and Eurasian plates. This is very likely to reflect rapid variations of horizontal flow in the upper mantle beneath the two plates.

Keywords: lithosphere, tomography, surface waves

(S) - IASPEI - *International Association of Seismology and Physics of the Earth's Interior*

JSS012

Poster presentation

2211

Body wave travel time anomalies caused by the stagnant slab

Dr. Hiroko Sugioka
IFREE JAMSTEC IASPEI

Daisuke Suetsugu, Masayuki Obayashi, Yoshio Fukao, Yuan Gao

Previous tomographic studies using short-period P times have commonly shown that the fast Pacific slab is stagnant in the mantle transition zone beneath the Philippine Sea and eastern Asia (e.g., Fukao et al., 2001). However, the fast S-velocity anomalies of the stagnant slab have been not commonly obtained from short-period S-wave time, which is based mostly on the ISC bulletin. The purpose of the present study is to determine whether the stagnant slab has fast S-velocity anomalies by analyzing arrival times picked from broadband waveforms and, if any, to determine the velocity perturbation ratio $\delta \ln V_s / \delta \ln V_p$ ($= R$) of the stagnant slab. The parameter R is useful to constrain whether a lateral velocity variation is caused by thermal and/or chemical origins. We analyzed seismograms of Izu-Bonin deep events observed by three broadband seismic networks of F-net, IRIS and CDSN (China Digital Seismographic Network). The CDSN data are important since body waves observed at the CDSN stations should travel a long distance in the stagnant slab. The observed first arrivals are significantly early relative to the Iasp91 model beneath northeastern China: Travel time residuals are -3~-4 s for P-wave and -6~-8 s for S-wave, which implies that the stagnant slab has fast S-velocity anomalies as well as fast P-velocity anomalies. We computed theoretical travel times of the first P arrivals with a three-dimensional P-velocity model (Obayashi et al., 2006) using the wave-front propagation method (Sakai, 1992) in which the stagnant slab beneath the studied region has fast P-velocity anomalies of 1-1.5 %. We calculated S-wave travel times with the S-velocity model constructed from the P-velocity model using a constant R . The theoretical travel times are in good agreement with the observed one for both P- and S-wave with the value of R of ~ 1.7 .

Keywords: stagnant slab, tomography



(S) - IASPEI - *International Association of Seismology and Physics of the Earth's Interior*

JSS012

Poster presentation

2212

Implication of low velocity anomaly found beneath the oceanward side of Honshu subduction zone: Interaction between the sinking hot anomaly and exothermic phase change

Dr. Satoru Honda

Earthquake Research Institute University of Tokyo IASPEI

Manabu Morishige, Yuji Orihashi

Tomographic results are important to understand the dynamics of the mantle. Recently, Obayashi et al. (2006) confirmed the existence of slow velocity anomaly under the ocean side of the Honshu subduction zone and they interpreted as hot anomaly around 200 degrees. This hot anomaly is closely related to the 410 km seismic discontinuity which is supposed to be related to the exothermic phase change from olivine to wadsleyite. Such a correlation appears to contradict our popular view of interaction between the exothermic phase change and convection that demands the promotion of the mantle flow. Here we consider a scenario in which a hot anomaly, whose origin might be a part of remains of hot plume(s) and/or stem(s), is dragged down by the slab and it interacts with the exothermic phase change near 410 km. The presence of exothermic phase change retards the downward movement of hot anomaly. Thus, the hot anomaly may stay near the 410 km for a while. To analyze this hypothesis, we have constructed a simple numerical model. We found that the hottest part is located above the 410 km discontinuity and stays there for a while. This may explain the observation and suggests that the determination of detailed distribution constrains the nature of the 410 km discontinuity. The time for the hot plume to stay near the 410 km discontinuity depends on many factors, such as the intensity of thermal anomalies and the viscosity. The hot anomaly whose size is equivalent to a few thousands km (horizontal) \times 100 km (vertical) may stay there \sim 100 million years. We shall discuss the geologic implication of this result.

Keywords: 410kmdiscontinuity, tomography, convection



(S) - IASPEI - *International Association of Seismology and Physics of the Earth's Interior*

JSS012

Poster presentation

2213

Mantle anisotropy beneath the eastern Asia

Dr. Yoko Tono
IFREE JAMSTEC IASPEI

Yoshio Fukao, Takashi Kunugi, Seiji Tsuboi

We made a detailed mapping of shear-wave splitting parameters of multiple ScS phases for the whole Japanese islands and their back-arc region. A set of multiple ScS phases (ScS, sScS, ScS2 and sScS2) has a mutually common source-receiver pair among the three nearby deep shocks and more than 550 stations of the Hi-net tiltmeter network and several IRIS stations situated in eastern Asia. The multiplicity of the ScS phases, three deep shocks with different focal mechanisms and an unprecedented number of stations made it possible to resolve mantle anisotropy into the two parts, anisotropy in the wedge mantle and the subducted Pacific-slab. The anisotropy of the wedge mantle shows a clear distinction of splitting pattern across the volcanic front. Such a distinction persists all along the southern Kuril, northern Honshu and Ryukyu arcs. On the Pacific side of the volcanic front vertically propagating shear wave is polarized with the fast direction approximately parallel to the trench, whereas it is polarized with the fast direction approximately parallel to the plate convergence direction on the marginal sea side of the volcanic front. This anisotropic system with the fast direction parallel to the plate convergence direction appears to extend to the Asian continent across the Japan Sea further away from the volcanic front. The Pacific-slab is anisotropic with the fast direction uniformly in the NNW, closely parallel to the Mesozoic fracture zones and perpendicular to the magnetic lineations on the northwestern Pacific seafloor. The NNW alignment extends into the β -spinel region well beyond the 400-km depth contour of the Wadati-Benioff zone but does not extend to the source region of the Vladivostok event at a depth of 566 km in the presumably oldest part of the subducted slab. The splitting parameters estimated from MDJ station, which is very close to the epicenter of the Vladivostok event, clearly shows a different anisotropy system with the fast direction roughly in EW.

Keywords: anisotropy, pacific slab, wedge mantle



(S) - IASPEI - *International Association of Seismology and Physics of the Earth's Interior*

JSS012

Poster presentation

2214

Thermal conductivity and thermal diffusivity of slab materials under high pressure

Dr. Masahiro Osako

Physical sciences and engineering National Museum of Nature and Science IASPEI

Akira Yoneda, Eiji Ito

Thermal properties of materials controls dynamics of the mantle and, in particular, behavior of descending slabs. The temperature contrast between slabs and its surroundings is due to thermal transport properties, i.e. thermal conductivity or thermal diffusivity, and the resulting density contrast can be a major source of the driving force. We determined thermal conductivity and thermal diffusivity of major mantle materials, olivine and garnet, and presented their values in the condition of the upper mantle, however, these data are for the materials of the non-hydrated mantle. Although these materials occupy considerable fractions in the mantle, minor constituents including hydrous phases are important to study behavior of the descending slabs. We proceed to measure thermal conductivity and thermal diffusivity for hydrous materials being characteristic of descending slabs. We use a pulse heating method for simultaneous thermal conductivity and thermal diffusivity measurement. The measurements are performed using a Kawai-type high-pressure apparatus at the Institute for Study of the Earth's Interior, Misasa. We have measured serpentine under pressure. The sample used was antigorite with light-greenish color and transparency. The result shows that serpentine has lower thermal conductivity and thermal diffusivity than dry mantle materials: at 2 GPa the values are about half of those of olivine. Moreover, their pressure derivatives are small to a pressure of 5 GPa compared with olivine, and show almost zero or slightly negative above this pressure. This behavior might be due to amorphization of serpentine under pressure. At 5 GPa serpentine could decompose above 800 K, because the thermal conductivity and thermal diffusivity were unobservable. It is said that serpentine is stable below 900 K at 5 GPa, and unstable just above the room temperature at 8.4 GPa. However at 8.4 GPa thermal conductivity and thermal diffusivity at high temperatures showed similar change. The measurements at 8.4 GPa were probably done for meta-stable state of serpentine. Decrease of thermal conductivity is smaller than that of thermal diffusivity; this will result in large change in the heat capacity at this temperature range, up to 800 K. Nevertheless, the measurements might be conducted during decomposing of serpentine, and therefore, additional measurements were needed to verify whether these results indicate intrinsic in serpentine or not. In any case, hydrous phases may show unexpected behavior in thermal properties, thermal conductivity or thermal diffusivity and heat capacity. Another measurements for hydrous phases, such as talc and amphibole are intended. Moreover, measurements of important high-pressure hydrous phases are needed. Samples of these phases prepared by sintering are far small, so the sample assembly is to reduce in its size, smaller than 3 mm in diameter. Although the experiments became troublesome, the upper pressure range of measurements can exceed 15 GPa.

Keywords: thermal conductivity, thermal diffusivity, high pressure

(S) - IASPEI - International Association of Seismology and Physics of the Earth's Interior

JSS012

Poster presentation

2215

Instantaneous mantle flow induced by subduction of a freely sinking slab

Dr. Claudia Piromallo

Seismology and Tectonophysics INGV-Roma IASPEI

Thorsten W. Becker, Francesca Funiciello, Claudio Faccenna

We conduct three-dimensional subduction experiments by a finite element approach to study flow around slabs, which are prescribed based on a transient stage of upper mantle subduction from a laboratory model. Instantaneous velocity field solutions are examined for a slab that sinks freely into the mantle, focusing on the toroidal vs. poloidal components as a function of boundary conditions (BCs), plate width, and viscosity contrast between slab and mantle. The 3-D approach shows that the toroidal flow plays a key role in affecting the circulation geometry in the vertical plane, compared to the 2-D case. In particular, the material resumed at surface in the back-arc wedge by the return flow cell below the slab tip is minimal with respect to 2-D models, in agreement with laboratory models. Furthermore, we find that circulation is characterized by a non-negligible upward flow component close to slab sides, that could have important implications to interpret local tectonic structure at slab edges. We show that BCs affect the magnitude as well as the pattern of the flow velocity field. In particular, in proximity of the slab the flow field is similar for no- and free-slip BCs, while strong variations exist elsewhere. Moreover, in our models of a transient subduction stage, the characteristic spatial length-scale influencing the flow pattern is given by the box height. By modelling different viscosity contrasts between slab and mantle (η), we find that significant return flow around edges can only be obtained for stiff slabs and that the strength of the Toroidal/Poloidal Ratio increases with η , nearly independent of slab width. We observe that for $\eta \geq 103$ the toroidal flow components make up about 60-70% of the poloidal ones, while we estimate about 40-50% for lower viscosity contrasts (~ 102). We note in our models that the toroidal term peaks for slab/mantle viscosity ratios $\eta_{\max} = 102$, independent of slab w . This trend is found not only for transient but also for steady-state, rollback subduction. Estimates for effective viscosity contrasts in nature are comparable to, or somewhat higher than η_{\max} .

Keywords: subduction, toroidal flow, mantle



(S) - IASPEI - *International Association of Seismology and Physics of the Earth's Interior*

JSS013

2216 - 2251

**Symposium
The lithosphere**

Convener : Prof. Sierd Cloetingh

Co-Convener : Prof. Hans Thybo

This session will include multi-disciplinary discussions of the continental lithosphere from geophysical, geochemical, and geologic data. The focus will be on probing the structure and composition of the lithosphere, including its physical properties, by both indirect and direct methods. Studies of the processes that have formed and modified the continental lithosphere since the Archean to the present are welcome. Some of the topics to be addressed include: (1) integrated thermal, gravity, electrical, and seismic models of lithospheric structure; (2) global and regional geophysical models of lithospheric structure; (3) studies of mantle xenoliths in the context of complementary geophysical results; (4) lithospheric stability; (5) models of lithospheric deformation from mantle xenoliths, seismic anisotropy, electrical properties, and other data. (6) discussions of the multitude of definitions of the lithosphere according to method, e.g. seismology, structural studies, electromagnetism, geothermology, and petrology.



(S) - IASPEI - *International Association of Seismology and Physics of the Earth's Interior*

JSS013

Oral Presentation

2216

Variations in mechanical anisotropy of the continental lithosphere

Dr. Jon Kirby

Spatial Sciences Curtin University of Technology IAG

Chris Swain, Steve Reddy

Spatial and azimuthal variations in the flexural rigidity of the lithosphere can be revealed through a wavelet analysis of gravity and topography data. The same method that we use to estimate elastic thickness variations is readily adaptable to such anisotropic studies. This mechanical anisotropy is thought to arise from gross alignment of olivine crystals in the upper mantle. Here we present results of such an analysis over continental lithosphere, and provide correlations with data from seismic anisotropy studies, whose variations are thought to arise from similar sources. These results show a good degree of correlation between mechanical and seismic anisotropies.

Keywords: anisotropy, wavelets

XXIV2007

PERUGIA
I T A L Y



(S) - IASPEI - *International Association of Seismology and Physics of the Earth's Interior*

JSS013

Oral Presentation

2217

A 3D shear wave velocity model of the Eastern Alpine crust from active source data

Dr. Michael Behm

Institute of Geodesy and Geophysics Vienna University of Technology IASPEI

Ewald Brckl, Celebration 2000 Working Group, Alp 2002 Working Group, Sudetes 2003 Working Group

Between 1997 and 2003, several large seismic 3D wide angle and reflection experiments were launched in Central Europe to explore the lithospheric structure. Seismic waves from shot points in boreholes (average charge 300 kg TNT) were recorded on a net of arbitrary oriented seismic profiles, thus enabling to identify inline and crossline wave arrivals (refractions and reflections from the crust and uppermost mantle). Despite that only vertical component geophones were used, good quality shear waves are also regularly observed in the seismic sections, in particular refractions (Sg) from the crust and reflections (SmS) from the Moho. We focus on a data subset of ~93,000 seismic traces from the CELEBRATION 2000, ALP 2002 and SUDETES 2003 experiments, which covers the area of the Eastern Alps and their transition to the surrounding tectonic provinces (Bohemian Massif, Southern Alps/Dinarides, Pannonian Domain). Sorting and stacking techniques are applied to increase the S/N ratio and to utilise as much 3D information as possible. As a first result we present a 3D seismic shear-wave velocity model of the crust derived from Sg arrivals. The middle and even lower crust of the Bohemian Massif is covered well by the model. In some parts of the orogenes (Eastern / Southern Alps) the energy loss due to the complicated tectonic structure allows for interpretation of the upper crust only. Based on this and previously determined P-wave velocities, the 3D distribution of Poissons ratio is calculated. S-wave velocities and Poissons ratio are related to the geological and tectonic structure.

Keywords: crust, s wave, alps



(S) - IASPEI - *International Association of Seismology and Physics of the Earth's Interior*

JSS013

Oral Presentation

2218

Beam Formed Receiver Functions from the

Mr. Will Levandowski

Department of Geosciences Princeton University IASPEI

Single station receiver functions in the southern Sierra Nevada, California show considerable variation in Moho P-S conversion intensity. Specifically, in the ranges western foothills, a region termed the Moho Hole (e.g. Zandt et al, 2004), the Moho appears to be completely absent on single station receiver functions. I explore the possibility that signal-generated reverberations have sufficiently obscured the seismograms to disguise a Moho P-S conversion. Using data from the 1997 Sierra Paradox Experiment, seismograms from 3 station sub-arrays (~20 km aperture) are slant-stacked to make the radial, transverse, and vertical components used in deconvolution. By stacking before deconvolution, signals from the Moho and intra-crustal discontinuities become more pronounced while reflections off of structures near individual receivers destructively interfere with one another. Receiver functions for these 3 station beams compare favorably with post-deconvolution stacking of the receiver functions calculated for their constituent stations. Of paramount interest is the use of this technique in the region interpreted as the Moho Hole. Here, beam formed receiver functions better constrain the extent and geometry of the small amplitude Moho conversion. In fact, it seems that this region is part of a larger trend: weakening of P-S conversion signals west from the range crest. This weakening trend mirrors a westward thickening of the crust observed in increasing P to P-S lag times. I propose that the two trends are cogenetic, caused by large scale (~100 km horizontally) downwarping of the Moho due to viscous coupling to downwelling delaminated lower lithosphere. This observed Moho geometry has implications for the mechanical response of upper crustal material to delamination events and the kinematics of uplift of the Sierra.

Keywords: delamination, receiver functions, beam forming



(S) - IASPEI - International Association of Seismology and Physics of the Earth's Interior

JSS013

Oral Presentation

2219

Nature of the South Indian precambrian crust

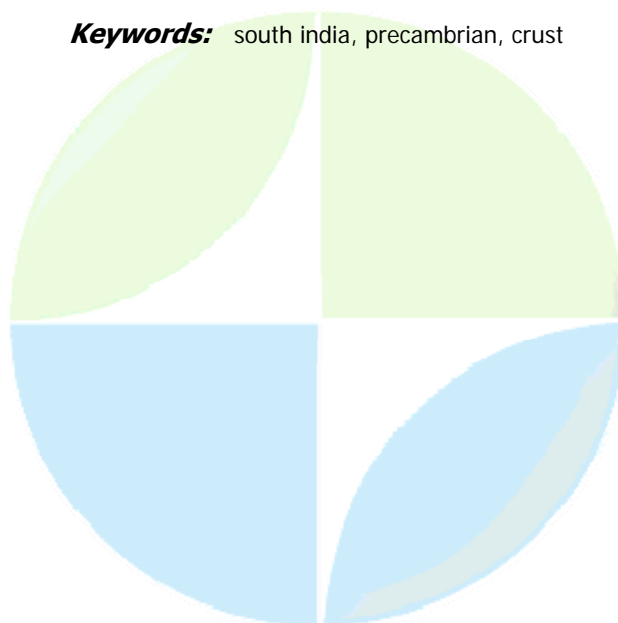
Dr. Shyam Rai

Seismic Tomography National Geophysical Research Institute IASPEI

Sandeep Gupta, S. Jagdeesh, Vinod Gaur

South India is a collage of several crustal blocks formed by geodynamic processes operating from mid-Archean to Neo-Proterozoic. The main geological province constitutes Dharwar craton, Granulite terrain and Cuddapah basin. Dharwar craton is an Archean continental fragment with a continuously exposed crustal section from low grade gneisses and greenstone belts in the north to granulites in south. Western part of craton hosts the 3.4 Ga greenstone belt while its northern part is covered with 65Ma Deccan volcanics. What forms the basement of the basalt is an unresolved issue. Eastern part of the Dharwar craton is wrapped by the Proterozoic Cuddapah basin. To the south of the craton is the high grade metamorphic terrain with imprint from Archean to late Proterozoic. These diverse crustal fragments of south India make it ideally suited to model the nature of the Archean crust and its possible deformation with time. We model the crustal structure of south India at 35 broadband seismograph locations through joint inversion of the receiver functions with the surface wave group velocity measurements. Moho depth varies significantly from 35 km beneath the late Archean eastern Dharwar craton (EDC), and Deccan volcanic province (DVP) to over 45 km beneath the mid Archean granite-greenstone belt in the western Dharwar craton (WDC), and ~40 km beneath the granulite terrain. The average shear velocity of south Indian crust varies from 3.66 km/s in upper part to ~ 3.9 km/s in the lower half and is higher than the global average for Precambrian terrains. We present the details of intra-terrain velocity variation in the crust, correlate with the surface geology and speculate the possible rock composition with depth in different terrains. These S- velocity derived composition sections along with recently acquired heat production in different rock types of south India have been used to infer the present day crustal contribution to the surface heat flow and therefore the mantle heat contribution. Together with these shear velocity and heat flow, we have used the reliable estimates of P-velocity with depth, nature of seismic reflector, conductivity variation with depth derived from MT measurements and the geochemical measurements to understand the crust composition and possible models of evolution.

Keywords: south india, precambrian, crust



(S) - IASPEI - International Association of Seismology and Physics of the Earth's Interior

JSS013

Oral Presentation

2220

Crust and upper mantle anisotropy in the Central Alborz Region

Dr. Ahmad Sadidkhouy

Seismology Institute of Geophysics, Tehran University

Gholam Javan Doloei

During the last 3 decades, the determination of anisotropy is a subject of interest for seismologists. In this study, we investigated anisotropy by shear wave splitting of Ps and SKS phases on broadband and short period seismograms. When a shear wave propagates through an anisotropic medium, energy is partitioned into orthogonally polarized fast and slow shear waves. This property is referred to as shear wave splitting. In this study we used shear wave splitting of Moho Ps and SKS phases from teleseismic to identify and estimate the shear wave anisotropy in the crust and upper mantle of the Alborz region (IRAN). The use of Moho Ps phase to study anisotropy is potentially valuable since it is one of the few ways to isolate the lower crust in the study of anisotropy. The SKS phase is a good tool for determining of anisotropy because in an isotropic medium, there is no SKS energy on the transverse component so that the presence of transverse energy indicates the rate of anisotropy. In this study, we selected teleseismic events (& for shear wave splitting of Ps method and for shear wave splitting of SKS method) which were recorded in 3 broadband seismic stations, DAMV, CHTH and THKV (International Institute of Earthquake Engineering and Seismology (IIEES)) and also 6 short period seismic stations, FIR, DMV, AFJ, SHR, MHD and GZV (Institute of Geophysics, Tehran University, (IGTU)) for determining anisotropy parameters in crust and upper mantle of the Alborz region. The majority of receiver functions showed two different Ps phases before Moho Ps on radial component. We believed in that the first Ps phase is generated in the upper crust ($h < 18$ km) while, the second one is belonging to the intermediate crust ($18 < h < 30$ km). The shear wave splitting of Ps phase is generated at the Moho, and thus any splitting must be due to an anisotropic region in lower crust. We estimated the average directions of anisotropy in crust of the Alborz region to be about 24 to 77 degree. Thus, the fast azimuth of anisotropy oriented approximately NE-SW as well. Moreover our results showed that the magnitude of anisotropy is about 0.22 to 0.29 seconds. The average direction of anisotropy in upper mantle of the Alborz region is estimated in a range of 35 to 71 degree by means of shear wave splitting SKS phase analysis. Moreover our results showed that the magnitude of anisotropy is about 1.2 to 1.9 seconds. The NE-SW trending fast azimuth calculated from this study is roughly perpendicular to the dominant fracture systems in the Alborz region. Our results were also in good agreement with results of previous studies. This strongly suggests coherent crust and upper mantle anisotropy in this region with a fast direction perpendicular to the strike of the Alborz mountain ranges.

Keywords: alborzmountainanisotropy, psconvertedphase, receiverfunctionskspase

(S) - IASPEI - *International Association of Seismology and Physics of the Earth's Interior*

JSS013

Oral Presentation

2221

Feedback between Andean mountain belt growth and plate convergence: a climate-driven process?

Mr. Giampiero Iaffaldano

Earth and Environmental Sciences Geophysics Section

Hans-Peter Bunge, Timothy H. Dixon, Martin Bcker

While it is generally assumed that global plate motions are driven by the pattern of convection in the Earth's mantle, the details of that linkage remain obscure. Buoyancy forces associated with subduction of cool, dense lithosphere at zones of plate convergence are thought to provide significant driving force, but the relative magnitudes of other driving and resisting forces are less clear. The ability to consider past as well as present plate motions provides significant additional constraints, because changes in plate motion are necessarily driven by changes in one or more driving or resisting forces, which may be inferred from independent data. Here we first exploit the capabilities of forward and inverse tectonic models of the Andean region to infer plate motion changes as far back as Miocene time. By accurately predicting observed convergence rates between Nazca and South America plates over the last 10 Myrs, we demonstrate that the growing topographic load of the Andes increases frictional resisting forces between downgoing and overriding plates and thus consumes a significant amount of the driving force available for plate tectonics. This result suggests a strong feedback between mountain belt growth and plate convergence. Finally, we speculate about the possibility of the role of climate in controlling such processes. Recently some authors have argued that climate may have strongly influenced the development and hence the morphology of the Andes. Climate variations occurring on the hemisphere scale generate in fact strong latitudinal precipitation gradients which result in large erosion variations along the mountain belt, from very high in the northern and southern parts to extremely low in the middle. Low erosion rates, however, have been implicated as a pre-requisite for the development of large plateaus such as the Puna and the Altiplano, which affect in turn the dynamics of Nazca and South America plates. In other words climate may potentially act as a force on plate tectonics.

Keywords: plate convergence, mountain building



(S) - IASPEI - *International Association of Seismology and Physics of the Earth's Interior*

JSS013

Oral Presentation

2222

High-Resolution 3D Anisotropic Structure of the North American Upper Mantle from Inversion of Body and Surface Waveform Data

Prof. Barbara Romanowicz

Berkeley Seismological Laboratory University of California at Berkeley IASPEI

Federica Marone

Seismic anisotropy provides insight into paleo and recent deformation processes and therefore mantle dynamics. Our knowledge of the upper mantle anisotropic structure under North America is based mainly on global tomographic models or SKS splitting studies which lack horizontal and vertical resolution respectively. In particular, the azimuthal anisotropy derived from local SKS splitting measurements and that predicted from surface wave inversions shows a well documented discrepancy especially under continents. We present here the first 3D regional tomographic model of the North American upper mantle, which simultaneously includes both radial and azimuthal anisotropy and reconciles this discrepancy. The novelty of our approach consists in the joint inversion of fundamental and higher mode surface waveforms together with constraints on azimuthal anisotropy derived from SKS splitting measurements, producing a 3D anisotropic model with enhanced depth resolution down to the transition zone. In a first step, we inverted long period waveform data simultaneously for perturbations in the isotropic S-velocity structure, the anisotropic parameter $\chi = (V_{sh}/V_{sv})^2$ and the depth to the Moho, in the framework of normal mode asymptotic theory (NACT) (Li and Romanowicz, 1995), correcting for 3D structure outside of the region of study using a global radially anisotropic model of the upper mantle, and correcting for crustal structure using a non-linear approach adapted to the large lateral variations of Moho depth. The resulting 2D broad-band sensitivity kernels allow us to exploit the information contained in long-period seismograms for body, fundamental and higher-mode surface waves at the same time. We have adapted the NACT algorithm for the regional case by implementing a lateral parametrization in terms of spherical splines on an inhomogeneous triangular grid of nodes, with the finest mesh for North America. The inverted dataset consists of more than 100,000 high quality 3-component body, fundamental and overtone surface waveforms, recorded at broad-band seismic stations in North America from teleseismic events. Notable features of the radially anisotropic part of the model are a positive ξ anomaly down to 300 km under cratons, indicating the presence of horizontal shear in the asthenosphere and a negative ξ anomaly beneath the Basin and Range province, which suggests the presence of mantle upwelling. Our 3D azimuthal anisotropic model indicates the presence of two layers of anisotropy with distinct fast axis directions under the stable part of the North American continent: a deeper layer with the fast axis direction aligned with the absolute plate motion direction suggesting lattice preferred orientation of anisotropic minerals in a present day asthenospheric flow and a shallower lithospheric layer likely showing records of past tectonic events. Under the tectonically active western US, where the lithosphere is thin, the direction of tomographically inferred anisotropy is stable with depth and compatible with the absolute plate motion direction. Synthetic SKS splitting parameters computed for this new 3D azimuthal anisotropic model are in good agreement with observations throughout North America. We believe that previous surface wave based models had rather low resolution power at depths greater than 200 km, and strongly underestimated the strength of the anisotropy at large depths beneath cratons. Still, the distribution of data, particularly SKS splitting data, across the US is very uneven, with large holes in the central and eastern US.

Keywords: lithosphere, asthenosphere, anisotropy

(S) - IASPEI - *International Association of Seismology and Physics of the Earth's Interior*

JSS013

Oral Presentation

2223

Deep density structure and EET of lithosphere in the NW Himalaya and Laddakh from analyses of gravity anomalies

Dr. Virendra Mani Tiwari

GRAVITY National Geophysical Research Institute IASPEI

V.M. Tiwari, P. Banerjee, B. Singh

We use recently recorded gravity data along a profile in the NW Himalaya along with data over Indian shield, Ganga basin and Laddakh to construct a deep density model across Himalayan orogeny belt. Density model constrained from all available geophysical observations such as teleseismic receiver functions and magnetotelluric results are utilised in defining subsurface load to estimate the effective elastic thickness (EET) of the lithosphere along a profile perpendicular to the Himalaya. Furthermore, we use a wavelet transform to compute coherence between Bouguer gravity and topography of existing data to map the variations of EET in the NW Himalaya. Our results confirm the earlier results that EET decreases to the north as Indian plate descends to the Himalaya.

Keywords: himalaya, gravity, lithosphere



(S) - IASPEI - *International Association of Seismology and Physics of the Earth's Interior*

JSS013

Oral Presentation

2224

Magmatic underplating of crust beneath the Laccadive Island, NW Indian Ocean

Dr. Sandeep Gupta

Seismic Tomography National Geophysical Research Institute, Hyderabad

Shyam Rai, Santosh Mishra

Laccadive Island is the northern segment of Chagos- Laccadive Ridge (CLR), a prominent aseismic topographic/tectonic feature in the NW Indian Ocean. Despite its significance in providing critical linkage between the hotspot and genesis of islands, it is poorly investigated using modern seismological tools. We investigate the crustal velocity structure beneath Laccadive Island through receiver function modelling of teleseismic waveform recorded on the island broadband station during January April 2005. The crustal velocity structure suggests ~16 km thick oceanic crust with layers of 0.5, 1.0, 6.0, 8.0 km thickness and shear velocities of 0.65, 2.2, 2.95, 3.98 km/s, respectively at depth. This is followed by ~10 km thick layer of shear velocity ~4.3 km/s layer. Further deep, at depth of 26 km, we observe uppermost mantle shear velocity 4.8 km/s. The presence of intermediate crust-mantle velocity layer could be interpreted as the underplating of mantle-derived melt at the base of oceanic crust which progressively deepens the crust-mantle boundary at 26 km. The melt was produced during the interaction of Indian plate with the Reunion hotspot. Continuity of crustal underplated material beneath Laccadive could be traced to Laxmi Ridge in the north and to Reunion Island in the south, suggesting this to be trace of the hotspot. This result along with measurements over other hotspot linked oceanic islands reinforces that crustal underplating is their common heritage.

Keywords: laccadive island, magmatic underplating, crustal structure



(S) - IASPEI - *International Association of Seismology and Physics of the Earth's Interior*

JSS013

Oral Presentation

2225

European mantle lithosphere as a mosaic of plates with their own pre-assembly anisotropy signature

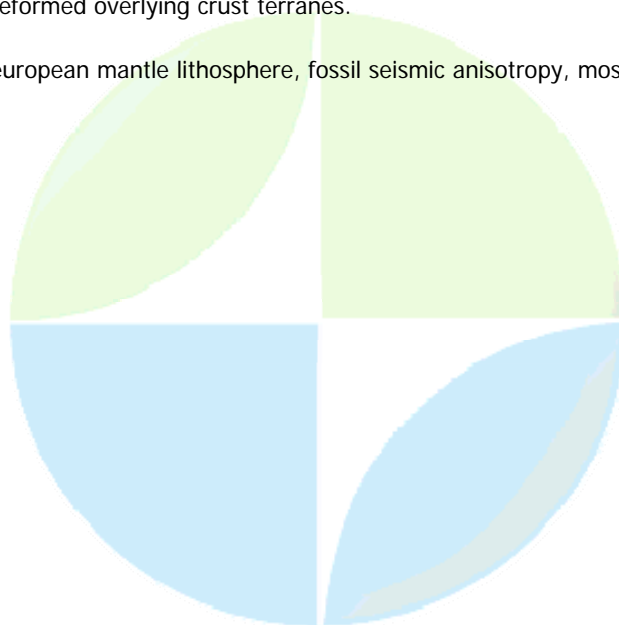
Dr. Vladislav Babuska

Seismology Geophysical Institute, Czech Acad. Sci. IASPEI

Jaroslava Plomerova

The concept of mobile terranes, or micro-continents, is considered as one of the most important additions to plate tectonics. However, we have only vague ideas about a role of large volumes of the mantle lithosphere in the formation of paleo-continents, in their break-up and in later assemblage of their pieces into a new continent. Knowledge of seismic anisotropy is key to our understanding of tectonic fabrics in the deep lithosphere and sublithospheric mantle. To study building elements of the European continent, we have modelled three-dimensional seismic anisotropy of the mantle lithosphere from anisotropic parameters of teleseismic body waves. We invert and interpret jointly shear-wave splitting parameters and P residual spheres based on data from dense networks of temporary and permanent stations in several European regions. Changes in orientation of the large-scale anisotropy, caused by systematic preferred orientation of olivine, identify boundaries of domains of mantle lithosphere. Individual domains are characterized by a consistent large-scale orientation of anisotropy approximated by hexagonal or orthorhombic symmetry with generally inclined symmetry axes. The domains are separated by mapped tectonic boundaries (sutures), which cut the entire lithosphere. Such boundaries play important role in the lithosphere architecture and its dynamics, e.g. in the location of intraplate earthquakes and volcanic fields. Besides the change of anisotropy orientation at domain boundaries, we often observe a change of the lithosphere and/or crust thicknesses. We do not detect any fabric of the mantle lithosphere, which could have been produced by a collision of microcontinents in a volume detectable by large-scale seismic anisotropy. The observations of consistent anisotropy within individual blocks of the mantle lithosphere reflect frozen-in olivine preferred orientation, most probably formed prior to the assembly of microcontinents that created the modern European landmass. Therefore, our findings support a plate-tectonic view of the continental lithosphere as a mosaic of rigid blocks of the mantle lithosphere with complicated but relatively sharp contact zones. These contacts are blurred by the easily deformed overlying crust terranes.

Keywords: european mantle lithosphere, fossil seismic anisotropy, mosaic of microplates



(S) - IASPEI - *International Association of Seismology and Physics of the Earth's Interior*

JSS013

Oral Presentation

2226

High resolution mapping of the lithospheric thickness with S receiver functions

Prof. Rainer Kind

Seismology GFZ Potsdam IASPEI

X. Yuan, F. Sodoudi, B. Heuer, W. Geissler, P. Kumar

The lithosphere is a mechanical definition, not a seismic one (in contrast to the crust-mantle boundary). Seismic low velocity zones have been discovered in the upper mantle (mainly with surface waves), which are associated with the asthenosphere. The boundary between lithosphere and asthenosphere (LAB) was considered a gradual transition zone. The still relatively seismic new technique of S receiver functions is able to resolve the LAB with much higher resolution than previously possible. This technique can be applied to seismic data of the many existing permanent stations and to data from temporarily deployed stations. We have used S receiver functions in Greece, central Europe, Iceland and Greenland for mapping the LAB. Beneath the northern Aegean we observe the African LAB at more than 200 km depth, in Germany and northern Bohemia it is near 80 km, whereas in southern Bohemia its depth reaches more than 100 km. The cratonic lithosphere east of the Trans European Suture Zone and in Greenland reaches 100-120 km. In Iceland we observe a clear negative discontinuity at about 80 km depth. If this is the LAB, it would be in contrast to the postglacial rebound data. We expect to have a global LAB map in the near future using this new body wave technique.

Keywords: lithospheric thickness, sreceiver functions, labmaps

PERUGIA
ITALY



(S) - IASPEI - *International Association of Seismology and Physics of the Earth's Interior*

JSS013

Oral Presentation

2227

Inversion of viscous properties of crust and mantle from the GPS temporal series measurements

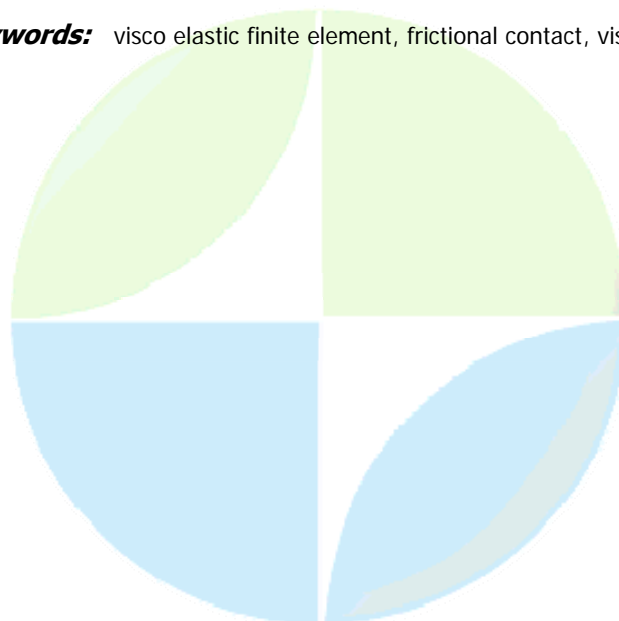
Dr. Shoubiao Zhu

Geophysics Institute of Crustal Dynamics, CEA IASPEI

Yongen Cai

The viscous properties of earth media are very important in geodynamics. Taking the physical property variation of focal media after earthquake into account, we propose the method to inverse the viscosities in lower crust and upper mantle from GPS temporal series measurements. Combining the genetic algorithm (GA) and Marquardt inversion, we regard the optimum model sought by GA as the initial one to carry out inversion by Marquardt method, in which the Jacobian matrix is produced by small perturbation. The areas of focal region are decided by aftershocks and by the velocity changes of seismic waves before and after the main shock. In inversion, visco-elastic finite element method (VFEM) is applied to calculate the surface displacements. The differences of the surface displacements in each time between the computed by VFEM and the observed by GPS are regarded as object function for optimization. The profile in which the GPS station 5936 in Taiwan, perpendicular to trace of Chelungpu fault is chosen as our model plane. The model consists of an upper crust overlying a lower crust and upper mantle. The parameters in the model are chosen as: the study plane is 230 km (west-east direction) by 120 km (deep from the surface). The boundary conditions are: the nodes on west side is fixed, the surface ground is free, the nodes on east side move westwards at constant velocity averaged by GPS measurements, the base of the model is stationary. In VFEM model, the number of triangular 6-node element is 3384 (6895 nodes). The rheology of the material is assumed to be linear Maxwellian. The shear modular, volume modular and density are chosen according to Preliminary Reference Earth Model. Noticing the substantial changes of both VP and VP/VS anomalies around epicentre before and after the Chi-Chi earthquake, we model the changes by assuming that the Poisson ratio of the media around the source region varies with time. Inversion computation and digital experiments show that the inversion method is high efficient and stable. The preliminary result suggests that viscosities of the lower crust and the upper mantle in Taiwan is 1.21018 pas and 3.61019 pas, respectively.

Keywords: visco elastic finite element, frictional contact, viscosity



(S) - IASPEI - *International Association of Seismology and Physics of the Earth's Interior*

JSS013

Oral Presentation

2228

Lithospheric structure and its relationship to diamond fertility of Dharwar and Bastar cratons of the Indian shield - a gravity perspective

Dr. Bijendra Singh

National Geophysical Research Institute, Hyderabad Scientist IASPEI

V. M. Tiwari, S. K. Verma

One of the unique features of the Indian shield is that it consists of number of Cratonic blocks bounded by mobile belts. The lithospheric structures across these terrains are not well resolved due to scanty of data. We have carried out gravity modeling along two long profiles cutting across the Indian shield to understand the lithospheric configuration below the Dharwar and Bastar Cratons. Modeling is constrained by the available geophysical results from deep seismic sounding, receiver function analysis, seismic tomography and magnetotelluric methods. After accounting for the anomalies due to known geological structures in the crust, long wavelength gravity response is interpreted in terms of variation in the thickness of the lithosphere. Modeling results suggest that the lithosphere below the western Dharwar Craton has got a maximum thickness of about 220-230 Km that reduces towards Eastern Dharwar Craton to about 150 Km. Under the Godavari rift, it further reduces to about 100-120 Km. North of Godavari in the Bastar Craton: the thickness again increases northward to about 200 Km. Interestingly, the study of 1.1 Ga mantle xenoliths from kimberlite of Dharwar Craton also provide similar depths. The lithospheric model thus obtained has significant implications on the geodynamic evolution of Dharwar and Bastar Cratons and Diamond fertility of Kimberlite fields north and south of Godavari rift. It is suggested that the Godavari rift represents the zone of suturing between Dharwar and Bastar Cratons during Archean period. The continent-continent collision of Dharwar and Bastar Cratons along Godavari suture zone (GSZ) gave rise to number of parallel fracture zones both north and south of the suture. The diamond fertility in Dharwar and Bastar Cratons are also governed by the GSZ below which the two Cratonic blocks show minimum thickness that is not conducive for diamond generation and stability. This is well reflected in the diamond barren kimberlite clusters belonging to Tokapal kimberlite field lying in the north and Narayanpet kimberlite field (NKF) lying to the south of GSZ. Kimberlite clusters further away from GZS are likely to be diamond fertile as they sample a thicker lithosphere providing necessary conditions for diamond generation and stability. Geochemical studies of mantle xenolith also reveal that these are derived from a 220-240 km thick lithosphere from less than 160 km lithosphere for the NKF. It is inferred that the Dharwar Craton in Peninsular India has not been subjected to any major destabilization during the past one billion years.

Keywords: kimberlite, cratons, gravity modeling

(S) - IASPEI - *International Association of Seismology and Physics of the Earth's Interior*

JSS013

Oral Presentation

2229

A new gravity model of the lithosphere of Northern Eurasia based on joint inversion of the gravity and seismic data.

Dr. Mikhail Kaban

Dept. 1 GeoForschungsZentrum IASPEI

Density structure of the crust and upper mantle represents a key, which helps to understand origin of tectonic processes and evolution of the lithosphere. Gravity, seismic and other available data are used to construct a new density model of the crust and upper mantle of Northern Eurasia. One of the most principal issues of the deep gravity modelling is the problem to eliminate the crustal effect from the observed gravity field. At the initial stage of this study we construct a new unified model of the crust, which is based on available seismic determinations. Compared to the previous models, it is principally improved for the territory of Western Europe (Tesauro et al., 2007) and Siberia. The new residual mantle gravity anomalies and residual topography are estimated based on these data. We invert these fields jointly with seismic tomography data to image density distribution within the crust and upper mantle. The inversion technique accounts for the fact that the residual gravity and residual topography are controlled by the same factors but in a different way, e.g. depending on depth. In the final stage we separate the effect of mantle temperature variations, which is estimated from seismic tomography models constrained by geothermal modelling. Some features of the composition density distribution, which are invisible in the seismic tomography data, are for the first time detected in the upper mantle. One important example is a strong positive density anomaly under significant part of the Alpine fold belt, which is likely related to remnants of the lithosphere plate. The constructed model also provides an explanation for the structure and tectonic evolution of the Siberian Platform. We can draw the conclusion that the density anomalies inferred in the subcrustal layer are related to variations in the upper mantle composition. In this case, the low-density zone in NW Eastern Siberia can be considered as a direct consequence of mantle plume activity that took place 251 Myr ago. This zone in the upper mantle also corresponds to the zone of the maximum thickness of trap formations.

Keywords: gravity model, mantle density



(S) - IASPEI - *International Association of Seismology and Physics of the Earth's Interior*

JSS013

Oral Presentation

2230

Layering of seismic anisotropy and the past and present deformation of the lithosphere and asthenosphere beneath Germany.

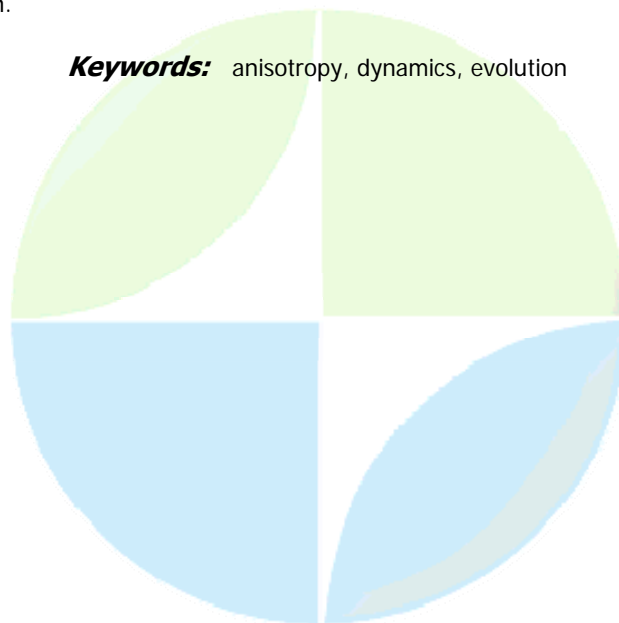
Dr. Sergei Lebedev

Earth Sciences Utrecht University IASPEI

Brigitte Endrun, Monika Bischoff, Thomas Meier

Dynamics of the lithosphere and asthenosphere has shaped and continues to re-shape the surface of Europe. We perform anisotropic array tomography with data from the German Regional Seismic Network and map--for the first time--stratification of seismic anisotropy beneath Germany within the entire lithosphere-asthenosphere depth range. Employing a new implementation of the two-station method, we measure interstation, surface-wave dispersion curves in broad period ranges (10-15 s to 250-400 s). We then invert the data for azimuthally anisotropic phase-velocity maps. Because surface waves at different periods sample different depths within the Earth, variations of anisotropy patterns with period (10--300 s) translate into tight constraints on the layering of seismic anisotropy within the lithosphere and asthenosphere. In both the lower crust and mantle lithosphere beneath the best-sampled western and central Germany, shear-wave fast-propagation directions are approximately NE, parallel to the strike of the Variscan suture. The lithospheric anisotropy is likely due to the fabric that has been created during the Variscan orogeny and frozen-in within the lithosphere ever since. The measured present thickness of this anisotropic layer thus constrains the thickness of the lithosphere at the end of the orogeny---important new information regarding the geodynamics of the continental collision. Between approximately 100 and 300 km depths, the anisotropic fast-propagation direction is distinctly different, striking East-West. This pattern is likely to reflect the strain in the asthenosphere due to the current and recent lithosphere-asthenosphere relative motion. The asthenospheric fast-propagation directions that we measure match those inferred from shear-wave splitting measurements; this shows that most of the splitting originates in the asthenosphere. Interestingly, the measured fast-propagation directions are also parallel to the published most conductive directions inferred from a magnetotelluric dataset, both in the lower crust (NE) and in the asthenosphere (E). The match of fast-propagation and high-conductivity directions has important implications for the origin of electrical anisotropy in the Earth.

Keywords: anisotropy, dynamics, evolution



(S) - IASPEI - *International Association of Seismology and Physics of the Earth's Interior*

JSS013

Oral Presentation

2231

Secular variations in the structure of the continental lithosphere over 3.5 Ga: A global analysis constrained by thermal data

Dr. Irina Artemieva

Geological Inst., Copenhagen Univ., Denmark IASPEI

Two global databases for the continents constrained on a 1 deg x 1 deg grid, (a) for tectono-thermal ages and (b) for lithospheric thermal thickness (Artemieva, Tectonophysics, 2006 and available for download at www.lithosphere.info), are used to analyse the age-dependence of structure and properties of the continental lithosphere. The analysis covers the entire geological history since the Archean until Cenozoic and includes global correlations between tectono-thermal ages of the continental lithosphere and (a) surface heat flow, (b) lithospheric thermal thickness, (c) seismic velocities in the upper mantle constrained by global tomography models, (d) compositional variations in the lithospheric mantle constrained by joint analysis of thermal and seismic tomography data. It is demonstrated that most of the physical properties of the post-Archean continental lithosphere show a strong age-dependence, while little variation with age is observed for the Archean lithosphere. A comparison with other geophysical and geochemical data (in particular, models of electrical conductivity for the mantle and xenoliths studies of mantle geotherms and mantle depletion) is presented.

Keywords: continental lithosphere, cratons, lithosphere thickness

PERUGIA
ITALY



(S) - IASPEI - *International Association of Seismology and Physics of the Earth's Interior*

JSS013

Poster presentation

2232

The Ypresian Lutetian boundary in the north of Tunisia, Biostratigraphy, Climatic, Tectonic and Environmental Events

Dr. Karoui- Yaakoub Narjess
geology facult des sciences de bizerte

Moufida Ben M'barek-Jemai, Nouredine Ben Ayed

The stratigraphic study of the Ypresian-Lutetian interval in the north of Tunisia is based on the planctic foraminifera distribution. Their analyses reveal that they are well preserved and very diversified and had permitted us to precise the biozonation of the Ypresian-Lutetian boundary. So we had identified the *Morozovella aragonensis* zone, the *Acarinina pentacamerata* zone and *Globigerinatheka subconglobata* zone. The simultaneous presence of the species *Hantkenina nuttalli*, *H. dumblei*, *Globigerinatheka mexicana mexicana* and *Morozovella lehneri* indicates that there is a hiatus of the *Hantkenina nuttalli* zone which is the first zone of early Lutetian. This hiatus doesn't exist in the center of Tunisia where limit was complete (Ben Ismail & Bobier, 1996). In the north of Tunisia, the hiatus of this zone would be linked to an active synsedimentary tectonics: the Eocene compression (Ben Ayed, 1986). The systematic and statistic analyses of benthic foraminifera at the Ypresian/Lutetian transition deposits, indicate that the benthic foraminifera are numerous, very diversified and are dominated by the infaunal groups. We note the co-existence of both the Midway and the Velasco type faunas. The most common Midwayan fauna species are: *Cibicidoides alleni*, *C. succedens*, *Anomalinoides acuta*, *A. midwayensis*, *Lenticulina midwayensis*, *Gavelinella dania*. The abundant Velascoan species are: *Nuttalides truempyi*, *Gavelinella rubiginosa*, *Gyroidinoides subangulatus*, *Gaudryina pyramidata*. The mineralogical and geochemical analyses of marls indicate the abundance of the kaolinite and smectite minerals, which indicate warm conditions. This warm climate is inherited since the Paleocene/Eocene boundary (Ben Ismail & Bobier, 1996; Bolle et al., 1999; Karoui-Yaakoub N., 1999; Thomas, E., J.C. Zachos & T.J. Bralower, 2000). At the upper of the Ypresian, the smectite is more abundant than the kaolinite with a pick 87%, this proves that the climate was warm with contrasted seasons: warm and dried periods alternated with warm and humid periods. At the base of the Lutetian the kaolinite became more abundant than the smectite, which indicates that the warm climate became more humid. In conclusion, the increase of planctic ratio, the highly diversified benthic fauna, the co-existence of both the Midway and Velasco type faunas and the abundance of the kaolinite and smectite minerals indicate probably a bathyal to deeper warm environment with some seasonal fluctuations. References Ben Ayed, N. (1986) - Evolution tectonique de l'avant-pays de la chaîne alpine de Tunisie du début du Mésozoïque à l'actuel. Thèse de Doctorat es-Sciences, Université Paris Sud Orsay. Edit. Office National Mines. Annales des Mines et de Géologie, 32, édition du Service géologique de Tunisie, 1993, 286 p. Ben Ismail & Bobier, 1996 Etude biostratigraphique, paléocologique et paléobiogéographique des séries éocènes (Yprésien-Lutétien basal) de Tunisie centrale. Géologie de l'Afrique et de l'Atlantique Sud, Actes Colloque Angers 1994, 563-583, 4 fig., 3 tab., 4 pl. Bolle Bolle, M.P., T. Adatte, G. Keller, K. Von Salis & S. Burns (1999) - The Paleocene-Eocene transition in southern Tethys (Tunisia): climatic and environmental fluctuations. Bulletin de la Société Géologique de France. 150 (5): 661-680. Karoui-Yaakoub N. (1999) - Le Paléocène en Tunisie septentrionale et centro-orientale: Systématique, biostratigraphie des Foraminifères et environnement de l'époque. Thèse de Doctorat, Université de Tunis II, 357 pp. Thomas, E., J.C. Zachos & T.J. Bralower (2000) - Deep-sea environments on a Warm Earth: Latest Paleocene-early Eocene. In: Huber, B.T. et al. (Eds). Warm climates in Earth History, Cambridge University Press, Cambridge, 132-160.

Keywords: ypresian lutetian interval, environment deposition, tunisia

(S) - IASPEI - *International Association of Seismology and Physics of the Earth's Interior*

JSS013

Poster presentation

2233

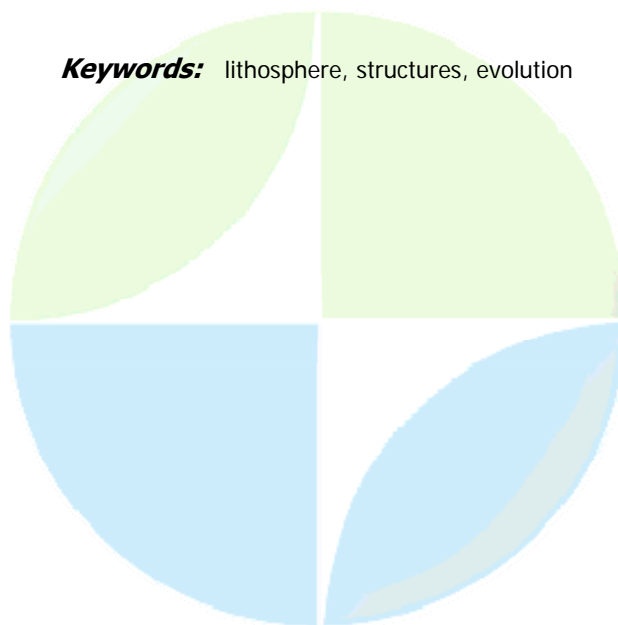
Deep lithospheric structures in geodynamical evolution of Middle Tien Shan

Dr. Irina Sidorova

Laboratory of Regional and Applied Geophysics Institute of Geology And Geophysics Academy of Sci IAMAS

This paper presents results of comprehensive analysis of the geologo-geophysical data in Uzbekistan using GIS&RS, which show in the spatial interrelations between the peculiarities of the Lithospheric structures of the region and geodynamic processes occurring there. Deciphering of structural units of western Uzbekistan territory using space images allows us to reveal regional, deeprooted lineaments, extending in latitudinal direction over Uzbekistan territory and neighboring countries. These lineaments or zone of lineaments with anomalous geoobjects widening from 50 up to 250 km are originated from a significant heterogeneity of upper mantle. The lineaments could penetrate the Earth up to deep lithosphere layers, inheriting a position of old fault-lineament systems which origin related to Precambrian to Paleocene tectonic processes. Some of these structural discontinuities are poorly expressed in surface geology, but can be detected by remote sensed methods, as well as by the magnetic and gravity anomalies. This study was made with complex geophysical and geological observations by the DSS-MOVZ profiles, that cross Uzbekistan and revealed a number of features, which are characteristic of the upper mantle rocks, related to morphology of bodies, their physical properties, consisting mainly in their contrasting values for contiguous blocks, and general increased velocity and density of the rocks they contain. Anomalous geological objects in Central Kyzylkum having anomalous high velocity and density values have been mapped at different depths within Central Kyzylkum: Muruntau, Kokpatas, Auminza-Beltau, Kuldjuktai, Darbazatau. The alteration zones, the tectonic lines and the circular structures related to the cones and calderas determined these methods and checked by group truth studies may be target areas to explore for some new deposits. New regional features have been revealed : they include peculiarities of the Earths crusts deep geological structure and spatial distribution of deposits; they are contact areas of the Earths crust geoblocks with anomalously high and low seismodensity parameters. Mapping of these zones helps select new ways in the search for mineral deposits.

Keywords: lithosphere, structures, evolution



(S) - IASPEI - *International Association of Seismology and Physics of the Earth's Interior*

JSS013

Poster presentation

2234

Comparison between fault lineaments on satellite images and Riedel model shear: a case study in Damavand Volcano, Central Alborz Mountains, Northern Iran

Mrs. Safieh Omidian

Department of Geology MSc. Student of Petrology, Department of Geology IASPEI

Jamshid Hassanzadeh, Mohsen Eliassi, Faribourz Gharib

The Alborz Mountains that fringe southern Caspian have deformed in response to the Arabia-Eurasia collision since ca. 12 Ma. An estimated shortening of 53–3 km has been accommodated by a combination of range-parallel, conjugate strike-slip faulting and range-normal thrusting. About 17 km of this shortening has been interpreted to be accommodated by westward relative motion of a crustal block bounded by conjugate dextral and sinistral strike-slip fault systems. It has also been shown that a change of dextral component of reverse faults to sinistral ones took place at 52 Ma ago. We have used remote sensing data in order to investigate the possible correlation between the lineaments pattern and Riedel model. The study was focused on Damavand volcano and its surrounding highlands; and Landsat ETM data were utilized to spot fault lineaments. By using several factors 2540 lineaments were distinguished. We discuss: 1) how comparable the rose diagram of these fault lineaments is with the Riedel model and 2) how a useful tool is this model to predict geometry of structures that may form in shallow crustal rocks deformed in a strike-slip regime. A principal displacement zone (PDZ) commonly forms parallel to the shear couple. Due to the direction of Arabia-Eurasia collision (N010-040), the prevailing structural trend is WNW-ESE; and 115° was taken as the dominant trend. Normal faults (T) should form perpendicular to the direction of maximum tensile stress. Riedel shears (R) form at an angle of (~15-20°) with the PDZ, where is the angle of internal friction for the faulted material (we considered which is typical of the upper crust). R shears will have the same sense of strike-slip motion as the PDZ, and they typically form a suite of en echelon fractures. Conjugate Riedel shears (R') can form at (~60-75°) relative to the PDZ. These conjugates have the opposite senses of strike-slip motion as the main fault. Finally, folds and thrust faults should form with their axes or traces, respectively, normal to the main compressive stress (P). Fold axes will initially be oriented at about 45° to the PDZ. Activation of first order phases results in second and third order R, R', T and P systematic fractures. Directions of the lineaments spotted on satellite images were tested with directions of the structural elements predicted by Riedel model for both sinistral and dextral systems. Most lineaments are compatible with this model. Exercising with Riedel model can provide indications for characteristics that fit each lineament.

Keywords: alborz, damavand, riedelmodel

(S) - IASPEI - *International Association of Seismology and Physics of the Earth's Interior*

JSS013

Poster presentation

2235

Petrology and geochemistry of Kuhe - Dom Volcanic Rocks in Ardestan, central Iran

Mrs. Neda Baranpourian
geology Petrology IAGA

Mohammad Hossain Razavi, Mohammad Hashem Emami

The Eocene volcano - sedimentary Rocks of Kuhe - Dom are located in Urmieh - Dokhtar magmatic belt in the northeast of Ardestan district, central Iran. The stratigraphic sequence is composed of lower Eocene Gorgab and Middle Eocene sahlab formations. The volcanic Rocks are olivine basalt, basaltic andesite, trachy basalt, trachy andesite andesite, dacite, rhyodacite and rhyolite. The pyroclastics rocks are less common in this area and consist of various types of crystal lithic tuffs and bereccias, in which crystals are essentially plagioclases and lithic fragments mainly basaltic-andesites and trachy-basalt-andesites. On the basis of trace and REE element diagrams, the Kuhe Dom rocks show characteristics of calcalkaline series. Petrological and geochemical investigations indicate that the Kuhe - Dom Volcanic Rocks are high k, Meta aluminous and are consistent to continental arc setting.

Keywords: magmaticbelt, geochemistry, petrology

PERUGIA
ITALY



(S) - IASPEI - International Association of Seismology and Physics of the Earth's Interior

JSS013

Poster presentation

2236

Modeling of the thermal structure of continental lithosphere

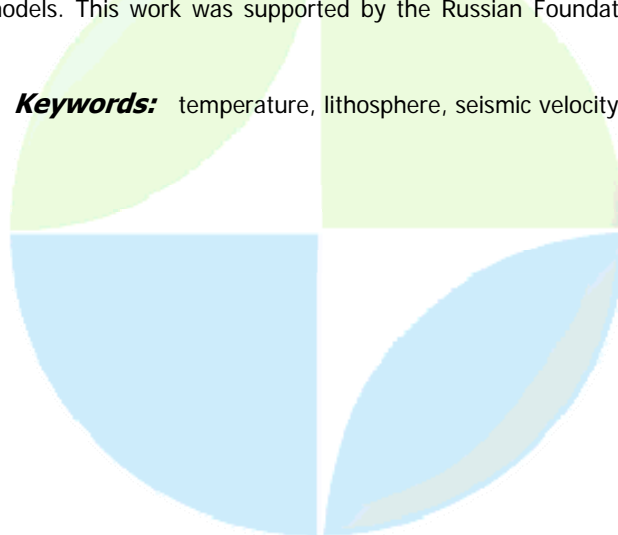
Prof. Victor Kronrod

Russian Academy of Sciences Vernadsky Institute of Geochemistry

Tatiana Kronrod

In this paper, a method is proposed for the calculation of the thermal regime of the crust and continental lithosphere (the temperature, heat flows, and heat generation). A specific feature of the method developed for solving the inverse thermophysical problem is the incorporation of constraints obtained from the seismic data inversion for the reconstruction of temperature. The input data are seismic velocities, surface heat flows, and the petrologic models of depleted garnet peridotites and fertile matter of the primitive mantle. We consider a region that comprises the crust (consisting of a few layers) and the lithosphere (where heat transfer is governed by the conductive mechanism). The thermal boundary of the lithosphere is defined by the intersection of the calculated temperature profile in the conductive region with the potential adiabat. The solution is divided into two stages. At the first stage, the temperature profile (T) is determined from absolute P and/or S wave velocities. The T profile is then adjusted to a thermophysical model of conductive transfer in the crust and mantle. Also at the second stage, the surface heat flow and the T profile are used to determine heat generation, the thicknesses of the crustal layers, and the heat flow components in the crust and lithosphere. The inverse problem of thermal conduction in a multilayer medium uses results of the temperature reconstruction by seismic data inversion. This allowed us to determine the analytical depth dependence of the temperature, the intensity of radiogenic heat sources in the crust, and the heat flow components in the crust and mantle. The procedure of converting seismic profiles into thermal ones is based on the equations of state of mantle material taking into account phase transformations and anharmonicity and anelasticity effects. To calculate the anelastic effects, a dimensionless coefficient is introduced into the standard procedure of calculating the Q factor; the value of this coefficient depends on the depth and is determined from the condition of minimization of a functional that characterizes the misfits between the temperature profile derived from the IASP91 model and the "average" geotherm for continents. We illustrate the application of our approach with the example of the lithosphere of the Archean Kaapvaal craton and the Earth's normal mantle (an "averaged" contemporary continental mantle). As a reference model, we take the model IASP91. In reconstructing the thermal regime and the thickness of the cratonic lithosphere, we use the BP11A regional model. Our modeling results show good agreement with modern geothermal models. This work was supported by the Russian Foundation for Basic Research, project 06-05-64151.

Keywords: temperature, lithosphere, seismic velocity



(S) - IASPEI - International Association of Seismology and Physics of the Earth's Interior

JSS013

Poster presentation

2237

Evaluation of the effects by heterogeneously inserted thin/thick high/low velocity layers in the part of crust

Dr. Kayoko Tsuruga

Japan Continental Shelf Survey Co. Ltd. IASPEI

Junzo Kasahara, Yoshihiro Naito, Azusa Nishizawa, Kentaro Kaneda

1. Introduction In the crustal structure studies using OBS and control sources, we frequently use arrival times and waveforms (e.g., refracted and wide-angle reflected arrivals, later phases of refracted and reflected arrivals, and P to S and S to P converted waves) and other data obtained by MCS and gravity data (Kasahara et al., 2007, this meeting). In our analysis, we use a forward modeling method simultaneously referring synthetic waveform and a travel time inversion. Real observed seismic records frequently show some complicated waveforms whose arrivals quickly decay with offset distance. They are usually interpreted by the presence of low/high velocity layer or negative gradient in velocity layers. Because such heterogeneous structures greatly influence the model construction, we have to explain these phases with geophysical interpretation of such phases. In this report, we, therefore, try to interpret particular seismic phases resulting from small-scale heterogeneous crustal structure in the ocean region by using FDM simulation of several models. 2. Numerical simulation Using horizontally inhomogeneous structure models, we synthesize waveforms by the FDM method (E3D developed by Larsen, 2000). We examined several numerical examples. Basic structural model was a horizontal multi-layered structure with 200km (H) x 20km (D). An oceanic crust with 7 km-thick was divided into four layers: (a) 0-1 km, (b) 1-2.5 km, (c) 2.5-3.5 km and (d) 3.5-7.0 km deep. We here show the following velocity gradient models for the layers (b) and (c) while the layers (a) and (d) has same velocity in any cases: Case-1: Velocity monotonously increases with depth for a whole model space (basic model) Case-2: Velocity in the both or either of layers (b) and (c) is constant Case-3: Velocity gradient changes at the interfaces such (a)-(b), (b)-(c) and (c)-(d). Case-4: Velocity discontinuity at the interfaces of such (a)-(b), (b)-(c) and (c)-(d). These models provides us a lot of in formations about the behaviors of amplitude observed in the cases of decollman, velocity reversal with depth and horizontal pinch-out of high velocity layer on OBS-airgun seismic records. We can also evaluate the characteristics of waveforms for thin high velocity layers such as chart and/or limestone layers at the shallow part and the fluid-filled layers existing in the crust of decollman. These inserted layers are frequently found in DSDP and ODP deep-sea drillings. Through the present case studies, seismic phases particularly with amplitude decay with offset distance are troublesome to construct the correct crustal velocity model because such phases are strongly affected by extremely local structure near receivers. So, in such case, we need to discard / screen such arrivals for the interpretation of long-offset arrivals because time delay through such local thin layers is very small, but the arrivals are very strong for shorter offset distance. 3. Summary Some OBS-airgun records show some arrivals which reflect the inhomogeneous velocity structure in space. The interpretation of such phase is not carried out by the usual interpretation method. In order to find the best treatment of such phases, we use FDM waveform simulation for several cases and screen the adequate data. Our results may greatly help for the interpretation of such troublesome phases.

Keywords: crustal structure, synthetic seismogram, fdm

(S) - IASPEI - International Association of Seismology and Physics of the Earth's Interior

JSS013

Poster presentation

2238

Evaluation of efficiencies of P-S conversion in T H E oceanic crust and Vp/Vs estimation

Dr. Kayoko Tsuruga

Japan Continental Shelf Survey Co. Ltd. IASPEI

Junzo Kasahara, Eiichiro Nishiyama, Kei Murase, Ryuji Kubota, Azusa Nishizawa

1. Introduction In the OBS-airgun records, P to S and/or S to P converted phases have been frequently observed by horizontal seismometers and vertical seismometer/hydrophone, respectively. Using such converted phases, we can estimate S wave structure in the crust and the mantle. In order to evaluate S wave velocities, the precise estimation of P and S velocity structures in the sediments is required. In this paper, we propose an evaluation method for the conversion efficiency of P to S and S to P and obtain S wave structure in the hard rock part of the crust. 2. Method In the oceanic region, S(V) waves observed in horizontal components are converted from P to S(V) at interfaces with large impedance contrast. We, here, simply evaluate a total energy flux of P-S conversion waves as follows: 1) We estimate efficiencies of transmission and conversion from P to S and/or S to V through the ocean bottom/sediments/hard-rock interfaces. 2) We evaluate relative converted P or S wave square amplitudes at OBS relative to the incident P waves penetrated into the ocean bottom. 3. Results The conversion from P to S occurs at (a) sediments/hard-rock interface or (b) seawater/bare rock interface. The case (a) occurs at the presence of thin unconsolidated sediment layer (P-wave velocity, V_p is less than 2.2km/s, S-wave velocity, V_s is less than 1.0 km/s) more than tens meters underlined by sedimentary rocks or hard rock layer (V_p is greater than 2.5km/s, V_p/V_s ratio is about 1.78). Such interface is often called as an acoustic basement by reflection seismics. The case (b) corresponds to bare rock layer exposed at the ocean bottom. For the present study, we assume the conversion occurs only at the ocean bottom and sediment layer /hard-rock interface and calculate the conversion rates in terms of relative energies. Among possible seven phases, large conversions are expected for (i) sediments/hard-rock interface at the incident side, (ii) at the ocean bottom of incident side, and (iii) at the sediments/hard-rock interface just beneath an OBS. Both of (i) and (ii) travel through whole crust as S wave. In the case of (iii), P wave converts to S wave only at the sediments/hard-rock interface just beneath an OBS. 4. Examples We examined real OBS-airgun data observed in the western part of the Pacific Ocean. It was found that most of conversions were observed on horizontal seismographs and they fit to the cases of (i) and (iii) for most of OBS records by comparing P-wave velocity crustal structure. The V_p/V_s ratios were estimated to be 3 to 20 for sedimentary layers whose V_s were to be 1.6-2.0 km/s beneath the western Pacific Ocean. V_s values were consistent with those measured by Hamilton (1976, 1979). We also found that V_p/V_s values of the upper and lower parts of the oceanic crust were extremely constant (i.e., 1.78) in the western Pacific and the ocean basins of NE Philippine Sea. We did not found V_p/V_s values of 2.0-2.5 which indicates the fractured crust and serpentinized mantle. On the other hand, S_n arrivals in two horizontally perpendicular directions suggest the presence of the anisotropy in the upper-most mantle. Although the V_p/V_s value in the upper-most mantle was 1.73, those in some areas were less than 1.70. We report the details and interpretation of V_p/V_s in the crust and the mantle. 5. Conclusion Because sea water can transmit only P wave, we have to use converted S waves in the crustal structure studies in the ocean region. Using converted phases from P to S and S to P waves, we can estimate the conversion rates and estimate the V_p/V_s in the crust.

Keywords: crustal structure, p s converted wave, s wave velocity

(S) - IASPEI - *International Association of Seismology and Physics of the Earth's Interior*

JSS013

Poster presentation

2239

A highly variable depth of the brittle/ductile transition in the lithosphere along the Andes Region

Dr. Miguel Muoz
IASPEI

Thermal and gravity data, together with rheological properties of rocks, are used to determine the brittle/ductile transition in the lithosphere along the Andes region. In the area of the Oca-Ancon fault system in northern Venezuela (heat flow (Q)=60-70 mWm⁻²), for acceptable thermal and rheological model parametrizations, the crustal brittle layer is not thicker than 11-18 km, in contrast to a maximum thickness of 23 km as suggested by the location of hypocentres. In the southern termination of the Bocono fault zone, where Q is of about 50 mWm⁻², the crustal seismogenic layer is not thicker than 20 km, and in models assuming a dry dunite upper mantle, a brittle layer is obtained beneath the crust/mantle boundary (CMB) down to about 55-60 km, in accordance to depth solutions of Kafka and Weidner (1981) where seismic activity at these depths is interpreted to be within the continental lithosphere and not related to the subducted ancient Farallon plate. In the Central Cordillera of Colombia and in the central northernmost area of Ecuador, the temperature at the CMB is close to 1000 C, and tectonic seismic activity can be expected to be generated only in the upper 13 km of the crust; in northeastern Ecuador, Kawakatsu and Proao-Cadena (1991) determined focal depths suggesting a seismogenic zone of 15 km thickness, and in the sub-Andes of Ecuador, focal depths larger than 30 km were relocated at 16 km and 10 km (Surez et al., 1983). In the Central Andes plateau, thermal models suggest that the crust below 15-20 km is in the ductile regime, in accordance with magnetotelluric (MT) observations and Q_p tomography; these last studies show no indication of a fluid curtain from the descending slab in the fore-arc region (Schilling et al., 2006). Thermal and rheological zonation in areas of generally low heat flow in Ecuador, Peru, Argentina and Chile indicate that earthquakes occurring at depths of 70-110 km are generated within the subcontinental upper mantle, and thus they are not associated to flat subduction of the oceanic lithosphere; in these areas there is no obvious correlation between the subduction of oceanic ridges a main subject for the flat-slab hypothesis and deformation processes and structural styles of the orogenic phases (Michaud et al., 2006; Aleman, 2006; Creixell et al., 2006). In the main Cordillera of central Chile (33 S-35 S), the strength envelope describes a brittle domain down to about 17-22 km, in accordance with crustal seismic activity. In southern Chile, in the south volcanic zone, only shallow tectonic seismic activity could be generated; most of the crust is ductile, and the temperature at the CMB is of about 880-1100 C. MT observations at latitudes of about 39 S show that high electrical conducting zones are encountered only beneath the volcanic front and eastwards from it, and also linked to some fault systems, the electrical conductance decreasing strongly towards de coastal range (Muoz et al., 1990; Brasse and Soyer, 2001); a down-going slab is not resolved by the MT soundings.

Keywords: andes, lithosphere, rheology

(S) - IASPEI - International Association of Seismology and Physics of the Earth's Interior

JSS013

Poster presentation

2240

Global rotation of lithosphere and position of seismic belts

Prof. Yury Barkin

Laboratory of Gravimetry Sternberg Astronomical Institute IAG

The general regularities in the motion of lithosphere plates and in spatial distribution of epicenters of the largest seismic events on the Earth surface in 20 century are investigated. Plates and earthquakes by the closest image are connected with each other. The seismicity is most brightly shown on boundaries of plates, and seismic belts (zones) determine these boundaries and configurations of the plates. On the other hand it is enough sure the parameters of global lithosphere rotation are determined (Greep, Gordon, 1990; Argus, Gordon, 1991; Barkin, 2000). The certain geometrical, kinematic and dynamic regularities of plate motion have been established (Barkin, 2000). The maximal tension at sliding of lithosphere and, accordingly, the strengthened accumulation of elastic energy and the most active displays of seismic activity should take place along the inclined equator of rotating lithosphere. Therefore we had the right to expect, that the pole P_w of the axis of global rotation of lithosphere, the pole P_m of the angular momentum of relative motion of plates and the pole P_s of a planetary (most active) seismic belt should have a close positions to each other. Results of the fulfilled research have confirmed the made assumption. Thus, the global rotation of lithosphere organizes (in planetary scale) and directs seismic events, and its equator of rotation is set actually the position of a planetary seismic belts (zones) of the most active seismic events, as it is observed actually. The dynamic model of lithosphere plates and lithosphere with various powers of oceanic and continental areas (Barkin, 2000) has been used for analysis. Only surface displacements are considered in this model in accordance with known kinematical theories NNR-1 and HS-2 (Greep, Gordon, 1990; Argus, Gordon, 1991). The special computer method of axography (Ferrandez Garcia et al., 2002) has been used for determination of the most active poles (P_s) of latitudinal and longitudinal alignment in positions of epicenters of large earthquakes in 20th century (coordinates in degrees): 1) 65.5 S, 60.5 E. (the analysis of 112 largest earthquakes in 20th century); 2) 53.5 S, 45.5 E (392 earthquakes with $M > 7$); 3) 54.5 S, 41.5 E (112 earthquakes); 4) 52.5 S, 56.5 E (392 earthquakes) etc. Various indexes of longitudinal (1), 2)), latitudinal (3)) and equatorial ordering (4)) (Ferrandez Garcia et al., 2000) have been used. The obtained coordinates of a pole of a seismic belt are coordinated with each other and with corresponding coordinates of the following poles (Barkin, 2000b): pole 49.0 S, 65.0 E of angular velocity of global rotation of lithosphere; pole 45.4 S, 57.6 E of the angular momentum of relative motion of lithospheres plates under theory HS2-NUVEL1; pole 48.1 S, 63.5 E of the angular momentum of global rotation of lithosphere. It is shown, that the vector of the principal moment of forces of inertia L_D of lithosphere (together with the Earth) is located in an equatorial plane and directed to descending node of seismic belt W_s (longitude 145.4 E). The centre of mass of lithosphere C_l with coordinates 41.0 N, 36.0 E is located near to the big seismic belt. The pole P_s is located on the other big seismic belt covering big northern arch of Pacific ocean, with ascending unit on equator (a longitude 105.0 E and an inclination about 55.0 degrees), up to seismic zones of South America. With poles of a vector of the moment of inertia forces of lithosphere, caused by the Earth rotation, the extended zones of active seismicity are connected. They form of the spirals located in the field of longitudes 90-180 E (spirals are twirled clockwise) and 270-360 E (are twirled counter-clockwise) with the general orientation in a direction the north - south. Their origin can be connected with the dynamic role of forces of inertia for non-spherical lithosphere. The moments of these forces and the corresponding motions of plates result in additional accumulation of elastic energy and influence on the spherical turns of plates. Three ring zones with the centers located on the basic seismic belt (with coordinates 30 N, 85 E; 15 N, 120 E; 5 S, 290 E) are

marked. Ring zones are closely connected to arc zones on plate boundaries and it serves as the indication, that activation of seismicity and structure and position of ring zones are determined by the general mechanism. References Barkin, Yu.V. (2000) About global rotation of the lithosphere. In: Towards an Integrated Global Geodetic Observing System (IGGOS). International Association of Geodesy Symposia. Vol. 120 (Eds. R. Rummel, H. Drewes, W. Bosch, H. Hornik). IAG Section II Symposium (October 5-9, 1998). Springer, Berlin. pp. 234-237. Barkin, Yu.V. (2000) The regular character of the plate motion: implication for Earth sciences. In: Towards an Integrated Global Geodetic Observing System (IGGOS). International Association of Geodesy Symposia. Vol. 120 (Eds. R. Rummel, H. Drewes, W. Bosch, H. Hornik). IAG Section II Symposium (October 5-9, 1998). Springer, Berlin. pp. 231-233. Barkin, Yu.V. (2000) Geometrical regularities of the lithosphere plate structure. Astronomical and Astrophysical transactions, Vol. 18, Issue 6, pp. 751-762. Barkin, Yu.V. (2000) Kinematical regularities in plate motion. Astronomical and Astrophysical Transactions, Vol. 18, Issue 6, pp. 763-778. Barkin, Yu.V. (2000) Dynamical regularities in the plate motion. Astronomical and Astrophysical Transactions, Vol. 19, Issue 1, pp. 1-12. Gripp A.E., Gordon R.G. (1990) Current plate velocities relative to the hot spots incorporating the NUVEL-1 global plate motion model. Geophys. Res. Lett., 1990, vol. 17, pp. 1109-1112. Argus D.F., Gordon R.G. (1991) No-net-rotation model of current plate velocities incorporating plate motion model NUVEL-1. // Geophysical Research Letters. Vol. 18. N 11. pp. 2039-2042. Ferrandez, M.G.; Barkin, Yu.V.; Ferrandiz, J.M. (2002) Ordered positions of formation centers of the earth-like planets and moons. In: Earth-like planets and moons. Proceedings of the 36th ESLAB Symposium, 3 - 8 June 2002, ESTEC, Noordwijk, The Netherlands. Eds.: B. Foing, B. Battrick. ESA SP-514, Noordwijk: ESA Publications Division, ISBN 92-9092-824-7, October 2002, pp. 129 - 135.

Keywords: lithosphere rotation, seismic belts positions, regularities

XXIV2007

PERUGIA
I T A L Y



(S) - IASPEI - *International Association of Seismology and Physics of the Earth's Interior*

JSS013

Poster presentation

2241

Crustal and uppermantle structure in the Eastern Mediterranean from the analysis of surface wave dispersion curves

Dr. Francesca Di Luccio

Seismology and Tectonophysics INGV IASPEI

Francesca Di Luccio, Mike E. Pasyanos

The dispersive properties of surface waves are used to infer earth structure in the Eastern Mediterranean region. Using group velocity maps for Rayleigh and Love waves from 7-100 s, we invert for the best 1D crust and upper-mantle structure at a regular series of points. Assembling the results produces a 3D lithospheric model, along with corresponding maps of sediment and crustal thickness. A comparison of our results to other studies finds the uncertainties of the Moho estimates to be about 5 km. We find thick sediments beneath most of the Eastern Mediterranean basin, in the Hellenic subduction zone and the Cyprus arc. The Ionian Sea is more characteristic of oceanic crust than the rest of the Eastern Mediterranean region as demonstrated in particular by the crustal thickness. We also find significant crustal thinning in the Aegean Sea portion of the back-arc, particularly towards the south. Notably slower S-wave velocities are found in the upper-mantle, especially in the northern Red Sea and Dead Sea Rift, central Turkey, and along the subduction zone. The low velocities in the upper-mantle that span from North Africa to Crete, in the Libyan Sea, might be an indication of serpentinized mantle from the subducting African lithosphere. We also find evidence of a strong reverse correlation between sediment and crustal thickness which, while previously demonstrated for extensional regions, also seems applicable for this convergence zone.

Keywords: surfacewaves, easternmediterranean, lithosphere



(S) - IASPEI - *International Association of Seismology and Physics of the Earth's Interior*

JSS013

Poster presentation

2242

Rayleigh Wave Group Velocity Tomography in Greenland from Correlation of Ambient Seismic Noise

Dr. Peter Voss
IASPEI

Peter Kyhl Knudsen, Olafur Gudmundsson, Sren Gregersen, Trine Dahl-Jensen, Winfried Hanka, Tine B. Larsen

Seismic tomography is traditionally based on known sources like explosions or earthquakes, in this study we have applied a technique of cross-correlation long time series of seismic recordings from pairs of broad band seismic stations, to extract information on surface wave velocities from the ambient seismic noise. From a cross-correlation of one month of vertical component recordings we show that the Rayleigh wave group velocity can be determined between station pairs in Greenland. Our result shows that the intensity of the ambient seismic noise is highest in coastal areas and that the intensity changes with the season, which correlates with the extent of sea ice around Greenland. The Rayleigh wave group velocity is obtained at three frequency intervals 5-10, 10-20 and 30-50 s. Tomography inversion at these frequency intervals is presented. Furthermore we present different aspects in the preparation and processing of the data set.

Keywords: seismictomography, noisecorrelation, greenland

PERUGIA
ITALY



(S) - IASPEI - *International Association of Seismology and Physics of the Earth's Interior*

JSS013

Poster presentation

2243

Exhumation of the Dabie UHP Metamorphic Terrane, China

Prof. Qingchen Wang

Institute of Geology and Geophysics Chinese Academy of Sciences IASPEI

Exhumation of deeply buried Ultra-high-pressure (UHP) terranes remains a puzzle in understanding lithospheric dynamic process. New evidence that constrains the exhumation process of the Dabie UHP terrane includes: (1) Structural geological data record the architecture of the Dabie UHP terrane. Three slices are recognized, i.e., from top to bottom, the Susong blueschist slice, the Huangzhen-Huangweihe (HH) HP slice, and the Jinheqiao-Shuanghe-Bixiling (JSB) UHP slice. These slices have been stacked and domed. (2) Geophysical data depict two offsets in the Moho. Offset-I separates the Dabie UHP terrane from the North China Craton and has served as a subduction channel, as well as an exhumation channel. Offset-II, separating the Dabie UHP terrane from the foreland belt, developed due to geodynamic regime reorganization. (3) Geochronological data reveal that the HP slice was exhumed earlier than the UHP slice. A northward younging exhumation polarity is implied with younger exhumation age closer to the exhumation channel. These evidences point to a multistage exhumation process. The Yangtze Craton collided with and subducted beneath the North China Craton in the very beginning of Triassic time. By 230 Ma, the Susong blueschist slice and the south end of the HH HP slice had arrived at a middle crustal level, while its north part was still at mantle depth. Such processes continued until the JSB UHP slice was exhumed to mid-crustal levels at 210 Ma. After geodynamic regime reorganization during 210~180 Ma, continuing compression of the Yangtze Craton and underthrusting along the offset-II in the Moho caused the dome structure and eventually brought the UHP rocks to the Earth's surface.

Keywords: uhp, dabieshan, exhumation



(S) - IASPEI - *International Association of Seismology and Physics of the Earth's Interior*

JSS013

Poster presentation

2244

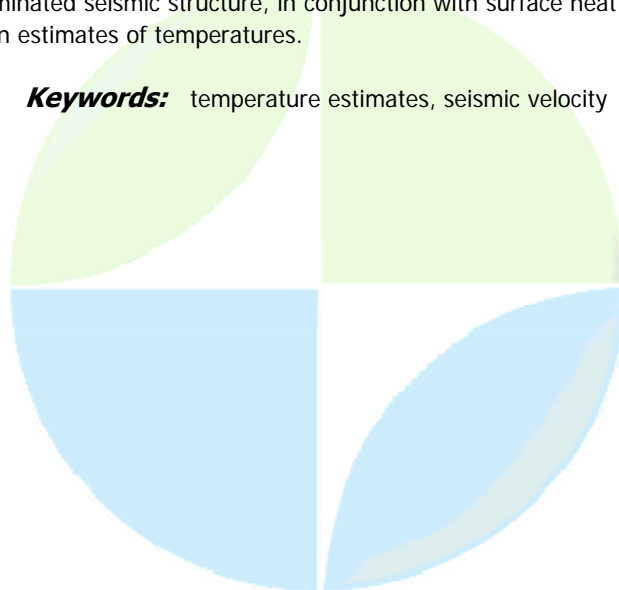
**Temperature estimates of the lithosphere on the romanian territory
constrained by seismic velocity data**

Dr. Maria Tumanian

Natural Fields Institute of Geodynamics, Bucharest, Romania IASPEI

Complex architecture of the lithosphere beneath the Romanian territory is interpreted as a direct result of the compressive tectonic interaction of three major tectonic compartments (East European Platform, Moesian Platform, Tisza-Dacia Alpaca terranes) during mountain building in the Carpathian Arc. The process of the Carpathian orogeny is considered the prevailing factor affecting the deep structure of the lithosphere, with major consequences on the seismic and magmatic activities. Geological, geophysical and seismological information collected during the last years indicated complicated thermo-mechanical structures of the crust and lithosphere and various seismic velocity-depth distributions for each of the mentioned tectonic units, especially at the plate margins contact. Temperature is a key physical parameter controlling the crustal and mantle dynamics. In the previous studies the thermal structure of the three tectonic units has been obtained indirectly through the extrapolation of the heat flow observations and by thermal modelling simulating the main geodynamic processes affecting the study area. During the intense processes - oceanic subduction, thickening-type compressive deformations, volcanic processes and surface geological processes (sedimentation and erosion in sedimentary basins, overthrusting and erosion in orogenic areas) - the entire lithosphere or parts of it have been involved. The previous evaluations of the lithosphere temperature required realistic estimates on crustal structure and distribution of the thermal parameters within the lithosphere. This study proposes a tool to better evaluate the spatial distribution of the thermal parameters and structures used in thermal modelling using information supplied by tomographic and seismic refraction experiments (CALIXTO99, Vrancea99 and Vrancea2001). Characteristics of the seismic wave propagation, strongly controlled by the thermal and mechanical properties of the rocks travelled across, provide an image of the heterogeneous nature of the lithosphere. A set of shear-wave velocity models determined by non-linear inversion of the surface wave velocity data are used in reducing the uncertainties in temperature estimates and to obtain a refinement of the temperature distribution in the lithosphere beneath the investigated tectonic units. The technique allows an analysis of the temperature effects in producing velocity variations and uses the thermally dominated seismic structure, in conjunction with surface heat flow observation, as an additional constraint on estimates of temperatures.

Keywords: temperature estimates, seismic velocity



(S) - IASPEI - *International Association of Seismology and Physics of the Earth's Interior*

JSS013

Poster presentation

2245

Tracking SKS shear-wave splitting across Central and Eastern Europe by using permanent networks and one single event

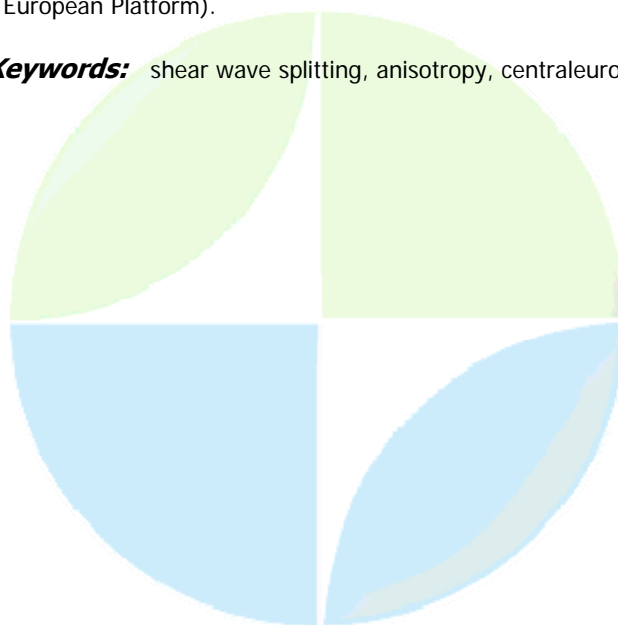
Dr. Thomas Plenefisch

Seismological Central Observatory BGR IASPEI

Marcus Walther

During the last decades a lot of SKS studies have been performed to detect and analyse seismic anisotropy in the upper mantle. Most of these investigations are based on temporary experiments. Usually these experiments cover regions of several hundred of kilometers with the scope to investigate one or two tectonic provinces or their transition zone respectively. Due to temporary limitations - usually 6 to 18 months - the experiments offer the possibility to record some events with reasonable SKS signal-to-noise ratio and under favourable circumstances one or two events with SKS showing high transversal SKS energy clearly above noise level. Here we propose another approach. Since the number of permanent stations has increased rapidly over Europe during the last years, we combine SKS records from several countries and institutions to investigate a broader region than those covered by temporary experiments. The second advantage of this philosophy comes from the long registration periods of the permanent stations, which allows to select SKS events with particular energetic SKS amplitudes. For a start we concentrate on records of one single event, namely the MW = 6.8 event of 13 November 2006 from the Santiago del Estero province (Argentina), a source region for which energetic SKS amplitudes have often been observed on European stations. For this event we collected data from permanent stations in Central and Eastern Europe (e.g. GEOFON (data from Poland, Czechia, Hungary, Russia etc.), GRSN (Germany), SED (Switzerland)) and we prepared seismogram sections in a narrow azimuth range. The sections cover the epicentral distance range between 93 to 115, e.g. from station GIMEL (Switzerland) in the southwest to station PUL (Russia) in the northwest of Europe. The SKS phase can be clearly correlated on the sections, most of the records show considerable SKS splitting. Since up to now, we have analysed only one single event, the resulting splitting parameters have still to be regarded as apparent splitting values. Nevertheless, the lateral variations of the splitting parameters over Central and Eastern Europe can be interpreted with respect to the major tectonic units (Alps, Varsican Orogen, East European Platform).

Keywords: shear wave splitting, anisotropy, centraleurope



(S) - IASPEI - *International Association of Seismology and Physics of the Earth's Interior*

JSS013

Poster presentation

2246

Application of integrated geophysical modelling for determination of the continental lithospheric structure in the Carpathian-Pannonian region - lithospheric thickness map

Dr. Jana Dererova

Geophysical Institute Slovak Academy of Sciences IASPEI

Miroslav Bielik, Hermann Zeyen, Karmah Salman

We applied integrated lithospheric modeling combining the interpretation of surface heat flow, geoid, gravity, and topography data for the determination of the lithospheric thermal structure along nine transects crossing the Western and Eastern Carpathians from the European Platform to the Pannonian Basin. Based on our calculations, we propose a new map of the lithospheric thickness in the Carpathian-Pannonian region. This map may serve as base for geodynamical reconstructions of this region and for a better understanding of the lithospheric processes governing its geodynamical evolution.

Keywords: integrated modelling, lithospheric structure, lithospheric thickness map



(S) - IASPEI - *International Association of Seismology and Physics of the Earth's Interior*

JSS013

Poster presentation

2247

Integrated lithospheric modelling in the Red Sea area

Dr. Jana Dererova

Geophysical Institute Slovak Academy of Sciences IASPEI

Miroslav Bielik, Anwar Hassan Ahmed Radwan, El-Sayed Abdel-Azim Issawy, Igor Koht

We applied 2D integrated geophysical modelling for the determination of the lithospheric structure and its thickness in the Red Sea area. The results show large differences between continental and oceanic lithospheric structure and thickness. The oceanic crust of the Red Sea is much thinner (12-15 km) in comparison with the continental crust which is located on both sides of the Red Sea, and reaches the thickness of around 28-33 km. The density of the lowermost part of the upper mantle in the Red Sea area is very low indicating possible presence of partial melting in the upper mantle and supporting the theory of uplift of the asthenospheric masses in the Red Sea that is accompanied by the process of underplating beneath the Moho discontinuity.

Keywords: integrated modelling, the red sea, lithospheric structure



(S) - IASPEI - *International Association of Seismology and Physics of the Earth's Interior*

JSS013

Poster presentation

2248

A new lithosphere model as input for the European Strength Map

Mrs. Magdala Tesauro
Tectonics Vrije Universiteit

Mikhail K. Kaban, Sierd Cloetingh

Tectonic studies made in intraplate Europe have shown that this area is more active than would be expected from its location far away from plate boundaries. The first strength map showed that the European lithosphere is characterized by major spatial mechanical strength variations, with a pronounced contrast between the strong lithosphere of the East-European Platform (EEP) east of the Teseyre-Tornquist Zone (TTZ) and the relatively weak lithosphere of Western Europe. In order to improve the results previously obtained, we have constructed a new crustal model, in which we implement the results of recent seismic studies. The new crustal model consists for continental realms, of two or three crustal layers and an overlying sedimentary cover layer, whereas for oceanic areas one crustal layer is used. The results of deep seismic reflection and refraction and/or receiver function studies are used to define the depth of the crustal interfaces and P-wave velocity distribution. The Moho depth variations are reconstructed by merging the most recent maps compiled for the European regions (e.g. Ziegler and Dzes, 2002, Kozlovskaja et al, 2004) and by ourselves using published interpretations of seismic profiles (e.g. in the Vring and Lofoten basins). To each layer of the model we associate a density value and corresponding lithology. Strong differences in the crustal structure are found between the areas east and west of the TTZ, respectively. The eastern region is mostly characterized by high velocity of the lowest layer ($V_p \sim 7.1 \text{ km/s}$) and thick crust, e.g. over the Baltica region ($\sim 42\text{-}44 \text{ km}$) with a maximum of over 60 km in the Baltic Shield. By contrast, crustal structure is more heterogeneous to the west from TTZ, being characterized by Variscan crust with slower P-wave velocity in the lower crust ($V_p \sim 6.8 \text{ km/s}$) and an average thickness of 30-35 km, orogens (e.g. the Alps and the Pyrenees), where the crustal thickness is increased up to 45-50 km, and locally by strong extensional deformation, which resulted in a very thin crust in the Pannonian Basin ($\sim 25 \text{ km}$) and in the Tyrrhenian Sea ($\sim 10 \text{ km}$). Concerning the oceanic domain, the crustal thickness is generally decreased towards the ridge (up to 10 km in the most western part), with local maxima up to 20-25 km (e.g. in the Vring and Lofoten basins) and up to 35-40 km beneath the islands (e.g. Iceland and Faeroe islands), on account of mantle underplating. Seismic tomography data are used to get the location of the lithosphere-asthenosphere boundary and calculate the temperature distribution. These results, jointly with the new crustal model, allowed us to refine the previous strength map. Furthermore, the gravity effect of the crustal model is calculated and removed from the observed gravity field in order to get residual mantle anomalies. These anomalies distribution are compared with the new strength results. Negative mantle gravity anomalies and relative low strength values characterize Western Europe, while the reverse is true for Eastern Europe. Large differences exist also for specific tectonic units: a pronounced contrast in lithosphere properties is found between the strong Adriatic plate and the weak Pannonian Basin area, as well as between the Baltic Shield and the North Sea rift system.

Keywords: crust, europe

(S) - IASPEI - *International Association of Seismology and Physics of the Earth's Interior*

JSS013

Poster presentation

2249

Surface wave tomography in Euro-Mediterranean region

Dr. Renata Schivardi

Andrea Morelli

We present a transversely isotropic shear wave velocity model of the upper mantle beneath Europe and the Mediterranean region, obtained by non-linear inversion of surface wave group velocity maps. Group velocity maps result from the regionalization of a dataset of measurements of fundamental mode Love and Rayleigh wave dispersion, carried out with iterated multiple filtering, and phase-matched filtering techniques. The linear inverse problem is stabilized using a priori information in the form of a global group velocity reference model, derived from the inversion of the phase velocity dataset of Ekstrom et al. (1997). The implications of different regularization constraints (mathematically equivalent to norm damping or smoothing with different criteria) are analyzed and compared. Both in group velocity maps and in shear velocity resulting model we find confirmation of the larger-scale deep geological features known for the region, namely the differentiation between fast old cratonic shields of Eastern Europe and North Western Africa and the slow seismic active Tethyan belt. At shorter scale length we image well slow anomalies associated with the magmatic provinces of the Sicily Channel, and the extensional zone of the Rhine graben. Fast anomalies are instead related to the Aegean and Hellenic Arc. Use of the dense European seismograph array results in maps with higher resolution than previously attained.

Keywords: surface waves, tomography

PERUGIA
ITALY



(S) - IASPEI - *International Association of Seismology and Physics of the Earth's Interior*

JSS013

Poster presentation

2250

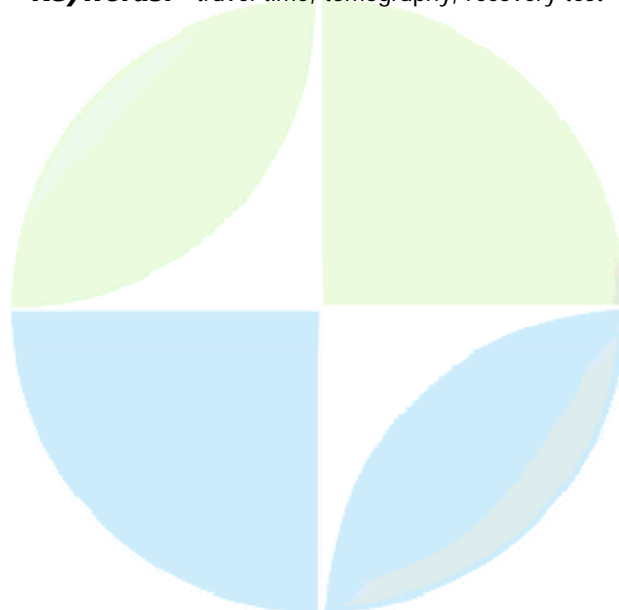
**Finite difference seismic travel times and non-linear seismic tomography:
recovery of slab-back-arc structures in the Mediterranean region**

Dr. Paola Serretti

Andrea Morelli

The main structural features in the upper mantle beneath the Africa-Eurasia collision belt are the seismically fast subducted lithosphere, and the slow back-arc basins. Seismic tomography has been able to image these features, with high relevance for tectonics and geodynamics, with increasing resolution. Although potentially affected by irregular spatial distribution, travel times of high-frequency P and S waves represent the data with best resolving power, and are often used in studies targeted at imaging the finer details of upper mantle structure. In strongly heterogeneous media, the seismic travel time inverse problem can be strongly non-linear, as ray paths in the real earth can significantly deviate from those computed in the reference model. We test recovery of upper mantle structures by nonlinear P-wave travel time tomography, trying to reconstruct a previously known, realistic wave speed structure. We use the real distribution of seismic sources and stations, and calculate P first arrival travel times by the accurate and efficient finite difference scheme of Podvin and Lecomte (1991), based on systematic application of Huygens principle, adapted to work in spherical geometry. We use different meshes for the crust (2 km spacing) and the mantle (6 km) to account for Moho depth with high precision. The same technique is used to compute synthetic data, and to calculate partial derivatives along the ray for the inversion. We use a perturbative iterative approach for the inversion, starting with a one dimensional prior model. Different strategies are tested and compared in the nonlinear inversion. We verify that realistic upper mantle structures strongly deflect seismic rays, and the correct paths can only be approached after a few iterations. Although linear inversion appears in fact able to delineate the main features quite well, general three-dimensional ray tracing -- capable of dealing with strong ray deflections -- and non-linear inversion show to be important to describe the finer details of the structure.

Keywords: travel time, tomography, recovery test



(S) - IASPEI - *International Association of Seismology and Physics of the Earth's Interior*

JSS013

Poster presentation

2251

Interpretation of mineralogic and geochemical results of clays from the Ypresian/Lutetian boundary in the North of Tunisia and the paleoenvironment reconstruction

Dr. Ben M'Barek Jema Moufida

Des Sciences de la Terre Facult des Sciences de Bizerte

Narjess Karoui Yaakoub, Nouredine Ben Ayed

The sejenen area is located at the border of north alpine zone in . It is characterised by the presence of the well developed Ypresien/Lutetian series which were composed of the clayey and calcareous series. These formations present some lateral variations of the thickness on relation with the large paleogeographic line of the Paleogene. The clayey assemblages were largely dominated by the kaolinite at the bottom and at the top of the lithostratigraphic series. At the middle the ratio of the kaolinite proportions increase. Indeed the illite presents the percentages little variable along all the series. Its index of the crystallinity is high at the base and at top of the Ypresian/Lutetian boundary series. It represents an average of 20% in the clayey mineralogic assemblage. The geochemical results show that the clayey samples at the bottom and at the top of the series are more rich on CaO, MgO, en Fe₂O₃ et en K₂O. The silica mineral (SiO₂) and the alumine oxide (Al₂O₃) present a higher concentration at the middle of the Ypresian/Lutetian boundary series. If we take into consideration the mineralogic content and the geochemical results of the major elements indicated previously, we can propose an interpretation of the paleoenvironment at the Ypresian/Lutetian boundary. So at this epoch, the kaolinite which is prevailing at the bottom and at the top of the series give evidence the presence of the alteration factors with a warm and humid climate. But the abundance of the smectite mineral at the middle of the series suggest a high marine level so that the environment become deeper.

Keywords: mineralogy paleoenvironment, ypresian lutetian, illite kaolinite smectite



(S) - IASPEI - *International Association of Seismology and Physics of the Earth's Interior*

JSS014

2252 - 2327

Symposium

Crustal structure and Tectonophysics - Crustal and lithospheric structure in active continental blocks and their boundaries

Convener : Prof. Kevin P Furlong

Although the concept of localized plate boundaries has been a foundation of modern plate tectonics, it is clear that deformation associated with the interaction of crustal and lithospheric blocks (or plates) is oftentimes distributed over a substantially broader region. This session will focus on studies aimed at defining the structure of plate boundaries, the regional extent of deformation associated with block interaction, the depth extent/distribution of plate boundaries, and innovative tools or approaches for defining the nature of plate (or crustal block) boundaries. We encourage contributions from the broad range of geophysical and geodetic studies, including modeling, that provide insight into the structure, deformational style, and the resulting diffuse or localized plate boundary structure.



(S) - IASPEI - *International Association of Seismology and Physics of the Earth's Interior*

JSS014

Oral Presentation

2252

Influence of the Along-Plate-Boundary rupturing on the subduction zone earthquake intensity pattern: the january 21 (22), 2003, Colima, Mexico, Across-Trench Earthquake (Mw 7.5)

Prof. Zobin Vyacheslav

Observatorio Vulcanologico Universidad de Colima, Mexico IAVCEI

The 2003 Colima earthquake (Mw 7.5) occurred along the across-trench structure of the El Gordo Graben, which constitutes a boundary between the Cocos and Rivera oceanic plates near Mexican coast. This earthquake was characterized by the down-dip across-trench directivity of its rupture, as reconstructed from seismic waveform modeling. It was a reason for the severe damage to buildings in the localities situated at distances where usual along-trench rupturing subduction earthquakes of the same magnitude do not produce any significant damage. A field investigation of residential house damage in 83 localities of the Occidental part of Mexico allowed construction of macroseismic map of the moment magnitude 7.5 2003 Colima earthquake. The macroseismic map of the 2003 earthquake shows that the narrow (30 km wide) intensity VII MM zone was elongated (up to 60 km) in the NE direction toward the continental part of Colima state. As a result, the intensity in Colima city was 1.5 grades larger than would be expected for this magnitude according to the proposed attenuation of intensity with distance relationship for earthquakes from the Mexican subduction zone.

Keywords: intensity, mexico, earthquake



(S) - IASPEI - *International Association of Seismology and Physics of the Earth's Interior*

JSS014

Oral Presentation

2253

Seismic image of the Central Himalaya (India) from broadband seismic network

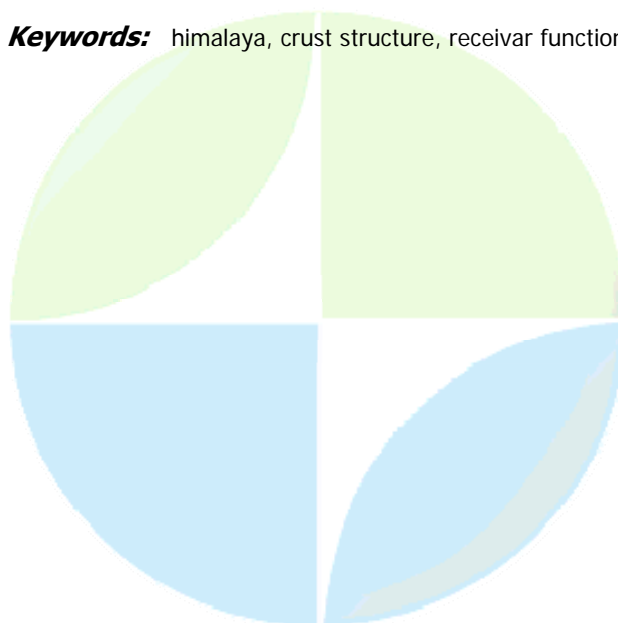
Mr. Ashish Kr.

Seismic Tomography Group National Geophysical Research Institute IASPEI

K. Sivaram, P. Rajgopala Sarma, K. Suryaprakasam, S. S. Rai

We investigate the variation in crustal S-wave velocity structure, 3-D distribution of seismic cloud and the nature of mantle layering from the exposed Indian shield (Aravalli craton) in south to the southern Tibetan Detachment (STD) in the Kumaon- Garhwal segment of the central Himalaya using a network of 25 broadband seismographs operating in the region since April 2005. The seismic network comprising of Guralp CMG-3T (120 s) seismometer and REFTEK data logger record the seismic waveform in continuous mode at 50s/s. The stations were aligned NE- SW direction almost perpendicular to the strike of the Himalaya. The stations were closely spaced at ~7-10 km interval from the Himalayan Frontal Thrust (HFT) in south to the STD in north and are widely spaced in Gangetic plain and Aravalli craton. We analysed over 100 teleseismic and 600 local earthquakes recorded by the network during April 2005- Oct 2006 to generate velocity model and the seismicity pattern. The 1-D shear velocity structure model at individual station is created through joint inversion of receiver functions from different azimuths with the surface wave group velocity measurements. Some of the important results include: 1.Northern Indian shield (Aravalli craton) characterized by a ~38 km thick crust with a comparatively lower velocity (<3.4 km/s) in the upper crust relative to the southern Indian shield (Dharwar craton) where it is >3.6 km/s. 2.Dip of the Indian Moho is 6-8 deg. beneath the lesser Himalaya with the average Pn and Sn velocity of 8.2 and 4.7 km/s, derived from the travel times of updip and downdip refracted waves. 3.Receiver function modeling results clearly map the Main Himalayan Thrust and also the Indian Moho, both showing significant change in their dip to the north of MCT. This is also supported by the seismic trend. 4.Presence of low velocity in the depth 20-30 km in the region between MCT and STD is modeled from receiver function time series. 5.Uplifted 410 discontinuity while the 660 km discontinuity split into 660 and 710km depths. 6.Seismicity is prevalent in the lower crust while it is nearly absent in the uppermost mantle.

Keywords: himalaya, crust structure, receiver function



(S) - IASPEI - International Association of Seismology and Physics of the Earth's Interior

JSS014

Oral Presentation

2254

Amurian a naissance plate: new GPS result supplemented by geological and geophysical evidence

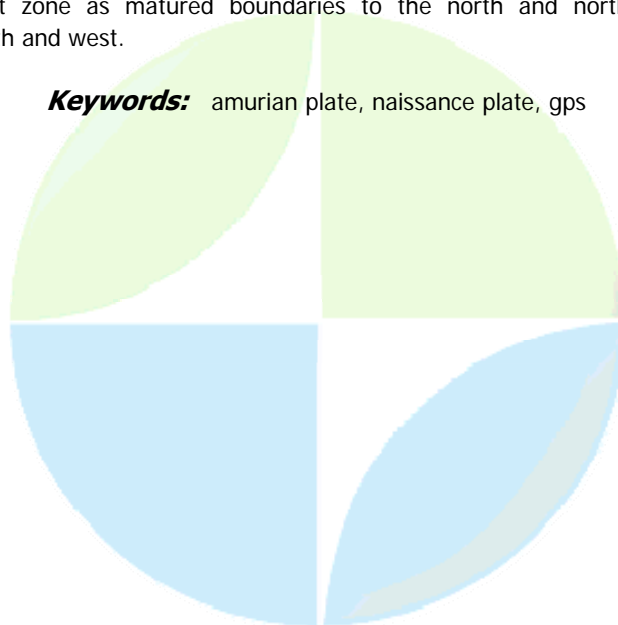
Prof. Xu Houze

Key Laboratory of Dynamic Geodesy Institutes of Geodesy and Geophysics, CAS IAG

Xiong Xiong, Pil-Ho Park, Teruyuki Kato, Jun Li

The tectonics and plate geometry in northeastern Asia has been a long-standing question, with a major issue being whether the Amurian plate (AM) is better regarded as part of the Eurasia or as a separate block. Complicated tectonic features, diffuse seismicity and poor coverage of GPS sites lead to ambiguity for determining the boundary of the AM. The surprising increment of GPS sites operated in eastern Asia in recent decade motivated in 2004 the start of a multilateral cooperation between the Institute of Geodesy and geophysics, Chinese Academy of Sciences, the Earthquake Research Institute, the University of Tokyo, and the Korea Astronomy and Space Science Institute. The cooperation resulted in a regional GPS network covering the proposed AM and surrounding areas. The data spanning 6 years (2000-2005) of 77 GPS sites, including 52 permanent and 25 yearly-surveyed ones, were compiled and processed by GAMIT/CLOBK software. The obtained velocities combined with published results yielded a consistent velocity map of the present-day crustal movement in northeast Asia, based on which the kinematics of the AM was discussed. The Eurasia-fixed Euler vector of AM, which was estimated with velocities at 12 sites on the stable part of the proposed AM, is located at 121.721.85oE and 60.6530.87oN, with a rate of 0.10210.002 deg/ma taking counterclockwise rotation as positive. The independence of the Amurian plate from the Eurasia was checked by statistical test. The results indicated that, in 95% confidence limit, the AM, comprised by the eastern Mongolia, southwest Russia, northeast China, Korean peninsula, is independent from the Eurasia. The southwest Japan and north China can be excluded from the AM. The western boundary of AM is defined by a diffuse deformation zone ranging between Mogolian Altai to the west and Hangay Plateau to the east. The southern boundary runs along extension basins in front of the south margin of the Yinshan-Yanshan Mts, and extends along Zhangbei-Shangzhi blind earthquake fracture belt. The kinematic results are consistent with geological and geophysical evidence, which suggest that the AM is a naissance plate with Stanovoy range and Baikal Rift zone as matured boundaries to the north and northwest, and developing boundaries to the south and west.

Keywords: amurian plate, naissance plate, gps



(S) - IASPEI - *International Association of Seismology and Physics of the Earth's Interior*

JSS014

Oral Presentation

2255

Active monitoring of asperities-reflectors system: time lapse monitoring of subducting interplate earthquakes and dynamics of magma reservoir

Dr. Junzo Kasahara

Advisory Department Japan Continental Shelf Survey, Japan IASPEI

Kayoko Tsuruga, Teruo Yamawaki, Naoyuki Fujii

Interplate earthquake activity strongly depends on physical coupling state at subducting plate boundaries, which can be classified as asperity and non-asperity. The strong PP wide-angle reflections from the subducting plate boundary were found in the aseismic subduction zones in the Japan Trench and in the slow slip region in the Nankai Trough. Those suggest the presence of low-Vp/soft materials and/or fluid at the subducting plate boundary. Such regions may cause slow-slip continuously or intermittently. In the volcanic region, magmatism is related to magma mobility and volcanism. Magma reservoirs have been identified by PxP, SxS, PxS, and/or SxP phases, and continuous monitoring of such reflected phases can inform us dynamic behavior of magma reservoirs. If we can map the areas of strong PP reflections by observations, we will be able to map the distribution of asperities along the plate boundary and/or magma reservoir, and we can actively monitor the physico-chemical state change of them. In order to actively monitor the physical and chemical state at the plate boundaries and of magma reservoirs, it is necessary to integrate mapping, active geophysical monitoring, continuous observation and petro-physical studies. We call such integrated studies as EARS (Exploration of Asperities and reflection System). The mapping and monitoring of the reflections at subducting plate boundaries and magma reservoir can be done by 2D, the 3D seismic reflection surveys, wide-angle reflection-refraction surveys and time-lapse measurements. To realize continuous monitoring of the seismic reflection intensity, we can use the ACROSS (Accurately-Controlled Routinely-Operated Signal System), which is an integrated active seismic monitoring system composed of a system synchronized by the GPS clock, and can repeatedly transmit frequency modulated seismic waves combined with sophisticated algorithm for signal analysis. In order to find best locations of active source and receivers pair in real field situation, we analyzed natural earthquakes, which have distinguished phase in central Japan. Those phases are interpreted as reflections from plate boundary. Examination of control source experiment in the central Japan also suggests strong reflected phase beneath Ontake volcano or Atera fault. We conducted some FDM seismic simulation using assumed ACROSS source for the fluid saturated plate boundary and magma reservoir beneath volcanoes. In synthetic seismogram calculation, strong SS and PS reflection phases appear at foot of volcano when a 6 km width of lens shape magma body is situated at 8 km deep.

Keywords: activemonitoring, interplate earthquakes, volcanism

(S) - IASPEI - *International Association of Seismology and Physics of the Earth's Interior*

JSS014

Oral Presentation

2256

Seismic Structure Beneath Tibet: Implications for Top-down Tectonics

Prof. James Ni

Department of Physics New Mexico State University IASPEI

Recent seismic studies in Tibet indicate that the transition from weak splitting in southern Tibet to strong azimuthal anisotropy in northern Tibet is exceptionally sharp, suggesting that the northern edge of the advancing Indian plate has reached ~32°N and plunges vertically downward to ~400 km depth as revealed from a tomographic image. In northern Tibet, a continental back-arc, the partially melted Asian mantle is highly anisotropic and is being squeezed and sheared between the Indian continental lithosphere to the south and Tsaidam and Tarim shields to the north, resulting in eastward mantle flow. In the eastern Himalayan Syntaxis region, where the Burma subduction zone meets the eastern Himalayas the fast directions of the split SKS waves are oriented approximately around the syntaxis which is consistent with the oroclinal bending hypothesis. The approximately N-S fast direction beneath easternmost Tibet and the E-W fast direction in southern Yunnan province are consistent with a coherent lithosphere-asthenosphere deformation as the Indian plate continues to underthrust beneath southern Tibet and the oceanic Indian plate subducts beneath Burma and southern Yunnan province.

Keywords: tibet, collision, himalayas



(S) - IASPEI - *International Association of Seismology and Physics of the Earth's Interior*

JSS014

Oral Presentation

2257

Deformation field and tectonics of Eastern Asia based on GPS observations

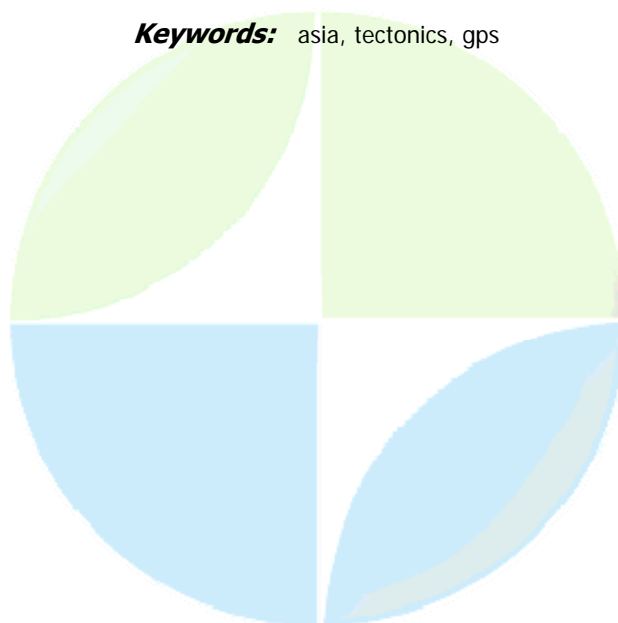
Prof. Teruyuki Kato

Earthquake Research Institute The University of Tokyo IAG

Makiko Iwakuni

East Asia is the largest field of plate convergence and deformation in the world. Although it is well known that its cause is due to the collision of Indian sub-continent to north, the mechanism of deformation of Chinese continent is not well known. Recent GPS measurements have clarified the velocity field of the area in unprecedented accuracy and in detail which provide us with much information to help us understand the mechanism of deformation of the region. We have conducted numerical modeling of such deformation based on the so-called block-slip deficit inversion. This presentation first reviews the recent results on the tectonics of the region using space geodesy. We then try to revise the velocity field of the region and re-analyze the field using the block-slip deficit model. Particular interests are paid to the Amurian plate and the Sichuan-Yunnan block rotation. Statistical tests fail to conclude that the hypothetical Amurian plate is independent of the surrounding blocks. Yet, change of data set suggests that it is independent. Since the south boundary of the Amurian plate is yet to be determined, the clear conclusion of the existence of the Amurian plate seems to be the open question to be solved in the future extensive studies. Another magnificent characteristic velocity field is the crustal rotation along the Sichuan-Yunnan tectonically active region. A lot of GPS observations have been conducted in this region, though its density is not like Japanese GEONET. We are conducting a cooperative project with Geological Institute, China Earthquake Administration, of permanent GPS observations along the Xianshuihe fault area. If the velocity field by GPS is obtained along these faults, we are able to estimate the expected maximum magnitude of earthquake using the knowledge of repeat interval of earthquakes and the time of the last event. Our preliminary results (e.g. Iwakuni [2004]) suggest that a M7 class earthquake is expected at a certain segment of the Xianshuihe fault. We would like also to argue why such magnificent rotation is occurring in the Sichuan-Yunnan tectonic zone by employing other geophysical data such as gravity anomaly or crustal seismic structures.

Keywords: asia, tectonics, gps



(S) - IASPEI - *International Association of Seismology and Physics of the Earth's Interior*

JSS014

Oral Presentation

2258

Estimating Moho Depth and 1-D Velocity Structure of the Himalaya Region using GA-MHYPO with HIMNT Earthquake Data

Prof. Woohan Kim
Seismology AGU IAVCEI

Charlotte Rowe

We present preliminary results of velocity analysis and hypocenter relocation for the Nepal/Tibet Himalaya. Based on the results of the Himalaya Nepal Tibet Seismic experiment (HIMNT), a Program for the Array Seismic Studies of the Crust and Lithosphere (PASSCAL) deployment that operated from 2001-2003, we have selected several earthquakes whose hypocenters place them within the upper mantle and crust. Phases were re-picked using amplitude and signal linearity measures (Park et al., 2004) to reduce reading error. We then jointly solved for new hypocentral parameters and average 1-D velocity structure for the source/network vicinity using GA-HYPO (Kim et al., 2006). GA-MHYPO is a genetic algorithm for optimizing hypocentral parameters and 1-D velocity structure by searching for a global solution to the 1-D velocity within prescribed ranges, seeking the minimum travel-time difference between observed and calculated phase arrivals. The velocity model (i.e., number of layers and their thickness) in this study is modified depending on the number of earthquakes and their depth distribution. Preliminary results indicate that the variation in Moho depth and velocity structure of the Himalaya region are significant, as has been proposed in previous analyses (e.g., Monsalve et al., 2006).

Keywords: moho depth, velocity, ga mhypo



(S) - IASPEI - *International Association of Seismology and Physics of the Earth's Interior*

JSS014

Oral Presentation

2259

GPS Constrain on Active Faulting and Block Rotation in deforming Asia

Dr. Wang Qi

Institute of Seismology China Earthquake Administration IASPEI

We explore a synthesized geodetic velocity field consisting ~2000 GPS velocities from the Crustal Movement Observation Network of China (CMONOC) and various campaigns throughout a period of 1991-2006. Our analysis of densified velocity data reveals a lot of unspecified features of active deformation. A velocity profile along the direction of N15E across Tibet shows a pattern of localized deformation on narrow zones of 50-100 km-wide associated with major Quaternary faults and sutures. The maximum velocity gradient is located on the E-W trending Gangdes, Gaize-Amdo and Fenghuoshan Thrusts. The thrusting slip rates are in range of 6-8 mm/yr comparable with striking-slip rates on the sub-parallel Karakorum-Jiali, Manyi-Ganzi and Kunlun faults. The geodetic slip rates of major faults in Tibet are 4-9 mm/yr. The fast rate of 14-18 mm/yr occurs on frontal thrusts at Himalaya, Pamir and southwest Tianshan, and less than 4 mm/yr elsewhere outside Tibet. The overall geodetic velocity field is predicted well within the uncertainty of 1-2 mm/yr in terms of rigid rotation model of 30 crustal blocks intersected by the Quaternary faults. The GPS inferred rates are in general agreement with that of long term faulting or its lower bound on the most faults. For example, the current geodetic rates are 1 one factor of 2-3 smaller than the long term rates of 20-30 mm/yr inferred from fault offset feature since Holocene on the Altyn Tagh fault and Karakorum fault. Internal deformation within ~30 intervening blocks hundreds of kilometers in dimension is relatively minor at level of several nano-strain /yr. The GPS-inferred slip rates on the major faults in Tibet indicate that the fault slip associated with a combination of crustal-scale block subducting, rifting and lateral extruding, has played a dominating role in accommodating continental convergence on India-Eurasia plate boundary. Our block model suggests that the tenet of plate tectonics may be applicable to characterize crustal deformation in Asia, though the large-scale extrusion out of Tibet through rapid slip-rate faulting is not necessarily invoked.

Keywords: gps, active deformation, china



(S) - IASPEI - International Association of Seismology and Physics of the Earth's Interior

JSS014

Oral Presentation

2260

Plate deformation and crustal structures at the southern end of the Ryukyu subduction zone off eastern Taiwan

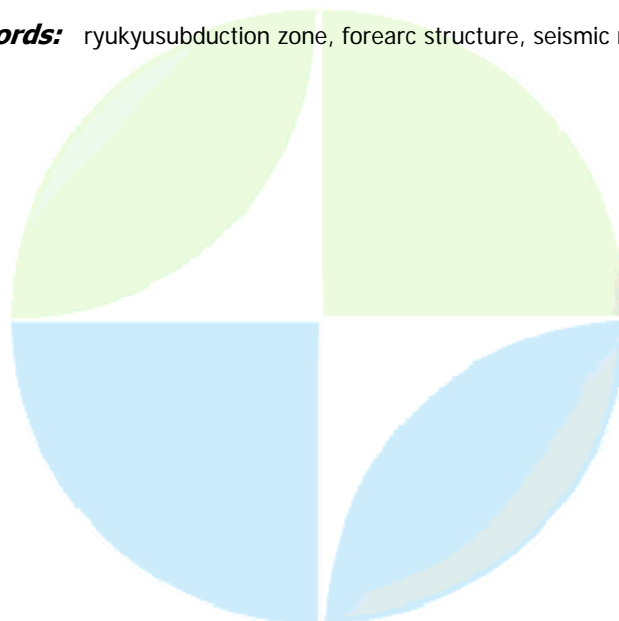
Prof. Char-Shine Liu

Institute of Oceanography National Taiwan University

Philippe Schnurle, Serge Lallemand, Yvonne Font

Multichannel seismic reflection profiles and swath bathymetry data reveal detailed morphotectonic structures of the southernmost Ryukyu arc-trench system east of Taiwan. Based on the different structural styles, the southernmost section of the Ryukyu arc-trench system can be divided into three zones. The first zone lies to the east of 123°E. It presents structures of a typical oblique subduction zone with frontal accretion of trench sediments, imbricated thrusts and folds in the accretionary wedge (the Yaeyama Ridge), and slightly folded forearc basin strata. A prominent right-lateral strike-slip fault is developed at the rear of the accretionary wedge which accounts for, at least partially, the lateral component of the oblique plate convergence, and may indicate the location of the southern boundary of the overriding Eurasia plate. The second zone lies between 123°E and 122°10'E where the Ryukyu subduction system is terminated by the impinging Luzon volcanic arc. Series of NW-SE trending shear faults cut through the thrust and folded ridges in the accretionary wedge. A NW-SE trending forearc basin (the Hoping Basin) lies between the accretionary wedge and the Ryukyu arc. Large earthquakes occur frequently along the eastern edge of the Hoping Basin. Seismic reflection data reveal that there is a basement high lies under the eastern half of the Hoping Basin, called the Hoping basement rise. This basement rise could be an uplifted feature due to the subduction (or the underplating) of some local asperities. Further investigation using deep seismic profiling and OBS array observation are planned in 2008 to better understand the seismogenic processes at this plate boundary and to evaluate the potential risks of earthquake hazards. Structures in the studied forearc region are mainly controlled by the high obliquity of convergence between the Philippine Sea and Eurasia plates, and by the collision of the Luzon arc with the Eurasia continental margin that terminates the Ryukyu subduction system to the west. Subduction of asperities may also play important roles in shaping the structures of the accretionary wedge and forearc basins here.

Keywords: ryukyusubduction zone, forearc structure, seismic reflection



(S) - IASPEI - *International Association of Seismology and Physics of the Earth's Interior*

JSS014

Oral Presentation

2261

Local Velocity Ratio Calculation for California A Simple Approach for Estimating Regional V_p/V_s

Mr. Gavin Hayes

Geosciences Penn State University, USA IASPEI

Kevin Furlong

For several decades, seismologists have used a variety of different methods to model the P-wave velocity structure of the Earth, and in particular, the Earth's crust. Modeling of the S-wave velocity field has been (and remains) more difficult, and as a result S-wave velocity structure is often directly related to P-wave models through empirical measurements of the velocity ratio in rocks. These velocity models are subsequently used in many different types of analyses, such as the calculation of strong ground motions in regional hazard maps, earthquake locations, and the inference of subsurface geology and other crustal properties. In all cases, better estimates of S-wave velocity models lead to more accurate models of the parameters they are used to describe, and can thus lead us to a more complete understanding of crustal structure. Here, we develop a straightforward technique for computing apparent velocity ratio of both the bulk seismogenic crust and shallow crust throughout California based on P- and S-wave travel-times from earthquakes to the dense network of broadband and short-period stations across the state. As the seismogenic zone is constrained to the shallow, brittlely deforming part of the crust, we can use these earthquake travel-times to estimate the apparent velocity ratio of that crust. Using this approach, we produce regional maps of V_p/V_s for all California, where station coverage is dense enough and rates of seismicity high enough to allow this type of analysis. We can also isolate the very shallow (generally aseismic) crustal section to construct a velocity ratio map of the near surface. This method, which we call the Local Velocity Ratio Calculation (LVRC), yields a simple yet powerful way to analyze the velocity ratio of the upper crust on a regional basis. Results may be related to geologic structure, can be used in conjunction with bulk crustal studies (such as receiver function analyses) to resolve upper and lower crustal properties and address issues related to crustal structure, or used to infer parameters such as ground shaking susceptibility in California and other similar areas worldwide, providing useful information to aid in the science of future hazard mitigation.



(S) - IASPEI - *International Association of Seismology and Physics of the Earth's Interior*

JSS014

Oral Presentation

2262

Distributed vs. narrow deformation in the mantle lithosphere beneath the central South Island, New Zealand: Insights from GPS and geology

Dr. Laura Wallace

Natural Hazards Group GNS Science

Susan Ellis

In the South Island, New Zealand, most of the crustal deformation between the Pacific and Australian plates occurs on known, active fault zones. GPS and geological data there can be explained (to first order) by the existence of a few, distinct tectonic (elastic) blocks with reasonably defined boundaries. However, there is ongoing debate regarding the nature of interplate deformation at depth, within the mantle lithosphere beneath the South Island. Some workers suggest that plate boundary deformation is broadly distributed within the mantle lithosphere (over a zone up to 400 km wide), while others contend that the overall relative plate motions are accommodated across comparatively narrow shear zones at depth. One of the assumptions of the elastic block model previously used in the interpretation of GPS and geological data in the South Island is that the relative plate motions occur at depth over a narrow zone. To assess the possibility of distributed deformation within the mantle lithosphere, we integrate the elastic block approach with analytical equations describing surface displacements due to a wide deformation zone at depth (below the elastic part of the crust). This is the first time that a fully three-dimensional inversion accounting for both localised and distributed shear within the lithosphere has been carried out. The GPS data (on its own) can be fit by either a wide or narrow shear zone at depth. However, the long-term surface deformation patterns we obtain for the two end-member models are quite distinct, suggesting that geological and geodetic studies together may help to distinguish between these two conceptual models for plate boundary deformation. In particular, to fit the GPS data with a wide shear zone in the mantle, we find that a quite unrealistic permanent deformation pattern in the upper crust (in comparison to the known active faulting) is needed.

Keywords: crustal deformation, tectonics, gps



(S) - IASPEI - International Association of Seismology and Physics of the Earth's Interior

JSS014

Oral Presentation

2263

Seismic velocity and anisotropy structures of the collision zone in Himalaya

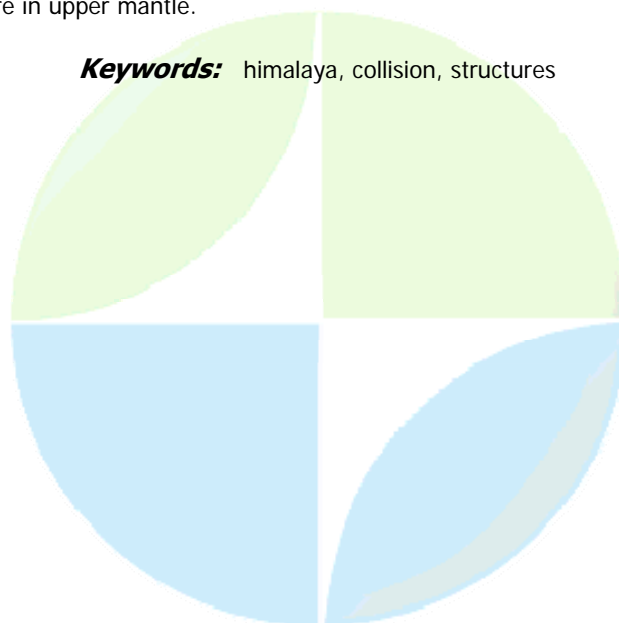
Prof. Zhifeng Ding

Institute of Geophysics, CEA IASPEI of China IASPEI

Wulin Liao, Hong Zhang, Guiyin Li, Hui Wang

Himalayan area is the collision zone of the Indian and Eurasian continents. With the increasing seismic observatory data, we can obtain more and more evidences of the collision processes. In this research, the seismic velocity map and the anisotropy of the lithospheric structures were used to study the collision features. The seismic arrivals of the regional and teleseismic events were collected and used to inverse the seismic structure in mid of the Himalayan area. These data were from the recordings of the permanent and portable seismic stations in and around the mid of Himalayan area during the past 15 years. The 3-D seismic structures in the research area were obtained by using the seismic tomography method (Zhao D., 1992, 1993). The shear wave anisotropies were also studied by using the seismic recordings from the portable seismic stations which were deployed in Himalayan area during 2000-2004. The results of the seismic tomography obviously show the collision structures in Himalayan area. The abnormal higher velocity zones can be traced from the southern part of Himalaya north to the mid of Tibetan region, with the increased depth. The images of the cross sections from to the northern part of the Plateau show the clear subduction and collision structures of the Indian plate and the Eurasian plate. The Indian lithosphere seemed to be delaminated into two subducting layers. The Lower part of Indian crust subducted below to the Moho of the south, which can be trace up to the Bangong-Nujiang suture; and the mantle lithosphere of the Indian continent subduct to the deeper part of the upper mantle beneath the southern. The shear wave splitting were observed in the 39 stations in Himalayan area. The fast polarization directions from the splitted S waves were vary in different part of the research area. The directions were NWW or NW in western part, and near NS in eastern part of the Himalayan area. Both the tomography and anisotropy research described the complicated collision structures in Himalayan area. The subduction mechanisms of the Indian plate were not alike along the collision front. The Indian plate may subduct to the Eurasian plate at some places which are low velocity and higher temperature in upper mantle.

Keywords: himalaya, collision, structures



(S) - IASPEI - *International Association of Seismology and Physics of the Earth's Interior*

JSS014

Oral Presentation

2264

Plate boundary deformation and microplates motion in the Central Mediterranean

Dr. Nicola D'Agostino

Istituto Nazionale Geofisica Vulcanologia IASPEI

Giulio Selvaggi, Antonio Avallone, Daniele Cheloni, Elisabetta D'Anastasio, Sergio Mantenuto

The Adriatic region has always puzzled and attracted the interest of the researchers involved in the studies of the Alpine-Mediterranean plate boundary zone. Whereas stratigraphic and paleomagnetic studies have described the Meso-Cenozoic evolution of the Adriatic region as a rigid promontory of the African plate, seismological and space geodetic information strongly support the evidence of an independent Adriatic microplate. In this study we use continuous and survey-style GPS measurements together with the analysis of earthquake slip vectors, to study the crustal motion and boundaries of the Adriatic region. Based on a rigorous statistical analysis of the data, we propose a set of Eulerian poles which describe the kinematics and the active deformation of the Central Mediterranean in terms of the relative motion between two microplates: Adria and Apulia. We propose that the Ionian region forms a single microplate with Apulia resolving the need for a discrete southern boundary between Adria and . We use a simple block model to illustrate how the microplates rotate to accommodate the Eurasia-Africa relative motion. The proposed present-day kinematics is then evaluated in relation to the evolution and fragmentation of the Adriatic promontory.

Keywords: mediterranean, microplate, geodesy



(S) - IASPEI - *International Association of Seismology and Physics of the Earth's Interior*

JSS014

Oral Presentation

2265

Interaction of active fault and fold development: the Balanegra-Sierra de Gador GPS network (Central Betic Cordillera, SE Spain)

Prof. Jesus Galindo-Zaldivar
Geodinamica Universidad de Granada

Antonio Gil, Carlos Marn-Lechado, Pedro Alfaro, Clara De Lacy, Francisco Jun Garca-Tortosa, Angel Carlos Lopez-Garrido, Antonio Pedrera-Parias, Isabel Ramos, Gracia Rodriguez-Caderot, Ana Ruiz-Constn, Carlos Sanz De Galdeano, Maria Jess Borque

The Betic-Rif cordilleras have been formed in the western Mediterranean by the oblique convergence related to the Eurasian-African plate boundary. The seismicity and the active tectonic structures are distributed along a band of more than 300 km wide. In the Internal Zones of the Betic Cordilleras, the development of large E-W oriented folds since the middle Miocene and related faults are the responsible of the present-day relief. These active upper crustal structures formed in the hanging wall of major detachments. The Balanegra-Sierra de Gador region is located in the boundary of the central Betic Cordillera and the Alboran Sea and shows a relatively more intense seismicity and tectonic activity than the surrounding areas. The last seismic series occurred in December 1994- January 1995 with two $M_b=4.9$ and $M_b=5.0$ mainshocks and more than 350 recorded events ($M_d>1.5$). This shallow activity occurred along the NW-SE oriented Balanegra normal fault, which determines the position of the coast line along more than 10 km and extends to the Alboran Sea. The Balanegra Fault zone is formed by several parallel faults with 1-10 m associated scarps producing a staircase morphology. The maximum vertical slip is generally of several hundred of meters. The fault zone is located southwest of the Sierra de Gador antiform that determines the highest relieves of this region. Minor NW-SE oriented normal faults indicate an ENE-WSW regional oriented extension. Seismic profiles points to the simultaneous development in the region of large ENE-WSW folds and minor faults since the Miocene. A new non-permanent GPS network has been installed in order to study more in detail the present-day relationships of large folds and faults development. For this purpose, in addition to measurement points installed in the Balanegra fault zone, other points have been located in the Sierra de Gador Antiform. A first measurement campaign has been developed during the spring-2006 and GPS locations have been determined with mm accuracy. In addition, two high precision leveling lines (accuracy of 0.2 mm) have been established across the fault. Anyway, taking into account the expected low rates of tectonic structures and the measurement precision, GPS network may provide accurate results after a period of more than 5 years and high precision leveling after 2 years if there are not new seismic series in the region. These data may help to quantify the tectonic model determined by NNW-SSE shortening accommodated by fold development and relief uplift and orthogonal ENE-WSW extension responsible of the normal fault activity.

Keywords: gps, faults folds, betics

(S) - IASPEI - *International Association of Seismology and Physics of the Earth's Interior*

JSS014

Oral Presentation

2266

Evolution of the Plate Boundary Through New Zealand since 25 Ma Spatial-temporal patterns of orogenesis

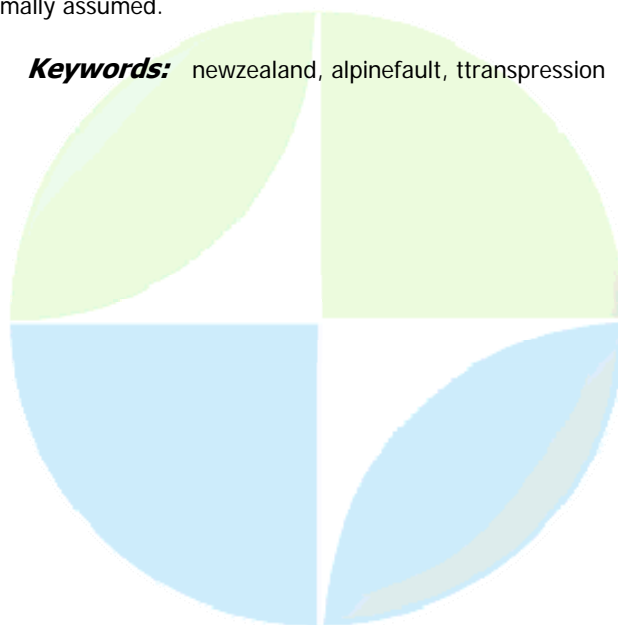
Prof. Kevin P Furlong

Department of Geosciences Penn State University IASPEI

P.J.J. Kamp, G.P. Hayes

The current plate boundary configuration through New Zealand of a (transpressional) continental transform linking two convergent/subduction zones initiated approximately 25 Ma. Its present configuration, kinematics, and patterns of deformation serve as a primary example of the tectonic response to transpressional plate interactions. Although the present situation is reasonably well constrained, the tectonic history of boundary is less clear. In particular, the extent, geometry, location, and deformational behavior of the plate boundary linking the Hikurangi and Puysegur subduction regimes the proto-Alpine Fault (AF) plate boundary structure prior to approximately 10 Ma is not well understood. Combining plate reconstructions, patterns of basin evolution and volcanism recording the southward migration of Hikurangi subduction, and plate kinematics through time allow us to place important constraints on the development of the proto-Alpine fault plate boundary through the Miocene. Results include (1) a substantial volume of crustal material must have been removed along the proto-AF adjacent/within the present North Island, implying transpression along that segment of the plate boundary in the Middle Miocene and the development of a Southern Alps-like orogen bounding the eastern margin of the present-day North Island; (2) The present North Island subduction margin and the accretionary margin forearc terranes were likely originally part of the Pacific plate (i.e. east of the proto-AF) and have been sequentially captured by the Australian plate in a manner similar to present capture by Australia of the Marlborough terranes in the northern South Island; (3) remnants of the proto-AF structures should lie inboard of these forearc terranes and may be associated with faults of the North Island Axial Ranges; and (4) the proto-AF plate boundary may have had different geometry, orientation, and attitude from the current Alpine Fault through the South Island characteristics that are in part controlled by the structure and mechanical properties of the Australia plate margin. This analysis implies that the Alpine Fault system was transpressional throughout much of its history and not only post-Miocene as is normally assumed.

Keywords: newzealand, alpinefault, ttranspression



(S) - IASPEI - *International Association of Seismology and Physics of the Earth's Interior*

JSS014

Oral Presentation

2267

New constraints on the motion and boundaries of the Sierra Nevada Block and Colorado Plateau from continuous GPS velocities

Dr. Corne Kreemer

Nevada Bureau of Mines and Geology University of Nevada, Reno IAG

William C. Hammond, Geoffrey Blewitt

We present a new GPS velocity solution for much of the western Basin and Range between the San Andreas Fault and the Rocky Mountains. This solution uses data from ~500 sites, including those from the BARD, SCIGN, EBRY, PANGA, BARGEN, CORS and PBO permanent arrays, as well as from our own semi-continuous MAGNET network in the western Basin and Range. Using the velocity solution we obtain better constraints for the motion of the Sierra Nevada block than was previously possible. Moreover, our analysis shows that all of the Sierra Nevada west of the crest moves as a rigid entity. Geodetic velocities in the Walker Lane are oriented parallel to the Sierra Nevada-North America small-circle, implying that most of the deformation to be accommodated as shear. However, many normal faults (particularly those bounding the eastern Sierran front) are oriented at ~45 degrees to the relative motion, suggesting regional strain partitioning. Overall, the deformation pattern is controlled by the geometry of the Sierras granite/metamorphic province as it moves along and away from the Basin and Ranges western margin. For the Colorado Plateau (CP) a consistent pattern is emerging with sites on the CP moving northwest, implying that the block is rigid and that the extension rate across the Rio Grande Rift is ~1 mm/yr. Our results also imply ~1-2 mm/yr of motion across the Hurricane Fault system between the CP and the Basin and Range. Anomalies to the observed velocity pattern exist near large urban areas (e.g., Phoenix, Las Vegas) or along the Colorado River. The anomalous velocities are probably due to loading effects from local ground-water variations. To obtain our solution we use the GIPSY-OASIS II software and apply a new ambiguity resolution technique that allows for fast and efficient processing of daily solutions for the entire network. Most of North America's Intermountain-West velocities relative to stable North America are very small and we would commonly need long time-series to infer significant motions in order to avoid seasonal effects and other long-term transients. Here we deploy a new regional filtering technique that allows us to include sites with relatively short observation span (~1 year). We create a regional-filter for each site by using residuals of all sites within 500-2000 km of that site (except the site itself). Those residuals are the result of fitting a linear rate and annual and semi-annual term to the unfiltered time-series. We solve for a linear rate simultaneously with seasonal parameters, and we infer white-, flicker-, and random-walk noise components for each individual time-series and apply those in the estimation of the rate uncertainties. The ITRF2000 velocities are transformed into the Stable North America Reference Frame (SNARF) by using ~30 velocities across the North American continent common with those in the SNARF solution. Using SNARF provides a clear demonstration that the Rio Grande Rift is separating CP from stable North America.

Keywords: gps velocities, sierra nevada, colorado plateau

(S) - IASPEI - *International Association of Seismology and Physics of the Earth's Interior*

JSS014

Oral Presentation

2268

Neotectonic model of the croatian external dinarides; a tectonic framework for the Adria Plate Margin and carbonate wedge tectonics

Mr. Gabriele Casale

Earth and Space Sciences University of Washington

Recently the Adria Microplate(s) has gained direct and indirect attention through several collaborative Peri-Adriatic projects. Despite these studies internal geometry and rates of motion remain elusive. As Adria is inaccessible for direct measurement geologic studies are confined to deformation along its margins. The strain accumulation within the external Dinarides is directly attributed to convergence Adria, and noticeable shortening across the Dinarides to 2 mm/yr is visible from available GPS data (Altiner 2001, Serpelloni 2005). Recent advances concerning structure, strain accumulation, erosion, and seismicity within accretionary wedges provide a context with which to understand convergent tectonics. Much field, geophysical, and borehole data exists within the external Dinarides, however, many of the exiting structural interpretations predate the Davis, Suppe, and Dahlen model of accretionary wedges or were constructed within a different context, such as hydrocarbon potential. We re-evaluate existing data to place the external Dinarides into a modern tectonic framework in terms of critical taper, overall structural pattern, and tectonic influx of the active portion of this convergent plate margin. This model comes as the pretext of a larger collaborative effort, and we describe synthesis of this model with geomorphic, geodetic, and long term tide gauge studies of modern and Plio-Quaternary vertical and horizontal displacement rates. Furthermore, we discuss the extension of this study to geodynamic models of accretionary wedges in terms of erosive flux distribution and mass balance.

Keywords: structure, accretionary wedge



(S) - IASPEI - *International Association of Seismology and Physics of the Earth's Interior*

JSS014

Oral Presentation

2269

Present-day horizontal and vertical tectonic motion of the Dinarides region, Croatia, from GPS data and tide gauge data

Mr. Goran Buble
IAG

Richard A. Bennett, Sigrun Hreinsdóttir, Gabriele Casale, Tomislav Baić, Eljko Bačić, Marijan Marjanović

Despite considerable attention directed towards Circum-Adriatic tectonics in the recent years, the rate and direction of Adria microplate motion and internal microplate fragmentation remain unresolved. We analyze tide gauge data from the eastern Adriatic Sea in order to assess spatial variation in vertical tectonics. Tide gauge data are available from eight sites in Italy, Slovenia, Croatia and Montenegro with long time series (30-95 years). Correlation among tide gauge records indicates that the interannual sealevel variations are common mode. We are thus able to mitigate bias in trend estimates associated with interannual variations by common-mode filtering (Wdowinski et al., 1997; Davis et al., 1999). We find relative vertical crustal rates (with respect to the geoid) along the coast that fluctuate between 0.7 mm/yr which may be indication of active tectonic processes. Preliminary vertical rates determined from a sparse network of continuous GPS sites (with respect to reference ellipsoid) in the region are in general agreement with the tide gauge results within uncertainties. We also analyzed campaign and continuous GPS data collected along the eastern Adriatic coast in 1994-2005 to investigate the pattern of horizontal deformation. We find that NE directed horizontal shortening across the Dinarides that varies along the coast of Croatia, revealing apparent rotations that are not well resolved by the present GPS data set, but which nevertheless provide new clues regarding the modern configuration and motion of the Adria microplate(s). Velocity estimates for Istria are compatible with previous models for Adria microplate motion (Battaglia et al., 2004; Calais et al. 2003). Sites in Istria have a Northward motion as expected but sites further south along the coast (latitude 44 to 45 degrees N) have a more westward motion, up to 40 degrees off from expected North Adria poles. Motions of sites on the Island of Palagruza, Croatia, outermost Dalmatian Island, and Matera, Italy, Puglia platform, respectively, differ by less than 0.20.3 mm/yr in magnitude and 03 degrees azimuth, which implies that Palagruza and Puglia lie on a common southern Adria microplate. We will also discuss a new project that will involve addition of a number of new continuous GPS stations, additional GPS campaigns, and other measurements.

Keywords: gps, tide gauge, dinarides

(S) - IASPEI - *International Association of Seismology and Physics of the Earth's Interior*

JSS014

Oral Presentation

2270

Significant lateral crustal elasticity contrast across the East Kunlun Fault in northern Tibet, inferred from co-seismic INSAR measurements of the 2001 MW 7.8 Kokoxili earthquake

Dr. Wei Tao

Institute of Geology China Earthquake Administration IASPEI

Zhengkang Shen, Yongge Wan, Xinjian Shan, Chao Ma

We use co-seismic deformation data of the 2001 Mw 7.8 Kokoxili earthquake obtained from InSAR measurements to study crustal elasticity contrast across the East Kunlun fault. Co-seismic deformation field of the earthquake documented by InSAR studies indicated that the displacements on the south side were 20-30% higher than that on the north side of the fault. We develop an elastic finite element model and invert InSAR data from two deformation profiles to estimate two parameters: the Young's modulus contrast across the fault and the fault rupture depth. The starting lithospheric structural model is adopted from a seismic reflection study on the north side of the East Kunlun fault. Our result places optimal estimates of the earthquake rupture depth as 20-22 km and the crustal Young's modulus contrast between the south and north side as 81-92%. Such a result, obtained from study of crustal deformation, suggests a softer crust south than north of the fault, which is consistent with previous tomographic and magnetotelluric studies of a low-velocity and high-conductivity layer existed in lower crust of the Kokoxili-qiangtang block south of the Kunlun Fault. The cause of the contrast must be related to the uplift and evolution process of the plateau. The rising of the Kunlun mountains may have resulted from the southward thrusting of the material in the Qaidam basin, producing relatively cold and strong mountain roots. On the other hand, south of the East Kunlun fault, the northeastward indentation of the India plate into Tibet has led to crustal thickening for the Kokoxili-Qiangtang block up to ~70 km, resulting in temperature increase in the crust and development of the slow-velocity and high-conductivity layers in the lithosphere. All of these should have reduced the strength of the crust on the south side of the fault, and led to the results we presented above.

Keywords: coseismic deformation, elasticity contrast, tibet



(S) - IASPEI - International Association of Seismology and Physics of the Earth's Interior

JSS014

Poster presentation

2271

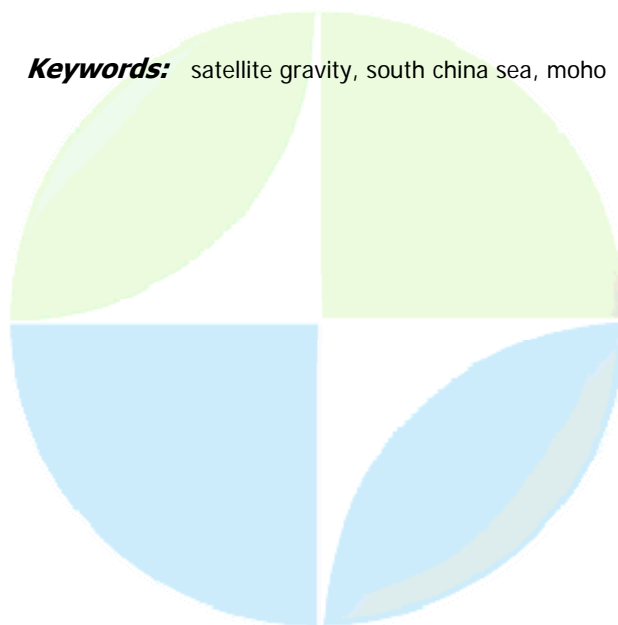
Moho and Crustal Structures of the South China sea from satellite gravity anomaly

Mr. Trung Nguyen Nhu

Department of Geomagnetic and Geoelectricity Institute for Marine Geology and Geophysics, VAST IAG

Satellite gravity is a superb tool for marine tectonic study. It provides a firsthand glimpse into seafloor morphology and tectonic elements such as spreading ridge, offset, continental-ocean boundary, faults, basins, volcanoes in the ocean. Interpretation of the gravity data constrained by the seismic data is most useful tools for investigating the crustal structure. In this paper, we present interpretation results of the satellite gravity data constrained by the deep seismic for predicting the Moho depth, fault systems and volcano/magma in the East Sea. The Moho surface was investigated by three different compute methods (i.e. isostatic model method, correlation regression method and 3D direct inversion) has shown that the given Moho depth has high accurate and reliable. Comparing to the seismic Moho depth, Comparing with the deep seismic data in the region (i.e. Sonobouy, OBS and ESP) reveals that the correlation regression and 3D gravity inversion solution give the RMS errors of 5, 7-5, 6 %, and RMS errors of the isostatic model is 9, 4%. The Moho depth in the East Sea changes in a wide range of 8-32 km. They are 10-14 km in the ocean Central Basin, 31-28 km along the coast of the margins and 28-18 km in the Hoangsa and Truongsa archipelagos. The crust of the East Sea consists of oceanic and continental crust. The crustal thickness is 4-10 km in the oceanic crust in which the northern side of the spreading ridge is thicker than that in the southern side. The crustal thickness is 31-12 km in the continental crust. The crust in the northern margin is thicker than that in the southern margin. The average crustal thickness is about 12-16 km in the southern margin and 16-20 km in the northern margin. The Red River, Phukhanh, Namconson, Tuchinh-Vungmay basins and Palawan trough lie on the thin continental crust (10-12 Km). Beibuwan, Pearl River Mouth and Cuulong basins lie on the thicker continental crust (20-24 Km). The results also determine the deep fault systems and volcano/magma that develop mainly in the NE-SW, NW-SE and NS directions and in the thin crust area. The volcano/magma activities in the southern side are stronger than that in the northern side of the East Sea.

Keywords: satellite gravity, south china sea, moho



(S) - IASPEI - International Association of Seismology and Physics of the Earth's Interior

JSS014

Poster presentation

2272

Seismotectonic models of the three recent devastating SCR earthquakes in India

Prof. Jnana Kayal

Department of Applied Geophysics Indian School of Mines IASPEI

During the last decade (1993-2003), three devastating earthquakes, Killari 1993, Jabalpur 1997 and Bhuj 2001, M 6.0 7.7, occurred in the Stable Continental Region (SCR) of India. These three earthquake sequences are well studied by deploying temporary microearthquake networks. The 1993 Killari earthquake (mb 6.3) is a typical shallow (0-10 km) SCR event. The 1997 Jabalpur earthquake (mb 6.0) and the 2001 Bhuj earthquake (MW 7.7) are, on the other hand, deeper (25-35 km) paleo-rift zone earthquakes within the continental region. The September 30, 1993 Killari earthquake (mb 6.3) occurred in the Deccan province of central India. The Killari earthquake and its 150 well located aftershocks were confined to a shallower depth (0-15 km), a common type of SCR seismicity. The main shock occurred by reverse faulting at a depth of 6 km; the deeper (6-15 km) aftershocks also occurred by reverse faulting. The shallower aftershocks, (0-<6 km), on the other hand, occurred by right-lateral strike-slip faulting. A south dipping hidden E-W fault generated the main shock and the deeper aftershocks (depth 6-15 km). The shallower aftershocks (depth 0-<6 km), on the other hand, were generated by shear adjustment along a hidden NW-SE fault by right-lateral strike-slip faulting. These fault zones are identified by detailed gravity and magnetotelluric (MT) studies. Seismic tomography study revealed a detailed velocity structure of the source area; the main shock occurred at the contact zone of a high velocity and low velocity zones (Kayal and Mukhopadhyay, 2002). The May 22, 1997 Jabalpur earthquake (mb 6.0) occurred at the base of the Narmada Rift Basin, within the stable continental region, at a depth of 35 km by reverse faulting with a left-lateral strike-slip motion. Only about 25 aftershocks were recorded that occurred at depth 35-40 km in the lower crust. The fault-plane solution of the aftershocks also reveals reverse faulting with left-lateral strike-slip motion. A tectonic model is proposed for the Jabalpur earthquake sequence. The model illustrates that south dipping Narmada South Fault (NSF), the southern margin fault of the Narmada Rift Basin, which was formed by tensional force in the geological past, now activated by reverse faulting due to compressional stress of the NE ward movement of the Indian plate (Kayal, 2000). Seismic tomography study of the source area could not be done due to meagre aftershock data. The deep rooted NSF is, however, reflected in gravity and MT studies. The most recent devastating Bhuj earthquake of January 26, 2001, MW = 7.7, is one of the rarest and largest events that occurred in a continental region of the world. This is the second largest event in the western margin of peninsular India continental region, after the 1819 Kutch earthquake of Mw = 7.8. The 2001 Bhuj earthquake is also an example of a deeper paleo-rift zone earthquake which occurred at a depth of 25 km in the Kutch Rift Basin. About 3000 aftershocks (M > 1.0) were recorded by a temporary network in two and a half months period after the main shock. The fault-plane solution of the main shock and the aftershocks show complicated seismogenic structures (Kayal et al., 2000a). The main shock shows reverse faulting with left-lateral strike-slip motion along a south dipping ENE-WSW trending fault. The well located aftershocks follow mainly two trends of fault/rupture at depth, one in NE direction and the other in NW direction. The aftershocks along the NE trending fault/rupture show reverse faulting with left -ateral strike slip-motion at the mid crustal (15-<25 km) as well as at the lower crustal (25-35 km) depth. The aftershocks along the NW trending fault or rupture occurred by pure reverse faulting at the mid crustal depth (15-<25 km), and by right-lateral strike-slip faulting at the shallow crustal (<10 km) and deeper crustal depth (25-38 km). Ground observations are compatible with the above. These observations suggest a fault interaction model,

which illustrates that the main shock originated at the base of the paleo-rift zone by reverse faulting, and it propagated ruptures along the NE as well as along the NW directions. Seismic tomography revealed more detailed picture of the complicated seismogenic structures in this rift-basin (Kayal et al., 2000b). It shows high V_p , low V_s and high V_p / V_s in the source area, which indicate that the source area is a fluid-filled fractured rock - matrix that triggered the main shock. References Kayal, J.R., 2000. Seismotectonic study of the two recent SCR earthquakes in central India, J. Geol. Soc. India, 55, 123-138. Kayal, J.R. and Mukhopadhyay, S., 2002. Seismic tomography structure of the 1993 Killari earthquake source area, Bull. Seism. Soc. Am., 92, 2036-2039. Kayal, J.R., De, R., Ram, S, Srirama, B.V., and Gaonkar, S. G. 2002a. Aftershocks of the January 26, 2001 Bhuj earthquake in the western India and its seismotectonic implications. J. Geol. Soc. India, 59, 395-417. Kayal, J.R., Zhao D, Mishra, O P, De R. and Singh, O P. 2002b. The 2001 Bhuj earthquake: Tomographic evidence for fluids at the hypocentre and its implications for rupture nucleation, Geophys. Res. Lett., 29(24), 51-54.

Keywords: fault plane solution, tomography, tectonic model

IUGG

XXIV2007

PERUGIA
I T A L Y



(S) - IASPEI - *International Association of Seismology and Physics of the Earth's Interior*

JSS014

Poster presentation

2273

Technology of the prediction of the tectonic and geomechanic processes at a selected areas for dispose radioactive waste

Dr. Tatarinov Victor
RAS Geophysical Center IASPEI

Morozov Vladislav, Belov Sergey, Kolesnikov Ilia

The possibility of using deep geological formations to dispose of high-level radioactive waste (HLW) is a subject raising heated debate among scientists. In Russia, the idea of constructing HLW repository in the Niznekansky granitoid massif in Krasnoyarsk area is widely discussed. To solve this problem we are elaborating a technology associated with time space stability prediction of the geological environment, which is subject to geodynamic processes evolutionary effects. It is based on the prediction of isolation properties stability in a structural tectonic block of the Earths crust for a given time. The danger is in the possibility that the selected structural block may be broken by new tectonic faults or movements on a passive fault may be activated and thus underground water may penetrate to HLW containers. Prediction technology elaboration is based on the following prerequisites. 1. The evolution of the Earths crust (velocity) is determined by the intensity of the tectonic process development in a region. The determining feature is the level of active tectonic stresses as well as physical and mechanical characteristics of rocks. 2.The tectonic stresses field varies in space and time, retaining tendencies inherited in the preceding period of the region tectonic development. 3.Modern stress strain state of the environment in combination with the inherited tendency of time space variation of the local fields tectonic stresses is the basis of geomechanical processes development in structural tectonic blocks. 4.The direction in which developing active tectonic faults spread is determined by inherited directions that depend on the tensor of active tectonic stresses. 5.The possibility of formation or development of tectonic faults (weak zones and others) is determined by the location of the fault as related to the major stresses axes. 6.The local zone of increased concentration of stresses makes potential places that initiate a likely development of the processes of geological environment destruction. The technology comprises the following complex of research methods. 1.Structural geology, engineering geology and geomorphology methods of fault block tectonics. 2.Heterogeneous finite-element modeling of stress fields distribution in structural blocks. 3.Paleotectonic reconstruction of stress strain state of the areas under investigation for a period of time of up to 1 million years. 4.Zoning of the area and separation of deep linear zones from geological and geophysical data that can be potential zones of tectonic faults on the basis of artificial intelligence methods. 5.GPS-observations of modern movements of the Earths crust. 6.The method of rock destruction time calculation on the basis of the kinetic theory of solid bodies strength.

Keywords: tectonic, radioactive, geomechanic

(S) - IASPEI - *International Association of Seismology and Physics of the Earth's Interior*

JSS014

Poster presentation

2274

Fine crustal structure in active tectonic area at Northwestern Edge of Tarism Basin Block

Dr. Zhaofan Xu

Geophysical Exploration Center, CEA 104 Wenhua Road, Zhengzhou 450002, China IASPEI

The northwestern edge of Tarism Basin and its adjacent area lies at the place where three tectonic units, i.e. Tianshan fold zone, Pamir tectonic arc and Tarim block, meet there and is one of the most active earthquake provinces at present in Chinese mainland. In the last century, about 3/4 strong earthquakes in Chinese mainland took place there. Especially from the twenty-first of January to sixteenth of April in 1997, at a very small area of 9x18km² near Jiashi city, where there was no any main fault found before, was hit by 7 strong earthquakes with the magnitude ranging from 6.0 to 6.9, and also no any seismic fault found after these shocks besides the macroscopic appearances of the destroyed villagers houses. It had never taken place before in Chinese mainland that a series of strong earthquakes shook a very small area in such a short period time of 85 days. In order to understand the crustal structure features beneath the strong earthquake swarm area, active source seismic investigation experiments with wide angle reflection/refraction, high resolution seismic refraction, near vertical seismic reflection profiles and a three-dimensional temporary seismic transmission array were carried out, respectively. The crustal structure features with different scales were determined by these seismic data and the hidden crustal faults were inferred. The high resolution seismic refraction results show that the upper crust is relatively well-distributed in laterally and the buried depth of crystalline basement is deeper in SW and shallower in NE, which forms a slope toward Tianshan Mt with a little uplift. The basement velocity is about 6.2km/s, which is comparatively higher than the other area in Chinese mainland. Though the crust show obviously layered structure features, the geometries of interior crust interfaces and Moho suggest that the crust had been suffered very strong deformations under the extrusion from Kunlun in south and Tianshan in north, and also suggest that the crustal deformations in the southern and deeper depth should stronger than in the northern and upper crust. The different deformation images between upper and lower crust, which are obtained from wide angle reflection/ refraction and high resolving seismic refraction surveys, respectively, imply that the geodynamics process should come from a rather large depth. Though the seismogenic tectonic background of Jiashi strong earthquake swarm maybe has something to do with the inferred crustal faults, no structure features show that these faults stretch to the near surface. Acknowledgments: This research was supported by the Joint Seismological Foundation of China Earthquake Administration, Grant 106076

Keywords: active tectonic area, active source seismic experime, crustal structure

(S) - IASPEI - *International Association of Seismology and Physics of the Earth's Interior*

JSS014

Poster presentation

2275

Three-Dimensional velocity structure of the South Fossa Magna, Central Japan

Dr. Haruhisa Nakamichi

Graduate School of Environmental Studies Nagoya University IAVCEI

Hidefumi Watanabe, Takao Ohminato

We present the three-dimensional structures of the P wave velocity (VP), S wave velocity (VS) as well as the P wave to S wave velocity ratio (VP/VS) beneath Mount Fuji and the South Fossa Magna, Japan, using arrival time data collected from 2002 to 2005 by a dense seismograph array. The high resolution data set and improved methodology reveal not only several velocity features that are consistent with previous studies, but also important new details that clarify the velocity structures associated with volcanic processes beneath Mount Fuji and the collision tectonics of the South Fossa Magna. One such particular feature is a low-VP, low-VS and low-VP/VS anomaly at depths of 7-17 km beneath Mount Fuji that corresponds with the locations of deep low-frequency (DLF) earthquakes. The coincidence of the velocity anomaly and the DLF locations suggests that supercritical volatile fluid, such as H₂O and CO₂, may be abundant in the low-VP/VS region and may play an important role in generating DLF earthquakes. This anomaly overlies a deeper low-VP, low-VS and high-VP/VS anomaly at depths of 15-25 km that may represent a zone of basaltic partial melt. Iso-velocity surfaces (VP = 6.0 km/s and VS = 3.5 km/s) corresponding to the upper limit of hypocenter distribution below Mount Fuji may define the upper surface of the Philippine Sea plate whose existence in a seismic gap beneath Mount Fuji has been controversial.

Keywords: fossa magna, mt fuji, tomography



(S) - IASPEI - *International Association of Seismology and Physics of the Earth's Interior*

JSS014

Poster presentation

2276

Is there the Amurian plate in northeast Asia?

Dr. Shuanggen Jin

Astro-Geodynamics Center Shanghai Astronomical Observatory, Chinese Aca.Sci IAG

Pil-Ho Park

The plate tectonics of Northeast (NE) Asia is very complex with diffuse and sparse seismicity in the broader plate deformation zone. Zonenshan and Savostin (1981) firstly proposed the existence of the Amurian plate in NE Asia based on the clear geographical boundary of Kuri-Japan trench and Baikal rift zone, but became diffuse throughout continental northeast Asia. This proposed Amurian plate (AM) is of special interest to constrain the relative motion of the major and minor plate in Northeast Asia and provides a rigorous framework for interpreting seismicity and the kinematics, especially for actively seismic Japan. However, whether it exists or not and its boundary geometry remain controversial, especially the location of the south boundary. Now the increasingly dense GPS networks operated by East Asian countries in this area provide an important tool to investigate plate tectonic movements and to identify the approximate location of plate boundaries. In this paper, the possibility of Amurian plate motion independent of Eurasia is tested rigorously using GPS velocities incorporating block modeling. The test has shown that the Amurian plate is independent of the Eurasian plate motion with statistical significance above 99% confidence level, and the south boundary of the Amuria is along the Yin-Yan Shan belt through to Japan.

Keywords: plate tectonics, amuria, gps

PERUGIA
ITALY



(S) - IASPEI - *International Association of Seismology and Physics of the Earth's Interior*

JSS014

Poster presentation

2277

Crust and upper mantle structure in continental China and its adjacent area from surface wave two-station analysis

Mrs. Guixi Yi

Information Engineering College Chengdu University of Technology IASPEI

Yao Huajian, Zhu Jie-Shou, Robert D, van der Hilst

Based on surface wave data recorded by 102 stations in China and adjacent area, we measure interstation Rayleigh-wave phase velocity dispersion data from two-station analysis and finally obtain dispersion curves in the period band 20-120s for 538 independent paths. Dispersion data are then used to invert for 21 phase velocity maps from 20s to 120s with 5s interval in the continental China and its adjacent regions (70-140E, 18-55N). Checkerboard tests show that the lateral resolution is about 3 in central-eastern China and about 5 in western China and adjacent regions. The main results obtained are shown as follows: (1) The spatial distribution of phase velocities in the studied area is significantly different for the western part and eastern part of China, which are approximately separated by the longitudinal line at 104E. (2) Phase velocity maps at shorter periods (20-35s) are influenced by topography and crustal thickness. On these maps, the western part is characterized by apparent low phase velocity, except Qaidam basin with high phase velocities. Tarim basin, Qinghai-Tibet plateau and its eastern margin-Songpan-Ganzi block, form the most prominent low velocity body in the studied area. A large-scale low velocity anomaly also appears in Western Mongolia. Yangtze block (including Sichuan Basin), south-China block, Songliao basin, Sea of Japan, and eastern Mongolia have apparent high phase velocities. (3) At the intermediate periods (40-75s) the area of low velocity anomaly in the west shrinks gradually as the period increases; the phase velocities beneath Himalayan thrust and Tarim Basin as well as Junggar basin become high, implying that Qinghai-Tibet low velocity area is surrounded by 3 high velocity bodies from south, northwest, and east, which may result in a southeastern migration of the low velocity material of the plateau. Meanwhile, the phase velocity distributions in the eastern part become disintegrated with relatively low velocity bodies beneath the East China Sea and Jilin region. (4) At longer period (80-100s) low velocity anomaly in Qinghai-Tibet plateau becomes weaker and weaker as period increases, and apparent low velocity bodies appear gradually beneath the eastern part of China. Northern Indo-China block and its adjacent sea area, East China Sea, Jilin region, and eastern Mongolia are dominated by prominent low velocity anomalies at the period 120s, which suggests a wide distribution of asthenosphere there. However, high phase velocities appear in Yangtze block (including Sichuan Basin), which may imply the absence of asthenosphere in the upper mantle beneath this relatively stable block. (5) North-South seismic belt in China has relatively low phase velocity from periods 20s to 120s, and becomes a natural boundary dividing the continental China into two parts with different phase velocity feature. In the next step, we will construct empirical Greens functions (EGFs) for pairs of stations from ambient seismic noise by using monthly or yearly data and measure shorter periods (e.g., 10-30s) surface-wave dispersion data from the obtained EGFs. Finally, we will combine phase velocity dispersion data from two-station analysis and EGFs to invert for crust and upper mantle structure in the continental China.

Keywords: rayleigh wave, phase velocity distribution, chinese continent

(S) - IASPEI - *International Association of Seismology and Physics of the Earth's Interior*

JSS014

Poster presentation

2278

Structure of earths crust and upper mantle, inland subduction and its coupling effects on the Dabie orogenic belt and the Tancheng-lujiang fault zone

Prof. Jiwen Teng

Institute of Geology and Geophysics Chinese Academy of Sciences IASPEI

Yan Yafen, Wang Guangjie, Xiong Xiong

The Dabieshan Mountains was a nearly EW trending collision orogenic belt under the roughly NS directed compressive force during the Indo-China and early Yanshan movement periods. It separates the North China and Yangtze continental blocks, between which exposed broad cores of metamorphic rocks. Since it lies at the west side of the place where the mountains and the Tanlu fault zone intersect and converge, the orogenic belt must be constrained by strong translational offset of the Tanlu fault zone during the late period (late Jurassic-early Cretaceous). This fault zone is an inland giant system of translational features on the eastern margin of the Chinese mainland, which appeared after the formation of the Dabieshan orogenic belt. Based on the rock chronology, the metamorphic pressure difference in the peak period and the discovered coesite in Alpine metamorphic sedimentary rock, the coesite and eclogite from the Dabie orogenic belt is inferred to be the consequence resulted from their reentry from mantle around the depth of the 120km to the shallow crust. To provide the quantitative evidence of the deep structure and dynamic process beneath the Dabie orogenic belt, we attempt to explore the 3-D velocity structure of S wave beneath this region by using the inversion method with 4 4 network based on the dispersion effect of Rayleigh wave. Our purpose is to reveal the formation mechanism of the UHPM zone in the Dabieshan, exchange of deep and shallow materials and energy, as well as deep dynamic processes of intraplate tectonics in terms of block-like features of structure in crust and upper mantle. Then we would propose new insights and evidence for the strong translational dislocation of the Dabieshan and the Tanlu fault zone, and the coupling effects of intraplate subduction. The results show that, there is a high-velocity subduction slab of tongue shape with underthrusting depth 160km extending from east to west. A low velocity mantle hotspot with a 500km wide head is found at depth of 70km in the upper mantle beneath the Qingling-Dabie orogenic belt. The outcrop of coesite and eclogites in the Dabie orogenic belt is the synthetic consequence of the movement and dynamic effects of deep (upper mantle) material results from the deep substance and energy exchange, strong strike-slip motion along the Tanlu fault zone and the inland subduction.

Keywords: dabie orogenic, inland subduction, deep process

(S) - IASPEI - International Association of Seismology and Physics of the Earth's Interior

JSS014

Poster presentation

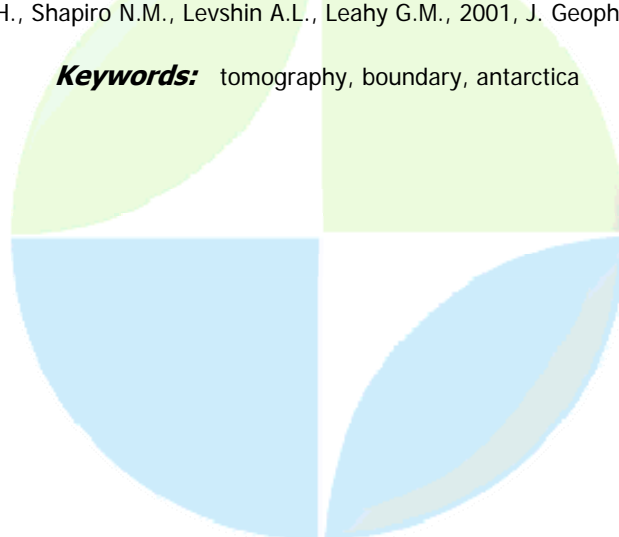
2279

Antarctic plate boundary with the gravimetric tomography data

Dr. Rudolf Greku
IASPEI IASPEI

Deep structure of the Antarctic plate boundary is obtained from surface up to the core for the space of 40,000 km using the gravimetric tomography method [1]. Coordinates of the boundary is used from [2]. This boundary is as contact zone with segments of other five large plates (Africa, Australia, Nazca, Pacific, South America) and four small plates (Shetland, Scotia, Sandwich, Somalia). It is obvious that the historical nature and tectonics of these plates are different for both the lithosphere and mantle layers. The structure shows a distribution of density inhomogeneities calculated as anomalies relatively the PREM density model using harmonic coefficients of the EGM96 global geoid model. Space resolution of the boundary vertical cross-section is of 60 km, radial resolutions on the image are different to show important features within distinct layers: solid surface-20 km, 20km-100km, 100km-750km, 750km-5300km. Data of the bottom topography (ETOPO5, NOAA-NGDC), free-air gravity anomalies [KMS2002, 3], and depths of Moho from the crustal model [Crust 2.0, 4] accompany our tomographic model. Several cross sections which are orthogonal to the boundary are calculated also to observe a structure and interaction of adjacent plates within the borderland and triple-junction points that are common to all segments. In the mantle dominate two bodies (plumes) with maximum depths near of 2800 km on the core-mantle boundary. Less dense masses which ascend from the Ross Sea plum become as three branches from depth of 200 km to the Australian-Antarctic Discordance (AAD, 124E), Ross Sea (175E) and to the boundary of the Nazca plate (100W). Dense masses descend from surface like subduction slabs and concentrate at depth of 60 km and 280 km. We discover a new information in area of the AAD structure where thinning hotter masses penetrate into the colder crust and lithosphere. Something similar to that is at the Nazca boundary. Gravimetric tomography data for the AAD area exhibit more detailed structure in comparison with the seismic tomography [5]. 1. Greku R.Kh., Kulikov A.A., Greku T.R., Earths structure with the gravimetric tomography method, this XXIV IUGG 2007, JSS011. 2. Bird P., An updated digital model of plate boundaries, An Electronic Journ. of the Earth Sci., Volume 4, Number 3, 14 March 2003, 10.1029/2001GC000252. 3. Andersen O.B., Dreyer S., Knudsen P, Berry P.A.M., Mathers E. L., Trimmer R., Kenyon S., Deriving 2Hz ERS-1 geodetic mission altimetry for gravity and marine geoid proposes, www.research.dk/GRAVITY. 4. Bassin, C., Laske, G. and Masters, G., The Current Limits of Resolution for Surface Wave Tomography in North America, EOS Trans AGU, 81, F897, 2000. 5. Ritzwoller M.H., Shapiro N.M., Levshin A.L., Leahy G.M., 2001, J. Geophys. Res., 106, 30645.

Keywords: tomography, boundary, antarctica



(S) - IASPEI - *International Association of Seismology and Physics of the Earth's Interior*

JSS014

Poster presentation

2280

Crustal configuration of NW Himalaya based on modeling of gravity data

Mr. Ashutosh Chamoli

Fractals in Geophysics National Geophysical Research Institute

A.K.Pandey, V.P. Dimri, P. Banerjee

The crustal structure of the Himalayan fold-thrust belt in NW Himalaya has been constrained using forward modeling and wavelet transform (WT) of the Bouguer gravity anomaly. The data covers the Himalayan range from the Sub Himalayan zone in the hanging wall of Himalayan Frontal Thrust (HFT) to the Karakoram fault across the Indus Tsangpo Suture Zone (ITSZ), from south to north, along about 450 km long (projected distance) the Kiratpur-Manali-Leh-Panamic transect. The spectral analysis of power spectrum of the gravity data has yielded the depths of layer interfaces in the crust. The long wavelength gravity data has been analysed using coherence method for isostatic compensation to obtain the average depth of effective elastic thickness. The Moho configuration and the locus of flexure of Indian crust has been constrained using forward modeling incorporating information from other studies. The Moho depth increases from approximately 35 km after MBT zone to about 60 km beneath higher Himalaya and it flattened northward with average depth of approximately 65 km till ITSZ. This suggests the MBT to be the locus of active tectonic loading in NW Himalaya rather than Main Central Thrust (MCT) as widely modeled in central Himalaya. The same is supported by presence of active microseismicity in the hanging wall of MBT and change in orographic front. The short wavelength data has been modeled on the basis of density contrast across the litho-tectonic boundaries and regional structural geometries along the profile section. The average depth and subsurface slope (dip) of the litho-tectonic boundaries has been obtained using the wavelet transform (WT), which shows good correlation with the major mapped tectonic boundaries including intracrustal/subcrustal faults in space scale domain. The combination of forward modeling and WT analysis of the data gives insight into the subsurface extent and geometry of regional structures for the first time from the NW Himalaya.

Keywords: himalaya, gravity, wavelet transform



(S) - IASPEI - *International Association of Seismology and Physics of the Earth's Interior*

JSS014

Poster presentation

2281

Can Amurian plate be discriminated from Eurasia: results from significance tests

Mrs. Dongmei Guo

Institute of Geodesy and Geophysics Chinese Academy of Sciences IASPEI

The independence of the Amurian Plate (AM) has been being an important issue of the geodynamics since the AM was proposed as a microplate within the Northeast Asia. Based on statistical methods, we conducted significance tests to investigate whether the AM is one part of the Eurasia (EU) or a separate block which is independent from EU. Furthermore, the ambiguous southern boundary of the AM is determined by statistical approaches. A consistent velocity field, which was employed as the database for significance test, was obtained by combining some new results of the ongoing China-Japan-Korea cooperative project and published ones. The velocities at GPS stations in the eastern Mongolia and Northeast China, that is believed to be the core stable part of the AM, were used to define the AM-EU Euler vector, with 55.7074N and 130.7404E as the pole and 0.0930/Ma as rotational rate taking counterclockwise as positive. The significance test with χ^2 -test method indicated that the AM is independent from the EU at a confidence level of 95%. In order to define the domain of the AM, we conducted significance test to check the differential movements between the core part of the AM and surrounding areas, including North China (NC), South China (SC), Western Mongolia(WM), Southern Korea (SK) and Southwestern Japan (SWJ). The F-test and χ^2 -test were used to investigate the differential movements between adjacent plate-pair, while the AIC (Akaike Information Criterion) was employed to test the independence of blocks within a multi-block system. The significance tests with F-test, χ^2 -test and AIC methods reached the consensus that there is significant relative movements between the AM and the NC, SC, WM and SWJ, while neglectable relative movement between the AM and SK. Therefore, we suggested that the SK is one part of the AM, and the others are independent from the AM. By statistical methods, we tried to define the southern boundary of the AM, which is very ambiguous due to complicated tectonic features and diffuse seismicity. We selected an area ranging from 110°E to 135°E in EW and 36°N to 50°N in NS, and covering the AM and NC to investigate the exact location of the southern boundary. Since the AM-NC boundary is almost E-W trending, we assumed a boundary located at latitude of 36°N and calculated c_2 value. Then, we calculated c_2 values with different locations of the assumed boundaries with an increment of 15' in latitude. In the c_2 values-latitude plot, the latitude corresponding to the minimum value of c_2 was suggested to be the location of the AM-NC boundary, which runs along northern margin of Erdos and Zhangbei earthquake belt.

Keywords: amurian, significance tests, boundary

(S) - IASPEI - *International Association of Seismology and Physics of the Earth's Interior*

JSS014

Poster presentation

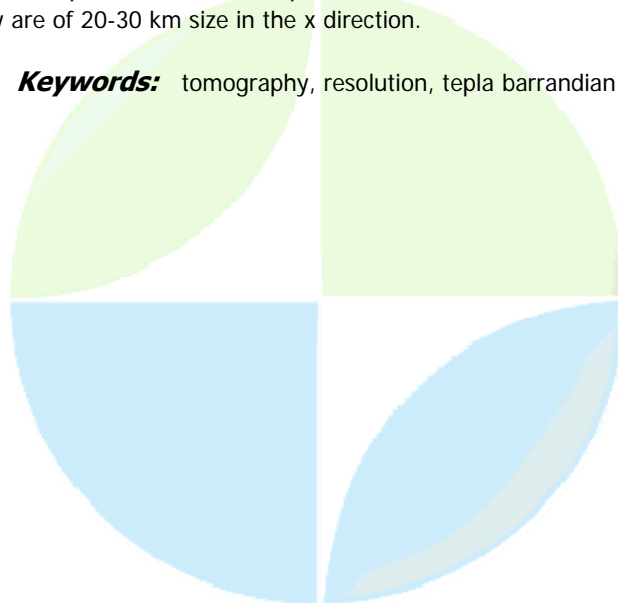
2282

High resolution refraction tomography - resolving the vertical displacement of Tepla-Barrandien unit of Bohemian Massif in the P-velocity sections on CEL9 LINE.

Dr. Miroslav Novotny
Seismic GFU CAS CR

The depth recursive tomography was used to the refraction data of the CEL9 profile. The applied grid inversion method (RTG) works in iterations and generates whenever a new set of probe rays for all gridpoints of the solution region. The velocity models resulting from the final iterations 2 and 3 yielded the RMS timefits comparable with the input RMS error. They provide an insight on interpretative reliability of single features occurring in output models, particularly near the expected resolution limits. The resolution limits were studied at three levels. First, uncertainties stemming from the input data incompleteness (gaps in deployment of sources and receivers, discrepancies in reciprocal traveltimes) were assessed. An integral transform was used to cast them in velocity sections. Second, the spatial response to one-node velocity excitation was found to give a superior resolution for studied velocity features. Third, ultimate lateral resolution was evaluated taking into account the magnitude of velocity anomalies and the time residua unresolved by RTG inversions at single depth levels. Thus, the minimum lateral sizes of 5% velocity anomaly, yet resolvable with high 95 % reliability, are 10-40 km in the depth range of 0-20 km. The exemplified CEL9 profile starts in Saxothuringian zone of Bohemian Massif, continues to SE across the 100-110 km narrow, ophiolite suture unit of Marinsk Lzně Complex (MLC), and then to the Tepla-Barrandian unit (TBU), 110-200 km. The TBU are bordered by steeply dipping shear zones, the West Bohemian Shear Zone (WBSH) in the west and the Central Bohemian Shear Zone (CBSZ) in the east, prompting that the crust thickened here during Variscan orogeny sank afterward down. An extensive velocity depression in the upper and middle crust of TBU can be followed at 110-170 km since the first iteration. It is placed under an elevation observed above in the uppermost crust corresponding to the ophiolites of MLC sature. The RTG tomography resolved the lateral sizes of 15 km for 5 % anomaly in the 10 km depth. Below the 12 km depth level both models exhibit a steep decrease of lateral resolution to more than 30 km. Thus, the velocity anomalies, about ~300 m/s, related to the MLC exposure or vertical displacement of the Tepl-Barrandian block exhibit a fair performance in final RTG models since they are of 20-30 km size in the x direction.

Keywords: tomography, resolution, tepla barrandian



(S) - IASPEI - *International Association of Seismology and Physics of the Earth's Interior*

JSS014

Poster presentation

2283

Seismic hazard assessment for east of Iran

Mrs. Elham Boustan

Geophysics Ph. d Student IASPEI

Dr. Noorbakhsh Mirzaei

In this research, deterministic seismic hazard assessment for Neyshaboor city in Khorasan province of NE Iran has been studied. In order to study, fault map of the study region including Mashhad, Torbatheydarieh, Sabzevar and Kashmar has been provided. Then based on available earthquake data (instrumental and historical) 15 potential seismic sources are determined. Using Donovan's (1973) attenuation relationship and surfer computer program, seismotectonic map for Neyshaboor has been provided and then seismic hazard assessment has been accomplished. Finally maximum acceleration in this city 0.43 g has calculated that is result from Neyshaboor fault.

Keywords: seismic hazard, neyshaboor, iran

XXIV2007

PERUGIA
I T A L Y



(S) - IASPEI - *International Association of Seismology and Physics of the Earth's Interior*

JSS014

Poster presentation

2284

Investigation of focal mechanism solutions of earthquakes in Iran

Mrs. Nadia Tahernai

Geophysics Ph.d student IASPEI

Dr. Mohammad Reza Gheitanchi

Iran is one of the most seismically active countries in the world because of settling on the Alpine-Himalayan Belt. For define the smaller plate in Iran, focal mechanism of large earthquakes has been investigate. Focal mechanism of earthquakes in the North Iran is thrust and sometimes strike- slip. The existence of normal mechanism in the Central Caspian Seismic Belt probability the northwest of the Caspian Sea. The Zagros Folded Belt in Iran and structurally appears to result from the collision of the continental plate of Arabia in the Southwest with Central Iran in the northeast. The most of mechanism solutions in the Zagros are of the simple thrust- type with nodal planes that approximately parallel the trend of the regional fold axes. The compressional axes have a NNE- SSW direction that indicates the general northeast movement of the Arabian plate. In Eastern Iran the seismically active zone is Lut. The rigidity problem of the Lut Block has been a matter of controversy for many years. Epicenters of earthquakes and trend of surface faulting by large earthquakes appear to mark the boundaries of the Lut plate. Focal mechanisms solutions are predominantly strike- slip faulting and sometimes have thrust components. The compressional axes nearly have a NE- SW direction. This is in agreement with the northeast movement of the Lut Block, but existence of right- lateral mechanism on the western edges of region, supports the argument against the rigidity of the Lut Block.

Keywords: iran, focal mechanism solution, seismicity



(S) - IASPEI - *International Association of Seismology and Physics of the Earth's Interior*

JSS014

Poster presentation

2285

Distribution of Seismic Energy Released in Iran

Mrs. Nadia Tahernai

Geophysics Ph.d student IASPEI

Dr. Mohammad Reza Gheitanchi

Iran is located along Alpine- Himalayan belt, and one of the seismically active regions in the world. Seismicity of Iranian plateau during the past 40 years from 1964 to 2004 is investigated in four 10-year successive time interval by analyzing about 1260 earthquakes in the region. The area was divided into quadrangles each covering half a degree of latitude and longitude, and the seismic energy and associated strain released of earthquakes which occurred within each quadrangle in different periods were computed and combined. The comparison of seismic energy maps indicates that the major zones of activity are, Zagros, Alborz and east-central Iran. Small plates in central Iran, the southern Caspian Sea, and Lut also show noticeable stability. The seismic gaps in early intervals were filled up by the seismic activities during the following time intervals. The maps of epicentral distribution and the frequency - magnitude diagrams during successive time intervals show that Alborz and Lut regions were seismically active and characterized by significant earthquakes. Zagros had a more regular pattern of seismic activity and experienced moderate and small earthquakes. The different seismic patterns suggest that the physical properties of fault systems are different in different regions and the crust is inhomogeneous in Iranian plateau.

Keywords: seismic energy, iran, seismicity



(S) - IASPEI - *International Association of Seismology and Physics of the Earth's Interior*

JSS014

Poster presentation

2286

A new sophisticated and integrated analysis for the crustal structure analysis using OBS and control sources

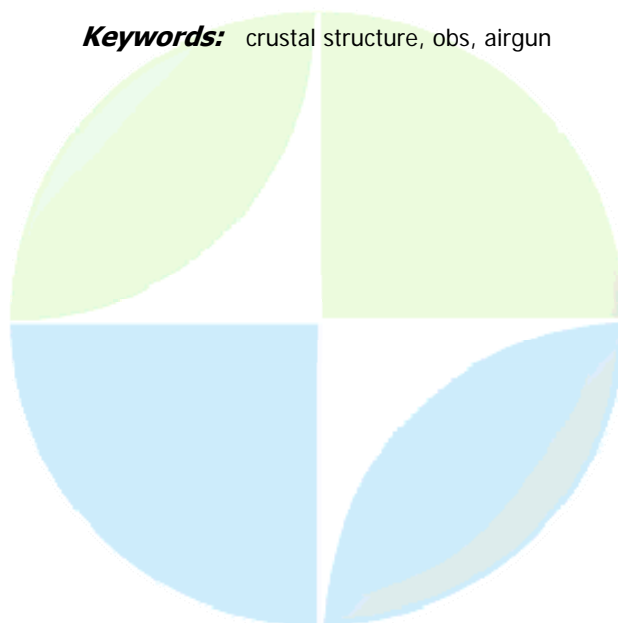
Dr. Junzo Kasahara

Advisory Department Japan Continental Shelf Survey, Japan IASPEI

Ryuji Kubota, Tomoyuki Tanaka, Shigeharu Mizohata, Eiichro Nishiyama, Azusa Nishizawa, Kentaro Kaneda

During recent a few years, a huge amount of seismic data to determine crustal structure in the oceanic region, has been collected using a set of digital OBSs and a large volume (e.g., ~8,000 cubic inches) tuned airgun-array. Such seismic surveys can provide full-waveform data of wide-angle reflected and refracted seismic arrivals. Most of previous analyses using OBS data have been carried out mainly by the travel-time inversion method using first arrivals. However, it is well known that the travel time inversion strongly depends on a starting model. In order to avoid the initial model dependence, it is necessary to use a reasonable crustal initial model to satisfy full-waveforms, MCS reflection data and geological and geophysical backgrounds. In our new sophisticated and integrated analysis we are adopting a combination of several datasets such as MCS data, Pg, Pn first and later arrivals, PmP and crustal reflected phases, P-S and S-P converted phases, and the amplitude of each phase. Travel-times and raypaths are calculated by the graph-method (Kubota et al., 2005). Synthetic waveforms are calculated by the finite difference method (Larsen, 2000). Travel-time inversion is carried out by Tomo2D developed by Korenaga et al. (2000). Seismic records are interactively processed using Pastup software developed by Fujie (1999). Those dataset are analyzed by the forward modeling, the ray tracing, the first-arrival and reflection travel-time tomography, and the calculation of synthetic seismograms. We have applied the above analysis for the crustal structure studies in the western Pacific Ocean near the Japanese archipelago. Crustal structures obtained by the above analysis stream satisfactory fit to the original waveforms and MCS reflection sections. Travel-time misfits between observed travel-times and theoretical travel-times are nearly 40 milliseconds or less. Most of analysis has been carried out by colleagues in Japan Continental Shelf Survey Co., JGI Inc., and Kawasaki Geological Engineering, Co. Ltd.

Keywords: crustal structure, obs, airgun



(S) - IASPEI - International Association of Seismology and Physics of the Earth's Interior

JSS014

Poster presentation

2287

Feasibility study for the continuous active monitoring of the temporal change and spatial movement of a magma reservoir beneath a volcano

Dr. Kayoko Tsuruga

Japan Continental Shelf Survey Co. Ltd. IASPEI

Junzo Kasahara, Naoyuki Fujii

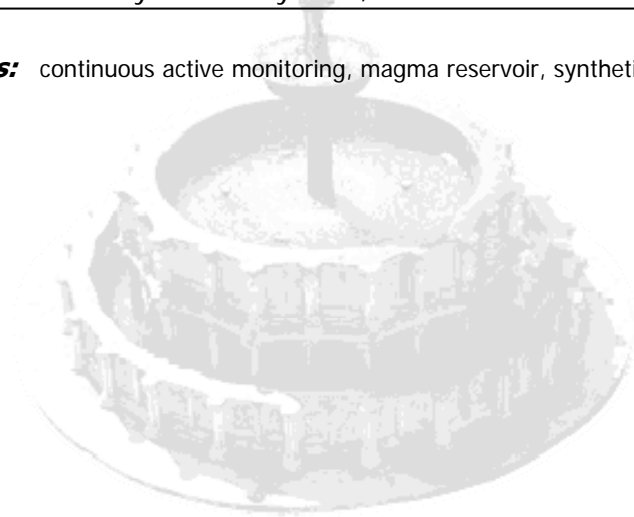
1. Introduction To quantify the temporal and spatial changes of underground geophysical state, we require an integrated mapping and monitoring system (Kasahara et al., in this meeting). A mapping of the crustal structure has been suggested by seismic reflection and refraction experiments by chemical explosive sources, other artificial sources and natural earthquakes. For example, across the central Japan the strong PxP reflection phase from the Philippine Sea plate boundary was identified (e.g., Iidaka et al.2003). The structures beneath volcanoes were also investigated at many sites (e.g., Izuoshima and Mt. Fuji volcanoes). On the other hand, we have proposed an observation system, ACROSS (Accurately-Controlled Routinely-Operated Signal System), for monitoring under the stable control for a long time period (Kumazawa et al., 2000). The array observation in Tokai area proved to observe the refracted and reflected P and S waves up to 75 km offset distance using two-week long stacking ACROSS data (Kasahara et al., 2004; Tsuruga et al., 2005). These results encourage us toward the continuous monitoring the magma reservoir and remarkable seismic reflectors in the crust. We here examine the potentiality of the active monitoring of for the magma reservoir and remarkable reflectors beneath a volcano by ACROSS through synthetic seismogram studies of appropriate reservoir models.

2. Simulation on the simple models with a low velocity zone beneath a volcano As a first step, we discuss the characteristics of wave propagation in the simple structure model including a low-velocity zone (LVZ) as a magma reservoir. We calculate the synthetic seismograms and travel times by FDM method (Larsen, 2000) and by a graph method developed by Kubota et al. (1995), respectively. The model space is 150-km wide and 30-km thick like as an island arc crustal structure. Models have two reservoir types: (A) a sheet-like reservoir with 10-km wide and 0.5-km thick and (B) a lens-like reservoir with 6-km wide and 3-km thick. Each one is located at the depth of 9 km around the center of the space. P-wave velocity, V_p , in LVZ is assumed to be 2 or 3 km/s. Seismic source is located near surface at 10-km offset distance from the center of LVZ and excites a single force in a horizontal plane like a seismic ACROSS source or an explosive pressure.

3. Results We obtained the preliminary results as follows: 1) In both cases of (A) and (B), remarkable strong S-wave reflections from the upper boundary of LVZ are observed together with relatively weak P-wave reflections and their diffractive waves. 2) Travel times depend on the shape of LVZ. 3) Amplitude of the S- and P-wave reflections from LVZ with $V_p=2$ km/s are relatively larger that with $V_p=3$ km/s. 4) Larger S-wave reflections from LVZ can be observed at 10-km offset distance from LVZ than those at the farther offset. 5) S-wave reflections from LVZ excited by a horizontal single force have relatively larger amplitude than those excited by an explosion source type. 6) In the model with a LVZ located at 9-km depth, amplitude of a vertical component is larger than the horizontal one. Thus the travel times and waveforms depend on the shape, properties and location of LVZ and also seismic source types. The remarkably strong S-wave reflections from LVZ particularly recommend us to use S-wave source.

4. Summary We examined the potentiality of the active monitoring of for the magma reservoir and remarkable reflectors beneath a volcano by ACROSS through synthetic seismogram studies of appropriate reservoir models. The variations of observed amplitude accompanying with the change of geophysical properties and location of LVZ suggest the high potential of continuous and real-time monitoring by the active sources as an ACROSS source and receivers array.

Keywords: continuous active monitoring, magma reservoir, synthetic waveforms



IUGG

XXIV2007

PERUGIA
I T A L Y



(S) - IASPEI - International Association of Seismology and Physics of the Earth's Interior

JSS014

Poster presentation

2288

Evaluation of the effects by heterogeneously inserted Thin/Thick High/Low velocity layers in the part of crust

Dr. Kayoko Tsuruga

Japan Continental Shelf Survey Co. Ltd. IASPEI

Junzo Kasahara, Ryuji Kubota, Yoshihiro Naito, Azusa Nishizawa, Kentaro Kaneda

1. Introduction In the crustal structure studies using OBS and control sources, we frequently use arrival times and waveforms (e.g., refracted and wide-angle reflected arrivals, later phases of refracted and reflected arrivals, and P to S and S to P converted waves) and other data obtained by MCS and gravity data (Kasahara et al., 2007, this meeting). In our analysis, we use a forward modeling method simultaneously referring synthetic waveform and a travel time inversion. Real observed seismic records frequently show some complicated waveforms whose arrivals quickly decay with offset distance. They are usually interpreted by the presence of low/high velocity layer or negative gradient in velocity layers. Because such heterogeneous structures greatly influence the model construction, we have to explain these phases with geophysical interpretation of such phases. In this report, we, therefore, try to interpret particular seismic phases resulting from small-scale heterogeneous crustal structure in the ocean region by using FDM simulation of several models. 2. Numerical simulation Using horizontally inhomogeneous structure models, we synthesize waveforms by the FDM method (E3D developed by Larsen, 2000). We examined several numerical examples. Basic structural model was a horizontal multi-layered structure with 200km (H) x 20km (D). An oceanic crust with 7 km-thick was divided into four layers: (a) 0-1 km, (b) 1-2.5 km, (c) 2.5-3.5 km and (d) 3.5-7.0 km deep. We here show the following velocity gradient models for the layers (b) and (c) while the layers (a) and (d) has same velocity in any cases: Case-1: Velocity monotonously increases with depth for a whole model space (basic model) Case-2: Velocity in the both or either of layers (b) and (c) is constant Case-3: Velocity gradient changes at the interfaces such (a)-(b), (b)-(c) and (c)-(d). Case-4: Velocity discontinuity at the interfaces of such (a)-(b), (b)-(c) and (c)-(d). These models provides us a lot of in formations about the behaviors of amplitude observed in the cases of decollement, velocity reversal with depth and horizontal pinch-out of high velocity layer on OBS-airgun seismic records. We can also evaluate the characteristics of waveforms for thin high velocity layers such as chart and/or limestone layers at the shallow part and the fluid-filled layers existing in the crust of decollemn. These inserted layers are frequently found in DSDP and ODP deep-sea drillings. Through the present case studies, seismic phases particularly with amplitude decay with offset distance are troublesome to construct the correct crustal velocity model because such phases are strongly affected by extremely local structure near receivers. So, in such case, we need to discard / screen such arrivals for the interpretation of long-offset arrivals because time delay through such local thin layers is very small, but the arrivals are very strong for shorter offset distance. 3. Summary Some OBS-airgun records show some arrivals which reflect the inhomogeneous velocity structure in space. The interpretation of such phase is not carried out by the usual interpretation method. In order to find the best treatment of such phases, we use FDM waveform simulation for several cases and screen the adequate data. Our results may greatly help for the interpretation of such troublesome phases.

Keywords: crustal structure, synthetic seismogram, fdm

(S) - IASPEI - *International Association of Seismology and Physics of the Earth's Interior*

JSS014

Poster presentation

2289

**A Interactive and integrated modeling tool for the crustal analysis using
OBS-control sources**

Dr. Junzo Kasahara

Advisory Department Japan Continental Shelf Survey, Japan IASPEI

**Gou Fujie, Kei Murase, Ryuji Kubota, Eiichiro Nishiyama, Tomoyuki Tanaka,
Kayoko Tsuruga, Shigeharu Mizohata, Shigeki Kawamura, Azusa Nishizawa,
Kentaro Kaneda**

In order to obtain an accurate best crustal velocity structure model, it is very important to make the best fit between the major seismic phases identified in the OBS wide-angle reflection and refraction survey data, and the MCS reflection sections. Recently, we have developed a new interactive software module for the Modeling-Pasteup crustal structure analysis tool, originally developed by Fujie et al. (2002), for OBS survey data. The improved interactive modeling module has two major functions: Modeling and Pasteup. Modeling and Pasteup can be run under X-Window circumstance of Linux OS. Under such computer circumstances, we can do the crustal structure analysis by a PC. Modeling is forward analysis software to carry out 1) crustal structure modeling, 2) travel time calculation for refracted first and later arrivals, reflected arrivals, arrivals of P-S converted waves, and headwaves, 3) raypath calculations, 4) depth to time conversion of layer boundaries and 5) gravity modeling. We define the crustal structure by several layers with velocity grids on the layer interface. When a discontinuous layer boundary is required, we can define two different velocities for the above and the below the particular layer boundary. We can compare traveltimes based on observed records and theoretical traveltimes on the Pasteup window. We also compute travel times of wide-angle reflections and superpose on the OBS seismic record sections. A part of software module can compute the two-way travel times of normal incident waves from the analyzed crustal structure model. The software module also superposes the time contours of the layers on the crustal structure model over the migrated time section of MCS using the Pasteup. Using a huge volume of real data, we confirmed that strong reflections from layers in the crust and the Moho seen in the OBS wide-angle reflection records are fairly consistent to the reflectors in the MCS section. By use of forward analysis, we also evaluate kind of waves for later arrivals. It is great help to the crustal modeling to use full wave information on seismic records. Synthetic waveforms calculated by FDM are also directly compared to observed ones. Gravity data are also used to evaluate the correctness of the resultant model. Through the interactive analysis, we can obtain the best fit model for observed data. Through above two processes, we can confirm the correctness of the resultant crustal structure model. We use the result of forward modeling as the input of traveltimes inversion to minimize non-linear effect of traveltimes inversion. The average rms misfit is approximately 30-40ms for 100 OBS data along 500km distance if arrivals are clear enough. In the actual processing, we used over 200 OBSs and every 200m airgun shots for the longest survey line.

Keywords: crustal structure, obs, interactive analysis

(S) - IASPEI - International Association of Seismology and Physics of the Earth's Interior

JSS014

Poster presentation

2290

Evaluation of efficiencies of P-S conversion in T H E oceanic crust and Vp/Vs estimation

Dr. Kayoko Tsuruga

Japan Continental Shelf Survey Co. Ltd. IASPEI

Junzo Kasahara, Eiichiro Nishiyama, Kei Murase, Ryuji Kubota, Azusa Nishizawa

1. Introduction In the OBS-airgun records, P to S and/or S to P converted phases have been frequently observed by horizontal seismometers and vertical seismometer/hydrophone, respectively. Using such converted phases, we can estimate S wave structure in the crust and the mantle. In order to evaluate S wave velocities, the precise estimation of P and S velocity structures in the sediments is required. In this paper, we propose an evaluation method for the conversion efficiency of P to S and S to P and obtain S wave structure in the hard rock part of the crust. 2. Method In the oceanic region, S(V) waves observed in horizontal components are converted from P to S(V) at interfaces with large impedance contrast. We, here, simply evaluate a total energy flux of P-S conversion waves as follows: 1) We estimate efficiencies of transmission and conversion from P to S and/or S to V through the ocean bottom/sediments/hard-rock interfaces. 2) We evaluate relative converted P or S wave square amplitudes at OBS relative to the incident P waves penetrated into the ocean bottom. 3. Results The conversion from P to S occurs at (a) sediments/hard-rock interface or (b) seawater/bare rock interface. The case (a) occurs at the presence of thin unconsolidated sediment layer (P-wave velocity, V_p is less than 2.2km/s, S-wave velocity, V_s is less than 1.0 km/s) more than tens meters underlined by sedimentary rocks or hard rock layer (V_p is greater than 2.5km/s, V_p/V_s ratio is about 1.78). Such interface is often called as an acoustic basement by reflection seismics. The case (b) corresponds to bare rock layer exposed at the ocean bottom. For the present study, we assume the conversion occurs only at the ocean bottom and sediment layer /hard-rock interface and calculate the conversion rates in terms of relative energies. Among possible seven cases, large conversions are expected for (i) sediments/hard-rock interface at the incident side, (ii) at the ocean bottom of incident side, and (iii) at the sediments/hard-rock interface just beneath an OBS. Both of (i) and (ii) travel through whole crust as S wave. In the case of (iii), P wave converts to S wave only at the sediments/hard-rock interface just beneath an OBS. 4. Examples We examined real OBS-airgun data observed in the western part of the Pacific Ocean. It was found that most of conversions were observed on horizontal seismographs and they fit to the cases of (i) and (iii) for most of OBS records by comparing P-wave velocity crustal structure. The V_p/V_s ratios were estimated to be 3 to 20 for sedimentary layers whose V_s were to be 1.6-2.0 km/s beneath the western Pacific Ocean. V_s values were consistent with those measured by Hamilton (1976, 1979). We also found that V_p/V_s values of the upper and lower parts of the oceanic crust were extremely constant (i.e., 1.78) in the western Pacific and the ocean basins of NE Philippine Sea. We did not find V_p/V_s values of 2.0-2.5 which indicates the fractured crust and serpentinized mantle. On the other hand, S_n arrivals in two horizontally perpendicular directions suggest the presence of the anisotropy in the upper-most mantle. Although the V_p/V_s value in the upper-most mantle was 1.73, those in some areas were less than 1.70. We report the details and interpretation of V_p/V_s in the crust and the mantle. 5. Conclusion Because sea water can transmit only P wave, we have to use converted S waves in the crustal structure studies in the ocean region. Using converted phases from P to S and S to P waves, we can estimate the conversion rates and estimate the V_p/V_s in the crust.

Keywords: crustal structure, p s converted wave, s wave velocity

(S) - IASPEI - *International Association of Seismology and Physics of the Earth's Interior*

JSS014

Poster presentation

2291

Crustal structure and Moho depth profile crossing the central Apennines (Italy) along the N42 parallel.

Dr. Francesco Pio Lucente
CNT INGV IASPEI

Massimo Di Bona, Nicola Piana Agostinetti

We present results from a teleseismic receiver function study of the crustal structure in the central Apennines (Italy). Data from fifteen stations installed during the GeoModAp project [Amato et al., 1998], deployed in a linear transect running along the N42 parallel, were used for analysis. A total number of about 350 receiver functions have been analysed. The crustal structure has been investigated using the neighbourhood algorithm inversion scheme proposed by Sambridge [1999a], obtaining crustal thicknesses, bulk crustal Vp/Vs ratio and velocity-depth models. The degree of constraint, resolution and trade-off between different parameters, for the results of the each inversion have been appraised applying the ensemble inference algorithm by Sambridge [1999b], returning the Bayesian indicators for each inverted parameter and for specific combinations of them. Although the seismic deployment crosses a region characterized by great crustal complexities and intense tectonic activity (recent volcanism, orogenesis, active extensional processes), which are reflected in the computed receiver functions, the relatively close spacing among the seismometers (about 20 km), and an ad hoc analysis and inversion strategy for each station, allow for a detailed reconstruction of the crustal structure and Moho geometry along the transect. We gain the picture of a classical moho-across-an-orogen profile: going from a relatively shallow depth (around 22 km) in the Tyrrhenian side, deepening down to 45 km depth beneath the highest Apennines, and rising up again to about 30 km depth value in correspondence of the Adriatic foreland.

Keywords: receiver function, apennines, crustal structure



(S) - IASPEI - *International Association of Seismology and Physics of the Earth's Interior*

JSS014

Poster presentation

2292

Large scale features of the south-easternmost TTZ as inferred from geophysical data

Dr. Lucian Besutiu

Dynamics of the Solid Earth Institute of Geodynamics of the Romanian Academy IAG

Unlike its northern and central part, thoroughly studied from the North Sea to the state-border of Romania through the large amount of works carried out during the EUROPROBE program and some later large scale seismic experiments, the path and structure of the SE extension of the Tornquist-Teisseyre Zone (TTZ) are still subject to debate. The paper represents an attempt to reveal TTZ large-scale peculiarities on the Romanian territory based on the available geophysical data interpretation. Several issues were targeted: (i) path, (ii) structure, (iii) nature, and (iv) SE end of the contact. The study started with the examination of the TTZ geophysical fingerprints along its known track. The TTZ path has been firstly outlined within the pattern of the airborne geomagnetic anomaly as separating the warmer (less magnetic) lithosphere of the Central European Plate (CEP) from the colder Precambrian lithosphere of the East European Plate (EEP) which allows the geomagnetic expression of its lower crust. The effect is still preserved at the altitude of the geomagnetic satellites. Both gravity and some DSS lines previously performed revealed a graben-like, or at least a step structure at the bottom of the crust all along the TTZ track. The TTZ path on the Romanian territory has been outlined both in the geomagnetic anomaly and heat-flow images, where parts of the CEP and EEP are clearly discriminated. The contact is also visible in pattern of the geomagnetic induction vectors. Modelling the TTZ large scale structure on the Romanian territory has been performed mainly based on gravity data interpretation under depth constraints provided by MTS and seismic data. More than 40,000 core samples from oil wells, and rock samples collected from hundreds outcrops located within East Carpathians and surrounding area were analysed in order to provide an appropriate density model for the main geological formations as known within the region. Gravity modelling confirmed the previous assumptions on the intricate alpine structures of East Carpathians with about 10 km thick nappes stack. Deeper on, the model revealed a graben-like structure at the bottom of the crust, with a 10 km step at the both Conrad and Moho discontinuities, quite similar to the TTZ features previously outlined along its north-western track. The regional stress tensor within Transylvanian Depression, pointing towards TTZ, and an accented crust deformation within the area seem to advocate for a compression contact in nature. The Moho keel seems to be well outlined in the gravity low (within both Bouguer and isostatic anomalies) extending from the North Sea to the bending area of East Carpathians (the Vrancea intermediate seismicity zone) where it suddenly ends. There is no gravity evidence on the TTZ extension towards the Black Sea as previously postulated. Due to data insufficiency, some speculations on the possible TTZ SE extent, beyond Vrancea zone, are made only. Acknowledgements. The research has been supported through the Romanian National Agency for Scientific Research grant CEEX-MENER no.732/2006.

Keywords: tornquist teisseyre, geophysics, romania

(S) - IASPEI - *International Association of Seismology and Physics of the Earth's Interior*

JSS014

Poster presentation

2293

Electrical resistivity imaging of seismically active frontal Himalaya

Mr. Gautam Rawat
Geophysics Group

Crustal seismicity in frontal Himalaya, like many seismically belts, exhibits sharp cut-off at depth of 15-20 km. This plane interpreted as basement thrust fault, separating the top of the underthrusting Indian plate from the over-riding sedimentary wedge of the Lesser Himalaya also defines the planar zone where foci of number of moderate to large earthquakes are aligned. Given the sensitivity of resistivity to rheology, magnetotelluric measurement are undertaken to study deep crustal structures and their possible linkage to the space-depth distribution of seismicity. Eighteen MT sites were occupied along a profile along Bijnaur - Mallari encompassing the major litho units of Indo-Gangetic Plains, Siwalik, Lesser Higher and Tethys Himalaya, separated respectively by the major thrusts of Himalaya namely HFT, MBT, MCT and STD. The tensor decomposition of robust impedances for the period band of 10 Hz - 1000 s suggest electrical strike coinciding with geological fabric. The most conspicuous feature of the inverted resistivity section is the low resistivity zone at a shallow depth of 10 km beneath the Indo-Gangetic Plains that dips down at a low-angle and extends as a continuous plane right up to the northern limit of the profile. The geometry of this low resistivity zone correlates well with the plane defined by the cutoff depth of seismicity in the region. The low resistivity of the layer may be attributed to accreted sedimentary rocks overlying the underthrust Indian plate or may mark the brittle-ductile transition beneath which the fluids generated by dehydration reactions are trapped. This visualization is supported by the fact the upper crustal section above this low resistivity zone is marked by high resistivity, interspersed by narrow low resistivity zone coinciding with surface exposure of the HFT, MBT and MCT. The interpreted resistivity section helps to image these major thrust zones as steeply north dipping interfaces near surface that flatten out at depth to merge with the mid-crustal low resistive layer. The paper will discuss the tectonic and rheological significance of the resistivity imaging to constrain the seismotectonic model of the frontal Himalaya.

Keywords: seismotectonic model, himalaya, resistivity



(S) - IASPEI - *International Association of Seismology and Physics of the Earth's Interior*

JSS014

Poster presentation

2294

Seismotectonic model for Kangra-Chamba Region of NW Himalaya

Mr. Naresh Kumar
Department of Geophysics

Jyoti Sharma, S.Mukhopadhyaya

A homogeneous earthquake catalogue with minimum detection threshold of $M=4.3$ for a period 1975 to 2004 shows that the rupture area of devastating Kangra earthquake of 1905 is still more active than the adjoining regions of NW Himalaya. Since 2004, a campaign mode seismic array is in operation in this region for constraining the seismotectonic model. With the improved detection threshold, local 174 earthquakes of magnitude ranging between 1 and 5 are inverted through Local Earthquake Tomography (LET) to simultaneously determining the average 1D velocity model. Further the data were inverted for 3 dimensional velocity variations that further reduced the location error. Mostly the seismic events are located in the upper crust above the detachment (decollement) plane, the surface separating the underthrusting Indian plate from over riding sedimentary wedge of Himalaya. In the depth section, the foci of large numbers of earthquakes show clear clustering along linear planes seen as sub-surface extension of the Main Boundary Thrust (MBT) and Punjal Thrust (PT). The first motion P-wave polarity of 22 well located events of magnitude more than 2.5 recorded at more than 12 stations are used for fault plane solutions to observe the sub-surface tectonic movement of the region. The clusters of other small magnitude events around these earthquakes are also used to obtain the composite fault plane solution for observing the slip movement along tectonic discontinuity. The majority of the fault mechanisms are of oblique types showing a combination of strike slip component with reverse and normal fault mechanisms. The north trending upper crustal fault movement is of reverse-faulting with right-lateral strike-slip motion whose dip angle goes on decreasing with depth. The locus of these fault plane solutions coupled with plane defined by sharp cut-off depth of crustal seismicity helps to trace the decolment beneath large part of the Kanra-Chamba of frontal Himalaya. However, in the eastern part of the region flanking the western part of the Punjab reentrant, a close clustering of epicenters is seen and in this section a few earthquakes below detachment zone are having normal movement. The deduced 3-D velocity model shows presence of NE-SW trending low velocity zone bordering the Punjab. It is inferred that the interaction of two thrust faults with perpendicular movement to each other in the deeper section of the eastern part of the study area is the source of stress concentration to generate the normal fault movement with left-lateral strike-slip motion in NW-SE direction. The seismic pattern, velocity structure, fault plane mechanism as well as emerging picture of stress distribution are integrated to constrain the seismotectonic model of the one of most active section of the NW Himalaya.

Keywords: himalaya, seismotectonics, velocity structure

(S) - IASPEI - *International Association of Seismology and Physics of the Earth's Interior*

JSS014

Poster presentation

2295

Crustal velocity structure of Northeast of Iran

Dr. Gholamreza Nowrouzi

IIEES & Birjand University Ph.D candidate IASPEI

Keith F. Priestley, Mohsen Ghafoury Ashtiany, Gholam Javan Doloei, Mohammad Mokhtary

Abstract: The tectonics of North-east of Iran is a key to understanding the closure processes of the Paleo-tethys oceanics realm as well as associated continental deformation. The crustal study is very important in understanding the tectonic evolution of an area but there is no a number of studies on crustal structure in this area then less is known and little has been published on this problem. This paper presents the results of seismic experiment aimed at the crustal structure beneath the 20 broadband and middle-band seismic stations in Northeast of Iran, using the joint inversion of teleseismic receiver functions and surface wave dispersion technique. Using the joint inversion of mentioned two data sets, the Moho and three main parts for crustal structure in Northeast of Iran is suggested as: - The upper part of crust has an S-wave velocity between 2.43.4 km/s and a 11 km thickness as an average with a 2.0 km standard deviation. - The middle part of crust has an S-wave velocity between 3.13.6 km/s and a 21 km thickness with a 3.3 km standard deviation. - The lower crust has an S-wave velocity between 3.6 4.3 km/s and a 16 km thickness with a 3.3 km estandard deviation. - The Moho depth is 49 km with 2.0 km standard deviation. In the Northeast of Iran, there is a Paleo-tethian geosuture but its place is questionable. We have tried to find an answer for this question.

Keywords: crustal velocity structure, northeast of iran, joint inversion



(S) - IASPEI - *International Association of Seismology and Physics of the Earth's Interior*

JSS014

Poster presentation

2296

Crustal structures in the rupture area of the 2003 Tokachi-oki earthquake (Mw=8.0)

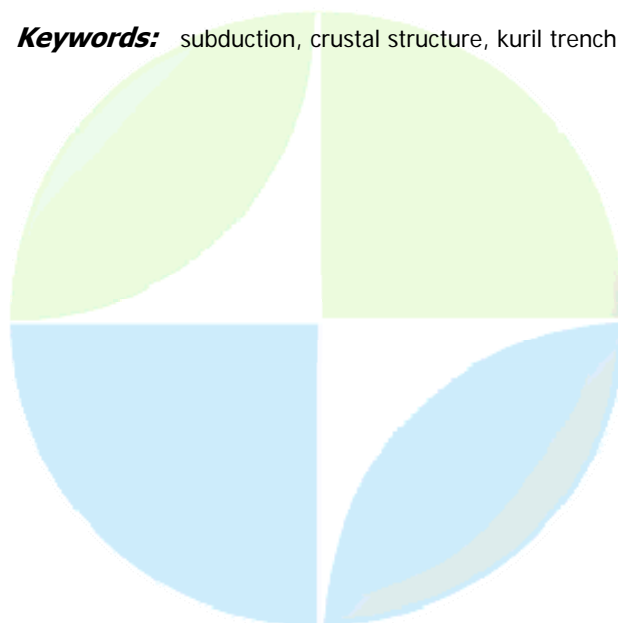
Dr. Tetsuo Takanami

Institute of Seismology and Volcanology Hokkaido University IASPEI

Yoshio Murai, Yuya Machida, Yumi Makino, Ryosuke Azuma, Ichisuke Saito, Toshihiko Kanazawa, Masanao Shinohara, Kimihiro Mochizuki, Tomoaki Yamada, Ryota Hino, Minoru Nishino, Kenji Uehira, Hiroki Miyamachi

The seismic velocity structure in and around the rupture area of the 2003 Tokachi-oki earthquake (Mw=8.0), in the southernmost part of Kuril trench, off Hokkaido, Japan was obtained by using air gun array and three-component ocean bottom seismometers (OBSs). The seismic P wave data have been modeled by ray tracing / inversion. The imaged structure along landward dipping oceanic crust suggests that the main event seems to have occurred in deeper extension of a series of subducting sea mounts though the resolution of inversion was insufficient there. In the main ruptured area showing the largest asperity, there are much fewer aftershocks. On the other hand, the zone with many afterslip events cumulated since the 2003 event corresponds with the zone having a comparatively stronger reflector in the upper plate boundary of subducting slab. Likewise, in the same rupture area, the three dimensional seismic velocity structure has been imaged by using P travel times of the aftershocks recorded by 47 OBSs and relocated the hypocenters simultaneously. The hypocenter distribution of aftershocks shows landward dipping planar shape with an increased dip angle of the hypocenter distribution at around the distance of 100 km from the trench axis. Furthermore, the hypocenter distribution projected on the parallel plane to the Kuril trench indicates that they also inclines gently to northeastward. Such a varied dip angle of the hypocenter distribution responds surely to the change of the depth of boundary of the subducting oceanic plate as evaluated from the wide-angle seismic survey using the air gun control sources. The rupture area of the 2003 Tokachi-oki earthquake and its neighbourhood can be thus interpreted as a highly deformed zone where the Northeastern Japan arc meets the Kuril arc moving westward, which is supported by the evidence that the Pacific plate is subducting obliquely under the Kuril arc.

Keywords: subduction, crustal structure, kuril trench



(S) - IASPEI - *International Association of Seismology and Physics of the Earth's Interior*

JSS014

Poster presentation

2297

Velocity structure in Naeen Region, Central Iran

Dr. Zohrehsadat Riazirad

Geophysics Azad University Science & Research branch M.Y.R.C IASPEI

In this study, seismic velocity of crust has been derived for Naeen region in south central of Iran. The velocities of layers were obtained from the time-distance curves by a least squares method. The average velocities for the events in a distance range 250-800 km provided the upper mantle velocity. Similarly, the mean value of seismic velocities for the distance range 110-150 km gave crustal velocity. Using data from International Institute of Earthquake Engineering and Seismology (IIEES) from recorded local earthquakes creates an opportunity to image crust and upper mantle in the region. At first step we obtained a 1-D velocity model by analysis of the travel-time curves for nearly 875 P and S wave arrival times from 647 local earthquakes. Recorded earthquakes were classified along the four separate profiles, and corresponding travel-time curves were analyzed. Seismic wave velocity of the crust is $V_{pg}=6.40.01$ (km/s) and $V_{sg}=3.50.2$ (km/s). Wave velocity of the Moho is $V_{pn}=8.050.02$ (km/s) and $V_{sn}=3.70.2$ (km/s). Depth for Moho discontinuities were obtained 391 km. This result is well correlates with the results of the previous gravimetric crustal studies.

Keywords: velocity, crust, iran



(S) - IASPEI - *International Association of Seismology and Physics of the Earth's Interior*

JSS014

Poster presentation

2298

Crustal structure in South of Zagros, from the 2005 Qeshm Island earthquake in Iran

Dr. Zohrehsadat Riazirad

Geophysics Azad University Science & Research branch M.Y.R.C IASPEI

Recently the seismic activity in south eastern extension of Zagros has been increased, remarkably. Among the several moderate earthquakes, several have occurred in Qeshm Island about 60 km southwest of Bandar-e-Abbas port city in south Iran. In this paper, the geology, including detailed fault map, and the seismicity, including teleseismic and locally recorded earthquakes. Focal mechanism of strong earthquakes were determined and discussed with the stress field in the region. The earthquakes that have occurred during that past 3 year were shallow events. On 27th November 2005, an earthquake occurred with $M_b=6.2$ in west of Qeshm about 57 km southwest of Bandar-e-Abbas and produced damages and destructions in the area. The mainshock was followed by considerable aftershock. According to this study the velocity of crust and under Moho and crustal depth is found. The velocities of layers were obtained from the time-distance curves by a least squares method. The apparent velocities for each event were obtained in a least squares manner. The average velocities for the events in a distance range 175-240 km provided the upper mantle velocity. Similarly, the mean value of apparent velocities for the distance range 120-145 km gave crust velocity. The best wave velocity of the crust is $V_{pg}=6.20.1$ (km/s) and $V_{sg}=3.550.05$ (km/s). Wave velocity of the Moho is $V_{pn}=8.050.05$ (km/s). In order to depth for Moho discontinuities were obtained 445 km in Bandar-e-abbas region. The computed curves for S arrivals by using several V_p/V_s ratios and comparison with the observed S waves, suggested a value of 1.75 for V_p/V_s . The observed later phases on the records of BNDS station were used as supplementary information.

Keywords: crust, qeshm island



(S) - IASPEI - *International Association of Seismology and Physics of the Earth's Interior*

JSS014

Poster presentation

2299

Seismic traveltime curves of the local earthquake in East- SouthEast of Iran

Dr. Zohrehsadat Riazirad

Geophysics Azad University Science & Research branch M.Y.R.C IASPEI

Seismic travel time for simultaneous determination of velocity and interface structure is presented that is applicable to any type of body wave seismic data. This study is velocity and depth of the crust in E-SE of Iran using local earthquakes. Wealth of data from recorded local earthquakes creates an opportunity to image crust and upper mantle in the region. These earthquakes on January 2005 to January 2006 were recorded in the BNDS, KRBR, NASN and ZHSE stations (IIEES) that $ML \geq 3$ were used to calculate the velocity of body wave and the thickness of the crust in these regions. The velocities of layers were obtained from the travel time curves by a least squares method. The apparent velocities for each event were obtained in a least squares manner. At first step we obtained a 1-D velocity model by analysis of the travel-time curves for nearly 20000 P, S wave arrival times from 647 local earthquakes. According to this study the velocity of crust is $V_{pg} = 6.30.01$ (km/s), $V_{sg} = 3.50.2$ (km/s) and suggested a 493 (km) crustal thickness. In additional velocity of upper mantel is $V_{pn} = 8.000.02$ (km/s) in Kerman region. The velocity of crust is $V_{pg} = 6.20.1$ (km/s), $V_{sg} = 3.550.05$ (km/s) and suggested a 445 (km) crustal thickness. In additional velocity of upper mantel is $V_{pn} = 8.050.05$ (km/s) in Bandar-e abbas region. The velocity of crust is $V_{sg} = 3.50.2$ (km/s). In additional velocity of upper mantel is $V_{pn} = 8.000.2$ (km/s) in Zahedan region. This well correlates with the results of the previous gravimetric crustal studies.

Keywords: earthquake, travel time



(S) - IASPEI - *International Association of Seismology and Physics of the Earth's Interior*

JSS014

Poster presentation

2300

Three-dimensional velocity structure of the convergent plate boundary in Eastern Taiwan from seismic and gravity data

Prof. Win-Bin Cheng

*Environmental and Property Management Jin-Wen University of Science and Technology
IASPEI*

The eastern Taiwan convergent plate boundary between 21 and 24°N, is undergoing a style of collision where obliquity plays a significant role. Earthquake data collected during 1986 to 2004 for the study area image crustal structures from oceanic crust to the continental part. This paper investigates three-dimensional velocity structural features of the plate boundary in eastern Taiwan by joint analysis of gravity anomaly and seismic arrival time data. We found two crustal anomalies: (1) two prominent high velocity/high Poisson's ratio anomalies in the mid to lower crust beneath the offshore area; (2) several volumes of relatively high-velocity/high Poisson's ratio rocks in the upper- to mid-crust beneath the Central Range. The former is interpreted as the Luzon arc and forearc blocks from east to west. The latter is interpreted as uplift material from the oceanic crust scraped from the Luzon forearc, which forms the core of the Central Range. The features of northward-narrowing in dimension and deepening in depth of the forearc block are revealed in the velocity solution, implying a subducting Luzon forearc fragment in eastern Taiwan. The values of Poisson's ratios and earthquake activity in the northern domain are generally larger than that in the southern domain, suggesting that the crustal accretion process has not been completed in the northern domain of the study area. Our resulting velocity and Poisson's ratio models provide some insight into the tectonic processes presently operating in eastern Taiwan. The subducting Luzon forearc acts as a backstop against which accreted rocks are thrust, and this contact may have seismogenic potential.

Keywords: seismic tomography, crustal structure, eastern taiwan



(S) - IASPEI - International Association of Seismology and Physics of the Earth's Interior

JSS014

Poster presentation

2301

Seismotectonics of Makran subduction zone

Dr. Kirti Srivastava

Fractals in Geophysics National Geophysics Research Institute IASPEI

V P Dimri

The seismicity patterns of Makran subduction zone has been analyzed by using the data of epicenters obtained from NEIC catalog for the duration of 1973-2005. All the earthquake magnitudes are body wave magnitudes (Mb). The minimum magnitude of the earthquakes is 4.0 whilst the maximum magnitude is 6.5. However, the focal depths of these earthquakes are not accurate as these have been located by global stations and hence, most of them are fixed at 33 km. The salient feature which is conspicuous from this analysis is the absence of shallow seismicity in western Makran whilst the eastern Makran has shallow interplate seismicity and coincides with the major deformation zone. The variation in b-value can be related to the stress distribution after the main-shock, as well as the history of previous ruptures. The regions with lower values of b are probably the regions under higher applied shear stress whereas the regions with higher values of b are the areas that experienced the slip or having lower stresses. From our study using the NEIC earthquake catalog the b-values have been separately estimated for the eastern and western segments. It is seen from the b-values that the eastern segment has a lower b-value and a higher fractal dimension whilst the western is in contrast with the b-value higher and lower fractal dimension.

Keywords: makran, b value, fractal dimension

PERUGIA
ITALY



(S) - IASPEI - *International Association of Seismology and Physics of the Earth's Interior*

JSS014

Poster presentation

2302

Analysis and modelling the recent vertical crustal movements and their relations with basement depth gravity anomaly and terrestrial heat flow

Prof. Istvan Joo

Geodynamics Fellow of IAG IAG

Timea Pajer

The subject of the paper: recent vertical crustal movements and the supposed occasionings as basement depth (D), Bouguer gravity anomaly (G) and the terrestrial heat flow (H). Among them the movemnets velocity had an important role in this study. The targets of the investiggations were: orientation of the face of vertical movemnets and modelling relationship among movement velocities and some geological characteristics. The method of investigation: regression correlation analysis and multivariable linear modelling of the connection betwenn vertical movements and the selected geological characteristics of the Carpathian Basin. There will be presented the method of investigation together with the results.

Keywords: correlation, modelling



(S) - IASPEI - *International Association of Seismology and Physics of the Earth's Interior*

JSS014

Poster presentation

2303

Active deformation in the Zanzan region, northwest Iran

Dr. Farhad Sobouti

Khaled Hesami, Reza Ghods

The Zanzan region in northwestern Iran is an area of intense deformation situated between two thrust belts of the Alborz to the north and the Zagros Mountains to the south. Offset geomorphic features along the major faults of the region suggest that the convergence between Arabia and Eurasia has been accommodated mainly through NW-trending right-lateral strike-slip faults in this region. These strike-slip faults appear to be the southeastern continuation of the North Tabriz fault and other right-lateral faults in SE Turkey. We combine results from the relocation of over 300 earthquakes with studies on geomorphic features to constrain active structural deformation in the Zanzan region. The seismic data were recorded by the University of Tehrans local short period networks during the period 1996-2005. The relocation process resulted in a revised seismicity map of the region. According to this new map, most of the seismicity in the region is concentrated on the fault zones of Talesh, Rudbar, Manjil and Taleghan in the northwestern edge of the region. While the Soltanieh, Zanzan and Mahneshan fault zones in the central parts, appear to be much more quiescent than were previously thought to be. On the other hand, geomorphic features show clear evidence of activity of these faults. Offset stream beds indicate right-lateral strike-slip motion along the NW-trending Soltanieh, Mahneshan and Manjil fault zones. The fact that the WNW trending active left-lateral Rudbar, Ipak, North Tehran, Mosha and Taleghan faults run sub-parallel to these right-lateral strike-slip faults suggests that shortening across the northwestern part of central Iran is accommodated by eastward relative motion of several crustal wedges bounded by conjugate dextral and sinistral strike-slip fault systems. This scenario is very similar to the proposed westward motion of the west-central Alborz. The existence of several active faults implies that this region contains an important seismic potential in spite of the fact that the Zanzan region has been seismically inactive during the last millennia.

Keywords: active deformation, seismicity, fault



(S) - IASPEI - *International Association of Seismology and Physics of the Earth's Interior*

JSS014

Poster presentation

2304

Short term (geodetic) and long term (geological) deformation patterns in the Northern Apennines

Dr. Nicola Cenni

Physics - Sector of Geophysics University of Bologna

Paolo Baldi, Enzo Mantovani, Maurizio Ferrini, Marcello Viti, Vittorio D'Intinosante, Daniele Babbuci, Dario Albarello

The Northern Apennines are constituted by remnants of the Alpine belt and by younger accretionary units stacked along the consuming border of the Adriatic domain. Present seismotectonic activity, associated with normal faults, is mostly concentrated in the axial part of the chain, where a NW-SE alignment of troughs is located. It is widely recognized that the average long-term displacement pattern could be significantly different from the short-term one, due to transient effects of post-seismic relaxation induced by strong earthquakes at major decoupling zones. A tentative estimate of both the short and long term behaviours is tried by mean of geodetic measurements and analysis of neotectonic deformation respectively. A reliable estimate of the velocity field in a zone is strongly conditioned by the high density of the geodetic network. This is particularly true for regions, like the Apennines belt, which are characterized by a complex tectonic setting and a strongly heterogenous strain pattern. In the Northern Apennines region a densification of the national geodetic network has been recently achieved by the installation of 8 GPS permanent stations, with the financial support of the Regione Toscana. The observations collected by these stations have been processed together with the ones provided by other 20 permanent stations in the surrounding regions which observed almost continuously from 2001 to 2006. Double-differenced phase measurements have been processed with the GAMIT software version 10.31 as single daily solutions. In data elaboration we have held fixed IGS final orbits, used coherent earth orientation parameters, removed outliers and cycle slips, estimated and applied tropospheric and ionospheric corrections and carried out a least square adjustment of the baseline elements. The present velocity field inferred from GPS data indicates that the central sector of the Apennines belt, the Umbro-Marchigiane-Romagnole Units, moves with a significantly higher velocity with respect to the adjacent sectors of that arc. This result is fairly consistent with the long term pattern, deduced by the time-space distribution of recent deformation (Quaternary). The reconstruction of this last pattern has also been carried out by a quantitative approach, based on finite element modelling. Both the short and long term patterns are consistent with the strain field inferred from the analysis of focal mechanisms of earthquakes. The geodynamic setting in the central Mediterranean region and the distribution of major earthquakes in the Apennines belt during the last centuries suggest that seismotectonic activity in the Northern Apennines is strongly influenced by the most intense decoupling earthquakes in the Latium-Abruzzi platform (Central Apennines). Since that platform has not been affected by strong earthquakes in the last 90 years, we suppose that this relatively long quiescence could explain the similarity between short and long term velocity and strain fields in the study area.

Keywords: gps, northern apennines, geological geodetic strain

(S) - IASPEI - *International Association of Seismology and Physics of the Earth's Interior*

JSS014

Poster presentation

2305

Structure of the crust and upper mantle in the Qinghai-Tibet Plateau and its adjacent areas

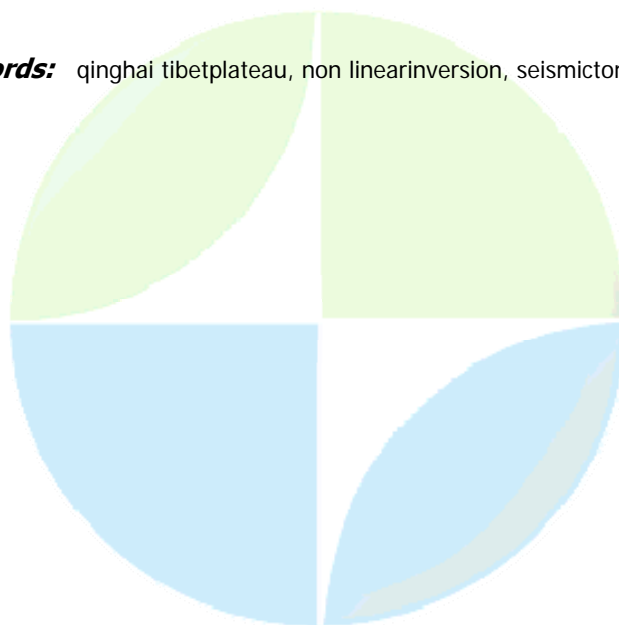
Dr. Xuemei Zhang

Institute of Geology and Geophysics Chinese Academy of Sciences IASPEI

Teng Jiwen

The Qinghai-Tibet Plateau, formed by the successive convergence and the continent-continent between Indian and Eurasian plates since 50Ma ago, is the key earth science laboratory for the understanding of the collision and mountain building mechanism. By their interaction the shallow and deep structures are very complicated. Many geophysicists gained a series of important accomplishment about the deep structure beneath the Qinghai-Tibet Plateau. However there are few studies on the fine structures of the lithosphere-asthenosphere system. Our study area is in the range of 18°N- 42°N and 70°E -106°E. In this study we collect long period (8s-150s) seismic records during the period of 1987-2003. In most of the Qinghai-Tibet plateau the horizontal resolution close to 200km. Based on our results of pure dispersions of Rayleigh wave tomography, taking S wave velocities from our linear inversion as the initial model, using simulated annealing algorithm, we carry out non-linear simultaneous inversion of the interface positions and S wave velocity. With the analyses of S wave velocity, we recognized the character of velocity structures and the thicknesses of the crust and the lithosphere. The results demonstrate the S wave velocity distribution and the crustal and the lithospheric thicknesses varying in different terranes. In the profiles, the Yarlung-Zangbo fault, Bangong-Nujiang fault, Jinshajiang fault and Altyn Tagh fault are obvious boundaries of velocity anomalies. The crust is rather thick with relatively lower velocity in the Qinghai-Tibet Plateau, varies from 60km to 80km, whereas the lithospheric thickness is thinner (130km-160 km) than its adjacent areas. Beneath the Qiantang Terrane where is a crust-mantle transition zone with no distinct velocity jump and Cenozoic lava with rich kalium element, the S wave velocity is relatively lower about 4.1-4.4km/s from 150km to 230km. The image of S wave velocities displays that the north-dipping higher velocity anomaly of the upper mantle is end at the Bangon-nujiang suture. has a thinner crust (32km-38km) with relatively higher velocity and rather thicker lithosphere of 190km. Sichuan and Tarim basins have the crust thickness less than 50km and thicker lithospheres.

Keywords: qinghai tibetplateau, non linearinversion, seismictomography



(S) - IASPEI - *International Association of Seismology and Physics of the Earth's Interior*

JSS014

Poster presentation

2306

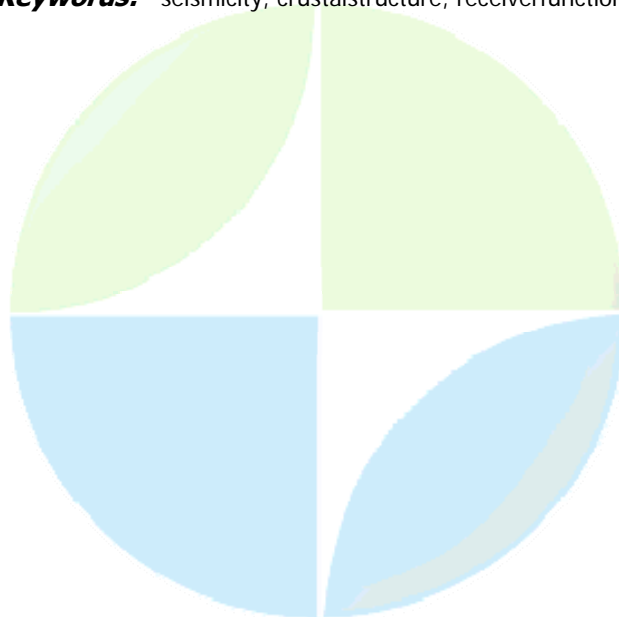
Preliminary Results of a Seismological Experiment on Mantle Dynamics and Crustal Structure beneath Isparta Angle

Mr. Ugur Mustafa Teoman

Eric Sandvol, Niyazi Turkelli, Dogan Aksari, Amanda Lough, Cem Destici, Sakir Sahin, Alev Berberoglu, DoğAn Kalafat

The Isparta Angle (IA) is formed by the intersection of two very different subduction zones: The Hellenic arc to the west and the Cyprian arc to the east. The Hellenic arc is characterized by a retreating and normal angle of subduction, whereas the arc appears to involve a shallow angle of subduction with two major seamounts (the Eratosthenes and Anixamander) impinging on the trench. There is substantial evidence that the Hellenic arc is retreating and the Cyprian arc is relatively stationary. The geometric difference between the Cyprian and Hellenic implies that there is a tear or gap in the subduction of African oceanic lithosphere beneath the Anatolian plate. This tear may be responsible for the seismically active structural features in the region as well as much of the active deformation within the Anatolian continental lithosphere, however, the nature and timing of this deformation has not been determined. In order to address these questions and further understand mantle dynamics and mantle flow through a possible tear in the subducting lithosphere in IA and the surroundings, 7 temporary Broadband instruments from University of Missouri-Columbia and 4 broadband instruments from PASSCAL were deployed in August 2006 in addition to the 23 permanent stations of Bogazici University, Kandilli Observatory and Earthquake Research Institute (KOERI) and Sleyman Demirel University (SDU) in the region. Also, KOERI will install 7 new broadband stations by the end of March, 2007. Using the enhanced detection capability and improved station coverage in the region, we will present some preliminary results, including the preliminary earthquake locations, seismic velocity structure and crustal thicknesses from Receiver functions for the selected stations. Through an improved understanding of this plate boundary, we will be able to further understand the nature of continental uplift, extension, and mantle dynamics in the region.

Keywords: seismicity, crustalstructure, receiverfunctions



(S) - IASPEI - *International Association of Seismology and Physics of the Earth's Interior*

JSS014

Poster presentation

2307

Gravity anomalies and lithospheric structure across the co-seismic rupture of great Sumatra-Andaman earthquake

Dr. Virendra Mani Tiwari

GRAVITY National Geophysical Research Institute IASPEI

V. M. Tiwari, K. Arora, B. Singh

The 26th December 2004 Sumatra-Andaman earthquake of $M_w=9.3$ ruptured a 1300-km-long portion of plate boundary, where the oceanic Indo-Australian plate underthrusts the Burmese plate. Rupture parameters derived from geodetic model suggest segmented asperity. Coincidentally, this segmentation has a visual correlation with gravity anomalies. Therefore, we have analysed gravity anomalies to define lithospheric structure and geometry of subduction zone along a few traverses to understand how the variations in the coseismic slip of the Sumatra earthquake correspond to the variations in the lithospheric/crustal structure?

Keywords: sumatra andaman, gravity anomalies, lithospheric structure



(S) - IASPEI - International Association of Seismology and Physics of the Earth's Interior

JSS014

Poster presentation

2308

Paleostresses and recent tectonic activity of the Palomares-Carboneras strike-slip faults (Eastern Betic Cordilleras, SE Spain)

Dr. Patricia Ruano

Dept. Geodinmica i Geofísica. U Barcelona Researcher

Jess Galindo-Zaldvar, Carlos Marr-Lechado

Palomares NNE-SSW and Carboneras NE-SW oriented strike-slip faults separate the southeastern end of the Betic Cordilleras and the Alboran Sea- South Balearic basin thin continental crust. These faults belong to the Trans Alboran shear zone- that has been considered a deep fracture zone with related volcanism, crossing the Betic-Rif Cordilleras. The age of their activity has been broadly discussed on the literature, and most of the authors suggest evidences of a minimum slip up to several tens of kilometers since the Miocene, with sinistral strike-slip regime and extensional episodes. Although these faults have not a clear present-day associated seismicity, there are local evidences of their recent activity. However, up to date, there is no detailed discussion or analysis of the interaction between these two oblique oriented major faults, with very straight cartographic traces. They should undergone a large geometrical interaction that is not evidenced at their intersection. This contribution aims to discuss the relationships between the activity of Palomares and Carboneras major faults, taking into account new field geological data on brittle deformation near faults zones. The palaeostresses determined from the analysis of microfaults and joints evidence NE-SW extension during the Tortonian, related to the development of normal faults, and local NW-SE compression. During the Messinian, compression rotates clockwise to the NNE-SSW and favors the sinistral strike-slip of the Carboneras Fault Zone, the dextral strike-slip of minor NW-SE oriented faults and the development of large folds such as the Sierra Alhamilla antiform. During the Pliocene, an anticlockwise rotation of stresses produces NNW-SSE oriented compression, which contributes to fold development. These stresses favoured the sinistral activity of the Palomares fault, with regard to Carboneras Fault. Finally, during the Quaternary an ENE-WSW extensional setting and NNW-SSW to NW-SE compression predominate, and secondary NW-SE normal faults develop. Local sinistral regime on Carboneras Fault may be consequence of the accommodation of the displacement of NW-SE normal faults, making it act as a transfer fault. In addition, local NW-SE extension has been also determined. NW-SE compression favoured the sinistral strike-slip activity of Palomares Fault regarding the orthogonally oriented Carboneras Fault. The geological field and geomorphological data also confirm the most intense recent activity of Palomares Fault zone, determining the orientation of the coast line. This fault zone, extending to the north along the Artea Fault, probably displaces Carboneras Fault which shows only local evidences of recent sediment deformation and physiographic feature displacements, typical of a relatively moderate activity.

Keywords: paleostress, palomares fault, recent tectonics

(S) - IASPEI - *International Association of Seismology and Physics of the Earth's Interior*

JSS014

Poster presentation

2309

Tectonophysical model of Tersko-Sunja segment of East Ciscaucasia based on seismotomography and lineament analysis.

Mrs. Galina Ivanchenko

Institute of Geospheres Dynamics Researcher IASPEI

The geodynamic situation in East Ciscaucasia in a fragment of the Scythian plate between Pericaspian rigid lithospheric inclusion and collision zone of the Great Caucasus is determined by horizontal compression. The area is in high tectonic stress condition and is deformed actively enough. Along the Caucasian ridge in a sedimentary cover the thrust series of N -Q age are developed. Reversed fault thrust character is established for Karpinsky Range (inversion structure at southern edge of the East Europe platform) tectonic boundaries. Intensity and style of deformations appreciably differ in the different strips of north - northeast (antiCaucasian) trend differentiated by elongated fracture zones. Usually it is activated fracture zones of the basement. The fragments of these zones are well fixed by geophysics. Many modern fractures, zones of localization of deformations and structural lines are established automated space image interpretation on technology LESSA. The area between the Caucasian ridge and Karpinsky Range is in a condition of strong compression and proceeding folds and thrust deformations of a sedimentary cover. The analysis and new interpretation of seismic records have allowed allocating in area Tersko-Sunja zone the set of earthquakes with deep the centers more than 70 kms [Godzikovskaja A.A. 1988]. Presence of such earthquakes, alongside with mantle earthquakes under the central part of Caspian sea, will be coordinated well to geodynamic model according to which deep shift or embryonic subduction zone, probably is formed here. We shall note, that it is cut in the west by an extended cross-Caucasian fracture zone of the north - northeast trend being also border of blocks with a various seismic mode. Seismotomographic analysis of Tersko-Sunja zone has shown a presence of structural heterogeneity in a transverse section, interpretive as a underthrust fault under the Caucasian ridge or thrust of a ridge on the Scythian plate, and heterogeneity of other type in a section along a ridge, interpretive as segmentation of underthrust fault zone. The presence of high-velocity anomaly under the Caucasian ridge on depths of 40-70 kms in a zone of the greatest gradients of a relief also does not contradict the given assumption. A set of thrusts, reversed faults and folds compensate in a sedimentary cover above the surface of detachment the movement of Transcaucasian-South-Caspian block (subplate) to Eurasia which is probably realized in depth by embryonic subduction zone. At least, under the Scythian plate the thickening of the crust compensating to deformation in a sedimentary cover is not fixed, though subduction or underthrust fault mechanism in continental conditions is limited enough and cannot accept scales of normal subduction of oceanic crust.

Keywords: seismotomography, lineament, subduction

(S) - IASPEI - *International Association of Seismology and Physics of the Earth's Interior*

JSS014

Poster presentation

2310

Spatial variation of the crustal stress field in Taiwan Region

Mr. Wen-Nan Wu

Institute of Geophysics National Central University Ph.D Candidate IASPEI

Taiwan is located along a strongly oblique convergent zone, where the Philippine Sea Plate (PSP) subducts northward beneath the Ryukyu Arc while the Eurasian Plate (EP) eastward beneath the Luzon Arc. In order to provide insight into the collision process and mountain-building for Taiwan, we applied a damped stress inversion technique (Hardebeck and Michael, 2006), which minimized the weighted sum of the data misfit and the model length, to the fault plane solutions which are shallower than 35 km from the Broadband Array in Taiwan for Seismology data center from 1995 July to 2006 December. region was gridded with 0.1 degree space grid and each earthquake was assigned to the nearest grid node. We next simultaneously inverted for stress in all grid nodes included all events within a 0.3 degree x 0.3 degree rectangle centered at the grid node, but the grid node with less than 8 earthquakes was abandoned. For the damped inversion, we chose the value of the damping parameter near the corner of the trade-off curve, in the lower left, where both the model length and data variance are relatively small, and stress orientation uncertainty was estimated using 2000 bootstrap resamplings of the entire data set. The 95% confidence region of the stress model is defined by the 95% of bootstrap solutions closest to the preferred solution. The result of the damped stress inversion indicates that in general the direction of compression is consistent with the relative plate motion direction of the PSP and EP but varies with the tectonic units. The direction of compression shows a significant clockwise rotation around the Lukang Magnetization High in mid-west, and the direction of extension is related to the rifting of the Okinawa Trough in northeastern. On the other hand, the Huatung Fault seems to dominate the crustal stress field in southeastern. Moreover, the spatial variation of the crustal stress field shows a significant stress boundary which is corresponding to the location of a possible tear fault at the northwestern tip of the subducting PSP.

Keywords: stress inversion, taiwan, focal mechanism



(S) - IASPEI - *International Association of Seismology and Physics of the Earth's Interior*

JSS014

Poster presentation

2311

Plate convergence at the Westernmost Philippine Sea plate

Mr. Wen-Nan Wu

Institute of Geophysics National Central University Ph.D Candidate IASPEI

To understand the convergent characteristics of the westernmost plate boundary between the Philippine Sea Plate and Eurasian Plate, we have calculated the stress states of plate motion by focal mechanisms. Cataloged by the Harvard centroid moment tensor solutions (Harvard CMT) and the Broadband Array in Taiwan (BATS) moment tensor, 251 focal mechanisms are used to determine the azimuths of the principal stress axes. We first used all the data to derive the mean stress tensor of the study area. The inversion result shows that the stress regime has a maximum compression along the direction of azimuth N299. This result is consistent with the general direction of the rigid plate motion between the PSP and EP in the study area. In order to understand the spatial variation of the regional stress pattern, we divided the study area into six sub-areas (blocks A to F) based on the feature of the free-air gravity anomaly. We compare the compressive directions obtained from the stress inversion with the plate motions calculated by the Euler pole and the Global Positioning System (GPS) analysis. As a result, the azimuth of the maximum stress axis, σ_1 , generally agrees with the directions of the theoretical plate motion and GPS velocity vectors except block C (Lanhsu region) and block F (Ilan plain region). The discrepancy of convergent direction near the Ilan plain region is probably caused by the rifting of the Okinawa Trough. The deviation of the σ_1 azimuth in the Lanhsu region could be attributed to a southwestward extrusion of the Luzon Arc block between 21N and 22N whose northern boundary may be associated with the right-lateral NE-SW trending fault (i.e. Huatung Fault, HF) along the Taitung Canyon. Comparing the σ_1 stress patterns between block C and block D, great strain energy along HF may not be completely released yet. Alternatively, the upper crust of block C may significantly have decoupled from its lower crust or uppermost mantle.

Keywords: stressinversion, philippinenseaplate, focalmechanism



(S) - IASPEI - *International Association of Seismology and Physics of the Earth's Interior*

JSS014

Poster presentation

2312

Temporal variation of the compressive direction in the hypocentral region after the 1999 Chi-Chi earthquake, Taiwan

Mr. Wen-Nan Wu

Institute of Geophysics National Central University Ph.D Candidate IASPEI

The state of tectonic stress variations in the hypocentral region of the 1999 Chi-Chi earthquake (Mw7.6) is investigated by applying the stress inversion to the focal mechanisms reported from the Broadband Array in for Seismology data center. First, the entire data sets before and after the Chi-Chi main shock are separately to perform the stress inversion. The result indicates that the direction of the maximum compressive axes, σ_1 , before the main shock is N1220 and the after becomes N3020, which both are consistent with the relative plate motion direction between the Philippine Sea and Eurasian plates. The stress inversion is then carried out by accumulating the focal mechanisms of aftershock sequences as a function of time. In general, the direction of σ_1 changes instantly and returns to its regional background stress state of prior to the Chi-Chi main shock and becomes stable less than two year. The recovery time of stress anomaly comparing to the recurrent interval of the Chelungpu fault is very short. Moreover, the 245 focal mechanisms of aftershocks were divided into 11 equal number of event windows with non-overlapping scheme to implement the stress inversion and concluded that the temporal variation of the direction of σ_1 is significantly oscillatory, rather than smoothly as reported by previous study.

Keywords: stressinversion, chi chiearthquake, focalmechanism



(S) - IASPEI - *International Association of Seismology and Physics of the Earth's Interior*

JSS014

Poster presentation

2313

Numerical simulation of the transition from subduction to arc-continent collision in offshore southeastern Taiwan

Prof. Wei-Hau Wang

Institute of Applied Geophysics National Chung Cheng University, Taiwan IASPEI

Hwong-Yi Wu

We conducted 2D finite element modeling to simulate the forearc structures adjacent to the Lutaobabuyan ridge in between the Philippines and Taiwan, where the North Luzon Trough, a typical forearc basin near the Philippines, gradually breaks down into two small basins around the offshore of southeastern Taiwan as the collision between the Luzon arc and the Eurasian plate initiates. Our simulation results suggest that the strength contrast between the accretionary wedge and the Luzon arc is the most important factor controlling regional tectonic style. Northwest of Luzon, the soft sediments in front of competent volcanic arc lead to a large strength contrast and result in a single forearc basin. As the Luzon arc moves closer to the Taiwan Island, the Taiwan orogeny would make the accretionary wedge uplift and lithified. Once the lithified accretionary wedge becomes 10 times stronger than the sediments deposited in the forearc basin, our model suggests that the lithified accretionary wedge would act as a new backstop that deforms the sediments in the forearc basin. As a result, a new ridge forms within the former forearc basin and divides it into two small basins. Our simulation results also suggest that the transition from unlithified to lithified accretionary wedge would lead to a stress change from the thrust type to strike-slip type, which is consistent with regional structures.

Keywords: forearc, lutaobabuyan, taiwan



(S) - IASPEI - *International Association of Seismology and Physics of the Earth's Interior*

JSS014

Poster presentation

2314

An extension of lower crust in central Kyushu, Japan, inferred from GPS derived velocity field- An Implication of Beppu-Shimabara graben structure

Dr. Keivan Hosseini

Physics Ferdowsi University of Mashhad IASPEI

Shoichi Yoshioka, Takeshi Matsushima, Sadaomi Suzuki

A dense array of GPS tracking network in provide us a good tool for monitoring crustal deformation. We carried out an inversion analysis of GPS derived velocity vectors, considering different model source regions during the period from Jan. 1, 1998 to Dec. 31, 2002. We proposed a dislocation model for the central Kyushu region where right lateral strike-slip is dominant in the lower crust at depths of 20-30 km. However, a NS oriented extensional model is also partly supported from Mt. Aso to the Shimabara peninsula which may shows the activity of a rift valley forming in the continental crust (Beppu-Shimabara Graben). This is consistent with the result obtained by the triangulation surveys conducted over the last 100 years (Tada, 1984) and the negative gravity anomalies (Komazawa and Kamata, 1985) and focal mechanisms of large earthquakes (Yamashina and Murai, 1975).

Keywords: gps, crustal deformation, beppu shimabara graben

PERUGIA
ITALY



(S) - IASPEI - *International Association of Seismology and Physics of the Earth's Interior*

JSS014

Poster presentation

2315

The mechanical role of the Philippine Sea Plate in Taiwan orogeny

Mrs. Yu-Yeh Lin

Institute of Applied Geophysics National Chung Cheng University IASPEI

Wei-Hau Wang

We use the finite element software ADEL1 to simulate the collision between the Eurasian and the Philippine Sea Plates in central Taiwan. The Taiwan mountain belt is characterized by an asymmetric wedge in E-W cross section, which is believed to be the result from an indentation of a strong backstop. However, the formation of this backstop is still unclear. We attempt to solve this puzzle by simulating the Taiwan mountain building with a thermomechanical model. Our simulation result shows that no distinct strength contrast between the Eurasian and the Philippine Sea plates can be found at depths shallower than 18 km. In depths of 18 to 42 km, the quartzo-feldsparic continental crust abruptly loses its strength while the colliding olivine-dominated Philippine Sea Plate remains strong. It is at this place the backstop effect appears. As a result, a highly deformed lower continental crust stands in front of a relatively undeformed Philippine Sea plate. By contrast, the upper continental crust above the toe of the Philippine Sea plate, where the Central Range is located, has been elevated by the deformed underlying lower crust but remains little deformation. This is consistent with recent observations that the Central Range has few earthquakes but with a moderate uplift rate. At both sides of the Central Range, stress accumulates in the upper crust. This results in two thrust belts in Western Foothills and Coastal Range respectively. Our model also suggests that the fastest uplift rate appears at eastern Central Range despite that its topography is not the highest. This implies that significant erosion must have been carrying on in this area, which has been supported by recent geochronological studies.

Keywords: taiwan, orogeny, backstop



(S) - IASPEI - International Association of Seismology and Physics of the Earth's Interior

JSS014

Poster presentation

2316

Shallow crustal geological signatures in electrical

Prof. Kalyan Kumar Roy

Dept. Geol.Sci.Jadavpur University,Kolkata,India Emeritus Scientist IAGA

N, Sri Rama Murthy, Lakshi Kanta Das, Kajal Kumar Mukherjee

Collinear dipole-dipole traversing across the Singhbhum shear zone, an Archean-Proterozoic contact, across the geological boundary of two Archean granite bodies of different ages and chemical compositions, across a Proterozoic volcanic body and across an Archean iron ore basin clearly depict shallow crustal inhomogeneity upto two kms from the surface. Scintrex 10 kilowatt transmitter and IPR-8 and 10 receivers were used to conduct this survey. 8 to 10 amperes of current could be sent through the ground and upto 500 microvolt potential could be measured in the potential dipole reliably. Both current and potential dipoles were of length 500 meters and dipole separation were varied from $n=1$ to 8. Global optimization tools, viz, Genetic Algorithm (GA) and Very Fast Simulated Annealing (VFSA) gave better convergence than conventional linearised least squares inversion, viz., weighted ridge regression approach for 2D resistivity modeling. Singhbhum shear zone could be clearly demarcated between the Archean Singhbhum craton and the Proterozoic North Singhbhum Fold Belt. The depth extent of an iron ore body in the Archean Noamundi iron ore basin on the western side of the Singhbhum craton could be mapped. The contact of two separate granite bodies of different geological ages could be deciphered. Signature of a volcanic body also could be seen in the electrical conductivity models below the Proterozoic Dhanjori volcanic basin. Advent of global positioning system (GPS) and easily available long distance communication system (cell phones) improved significantly the practical feasibility of use of high power DC resistivity set up for shallow crustal studies where magnetotelluric method fails because of very high cultural noise.

Keywords: electrical conductivity, precambrians, singhbhum



(S) - IASPEI - *International Association of Seismology and Physics of the Earth's Interior*

JSS014

Poster presentation

2317

P-Wave velocity perturbations of the crust beneath Georgia

Dr. Tea Mumladze

Seismic Data Processing Seismic Monitoring Centre of Georgia

We determined the first high-resolution tomographic image of the crust beneath applying the local tomography method of Zhao et al. (1992). The study area was divided into four layers vertically and a 3-D grid net was set up in the modeling space. Velocities at grid nodes were taken as unknown parameters. The velocity at any point in the model was computed by linearly interpolating the velocities at the eight grid nodes surrounding that point. The grid spacing was 30 km in the horizontal and 5 to 20 km in the vertical direction, respectively. We used 78,454 P and 67,105 S wave arrival times from 6750 earthquakes recorded by 98 seismic stations of the regional seismic network of and seismic networks of and . Our results show strong lateral heterogeneity in the crust under and correlation among the velocity variations, seismicity, active faults, and Quaternary volcanic centers. Our tomography image of the uppermost mantle reflects the depth variation of the Moho discontinuity.

Keywords: crust, structure, velocity



(S) - IASPEI - *International Association of Seismology and Physics of the Earth's Interior*

JSS014

Poster presentation

2318

Origin of tectonic stresses in the chinese continent and adjacent areas

Dr. Shoubiao Zhu

Geophysics Institute of Crustal Dynamics, CEA IASPEI

Yaolin Shi

Based on data of principal stress orientation from focal mechanism and of geological features in China, we made pseudo-3D genetic algorithm finite element (GA-FEM) inversion to investigate the main forces acting on the Chinese continent and adjacent areas which form the Chinese tectonic stress field. The results confirm that plate boundary forces play the dominant role in forming the stress field in China, as noticed by many previous researchers. However, we also find that topographic spreading forces, as well as basal drag forces of the lower crust to the upper crust, make significant contribution to stresses in regional scale. Forces acting on the Chinese continent can be outlined as follows: the collision of the India plate to the NNE is the most important action, whereby forces oriented to the NW by the Philippine plate and forces oriented to the SWW by the Pacific plate are also important. Topographic spreading forces are not negligible at high topographic gradient zones, these forces are perpendicular to edges of the Tibetan Plateau and a topographic gradient belt running in the NNE direction across Eastern China. Basal drag forces applied by the ductile flow of the lower crust to the base of upper crust affect the regional stress field in the Tibetan Plateau remarkably, producing the clockwise rotation around the eastern Himalaya syntax.

Keywords: finite element, genetic algorithm, chinese continent

PERUGIA
I T A L Y



(S) - IASPEI - *International Association of Seismology and Physics of the Earth's Interior*

JSS014

Poster presentation

2319

Simulation of earthquake processes by finite element method: the case of megathrust earthquakes on the Sumatra subduction zone

Dr. Shoubiao Zhu

Geophysics Institute of Crustal Dynamics, CEA IASPEI

Huilin Xing, Furen Xie, Yaolin Shi

Numerical simulation of the earthquake processes is a key method to carry out physical accurate earthquake forecast in the future, but today empirical method is used in earthquake prediction, which is seldom successful. In this paper, we use a unified rate-dependent frictional law to formulate two different frictional states, one is sticking, and another is sliding. Based on R-minimum, time integration method with static explicit is adopted in finite element analysis in order to make the result convergent in calculation. Taken the Sumatra subduction zone as an example, where the major earthquake with $M_m=9.3$ occurred in 2004, the process of locking, unlocking, and sliding between the subduction plate and the overriding plate is modeled. There are 72000 hexahedral elements with 80820 nodes in the model, which covers some areas of the India Ocean plate, of the Sunda subplate, and the Sumatra-Andaman subduction zones. Contact elements are used to model the behaviors of the subduction in finite element computation. The boundary conditions are applied to the model according to GPS measurements. The media in the study areas is regarded as linear elastic with the Young's modulus being 70GPa, and Poisson ratio 0.25, and the density is chosen as 2700kg/m³. The computed result shows that a large area of homogeneous media with the same frictional coefficient is a prerequisite for forming large scale of sudden sliding, which is regarded as an event. The earthquakes simulated by the model on the Sumatra subduction zone have characteristics of quasi-cycle in time and of transference in space. The rupture causing earthquakes propagates from down to upward. Moreover, the geometry of the subduction zone has much influence on the location of the large event.

Keywords: finite element, frictional contact, sumatra subduction zone



(S) - IASPEI - *International Association of Seismology and Physics of the Earth's Interior*

JSS014

Poster presentation

2320

Folding of MOHO beneath Tibet and South Korea

Dr. Young Hong Shin

Space Geodesy Korea Astronomy & Space Science Institute IASPEI

Houze Xu, Pil Ho Park, Jong Uk Park, Jeong Ho Baek

We present the folding structures of Moho beneath the Tibetan Plateau and the southern part of the Korean Peninsula, which show good coincidence with observations from modern global positioning system (GPS). The Tibetan Plateau is greatly affected by heavy compression between Eurasian and Indian Plates. The Korean Peninsula is closely located to the collisional boundary between Eurasian, Pacific, and Philippine Plates, resulting in a compressional force. Thus the study areas possibly have particular deformation structures related with the tectonic environment. Our Moho folding model is based on the gravimetric Moho undulation model and the flexural isostasy model. To estimate the deformation of the Tibetan Moho, we use the recent GRACE satellite-based gravity model, GGM02C as the principle gravity data. Finding out some defects of the former method in estimating the prevailing wavelengths of the folding structure, we suggest a new method producing different results. Our Moho folding model shows: (a) EW directional trend is prominent in western Tibet, while NS directional one in eastern Tibet, (b) the folding structures are not limited to the inside of the plateau but extended to the near surroundings of the plateau, (c) the amplitude of the folding is about 7.5km inside the plateau, (d) rapid decreasing of the amplitude is observed outside the plateau, (e) the intervals between the folding troughs are observed to keep a semi-constant distance of about 330-340km, which is quite smaller than that of the previous study of about 500~700km, and (f) our results are in good agreement with the modern GPS measurements and relate with weakness and partial melting of the Tibetan lithosphere. In examining the southern part of the Korean Peninsula, we use surface gravity data as the principle data. Our model of the Moho deformation shows: (a) the Moho folding structure is parallel to SKTL (South Korean Tectonic Line), which indicates a positive association with the collision of the Yeongnam and Gyeonggi Massifs and a repeated compression afterwards, (b) the amplitude of the folding is about 1.5km and wavelength about 150-200km, (c) the Moho beneath the Gyeongsang Basin has remarkably risen; this seems to result from both collisional compression and buoyancy caused by magmatic underplating, (d) the Moho deformation is the shallowest east of the Taebaek Mountains and deepens toward the west direction, which can be interpreted as the results of opening of East Sea (Japan Sea) and Ulleung Basin. The Moho deformation model in this area correlates well with earthquake distribution and crustal movement measured by GPS. The observed prevailing wavelengths of the folding structures of the two areas are compatible with predicted ones of elastic plates

Keywords: folding, moho, tectonics

(S) - IASPEI - *International Association of Seismology and Physics of the Earth's Interior*

JSS014

Poster presentation

2321

Lithosphere-asthenosphere system beneath The Carpathian Bending Zone by seismic attenuation and satellite geodesy

Dr. Victor Mocanu

Geophysics University of Bucharest

Ray Russo, Boudewijn Ambrosius

The origin of the unusual high seismic activity beneath the Carpathian Bending Zone is a long-term debate and keeps the geoscientific efforts at high level in this area. The processes involved are complex and their nature could be eventually associated with several hypothesis: (1) subduction of an oceanic lithosphere (and eventually a remnant of this being just now detaching from the continental lithosphere of the East European Platform and Moesian Platforms), (2) the oceanic slab subduction ended sometimes in late Miocene and then a part of the continental lithosphere of the mentioned platforms has been delaminated. Various models of the lithosphere asthenosphere system take into account for example the seismic attenuation and shear wave splitting. Different geometry of the lithosphere asthenosphere system as well as the mantle flow around the slabs generate intriguing questions. We consider another constraint to the various methodological approaches by taking into account the kinematics of the crustal blocks as suggested by robust outcomes of the satellite geodesy. We will integrate results of seismic attenuation, mantle anisotropy and GPS in order to test the deep feedback to the Tethyan closure, including the asthenosphere lithosphere system, trying to explain the very unusual high Carpathian seismicity.

Keywords: earthquakes, attenuation, gps



(S) - IASPEI - *International Association of Seismology and Physics of the Earth's Interior*

JSS014

Poster presentation

2322

Crustal structure of the Abruzzo Apennines (Central Italy) through the analysis of seismic data registered by a local network

Dr. Samer Bagh

Centro Nazionale Terremoti Istituto Nazionale di Geofisica e Vulcanologia

Claudio Chiarabba, Pasquale De Gori, Nicola Piana Agostinetti

In this study the background seismic activity and crustal structure of the Abruzzo Apennines (Central Italy) were investigated by analyzing and processing about 850 local earthquakes and 30 teleseisms, recorded from April 2003 to September 2004 by a dense temporary seismic network, composed of 30 digital three-component stations. Velocity models computed by local earthquake tomography and receiver function analysis were used to investigate the crustal structure of the study region. The computed 3-D tomographic model shows two clear, high Vp features. The shape of the shallower one (down to 9-10 km depth), resembles in cross section thrust-sheets with E to NE vergence, in good agreement with the imbricates of the regional thrust systems of the Abruzzo Apennines. The geometry of this high-Vp anomaly suggests multiple detachment levels, implying a thin-skinned component in the Mio-Pliocene orogenic building of the region. The deeper high Vp feature, visible between 9 and 15 km depth (i.e., the lowermost limit of the Vp model resolution), has higher velocities (> 7 km/s). This relatively thick high Vp feature may represent thick Triassic successions (evaporites and dolomites) deposited in the hanging-wall of pre-orogenic extensional faults. This suggests a tectonic inversion component in the compressive tectonics, which may indicate an involvement of, at least, the basement-top formation in the compressive tectonics. S-wave velocity model obtained by the receiver function analysis provides valuable information on the basement depth. A low velocity layer ($V_s = 2.8$ km/s, $V_p = 5.0$ km/s) is imaged at about 15 km depth. This layer is interpreted as Permo-Triassic clastic successions overlying the crystalline metamorphic basement. Based on the obtained velocity structure and other available geophysical data, a structural model including elements of both thin and thick-skinned tectonics is suggested for this sector of the Apennines.

Keywords: local earthquake tomography, receiver function, crustal structure



(S) - IASPEI - *International Association of Seismology and Physics of the Earth's Interior*

JSS014

Poster presentation

2323

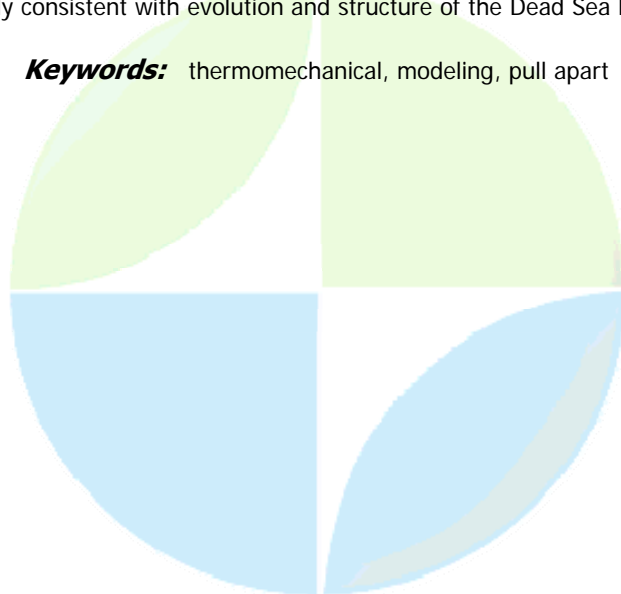
Modeling formation and development of a pull-apart basin effect of crustal rheology

Dr. Alexey Petrunin

Stephan V. Sobolev

Pull-apart basins belong to a special type of sedimentary basins formed at overstepping or bending of an active continental transform fault. An example of a pull-apart basin is the Dead Sea basin (DSB) which is located at the Dead Sea transform (DST) boundary, dividing the African and Arabian plates. The basin formed as a result of crustal extension in domain where the DST has left-side overstepping and accommodation of 105 km sinistral displacement along the DST has led to formation of 150 km long and more than 8-10 km deep pull-apart basin during last 17 Myr. Previous generic modeling results (Petrunin and Sobolev, 2006) demonstrated that the thickness of the brittle layer and friction strength at major faults as well as the magnitude of strike-slip displacement control thickness of sediments and deformation pattern beneath the basin. However the generic models predict decrease of the sedimentation rate in a pull-apart basin with time although there is an indication that the sedimentation rate in the Southern Dead Sea Basin remained high or even increased during the last few million years resulting in the deepest Cenozoic sedimentary basin on the Earth. In present study we consider effect of lower crustal viscosity and rate of friction softening on sedimentation rate. The modeling shows that both those parameters significantly influence maximum thickness of sedimentary layer, shape of the basin and sedimentation rate. Under very fast softening rate (five times friction coefficient dropping at differential displacement of few km) all models with reasonable lower crustal viscosity generate maximal subsidence rate at the beginning of the basin formation and decreasing sedimentation rate (up to zero) at the late stage of evolution during the model time of 20 million years. Under the very slow softening rate (five times friction coefficient dropping at differential displacement of few hundred km) models with any reasonable crustal rheology show acceleration of sedimentation with time but the rates are too low to form 10 km deep basin during 20 million years. The models with medium softening rate (five times friction coefficient dropping at differential displacement of few tens of km) and strong lower crust, generate near constant or even increasing sedimentation rate with time as well as deep sedimentary basin which is generally consistent with evolution and structure of the Dead Sea Basin.

Keywords: thermomechanical, modeling, pull apart



(S) - IASPEI - *International Association of Seismology and Physics of the Earth's Interior*

JSS014

Poster presentation

2324

Imaging the structure-sensitive bodies in seismogenic zone by across

Dr. Naoyuki Fujii

*Institute of Geosciences, Shizuoka University Institute of Geosciences, Shizuoka University
IASPEI*

Mineo Kumazawa, Junzo Kasahara, Takahiro Kunitomo, Takahiro Nakajima, Ken Hasegawa, Yoko Hasada, Toshikiwatanabe, Weipeng Huang, Toshiaki Masuda, Mikio Satomura, Katsuyoshi Michibayashi

We have developed an active monitoring system named the ACROSS (Accurately Controlled Routinely Operated Signal System) in which a tensor transfer function with highly reliable error estimation. This approach will be the best way to discriminate very small temporal changes of the physical properties (material dispersion) and heterogeneous structures in the crust. Observation by ACROSS provides a tensor transfer (Greens) function sampled at finite discrete frequencies in a limited frequency range. From the Toki transmission site we have continuously transmitted circularly (horizontally) polarized seismic waves with modulated frequencies from 10 to 20 Hz for more than five years. Newly installed seismic ACROSS transmitter at Mori-machi, (Shizuoka Pref. by MRI), can generate more powerful energy with frequencies from 3.5 Hz to 8 Hz continuously from October, 2006. Observable phenomena that can cause temporal variations of stress field related to generations of earthquakes and volcanic eruptions could be reflected to the scattered or reflected waves interacted with Active scattering sources. The heterogeneity in the lithosphere originated from both stress state and heterogeneous distribution of fluid-bearing rocks can be the scattering sources. Temporal variation of such scattering sources due to the structure sensitivity of rocks is an essential characteristics of seismogenic regions as well as the active volcanic regions. The active geophysical monitoring would be the essential tool to detect and clarify such an evolving process that governed by the structure sensitivity of rocks in the crust and upper mantle. Among many structure sensitive phenomena, probable changes in the reflected or scattered seismic or electromagnetic signals are expected. Temporal variations of impedance and anisotropic dispersion of the transmitted signals are likely to occur in the subduction zones where the scattering sources are evolving associated with the movement of the fluid mainly composed of supercritical water in the crust and upper mantle conditions. Recent discoveries of intermittent occurrence of slow slip events and deep non-volcanic tremors in the subduction zone could be one of the most challenging targets to clarify their characteristics by using the active monitoring techniques, as well as the dense networks of GPS and the seismometers (with tilt meters). The acquired data by several permanent and temporary stations have been analyzed for various purposes to discriminate signals of the heterogeneous crust from various noises. We have found that the data acquired by seismic ACROSS often show highly frequency-dependent features. There are at least three possible causes for it; (1) frequency characteristics of the transmitted waves governed by nearby structure, (2) material dispersion of the propagating media, and (3) multi-path caused by heterogeneities of the media. Factor (1) can easily be eliminated, since they are common for all the receiving sites surrounding the transmitter. Different signatures of frequency dependencies of each tensor component of transfer function would also reflect from combinations of the above causes presumably material dispersion and heterogeneities of the propagating media. Now we have a basic data set on the frequency dependent vision (color vision) of the complex structures of the Earth's crust. In addition to Seismic ACROSS, we are developing Electromagnetic (EM-) ACROSS with a 600m long and 10A current dipole source in Shizuoka University, in order to physically visible images of re-flectors and scatterers in the crust.

Keywords: structure sensitive, scatterer, active monitoring



IUGG

XXIV2007

PERUGIA

I T A L Y



(S) - IASPEI - *International Association of Seismology and Physics of the Earth's Interior*

JSS014

Poster presentation

2325

Karst Drainage and Erosion Patterns: Implications for Erosional and Depositional Flux in an Accretionary Wedge

Mr. Andrew Gendaszek

Dept. of Earth and Space Sciences University of Washington

Gabe Casale

Recent studies indicate that erosion and deposition within an active accretionary wedge influence strain distribution, seismicity and the overall geometry of an accretionary wedge. The External Dinarides form the eastern margin of the Adriatic micro-plate and are comprised primarily of carbonate lithologies. Dissolution dominates as the primary erosional process within the External Dinarides. The complex karstic drainage network transporting dissolved load out of the External Dinarides is capable of only proximal transport of clastic sediments. The Neretva River in the southern External Dinarides forms the only major conduit for clastic sediments from the interior of the Dinarides to its foredeep in the Adriatic. We compare surface drainage networks across the External Dinarides against off-shore well-logs and seismic sections to establish a relationship between clastic mass-transport and deposition at the toe of the wedge. This has implications for the overall geometry of the accretionary wedge in particular the alpha angle. Finally we discuss the drainage network and thickness of sediments in the foredeep in terms of strain distribution and surface velocities from geodetic surveys.

Keywords: erosion, accretionary wedge, dinarides



(S) - IASPEI - International Association of Seismology and Physics of the Earth's Interior

JSS014

Poster presentation

2326

To the global factors, stimulating tectonic movements

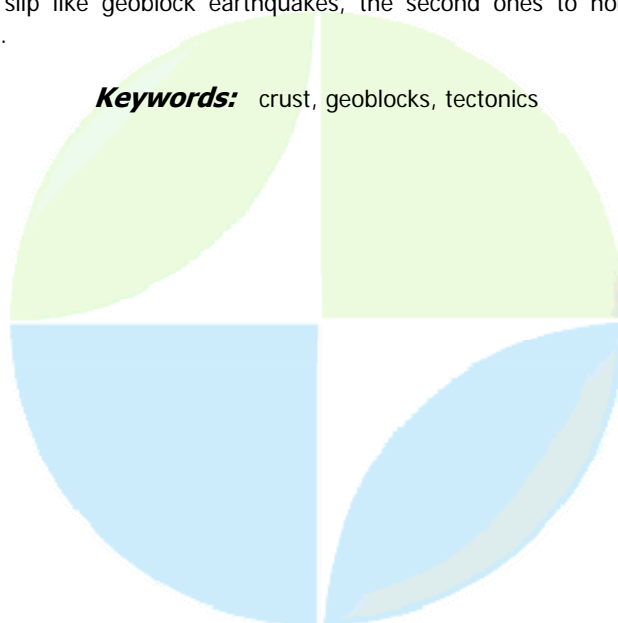
Dr. Farshed Karimov

Seismology Institute of Earthquake Engineering and Seismology IASPEI

Zafar Usmanov

At the present investigation an attempt has been undertaken to learn possible origin of geoblocks equilibrium loss, raising tectonic stresses at the geoblocks contact juncture, leading to earthquake and creep shifting. The model chosen presents equilibrium state of the material point on a rotating sphere surface. For the investigation gravity, dry friction and inertia forces have been taken into consideration. The method suggested can be applied for analyses of screw oscillations of the globe, Chandler's ones in part, and to study geoblocks equilibrium exposed breaking and earthquake as a result of Earth speed variations and thus tectonic stresses accumulation. Coriolis force is neglected due to very initial situation is under the consideration, when point's velocity is negligibly small. For the stable states the point's velocity and acceleration are identically equal zero. The following equation has been obtained for critical equilibrium conditions $f^2 = m^2 \cdot R^6 \cdot \cos^2\theta_0 \cdot (\Omega'^2 + \Omega^4 \cdot \sin^2\theta_0) / (\mu \cdot M \cdot m + \Omega^2 \cdot R^3 \cdot \cos^2\theta_0)^2$, where f is the friction coefficient, M is the Earth mass, μ is the gravity constant, m is the physical point mass, R is the globe radius, $\Omega = \Omega(t)$ is angle velocity dependent on time factor t , $\theta(t) = \theta_0$ determines critical latitude for stability positions. If $\Omega' = 0$, $\Omega = \Omega_0$, then at the latitudes $\theta_1 \leq \theta_0 \leq \theta_2$ and $-\theta_2 \leq \theta_0 \leq -\theta_1$ under $\theta_1 < \theta_2$ there are belts, where stable equilibrium is losing. And there will be three stable equilibrium areas, polar caps and equatorial belt, divided by two unstable latitude belt states symmetrically situated relatively equator ring. The ratio $m_0 / M = q$ is equal to ratio of gravity force to centripetal force, which is connected with β parameter from the well known A. Clairaut's formulas for the gravity force acceleration on the Earth surface spheroid. At the polar vicinity gravity force and reaction of rest are playing the major role in geoblocks stability. At the equatorial belt centripetal force is joining them. Friction forces are sufficient at the middle, transition belts. Critical places determined on the Earth surface for equilibrium states are responding to geoblocks more stressed by surface forces and therefore more likely to undergone shifting and generation earthquakes. At that surface forces can generate both normal pressures and tangential strengths between adjacent geoblocks. The first ones can lead to uplift or slip like geoblock earthquakes, the second ones to horizontal mutual shifting geoblock earthquakes..

Keywords: crust, geoblocks, tectonics



(S) - IASPEI - *International Association of Seismology and Physics of the Earth's Interior*

JSS014

Poster presentation

2327

Spatial pattern similarities between small magnitude seismicity in the argentinian backarc continental crust ($m < 3.5$) and in the Nazca Plate ($M < 4.5$) at its transition from flat to normal subduction

Prof. Enrique Triep

Subcom. de Sismologia y Fs. del Int. de la Tierra Member

Renzo Furlani

It is generally accepted that the flat subduction process between latitudes ~ 28 - 33 S is at least in part a consequence of the thickened oceanic crust of the Juan Fernndez ridge, and that it is related to the high crustal upper plate seismicity and to the broad scale uplift process of the Precordillera and Sierras Pampeanas. Small earthquakes from a three months broadband experiment deployed mainly in the backarc of west-central Argentina, between latitudes 31.5 - 33.5 S, show pattern similarities between the seismicities in the double lithosphere: the one in the subducted Nazca plate within the ~ 100 - 250 km depth range and the one in the continental crust of the South America plate. Clusters and alignments in both seismicities have spatial correspondences. Two neighboring zones are distinguished: 1) North of ~ 31.7 S, just above the Juan Fernndez ridge trace, the superficial seismicity is displaced eastward with respect to deeper one due to the predominant direction progression of the ridge. Vertical stresses are favourably transferred by a continental upper mantle without an asthenospheric wedge. The consequence is the high seismicity of the zone. Also, as one example, the vertical component of accumulated stresses could be linked to the uplift of the Sierra de Pie de Palo. 2) Between ~ 31.7 - 33.5 S, where there is the major transition from flat to normal subduction, the superficial seismicity is displaced southeastward with respect to the deeper one. Both seismicities have lined shapes branches that embrace the base and top of an aseismic continental lithospheric volume, some what like an inclined cylinder, that help to visualize their spatial connection. The base of the volume at 105 km depth is on the strong bending of the contorted plate, and the top includes some crustal regions of Precordillera, Cerrillada Pedemontana, Huayqueras and eastern plains. The volume coincides with a feature determined by tomography and characterized by high V_p , high V_s velocity values and relatively high V_p/V_s ratio, which are consistent with upper mantle mineralogies no longer hydrated or melted to any significant extent. In these conditions the volume seams to perform as an efficient stress guide. The stresses can be originated at the deep boundary between the two lithospheres and/or from the deformation process in the continental upper mantle that fills the space pinched out by the Nazca plate strong bend. Then, at least for the region and the earthquake range magnitude here considered and besides the horizontal stresses coming from the relative plate movement, the spatial pattern similarities between the seismicities in the subducted plate and continental crust show a case of a noticeable effect of the vertical stress components coming from the deep boundary of the two involved lithospheres and/or the deformation process of the continental upper mantle produced by the contorted plate.

Keywords: lithosphere, boundary, interaction

(S) - IASPEI - *International Association of Seismology and Physics of the Earth's Interior*

JSS015

2328 - 2338

Symposium

Crustal structure and Tectonophysics - Large-scale multi-disciplinary programs for continental imaging

Convener : Prof. Hans Thybo

Imaging experiments that incorporate multiple geophysical tools (e.g. active and passive seismology, MT, GPS, heat flow, etc.) provide significantly improved images of the structure and composition of the continents. In this session we will highlight those multi-disciplinary experiments that are aimed at improving our understanding of the continental lithosphere. Contributions describing both existing and planned experiments along with contributions focusing on the benefits of including specific techniques are encouraged for this session.

IUGG
XXIV2007
PERUGIA
ITALY



(S) - IASPEI - *International Association of Seismology and Physics of the Earth's Interior*

JSS015

Oral Presentation

2328

3-D crustal velocity tomography in south of Jiangsu Province and adjacent area, China

Prof. Qinghe Li

Earthquake Administration of Jiangsu province China Earthquake Administration IASPEI

Zhang Yuiansheng, Jin Shumei

The Method MULTiphase Traveltime Inversion(MUTI) has been improved and optimized. We get 3-D velocity tomography in south of Jiangsu province and adjacent area(29-34N, 117.5-122.5E), China, by using seismic data after relocation by DD and GA jointly. The crust can divided into upper, middle and lower part. The buried depth of upper crust is 10-12km with velocity 6.24km/s, the buried depth of middle crust is 22-23km with 6.77km/s. The depth of Moho is 28.2-38.1km, appear shallower in northeast and deeper in southwest. Stronger heterogeneity in various layer has been found. According to analyzing focus and deep structure, we can estimate the deep geometry of Maoshan Fault on which occurred M6 earthquake in 1979, and the deep geometry of Taicang-Fengxian Fault on which occurred M5.1 earthquake in 1990. we also can analyze the features of deep structure.

Keywords: 3 d velocity tomography, features of deep structure



(S) - IASPEI - *International Association of Seismology and Physics of the Earth's Interior*

JSS015

Oral Presentation

2329

Single-Station Passive Seismic Stratigraphy to 2km depth in sedimentary basins

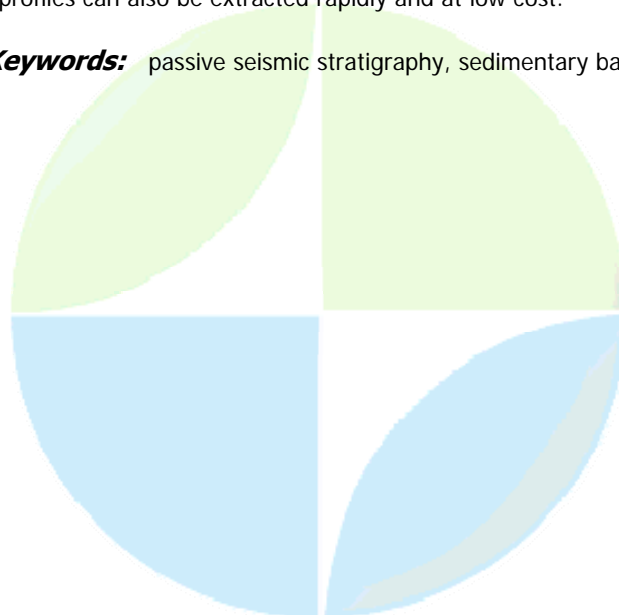
Prof. Francesco Mulargia

Fisica, settore Geofisica Universit di Bologna

Silvia Castellaro

Passive seismic 3D stratigraphy is commonly effected by reconstructing the noise wavefield that crosses an array of seismometers. The range of wavelengths that can be analysed is tied to the size and layout of the array, with bandwidth and resolving power generally proportional to the degree of compicacy of the measuring network. At the other extreme, maximum simplicity is achieved by the Single-Station Passive Seismic Stratigraphy (S-SPSS) approach, which has been so far essentially based on the Horizontal to Vertical Spectral Ratio (HVSr). The latter, in spite of its hazy theoretical bases, has been successful in 1-D subsoil mapping up to depths of some tens of meters. In light of tremor composition, both a theoretical analysis as well as numerical simulations suggests that the Airy phases are a fingerprint more reliable and effective than HVSr for stratigraphic applications. In a series of tests on a variety of sites on large sedimentary basins of the Italian territory, where direct deep well data are available from oil exploration, we positively identified the bedrock interface down to depths of 1700 m. Tremor illumination was found to be sufficient under all weather conditions, although the reflections from interfaces deeper than 500 m were more evident under stormy weather and became very clear in concomitance with sea storms. Under good weather conditions in the whole Mediterranean basin we failed to identify the bedrock interface when sited at 2000 m or deeper. A tremor acquisition for passive stratigraphy requires typically 30 minutes, with only marginal improvement brought in by longer recording times. Several strata at different depths can be usually resolved at each site. We find that inverting tremor data for depth by using a fixed general parametrization leads to an accuracy on depth estimates around 20%. This suggests the use of S-SPSS as a fast and inexpensive tool to build starting models for accurate stratigraphic analysis. Alternatively, by tuning the parameters at a site where stratigraphy is known by direct exploration, S-SPSS can accurately extend subsurface mapping to all the regions where a similar structural pattern applies and where the depth of the interfaces may vary. In this case, the velocity profiles can also be extracted rapidly and at low cost.

Keywords: passive seismic stratigraphy, sedimentary basin



(S) - IASPEI - International Association of Seismology and Physics of the Earth's Interior

JSS015

Oral Presentation

2330

Seismic imaging of the lithosphere beneath southeast Australia using data from multiple array deployments

Dr. Nick Rawlinson

Research School of Earth Sciences Australian National University

Brian L. N. Kennett

Over the past five years, the Research School of Earth Sciences at the Australian National University has pursued a vigorous campaign of passive seismic array deployments to substantially increase the high density data coverage of the lithosphere beneath southeast Australia. To date, a total of eight separate seismic arrays have been deployed for periods ranging between 5-8 months in Tasmania, Victoria, eastern South Australia and southern New South Wales. When combined, this cluster of adjacent arrays comprises nearly 350 recorders (mostly short period), with station spacings ranging between 15-50 km. With the long term goal of covering much of eastern Australia at high density for the purposes of passive seismic imaging, including teleseismic and ambient noise tomography, this ambitious project has the potential to make a significant contribution to seismology and the understanding of the Australian continent. In this presentation, we will focus on results from several recent studies that have been undertaken using data from the multiple seismic arrays in southeast Australia. The SEAL (2004-2005) and EVA (2005-2006) experiments, which involved two adjacent deployments in eastern Victoria and southern New South Wales, yielded high quality teleseismic data that have been mapped as 3-D variations in P-wavespeed. This was done using a new iterative non-linear tomography scheme which makes use of a robust grid based wavefront tracking technique to solve the forward problem of data prediction, and a subspace inversion method to reconcile the predictions with observations by adjusting the model parameters. Analysis of the tomographic images reveals a distinctly faster upper mantle beneath the Delamerian Orogen compared to the western Lachlan Orogen which lies to the east. This suggests that the former is underlain by Proterozoic lithosphere, and the latter by Palaeozoic lithosphere. One advantage of having high density passive seismic data spanning a large region is that it has the potential to be combined with more focused active source experiments. For example, the island of Tasmania, which lies at the southern tip of southeast Australia, hosted a large 3-D crustal refraction and wide-angle reflection experiment in 1995, which comprised some 44 land-based stations and 36,000 marine airgun shots. Recently, this dataset was combined with teleseismic arrival time data from the 2002 TIGGER experiment of Tasmania in a simultaneous inversion for 3-D lithospheric P-wavespeed and Moho geometry. In contrast to previous results from separate inversions of the active and passive source datasets, the new images reveal a zone of elevated wavespeed beneath the Cambrian Mt. Read Volcanics, and indicate that both crustal thinning and elevated wavespeeds occur beneath northeast Tasmania, which supports the case for the existence of a prior passive margin.

Keywords: seismic tomography, australia, lithosphere

(S) - IASPEI - *International Association of Seismology and Physics of the Earth's Interior*

JSS015

Oral Presentation

2331

Deep seismic reflection image and seismic refraction study across the Achan Kovil Shear Zone (AKSZ) Suggest a major panafrikan tectonic event

Dr. Rajendra Prasad Bitragunta

Project Leader, CSS Project National Geophysical Research Institute IASPEI

B.Rajendra Prasad, P.Koteswara Rao, G. Kesava Rao

The Southern Granulite Terrain (SGT) of south is one of few terrains in the world that has preserved Achaean crust with extensive granulites essentially of lower crustal origin. The intervening shear zones between the highland granulite massifs might have acted as conduits for exhumation of these high pressure and temperature rocks to their present position probably during Pan-African rifting (~500 Ma). The SGT is divided into three major blocks. The northern granulite block occupies the area between Dharwar craton and Palghat-Cauvery Shear (PCS) zone and defines transition between low and high grade terrains. The region between PCS and Achan Kovil Shear Zone (AKSZ) zone is southern granulite block (0.50.7 Ga) including most of the highlands with amphibolites facies gneisses and supracrustal rocks in addition to charnockite, granulites and khondalites. The NW-SE trending AKSZ is more prominent toward southern end of SGT and indicates Proterozoic tectonic activity [Santosh et al., 2003]. The granulites were formed at average 710 kbar and 700800 °C corresponding to burial depths of about 2025 km (Rao et al., 2003). To understand the complex geology and tectonic settings of SGT, a 220 km long N-S trending deep seismic Reflection/refraction traverse was recorded from Vattalkundu to Kanyakumari in 2005-2006 traversing across different shear zones. Deep seismic reflection data were acquired using a state of the art 240-channel, 24-bit Radio Frequency Telemetry System with all its accessories for the first time, along the Vattalkundu-Kanyakumari. (Rajendra Prasad, et. al., 2007) Symmetric split spread geometry with 75/90 data channels on either side of the shot point was used for recording 24 s long seismic reflection data along the profile. A shot interval of 200 m and geophone group interval of 100 m were used to generate a nominal foldage of more than 30. Each receiver consisted of 20 geophone series string of 4.5 Hz natural frequency provided enough signal strength for recording the seismic events with high fidelity in a wide frequency band at 2ms sampling interval (4.5-250 Hz). The commands and data transfer were accomplished through a bidirectional and reliable VHF radio link between remote units and the recording unit. The seismic source comprised of buried charge of 50 Kg in 25 m specially drilled shot hole. The data thus acquired is subjected to pre-processing for eliminating the coherent noises and standard crustal seismic data processing sequence to generate high resolution seismic images of the region. The AKSZ shows up a series of south dipping, continuous parallel reflectors over an area of 30-40 km originating at mid-crustal levels complementing our seismic tomographic image (Rajendra Prasad, et .al., 2006).

Keywords: southerngranuliteterrain, achankovilshearzone, seismicreflectionrefraction

(S) - IASPEI - *International Association of Seismology and Physics of the Earth's Interior*

JSS015

Oral Presentation

2332

Implications of transitional structure across Central Taiwan from studies of wide-aperture seismic, receiver functions, stress field and earthquake data

Prof. How-Wei Chen

Institute of Geophysics Professor

We present our integrated study on delineating the transitional structure related to the subduction-collision tectonic features beneath Central Taiwan. Four types of studies were conducted including: a wide-angle active source experiment; teleseismic receiver function analysis to identify regional crust structure features; spatio-temporal stress field analysis from BATS and CWB data and co-seismic Chi-Chi earthquake source rupture and strong motion analysis. Four different types of datasets all reflect strong coupling between source rupture and wave generation processes due to lateral variations of crust-scale structure. Wide-aperture seismic experiment from a 500kg explosive source and datasets collected from a fairly dense seismic array consisting of 150 IRIS stations, 33 portable 3-component strong motion stations and island-wide broadband and short-period seismic monitoring stations are used. The data processing is implemented including noise reduction; depth filtering for direct arrivals and surface waves; multiple attenuation and prestack reverse-time depth imaging. From receiver function analysis, the best estimated Moho depth from 41 broadband stations on average is 30 km. The results reveal a westward crustal thinning from 37.5 km in eastern Taiwan to 30 km in the east coast of mainland China. In the north, the averaged Moho depth is 25 km and deepens to 34 km in southern Taiwan. Notable crustal thinning under northern Taiwan may associate with back-arc opening and magmatic activities. Variation of H and V_p/V_s ratio (κ) across SSLB (52 km, 1.77), YULB (39.5 km, 1.59) marks the strong lateral change in the Moho topography. Relatively low κ at YULB and LYUB (29.49km, 1.56) together with SSLB may indicate a possible trace of active collision and orogenic processes involved beneath central Taiwan. The overall thickened crust in the south, thin crust in the north and possible transition in the central Taiwan marks the different tectonic units between the subduction wedge and the collision prism onshore. Spatiotemporal evolution of tectonic stress state within the seismogenic zone associated with Chelungpu fault indicate that the maximum compressive stress (σ_1) axis is highly correlated with plate motion between Philippine Sea and Eurasian plates. The temporal variation of σ_1 axis base on aftershock sequences has fairly unique short recurrence interval of 300 days or more. Rather distinct temporal oscillatory pattern of σ_1 axis directions indicate an under-damped forced oscillation system associated with Chi-Chi earthquake rather than over-damped situation reported by Zhao et al, (1997). Study of Chi-Chi earthquake including 3D fault plane geometry, co-seismic source rupture processes follow by strong motion simulation and prediction. The largest Chi-Chi earthquake over last century associated with others studies all indicate that the most damaged event is highly influence by the crustal structure. All studies confirm that heterogeneous and possibly north extension of subducted crust-scale structure have significant effects on waveform and travel-times.

Keywords: stress inversion, central taiwan, receiver function

(S) - IASPEI - *International Association of Seismology and Physics of the Earth's Interior*

JSS015

Oral Presentation

2333

Possibility of the Earth's global tomography with the use of vibrating sources

Dr. Valery Kovalevsky

Geophysical Department of ICM&MG SB RAS Secretary of science ICM&MG SB RAS IASPEI

Anatoly Alekseev, Boris Glinsky

The paper considers the possibility of the use of artificial vibrating high-power sources for global tomography of the Earth. The analysis of the results of the works carried out in USA, Russia and Japan of vibrating sources application for sounding of the Earth's crust and the upper mantle is executed. The most powerful today 100 - ton seismic vibrators allow us to record vibrating signals at the distances of 400-1000 km in various modes of radiation. Results of the vibroseismic researches of the Earth's crust structure and monitoring its stress state executed in the Siberian branch of the Russian Academy of Science are submitted. Estimates of the vibroseismic signals amplitudes and the required vibrating sources power for recording at the teleseismic distances are received. The principles of the construction of super-power vibrators, problems of the creation of resonant oscillatory systems and problems of their precise control are analyzed. Variants of constructions of super-power vibrating sources with the force of 1-10 thousand tons for the operation on continents and in the sea are offered. The worldwide super-power vibrating sources network for realization global tomography of the Earth is proposed. Possible research problems of the Earth's global tomography are considered. One of them is the study the medium movement in internal areas of the Earth and, in particular, rotation of the Earth core.

Keywords: tomography, vibrators, research



(S) - IASPEI - *International Association of Seismology and Physics of the Earth's Interior*

JSS015

Oral Presentation

2334

Vibroseismic Earths crust structure research in Siberia.

Dr. Valery Kovalevsky

Geophysical Department of ICM&MG SB RAS Secretary of science ICM&MG SB RAS IASPEI

Boris Glinsky, Marat Khairetdinov, Victor Seleznev, Alexander Emanov, Victor Soloviev

The paper presents results of the experimental works with powerful seismic vibrational sources carried out by geophysicists of Siberian Branch of RAS. The materials of the deep vibroseismic researches of the Earth crust of the Altay-Sayan and Okhotsko-Chukotski regions and the Baikal rift zone are presented. The detail deep cross-sections of the Earths crust and upper mantle including time-sections of CDP-DSS up to depth of 80km were received. The paper presents experimental data of the 10-days active vibroseismic monitoring of the Baikal rift zones where the attempt to estimate the top border of the reactive and dissipative strain-sensitivity of the crust in seismic active Baikal zone is made. The waves from vibrator reflected from Moho boundary at the distance of 125 kms were recorded and variations of the arrival times were analyzed. The results of the long-term experiment on vibroseismic monitoring for investigation of the seasonal variations of the vibrational wave field and experiment of the detection the influence of the Earths crust tides on seismic wave velocities are presented too. In the paper are discussing new vibration geotechnologies based on the using of powerful seismic vibrators: detail deep seismic investigations of the Earths crust and the upper mantle, diagnostics of physical state of buildings and structures, active vibroseismic monitoring of the seismic-prone zones and studying of the geodynamic processes, vibroseismic calibration of international network stations, seismic ecology.

Keywords: vibroseismic, research, crust



(S) - IASPEI - *International Association of Seismology and Physics of the Earth's Interior*

JSS015

Oral Presentation

2335

Project INDEPTH and the Deep Structure of the Tibetan Plateau

Prof. Larry Brown

Institute for the Study of the Continents Cornell University IASPEI

Wenjin Zhao

Project INDEPTH is a multinational, multidisciplinary initiative that has now collected an extensive suite of geophysical data extending from the high Himalayas to the central portion of the Tibetan plateau. INDEPTH I detailed the geometry of the Main Himalayan detachment beneath which Indian continental crust is subducting beneath the deforming leading edge of Asia, providing an important new constraint on the amount of plate convergence that could be attributed to crustal shortening in the Himalaya. INDEPTH II seismic and magnetotelluric indications of partial melt in southern have lent support to tectonic models involving warm, weak crust and attendant material flow at depth. INDEPTH III results that are consistent with such flow beneath the central plateau include a highly conductive crust, restriction of local seismicity to the uppermost crust, reflective lamination in the lower crust, and coherent crustal anisotropy. Mantle tomography of INDEPTH III teleseismic recordings indicate a steeply dipping zone of anomalously fast (cold?) material in the mantle beneath central Tibet that likely marks subducted Indian lithosphere, an interpretation consistent with the gravity field over Tibet. Receiver functions computed beneath INDEPTH stations indicate a segmentation of the Moho that may reflect post-collisional reactivation of older accreted terranes. INDEPTH IV is now poised to complete its megatranssect with new surveys across the northeast boundary of the Tibet Plateau as represented by the Kunlun Mountains and Qaidam Basins. INDEPTH IV will begin in the Spring of 2007 to address outstanding crustal issues such as the role of Moho faults, the extent of lower crustal flow, and possible subduction of Asian lithosphere beneath the northern plateau.

Keywords: tibet, lithosphere, orogeny



(S) - IASPEI - International Association of Seismology and Physics of the Earth's Interior

JSS015

Poster presentation

2336

Geophysical investigations of the Eastern Alpine crust and upper mantle

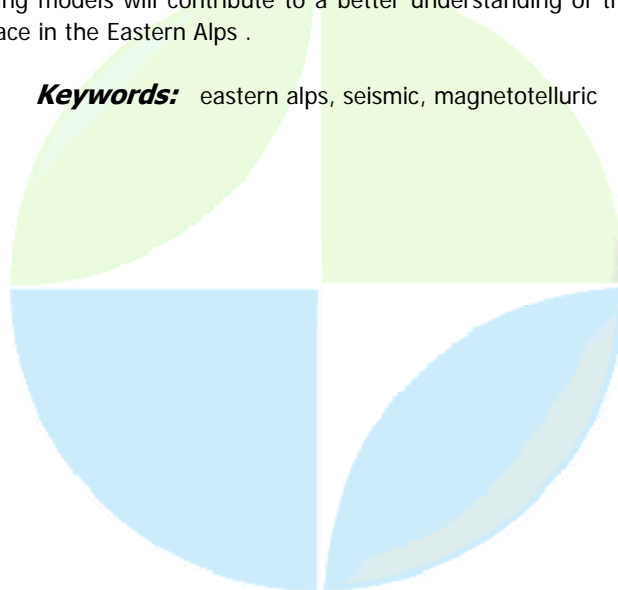
Dr. Michael Behm

Institute of Geodesy and Geophysics Vienna University of Technology IASPEI

Ewald Brckl, Franz Kohlbeck, Ulrike Mitterbauer, Laszlo Szarka, Alpess Working Group, Hungarian Mt Team

Currently the deep structure of the Eastern Alps and their surroundings is intensively studied by several large-scale geophysical investigations. We present latest results and ongoing projects. The 3D seismic refraction experiments CELEBRATION 2000 and ALP 2002 delivered much new insight into the P-wave velocity distribution of the crust and the structure of the complex Moho boundary in the area. In both experiments, seismic waves generated by 55 and 39 blasts, respectively, were recorded each with approximately 900 recorders. The results are a 3D velocity model of the crust, a new Moho depth map and 2D interpretations along selected profiles. The most important outcome is the determination of a pronounced fragmentation of the crust, including the new interpretation of the crustal block Pannonia which may be related to Miocene-to-date extrusion tectonics. Based on these results, the ALPASS experiment was launched to investigate the structure of the upper mantle down to the 660 km discontinuity. 110 permanent and 79 temporarily deployed stations recorded earthquake waveforms in the time from May 2005 to April 2006. These data provide the input for surface wave inversion, receiver functions, and teleseismic tomography. Seismic recordings from 144 earthquakes have been selected for a teleseismic tomographic inversion. A preliminary first model of the P-wave velocity structure of the upper mantle will be presented. Of particular interest is the direction of subduction below the Eastern Alps, since previous investigations yield contradicting results. Magnetotelluric soundings targeting the crust have been performed in the frame of the DIMS project. Ten test measurements with different instruments were carried out along the Hungarian-Austrian border. Another 33 measurements followed a seismic profile from the Hungarian border toward NW. Preliminary results indicate low resistivity of sediments in the Graz Basin in the SE part of the profile, as opposed to the highly resistive Eastern Alps in the NW. Large-scale tectonic fractures appear as conductive dikes. The long period soundings along the Hungarian-Austrian border might delineate the asthenosphere. We conclude that all three projects deliver much new insight into the deep structure of the investigated area. The joint interpretation of the existing and forthcoming models will contribute to a better understanding of the complex geodynamic processes that took place in the Eastern Alps.

Keywords: eastern alps, seismic, magnetotelluric



(S) - IASPEI - *International Association of Seismology and Physics of the Earth's Interior*

JSS015

Poster presentation

2337

P-Wave velocity structures, reflectors and seismic activity from seismic surveys in Kinki district, Southwest Japan

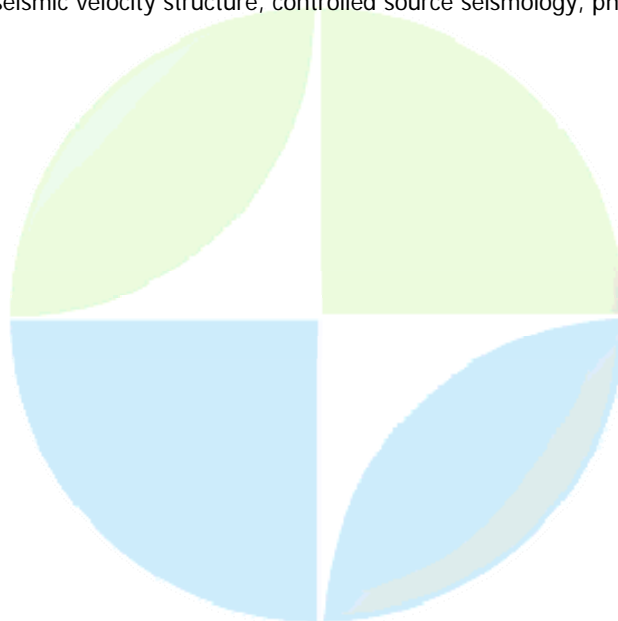
Prof. Kiyoshi Ito

Disaster Prevention Research Institute Kyoto University IASPEI

Issei Hirose, Yasuhiro Umeda, Hiroshi Sato, Naoshi Hirata, Tanio Ito, Susumu Abe, Taku Kawanaka, Takeshi Ikawa

A large-scale seismic survey was conducted across the Kinki district from the Pacific to the Sea of Japan (Shingu-Maizuru line) in 2004, under the Special Project for the Strong Motion Evaluation in the Urban Areas. In the profile, 13 shots (100-700kg) of dynamite and 3 multivibrator (a few hundreds of sweeps) with 4 vibroseis trucks were used for refraction and wide-angle reflection surveys along a line of 220km long. More than 2200 seismometer stations were set at intervals of 50-100m all along the line. Clear first arrivals and reflections from the Philippine Sea plate (PSP) and reflectors in the crust were obtained at almost stations. Shallow P-wave velocity structure less than about 7km was well determined from refraction analyses and the resultant velocity changes of the surface layer are well correspond to the large-scale geological features. P-wave velocity structure of the whole crust and upper mantle was also determined from refracted and reflected waves. The reflections from the PSP are very clear beneath Kii Peninsula and are still visible under the northern Kinki district at depth of about 50-70km. Double reflectors with related to the subducting PSP were well recorded and the lower reflector is well coincident with the upper boundary of the mantle earthquakes. Therefore, the upper boundary, which seems to be the plate boundary, is shallower than the depth that has been determined from earthquake distributions by 7-10km. Besides, many north-dipping seismic reflectors in the lower crust in the middle and southern Kinki district were detected and some of them seem to be connected to the large active faults, such as the Median and the Arima-Takatsuki Tectonic Lines. In northern Kinki district, two near horizontal reflectors of 15 and 25 km deep were found and the shallower reflector is coincident to the base of the crustal seismicity. Thus the results are useful for the estimation of strong motion as well as the nucleation process of the large earthquakes.

Keywords: seismic velocity structure, controlled source seismology, philippine sera plate



(S) - IASPEI - International Association of Seismology and Physics of the Earth's Interior

JSS015

Poster presentation

2338

Crustal structure and stress field for southern Apennines region from local earthquakes

Dr. Annalisa Romeo

Dipartimento di Scienze Fisiche Universit di Napoli Federico II, RISSC-Lab

Giuseppe Pasquale, Raffaella De Matteis, Giovanni Iannaccone, Aldo Zollo

The Southern Apennines is one of the Italian areas characterized by most intense geodynamic activity; as evidenced by the seismic catalogues in historical time it was struck by several destructive earthquakes (Boschi et al., 1998). The most recent one occurred on 1980, 23 november, M 6.9, producing more than 3000 casualties and extended damages in all the region. Nowadays the seismic activity is characterized by low-moderate earthquakes. In this work we present a three-dimensional P-wave velocity crustal model of Southern Apennines region using travel time of local earthquakes. In this model we re-localize the earthquakes and then we compute the focal mechanisms in order to estimate the stress field acting in the area. In order to obtain a 3D velocity model we merged the data collected from 1988 to 2003 by Istituto Nazionale di Geofisica e Vulcanologia (INGV) network (Italian National Seismic Network) with arrival time of aftershocks of 1980 M 6.9 Irpinia earthquake recorded by a temporary network. Only the earthquakes which were recorded at least eight stations were considered and the final database consist of 1196 earthquakes with 15500 P and 7000 S arrival time readings. We used the linearized, iterative tomographic approach proposed by Benz et al. (1996), which allows inversion of local earthquakes first-arrival travel-time to solve simultaneous velocity model parameters and hypocentral parameters. The iterative technique takes into account the nonlinearity of the problem but in each iteration the method is based on a linear approach. This means that the starting model will influence the inversion process. In order to avoid falling in a local minimum, the final velocity model was obtained as the mean of the 250 velocity values assumed by each cell in the 3D inversions performed with different 1D reference models randomly generated in a selected range. Uncertainty associated to the velocity value for each cell has been analyzed and the model resolution has been evaluated through a standard checkerboard test. In order to give an improved representation of the seismicity pattern, we have re-localized the 1196 earthquakes in the 3D final velocity model using a probabilistic, non-linear, global-search earthquake location method (NonLinLoc code, Lomax et al., 2000). The relocated seismicity is shifted eastward caused by a low velocity zone in the eastern part of the investigated area. It is clustered around the system fault of the 1980 Irpinia earthquake and have a depth ranging between 0-20 km. For the computation of best fit double-couple focal mechanisms we used the fault-plane fit grid-search algorithm (FPFIT) of Reasenberg & Oppenheir (1985). Restrictions are place on the minimum number of first arrival polarities (six polarities), maximum acceptable RMS residual (≤ 0.5 s) and maximum values for ERX (≤ 0.8 km), ERY (≤ 0.8 km), ERZ (≤ 0.8 km) and gap ≤ 180 . The FPFIT algorithm computes the orientation of the P and T axes, but there is no correspondence between P and T axes and the principal stress orientations. With the purpose of investigating the stress field in this region, we applied the Michael (1984) procedure to our data set of fault-plane solutions. It computes the best uniform stress field for the dataset and meaningful confidence regions using a statistical tool known as bootstrap resampling. Stress inversion shows a nearly horizontal NE-SW minimum compressive stress axis (σ_3), while maximum compressive axis (σ_1) is vertical. This result reveals that Southern Apennines is generally ongoing through NE-SW extension, as evidenced by the fault-plane solutions of major earthquakes occurring along the Apenninic Belt.

Keywords: tomography, stress field, focal mechanism

(S) - IASPEI - *International Association of Seismology and Physics of the Earth's Interior*

JSS016

2339 - 2358

**Symposium
Underwater observatories**

Convener : Prof. Barbara Romanowicz

The international earth and ocean sciences community recognizes the need for long-term observatories in the oceans in order to provide optimally sampled observations of global scale processes, in real-time when appropriate, and for the long-term monitoring of time dependent processes on the regional and local scales. International Ocean Network (ION) was formed to foster synergies among different disciplines, and to facilitate cooperation in the development of critical elements of the observing systems, harmonization of those elements of the system. In order to achieve these goals, technical developments are required that should provide the prolongation of the study of investigated parameters from the land to the ocean bottom. The session interests will be concentrated on the discussion of scientific tasks which need joining of international efforts for their realization as well as on technological problems solution to create new generation of inexpensive ocean/sea bottom long-term observatories but with sufficiently high level of parameters, development of sensors that can operate stably over long times and take advantage of observatory infrastructure. Harmonization of interfaces to facilitate the interchangeability of instruments and the sharing of maintenance tasks is also between sessions interests.

XXIV2007

PERUGIA
I T A L Y



(S) - IASPEI - International Association of Seismology and Physics of the Earth's Interior

JSS016

Oral Presentation

2339

Inexpensive ocean bottom long-term geomagnetic observatory

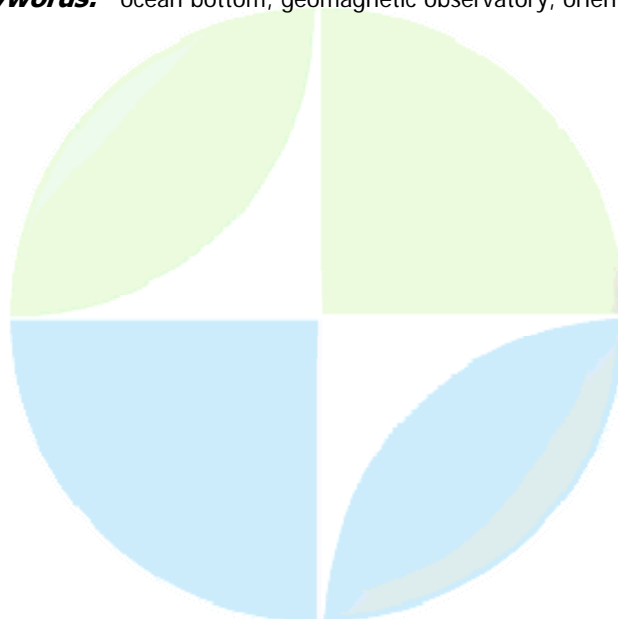
Prof. Valery Korepanov

Laboratory for EM Investigations Lviv Center of Institute of Space Research IAGA

Andriy Prystai, Yevhen Klymovych, Oleksandr Kuznetsov

The need for long-term geomagnetic observatories at the ocean bottom is widely recognized by international scientific community in order to provide optimally sampled observations of geomagnetic field variations. Such a global coverage is necessary to improve the magnetic dynamo model as well as to monitor time-dependent processes in the Earth's interior on global and regional scale. The technological problems of the realization of such a long-term geomagnetic observatory are analyzed. At the present state of the electronic components and microprocessor technique development the major difficulty presents not technological, but specific methodological aspects of the magnetic field measurement and data transmission. First the electromagnetic environment at deep sea is considered and expected spectral density of magnetic oscillations is estimated with the aim to determine necessary measurements resolution and sampling rate. Next the most important aspect magnetometer sensor orientation and calibration in automated mode without moving parts is discussed. It is proposed to use the method of Euler angles determination of the randomly oriented coordinates frame of the station at the sea bed relatively to the reference Earth's geomagnetic coordinates frame. It is shown that having the magnetometer data collected in this randomly oriented frame plus information about Z axis deviation from vertical position and the data from nearby geomagnetic observatory it is possible to calculate the corresponding Euler angles and to rotate virtually the randomly oriented sensitivity axes of the sea-bed magnetometer in order to reduce the data obtained in the random frame to the reference geomagnetic frame. Following the obtained recommendation an inexpensive autonomous sea-bed automatic magnetometer is constructed and successfully tested. The efficiency of the proposed methodology was experimentally confirmed. The peculiarities of the sea-bed magnetometer design destined for the International Ocean Network and its performances are presented. This study was partially supported by the STCU Project -3165.

Keywords: ocean bottom, geomagnetic observatory, orientation



(S) - IASPEI - *International Association of Seismology and Physics of the Earth's Interior*

JSS016

Oral Presentation

2340

A New Method for the Mosaic of Multibeam Bathymetry Data

Mr. Fanlin Yang

Key Laboratory of Foundational Geo-information Shandong University of Science & Technology IASPEI

Cuiyu Sun, Xiangwei Zhao, Xinzhou Wang

Multibeam sonar system (MBES) usually has a wide swath. Refraction artifacts and Roll residuals are usually presented in multibeam survey and more obvious in flat seafloor and shallow water environment. They are very serious for the edge beams of swath and very trivial at nadir, so the mosaic for neighboring swaths is difficult because of these errors. Roll residuals are obvious on orthogonal plane, so they can be solved easily. However, in some situations, especially in the estuary, sound speed changes rapidly. SSP can not be accurately obtained while surveying. Sound refraction artifacts can seriously degrade the quality of final result. A postprocessing method for the removal of roll system residuals and sound refraction artifacts must be researched as early as possible. A new method for solving this problem is presented by this paper. Because of the limit of mounting method, the transducer can not be placed in ideal position. A patch test may not solve this problem perfectly, too. If some swath data in a flat seafloor are projected along orthogonal direction, the shape of data on projection plane likes V. When we change the roll parameter, the shape of artifacts will vary as roll parameter modulates. When the V is disappeared, this roll parameter in this time is that we need. Then sound refraction is removed by one kind of postprocessing method based on equivalent SSP theory. According to former research, a real SSP can be displaced by a new SSP under the some prerequisites. We present a new SSP model. It has three water layers. The two upper layers are constant sound speed gradient layers, and the third layer has same sound speed gradient and sound speed with the deepest layer of measured SSP. The unknown parameters include surficial sound speed c_0 , the sound speed c_1 in first and second layer interface, the bottom depth z_1 of first layer and the bottom depth z_2 of second layer. In order to simplify the algorithm and retain the basic shape of raw profile of each ping, we correct the raw data on the basis of their raw positions and depths. We assume that the original water column only has one layer and the sound speed is 1500m/s. Travel time and arrival angle of each beam can be recalculated according to the raw across-track distance and depth, instead of raw record. So c_0 is 1500m/s. The total depths of first and second layer are known. If we assume that the two upper layers have the same thickness, the unknown parameter will only leave one, i.e. c_1 . Then a search algorithm is adopted to obtain the sound speed c_1 in first and second layer interface. The spatial position of each beam will be recalculated according to the new SSP. To avoid a local optimization, the depth at nadir must control the final result. In order to limit the impact of terrain, multibeam data must be divided into many sub-regions. Each ping in sub-regions is projected along track direction. However, a discontinuity will occur at the edges of sub-regions. In order to solve this problem, the parameters of each sub-region will be only owned by the central ping. All other pings will be calculated through the interpolation between sub-regions. Finally, the redundant beams for two neighboring swaths are removed. After all procedures have been finished, the fine mosaic can be obtained. The method is verified by the simulated and real data and has been applied in processing a large area data.

Keywords: multibeam sonar, roll residual, refraction

(S) - IASPEI - *International Association of Seismology and Physics of the Earth's Interior*

JSS016

Oral Presentation

2341

MOBB: A Long Term Broadband Seafloor Observatory in Monterey Bay:

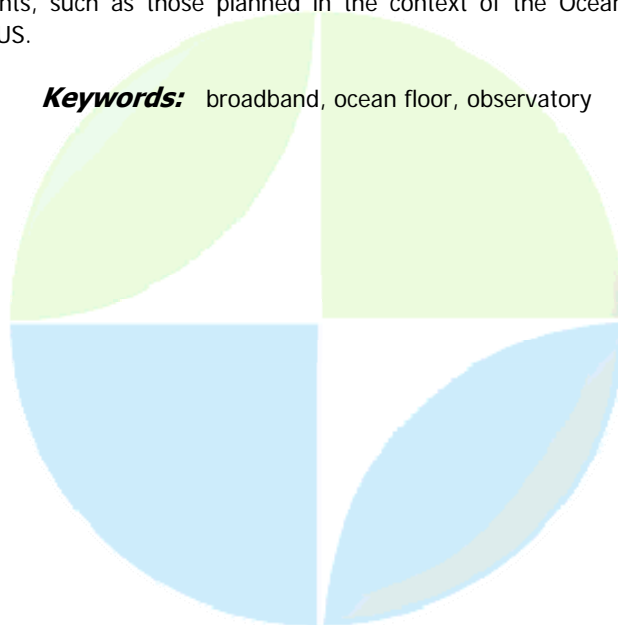
Prof. Barbara Romanowicz

Berkeley Seismological Laboratory University of California at Berkeley IASPEI

***Paul McGill, Doug Neuhauser, David Dolenc, Debra Stakes, Robert Uhrhammer,
Tony Ramirez***

A continuously recording autonomous broadband seismic station was installed in April 2002 in Monterey Bay (California), 40 km off-shore at a water depth of 1000m, and has been operating ever since. MOBB (Monterey bay Ocean floor Broad Band project) is a collaborative project between the Monterey Bay Aquarium Research Institute (MBARI) and the Berkeley Seismological Laboratory (BSL). This is a pilot project towards extending the on-shore broadband seismic network in northern California, to the seaside of the North-America/Pacific plate boundary, providing better azimuthal coverage for regional earthquake and structure studies. The system comprises a three component Guralp CMG-1 seismometer with a 360 s corner period, buried below the ocean floor, as well as a current meter and DPG (differential pressure gauge) installed in the vicinity of the seismometer. The recording and battery package, which is installed nearby in an anti-trawling device, is exchanged every 3-4 months with the help of the MBARI ROV Ventana. The data are archived at the Northern California Earthquake Data Center (NCEDC: <http://www.ncedc.org>). The data accumulated over the past 5 years has enabled studies of long period seismic noise in shallow buried near-coast ocean floor environments. We discuss the sources of this noise, which are either signal-generated (due to reverberation of seismic waves in the shallow seafloor sediments), or due to ocean processes such as infragravity waves. We have developed procedures to reduce the level of this noise by post-processing and illustrate this with some examples. During the next year, we will develop an interface to connect the MOBB system to the MARS cable (Monterey Accelerated Research System; url {<http://www.mbari.org/mars/>}) whose termination is less than 4 km from our site. Connection to the cable will provide real-time, continuous seismic data which will be merged with the rest of the northern California real-time seismic system, as part of the Berkeley Digital Seismic Network (BDSN). This will serve as prototype for other real-time multi-parameter cabled systems which comprise both analog and digital devices with a variety of sampling and timing requirements, such as those planned in the context of the Ocean Observatory Initiative (OOI) program in the US.

Keywords: broadband, ocean floor, observatory



(S) - IASPEI - *International Association of Seismology and Physics of the Earth's Interior*

JSS016

Oral Presentation

2342

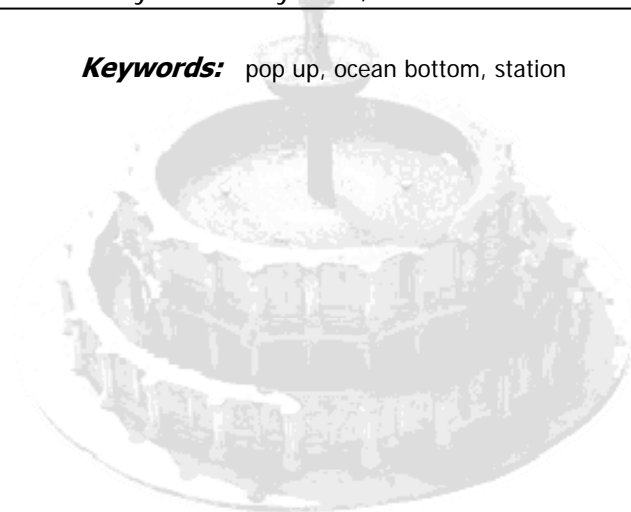
Development of a pop-up ocean bottom station for investigations of groundwater seepage and underwater earthquakes

Dr. Aleksey Kontar

Geophysics P.P. Shirshov Institute of Oceanology IASPEI

Submarine groundwater seepage could be of importance for various underwater operations (acoustic interference, etc.). Radon (Rn-222) can be a valuable tracer of direct groundwater discharge on the ocean floor. Also changes in the radon emission of groundwater have come to be known as one of the precursory phenomena of a submarine earthquake. Although Rn-222 in water may be measured reliably by classical methods such as radon emanation techniques, this approach can only provide information about water bodies over limited time periods. Ideally, studies of groundwater discharge would include measurements on the bottom of the ocean of dissolved radon concentrations integrated over various periods including time scales of days to weeks using a pop-up bottom station. Unfortunately, fine-scale temporal analysis is invariably limited by sampling logistics and time constraints. Therefore, it is desirable to develop a detection system which could be deployed on the bottom of the ocean and provide monitoring either in real time, for a rapid site assessment, or moored for a more extended period to provide a continuous record. We have designed a few varieties of an underwater radon detection system, suitable for deployment on the bottom of the ocean. One design is based on a new plastic scintillator with unique features that make it appropriate for in situ measurement of the alpha-activity of natural waters. A negative charge on the detector is used to attract positively-charged Rn-222 daughters to the detector surface. Monitoring of the 6.0 MeV alpha particles associated with the decay of Po-218 allowed concentrations of 4 pCi/L to be determined in 15 minutes with an uncertainty of 11%. The detector is made of a silicon semi-conducting PIN photodiode, an amplifier module, a water-proof connector and a bias battery. All of these are protected from water by a hydrophobic microporous membrane which allows diffusion of radon gas, but excludes water. The 25 μ m thick polypropylene hydrophobic membrane has a pore size of 0.04 \times 0.12 μ m and a 35% porosity, and is attached as a flat sheet to the end of the cylindrical container. The microporous membrane is pinched between flanges of the container and reinforced with a chlorovinyl board with 56 openings (1.0 cm ID each). These characteristics allow only gas dissolved in the water to pass into the detector chamber, except at very high pressures when water will move through the pores. A hydrophobic and insoluble polymer is used as a polymer base for the plastic scintillator. This material is superior to such polymers as polycarbonate and polyethylene-terephthalate with respect to size stability when humidity increases. The thickness of the plastic scintillator is set equal to an average path length of the alpha-particles. The scintillator is placed on the outer surface of a transparent (visual spectrum band of the electrical wave range) waterproof case so direct contact with the environment is achieved. A photo-detector with a large diameter (370-382 mm) hemispheric photoelectric cathode is located inside the waterproof case. This scheme permits monitoring large water volumes with a relatively small sized counter (a 450-500 mm diameter sphere) with low background (less than one background pulse per minute). The electronic equipment consists of a threshold anode pulse discriminator; a transformation unit for converting battery voltage into rated voltage values to supply the photo-detector and electronic equipment; a counter, timer, and buffer memory for brief and permanent data storage; a signal forming unit with a hydroacoustic package unit; and a hydroacoustic release mechanism. Data may be transmitted over the hydroacoustic channel and written on the permanent data carrier. A lithium battery supply unit could supply a minimum of 4,500 hours of continuous operation. Various deployment scenarios of a new pop-up ocean bottom station also were proposed.

Keywords: pop up, ocean bottom, station



IUGG

XXIV2007

PERUGIA
I T A L Y



(S) - IASPEI - *International Association of Seismology and Physics of the Earth's Interior*

JSS016

Oral Presentation

2343

Surprising Science Arising from Exploring the Earth from Deep Ocean Observatories

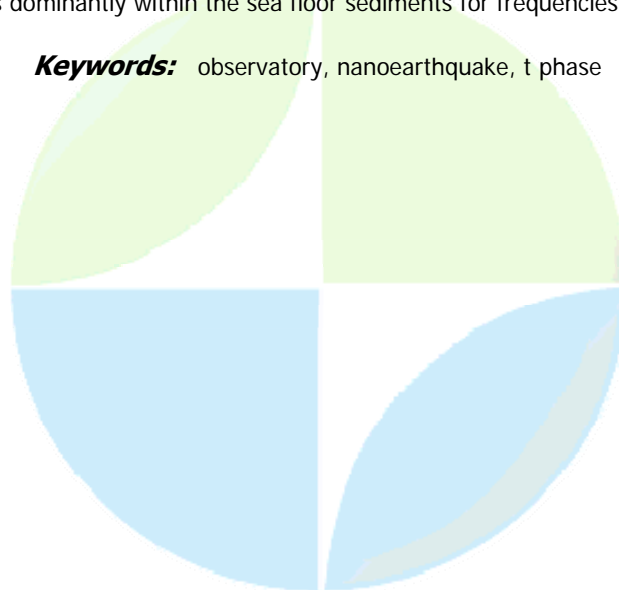
Dr. Rhett Butler

Global Seismographic Network The IRIS Consortium IASPEI

Fred Duennebier, Cinna Lomnitz

The Hawaii-2 Observatory (H2O) deployed at the sea floor between Hawaii and California from 1998-2003 and the Ocean Seismic Network Pilot Experiment (OSN1) deployed in 1998 225 km SSW of Oahu each yielded scientific results which were unanticipated when the observatories were planned and funded. These 'surprises' present the essence of discovery in science and offer compelling motivations for continuing our scientific exploration of Earth in the deep oceans, not simply for what we hope to find, but rather for what we have not yet even imagined. Nanoearthquakes ($M < 0$) have been observed in the 45-50 m.y. age upper oceanic crust at H2O. These tiny events illuminate the crust and yield direct observations of shear-wave birefringence, indicating 3% anisotropy in the basalt. High-frequency (up to 20 Hz) seismic P waves propagating in the oceanic lithosphere have been routinely observed at H2O propagating from earthquakes from the Aleutians to California and from Hawaii. However, corresponding shear-waves have been seen at H2O only from Hawaii, indicating significant propagation variability in the northeast Pacific lithosphere. T-waves from earthquakes (1,000-10,000 km distance range) have been observed not only at the sea floor H2O site, which is more than a km below the conjugate depth of the SOFAR channel, but also 245 m below the sea floor in an ODP borehole at the OSN1 site. T-waves at H2O are observed in this 'shadow zone' as undispersed high-mode Rayleigh/Scholte waves seismoacoustically coupled at the sea floor interface. Acoustic scattering processes from internal waves and thermohaline covariation (spice) in the upper ocean have not been able explain these observations, which may represent a new, coupled-mode interface wave propagating at the sea floor. The observation of T-waves from an earthquake in Guatemala at OSN1, whose path is blocked by the Island of Hawaii, is consistent with scattering from the vicinity of the Cross Seamount. The seismoacoustic T-waves observed by shallow-buried seismometers at both H2O and OSN1 are strongly radially polarized, whereas the OSN1 borehole sensor shows vertical polarization consistent with an evanescent wave. At the H2O site where both a seismometer and hydrophone were deployed, T-wave energy resides dominantly within the sea floor sediments for frequencies below 5 Hz.

Keywords: observatory, nanoearthquake, t phase



(S) - IASPEI - *International Association of Seismology and Physics of the Earth's Interior*

JSS016

Oral Presentation

2344

A new ocean bottom cable system for dense observations of earthquakes on the seafloor

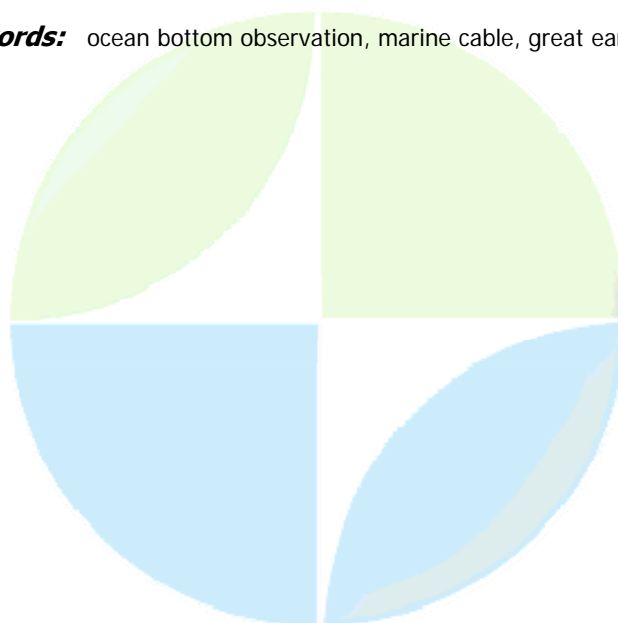
Dr. Toshihiko Kanazawa

Earthquake Research Institute, Univ. of Tokyo Professor IASPEI

Masanao Shinohara, Shinichi Sakai, Osamu Sano, Hisashi Utada, Hajime Shiobara, Yuichi Morita, Tomoaki Yamada, Katsuyuki Yamazaki

M8-class damaging submarine earthquakes occurred repeatedly at almost regular intervals at the subduction plate boundaries around Japan. The Pacific plate and the Philippine Sea plate subduct beneath the Japan Islands along ocean trenches of the Kuril Trench, the Japan Trench and the Nankai Trough, which locate off the east coast of Japan. Plate subducting causes repetitive occurrences of damaging earthquakes in Japan. Therefore the monitoring of seismic activities in the focal region of the damaging earthquakes is very important for earthquake forecasting. We have developed a new long-term ocean bottom seismometer (LT-OBS), which has an ability to record seismic signals continuously over one-year period. The LT-OBS is the most effective instrument to study seismic activities in the sea by a dense seismic network on the sea floor. However, OBS does not provide earthquake data in real time. Ocean bottom cable systems (OBCS) can optimize a real-time earthquake monitoring in the focal region of the damaging earthquakes. We have designed a new cost effective OBCS, jointly with engineers of various fields such as communication engineering, ocean engineering, metrology, electronics, and mechanical engineering. A main specification of a stationary type OBCS is as follows, 1. Landing Station: two place; both stations have power-feeding units for redundancy 2. Sensor: 40 of Seismometers and 3 of Tsunami sensors 3. Sensor interval: 20km for dense observation 4. Cable length: 900km 5. Dual Ring structured network of Ethernet switch for fault-tolerant and redundancy 6. Smaller sized OBCS housing for lower cost and easy handling onboard. 7. Delivery accuracy of time stamp: more than 0.1ms by PTP 8. Operational life: 20 years Authors will discuss new cost effective OBCS in detail in a paper, especially, new network structure for the OBCS, high precision time stamping, and high reliable analog signal digitizer interface design. Mobile type OBCS is within our system design target, too.

Keywords: ocean bottom observation, marine cable, great earthquake



(S) - IASPEI - *International Association of Seismology and Physics of the Earth's Interior*

JSS016

Oral Presentation

2345

Present status of seafloor electromagnetic stations in the northwest Pacific

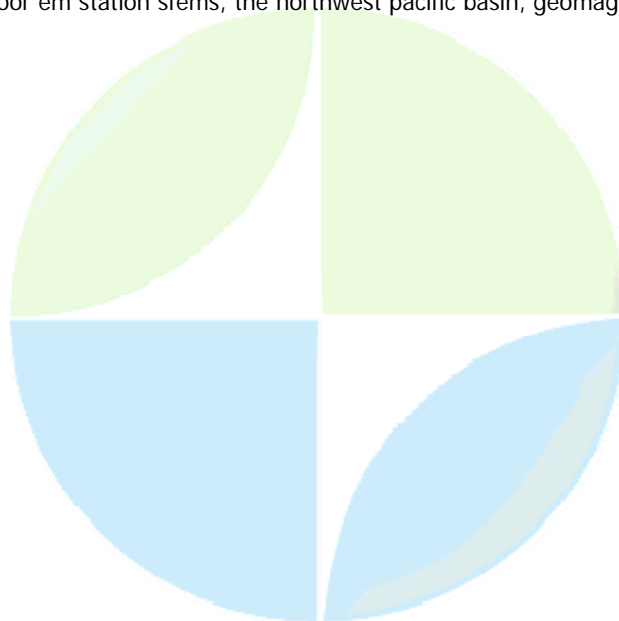
Dr. Hiroaki Toh

Earth Sciences University of Toyama IAGA

Yozo Hamano

WP1 and WP2 are known as the locations of borehole seismometers in the northwest Pacific. Close to each site, we are maintaining SeaFloor ElectroMagnetic Stations (SFEMSs) that monitor the geomagnetic field as well as the short-period geoelectric field. The EM sites are respectively called WPB (West Philippine Basin) and NWP (North West Pacific). SFEMS measures the absolute scalar geomagnetic total force by an Overhauser proton precession magnetometer, geomagnetic three components by a fluxgate vector magnetometer, horizontal two components of the geoelectric field and tilts in addition to temperature and the instruments azimuth at the seafloor by a fibre optical gyro. The 3.5-year long EM time series observed at NWP have been analyzed to yield the following two results: (1) Absolute measurements of not only the scalar geomagnetic total force but also the vector geomagnetic field components have been successfully conducted even by unmanned and pop-up type seafloor instruments. (2) The electrical structure beneath the 129Ma-old seafloor has been revealed as deep as 850 km using both magnetotelluric and geomagnetic deep sounding signals. It was not until we were able to acquire precise attitude data at the seafloor such as tilts and orientation that the former result was achieved. The scalar and vector secular variations at the seafloor were further confirmed by comparison with a couple of global geomagnetic field models based on recent magnetic satellite data (Oersted and CHAMP). It was a good surprise to see an excellent agreement between the observed and predicted geomagnetic scalar and vector secular variations, even though the seafloor and satellite measurements were completely independent. In this paper, we will report the present status of SFEMSs operated in the northwest Pacific, which covers the details of SFEMS, ability and limitation of the present instruments, the quality of the EM data derived so far, and possible future plans. Necessity of measuring precise tilts to recover the vector geomagnetic secular variation will also be emphasized.

Keywords: seafloor em station sfems, the northwest pacific basin, geomagnetic secular variation



(S) - IASPEI - *International Association of Seismology and Physics of the Earth's Interior*

JSS016

Oral Presentation

2346

The NEMO station deployment first result

Dr. Mario Salvatore Musumeci

Laboratori Nazionali del Sud Istituto Nazionale di Fisica Nucleare IAPSO

The Nemo Collaboration

The NEMO collaboration is carrying out an R&D activity aimed at the realization of a km³ an underwater Cherenkov neutrino detector. Long-term exploration of a 3500 m deep-sea site located at about 50 NM offshore the Sicilian coast (Capo Passero) has shown that it is optimal for the installation of the detector. The technological solutions proposed for the detector realization have been validated through a Phase-1 project, culminated in December 2006 with the deployment of a junction box and a prototype detector structure at a Test Site 14 nautical miles offshore the Catania harbour at 2000 m depth. The realization of a new infrastructure with a 100 km long electro-optical cable on the candidate site is under way. This Phase-2 project will provide the possibility to test detector components at 3500 m depth and will allow for a continuous monitoring of the site environmental properties. Both these cabled infrastructures, which were fully funded by the INFN (Istituto Nazionale di Fisica Nucleare), are planned to be part of the future European underwater research infrastructure recently defined by ESFRI.

Keywords: neutrino, cabled, infrastructures

PERUGIA
ITALY



(S) - IASPEI - *International Association of Seismology and Physics of the Earth's Interior*

JSS016

Oral Presentation

2347

European experience on Multiparameter Seafloor Observatories, technical-scientific solutions and open questions on sensors and data

Prof. Paolo Favali

Marine Unit RIDGE - Dept. Roma 2 Istituto Nazionale di Geofisica e Vulcanologia IASPEI

L. Beranzoli, M. Calcara, A. De Santis, G. Etiope, F. Gasparoni, N. Lo Bue, G. Marinaro, S. Monna

Almost 10 years have passed from the 1st experiment in Europe with GEOSTAR multiparameter seafloor observatory developed within EC projects. After that experience, many other developments and experiments has been completed both at European level (GEOSTAR-2, ORION-GEOSTAR-3, ASSEM) and at National level (NEMO-SN1). The presentation gives an overview of the technical-scientific solutions adopted for realisation of sensor prototypes, sensors installation and data quality control. The inadequacy of some sensors is also discussed. Finally the benefits of a multiparameter approach for the data quality assessment will be presented.

Keywords: multiparameter, sefloor, observatory



(S) - IASPEI - *International Association of Seismology and Physics of the Earth's Interior*

JSS016

Oral Presentation

2348

Multiparameter seafloor observatory deployed for tsunami warning

Dr. Francesco Chierici

Istituto di Radioastronomia Istituto Nazionale di Astrofisica

Luca Pignagnoli, Laura Beranzoli, Francesco Gasparoni, Luis Manuel Marques Matias, Davide Embriaco, Paolo Favali, Giuditta Marinaro, Nevio Zitellini

On September 2007 a multi-parameter observatory, equipped with a tsunami detector, will be deployed in the Gulf of Cadiz, in the framework of NEAREST EC Project. NEAREST is particularly addressed to tsunami detection and early warning in the tsunami-prone areas of the Portugal, Spain and Morocco Atlantic coasts. Among other deliverables, NEAREST project will produce and test basic parts of an operational prototype of near field tsunami warning system. This system is based on a onshore warning centre in charge of collecting, integrating, and processing data from the already operating geophysical monitoring networks. The seaside part of the system is an advanced type of tsunami detector, integrating a pressure sensor with a seismometer and accelerometers, installed on board of the sea bottom multi-parametric observatory GEOSTAR, capable of two way acoustic communication with a surface buoy. The buoy, equipped with meteo station and GPS, is connected to a shore station via radio and satellite links. This way we intend to combine the typical warning approach with the acquisition of geophysical, geochemical and oceanographic data.

Keywords: underwater observatory, tsunami warning, south west iberia

PERUGIA
ITALY



(S) - IASPEI - *International Association of Seismology and Physics of the Earth's Interior*

JSS016

Oral Presentation

2349

Permanent (OBS ALBORAN) and long term (RED FOMAR) OBS deployment at Gulf of Cadiz Alboran Sea (Ibero-Maghrebian Region).

Dr. Antonio Pazos Garca
FDSN member IASPEI

Jos Martn Davila, Elisa Buforn, Agustn Udas, Winfried Hanka

The Eurasian-African plate boundary crosses the called "Ibero-Maghrebian" region from the San Vicente Cape (SW Portugal) to Tunisia including the south Iberia, Alborn Sea, and northern of Morocco and Algeria. The low convergence rate at this plateboundary produces a continuous moderate seismic activity of low magnitude and shallow depth, where the occurrence of large earthquakes is separated by long time intervals. In this region, there are also intermediate and very deep earthquakes. To study this complex area, the Royal Naval Observatory in San Fernando (ROA) and the Universidad Complutense of Madrid (UCM), with the collaboration of the GeoForschungZentrum of Potsdam (GFZ), have deployed the Western Mediterranean Broad Band seismic network (WM), with stations located in southern Spain and Northern Africa, surrounding the Alboran sea and the Cadiz Gulf. Due to the fact of that many events are located at marine areas, and the poor geographic azimuthal coverage at some zones provided by land stations, the WM network will be complemented with a deployment of several broad band Ocean Bottom Seismometers (OBS) in the Gulf of Cdiz and the Alborn sea. One permanent OBS will be deployed in the vicinities of the Alborn island (OBS Alborn) and four long term (three years) temporal OBS's will be deployed at the Gulf of Cdiz and the Alborn sea (Red FOMAR), with the support of the Spanish Navy facilities (ships, divers,...). All them have been funded by the Spanish "Ministerio de Educacin y Ciencia" under the projects RIOA05-23-002 and CGL2005-24194-E. In this work we describe the present status of the OBS deployment, and the future planned steps, in the frame of the Western Mediterranean (WM) network activities.

Keywords: obs, western mediterranean



(S) - IASPEI - *International Association of Seismology and Physics of the Earth's Interior*

JSS016

Oral Presentation

2350

**Long-term Seismic Monitoring of the East Pacific Rise at 950 N ---
Scientific Findings and Implications for Future Permanent Ocean
Observatories**

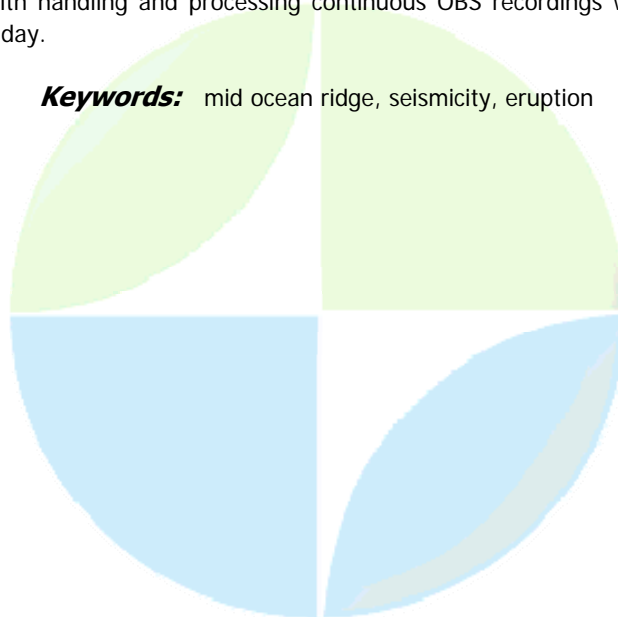
Dr. Felix Waldhauser

Lamont-Doherty Earth Observatory Columbia University IASPEI

Maya Tolstoy

An array of up to twelve short period Ocean Bottom Seismometers (OBSs) (Scripps L-CHEAPO) have been deployed at the Ridge 2000 East Pacific Rise Integrated Studies Site Bulls Eye at 950 N since October 2003. The array, occupying an area of approximately 4 by 4 km, has been turned-around on an approximately annual basis. It has been pulled out in January 2007, ending the longest continuous recording of local microearthquake activity at a Mid Ocean Ridge (MOR). The array captured the onset of a ramp up in the seismicity rate from ~36 events per day in 2003 to ~600 events per day in 2005 leading up to January 2006, when an eruption occurred within and near the array. While eight OBSs were either lost or buried in fresh lava, four were recovered, and at least two and possibly all four OBSs recorded the eruption and its seismic aftermath. Data from the first deployment (Oct 2003 - April 2004) has been analyzed and a total of 16,079 events were detected and located, of which approximately 7,300 events locate within the array (azimuthal station gap less than 180). High-resolution event locations based on hand-picked P- and S-wave arrival times image, for the first time, the basic structure of a hydrothermal circulation cell. In particular, we interpret a near vertical pipe of seismicity as an on-axis down-flow zone. The lateral positions of the shallow earthquakes in the pipe correlate with a kink in the axial summit trough, and an absence of nearby active hot vents. The deeper events are consistent with measured axial magma chamber depths (~1.4 km) and widths in the 950 N area. Data from later deployments are currently being analyzed and we expected that they provide insight into the temporal and spatial evolution of the eruption that occurred in January 2006. We use this experiment and associated data and results to highlight the scientific value of long-term local-scale seismic monitoring of MOR systems to further our understanding of the strongly time-dependent processes that drive divergent plate boundaries. We report on the characteristics and quality of the seismic data collected and our experience with handling and processing continuous OBS recordings with peak rates of over 2000 earthquakes per day.

Keywords: mid ocean ridge, seismicity, eruption



(S) - IASPEI - *International Association of Seismology and Physics of the Earth's Interior*

JSS016

Poster presentation

2351

Development of a new method of geophysical survey of saltwater-freshwater interface in the coastal zone

Prof. Evgeny Kontar

Experimental Methods Lab P.P. Shirshov Institute of Oceanology IAPSO

Yuriy Ozorovich

We report here some results of development of new method of geophysical survey of saltwater-freshwater interface in the coastal zone and mathematical analysis of the 3-D structure of the geo-electrical data obtained near the boat basin in Donnalucata in the province of Ragusa along the southeastern coast of Sicily, Italy. This geophysical survey and geo-mapping spatial distribution of the saltwater-freshwater interface in the coastal zone were conducted during the IAEA submarine groundwater discharge (SGD) experiment in Sicily. We have been using the MARSSES TEM sounding instrument, which has been developed at the Russian Academy of Sciences, based on time-domain electromagnetic sounding technology. Using TEM technology it is possible to conduct a subsurface sounding to a depth of up to 300 m. Our study have shown the presence of two layers with various mineralization of subsurface waters in the coastal zone of Donnalucata. The geo-electrical data have been taken for two subsurface zones with different type of subsurface water: resistivity = 5.37 Om-m and with mineralization of the groundwater on the order of 2000-2500 mg/L (basic water-sated horizon from 5 meters up to 15 meters in depth), and a second zone (depths from 50 meters up to 70 meters) with resistivity = 3.32 Om-m and mineralization of groundwater on the order of 4500 - 5000 mg/L. The analysis of the geophysical data have show the reason for the increase maximum SGD in the domain of measurements as revealed according to the results obtained by some other methods and different tools used in the offshore zone in the channel between two piers of the boat basin. This maximum discharge reflects the specific geological structure in the display of karstic groundwater phenomena of the coastal zone of Donnalucata, and provide a conceptual framework for understanding the effects of SGD processes in the coastal zone.

Keywords: submarine groundwater, coastal zone, underwater observatories



(S) - IASPEI - *International Association of Seismology and Physics of the Earth's Interior*

JSS016

Poster presentation

2352

Seafloor borehole seismic observatories in the western Pacific and upper mantle and crustal structure beneath the northwestern Pacific basin

Dr. Masanao Shinohara

Earthquake Research Institute University of Tokyo IASPEI

Tetsuo Fukano, Toshihiko Kanazawa, Eiichiro Araki, Kiyoshi Suyehiro, Masashi Mochizuki, Kazuo Nakahigashi, Yuka Kaiho, Tomoaki Yamada

Geophysical networks provide data for better understanding of the dynamics in the Earth. However, a great limitation on existing networks is the uneven distribution of stations, especially lack of stations in the ocean such as the Pacific. For uniform distribution of stations on the Earth, we need to construct observatories in the sea. The western Pacific area has been selected for installation of ocean-bottom observatories because it is ideal for problems related to plate subduction. Boreholes are considered to give best environment for geophysical observations in the sea. Four borehole geophysical observatories at three areas have been installed during ODP Leg186, 191 and 195. Two stations (JT-1 and JT-2) are located on the landward side of the Japan Trench. The observatories WP-1 and WP-2 are effectively located to complete a 1000-km span network in the western Pacific area. The WP-1 site is in the west Philippine Basin west of the Kyushu-Palau Ridge. The WP-2 observatory is situated in the northwestern Pacific Basin. Both the stations fill gap for global seismic networks. The WP-1 observatory was activated in March 2002 using an ROV and long-term observation started. In June 2006, an ROV dived to the WP-1 (fourth visit) and recovered the data. At this visit, data recording was discontinued. At present, seismic records of 692-days (Mar. 2002 - Feb. 2004) have been obtained from the WP-1. The WP-2 observatory was activated in October 2000 using an ROV. In June 2005, an ROV made fourth visit to the WP-2 and recovered the data. Recording at the WP-2 has been suspended from the fourth ROV visit. In total, 436-days data (Oct. 2000 - Jan. 2001, Aug. 2001 - July 2002) were retrieved. A detailed structure of an oceanic plate is important information to consider a dynamics of oceanic plate. Geomagnetic studies in the WP-2 area indicate the crust was formed 129 Ma. The seismic experiments with ocean bottom seismometers (OBSs), the WP-2 and airguns were performed around the WP-2 in July 2001, July 2002 and July 2005. To detect a seismic anisotropy in the uppermost mantle, the experiments had four profiles with different directions. Broadband seismic records for 436 days in total were retrieved from the WP-2. Reflecting low noise environment, many teleseismic events were recorded. The purposes of the present study are to obtain a detail seismic structure of crust and uppermost mantle including a seismic anisotropy from the seismic surveys and to estimate a upper mantle structure including depths of discontinuities using the WP-2 records. Shallow seismic velocity models just below OBS were derived from using tau-p method and records of a hydrophone streamer. The obtained seismic models were confirmed using the ODP logging data. Deep structures were estimated by forward modeling using a two dimensional ray tracing method. The estimated crustal structures beneath each line are almost identical. In a sediment layer, P-wave structure is 1.6km/s, S-wave is about 0.2km/s, the thickness of this layer is approximately 0.4km. The layer 2 is divided into two layers which have different vertical velocity gradients (layer 2A and layer 2B). The P- and S-wave velocities at the top of the layer 2A are 4.6km/s and 2.7km/s, respectively. The layer 2B has P- and S-wave velocities of 5.3km/s and 3.1km/s at the top of the layer, respectively. Total thickness of the layer 2 is about 1.4 km. The data from the WP-2 were useful to estimate the detailed structure of the layer 2. The uppermost Layer 3 has P- and S-wave velocities of 6.8km/s and 3.8km/s, respectively. The layer 3 is about 5km thick. To explain large amplitudes of Pn phase, a crust-mantle transition layer is required at the bottom of the crust. The Pn velocities are different in each profile. Average velocities of Pn and

V_p and V_s are 8.2 km/s and 4.7 km/s, respectively. The velocity variations are about 5% for P-wave and about 3.5% for S-wave. From this result, a seismic anisotropy of the uppermost mantle is suggested, and the fast direction seems to be perpendicular to the magnetic lineations. Therefore the anisotropy below the WP-2 is suggested to originate in a preferred orientation of olivine crystals in the uppermost mantle. The upper mantle velocity structure is inferred from travel times of earthquakes recorded by the WP-2 and the previous studies of the northwestern Pacific basin. To explain late first arrivals from the earthquakes with epicentral distances smaller than 2200 km, a low velocity zone below a depth of 30 km and a rapid increase of velocity at a depth of 210 km are needed. To perform receiver function analysis, we selected 16 events with a magnitude greater than 6, that have epicentral distance ranging from 30 degrees to 90 degrees, and have high signal-to-noise (S/N) ratio from the WP-2 data. A bandpass filter of 8-360 seconds was applied for the receiver function analysis. A velocity model named the WP-2 model which is modified Iasp91 model where crustal layers are replaced by the results of the airgun experiment was constructed. After the theoretical Ps-P times are calculated using the WP-2 model, travel times for large amplitudes of the receiver function corresponding to 410 km and 660 km discontinuities were read. Averaging the read times, conversion depths of 416 km and 666 km were obtained.

Keywords: seafloor seismic observatory, lithosphere, seismic anisotropy

IUGG
XXIV2007
PERUGIA
ITALY



(S) - IASPEI - *International Association of Seismology and Physics of the Earth's Interior*

JSS016

Poster presentation

2353

Underwater observation with new tool makes it different: Concept is not new, but the result is worth nugget

Mr. Kiyoyuki Kisimoto

Institute of Geology and Geoinformation Geological Survey of Japan, AIST IASPEI

Masato Joshima, Kiyokazu Nishimura

Whenever locally collected long-term observational data is to be analyzed to extract global phenomena, correction/estimation of local/regional effects on the data is always important. Especially in case of the ocean bottom observations with multi-disciplinary collaboration, careful site selection procedure or pre-survey is essential. Recent advancement of the swath bathymetric surveys provides us more and more accurate and high resolution topographic data and imagery of the seafloor. This is good news, however, we still have little data of even the shallowest part of the subbottom of the deep seafloor. Various kinds of deep submergence vehicles (DSVs) are now available for detailed ocean bottom experiments, such as ROV, AUV and HOV. In our presentation we show several new findings obtained by our latest tool called DAI-PACK (Deep-sea Acoustic Imaging Package) system, which is a portable piggy-back system to be accommodated on various DSVs. The DAI-PACK has two sensors, i.e. (1) deep-sea side-scan sonar and (2) deep-sea sub-bottom profiler and all components except sensors are packaged in an aluminum pressure sphere, which has been successfully installed as a piggy-back payload on several vehicles. The DAI-PACK is an off-line (stand-alone) system to avoid the interference with the DSVs. We have produced good results so far (1) detailed side-scan imagery of a hydrothermal area of deep-sea caldera in Izu-Bonin ridge, (2) subbottom layer profiles of very thinly sedimented off-ridge volcanoes near the southern East Pacific Rise, which is useful to infer the eruption dates, (3) underwater observation of 2004 Sumatra earthquake epicentral region using ROV, (4) mapping of the depth change of Gas-Hydrate sub-layers near the seabottom, which led to find the hydrate-ice exposure on the bottom surface near coast of Japan in 2006. The DAI-PACK system is a very useful site-survey tool for many ocean bottom observations.

Keywords: acoustic imaging, subbottom profiling, dai pack



(S) - IASPEI - *International Association of Seismology and Physics of the Earth's Interior*

JSS016

Poster presentation

2354

Effects of bias of reference GPS position on observation for ocean bottom crustal deformation

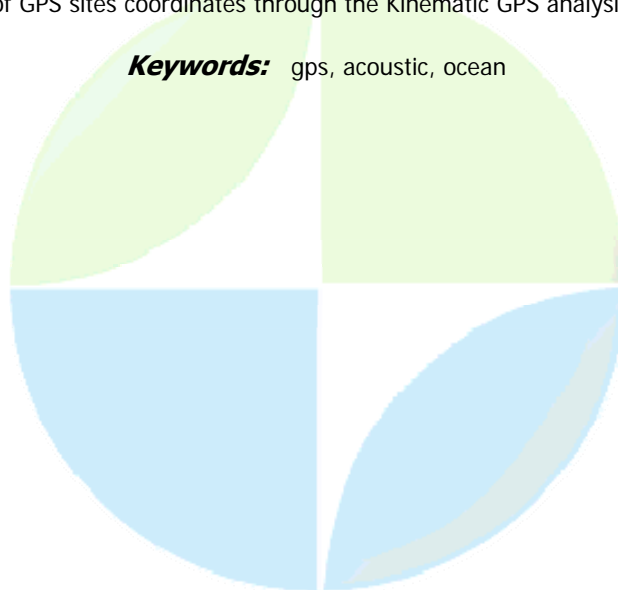
Dr. Tsuyoshi Watanabe

Graduate School of Environmental Studies RCSVDM, Nagoya University IAG

Keiichi Tadokoro, Takashi Okuda, Yoshitaka Aizawa, Shingo Sugimoto, Jin Yasuda, Daisuke Muto, Masataka Ando

Our research group, Nagoya Univ., has conducted the observation of ocean bottom crustal deformation by using GPS/Acoustic techniques to know the process of subduction of the Philippine Sea plate around the Nankai and Suruga Trough. In this system, we estimate the position of a surveying vessel by Kinematic GPS analysis and measure the distance between the vessel and the benchmark on the sea floor by Acoustic measurements. Next we determine the location of the benchmark. Repeated GPS/Acoustic observation has been conducted at the Kumano Basin and Suruga Bay since 2004 and 2005, respectively. For the repeatability of observation, the location of benchmark is determined within a precision of 2-3 cm at horizontal components at the Kumano Basin (Tadokoro et al., 2006). We have three continuous GPS sites on land for Kinematic GPS analysis, where a choke ring antenna is mounted on the top of the pillar and dual-frequency GPS data are collected every 0.2 second. each receiver records GPS signals continuously with a sampling interval of 0.2 seconds. However estimated GPS sites velocities are inconsistent with those obtained by GEONET. This difference may be caused by following two factors. The first factor is the difference of observation period. The second factor is annual and semiannual variations of GPS time series. We neglect annual and semiannual variations when we estimate GPS sites velocities. GPS/Acoustic observation is conducted for 2-4 days par one campaign. As for GPS site coordinate, we adopt the average coordinate for about 20 days, which includes one-week before and after observational days on the sea, as the reference coordinate for Kinematic GPS analysis. There is a possibility that GPS sites coordinates have some bias, because annual and semiannual variations are contained for about 20 days. In this study, we investigate how the determination of GPS sites coordinates affects the estimation of the location of benchmark on the sea floor. We use data between November 2005 and October 2006 at the Kumano Basin and estimate GPS sites coordinates using Bernese (Ver 5.0) software. Then we calculate the variation of the location of benchmark according to the bias of GPS sites coordinates through the Kinematic GPS analysis.

Keywords: gps, acoustic, ocean



(S) - IASPEI - International Association of Seismology and Physics of the Earth's Interior

JSS016

Poster presentation

2355

Gas-hydrates: a future potential source of energy in India

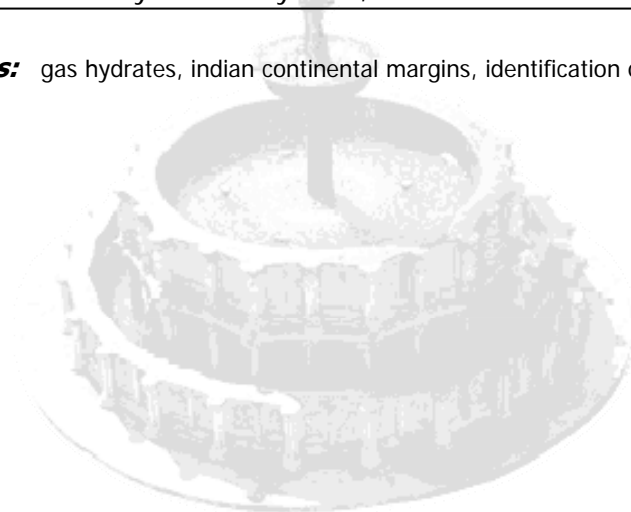
Dr. Kalachand Sain

Marine Geophysical Group National Geophysical Research Institute

KALACHAND SAIN National Geophysical Research Institute, Uppal Road, Hyderabad - 500 007, India

The energy-demand in developing countries like is growing very fast compared to industrial countries of the world. At present we import more than ~70% of our energy requirement and major discovery of hydrocarbons have not taken place during the last couple of decades. Since the economic growth with our huge population depends heavily on the energy security, we are desperately looking for an alternate form of energy. Gas-hydrates seem to be the best alternative. Gas-hydrates are crystalline form of water and low molecular weight hydrocarbons (mainly methane), and are formed at high pressure and low temperature in the outer continental margins and permafrost regions. These have attracted the global attention due to their wide-spread occurrences and potential as future major energy resources. Parameters such as bathymetry, seafloor temperature, sedimentary thicknesses, rate of sedimentation, total organic carbon content etc. indicate good prospects of gas-hydrates in the huge continental margins of . The methane gas stored in the form of gas-hydrates and underlying free-gas within our exclusive economic zone is estimated to be of the order of trillion meter cube, which can take care of our energy requirements for several tens of decades. The National Gas Hydrates Programs under the aegis of the Ministry of Petroleum & Natural Gas and the Ministry of Earth Sciences have initiated a lot of scientific plans and technological advancement for the exploration and exploitation of gas-hydrates. As a member of the national program, we are mainly involved in finding out the prospective zones and evaluating the resource potential using geophysical (seismic) data. Gas-hydrates are mostly detected by identifying an anomalous reflector, known as the bottom simulating reflectors or BSR on seismic data based on its characteristic features. We identified BSRs on available seismic data in the Kerala-Konkon, Krishna-Godavari andMahanadi basins and the Andaman region. The recent drilling expedition at the identified locations of gas-hydrates occurrences delineated a rich gas-hydrates deposit in the Krishna-Godavari basin. The Mahanadi basin and the Andaman region have been found very prospective for gas-hydrates. Much of the deep-water regions are yet to be explored. New data sets with suitable parameters are to be acquired to comprehend the lateral/areal extension of gas-hydrates, and assess their resource potential along the margins of Indian continent. As gas-hydrates are not stable at NTP, the existing technique, generally used for conventional hydrocarbons, cannot be used for exploitation. A concerted effort is going on in this direction. With the growth of technology, it is expected that methane from below the gas-hydrates can be exploited economically in near future. It may take a decade or so to produce gas from gas-hydrates. Therefore, it is high time to map the prospective zones of gas-hydrates and evaluate the resource potential. For this purpose, we have developed several seismic tools like travelttime tomography; waveform inversion; AVO inversion; AVO attributes; quality factors, seismic attributes etc. and will demonstrate their application to multi-channel marine seismic reflection data. We will also show that studies of quality factor and proxies like pockmark and gas escape features (like faulting or gas-chimney) offer indirect evidences for the identification of gas-hydrates in absence of BSR. As pure gas-hydrates have much higher seismic velocities than that of host sediments, presence of gas-hydrates increases seismic velocities, whereas free-gas below the hydrates-bearing sediments reduces the seismic velocity. Thus estimating accurate velocities using waveform tomography followed by rock physics modeling or invoking effective medium theory provide an excellent tool for quantifying gas-hydrates and/or free-gas across a BSR.

Keywords: gas hydrates, indian continental margins, identification quantification



IUGG

XXIV2007

PERUGIA
I T A L Y



(S) - IASPEI - *International Association of Seismology and Physics of the Earth's Interior*

JSS016

Poster presentation

2356

Repeated Observation of Seafloor Crustal Deformation Using a GPS/Acoustic System

Prof. Keiichi Tadokoro

Research Center of seismology and Volcanology Nagoya University IASPEI

Masataka Ando, Shingo Sugimoto, Takashi Okuda, Ryoya Ikuta, Tsuyoshi Watanabe, Keizo Sayanagi, Masahiro Kuno, Jin Yasuda, Daisuke Muto

The Nankai Trough is one of the active plate boundaries where the major subduction earthquakes, Nankai and Tonankai earthquakes, repeatedly occur. The source regions of the earthquakes are located beneath the sea bottom, and it is necessary to monitor the crustal activities, such as seismicity and crustal deformation, for the sake of earthquake prediction and disaster prevention. One of the useful tools to monitor seafloor crustal deformation is the observation system composed of the acoustic ranging and kinematic GPS positioning techniques. We install seafloor benchmark composed of three sea bottom transponders for acoustic ranging. We have installed the seafloor benchmarks at three sites close to the mid-Nankai Trough. We repeatedly observed at the two sites among them ten times at each benchmark from 2004. The result of the repeated observation shows that the repeatability of the measurement is about ± 3 cm for each horizontal component. The coseismic crustal deformation due to M7 class earthquakes was also detected at the sea bottom benchmark. We installed four benchmarks also at the Suruga Trough which is located at the northern margin of the Nankai Trough. We measured the benchmark 14 times for about a year. We observed a displacement vector of $(-3.8 \pm 3.3, 0.5 \pm 2.1)$, which is consistent with plate convergence at the region considering the error values.

Keywords: seafloor crustal deformation, nankai trough, acoustic ranging



(S) - IASPEI - *International Association of Seismology and Physics of the Earth's Interior*

JSS016

Poster presentation

2357

Evaluation of analysis method for GPS/Acoustic seafloor geodetic observation

Dr. Shingo Sugimoto

RSVD Nagoya University IASPEI

Keiichi Tadokoro, Ryoya Ikuta, Takashi Okuda, Yoshitaka Aizawa, Tsuyoshi Watanabe, Jin Yasuda, Daisuke Muto, Keizo Sayanagi, Toshiyasu Nagao, Masataka Ando

Observations of seafloor crustal deformation is very important to understand the dynamics of plate boundary that include the strain accumulation processes, great interplate earthquakes mechanisms, and submarine volcanoes activities. Since 2002, we have been developing an observation system with the GPS/Acoustic combination technique for monitoring of seafloor crustal deformation at the Suruga trough, central Japan. Repeated measurements of seafloor transponder can reveal directly the seafloor crustal deformation in the focal area of the subduction zone. The primary purpose of our observation is to detect and monitor the crustal deformation caused by the subduction where huge earthquakes repeatedly occur. GPS/Acoustic seafloor positioning determines both the weighted center of a seafloor transponder array and temporal change of acoustic velocity. We used cubic B-spline functions as basis functions to express the smoothed temporal change of acoustic velocity. The smoothness was represented by first order derivative of temporal change of acoustic velocity. We determined the hyper parameter which gives the most suitable smoothness by following two steps. 1) After dividing the two group dataset from all dataset with keeping the distribution, we carry out the seafloor positioning analysis for two halves and full dataset with various hyper parameters. 2) We adopted a best hyper parameter which calculates the closest seafloor positions by between each half and full dataset. Underwater acoustic ranging with respect to two or three seafloor transponders can estimate the temporal change of acoustic velocity accurately. On the other hand, Acoustic ranging with respect to one seafloor transponder continuously can not estimate the suitable temporal change of it. To estimate the temporal change of acoustic velocity correctly, we constrained the height component of all seafloor transponders on seafloor positioning. As a result for several observations, RMS of determined weight center of seafloor transponders array was 3-4 cm in horizontal. To evaluate the performance of this analysis and to evaluate the result, we carried out a synthetic experiment. We made synthetic travel-time data using certain velocity models and proper accidental errors with actual vessel positions. Through the synthetic experiments, we will discuss conditions for good repeatability of seafloor positioning.

Keywords: geodesy, underwater

(S) - IASPEI - *International Association of Seismology and Physics of the Earth's Interior*

JSS016

Poster presentation

2358

ESONET: a network to integrate European research on sea observatories

Prof. Paolo Favali

Marine Unit RIDGE - Dept. Roma 2 Istituto Nazionale di Geofisica e Vulcanologia IASPEI

R. Person, C. Berndt, J.J. Danobeitia, M. Gillooly, J. Mienert, J.M. Miranda, A. Tselepidis, T. Van Weering, C. Waldmann

ESONET (European Seas Observatory Network) is a European Network of Excellence (NoE) associating 50 partners (research centres, universities, industrials and SMEs) from 14 countries. More than 300 scientists and engineers will participate to its activities. The goal of the ESONET NOE is the lasting integration of European research on deep-sea multidisciplinary observatories. Over the initial 4 years, the approach will be to merge the programmes of members Organisations through research activities addressing the scientific objectives and networking activities specially designed for integration and spreading Excellence. ESONET NoE will create an organisation capable of implementing, operating and maintaining a network of multidisciplinary ocean observatories in deep waters around Europe from the Arctic Ocean to the Black Sea. The NoE will structure the resources of the participating institutes to create the necessary critical mass, remove barriers and through a joint programme of activities arrive at durable solutions for this future organisation. Long-term observatories are crucial for European scientists to maintain world leadership that was developed through past and present framework programs. Only long-term observatories allow continuous observation of large numbers of parameters collected through power intensive sensors. This capability is crucial for observing natural processes that are either very episodic or statistically require long time series to detect because they are hidden by noise of higher frequency. The most important ones are: (1) the episodic release of methane from the seabed affecting climate change, (2) the relationship between earthquakes, tsunami generation and submarine slope failures, and (3) the short term biogeochemical processes affecting the marine ecosystems. The ESONET observatories will provide information on global change, warnings of natural hazards and a basis for sustainable management of the European Seas. They will be a sub-sea segment of the GMES and GEOSS initiatives and linked to the EU INSPIRE initiative. A network of observatories around Europe will lead to unprecedented scientific advances in knowledge of submarine geology, the ecosystem of the seas and the environment around Europe. ESONET efforts will be part of a system extending around the world in co-operation with , and . The integration process will permanently underlie ESONET NoE action. ESONET NoE will foster energies in Europe to constitute a permanent organisation, promoting infrastructures that will operate for 10 to 30 years. A strong link has also to be established with the EMSO (European Multidisciplinary Sea Observatories) proposal, one of the main components of ESFRI in the FP7.

Keywords: deep sea, observatory, network

(S) - IASPEI - *International Association of Seismology and Physics of the Earth's Interior*

JSS017

2359 - 2394

Symposium

Lithosphere thermal state and geodynamic processes: from measurements to models

Convener : Prof. David Chapman

The lithosphere is identified as the outer layer of the Earth that is sufficiently cool and therefore rigid to act as a coherent tectonic unit. This symposium seeks papers from the many branches of geology and geophysics that relate to the thermal state of the lithosphere (heat flow, seismology, electromagnetism, petrology, etc) either from the perspective of measurements and data sets, or from creating models constrained by these data. Papers addressing geodynamic processes such as rifting, plate convergence, mid plate volcanism, delamination, underplating, etc. and their consequence for lithosphere evolution are especially welcome.

IUGG
XXIV2007
PERUGIA
ITALY



(S) - IASPEI - *International Association of Seismology and Physics of the Earth's Interior*

JSS017

Oral Presentation

2359

Temperature-time series, thermal regime and the instability of the fluid column in a borehole

Dr. Vladimír Cermak

Geophysical Institute Academy of Sciences of the Czech Republic IASPEI

The increase in sensitivity together with extended data storage capacity of data loggers has opened new horizons for detailed in-situ borehole experiments. Observational evidence proved that even when a borehole is in apparently well stabilized conditions, temperature data may exhibit certain unrest resembling irregular oscillations. (1) We demonstrate the results of monitoring experiments performed in widely different geological settings: incidental observations from Kamchatka, Finland and Mexico together with systematic studies performed in the test hole in Prague (Czech Rep.) covering time span of various length (days to months) with sampling interval varying from seconds to minutes. (2) Temperature in the borehole fluid (water) exhibits oscillation of the order of several thousandths or even hundredths of degree. (3) The character of the oscillation may differ depth to depth and (probably) also time to time. (4) Obtained temperature-time series displayed intermittent, non-periodic oscillations of temperature with sharp gradients and large fluctuations over all observed time scales. (5) Local growth of the second moment technique revealed the presence of at least two distinct temperature forming processes. One of them can be related to heat transfer in the structurally and compositionally complex subsurface. The second of them, which presents the bulk of the measured signal, probably reflects intra-hole convection. It can be demonstrated that at higher Rayleigh numbers the periodic character of oscillations characteristic for quiescent regime is superseded by stochastic features. The oscillatory convection occurs due to instability of the horizontal boundary layers. In spite of the fact that convection is characterized by slow motion, the oscillatory intra-hole flow and corresponding temperature patterns may exhibit features typical of turbulence. The synchronous arrangement of several data loggers (up to five) located at close depth intervals (a few meters) enabled to map time variation of the local temperature patterns at depth.

Keywords: geothermics, temperature time monitoring, borehole convection



(S) - IASPEI - *International Association of Seismology and Physics of the Earth's Interior*

JSS017

Oral Presentation

2360

withdrawn

Dr. Jacek Majorowicz
IASPEI

IUGG

XXIV2007

PERUGIA
I T A L Y



(S) - IASPEI - *International Association of Seismology and Physics of the Earth's Interior*

JSS017

Oral Presentation

2361

Heat flow variation with depth in Poland and Central Europe from deep equilibrium temperature logs and lithosphere thermal state

Dr. Jacek Majorowicz
IASPEI

Jan Safanda, Vladimir Cermak, Marta Wroblewska, Jan Szewczyk, Stanislaw Wybraniec, Marek Grad, Aleksander Guterch

High precision, deep, temperature depth (T-z) logs were obtained in three deep wells in Poland some three decades after the drilling ceased. These new logs give unique thermal equilibrium information for the western margin of the Precambrian craton and the Variscan accreted terranes. A heat flow of 50-60 mW m⁻² was determined in the lower 900 m of a 2900 m deep well at Torun (western part of the Precambrian craton) using estimated thermal conductivities from net rock analyses and measured thermal conductivities on core samples. We determined, using functional space inversion of the entire temperature-depth profile, that postglacial warming at Torun was 10-15 C. A 1044 m T-z profile at Czeszewo well (the Variscan platform) does not sample the region below the post-glacial warming signal, but our analysis also showed an increase in heat flow with depth in the region. The estimated heat flow is 65.1 mW/m². After correcting for the transient effects of post-glacial warming in the Czeszewo well, we estimated steady-state heat flow at 2 km depth to be 84.7 mW m⁻² to 86.6 mW/m², which agrees with heat flow estimates from below 2 km in other wells in the area. These changes in heat flow with depth are consistent with a model of the glacial cycles (90 - 25 - 90 - 25 - ...ka) with temperatures (0 - 14 - 0 - 14C - ...) and temperature before the onset of the cycles equal to the weighted average of one cycle [(90*0C + 25*14C)/115ka = 3.05 C]. In Udryn-Sidorowka wells (low heat generation norite -anorthosite intrusion in NE Poland - Precambrian craton) combined T-z from 2 profiles gives significant increase of heat flow with depth. Deep heat flow is 40 mWm⁻² at 2.3km. The estimated paleosurface temperature is -10C (Safanda, Szewczyk, Majorowicz.,2004 GRL). It is consistent with other studies in Central Europe in deep wells in Czech Republic, Slovenia and in the KTB well in Germany (Safanda & Rajver, 2001 GPCH; Clauser et. al, 1997 JGR). These study confirm that deep heat flow map of Central Europe requires correction and only deepwell heat flow determinations are useful for lithosphere modeling. These corrected deep heat flow values were used through Central Europe to study thermal lithospheric state. Large variations in the uppermost mantle velocity (from less than 7.9 km/s to >8.5 km/s) through the area of Poland and Central Europe suggest a transition between low velocity hot southern southwestern part and high velocity cold mostly northern and north-eastern part. This does not exactly agree with deep heat flow data in many areas of the Variscan inner and outer zones. High heat flow zones (>80mW/m²) occur in the areas of highest Pn velocities (>8.2 km/s) while low heat flow zones (40-60 mW/m²) occur in areas having relatively low Pn velocities (7.9-8.05 km/s). On the other hand, there is a good relationship between heat flow, crustal thickness, and elevation that is consistent with a simple isostatic model of the major tectonic units in Central Europe. This suggests to us that large compositional changes exist in the mantle below the Variscan foreland in TESZ (Trans-European Suture) zone.

Keywords: paleo heat flow, thermal lithosphere, permian basin

(S) - IASPEI - *International Association of Seismology and Physics of the Earth's Interior*

JSS017

Oral Presentation

2362

Interpretation and mathematical modelling of temporal changes of temperature observed in borehole YAXCOPOIL-1 within the CHICXULUB impact structure, Mexico

Dr. Jan Safanda

Department of Geothermics Geophysical Institute Prague IASPEI

Helmut Wilhelm, Philipp Heidinger, Vladimir Cermak

The geothermal research of the Chicxulub impact structure on the Yucatan Peninsula, Mexico, included repeated temperature logs of the 1.5 km deep borehole Yaxcopoil-1, which were done following 0.3-0.8, 15, 24, 34 and 50 months after shut-in of drilling operations. A gradual distortion of the linear temperature profile by a cold wave of the 0.8 -1.6 C amplitude was detected propagating downward from 145 m to 317 m within the observational period of 50 months (March 2002 April 2006). As an explanation of this unusual phenomenon, the hypothesis of a downward migration of the drilling mud, accumulated within the overlying and cooler highly porous and permeable karstic rocks during the drilling, was proposed. Velocity of the downward propagation of the cold wave decreased appreciably between the last two logs (December 2004 April 2006). It may indicate that the mud migrating downward through the system of interconnected caverns and conduits reached a bottom of the secondary porosity zone. We present results of simulations of thermal effects of the downward migrating drilling mud, obtained by a numerical solution of the heat transfer equation in a set of geothermal models of the borehole and its surroundings.

Keywords: yucatan peninsula, thermal conditions, hydraulic properties



(S) - IASPEI - *International Association of Seismology and Physics of the Earth's Interior*

JSS017

Oral Presentation

2363

Evolution of shallow crustal thermal structures from subduction to collision in Taiwan Region

Dr. Wu-Cheng Chi

Institute of Earth Sciences Academia Sinica IASPEI

Donald L. Reed

We study crustal thermal evolution by examining heat flow patterns along a convergent boundary from a young subduction zone to a more structurally-mature collision zone. More than 8000 km of seismic profiles covering a region of 45,000 km² offshore southern Taiwan show wide spread bottom simulating reflectors (BSRs). We derived 1107 BSR-based heat flows before combining additional 42 published offshore thermal probe data and 86 onland heat flow data to document the shallow forearc thermal structures from the subduction zone to the collision zone. In the subduction zone geothermal gradient ranges mostly within 30 to 80 °C/km, and decreases toward the ridge due to intensive dewatering at the toe, sediment blanketing effect, topographic effect, cooling from the subducting plate, and other processes. The temperature-depth relation derived from BSRs in the initial collision zone can be explained by a model with a maximum vertical steady-state flow rate of 6.7 mm/yr, suggesting possible upward fluid migration at the shallow depths. The heat flow reduction from blanketing effect can be reduced up to 50% due to fast sedimentation rates near the continental slope. The geothermal gradients range mostly from 30 to 90 °C/km in the collision zone, and increase, instead of decrease, toward the ridge, possibly caused by exhumation, erosion, topographic-induced ground water circulation, and some upper mantle processes related to collision. Heat flow in collision zone ranges from 80 to 250 mW/m². The high heat flow in collision zone correlates with shallower seismicity zone and high seismic attenuation. While the lower heat flow in the subduction zone might allow the earthquakes rupture to greater depth. The drastic increase in heat flow along the ridge from subduction to collision zone may cause overestimates in exhumation rates if a constant 30 °C/km geothermal gradient was used in fission track studies.

Keywords: heat flow, collision zone, bsr



(S) - IASPEI - *International Association of Seismology and Physics of the Earth's Interior*

JSS017

Oral Presentation

2364

Altiplano-Puna Elevation and the role of thermal isostasy

Dr. Claudia Prezzi

*Universidad de Buenos Aires - Ciencias Geológicas Universidad de Buenos Aires - CONICET
IAGA*

Hans-Jürgen Gtze, Sabine Schmidt

The most remarkable feature of the Central Andes is the Altiplano-Puna plateau. This plateau is characterized by 3.5 km average elevation, approximately 70 km crustal thickness and very high heat flow. Furthermore, below the Altiplano-Puna the existence of a partial melting zone at mid-crustal depth has been established by a number of independent observations (e.g. extreme high conductivity zones, broad low seismic velocity zones, etc.). This interpretation is strongly supported by the presence of a huge concentration of Neogene ignimbrites (most of them derived from crustal melting): the Altiplano-Puna Volcanic Complex. On the other hand, the forearc and the foreland basins have lower heat flow, thinner crust, and lower altitude. These features suggest that thermal isostasy could play a role in the compensation of the Altiplano-Puna. Thermal isostasy is the geodynamic process whereby regional variations in the lithospheric thermal regime cause changes in elevation. Elevation changes result from variations in rock density in response to thermal expansion. However the thermal contribution to continental elevation is difficult to assess, because variations in crustal density and thickness can mask it. This study estimates the elevation effect due to compositional variations and removes it by an isostatic adjustment, revealing the thermal and geodynamic effects on elevation. The effects of compositional and thickness variations within the crust were removed using the crustal density structure obtained for the Central Andes between 19S and 30S from 3D forward gravity modelling. The gravity model is very well constrained by a large amount of geophysical, geological, petrological and geochemical data. The elevation was adjusted for compositional buoyancy by calculating the density-thickness product from our 3D gravity model, relative to a reference crustal section (average crustal density: 2850 kg/m³, average mantle density: 3350 kg/m³, crustal thickness: 40 km). GTOPO30 digital elevation model was used to estimate the actual topography. The heat flow data base considered in this study includes new values recently published. The thermal isostatic relationship describing the thermal contributions to the elevation was determined using a reference geotherm corresponding to a surface heat flow of 30 mW/m² and assigning a lithosphere having this thermal estate an elevation of 0 km. Average elevation adjustments range between 300 and 3000 m, with maximum values of approximately 6000 m. It is observed that no correlation exists between the actual elevation and the corresponding heat flow values. In contrast, the compositionally adjusted elevation shows direct correlation with heat flow, with an increase of around 3000 m elevation between low and high heat flow zones. The forearc and the foreland basins areas are characterized by lower heat flow and lower elevation adjustments, whereas the Altiplano-Puna plateau, the Western Cordillera and the Eastern Cordillera, show higher heat flow and higher elevation adjustments. Our results suggest that while the thermal component of the Altiplano elevation would be of 1 km, the thermal contribution to the Puna elevation would be of 2 km. Previous works highlighted the fact that the Puna and the Altiplano have uniform average elevation in spite of showing great variation in the amount of structural shortening. Shortening estimates are sufficient to account for crustal cross sectional area in the Altiplano north of 22S, but are less than that needed in the Puna south of 22S. Other authors suggested that thermal heating and crustal flow would explain the uniform altitude of the Altiplano-Puna, in coincidence with our results. Moreover, it was determined that the above mentioned partially molten zone would extend in the backarc region between about 22 and 24 S and below the Altiplano-Puna Volcanic Complex area of caldera

concentration. On the other hand, our 3D gravity model shows the presence of shallower asthenosphere below the Puna than below the Altiplano, suggesting a possible relationship between the depth to the top of the asthenosphere and the higher heat flow, the existence of a mid-crustal partially molten zone and of the Altiplano-Puna Volcanic Complex in the Puna. The obtained results would suggest that the thermal state of the lithosphere could play a significant role in the elevation of the Central Andes.

Keywords: altiplano puna, thermal state, elevation



IUGG

XXIV2007

PERUGIA
I T A L Y



(S) - IASPEI - *International Association of Seismology and Physics of the Earth's Interior*

JSS017

Oral Presentation

2365

Thermal diffusivity of granulite rocks at elevated temperatures

Dr. Labani Ray

*Heat Flow and Heat Production Study National Geophysical Research Institute, Hyderabad
IASPEI*

H.-J. Frster, F.R. Schilling, A. Frster

The thermal diffusivity of felsic, intermediate, and mafic granulites from the South Indian Granulite Province has been measured at elevated temperatures (up to 550 C), using a transient technique. Measurements were carried out at intervals of 25 oC up to 100 C, and 50 oC at temperatures above 100 C. At room temperature, the thermal diffusivity of felsic and intermediate granulites ranges between 1.3 and 2.2 mm² s⁻¹, whereas that of the mafic granulites ranges between 1.2 and 1.4 mm² s⁻¹. The effect of radiative heat transfer is generally observed above 450 C. Below 450 C, i.e., in the conductive heat transfer zone, thermal diffusivity decreases between 35% and 45%. Rocks having a high thermal diffusivity at room temperature show a greater proportional decrease in diffusivity with increasing temperature and vice versa. The parameter, which has the greatest impact on the temperature dependence of thermal diffusivity, is the room-temperature thermal diffusivity, which itself is a function of the mineralogical composition of the rock. An equation has been derived for estimating thermal diffusivity D of granulites at higher temperature (T) and pressure (P) as $D = 0.7 \text{ mm}^2\text{s}^{-1} + 144 \text{ K} (DRT - 0.7 \text{ mm}^2\text{s}^{-1}) \times (0.1 \text{ GPa}^{-1}) / (T - 150 \text{ K}) + CT^3$ where DRT is room-temperature thermal diffusivity, T is the absolute temperature in Kelvin, constant C varies from 10⁻⁹ to 10⁻¹⁰ depending on intrinsic rock properties (opacity, absorption behavior, grain size, grain boundary, etc). This equation may be used in thermal modeling of deep crustal sections involving granulitic rocks, with the room-temperature thermal diffusivity being the only parameter to measure if heat transport by radiation can be neglected

Keywords: thermal diffusivity, temperature dependence, granulite rock



(S) - IASPEI - *International Association of Seismology and Physics of the Earth's Interior*

JSS017

Oral Presentation

2366

Brittle-ductile transition and cutoff depth of seismicity in the Apennines belt

Prof. Vincenzo Pasquale

DIPTERIS Universit di Genova Universit di Genova IASPEI

Paolo Chiozzi, Gianluca Gola

The thickness of the seismogenic layer in the continents is closely related to the mechanical strength of the lithosphere and accordingly to the occurrence of large earthquakes. The seismicaseismic boundary is thought to be related to the thermally-controlled brittle-ductile transition and the largest earthquakes in the crust occur near the cutoff depth of seismicity. Nevertheless, in some young orogenic belts, the connection between the thermal field and mechanical properties is still unclear. The paper focuses on this topic and analyses lateral variation of lithosphere rheology beneath the central-northern sector of the Apennines belt (Italy). The seismic activity recorded in the time period 1981-2002 is scattered along the entire belt. The number of quakes and the energy released are larger in the Internal Zone of the belt, where the maximum focal depth is 97 km. In this zone, the quakes define a slab dipping westward at an angle of 45 and the event with maximum local magnitude (5.9) occurred at 21 km depth. In the eastern part of the belt (External zone), the distribution of earthquakes versus depth presents two peaks; one at 5 km and another, more prominent, at 25 km narily at the depth of the maximum magnitude (5.1) earthquake. The b-value of the frequency-magnitude relation decreases with depth and eastwards; the largest value (0.955) is inferred in the western part of the belt (Peri-Tyrrhenian Zone), which shows extensional tectonics, few earthquakes (maximum magnitude 4.3) and higher terrestrial heat-flow density (80-120 mW/m²). Since the lithosphere thermal state across the belt is far from equilibrium and at different stages of relaxation, rheological modelling was based on a transient thermal approach. Consequently, the expected mechanical behaviour is a function of time and position. The bottom depth of the brittle layer is 10 km in the Peri-Tyrrhenian Zone and 28 km in the External Zone, and the corresponding temperature range is of 310-380 C. In the External Zone, characterized by a compressional tectonic regime and large average mechanical strength, a 6 km thick brittle layer in the upper mantle with limiting temperature of 600 C below a ductile crustal layer is expected. In the Internal Zone, the deeper earthquakes are related to thermal conditions controlled by the vertical descent rate and time since the beginning of the lithosphere subduction. The empirical relation between the maximum depth of seismicity and the age of subduction allowed us to infer a convergence velocity of 2 cm/yr and a minimum temperature at the seismicity cutoff depth of 750 C.

Keywords: heat flux, rheology, seismicity

(S) - IASPEI - *International Association of Seismology and Physics of the Earth's Interior*

JSS017

Oral Presentation

2367

Mantle contributions to elevation in China continent: results of thermal isostasy analysis

Mr. Shan Bin

Key Laboratory of Dynamic Geodesy Institute of Geodesy and Geophysics, CAS IASPEI

Xiong Xiong

The failure of simple isostasy models which involve crustal density and crustal thickness alone, to explain the surprising observations of high elevation over thin crust and low elevation over thick crust in some tectonic blocks of China continent, suggests that the contribution of lithospheric mantle for isostasy should be incorporated. Thermal isostasy, which is based on the fact that a change in temperature results in a change in volume and therefore in density, should be taken into account. In this study, using mass balance model, we conducted thermal isostasy analysis to separate the contributions of crust and mantle to surface elevation. Based on 723 heatflow measurements in China mainland and additional data from the global heatflow dataset, we divided China mainland and its adjacent area into nineteen tectonic units to exhibit overall variations of heat flow pattern. The contribution of crust to elevation was calculated with crustal structure and related parameters which were derived from seismological studies. Introducing temperatures of Moho and thickness of lithospheric mantle, and applying mass balance model, we calculated the contribution to elevation from the buoyancy of lithosphere mantle. The results suggest that the elevation of most tectonic units could be explained well by integrating the contributions from crust and lithospheric mantle. For instance, the elevations of the Cuxiong and Tarim basins, 1900m and 1230m, are far from the predictions by Airy isostasy model, which are ~2275m and ~2050m, respectively. By assigning Moho temperatures of Cuxiong and Tarim basins, 900°C and 500°C, we obtained the results that the elevations were reduced by the mantle lithosphere contribution of ~-320m for the Cuxiong and ~-980m for the Tarim, resulting in a combined elevation of ~1955m for the Cuxiong and ~1070m for the Tarim, respectively. Therefore, after integrating the two contributions together, we found the elevation difference calculated by the mass balance model between the two tectonic units fitted well with the observed one. The contribution of lithospheric mantle can be understood in the way that high temperatures in the upper mantle reduce density by thermal expansion and compensate for thin high density crust, and vice versa. The compensation status was also in good agreement with the results of vertical crustal movement derived from geodetic studies. Our study suggests that mantle contribution to lithosphere isostasy is so important that it should be taken into account in isostasy analysis. Furthermore, since mantle contribution is estimated from lithosphere thickness and average temperature of lithospheric mantle, thermal isostasy analysis provides an effective way to constrain roughly the temperature of Moho in the areas where geothermal observations are not available.

Keywords: thermal isostasy, elevation, china

(S) - IASPEI - *International Association of Seismology and Physics of the Earth's Interior*

JSS017

Oral Presentation

2368

Thermal evolution and stability of the cratonic lithosphere

Prof. Jean-Claude Mareschal

GEOTOP-UQAM-McGill University of Quebec at Montreal

Claire Perry, Claude Jaupart

The Archean geological record indicates elevated temperatures in the lower crust while the preservation of Archean features in the mantle requires mantle temperatures to remain sufficiently low. Archean provinces are presently characterized by low heat flow, with an average of 41 mW m², i.e. less than the global continental average (56mW m²). The range of regionally averaged heat flow values in Archean Provinces (18-54mW m²) is narrower than in younger terranes. But there are important variations in crustal heat production between different Archean Provinces. At the end of the Archean, when crustal heat production was double the present, surface heat flow varied over a range (45-90 mW m²) as wide as that presently observed in Paleozoic Provinces. For the present-day vertical distribution of radio-elements, high heat production during the Archean is insufficient to account for elevated lower crustal temperatures. High temperature-low pressure metamorphism conditions require additional heat input, for example by emplacement of large volumes of basaltic melts, crustal thickening or higher concentrations of radio-elements in the lower crust than at present. In the Archean, with a crust thicker than 40km or with the radio-elements uniformly distributed throughout a 40km thick crust, the lower crust was near melting and, with an effective viscosity 10¹⁹ Pa s, it could not sustain the stress due to crustal thickening. Long-term crustal stability requires the enrichment of the upper crust in radio-elements through melt extraction from the lower crust. After root emplacement, thermal conditions in cratons remained far from equilibrium for 1-2Gyr. Depending on the mechanism of root formation, temperature at 150km might only be 150K higher than present, implying that the lithospheric mantle remained sufficiently cold and strong to preserve Archean features. In thick continental lithosphere, temperatures in the crust and deep in the continental root are effectively decoupled for a long time

Keywords: heatflow, craton



(S) - IASPEI - *International Association of Seismology and Physics of the Earth's Interior*

JSS017

Oral Presentation

2369

New heat flow data in the Indian Shield: implications for mantle heterogeneity beneath different terranes

Dr. Sukanta Roy

National Geophysical Research Institute, India Tectonophysics IASPEI

R. Srinivasan

Thirty-five new heat flow values have been determined in the greenstone-granite-gneiss and gneiss-granulite provinces of the southern Indian shield. The new sites include 11 in the largely tonalitic Western Dharwar Craton (WDC) where the rocks are in the age range of 3.3 to 2.6 Ga, 9 in the 2.5 Ga Closepet Granite (CG) batholith, and 15 in the Late Archaean and Pan-African gneiss-granulite terrain. Together with the data obtained earlier from measurements at 42 sites in the 2.6 to 2.5 Ga largely granodioritic Eastern Dharwar Craton (EDC), 4 sites in the WDC, and 21 sites in the gneiss-granulite province to their south, the present data set contributes to improved characterization of the thermal state of the southern Indian Precambrian crust. Results emerging from the study are as follows: (i) the WDC is characterized by low heat flow (range 29-32 mW m⁻²) relative to the EDC (range 25-51 mW m⁻²). (ii) The previously reported 28-45 mW m⁻², heat flow range for the gneiss-granulite terrain of south India, stands revised in the light of new heat flow value of 58 mW m⁻² determined in the Kerala Khondalite Belt. (iii) Measurements at two different crustal levels within a single pluton the Closepet Granite demonstrate that, heat flow variations in a batholithic unit can be explained by variations in radiogenic heat production at different crustal levels. Heat production generally decreases with depth in plutons although not necessarily in a systematic way. (iv) Mantle heat flow estimates in the Dharwar greenstone-granite gneiss province vary as follows: 11 mW m⁻² beneath the region of the oldest, unmodified tonalitic crust of the WDC; 12 -14 mW m⁻² in the Closepet Granite terrain, and 12-19 mW m⁻² in the EDC. While these estimates of mantle heat flow are consistent with the range observed in other Precambrian provinces (e.g., Canadian, African and Baltic shields), the region beneath the Late Archaean granulites south of the EDC and WDC but north of the Palghat-Cauvery lineament zone exhibits distinctly higher estimates in the range 23-32 mW m⁻². Crustal thermal models derived on the basis of heat flow and heat production datasets demonstrate that the variations in heat flow within the greenstone-granite-gneiss province of the Dharwar craton are explained by variations in heat production of upper crustal rocks. On the other hand, the granulitic terrain of the Dharwar craton exhibits a similar heat flow regime but a distinctly lower heat production in the upper crust relative to the greenstone-granite-gneiss terrain, which results in a higher component of mantle heat flow. Contrary to previous hypotheses, the Precambrian terrain of southern India cannot be represented by a single thermal model covering all the geological sub-provinces, but represents a mosaic of terrains with varying infra- and sub-crustal thermal regimes.

Keywords: heat flow, heat production, crustal thermal structure

(S) - IASPEI - *International Association of Seismology and Physics of the Earth's Interior*

JSS017

Oral Presentation

2370

High mantle heat flow and thermally induced stresses below Latur and Koyna seismogenic regions of Deccan volcanic Province, India: a case study

Dr. O.P. Pandey

Theoretical Geophysics National Geophysical Research Institute (NGRI) IASPEI

65 Ma old Deccan volcanic province, covered by a thick suite of tholeiitic basalt flows spread over almost 1/6th of Indian landmass near western margin, has been experiencing large number of moderate earthquakes since historical times. Many of these earthquakes like Koyna (1967), Latur (1993) and Bhuj (2003) etc. were of devastating in nature claiming heavy loss of human life and property. In spite of large number of studies in the past, possible seismogenic cause of such events are still not understood clearly. In this view, an attempt is made here to study in detail the prevailing thermal regime of the lithosphere beneath Latur and Koyna seismogenic regions, where a fairly accurate crustal and compositional structure has now become available through recent initiatives. This study indicates presence of high input of heat from the mantle (29-35 mW/m²) below these regions with temperatures at Moho reaching between 490oC and 600oC. Similarly, these regions are also characterized by a thin lithosphere, varying approximately between 90 km and 110 km, which is less than half to that usually found in comparable late Archean shield terrains elsewhere. In some segments, close to western margin of the Deccan volcanic province, where earthquakes are quite frequent, lithosphere has thinned down to as much as 40 to 50 km with Moho temperatures exceeding 800oC. It is felt that the lithosphere beneath Deccan volcanic terrain is quite warm which besides weakening the lithosphere, creating additional intraplate thermal stresses which is getting accumulated in apparently exhumed denser crust, where average crustal S velocities sometimes reach as high as 4.0 km/s. These thermal stresses act over and above to that generated by northward movement of Indian plate, thereby accelerating the process of earthquake nucleation beneath these regions.

Keywords: lithosphere, thermal state, seismogenesis



(S) - IASPEI - *International Association of Seismology and Physics of the Earth's Interior*

JSS017

Oral Presentation

2371

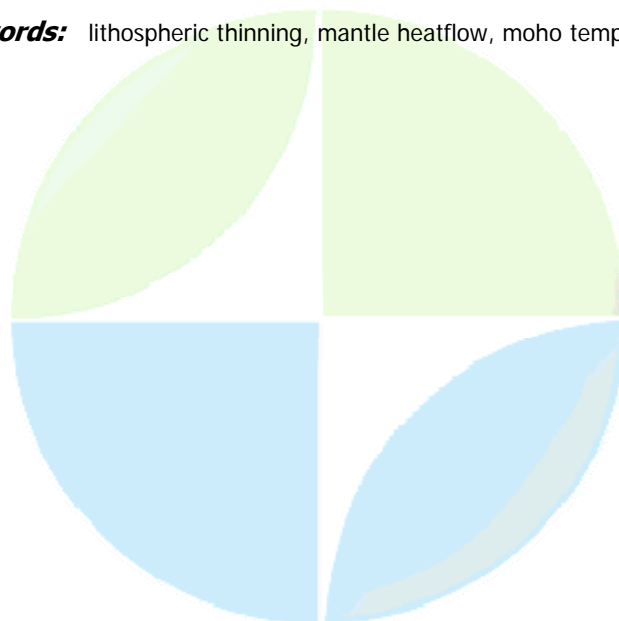
Thinning of hot Indian lithosphere : causes and consequences

Dr. O.P. Pandey

Theoretical Geophysics National Geophysical Research Institute (NGRI) IASPEI

Indian shield is unique and differs considerably from other stable areas of the earth. It has remained dynamic since at least late Archeans due to a number of long sustained tectonothermal events which repeatedly rejuvenated and remobilized the entire lithosphere. The continued reactivation over such a long period of time, which continues even now is not evident elsewhere. About two decades back, a preliminary attempt was made to study the thermal regime of the Indian lithosphere using the then available meager heat flow data set, which indicated the possibility of a quite thin and warm lithosphere beneath Indian shield. Since then, there has been a dramatic increase in heat flow numbers as well as new geological and geophysical informations. Consequently, the crustal structure is now better understood warranting a fresh look over the Indian shields thermal regime. Present study validates the presence of a thin lithosphere (average ~ 105 km compared to 250-300 km in similar terrains elsewhere) and a quite warm Moho with an average temperature close to 600°C beneath Indian cratonic shield. Thinning of the lithosphere has now been confirmed by recent multimode surface waveform tomographic and other geophysical studies. Beneath many of the late Archean segments, heat flow from the mantle exceeds 30 mW/m². An interesting inference which emerges from this study is that beneath certain ancient cratons, where gravity bias is distinctly positive, Moho temperatures and mantle heat flow reaches as high as 800°C and 45 mW/m² respectively with depth to the asthenosphere at only 65 km. It is felt that the long sustained reactivation may have led to the enrichment of lithophilic/radioactive elements at shallow mantle levels, which made it buoyant and fertile, thereby allowing for a thinner and weaker lithosphere. Such an order of thinning would result into the underlying lithosphere being subjected to a much higher insitu temperatures leading to sustained regional uplifting and exhumation of deeper crustal layers, which now appears to be so prevalent in the Indian shield. It may not be just a coincidence that almost all the catastrophic/damaging earthquakes which occurred since 1618 lie either on uplifted blocks or on their escarpment edges.

Keywords: lithospheric thinning, mantle heatflow, moho temperatures



(S) - IASPEI - *International Association of Seismology and Physics of the Earth's Interior*

JSS017

Oral Presentation

2372

Characterising the influence of latent heat effects on GST history

Prof. Christoph Clauser

Applied Geophysics RWTH Aachen University IASPEI

Darius Mottaghy

In moderate and high latitudes, the signature in borehole temperatures due to past surface temperature variations can be significantly influenced by latent heat liberated or consumed by freezing or thawing pore water, respectively. The magnitude of the effect depends on several parameters, most important porosity, but also the present-day and past ground surface temperature (GST), and basal heat flow. Depending on the depth of available borehole temperatures, we studied the impact on short term GST history inversions, as well as long term histories as far back as to the last glaciation. The influence of different parameters is investigated by generating a number of synthetic temperature logs and inverting them for ground surface temperature histories by a regularised Tikhonov inversion scheme. To this end we used a simple step forcing function. These simulations are performed both with and without latent heat effects. Regarding long-term GST history reconstructions and in view of possible corrections applied to inversions which neglect the latent heat effect, we find the difference between present-day and glaciation temperatures useful to quantify this effect. To illustrate possible corrections, we plot the dependence of this temperature difference (as a function of the latent heat effect) versus porosity, basal heat flow, present-day and past GST. Depending on parameter combination and present-day surface temperature, the neglect of freezing and thawing processes results in an overestimation of the postglacial warming of up to 4 K. We also studied the impact of the latent heat effect on GST history inversions on shorter time scales. Using a simplified, synthetic model for the temperature variations within the last 1000 years, we find that amplitude and duration of the cool period of the Little Ice Age and the recent warming are not large enough to cause a significant influence of the latent heat effect. However, neglect of this effect results in a clearly deteriorated timing.

Keywords: paleoclimate, borehole temperature, inversion



(S) - IASPEI - *International Association of Seismology and Physics of the Earth's Interior*

JSS017

Oral Presentation

2373

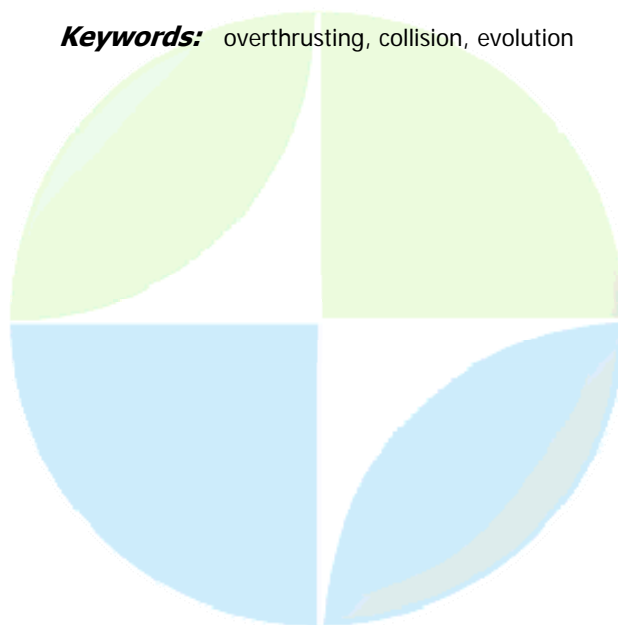
The influence of deformations on the P-T-t conditions in continental collisional structures

Dr. Olga Parphenuk

Physical processes of the Earth's interiors Institute of Physics of the Earth Russ. Ac. Sci.

Extensive development of horizontal and oblique motions of crustal plates and blocks leads to nonstationary disturbances in the thermal regime, the heat flow and the surface and Moho topography. Thermal-mechanical models of continental collision including horizontal shortening and brittle overthrusting in the upper crust and lower crustal viscous flow are applied to the simulation of the thermal and tectonic evolution of the overthrust structures. Finite-element 2-D modeling was used to examine the conditions under which ductile flow of the rheologically layered lower crust and upper mantle can produce the structure with crustal roots and surface uplift as a result of shortening, loading and erosion. The thermal effects of collisional process and postorogenic stage are studied. Thermal calculations show that the main temperature increase is observed at depths of the middle and lower crust and is fairly significant (up to 250K). In other words, the temperature characteristic of depths of 40-60 km is attained at depths of 20-40 km, creating there conditions for the partial melting. At the deeper mantle levels the collisional geotherms mainly follow the deformation. Since the collisional model is predominantly two-dimensional, it can provide insights into the variety of metamorphic conditions in a region that experiences deformations in a horizontal compression setting. Different P-T histories and the variety of metamorphic conditions at the surface are obtained as a result of the upward movement along the fault, the additional loading redistribution due to erosion, and the viscous compensation at the level of the lower crust. The final and postcollisional stages are characterized by the significant heat flow increase because of the thickening of the heat producing upper crust layer. The sedimentary basins are formed at the edges of the collisional uplift by the rocks denudated from the surface elavation. At the frontal edge of the thrust sheet the basin depth reaches the value of ~ 4 km with the maximum erosion level of ~9 km. At the postcollisional stage the compressional regime is changed by extension but under the stresses of an order of magnitude less. The research is supported by the Russian Foundation for the Basic Research (grant 06-05-65221).

Keywords: overthrusting, collision, evolution



(S) - IASPEI - *International Association of Seismology and Physics of the Earth's Interior*

JSS017

Oral Presentation

2374

Continental crust-rheology, thermal state and petrology

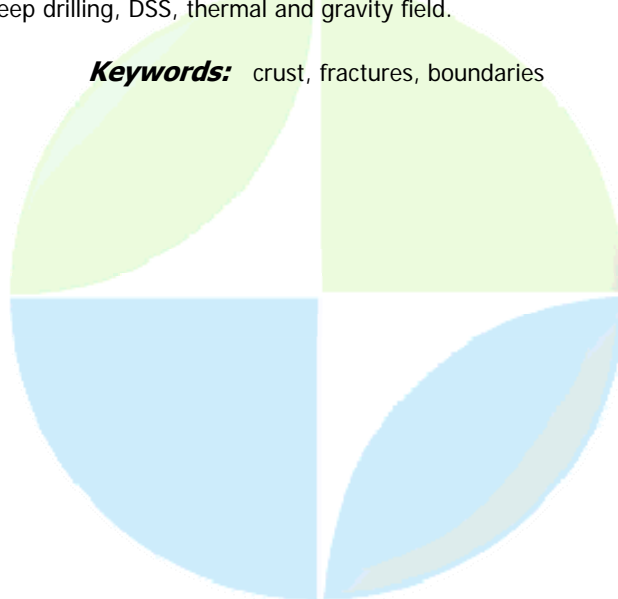
Dr. Svyatoslav Milanovskiy

Institute Physics of the Earth Russian Academy of Science IAHS

Nikolaevskiy Viktor Nikolaevich, Kaban Mihail Konstantinovich

Shear fracture of rocks depends on general level of pressure and temperature and is generated by the tectonic stress difference. Corresponding correlation of triaxial experimental data of core fracturing with deep seismic sounding leads to the concept of the Earth crust stratification by the fracture intensity. Types of rupture of rock materials are classified according to their changes with pressure and temperature. Granite is selected as a typical geomaterial of the continental crust. There are two distinct criteria of brittle-ductile transition. The first one is defined by disappearance of stress drop and corresponds to the Conrad boundary. The second is disappearance of stable cracks in finite state and corresponds to the Mohorovichich boundary. It explains low velocity and electric resistance zones by cataclastic (semi-brittle) geomaterial states that possess high fluid permeability (due to dilatancy) and therefore admit intense mass transfer. However, at the Mohorovichich boundary the thermodynamic state corresponds to true plastic failure, correspondingly the rock permeability for fluids is annihilated and phase transition to mantle rocks occurs at the Moho. Stresses that are necessary for tectonic rupture and crust dynamic are estimated. Seismic reflectors are explained by deep listric faults filled with crushed or intruded geomaterials. Deep fault inclination can be used for estimation of stress anisotropy. Waveguides are presented by bands of dilatant crack localization. Between the Conrad and Mohorovichich boundary the geomaterials are in cataclastic state with special dilatant rheology. The absence of elastic energy accumulation in the mantle is explained by rock strength dependence on strain rate. As a sequence earthquake hypocenters are concentrated above the Conrad boundary but they are absent beneath the Mohorovichich boundary. The Mohorovichich boundary the thermodynamic state corresponds to true plastic failure. This means the fracture permeability annihilation in rocks and transition to the upper mantle can take place. However, faults can cross the whole lithosphere in a brittle manner during earthquake events with high rate. Faults can exist in the lower crust beneath sedimentary basins. It explains fluidodynamics of mantle helium, hydrocarbons, etc., and their accumulation. In this work are presented results obtained during years of case study of continental crust based on superdeep drilling, DSS, thermal and gravity field.

Keywords: crust, fractures, boundaries



(S) - IASPEI - *International Association of Seismology and Physics of the Earth's Interior*

JSS017

Oral Presentation

2375

Surface elevation and stress regime derived from the thermal and compositional structure of continental lithosphere

Dr. Claire Perry
IASPEI

Jean-Claude Mareschal

The elevation of the continents is governed in part by the thermal and compositional structure of the lithosphere and in part by mantle dynamics. Heat flow and seismic data sets constrain the lithospheric temperature and compositional anomalies. In active tectonic regions, non-steady state geotherms are used to include the effect of extension, and possibly recent delamination events. We calculate the surface elevation of North America from the thermal buoyancy of the mantle lid and from crustal thickness and density. We also include variations in the composition of the mantle lid. Relative mantle lid density anomalies between the Archean, Proterozoic and Phanerozoic terranes of North America are presented and the residual topography is used to estimate the effect of compositional differences or dynamic mantle flow. The gravitational potential energy is calculated to determine how the distribution of lithospheric stresses in the continent affects the extensional regime.

Keywords: heat flow, upper mantle density, lithospheric stress

PERUGIA
ITALY



(S) - IASPEI - *International Association of Seismology and Physics of the Earth's Interior*

JSS017

Oral Presentation

2376

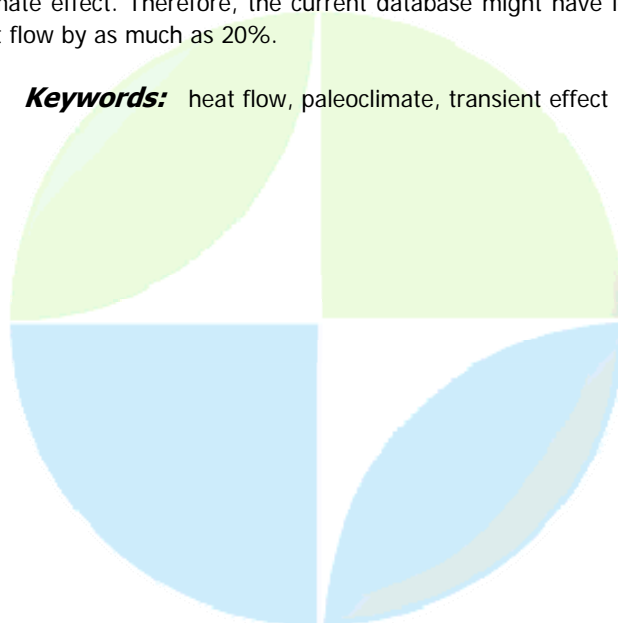
Transient effect of the last glaciation on the continental heat flow

Dr. Shaopeng Huang

Department of Geological Sciences University of Michigan IASPEI

Terrestrial heat flow is a measure of energy flux outward from the interior of Earth. On the one hand, it carries rich information about the tectonic history, the thermal structure of the lithosphere, and the bulk chemical composition of the crust on regional and global scales. On the other hand, a heat flow measurement is subject to the perturbation of various sources including past climate change. The assessment of the paleoclimate effect on a heat flow measurement requires a good understanding of the paleoclimate history. Taking advantage of the recent advances in paleoclimate research, I reevaluate the transient effect of the last glaciation on the continental heat flow. Ice core records (Dahl-Jensen et al., 1998, *Science*; Alley, 2000, *Quaternary Sci. Rev.*) show that the ice sheet temperature in Greenland was at least 20 degrees Celsius colder at the last glacial maximum than at the present. An array of GCM models (Winton, 2006, *Geophys. Res. Lett.*) confirm that climate change is amplified in arctic areas by almost a factor of two. Accordingly, I approximated the global ground surface temperature history over the past 50,000 years with an amplitude-reduced version of the Greenland ice core paleotemperature record, and supplemented the adjusted ice core record with the borehole-proxy integrated climate reconstruction over the past 500 years (Huang, 2004, *Geophys. Res. Lett.*) and the meteorological record over the past 150 years (Brohan et al., 2006, *J. Geophys. Res.-Atm.*). Additionally I assumed a progressively increasing uncertainty up to 50% at 50,000 years before present. A set of subsurface temperature models are then synthesized by forward simulation. The results show that the apparent heat flow within the upper 2000 m of the crust is systematically lower than the actual terrestrial heat flow because of the impact of the last glaciation. For example, the estimated discrepancies between the true and apparent heat flows at the depth of 500 m fall in the range of 14 +/- 6 milliwatts per square meter in these models. The last glaciation transient perturbation is generally more profound at shallower depths. The uppermost 500 m of the crust embraces over 60% of the continental measurements residing in the global heat flow database (Pollack et al., 1993, *Rev. Geophys.*) of the International Heat Flow Commission. Most of those measurements have not been corrected for paleoclimate effect. Therefore, the current database might have led to an underestimate of the continental heat flow by as much as 20%.

Keywords: heat flow, paleoclimate, transient effect



(S) - IASPEI - *International Association of Seismology and Physics of the Earth's Interior*

JSS017

Oral Presentation

2377

Thermal state of the upper mantle beneath the Japanese Islands inferred from seismic tomography

Dr. Alik Ismail-Zadeh

Geophysical Institute Karlsruhe University IASPEI

Satoru Honda

Constraints on present temperature are essential for understanding mantle dynamics at present and in the past. We develop a model of the present thermal state of the upper mantle beneath the Japanese islands and surrounding area by inverting P-wave velocity anomalies of the high-resolution global seismic tomography. In the forward modeling of synthetic seismic velocity anomalies the effects of anharmonicity, anelasticity, and partial melting on seismic velocities are considered. To the east and southeast of the Japanese islands seismic temperature anomalies (with respect to the adiabatic geotherm) indicate relatively cold (down to about 190 km) lithosphere of the Philippine Sea plate subducting beneath the Japanese islands. The upper mantle beneath the region warms with depths, and the temperature anomalies reach up to 300 deg. at the depth interval of 348 to 410 km remaining relatively warm down to the bottom of the upper mantle and perhaps even deeper. To the west of the Japanese islands warm uppermost mantle becomes cooler at the depths of about 220 km to 500 km and warms up below the depths. To the southwest of the islands the upper mantle is relatively warm (temperature anomalies are up to about 200 deg.) and cools at the depths below the transition zone where a huge pile of cold lithosphere (temperature anomalies are down to about 300 deg.) is believed to stagnate at the boundary between the upper and lower mantle. We analyse a sensitivity of the temperature model with respect to dry and wet solidus and estimate regions of possible melting. The thermal model is constrained by measured heat flow in the region.

Keywords: seismic temperature, velocity anomaly, japan



(S) - IASPEI - International Association of Seismology and Physics of the Earth's Interior

JSS017

Oral Presentation

2378

New geothermal data from URAL SUPERDEEP WELL SG-4

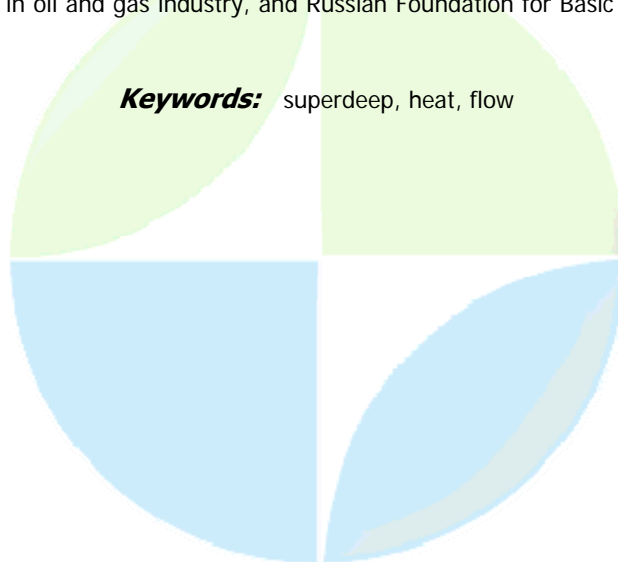
Prof. Yuri Popov

Technical Physics and Rock Physics Russian State Geological Prospecting University IASPEI

Dmitriy Miklashevskiy, Raisa Romushkevich, Dmitriy Korobkov, Oleg Esipko

Previous determinations of conductive component of heat flow density (HFD) for the Ural deep well SG-4 has been done within a depth interval 400-4800 m (Popov et al., 1999) using results of the measurements of rock thermal properties on 4160 cores at normal conditions and temperature logging data for the well shut-in time of 5305 days. Influence of formation pressure and temperature on thermal conductivity (TC) has been estimated as negligible from literature data taking into account low temperatures of the formation (about 77 °C for 4800 m). The results have shown a significant increase in HFD with a depth from 23 to 60 mW/m². New experimental geothermal data have been obtained in 2005-2006 after the SG-4 well bottom has reached 6000 m. Equilibrium temperature gradient values have been estimated from the temperature logs recorded within a depth interval 376-1000 m. Additional measurements of rock TC have been performed on 416 cores from a depth interval of 4800-5951 m. Total length of cores studied reached ~600 m that is about 10% of a well length. Increase in rock thermal conductivity at water-saturation was established to be 520%. Amount of SG-4 cores studied exceeds by ~1.6 times a total amount of rock samples studied in geothermal investigations of the Ural earlier (near to 2800 samples acc. to I. Golovanova, 2005). Our new instrument has been applied to measure rock TC in-situ conditions at simultaneous influence of elevated temperature and pressure on 19 cores uniformly selected from a depth interval of 6505-939 m. The measurements confirmed that rock TC does not change essentially at formation pressure and temperature and decreases by 4% in average without a certain regularity with a depth. The HFD values have been determined for every depth interval of 100 m with slimming along the well by 10 m within a depth interval of 3005-950 m. Within 3001-1000 m average HFD value (26-29 mW/m²) is in good accordance to previous data inferred from shallow wells (21-32 mW/m²). Essential HFD increase is observed below 1200 m. As a result, the HFD value reaches 53-62 mW/m² within a depth interval of 3500-5950 m with average value of 55 mW/m². The obtained HFD data prejudice previous HFD estimates in the SG-4 drilling site, which could be understated, and raise a question on previous conclusions about abnormally low values of terrestrial HFD in the region. Authors wish to acknowledge generous support of Schlumberger Oilfield Services, an international company in oil and gas industry, and Russian Foundation for Basic Research (grant 05-05-64879).

Keywords: superdeep, heat, flow



(S) - IASPEI - *International Association of Seismology and Physics of the Earth's Interior*

JSS017

Oral Presentation

2379

Continental Elevation and Upper Crustal Radioactivity

Prof. David Chapman

Geology and Geophysics University of Utah IASPEI

Derrick Hasterok

Continental elevation is an accurate and easily observable dataset that may be used as a constraint on geodynamic processes. Elevation contributions due to geodynamic processes are typically on the order of 10s to 1-2000 meters, which can be easily masked due to the larger contributions of compositional and thermal buoyancy. In order to observe the geodynamic contributions to elevation, the compositional and thermal effects must be estimated and removed. Our ability to identify the geodynamic contributions to elevation is made possible when uncertainties related to the compositional buoyancy can be accurately determined. In this study, we make an isostatic correction for compositional buoyancy, develop a general thermal isostatic model for the continents, and explore heat production as a large potential contributor to observed elevation. The elevation of 73 global tectonic provinces are adjusted for the effect of compositional buoyancy by computing an isostatic adjustment relative to a standard crustal section (average density of 2850 kg/m³ and a 39 km thick crust). The crustal thickness and P-wave seismic velocity (VP) structure are determined for each province from seismic models; densities are computed using an empirical relationship derived from laboratory pressure-temperature-velocity-density data. Uncertainties in the elevation adjustment are estimated using a Monte Carlo analysis. Compositional elevation adjustments applied to a global set of tectonic provinces range from ~-1600 m in the Ukrainian Shield to 2300 m in the Gulf of California. Estimated uncertainties range from ~200 m to >600 m. Thermal buoyancy is estimated by integrating the difference between a geotherm derived from observed values of heat flow and a reference geotherm. The best fitting continental heat flow-elevation model has a reference heat flow of 43 mW/m² at 0 km elevation and a 70:30 partitioning of surface heat flow between reduced heat flow and upper crustal radioactive heat production. A set of North American-only provinces show a 60:40 partitioning. Whereas raw elevations of continental provinces show little correlation with heat flow, the compositionally adjusted elevations show a clear trend with about 4 km difference between cold and hot provinces. A continental heat flow-elevation plot is used to identify outliers in adjusted province elevations. A three provinces with anomalously high upper crustal heat production, the Wopmay orogen and the North and South Australian cratons, fall >1 km below the thermal isostatic modeled elevation. These regions illustrate the importance of constraining lithospheric heat production variations prior to estimating the geodynamic contributions to elevation.

Keywords: lithosphere, elevation, heatflow

(S) - IASPEI - *International Association of Seismology and Physics of the Earth's Interior*

JSS017

Oral Presentation

2380

The Carpathian Basins Project: an investigation of the evolution of the Pannonian-Carpathian orogenic system

Prof. Gregory Houseman

School of Earth and Environment University of Leeds IASPEI

G. Stuart, E. Hegeds, E. Brckl, S. Radovanovic, U. Achauer, A. Brisbane, A. Horleston, D. Hawthorn, P. Lorinczi, B. Dando, G. Falus, A. Kovcs, I. Trk, H. Hausmann, W. Loderer, V. Kovacevic, S. Petrovic, D. Valcic

The Pannonian Basin is the largest of a group of Miocene-age extensional basins within the arc of the Alpine-Carpathian Mountain Ranges. These basins are generally recognized as extensional in origin, but their formation is paradoxical because they are almost entirely surrounded by mountain chains of a similar age, which result from sustained convergence throughout and since the period of lithospheric extension. The lithospheric extension within the Pannonian region is usually attributed to the roll-back of subduction systems in which oceanic lithosphere was subducted beneath the outer Carpathians as the crust and lithosphere within extended. An alternative class of models relies on the idea of gravitational instability of the mantle lithosphere in which synchronous extension of the basin, and convergence of the peripheral mountain belts is driven by a convective overturn of the upper mantle. In either case however, these models remain conceptual and require further quantitative development and testing against observation. The Carpathian Basins Project (CBP) is a major international seismology collaboration within the framework of Topo-Europe, designed to provide much improved spatial resolution on the seismic velocity structure of the Pannonian and Vienna Basins. Starting in September 2005 we commenced the deployment of 60 portable broadband seismic stations in Austria, Hungary and Serbia. The CBP array has two major components: a regional broadband (to 100 sec period) array (RBB) of 10 stations across the interior of the Pannonian Basin, and a High-resolution Seismic Tomography array (HST) of 50 stations (broadband to 30 sec), spanning the Vienna Basin and the western part of the Pannonian Basin. Continuously recording for two years (RBB) and for one year (HST) respectively, these data will enable relatively high-resolution seismic tomography images of the lithosphere and upper mantle beneath the western part of the Vienna/Pannonia region to be obtained. The data also will enable receiver-function analysis, surface-wave analysis, and seismic anisotropy (SKS) measurements to be carried out. The object of these analyses is to examine the evidence for deformation of the mantle lithosphere and anomalous properties within the asthenosphere and upper mantle, in order to discriminate between different models for how this orogenic system evolved. The project is supported by a numerical modelling effort using 3D finite element methods to examine mechanical models of the formation and evolution of the basin. In these finite deformation models we track the development of stress and deformation in crust and lithosphere as the basin extends. We will report on progress to date in the CBP project.

Keywords: lithosphere, orogeny, stress

(S) - IASPEI - *International Association of Seismology and Physics of the Earth's Interior*

JSS017

Oral Presentation

2381

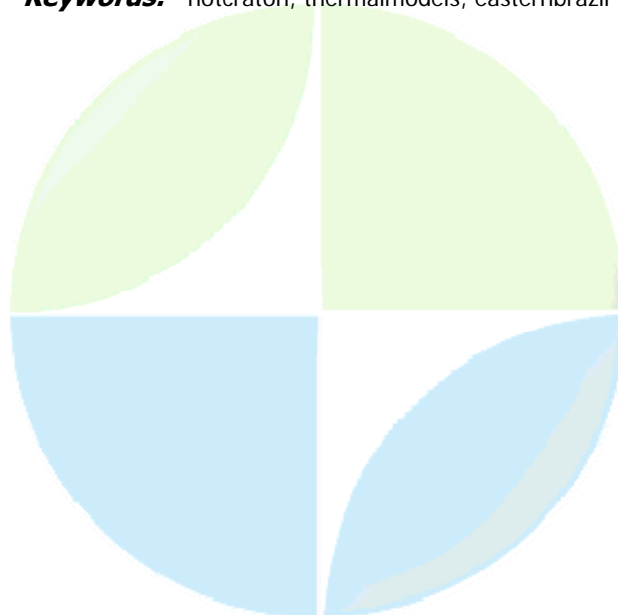
Heat flow and thermal models of a hot craton in the South American continental lithosphere

Prof. Valiya Hamza

Geofísica Observatório Nacional-ON, Rio de Janeiro, Brazil IASPEI

A detailed analysis of geothermal data from the highland area of eastern Brazil has been carried out as part of an attempt to understand regional variations in geothermal gradients and heat flow across the So Francisco craton and the neighboring metamorphic fold belts. The database employed includes results of geothermal measurements at 53 localities. The results indicate that the craton and the adjacent metamorphic fold belts are characterized by geothermal gradients in the range of 8 to 270C/km, with a mean of 14.3 0.8C/km. The estimated heat flow values are found to fall in the range of 30 to 70mW/m², with low values in the northern parts of the craton. Superimposed on this regional trend are the occurrences of several isolated small-scale anomalies with thermal gradients of greater than 40C/km (with corresponding heat flow values in excess of 80mW/m²). These are in general associated with over-thrust terrains on the eastern and western border of the craton. There are indications that lateral heat transfer by subsurface fluid circulation is responsible for the occurrence of such anomalous thermal belts. Crustal temperatures were calculated using based on a procedure that makes simultaneous use of the Kirchoff and Generalized Integral Transforms. The thermal models take into consideration variation of thermal conductivity with temperature as well as change of radiogenic heat generation with depth. Vertical distributions of seismic velocities were used in obtaining estimates of radiogenic heat production in crustal layers. The results point to temperature variations of up to 250oC at the Moho depth, between the cold northern and hot sothern parts of the craton. There are indications that such differences are responsible for the contrasting styles of deformation patterns in the metamorphic fold belts. 1. JSS017 2. Lithosphere thermal state and geodynamic processes: from measurements to models 3. So Francisco Craton, Thermal Models 4. Valiya Hamza, Observatório Nacional, Rua General Jos Cristino, 77, Rio de Janeiro Brazil, Tel. +55 21 2580 7081, Fax +5 21 2560 7081, e-mail: hamza@on.br 5. O 6. PC 7. NO 8. Carlos Alexandrino: NO, Valiya Hamza: YES 9. NONE

Keywords: hotcraton, thermalmodels, easternbrazil



(S) - IASPEI - International Association of Seismology and Physics of the Earth's Interior

JSS017

Oral Presentation

2382

The Post-Glacial Warming Signal in Heat Flow

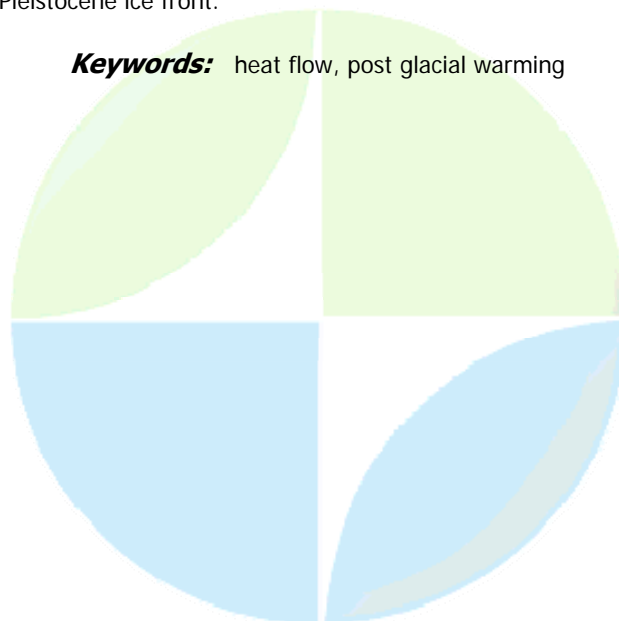
Dr. Will Gosnold

Geology and Geological Engineering University of North Dakota IASPEI

Jacek Majorowicz

We advance the hypothesis that post-glacial warming in northern hemisphere continents may have been of the order of 10 to 15 C rather than 3 to 5 C as is generally accepted in terrestrial heat flow research. If this hypothesis is correct, some northern hemisphere heat flow values may require revision by as much as 30 to 60 percent. We present several lines of reasoning that tend to support this hypothesis. First, analyses of ensembles of heat flow determinations in parts of Europe and North America show a systematic increase in heat flow with depth. These observations are not from analyses of heat flow variation in individual boreholes, but are of heat flow determinations at different depths in different boreholes. In Europe, the increase in heat flow with depth has been observed by analysis of more than 1500 deep boreholes located throughout the Fennoscandian Shield, East European Platform, Danish Basin, Czech Republic, and . There are significantly fewer deep boreholes in North America, but the increase in heat flow with depth appears in examination of a suite of 759 sites in the IHFC Global Heat Flow Database for the region east of the Rocky Mountains and north of latitude 40 N. Second, surface heat flow values in southern hemisphere shields average approximately 61 mWm⁻², but surface heat flow values in northern hemisphere shields average approximately 37 mWm⁻². There must be a physical or chemical reason for northern and southern shield areas of similar ages to have different heat flow values. The northern hemisphere post-glacial warming signal may be part of a combination of several possible explanations. A third line of reasoning is that the signal is subtle and cannot be recognized using the conventional heat flow practice of determining thermal conductivity and thermal gradients on only a short section of a borehole. Of special significance to this particular argument is the fact that two-thirds of all terrestrial heat flow determinations have been made in boreholes less than 1000 m deep and 87 percent of heat flow determinations in North America have been made in boreholes less than 500 m deep becomes more critical where. Finally, models T-z profiles based on warming by 15 C closely reproduce observed T-z profiles in 2 km deep boreholes in a region of North America that lies along the edge of the Pleistocene ice front.

Keywords: heat flow, post glacial warming



(S) - IASPEI - *International Association of Seismology and Physics of the Earth's Interior*

JSS017

Oral Presentation

2383

Conductive heat flow in the mediterranean region: pitfalls in low degree harmonic representations

Prof. Valiya Hamza

Geofisica Observatorio Nacional-ON, Rio de Janeiro, Brazil IASPEI

A comparative study numerical and spherical harmonic representation of conductive heat flow of the Mediterranean region has been attempted. The numerical representation indicate that heat flow is relatively high in the western half of the Mediterranean compared to its eastern parts, the exception being the area of the Aegean sea. However, harmonic representations based on the set of Legendre coefficients, published in 1993 (SHC93), are found to lead to regional heat flow trends characterized by a broad east-west anomaly but with subdued heat flow values. There are indications that this discrepancy in the regional trend between the numerical and SHC93maps arise from the lack of adequate spatial resolution in low degree harmonic representations. In an attempt to improve the spatial resolution regional heat flow maps were derived on the basis of new set of Legendre coefficients for 36 degree expansion. These maps reveal a pattern indicating high heat flow in the western parts relative to the eastern parts of the Mediterranean. The central segment of the heat flow anomaly is situated in the western off-shore region of the Italian Peninsula. The overall trend is thus similar to that observed in numerical representations.

Keywords: mediterranean, harmonicrepresentation, conductiveheatflow



(S) - IASPEI - *International Association of Seismology and Physics of the Earth's Interior*

JSS017

Poster presentation

2384

**The evaluation of the heat flow in the area of the Uralian Superdeep well
CF-4**

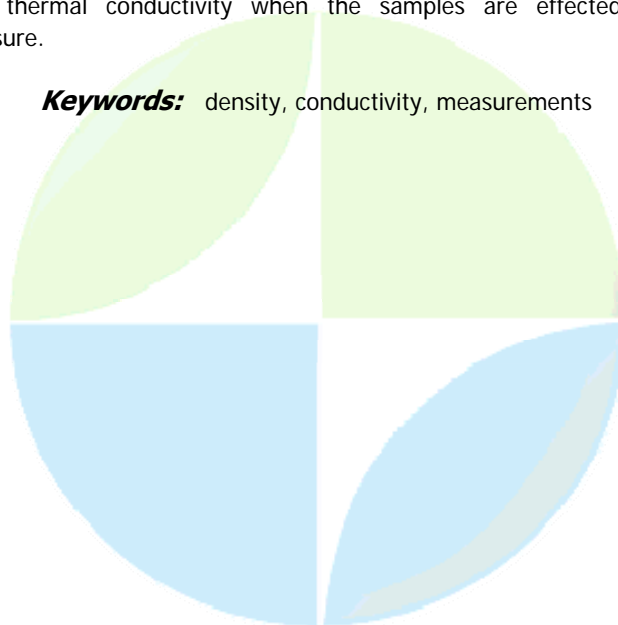
Prof. Aleksander Lipaev

development of oil and gas fields almetyevsk state oil institute IASPEI

Sergey Lipaev

In order to improve the accuracy of the heat flow value (q) the authors have carried out the measurements of the basalt samples thermal conductivity from the well CF-4 taken from the depths of 5010-5090 metres. The results of the investigations show that in the conditions of temperature increasing from 20 C up to 80 C with the constant pressure ($p=0,1$ MPa) all the investigated samples show the average 9-10 % decreasing of thermal conductivity (λ). At the same time in the conditions of the temperature changing from 20 C and pressure 0,1 MPa to the thermodynamic conditions of the basalt formation ($t=80$ C, $P=150$ MPa) the average 7-8 % λ increasing is observed which is the result of the temperature and pressure effects. The noted effect of the thermal conductivity increasing with the increasing of the reservoir depth is mostly characteristic for the Uralian area where the relatively low values of the depth temperature are observed. In this case the influence of the high formation pressure on the thermal conductivity may reduce the effect of the thermal conductivity decreasing on the temperature increasing and even surpass it. Three variants of the heat flow density evaluation have been carried out: 1) in the case when the thermal conductivity value is considered under the temperature of 20 C and atmospheric pressure, the heat flow for the depths range from 5010 to 5090 metres makes up 40,1 mW/m². 2) in the case when the only factor that is the temperature (80 C) influences the rock the nominal (calculated) value of the heat flow makes up 35,6 mW/m²; 3) the full consideration of the temperature and pressure effects on the rock thermal conductivity leads to the value of $q=42,9$ mW/m². The authors believe that the most true (reliable) q value is the last one, while measurements of rock thermal conductivity under the atmospheric conditions lead to the certain reducing of the heat flow value. And though it seems paradoxical, the consideration of only one of the two opposite factors of the influence on the rock λ , that is of the temperature factor, may lead to even more distorted result obtained. The paper, therefore, suggests the necessity of a methodology for measuring the rock thermal conductivity when the samples are effected by both parameters temperature and pressure.

Keywords: density, conductivity, measurements



(S) - IASPEI - *International Association of Seismology and Physics of the Earth's Interior*

JSS017

Poster presentation

2385

Temperature-time series, thermal regime and the instability of the fluid column in a borehole

Dr. Vladimír Cermak

Geophysical Institute Academy of Sciences of the Czech Republic IASPEI

The increase in sensitivity together with extended data storage capacity of data loggers has opened new horizons for detailed in-situ borehole experiments. Observational evidence proved that even when a borehole is in apparently well stabilized conditions, temperature data may exhibit certain unrest resembling irregular oscillations. (1) We demonstrate the results of monitoring experiments performed in widely different geological settings: incidental observations from Kamchatka, Finland and Mexico together with systematic studies performed in the test hole in Prague (Czech Rep.) covering time span of various length (days to months) with sampling interval varying from seconds to minutes. (2) Temperature in the borehole fluid (water) exhibits oscillation of the order of several thousandths or even hundredths of degree. (3) The character of the oscillation may differ depth to depth and (probably) also time to time. (4) Obtained temperature-time series displayed intermittent, non-periodic oscillations of temperature with sharp gradients and large fluctuations over all observed time scales. (5) Local growth of the second moment technique revealed the presence of at least two distinct temperature forming processes. One of them can be related to heat transfer in the structurally and compositionally complex subsurface. The second of them, which presents the bulk of the measured signal, probably reflects intra-hole convection. It can be demonstrated that at higher Rayleigh numbers the periodic character of oscillations characteristic for quiescent regime is superseded by stochastic features. The oscillatory convection occurs due to instability of the horizontal boundary layers. In spite of the fact that convection is characterized by slow motion, the oscillatory intra-hole flow and corresponding temperature patterns may exhibit features typical of turbulence. The synchronous arrangement of several data loggers (up to five) located at close depth intervals (a few meters) enabled to map time variation of the local temperature patterns at depth.

Keywords: borehole temperature, convection, temperature time monitoring



(S) - IASPEI - *International Association of Seismology and Physics of the Earth's Interior*

JSS017

Poster presentation

2386

Resolving terrain effects in borehole temperature profiles

Mrs. Shannon Heinle

Geology and Geological Engineering University of North Dakota IASPEI

William Gosnold

Reliable borehole temperature profiles are critical for paleoclimate analysis. As many climate workers have discovered, T-z profiles in boreholes can contain a variety of steady-state and transient non-climate-related signals. These noise signals include terrain effects such as, topography, land use, land cover, direct and diffused sun radiation, slope angle, and dynamic elements such as groundwater flow and variable precipitation, wind, and snow cover. Few of these effects can be quantified and therefore it is difficult to apply corrections to profiles. However, several studies have concluded that topographical effects, which exert the largest influence on temperature profiles, may be modeled with some degree of confidence. We are attempting to determine the specific terrain effects affecting borehole temperature profiles in the 130 United States boreholes included in the IHFC borehole paleoclimate data set and to determine the feasibility of correcting terrain effects on these boreholes. We are using a combination of remote sensing and field site visits in our analysis. Temperature profiles we have studied have shown promise in categorizing terrain effects.

Keywords: terrain effect, borehole, climate

PERUGIA
ITALY



(S) - IASPEI - *International Association of Seismology and Physics of the Earth's Interior*

JSS017

Poster presentation

2387

Hydro-geothermal characters of the Moroccan Atlas

Dr. Massimo Verdoya

Dip. Te. Ris. Universit di Genova IASPEI

**Yassine Zarhloule, Abdenbi El Mandour, Paolo Chiozzi, Mimoun Boughriba,
Abderrahim Lahrach**

The geological setting of northwestern Morocco is characterized to the west by the Maghrebide orogenic system, of Alpine age and referred as to the Rif domain, and to the east by the intra-continental Mesozoic-Cenozoic belt of the Middle Atlas. These ranges form the main recharge zones of deep water reservoirs. In the Middle Atlas there are several hydrogeological basins with minor shallow aquifers in the Plio-Quaternary terrains. A marly substratum separates the shallow groundwater from the deeper artesian aquifer, occurring in the high-permeability Liassic carbonatic sequences and extending throughout the region. The top of the carbonatic aquifer ranges from 200 to 1300 m depth, and water temperatures as higher as 50 C were recorded to about 500 m depth. Moreover, numerous springs with temperature larger than 40 C and a flow which may reach 40 l/s occur in this area. Geothermal data so far achieved, especially from deep exploration oil wells, point to an increase of terrestrial heat-flow density from the Rif to the Middle Atlas zone, from about 60 to more than 80 mW/m², respectively. Possible explanations should be searched in the regional extensional tectonics which has affected this area in Plio-Quaternary times yielding intensive volcanic activity. The aim of this paper is to contribute to the hydro-geothermal characterization of northwestern Morocco by presenting results of measurements of rock thermo-physical properties and analyzing temperature data available from water wells reaching the Mesozoic terrains. A number of thermal conductivity measurements were carried out on a set of samples representative of the stratigraphic sequence of the Middle Atlas. The carbonatic lithotypes forming the deep aquifer show a relatively high thermal conductivity. Values range from 2.0-3.1 W/(m K) in limestones to 4.6-5.0 W/(m K) in dolomites. Temperature depth profiles from boreholes characterized by upward flow of hot water fed by the carbonatic formation are available to 350-500 m depth. Temperature logs were analyzed by matching thermal data with models of vertical temperature distribution, which incorporate both heat and mass transfer. Thermo-hydraulic parameters were calculated from the coefficients of the advective models obtained by means of the least-square fitting method. The inferred temperature gradient above the advectively perturbed carbonatic formation exceeds 50 mK/m, thus locally boosting the heat-flow density to values larger than 100 mW/m². Analytical modeling of heat and water transfer involved in the deep circulation was attempted along selected hydro-geological cross-sections. Several hypotheses of basal heat-flow density, porosity, aquifer thickness and water velocity were tested in order to fit the borehole thermal records. The results show that temperatures of the deep aquifer are compatible with a topographically driven flow in the carbonatic formations down to 600-1500 m depth, under conditions of enhanced geothermal gradient.

Keywords: advection, deep aquifers

(S) - IASPEI - *International Association of Seismology and Physics of the Earth's Interior*

JSS017

Poster presentation

2388

Time-dependent lithosphere thermal state in the Carpatho-Pannonian Area. a review based on heat flow data and modeling

Dr. Crisan Demetrescu

Natural Fields Institute of Geodynamics, Bucharest, Romania IASPEI

Maria Tumanian

The formation of the Carpathians, their relationship with the foreland, as well as the present configuration and structure of the Carpatho-Pannonian area are the result of a long-term tectonic evolution of lithosphere under global and local forces. The evolution starts with the extensional regime of Triassic and Jurassic, includes the emplacement of Inner, Median and outer Dacides and of Transylvanides in Cretaceous, followed by the deposition of the post-tectonic cover in the Transylvanian and Pannonian domains, and ends in Neogene, with overthrusting of Moldavides in the Eastern Carpathians and the formation of Transylvanian and Pannonian basins as a result of compressional and, respectively, of extensional deformation of lithosphere. Episodes of volcanism accompany these processes. The paper reviews the time-dependent thermal effects of tectonic processes involving the entire lithosphere (pre-Miocene oceanic subduction and Miocene continental collision in the Eastern Carpathians, extension in the Pannonian basin) or only its upper part (flysch nappes formation in the Eastern Carpathians, Neogene volcanism, Neogene sedimentation and erosion in the main subsident areas, namely the Pannonian, Transylvanian and Focșani depressions), discussed the heat flux budget of the lithosphere based on surface heat flux data and tectonic processes modeling and attempts at obtaining a comprehensive image of the temperature field and rheological structure of the lithosphere in the study area.

Keywords: heat flow, geodynamic processes, thermal structure



(S) - IASPEI - *International Association of Seismology and Physics of the Earth's Interior*

JSS017

Poster presentation

2389

Heat and groundwater flow modeling in the lithosphere of the Eastern Carpathians Bend

Dr. Venera Dobrica

Natural Fields Institute of Geodynamics, Bucharest, Romania IASPEI

Helmut Wilhelm

The geothermal regime in the Earth's lithosphere is given mainly by the transport to the surface of heat from the mantle and of heat that is generated by the decay of radioactive isotopes in the rocks. The main mechanisms of heat transfer are conduction and convection by moving fluids. The circulating fluids can have an important effect on the heat transport in sediments during basin development, producing deviations from a purely conductive thermal regime within sedimentary basins. The thermal regime of the lithosphere in the East Carpathian bend and its foreland was analyzed, based on geothermal measurements performed in 41 boreholes. The temperature-depth profiles show a large range of the lateral variation of geothermal gradients, from 23 mK^m-1 to 53 mK^m-1, and an increase of the gradient with depth, in the studied area. The increase of the temperature gradients with depth may be a consequence of the presence of a fluid flow component, but it may also be explained by a decrease of the thermal conductivity with depth which may follow from transition from wet to dry conditions or by undercompaction. We modeled the thermal regime of the foreland of the Eastern Carpathians from the point of view of groundwater flow in relation to the heat transfer. Depending on the flow strength, the geothermal regime in the basin can be influenced, with cooling effects in recharge areas, and warming effects in discharge areas. Using quantitative modeling techniques, models which take into account the coupled effects of heat and migration of water given by topographic relief, buoyancy forces and sediment compaction, would be constructed. The accuracy of models depends on hydrologic properties of sediments.

Keywords: heat flow data, basin scale fluid flow, modeling



(S) - IASPEI - *International Association of Seismology and Physics of the Earth's Interior*

JSS017

Poster presentation

2390

Hydrothermal circulation within subducting crust: Implications for subduction zone temperature

Mr. Troy Kummer

Glenn Spinelli

Hydrothermal circulation plays an important role in cooling and redistributing heat within high-permeability ocean crust. We examine the effect of hydrothermal circulation on subduction zone temperature by modeling 2D fluid and heat transport within subducting ocean crust using a finite element heat and mass transport code. The effect of hydrothermal circulation is quantified by comparing results from simulations with coupled fluid and heat transport to those from simulations with only heat conduction (no fluid flow). We examine how convergence rate and subduction geometry influence hydrothermal circulation and temperatures within the subduction zone. Modeled geometries mimic the Middle America subduction zone off Nicoya Peninsula, and the subduction zone. We simulate fluid and heat flow for systems with upper basaltic basement permeability ranging from 10⁻¹³ to 10⁻¹⁰ m². Additionally, we examine the effect of permeability reduction within the basaltic basement as it is subducted. For lower permeabilities, the models with fluid transport show suppressed temperatures along the subducting slab relative to purely conductive models. At higher permeabilities, large convection cells reduce temperatures far into the subduction zone and transport heat seaward towards the trench; temperatures at the toe of the margin wedge become elevated relative to the case with no fluid flow. Permeability reduction with depth limits how far into the subduction zone significant hydrothermal circulation can persist.

Keywords: subduction, zone, hydrothermal



(S) - IASPEI - *International Association of Seismology and Physics of the Earth's Interior*

JSS017

Poster presentation

2391

Crustal rheology along the Neapolitan Volcanic Zone-Apennine-Apulia foreland transect, (Southern Italy)

Dr. Giuseppe Solaro
INGV Osservatorio Vesuviano IASPEI

We investigated the crustal rheology of the Southern Apennine chain along a WSW-ENE oriented cross-section, running from Neapolitan Volcanic Zone to Apulia foreland. A computed thermal modelling and re-localized hypocentral distribution of earthquakes of the area, spanning from 1993 to 2005, have been used to constrain the rheological model. Results show that beneath the Neapolitan Volcanic Zone the brittle/ductile transition is located at about 8 km of depth, whereas in correspondence with the axial zone of the chain the rheology shows two brittle horizons, whose top are located at 20 km and 30 km depth, respectively. Our results show that the horizontal rheological variations are quite predominant with respect to vertical ones in this sector of the Apennine belt. This fact can be helpful to discriminate which of tectonic processes have played a major role to construct the belt and/or is still active. In conclusion, the rheological model and the strength envelopes obtained from our modelling could be taken into account, as a first order approximation, to better understand the mechanical behaviour of the Southern Apennine crust.

Keywords: rheology, tectonics, apennine

PERUGIA
ITALY



(S) - IASPEI - *International Association of Seismology and Physics of the Earth's Interior*

JSS017

Poster presentation

2392

Studying thermal properties of sedimentary and crystalline rocks at elevated temperature and pressures: equipment, methodology and results

Mr. Dmitriy Miklashevskiy

Technical Physics and Rock Physics Russian State Geological Prospecting University IASPEI

Yuri Popov, Vladimir Tertychnyi, Irina Bayuk, Raisa Romushkevich, Christof Clauser, Renate Pechnig

Rocks thermal properties - thermal conductivity (TC), thermal diffusivity (TD) and volumetric heat capacity (VHC) - have been studied using a newly developed instrument which allows the measurements with simultaneous influence of temperature, pore and two components of lithostatic pressures. A special methodology has been elaborated to study rock matrix properties and pore space geometry before and after the measurements at elevated temperature and pressure. The methodology provides a control of changes in inner pore structure and matrix thermal properties during PT measurements and is based on (1) experimental results on thermal conductivity, thermal diffusivity and volumetric heat capacity of rocks at normal conditions using the precise optical scanning instrument; (2) estimation of inner pore space structure and matrix thermal properties with theoretical modeling. Two rock collections have been studied. Collection 1: 59 sedimentary rocks included feldspar-quartz and quartz feldspar-sandstone samples, carbonate and sulphate rocks. Porosity values varied within a range of (0.236)%. According to the results of thermal property measurements at elevated temperature (25180) oC and equal vertical and horizontal components of lithostatic pressure (up to 180 MPa) and pore pressure (up to 80 MPa) TC, TD and VHC have varied at pressure of 180 MPa and temperature of 120 oC by -9.246%, -64-14% and 0.9171%, respectively. Variations of TC bersus PT conditions are close to linear low. Correlation between slope angle of TC(P,T) curves and TC values at normal PT conditions has been found to be close for sandstones and carbonate rocks with correlation coefficients - 0.81 and -0.91, correspondingly. Collection 2: 19 cores from the Ural superdeep well SG-3 (Russia) were sampled within depth interval of (6505939) m. Porosity of the studied rocks varied within range of (0.11.5)%. Results of thermal property measurements at elevated temperature (25120) oC and equal vertical and horizontal components of lithostatic pressure have shown that thermal conductivity, thermal diffusivity and volumetric heat capacity vary at pressure of 170 MPa and temperature of 120 oC by -5.9-26 %, -11.2-33% and 2.732%, respectively. Decrease in TC values for PT conditions corresponding to the sampling depths has been found to be equal to 4% in average in comparison to TC values at normal conditions that allows correction of previous estimates of heat flow density done with thermal conductivity values obtained from the measurements at normal conditions. Authors wish to acknowledge generous support of Schlumberger Oilfield Services, an international company in oil and gas industry, and Russian Foundation for Basic Research (grant 05-05-64879).

Keywords: measurements, thermal, properties

(S) - IASPEI - *International Association of Seismology and Physics of the Earth's Interior*

JSS017

Poster presentation

2393

Temperature dependence of the relationship of thermal diffusivity versus thermal conductivity for crystalline rocks

Prof. Christoph Clauser

Applied Geophysics RWTH Aachen University IASPEI

Darius Mottaghy, Hans-Dieter Vosteen, Rüdiger Schellschmidt

Thermal diffusivity governs the transient heat transport equation. Thus, a realistic characterisation of this parameter and its temperature dependence is crucial for geothermal modelling. Due to sparse information from boreholes, lack of samples, and elaborate measurement procedures, there is often insufficient data on thermal diffusivity at elevated temperatures. We make use of existing data on crystalline (metamorphic and magmatic) rock samples from the Kola peninsula and the Eastern Alps and develop a general relationship for the temperature dependence of thermal diffusivity up to 300 C. The temperature dependence of thermal conductivity is parameterised itself, using an empirical relationship which is set up for both data sets as well. Hence, only thermal conductivity at ambient temperatures is required for determining the temperature dependence of thermal diffusivity. We obtain different coefficients for both data sets which can be explained by different geological settings. Comparisons with other expressions for these rock physical parameters show a good agreement at ambient conditions. General relations for thermal diffusivity at elevated temperatures are rare. A comparison of our results with data from two crystalline samples from the KTB highlights the need for further data, which will help to quantify uncertainties.

Keywords: geothermics, temperature dependence, thermal diffusivity



(S) - IASPEI - *International Association of Seismology and Physics of the Earth's Interior*

JSS017

Poster presentation

2394

Estimation of formation temperature from measurements in near bottom zone

Mrs. Anna Semenova

Technical Physics and Rock Physics Russian State Geological Prospecting University IASPEI

Yury Popov, Vyacheslav Pimenov

A. Semenova, Yu. Popov, V. Pimenov Russian State Geological Prospecting University, Moscow, Russia
Experimental data on bottom hole temperature (BHT) are important in geothermal research when it is impossible to obtain undisturbed formation temperature distribution or when temperature logging could not be performed. Sometimes BHT measured in several depth levels during drilling company are used to give information on equilibrium temperature gradient for heat flow density estimations. It is important (1) to know conditions of BHT measurements which can exclude significant discrepancy in experimental temperature data and real formation temperature, and (2) to estimate possible systematic difference between experimental data and undisturbed formation temperature to provide necessary corrections in the experimental results. We calculated 2D temperature field for several typical wells and considered dependence of well axis temperature on time in different distances from a bottom-hole (1-20 m). Possible natural convection in the well was taken into account using different values of mud effective thermal conductivity in the calculations. Calculation results show that the temperature measured in the well axis near the bottom can differ significantly from undisturbed formation temperature (1-10 K depending on a well depth within a range 500-5000 m) if optimal regime parameters for temperature measurements are not used. Our calculations result in recommendations for the measurements of bottom hole temperatures with optimal conditions providing accepted correspondence between the measurement data and undisturbed formation temperature. Authors wish to acknowledge generous support of Schlumberger Oilfield Services, an international company in oil and gas industry.

Keywords: bottom, hole, temperature



(S) - IASPEI - *International Association of Seismology and Physics of the Earth's Interior*

JSW001

2395 - 2399

Workshop

Subduction zone related volcanism and hazard mitigation

Convener : Prof. Sri Widiyantoro

Many densely populated countries are situated along major subduction zones whose seismic and volcanic hazards may have severe consequences on the socio-economic conditions of these countries. The 2004 Sumatran great earthquake with its attendant devastating tsunami highlighted the need to study such areas in order to understand the nature of subduction processes and provide a coherent picture to understand its possible effects. Several eruptions occurred in the 20th century in developing countries located along subduction zones. Some of them have caused a large number of casualties and great damage to infrastructure. The symposium on "subduction zone related volcanism and hazard mitigation" is to bring together people working on volcanological studies along subduction zones and especially in volcanic hazard mitigation. Research on topics like: i) Volcano hazard mapping, ii) Mitigation strategies for subduction zone related hazards, iii) Development of integrated emergency plans to reduce risk in subduction zones, iv) General volcanological studies focused in improving volcanic hazard knowledge, and v) Integrated geophysical, geological and geochemical studies to improve volcanic hazard mitigation would be most welcome.

XXIV2007

PERUGIA
I T A L Y



(S) - IASPEI - *International Association of Seismology and Physics of the Earth's Interior*

JSW001

Oral Presentation

2395

Volcanic gases in subduction zones : Documentation of temperature measurements of the fumaroles at Vulcano island, Italy - a case study

Mr. Eric Reiter
none none

INTRODUCTION Since a few years, Information Technology (IT) is more and more important in geosciences and especially in volcanology. A Geographical Information System (GIS) is a great way to organize and maintain your data for volcanology. GIS FOR VULCANO'S TEMPERATURE MEASUREMENTS The purpose of the project is to create an internet resource which saves time to all researchers as it will publish available and future temperature measurements of fumaroles. The base of the system consists of interactive digital maps. Each map is a layer of the system. Each layer represents data for a date of temperature measurements. The user can select in a menu one or more layers to be seen in the interface. The background of all layers is the geological map of Vulcano Island or an aerial photo of La Fossa crater. The temperature's evolution vs time can be seen too. During the same project, we develop an add-on for Google Earth allowing a nicer interface to locate the fumaroles vents. Links between the add-on and the web site exist to view the temperatures evolution of each fumarole. OUTLOOK OF THE PROJECT A version of the project is already on line. The add-on can be downloaded too. This program can be adapted for all volcanoes and a lot of kind of data (isotopic compositions, deformation, epicenters location, etc.). It will run on and off-line. So you can have it on CD-Rom with your own data to study them. An internet GIS can also be a source of information for the educated tourists and a base to train local guides.

Keywords: vulcano, gas, survey



(S) - IASPEI - *International Association of Seismology and Physics of the Earth's Interior*

JSW001

Oral Presentation

2396

Ancient subduction zone in the Sakhalin Island (the Sea of Okhotsk)

Prof. Alexander Rodnikov

Geophysical Center Russian Academy of Sciences IAVCEI

In the Sea of Okhotsk in Eastern Sakhalin an ancient (Upper Cretaceous-Paleogene) subduction zone is distinguished. On the surface it is manifested by an ophiolite complex, which separates North Sakhalin oil and gas basin from Deryugin basin of the Sea of Okhotsk. This complex is represented with harzburgite, dunite, wehrlite, rodingite, gabbro and amphibolite forming ophiolite plates. It is supposed that 100 million years ago, the oceanic lithosphere of the Sea of Okhotsk subducted under Sakhalin, the eastern part of which was an andesite island arc. Behind andesite island arc, in western Sakhalin there was a back-arc basin where sandy clayey deposits accumulated in the Late Cretaceous- Paleogene, which subsequently formed the basement of Cenozoic North Sakhalin oil and gas basin. Approximately 10-15 million years ago subduction of the lithosphere of the Sea of Okhotsk apparently ceased. It is established that the Deryugin basin was formed at the place of ancient deep trench, and Sakhalin basin is located above the ancient (Late Cretaceous- Paleogene) subduction zone. So, the Late Cretaceous- Paleogene rocks of the North Sakhalin sedimentary basin formed in the conditions of back-arc basin may be favorable for generation, accumulation and conservation of hydrocarbons.

Keywords: subduction zone, geodynamics, sakhalin

PERUGIA
ITALY



(S) - IASPEI - *International Association of Seismology and Physics of the Earth's Interior*

JSW001

Oral Presentation

2397

Tomographic Inversion of Local P and S Data for Structure below the Toba Caldera Complex in North Sumatra

Prof. Sri Widiyantoro

Geophysics Bandung Institute of Technology IASPEI

Wandono

We have conducted a tomographic imaging for the Toba caldera, a 30 km x 90 km topographic depression, located in North Sumatra that represents one of the largest Quaternary calderas in the world. We estimate the 3D P- and S-wave velocity structures beneath the caldera complex using arrival time data of local earthquakes recorded by a 40-station seismic network which had been operated for 4 months (data by courtesy of a PASSCAL program) combined with data from a local network operated by BMG. The resulting tomographic images reveal the presence of pronounced low P and S velocity anomalies that are likely to map the distribution of magma within this subduction-related volcanic system. In the upper 10 km of crust the largest low-velocity region underlies a part of the great Sumatran fault and the southern part of the Toba depression and coincides with a gravity low centered over the regional uplift of a resurgent dome. The imaged low-velocity anomalies extending down to about 100 km depth may be related to the potency of a remaining supervolcano below the study region which will need further investigation.

Keywords: toba caldera, tomography, supervolcano



(S) - IASPEI - International Association of Seismology and Physics of the Earth's Interior

JSW001

Oral Presentation

2398

Drift of the earth core to the North and inversion of global volcanic process

Prof. Yury Barkin

Laboratory of Gravimetry Sternberg Astronomical Institute IAG

The analysis of modern data of geodetic, gravimetry and geophysical observations testify a reality of the phenomena of a drift of outer core of the Earth and its translational oscillations with a wide spectrum of frequencies relatively to elastic mantle (Barkin, 1995, 2002; Barkin, Vilke, 2004; Barkin, Shuanggen, 2006). Displacements of the core are accompanied by elastic deformations of the mantle and by variations of its tension state which in turn find reflection in variations of seismic, volcanic and, generally speaking, in all planetary natural processes. This phenomenon is characterized by the slow secular component of process and by periodic variations with interannual, decadal and more long periods, and have inversion character. Activity of process increase in one hemisphere (on direction of the core drift) and activity decrease in opposite hemisphere. It is principal property of considered phenomenon. This theoretical conclusion based on a geodynamical model about forced small relative displacements and rotations of the Earth shells under action of a gravitational attraction of the Moon, the Sun and other celestial bodies, has obtained a set of confirmations at the analysis of variations of natural processes in opposite hemispheres of the Earth (Barkin, 2000, 2002, 2006). In particular the drift of the core causes the phenomenon of inversion in activity of volcanic processes in northern and southern hemispheres. Dynamic studies and the satellite data about geocenter motion have confirmed the displacement of the core in present epoch (predicted by author) to the north in the direction of a geographical point 70 N, 104 E (Barkin, 1997). In hemispheres N and S, separated by a plane of inclined equator, the subduction zones and zones of rifting are located asymmetrically. In hemisphere N the magmatic volcanos of belts of compression (of subduction zones) are mainly located, and magmatic volcanos of rifting zones (of spreading zones) are located in opposite hemisphere. On our model the changes of tension states in zones of volcanos in northern hemisphere will result in their activation. In southern hemisphere S the changes of volcano activity will have the opposite tendency. The specified phenomenon is observed actually. The number of eruptions of volcanos of subduction zones linearly increase with velocity about 5 eruptions per one year (for the period in hundred years). Thus the number of eruptions of volcanos of rifting zones on the contrary decreases. This phenomenon was open as a result of the analysis of the known data on volcanic activity for a time interval with 1850 on 1977 (Mekhtiev, Khalilov, 1987). By the method of sliding average the diagrams of temporal series of numbers of eruptions of volcanos for the period 1800 - 2000 have been constructed (Khain, Khalilov, Ismail-Zade, 2004). The geodynamic model of the forced displacements of the core allows to describe a wide spectrum of its cyclic oscillations, in particular with the decade periods. By reflection of cyclic polar displacements of the core between hemispheres N and S will be corresponding cyclic antiphase variations of volcanic activity in the specified hemispheres. It was actually revealed, that peaks of activation of volcanos of subduction zones, falling on 1885, 1950, coincide with peaks of passivity of volcanos of rifting zones. Peaks of the periods of passive volcanism of subduction zones of 1860, 1900, 1910, 1960 will be coordinated to peaks of increase of activity of volcanos of rifting zones. Only to peaks of activity of volcanos of subduction zones 1910, 1930 and to the peak of passivity of 1940 are not strongly pronounced antiphase of zones of activity. These moments can be explain as result of some imposing of corresponding zones of subduction and rifting with respect to hemispheres N and S. Thus, changes of intensity of volcanism in the specified period of time in 127 years confirm prospective displacement of the Earth core and developed geodynamical model of the forced swing of the Earth shells as a whole. The cyclicities of volcanic eruptions revealed at the spectral analysis with the periods 20, 40 years and

others (Khain, Khalilov, Ismail-Zade, 2004) have been predicted earlier on the basis of a hypothesis about unity of cyclicities of variations of all planetary processes, caused by the uniform mechanism of core oscillations ("a motor", "a heart" or "a engine") (Barkin, 2002). References Barkin Yu.V.(1997) Secular Redistribution of the External and Internal Masses of the Earth and Their Role in the Variations of the Geopotential and Earth's Rotation. XXII General Assembly of EGS (Vienna, 21-25 April 1997). Annales Geophysicae, Supplement 1 to Volume 15. Part 1, p. 32. Barkin, Yu.V. (2000) A mechanism of variations of the Earth rotation at different timescales. In: Polar Motion: Historical and Scientific Problems (Eds. Steven Dick, Dennis McCarthy, and Brian Luzum)/ Proceedings of IAU Colloquium 178 (Cagliari, Sardinia, Italy, 27-30 September 1999). Astronomical Society of the Pacific conference series, V. 208. Sheridan Books, Chelsea, Michigan. pp. 373-379. Barkin, Yu.V. (2002) Explanation of endogenous activity of planets and satellites and its cyclicity. Izvestia cekzii nauk o Zemle. Rus. Acad. of Nat. Sciences, Issue 9, December 2002, M.: VINITI, pp. 45-97. In Russian. Barkin, Yu.V. and Shuanggen, J. (2006) Kinematics and dynamics of the Earth hemispheres. EGU General Assembly (Vienna, Austria, 2-7 April 2006). Geophysical Research Abstracts, Volume 8, abstract # EGU06-A-01680. Khain V.E., Khalilov E.N., Ismail-Zade T.A. (2004) Periodicity of volcanic activity in various geodynamics states and possible pulsation of the Earth radius. Publications of section of the Earth sciences, issue 12, pp. 9-16. In Russian. Mekhtiev Sh.F., Khalilov E.N. (1987) Volcanoes and geodynamics. Nature (Moscow), No.5, pp. 46- 49. In Russian.

Keywords: subduction, volcanos, inversion



(S) - IASPEI - *International Association of Seismology and Physics of the Earth's Interior*

JSW001

Oral Presentation

2399

Temporal evolution and migration of volcanism in Northern Martinique Island (Lesser Antilles, French West Indies)

Mrs. Aurelie Germa

Laboratoire de geochronologie, UMR IDES Universit Paris Sud (PARIS XI) IAVCEI

Quidelleur Xavier, Labanieh Shasa, Chauvel Catherine

Martinique (14N, 61W) is the Lesser Antilles Island where the most complete volcanic history of the arc can be found. However, most studies have been restricted to Mount Pele volcano, more particularly to the destructive 1902 and 1929 A.D. eruptions, rather than on the older zones from the recent arc (Morne Jacob, Pitons du Carbet and Mount Conil complexes), which recorded at least five events of flank collapse. The aim of this study is to determine the volcanic evolution of the recent arc in Martinique Island by constraining the building and destructive rates of the different volcanic complexes in order to improve the knowledge of its recent activity. Dating of nearly thirty selected representative samples from the northern volcanic complexes has been obtained by K-Ar, based on the Cassignol-Gillot technique. Together with these radiometric ages, ongoing morphological works and field observations will help us to better reconstruct the volcanic history of the Morne Jacob, Pitons du Carbet and Mont Conil complexes, and to characterize their relationship with the active volcano of Mount Pele. First results show that Morne Jacob volcano has a longer history than previously inferred: the different stages of activity range between 5.5 and 1.5 Ma. A large basaltic to andesitic shield volcano was built between 5.5 and 2.1 Ma. At the end of this first stage, the northeastern flank collapsed. A new andesitic centre erupted into the depression, and peripheric vents emitted lava flows down to the Caribbean coasts, between 2.04 and 1.5 Ma. Piton du Carbet complex is younger than estimated before: a first stage of activity occurred with the construction of an andesitic volcano between 1 Ma and 770 ka, which ended by a large flank collapse southwest directed. The loss of lithostatic load favoured more basic magma ascent and eruption of Pitons du Carbet s.s. inside the depression. The mean emplacement age of the Pitons du Carbet being of 337.5 ka (Samper et al., 2007), it is interpreted as the flank collapse age. Pitons Mont Conil and Mount Pele constitute the northernmost compartment of the island. Piton Mont Conil complex started its activity while the Carbet complex was still active, with andesites emitted between 543.8 ka and 189.3 ka. Its evolution and the relationship with the subsequent stages remains to be better constrained because its activity preceded that of Mount Pele, the active volcano. Finally, our combined approach based on geochronological, geochemistry, geomorphological and fieldwork studies, will allow us to propose a general evolution model for the recent arc volcanism in northern Martinique island, from 5.5 Ma to present.

Keywords: martinique, k ar geochronology, flank collapse

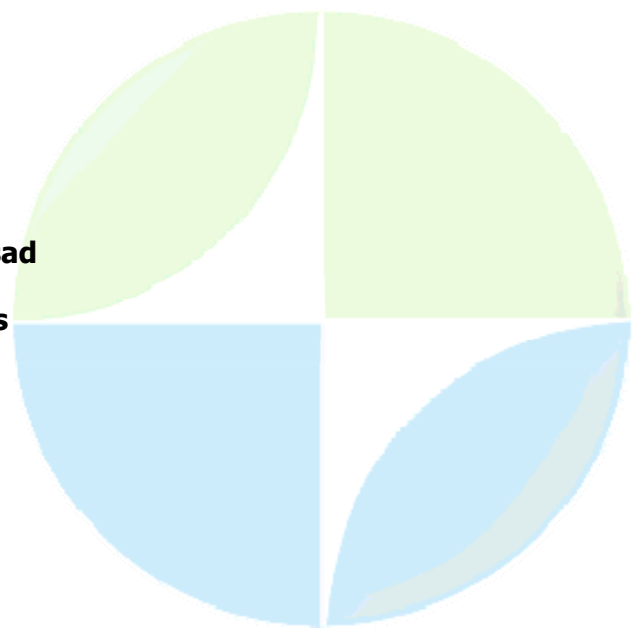
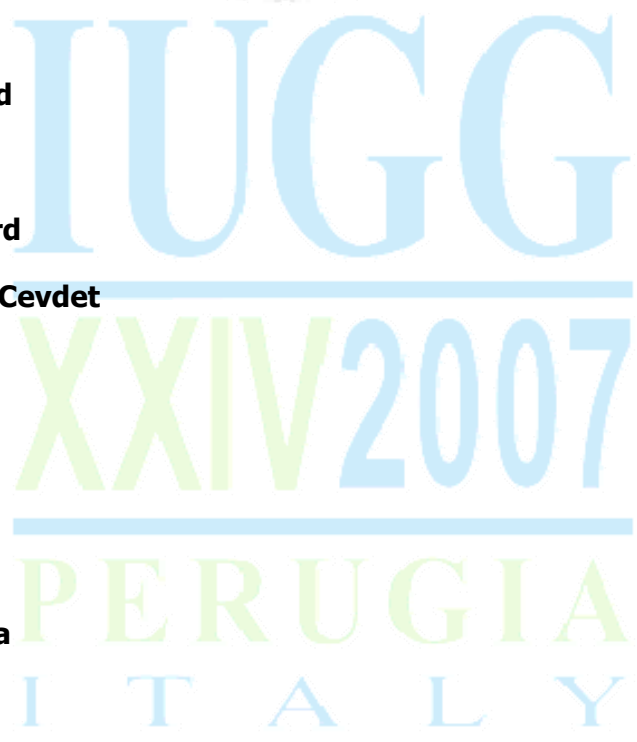
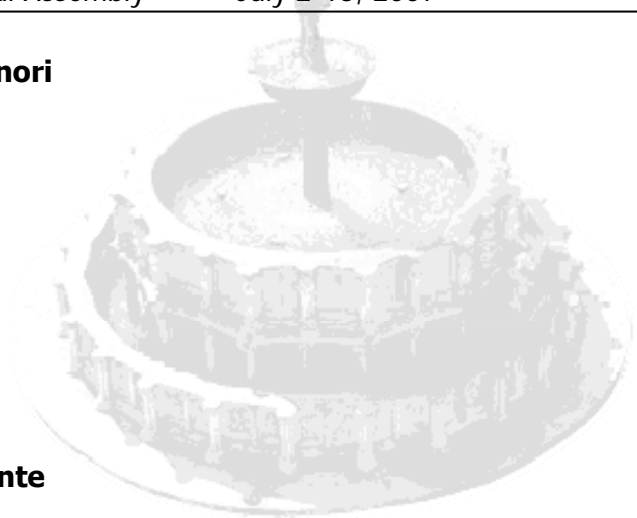
Ghorab Mahmoud	1716
Mehrabian Shayesteh	1717
Mizani Shervin	1718
Khan Amir	1719
Irifune Tetsuo	1720
Jackson Ian	1721
Barnhoorn Auke	1722
Italiano Francesco	1723
Russell Kelly	1724
Tamrazyan Artush	1725
Alva-Valdivia Luis M.	1726
Shariatinia Zeinab	1727
Karnaukhova Elena	1728
Korchin Valery	1729
Singh Kripa Shanker	1730
Mehrabian Shayesteh	1731
Chaudhari Lalit	1732
Marra John	1733
Costa Pedro J M	1734
Horrillo Juan	1735
Greenslade Diana	1736
Gonzalez-Ferran Oscar	1737
Bernard Eddie	1738
Wong Wing Tak	1739
Liu Philip	1740
Mercado-Irizarry Aurelio	1741



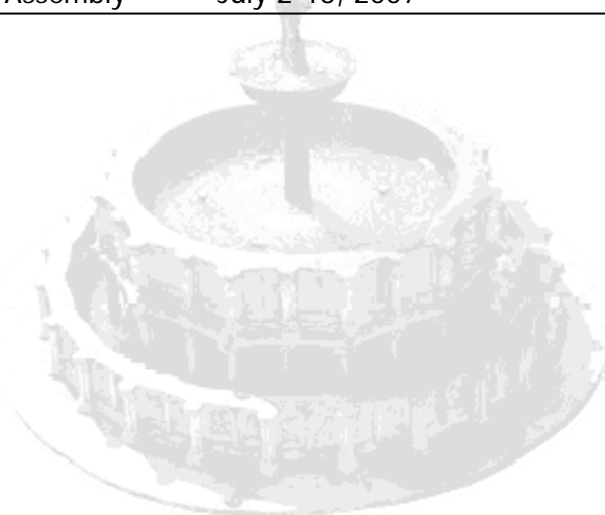
Matsutomi Hideo	1742
Coppo Nicolas	1743
Tanioka Yuichiro	1744
Gusiakov Viacheslav	1745
Vilibic Ivica	1746
Takahashi Tomoyuki	1747
Rabinovich Alexander	1748
Grilli Stephan	1749
Imamura Fumihiko	1750
Pelinovsky Efim	1751
Kato Teruyuki	1752
Power William	1753
Downes Gaye	1754
Santos Angela	1755
Nadya Razzhigaeva	1756
Fokaefs Anna	1757
Papadopoulos Gerassimos	1758
Armigliato Alberto	1759
Gill Stephen	1760
Suleimani Elena	1761
Kulikov Evgueni	1762
Bermudez Luis	1763
Dunbar Paula	1764
Fujima Koji	1765
Cherniawsky Josef	1766
Koshimura Shunichi	1767



Shigihara Yoshinori	1768
Cummins Phil	1769
Lorito Stefano	1770
Kanoglu Utku	1771
Stroker Kelly	1772
Dengler Lori	1773
Crescenzo Violante	1774
Tang Liujuan	1775
Stephenson Fred	1776
Abe Kuniaki	1777
Thomson Richard	1778
Yalciner Ahmet Cevdet	1779
Kongko Widjo	1780
Kong Laura	1781
Thio Hong Kie	1782
Kontar Evgeny	1783
Kanbua Wattana	1784
Kumar Arun	1785
Voronina Tatiana	1786
Wilson Chris	1787
Allen Stewart	1788
Fujii Yushiro	1789
Dimri Vijay Prasad	1790
Reicherter Klaus	1791
Mindlin Ilia	1792
Grilli Stephan	1793



Zahibo Narcisse	1794
Fujii Hiroyuki	1795
Imai Sayaka	1796
Troitskaya Yuliya	1797
Saito Tatsuhiko	1798
Tanioka Yuichiro	1799
Abe Ikuo	1800
Violante Roberto Antonio	1801
Power William	1802
Downes Gaye	1803
Murashima Yoichi	1804
Tsushima Hiroaki	1805
Fujii Naoki	1806
Marchuk Andrey	1807
Marchuk Andrey	1808
Nadya Razzhigaeva	1809
Didenkulova Ira	1810
Armigliato Alberto	1811
Dunbar Paula	1812
Baptista Maria Ana	1813
Hanifa N. Rahma	1814
Minoura Koji	1815
Morozov Victor	1816
Iwabuchi Yoko	1817
Simanjuntak Arthur	1818
Inoue Shusaku	1819



IUGG

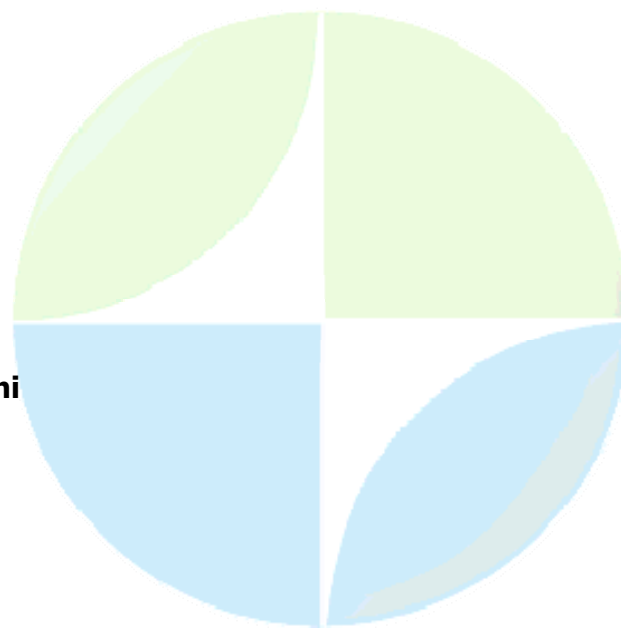
XXIV 2007

PERUGIA

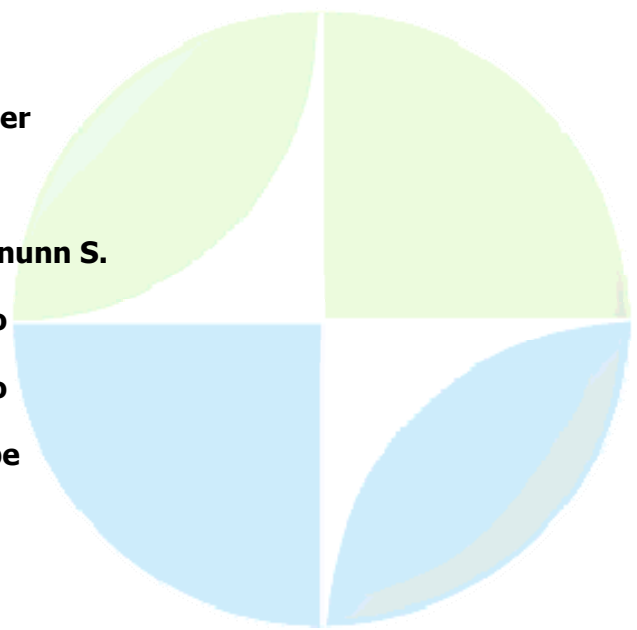
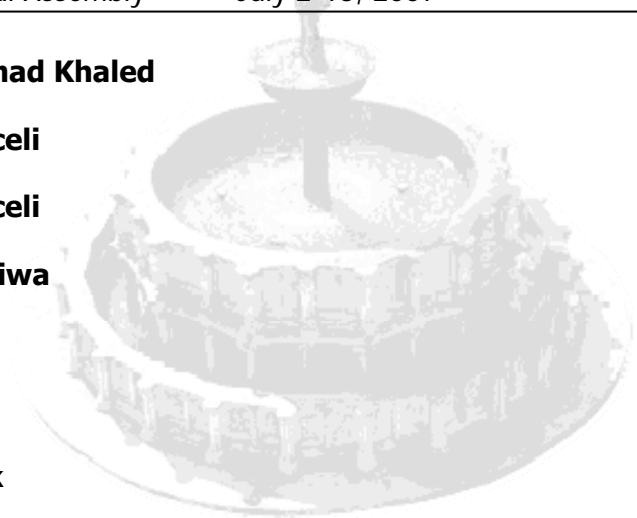
ITALY




Cummins Phil	1820
Cummins Phil	1821
Armigliato Alberto	1822
Korolev Pavel	1823
Armigliato Alberto	1824
Harada Tomoya	1825
Lima Vnia	1826
Kaystrenko Victor	1827
Ogasawara Toshinori	1828
Lorito Stefano	1829
Mercado-Irizarry Aurelio	1830
Brocko Vinita Ruth	1831
Kanoglu Utku	1832
Harada Kenji	1833
Yalciner Ahmet Cevdet	1834
Abdelkarim Yelles-Chaouche	1835
Tsuji Yoshinobu	1836
Tsuji Yoshinobu	1837
Tachibana Toru	1838
Fritz Hermann	1839
Fritz Hermann	1840
Taylor Lisa	1841
Odido Mika	1842
Yoshida Kenichi	1843
Namegaya Yuichi	1844
Maggero Balla	1845

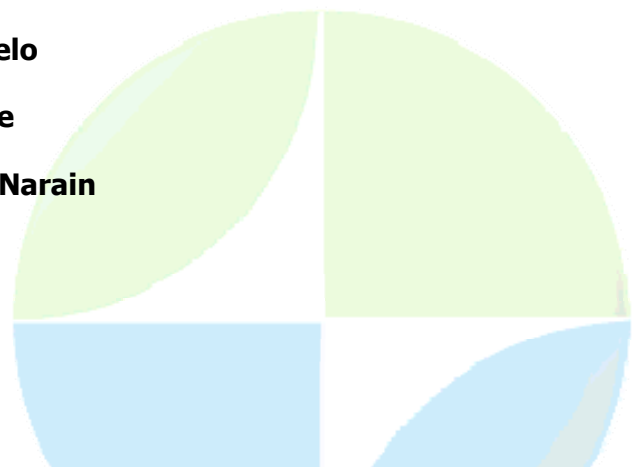



Akhtar Mohammad Khaled	1846
Pi Figueroa Araceli	1847
Pi Figueroa Araceli	1848
Sonuga Olumuyiwa	1849
Frolova Nina	1850
Price Colin	1851
Simons Frederik	1852
Mandal Prantik	1853
Taramelli Andrea	1854
Olorode Deborah	1855
Lancieri Maria	1856
Garces Milton	1857
Satriano Claudio	1858
Shevtsov Boris	1859
Trichtchenko Larisa	1860
Cummins Phil	1861
Korolev Yury	1862
Saleh Hussain	1863
Cechet Bob	1864
Wang Shiyu	1865
Rudloff Alexander	1866
Traversa Paola	1867
Jakobsdttir Steinunn S.	1868
Lacava Teodosio	1869
Lacava Teodosio	1870
Mazzeo Giuseppe	1871







Filizzola Carolina	1872
Zitellini Nevio	1873
Olivieri Marco	1874
Convertito Vincenzo	1875
Prachuab Sumalee	1876
Kontar Evgeny	1877
Palchik Vyacheslav	1878
Browitt Chris	1879
Egorov Nikolay	1880
Marapulets Yury	1881
Antonyan Alvaro	1882
Matsumoto Hiroyuki	1883
You Sung Hyup	1884
Stanica Dumitru	1885
Pinsky Vladimir	1886
Holgate Simon	1887
Chavez_campos Teodosio	1888
Labak Peter	1889
Turino Chiara	1890
Gerardo Colangelo	1891
Casciello Daniele	1892
Srivastava Hari Narain	1893
Stiros Stathis	1894
Yildirim Cengiz	1895
Adams John	1896
Schwartz David	1897



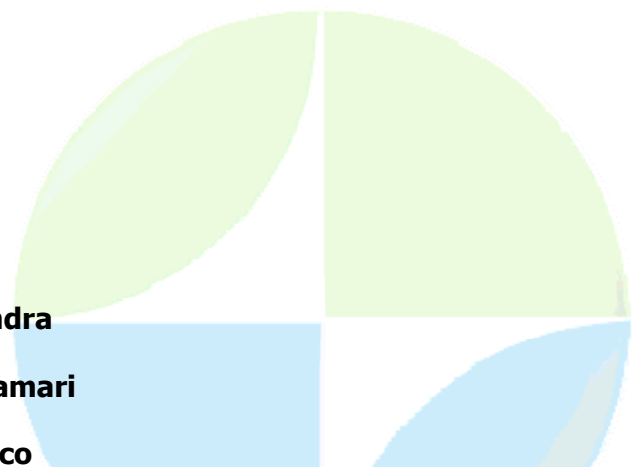



Mazzotti Stephane	1898
Caputo Riccardo	1899
Basili Roberto	1900
Barba Salvatore	1901
Adams John	1902
Ariyoshi Keisuke	1903
Leonard Mark	1904
Zielke Olaf	1905
Meghraoui Mustapha	1906
Mouslopoulou Vasiliki	1907
Yoshioka Toshikazu	1908
Emre Omer	1909
Caputo Riccardo	1910
Hecker Suzanne	1911
Awata Yasuo	1912
Leonard Mark	1913
Rockwell Thomas	1914
Villamor Pilar	1915
Berryman Kelvin	1916
Walsh John	1917
Nicol Andy	1918
Abd Etedal Mahsa	1919
Nemati Azam	1920
Caputo Riccardo	1921
Leonard Mark	1922
Nappi Rosa	1923





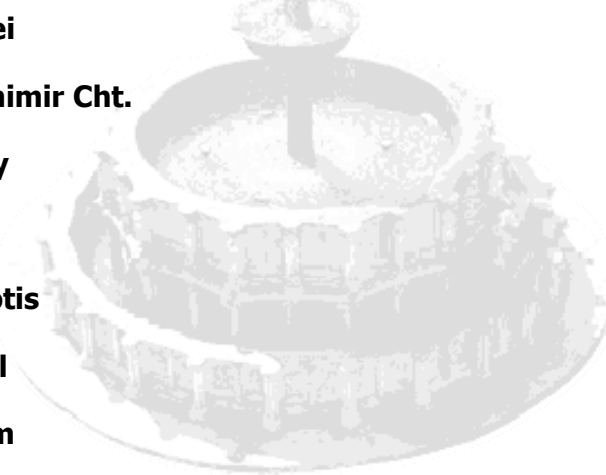
Youcef Bouhadad	1924
Wilson Kate	1925
Meghraoui Mustapha	1926
Reicherter Klaus	1927
Gracia Eulalia	1928
Gribovszki Katalin	1929
Marco Shmuel	1930
Toda Shinji	1931
Rockwell Thomas	1932
Biasi Glenn	1933
Masana Eullia	1934
Agnon Amotz	1935
Fonseca Joao	1936
Perea Hector	1937
Pandey Prabha	1938
Gruetzner Christoph	1939
Babaie Mahani Alireza	1940
Kastelic Vanja	1941
Babonneau Nathalie	1942
Kondo Hisao	1943
Leonard Mark	1944
Pandey Anand	1945
Moreno Ximena	1946
Smedile Alessandra	1947
Tsamalashvili Tamari	1948
Gutierrez Francisco	1949







Pucci Stefano	1950
Ragona Daniel	1951
Spichak Viacheslav	1952
Verma Saurabh	1953
Saracco Ginette	1954
Utsugi Mitsuru	1955
Currenti Gilda	1956
Hase Hideaki	1957
Gvishiani Alexey	1958
Jacques Zlotnicki	1959
Napoli Rosalba	1960
Hashimoto Takeshi	1961
Ishido Tsuneo	1962
Koyama Takao	1963
Sasai Yoichi	1964
Sasai Yoichi	1965
Utsugi Mitsuru	1966
Okubo Ayako	1967
Aizawa Koki	1968
Blanco-Montenegro Isabel	1969
Garcia Alicia	1970
Thomas Ronald	1971
K. K. Abdul Azeez	1972
Kanda Wataru	1973
Legaz Aurlie	1974
Ogawa Yasuo	1975





Yoshimura Ryohei	1976
Mavrodiev Strachimir Cht.	1977
Korepanov Valery	1978
Thomas Jeremy	1979
Varotsos Panayiotis	1980
Gokhberg Mikhail	1981
Johnston Malcolm	1982
Savchenko Tymur	1983
Ichihara Hiroshi	1984
Cukavac Milena	1985
Kato Mamoru	1986
Chand Ramesh	1987
Hollis-Watts Phillip	1988
Pulinets Sergey	1989
Bortnik Jacob	1990
Freund Friedemann	1991
Hattori Katsumi	1992
Hata Masayasu	1993
Mogi Toru	1994
Nenovski Petko	1995
Dunson Clark	1996
Duba Al	1997
Cutler James	1998
Karimov Farshed	1999
Guglielmi Anatol	2000
Fan Xiaoping	2001





Ruzhin Yuri	2002
Shpakovski Vitali	2003
Nishida Yasunori	2004
Iren-Adelina Moldovan	2005
Moldovan Adrian-Septimiu	2006
Qian Wei	2007
Esaki Yuko	2008
Moghadas Davood	2009
Yamazaki Ken'Ichi	2010
Ansari Masoud	2011
Jacques Zlotnicki	2012
Masci Fabrizio	2013
Uyeshima Makoto	2014
Honkura Yoshimori	2015
Kuwano Osamu	2016
Mogi Toru	2017
Oshiman Naoto	2018
Yoshimura Ryokei	2019
Koppireddi Veeraswamy	2020
Di Mauro Domenico	2021
Varotsos Panayiotis	2022
Varotsos Panayiotis	2023
Rozhnoi Alexander	2024
Rozhnoi Alexander	2025
Uyeda Seiya	2026
Biagi Pier Francesco	2027

Castellana Laura	2028
Stanica Dumitru	2029
Uyeda Seiya	2030
Srivastava Hari Narain	2031
Gao Yougang	2032
Gupta Harsh	2033
Kamogawa Masashi	2034
Nagao Toshiyasu	2035
Izutsu Jun	2036
Jiping Dong	2037
Freund Friedemann	2038
Liu Jann-Yenq	2039
Poscolieri Maurizio	2040
Sayanagi Keizo	2041
Gerardo Colangelo	2042
Sengor Taner	2043
Quattrocchi Fedora	2044
Varotsos Panayiotis	2045
Schekotov Alexandr	2046
Molchanov Oleg	2047
Molchanov Oleg	2048
Biagi Pier Francesco	2049
Maggipinto Tommaso	2050
Uyeda Seiya	2051
Smirnov Sergey	2052
Blecki Jan	2053



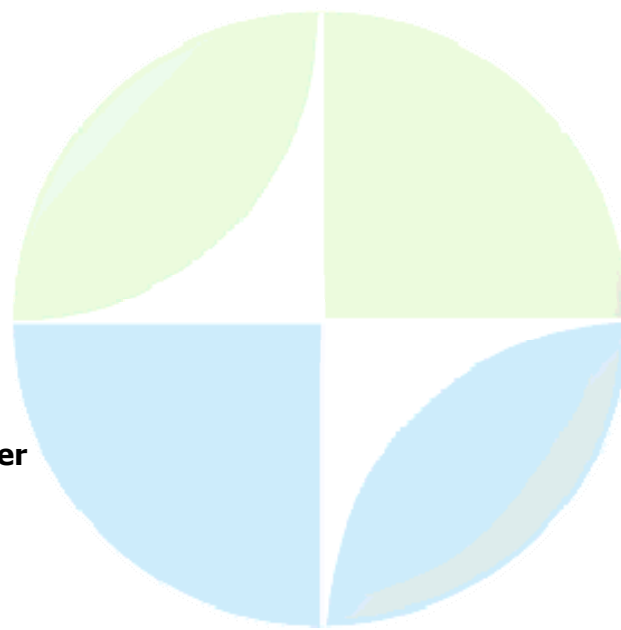
Cas Ray	2054
Stavrakas Ilias	2055
Rodkin Mikhail	2056
Nishihashi Masahide	2057
Palangio Paolo	2058
Hattori Katsumi	2059
Hattori Katsumi	2060
Baldacci Francesco	2061
Mogi Toru	2062
Hloupis George	2063
De La Torre Cervantes	2064
De La Torre Cervantes	2065
Sigaeva Ekaterina	2066
Bhattacharya Shourabh	2067
Korepanov Valery	2068
Pulinets Sergey	2069
Ouzounov Dimitar	2070
Jambulingam Senthilkumar	2071
Conti Livio	2072
Liu Jann-Yenq	2073
Kamogawa Masashi	2074
Marchese Francesco	2075
Aliano Carolina	2076
Singh Ramesh	2077
Parrot Michel	2078
Condadakis Michael	2079



Khegai Valeri	2080
Kaynak Ugur	2081
Marapulets Yury	2082
Zakharenkova Irina	2083
Zakharenkova Irina	2084
Nishihashi Masahide	2085
Ouzounov Dimitar	2086
Freund Friedemann	2087
Sigaeva Ekaterina	2088
Onishi Tatsuo	2089
Buzzi Aurora	2090
Zakharenkova Irina	2091
Ho Yi-Ying	2092
Walzer Uwe	2093
Mandal Prantik	2094
Salah Mohamed	2095
Zhng Shijie	2096
Rai Shyam	2097
Xiong Xiong	2098
Usui Yusuke	2099
Tanaka Satoru	2100
Steinberger Bernhard	2101
Isse Takehi	2102
Margheriti Lucia	2103
Takeuchi Nozomu	2104
Osmaston Miles	2105



Tondi Rosaria	2106
Ismail-Zadeh Alik	2107
Scafidi Davide	2108
Larson Angela Marie	2109
Romanowicz Barbara	2110
Romanowicz Barbara	2111
Scalera Giancarlo	2112
Cammarano Fabio	2113
Key Kerry	2114
Mittelstaedt Eric	2115
Tonegawa Takashi	2116
Tsuchiya Taku	2117
Tabatabai Shadi	2118
Guidarelli Mariangela	2119
Plomerova Jaroslava	2120
Deuss Arwen	2121
Zhu Shoubiao	2122
Cardellini Carlo	2123
Montagner Jean-Paul	2124
Lowman Julian	2125
Kaban Mikhail	2126
Lebedev Sergei	2127
Davaille Anne	2128
Lay Thorne	2129
Watada Shingo	2130
Bobrov Alexander	2131



Rodnikov Alexander	2132
Mordvintsev Oleg	2133
Mkrtchyan Mariam	2134
Wang Wen-Jun	2135
Hovhannisian Hmayak	2136
Greku Rudolf	2137
Mohamed Abdel-Monem	2138
Du Zhixing	2139
Uehira Kenji	2140
Sidorenkov Nikolay	2141
Yamamoto Yojiro	2142
Kuge Keiko	2143
Margheriti Lucia	2144
Manthilake M.A. Geeth Mahinda	2145
Zlagnean Luminita	2146
Ballani Ludwig	2147
Prasad S N	2148
Barkin Yury	2149
Cinti Francesca R.	2150
Barkin Yury	2151
Polet Jascha	2152
Yoshida Masaki	2153
Pedrera Antonio	2154
Kuwano Asako	2155
Yamagishi Yasuko	2156
Mkrtchyan Mariam	2157



Zhang Xiaomei	2158
Al-Lazki Ali	2159
Yoshizawa Kazunori	2160
Yoshizawa Kazunori	2161
Nakahigashi Kazuo	2162
Enescu Bogdan	2163
Presti Debora	2164
Pondrelli Silvia	2165
Lekic Vedran	2166
Obayashi Masayuki	2167
Nakayama Shotaro	2168
Gyodakyan Eduard	2169
Salimbeni Simone	2170
Gollapally Mohan	2171
Kerimov Ikram	2172
Zhu Shoubiao	2173
Mohammadi Elham	2174
Chaloner Jeremy	2175
Thomas Christine	2176
Dilmaghani Masoumeh	2177
Bayramnejad Esmaeil	2178
Alikhani Zahra	2179
Hutko Alexander	2180
Naira Gedakian	2181
R. Ghias Sanaz	2182
Crossley David	2183



Bulatova Natalia	2184
Ioganson Lidia	2185
Furlani Renzo	2186
Kawakatsu Hitoshi	2187
Tajima Fumiko	2188
Suetsugu Daisuke	2189
Tarits Pascal	2190
Isse Takehi	2191
Hirose Kei	2192
Irifune Tetsuo	2193
Aizawa Yoshitaka	2194
Baba Kiyoshi	2195
Polat Gulden	2196
Obayashi Masayuki	2197
Bina Craig	2198
Fukao Yoshio	2199
Jarvis Gary	2200
Suetsugu Daisuke	2201
Litasov Konstantin	2202
Yomogida Kiyoshi	2203
Yoshioka Shoichi	2204
Shito Azusa	2205
Tibi Rigobert	2206
Shiraishi Rei	2207
Shimizu Hisayoshi	2208
Hirahara Kazuro	2209



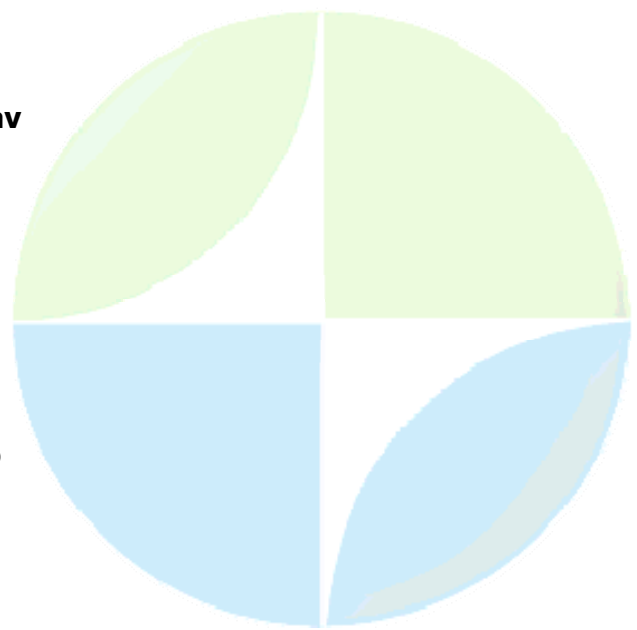
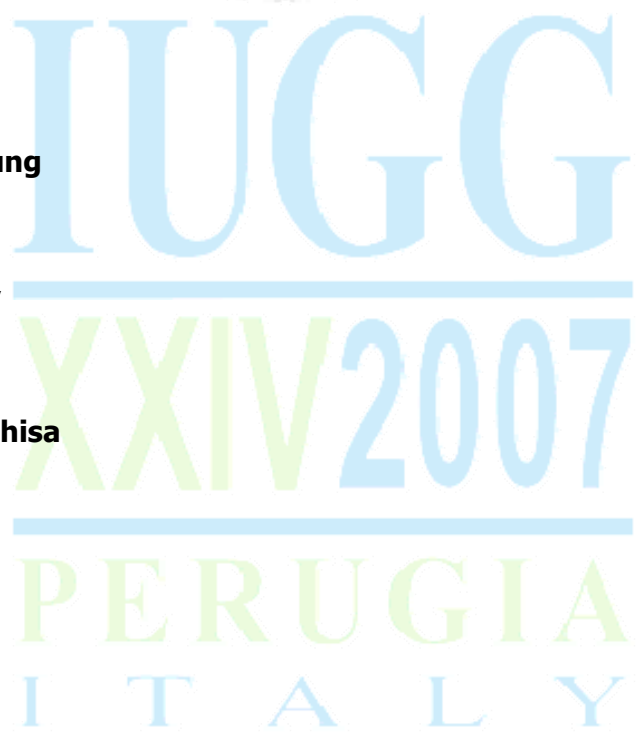
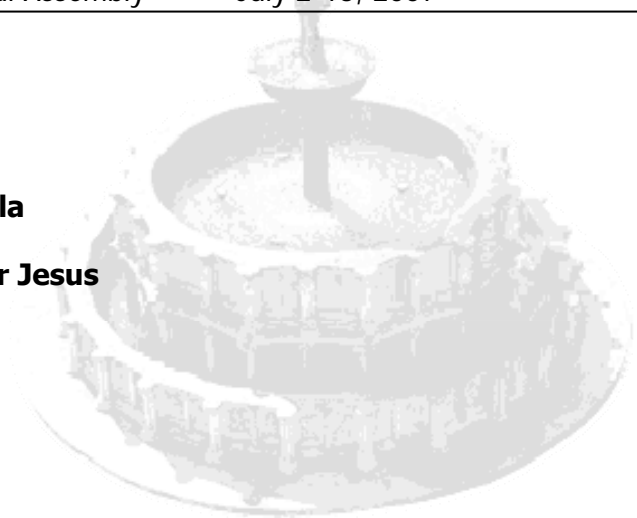
Litvina Ekaterina	2210
Sugioka Hiroko	2211
Honda Satoru	2212
Tono Yoko	2213
Osako Masahiro	2214
Piromallo Claudia	2215
Kirby Jon	2216
Behm Michael	2217
Levandowski Will	2218
Rai Shyam	2219
Sadidkhoy Ahmad	2220
Iaffaldano Giampiero	2221
Romanowicz Barbara	2222
Tiwari Virendra Mani	2223
Gupta Sandeep	2224
Babuska Vladislav	2225
Kind Rainer	2226
Zhu Shoubiao	2227
Singh Bijendra	2228
Kaban Mikhail	2229
Lebedev Sergei	2230
Artemieva Irina	2231
Narjess Karoui- Yaakoub	2232
Sidorova Irina	2233
Omidian Safieh	2234
Baranpourian Neda	2235



Kronrod Victor	2236
Tsuruga Kayoko	2237
Tsuruga Kayoko	2238
Muoz Miguel	2239
Barkin Yury	2240
Di Luccio Francesca	2241
Voss Peter	2242
Wang Qingchen	2243
Tumanian Maria	2244
Plenefisch Thomas	2245
Dererova Jana	2246
Dererova Jana	2247
Tesauro Magdala	2248
Schivardi Renata	2249
Serretti Paola	2250
Moufida Ben M'Barek Jema	2251
Vyacheslav Zobin	2252
Kr. Ashish	2253
Houze Xu	2254
Kasahara Junzo	2255
Ni James	2256
Kato Teruyuki	2257
Kim Woohan	2258
Qi Wang	2259
Liu Char-Shine	2260
Hayes Gavin	2261



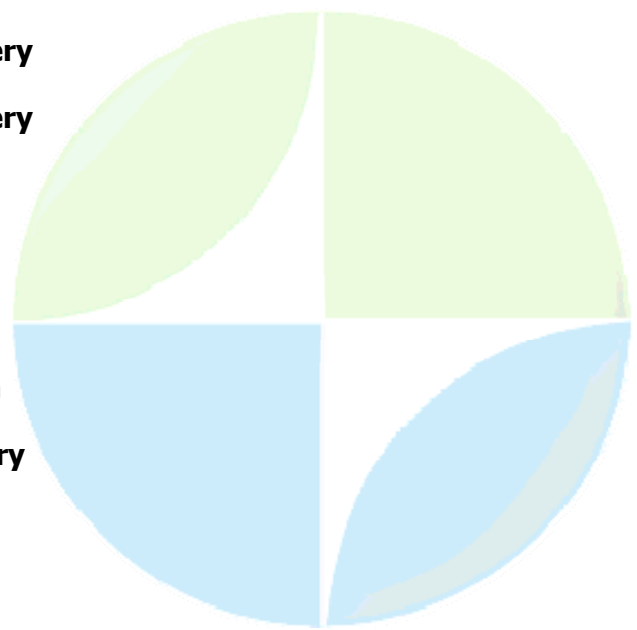
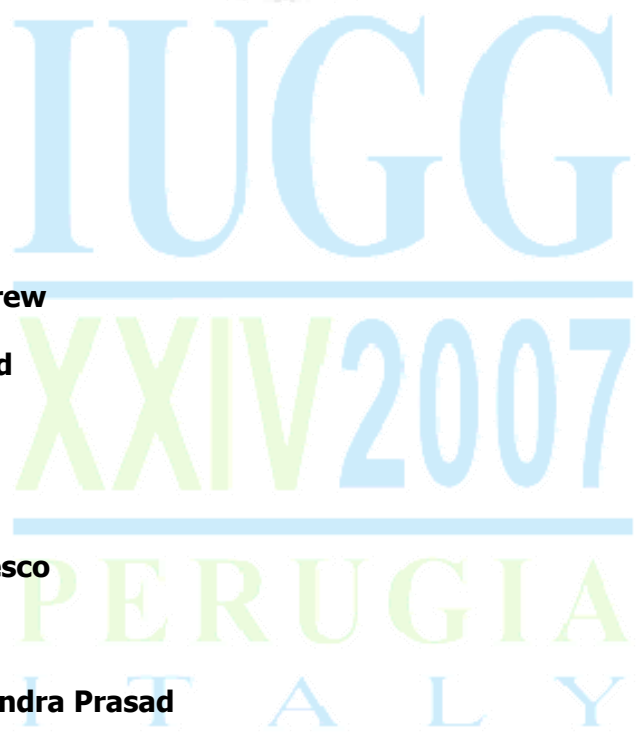
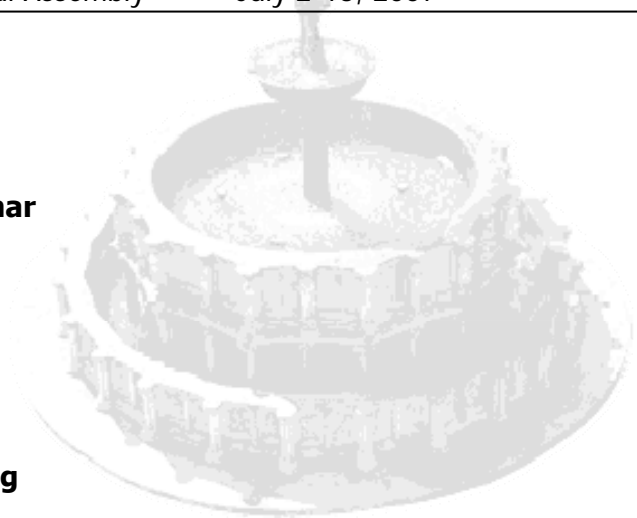
Wallace Laura	2262
Ding Zhifeng	2263
D'Agostino Nicola	2264
Galindo-Zaldivar Jesus	2265
Furlong Kevin P	2266
Kreemer Corne	2267
Casale Gabriele	2268
Buble Goran	2269
Tao Wei	2270
Nguyen Nhu Trung	2271
Kayal Jnana	2272
Victor Tatarinov	2273
Xu Zhaofan	2274
Nakamichi Haruhisa	2275
Jin Shuanggen	2276
Yi Guixi	2277
Teng Jiwen	2278
Greku Rudolf	2279
Chamoli Ashutosh	2280
Guo Dongmei	2281
Novotny Miroslav	2282
Boustan Elham	2283
Tahernai Nadia	2284
Tahernai Nadia	2285
Kasahara Junzo	2286
Tsuruga Kayoko	2287



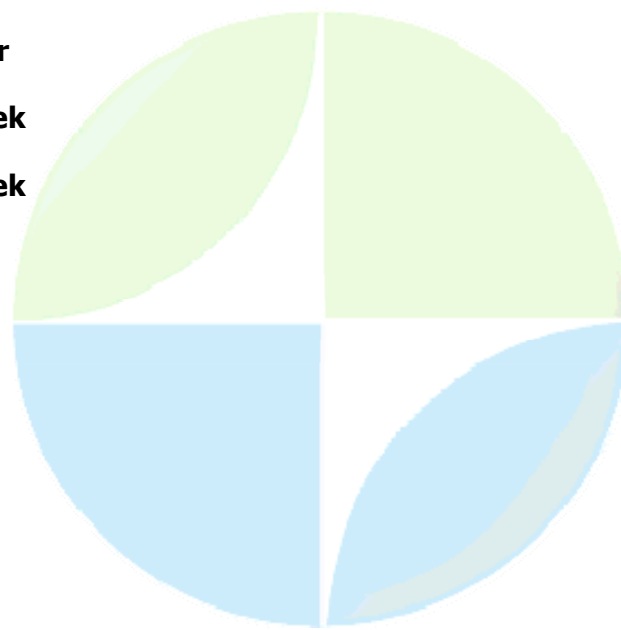
Tsuruga Kayoko	2288
Kasahara Junzo	2289
Tsuruga Kayoko	2290
Lucente Francesco Pio	2291
Besutiu Lucian	2292
Rawat Gautam	2293
Kumar Naresh	2294
Nowrouzi Gholamreza	2295
Takanami Tetsuo	2296
Riazirad Zohrehsadat	2297
Riazirad Zohrehsadat	2298
Riazirad Zohrehsadat	2299
Cheng Win-Bin	2300
Srivastava Kirti	2301
Joo Istvan	2302
Sobouti Farhad	2303
Cenni Nicola	2304
Zhang Xuemei	2305
Teoman Ugur Mustafa	2306
Tiwari Virendra Mani	2307
Ruano Patricia	2308
Ivanchenko Galina	2309
Wu Wen-Nan	2310
Wu Wen-Nan	2311
Wu Wen-Nan	2312
Wang Wei-Hau	2313



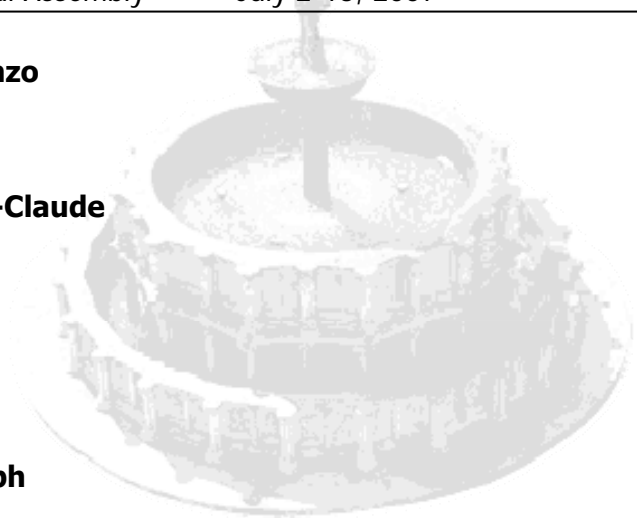
Hosseini Keivan	2314
Lin Yu-Yeh	2315
Roy Kalyan Kumar	2316
Mumladze Tea	2317
Zhu Shoubiao	2318
Zhu Shoubiao	2319
Shin Young Hong	2320
Mocanu Victor	2321
Bagh Samer	2322
Petrinin Alexey	2323
Fujii Naoyuki	2324
Gendaszek Andrew	2325
Karimov Farshed	2326
Triep Enrique	2327
Li Qinghe	2328
Mulargia Francesco	2329
Rawlinson Nick	2330
Bitragunta Rajendra Prasad	2331
Chen How-Wei	2332
Kovalevsky Valery	2333
Kovalevsky Valery	2334
Brown Larry	2335
Behm Michael	2336
Ito Kiyoshi	2337
Romeo Annalisa	2338
Korepanov Valery	2339



Yang Fanlin	2340
Romanowicz Barbara	2341
Kontar Aleksey	2342
Butler Rhett	2343
Kanazawa Toshihiko	2344
Toh Hiroaki	2345
Musumeci Mario Salvatore	2346
Favali Paolo	2347
Chierici Francesco	2348
Pazos Garca Antonio	2349
Waldhauser Felix	2350
Kontar Evgeny	2351
Shinohara Masanao	2352
Kisimoto Kiyoyuki	2353
Watanabe Tsuyoshi	2354
Sain Kalachand	2355
Tadokoro Keiichi	2356
Sugimoto Shingo	2357
Favali Paolo	2358
Cermak Vladimir	2359
Majorowicz Jacek	2360
Majorowicz Jacek	2361
Safanda Jan	2362
Chi Wu-Cheng	2363
Prezzi Claudia	2364
Ray Labani	2365



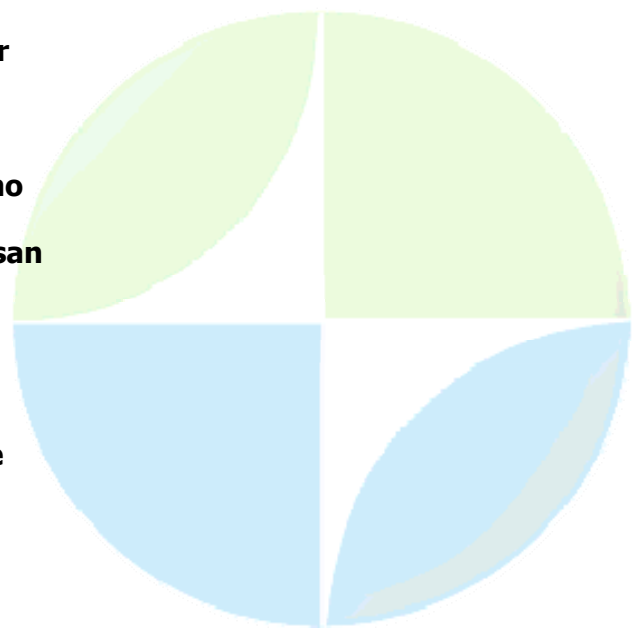
Pasquale Vincenzo	2366
Bin Shan	2367
Mareschal Jean-Claude	2368
Roy Sukanta	2369
Pandey O.P.	2370
Pandey O.P.	2371
Clauser Christoph	2372
Parphenuk Olga	2373
Milanovskiy Svyatoslav	2374
Perry Claire	2375
Huang Shaopeng	2376
Ismail-Zadeh Alik	2377
Popov Yuri	2378
Chapman David	2379
Houseman Gregory	2380
Hamza Valiya	2381
Gosnold Will	2382
Hamza Valiya	2383
Lipaev Aleksander	2384
Cermak Vladimir	2385
Heinle Shannon	2386
Verdoya Massimo	2387
Demetrescu Crisan	2388
Dobrica Venera	2389
Kummer Troy	2390
Solaro Giuseppe	2391



IUGG

XXIV2007

PERUGIA
I T A L Y



Miklashevskiy Dmitriy

2392

Clauser Christoph

2393

Semenova Anna

2394

Reiter Eric

2395

Rodnikov Alexander

2396

Widiyantoro Sri

2397

Barkin Yury

2398

Germa Aurelie

2399



IUGG

XXIV2007

PERUGIA
I T A L Y



In collaboration with



Sponsored by



Endorsed by



Thanks to



Touring Club Italiano



Media Partners



Sede regionale per l'Umbria





IUGG

XXIV2007

PERUGIA
I T A L Y



Published and Distributed by

USMA 2007

Umbria Scientific Meeting Association 2007

c/o IRPI CNR

Via della Madonna Alta, 126 - 06128 Perugia - Italy

e-mail: protocol@iugg2007perugia.it

website: www.iugg2007perugia.it

Printed in Italy, March 2008